CURRENT RESEARCH IN GEOLOGY APPLIED TO ORE DEPOSITS

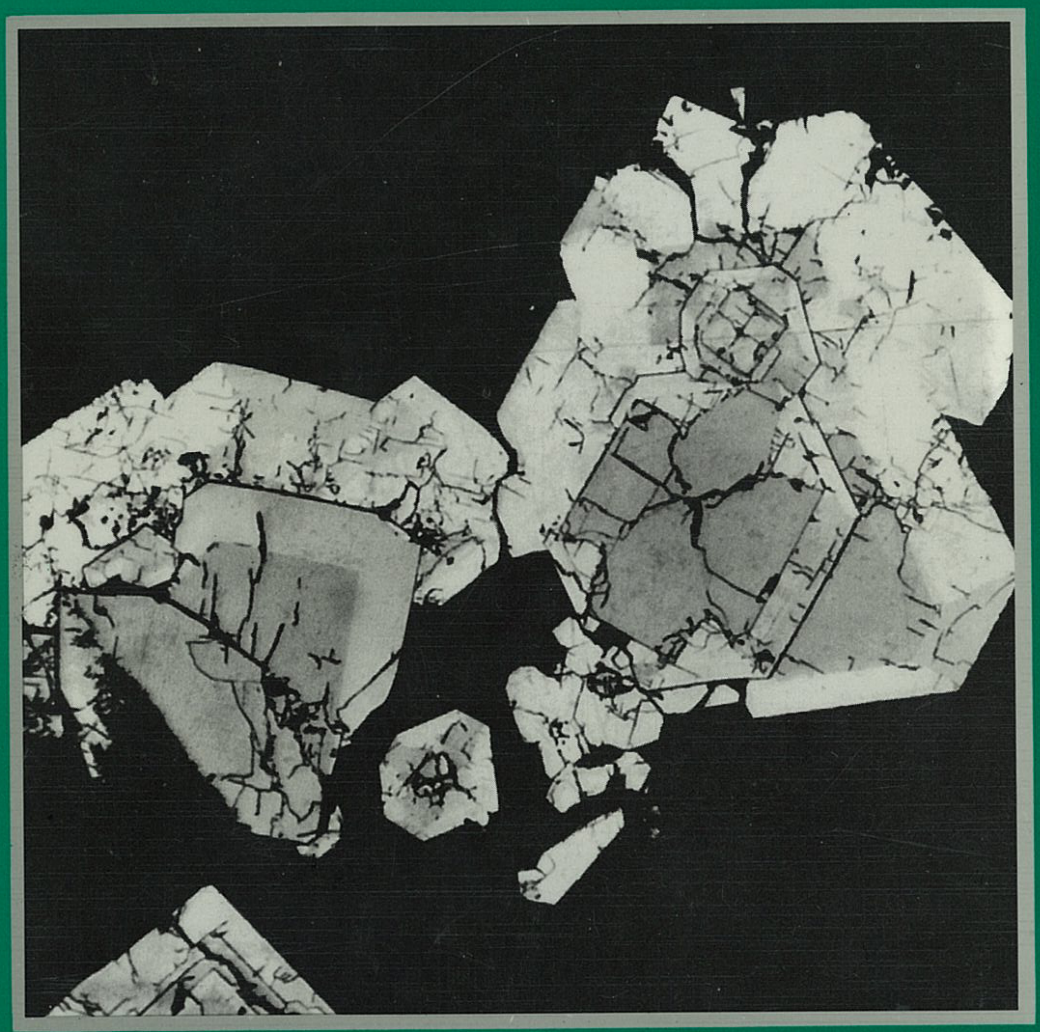

Edited by Purificación Fenoll Hach-Alí, José Torres-Ruiz & Fernando Gervilla

PROCEEDINGS OF THE SECOND BIENNIAL SGA MEETING
GRANADA / 9 - 11 SEPTEMBER 1993

CURRENT RESEARCH IN GEOLOGY APPLIED TO ORE DEPOSITS

Edited by

Purificación FENOLL HACH-ALI
José TORRES-RUIZ
Fernando GERVILLA

Departamento de Mineralogía y Petrología,
Universidad de Granada, Granada, Spain

Cover photograph in memory of our colleague and friend Prof. Dr. Günter A. Moh (1929–1993)
Cubooctahedral crystals of villamaninite, sector and concentrically zoned.
Providence mine (North Spain).
Microphotograph by A. Paniagua

Published by
University of Granada. Granada, Spain.
ISBN 84–338–1772–8. Depósito Legal GR–5299.1993

Printed by
La Guioconda, Granada 1993, Spain

Current Research in Geology Applied to Ore Deposits. Fenoll Hach-Ali, Torres-Ruiz & Gervilla (eds) (1993). ISBN 84-338-1772-8

Contents

2. *Massive and stratabound sulphide deposits in volcanic and sedimentary sequences*

3. Gold and other precious metals

5. Industrial mineral deposits

6. *Open session*

SPONSORED BY

Ministerio de Educación y Ciencia

Universidad de Granada

Consejo Superior de Investigaciones Científicas

The Society for Geology Applied to Mineral Deposits

Sociedad Española de Mineralogía

The Society of Economic Geologists
The IGCP 336
The IGCP 357

International Science Foundation

Excma. Diputacion Provincial de Granada

Excmo. Ayuntamiento de Granada

Springer Verlag

Caja General de Ahorros de Granada

Hipercor

FIELD TRIPS IN COOPERATION WITH

Riotinto Minera S.A.
Andaluza de Piritas S.A. (Minas de Aznalcollar)
SOMINCOR (Minas de Neves–Corvo)
Tolsa S.A.
Minas de Gador S.A.

Current Research in Geology Applied to Ore Deposits.Fenoll Hach-Alí, Torres-Ruiz & Gervilla(eds)(1993).ISBN 84-338-1772-8

Preface and Editorial Comments

During the 25th SGA Anniversary Meeting in Nancy, France, the SGA decided to hold its Second Biennial Meeting in Granada, Spain being one of Europe's most active countries as far as the mining of ore deposits is concerned.

The meeting has been organised by a group of researchers belonging to the Department of Mineralogy and Petrology of the University of Granada, together with the Andalucian Institute of Mediterranean Geology and the University of the Basque Country, to all of whom I extend my grateful thanks for their help and logistic support.

On behalf of the organising committee of the SGA I also wish to thank the Spanish Ministry of Education and Science and all the other institutions who have helped in the organisation of this meeting and have made it possible for scientists from developing countries to be able to take part.

And my thanks are of course due to all those researchers from five continents (191 from Europe, with a large contingent from the eastern countries, 20 from America, and 44 from Asia, Africa and Australia) who have contributed to the meeting with their presence and their scientific contributions to the volume *Current Research in Geology Applied to Ore Deposits*, in which all the communications presented during the Second Biennial Meeting of the SGA in Granada (9 to 11 September, 1993) are published. These communications are grouped into the following topics: mineralogical and geochemical studies applied to ore deposits; massive and stratabound sulphide deposits in volcanic and sedimentary sequences; gold and other precious metals; rare elements and other mineralizations associated with granitic rocks; and industrial mineral deposits.

I must also acknowledge the help given by María del Mar Abad and Salvador Morales in the publication of this volume, with their unstinting efforts in the composition of texts and correction of errors. Lastly, my thanks go to the printing house La Guioconda and to all those who have contributed in any way to ensuring that the volume came out before the meeting.

It is a pleasure for the Organizing Committee and SGA to wish you a pleasant stay in Granada during the meeting.

Granada, June 30
Puri Fenoll Hach-Alí

LOCAL ORGANIZING COMMITTEE

Departamento de Mineralogía y Petrología
Universidad de Granada

Departamento de Mineralogía y Petrología
Universidad del País Vasco

Instituto Andaluz de Geología Mediterránea (IAGM)
Consejo Superior de Investigaciones Científicas - Universidad de Granada

MEETING COMMITTEE

Secretary General:	Puri Fenoll Hach-Alí
General Affairs:	Fernando Gervilla Linares, Alberto Lopez Galindo, Miguel Ortega Huertas, José Torres-Ruiz.
Abstracts:	Fernando Gervilla Linares, José Torres-Ruiz
Field Trips:	Fernando Gervilla Linares, José Torres-Ruiz, Francisco Velasco Roldán
Budget:	Alberto Lopez Galindo
Advisory Members:	Antonio Arribas Moreno, José Linares Gonzalez, José Lopez Ruiz, Manuel Rodriguez Gallego, Francisco Velasco Roldán

Current Research in Geology Applied to Ore Deposits.Fenoll Hach-Alí, Torres-Ruiz & Gervilla(eds)(1993).ISBN 84-338-1772-8

Society for Geology Applied to Mineral Deposits

COUNCIL FOR 1993

Executive Committee

President: I. Plimer (Australia)
Vice-President: J.C. Touray (France)
President-Elect: Z. Johan (France)
Vice President-Elect: B. Lehmann (Germany)
Secretary: M. Pagel (France)
Treasurer: R. Höll (Germany)
Chief Editor: D. Rickard (United Kingdom)

Regional Vice-Presidents

N. America: J. Guha (Canada)
S. America: W. Vivallo (South America)
Asia: H. Shimazaki (Japan)
Australia: H. Etminan (Australia)
S. Africa: M.J. Viljoen (South Africa)

Councillors:

Terms ending on December 31, 1996
L. Fontboté (Switzerland)
K. Sundblad (Sweden)
J. Boulègue (France)
J.F. Sureau (France)
O. Thalhammer (Austria)
B. Stribny (Germany)

Terms ending on December 31, 1994
G.C. Amstutz (Germany)
M. Boni (Italy)
A.M. Evans (United Kingdom)
P. Fenoll Hach-Alí (Spain)
J. Aichler (Czech)
C. Marignac (France)
D. Rickard (United Kingdom)
S. Scott (Canada)

Ex-Officio Councillors (SEG)

President: Samuel S. Adams (USA)
Executive Secretary: John A. Thoms (USA)

Invited lectures

Current Research in Geology Applied to Ore Deposits. Fenoll Hach-Alí, Torres-Ruiz & Gervilla (eds) (1993). ISBN 84-338-1772-8

SUBMARINE HYDROTHERMAL AND EVAPORITE-RELATED BASE METAL, RARE METAL AND PGE MINERALIZATION IN THE LOWER PROTEROZOIC OLARY BLOCK, SOUTH AUSTRALIA

Plimer, I.
School of Earth Sciences, The University of Melbourne, Parkville Vic, 3052, Australia

The Lower-Middle Proterozoic Olary Block of South Australia comprises multiply deformed high metamorphic grade metasediments and metavolcanics. The rocks form part of the Willyama Supergroup which, 100km to the east, hosts the giant Broken Hill Pb-Zn-Ag deposits. Hundreds of small base metal and uranium ore deposits occur in the Olary Block, the largest of which was the Radium Hill uranium deposits. There are no base metal deposits in the Olary Block which closely resemble the Broken Hill Pb-Zn-Ag mineralisation.

The Olary Block has enjoyed Lower Proterozoic coeval D1-M1 resulting in amphibolite facies metamorphism and recumbent folds. Coeval D2-M2 upright, open to tight folds and amphibolite facies metamorphism are overprinted by D3 which is expressed as gentle warps of pre-existing fabrics and dissection by retrograde shear zones. The small time difference between deposition of the Willyama Supergroup and the coeval D1-M1 and D2-D2-M2 events suggests that deposition and tectonism were a continuum of the same process. Retrogression of the Willyama Supergroup began in D3. However, the retrograde events D4-D5 affected both the Willyama Supergroup and the overlying Adelaidean sequence. The D4-D5 events are dated at about 500 Ma.

The Willyama Supergroup in the Olary Block comprises a number of unusual lithologies. The basal part of the stratigraphy comprises migmatite and composite gneiss and there are indications that this is Archaean-Lower Proterozoic basement. Overlying the composite gneiss is the quartzofeldspathic suite comprising a basal Middle Proterozoic felsic gneiss of granitic composition containing bipyramidal quartz and tabular feldspars which is interpreted as a felsic volcanic rock. Stratigraphically above this gneiss is a sequence of psammopelitic to pelitic gneiss in a sequence dominated by quartzofeldspathic gneiss. Lithological boundaries within the quartzofeldspathic gneiss are gradational. The quartzofeldspathic horizons contain K feldspar-biotite-quartz gneiss, quartz-albite rocks and calc-albitites. Minor discordant and concordant amphibolite masses are present.

Horizons of laminated quartz-magnetite$\pm$hematite and quartz-magnetite-barite$\pm$hematite rocks (iron formations) occur at the top of the quartzofeldspathic suite and are the most economically interesting parts of the quartzofeldspathic suite and are traditionally thought to represent submarine hydrothermal precipitates. These iron formations contain both primary and secondary hematite, have the REE signature of hydrothermal fluids and, in high strain areas, are well laminated with laminae defined by schlieren of magnetite and magnetite-hematite. Much of the "bedding" in these banded iron formations is of tectonic origin. In low strain areas, a gradation from calc-albitite into magnetite albitite, magnetite pseudomorphs after a rhombohedral mineral (? primary dolomite) and bedding characteristics identical to that observed in the overlying calc-albitites are present. Calc-albitite rocks have textures

suggesting that primary evaporitic dolomite and gypsum were replaced by calc-silicate minerals and, by analogy, it appears that the iron formations result from the pre-metamorphic sub-sea floor replacement of evaporite minerals such as dolomite and gypsum by an extremely oxidised hydrothermal fluid. There is no evidence to suggest that the iron formations formed as a result of precipitation on the sea floor from submarine hydrothermal activity.

Overlying the quartzofeldspathic suite is a package of sediments dominated by a diversity of calc-silicate rocks, quartz-albite±cobaltian pyrite rocks and metasediments (psammopelites, pelites) and rare piemontite-, magnetite-garnet-, quartz-iron sulphide- and sulphide-bearing rocks. Lithological boundaries are commonly gradational, especially between the albitite, calc-albitite and calc-silicate rocks. The rare Mn- and Fe-rich rocks represent highly oxidised submarine hydrothermal precipitates.

Calc-silicate rocks grade from laminated calc-silicate units, to calc-silicate-albite rocks, to calc-silicate-albite-magnetite rocks to quartz-magnetite±hematite rocks. Retrograde metamorphic (? M3) andradite and epidote are well developed along bedding and in fractures in the calc-silicate rocks. The prograde diopside-grossular-plagiocase calc-silicate rocks display bedding, pseudomorphs after dolomite and gypsum, hypersaline fluid inclusions and variable contents of scapolite, scheelite, pyrite, chalcopyrite, cobaltian arsenopyrite, galena, sphalerite and gold.

A great diversity of calc-silicate breccias occur. The breccias contain clasts of albitite or calc-albite and a calc-silicate matrix however, in one place, the matrix is composed of magnetite-hematite. Some breccias are possibly karstic in origin related to the replacement, solution and collapse of evaporitic rocks by diagenetic and hydrothermal fluids whereas other breccias are related to competency differences during D2 deformation and post-D2 brittle deformation. A number of these calc-silicate breccias contain minor Fe, Cu and Au mineralisation.

On the basis of chemistry, fluid inclusions, evaporite pseudomorphs and boron isotope geochemistry, the calc-silicate and calc-albitite rocks are interpreted as metamorphosed continental evaporites intercalated with both oxidised and reduced sediments, analcime-rich rocks and felsic volcanics. This Middle Proterozoic evaporite-volcanic-clastic sediment sequence overlies Archaean to Lower Proterozoic continental basement. It is proposed that dewatering of the clastic sediment-continental evaporite pile has resulted in hypersaline oxidised diagenetic fluids which, at redox interfaces in the pelitic-psammopelitic-calc-silicate rocks, deposited sulphides. The redox interface is characterised by sulphide minerals of the transition elements such as Fe, Cu, Co and Ni and minerals of other variable valence elements (U, Au). Minor platinoids (Pd>>Pt) also occur at this horizon of redox-controlled sulphide deposits however the source and sink of the platinum group elements is not known. Platinoids are enriched in some gossans developed at redox interfaces.

The uppermost part of the Willyama Supergroup in the Olary Block comprises a pelite suite. The pelite suite has been subdivided into a lower pelite suite within which calc-silicate ellipsoids, tourmalinite and tourmaline-rich pelite are characteristic. Boron isotope data from the tourmalinite suggests that the boron is of continental evaporite origin. The upper part of

the pelite suite is somewhat more psammopelitic, contains chiastolite-bearing carbonaceous pelites, psammites, minor calc-silicate rocks and quartz-garnet rocks. Both the tourmaline- and garnet-rich rocks are interpreted as submarine hydrothermal precipitates or sub-sea floor replacements of pelitic sediments.

The Middle Proterozoic Willyama Supergroup rocks were deposited on rifted Archaean-Lower Proterozoic basement. Bimodal volcanism occurred and initial continental rifting was associated with an abundance of felsic volcanics. Ash falls into alkaline lakes, somewhat akin to the modern East African Rift, produced analcime-rich rocks. Evaporites and possibly lacustrine clastic sediments also formed in this rift. The sequence comprising evaporite-felsic volcanic-clastic sediment underwent dewatering and diagenesis resulting in the extensive replacement of sediments by minerals precipitated from the resultant supersaline brines. Oxidised supersaline hydrothermal fluids cooled the new crust and precipitated mineralisation below and on the rift floor. Hydrothermal activity persisted during relaxation phase of the rift wherein the rift was being filled with clastic sediments, boron was leached from continental evaporites deeper in the pile and deposited as sub-rift floor replacements and rift floor precipitates, and hot springs precipitated iron- and manganese-rich sediments on the rift floor. It is suggested that there is a continuum of related Middle Proterozoic events commencing with continental margin extension followed by rifting, subsidence, compression and uplift.

A correlation of the Willyama Supergroup in the Olary Block with the Supergroup in the adjacent Broken Hill Block suggests that an event of sudden deepening coeval with granite emplacement, a high geothermal gradient and resultant submarine hydrothermal activity was absent in the Olary Block. The giant Broken Hill Pb-Zn-Ag deposits formed during this event of high geothermal gradient when an energy source (plutons, thin crust) produced focussed magmatic fluids mixed with supersaline evaporite-derived hydrothermal fluids. These fluids ascended a fault, underwent instantaneous P-T-X changes in the rift graben, and precipitated the Broken Hill sulphide deposits.

Deformation of the Willyama Supergroup in the Olary Block has resulted in the generation of quartz-feldspar-rare metal pegmatites (D1) and quartz-feldspar pegmatite (D2, D3). The D1 pegmatites contain beryl, retrograde bertrandite and muscovite, phosphates and rare Li minerals. These pegmatites commonly have a minor sillimanite-rich aureole, the pegmatite composition reflects the composition of the intruded rocks and the D1 pegmatites are controlled by D1 structures. For example, tourmaline-rich pegmatites only occur in the pelite suite (which contains tourmalinite and tourmaline-rich pelite) and Mn-Fe phosphate-bearing pegmatites only occur in the stratigraphic package containing piemontite- and magnetite-hematite-bearing rocks. The D2 pegmatites are far less voluminous than D1 pegmatites and contain no ore minerals as the first melting batch appears to have efficiently removed the incompatible elements. Two generations of relatively oxidised syn-tectonic granitoids and one post-tectonic granite have intruded the sequence.

Uranium mineralisation is associated with the second phase of syn-tectonic granite. The second generation of syntectonic granites are sodic in contrast to the potassic first generation of granites. Uranium mineralisation occurs in brecciated sodic granitoids which have a matrix

of F-phlogopite and quartz. Uranium minerals occur in veins, in shear/fault zones and as minor disseminations.

Overlying the Willyama Supergroup is the Late Proterozoic Adelaidean Sequence comprising weakly deformed greenschist facies metamorphosed psammitic, pelitic, and carbonate sediments of glacial, shallow marine and evaporitic origin. Minor carbonate-hosted Pb-Zn deposits and minor slate-belt-type axial plane quartz-pyrite-arsenopyrite veins in anticlines occur in the Adelaidean sequence.

A small carbonatite with associated sheared retrogressed alkaline pyroxenites (e.g. jacupirangite, ijolite) occurs within a shear zone. The shear zone may be associated with the 500 Ma D4-D5 events. The emplacement of the undated carbonatite complex is probably related to extension resulting in the opening of the Bancannia Trough to the north-east at 480 Ma. The carbonatite is poorly exposed, covered by calcrete and deeply weathered and only primary coarse grained ferroan calcite, LREE-enriched apatite and chalcopyrite have been identified.

Although the topography is controlled by Tertiary uplift, weathering probably commenced immediately after the Permian glaciation. The freshness of outcrop and juvenile topography suggest a very recent uplift. Outcropping sulphide deposits have a spectacular array of secondary copper, cobalt and iron arsenates, carbonates and silicates, gossans are widespread and groundwaters are enriched in heavy metals. The intense weathering and northward drainage into salt lakes has resulted in Tertiary calcrete-type and fluvial channel uranium deposits which derived the uranium from long intense weathering of the syntectonic uraniferous sodic granitoids and U-rich metasediments.

This project forms part of a mining industry-Australian Research Council supported Olary Research Project in the Olary Block initiated and supervised by Dr Paul Ashley (University of New England), Assoc. Prof. Phil Seccombe (University of Newcastle) and the author. It has used the unusual approach of mapping a 4500 km^2 area of the Olary Block rocks before detailed mineralogical, petrological, geochemical, stable isotopic and geochronological studies.

Current Research in Geology Applied to Ore Deposits. Fenoll Hach-Alí, Torres-Ruiz & Gervilla (eds). (1993) ISBN 84-338-1772-8

RECENT EVOLUTION OF MINERALOGICAL AND GEOCHEMICAL TECHNIQUES APPLIED TO ORE DEPOSITS: SELECTED ILLUSTRATIONS

Touray, J.C.
Université d'Orléans, ESEM, Rue Léonard de Vinci, 45072 Orléans Cedex 2, France. URA 1366 du CNRS et GdR. "Métallogénie et Matériaux Minéraux".

Improvements in scientific knowledge depend both on a renewal of concepts and upon an evolution of techniques. In this last respect, absolute dating which has strongly improved since the sixties, is now usable in a routine way to constrain metallogenic models. For example, in order to bracket the timing of Archean gold mineralization in the Superior Province, a number of dating methods have been applied (Classical Rb-Sr, ^{40}Ar-^{39}Ar step heating of vein related muscovite and metamorphic amphibole, U-Pb dating of zircon, rutile and sphene, Sm-Nd dating of scheelite.). The results give evidence for a 70-100 m.y time gap between plutonism-metamorphism and mineralization (Hanes et al., 1992).

Analytical devices for isotopic dating were developed in strong relation with applications to geosciences. However, in a more general way, mineralogy and geochemistry have benefited from an accelerated development of analytical methods firstly devolved to other domains such as solid physics, materials science or chemistry.

Within the bunch of recently introduced methods, I selected four approaches in order to "sample" different analytical fields. These approaches deal with isotope and trace elements studies, mineral imaging and computer geochemistry.

ION MICROPROBE GEOISOTOPY

Since the pioneering work of Deloule et al (1986) about "lead and sulfur microstratigraphy in galena crystals from MVT deposits", a limited number of applications to Ore Geochemistry have been published. A possible reason is the relatively low present accuracy (0.8 to 1 permil) which limits investigations to particular problems involving high variations of isotopic ratios. In this respect, Pb and S presently remain the best candidates for ion microprobe isotopic investigations. When higher precisions will be attained with ion microprobes of the new generation, a number of other applications, including Oxygen thermometry, will become possible.

Profiles of lead isotope composition were measured, normal to the growth zoning of PbS (Mc Farlane and Petersen, 1990). For adequate precision, only $^{207}Pb/^{206}Pb$ and $^{208}Pb/^{206}Pb$ ratios were measured. In samples from Hualgayoc area (Peru), the maximum variation of lead isotopic ratios was found only slightly higher than the analytical uncertainty. This lack of zoning indicates either a single source of lead or a thorough homogenization of Pb from diverse sources prior to galena deposition. Ion microprobe measurement of $\delta^{34}S$ may give informations on variations of the fluid composition and temperature or on the crystallization history of the ores. Isotopic zoning at a 0.1 mm scale has been observed in one hydrothermal sulfide rich chimney from the EPR with $\delta^{34}S$ scattering from -1 to +7 permil (Chaussidon et

al., 1991). Temperature changes (reflected by variable Se contents in chalcopyrite) and variable amounts of sulphate reduction may explain the observed $\delta^{34}S$ variations. The HYC deposit at Mc Arthur River (Australia) is an example of sediment-hosted massive deposit made of finely intergrown sulfides in which a very large sulfur isotope variability has been determined using an ion microprobe (Eldridge et al, 1993). A key issue was to define, through $\delta^{34}S$ measurements, the genetic relations between primary pyrites and the base metals mineralization. Extreme variations reaching 50 permil have been observed in pyrites while sphalerite, galena and chalcopyrite displayed more restricted $\delta^{34}S$ values. These data suggest a syndiagenetic formation of pyrite involving biogenic H_2S and an epigenetic origin for the base metal sulfides, which precludes any "Sedex-type" accumulation of Zn, Pb and Cu.

ICP-MS INDUCTIVELY COUPLED PLASMA-MASS SPECTROMETRY

Inductively coupled Plasma-Mass Spectrometry (ICP-MS) is a relatively new, highly sensitive method for elemental and isotopic analysis. A survey of applications in geoanalysis (Hall, 1992) and a list of some 70 references about geological applications have recently been published (Mc Larren, 1992). Accuracy depends mainly on the possibility of eliminating spectral interferences; high sensitivity stems from the excitation source which reaches about 8 000 to 10 000°K. The ICP-MS can be utilized in two operating modes : a) quantitative or semiquantitative analysis with routine accuracy of 10 to 20%, more than 80 elements being typically determined in about 5 minutes with evident applications to geochemical prospection; b) isotope dilution analysis, allowing very accurate quantifications of 0.1 to 0.5%.

The main advantages of ICP-MS compared to ICP Emission Spectrometry are better detection limits (typically ppb and sub-ppb level) and possibility of detecting refractory elements (Brenner and Taylor, 1992). REE detection limits in aqueous solutions are up to four orders of magnitude lower than the concentrations determined in groundwater samples (Stroh, 1992) which indicates potential applications to fluid inclusions leachates. Regarding fluid and solid inclusions, the laser ablation technique (ablated spot about 50 μm^2) may be used for direct analysis with detection limits in the ppb concentration range. A joint innovation is the development of fast electronics capable of scanning the entire mass range in 0.1s, which enables measurement of fast analytical transient signals such as emitted by laser ablation. Promising studies, in the field of hydrogeochemical prospecting of ore deposits, deal with determinations of precious (Pt, Pd, Os, Au) and other trace metals (e.g. W, Mo, U, REE).

RAMAN IMAGING WITH CONFOCAL SCANNING

Raman micro-spectroscopy is a molecular technique whose applications during the eighties led to significant progresses in micromineralogy and in fluid inclusions geochemistry. Although known for at least two decades, Raman imaging is only developed at present.

This new facility complements conventional mono or multichannel spectroscopic devices. The main purpose of the different laser Raman imaging and mapping techniques is to map out the distribution of a given chemical compound in the depth of a transparent mineral. The observed zone is divided in elementary pixels whose spectral intensities are measured for selected Raman bands. Spectral and spatial data are stored, then an image is reconstructed for each band, leading to "optical sections" i.e. "Raman tomographies". Different technical methods may be used : in the Ramascope, the whole observed field is illuminated by the laser excitation radiation. After optical spectral filtering of the selected band, the spectral intensities are simultaneously measured in the 2D by means of a CCD camera, before subsequent processing. In the Dilor "confocal laser Raman system" (Da Silva, 1991), the system is kept confocal and stigmatic for every pixel. Unlike the conventional optical microscope, the confocal arrangement uses a point light-source (usually a laser beam) sharply focused onto the specimen. A pinhole aperture isolates in the enlarged image a region exactly corresponding to the illuminated pixel. After photoelectron detection, computer data processing enables a reconstruction of microscope images. The confocal systems offer an enhanced contrast, an improved depth of field and axial resolution permitting "optical sectioning". These properties lead to high accuracy in Raman imaging, as displayed in the Dilor System, whose principle is as following : two optical deflectors (one for lateral scanning of the laser beam, the other for selection of the image point) are installed within a confocal microscope transfer optics. A dispersive spectral analyzer permits then to choose a selected Raman band. Using this facility, Raman tomographies of fluid inclusions may currently be performed, permitting the localization of fluid components and sometimes of unexpected solids.

GEOCHEMICAL SIMULATORS

Computer codes for chemical modelling of natural systems and sometimes involving ore genesis are now of routine use (Jamet et al., 1993). Amongst recent progresses, one may quote a) the coupling of speciation of water solutes and water-rock interactions with hydrodynamics, in order to explain the migration of species through the geological medium; b) the improvement of chemical codes for accomodating a large number of elements and species and resolve new problems. In this respect, the BRGM has recently developed a combination of a simulation software package (NEPTUNIX) with a general application graphic system (ALLAN). Using this new strategy makes it possible to improve the solving of thermodynamic and kinetic problems and explore mechanisms hitherto rarely taken into account (e.g. redox reactions kinetics, crystal growth etc...); specific simulators may be created for each application, code writing and solving of equations being no longer a concern. Applications to metallogeny are still preliminary but potential developments in this field are important. An example of geochemical problem, the interaction of sea water with a sandstone-type aquifer has been simulated with 12 elements, 86 aqueous species and 8 minerals. The results indicate that a state of general redox equilibrium is reached after 80 days at 25°C (Fabriol and Czernichowski, 1992).

CONCLUSION

Current research in Ore Mineralogy and Geochemistry is regularly replenished by new techniques giving new informations or data, more accurate or easier to obtain than before. Present routine use of Electron Microprobe, Raman microspectrometers or Scanning Electron Microscope are familiar examples.

In my opinion and as presented in this lecture, future progresses lie in the following fields : Extension of microprobing to geoisotopy; development of high sensitivity multielement trace analysis (ICP-MS); new imaging techniques (Raman "tomographies") and geochemical simulation.

The main wager is about the long range validity of this choice, a number of new devices lying rapidly in the cemetery of the stillborn "promising techniques".

C. Beny, M. Chaussidon and R. Fabriol are acknowledged for helpful dicussions.

REFERENCES

Brenner J.B.and Taylor H.E. (1992). Critical Reviews in Analytical Chemistry, 23 : 355-367.

Chaussidon M., Albarède F. and Sheppard S.M.F. (1991). Source Transport and Deposition of Metals; Pagel and Leroy (eds). Balkema, Rotterdam : 609-614.

Da Silva E. (1991).Unpublished DILOR documentation.

Deloule E., Allègre C.J. and Doe B. (1986). Economic Geology, 81 : 1307-1321.

Eldridge C.S., Williams N. and Walshe J.L. (1993). Economic Geology, 88 : 1-26.

Fabriol R. and Czernichowski I. (1992). Proceedings of 7th Water-Rock Interactions. Balkema, Rotterdam : 213-216.

Hall G.E.M. (1992). Journal of Geochemical Exploration, 44 : 201-249.

Hanes J.A., Archibald D.A. and Hodgson C.J. (1992). Economic Geology, 87 : 1849-1861.

Jamet P., Hooker P.J., Schmitt J.M , Ledoux E. and Escalier des Orres P. (1993). Mineralium Deposita, 28 : 66-76.

Mc Farlane A.W. and Petersen V. (1990). Economic Geology, 85 : 1303-1327.

Mc Larren (1992). Atomic Spectroscopy, 13 : 81-88.

Stroh A. (1992). Atomic Spectroscopy, 13 : 89-92.

Current Research in Geology Applied to Ore Deposits. Fenoll Hach-Alí, Torres-Ruiz & Gervilla (eds) (1993). ISBN 84-338-1772-8

SELF-ORGANIZATION FABRICS IN CARBONATE-HOSTED ORE DEPOSITS: THE EXAMPLE OF DIAGENETIC CRYSTALLIZATION RHYTHMITES (DCRs)

Fontboté, L.
Dépt. de Minéralogie, 13 Rue des Maraîchers, 1211 Geneva 4, Switzeland.

Introduction

The scope of this contribution is to present an example of macroscopic rhythmic banding created at the interaction site between mineralizing brine(s) and host rock. It will be shown that certain rhythmic fabrics described below and which are typical for many carbonate-hosted ore deposits are not determined by a possible original depositional or tectonic rhythmicity. It is rather suggested that they are due completely or in part to "self-organization" processes, i.e., ."the spontaneous transition of a non-equilibrium system from a non-patterned state to a patterned state without the intervention of patterned external cause" (Chadam and Ortoleva, 1990, p. 175).

Rhythmic banded textures in carbonate-hosted ore deposits

Figure 1 shows an example of the banded textures discussed in the present contribution. They are characterized by rhyhtmic alternance of dark and light bands which correspond petrographically to distinct carbonate generations. In general, the dark bands or "*generation I*" correspond to a fine- to medium grained aggregate of dolomite with or without fine-grained sphalerite and subordinate pyrite. The light bands consist of coarse to very coarse subhedral crystals of dolomite or sphalerite arranged in a bipolar pattern ("*generation II*"). In places, a xenomorphic filling of white sparry dolomite, galena, calcite or bitumen is observed in the center of the light bands ("*generation III*"). The petrographic character of the dark and the light bands is essentially different. Whereas the dark bands correspond to the strongly replaced and completely recrystallized host rock, the light bands are open-space filling precipitates. There exist different lines of evidences indicating that the space filled by white sparry dolomite, sphalerite and the other minerals ocurring in generations II and III has been produced mainly by dissolution of the host rock.

Characteristic rhythmic fabrics similar to those shown in Fig.1 occur in numerous carbonate-hosted ore deposits. The most common composition is dolomite with or without sphalerite and galena. However, numerous other compositions are known, including barite or fluorite (Gorzawski et al., 1989), ankerite and siderite (Gil et al. 1984), magnesite (Velasco et al. 1987), dolomite, pyrite and sphalerite (Arne & Kissin, 1989). These fabrics are generally referred to as "zebra ore" or "zebra rock" but other local names are also used ("coon-tail" fluorite ore in southern Illinois; "franciscana dolomite" in southern Spain, and "mineral rubanné" in the French literature). Fontboté and Amstutz (1983) presented a review of these fabrics and concluded from geometrical observations that in many cases the rhythmic banding is basically not inherited from an original depositional rhythmicity but rather created by the process of diagenetic crystallization and recrystallization itself and proposed the term "diagenetic crystallization rhythmite (DCR)".

Fig. 1 Example of irregular dolomitic DCR in a mine wall of the San Vicente Zn-Pb deposit. Scale is given by the hammer at the left side.

If, as discussed below, the conclusion that the rhythmicity basically is not inherited can be mantained, subsequent geochemical investigations do not support other assertions proposed by Fontboté and Amstutz (1983). In particular, it was suggested that DCRs form during early diagenesis by a process of differentiation by crystallization fractionation in the sense of Amstutz and Park (1971), implicitly assuming a closed system during diagenetic crystallization. However, as already noted by Fontboté and Gorzawski (1990) and discussed in the next section, all DCRs known to the author are the result of the interaction of brine(s) and the host rock in an open system long after lithification. Arne and Kissin (1989) concluded similarly by describing DCRs of the Nanisivik Pb-Zn-Ag deposit.

Isotopic characteristics and precipitation conditions

Carbon, oxygen, and strontium isotopic determinations carried out on dolomite, calcite and sphalerite of DCRs of different localities display marked compositional patterns (Gorzawski et al., 1989, and 1990, Fontboté and Gorzawski,1990., Moritz et al.,1993, Spangenberg et al., this vol.). In general, stable isotopes tend to be lighter and strontium isotopes more radiogenic in the later open space-filling generations II and III than in generation I which is a replacement and recrystallization of the original host rock. This general behaviour can be explained in terms of different mixing ratios between influxing brine(s) and the original carbonate rock. In generation I, where relicts of the original host rock are still preserved, the fluid/rock ratio is lower that in generations II and III which are open space precipitates. Therefore, the isotopic composition of the later filling minerals reflect better the characteristics of the influxing brine(s).

In summary, these considerations are in agreement with the conclusion avanced by Fontboté and Gorzawski (1990, p. 1415-1418) that DCRs at San Vicente formed during "late stages of diagenesis, under a burial of two to three kilometers by a reaction of the original carbonate rock with an influxing basinal brine". In fact, all DCRs studied in some detail (e.g., Fontboté and Gorzawski, 1990, Gorzwski et al., 1989, Landis and Tschauder, 1990, Moritz et al., this volume) show that the coarsely crystalline generation II has formed by precipitation of hot, saline, and strontium radiogenic brines, i.e., brines similar to those which form MVT ore deposits.

Detailed analyses on a dolomitic DCR of San Vicente carried out by Spangenberg et al. (this vol.) show small but measurable differences in the stable isotope composition of paragenetic coeval sparry dolomite of generation II. This indicaties that compositional gradients existed at the sample scale during crystallization. This supports the hypothesis of Machel (1990) that diagenetic recrystallization and in some cases precipitation of carbonates in aquous fluids may occur commonly in thermodynamic *disequilibrium* with the bulk solution. The compositional gradients could be due to different fluid/rock ratios or different brine mixing ratios or to the existence of thin surface-absorbed or surface-bonded fluid layers.

The rhythmic banding of DCRs

Interpretations which explain the banding of DCRs as mimic replacement of depositional rhythmicity (e.g., Bogacz et al. 1973) can not be retained since abundant petrographic evidences show that DCRs develop a rhythmicity non related to fabrics of the original host rock. Although in many cases the rhythmic banding of DCRs incorporates original features like bedding, algal mat lamination or cross-cutting patterns produced by stress (Fig. 1), the rhythmicity in DCRs is much more "cyclic" than that of the original fabric. Extreme examples of almost perfect "cyclicity" are shown in Fig. 1 of Spangenberg et al. (this vol). In addition, DCRs are often generated in rocks devoid of any bedding or other type of original rhythmicity at the scale of DCR banding. For example, many of the DCRs studied in the San Vicente deposit overprint unpatterned oolitic dolostones (Fontboté and Gorzawski, 1990). One example of this is shown in Fig. 1 where areas with different rhythm thickness and different ratios between dark and sparry dolomite occur in lateral continuity overprinting an oolitic dolostone. A similar observation is made by Landis and Tschauder (1990, p. 341) by describing zebra rocks in Central Colorado: "Variations in bedding at the scale of zebra banding cannot be discerned in adjacent gray dolostone. Zebra rock cannot be related to replacement of favorable laminae".

The geometric key in order to understand the formation of the evenly spaced bands of DCRs is the observation that the development of a rhythm is interpendent with that of the contiguous ones. This feature can be observed in Fig. 1 where it can be seen that adjacent rhythms tend to have similar widths. For example, the right half of Fig. 1 shows areas with thin (at the mm scale) and thick

rhythms (at the cm scale). Transition between thin- and thick-banded areas is gradual, indicating that the thickness of a rhythm influences in some way that of the contiguous one. This phenomenon can be generalized to numerous examples of DCRs of different parts of the world as analyzed statistically by Fontboté and Amstutz (1983). It appears that the development of each rhythm has a range of influence which is determined by the growth of the neighbour ones. The existence of this feedback indicates that the rhythmicity is dependent of the growth process itself and not due to external factors like an inherited depositional rhythmicity (Bogacz et al. 1973), replacement of stromatactis (Landis and Tschauder, 1991), replacement of evaporite layers (Beales and Hardy, 1980), or pulsatory influx of ore fluid (Ghazban et al., 1990, Arne et al., 1991).

Hydraulic fracturing and brecciation often occur associated with DCRs. It could be argued that DCRs could also develop through injection and hydraulic fracturing of a fluid in the host rock pulling apart rhyhmically the host rock. Petrographic evidence indicates that this is not the essential mechanism as the sparry dolomite of generation II has precipitated in a space open mainly by dissolution of the host rock (see for example Fig. 1). Transitions between both types of fabrics are however observed.

Self organization processes

If the striking rhythmic banding is not inherited from an original sedimentary or tectonic banding, how was it developed? An answer may be been found in the investigations on self-organization systems. A number of geological examples in which ordered distribution arises without the mediation of an initial patterned texture are described in a special volume on "Self organization in geological systems" (Ortoleva, 1990b). These include oscillatory zoning and complex morphology of crystals, ordered geomorphological patterns, as well as a variety of periodic - in part fractal- geometric patterns in diagenetic, metamorphic and igneous environment. Dewers & Ortoleva (1990) explain many of these phenomena in terms of coupling between mechanical forces, chemical reactions and solute transport. Self-organization necessarely involves disequilibrium and feedback loops. In addition, Chadam and Ortolewa (1990) mention the existence of "noise" (heterogeneties) in the system.

These three "physical" requirements, i. e. disequilibrium, feedback and "noise" for generating self-organization textures may be present during formation of DCRs. It has been shown above that disequilibrium probably existed between carbonates precipitated as generation II and the bulk fluid. Feedback loops are required to explain the interdependence between the growth of contiguous rhythms. Finally, different hetereogeneties like bedding, different grain size or tectonic disturbances may provide the "noise" necessary to start the process of differential replacement, dissolution and open-space filling leading to the generation of DCRs.

In other self-organization textures formed at low temperatures, as for example Ostwald-Liesegang rings (Sultan et al. 1990), calcite concretions in sediments (Bjørkum and Walderhaug, 1990), or "diagenetic bedding" in the sense of Ricken (1986), interdiffusion appears to play a main role. If mass transport in DCRs is also assured by diffusion or if advection plays a role must be investigated. A difference compared to the textures mentioned above is the coarse grain size of the light bands of DCRs.

Conclusion

It appears that the rhythmicity in DCRs is given because of the alternancy of (light colored) bands in which complete dissolution occurs within (dark) bands in which replacement with certain preservation of the original sedimentary fabric dominates. The spacing of the dissolution-dominated bands within the dark replacing host rock is cyclic suggesting that this is what produces the rhythmicity. The periodicity could result from a kinetik feedback between areas of dissolution. A possible analogue has been discussed by Merino et al. (1983) who presents a kinetic theory to the generation of evenly-spaced pressure solution seams during late diagenesis.

Initial hetereogeneities are seen to influence, yet no to fully determine, the textural evolution leading to DCRs. In this way the rhythmic zoning of DCRs may generate "without the intervention of externally imposed periodicities in the state (pressure, temperature, or composition" of the fluid (Ortoleva, 1990a, p. 3), or without the intervention of inherited gemetric pattern in the carbonate rock being replaced.

Acknowledgements: This study is supported by the Swiss National Science Foundation (Grant nr. 20-36397.92). Discussions with R. Moritz and J. Spangenberg (Geneva), L. Oldham (Clitheroe) and J. M. García-Ruiz (Granada) are warmly thanked.

References

Amstutz, G.C. & Park, W.C. (1971) The paragenetic position of sulfides in the diagenetic crystallization sequence. Soc. Mining Geol. Japan, Spec. Issue 3, 280-282.

Arne, D.C., Curtis, L.W., & Kissin, S.A. (1991) Internal zonation in a carbonate-hosted Zn-Pb-Ag deposit.Nanisivik, Baffin Island, Canada. Economic Geology, v. 86, p.699-717.

Arne, D.C. & Kissin, S.A. (1989) The significance of "diagenetic crystallization rhythmites" at the Nanisivik Pb-Zn-Ag deposit, Baffin Island, Canada. Mineralium Deposita v. 24, p. 210-218

Beales, F.W., & Hardy, J.L. (1980) Criteria for the recognition of diverse dolomite type with an emphasis on studies on host rocks for Mississippi Valley-Type ore deposits. SEP; special publication, n. 28, p. 197-213.

Bjørkum, P.A. & Walderhaug, O. (1990) Geometrical arrangement of calcite cementation within shallow marine sandstones. Earth Sciences Reviews, v. 29, p. 145-161.

Bogacz, K., Dzulynski, S., Haranczyk, C. & Sobczynsky, P (1973) Sphalerite Ores Reflecting the Pattern of Primary Stratification in the Triassic of the Cracow-Silesian Region. Ann. Soc. Geol. Pol., v. 43, 3, p. 285-300, Krakow.

Chadam, J. & Ortoleva, P. (1990) Morphological instabilities in physico-chemical systems. Earth Sciences Reviews, v. 29, p. 175-181.

Dewers, Th. & Ortoleva, P. (1990) Differentiated structures arising from mechano-chemical feedback in stressed rocks. Earth Sciences Reviews, v. 29, p. 283-298.

Dewers, Th. & Ortoleva, P. J. (1990) Iteraction of Reaction, mass trasnport, and rock deformation during diagenesis: Mathematical modeling of intergranular pressure solution, stylolites, and differential compaction/cementation. In: Meshri, I.D. & Ortoleva, P.J. Prediction of reservoir quality through chemical modeling. AAPG Memoir 49, Tulsa, p. 147-160.

Fontboté, L. & Amstutz, G. C. (1983) Facies and sequence analysis of diagenetic crystallization rhythmites in strata-bound Pb-Zn-(Ba-F) deposits in the Triassic of Central and Southern Europe. In: H.G. Sschneider (Ed.) Mineral Deposits of the Alps and of the Alpine Epoch in Europe, Springer, Heidelberg, p. 347-358.

Fontboté, L., & Gorzawski, H. (1990) Genesis of the Mississippi Valley-type Zn-Pb deposit of San Vicente. Central Peru: geological and isotopic (Sr, O, C, S) evidences. Economic Geology, v. 85, p. 1402-1437.

Ghazban, F., Schwarcz, H.P., & Ford, D.C. (1990) Carbon and sulfur isotope evidence for in situ reduction of sulfate, Nanisivik lead-zinc deposits, Northwest Territories, Baffin Island, Canada. Economic Geology, v. 85, p. 360-375.

Gil, P.P., Martíinez, R. & Velasco, F. (1984) Ritmitas diagenéticas en las mineralizaciones de siderita de Bilbao. I Congr. Español de Geologia, Segovia, v. II, P. 491-499.

Gorzawski, H., Fontboté, L., Sureau, A., & Calvez, J.Y. (1989) Strontium isotope trends during diagenesis in ore-bearing carbonate basins. Geologische Rundschau, v. 78, p. 269-290.

Landis, G.P. Tschauder, R.J. (1990) Late Mississippian karst caves and Ba-Ag-Pb-Zn mineralization in Central colorado: Part II Fluid inclusion, stable isotope, and rock geochemistry data and a model of ore deposition. In: Beaty, D.W., Landis, G.P., and Thomson, T.B. (eds). carbonate-hosted sulfide deposits of the Central Colorado Mineral Belt. Economic geology, monograph 7, p. 339-366.

Machel, H.-G. (1990) Bulk solution disequilibrium in aqueous fluids as exemplified by diagenetic carbonates. In: Meshri, I.D. & Ortoleva, P.J. (Eds.) Prediction of reservoir quality through chemical modeling. AAPG Memoir nr. 49, p. 71-175.

Merino, E., Ortoleva, P., & Strickholm, P. (1983) Generation of evenly spaced pressure solution seams during late diagenesis: a kinetik theory. Contributions to Mineralogy and Petrology, v. 82, p. 360-370.

Moritz, R., Fontboté, L., Spangenberg, J. Rosas, S., & Fontignie, D. (1993) Strontium, carbon, and oxygen isotope trends in the Pucará Basin, Peru: Brine evolution and formation of Mississippi Valley-type deposits. Geofluids '93, 4th-7th May 1993, Torquay, England

Moritz, R., Spangenberg, J. & Fontboté, L. (1993) Evaluation of fluid mixing and fluid-rock interaction processes during genesis of the San Vicente Zn-Pb MVT deposit, central Peru, based on Sr, O, and C isotopic covariations. Second Biennial SGA Meeting, Granada, Spain, Sept. 9-13 1993

Ortoleva, P. (1990) Role of attachment kinetic feedback in the oscillatory zoing of crystals grown from melts. Earth Sciences Reviews, v. 29, p. 3-8.

Ortoleva, P. (Ed.) (1990) Special issue "Self-organization in geological systems". Earth Sciences Reviews, v. 29, p. 1-417.

Ricken, W. (1986) Diagenetic bedding: A model for marl-limestone alternations. Lecture notes in Earth Sciences, Springer, New York, v. 6, 210 p.

Spangenberg, J., Sharp, Z., & Fontboté, L. (1993) Apparent stable isotope heterogeneities in carbonatesdue to teh effect of organic matter and sulfides: case study on theSan Vicente MVT zinc-lead deposit, Peru Second Biennial SGA Meeting, Granada, Spain, Sept. 9-11, 1993

Sulatan, R. ,Ortoleva, P., De Paquale F. & Tartaglia, P. (1990) Bifurcation of the ostwald-Liesegangsupersaturation-nucleation-depletion cycle. Earth Sciences Reviews, v. 29, p. 1613-173.

Thomson, T.B. & Arehart, G.B. (1990) Geology and the origin of ore deposits in the Leadville district, Colorado: Part I. Geological studies of orebodies and wall rocks. In: Beaty, D.W., Landis, G.P., and Thomson, T.B. (eds). carbonate-hosted sulfide deposits of the Central Colorado Mineral Belt. Economic geology, monograph 7, p.130-155.

Velasco, F., Pesquera, A., Arce, R. & Olmedo, F. (1986) A contribution to the ore genesis of the magnesite deposit of Eugui, Navarra (Spain) Mineralium Deposita, v. 22, p. 33-41.

Current Research in Geology Applied to Ore Deposits. Fenoll Hach-Alí, Torres-Ruiz & Gervilla (eds) (1993). ISBN 84-338-1772-8

FLUIDS: A PREREQUISITE FOR PLATINUM METALS MINERALIZATION

Stumpfl, E.F.
Inst. of Geological Sciences, Mining University, A-8700 Leoben, Austria

ABSTRACT: A vast amount of new data on the importance of metasomatic replacement and hydrothermal regimes in layered igneous complexes (Bushveld, Skaergaard, Great Dyke, Stillwater, Duluth) has emerged in recent years. Finally, the significance of fluid regimes - long accepted as integral features of acid igneous rocks - is being recognized in the mafic/ultramafic field. Parallel to these developments, our knowledge expanded on processes of precious metals concentration. We shall focus here on the role of fluids for PGE genesis and consider relevant field evidence, mineralogical observations, analytical data and experimental results. These considerations are of importance for conceptual modelling in ore genesis and for exploration.

Field evidence

1. Potholes

Potholes in layered igneous complexes, long considered enigmatic features, have emerged as the most impressive, large-scale results of fluid activity. The first comprehensive model of pothole formation in the Bushveld Complex has been presented by Ballhaus (1988); potholes have since also been recorded from the mafic complexes of Northern Finland, from the Stillwater Complex and from the Skaergaard intrusion.

Potholes are circular to elliptic features of up to 1000 m diameter, within which deposition of the "normal" stratigraphy of mafic igneous rocks has been interrupted because of lowering of the liquidus temperature due to the presence of volatiles. Pegmatoids, graphite, hydrous silicates and PGE associations differing from those in normal PGE-bearing horizons are characteristic aspects of potholes.

In potholed areas, the ore-bearing reef (e.g. Merensky Reef) leaves its position in the stratigraphic sequence to "descend" to a lower level which may be up to 20 m below its original position. The resulting pothole is filled by pegmatoids, which may carry up to 80 % graphite, and by rocks from the hanging wall sequence. PGM associations in potholes and in normal reef differ significantly, with a preponderance of Pt-Fe alloys in the former and Pt-Pd-sulphides and tellurides in the latter. While potholes are co-genetic with the respective PGE reef, ultramafic pipes (discussed below) are not. Again, there is the dominance of Pt-Fe alloys in and near the pipes with increasing proportions of sulphides and tellurides away from it. The features discussed above are ascribed to the activity of volatiles associated with the formation of potholes and pipes, respectively.

2. Pipes

Ultramafic pipes represent another remarkable product of the activity of fluids in layered igneous complexes. They have been recorded from the Bushveld, Finland, Stillwater, Skaergaard and from the Duluth Complex, Minnesota. In the Bushveld crosscutting pegmatoids carry Fe-rich olivine, tremolitic amphibole, albitic plagioclase, talc and Fe-Ti-oxides rather than chromite. They also reveal a linear positive

relationship between SiO_2 and H_2O contents. Estimates of maximum temperatures for the metasomatic processes involved range from 670° - 800°C; these are in the same order of magnitude as temperatures obtained from fluid inclusion studies in the Merensky Reef (720°C; Ballhaus and Stumpfl, 1986). Where pipes cut the PGE-bearing horizon, such as the Merensky or the UG2 chromitite in the Bushveld Complex, modifications of "standard" PGM mineralogy can be observed up to 3000 m away from ultramafic pipes.

3. Ophiolite chromitites

In the giant ophiolitic chromitite deposits of Kempirsai, Kazakhstan (annual production, 4 mt of chromitite), orbicular-type chromitites (leopard ore) with large proportions of hydrous silicates preferentially occur in the hanging wall of massive chromitite bodies. This is interpreted as a result of volatiles migrating towards the roof; pronounced effects of a volatile regime have also been reported from the stratigraphically higher chromitite layers in the Troodos ophiolite. At Kempirsai, fluids are considered polygenetic; there is a magmatic contribution but crustal contamination also plays a role. This is documented by the occurrence of blocks of mafic/ultramafic country rocks in massive chromitites. These are strongly altered and change gradually into disseminated, orbicular, rich disseminated and finally, into massive chromitites. Chromitites at Kempirsai carry in average 1 ppm PGE part of which is located in laurite (RuS_2) and erlichmanite (OsS_2); this is presently not recovered but the problem is the subject of a cooperative research project between the Institut für Geowissenschaften, Leoben and IGEM, Moscow.

The upwards-migrating fluids responsible for pothole and pipe formation have been derived from the intercumulus liquid by fluid-melt unmixing. This is not to exclude the possibility of fluid contributions from country rocks which, e.g. Duluth, has been proven by isotopic evidence. Pothole and pipe formation, however, has taken place on such a scale that it can largely be attributed to the activity of intercumulus-derived fluids. In the Lukkulaisvaara intrusion (Kola Peninsula, Russia), sulfide and associated PGE mineralization is hosted in pegmatites surrounding microgabbro norites; the latter are interpreted as the results of a sudden loss of volatiles.

Mineralogy and geochemistry

The ortho-magmatic concept of PGE concentration postulates sulphide precipitation in the course of magma mixing due to input of pulses of new magma into the chamber. The turbulence associated with plume emplacement leads to high "R" factors. Sulphide globules then move under the influence of gravity towards the bottom of the chamber, scavenging, en route, PGE from the magma. This process would lead to associations of magmatic sulphides with globular textures preserved in places, with cumulus silicates in layers such as the J.M., Merensky or Skaergaard reefs. What we do, in fact, encounter differs significantly from the above assumption: a wide compositional spectrum of discrete PGM, associated with hydrous silicates, altered feldspars, graphite and Fl-bearing quartz. At Stillwater, the J.M. reef is in parts enveloped by up to 200 m thick zones of pegmatoids and alteration features, which extend into footwall and hanging wall. "De-coupling" of S and PGE is a world-wide feature in layered igneous complexes (Fig.1). The distribution patterns shown suggest that transport and deposition of PGE is not necessarily linked to sulphides.

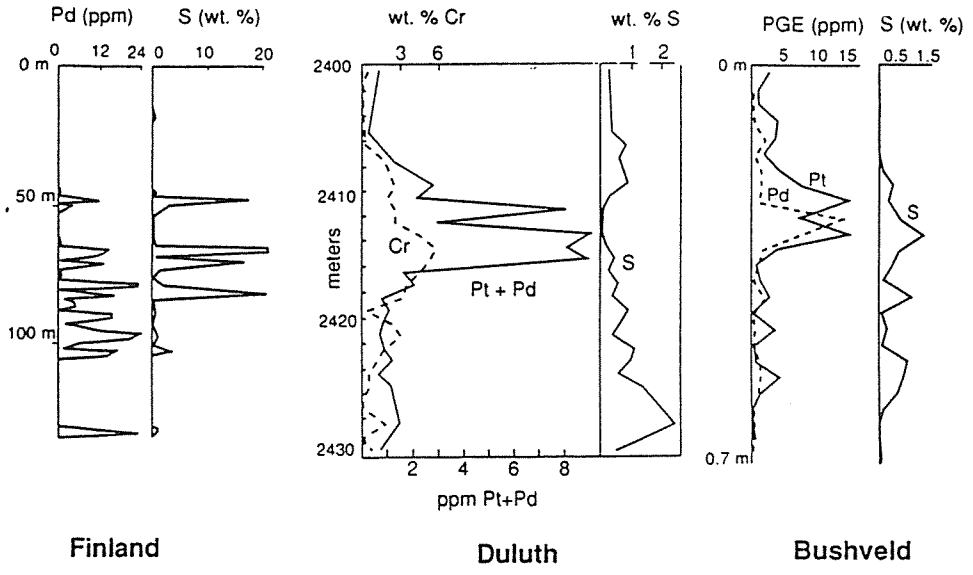

Fig.1: PGE and S distribution in drillholes from the Suhanko Complex, Finland (Huhtelin et al., 1989), the Duluth Complex, Minnesota (Sabelin et al., 1986) and from the Merensky Reef, Bushveld (Crocket et al. 1976). At Suhanko, there is significant Pd mineralization without sulphides, at Duluth Pt+Pd are concentrated about 15 metres above a sulphide-rich layer, and in the Merensky Reef, the Pd but not the Pt peak coincides with a sulphur peak.

Detailed investigation of mineral textures in supposedly unaltered layered rocks of the Upper Criticial Zone of the Bushveld Complex reveals alteration reactions similar to those in surrounding ultramafic pegmatoids. These include clinopyroxene coronas surrounding orthopyroxene, hornblende and biotite lamellae in orthopyroxene, and the formation of olivine, talc and serpentine from orthopyroxene (Zingg, 1988). These alteration phenomena are attributed to a fluid regime linked to the emplacement of concordant pegmatites. The highest grade of PGE mineralization (>2 kg/ton) known in "primary" (non-placer) deposits was encountered in dunite pipes of the Eastern Bushveld.

A remarkable aspect of the 2.4 b.y. Finnish intrusions is the frequent occurrence, within the same igneous body, of stratiform PGE concentrations associated with sulphides, with silicates or with oxides. This has been ascribed to a polyphase evolution, with possible premagmatic mantle PGE enrichment due to depletion, high degree of melting during the partial mantle event, crustal contamination, interaction between two magmas and activity of magmatic volatiles(Saini-Eidukat et al., 1993, this vol.).

Impressive examples for PGE mineralization occurring without sulphides have been reported from the Rytikangas PGE Reef in the Suhanko-Konttijärvi area, Finland. Out of 87 identifications of PGM, 64 % are associated with silicates only. In these

deposits, the presence of Pd-selenides and Pd-Sn phases also points towards low-temperature hydrothermal processes (Iljina, Ph.D. thesis, University of Oulu, 1993).

There is also disseminated PGE mineralization, with galena, in basement granitoids, pointing to a volatile phase as transporting agent. The Rytikangas Reef occurs in pegmatoids and poikilitic orthocumulates which cross-cut the underlying adcumulates - a situation not dissimilar to parts of the J.M. Reef at Stillwater. Formation of the Rytikangas Reef has been ascribed to upward-moving intercumulus fluids. In the Narkaus Complex, N.Finland, silicate-associated PGE mineralization occurs in chlorite schists of unusual chemical composition (Thalhammer et al., this volume). This cannot be explained by magmatic processes.

These observations further underline the fact that scavenging of PGE by sulphides is by no means a prerequisite for the formation of economic PGE concentrations. The same applies to the Skaergaard intrusion, East Greenland, where saline, CH_4-bearing fluid inclusions have recently been described. These have been trapped at 655 to 770°C, at fO_2 1.5 and 2.0 log units below the QFM oxygen buffer (Larsen et al., 1992). They also occur in the Triple Group horizon of the Middle Zone, which carries gold and platinum-rich horizons (Bird et al., 1991).

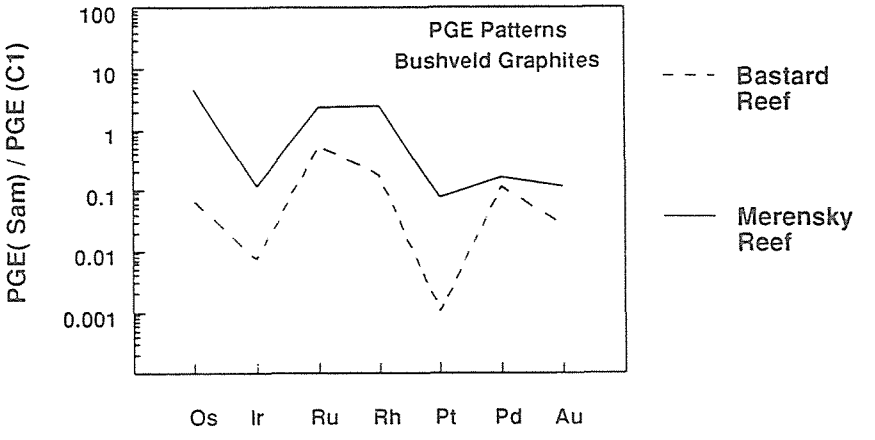

Fig.2: PGE contents in graphite from the Merensky Reef (NaCl-rich fluid inclusions in quartz, economic PGE contents) and from the barren Bastard Reef (CO_2-rich fluid inclusions in quartz) (from Wilson et al., 1992). This illustrates the significance of volatiles in the system C-O-H-Cl for PGE mineralization.

A complex association of fluid inclusions occur in quartz in the Merensky Reef (Ballhaus and Stumpfl, 1986). These comprise, amongst others, highly saline FI with up to 80 % w.t. NaCl. Maximum temperatures of entrapment have been estimated at 730°C at 4-5 kb.The PGE-rich Merensky Reef also carries graphite with significant PGE-contents; graphite in the PGE-poor, uneconomic Bastard Reef which occurs above the MR and is characterised by CO_2-rich FI shows significantly lower PGE contents (Fig.2). However, NaCl-bearing FI are only one expression of the Cl-contents of those late-magmatic fluids. A hydrous iron chloride, hibbingite, has recently been

described (Saini-Eidukat et al., 1993). This mineral is widespread and occurs over significant volumes of rock. It can be considered a final product of late-magmatic chlorine-rich fluids; hibbingite is inconspicuous under the microscope and easily dissolves in H_2O. This has probably prevented its recognition until recently.

In the Coronation Hill - El Sharana region, Northern Territory, Australia, unconformity-related Au-Pt-Pd-U mineralization has been deposited at 140 °C from a boiling, strongly saline fluid with high $CaCl_2$ contents. Oxygen isotopes measured from quartz and carbonate veins at Coronation Hill have average values of 13.3 ‰ + 5 ‰ ^{18}O. The descending ore-forming fluids had average $\delta\ ^{18}O$ values of -3.6 ‰, pointing towards a mineralizing fluid of meteoric origin; this was highly oxidized and carried the precious metals as chloride complexes, such as as $AuCl_2$ and $PtCl_4$: Interaction of these fluids with carbonaceous or sulphide-bearing rocks resulted in precipitation of the metals (Fig.3). The Coronation Hill example is considered particularly relevant because it represents a comparatively simple, one-stage precious metals depositing system where relevant parameters (FI, geochemistry, stable isotopes) have been determined quantatively (Mernagh, 1992), and a convincing case has been made for transport and concentration of PGE and gold by low-temperature meteoric fluids.

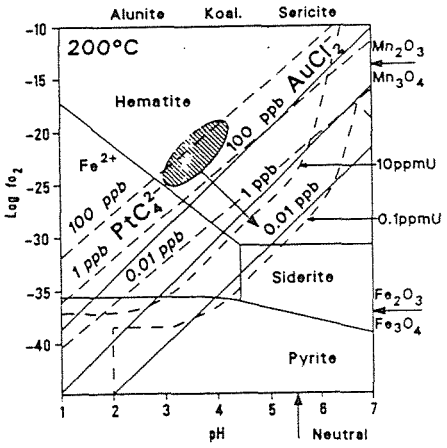

Fig.3: Log fO_2.pH diagram, showing the distribution of iron phases, and the solubility of U oxides, $AuCl_2$, and $PtCl_4^{2-}$ in solution at 200°C. Heavy arrows on the right ordinate mark the position of the hematite+magnetite and Mn_3O_4 + Mn_2O_3 redox buffer assemblages. The hatching indicates the possible pH and oxidation state of the original ore fluid, and the light arrow a possible reaction path (from Mernagh, 1992).

The mobility of PGE at surface temperatures has been documented in the lateritic environments in W.Australia. Saprolites above ultramafic bodies in the New Norcia area carry up to 1 ppm Pd over 30 m. Chromitites at Niquelandia, Brazil, have been exposed to lateritic weathering; goethite fillings between chromite grains carry a variety of PGE. There is also goethite with up to 37 % Ru and 15 % Fe. In some grains, Ru may reach 45 % and Ir 10 %. Os as well as Pt, Pd and Rh are absent or occur as trace components only.This is the first reported occurrence of hydroxides of Rh, Pd, Fe and Cu (Milliotti and Stumpfl, 1993).

Although oxidizing conditions are not conducive to PGE transport at high (late-magmatic) temperatures, this is not the case in the low-temperature environment. The goethite-PGM association appears to be a result of weathering under tropical conditions; it has not been reported from occurrences in higher latitudes.

Experimental data

There is now experimental evidence for PGE transport by fluids over a wide range of temperatures. Synthetic fluid inclusions obtained by equilibration of H_2O-NaCl-+ (CH_4-CO_2-H_2S) with metallic Pt and Au and (FeNiCu)S monosulphide solid solution doped with PtS and Au at 900°C and 0.5-1 GPa carry, amongst others, H_20, NaCl, Pt or Au-bearing mss, PtFe alloy and PtS (Ballhaus et al., oral comm.,1991). These results suggest that high-T fluid transport may be relevant for Pt concentrations in layered intrusions at low $f0_2$ and for the formation of fluid inclusions in the Merensky Reef and other layered complexes.

PGE volatilities determined experimentally by Fleet (1992) are much higher than those calculated from thermo-chemical data. The results suggest significant transport of PGE in volatile phases in largely solidified magmatic systems. In the 200 to 400°C range, Mackovicky et al. (1990) have documented the low formation temperatures of PGM in the Pd-Pt-S and Pd-Te-S systems.

In addition to transport of PGE in chloride solutions, other modes of transport should also be considered. It has been suggested that particulate clusters of <100 PGE atoms may occur in silicate melts (McDonald and Tredoux, 1991). These are not bonded to the silicate melt and could become enriched in the residual melts; from there they can be transported as carbonyl complexes in a carbonaceous volatile phase. Thus, PGE can be removed from large volumes of intercumulus melt and concentrated in specific sites.

Conclusions

Pegmatites, hydrothermal veins and alteration zones have, traditionally, been considered a by-product of the emplacement of granitoid rocks. The geological and economic importance of porphyry copper systems has, no doubt, strengthened this attitude. However, there is now comprehensive evidence for the activity of fluids in mafic-ultramafic intrusions and ophiolites. A vast spectrum of concordant and discordant pegmatoids, cross-cutting pipes, potholes and alteration zones has been recognized world-wide in recent years. A comprehensive fluid regime which ranges from high-temperature volatiles separating from the intercumulus liquid, to late-magmatic hydrothermal and even meteoric fluids forms an integral part of the evolution of mafic-ultramafic rocks.

Observations on the field scale have been augmented by microscopic, analytical and isotopic evidence. Fluids have been involved in transport and deposition of PGE and Au from the major mafic/ultramafic complexes (Bushveld, Stillwater, Finland, Duluth, Skaergaard) to Alaskan type complexes (Fifield; NSW) and ophiolites. They very likely also play a role in the formation of chromitite horizons and pipes. Experimental evidence points towards precious metal transport in chloride complexes at high temperatures and low $f0_2$. Other modes of transport should not be excluded. Clusters of PGE atoms may be transported as carbonyles. Low-temperature solubility

of PGE is documented by Pd-bearing saprolites (W.Australia) and by the recently discovered goethite-PGE association (Brazil).

References

Ballhaus, C.G. 1988. Potholes of the Merensky Reef at Brakspruit Shaft, Rustenburg Platinum Mines; primary disturbance in the magmatic stratigraphy.: Econ.Geol 83: 1140 - 1158.

Ballhaus, C.G. & Stumpfl, E.F., 1986. Sulfide and platinum mineralization in the Merensky Reef: evidence from hydrous silicates and fluid inclusions. Contrib.Mineral.Petrol.94, 193-204.

Bird, D.K., Brooks, C.K., Gannicott, R.A., and Turner, P.A., 1991. A gold-bearing horizon in the Skaergaard intrusion, East Greenland. Econ.Geol. 86, 1083-1092.

Donald, M. & Tredoux M. 1991. Thoughts on the transport of the Platinum-Group-Elements as volatile carbonyls in late stage magmatic fluids. Abstract in: Workshop on medium and small-scale structures in mafic and ultramafic rocks, Univ.of Natal.

Fleet, M.E., 1992. Experiments on the volatility of Fe, Ni, Cu, and Platinum Group Elements (PGE) in sulfide assemblages at 1000°C. Abstract, EOS, Trans.Amer.Geophys.Union, 73 (14), Spring Meeting Supplement, 372.

Huhtelin, T.A.,Lahtinen, J.J., Alapieti, T.T., Korvuo, E. and Sotka, P., 1989. The Narkaus intrusion and related PGE and sulphide mineralizations, in Alapieti, T., ed., 5th International Platinum Symposium - Guide to the Post-Symposium Field Trip: Espoo, Geological Survey of Finland, p.145-161 (fig.7.4, p.152).

Mackovicky, E., Karup-Møller, S., Mackovicky, M., Rose-Hansen, J., 1990. Experimental studies on the phase systems Fe-Ni-Pt-S and Fe-Pt-Pd-As-S applied to PGE deposits. Mineral.Petr...42, 307-320.

Mernagh, T. 1992. Fluid inclusion and oxygen-isotope evidence for low- temperatur Au-Pt-Pd (+-U) mineralization at Coronation Hill, NT.BMR Research Newsletter 16, 3 - 4.

Milliotti, C. and Stumpfl, E.F. 1993. Platinum-Group mineral inclusions, textures and distribution in the Chromitites of the Niquelandia Complex, Brazil. Abstract, First Brazilian Conference on Platinum Group Elements, Brasilia.

Mogessie, A. & Stumpfl E.F. 1992. Platinum-group element and stable isotope geochemistry of PGM-bearing troctolitic rocks of the Duluth Complex, Minnesota. Austral.J.Earth.Sc.39, 315 - 325.

Sabelin, T., Iwasaki, I., and Ried, K.J., 1986. Platinum group minerals in the Duluth Complex and their beneficiation behaviors: Skillings'Mining Review, v.August 23, p.4-7.

Saini-Eidukat, B., Thalhammer, O.A.R., Iljina, M., Halkoaho, T., Alapieti, T. 1993. Controls on PGE mineralization in the paleoproterozoic Kemi- Koillismaa-Olanga mafic intrusion belt, Fennoscandian shield (this volume).

Thalhammer, O.A.R., Saini-Eidukat, B., Iljina, M., Alapieti, T.T. 1993. PGE mineralization associated with silicates within the Siika-Kämä PGE Reef, Portimo Layered Complex, Fennoscandian shield, Finland: an unusual mineralization type (this volume).

Wilson, G.C., Kilius, L.R., Rucklidge, J.C. 1992. Precious metal contents of sulfide, oxide, and graphite crystals: Determinations by accelerator mass spectrometry. Iso Trace Report 92-01, Isotrace Laboratory, University of Toronto.

Zingg, A.J. 1988. The nature and origin of some pegmatoids and associated rocks in the Western Bushveld Complex, South Africa. Ph.D. Thesis, Mining University, Leoben, 207 pp.

Current Research in Geology Applied to Ore Deposits. Fenoll Hach-Alí, Torres-Ruiz & Gervilla (eds) (1993). ISBN 84-338-1772-8

FRACTIONATION IN GRANITE + RARE-ELEMENT PEGMATITE SYSTEMS. FACTS AND FICTION.

Černý, P.
Dept. of Geological Sciences, University of Manitoba, Winnipeg, Manitoba, Canada R3T 2N2.

ABSTRACT: Textural, paragenetic and geochemical features of fractionation in cogenetic suites of fertile granites and their rare-element pegmatite aureoles are fairly well established. They locally represent the most extreme fractionation gradients encountered in any magmatic system. However, the mechanisms facilitating this fractionation are much less known. The principal expressions of fractionation in granite + rare-element pegmatite systems are reviewed, and the probable, potential and unlikely mechanisms are discussed.

Historically, numerous competing hypotheses have been forwarded to explain the origin of rare-element granitic pegmatites. During the last two decades, field observations, paragenetic and geochemical data plus experimental studies have clearly established complex magmas as the parent medium, generated by differentiation/fractionation from fertile granitic intrusions (e.g., Černý 1982, 1992a,b; Černý and Meintzer 1988; Shearer et al. 1987, 1992). Common metamorphic and tectonic setting, physical continuity and gradual changes in texture, mineral assemblages and geochemistry are the most significant features linking the parent granites and their pegmatite progeny. However, the specific nature of the fertile granitic magmas and their pegmatite-generating residua is still being examined and discussed. Consequently, the mechanisms of fractionation that extract high concentrations of numerous LILE and HFSE elements into the tail-end differentiates also are debatable, and in some cases questionable. Let us review the salient characteristics of the granite + rare-element pegmatite systems, and discuss the diverse mechanisms offered over the past ~80 years to explain the fractionation phenomena.

The fertile granites display solidification trends advancing either from early peripheral consolidation inwards (with pegmatites penetrating this crust and its metamorphic envelope) or from primitive lithologies at deep levels upwards (with pegmatites penetrating the roof as a direct extension of the most evolved, topmost granite facies). The trend progresses from biotite-bearing to leucocratic granites, with more or less concurrent coarsening of grain size, development of aplitic, graphic and blocky textures, and local appearance of internal pegmatitic pods, gradually evolving from the surrounding granite. Pegmatitic leucogranites commonly grade into poorly zoned barren pegmatite bodies; in many cases, the two categories cannot be clearly distinguished.

Pegmatite aureoles surrounding the parent granites are commonly zoned, from the primitive interior through marginal to the most complex exterior pegmatites. Zoning is particularly well developed in the peraluminous LCT family, grading from barren and beryl-columbite pegmatites through intermediate subtypes to complex Li-rich pegmatites, albite-spodumene bodies and the albite type. Except the last two categories (which are still insufficiently understood), the textural and paragenetic complexity remarkably increases through this sequence, and so does the geochemical diversity.

Compositional features gradually change from the most primitive granite facies to the most evolved pegmatites. In the peraluminous LCT family, Ca,Sr,Ba,Mg,Fe,REE's, Y,Ti and Zr are compatible, extracted in early stages of crystallization, whereas Li,Rb,Cs,Tl,Be,Mn,Ga,Ge,Sn,Hf,Nb,Ta,B,F and P behave in an incompatible manner, enriched in residual magmas. In the subaluminous NYF family, Ca,Sr,Ba,Mg and Fe are compatible but REE's,Y,Zr and Ti seem to

increase with differentiation to the pegmatites, along with the incompatible elements typical of the LCT systems. This condensed "classification" of element behaviour is, of course, oversimplified: perceptible deviations from these generalized trends are observed in geochemically specialized granite + pegmatite systems, and among peraluminous LCT suites with different anionic dominances. In all cases, strong fractionation is shown by decreasing K/Rb, K/Cs, Rb/Cs, K/Tl, Ba/Rb, Sr/Rb, Mg/Fe, Fe/Mn, Ti/Sn, Th/U, Zr/Hf, Nb/Ta, Ti/(Nb,Ta) and W/Ta, whereas that of Rb/Tl, Al/Ga, Si/Ge, Ca/Sr is less pronounced, and reversals in LREE/HREE, Ca/Y and Fe/Sc are observed, superposed on their general decrease. The negative Eu anomaly initially increases but becomes greatly reduced in highly fractionated pegmatites.

In general, the facts of fractionation outlined above are reasonably well known. In contrast, much of our understanding of the underlying mechanisms is speculative at best, and occasionally rather nebulous. This is in part due to insufficient study of these phenomena, generated by an environment changing from magmatic through supercritical to hydrothermal + gaseous, in which a single element may be controlled by several factors in different stages of the process.

(1) Crystal-melt partitioning (Goldschmidt 1930; Ringwood 1955; Mittlefehldt and Miller 1983; Mahood and Hildreth 1983; Michael 1983) removes some cations that form early accessory minerals (REE's in monazite, Ti in ilmenite, Zr in zircon). Conversely, cations excluded from early accessory minerals and most rock-forming phases on crystal-chemical grounds accumulate in the residual melts (e.g., Li,Be). Compatible trace elements capable of substituting for major cations are preferentially extracted from the melt (Ba,Sr in K-feldspar and micas), whereas their incompatible counterparts are enriched in residual melts and enter in increasing quantities only the late generations of the same species (e.g., Rb,Cs).

(2) Fluid transport (e.g., Shaw 1968) may become significant in the advanced stages of evolution of the fertile granites. Extensively hydrated cations may essentially follow upward migration and accumulation of volatile components within homogeneous, highly hydrous but still undersaturated magmas. This may be particularly significant for non-complexing cations.

(3) Thermogravitational diffusion/convection in sizeable magma reservoirs (Hildreth 1979, 1981) may very effectively promote the above fluid transport of lithophile rare elements (Li,Rb,Cs,Tl,Be,Mn,Sc,Y,HREE's,Sn,U,Th, Mo,Nb,Ta and W), generating volatile-enriched and highly fractionated magma layers beneath the roof of plutonic intrusions. However, this mechanism seems to be more viable in basaltic magmas rather than the relatively viscous granite melts (Lesher et al. 1982).

(4) Zone refining and the concept of buoyant boundary layers are worth consideration but so far they seem to stumble over the same viscosity obstacle as the preceding mechanism of the modified Soret effect. They might probably apply to smaller-scale phenomena in layered tops of stratified fertile plutons.

(5) Whereas the above mechanisms can be effective during plutonic differentiation, complexing (Ringwood 1955; Beus 1966) conserves rare lithophile elements for late-stage crystallization at different stages of the pegmatite-generating and -consolidating process. Complexes stable under magmatic conditions preserve rare-element cations till their breakdown triggered by cooling, decompression, changes in pH *et similia*. Numerous complexes were examined experimentally (incorporating, e.g., Be,Sn,Ga,Nb and Ta). However, our understanding of speciation of rare elements in pegmatite melts and fluids is still rudimentary, and only a few elements are justifiably suspect of being controlled, in part, by complexing (such as fractionation of Al-Ga, Nb-Ta or HREE-LREE). Speculations abound about complexing of many other cations, including the rare alkalis.

(6) "Crystal-crystal" fractionation may also play a role at different stages of the whole granite-to-pegmatite evolution. Substitutions subject to significant crystal-chemical controls can strongly affect partitioning of trace elements in differentiating suites with diverse mineral assemblages (e.g., micas ≫ feldspars preference for Ga; Černý and Hawthorne 1989).

(7) Liquid-liquid fractionation might possibly play a role at the highly fractionated level of evolved pegmatite magmas. Liquid immiscibility is advocated for F-rich systems on experimental grounds (e.g., Melentyev et al. 1967). So far it was demonstrated for simple haplogranitic systems in the presence of ≥ 4 wt.%F, which is considerably in excess of the F contents known from bulk pegmatite compositions. However, the F content of pegmatite melts could be distinctly higher than that of the solid products of their crystallization, and we have no information about the possibly compounding effects of other volatile components such as B,P or Li.

(8) Melt-vapour fractionation was assigned a significant role by Jahns and Burnham (e.g., 1969) who advocated the appearance of an exsolved supercritical fluid at the onset of coarse pegmatitic textures in granite or pegmatite zoning. This concept was uprooted by the recent experimental work of London et al. (1988, 1989), in which H_2O-oversaturated melts yielded fine-grained anchi-homogeneous products. However, H_2O-rich but H_2O-undersaturated melts solidified into miniature replicas of zoned pegmatites, with strong fractionation gradients from margin to core. The only stage at which supercritical fluid appears along with the melt is a very late period of vug formation and/or fluid exomorphism. London's experiments have also shown moderate to strong preference of the lithophile rare elements, F and P for melt, rather than for the exsolved fluid (the only exception being B).

(9) The last factor to be considered is acting at the smallest scale of fractionation, during the growth of individual crystals. Diffusion through melt or fluid controlled by mass effect may be effective in fractionation of closely related cations which differ substantially in atomic masses, such as Zr-Hf or Nb-Ta (Butler and Thompson 1965). Progressive zoning in zircon or columbite-tantalite and related minerals may result from this mechanism.

This review indicates that a multitude of fractionation vehicles is available for diverse stages of granite + pegmatite evolution but only a few of them are reasonably documented, and some classic concepts are being dismantled by thorough testing. Not only that the current scrutiny modifies the number and character of possible mechanisms, but the traditional features of fractionation become expanded by new observations: large-scale gradients in thin, tabular, subhorizontal pegmatite bodies; widespread oscillatory zoning in Nb,Ta oxide minerals; homogeneous masses of lepidolite vs. extreme muscovite-to-lepidolite zoning within individual microcrystals; homogeneous vs. extremely zoned zircon-hafnon; and very late appearance of significant concentrations of Ca,Ba,Sr,Fe,Mg and/or Cl. All these and other phenomena will require a thorough study and interpretation.

References

A.A. Beus, 1966, Geochemistry of Beryllium and the Genetic Types of Beryllium Deposits, Freeman & Co., 401pp.
J.R. Butler and A.J. Thompson, 1965, Geochim.Cosmochim.Acta 29, 167-175.
P. Černý, 1982, Mineral. Assoc. Canada Sh. Course Handb. 8, 405-461.
P. Černý, 1991a, Geosci. Canada 18, 49-67.
P. Černý, 1991b, Geosci. Canada 18, 68-81.
P. Černý, 1989, GAC-MAC Ann. Meeting Montreal, Progr. Abstr. 21, A21.
P. Černý and R.E. Meintzer, 1988, CIM Spec. Vol. 39, 170-207.
V.M. Goldschmidt, 1930, Nachr. Ges. Wissensch. Gottingen, Mat.-phys.Kl., 370-378.

W. Hildreth, 1979, Geol. Soc. America Spec. Pap. 180, 43-75.
W. Hildreth, 1981, Jour. Geophys. Res. 86, B11, 10153-10192.
R.H. Jahns and C.W. Burnham, 1969, Econ. Geol. 64, 843-864.
C.E. Lesher, D. Walker, P. Candela, J.F. Hays, 1982, GSA-MSA Ann. Meeting Progr. Abstracts 14, p. 545.
D. London, 1986, Amer. Mineral. 71, 376-395.
D. London, 1990, Geol. Soc. America Spec. Paper 246, 35-50.
D. London, R.L. Hervig and G.B. Morgan VI, 1988, Contrib. Mineral. Petrol. 99, 360-373.
D. London, G.B. Morgan IV and R.L. Hervig, 1989, Contrib. Mineral. Petrol. 102, 1-17.
G. Mahood and W. Hildereth, 1983, Geochim. Cosmochim. Acta 47, 11-30.
B.N. Melentyev, L.M. Delitsyn and G.B. Melentyev, 1967, Dokl. Acad. Sci. USSR, Earth Sci. Sect. 175, 180-183.
P.J. Michael, 1983, Geology 11, 31-34.
D.W. Mittlefehldt and C.F. Miller, 1983, Geochim. Cosmochim. Acta 47, 109-124.
A.E. Ringwood, 1955, Geochim. Cosmochim. Acta 7, 242-254.
D.M. Shaw, 1968, Geochim. Cosmochim. Acta 32, 573-601.
C.K. Shearer, J.J. Papike and J.C. Laul, 1987, Geochim. Cosmochim. Acta. 51, 473-486.
C.K. Shearer, J.J. Papike, and B.L. Jolliff, 1992, Canad. Mineral. 30, 785-809.

1 Mineralogical and geochemical studies applied to ore deposits

Current Research in Geology Applied to Ore Deposits.Fenoll Hach-Ali, Torres-Ruiz & Gervilla(eds)(1993).ISBN 84-338-1772-8

OBSERVATIONS ON THE ISOTOPIC COMPOSITION OF ORE Pb IN THE IBERIAN PENINSULA

Arribas Jr A.
Geological Survey of Japan, 1-1-3 Higashi, Tsukuba, 305 Japan

ABSTRACT: Comparison of recently published Pb-isotope data from ore deposits of the Iberian peninsula with data for selected Pb-Zn deposits in southern Europe indicates the importance of the Hercynian metasedimentary basement as a source of ore-Pb. Sedimentary-exhalative-type deposits and some epigenetic vein- and manto-type deposits contain basement Pb. An igneous rock source of Pb is suggested for Hercynian vein-type and Miocene volcanic-hosted deposits.

INTRODUCTION

Recent Pb-isotope studies of Cambrian to Miocene age ore deposits in Spain and Portugal provide insight into the metallogeny and crustal evolution of the Iberian peninsula. This paper discusses the relationship of Pb-isotope data for Iberian ores with data from southern European deposits, with an emphasis on the various metal sources (e.g., basement vs. intrusive rock sources). Furthermore, the Pb-isotopic evolution of the basement rocks provides the geochemical framework to discuss questions of broad geologic interest in the region.

GEOLOGIC SETTING AND ORE DEPOSIT TYPES

Most of the pre-Mesozoic basement of the Iberian peninsula consists of terranes of late Proterozoic to Devonian age, similar to other regions of western Europe. These terranes were deformed, metamorphosed, and intruded by various granitoids before the Lower Permian, during the Hercynian orogeny. In Spain and Portugal these terranes form the stable platform beneath Neogene basins, and outcrop in the Iberian Massif and internal zones of the Betic and Pyrenean Alpine chains (Fig. 1).

The ore deposits from the Iberian peninsula considered in this paper occur in the following settings: (1) within the pre-Mesozoic basement in relation to Cambrian (*Rubiales*), Ordovician to Devonian (*central and eastern Pyrenees*), and Carboniferous (*Iberian Pyrite Belt, Linares*) mineralization events, (2) in Triassic carbonate rocks deformed during the Alpine orogeny (*Betic Cordillera*), and (3) cross-cutting Paleozoic to Miocene rocks, in association with Miocene post-collisional volcanism (*Cartagena, Mazarrón, Rodalquilar, Almagrera*).

The Pb-isotope fields of these deposits are shown in Figure 2, together with the fields of Pb-Zn deposits of southern Europe that have homogeneous Pb-isotopic compositions and occur within the same basement terrane (except for the Iberian Pyrite Belt; see Matte, 1991). The ores shown in Figure 2 may be grouped genetically as follows (in parentheses, references to Pb-isotope data):(1) sedimentary exhalative deposits, Montagne Noire (Brévart et al., 1982), southwestern Sardinia (Boni & Köppel, 1985; Ludwig et al., 1989), central and eastern Pyrenees (Marcoux et al., 1992; Pujals, 1993), Graz (Köppel & Schroll, 1983), southern and eastern Alps (Köppel & Schroll, 1988), Betic Cordillera (Arribas et al., 1991). (2) volcanogenic massive sulfide deposits, Iberian Pyrite Belt (IPB)

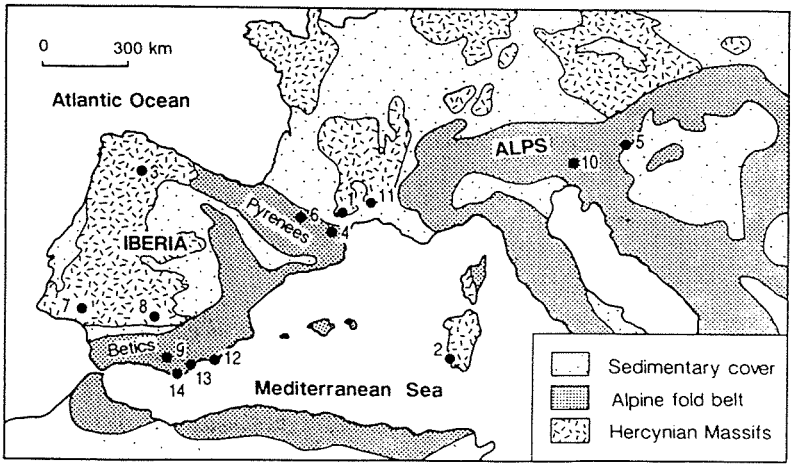

Fig. 1. Simplified structural map of southern Europe, showing location of mining districts considered in this study (for the names of deposits, see Fig. 2).

(Marcoux et al., 1992). (3) epigenetic hydrothermal deposits, including veins related to Hercynian magmas at Linares (Arribas & Tosdal, 1991, unpub. data), vein and/or replacement mantos at Cartagena, Almagrera, and Mazarrón (Arribas et al., 1991), epithermal, volcanic-hosted Au at Rodalquilar (Arribas et al., 1991), and complex ores at Les Malines (Le Guen et al., 1991).

SOURCES OF ORE LEAD

On the basis of the well-understood geologic setting and similarity between rock-Pb and ore-Pb data, it appears that Pb in the Linares and Rodalquilar deposits was derived from Hercynian granitoids and Miocene calc-akaline volcanic host-rocks, respectively (Fig. 2).

For the rest of the Pb-isotope data, except for the IPB (see below), a pre-Mesozoic basement rock source is suggested. This interpretation is consistent with previous studies of some individual ore deposits and is confirmed by the rock-Pb data; the trends defined by the ore samples in Pb-variation diagrams are similar to those of whole-rock and feldspar samples from basement rocks in Spain, France, and the Alps (see Köppel & Schroll, 1988; Arribas et al., 1991; Le Guen et al., 1991). The contribution of basement Pb could have occured by direct leaching, or, in the case of post-Hercynian deposits, from leaching of first-cycle sediments derived from the basement rocks. Howeˊver, the coherence of the Pb-isotope trends among all deposits suggests that Pb was extracted at various times from sources with similar U/Pb, Th/Pb, and Th/U ratios. This was most likely a common source, such as the metamorphic rocks of the Vendée Cévennes-Drosendorf terrane of southern Europe (see the paleogeographic reconstruction of Matte, 1991). Geologic factors that contributed to produce consistent ore Pb-isotopic compositions with such limited ranges (Fig. 2) include homogenization of the original Archean or early Proterozoic crystalline basement by erosion and deposition of thick sedimentary Paleozoic sequences, and hydrothermal convection during ore-forming processes.

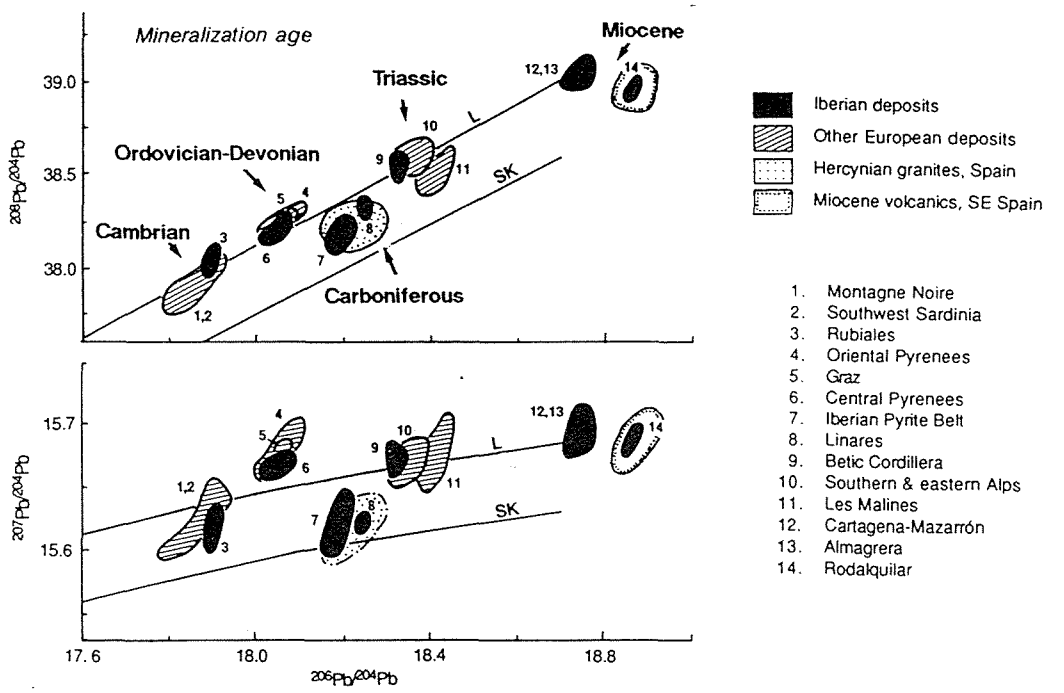

Fig. 2. Summary Pb-isotope variation diagrams of ores from the Iberian peninsula and selected Pb-Zn deposits of southern Europe. SK is Stacey and Kramers (1975) growth curve and (L) is a two-stage Pb evolution curve proposed by Ludwig et al. (1989) for Sardinia. Rock Pb data for Hercynian granites and Miocene volcanic rocks in Spain are from Michard-Vitrac et al. (1981) and Arribas et al. (1991), respectively.

With respect to the IPB, it may be argued that Pb in these ores is similar in origin to the Linares deposit (magmatogenic), originating perhaps from early Hercynian intrusive rocks. However, the IPB is located within a different basement terrane (Cornwall-Rhenish; Matte, 1991) and the Pb-isotope trends of this terrane are not well known.

CONCLUSIONS AND IMPLICATIONS

The Pb-isotope data for major base-metal ores in southern Europe suggest extensive leaching of Pb from the late Proterozoic to Devonian (Hercynian) basement rocks. Other deposits, such as Miocene volcanic-hosted epithermal Au deposits and Hercynian vein deposits show a dominant magmatic source for the Pb.

Identification of the basement Pb-isotopic signature for southern Europe provides a useful constraint in the discussion of regional metallogenic, petrogenetic, and structural questions. Three examples are: (1) the Rubiales Pb-Zn deposit in northwestern Spain is considered to be controlled by a Hercynian shear zone (Tornos & Arias, 1993); however, the Pb-isotope data suggest remobilization of lower Cambrian stratabound mineralization, similar to carbonate-hosted deposits in the Montagne Noire and southwestern Sardinia (fields 1, 2 and 3, Fig. 2); (2) extensive crustal contamination of

Miocene to Pliocene volcanic rocks in southeastern Spain (also in central Italy) is indicated by the large component of crustal Pb in these rocks; and (3) the similarity between the Pb-isotope data for basement and volcanic rocks of southern Spain and southern Greece (Milos Island; Pflumio et al., 1993) suggests that the pre-Alpine basement in the Aegean region is also Hercynian.

REFERENCES

Arribas, A., Tosdal, R.M. & Wooden, J.L. 1991. Lead isotope constraints on the origin of base- and precious-metal deposits from southeastern Spain. In: Pagel & Leroy (eds.) Source, Transport and Deposition of Metals. Balkema Rotterdam, pp 241-244

Boni, M. & Köppel, V. 1985. Ore-lead isotope pattern from the Iglesiente-Sulcis area (SW Sardinia) and the problem of remobilization of metals. Mineral. Deposita 20:185-193

Brévart, O., Dupré, B., & Allègre, J.C. 1982. Metallogenic provinces and the remobilization process studied by Pb isotopes:Pb-Zn ore deposits from the southern Massif Central. Econ. Geol. 77:564-575.

Köppel, V., & Scroll, E. 1983. Lead isotopes of Paleozoic, strata-bound to stratiform galena bearing sulfide deposits of the eastern Alps (Austria); implications for their geotectonic setting. Schwerz. Min. Petr. Mitt. 63:347-360

Köppel, V., & Schroll, E. 1988. Pb-isotope evidence for the origin of Pb in strata-bound Pb-Zn deposits in Triassic carbonates of the Eastern and Southern Alps. Mineral. Deposita 23:96-103

Le Guen, M., Orgeval, J.J. & Lancelot, J.R. 1991. Lead isotope behaviour in a polyphased Pb-Zn ore deposit Les Malines (Cévennes, France). Mineral. Deposita 26:180-188

Ludwig, K.R., Vollmer, R., Turi, B., Simmons, K. R. & Perna, G., 1989. Isotopic constraints on the genesis of base-metal ores in southern Sardinia. Eur. Jour. Mineral. 1:657-666

Marcoux, E., Leistel, J.M., Sobol, F., Milesi, J.P., Lescuyer, J.L. & Leca, X. 1992, Signature isotopique du plomb des amas sulfurés de la province de Huelva, Espagne. Conséquences métallogéniques et géodynamiques. C.R. Acad. Sci. Paris, 314-II:1469-1476

Marcoux, E., Joubert, M. & Lescuyer, J.J. 1991. Origine des minéralisations stratiformes de la bordure du Canigou (Pyrénées-orientales, France): apport de la géochimie isotopique du plomb. C.R. Acad. Sci. Paris, 312-II:281-287

Matte, P. 1991. Accretionary history and crustal evolution of the Variscan belt in Western Europe. Tectonophysics 196:309-337

Michard-Vitrac, A., Albarede, F. and Allègre, C.J. 1981. Lead isotopic composition of Hercynian granitic K-feldspars constrains continental genesis. Nature 291:460-464

Pflumio, C., Briqueu, L., Boulegue, J., & Liakopoulos, A. 1993. Geochemical and isotopic characteristics of present-day and past geothermal systems of Milos island (Aegean arc). Jour. Resource Geology, Japan, Spec. Issue (in press)

Pujals, I. 1993. Las mineralizaciones de sulfuros en el cambro-Ordovicico de la Val d'Aran (Pirineo central, Lerida). Unpub. PhD. Univ. of Barcelona, 310 pp

Stacey, J.S. & Kramers, J.D. 1975. Approximation of terrestrial Pb isotope evolution by a two-stage model. Earth Planet. Sci. Lett. 26:207-221

Tornos, F. & Arias, D. 1993. Sulfur and Pb isotope geochemistry of the Rubiales Zn-Pb deposit (Spain). Eur. Jour. Mineral.(in press)

Current Research in Geology Applied to Ore Deposits. Fenoll Hach-Alí, Torres-Ruiz & Gervilla (eds) (1993). ISBN 84-338-1772-8

SULPHUR ISOTOPE COMPOSITION OF Cu-Pb-Zn MINERALIZATION FROM THE PYRITE DEPOSIT OF CAMPIANO (SOUTHERN TUSCANY)

Benvenuti, M. (1); Morelli, F. (1); Corsini, F. (1); Lattanzi, P. (1) & Tanelli, G. (2)
(1) Dip.to Scienze della Terra, Firenze, Italy
(2) Dip.to Scienze della Terra, Napoli, Italy

Abstract: Cu-Pb-Zn±Ag polymetallic mineralization associated with massive pyrite at Campiano mine has been analyzed for sulfur isotope composition. In particular, the S-isotope signatures of galena and sphalerite points to deposition at about 340°C, under relatively high fS_2 values, from fluids with $\delta^{34}S_{\Sigma S}$ around +6.3 per mil. These values compare with a previous $\delta^{34}S_{\Sigma S}$ estimate of +8 per mil for the skarn Cu-Pb-Zn deposit of Campiglia Marittima (southern Tuscany).

Introduction

The Campiano deposit is one of the largest pyrite (±Cu,Pb,Zn) deposits of southern Tuscany. The origin of these deposits has been ascribed to an early (pre-Tethydean) sedimentary-hydrothermal stage leading to massive pyrite (±Cu,Pb,Zn sulfide) deposition, followed by a late-Apenninic hydrothermal event of (re)mobilization and (re)deposition of metals in structurally-controlled sites (Tanelli & Lattanzi, 1986). The Campiano deposit, however, appears quite peculiar at the district scale with respect to ore setting, mineral associations and ore textures (Morelli, 1990).
In this communication, we present new data on the S-isotope composition of sulfide minerals at Campiano, in order to better understand the ore-forming environment.

Geologic framework

The Campiano deposit consists of 25 Mt pyrite, currently exploited between levels -20 and -300 meters below sea level. The whole area is characterized by a high geothermal gradient (about 100°C/Km) presumably linked to the presence of a magmatic body at shallow depths. The Campiano deposit is strictly associated with a major tectonic lineament, the "Boccheggiano fault", a normal structure trending NW-SE and extending downdip (45°NE) for several hundreds of meters. The footwall rocks belong to the "Filladi di Boccheggiano" formation, consisting of a dominantly phyllitic complex with interlayered sulphatic-carbonatic masses, locally metasomatized to skarn. The hangingwall rocks are represented by flysch sequences (Ligurids) and underlying (Late Triassic?) evaporites.
Polymetallic mineralization (the so-called "Filone quarzoso-cuprifero") has been exploited in the past in the upper portion of the Boccheggiano fault. Significant, although uneconomic, amounts of polymetallic minerals have been also discovered at greater depth in association with the massive pyrite body of Campiano. The investigated samples were preferentially taken from this Cu-Pb-Zn (Ag) mineralization.

Mineralogy and textures

Main ore minerals in the polymetallic sulfide assemblage commonly include chalcopyrite, sphalerite, galena, pyrite,

pyrrhotite, and magnetite (Morelli, 1990). The polymetallic sulfide assemblage overprints an earlier, quantitatively more abundant Fe-mineral association (pyrite, magnetite, hematite, and pyrrhotite), typically displaying a strong metamorphic imprint. Sphalerite and galena usually show mutual grain boundaries. Pb-Cu-Zn minerals may show textural equilibrium with a late pyrite generation.

Sulfur isotope data: results and discussion

S-isotope analyses were performed on sphalerite (N=8), galena (N=5), pyrite (N=9), pyrrhotite (N=1) and anhydrite (N=2) by Krueger Enterprise Inc. (Cambridge, Massachussetts). The reported analytical uncertainty is ±0.1 per mil or better. Results are depicted in Fig.1 together with previous S-isotope data by Cortecci et al. (1983). Sulfides show a large spread of $\delta^{34}S$ values (4.2÷13.9 per mil), with a frequency peak at about 7 per mil. The widest variations are shown by pyrite and pyrrhotite ($\delta^{34}S$=6.0÷13.8 and 4.2÷13.9 per mil, respectively), whereas base-metal sulfides have fairly homogeneous compositions (average $\delta^{34}S$= 6.6±0.4 per mil, sphalerite, and 4.6±0.5 per mil, galena). No significant correlation between S-isotope composition and depth, type of setting and/or mineral assemblage is evident. On the other hand, the order of enrichment in ^{34}S among the various sulfur compounds is indicative that isotopic equilibrium was approached, at least at large scale.

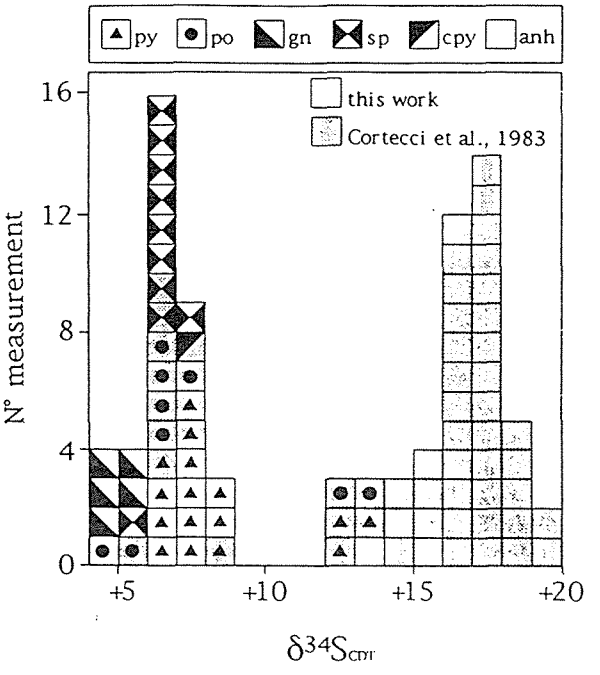

Fig.1 - $\delta^{34}S$ values of sulfides and sulfates from Campiano.

Base-metal sulfides in veins cutting through massive pyrite are probably in isotopic disequilibrium with massive pyrite, because apparent isotopic temperatures for pyrite-sphalerite and pyrite-galena pairs are seemingly too high (≥500°C). When pyrite, sphalerite and galena all belong to the same vein assemblage, isotope geothermometry gives consistently lower values (T=140-275°C). The most consistent isotopic temperatures were given by several sphalerite-galena pairs, which provided an average temperature estimate of 348±45°C. Such a value is in good agreement with temperatures estimated by other methods, such as stannite(kesterite)-sphalerite geothermometry (T=245-360°C: Corsini et al., 1991), fluid inclusion microthermometry (T=310-340°C:

Garrone, 1988), and Cd partitioning between sphalerite and galena in one sample (T=350°C: Garrone, 1988). Therefore, a value of 340°C seems a reasonable temperature estimate for deposition of polymetallic mineralization at Campiano.

We can also attempt to define other physico-chemical parameters such as sulfur and oxygen fugacities by combining phase equilibria and mineral chemistry data. The FeS content of sphalerite (FeS_{sp}) ranges between 3.6 and 18.3 mol% (average values), with a marked tendency to be higher in sphalerites associated with pyrite and hexagonal pyrrhotite than in sphalerites from pyrrhotite-free samples. The bulk of mineralogical and textural features indicates that sphalerite deposition was accomplished under relatively high fS_2 values, predominantly in the pyrite-stability field. More in detail, at about 340°C and low pressure, a fS_2 range of 10^{-8}-10^{-9} can be calculated from the equation of Barton & Skinner (1979, p.369). The corresponding compositional field of mineralizing fluids in a pH-fO_2 diagram (Fig.2) falls entirely within the $H_2S_{(aq)}$-dominant region. In addition, considering the common occurrence of muscovite and quartz, a pH range of 2.7 to 5.9 can be assumed. Using Ohmoto & Rye's (1979) isotope fractionation factors between sulfides and $H_2S_{(aq)}$, a $\delta^{34}S_{\Sigma S}$ of approximately 6.3-6.4 per mil may be thus calculated for fluids in equilibrium with sphalerite and galena with the measured S-isotope signature.

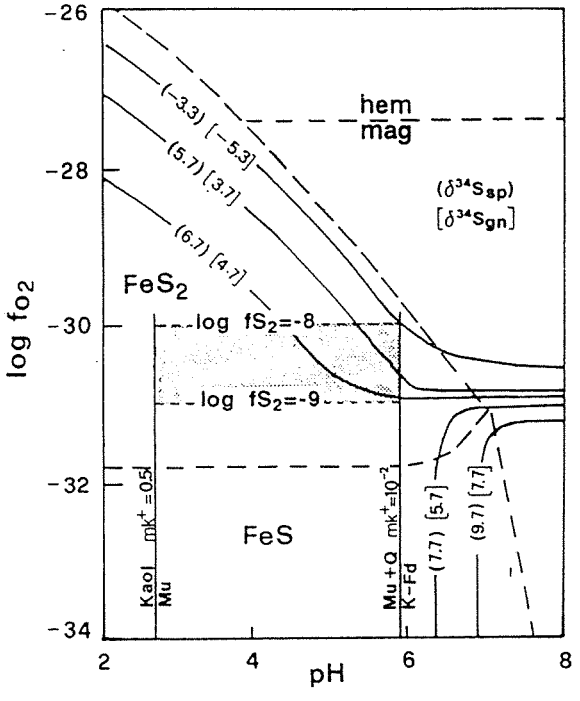

Fig.2 - Comparison of the position of $\delta^{34}S$ contours of sphalerite (sp) and galena (gn) with the stability fields of Fe-S-O minerals and muscovite (mu). T=340°C, $\delta^{34}S_{\Sigma S}$=6.3-6.4 per mil, ΣS=0.01 moles/Kg H_2O, m_{K^+}=0.01 to 0.5 moles/Kg H_2O. The shaded area represents the stability field of mineralizing fluids.

Conclusions

On the basis of several independent geothermometers, a temperature estimate in the order of 340°C has been proposed for polymetallic sulfide deposition at Campiano. Calculated $\delta^{34}S_{\Sigma S}$ of ore-forming fluids compares well with that determined for other deposits in southern Tuscany, namely the polymetallic skarn mineralization at Valle del Temperino, Campiglia Marittima ($\delta^{34}S_{\Sigma S}\cong 8$ per mil: Corsini et al., 1980). This feature, in conjunction with other geological,

mineralogical, textural and compositional evidences (cfr. Tanelli, 1983, and references therein), is consistent with a similar evolutionary trend of Campiano and other polymetallic mineralization throughout southern Tuscany. Their emplacement would have been promoted by hydrothermal activity extensively affecting the district at a late-Apenninic stage. With respect to this picture, the Campiano deposit shows some peculiar and still controversial aspects. In particular, it is not clear whether the massive pyrite bodies must be included among the products of such a late hydrothermal activity or, alternatively, they could represent a pre-Tethydean massive sulfide deposit (pyrite±Cu,Pb,Zn,Ag) subsequently affected by (re)mobilization processes. In this respect, the observed textural and isotopic features of pyrite could reflect a multi-stage deposition of this phase, each generation recording different chemico-physical conditions, whereas base-metal sulfides could have formed by a single-stage process and/or under more uniform environmental conditions.

The researches were financially supported by MURST (40% and 60% University of Florence and University "Federico II" of Naples) and CNR (Centro di Minerogenesi e Geochimica Applicata of Florence).

References

Barton, P.B. & Skinner, B.J. 1979. Sulfide mineral stabilities. In: Barnes, H.L. (ed.) Geochemistry of hydrothermal ore deposits, 2nd Edn. Wiley & Sons New York, pp.278-403

Corsini, F., Morelli, F. & Tanelli, G. 1991. A polymetallic sulfide (Cu-Pb-Zn) assemblage from the Boccheggiano-Campiano (Tuscany) pyrite deposit: Application of the stannite-sphalerite geothermometer. N.Jb.Miner.Mh. 11:523-528

Corsini, F., Cortecci, G., Leone, G. & Tanelli, G. 1980. Sulfur isotope study of the skarn-(Cu-Pb-Zn) sulfide deposit of Valle del Temperino, Campiglia Marittima, Tuscany, Italy. Econ. Geol. 75:83-96

Cortecci, G., Klemm, D.D., Lattanzi, P., Tanelli, G. & Wagner, J. 1983. A sulfur isotope study on pyrite deposits of southern Tuscany, Italy. Mineral. Deposita 18:285-297

Garrone, G. 1988. Il giacimento a pirite e solfuri misti di Campiano: studio geochimico mineralogico. Tesi di laurea in Sc. Geologiche, Università di Torino

Morelli, F. 1990. Studio mineralogico del giacimento a pirite e solfuri di Cu-Pb-Zn di Boccheggiano-Campiano. Tesi di laurea in Sc. Geologiche, Università di Firenze

Ohmoto, H. & Rye, R.O. 1979. Isotopes of sulfur and carbon. In: Barnes H.L. (ed.) Geochemistry of hydrothermal ore deposits, 2nd Edn., Wiley & Sons New York, pp 509-567

Tanelli, G. 1983. Mineralizzazioni metallifere e minerogenesi della Toscana. Mem. Soc. Geol. It. 25:91-109

Tanelli, G. & Lattanzi P. 1986. Metallogeny and mineral exploration in Tuscany: state of the art. Mem. Soc. Geol. It. 31:299-304

Current Research in Geology Applied to Ore Deposits.Fenoll Hach-Alí, Torres-Ruiz & Gervilla(eds)(1993).ISBN 84-338-1772-8

STABLE ISOTOPE EVIDENCE FOR THE GENESIS OF THE MADAN VEIN AND REPLACEMENT LEAD-ZINC DEPOSITS, CENTRAL RODHOPES, BULGARIA

Bonev, I.K. (1); Boyce, A.J. (2); Fallick, A.E. (2) & Rice, C.M. (3)
(1) Geological Inst., Bulgarian Academy of Sciences, 1113 Sofia, Bulgaria
(2) Scottish Universities Research and Reactor Centre -SURRC, East Kilbride, Glasgow, G75 0QU, U.K.
(3) Dept. of Geology and Petroleum Geology, University of Aberdeen, AB9 2UE, U.K.

ABSTRACT: The primary fluid macroinclusions located in some galena crystals permit direct determination of δD and $\delta^{18}O$ of the hydrothermal fluids using special techniques. The δD values (-62.4 ± 7‰) and the $\delta^{18}O$ values (dispersed mainly between 0 and -15‰) indicate a meteoric origin of the main water constituent of solutions. The $\delta^{34}S$ composition of the major sulphides (+1 to +7‰) coincides with those of premetamorphic pyrrhotite layers concordant to the embedding gneiss rocks ($\delta^{34}S$ 4‰) suggesting them as a probable source of S. The base metals seem to have been mobilized from a deep seated magmatic body connected with the Tertiary volcanic activity. The ore deposition is the result of convective circulation of solutions along large, partly opened faults in the thermal field of this body.

Introduction. The Madan ore district situated in the southern part of the Rhodope Mountains is the Bulgarian largest and most productive lead-zinc mining area, intensively worked during the last 4-5 decades. The Tertiary (30-40 Ma) ore mineralizations of vein and skarn-replacement type emplaced mainly in metamorphic rocks are relatively well studied. However, a study of S, H and O stable isotopes may provide important data for better understanding of the ore-forming processes. The sulphide ore deposits in Thermes, NE Greece, are a natural southern extension of the Madan district and have the same genetic problems.

Primary fluid inclusions of macroscopic (up to mm) size are known from some large galena crystals (Bonev, 1977). The ore solutions, as found by direct analysis in such fluid inclusions (Piperov et al., 1977), represent slightly acidic, comparatively diluted chloride-sodium-potassium aqueous solutions of 4-5‰ total salinity and Na:K:Ca molar ratio of about 11:2:1 with some Fe and Mn content. The gas phase is mainly CO_2. Homogenization temperatures are 360-300°C for the main sulphide assemblages, and 280-200°C for the late quartz-carbonate assemblage. The average pressure has been estimated as 100 bars.

The ore deposition is the effect of the physico-chemical (mainly pH) changes in the fluids as the result of: 1) interaction with pyroxene skarns, 2) interaction with the host gneiss rocks, and 3) boiling of solutions (Bonev, 1984).

Samples studied. Samples of coexisting sulphides from the vein and metasomatic ores of the main deposits in the district were used for isotopic studies. Quartz specimens analysed for $\delta^{18}O$ were single crystals coexistent with galena and sphalerite.

Experimental. Sulphur isotopic ratios were measured by standard mass spectroscopic techniques after transforming the sulphides into SO_2. Standard techniques were also used in the production of quartz $\delta^{18}O$ data. δD isotopic values were determined from the fluid macroinclusions in galena crystals. Two main

methods were developed for this study: 1) extraction of fluids from the thoroughly prepared crystals through crushing and subsequent decrepitation under vacuum at high temperatures (400°C) in a special crushing device-ampoule, and 2) extraction of water from macroinclusions near the galena crystal surfaces by puncturing and direct collection in capillaries. The extracted waters were saturated by standard CO_2 and, after equilibration and separation, the O isotope ratio was determined from the exchanged CO_2 gas, as recommended by Ohba (1987).By using U-furnace the water was transformed into H for the δD mass spectroscopic determination.

Results and discussion.

$\delta^{34}S$. The $\delta^{34}S$ composition of sulphide minerals (~60 analyses) varies in a relatively narrow range, (0 to +7.5 ‰, Fig. 1). The measured $\delta^{34}S$ differences for the simultaneous galena and sphalerite are close to the equilibrium fractionation values, and the calculated for these pairs temperatures (355-320-260°C) are compatible with the homogenization temperatures in associated quartz. In cases of successive precipitation the $\delta^{34}S$ differences are smaller and the calculated temperatures are not realistic.

It is worth noting that the $\delta^{34}S$ values for the lead-zinc mineralization in the Thermes area (Changkakoti et al., 1990) are very similar, grouped in a narrow range from -0.8 to +6.1‰. However, a small systematic shift towards the lighter values characterize these data.

In one of the underground mines (Murzyan), a pyrrhotite-amphibole layered body was revealed. It interlayers concordantly the gneiss rocks as part of the metamorphic complex but has not visible link with the ore veins. The $\delta^{34}S$ values of this pyrrhotite (4.04‰) are very close to the average for the whole district, which suggests the possible role of such premetamorphic sulphides as a S-source.

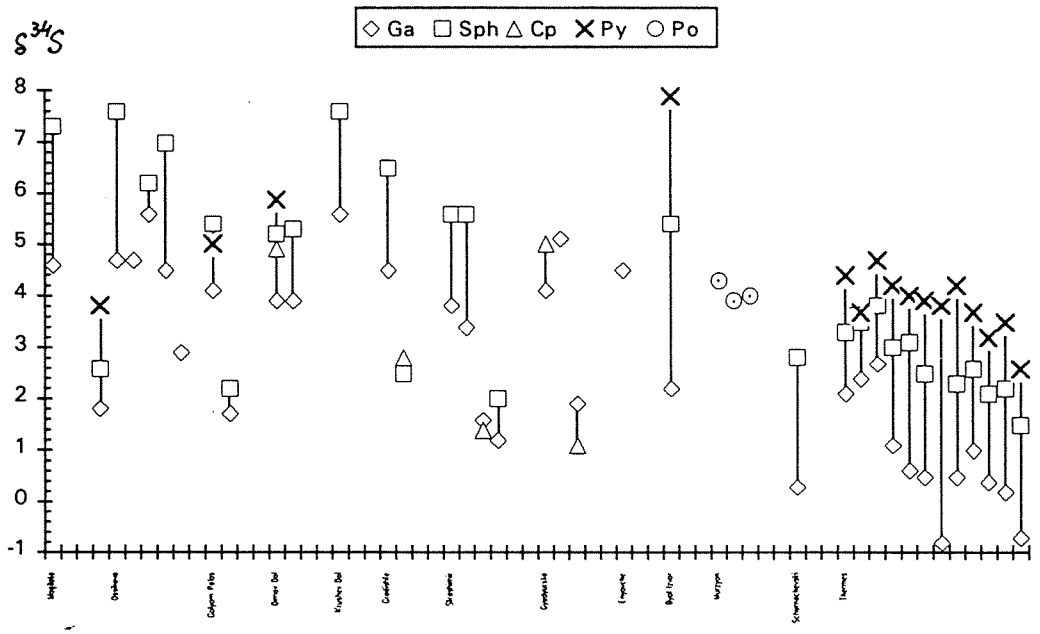

Fig.1 $\delta^{34}S$ of sulphides from different deposits in the Madan district and the Thermes area

δD. The δD values measured from the water of the fluid inclusions in galena are grouped in the range between -10 and -70‰, with a mean value of -62.4 ± 7.0‰ gained from 27 analyses, including the data of Piperov and Penchev (1982). This value agrees very well with that of the modern meteoric waters in the area: -66 ± 5‰, according to the above authors (Fig 2).

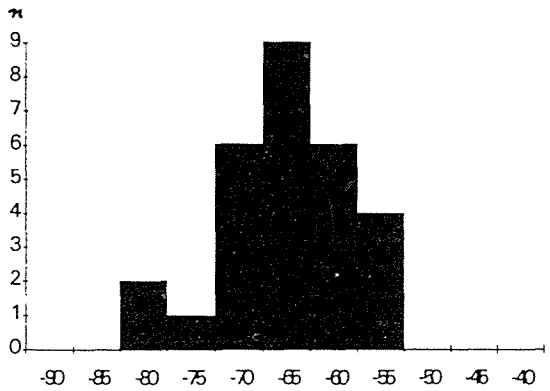

Fig 2. Frequency diagram of δD content of inclusion fluids extracted from galena crystals

$\delta^{18}O$. The direct $\delta^{18}O$ determinations of inclusion fluids exracted from galena crystals are dispersed in a wide range of light negative (<0) values (Fig. 3) with a mean value of -9.6 ± 5.7‰ (9 analyses). The average $\delta^{18}O$ ratio for these waters is located exactly on the line of meteoric waters. Indirect methods for ascertaining the O isotopic composition were also applied - determining the $\delta^{18}O$ of quartz crystals contemporarenous with the main sulphides. The $\delta^{18}O$ values of fluids in equilibrium with such quartz were calculated using the water-quartz fractionation factor for temperatures characteristic of the ore mineralization. The light $\delta^{18}O$ values obtained are grouped in a narrow range between 0 and -5‰, average -2.40 ± 1.60 (18 analyses).

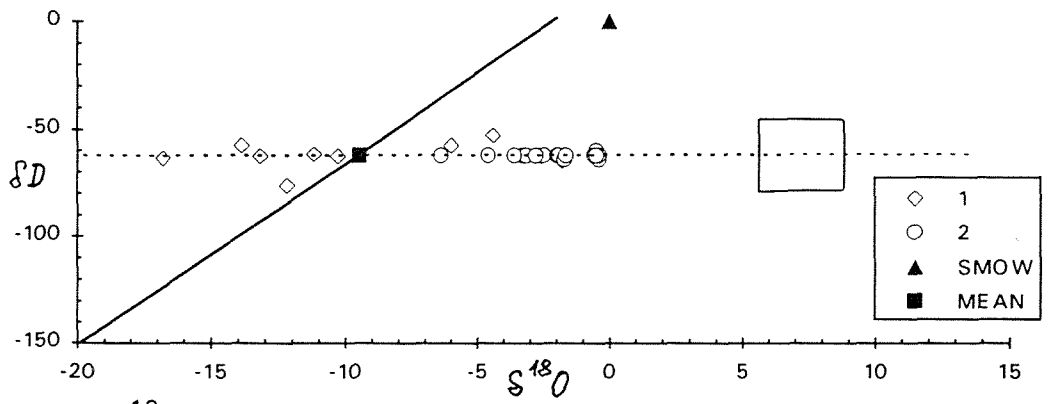

Fig.3. $\delta D/\delta^{18}O$ isotropic composition of the hydrothermal fluids: from inclusions in galena (individual values - 1, and mean value solid square) as compared to the primary magmatic water area (in the square) and SMOW

As compared to $\delta^{18}O$ data produced from solid quartz, the $\delta^{18}O$ values of inclusion fluids scatter in a larger area, partly also to the left of the meteoric water line (Fig. 3). It must be taken in consideration that vapour bubbles enriched in light isotopes have played a substantial role during trapping of the macroinclusions in galena from the boiling solutions, and the liquid:vapour ratio in the different inclusions is highly variable (e.g. 1:1, Piperov et al., 1977; Bonev, 1977).

Genetic model. The results of the isotopic studies indicate that the ore deposition in the Madan district (including the area of Thermes) took place in a high-temperature meteoric-hydrothermal system (as these discussed by Criss and Taylor, 1986). The convective circulation of the deeply penetrating predominantly surfacial waters was generated by the thermal energy of a magmatic heat source, and was strongly controlled by the fracture network in the weakly permeable country rocks.

Most likely, such a model is applicable and to the other geologically and mineralogically very similar Tertiary lead-zinc ore fields in the Rhodopes, as well as in the Serbian-Macedonian Massif, incliding in Bulgaria, Greece and Macedonia.

Acknowledgements. Financial and technical support from the Royal Society, SURRC - East Kilbride, University of Aberdeen, and the Bulgarian National Science Foundation is gratefully acknowledged.

References

Bonev, I. 1977. Primary fluid inclusions in galena crystals. I. Morphology and origin. Mineral. Deposita. 12:64-76.

Bonev, I. 1984. Mechanisms of the hydrothermal ore deposition in the Madan lead-zinc deposits, Central Rhodopes, Bulgaria. In: Proc. Sixth. Quadr. IAGOD Symp. E. Shweizerbart'sche Verlagsbuchhandlung , Stuttgart: pp 69-73.

Changkakoti, A., R. Dimitrakopoulos, J. Gray, H. R. Krouse, D. Krstic, S. I. Kalogeropoulos, N. D. Arvanitidis. 1990. Sulfur and lead isotopic composition of sulfide minerals from Thermes and Esimi, Rhodope Massif, Greece. N. Jb. Miner. Mh. 9:413-430.

Criss, R. E., H. P. Taylor, Jr. 1986. Meteoric-hydrothermal systems. In: Valley, J. W.,H. P. Taylor, Jr., J. R. O'Neil (eds.). Stable isotopes, Rev. in Mineralogy. 16:373-424.

Ohba, T. 1987 18O/16O and D/H ratio determination for small amounts of water. Geochem. J. 21:183-186.

Piperov, N. B., N. P. Penchev, I. K. Bonev. 1977. Primary fluid inclusions in galena crystals. II. Chemical composition of the liquid and gas phases. Mineral. Deposita. 12:77-89.

Piperov, N. B., N. P. Penchev. 1982. Deuterium content of the inclusion water from hydrothermal galenas, Madan, Bulgaria: Preliminary investigation. Econ. Geol. 77, 1-2: 195-197.

Current Research in Geology Applied to Ore Deposits.Fenoll Hach-Alí, Torres-Ruiz & Gervilla(eds)(1993).ISBN 84-338-1772-8

AUTHIGENESIS IN SEDIMENTS OF THE MIDDLE VALLEY, NORTHERN JUAN DE FUCA (ODP LEG 139): A RECORD OF CONVECTIVE HYDROTHERMAL CIRCULATION ON A SULPHIDE BEARING, SEDIMENTED RIDGE

Boni, M. (1); Früh-Green, G.L. (2); Mckenzie, J.A. (2) & Buatier, J. (3)
(1) Dip.to Scienze della Terra. Univertita' di Napoli, Largo S. Marcellino 10, 80138 Napoli, Italy
(2) Geologisches Inst., ETH-Zürich, ETH Zentrum, 8092 Zürich, Switzerland
(3) Sciences de la Terre. Université de Lille, 59655 Villeneuve D'Ascq, France

Abstract: Mineralogical, petrographical and stable isotope investigations of authigenic minerals recovered from the sediments cored at Middle Valley have allowed a better insight into hydrothermal processes in an area where significant massive sulfides have been discovered recently. In particular, both mineralogical and geochemical composition, as well as stable isotopes have proven to be excellent tracers of the temperatures and geochemical conditions under which in situ reactions occurred. The results of this study have provided important information to define the fluid pathways and temperature gradients in both active and fossil hydrothermal systems of sedimented ridges.

Middle Valley is a fault-bounded rift valley, situated at the northern extremity of the Juan de Fuca Ridge, just south of the Sovanco fracture zone (Davis & Villinger, 1992). Because of its proximity to the North American continental margin, Middle Valley is predominantly filled by terrigenous sediments (Goodfellow & Blaise, 1988). The sedimentary sequences are characterized by turbidite units of variable thickness (300-1500 m), interbedded with pelagic to hemipelagic sediments.
The sediment/basement interface in Middle Valley is transitional rather than sharp. The top of the igneous crust is characterized by a gradual transition zone of intercalated sediments and basaltic sills and flows. Numerous local heat flow anomalies occur in the valley (Davis & Villinger, 1992). The elevated basement temperatures probably reflect a high thermal insulating capacity and low permeability of the sedimentary sequences. This plays an important role in maintaining high fluid temperatures and facilitating hydrothermal discharge at a restricted number of vent sites (Goodfellow & Blaise, 1988).

The four sites drilled in the eastern part of Middle Valley during ODP Leg 139 are characterized by distinct hydrologic environments which include an area of fluid recharge at lower temperatures (Site 855), an area of active discharge characterized by high flow (Site 858), and a "hydrothermal reservoir" (Site 857), with high temperature fluids well-sealed with sediments. Site 856 is considered to be an area of fossil discharge where an older event of hydrothermal activity, possibly reactivated, led to strong alteration of the sedimentary cover and to the deposition of a large body of over 95m in thickness of massive sulfides (Davis et al.,1992). Main components of the ore are the iron minerals pyrite, pyrrhotite, magnetite and marcasite. Chalcopyrite and sphalerite are present only in minor amounts. As gangue minerals associated to the sulfides quartz, talc, dolomite and siderite have been observed.
However, among the various hydrothermal authigenic phases recovered from the sedimentary piles cored during the Leg, the more abundant are silicates and carbonates. Authigenic silicate, prevailing in deepest layers downhole,are mostly Mg-chlorite, but in Site 858 the

silicate sequences from sea-water interface to the deepest levels of the holes reflect a thermal gradient with depth, related to the vertical influence of the intrusive fluids. Carbonate nodules and concretions (Al-Aasm & Blaise, 1991) have been sampled at several depths from Sites 856, 857 and 858 and consist mostly of Ca-carbonate concentrations of various shapes, impregnating and/or substituting for both hemipelagic and coarse-to-fine turbiditic sediments. In the coarser lithologies they form a cement network between detrital grains. In the finer silty clays the carbonates can be (1) unevenly diffused as microcrystalline cement, whose distribution follows generally traces of burrowing organisms, and as (2) fibrous calcite macrocrystals growing in the form of rounded concretions throughout the silty sediment. In the latter case, calcite nodules contain pyrite crystals and framboids as well as Mn-dendrites. Observed under cathodic light, the carbonates are all luminescing, with different degrees of colour and brightness. Higher cathodoluminescence colours, however, appear to be related to Mn-values > 0.7 wt.% (Mn/Ca > 0.02) in the calcite. These higher Mn/Ca ratios are common both in the nodules sampled from Sites 856 and 857, below 40 meter below sea floor, as well as in few nodules from Site 858, below 20 m. Mn-richer carbonates have been deposited in more advanced diagenetic stages compared with those recovered at shallower depths, whose carbonates have lower Mn/Ca ratios (Buatier et al., in press). The same characters have been deduced from the stable isotope ratios, where the shallow/low-Mn nodules show positive ∂18O (PDB) and more negative (< -25‰ PDB) ∂13C, compared with late-diagenetic/high-Mn nodules (negative ∂18O and more positive ∂13C).

Moreover, oxygen and carbon isotope measurements on authigenic carbonates, integrated also by the data recorded from the silicates, provide a record of present and fossil convective fluid circulation and high temperature gradients associated with the hydrothermal alteration of the sediments of Middle Valley (Früh-Green et al., in press). Oxygen isotope compositions of authigenic carbonates from the active hydrothermal field at Site 858 show vertical thermal gradients of 2.2°C/m in the more distal holes, and of 10°C/m at the central vent areas.

As anticipated, the higher thermal gradient is consistent with oxygen isotope data for Mg-rich authigenic clays and quartz, which yield isotope fractionation temperatures of 280°C at 32 mbsf in a hole (858B) where no authigenic carbonates have been recorded. Extrapolation of the latter gradient to greater depths indicates temperatures of approximately 400°C at depths of 40-45 mbsf in the sedimentary sequence, approaching values which are sufficiently high enough to generate ore-forming fluids at these shallow depths. Furthermore, the calculated thermal gradients from the active vent area are similar to paleo-geothermal gradients recorded in the oxygen isotopic composition of carbonates from the fossil hydrothermal field at Site 856 (with its massive sulfides), which are higher than the modern measured geothermal gradient.

Carbon and oxygen isotope data of shallow carbonates at the active hydrothermal field are consistent with methane oxidation and, together with the presence of dolomite and Mg in pore-water profiles, provide evidence for advection of cold, oxidizing surface waters at shallow depths. From about 5 mbsf (carbonate cements) and 20 mbsf (nodules) respectively, to the base of the cored section at Site 858 and throughout the hydrothermal reservoir at Site 857, the carbonate minerals with ∂13C values between -10 and -25‰ reflect sulfate

reduction, demonstrating that the circulating hydrothermal fluids were reducing. The same reducing conditions can be deduced also by the presence of Mn-bearing carbonates in the deeper carbonate nodules.
The results of this integrated study, combined with pore water and sediment geochemistry, delineate a system of large scale convective hydrothermal circulation through the sedimentary sequence. In addition, smaller scale fluid advection in the shallowest parts of the section occurs. The oxygen isotope data imply an altered isotopic composition for the circulating fluids, indicating that the reaction rates or fluid/rock interactions must be high, relative to the fluid flux rates.

References

Al-Aasm I.S. and Blaise B. 1991. Interaction between hemipelagic sediment and a hydrothermal system: Middle Valley, northern Juan de Fuca Ridge, subarctic northeast Pacific. Marine Geology. 98:25-40.

Buatier M., Boni M., Karpoff A.M., McKenzie J.A. and Früh-Green G.L. in press. Mineralogical and petrographical records of sediment-fluid interactions in the sedimentary sequence of Middle Valley, Juan de Fuca Ridge, ODP Leg 139. ODP Scientific Results Volume B.

Davis E.E. and Villinger A.W. 1992. Tectonic and thermal structure of the Middle Valley sedimented rift, northern Juan de Fuca Ridge. In Davis E.E., Mottl M., Fisher A. et al., 1992, Initial Reports, ODP Leg 139, Middle Valley: 9-41.

Davis E.E.,Mottl M., Fisher A. and Scientific Party 1992. Initial Reports, ODP LEG 139, Middle Valley, 4 July - 11 September 1991, Volume A.

Früh-Green G.L., McKenzie J.A., Boni M., Karpoff A.M. and Buatier M. in press. Stable isotope and geochemical record of convective hydrothermal circulation in the sedimentary sequence of Middle Valley, Juan de Fuca Ridge, ODP Leg 139. ODP Scientific Results Volume B.

Goodfellow W.D. and Blaise B. 1988. Sulphide formation and hydrothermal alteration of hemipelagic sediments in Middle Valley, Northern Juan de Fuca Ridge. Canad.Mineral. 26:675-696.

Current Research in Geology Applied to Ore Deposits. Fenoll Hach-Ali, Torres-Ruiz & Gervilla (eds) (1993). ISBN 84-338-1772-8

DEPOSITION ENVIRONMENT OF GOLD-BEARING ARSENOPYRITE IN MESOTHERMAL DEPOSITS

Bortnikov, N.S. (1); Genkin, A.D. (1); Chryssoulis, S. (2)
(1) IGEM, Russian Acad. Sci., 35 Staromonetny, Moscow, Russia
(2) University of Wester Ontario, London, Ontario, Canada N6A 5B7

ABSTRACT: SIMS analyses revealed that arsenopyrite contained 1.2 to 74 ppm "invisible gold". PT conditions are estimated to have ranged from 190 to 380°C and 0.9 to 2.7 kb.

1 INTRODUCTION

Gold occurs usually as isolated grains of native gold in quartz veins or gold and silver tellurides intimately associated with sulfides (Boyle,1979). "Invisible gold" incorporated in sulfides minerals has been found to play an important role in many low grade deposits (Boiron et al.,1989; Chryssoulis,1989; Cabri et al.,1989). Arsenopyrite is a principal mineral containing invisible gold. Paragenesis and crystallization conditions of Au-bearing arsenopyrite are poorly documented. This paper presents an attempt to shed new light on paragenesis, chemical composition and condition of formation of Au-bearing arsenopyrite in the mesothermal deposits.

2 GEOLOGY OF DEPOSITS

Au-bearing arsenopyrite has been found in mesothermal deposits Nezhdaninskoye (Russia), Charmitan (Uzbekistan) and Delita (Cuba).

The Charmitan gold deposit is located within the North Nurata anticlinorium in endo- and exocontact zones of the Koschrabad granosyenite body intruded in the metamorphosed sedimentary sequence (sericite-chlorite, quartz-sericite shists, carbonaceous and clay shales). The metamorphosed rocks are folded in an isoclinal anticline. The zone of the regional faults in the southern exocontact of the intrusive body has been mapped. Quartz veins and mineralized zones are located in the fractures related to this fault zone.

The Delita deposit is located within the anticlinal fold and is hosted by the metamorphic quartz-sericite shists with the beds enriched in graphite and the carbonaceous matter. The large magmatic bodies were not found, but small dykes of rhyolite has been recognized. Ore bodies are the quartz veins, containing 3-15% opaque minerals.

The Nezhdaninskoye deposit is located in South-Verkhoyansk synclinorium. It is hosted by a 400-m-thick sequence of black aleurolites with thin sandstone beds and a 800-m-thick sequence of carbonaceous argillites. These rocks contain up to 2 wt. per cent of organic matter and disseminated fine-grained pyrite and marcasite. Host rocks have been metamorphosed to low greenschist facies. The principal fold of the district is the Dybinskaya anticline. This fold is asymmetric and has a north-east (15-20^{o}) axial surface. Its limbs are undisturbed by faulting. North-North-westerly trending (350^{o}) and north-easterly (60^{o}) trending faults are components of a conjugate system that dominates the tectonic pattern of the Nezhdaninskoye area. The ore bodies are controlled by the Nezhdaninskaya tectonic zone which includes the foliation, brecciation, shear zones. The sedimentary sequence is intruded by small stocks of gabbro-diorite and numerous dykes of aplite, spessartite, kersantite and diorite porphyrites.

3 MINERAL PARAGENESIS OF GOLD-BEARING ARSENOPYRITE

The multistage ore forming process was responsible for the formation of gold deposits with very complex mineral composition. Two generations of Au-bearing arsenopyrite have been recognized. Earlier arsenopyrite is coarse grained and comprises the ribbons, veinlets, and pockets in the quartz veins. It associates with pyrite and native gold. Native gold (fineness ranges from 740 to 950) replaces earlier arsenopyrite. The late arsenopyrite is fine grained and associates with pyrite, tetrahedrite, Pb-Sb sulphosalts (jamesonite, boulangerite, zinckenite) and Pb-Ag-Sb sulphosalts (owyheeite, diaphorite) The grains of the late arsenopyrite are crosscut by late electrum (the fineness is 480-560).

4 GOLD IN SULFIDES

Secondary ion microprobe analyses has been used to determine a gold content in sulfides. Analytical procedure has been described in detail by Chryssolius (1989). The results are given in Table.

Table

Gold contents (in ppm) in sulphide minerals

Deposit	Mineral	Range	Average
Nezhdaninskoye	Asp I	1.5 - 48 (9)	12.4+9.43
	Asp II	10.0 - 35 (10)	22.4+5.79
	Py	1.4 (1)	
	Po	0.78- 1.2 (2)	
Charmitan	Asp I	1.2 - 23 (15)	5.4+2.9
	Asp II	2.7 - 74 (8)	30.1+15.9
	Py	4.4	
Delita	Asp	5.4 - 56 (17)	26.3+7.69
	Po	0.38- 0.68 (2)	

Note. Asp I - coarse grained arsenopyrite, Asp II - fine grained arsenopyrite, Py - pyrite, Po - pyrrhotite, Number of analyses is given in parentheses.

5 CHEMICAL COMPOSITION OF ARSENOPYRITE

Microprobe analyses have revealed the wide compositional variations in Au-bearing arsenopyrite. The As content in earlier arsenopyrite varies from 28.8 to 32.1 at.% in the Charmitan deposit, from 31.2 to 32.2 at.% in the Nezhdaninskoye deposit, and from 30.3 to 32.4 at.% in the Delita deposit. The similar ranges of the composition were found for arsenopyrite of the late generation. They are from 28.6 to 31.7 in the Charmitan deposit, from 32.6 to 33.3 in the Nezhdaninskoye deposit, and from 30.5 to 32.8 at.% in the Delita deposit. Therefore, gold-bearing arsenopyrite is As-deficient in relation to the stoichiometric FeAsS. The ranges found coincide well with the compositional variations of arsenopyrite in equilibrium with pyrite as it has been recognized in the experimental study of the Fe-As-S system.

6 PHYSICAL AND CHEMICAL CONDITIONS OF ARSENOPYRITE CRYSTALLIZATION

The data on mineral paragenesis, fluid inclusion and stable isotope studies (Bortnikov et al.,1989,1991,1993) were used to evaluate physico-chemical parameters of Au-arsenopyrite-forming process. Ore fluids have low to moderate salinity and consist of $H_2O>CO_2>CH_4=N_2>H_2S$. T-P conditions for the auriferous mineralization are estimated to have been ranged from 190 to 380°C and 0.9 to 2.7kb. Boiling may result in mineral deposition at pH values of 4 to 6 and a_{O2} and a_{S2} of the mineralizing fluids were in the range about 10^{-31} to 10^{-36} and 10^{-7} to 10^{-12}, respective-ly. The CO_2 and CH_4 fugacities were up to $10^{2.5}$ and $10^{1.4}$ bars.

REFERENCES

Boiron,M.-C., Cathelineau,M., Trescases,J.-J., 1989. Conditions of gold-bearing arsenopyrite crystallization in the Villeranges Basin, Marche-Combrailles Shear zone, France: a mineralogical and fluid inclusion study. Econ.Geol.,v.84,p.1340-1362.

Bortnikov,N.S., Gamyanin,G.N., Naumov,V.B., Nosik,L.P., 1993. The Nezhdaninskoye mesothermal gold deposit, Russia: Ore-forming fluid and deposition environment. This volume.

Bortnikov,N.S., Kramer,H.L., Genkin,A.D., Kulnev,A.S., 1989. Mineral composition and formation conditions of the Delita gold deposit (Republic of Cuba). Geol.rudn.mestorozhd.,N 5,p.3-7.

Bortnikov,N.S., Prokof'ev,V.Ju., Rasdolina, N.V., 1992. Environment of ore deposition in the Charmitan gold vein deposit, Nurata Mountains, Uzbekistan, USSR. 29th IGC. Abstract volume 3, p.746.

Boyle, R.W., 1979.The geochemistry of gold and its deposits: Canad.Geol.Survey Bull.,280,544p.

Cabri, L.J., Chryssoulis, S.L., de Villiers, J.P.R., Laflamme, J.H.G., Buseck, P., 1989. The nature of "invisible" gold in arsenopyrite. Canad.Mineralogist,v.27,p.353-362.

Chryssoulis, S.L.,1989. Ion probe microanalysis of gold in common sulphide minerals and implications for enhanced recovery from refractory gold ores. CANMET Contract Report,79037-01-99.

Current Research in Geology Applied to Ore Deposits.Fenoll Hach-Alí, Torres-Ruiz & Gervilla(eds)(1993).ISBN 84-338-1772-8

THE MOONTA COPPER DEPOSITS, SOUTH AUSTRALIA: GEOLOGY AND ORE GENESIS OF THE POONA AND WHEAL HUGHES ORE BODIES

Both, R.A.(1); Hafer, M.R. (1); Mendis, D.P.J. (1) & Kelty, B. (2)
(1) Dept. of Geology and Geophysics, University of Adelaide, South Australia
(2) Moonta Mining Joint Venture, Moonta, South Australia

ABSTRACT: Recent exploration in the Moonta area, South Australia, has resulted in the development of two new mining operations in this previously important copper field. The Poona and Wheal Hughes ore bodies are vein deposits located in shear zones in the Mid-Proterozoic Moonta Porphyry. The major minerals are chalcopyrite, pyrite, hematite, quartz, chlorite and tourmaline. Fluid inclusions in quartz have homogenization temperatures between 140° and 388°C and salinities between 0.2 and 22.7 wt % NaCl equivalent. Temperatures calculated from chlorite analyses range from 163° to 326°C, with log fO_2 values from -50.9 to -31.4. $\delta^{34}S$ values of chalcopyrite, pyrite and bornite vary from -1.3 to 6.4 per mil. A magmatic hydrothermal origin is suggested (but not proved) by the association with pegmatites, the presence of tourmaline and minor molybdenite, and near-zero $\delta^{34}S$ values.

1. INTRODUCTION

The Moonta copper deposits in South Australia were discovered in 1860 and worked continuously until 1923. During this time the Moonta and adjacent Wallaroo fields were important copper producers, yielding 6,250,000 tons of ore at an average grade of 5.3% copper. After closure of the mines, these fields remained dormant until recent exploration by Western Mining Corporation discovered further deposits at Moonta by means of SIRO TEM surveys, leading to the development of mining operations at Poona and Wheal Hughes (Fig. 1) by Moonta Mining Joint Venture. The Poona mine was worked from 1988 to 1992, producing 150,000 tons of ore at 4.8% Cu and 1.5g/t Au from the open cut and 37,000 tons at 4.6% Cu and 1.3g/t Au from the underground mine. Wheal Hughes commenced operations in 1991 and produced 140,000 tons of ore from the open cut; an ongoing drilling program has so far proved 160,000 tons of ore at 5.2% Cu and 0.7g/t Au underground, of which 50,000 tons have been mined to date. Although not large, these discoveries have provided the first opportunity in recent years to investigate the origin of the Moonta deposits, since lack of access to old workings and complete absence of outcrop in the area had previously prevented such studies.

2. REGIONAL GEOLOGICAL SETTING

The copper deposts of Moonta and Wallaroo are located within the Gawler Craton (Parker, 1990), and hosted by the Proterozoic Moonta Porphyry and Doora Schist, respectively (Fig. 1). The Moonta Porphyry is a strongly foliated, porphyritic rhyolite interpreted by Lemar (1975), on the basis of relic primary textures, as representing a sequence of comagmatic ash flow tuffs and tuff breccias and intrusive microgranites. Fanning et al. (1988) have reported a U-Pb zircon age of 1741 ± 9 Ma for the Moonta Porphyry. The Doora Schist is interlayered with the Moonta Porphyry (Fig. 2). The Kimban Orogeny (1950 to 1700 Ma; Parker, 1990) was followed by emplacement of the Arthurton-Tickera granite suite and deposition of Proterozoic and Cambrian sediments (Fig. 2). The granite has been dated by zircon at 1585 ± 3 Ma (Creaser, 1989). Pegmatite bodies are common throughout the region, including the ore zones, and are apparently a late stage fractionation of the granite.

3. MINERALIZATION AND PARAGENESIS

Mineralization in the Moonta field typically consists of tabular veins within fractures and shear zones in the Moonta Porphyry. The majority of the veins are located in a series of concentric arcs trending from NNE to ENE. The Poona vein stikes E-W and dips approximately 45°N, within a shear zone, and is offset into 3 segments by faults perpendicular to the shear plane. The Wheal Hughes deposit is unusual for the Moonta field, in that the main part consists of a sheeted vein system. The veins strike NE-SW and dip 45°NW, and are hosted by a 25m thick shear zone. The NE part of the Wheal Hughes deposit, known as Leighton's lode, consists of a single vein separated from the main part by a cross-cutting fault. Post-mineralization shearing of both the Poona and Wheal Hughes deposits has produced pinch and swell boudinage structures in the ore, with copper enrichment in both the boudin and neck zones.

The Poona and Wheal Hughes ores contain similar mineral assemblages, but with some differences in mineral proportions and paragenesis (Fig. 3). The dominant metallic minerals at Poona are chalcopyrite, pyrite and hematite, with

minor amounts of magnetite and bornite, and trace amounts of carrollite, gold and marcasite. At Wheal Hughes chalcopyrite and pyrite dominate, with only minor hematite, and traces of magnetite, carrollite, gold and marcasite. Minor molybdenite is also present at Wheal Hughes. Non-metallic minerals in the ores are quartz, chlorite, sericite and tourmaline. Both deposits have undergone supergene alteration in the upper levels. Patches of atacamite, cuprite and malachite occur at the base of the oxidized zone and pods of native copper have been found in the gradational boundary between the oxidized and supergene sulphide zones. The main secondary sulphides are chalcocite and covellite, with minor digenite found only at Poona.

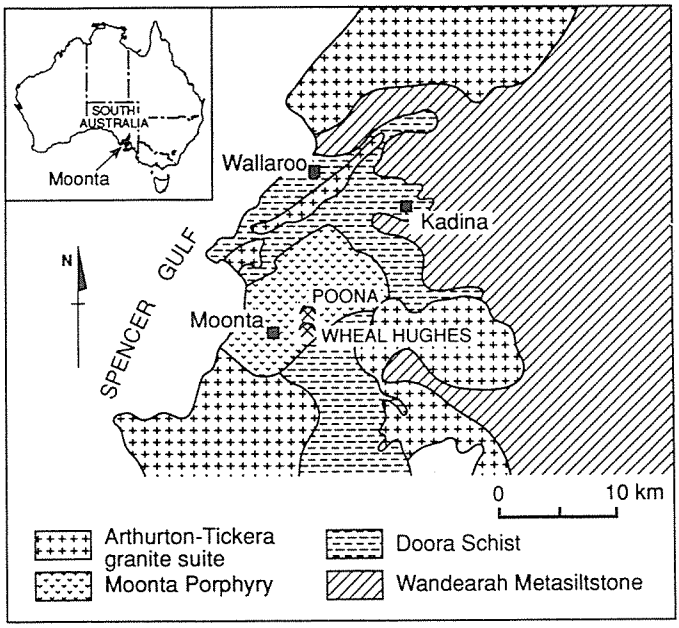

Fig. 1: Generalized regional geology (after Hafer, 1991).

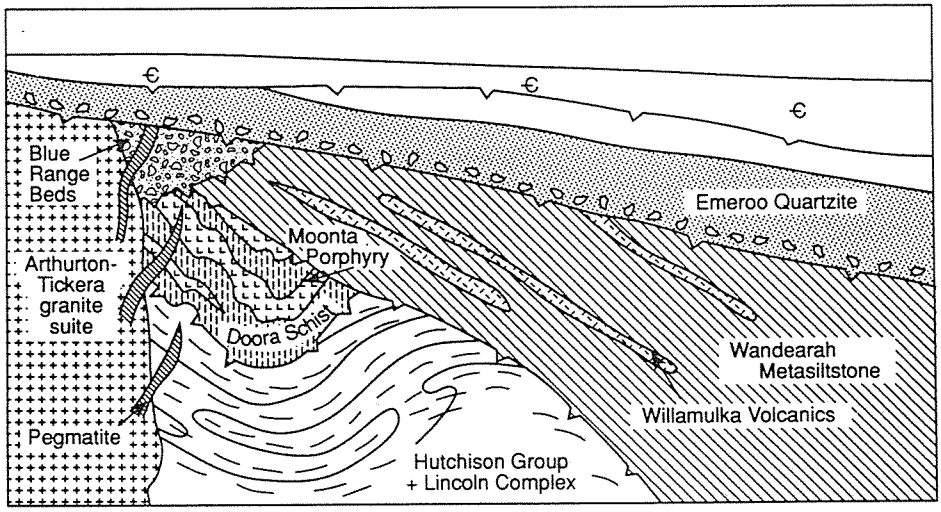

Fig. 2: Schematic diagram of rock relationships, Moonta region (after A. J. Parker, pers. comm.; Hafer, 1991).

Adjacent to the ores bodies the host porphyry has been altered to chlorite, tourmaline and sericite. Tourmaline is more abundant in the alteration zone associated with the main part of the Wheal Hughes orebody, where the zone is up to several metres in thickness. The Leighton's lode segment and Poona have narrower alteration zones. The oxidized porphyry above both deposits, as well as the feldspathic sandstone of the Blue Range Beds (Fig. 2) that partly overlie the Wheal Hughes deposit, are extensively kaolinized. This kaolinite is clearly supergene, but the Wheal Hughes veins are also partly surrounded by a zone of kaolinite that could, at least in part, be hypogene in origin.

The paragenetic sequence shows only minor differences between the two deposits (Fig. 3). Mineralization was deposited in 3 hydrothermal stages separated by episodes of fracturing associated with shearing. The first stage was characterized by Fe oxides; magnetite was deposited initially and subsequently almost entirely replaced by hematite. The second stage was dominated by Fe sulphides, mainly pyrite with minor marcasite. The final hydrothermal stage involved deposition of Cu–Co–Fe–Au mineralization. The major mineral is chalcopyrite, which replaced earlier minerals along fractures. Carrollite is closely associated with chalcopyrite and shows similar textural relationships. Bornite and gold both occur mainly as small inclusions within chalcopyrite. The main paragenetic difference between the two deposits is the presence at Poona of a second generation of hematite, in the form of thin tabular crystals that form a network within fractures in earlier hematite and pyrite. The spaces in the network have been filled with chalcopyrite and associated third stage minerals. Although molybdenite is present at Wheal Hughes it has not been observed in contact with other metallic minerals and, hence, its paragenetic relationships are not known. Quartz appears to have been deposited in all stages. Deposition of chlorite, sericite and tourmaline commenced in the second stage and continued through the third stage.

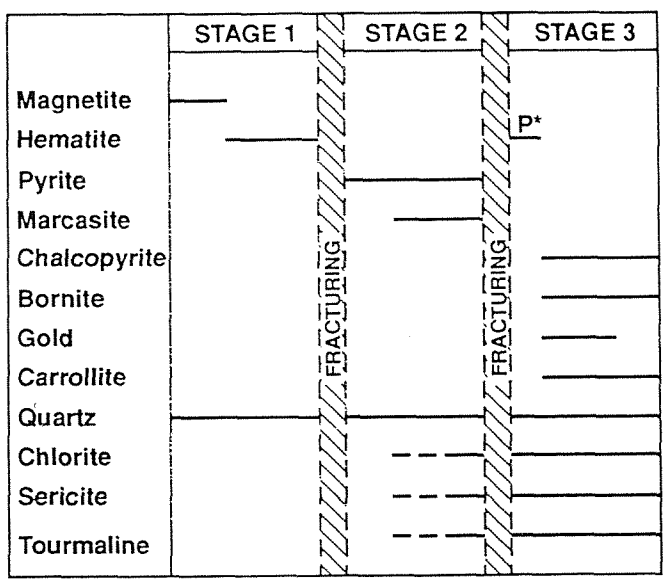

Fig. 3: Paragenetic sequence of mineralization, Poona and Wheal Hughes ore bodies. P* indicates observed at Poona only.

4. FLUID INCLUSIONS

Fluid inclusions in quartz associated with the ore minerals are small (maximum size 15 x 12μm) and mainly 2-phase liquid-rich inclusions. Small daughter crystals were observed in some fluid inclusions and appear to be halite and hematite. Discrimination between primary and secondary fluid inclusions was difficult in the absence of growth zoning in the quartz.

First melting temperatures of fluid inclusions classified as primary ranged from -63.0^{0} to -23.6^{0}C, indicating the presence in the fluid of components such as $CaCl_2$ and/or $MgCl_2$ in addition to NaCl. Final melting temperatures

correspond to a salinity range of 0.2 to 22.7 wt. % NaCl equivalent. Homogenization temperatures show a range of 139.8° to 387.8°C, with the data suggesting 2 groups, viz. a higher temperature group with a mode around 340°C and a lower temperature group with a mode around 180°C. The latter group overlaps with homogenization temperatures of fluid inclusions identified as secondary.

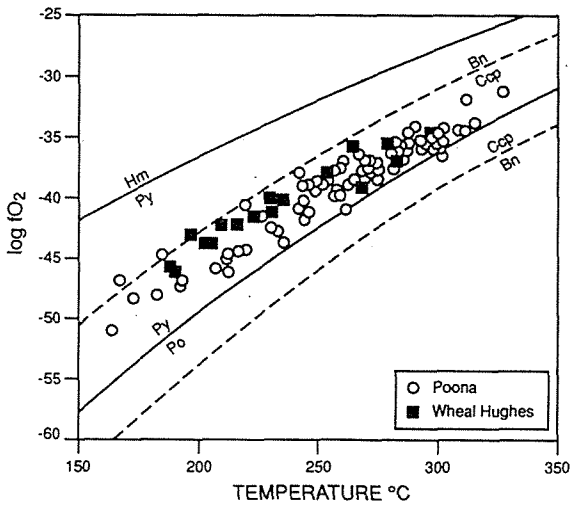

Fig. 4: Log fO_2 vs. T diagram showing chlorite data in relation to stability fields of pyrite (Py), pyrrhotite (Po), hematite (Hm), chalcopyrite (Ccp) and bornite (Bn). Calculated for pH=4.5.

5. CHLORITES

Electron microprobe analyses of chlorites were used to calculate temperatures and fO_2 values, using the 6-component solid solution model of Walshe (1986). Chlorites intergrown with chalcopyrite and/or pyrite give a range of calculated temperatures of 163° to 326°C, with a mode around 280°C and log fO_2 values ranging from -50.9 to -31.4. The data define a trend of decreasing fO_2 with temperature (Fig. 4), presumably reflecting a waning hydrothermal system.

6. SULPHUR ISOTOPES

$\delta^{34}S$ values of 13 chalcopyrites from Poona range from -1.3 to 5.5 per mil and 12 from Wheal Hughes range from 2.5 to 6.4 per mil. In addition, 7 pyrites and 1 bornite from Poona and 2 pyrites from Wheal Hughes lie within the respective chalcopyrite $\delta^{34}S$ ranges for the deposits. T-fO_2-pH considerations indicate that the dominant sulphur species in the fluid was H_2S and that $\delta^{34}S_{sulphide\ minerals} = \delta^{34}S_{fluid}$.

7. ORE GENESIS

Several features of the Poona and Wheal Hughes ore bodies are consistent with a magmatic origin for the hydrothermal fluids responsible for the deposits and, by implication, for other deposits in the Moonta field. These features include the common association of pegmatites with the ore zones, the presence of abundant tourmaline as a gangue component of the ores and in the wallrock alteration assemblages, and the occurrence of molybdenite as a minor component in the Wheal Hughes ore (a feature also of many other Moonta deposits). The near-zero $\delta^{34}S$ values of the sulphide minerals are also in keeping with a magmatic origin for the sulphur. In terms of both time and space, the Arthurton-Tickera granite suite (Figs. 1 and 2) represents a possible source of the hydrothermal fluid. However, none of the above characteristics proves a magmatic origin and further stable isotope analyses ($\delta^{18}O$ of quartz and $\delta^{18}O$ and δD of chlorite) are currently being undertaken in an attempt to further constrain the fluid source.

REFERENCES

Creaser, R.A. 1989. The geology and petrology of Middle Proterozoic felsic magmatism of the Stuart Shelf, South Australia. PhD thesis (unpubl), LaTrobe Univ.

Fanning, C.M., Flint, R.B., Parker, A.J., Ludwig, K.R. & Blissett, A.H. 1988. Refined Proterozoic evolution of the Gawler Craton, South Australia, through U-Pb zircon geochronology. Precamb. Res.. 40/41:363-386.

Hafer, M.R. 1991. Origin and controls of deposition of the Wheal Hughes and Poona copper deposits, Moonta, South Australia. Hons. thesis (unpubl.), Univ. of Adelaide.

Lemar, R.C. 1975. The origin of the Moonta Porphyry. Grad. Dipl. thesis (unpubl.), South Aust. Inst. Technology.

Parker, A.J. 1990. Gawler Craton and Stuart Shelf - regional geology and mineralisation. In: Hughes F.E. (ed.) Geology of the mineral deposits of Australia and Papua New Guinea. Australas. Inst. Min. Metall, Melbourne, pp 999-1008.

Walshe, J.L. 1986. A six-component solid solution model and the conditions of chlorite formation in hydrothermal and geothermal systems. Econ.Geol. 81:681-703.

Current Research in Geology Applied to Ore Deposits. Fenoll Hach-Alí, Torres-Ruiz & Gervilla (eds) (1993). ISBN 84-338-1772-8

PETROGRAPHIC AND $\delta^{34}S$ STUDY OF LOWER PALAEOZOIC ROCKS UNDER THE NAVAN Zn+Pb DEPOSITS: A SOURCE OF HYDROTHERMAL SULPHUR

Boyce, A.J. (1); Fletcher, T.J. (1); Fallick, A.E. (1); Ashton, J. (2) & Russell, M.J. (3)
(1) Isotope Geology Unit, SURRC, East Kilbride, Glasgow, G75 0QU, Scotland
(2) Geology Dept., Outokumpu Zinc-Tara Mines, Navan, Co. Meath, Ireland
(3) Dept. of Geology and Applied Geology, University of Glasgow, Glasgow, G12 8QQ, Scotland

Abstract

Pyrite in the Lower Palaeozoic sequences below the giant Lower Carboniferous Sedex base-metal ore deposit at Navan exhibits at least four generations of growth, dominated by growth during early to late Lower Palaeozoic diagenesis. The pyrite exhibits an extraordinary range in $\partial^{34}S$, between -33.4‰ and +61.7‰, with the bulk of the data (80%) falling between 0‰ and +30‰, with a mode around +16‰. This mode is very similar to the $\partial^{34}S_{H_2S}$ of hydrothermal sulphide in the main ore horizons (~+15‰), suggesting a genetic link between the two: that is, the Lower Palaeozoic-hosted sulphide was leached with base-metals during the hydrothermal convection which led to the deposition of the deposit.

Introduction

The Navan Zn+Pb deposit is a world-class base-metal orebody (~69.9Mt at 10.1% Zn and 2.6% Pb), with the ores occurring in complex stratiform to stratabound tabular lenses. It is hosted in Lower Carboniferous shallow-water carbonate lithologies, during the diagenesis of which, the base-metal sulphides were precipitated (Ashton, *et al*, 1992).

Anderson's (1990) detailed petrographic and sulphur isotopic study showed that, although most of the sulphide ore was precipitated via the combination of hydrothermally exhaled metals and local bacteriogenic sulphide, a small but significant component of the ore was deposited using a hydrothermal sulphide source: that is, sulphide entrained in the hydrothermal solutions along with the metals. The two sulphide components have distinctly different $\partial^{34}S$: the "bacteriogenic" ores having $\partial^{34}S$ around -15‰, and the "hydrothermal" sulphides having a calculated $\partial^{34}S_{H_2S}$ around +15‰ (Anderson, 1990). This dual source of sulphide is also seen in the two other major base-metal ore producers in Ireland (Silvermines and Tynagh; Anderson *et al*, 1989).

The currently dominant genetic model for the Irish base-metal ores is the "convective" leaching model, which envisages the metals and some sulphur being derived from the thick sequence of Silurian and Ordovician turbiditic shales and siltstones, and volcanics which underlie the deposit (on the southern flank of the Longford-Down Inlier). The solutions are transported to the depositional site by large scale (≥30km diameter) convecting hydrothermal systems (Russell, 1978; Mills *et al*, 1987). The hydrothermal sulphur is suggested to be leached from diagenetic pyrite in the Lower Palaeozoic rocks.

Anderson *et al* (1989) published preliminary $\partial^{34}S$ data on 7 samples from beneath the Navan deposit, and suggested that the unusually isotopically heavy mean $\partial^{34}S$ of this "diagenetic" pyrite (~+16‰) correlated well with the hydrothermal signature in the base-metal deposit. It was also clear that the $\partial^{34}S$ of supposed diagenetic pyrite was significantly ^{34}S-enriched. A $\partial^{34}S$ range around 0‰ to -15‰ is expected from general considerations of diagenetic sulphide origins, and confirmed in the laterally equivalent Moffat Shale in southern Scotland (0‰ to -17‰; Anderson *et al*, 1989).

Our study aims to test the link between the hydrothermal and Lower Palaeozoic sulphides, while assessing the nature of the latter sulphide - is it truly diagenetic? To this end, we have accessed new Lower Palaeozoic core material from the deposit vicinity.

Lower Palaeozoic Pyrite

The Lower Palaeozoic sulphide is overwhelmingly in the form of pyrite in all lithologies, and is locally very abundant. Petrographic analysis reveals at least four generations of this pyrite (Fig. 1). Host sediments are mostly mildly deformed mudstones, with a weak slatey cleavage occasionally present. Small scale shearing and slumping (mm scale) are considered to be original sedimentary features. More intense deformation is localised, consisting of faulting and brecciation (accompanied by quartz±carbonate veining). The latter are related to major tectonic structures, which slice the Lower Palaeozoic succession in the area (Vaughan, 1992).

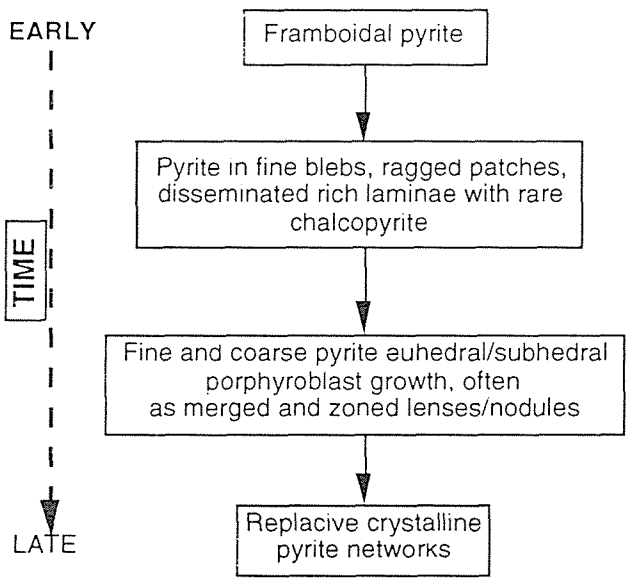

Figure 1: Preliminary Navan paragenesis in Lower Palaeozoic lithologies in borehole N1014

The pyrite exhibits a wide and complex range of textural forms, the paragenesis of which can be simplified as follows. Early diagenetic types are dominated by framboids (~10μm, locally abundant) and fine disseminated coatings on graptolites. The succeeding pyrite is in the form of ragged or rounded blebs which occur as disseminations or thin lenses (≤0.5mm). The next stages of growth exhibit a gradation from fine euhedral porphyroblasts, which appear then to coarsen, and finally to merge into large pyrite lenses and nodules (≤5cm, dictated by core diameter). These nodules sometimes exhibit zoning defined by variations in the amount of interstitial silicate material, or in the size of the pyrite subhedra. The fact that porphyroblasts and most lenses generally cross-cut sedimentary laminae and fossils, indicates that they have been deposited post-lithification. Flexuring of sedimentary laminae above and below these lenses, however, suggests that the growth may have been late diagenetic (rather than much later). A final stage of growth is associated with a phase of brittle deformation which fractures earlier lenses and is accompanied by the deposition of fine, replacive, pyrite networks. At least three phases of quartz±carbonate veining are also noted.

Sulphur Isotopes

Concentrating on Hole N1014, coarsely sampled pyrite (from all generations) show extreme variation in $\partial^{34}S$, between -33.4‰ to +51.9‰ (Fig. 2): 80% of the data, however, fall in the range -2.1‰ to +32‰, with a mode around +16‰. There is no systematic variation with depth in the hole. The same textural style can show a wide variation in $\partial^{34}S$, but co-existing early and late generations of pyrite showed notable variations up to 15.4‰, with the later pyrite usually (but not exclusively) being isotopically heavier. Locally extreme variations in $\partial^{34}S$ correlate with particularly tectonised and altered drillcore.

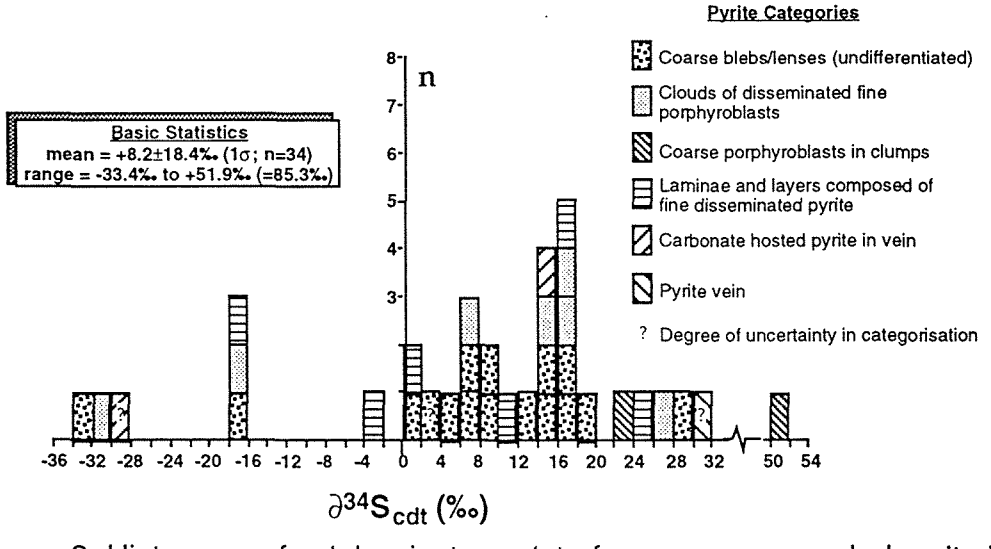

Figure 2: Histogram of sulphur isotope data from coarse-sampled pyrite in Lower Palaeozoic lithologies of Hole N1014.

Laser $\partial^{34}S$ analyses reveal a systematic variation in $\partial^{34}S$ within zoned nodules, in which ^{34}S is progressively enriched from core to rim, resulting in the rim being ≤10‰ heavier than the core. This is typical of the pattern of diagenetic nodule growth reported by Raiswell (1982), in which the bacteriogenic sulphate reduction system (supplying sulphide) becomes progressively closed as the pyrite grows outwards.

Conclusions

Incorporating the data of Anderson *et al*(1989), we confirm the unusually heavy $\partial^{34}S$ of Lower Palaeozoic-hosted pyrite under the Navan deposit, which appears principally to be the result of prolonged, periodic deposition of pyrite during the diagenesis of the Lower Palaeozoic sequence. The correlation of mean $\partial^{34}S$ of Lower Palaeozoic pyrite (~+16‰) with the calculated $\partial^{34}S_{H_2S}$ of ore precipitated with hydrothermal sulphide (~+15‰) is consistent with the convection hypothesis which postulates that the hydrothermal solutions at Navan leached sulphur from the underlying Lower Palaeozoic lithologies.

References

Anderson, I.K. 1990. Ore depositional processes in the formation of the Navan zinc/lead deposit, Co. Meath, Ireland. PhD Thesis, Univ. of Strathclyde.

Anderson, I.K. *et al* 1989. Preliminary sulphur isotope data of diagenetic and vein sulphides in the Lower Palaeozoic strata of Ireland and southern Scotland: implications for Zn+Pb+Ba mineralization. J. Geol. Soc. London, **146:**715-720.

Ashton, J.H., Black, A., Geraghty, J., Holdstock, M and Hyland, E. 1992. The geological setting and base-metal distribution in the Navan Boulder Conglomerate. In,Bowden, A.A. *et al* (eds) The Irish Minerals Industry 1980-1990. Irish Association for Economic Geology.

Mills, H, Halliday, A.N., Ashton, J.H., Anderson, I.K. and Russell, M.J. 1987. Origin of a giant orebody at Navan, Ireland. Nature, 327:223-226.

Raiswell, R. 1982. Pyrite texture, isotopic composition and the availability of iron. Am. J. Sci., **282**:1244-1263.

Russell, M.J. 1978. Downward excavating hydrothermal cells and Irish-type ore deposits: importance of an underlying thick Caledonian prism. Trans. Instn. Min. Metall., **B87:**168-171.

Vaughan, A. 1991. The Lower Palaeozoic of the Iapetus Suture Zone in eastern Ireland. PhD Thesis, Trinity College, Dublin.

Current Research in Geology Applied to Ore Deposits.Fenoll Hach-Alí, Torres-Ruiz & Gervilla(eds)(1993).ISBN 84-338-1772-8

NEW DATA ON THE ORE MINERALOGY OF THE UPULUNGOS MINE, LA MEJICANA DISTRICT, SIERRA DE FAMATINA, ARGENTINA

Brodtkorb, M.K. de (1) & Paar, W.H. (2)
(1) Consejo Nacional de Investigaciones Científicas y Tecnológicas, Paso 258, 1640 Martínez, Argentina
(2) Inst. of Mineralogy and Petrology, University Hellbrunnerstr. 34, A-5020 Salzburg, Austria

ABSTRACT: Ore samples from the Upulungos mine, La Mejicana District,Rioja Province of Argentina, were investigated by reflected light microscopy, electron microprobe analyses and x-ray methods.- The ore assemblage consists of pyrite, chalcopyrite, enargite-stibioenargite, luzonite-stibioluzonite, fahlores, colusite and aikinite. A Ag-Bi phase related to Pb-free benjaminite also occurs. A very pronounced chemical zonality is typical for most phases.

Introduction

The Nevado de Famatina Mining District is located in the Famatina Range, La Rioja Province of Argentina, at an altitude between 2600 and 4600 m above sea level. The district is well known for extensive vein-type copper (Angelelli,1983; Mendez,1981) and a porphyry type mineralisation. The latter was proved during an exploration campaign from 1976-1983 (Marcos and Zannetini,1982).
The most important veins were exploited in the La Mejicana (Upulungos and San Pedro mines), Los Bayos and Ophir districts.
The mining activity was important only early this century. More than 1 million tons of ore grading 10% Cu, 8 g/t Au, 70 g/t Ag (San Pedro) and 3% Cu, 20 g/t Au, 300 g/t Ag (Upulungos) were produced during that time.
The complex mineralogy of the copper veins was only incompletely studied so far. According to earlier investigations (Angelelli et al.,1970; Brodtkorb and Klemm, 1980) the mineral association of La Mejicana is composed of luzonite-stibioluzonite (famatinite), enargite-stibioenargite, pyrite, tetrahedrite-tennantite, chalcopyrite, sphalerite, galena, native gold, native silver, wittichenite-emplectite, ? boulangerite, mineral "X" and secondary covellite. Gangue minerals are quartz, barite and alunite. Malachite, azurite, chalcanthite and goslarite are weathering products of the primary mineralisation.
In this note new microprobe analyses of luzonite-stibioluzonite, enargite-stibioenargite, fahlores, aikinite and colusite are presented. The latter represents the first occurrence of this mineral in Argentina.

Geology

The structure of the Sierra de Famatina is relatively simple. Besides an important Taconic phase, the present structure of uplifted longitudinal ranges and downfaulted intermontane valleys is due to Tertiary (Lower Miocene-Pliocene) movements.
The stratigraphic sequence in this region begins with sediments of the Negro Peinado Formation, deposited during the Cambrian to early Ordovician. They were metamorphosed and deformed during the late Ordovician. The prevailing rocks range from dark green siltstones to gray-black sandstones. In the southern part of the mining district, the Negro Peinado Formation has been intruded by granites and granodiorites, which were correlated by Marcos and Zanettini (1982) with the Nunorco Batholith of late Ordovician to Carboniferous age (Turner,1971). Late Paleozoic continental sediments

(Agua Colorada and Patquia Formations) overlie unconformably the older rocks. Small bodies of porphyritic rocks have intruded the Negro Peinado Formation during the late Tertiary; those are known as the Mogote Formation. The apparent spatial relationship between the mineralisation and the dacitic rocks of the Mogote Formation suggests a genetic link between them (Angelelli, 1983; Marcos and Zanettini, 1982).

Mineralogy

Two specimens from the Upulungos mine were studied by reflected light microscopy, electron microprobe analyses and x-ray methods.
The mineral assemblage consists of predominating enargite and luzonite-stibioluzonite (famatinite) associated with minor amounts of pyrite, different fahlores, colusite, chalcopyrite, galena, sphalerite, aikinite and a phase probably related to Pb-free benjaminite.

The minerals of the luzonite-stibioluzonite and enargite groups have all the typical properties described in detail by previous investigators (Gaines, 1957; Ramdohr, 1969; Brodtkorb and Klemm, 1980). Electron microprobe analyses (Table) show very distinct chemical zonality and tin contents, which have not been recognised so far.

Table. Electron microprobe analyses of various minerals from the Upulungos mine, La Mejicana District, Sierra de Famatina (Argentina).- Cameca Camebax Microprobe, operated at 25 kV and 20 nA. The results were processed by the Cameca PAP program. Synthetic sphalerite (ZnK_α,SK_α), covellite (CuK_α), stibnite (SbL_α) bismuthinite (BiL_α), galena (PbL_α), GaAs (AsK_α), SnS (SnI_α), pyrite (FeK_α), as well as pure metals (Ag,V)(AgL_α, VK_α) were used as standards (x-ray lines in brackets).

	1	2	3	4	5	6	7
Cu	46.5	45.1-49.7	47.9-49.6	39.6-40.7	40.4	43.8	36.2-38.3
Ag				0.9- 1.7	3.0	1.2	1.7- 2.9
Fe		0.1- 0.6	0.3- 0.6	0.6- 0.7	2.1	3.2	0.6- 1.2
Zn			0.1	6.2- 6.7	4.1	2.5	4.6- 6.1
Sb	0.1	3.3-19.7	4.8- 7.0	18.9-19.5	10.8	3.1	15.7-17.3
As	19.2	5.6-15.2	3.6- 7.2	5.8- 7.8	13.2	18.6	4.1- 6.1
Bi					0.1	0.1	6.3- 9.2
Sn		0.1-1.9	5.5- 9.0				
V			2.0- 2.9				
S	33.3	28.9-32.3	27.6-29.6	24.5-24.9	27.1	28.2	23.3-24.0

1: enargite; 2: luzonite-stibioluzonite; 3: colusite; 4-6: tetrahedrite-tennanite; 7: annivite.

Colusite (Figs.1,2) is the interesting discovery of this study. It corresponds to the mineral "X" from the Upulungos and Melliza mines (Brodtkorb and Klemm, 1980). C. in the studied material appears cream to brownish colored in reflected light and has no internal reflections. Reflectances were measured in air using tungsten carbide No 044 (Zeiss) as a standard. Values at the four standard wavelength are (λ,%): 470,26.7; 546,29.2; 589,31.1; 650,31.8. The microhardness (100 g load) is ranging between 330-365 $kp.mm^{-2}$.
Colusite occurs as distinctly zoned irregular veinlets and grains intergrown with or as inclusions in enargite-luzonite type phases, fahlore and pyrite. The variation in chemical composition is obvious (Table) and is the explanation for the slightly differing reflection colors.
On the basis of an average composition (wt.%) of colusite-Cu 49.6, As 7.0, Sb 5.2, Fe 0.3, Sn 5.7, V 2.9, S 29.6- the formula is ($\Sigma M+S=66$): $Cu_{26.4}V_{1.9}(As_{3.3}Sb_{1.32})_{\Sigma 6.17}S_{31.3}$. Several grains gave tungsten contents up to 3 wt.%.

Colusite is a not too widespread phase in mineral deposits but is occasionally associated with enargite-luzonite in hydrothermal Cu-As deposits (Orlandi et al.,1981).

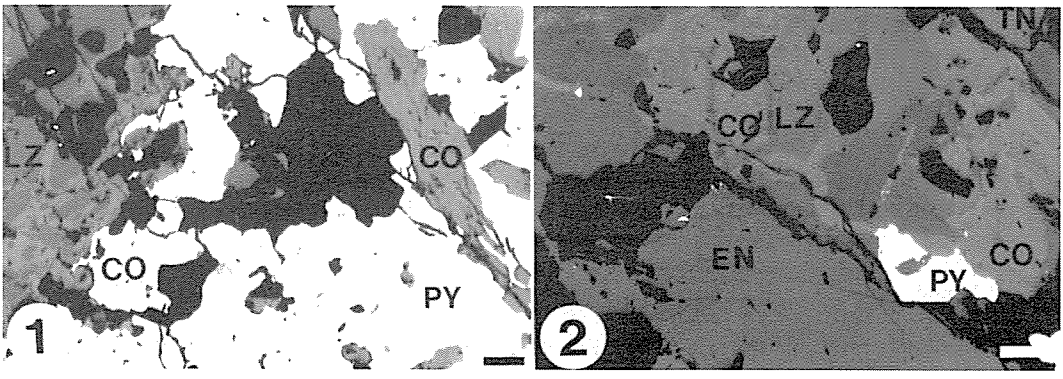

Figs.1+2 Colusite (CO) as inclusions in pyrite (PY) and as irregular network replacing luzonite/stibioluzonite (LZ). The zonal texture is well visible in Fig.2. EN,enargite; TN,tennantite. - Length of bar : 25 µm.

The chemistry of the fahlores is quite variable. Tetrahedrite-tennantite phases with up to 3 wt.% Ag are always intergrown with enargite-luzonite. The high bismuth-containing fahlore (annivite) is associated with aikinite (Cu 11.0, Pb 35.6, Bi 36.9, S 16.9 wt.%) and a Ag-Bi compound related to Pb-free benjaminite.-

Acknowledgement. WHP is most thankful to Dr.A.C.Roberts (Ottawa; Geolog. Survey of Canada) for confirmation of the colusite by x-ray work.

References

Angelelli,V.,Fernàndez Lima,J.C.,Herrera,A.& Aristarain,L. 1970. Descripción del Mapa Metalogenético de la República Argentina.Dir.Nac.Geol.Min.,Anales XV

Angelelli,V.,1983. Yacimientos metaliferos de la República Argentina. Com.Inv. Cient.Prov.Buenos Aires

Brodtkorb,M.K.de & Klemm,D.D.,1980. Estudio mineralogico de enargitas y luzonitas de la Sierra de Famatina, Provincia de la Rioja, y la supresion del termino famatinita. Asoc.Geol.Argentina,Revista,XXXV(3):348-354

Marcos,O. & Zanettini,J.C.1982. Geologia y exploración del proyecto Nevados de Famatina. Serv.Geol.Nac.Buenos Aires, unpublished report

Mendez,V.1981. Exploración geológica del Nevado de Famatina. Acad.Nac.de Cs.Fis. y Naturales,Anales 33:151-169

Orlandi,P.,Merlino,St.,Duchi,G. & Vezzalini,G.1981. Colusite: A new occurrence and crystal chemistry. Canad.Min.19 : 423-427

Ramdohr,P.1969. The ore minerals and their intergrowths. Pergamon Press.

Turner,J.C.M.,1971. Descripción geológica de la Hoja 15 d,Famatina, Prov.de la Rioja. Dir.Nac.Geol.Min., Boletin 126

Current Research in Geology Applied to Ore Deposits.Fenoll Hach-Alí, Torres-Ruiz & Gervilla(eds)(1993).ISBN 84-338-1772-8

THE GEOCHEMICAL PROSPECTION OF Cu AND Co MINERALIZATION IN THE KASTAMONU REGION (NORTHERN ANATOLIA)

Bürküt, Y.; Suner, F. & Kirikoğlu, S.
ITÜ Mining Faculty, Dept. of Geology, Ore Deposits-Geochemistry Section, 80670 Maslak Istanbul, Turkey

ABSTRACT : In this study, the Kastamonu Region was prospected. For this aim, the samples of stream sediments and rocks were collected and analyzed using different methods. It was concluded that the fractures and faults were the most favorable places for the deposition of the ore. The determined main ore was Cu in the area with the minor amount of Co and Au. The estimated reserve was about 1 million metric ton of Cu with the maximum grade of 1.5 % Cu. The main ore mineral was Chalcopyrite in which the determined maximum Au and Co contents were 1.5 and 2000 ppm.

The studied area is located on the Northern part of the Anatolian Peninsula, in the province of Kastamonu. This area is also part of the metalogenetic Pontid area. İn this study, it was prospected an area of about 600 km^2 appoximately.

As a part of Black Sea oceanic crust, the region was consisted of ophiolitic formations, named as the Çangal Metaophiolitic Massive. As the result of the field observations and investigations, the geology of studied and surrounding areas was determined as it was explained below. The bottom levels have been characterized by ultramafic and peridotitic rocks most of which were serpantinized. The gabroic, diabasic and doleritic rocks which generally cut the former formations were observed on the top of ultrabasics. On the upper levels of these formations, it was found spilitic pillow lawas and tuffs together with other volcanic products.

It was determined that some parts of this ophiolitic series were highly affected by dynamic-methamorphic processes because of which a metaophiolitic series were formed. The metagabbro, metaspilitic rocks and serpartin were also the observed rocks in the region. The upper levels of these rocks were consisted mainly of shales and phyllites the mineralogical composition of which were determined as the paragenesis of chlorite + sericite + quartz. All these rocks mentioned above were cut by the Çangal Granitoid that has caused the contact metamormism in the studied area. This complex was overlain discordantly by Alpidic sedimentary sequences which were mainly consisted of agglomera, sandstone and limestone.

The studied area, which exhibits typical subduction zone properties, has been affected largely by tectonic procedures. A lot of deep faults were observed in the area, which have generally cut the all rocks mentioned above. The main fault in the prospected area is the Northern Anatolian Fault and related to that other big and small antitetic - syntetic faults were formed. The ore formation were observed in these faults and also fractures which were very common in the region, as a result of deposition of ore minerals which were transported into these tectonic environments by means of hydrothermal solutions. These ore-bearing solutions were originated from the Çangal Granitoid which was the productive pluton in this region.

In the prospected area, among the other mentioned rocks, the doleritic and diabasic rocks were the most suitable rocks as the results of the field observations and microscopic studies for these kinds of ore depositions. Eventhough the other basic and ultrabasic rocks observed in the area were subjected to alteration procedures and also to the same tectonic movements, the highest metalic concentrations were measured on the samples of the doleritic and diabasic rocks.

Our studies have revealed that the dominant ore formation in the region was the copper mineralization. The measured grade of copper were changed from 250 ppm to

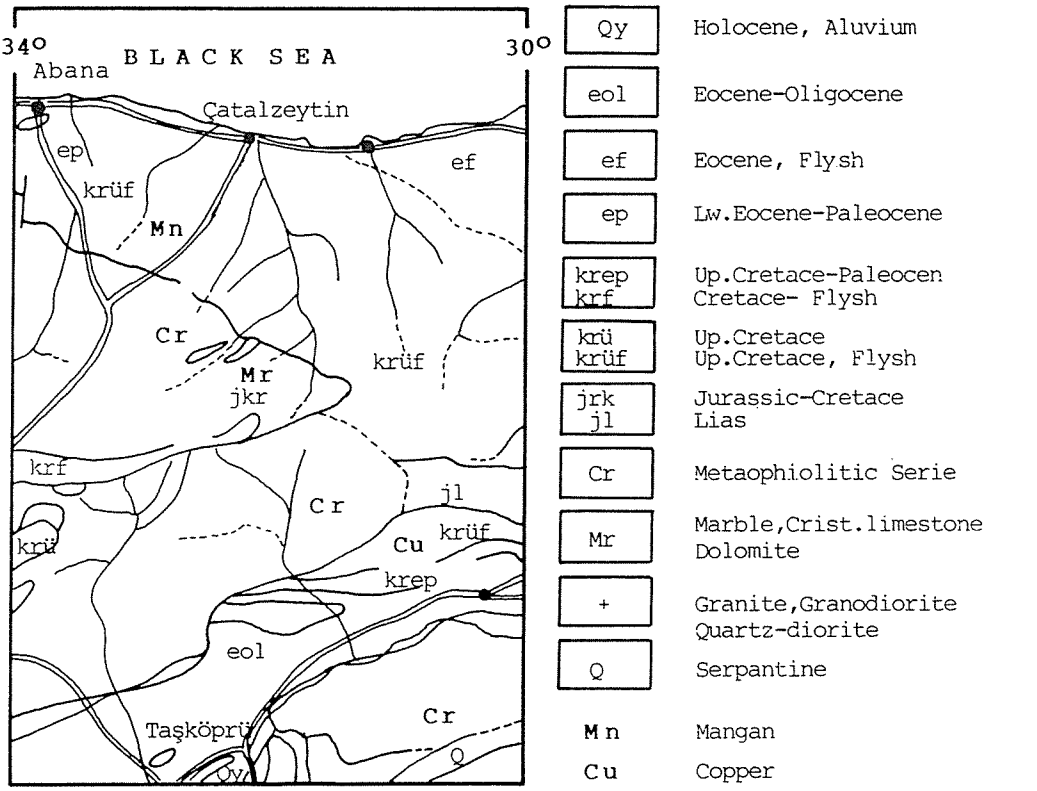

Figure 1. The geological map of the studied and surrounding areas.The scale is 1/25000.

1.5 % and,in this study, it was evaluated merely the samples that have carried more than 0.5 %. The reserve estimations and the geochemical maps were calculated and prepared by taking into account this limitation. Ore mineral paragenesis was determined as pyrite + chalcopyrite. In addition to the copper concentration, in these minerals, especially in chalcopyrites, cobalt and gold presences were investigated in significant levels. As a result of the chemical analyses, the determined cobalt level was between 0.1 and 0.2 %, and gold level was between 0.0 and 1.5 ppm. In the view the mineralogy, cobalt was observed in the form of Co-Pendlandite ; gold in the elementary form.

In the region, as it was pointed out before, fractures and faults were the ore deposition places where hydrothermal solutions were circulated which were the reason not only ore-transportation-crystallization proces but also alterations of rocks. These alterations around deposits exhibit various properties and a series of alterated rocks.These alterations are also very important in covering a much greater area than the deposits itself and reveal generally the presence of a deposit before mineralization has been ascertained.In the prospected area this kind of alteration has included chloritization, epidotization and serpantinization were observed. Especially, chloritization was determined within the dyke system where diabas and dolerites were very common. These rocks and alterations, particularly,chloritization, could serve as a guide for mineralization in the form of pyrite and chalcopyrite in the region.

The topography of this mineralized area was hard and also covered mostly by forests. On the other hand, the tectonism was very effective and caused many cracks, fractures and faults. In such a hardly conditioned area, in order to work effectively and to prospect in detail, it was planned to collect the samples from a very large area, not only from the rocks but also from the rivers which were common in the region. For this aim the samples of the rocks and stream sediments were analyzed using different chemical methods. The major and minor elements contents were determined using Atomic Absorption, Flame Photometry, Spectrophotometry and also gravimetrical methods. The Atomic Absorption was the most used method in determining the levels of Cu, Pb, Zn, Au, Co and other elements. The results of the analyses were evaluated statistically and the target localities were chosen. After this step was proceded, the detailed explorations were applied and the sampling were repeated in hopeful places. The analyses of all samples were performed using the methods mentioned earlier. By taking into account the all results, the geological and isoproperty maps, such as isograde map of Cu, of Zn, isolithology map, were prepared in scale of 1/1000. As a result of the evaluations the data, the lowest level of ore, in productions, were chosen as 0.5 % Cu.

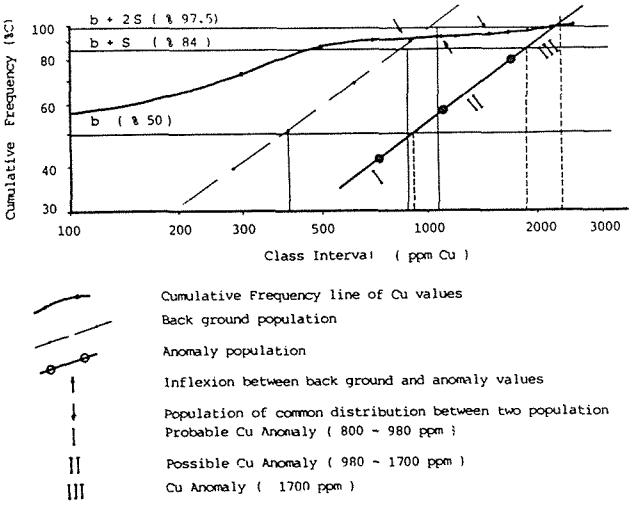

Figure 2. The determination of geochemical parameters in the studied area.

After the anomalous areas were found out as the results of mineralogical, petrographical and geochemical studies ; it was planned to control the determinations and the hopuful localities. Furhtermore, it was tried to find the exact depth of the ore. For this aim, the P.S. geophysical method were applied to the region where the geochemical studies have revealed the anomalies. The data of the geophysical workings were evaluated also statistically and the results were correlated with those of the geochemical studies. The P.S. method has supported the results of the geochemically determined anomalous localities. The geophysical and geochemical maps have definitely indicated the same point as a location of ore deposition. The estimated ore depth was 150 m. below the surface. As the conclusion of the studies, it was observed that the places where the oxidation processes has been worked and produced the minerals such as malachite, azurite and brochantite, were also very important in indicating to ore depositions. The oxidation processes have been largely developped and many secondary minerals were formed.

The reserve estimation calculations have been also evaluated. For this aim , all chemical analyses and maps prepared before were studied geostatistically. The isograde maps and geologic cross sections were evaluated together . As a result of these detailed geostatistical methods, the reserve of copper were estimated, approximately, one million metric ton of 0.5 - 1.5 % Cu. On the other hand, the results of the geochemical and microscopic workings were revealed that a very wide area of poorly mineralized were yielded in the surrounding part of the investigated region.

Evaluating the geological and geophysical data, it was also studied on a drilling programme with the aim the determination of the border of the deposit. According to the data it was proposed a series of drill the depht of which must be between 100 m. and 300 m. by taking into account of the topographic conditions.

Finally, the interpretation and evaluation of all data, it was assumed that there was many deposits carrying similar properties in the same geologic formations in the E - W , the direction of the Northern Anatolian Fault.

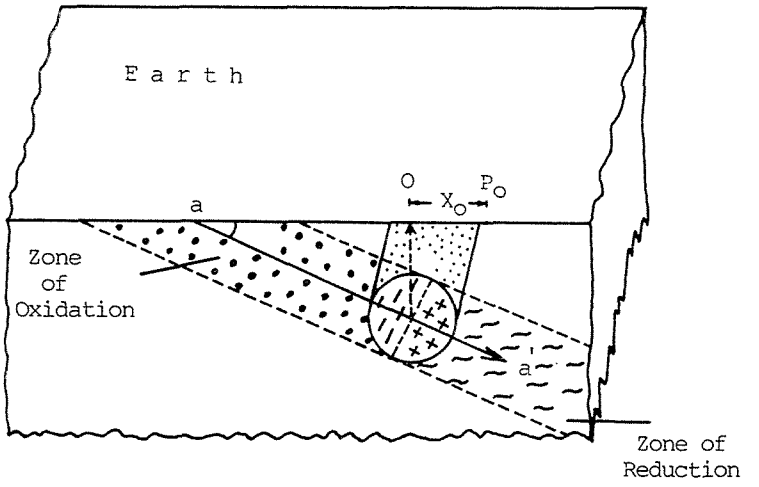

Figure 3. The estimated model of the ore formation.

References

Bürküt, Y. 1992. The Kastamonu Cu,Zn,Co Prospections, The DPT Project,İstanbul

Kuzvart, M. & Böhmer, M. Prospecting and Exploration of Mineral Deposits, Elsevier, Amsterdam.

Kovenko, V. 1989. Küre Madenleri Jeolojisi ve çalışmaları hakkında,MTA Rapor No 860, Ankara.

Köksoy,M. & Turan,Y. 1973. Kastamonu Küre sahasının genel Jeoşimik Etüdü. MTA Rapor No.1400, Ankara.

Current Research in Geology Applied to Ore Deposits.Fenoll Hach-Alí, Torres-Ruiz & Gervilla(eds)(1993).ISBN 84-338-1772-8

THE COLL DE PAL KARSTIC BARITE DEPOSITS (EASTERN PYRENEES, SPAIN): FLUID CHEMISTRY AND STABLE ISOTOPES

Cardellach, E. (1); Canals, A. (2) & Ayora, C. (3)
(1) Dept. de Geología. Universitat Autònoma de Barcelona, 08193 Bellaterra, Spain
(2) Dept. de Cristal.lografía, Mineralogía i Dipòsit Minerals. Universitat de Barcelona, Barcelona, Spain
(3) Inst. de Geología Jaume Almera, CSIC, Barcelona, Spain

ABSTRACT: The karstic barite deposits of the Coll de Pal area developed in cavities of dolomitized limestones of Devonian age. Paragenesis is constituted by saddle dolomite, pyrite, chalcopyrite, calcite, quartz and barite. The saddle dolomite and sulfides are related by a sulfate reduction process that took place between 125 and 150°C. Barite precipitation is explained by a mixing between sulfate-rich solutions of probable marine origin and hot, $CaCl_2$-rich brines of evolved meteoric or connate origin.

INTRODUCTION

The infilling of karstic structures by mineralization occurred in Cambrian and Devonian carbonates from the Eastern Pyrenees. This type of mineralization is characterized by the presence of barite and minor amounts of Fe and Cu sulfides associated with a widespread phase of dolomitization. One of the best examples, due to its accessibility and good outcrop, is the Coll de Pal deposit. It was mined for barite until the 80's. This deposit is similar to the low-temperature Ba-F-base metal vein mineralizations enclosed within the Paleozoic basement of the Catalonian Coastal Ranges (NE Spain) with an age ranging from late Triassic to Jurassic, that have been described by Canals and Cardellach (1993).

The purpose of this work is to constrain the age, chemistry, and origin of the mineralizing fluids that formed the karst-filling deposits, using stable isotope and fluid inclusion data. In so doing, a genetic model extensible to similar deposits of the Eastern Pyrenees is developed and a comparison with the vein-type deposits of the Catalonian Coastal Ranges is established.

GEOLOGY AND MINERALOGY

The studied area is located in the Tossa d'Alp massif, Eastern Pyrenees, about 150 km to the NW of Barcelona. The Tossa d'Alp massif is made up of materials of upper Paleozoic to Cenozoic age. The upper Paleozoic is represented by the Devonian (limestones) and Carboniferous (detrital materials of Culm facies, schists and conglomerates) unconformably covered by volcanics (rhyolites and ignimbrites) of Stephanian to Permian age (Domingo et al., 1988). The Mesozoic sediments unconformably overlie the peneplane formed by the Hercynian basement and are represented by the lower Triassic and the Cretaceous. The Triassic section is represented by red-bed facies: conglomerates,

sandstones and shales (Buntsandstein facies) and the Cretaceous (deposited discordantly on the Triassic) by limestones. The Cenozoic is constituted by red sandstones and shales. The area has been affected by the Hercynian and Alpine orogenies, which have given rise to a complex succession of thrusts and faults.

The Coll de Pal deposits are situated within dolomitized limestones of upper Devonian age. They consist of several dolomitized cavities of karstic morphology. Previous to mineralization the cavities were partially filled with banded speleothems of dolomite and by large crystals of calcite. No clear relationship between these two fillings has been found. Pervasive dolomite replacement of the regional limestone developed around fractures and karstic cavities. The mineralizing stage consists of a first generation of dolomite (nonplanar dolomite of Sibley and Gregg, 1987) followed by the precipitation of a millimetric to centimetric-size band of saddle dolomite and sulfides (chalcopyrite and pyrite). A later generation of quartz and calcite preceeds the precipitation of white barite, the most abundant mineral, which is present as large radial crystals. A last generation of late calcite can also be recognized.

FLUID INCLUSION DATA

Fluid inclusion studies were made on quartz and saddle dolomite. The size of the fluid inclusions in dolomite (<5μ) only allowed to obtain homogenization temperatures (Th). Primary fluid inclusions in quartz and dolomite are composed of two phases, liquid and vapor, at room temperature. Th for inclusions in saddle dolomite are around 125°C (n=11). Th in quartz inclusions are aroud 150°C (n=27). Ice melting temperature is around -16.2°C, pointing to a salinity of 20 wt% eq. NaCl. Eutectic temperatures are as low as -57°C indicating the existence of a polysaline brine. SEM-EDS analyses on frozen fluid inclusions show that the fluid is composed of NaCl and CaCl2, with minor amounts of KCl. No SO_4, Fe or Mg have been detected (<0.5%). Many inclusions show trapped crystals of platy morphology, with Si, Al and K in their chemical composition (SEM-EDS analyses) which have been interpreted as muscovite. These $CaCl_2$-rich brines are like those found in the Ba-F vein type deposits in the Catalonian Coastal Ranges, or in the Variscan domain of Western Europe and Northern Africa.

ISOTOPE DATA

24 carbonates (12 calcites and 12 dolomites) have been analyzed for their stable isotopic composition (Fig 1). Dolomite around the cavities has a $\delta^{13}C$=+1‰ (PDB) and $\delta^{18}O$=23.2‰ (SMOW); these values are heavier than the regional Devonian limestone: values for $\delta^{13}C$=+0.5‰ and $\delta^{18}O$=21.8‰ suggest that the first dolomitization phase was due to ^{18}O-rich solutions, probably representing evaporated seawater. Nonplanar and saddle dolomite show similar isotopic signatures: from +1 to -2‰ in $\delta^{13}C$ and from 22 to 23‰ in $\delta^{18}O$. As the dolomitization took place at

125°C, the $\delta^{18}O$ of water in equilibrium with the dolomite had a value of about +4.7‰ (fractionation equation of Land, 1983). Hydrothermal calcite shows almost constant $\delta^{13}C$~0‰ but variable $\delta^{18}O$ (20 to 18‰) which is compatible with a precipitation from a fluid of constant composition and at an increasing temperature from 125 to 150°C. $\delta^{18}O$ of quartz is around 21‰; at 150°C $\delta^{18}O$ of water in equilibrium with the quartz is 4.9‰.

$\delta^{34}S$ of chalcopyrites ranges from -1‰ (mean of 2 values) to +10.5 (CDT) (mean of 2 values). $\delta^{34}S$ of barite is 15.3‰ (mean of 10 analyses).

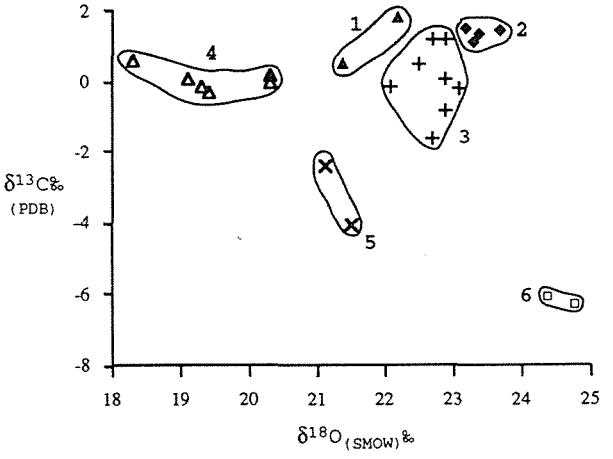

Fig. 1.- *Carbon and oxygen isotopic composition of carbonates. Devonian limestones (1);regional dolomites (2);saddle dolomite (3); hydrothermal calcite (4); calcite speleothems(5); late calcite (6).*

DISCUSSION AND CONCLUSIONS

The fluid inclusion and isotope data allow us to determine the composition of the hydrothermal solution(s) from which the mineralization at Coll de Pal formed. The age of formation of the karst system is not known. The first dolomitization phase developed around the karstic cavities and along joints and fractures and was probably due to the interaction with evaporated ^{18}O-rich marine waters. Banded dolomitic sedimentation (speleothems) formed at the bottom of some cavities during this process. A rise in the temperature, probably due to an influx of hot waters into the system, induced the recrystallization of the former dolomite to nonplanar dolomite and the precipitation of the saddle dolomite. This process took place around 125°C, resulting in the cavities being surrounded by a cm-thick dark brown dolomite followed by the saddle dolomite. An apparently simultaneous process was the precipitation of minor amounts of pyrite and chalcopyrite. The relationship between saddle dolomite and sulfide precipitation can be linked through a reaction as:

$$2Ca^{2+}+2SO_4+Mg^{2+}+2CH_4 \leftrightarrow CaMg(CO_3)_2+Ca^{2+}+2H_2O+2H_2S$$

which involves the reduction of sulfate by organic matter, represented

here by methane. This reaction produces H_2S which can combine with metals (Fe, Cu...) to give the sulfides. The small amount of saddle dolomite and sulfides indicates that reduction of sulfate was not a quantitatively important process. This is supported by the lack of carbonate dissolution accompanying the sulfide precipitation. The coexistence of quartz with calcite and the presence of muscovite in quartz fluid inclusions constraining the pH from 5.5 to 6.5 at 150°C supports the idea of minor pH changes due to sulfide precipitation. Sulfate reduction took place between the T recorded by the saddle dolomite (125°C) and the quartz (150°C). The coexisting light and heavy $\delta^{34}S$ values of chalcopyrite could be indicative of reduction of sulfate molecules in locally closed systems. The reduction of sulfate did not affect the overall $\delta^{34}S$ of the dissolved sulfate as the sulfur isotopic composition of barite is constant in all the samples.

The model assumes that the karst system was saturated with SO_4-rich water. The most probable candidate for this type of solution is seawater. In fact, the $\delta^{34}S$ of barite is similar to the isotopic sulfate values recorded in Triassic evaporites in NE Spain by Utrilla (1992). The inflow of a hot, Ba-bearing brine could have caused the precipitation.

The oxygen isotopic composition of water in equilibrium with saddle dolomite and quartz is around 4.5‰. This light value seems to indicate a non magmatic origin for the hot fluids. The chemical composition of these fluids (polysaline $CaCl_2$-rich brines with minor amounts of KCl) and saturated with muscovite together with its oxygen isotopic composition point to an evolved meteoric water or connate water that interacted with basement. The genetic model is similar to that proposed for the Ba-sulfide bearing veins in the Catalonian Coastal Ranges.

REFERENCES

Canals, A. & Cardellach, E. 1993.Strontium and sulphur isotope geochemistry of low-temperature Barite-Fluorite veins of the Catalonian Coastal Ranges (NE Spain): a fluid mixing model and age constraints. Chem. Geol. 104:269-280

Domingo, F., Muñoz, J.A., Santanach, P. 1988. Estructures d'encavalcament en els materials del sòcol hercinià del Massís de la Tossa d'Alp (Pirineu Oriental). Acta. Geol. Hisp. 23-2:141-153.

Land, L.S. 1983. The application of stable isotopes to studies of the origin of dolomite and to problems of diagenesis of clastic sediments. Soc. Econ. Paleontologists and Mineralogists Short Course Note Series No 10. 4.1-4.22.

Sibley, D.F. & Gregg, J.M. 1987. Classification of dolomite rock textures. Jour. Sed. Petrology. 57:967-975

Utrilla, R., Pierre, C., Ortí, F. & Pueyo, J.J. 1992. Oxygen and sulphur isotope compositions as indicators of the origin of Mesozoic and Cenozoic evaporites from Spain. Chem. Geol. (Isot. Geosci. Sect.). 102:229-244.

Current Research in Geology Applied to Ore Deposits. Fenoll Hach-Alí, Torres-Ruiz & Gervilla (eds) (1993). ISBN 84-338-1772-8

A MIXED CRUSTAL SOURCE MODEL FOR THE IGLESIENTE Pb-Zn ORE DEPOSITS (S.W. SARDINIA): LEAD ISOTOPE EVIDENCE

Caron, C.(1); Lancelot, J.R.(1) & Orgeval, J.J.(2)
(1) URA 1371, Université Montpellier II, France
(2) Dept. Explo. BRGM, Orléans, France

ABSTRACT Lead isotope evidence shows that the major stratabound Pb-Zn ore deposits in the Lower Cambrian carbonates of SW Sardinia (Iglesiente) were derived from mixed crustal sources, clearly identified as the continental basements of SW Sardinia and the Eastern Pyrenees. A comparison between the lead isotope compositions of the Iglesiente Pb-Zn sulfides and those of representative country rocks supports the long-held assumption of a Mississippi-Valley type origin for these deposits, but involving a major remobilization of pre-existing Cambrian ores during the Early Ordovician "Sardic tectonic phase".

Most Cambrian-hosted Pb-Zn orebodies in the Iglesiente area are considered to be stratabound deposits formed according to a Mississippi Valley type model, through Cambrian sedimentary-diagenetic processes (Boni and Koeppel 1985). Some Pb-Zn orebodies, previously ascribed to supergene processes in relation to Ordovician and Permo-Triassic erosion surfaces, are now shown to result from late- to post-Hercynian hydrothermal activity (Boni et al 1992). Furthermore, in the vicinity of late-Hercynian intrusions, lead isotope data on galenas (Boni and Koeppel 1985, Ludwig et al 1989) have revealed local remobilization of pre-existing Pb-Zn ores with mixing of Lower Paleozoic and Carboniferous leads. Lead of the Cambrian stratabound deposits was believed to derive from a single homogeneous source, in agreement with the observed homogeneity of lead isotope compositions. The anomalous $^{207}Pb/^{204}Pb$ ratios and old model ages of the Sardinian Pb-Zn ores suggested a crustal, but U-depleted Precambrian source (Boni and Koeppel 1985). These particularities were also explained by a two-stage Pb-evolution model involving a single-age igneous source of maximum Cambrian age, virtually absent in SW Sardinia, but considered to be similar, even if slightly older, to known occurrences of Cambrian orthogneisses and "porphyroids" in the French Massif Central (Ludwig et al 1989). The assumption of a MVT origin for the Iglesiente Pb-Zn deposits tended nevertheless to be unsatisfactory, since inconsistent with the observed narrow range of lead isotope compositions and with the poor radiogenic values which characterize the oldest Cambrian-stratabound deposits from SW Sardinia.

In order to provide new isotopic constraints on the genesis of these deposits and since all the lead isotope studies carriêd out up today only took into account the analysis of galenas, even though sphalerite is generally by far the most abundant ore mineral, systematic lead isotope analyses were performed on

a variety of sulfides (sphalerite, pyrite, galena) selected from the main mining districts of the Iglesiente province. Further, so as to determine the origin(s) of the lead, representative country rocks were also analyzed for lead isotopes. At first sight, a minimum Cambrian age can be inferred for these deposits since, plotted on a Pb isotope diagram, as many as 50 data points define a tight domain close to the 600 Ma secondary isochron of the Stacey-Kramers model. Systematic analyses of the sulfides however show a peculiar, almost vertical trend, leading to high $^{207}Pb/^{204}Pb$ ratios, especially for the sulfides of the stratigraphically higher deposits located within the Ceroide limestones ; the scatter in $^{207}Pb/^{204}Pb$ ratios is particularly well recorded in the successive generations of sulfides (Fig 1). Moreover, for each mine, and even for each given sample in a studied mine, significant heterogeneities are seen between the Cambrian host rocks and the associated sphalerites and galenas. Most of the analyzed galenas from Ceroide limestone-hosted deposits are significantly ^{207}Pb-enriched with respect to the other associated sulfides and preferentially belong to the latest stages of ore deposition. Variations in the $^{207}Pb/^{204}Pb$ ratios are systematically and distinctly higher than those in the $^{206}Pb/^{204}Pb$ ratios. Such trends cannot be accounted for by a simple radioactive decay model following possible lead remobilization, since the time interval necessary to produce the $^{207}Pb/^{204}Pb$ variations is about 10 times greater than that required for the $^{206}Pb/^{204}Pb$ variations. Consequently, the most appropriate mechanism to explain such small-scale but noticeable inhomogeneities would be the contribution of extraneous lead in the immediate vicinity of the orebodies. The observed trends suggest the existence of an heterogeneous crustal source for the metals and, more precisely, the involvement of a significantly older (probably late Precambrian) crustal component responsible for the observed elevated $^{207}Pb/^{204}Pb$ ratios in the higher ore deposits. At least two crustal sources, with distinct μ values, may be regarded as lead sources for Pb-Zn Iglesiente ores (Fig 2). One source, with a μ value of 9.95 can be clearly identified as the Iglesiente continental basement, according to three sets of data : K-feldspars from the Nebida sandstones (Early Cambrian detrital sequence), sulfides from the stratigraphically lower deposits (Laminated Dolomite member) and K-feldspars from several Iglesiente Variscan granites. The second source, characterized by a higher μ value of about 10.10 could account, through mixing, for the significant ^{207}Pb enrichment displayed by sulfides from the stratigraphically higher deposits (Ceroide limestones). A comparison between lead isotope compositions in granitic K-feldspars from SW

Sardinia and the Eastern Pyrenees (Michard-Vitrac et al 1981) indicates that this second source could correspond to the pre-Variscan basement of the Eastern Pyrenees. This analogy between the Eastern Pyrenees and the Iglesiente both areas seems quite reasonable since formed part of a single crustal segment in pre-Oligocene times. Finally, Cambrian limestones, sampled in subsurface conditions and far from any mineralized zone, exhibit an interesting lead isotopic composition. This composition, corrected for in situ U decay, suggests that an isotopic heterogeneity exists between the Cambrian host rocks and the associated sulfides and that remobilization of the sulfides occurred at least 60 Ma after the sediment deposition, i.e circa 480 Ma, in Early Ordovician times, assuming an age of 540 Ma for the sediment deposition. Thus the observed heterogeneities between various sulfides and related host rocks in a given mine could result from the remobilization of lead and its reconcentration with the addition of a more radiogenic component.

In conclusion, these latest lead isotope analyses suggest that the Pb-Zn ore deposits of the Iglesiente area may not be early diagenetic deposits of Cambrian age, emplaced through purely sedimentary processes, but Mississippi-Valley-type deposits related to a regional hydrothermal system in Early Ordovician times (Sardic phase) and characterized, unlike North American MVT deposits, by a relatively short time interval between sediment deposition and Pb-Zn ore formation. This peculiarity results in an apparent homogeneous pattern for the lead isotope compositions, in contrast with the widely ranging radiogenic character of North American MVT leads, owing to the long interval (at least 140 to 180 Ma) between sediment deposition and lead remobilization. The Early Ordovician event, evoked for the emplacement of infra-economic mineralization at the mid-Ordovician unconformity (Boni et al 1991) in Iglesiente-Sulcis, would not have been restricted to this specific stratigraphic stage but would have operated on a large scale in the overall Lower Cambrian sequence. Although a minor tectonic event, poorly documented and diversely interpreted owing to the superimposition of Hercynian structures, the Sardic phase may have played a significant metallogenic role. This episode may have induced the circulation of hydrothermal fluids likely to reconcentrate pre-existing Cambrian ores, in an extensional tectonic setting characterized by the break-up of the Cambrian carbonate platform into northerly-trending horsts and grabens (Laurent and Arthaud 1993). The analyses have also been used to propose a mixed crustal source model for the Pb-Zn Iglesiente ores, involving the

Sardinian continental basement and an old crustal component recognized as the pre-Variscan basement of the Eastern Pyrenees.

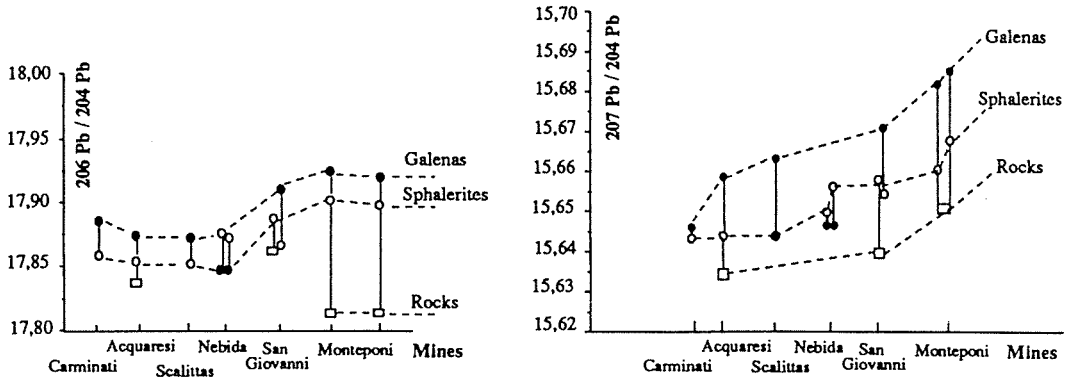

Figure 1 - Variations of 206Pb/204Pb and 207Pb/204Pb ratios between host-rocks, sphalerites and galenas in each studied mine

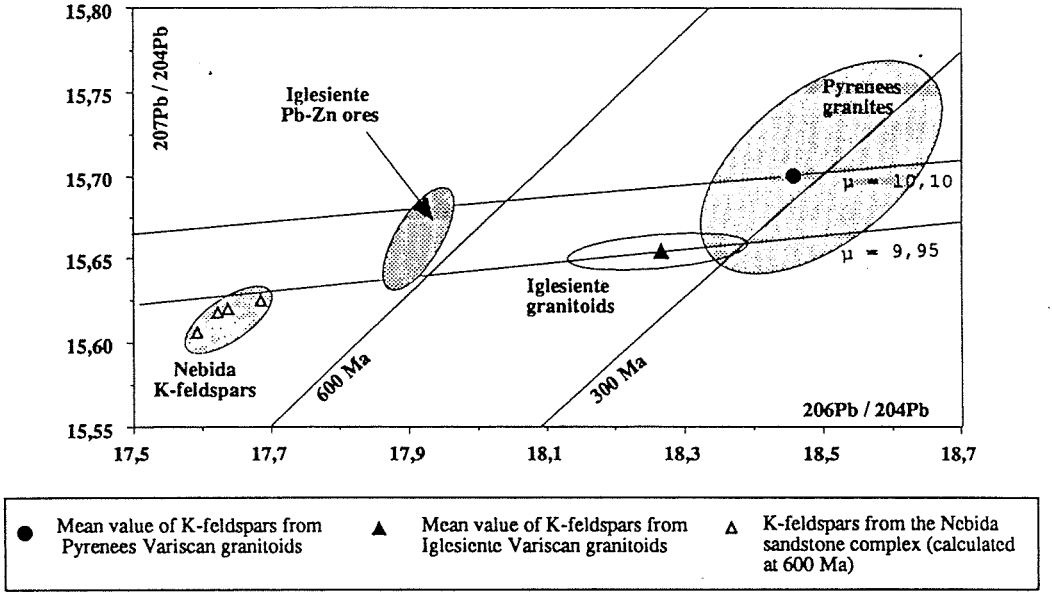

Figure 2 - Lead isotope plot for Iglesiente and Eastern Pyrenees formations

Boni, M.& Koeppel, V. 1985. Ore-lead isotope pattern from the Iglesiente-Sulcis Area (SW Sardinia) and the problem of remobilization of metals. Mineral.Deposita. 20 : 185-193

Boni, M. & al. 1991. Stratabound ores at the mid-Ordovician unconformity in SW Sardinia, EUG VI, Strasbourg, Abstract, 410.

Boni, M.& al. 1992 . Late to Post-Hercynian Hydrothermal Activity and Mineralization in Southwest Sardinia (Italy). Econ.Geol.87 : 2113-2137

Laurent, Ph. & Arthaud, F. 1993. "Sardic orogeny" : a distensive event during Ordovician. EUG VII, Strasbourg, Abstract, 207

Ludwig, K.R.& al. 1989. Isotopic constraints on the genesis of base-metal ores in southern and central Sardinia. Eur.J.Mineral. 1 : 657-666

Michard Vitrac, A. & al. 1981. Lead isotopic composition of Hercynian granitic K-feldspars constrains continental genesis. Nature. 291 : 460-464

Current Research in Geology Applied to Ore Deposits.Fenoll Hach-Alí, Torres-Ruiz & Gervilla(eds)(1993).ISBN 84-338-1772-8

THE TELLURIDES OF THE ROMANIAN NEOGENE ORE DEPOSITS

Cioflica, G.; Jude, R.; Lupulescu, M.; Simon, Gr. & Damian, Gh.
Dept. of Mineralogy, University of Bucharest, Bucharest, Romania

The mineralogical investigation of the tellurides of ore deposits related to Neogene volcanic and subvolcanic structures in Romania pointed out as follow: new compositional data about altaite, coloradoite, hessite, krennerite, sylvanite, nagyagite; an unnamed $SbTe_2$ has been identifyed as well as two nagyagite phases which are different in Te, Sb and Au, Ag contents.

The Tertiary subduction in the Carpathian regions gave rise to various volcanic and subvolcanic structures,especially andesites.These structures constitute the Volcanic Zone of the East Carpathian and the Volcanic Zone of the Metaliferi Mts. and contain hydrothermal ore deposits of Au-Ag,Au-Ag-Te ,Cu, base-metal type with subordinate amounts of Hg, solfatarian S and hydrometasomatic Fe ores. The mineralisations constitute veins, breccia pipes, stockworks, impregnation and metasomatic irregular bodies in carbonatic rocks. Among these, the porphyry-copper mineralisations (Cu-Mo or Cu-Au) are known only in the Volcanic Zone of the Metaliferi Mts.(fig.1); here they are centred on subvolcanic bodies of andesitic - microdioritic composition. In the upper part of these structures, Au-Ag or Pb-Zn vein systems are usually found. Occurences of tellurides, are known especially at Sacarimb, Stanija, Baia de Aries, Caraci, Barza, Bucium, Fata Baii, Magura-Hondol and Techerau in the Volcanic Zone of the Metaliferi Mts.(Helke,1933; Giusca,1935,1937; Ghitulescu and Socolescu,1941); other occurences have been identifyed at Baita in Gutai Mts. (Butucescu et.al.,1963) and at Cobasel and Izvorul Rosu in Rodna Mts.,in the Northern part of the Volcanic Zone of the Carpathians (Constantiniuc et al. 1988; Jude et al.,1991).

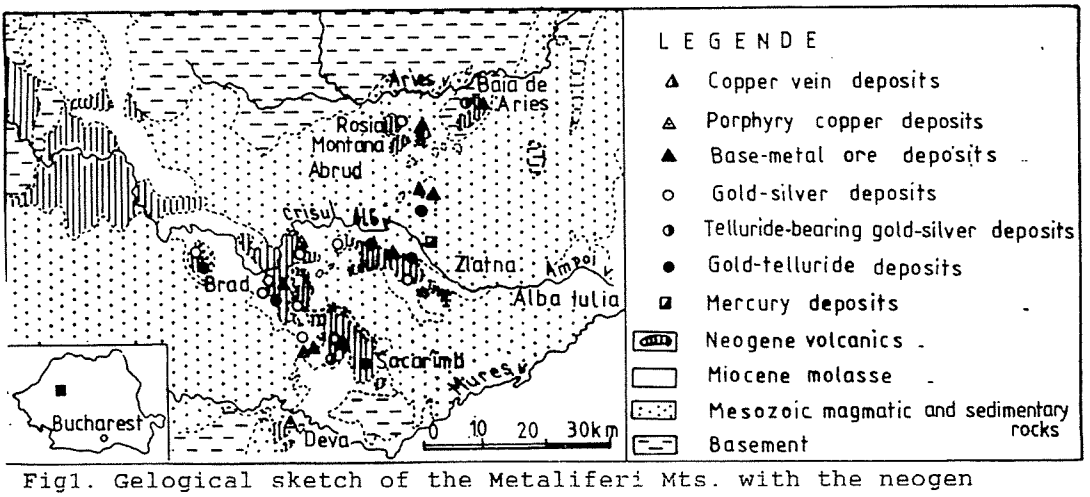

Fig1. Gelogical sketch of the Metaliferi Mts. with the neogen volcanics and related ore deposits.

At Sacarimb, a classic gold - telluride ore deposit, mineralisations occur as veins located in a volcanic structure built up of quartz-andesites of Sarmatian age. About 230 veins, very rich in mineral species, have been known. More than 100 minerals have been identifyed here, the more important being the tellurides. Until now 14 tellurides have been found here: tellurium, tellurite, frohbergite, muthmanite, calaverite, krennerite, altaite, nagyagite, sylvanite, petzite, hessite, coloradoite, stuetzite and tellurantimony. The tellurides have a random distribution in the four vein groups: Magdalena vein group which contains especially nagyagite and altaite with common sulphides; Longin and Antelongin vein group consisted of krennerite, sylvanite and gold together with common sulphides; Nepomuc vein group for which petzite and hessite are characteristic; Erzbau vein group includes especially common sulphides and minor amounts of nagyagite.

At Stanija occur the telluride-bearing gold veins located in a volcanic structure built up of andesites of Sarmatian age in the Ungurelu Hill or in Cretaceus sedimentary formation in the Fericelii Hill. The vein complex in Fericelii Hill is related to an andesitic subvolcanic body seated at depth. Among the tellurides identifyed here we may note: sylvanite, calaverite, hessite, petzite, altaite, tetradymite, stuetzite, coloradoite and tellurium; an unnamed $SbTe_2$ must be added.

At Baia de Aries, the telluride mineralisations as veins are well differentiated in space, together with Au-Ag and Pb-Zn veins, breccia pipes and metasomatic irregular bodies being related to volcanic and subvolcanic andesitic structures of Sarmatian age. Here are mentioned: altaite, nagyagite, sylvanite and hessite.The tellurides veins cross the Au-Ag veins, proving their subsequent emplacement.

At Caraci, in a volcanic structure built up of andesite of Sarmatian age, there are Au-Ag veins in which the tellurides such as: nagyagite, sylvanite and hessite, are locally developed.

At Fata Baii some tellurides, such as: tellurium, tellurite and nagyagite, have been mentioned and at Bradisor mine, in Barza volcanic structures, there are gold veins with local concentrations of telluride minerals (altaite, sylvanite, petzite and tellurium).

In Arama copper vein from Bucium, and less at Botes, a telluride sequence has been identifyed (altaite, sylvanite, petzite and hessite) in the same occurence with native gold and various copper sulphides and sulphosalts. At Magura-Hondol tellurides (calaverite, sylvanite, petzite, altaite and tellurantimony) have been described only recently (Simon & Ioan,1993 unpubl.data) and occur as veinlets into a gold and base-metal ore deposit. At Techerau only native tellurium has been mentioned till now.

At Baita, in Gutai Mts, have been mentioned veinlets with tellurides (hessite, petzite, sylvanite and altaite) in the same occurence with native gold and common sulphides. Also, at Cobasel and Izvoru Rosu in Rodna Mts has been described a sequence of tellurides (altaite, sylvanite, nagyagite and hessite) associated with native gold and common sulphides in breccia pipes and veins; here the mineralisations are related to lati-andesites.

Mineralogical features. The reflectance (R%) and chemical composition data for altaite, coloradoite, hessite, krennerite, sylvanite and nagyagite, to which an unnamed $SbTe_2$ is added, are listed in Table 1 and 2.

Table 1. Reflectance data for some tellurides from Romania.

Nr.	Mineral	R	Wavelenght 486	552	589	656	Location
1.	Altaite	R	69.7	66.5	64.5	61.0	Sacarimb
2.	Altaite	R	69.7	68.5	66.0	62.5	Stanija
3.	Coloradoite	R	37.0	36.0	39.1	37.5	Sacarimb
4.	Coloradoite	R	36.5	37.0	38.5	36.0	Stanija
5.	Hessite	R1	40.0	40.0	41.5	42.5	Sacarimb
		R2	37.2	37.5	37.0	37.0	
6.	Hessite	R1	40.2	41.0	43.0	45.0	Stanija
		R2	38.0	37.8	38.5	38.7	
7.	Krennerite	R1	62.0	63.0	63.3	64.0	Sacarimb
		R2	53.5	50.8	56.5	57.5	
8.	Sylvanite	R1	59.2	61.0	61.9	64.0	Sacarimb
		R2	50.6	51.6	52.1	54.5	
9.	Sylvanite	R1	57.0	58.2	58.5	60.5	Stanija
		R2	45.5	46.0	46.8	49.0	
10.	Sylvanite	R1	57.5	58.5	58.0	59.8	Baia de
		R2	42.0	44.0	45.0	46.0	Aries
11.	Petzite	R	41.5	38.0	38.0	39.5	Sacarimb
12.	Petzite	R	40.8	39.0	39.0	39.0	Stanija
13.	Nagyagite I	R1	42.5	40.2	39.8	37.8	Sacarimb
		R2	42.0	38.9	38.4	37.0	
14.	Unamed $SbTe_2$	R1	66.1	66.5	67.5	67.0	Scanija
		R2	61.3	61.5	62.5	62.0	

Note. Nr.4 Coloradoite : Data - Popescu & Constantinescu (1992)

Table 2. Compositional data for some tellurides from Romania. (wt%)

	Mineral	Pb	Hg	Au	Ag	Sb	Fe	Cu	Bi	Ni	Mo	Te	S	Total
1.	Altaite	61.54		0.16	0.17	0.27	0.04	0.04				37.08	0.04	99.35
2.	Altaite	95.30										40.20		99.50
3.	Coloradoite		56.50		0.20						2.76	40.50		100.0
4.	Hessite	0.12		0.11	63.23	0.14	0.02					37.77		100.4
5.	Hessite				65.43							34.57		100.0
6.	Krennerite			34.75	5.47						0.17	60.00		100.4
7.	Sylvanite			25.21	12.64	0.30		0.02	0.12	0.02		61.64	0.05	100.0
8.	Sylvanite			22.87	11.69						0.10	62.83		97.5
9.	Sylvanite			25.30	14.30						0.13	62.70		102.4
10.	Petzite			22.25	39.30							38.45		100.0
11.	Nagyagite I	57.74		5.66	0.28	7.97				0.03		17.31	12.08	101.0
12.	NagyagiteII	57.22		3.62	0.03	9.87				0.01		18.22	12.85	101.8
13.	Unamed $SbTe_2$					34.03						67.97		102.0

Location : 1,3,4,6,7,11,12 Sacarimb; 2,5,8,10,13 Stanija; 9 Baia de Aries

Calculated chemical formula: 1. $Pb_{1.02}Te$; 2. $Pb_{0.91}Te$; 3. $Hg_{0.98}Mo_{0.09}Ag_{0.007}Te$; 4. $Ag_{1.98}Te$; 5. $Ag_{2.24}Te$; 6. $Au_{0.75}Ag_{0.25}Te_2$; 7. $Au_{0.97}Ag_{1.06}Te_4$; 8. $Au_{0.92}Ag_{0.88}Te_4$; 9. $Au_{1.05}Ag_{1.08}Te_4$; 10. $Ag_{2.41}Au_{0.74}Te_2$; 11. $Au_{0.714}Ag_{0.063}Pb_7Sb_{1.638}Te_{3.402}S_{9.464}$; 12. $Au_{0.462}Ag_{0.007}Pb_7Sb_{2.058}Te_{3.626}S_{10.15}$; 13. $SbTe_{1.88}$

These data are similar with those from mineralogical literature; only for nagyagite some contrasting data have been found. In polished sections examinated by us, constantly two nagyagite phases have been identifyed which are different in optical and chemical features. These are: Nagyagite I - is earlier, and it has a very clear plate habit, a greyish white colour with a slightly creamy tint.It's anisotropy is weak in brownish to bluish colours and the chemical analysis constantly show higher values of Au and Ag and lower values of Te and Sb when compared with nagyagite II ; Nagyagite II - occurs usually as rims which substitute the earlier nagyagite I. It has a greyish white colour with a slightly greenish tint, the polishing hardness is lower than nagyagite I. The anisotropy is distinct and it's chemical analysis constantly exhibits higher values of Te and Sb and lower values of Au and Ag when compared with nagyagite I. The identification and characteristics of these phases, confirm partly the Giusca's (1937) observations involving the unhomogenity of nagyagite.

Conclusions: The following conclusions might be pointed out: the telluride minerals occur as gold-telluride ore deposits (i.g.Sacarimb) or as telluride-bearing gold-silver and less base-metal ore deposits; new compositional data about altaite, coloradoite, hessite, krennerite, sylvanite and nagyagite are here presented in agreement with those from mineralogical literature; also an unnamed $SbTe_2$ has been described; two nagyagite phase different in optical and compositional characteristics have been identifyed.

References:

Butucescu,N., Bonea,N., Bodnarencu,A., Stoicescu,Gh., Stoicescu,E. 1963. Mineralizatia cu telururi auro-argentifere din zacamintul Baita - Nistru (Baia Mare). Rev.Min.,14, 5.

Cioflica,G., Damian,Gh., Jude,R., Lupulescu,M. 1992.A new telluride mineral from Stanija area, Met_aliferi Mts. Rom.J.Mineralogy, 75, p.65-68.

Ghitulescu,T.P. & Socolescu,M. 1941. Etude geologique et miniere des Monts Metalliferes. An.Inst.Geol. al Romaniei, XXI,p.181-284.

Giusca,D. 1935. Note preliminaire sur la genese du gisement aurifer de Sacarimb. Bul.Lab.de Mineralogie, Universsite de Bucharest

Giusca,D. 1936. Le chimisme de la nagyagite. Bul. Soc. Rom.Geol.,v. III,p 118-284.

Helke,A. 1933. Beitrage zur Kenntnis der Golderzgange am Ungarberge und am Fericel (Stanija) in Siebenburgischen Erzgebirge Romanien. Min.Petr.Mitt. 44, p.265-324.

Jude,R., Jude,Lidia , Popescu,Rodica , Lupulescu,M. 1990. The Cobasel andesitic stock (Rodna Mts.) - petrological and metallogenetical features. Anal.Universitatii Bucuresti 39,p.3-12

Popescu,Gh. & Constantinescu,E. 1992. First occurence of the coloradoite in Romania. Rev.Roum.Geologie, t.36,p.33-34.

Popescu,Gh. & Simon,Gr. 1992. New tellurides from Sacarimb (Nagyag) Metaliferi Mts. Rom.J.Mineralogy,75 ,Supplem.1.

Ramdohr,P. & Udubasa,Gh. 1973. Frohbergit - Vorkommen in den Golderzlagerstadten von Sacarimb und Fata Baii (Rumanien).Mineral Deposita (Berl.) 8, p.179-182.

Current Research in Geology Applied to Ore Deposits.Fenoll Hach-Alí, Torres-Ruiz & Gervilla(eds)(1993).ISBN 84-338-1772-8

PLIOCENE TO QUATERNARY VOLCANIC-RELATED (HOT-SPRING) EPITHERMAL Mn-(Co)-Fe DEPOSITS: THE CALATRAVA VOLCANIC FIELD (SPAIN)

Crespo Zamorano, A. (1); Lunar, R. (2); Oyarzun, R. (2) & Doblas, M. (3)

(1) Empresa Nacional ADARO, Ciudad Real, Spain

(2) Dept. Cristalografía y Mineralogía. Facultad de Geología. Universidad Complutense, Avda Complutense s/n, 28040 Madrid, Spain

(3) Museo Nacional de Ciencias Naturales, CSIC, Madrid, Spain

ABSTRACT: The Calatrava Volcanic Field (CVF) hosts a series of Mn-(Co)-Fe deposits displaying different morphologies: spring aprons, veins (proximal facies), disseminations, wad and pisolitic beds (distal facies). The deposits formed in relation to epithermal hydrothermal systems driven by the Pliocene volcanic activity. In terms of the high-Co values and Mn-oxide mineralogy (todorokite, lithiophorite, birnessite, cryptomelane) the deposits can be regarded as 'rare' as none of these features is common in environments such as the one of the CVF.

GEOLOGY

The Calatrava Volcanic Field (CVF) (Fig. 1) developed within an area characterized by an Hercynian basement (quartzites, limestones, slates; Ordovician-Silurian) covered by upper Miocene to Quaternary fluvial and lacustrine sediments. The sediments were deposited within fault bounded basins that formed as the result of extensional tectonics (López Ruíz et al., 1993). Alkaline volcanism began in late Miocene time (8.7-6.4 Ma) with the extrusion of leucitites. Most of the volcanic activity concentrated in Pliocene-Quaternary time (4.7-1.6 Ma) with emissions of olivine leucitites, olivine nephelinites, and alkali olivine basalts. Volcanism and sedimentary processes developed contemporaneously within the extensional basins (López Ruíz et al., 1993).

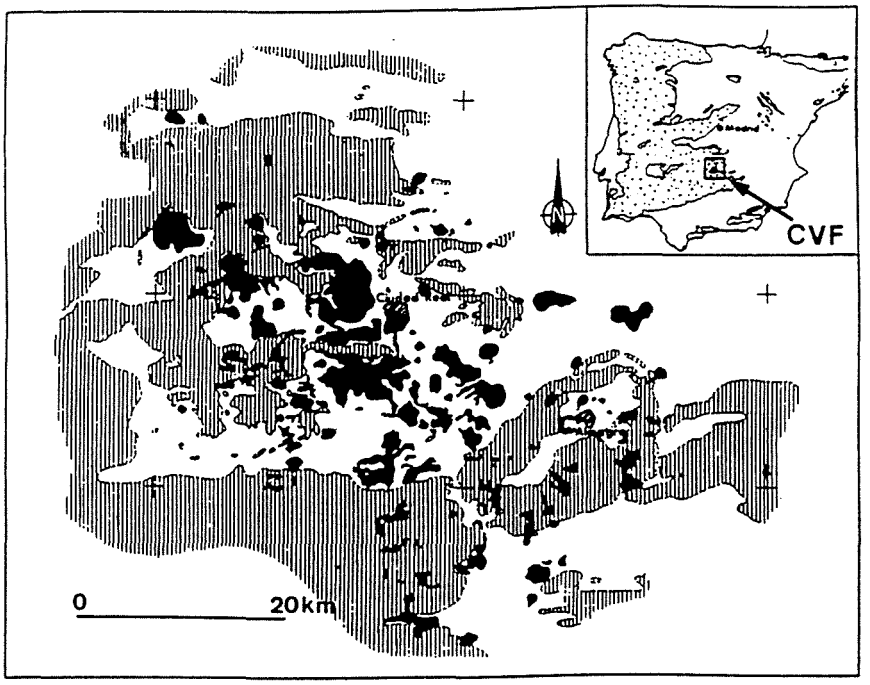

Fig. 1. Location map (see inlet) and local geology of the CVF. The NW volcanic trend is depicted by the areas shown in black (alkaline volcanics). After Crespo Zamorano (1992). Vertical lines: Hercynian basement

Pyroclasts and lavas were ejected from more than 240 emission centers within a subcircular-shaped area where a dominant NW-SE volcanic trend can be recognized (López Ruíz et al., 1993). As shown by mining/exploration works in the CVF, volcanism was clearly related to extensional faults, which also acted as preferred conduits for the migration of hydrothermal fluids leading to the formation of Mn-(Co) and Fe deposits (Crespo Zamorano, 1992; López Ruíz et al., 1993). Geothermal activity is still active within the area as shown by the existence of the so-called "hervideros" (boiling spots).

THE Mn-(Co)-Fe MINERALIZATION

The CVF Mn-(Co)-Fe deposits were discontinuously mined from 1880 to 1963. A renewed economic interest in the area came in the last years as a result of the findings of high Co-(Ni) values (up to 2.08 % Co) in the Mn oxides.

The mineralized bodies display a series of different morphologies that can be grouped into five types: disseminations, wad beds, pisolitic beds, crusts and veins. Gradual transitions have been found between some them. The morphological differences have no chemical expression in terms of Mn, Fe, Co or Ni.

Ore mineralogy was studied by optical microscopy, XRD, infrared spectroscopy, and EMP. The following Mn and Fe oxides were identified: cryptomelane, todorokite, birnessite, lithiophorite, goethite, and hematite. The Mn oxides are cobalt-rich with values of up to 2.08 % Co (range: 0.02-2.08 %).

a) Proximal Facies

Proximal facies (crusts) developed in close proximity to fault-controlled hydrothermal vents (the so-called "hervideros") that formed along the margins of the different basins (Fig. 2). The higher levels are of Quaternary age and Fe-rich. The Mn-(Co)-Fe spring aprons laterally overlap volcaniclastic and sedimentary facies and display average thicknesses of 0.7 m extending for no more than a hundred of meters. Average grades (62 crusts) give the following values: 7.50 % Mn, 10.95 % Fe, 0.15 % Co, and 0.02 % Ni. The evolution of of the hydrothermal systems led to early Mn-(Co) oxide mineralization that was followed in time by deposition of Fe oxides.

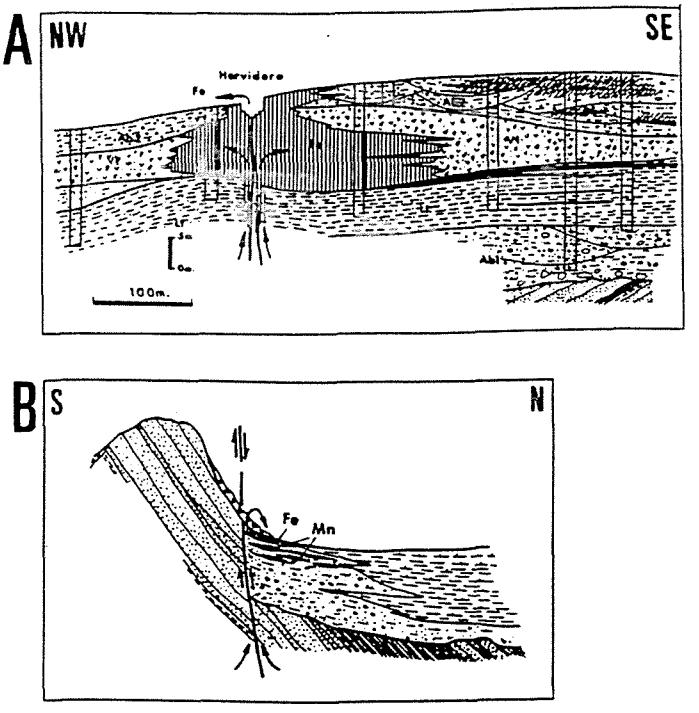

Fig. 2. A) the so-called "hervideros", vertical lines: Fe, black: Mn. B) a fault controlled spring apron.

b) Distal Facies

These are typical stratabound deposits of clear sedimentary affinities. Grades are generally low (average: 3.4 % Mn). Three sub-types of distal facies are recognized: disseminations, wad beds and pisolitic beds.

The disseminations are the most common morphology and can be regarded as stratabound deposits. Mn deposition occurred as a combination of detrital, chemical and biochemical processes. The Mn source were the hydrothermal vents, from where solutions were expelled flowing down the slopes or directly spilled onto the sediments and later deposited as sedimentary facies.

The wad beds constitute around 16 % of the distal facies. The beds are formed by an earthy variety of wad, and typically display lensoid morphologies. The mineralized bodies can extend for several hundred of meters, with an average thickness of 0.7 m. Average grades indicate values 5.85 % Mn, 4.96 % Fe, 0.13 % Co, and 0.01 % Ni.

The pisolitic beds are not abundant, constituting less than 4 % of the distal facies. The beds are formed by pisolitic Mn oxides within a clay/sandy matrix. Average thickness of these bodies is 0.96 m, and grades are 3.21 % Mn, 8.47 % Fe, 0.07 % Co, and 0.02 % Ni.

SOME CONSIDERATIONS REGARDING THE GENESIS OF THE CVF Mn-(Co)-Fe DEPOSITS

A volcanogenic origin for the CVF Mn-(Co)-Fe deposits seems clear: 1) The deposits formed in close proximity to the volcanic facies, 2) volcanism, Mn-(Co)-Fe mineralization, and sedimentation developed within a generalized extensional episode, and 3) at a global scale the whole CVF seems to have formed within a 'failed rift' tectonic scenario.

Up to here the CVF Mn-(Co)-Fe deposits seem rather 'normal' i.e. a clear link to volcanism and extensional conditions has been established. However, the high contents in cobalt (up to 2.08 % Co) make the CVF Mn-(Co)-Fe deposits rather 'unique'. The only examples of high-Co Mn-oxides are those of the present-day manganiferous nodules formed in seamounts and active ridges (1.15 % Co and 0.40 % Co respectively; Glasby, 1977). Furthermore, only hydrogenous ferromanganese deposits are clearly Co-rich (as compared to the submarine hydrothermal deposits).

This is in open contradiction with the geological framework of the CVF Mn-(Co)-Fe deposits as they formed within shallow continental, volcanic, lacustrine-fluvial basins.

Perhaps the answer must not be searched in the geologic-tectonic framework but in the mineralogy of the CVF Mn-(Co)-Fe deposits. Of the four Mn-oxides found in the CVF, two have tunnel structure (todorokite and cryptomelane) and two have a layered structure (lithiophorite and birnessite). The tunnel structure todorokites can admit Co^{2+} in the M2-type octahedral sites (Roy, 1992). On the other hand, layered structures (e.g. lithiophorite) can adsorb and display high contents of Co (e.g. 2.8 % CoO in lithiophorite; Roy, 1981).

Since the alkaline volcanics of the CVF are neither enriched nor depleted in cobalt, the problem should not be addressed in terms of the source but on the 'ability' of some minerals to scavenge cobalt from solutions. Both the tunnel and layered structure minerals (todorokite-cryptomelane, lithiophorite-birnessite respectively) have this potential ability to scavenge cobalt. In fact, EMP analyses performed on cryptomelane and lithiophorite samples from the CVF give values of up to 1.14 % Co and 8.11 % Co respectively.

This is what could be termed the 'mineralogical approach' to the problem. However, even if this approach apparently explains the Co-rich Mn-oxide facies, a major problem still remain to be solved. None of these minerals can be regarded as 'common' within environments such as the one of the CVF (hot-springs). In fact, only birnessite and cryptomelane have been observed in such environments (Nicholson, 1992). Nevertheless, Nicholson (1992) only give them the status of 'known' (by contrast to the 'common' status of other minerals). The CVF Mn-oxides are 'common' in environments such as weathering deposits in arid climates (birnessite, cryptomelane), soil profiles including swamp and bog deposits (birnessite, lithiophorite), weathering of mineralized sequences (cryptomelane) or seawater nodules (todorokite) (Nicholson, 1992).

Since the CVF Mn-(Co)-Fe deposits have clear-cut indicators of a hot-spring source, their origin is rare and therefore quite 'unique' in terms of the high-Co values and Mn-oxide mineralogy. Until a plausible explanation for the presence of these oxides can be given, the following ideas on the CVF Mn-(Co)-Fe deposits metallogenesis can be advanced:

1) The deposits formed within a volcanisedimentary environment during Pliocene-Quaternary time, within lacustrine-fluvial extensional basins.
2) Transport mechanism for the metals were epithermal hydrothermal solutions of

high-fO_2 that precipitated their metal load as manganiferous sinters (proximal facies, spring aprons).
3) Part of the manganese (and cobalt) migrated towards the inner parts of the basins forming stratabound deposits (distal facies).

REFERENCES

Crespo Zamorano, A. 1992. Geología, mineralogía y génesis de los yacimientos de manganeso cobaltíferos del Campo de Calatrava (Ciudad Real). PhD. thesis, Universidad Complutense, Madrid, 389 pp.

Glasby, G.P. 1977. Marine Manganese Deposits. Elsevier, Amsterdam, 523 pp.

López Ruíz, J., Cebriá, J.M., Doblas, M., Oyarzun, R., Hoyos, M. & Martín, C. 1993. The Late Cenozoic alkaline volcanism of the Central Iberian Peninsula (Calatrava Volcanic Province, Spain): intraplate volcanism related to extensional tectonics. J. Geol. Soc., in press.

Nicholson, K. 1992. Contrasting mineralogical-geochemical signatures of manganese oxides: guides to metallogenesis. Econ. Geol. 87: 1253-1264.

Roy, S. 1981. Manganese Deposits. Academic Press, London, 458 pp.

Roy, S. 1992. Environments and processes of manganese deposition. Econ. Geol. 87: 1218-1236.

Current Research in Geology Applied to Ore Deposits.Fenoll Hach-Alí, Torres-Ruiz & Gervilla(eds)(1993).ISBN 84-338-1772-8

GEOCHEMICAL CONSTRAINTS OF FORMATION OF Au-BEARING AND BARREN SKARNS ALONG THE NORTHERN CONTACT OF THE MALADETA BATHOLITH (CENTRAL PYRENEES, SPAIN)

Delgado, J. (1); Soler, A. (1); Arcos, D. (1) & Ayora, C. (2)
(1) Dept. Cristal.lografia, Mineralogía i Depòsit Minerals. Universitat de Barcelona, Barcelona, Spain
(2) Inst. de Geología Jaume Almera, CSIC, Barcelona, Spain

Abstract: Three skarns from a small area in the northern contact of the Maladeta batolith (Central Pyrenees, Spain) have been studied in order to determine the physic-chemical parameters of formation and to point out the differences existing between one Au-bearing and two barren skarns. The three skarns show very similar evolution paths for fO_2, between the NNO and the QFM buffers, and fS_2, ranging between 10^{-8} to 10^{-10} bar. Neither fluid salinities nor pH differences account for the distinct mineralogy observed. Physic-chemical characters, although necessary for a complete understanding of the geochemical systems, do not explain the observed differences among the deposits studied. Therefore, the mineralogical variations observed could be the result of the interaction by distinct fluid sources and may be proved with the aid of accurate stable and/or radiogenic isotope studies.

Introduction: Field surveys along the north contact of the Maladeta batholith have revealed the existence of more than thirty W-bearing skarns and at least one As-Au-bearing hedenbergite skarn with sizes ranging from meters to tens of meters. Among them, three well exposed and mineralogically distinct skarns have been selected in order to constrain and compare their physic-chemical conditions of formation: an As-Au bearing, sulfide-rich and boron-silicate absent skarn (Sarraera) and two barren, sulfide-poor and boron-silicate mineralized skarns (Arties and Escunyau). All three are supposed to be coeval and they are located in a restricted mapping area of less than 2 km length along the northern contact of the pluton.

The observed differences may be explained by two hypotheses: 1) variation in the physic-chemical parameters of the mineralization and 2) fluid differences related to their source, composition and relative amount of fluid circulating through the skarns.

Geological setting: The Maladeta batholith is a late Hercynian igneous complex (277±7 ma, Rb-Sr isochron, $\lambda=1.44\times10^{-11}$ $year^{-1}$; Michard-Vitrac et al., 1980) mainly composed of granodioritic rocks and subordinate gabronorites and two-mica granites situated in the central segment of the Pyrenean Axial Zone (Aran and Benasque Valleys, Spain). This complex intruded Paleozoic rocks ranging from Cambro-Ordovician to Carboniferous age although most of the rocks outcropping along north and south flanks are Devonian limestones and marls. A thermal contact aureole of more than 300 m width overprinted the effects of the low grade regional metamorphism of this area (Greenschist facies). Tectonics of the area are related with the complex history common to the whole Pyrenees: an Hercynian polyphase folding and E-W thrusting events (both pre-intrusive) and Alpine age E-W thrusting that gave rise to the physiographically distinctive Pyrenean Range. Magma emplacement studies have been undertaken by Delgado et al. (1993) who estimated 2.5±0.5 kbar and 625±25 °C as maximum P-T conditions for rocks within the innermost zone of the contact aureole, according to several independent exchange geothermometers and the univariant assemblage hercynite+corundum+sillimanite+almandine.

Skarn description: The studied skarns belong to the W-bearing calcic-reduced hedenbergitic skarns of Einaudi et al. (1981) that are widespread throughout the Pyrenees. Tungsten mineralization is

irregular in the studied skarns and, in general, contents are low. Mineralization may be divided into two major stages for all the skarns, the first stage being characterized by the development of a thick monomineralic hedenbergitic zone (up to 45 m), sometimes overprinting a previous metasomatic column of wollastonite, vesuvianite, diopside and a grossularitic garnet of less than 10-15 cm. This first stage is roughly the same for the three studied skarns. The second stage accounts for much of the differences observed in the skarns. In the Au-mineralized skarn of Sarraera, the 2nd stage is characterized by the development of a complex retrograde assemblage made up of ferroactinolite, ilvaite, quartz, calcite, stilpnomelane, chlorite, magnetite, scheelite and sulfides (arsenopyrite, pyrrhotite, chalcopyrite, pyrite, bismuthinite and joseite) as major components together with other metals (löllingite, gold, bismuth). From the sequence point of view, ilvaite is previous to ferroactinolite, stilpnomelane and chlorite. Calcite and quartz are distributed throughout the second stage. Metals start with löllingite and end with an arsenopyrite-pyrite assemblage. The second stage in the skarn of Escunyau is characterized by the development of minute amounts of ilvaite plus magnetite retrograding the pyroxenes and a zone of grossularitic garnet followed by an assemblage of epidote, quartz, calcite, axinite, actinolite, stilpnomelane and chlorite. Sulfide mineralization is very poor and is restricted to small masses of pyrite crossed by late pyrrhotite, magnetite and small crystals of sulfo-arsenides of Co and/or Ni. Arties skarn is rather simple compared with the other two. Second stage begins with the filling of geodic cavities and veins by idiomorphic crystals of quartz, axinite, epidote and calcite (±stilpnomelane), followed by a ferroactinolite, stilpnomelane, calcite and sulfides assemblage along joints that crosscut hedenbergite crystals. Ilvaite and magnetite are also present in small amounts. Sulfides are basically pyrrhotite with small quantities of chalcopyrite and arsenopyrite.

Physic-chemical characterization: Accurate mineralogical and phase equilibria studies have been carried out to see what are the differences, if any, between each mineralization. These studies include temperature, fO_2, fS_2 fluid composition determinations. Ilvaite, ferroactinolite and other mineral phases belonging to the Ca-Fe-Si-H-O system stability fields have been constrained in order to achieve a better understanding of the natural systems.

***Oxygen fugacity*:** The oxidation state of the metasomatic fluid is reflected in the skarns' mineral paragenesis. A tight control of fO_2 has been established for the skarn of Sarraera. Hedenbergite and andradite limit the initial fO_2 below the QFM oxygen buffer or between QFM and NNO during 1st stage mineralization. The ilvaite stability field and the sequence of the retrograde reactions suggest

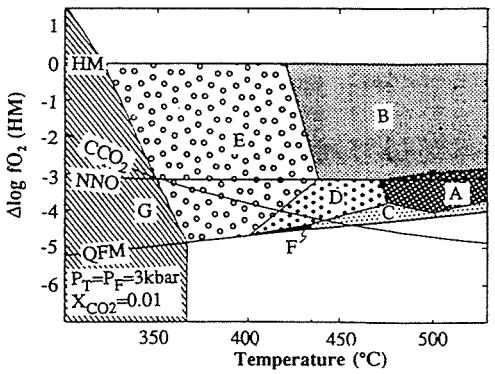

Fig. 1: *T-fO_2 diagram (referred to HM buffer). A) Hedenbergite+andradite+magnetite; B) Andradite+magnetite; C) Hedenbergite+ magnetite; D) Ilvaite+quartz+calcite; E) Magnetite+quartz+calcite; F) Ferroactinolite+ magnetite; G) Siderite.*

that fO_2 evolution in this skarn followed a constant redox path, between NNO and QFM for a temperature interval from 625 °C to 300 °C. Small graphite plates associated with the latest sulfides may indicate a small rise in fO_2 (over NNO) or a decrease in fluid X_{CO2}. No additional controls are

supplied by the mineralogy of Arties and Escunyau skarns although a similar path may be inferred from their semblance (Fig. 1).

Sulfur fugacity: The existence of two generations of arsenopyrite in the Sarraera skarn as well as the composition and mineral association for them both impose important constraints on the fS_2 of the system. The first arsenopyrite generation consists of As-rich crystals (35-36 at.% As) with common inclusions of löllingite, pyrrhotite and native bismuth. The second generation (31-32 at.% As) is associated with pyrite, native bismuth and bismutinite and it has been studied in detail by Delgado and Soler (1992). Arsenopyrite composition agrees with the expected paragenetic pyrrhotite composition (Delgado et al., 1993) and ilvaite in equilibrium with pyrrhotite and magnetite. The evolution of the Sarraera mineralization shows constant fS_2 values of about 10^{-8} to 10^{-9} bar between 500 and 300 °C (Fig. 2). fS_2 in the Arties skarn is determined by the presence of a unique generation of arsenopyrite (33.5-34.5 at.% As), and the composition of pyrrhotite and the ilvaite+magnetite+pyrrhotite stability field overlapping an area around 10^{-9} bar. The Escunyau skarn shows a noticeable decrease in fS_2 due to the drop from pyrite field to that of pyrrhotite. If we trust the pyrrhotite composition and the ilvaite+magnetite+pyrrhotite stability field, fS_2 is slightly lower than the two preceding cases (10^{-10} bar), although this value could be much higher at the beginning of the sulfidation stage (2nd stage).

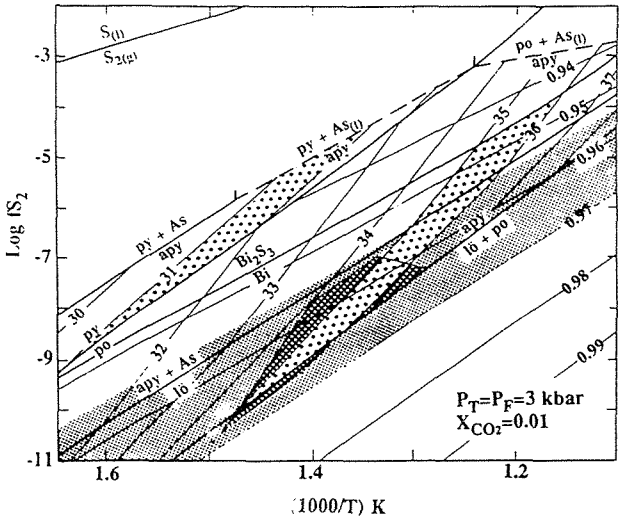

Fig. 2: *T-fS_2 diagram for the Sarraera skarn. Black dotted areas are the compositional range of the arsenopyrites analyzed. Shadowed area is the compositional range of pyrrhotites from this skarn. Both areas superpose on the ilvaite+pyrrhotite+magnetite stability field (dark area). Numbers 0.94 to 0.99 are N_{FeS} in pyrrhotite. Numbers 30 to 37 are atomic As % in arsenopyrite.*

Temperature: The starting temperature for all three skarns is not clearly established. It seems reasonable to believe that the maximum temperature has to be equal or close to that observed in the innermost zone of the contact thermal aureole. The beginning of the 2nd stage retrogradation may be associated with the growing of ilvaite which is more or less abundant in all the skarns. The maximum thermal stability of this mineral at P_F=3 kbar is 525 °C. Ferroactinolite maximum stability is about 475 °C for the same fluid pressure and its destruction at lower temperatures to give a siderite+quartz+calcite assemblage depends strongly on fluid X_{CO2}. Sulfides give some more restriction on temperatures. In the Sarraera skarn, 1st arsenopyrite generation seems to have grown between 400 and 500 °C, whilst 2nd generation is around 275-325 °C. In Arties, arsenopyrite crystallization seems to have ocured at about 450 °C and in Escunyau a temperature slightly over 400 °C may be inferred from pyrrhotite composition and the ilvaite+magnetite+pyrrhotite stability

field. In the last case, pyrite crystals precede pyrrhotite and other sulfides so a temperature in excess of 400 °C may be assumed. Topological stability relations among the different paragenetic minerals depend on fluid composition (f_{H2O}) and, consequently, temperatures may suffer displacements.

Fluid composition: According to Ohmoto and Kerrick (1977), volatile fluid speciation may be estimated if we know fO_2 and fS_2 for a given temperature gap. With the adequate Gibbs free energy data and gas fugacity coefficients it is possible to calculate fluid speciation. For fO_2 between NNO and QFM and fS_2 around 10^{-8}-10^{-9} bar, which are consistent with all three skarns, the most important fluid species is H_2O with CO_2 being the most important carbon-bearing species and H_2S (predominant sulfur species).

An acidic pH is constrained by the presence of muscovite+quartz+K-feldspar as a common assemblage in the three skarns. No accurate numerical value may be given due to the absence of data on a_{K+} in the fluid. However, a similar pH value may be assumed for three mineralizations.

Fluid inclusion studies are seriously hampered by the intense tectonization of the skarns. CO_2 phases have not been observed in any fluid inclusion from any skarn. Fluid appears as an hypersaline brine, NaCl sometimes oversaturated at room temperature. Freezing temperatures and maximum eutectic measurements point to a polysaline system dominated by NaCl-H_2O although the presence of additional components ($CaCl_2$, KCl,..) may not be disregarded. Salinities of primary and pseudosecondary inclusions are around 22-26% in Arties and Escunyau, and 28-34% in Sarraera (all in wt.% eq. NaCl). Secondary inclusions have about 12-14 wt.% eq. NaCl. A pattern of variable homogenization temperatures and constant salinities suggest recrystallization phenomena.

Conclusions: Physic-chemical characterization of three distinct-mineralized skarns suggests that all three deposits formed in a very similar environment (fO_2, fS_2, P_F, temperature interval and salinity). No reason has been found to attribute the mineralogical differences among Sarraera, Arties and Escunyau skarns to changes in these intensive variables. This conclusion rules out the hypothesis of a different physic-chemical environment as being responsible for gold mineralization in the Sarraera skarn and its absence in Arties and Escunyau skarns.

Differences are therefore the result of changes in fluid source, composition (As, Au, B,...) and/or the fluid's availability during skarn formation also related with system permeability. To test this hypothesis further work, mainly stable and/or radiogenic isotope geochemistry, is required.

Acknowledgements: This research has been financed by the CICYT project GEO90-0507.

References

Delgado, J. & Soler, A. 1993. Precisiones sobre el locus del punto isobárico invariante Bi-Bi_2S_3-FeS-FeS_2-S_2 a partir de una paragénesis natural y cálculos termodinámicos. Bol. Soc. Esp. Min. (in press)

Delgado, J., Soler, A. & Arcos, D. 1993. La composición de la pirrotina y su aplicación en la determinación de las condiciones de formación del los skarns de La Maladeta (Pirineo Central, Lleida). Actas XIII Reunión Soc. Esp. Min. (in press)

Delgado, J., Soler, A. & Arcos, D. 1993. Thermobarometric constraints for the emplacement of the Maladeta batholith, Central Pyrenees, Spain. EUG-VII (in press)

Einaudi, M., Meinert, L. & Newberry, R. 1981. Skarn deposits. Econ. Geol. 75th Anniv. p. 317-391

Michard-Vitrac, A., Albarède, F., Dupuis, C. & Taylor Jr., H.P. 1980. The genesis of Variscan (Hercynian) plutonic rocks: Inferences from Sr, Pb and O studies on the Maladeta igneous complex, Central Pyrenees (Spain). Cont. Min. Petrol. 72:57-72

Ohmoto, H. & Kerrick, D.M. 1977. Devolatilization equilibria in graphitic systems. Am. Jour. Sci. 277:1013-1044

Current Research in Geology Applied to Ore Deposits.Fenoll Hach-Alí, Torres-Ruiz & Gervilla(eds)(1993).ISBN 84-338-1772-8

ORGANIC MATTER AND Zn-Pb-(Ba) MINERALIZATION AT THE LES MALINES MINE (GARD, FRANCE): A REASSESSMENT.

Disnar, J.R. (1) & Orgeval, J.J. (2)
(1) URA 724, bât. Géosciences, Université d'Orléans, B.P. 6759, 45067 Orléans Cedex 2, France
(2) BRGM, DMM/DEX/UR, Av. de Concyr, B.P. 6009, 45060 Orléans Cédex 2, France

ABSTRACT: The Triassic marls and the Georgian basement both contain too low amounts of autochtonous organic matter - too low and to highly mature, respectively - to have produced the oil and bitumens frequently found in fissures and voids. The association of the bitumens with barite-rich ores precipitated by hot hydrothermal fluids (i) indicate that they have very lilely been brought in by these solutions and (ii) their alteration as a result of water washing, "chromatographic" segregation and thermal cracking. Increasing amounts of these bitumens, from W to E in the mine, may indicate that they originated from SE basin formations.

INTRODUCTION

Les Malines, the largest french MVT deposit (1Mt Zn+Pb), has been the object of continuous studies for decades (Disnar and Defoix, 1991). However, no detailed investigation of the associated organic materials has been undertaken since the pioneering work of Connan and Orgeval (1977). The present paper reports on new organic geochemical data which benefit from the use of new technologies (Rock-Eval pyrolysis and GC-MS) and also from recent information brought by other approaches (e.g. fluid inclusions studies; Ramboz and Charef, 1988).

SAMPLING AND METHODS

This study delt with 19 samples taken in different mine works and representative of the various types of ores encountered in the Cambrian basement and in the Triassic as well as of the barren host-rocks (see Table).

Organic geochemical investigations included: Leco C, S determination, Rock-Eval pyrolysis, bitumen extraction and fractionation, Gas Chromatography and GC-Mass Spectrometry (GC-MS) of the saturated and aromatic hydrocarbons.

Major and trace elements were determined by ICP-spectrometry and atomic absorption.

RESULTS AND DISCUSSION

Two Triassic marls samples taken from the Ratonneau works revealed TOC values of 0.42 and 0.70 %, respectively. Identical Tmax and OPI values of 430°C and 0.22, respectively, attest their low maturity (onset of the oil-window). Unimodal n-alkane distributions dominated by the n-C17 reveal the exclusively marine origin of the organic matter. The presence: (i) of a complete series of C15+ n-alkanes and (ii) of the isoprenoids pristane and phytane in proportions relative to the n-alkanes that is compatible with the maturity the samples (Pr+ Ph/nC17+nC18 = 0.55 and 0.37),

Mine area	Sample	Zn %	Pb %	Ba %	TOC %	S %	DESCRIPTION
RATONNEAU	R 163	<0.10	<0.10	<0.10	0.18	0.08	DOLOMITE, IN DECIMETER-THICK BEDS (GEORGIAN).
	R 164	<0.10	<0.10	<0.10	0.42	2.15	BLACK DOLOMITE MARL BEDS (TRIASSIC) IN CONTACT WITH THE GEORGIAN BASEMENT.
	R 165	<0.10	<0.10	<0.10	0.70	3.87	IDEM
	R 166	0.15	<0.10	<0.10	0.35	16.80	BRECCIA WITH CLASTS OF GEORGIAN GREY DOLOMITE AND BARITE CRYSTALS IN THE CEMENT : AUREOLE OF THE OREBODY.
VIEILLE MINE	VM 168	0.11	<0.10	0.15	0.11	0.65	GREENISH TO BLACK DOLOMITIC MARL (TRIASSIC) : HANGING WALL OF THE MINERALIZATION.
	VM 169	5.60	1.10	<0.10	0.26	7.45	GREY DOLOMITIC MARL (TRIASSIC) AS FILL IN THE GEORGIAN BASEMENT.
	VM 170	9.25	3.30	21.30	0.22	20.65	FILL (TRIASSIC) IN A DETACHED PART OF THE GEORGIAN BASEMENT.
	VM 171	11.70	1.30	57.60	0.09	15.30	KARST OREBODY (ASTERIX DEPOSIT) WITH SPHALERITE, GALENA AND BARITE.
ESPERANCE	E 172	<0.10	<0.10	48.40	1.20	24.40	TECTONIC BRECCIA WITH CLASTS OF GEORGIAN BASEMENT CEMENTED BY BARITE AND GALENA.
	E 173A	<0.10	<0.10	0.22	0.15	1.43	GREY-BLACK DOLOMITIC MARL (TRIASSIC) : HANGING WALL OF THE MINERALIZATION.
	E 173B	6.30	1.05	16.00	1.17	9.40	INTERBEDDED GREY DOLOMITE AND BLACK MARL (TRIASSIC).
	E 174	9.10	3.55	8.90	1.20	8.35	TECTONIC BRECCIA WITH CLASTS OF GREY GEORGIAN BASEMENT : CEMENT OF SPHALERITE, GALENA, BARITE, PLUS BITUMENS.
MONDARDIER	M 175	5.15	0.20	<0.10	n.d.	3.00	CONGLOMERATE WITH CLASTS OF GREY AND PINK GEORGIAN BASEMENT ; SPHALERITE CEMENT.
	M 176	39.00	0.85	<0.10	0.05	20.35	RECONCENTRATION OF SPHALERITE ALONG A FAULT IN THE CONGLOMERATE (cf. M 175).
	M 177	0.15	<0.10	<0.10	0.03	0.09	GREY-BLACK DOLOMITIC INTERBEDS (TRIASSIC) : HANGING WALL OF THE MINERALIZATION.
	M 178	<0.10	<0.10	0.12	0.16	0.09	RED MARL (TRIASSIC).
	M 179	12.20	1.00	<0.10	0.48	16.65	BLACK DOLOMITIC BASEMENT (GEORGIAN) : FINELY DISSEMINATED SPHALERITE.
	M 180	32.00	5.60	<0.10	n.a.	19.00	GREY-BLACK DOLOMITIC BASEMENT (GEORGIAN) : FINELY DISSEMINATED SPHALERITE
SANGUINEDE	S 185	5.25	0.40	<0.10	0.46	7.20	SPHALERITE, BOURNONITE, GALENA MINERALIZATION IN THE BLACK DOLOMITIC BAS^{t}. (GEORGIAN).

n.d. = not detected ; n.a. = not analyzed

Table 1 : Location and assay values of the studied samples.

testify that they have not undergone any alteration, namely by water washing or by biodegradation. As a consequence of the algal origin of the organic matter and of its low maturity, the very low IH values given by these two samples (130 and 80 mg hydrocarbons. g-1 TOC, respectively) can be taken as an indication about a severe degradation of the primary organic inputs during sedimentation and/or subsequent early diagenesis. This interpretation is supported by GC-MS data revealing the presence of only very low amounts of steranes - inherited from eukaryotes - in these two samples. GC-MS analysis also revealed the presence of notable amounts of hopanes - derived from prokaryotes - the presence of which testify to an intense bacterial activity during early diagenesis.

Another sample of Triassic marls originating from the Vieille Mine works revealed much lower TOC (0.11 %) and HI values (22 mg hydrocarbons. g-1 TOC) than in the two previous ones, and also a slightly higher maturity (Tmax 436°C). Its saturated hydrocarbon distribution differs from the two previous ones by a mode in n-C21 and a marked odd over even predominance of the C20+ n-alkanes. These features: (i) indicate a notable terrestrial plant contribution to the primary organic inputs and (ii) confirm the maturity assessment given by Tmax. The rapid decrease of the C21- n-alkanes with decreasing molecular weight, the very low proportions of the isoprenoids and the relative importance of the hump of the UCM (Unresolved Complex Mixture), indicate a loss of hydrocarbons attributable to water washing.

Four samples of black dolomites of the Georgian basement revealed TOC contents which never reach 0.5 %. Tmax values

approaching or higher than 500°C confirm the high maturity awaited for these metamorphosed sediments. One of these samples produced anomalously high amounts of CHCl3 extractable organic material (1030 ppm) very rich in hydrocarbons (39 %saturated, 9 % aromatics). The gas chromatogram of the saturated hydrocarbons shows: (i) a very large bell-shaped hump of UCM; (ii) notable of amounts of low-molecular weight n-alkanes dominated by the n-C17 and the n-C18; (iii) rather high amounts of the isoprenoids pristane and phytane (Pr+Ph/nC17+nC18 = 0.54). These unusual characteristics can interpreted as the result of a molecular "chromatographic" segregation that occurred in the course of oil migration.

All of the other samples which contain notable amounts of OM, originated from barite-rich orebodies hosted by the Cambrian basement (Vielle Mine and Esperance). All these samples contain allochtonous bitumens accumulated in fissures and/or voids. GC analysis of the saturated hydrocarbons mainly revealed a large hump of UCM with variable amounts of n-alkanes. The variations of the amounts of the n-alkanes and of their distribution can be interpreted as resulting from water washing, "chromatographic" segregation and thermal cracking provoked by the hot waters which brought the bitumens (~300°C; Ramboz and Charef, 1988). Consequently, the latter compounds are called "pyrobitumens" in the following discussion.

GENERAL DISCUSSION AND CONCLUSIONS

Consistently with previous work (Gauthier et al., 1988), the results of the present study indicate that autochtonous organic matter is not very abundant in the environment of the Les Malines mine. TOC values seldom exceed 0.5 % in the Triassic dolomitic marls. Comparable or even higher amounts of organic matter - which may exceptionnaly reach 2.7 % TOC (Gauthier et al., 1988)- have been found in the dolomitic Georgian basement. TOC values greater than 1 % appear most frequently due to allochtonous oil and/or bitumens (Connan and Orgeval, 1977; Gauthier et al., 1988; this study) and are very little meaningfull because of the inhomogeneous repartition of this material, usually accumulated in fissures and voids.

Autochtonous organic matter is - as expected - very mature in the metamorphosed basement, but only slightly mature in the Triassic marls (onset of the oil window). Except a low mature oil impregnating the old basement in the Montdardier works, the allochtonous material is represented by pyrobitumens associated with barite precipitated by hydrothermal fluids (Ramboz and Charef, 1988). Despite the extent of the hydrothermal alteration undergone by the pyrobitumens, they produced Tmax values in the same range than those given by the Triassic marls and thus consistent with maturation caused by burial diagenesis. This observation indicates that oil and bitumen migration and emplacement, certainly occurred early during the deposition history of the sedimentary cover. Because of low organic matter contents, low maturity and the absence of any mark of alteration of the associated hydrocarbons, the Triassic marls, sole formations to have some oil potential in the mine area, can hardly be regarded as the source of the bitumens

as hypothesized in previous work (Connan and Orgeval, 1977). Another argument in favor of a non local origin of these compounds is their relative abundance in the basement - in association with mineralization - and especially in mine areas where the Triassic is thin and even locally absent (i.e. Vielle Mine). The mineralizing character of the oil-bearing brines is highly suggested by the general association between migrated oil and/or bitumens and ore, both accumulated in paleo-reservoirs and drains (conglomerates, breccias, faults and fractures). Increasing amounts of bitumens from E to W suggest that these products could have originated from sedimentary formations of the SE Languedoc basin. More data would be necessary to verify this hypothesis.

The part that organic materials could have played in the mineralizing events remains conjectural. However, the involvement of n-alkanes biodegradation in the ore deposition hypothesized in previous work (Connan and Orgeval, 1977) must be rejected for the following reasons: (i) the alteration of the n-alkane signatures of allochtonous bitumens can be attributed to the various physico-chemical processes mentionned here above, rather than to bacterial activity; (ii) because of low TOC contents and low maturity, the Triassic marls could have only produced very low amounts of n-alkanes; (iii) the n-alkanes were obviously produced as a result of burial diagenesis, and thus necessarily long time after ore deposition.

ACKNOWLEDGEMENTS : This work was carried out with funds granted under the E.E.C. CREST contract n° MA1M1-0003C.

REFERENCES

Connan J. and Orgeval J. J. (1977) Un exemple d'application de la géochimie organique en métallogénie: la mine des Malines (Gard, France). Bull. Cent. Rech. Explor.-Prod. Elf-Aquitaine 1: 59-105.

Disnar J. R. and Defoix D. (1991) Géochimie organique des hydrocarbures gazeux: analyse et application à la propection minière (bordure orientale des Causses et gisement Zn-Pb des Malines (Gard, France). BRGM report n° R 32 546, 131 p.

Gauthier B., Disnar J. R., Fourmont P. and Trichet J. (1988) Utilisation de la matière organique comme outil de prospection tactique: exemple du gisement Zn-Pb des Malines (Gard, France). Doc. BRGM n° 158, vol. II: 843-862. Editions du BRGM, Orléans.

Ramboz C. and Charef A. (1988) Temperature, burial history, and paleohydrology of the Les Malines Pb-Zn deposit: reconstruction from aqueous inclusions in barite. Econ. Geol. 83: 784-800.

Current Research in Geology Applied to Ore Deposits. Fenoll Hach-Alí, Torres-Ruiz & Gervilla (eds) (1993). ISBN 84-338-1772-8

PETROGENESIS OF CORDIERITE-ANTHOPHYLLITE ROCKS, TUNABERG, SWEDEN

Dobbe, R.
Inst. of Earth Sciences, Free University, De Boelelaan 1085, 1081 HV Amsterdam, The Netherlands

ABSTRACT: High amphibolite-facies cordierite-anthophyllite rocks occur in discordant alteration zones in the wall-rocks of stratiform iron ores at Tunaberg, Sweden. One association of altered rocks is derived from an acid volcanic protolith and shows gradations from cordierite-bearing acid metavolcanics to quartz-cordierite-anthophyllite-biotite schists. Another association of altered rocks is derived from a basic rock protolith and consists of quartz-free, highly aluminous cordierite-anthophyllite/gedrite(±plagioclase) rocks occurring in an inner zone of strongest alteration and grading into successively less altered, more outward zones of plagioclase-anthophyllite rock, plagioclase-hornblende-cummingtonite rock and plagioclase-hornblende amphibolite, respectively. The observed mineral assemblages in the latter association of altered rocks indicate progressive loss of SiO_2, CaO and Na_2O during alteration and progressive decrease of Ca-contents from the inner alteration zone towards the outermost zone of virtually unaltered amphibolite. Residual enrichment in the immobile components Al_2O_3, TiO_2, FeO and MgO caused the formation in the alteration zones of metamorphic mineral assemblages with cordierite and anthophyllite/gedrite, and locally corundum and högbomite.

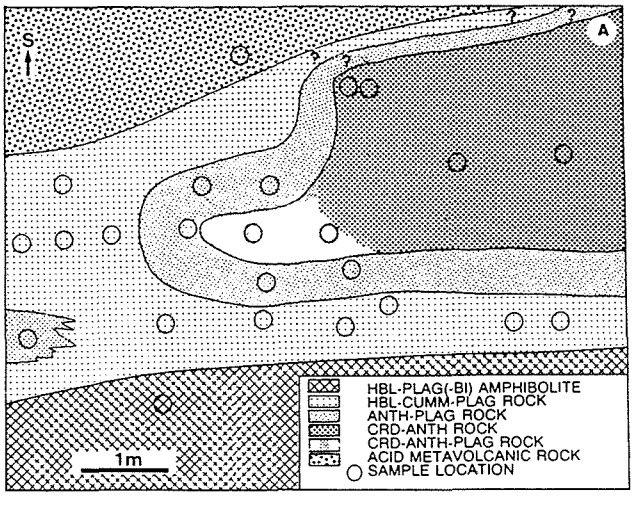

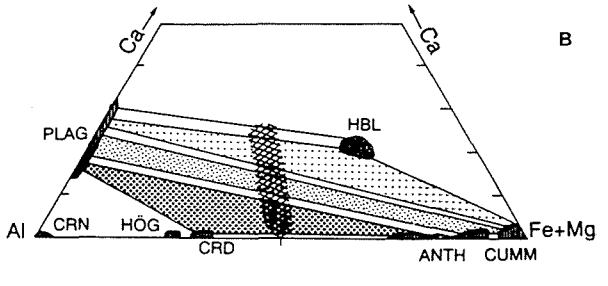

Fig. 1.(A) Sketch of alteration zones with inner zone of cordierite-anthophyllite rock, intermediate zone of plagioclase-anthophyllite rock and outer zone of plagioclase-hornblende-cummingtonite rock; zone boundaries and boundary with plagioclase-hornblende(-biotite) amphibolite are gradual. (B) projection from the Si-apex onto the plane Ca-Al-(Fe+Mg) illustrating chemographic and phase relations of the rocks shown in Figure 1A; Striped areas indicate composition limits of mineral phases; light, intermediate and dark dotted fields correspond to mineral assemblages of rocks from the outer, intermediate and inner zone in Figure 1A, respectively; cross-hatched field indicate compositions between plagioclase(PLAG)-hornblende (HBL)-cummingtonite (CUMM) amphibolites and cordierite (CRD)-anthophyllite/ gedrite (ANTH) rocks, the latter locally with corundum (CRN) and högbomite (HÖG).

1 INTRODUCTION AND GEOLOGICAL SETTING

In the Baltic shield Mg-rich schists are commonly associated with massive Fe-Cu-Zn-Pb sulphide and Fe-oxide ores. In the western part of the Early Proterozoic (1.9-1.8 Ga) Bergslagen metallogenetic province Mg-alteration occurs in extensive zones of greenschist facies Mg-chlorite-quartz-sericite (Baker & De Groot, 1983) and amphibolite facies cordierite-bearing (Trägårdh, 1988) schists that often show discordant relationships to exhalative-sedimentary iron ores and their host rocks of predominantly felsic volcanics; the strong Mg-enrichment and Fe(-Mn)-depletion in these schists are ascribed to processes related to felsic rock-seawater interaction in a sub-seafloor hydrothermal system. In the high amphibolite-facies metamorphosed Tunaberg area, SE Bergslagen, Sweden, a thin volcanic succession is underlain by a thick sequence of metasediments. A 200 m thick lower mineralized horizon in the metasediments shows intercalations of acid metatuffites associated with exhalative-sedimentary Fe-oxide ores, Mn-silicate ores (eulysites) and Mg-Fe-rich alteration zones. This paper describes one such Mg-Fe-rich alteration zone in the Tunaberg area, where a zone of cordierite-anthophyllite/gedrite and plagioclase-anthophyllite-cummingtonite rocks is found sandwiched between a layer of quartz-plagioclase-biotite metavolcanite and a layer of plagioclase-hornblende(-biotite) amphibolite (Fig. 1A).

2 PETROGRAPHY AND MINERAL CHEMISTRY

The Mg-Fe-rich alteration zones at Tunaberg show semi-conformable relationships to magnetite-hornblende skarns. The altered rocks show strong mineralogical and chemical variation. Figure 1 shows an alteration zone with the following quartz-free rock types: outer zone of plagioclase-hornblende-cummingtonite rock; intermediate zone of plagioclase-anthophyllite rock; inner zone of cordierite-anthophyllite/gedrite-biotite rock, locally with some plagioclase. The fine- to medium-grained rocks show a strong lineation due to alignment of 1-2 mm long amphibole crystals. On rock exposures in the inner zone, protruding nodules of coarse-grained cordierite-anthophyllite/gedrite(-biotite) rock form characteristic cigar-like bodies in a matrix of anastomising schlieren showing abundant anthophyllite and biotite. Composition limits of mineral phases are shown in Figure 1B. Anthophyllite in plagioclase-hornblende-cummingtonite and plagioclase-anthophyllite rocks of the outer and intermediate zones shows lower Na, Al and Fe/(Fe + Mg) compared to anthophyllite-gedrite in cordierite-anthophyllite/gedrite rocks from the inner zone. Anthophyllite-gedrite shows positive correlation of Al(IV) and Na, Al(VI) and Na, Al and Fe/(Fe+Mg), and Na and Fe/(Fe+Mg).

3 PHASE RELATIONS

The quartz-absent mineral assemblages from the described alteration zones are shown projected from the Si-apex onto the plane Ca-Al-(Fe+Mg) of Figure 1B. The strong influence of bulk CaO-contents on the composition of plagioclase coexisting with different (Fe,Mg)-silicates is illustrated in Figure 1B. The intensely altered rocks of the inner zone show low Ca-contents (Fig. 2A) characterized by the mineral assemblage of cordierite + Na,Al-rich anthophyllite/gedrite ± plagioclase (An_{26}). Increasing Ca-content towards the outer alteration zones moves the bulk composition into the fields of the assemblages plagioclase (An_{36}) + Na,Al-poor anthophyllite ± cummingtonite, plagioclase (An_{47}) + hornblende + cummingtonite ± Na,Al-poor anthophyllite, and plagioclase (An_{71}) + hornblende, respectively.

4 ROCK CHEMISTRY

Mafic rock protoliths of cordierite-anthophyllite rocks have been suggested by e.g. Vallance (1967), Treolar & Putnis (1982), Schneiderman & Tracy (1991). On the other hand, acid volcanic protoliths of cordierite-anthophyllite rocks in W. Bergslagen have been suggested by e.g. Wolter & Seifert (1984) and Trägårdh (1988). Trägårdh (1988) noticed that cordierite-anthophyllite-bearing wall-rocks close to iron ores show strong Fe-Mg-enrichment (with low MgO/FeO_{tot}) and depletion in Si and alkalis. At Tunaberg the wall rocks of the iron ores show chemical and mineralogical graduations from quartz-plagioclase-biotite acid metavolcanics to cordierite-anthophyllite-bearing acid metavolcanics, and to quartz-cordierite-anthophyllite-biotite schists, suggesting a derivation of cordierite-anthophyllite rocks from acid metavolcanics (Dobbe, in prep.). However, in this study a case is described of cordierite-anthophyllite rocks representing altered plagioclase-hornblende amphibolite. Evidence is provided by 1) the silica-undersaturated, highly aluminous nature of the altered rocks, occurring adjacent to amphibolite (Fig. 1A), 2) the gradation of chemical and mineralogical composition of rocks from inner to outer alteration zone, 3) the immobile behaviour of Al_2O_3, TiO_2, Zr, Hf, and Nb (see below), and 4) the presence in the alteration zones of Cr-V-bearing magnetite and other characteristic oxide minerals of basic rocks and their cordierite-orthoamphibole-bearing altered derivatives (Bernier, 1990). The Al_2O_3-CaO diagram (Fig. 2A) clearly shows that in the Tunaberg area there are quartz-cordierite-anthophyllite-schists derived from acid rocks, and quartz-undersaturated highly aluminous cordierite-anthophyllite-schists derived from basic rocks. Figure 2B shows an isocon diagram (Grant, 1986) based on the averages of 6 analyses of weakly altered outer zone plagioclase-hornblende-cummingtonite rocks and 6 analyses of pervasively altered inner zone cordierite-anthophyllite rocks. The plagioclase-hornblende(-biotite) amphibolites and their incipient alteration products of plagioclase-horn-

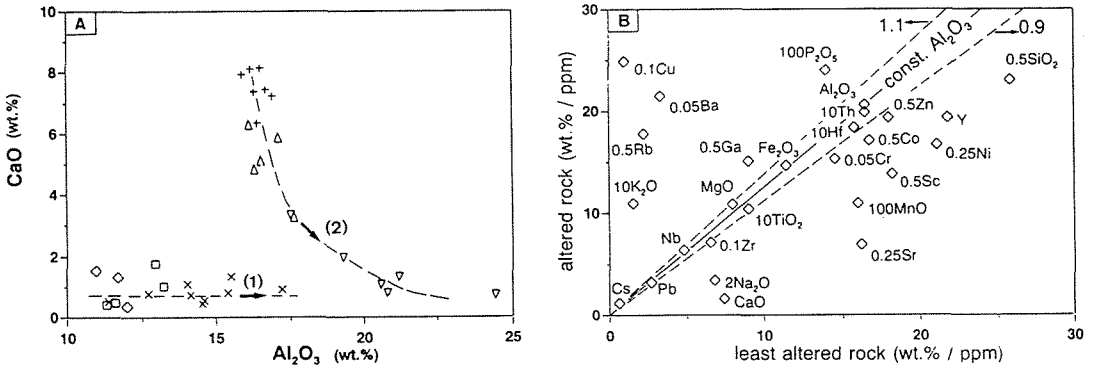

Fig. 2.(A) Al_2O_3-CaO plots of cordierite-anthophyllite and associated rocks from the Tunaberg area; the diagram clearly shows two alteration trends: (1) from acid metavolcanics (◇) and quartz-biotite schists (□) to quartz-cordierite-anthophyllite-biotite schists (x), and 2) from plagioclase-hornblende(±cummingtonite) rocks (+) to plagioclase-anthophyllite rocks (△), and to cordierite-anthophyllite/gedrite rocks (▽). (B) Isocon diagram (Grant, 1986) showing outer zone hornblende-plagioclase(±cummingtonite) amphibolites versus inner zone cordierite-anthophyllite rocks. Oxides are plotted in weight percent, elements in ppm. Isocon line assumes constant alumina; elements with ~10 percent gain plot on 1.1 line, elements with ~10 percent losses plot on 0.9 line.

blende-cummingtonite rocks show similar major, minor and REE element chemistry, except for lower K, Rb, Sr, and Ba in the slightly altered rocks. Immobile components, defining a best-fit isocon showing a linear array through the origin (Fig. 2B), are Al_2O_3, FeO_{tot}, MgO, TiO_2, Zr, Hf, Nb, Pb, Th and Cr. On the basis of constant Al the slope of the alumina isocon is 1.23 (Fig. 2B); this corresponds to a mass decrease of 19 percent and, including density in the calculations, a volume decrease of 22 percent. Assuming constant Al mobile components lost during alteration are SiO_2, CaO, Na_2O, MnO, Sr, Sc Ni and Y, mobile components gained are P_2O_5, K_2O, Rb, Ba, Cs, Cu and Ga. Comparison of the normalized REE patterns of cordierite-anthophyllite/gedrite rocks and plagioclase-hornblende-cummingtonite rocks shows that of the REE Eu has behaved as relatively mobile element lost during alteration.

5 CONCLUSIONS

- Mg-Fe-enriched alteration zones occur in discordant zones in the high amphibolite-facies metamorphosed wall-rocks of stratiform iron ores in the Tunaberg area.
- Quartz-free, highly aluminous cordierite-anthophyllite/gedrite(-plagioclase) rocks represent altered equivalents of plagioclase-hornblende amphibolites; intermediate alteration is represented by plagioclase-hornblende-cummingtonite and plagioclase-anthophyllite rocks.
- Alteration is attended by loss of SiO_2, CaO and Na_2O, resulting in progressively lower Ca-content and Ca-poor mineral parageneses towards the inner zone of strongest alteration.
- Residual enrichment in the immobile components Al_2O_3, TiO_2, FeO and MgO resulted in assemblages with cordierite and anthophyllite, and other aluminium-rich minerals such as corundum and högbomite.
- Cordierite-anthophyllite rocks in the Tunaberg area show two chemically distinct alteration trends indicating their derivation from an acid volcanic protolith in one case, and from a basic rock protolith in the other case.

REFERENCES

Baker, J.H & De Groot, P.A. 1983. Proterozoic seawater - felsic volcanics interaction W. Bergslagen, Sweden. Evidence for high REE mobility and implications for 1.8Ga seawater compositions. Contrib. Mineral. Petrol. 82: 119-130

Bernier, L.R. 1990. Vanadiferous zincian-chromian hercynite in a metamorphosed basalt-hosted alteration zone, Atik Lake, Manitoba. Can. Mineral. 28: 37-50

Grant, J.A. 1986. The Isocon Diagram - A Simple Solution to Gresens' Equation for Metasomatic Alteration. Econ. Geol. 81: 1976-1982

Schneiderman, J.S. & Tracy, R.J. 1991. Petrology of orthoamphibole-cordierite gneisses from the Orijärvi area, southwest Finland. Amer. Mineral. 76: 942-955

Trägårdh, J. 1988. Cordierite-mica-quartz schists in a Proterozoic volcanic iron ore-bearing terrain, Riddarhyttan area, Bergslagen, Sweden. Geol. Mijnbouw 67: 397-409

Treolar, P.J. & Putnis, A. 1982. Chemistry and microstructure of orthoamphiboles from cordierite-amphibole rocks at Outokumpu, North Karelia, Finland. Mineral. Mag. 45: 55-62

Vallance, T.G. 1967. Mafic rock alteration and isochemical development of some cordierite-anthophyllite rocks. J. Petrol. 8: 84-96

Wolter, H.U. & Seifert, F. 1984. Mineralogy and genesis of cordierite-anthophyllite rocks from the sulfide deposit of Falun, Sweden. Lithos 17: 147-152

Current Research in Geology Applied to Ore Deposits.Fenoll Hach-Ali, Torres-Ruiz & Gervilla(eds)(1993).ISBN 84-338-1772-8

A SANDSTONE Pb-Ba DEPOSIT AT THE BASE OF THE MIOCENE IN WESTERN SARDINIA, ITALY

Fadda, S. (1); Fiori, M. (1); Pretti, S. (2) & Spiga, G. (3)
(1) Centro Studi Geominerari e Mineralurgici del CNR, Cagliari, Italy
(2) Istituto Giacimenti Minerali, Universita' di Cagliari, Italy
(3) Alfalab SGS, Assemini, Cagliari, Italy

Abstract
The recent development of studies on mineral occurrences related with Tertiary volcanics in Sardinia led to the discovery of an interesting cerussite - barite indication in clastic sediments of Upper Oligocene-Lower Miocene age. The characteristics of these occurrences indicate the calc-alkaline volcanics, affected by epithermal alteration and mineralization, as the source of the metals as well as oxidizing early diagenetic conditions for the deposition environment.

Foreword

The ore occurrences hosted in Tertiary terrains in Sardinia have been carefully investigated only for a few years. In particular, epithermal and porphyry-type bodies have been discovered (Pretti, 1988; Garbarino et al., 1991). The only occurrences of supergenic origin already known up to now were of Mn oxides and Cu carbonates, but the relative literature is very scarce (Millosevich, 1906). The studies in progress on the epithermal system of Monti Ferru (central-western Sardinia) recently led to the discovery of Ba-Pb bearing clastic beds, which are the subject of the present communication.

Geological framework of the area

At the end of the important phase of calc-alkaline volcanism related with the eastward drift of Sardinia in Oligocene-Miocene times, an epithermal activity developed, which produced important alteration phenomena, including pervasive potassic alteration, and mineralization, particularly of base metals. At the end of all these phenomena, a sedimentary series of Upper Oligocene-Miocene age was deposited during a transgressive phase. The basal, clastic beds of this series commonly include clasts deriving from the erosion of the above said volcanic rocks. The rest of the series, which does not exceed a few hundreds of metres, is mostly formed by marls and limestones of platform environment.
In the investigated area all these terms outcrop, with the calc-alkaline volcanics on the eastern side and the sedimentary series between the volcanics and the sea westwards. The basal clastic beds outcrop in the valley of Rio Pischinappiu thanks to the combined effects of the erosion of the stream and of the offset of a local fault. Of the two outcrops, the northern is very small, while the southern has an extension of some 20 hectares and displays a good section in correspondence of the fault.

The local clastic series

The cited series has been carefully studied and sampled. Its total thickness is of some 40 m and has been subdivided into 12 beds on the basis of the macroscopic characteristics. It starts with reworked pyroclastics, and then passes on to sandstones-microconglomerates. Coarse conglomerates appear in the upper part. The last two beds lie unconformably on the rest of the series.
The beds below the unconformity show a very low maturity and are mostly formed of K-feldspar and quartz, deriving from the epithermally K-altered calc-alkaline volcanics and the quartz veins of Monti Ferru. The main component of their cement is authigenic K-feldspar. Their porosity is fairly high (about 15-20%) and soluble chlorides of K, Na, Mg and Ca are still present in the pores.

The beds above the unconformity are much more mature, with predominantly rounded quartz clasts and cement made of Fe-hydroxides.

The mineralization

The analysis of the samples showed anomalous contents in a few elements, particularly Pb and Ba. The latter occurs as barite and the former mostly as cerussite. With the exception of the first bed (a), the metal content of the lower beds (b-c) is comparatively low, even though anomalous in Pb (around 200-400 ppm). Starting from bed (d), Pb sharply increases and rapidly reaches values of tens of percent in bed (e) (Fig.1), then normally keeps high values (thousands of ppm) up to the top of the series.

Ba is also low in the lower beds (a-d) then increases to thousands of ppm im the upper beds, with particularly rich levels mostly in the upper parts of some beds- e.g. bed (f)- where barite occurs as crystals and small lenses (Fig.1). Zn reaches high values (more than 1%) only in the lower level, then decreases to normal geochemical contents. Cu is also commonly present in normal geochemical values, with the exception of bed (e), where it reaches hundreds of ppm (Fig.1).

Discussion

In synthesis, the above exposition shows that in a clastic series of Upper Oligocene-Lower Miocene age, derived from calc-alkaline volcanics affected by epithermal alteration and mineralization, a supergenic mineralization including barite and cerussite formed, particularly high Pb values in level (e), which has a thickness of 0.6-1 m.

The fact that epithermal ore bodies, known in a locality in the vicinity of the studied outcrops, mostly contain Zn-Pb, with minor Cu, is the best explanation for the origin of the Pb. The conditions favourable to the enrichment of this metal appear related to the climatic condition at deposition time, which were similar to the present conditions, i.e. warm and semiarid (Biondi & Filigheddu, 1988). These would be the conditions favourable for bisiallitization, which leads to a preferable, residual Pb concentration (Samama, 1973).

This is also confirmed by the appearance of the sediments below the unconformity, whose reddening is clearly superficial, related to the present weathering.

The origin of Ba would also be related with the altered volcanic rocks, whose K-feldspar content is high enough to ensure a good supply of this element. The Pb occurrence as cerussite is clearly primary. Since the scarce Fe also occurs as hematite, and sulphides such as galena, pyrite and covellite occur in absolutely negligible quantity, all suggest an environment characterized by oxidizing conditions and elevated pH (Fig.2) (Garrels & Christ, 1965). The oxidizing environment could indicate both synsedimentary deposition and eodiagenetic, near-surface formation. The first possibility cannot represent the main deposition mechanism at least for bed (e), where about 35% cerussite is present. In turn, the near-surface, early condition of diagenesis of the beds are confirmed by the comparatively high porosity of all the beds and by the predominating authigenic K-feldspar as cement (Pettijohn et al., 1973). The abundance of the latter mineral, together with the presence of soluble K in the pores, clearly indicate abudance of this element in the waters, thus an alkaline environment.

It is likely that the solutions which carried the Pb initially were of a lower pH, mostly by sulphuric ion (after oxidation of the epithermal sulphides), but it was gradually eliminated by barite precipitation. The possibly formed Pb sulphates (anglesite and lanarkite) are much more soluble than cerussite and barite; thus they may have been displaced by them.

The high concentration of cerussite in bed (e) indicates that this bed formed the main "trap" for the percolating Pb.This means that:

- along bed (e) the C species were comparatively abundant in the waters: this

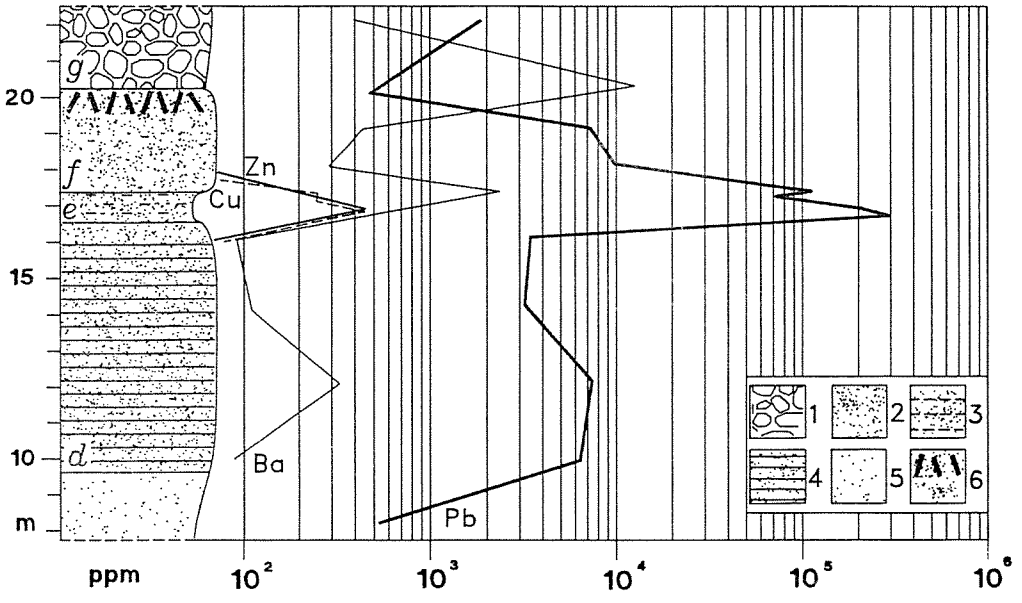

Fig. 1 (up) part of the stratigraphic column of the main outcrop, including the highly mineralized bed. Zn and Cu also reach the highest values in the same bed, but their content is negligible as compared to that of Pb. Note that Ba, mostly as barite, reaches higher values in the upper beds.

1– Conglomerate ; 2– Fine sandstone
3– K–Feldspar–cerussite bed
4– Bedded fine sandstone
5– Coarse sandstone ; 6– Barite crystals

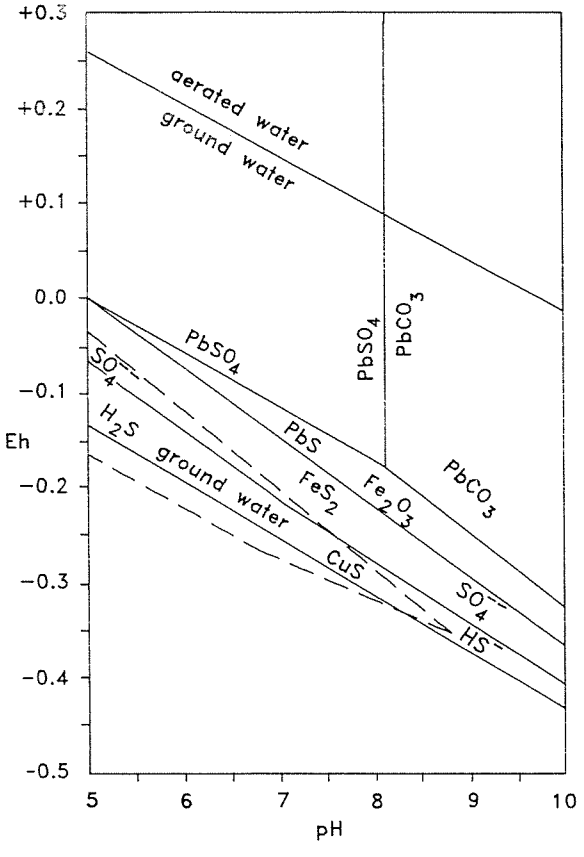

Fig. 2 (left) pH – Eh diagram representing the formation field of the observed minerals at 1 atm and 25 °C, not far from the true conditions in the mineralized beds (after Garrels and Christ, 1965, modified).
The main constraints concern the lower limit, which is the cerussite – galena boundary, with locally and temporally very limited Eh variations as far as the covellite field.
The upper limit should be that of ground waters, but synsedimentary precipitation of cerussite (surface waters) is not excluded.
The lateral limits should be those of natural waters (pH c.a 6.5 – 8.5).

may be explained in several manners, some of which imply that this bed represented a permeability barrier;
- bed (e) contained substances that were easily soluble, in order to give place to the final minerals, which are mostly authigenic cerussite and K-feldspar. Both conditions could be satisfied if this bed were formed mainly of volcanic glass, related with the final volcanic episodes, which are known to occur near the base of the Miocene sedimentary series.

Acknowledgements
Study supported by the contribution of "Centro Studi Geominerari e Mineralurgici del C.N.R.", Piazza D'Armi, Cagliari, Italy.

References

Biondi E. & Filigheddu P.,1988. A palm fossil closely related to Chamaerops humilis L. from the Lower Miocene of Sardinia (Italy). Giorn. Bot.Ital., in press.

Garbarino C., Grillo S.M., Marcello A., Pretti S.,Uras I. & Fiori M., 1991. First data on Tertiary epithermal occurrences in Sardinia, Italy. Proc. Symp. "Brazil Gold 91", Belo Horizonte, 143-150.

Garrels R.M. & Christ C.L., 1965. Solutions, Minerals and Equilibria. Harper & Row (New York) and J. Weatherhill, Inc. (Tokio).

Millosevich F., 1906. Appunti di mineralogia sarda. Il giacimento di azzurrite del castello di Bonvei, presso Mara, con alcune considerazioni sulla formazione dei carbonati di rocce naturali.Rend. R. Acc. Lincei, XV, 732-740.

Pretti S., 1988. Mineralization related to Tertiary volcanism in Sardinia: opportuneness of a re-examination. Proc. Symp. "Zuffar' days", Cagliari, 89-100.

Samama J.C., 1973. Ore deposits and continental weathering: a contribution to the problem of geochemical inheritance of heavy metal contents of basement areas and of sedimentary basins. "Ores in sediments", Springer, 247-265.

Current Research in Geology Applied to Ore Deposits. Fenoll Hach-Alí, Torres-Ruiz & Gervilla (eds) (1993). ISBN 84-338-1772-8

TRACE ELEMENT CONTENTS IN PYRITES FROM THE TERTIARY AND PRE-MESOZOIC SULPHIDE DEPOSITS OF THE KIRKI-LEPTOKARIA-ESSIMI AREA, THRACE, GREECE

Filippidis, A. (1); Chatzikirkou, A. (2); Katirtzoglou, C.(2); Skounakis, S. (3); Michailidis, K. (1) & Kassoli-Fournaraki, A. (1)

(1) Aristotle University of Thessaloniki, Greece

(2) Inst. of Geology and Mineral Exploration, Thessaloniki, Greece

(3) University of Athens, Greece

ABSTRACT: Pyrites from the Tertiary and Pre-Mesozoic sulfide deposits of the Kirki-Leptokaria-Essimi area were analyzed for their Cr, Co, Ni, As, V, Nb, Mo, Sn and W contents. The trace elements composition shows the lack of any discrimination between the Tertiary and the Pre-Mesozoic sulfide deposits. The Co/Ni ratio values varying within the range 0.72-4.38 and the way of their distribution might indicate that the Oligocene magmatic activity, which was responsible for the formation of the hydrothermal Tertiary sulfide deposits, has chemically affected and/or remobilized the sedimentary Priabonian and volcanogenic Pre-Mesozoic ones.

INTRODUCTION

The trace element contents of pyrite have been used to distinguish various ore forming environments (e.g., Mookherjee & Philip 1979, Xuexin 1984). A previous work (Filippidis 1992) concentrated on some trace elements in pyrites from the Tertiary sulfide deposits of the Kirki-Essimi basin, Thrace, Greece. The main purpose of this study is to compare some trace element contents of the pyrites between the Tertiary and Pre-Mesozoic sulfide deposits of the Kirki-Leptokaria-Essimi area, Thrace, Greece. Questions concerning the probable variations in the trace element contents of pyrites within an ore deposit are not in the scope of this study.

GEOLOGICAL SETTING

The analyzed pyrites were collected from four Tertiary and three Pre-Mesozoic sulfide deposits (Fig. 1) hosted within the Tertiary volcanosedimentary

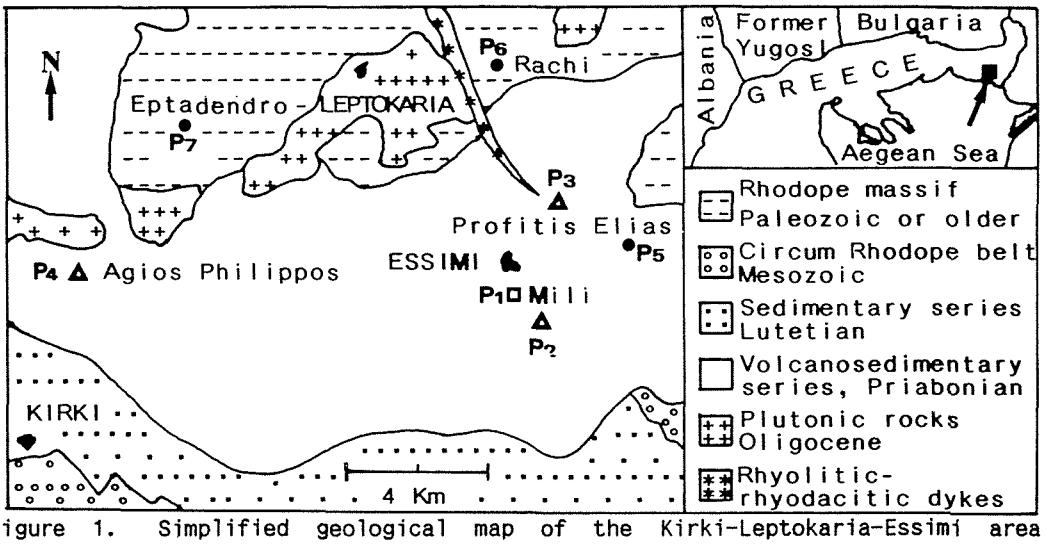

Figure 1. Simplified geological map of the Kirki-Leptokaria-Essimi area (Katirtzoglou 1986) and sample location. P1: Priabonian deposit. P2-P4: Oligocene-Miocene deposits. P5-P7: Pre-Mesozoic deposits. Sample position: Drill cores (P1, P2, P4, P5), galleries (P3, P7), shafts (P6).

Table 1. The main features of the investigated sulfide deposits

Sample No. Locality	Main features of the sulfide deposits
P1 Mili	sedimentary, stratiform, massive. Py(90%), Ga(5%) & Sph(5%). Host rock: metapelite-sandstone (Priabonian).
P2 Mili	hydrothermal, disseminated, veinlet - infillings. Py(90%), Ga(5%) & Sph(5%). Host rock: andesitic porphyry (Priabonian).
P3 Profitis Elias	hydrothermal, massive, vein type. Py(35%), Cpy(35%), Sph(20%) & Ga(10%). Host rock: metasedimentary (Priabonian).
P4 Agios Philippos	hydrothermal, massive, vein type. Py(100%). Host rock: metasedimentary (Priabonian).
P5 Profitis Elias	reformed post-volcanogenic, stratiform, massive. Cpy(50%), Py(40%), Ga+Sph+Po(10%). Host rock: chlorite schist (Paleozoic or older)
P6 Rachi	reformed post-volcanogenic, stratiform, massive to disseminated. Py(50%) & Cpy(50%). Host rock: amphibolite (Paleozoic or older).
P7 Eptadendro	reformed post-volcanogenic, stratiform, massive. Cpy(90%) & Py(10%) Host rock: amphibolite (Paleozoic or older).

Cpy=Chalcopyrite, Ga=Galena, Po=Pyrrhotite, Py=Pyrite, Sph=Sphalerite

Table 2. Pyrite composition (in ppm) from the investigated sulfide deposits

Sample No.	P1*	P2*	P3*	P4*	P5*	P6*	P7*
V (2)**	13	5	<2	3	<2	<2	<2
Cr (2)	65	25	10	5	64	12	662
Co (2)	275	103	160	274	408	263	1801
Ni (2)	382	127	100	105	243	60	2047
As(10)	380	315	750	220	970	30	241
Nb(10)	<10	<10	<10	<10	<10	<10	<10
Mo(10)	20	<10	<10	<10	<10	<10	<10
Sn(10)	<10	<10	<10	<10	<10	<10	<10
W (10)	<10	<10	<10	<10	<10	<10	<10
Co/Ni	0.72	0.81	1.60	2.61	1.68	4.38	0.88

*)Average of 3 analyses. **)Detection limit. P1-P4=Tertiary, P5-P7=Pre-Mesozoic

formation and the Rhodope metamorphic basement of the Kirki-Leptokaria-Essimi area. Up to 1970, there was an intense mining activity for some of these sulfide deposits. The Rhodope metamorphic basement (Paleozoic or older) is overlain by the Circum Rhodope belt (Mesozoic), represented in the study area by the Makri and Drimou Melia units. The Rhodope metamorphic basement, the Circum Rhodope belt and the Tertiary sedimentary formations are intruded by Oligocene plutonic rocks and crosscut by rhyolitic-rhyodacitic dykes (Katirtzoglou 1986).

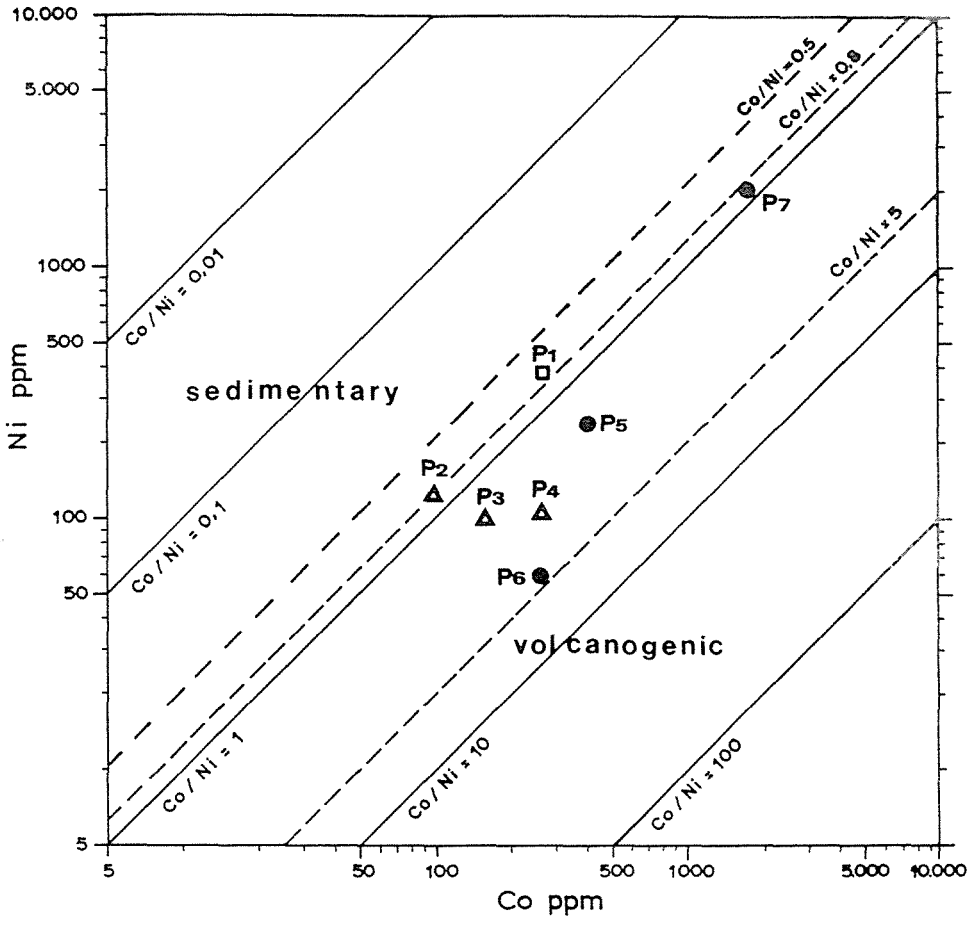

Figure 2. Ni-Co relationships of pyrites from Tertiary & Pre-Mesozoic sulfide deposits in the Kirki-Leptokaria-Essimi area. P1=sedimentary (Priabonian), P2-P4=hydrothermal (Oligocene-Miocene) and P5-P7=reformed post-volcanogenic (Pre-Mesozoic) deposits.

MATERIALS AND METHODS

Fifteen ore samples (≈1 kg each) were collected from drill hole cores, galleries and shafts. Each ore sample was examined in reflected light microscope. Point counting (three polished sections) was used to estimate the proportions of the predominant ore minerals. The main features of the sulfide deposits are given in Table 1. Details for the Agios Philippos polymetallic ore mineralization are given by Vavelidis et al. (1989). The ore material was gently fragmented for several times and pyrite was separated under a stereomicroscope. XRD analyses revealed only pyrite to be present in the separates. The trace element analyses of the pyrites (Table 2), were performed by Inductively Coupled Plasma (ICP). An estimation of the purity of the separates was made by determining elements such as Si, Ca, Mg, Cu, Zn, Pb for each sample. These elements indicate the magnitude of contamination by the gangue minerals as well as by the chalcopyrite, sphalerite and galena in cases of very small inclusions present in the pyrite. Hence, six out of the fifteen analyses were excluded due to high contamination.

RESULTS AND DISCUSSION

The correlation of the analyzed trace elements in pairs (Co-Cr, Ni-Cr, Cr-As, Co-As, Ni-As, Ni-Co) showed that no one discrimination exists between the Tertiary and Pre-Mesozoic sulfide deposits. The Co/Ni ratio values in pyrites were widely used to discriminate between ore forming environments of sulfide deposits (e.g., Bralia et al. 1979, Mookherjee & Philip 1979, Raiswell & Plant 1980, Duchesne et al. 1983, Xuexin 1984). However, a wide dispersion exists even in the same ore type (e.g., 0.01-1.0 for sedimentary and 3.5-50 for volcanogenic pyrites). Reviewing the literature, the Co/Ni ratio values can be broadly summarized as following: the sedimentary pyrites show a Co/Ni ratio approximately <0.5-0.8, while the volcanogenic ones approximately >5. Between these values pyrites from different ore types (e.g., reformed, metamorphosed, skarn-hydrothermal and hydrothermal) can be placed.

The pyrite from the sedimentary Priabonian sulfide deposit shows a Co/Ni ratio value of 0.72, the hydrothermal Oligocene-Miocene deposits show a ratio of 0.81-2.61 and the reformed post-volcanogenic Pre-Mesozoic ones of 0.88-4.38. These Co/Ni ratio values lying between 0.72 and 4.38 are plotted in the 0.5 to 5 field of Fig. 2. That is, there is an inclination of the Co/Ni ratio values from the sedimentary (P1) and volcanogenic (P5-P7) pyrites towards the inner field.

The Oligocene to Miocene magmatism was the latest endogenic episode in the area. The very close vicinity of the magmatic rocks to the older sedimentary and post-volcanogenic sulfide deposits indicates that the Oligocene magmatism could thermally act on the deeper parts of these deposits and more or less change their textural features. Besides, the released magmatic fluids may have chemically affected the pre-existing mineralizations in the area.

Considering the Co/Ni ratio values of the examined pyrites and the absence of any discrimination between the different sulfide deposits, it can be concluded that most probably the latest Oligocene magmatic activity, which was responsible for the formation of the hydrothermal sulfide deposits, chemically affected and/or remobilized the stratiform Priabonian and Pre-Mesozoic ones.

REFERENCES

Bralia, A., Sabatini, G. & Troja, F. 1979. A revaluation of the Co/Ni ratio in pyrite as geochemical tool in ore genesis problems. Mineral. Deposita 14:353-374.

Duchesne, J.C., Rouhart, A., Schoumacher, C. & Dillen, H. 1983. Thallium, nickel, cobalt and other trace elements in iron sulfides from Belgian lead-zinc vein deposits. Mineral. Deposita 18:303-313.

Filippidis, A. 1992. Trace element contents of pyrites from Tertiary sulfide deposits of the Kirki-Essimi basin, Northeastern Greece. Mineral Wealth 78:45-52.

Katirtzoglou, C. 1986. The metallogenesis of the Tertiary sulfide mineralization of the Essimi region. Ph.D. thesis, Univ. Athens (in Greek).

Mookherjee, A. & Philip, R. 1979. Distribution of copper, cobalt and nickel in ores and host-rocks, Ingladhal, Karnataka, India. Mineral. Deposita 14:33-55.

Raiswell, R. & Plant, J. 1980. The incorporation of trace elements into pyrite during diagenesis of black shales, Yorkshire, England. Econ. Geology 75:684-699.

Vavelidis, M., Filippidis, A., Michailidis, K. & Evangelou, E. 1989. The polymetallic ore mineralization of the Kirki area, Alexandroupolis district, Northeast Greece. Geol. Rhodopica 1:350-365.

Xuexin, S. 1984. Minor elements and ore genesis of the Fankou lead-zinc deposit, China. Mineral. Deposita 19:95-104.

Current Research in Geology Applied to Ore Deposits.Fenoll Hach-Alí, Torres-Ruiz & Gervilla(eds)(1993).ISBN 84-338-1772-8

PARAGENETIC AND FLUID INCLUSION STUDIES OF POLYMETALLIC MINERALIZATION IN THE PALAEOZOIC RIF (NORTH TETOUAN, MOROCCO)

Fkihech, A. & Fenoll Hach-Alí, P.
Dept. de Mineralogía y Petrología, Universidad de Granada, Granada, Spain

Abstract: Mineral deposits in the region between Sebta and Tetouan are dominantly hydrothermal veins rich in Co-Ni-As-(Au) and Cu-Pb-Zn-Sb-Ag. The deposits occur in a NE-SW zone parallel to the thrust contact between the Ghomarides and Sebtides tectonostratigraphic units of the internal Rif. Mineralogical and microthermometric studies suggest a deep origin for the metals, probably related to ultramafic rocks and migmatites at the base of the Sebtides. The metals were transported to higher levels in the crust by fluids that ranged in temperature from as high as 400ºC down to 120ºC and deposited the minerals through a paragenetic sequence of five stages.

Introduction and geological setting

Metallic mineralization in the Sebta-Tetouan region (N. Morocco) consists predominantly of hydrothermal deposits, mainly vein type, with complex parageneses; some are rich in Co-Ni-As-(Au) and others in Pb-Zn and/or Cu-Sb-Ag.

From a structural point of view (Fig.1), the region is

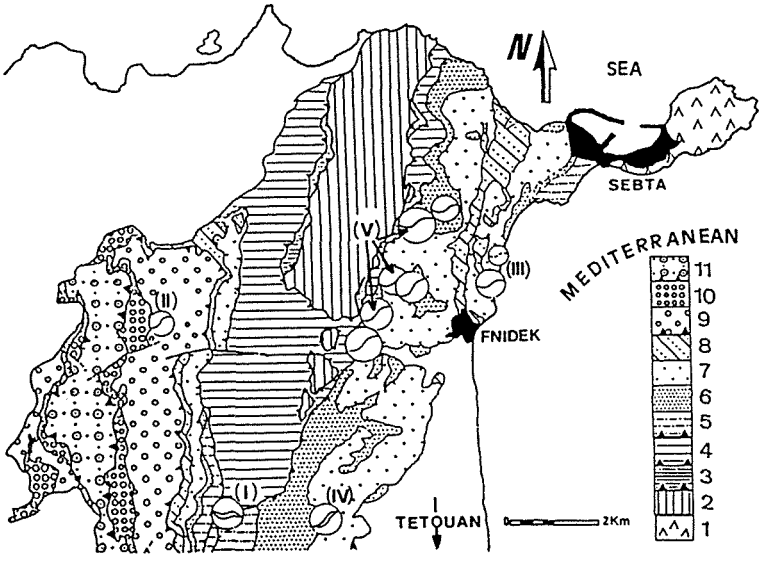

Fig.1: Geology and location of ore deposits in the Sebtides and Ghomarides tectonostratigraphic units, North Tetouan, Morocco.Sebtides: (1) Monte Hacho gneiss and serpentinite; (2) Beni-Mzala unit- schist (Permian), quartzite (Scythian), marble and dolomite (Anisian?); (3) Bouquette d'Anjera unit- schist (Permien), sandstone (Scythian), massive dolomite (Anisian); (4) Tizgarine unit- greywacke schist (Permien), quartzite (Scythian), massive calcareous dolomite (Anisian). Ghomarides: Akaïli unit- (5) greywacke schist (Silurian), (6) highly deformed limestone (Devonian), (7) flysch (Carboniferous), (8) sandstone and conglomerate (Permo-Triassic); Koudiat-Tizian unit- (9) pelitic greywacke flysch (Devono-Carboniferous), (10) sandstone and conglomerate (Permo-Triassic); (11) Beni-Hozmar unit- "flysch" (Devono-Carboniferous), sandstone and conglomerate (Permo-Triassic). Ore deposits: I) Hriyech; II) Aïn-Jir; III) Aïn-Gharnoq and Kurb-El-Hudoud; IV) Haïdra; V) Beni-Mzala district.

characterized by the superposition of two large tectonostratigraphic units, known (from lower to upper) as the Sebtides and Ghomarides, of Devono-Carboniferous to Anisian and Silurian to Permo-Triassic age, respectively. The Sebtides consist of a metapelitic sequence showing a decrease in metamorphic grade from the muscovite-biotite-kyanite or staurolite-andalusite schists and quartzites of the lower, or Beni-Mzala, unit to the phyllites of the upper, or Tizgarine, unit. The Ghomarides are comprised of three superposed thrust sheets known, from lower to upper, as the Akaïli, Koudiat-Tizian and Beni-Hozmar units. These consist of various alternating sequences of limestones, sandstones and shales or phyllites of very low metamorphic grade (Chalouan,1986; Ouzzani,1986). The thrusting of the Ghomarides over the Sebtides took place during the Oligo-Miocene, and the thrust surfaces may also have acted as faults in a complex regional extension regime after the Burdigalian (García-Dueñas et al., 1990). The Alpine metamorphism that affected the contact between the Sebtides and Ghomarides has been dated at 22 Ma by K/Ar methods (Ouazani, 1986).

The mineral deposits are mainly located in a zone close to, and parallel with, the thrust contact between the Ghomarides and the Sebtides, in a NE-SW direction. The region has also been affected by later E-W faults.The majority of the deposits (Aïn-Gharnoq, Kurb-El Hudoud, Haïdra, and Beni-Mzala) occur in rocks of Devonian or Carboniferous age within the Akaïli unit of the Ghomarides. However, the Hriyech deposit is located in a structurally lower position, in phyllites of the Tizgarine unit of the Sebtides, and the Aïn-Jir prospect is a special case in that it occurs in rocks representing a much high structural position, the Devonian Koudiat-Tizian unit of the Ghomarides.

Mineralogy and fluid inclusions

On the basis of the mineral assemblages and mineral compositions, 5 types of mineral deposits can be recognized:

Type-I : Cu-Sb-As-Co-Ni (Hriyech deposit).
Type-II : Cu-Pb-Zn-As-Ni-(Co) (Aïn-Jir prospect).
Type-III: Cu-Pb-Zn (Aïn-Gharnoq and Kurb-El Hudoud deposits).
Type-IV : Pb-Zn-Cu-Sb-Ag (Haïdra deposits).
Type-V : Sb-As-(Au) (Beni-Mzala deposits, Fnidek district).

From mineralogical and textural studies of the different mineral associations, a generalized paragenetic sequence for the deposits has been established (Fig.2) for these deposits. The first stage is characterized by the presence of pyrite and minor chalcopyrite in all 5 types of deposits, accompanied by gersdorffite and cobaltite in types I and II and by Au-bearing arsenopyrite in type V. The second stage is represented by chalcopyrite, sphalerite and galena in types II, III and IV, and by bornite in type II only. During the third stage, silver-poor tetrahedrite was deposited in types I and II, and bournonite and ullmannite in type I. Silver-rich sulphosalts (Ag-tetrahedrite, freibergite and pyrargyrite) characterize the fourth stage, but are found only in deposits of type IV. The final stage of mineralization is represented exclusively by the presence of stibnite in type V deposits.

Preliminary investigations have been made of chlorites associated with mineralization of types I and III. Temperatures calculated from microprobe analyse of chlorite associated with quartz

and pyrite, according to the 6-component solid solution model of Walshe (1986), range from 200° to 400°C for both types of deposits. More detailed studies are in progress.

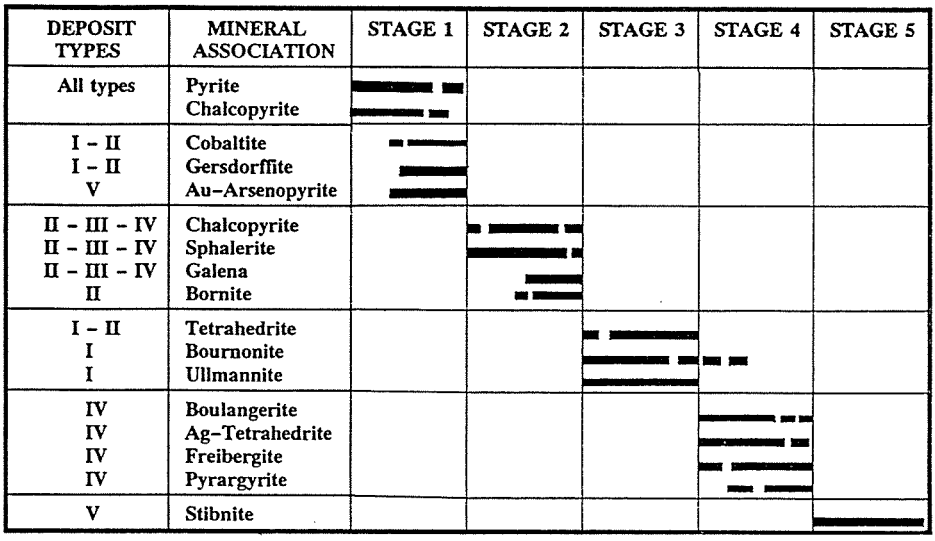

Figure 2: Paragenetic sequence of mineral deposition for deposit types (see text)

Fluid inclusion studies of quartz, calcite and fluorite demonstrate two intervals of homogenisation temperatures (viz. 120°-140°C and 230°-250°C) for 4 types of deposits. Where data were obtained on 2 minerals from the same deposit (Table 1), these temperature ranges were observed in both minerals. A third

Table 1. Fluid inclusion data (* indicates smaller number of measurements)

Deposit	(type)	Minerals	wt% NaCl equiv.	T ºC
HRIYECH	(I)	quartz	2 – 8	120 – 140 230 – 250 370 – 380 *
AIN GHARNOQ	(III)	quartz + calcite	4 – 8.5	110 –130 220 – 240
HAIDRA	(IV)	quartz + fluorite	6 – 14	120 – 140 210 – 230 *
BENI MEZALA	(V)	quartz	14 – 23	120 – 140 240 – 250 330 – 350

temperature interval (300°- 400°C) was detected only in the Beni-Mzala (type V) and Hriyech (type I) deposits. The fluid inclusions show a large range in salinity, from 2-8 wt% NaCl equivalent in the Hriyech deposit (type I), 4-8.5 wt% in the Aïn-Gharnoq deposit (type III), and 6-14 wt% in the Haïdra deposits (type IV), to 14-23 wt% in the

Beni-Mzala deposits (type V). Fluid inclusions suitable for microthermometric measurements were not found in the samples from the Aïn-Jir prospect (type II).

Conclusions

The presence of mineralization rich in Co-Ni-As-(Au) as well as assemblages of Cu-Pb-Zn-Sb-Ag minerals, in some cases in the same deposits, suggests a deep origin for the metals, possibly related to ultramafic rocks and migmatites located at the base of the Sebtides. The thrust surface between the Ghomarides and Sebtides tectonstratigraphic units may have played a role in deep circulation of the fluids, as well as their subsequent migration to higher levels, especially during the post-Burdigalian extensional tectonic phase.

During their migration towards the surface, the fluids may have undergone temporal and spatial evolution, as can be seen from the fluids inclusion data:

(1) Although not yet complete, the fluid inclusion study suggests a variation in temperature of formation between the different stages of mineralization (Table 1; Fig.2). The high temperature interval (300°-400°C) may correspond to stage 1 of the paragenetic sequence, the second interval (230°-250°C) to stages 2 and 3, and the low temperature interval (120°-140°C) to stages 4 and 5.

The preliminary temperature data for chlorite associated with the mineralization in deposits of types I and III are in agreement with this interpretation of the fluid inclusion data, in that a temperature range of 200°-400°C is indicated for stages 1 to 3 of the paragenesis (see Fig.2).

(2) The large variation in salinity of the fluids between deposits (Table 1), with values ranging from 2-8 wt% NaCl equivalent for the Hriyech deposit (type I) to 14-23 wt% for the Beni-Mzala deposit (type V) (Table 1), also reflects a temporal and spatial evolution.

References

Chalouan, A. 1986. Les nappes Ghomarides (Rif septentrional, Maroc), un terrain varisque dans la chaine alpine. Thése, Univ. Strasbourg, France.

García-Dueñas, V., Balanyá, J.C., Esteras, M., Sandoval, N., and Bahmad, A. 1990. La formación del arco de Gibraltar y su evolución tectónica neógena. III^{er} Colloque Inter. sur le Lieson Fixe Europe-Afrique a travers de Detroit de Gibraltar. Donnèes du site. Geologie. 1-21. Marrakech (Maroc).

Ouazzani-Thouhami, M. 1986. Structures et recristalisations associées dans des zones de cisaillement: nappes de Mascate (Oman) et nappes de Federico s.l. (Rif interne, Maroc). Thése, Univ. Strasbourg, France.

Walshe, J.L. 1986. A 6-component chlorite solid solution model and the conditions of the chlorite formation in hydrothermal and geothermal systems. Econ. Geology. 81:681-703.

This study has been supported by the Research Group 4028 of the Junta Andalucia and by the DGICYT Project PB-0107 We are grateful to Dr. Ross A. Both (University of Adelaide) for his assistence in traslating the original text.

Current Research in Geology Applied to Ore Deposits.Fenoll Hach-Alí, Torres-Ruiz & Gervilla(eds)(1993).ISBN 84-338-1772-8

GEOCHEMISTRY AND ORIGIN OF THE EMERALD DEPOSITS OF COLOMBIA

Giuliani, G. (1); Cheilletz, A. (2); Sheppard, S.M.F. (3) & Arboleda, C. (4)
(1) ORSTOM et CRPG, BP 20, 54501 Vandoeuvre, France
(2) ENSG et CRPG, BP 20, 54501 Vandoeuvre, France
(3) ENS, 46 Allée d'Italie, 69364 Lyon, France
(4) Mineralco, S.A., Calle 32, nº 13-07, AE 17878, Bogotá, Colombia

Abstract. The emerald deposits of Colombia are related to huge hydrothermal fluid infiltration vein networks which develop an intense sodium and carbonate metasomatic halo within the enclosing black shales. Leaching of major (K,Al, Si,Ti,Mg,P), trace (Ba,Be,Cr,Rb, Sc,U,V,B,C) and REE elements from black shales is accompanied by their partial redistribution as in-filling vein-system minerals. Oxygen isotope geochemistry of the hydrothermal carbonates and quartz indicates a strong enrichment in $\delta^{18}O$ of the waters in equilibrium with the mineralization ($+10 < \delta^{18}O\ H_2O < +18‰$), which correspond to metamorphic or basinal formation waters. The proposed model of emerald genesis involves a local sedimentary origin for beryllium and a metamorphic origin for the fluids.

INTRODUCTION

The emerald mineralization of Colombia consists of carbonate-pyrite breccia, veins, veinlets and pockets which are hosted by Lower Cretaceous black shales (BS). The ore formation is complex and involves a multiple stage process by the way of moderate temperature (300°c) fluid transfers through the sedimentary pile at 32-38 Ma (Cheilletz et al., 1993) without magmatic manifestation. The origin of the mineralizing fluids and the source of beryllium has been long time debated. A strong convergence appears concerning the removal of beryllium from the hosting-BS (Beus, 1979; Kozlowski et al., 1988; Giuliani et al., 1990a; Ottaway and Wicks, 1991) but not yet proved.

The purpose of this paper is to add new geological and geochemical constraints to the emerald-forming process, particularly concerning the behaviour of major, trace and rare earth elements (REE) during fluid-rock interactions and to discuss the probable origin of the hydrothermal fluids through O-isotope geochemistry of gangue minerals as quartz and carbonates.

GEOLOGICAL SETTING

The Colombian emerald deposits are located within two narrow belts of the eastern Cordillera Lower Cretaceous sedimentary formations. The eastern belt includes the mining districts of Gachalá and Chivor, and the western belt, the districts of Coscuez, Muzo and La Palma-Yacopí. The mineralization is hosted by breccias, shear faults and tension gashes with hydrofracturing (Giuliani et al., 1990b) acting as a major process of the fracture-system development. The hydrothermal fluid circulation is accompanied by an intense fluid-rock interaction and metasomatic alterations of the enclosing BS (Baker, 1975; Beus, 1979; Giuliani et al., 1990b) consisting in carbonatization, albitization and pyritisation halos developed around the emerald-bearing carbonate vein network. The carbonate and pyrite infilling of the vein system has been divided into three successive stages: (I) white fibrous calcite with cubic pyrite, albite and green micas, (II) rhomboedral-white to grey calcite or dolomite with cubic or dodecaedric pyrite, albite and quartz, (III) REE-dolomite, pyritohedral or dodocaedral pyrite, quartz, fluorite, parisite (in Muzo district). Stage III represents the main productive emerald period.

NEW GEOCHEMICAL DATA

Microscopic and X-Ray diffraction studies reveal that the BS around the mineralized zones have undergone strong carbonatization and albitization. The albitized BS (Ab BS) are composed mainly by albite (45 to 92% of the rock), micas (up to 20%), quartz (up to 19%) and pyrite (up to 10%). The calcitized BS (Ab-Ca BS) are composed by calcite and/or dolomite (5 to 55%), albite (25 to 45 %), quartz (5 to 48%) and pyrite (up to 10%). The spatial relationships between Ab BS (albitites) and Ab-Ca BS is unknown, however, the stage of carbonatization appears evidently well developed around the carbonated breccia and vein systems.

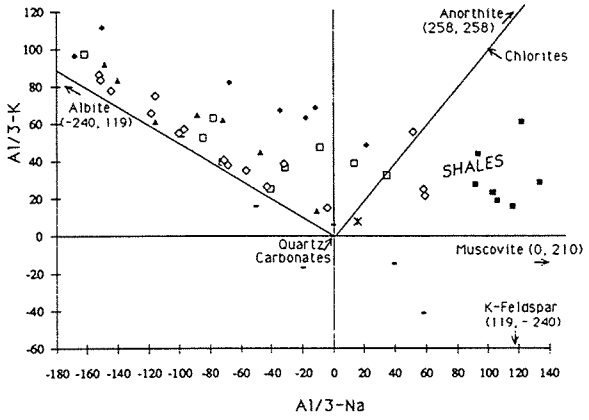

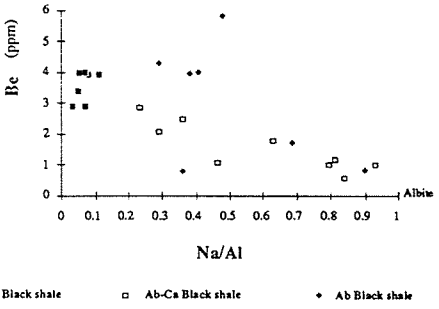

Sedimentary formations: BS; "Kaolin"

Metazomatized rocks: Ab-Ca BS; Ab BS

Breccia: B-Ab BS; B-BS; B-"Kaolin"

Figure 1-a: Al/3-K versus Al/3-Na diagram; -b: Beryllium versus Na/Al diagram for the deposits of Chivor, El Toro, Quipama, Tequendama, La Pava and Yacopí.

Representative rock-types of several deposits from the different mining districts were chemically analyzed by ICP spectrography at the CRPG (Vandoeuvre). The diagram Al/3-K versus Al/3-Na (Fig.1a) underlines the albitization and carbonatization trends of the BS. Breccia lies on the albite-carbonate joint confirming that albite is still precipitating with carbonates during the main ore-forming process. A geochemical major and trace elements profile realized through the mining gallery from El Toro (Gachalà district, Fig.2) shows that albitization is well developed in the immediate outer zone

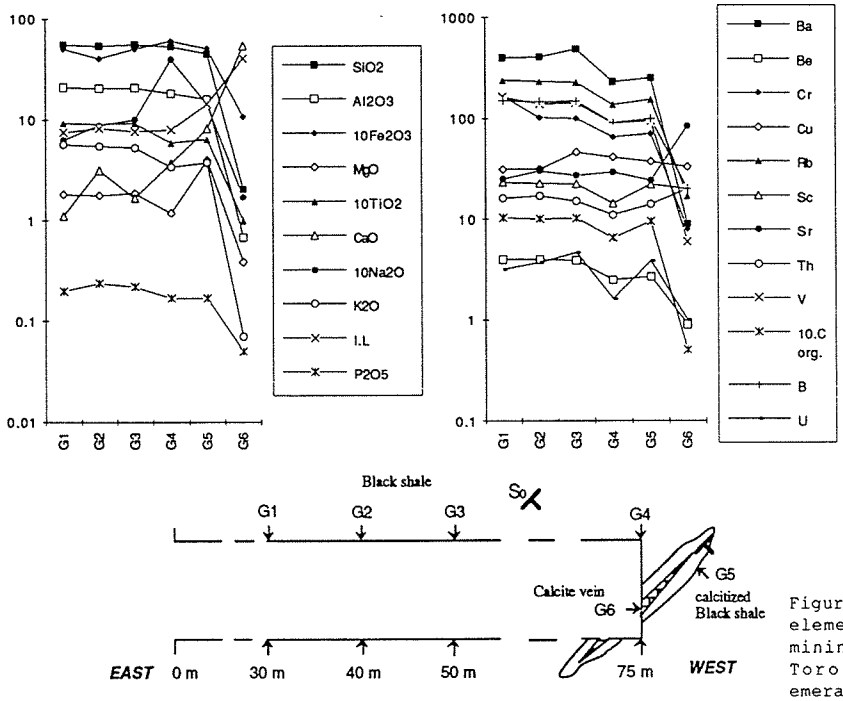

Figure 2. Major and trace elements behaviour of a mining gallery from El Toro mines (eastern emerald belt).

Sketch Map of El Toro horizontal mining gallery

(G4) of an emerald-free calcite vein (G6). In G4 zone, the increase in Na is acompanied by decreases of K, Al, Ti, Si, Mg and P from the BS (density BS= 2.45; ds Na-Ca BS= 2.44); G5 shows an increase of Ca and Mg relatively to G4. Comparison of trace elements distribution in the BS and within G4 and G5 zones (Fig 2), evidences an intense leaching of almost all trace elements from the BS with huge depletion in Ba,Be,Cr,Rb,Sc,U,V,B,Th and organic carbon. These observations can be generalized to the other emerald deposits (Giuliani et al., 1990a) with particular emphasis of *the progressive leaching of Be at the same time as the BS metasomatic albitization* (Fig.1b).

The REE behaviour during the fluid-rock interactions and the development of the metasomatic alteration halos has been particularly emphasized. The shape of the REE patterns of the Ab-Ca and Ab BS looks like those of BS. However, they are depleted in light REE (LREE), especially Ce and Nd. The REE patterns of the vein-filling minerals show (Fig.3): (1) calcite from stage II is LREE

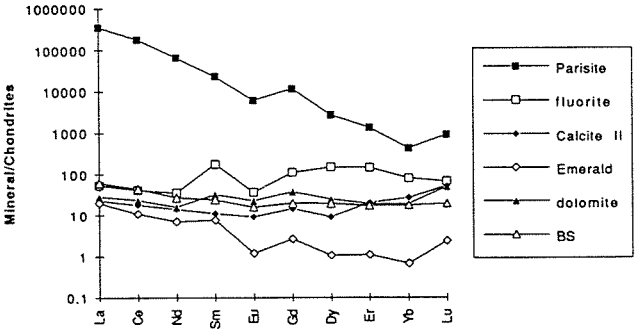

Figure 3. REE patterns of vein-filling minerals associated to the stage III of a emerald-bearing carbonate vein from Quipama mine (Cincho workings, Muzo District).

depleted relative to the BS. This behaviour is typical of calcite and dolomite from stages I and II of the whole deposits. It indicates that the solutions must have been initially LREE depleted, considering that fractionation of REE between calcite and brine is low (Graf, 1988); (2) the parisite deposition in the coeval association of parisite, fluorite, dolomite and emerald (stage III), provokes the depletion of $\sum$REE and LREE in the fluid. In consequence, emerald and fluorite have the same Eu anomaly as parisite (Eu/Eu*= 0.30) but are both LREE depleted. Besides, fluorite is HREE enriched meanwhile emerald shows exactly the opposite pattern. Dolomite and emerald present, excepted for the Eu anomaly (Eu/Eu*$_{dolomite}$= 0.65) and their total REE concentrations, the same pattern, especially concerning the LREE.

$^{18}O/^{16}O$ ISOTOPIC GEOCHEMISTRY

Oxygen isotope studies of quartz and carbonates associated with emerald from Cincho, Coscuez, Yacopí, Tequendama and Chivor mines were realized at the CRPG (Giuliani et al., 1992). The data show a strong enrichment in ^{18}O (Fig.4).

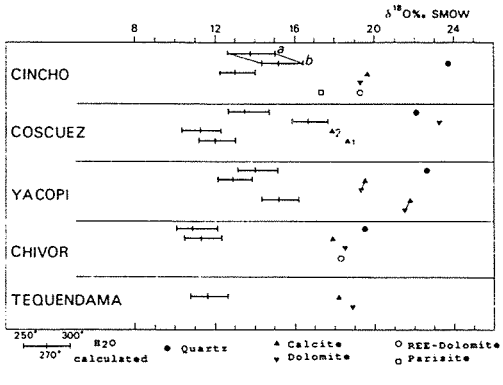

Figure 4. $\delta^{18}O$ data of the carbonates and quartz from the studied deposits. The $\delta^{18}O$ data in equilibrium with quartz and calcite are calculated at 250, 270 and 300°C. a: Fractionation factors of Bottinga and Javoy (1973), b: fractionation factor of Clayton and Mayeda (1972) applied to all the others quartz. 1= calcite stage I; 2= calcite stage II

The $\delta^{18}O$ from the different types of carbonates varies over a range of 2.2‰ for the all of the samples and appears more variable for quartz (4‰). The waters in equilibrium with the mineralization are generally enriched in ^{18}O (+10‰ < $\delta^{18}O$ < +18‰) for a temperature of formation estimated at 300°C. The calculated $\delta^{18}O$ H_2O for the different deposits yield values of metamorphic waters or basinal formation waters. In contrast, the $\delta^{18}O$ H_2O are higher than the values measured in such waters (T<150°C) and imply that the $\delta^{18}O$ is controlled by the low-temperature sedimentary origin of the metasediments. Following these results, the origin of the fluids can be considered as metamorphic.

CONCLUSIONS

The emerald deposits of Colombia are characterized by a strong fluid-rock interaction process leading to sodium and carbonate metasomatism of enclosing BS which conversely are leached in major, trace and REE elements, redeposited as in-filling vein minerals. The depletion in Al,Si,Be,Cr and V particularly evidences a wall-rock BS source for these elements recovered within the crystallochemical structure of emerald in the vein system. Therefore, a model based on a local sedimentary origin for Be can be proposed for the genesis of emerald. The origin of the hydrothermal fluids responsible of cationic transfers has been approached by oxygen isotopic measurements. The calculated $\delta^{18}O$ H_2O for carbonates and quartz indicate values of metamorphic or basinal formation waters. Considering the 300°C temperature of emerald formation, these fluids are considered to be of metamorphic origin with high $\delta^{18}O$ values being controlled by the low temperature sedimentary origin of the metasediments.

REFERENCES

Baker, P.J., 1975. Projecto de esmeraldas, informe tecnico final, Naciones Unidas-Ingeominas, COL-72/004, 71p.

Beus,.A.A., 1979. Sodium: a geochemical indicator of emerald mineralization in the Cordillera Oriental: Colombia: J. Geochem. Explor., II :195-208.

Cheilletz, A., Féraud, G., Giuliani, G. and Rodriguez, C., 1993. Time-pressure-temperature formation of Colombian emeralds: an 40Ar/39Ar laser-probe and fluid inclusion microthermometry contribution. Econ. Geol. (accepted).

Giuliani, G., Cheilletz, A. and Rodriguez, C.T., 1990a. New metallogenic data on the emerald deposits of Colombia: 8th IAGOD Symposium, Ottawa, 12-18 August 1990, Abstracts: 185-186.

Giuliani, G., Rodriguez, C.T., and Rueda, F., 1990b. Les gisements d'émeraude de la Cordillère orientale de la Colombie: nouvelles données métallogéniques: Mineralium Deposita, 25: 105-111.

Giuliani, G., Sheppard, S.M.F., and Cheilletz, A., 1992. Fluid inclusions and $^{18}O/^{16}O$, $^{13}C/^{12}C$ isotope geochemistry contribution to the genesis of emerald deposits from the Oriental Cordillera of Colombia: C. R. Acad. Sci. Paris, t. 314, II: 269-274.

Graf Jr., J.L., 1988. Rare earth element studies of Mississippi Valley type (MVT), Pb-Zn-Cu deposits in Kansas, Oklahoma and Missouri (USA).Document BRGM, 183: 75-88.

Kozlowski, A., Metz, P., and Jaramillo, H.A.E., 1988. Emeralds from Somondoco, Colombia: chemical composition, fluid inclusions and origin: N. Jahrb. Mineral. Abh., 159: 23-49.

Ottaway, T.L. and Wicks, F.J., 1991. Sulfate reduction at the Muzo emerald deposit. In: Proceedings of the International Gemological Symposium, Toronto, 27-29 May, 16: A93

Current Research in Geology Applied to Ore Deposits.Fenoll Hach-Alí, Torres-Ruiz & Gervilla(eds)(1993).ISBN 84-338-1772-8

MINERALOGY AND GEOCHEMISTRY OF THE KERCH OOLITIC IRON ORES

Golubovskaya, E.V.
Geological Inst., Russian Academy of Sciences, Moscow, Russia

Abstract. Essentially new characteristics have been proposed for the silicates of the iron ores of the Kerch deposits. The chief mineral phase is thrioctachedral Fe^{2+}-smectite, which get transformation by the contact with air oxygen to dioctachedral smectite.Geochemical specification of principal components has been defined.

The mineralogy and genesis of Kerch iron ores have been studied for many years by different scientists. However, no commonly accepted theory on the origin and mineral composition of these ores has emerged. Recently, the Geological Institute of the Academy of Sciences of Russia developed a new approach of the study of natural entities, geomineralogy, which is based on a comprehensive investigation of natural objects. It includes a description of the general "geological situation" in terms of geologic formations and facies, as a background for describing the material composition of rocks, the paragenetic mineral associations, and fine structural and crystallochemical investigations of the main minerals, whose indicator characteristics may reflect the rock formation and alteration history and geochemistry. In the present study this methodology is applied to iron ore deposits.

The Kerch iron ore deposits in the eastern part of Kerch Peninsula are an element of the extensive Niogene (Kimmerian) Azov-Black Sea iron ore province. Tectonically, the basin is connected with the Indol-Kuban trough, formed during the Neogene along the perimeter of the meganticlinorium of the Greater Caucasus and the Crimean Mountains, and along the Kerch-Taman subsidence region separating these two Alpaine structures. Ore horizons confin to the Middle Pliocene-Kimmerian.Kerch ore deposits are associated with large brachysynclinal folds and concentrate most of the commercial reserves of the basin. These are ore bodies occurring subhorizontally with dip angles of $1-3^{o}$, less often $5-7^{o}$. Three types of ore are distinguished by tradition - tobacco, brown, and caviar - each with a different morphology, chemistry, and mineralogy. Tobacco ores occur at the base of ore horizon. They are found disconformably on sand-clay coquina of a Pontian age, or conformally on Lower Kimmerian clays in central most subside parts of troughs at depths of 30-50 m. The contacts of tobacco ores with underlying rocks are sharp. Brown ores rim margins of troughs as strips and cover tobacco ores in isolated locations. They vary in thickness from 3 to 25 m. Caviar ores are found on the sides of troughs as lenses at the top of the ore bed. Toward the central parts of troughs they wedge out and are succeeded by brown varieties. The thickness of these ores is 6-12 m. The oolitic iron ores in Neogene Kerch deposits have been approached in the integrated studies. New facies have been established for all types of ores. Tobacco ores were formed in silt depressions in which different components accumulated mechanically (in iron reducing conditions): from oolites and exotic inclusions to the colloid

silico-ferruginous mass (at present the cement of ores). All above cited components got into depressions by various means. The brown ores are a polyfacies complex. The main role is played by the deposits of high-energy environments, submarine barriers and bars, in which oolitic sands were accumulated, and subfacies of ferruginous beachrocks formed at the interface of the subaquatic and subaerial environments, under the influence of ferruginous solution on the organic sandy clays accumulation. The caviare ores, on the whole, are the deposits of nearshore sandy fields, at times and in places flooded by water. The regression evolution of the Kerch iron ores basin has been shown to reflect the change of facies from marginal (silt depression) to nearshore to subaerial. These modifications of facies are reflected by the definite position of various genetic types of ores in this row. The original sedimentological model was suggested for the Kerch deposits. The indicator minerals were determined and mineral associations systematized for the main facies-genetic types of ores. The tobacco ores have the following series of characteristic minerals: Fe^{2+}-Fe^{3+}-allophane, trioctahedral Fe^{2+}-smectite, anapaite, vivianite, olygonite, and pyrite. The brown ores: dioctahedral smectite (nontronite and Fe-Al-beidellite), berthierine, Fe^{3+}-allophane, hydrogoethite, oxides of manganese, siderite and also the group of phosphates: mitridatite, picite, kerchenite, bosphorite. The caviare ores: dioctahedral smectites (nontronite, Fe-Al-beidellite), hydrogoethite, oxides of manganese (bernessite, todorokite, vernadite) in the cement and clastics of ores, and rhodochrosite. New characteristics have been proposed for the silicates of the tobacco ores of these deposits. We disagree with the wide spread view-point about the main role of chlorite minerals in the Kerch ores. The chief mineral phase is the trioctahedral Fe-smectite, which was altered by its contact with air oxygen to the dioctahedral smectite.

We should note that Fe^{2+}-containing trioctahedral smectite has been discovered in sedimentary iron ore deposites for the first time. It exists due to the presence of organic matter, which creates a reductive environment and functions as a sort of buffer, shielding Fe^{2+} from oxidation. The existence of this smectite in tobacco ore was established by applying, for the first time, specimen conservation in argon during field sampling. Argon creates an inert medium and prevents the rock from oxidation. The nature of the organic matter, the forms in which it is found, and the causes of the reductive setting {for Fe^{2+}} in fossil condition are subjects for future study, but it is possible that these factors {as well as the presence of organics in the interlayer space of smectites} are associated with the influx of hydrocarbon gases, since the iron ore deposits are situated in an area of oil and gas shows and mud volcanos.

Differential analysis has been performed indicating the chemical minor elements distribution in different facies types. Geochemical specification of principal components has been defined. In all the above types, phosphorus, arsenic, lead and zinc have been shown to directly correlate with iron, and cobalt - with manganese.

The matrix in all ores types shown an average contents of all elements which is approaching the clarke value. Tobacco ores for-ming in silt basins show higher phosphorus, arsenic, lead and co-balt contents; caviare and brown ores accumulating in the nearshore

contain more nickel, manganese and rare earth elements (yttrium, ytterbium).

All types of ore oolites enriched by phosphorus, arsenic, lead, zinc, molybdenum and poor in vanadium, chromium and nickel. The clarkes of concentrations of titanium and gallium are always less than 1; their average value is 0,4. However, the oolites present in brown and caviare ores are generally enriched by manganese and iron, while in fragments of clay-ferruginous rocks of these ores are enriched by vanadium, titanium and gallium.

Hence,the geochemical characteristics may reflect the facies-genetic environments through the contents and specific distribution of minor elements. Substantial differences existing in geochemical specialization of brown and caviare ores do not allow us to agree with the wide spread concept of their formation and to treat them as the products of tobacco ores alteration to accompany their oxidation.

Tsipursky,S.I.& Golubovskaya, E.V. 1989. Smectites of the tobacco ores of the Kerch deposits. Litologiya i Polezn. iskop., 2:58-73.

Current Research in Geology Applied to Ore Deposits. Fenoll Hach-Alí, Torres-Ruiz & Gervilla (eds)(1993). ISBN 84-338-1772-8

METALLOGENY OF THE Zn-Pb DEPOSITS OF THE SOUTHEASTERN REGION OF THE PICOS DE EUROPA (CANTABRIA, SPAIN)

Gómez-Fernández, F. (1); Mangas, J. (2); Both, R.A. (3) & Arribas, A. (4)
(1) Apdo 261, Torrelavega, 39300 Cantabria, Spain.
(2) Dept. de Física-Geología, Universidad de Las Palmas, 35080 Las Palmas de Gran Canaria, Spain
(3) Dept. of Geology and Geophysics, University of Adelaide, Adelaide, South Australia
(4) Dept. de Ingeniería Geológica, Escuela Técnica Superior de Ingenieros de Minas, 28003 Madrid, Spain

ABSTRACT: The Zn-Pb (Cu, Fe, Sb, Hg and F) mineralization in the SE part of the Picos de Europa consists of epigenetic carbonate-hosted deposits formed from moderate temperature hydrothermal fluids. The occurrence of the deposits is controlled by an association with faults and dolostones. Stable isotope data suggest that the mineralizing fluids were derived from formation waters of the sediments of the Pisuerga-Carrión region and that the sulphur was of crustal origin. In the Permian, possibly during an extension tectonic phase, these fluids migrated through late-Hercynian fractures to deposit the mineralization in the Picos de Europa region.

GEOLOGICAL SETTING

The Cantabrian Zone, described by Lotze (1945), has been subdivided into 5 structural regions by Julivert (1971). The mineral deposits included in this study are located in the Picos de Europa region, near the overthrust boundary with the Pisuerga-Carrion region. The stratigraphic sequence consists of several units made up mainly of Carboniferous limestones. These units were repeatedly thrust faulted, so that the region has an overall imbricated structure. Another important tectonic feature is the late-Hercynian subvertical fault system which strikes N105-120E and gave rise to the block tectonics in the area. A process of dolomitization, affecting large volumes of rock of the lower structural units and smaller volumes of upper units, preceded the formation of the Zn-Pb deposits (Gómez-Fernandez, 1992).

MINERALIZATION

Zn-Pb (Cu, Fe, Sb, Hg and F) mineralization in the SE part of the Picos de Europa is represented by a large number of mines and smaller occurrences, the most important being the Aliva and Andara mines. These are relatively small carbonate-hosted deposits (the Aliva mine produced 600,000 tons of ore at an average grade of 13% Zn and 2% Pb) showing many similarities to those of the Mississippi Valley and the Irish types. The mineralized bodies are located close to late-Hercynian faults, generally on the southern side of the principal faults that affect both the Caliza de Montaña and the Picos de Europa Formations. The geometry of the mineralized bodies is controlled by the presence not only of fractures but also of dolostones.

Two types of mineralization have been observed in most of the deposits. Type I mineralization consists of granular sphalerite, galena, dolomite and calcite, with minor amounts of chalcopyrite, tetrahedrite and pyrite. This mineralization has granular, laminated and botryoidal textures. Type II mineralization is characterized by yellow sphalerite, with galena and calcite and minor amounts of dolomite, pyrite and quartz. Large crystals of type II sphalerite and galena are quite common. Associated with this type of mineralization is fluorite that was deposited at a later stage. The mineralization of both types is accompanied by graphitic matter, as well as sericite,

microcrystalline quartz and carbonate minerals that were formed as a result of hydrothermal alteration of the host carbonate rocks.

Type II mineralization post-dated type I and the two types essentially represent the two principal depositional phases shown in Figure 1. Following these two phases, late stage dolomite, calcite, galena, pyrite and fluorite were deposited, and subsequently hydrozincite, azurite, malachite, chalcocite, aurichalcite, cinnabar and Fe oxides were formed by supergene alteration.

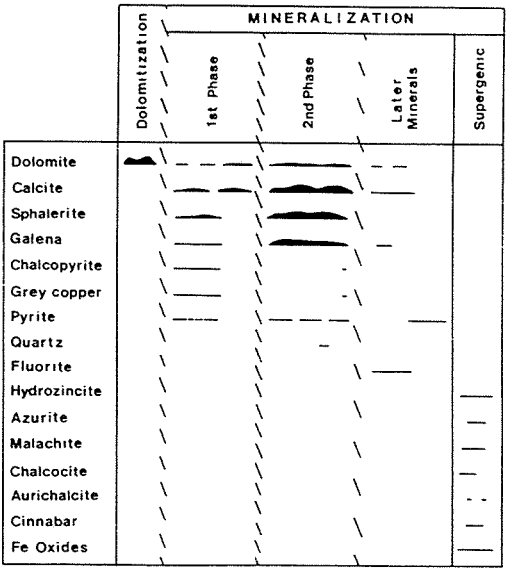

Figure 1. General paragenesis of the deposits.

GEOCHEMISTRY

Fluid Inclusions

A study has been made of fluid inclusions in minerals from Aliva (sphalerite I, dolomite I, sphalerite II, calcite II and fluorite) and Andara (sphalerite II). Microthermometric measurements and X-ray microanalysis of frozen inclusions show that the trapped fluids belong to the H_2O-NaCl system, with low concentrations of other salts in solution. The inclusions show the following phase changes: Tn= -50^{o} to -75^{o}C, Te= -45^{o} to -55^{o}C, Tm ice= -4^{o} to -21.3^{o}C, and Th= 80^{o} to 175^{o}C. Taking into account field evidence and the mean value for the mineralizing solution (Th= 150^{o}C and salinity = 15 wt.% eq. NaCl), the minimum temperature corrections due to hydrostatic and lithostatic pressures would be between 20^{o} and 50^{o}C, respectively. Hence, a minimum temperature of formation of between 170^{o} and 200^{o}C is indicated for the sulphide and carbonate minerals of the two types of mineralization in the Aliva deposit, whereas the fluorite would have precipitated at lower temperatures (Th range between 80^{o} and 145^{o}C).

Rare Earth Elements

Analyses of rare earth elements in carbonates of the Aliva mine show that both the carbonate rocks hosting the mineralization and the gangue carbonate minerals within the mineralization have similar Yb/La and Yb/Ca ratios, and plot within or near the field for hydrothermal carbonates in the diagram of Parekh and Möller (1977).

Stable Isotopes

$\delta^{13}C_{PDB}$ values of the host carbonates of the Aliva mine vary from 2.7 to 5.5 per mil and $\delta^{18}O_{SMOW}$ values vary from 13.9 to 22.6 per mil. These $\delta^{18}O$ values are considerably lower than those expected for sedimentary carbonate rocks of Carboniferous age (Veizer and Hoefs, 1976).

Carbon and oxygen isotope analyses have also been made of gangue carbonates, as well as sulphur isotope analyses of sulphides from several deposits. The gangue carbonates have $\delta^{13}C_{PDB}$ values between 1.0 and 2.9 per mil and $\delta^{18}O_{SMOW}$ values between 11.5 and 16.2 per mil. $\delta^{34}S$ values of sphalerite and galena range from −9.3 to 12.9 to per mil for type I and from −4.8 to 4.2 for type II. For each deposit sampled, the mean $\delta^{34}S$ values of type II sphalerite and galena are lighter than those of type I.

DISCUSSION

By consideration of the geochemical data together with information provided by the paragenesis, the formation conditions of mineralization in the Aliva mine can be deduced. Taking the mean temperature for deposition for both types of mineralization as 170°C, a relatively low pH for the fluid (approximately 4.3 ±1) is indicated by the presence of sericite as a wallrock alteration product associated with both types. The iron contents of sphalerite indicate little variation in oxygen fugacity during deposition of each type (log fO_2 approximately −47 to −46).

Under these conditions the variation in sulphur isotope composition between the two generations of mineralization cannot be explained on the basis of a fluid with constant $\delta^{34}S$ undergoing changes in oxidation state and/or pH. On the contrary, it is apparent that $\delta^{34}S_{fluid}$ was very different during the two mineralization phases, whereas fO_2 and pH conditions were relatively constant. According to the fractionation data of Ohmoto and Rye (1979), $\delta^{34}S_{fluid}$ for the Aliva deposit would have been approximately 12 per mil during deposition of type I mineralization and approximately −0.5 per mil during deposition of type II mineralization.

The field and isotopic evidence points to a crustal origin of the mineralizing fluids, there being no evidence of involvement of magmatic fluids. The oxygen and carbon isotope data are in accordance with the fluids having been derived from formation waters of the sediments of the Pisuerga–Carrión region. It is probable that during the Permian, coinciding with the development of extension tectonics, these fluids migrated to the Picos de Europa region, ascending by way of fractures that had originated at the end of the Hercynian orogeny. During their migration to, and/or at, the site of deposition the fluids could have become enriched in isotopically light sulphur as a result of contact with biogenic sulphur (in the form of pyrite or H_2S) in organic limestone. The lower mean $\delta^{34}S$ value of type II mineralization, compared to type I, could be a consequence of greater interaction between the type II fluid and the host rocks.

The $\delta^{13}C$ and $\delta^{18}O$ data of the host carbonates demonstrate that the wallrocks underwent isotope exchange, apparently during hydrothermal activity related to ore deposition. This is further supported by the fact that the Aliva deposit host carbonates have Yb/La and Yb/Ca relations similar to those expected for hydrothermal carbonates. In Aliva, the isotopic alteration is evident not only in the proximity of the mineralization but also over a relatively large area.

REFERENCES

Gómez-Fernandez, F. 1992. Metalogenia de los yacimientos de Pb–Zn del sector sudeste de Picos de Europa. Tesis Doctoral. Universidad de Salamanca. 241 p.

Julivert, M. 1971. Décollement tectonics in the Hercynian Cordillera of northwest Spain. Am. Jour. Sci., 170: 1–29.

Lotze, F. 1945. Zur Gliederung der Varisziden der Iberischen Meseta. Geotekt. Forsch., 6: 78–92.

Ohmoto, H. & Rye, R.O. 1979. Isotopes of sulfur and carbon. In: H.L. Barnes (ed.), Geochemistry of Hydrothermal Ore deposits, 2nd ed., John Wiley, New York, pp. 509–567.

Parekh, P.P. & Möller, P. 1977. Revelation on the genesis of minerals in paragenesis with fluorites, calcites and phosphates via rare earth fractionation. In: Nuclear Techniques and Mineral Resources. International Atomic Energy Agency Vienna, pp. 353–369.

Veizer, J. & Hoefs, J. 1976. The nature of O^{18}/O^{16} and C^{13}/C^{12} secular trends in sedimentary carbonate rocks. Geochim. Cosmochim. Acta, 40: 1387–1395.

Current Research in Geology Applied to Ore Deposits.Fenoll Hach-Ali, Torres-Ruiz & Gervilla(eds)(1993).ISBN 84-338-1772-8

TEXTURES OF PODIFORM CHROMITITE, SOUTHEASTERN AUSTRALIA

Graham, I.T.; Marshall, B. & Franklin, B.J.
Dept. of Applied Geology. University of Technology. Sydney, PO Box 123 Broadway, Australia 2007.

ABSTRACT: Podiform chromitite deposits displaying a wide variety of both formational and post-formational textures occur within the southern serpentinite belts of southeastern Australia. In the past, these textures have been ascribed to primary magmatism and/or secondary tectonism. However, the formational textures within these deposits are here ascribed to the metasomatic replacement of olivine (in the dunitic host rock) by chromite. The post-formational textures reflect fracturing under high fluid pressures during substantially later serpentinisation

INTRODUCTION

The origin of podiform chromitite in alpine-type ultramafic bodies is still disputed (e.g. Lago *et al.* 1982, Johan 1986). The textures are ambiguous with many of the same textures being interpreted in terms of primary magmatism (Leblanc 1980) and secondary tectonism (Gates 1991). In the present paper, we describe and genetically interpret chromitite textures from podiform chromitite deposits from the southern serpentinite belts of NSW, southeastern Australia.

The serpentinite belts are sub-vertical, alpine-type ultramafic bodies lying within an early to middle Palaeozoic fold belt - the Lachlan Fold Belt (LFB) - and outcropping over a total linear distance of 230km. The belts are individually up to 1.2km in width and 56km in length (Franklin *et al.* 1992). The longest belt is known as the Coolac Serpentinite Belt (CSB). The ultramafic belts are composed of variably serpentinised, metamorphosed and deformed peridotite. Structural features include gross lithological and meso-scale mineral layering, fibre-vein foliations and S-C dominated shear zone fabrics.

THE CHROMITITE DEPOSITS

Textural analysis is mainly based on the well-exposed Mount Lightning Adit (MLA) and Quilter's Open-Cut (QOC) deposits (both within the CSB). The MLA chromitite has a thin (0.5 to 2m), essentially unfoliated, dunitic halo which is enclosed within a zone (approximately 5m thick) of schistose harzburgite. At the QOC deposit the podiform chromitite bodies are enclosed within a zone of schistose dunitic serpentinite which is approximately 4m thick. The serpentinite contains diffuse-margined cores of partially serpentinised, altered, massive pseudoporphyritic harzburgite. Both bodies are tabulate and dip shallowly (20° NW) whereas the enclosing harzburgite body is vertical to steeply dipping (60° WSW) and its internal primary layering (defined by varying proportions of olivine and orthopyroxene) dips 60° ENE (Graham *et al.* 1991a).

Fracture-fill minerals within the chromitites consist of lizardite, chrysotile, talc, magnesite, ferritchromit, awaruite, nickel sulphides, chromian clinochlore and within the MLA deposit, uvarovite garnet (Graham & Colchester in preparation).

TEXTURAL STUDIES

The chromitites display a wide variety of formational and post-formational textures. The relative degrees of development of both textural groupings varies from the margin (where disseminated chromitite occurs) to the core of the bodies (where massive polycrystalline chromitite occurs). It also varies as a function of the size of the bodies, this particularly impacting on the intensity of post-formational fracturing. These spatial distributions have bearing on the interpretation of the textures.

Meso-scale observations

(a) MLA deposit

The following progression from margin to core is observed: disseminated chromitite (containing up to 20% chromite), nodular chromitite (containing between 20 and 60% chromite) and massive polycrystalline chromitite (containing more than 60% chromite).

Disseminated chromitite consists of cuspate or lobate anhedral chromite grains (< 1mm to 10mm in size), with rare clots (up to 5mm in diameter) comprising aggregates of smaller chromite grains within a matrix of alumian lizardite and chrysotile 2M. Some of the chromite

grains have hollow cores. Other forms of dissemination include trains of elongate chromite grains which define planar and linear preferred orientations, and layering defined by chromite-poor and chromite-rich bands of variable grainsize.

Nodular chromitite consists of hollow, angular to sub-rounded, equant to elongate ellipsoidal chromite grains within a matrix of serpentine. The nodules range in size from less than 1mm in diameter to 7mm but the average grainsize is some 3-4mm. The nodules are evenly and closely spaced (usually less than 2mm).

Massive polycrystalline chromitite consists of highly fractured, subrounded chromite nodules ranging in diameter from 1mm to 7mm. The nodules are closely packed with less than 5% internodular space infilled with serpentine.

Post-formational features range from discrete fractures to intense brecciation. The amount of dilation is very small (from 0.5mm down to resolution limits) and they lack significant shear components.

(b) QOC deposit

Whereas formational features are well preserved in the MLA deposit, the QOC deposit is dominated by post-formational deformation textures. This is ascribed to the QOC chromitite forming small, easily disrupted lenses within sheared (S-C fabric foliation) dunite.

Formational textures which are preserved include "vein-like" bodies (up to 400mm in length and 100mm in width, but with highly variable widths over short distances) comprising aggregates of highly fractured and brecciated angular chromite grains up to 2mm in diameter.

The dominant formational texture within this deposit was probably massive polycrystalline chromitite and the dominant post-formational effect has been to turn this into a compact, cohesive crush microbreccia (Sibson 1977) consisting of highly angular, equant, fractured chromite grains up to 1mm in diameter. The contact between this massive chromitite and the host rock carries slickenlines.

Micro-scale observations

(a) MLA deposit

Formational textures comprise poor to well-developed chromite-olivine pseudo net texture progressing into poor to well-developed massive polycrystalline chromitite. This reflects the increasing chromite/olivine ratio from disseminated chromitite to massive polycrystalline chromitite at meso-scale.

Olivine inclusions (ranging in size from 100 microns to 0.1mm) in the chromite are ovoid in shape, well-rounded and usually contain tiny (<2 microns) inclusions of nickel sulphides. Both single and multiple ovoid-shaped serpentine pseudomorphs of olivine (of a similar size to the olivine inclusions) occur within the chromitites.

Post-formational textures comprise fracturing and replacement relationships. Fracturing is systematic and consists of an orthogonal pair; one striking parallel to the long axis of the orebody. The fractures have large aspect ratios (> 1000) in that they have lengths greater than 10mm and widths less than 0.001mm. Cataclasis is apparent where the fractures intersect. In the breccia and along the main fractures, pre-fracture grain boundaries can be matched across the fractures. This is consistent with no rotation of fragments and negligible shear components.

In elongate chromite grains, one fracture of the orthogonal pair parallels the elongation direction. Also, trails of fine-grained, euhedral magnetite grains parallel the elongation direction. Ferritchromit replaces primary chromite along the fractures which are commonly filled by chrysotile, talc, magnesite and secondary nickel sulphides which themselves replace earlier-formed secondary phases such as chrysotile (in fact, the long axes of the nickel sulphide grains is normal to the chrysotile vein fibres which are perpendicular to the vein walls).

(b) QOC deposit

The dominant micro-textures within the QOC deposit are of post-formational origin. The chromitites can be described as crush microbreccias with fragments ranging in size from 1mm down to sub-micron size. The angular chromite fragments have preserved their relative positions (consistent with dilation without significant rotation). Fracture-related replacement

of chromite by ferritchromit is common and the main fracture-fill mineralogy consists of chrysotile, ferritchromit, magnetite and awaruite.

DISCUSSION AND INTERPRETATIONS

Formational features

Mesoscale disseminated chromitite exhibits poorly developed chromite-olivine pseudo net texture at microscale. It occupies the marginal portions of the deposits, similar to the GR2H deposit, New Caledonia, where massive chromitite becomes more disseminated towards the footwall (Johan 1986). The microtexture could be primary magmatic with concurrent crystallisation of olivine and chromite. It is alternatively consistent with progressive replacement of olivine by chromite. Johan (1986), advocated the replacement model and despite the difficulty of transporting chromite in solution (Graham *et al.* 1991b), we support this model, since it best fits the meso and microscale textural observations.

This in turn raises the question of the origin of the olivine (the dunitic host). We again support metasomatic conversion of harzburgite to dunite (Johan *et al.* 1983) based on the presence of diffuse margined harzburgitic residuals (or cores) within the dunite. Leblanc & Ceuleneer (1992), also indicated a replacement model within the Oman ophiolite where they suggested that the dunitic host rock of a chromitite dyke was in the solid state before the chromite-forming fluid flowed through it.

Gates (1991), suggested that linear trails of chromite fragments within the chromite deposits of the State-Line serpentinite resulted from secondary shear processes. However, there is no evidence of shearing (such as rotation of fragmented chromite grains) within the lineated disseminated chromitite of the MLA deposit. These linear trails occur within "normal" disseminated chromitite. The MLA texture therefore remains a complex formational feature of uncertain genesis .

Golding (1975) proposed that the clots of chromite grains within disseminated chromitite were former polyhedra which were disaggregated by secondary tectonism. There is no evidence of preferred orientation of the clots or of the surrounding disseminated chromite, such as would support secondary tectonism. Nor is there any obvious foliation in the chrysotile-lizardite matrix. The texture in isolation could be primary magmatic, but we would explain it as a replacement heterogeneity to preserve consistency with the concept of metasomatic olivine pseudomorphed by chromite.

Olivine inclusions in chromite, hollow cores of chromite , chromite-olivine pseudo net textures and massive polycrystalline textures are all interpreted in terms of partial to complete replacement of metasomatic olivine by chromite.

The diffuse margined chromitite veins are interpreted as having formed from chromite-rich fluids migrating along fractures within the outer margins of the solid dunite, and metasomatically replacing the dunite along the fracture walls. Previous explanations have included dykes of crystal mush, magmatic replacement dykes or inhomogenous magmatic concentrations. We prefer the metasomatic replacement model above as it best describes the geometry and textures of the veins but concede that the relationship is still somewhat ambiguous.

Post-formational textures

Secondary tectonic processes have affected both of the deposits to some degree with the smallest chromitite pods being the most affected. This is simply because the smaller bodies will experience a greater stress (as they have smaller surface areas and stress is force/area). Also, the capacity to transmit stress through a body tends to decrease from the margin to the core.

Within the MLA deposit, two distinct fracture orientations occur. These two sets of fractures must have formed concurrently because they are both dilatant, show no offset effects, have cataclasis at interstices and have the same continuous fracture-fill minerals and ferritchromit alteration. Minor ductile deformation as evidenced by elongate chromite grains may belong to the same deformation event as one set of the fractures parallel the elongation direction of these grains while the other set is perpendicular to it, with both sets of fractures cutting through the grains. The fine grained magnetite trails that parallel the elongation direction of these chromite grains may also have formed during this single deformation event

or soon after it, by the invasion of hydrothermal fluids along the fractures causing partial dissolution of the chromite and precipitating out chromitiferous magnetite.

The fracturing and brecciation are due to hydraulic fracturing with only minor dilation and with little shear displacement. This requires that the fracturing occurred in a regime where $P_f - \sigma_3 > T$.

Secondary tectonism mainly comprises brittle failure concurrent with high fluid pressures and most probably equates with serpentinisation with fibrous serpentine minerals in the fracture-fill and fibre axes tracking the extensional opening.

CONCLUSIONS

The chromitite deposits of the CSB and WSB display a wide variety of textures. The formational textures form an inadequate basis for reaching definitive conclusions regarding chromitite genesis. However, evidence for the metasomatic origin of the dunite is strong, and this mitigates against the chromitite being primary magmatic. The chromitite formational textures have therefore been interpreted in terms of a metasomatic replacement model. This model is consistent with both meso- and micro-textural observations and best explains the grading of massive into disseminated chromitite. The most obvious deficiency of the model lies in the chemistry of chromium; we do not know of any fluid that will transport it over the distances that would be required, although Johan (1986) believes that it must be a reducing fluid at a temperature lower than 1050°C.

In applying this model to other podiform chromitite deposits the essential factors are: (1) the amount of replacement of olivine by chromite from the chromite-forming fluid, and (2) the duration of the ore-forming system. Any change in either of these two factors will result in a change in the zonation and geometry of the chromitite pods as well as in the formational textures.

REFERENCES

Franklin, B.J., Graham, I.T. & Marshall, B. 1992. The serpentinite belts of southern New South Wales - slices of Palaeozoic upper mantle? Geological Society of Australia Abstracts, 32:32-33.

Gates, A.E. 1991. Shear zone control on mineral deposits in the State-Line serpentinite, Pennsylvania Piedmont. Ore Geology Reviews, 6:171-184.

Golding, H.G. 1975. Relict textures of chromitites from New South Wales. Journal of the Geological Society of Australia 22:397-412.

Graham, I.T., Marshall, B. & Franklin, B.J. 1991a. Fluid-controlled formation and evolution of chromite, sulphides and PGE's in podiform chromitite in the Coolac Serpentinite Belt, NSW. Bureau of Mineral Resources Record 1990/95:25.

Graham, I.T., Marshall, B. & Franklin, B.J. 1991b. PGE remobilization, Coolac Serpentinite, Australia. In: Pagel, M. & Leroy, J.L.(eds), Source,Transport and Deposition of Metals. Proceedings of the 25 years SGA Anniversary Meeting, Nancy, 30 August-3 September, 1991, Balkema Rotterdam:619-622.

Johan, Z. 1986. Chromite deposits in the Massif du Sud ophiolite, New Caledonia: Genetic considerations. In: Stowe, C.W.(ed), Evolution of Chromium Ore Fields. Van Nostrand Reinhold New York:311-339.

Johan, Z., Dunlop, H., Le Bel, L., Robert, J.L. & Volfinger, M. 1983. Origin of chromite deposits in ophiolitic complexes: evidence for a volatile and sodium-rich reducing fluid phase. Fortschrift Mineralogische, 61:105-107.

Lago, B.L., Rabinowicz, M. & Nicolas, A. 1982. Podiform chromite orebodies: a genetic model. Journal of Petrology, 23:103-125.

Leblanc, M. 1980. Chromite growth, dissolution and deformation from a morphological view point: SEM investigations. Mineralium Deposita, 16:269-282.

Leblanc, M. & Ceuleneer, G. 1992. Chromite crystallization in a multicellular magma flow: Evidence from a chromitite dike in the Oman ophiolite. Lithos, 27:231-257.

Sibson, R.H. 1977. Fault rocks and fault mechanisms. Journal of the Geological Society, London, 133:191-213.

Current Research in Geology Applied to Ore Deposits. Fenoll Hach-Alí, Torres-Ruiz & Gervilla (eds) (1993). ISBN 84-338-1772-8

Sr-ISOTOPIC AND WHOLE ROCK GEOCHEMICAL STUDY ON THE GENESIS OF THE SCHLAINING STIBNITE DEPOSIT (AUSTRIA)

Grum, W. (1); Frimmel, H.E. (2) & Koller, F. (3)
(1) Inst. of Geosciences, Mining University Leoben, A-8700 Leoben, Austria
(2) Dept. of Geology, University of Cape Town, Rondebosch 7700, South Africa
(3) Inst. of Petrology, University Vienna, A-1010 Vienna, Austria

ABSTRACT: Data on the whole rock composition and Sr isotopic signatures of host rock, ore and water samples from the Schlaining stibnite deposit (Penninic unit, Eastern Alps) indicate a hydrothermal origin of the Sb mineralization, related to fluids convecting through faults of Tertiary age (<19 Ma). The Sb could have been either mobilized by ascending metamorphic fluids from older Sb mineralizations of Kreuzeck or Rabant type within equivalents of the Penninic "Untere Schieferhülle", or leached from tectonically overlying Lower Austroalpine unit and subsequently circulated into greater depth by descending waters.

1) INTRODUCTION

The Schlaining stibnite deposit is known for its high grade ore which is exceptionally poor in As, Hg and W. It is hosted by Mesozoic metasedimentary rocks of the Penninic unit, which is exposed in the tectonic window of Rechnitz (Burgenland, Austria). The origin of this type of Sb mineralization has been highly controversial. Hiessleitner (1952) and more recently Belocky et al (1991) compared the Schlaining deposit with those in SE-Europe and suggested a genetic relationship with the Miocene andesitic volcanism along the eastern margin of the Alps. In contrast, Nawaratne (1989) has proposed a synsedimentary origin. The aim of this study is to set some geochemical, particularly Sr isotopic, constraints on the possible genetic models for the Schlaining deposit.

2) GEOLOGICAL SETTING AND MINERALOGY

The Sb mineralization occurs within 60-80 m thick Lower Cretaceous to Upper Jurassic calcareous micaschists, with ophiolitic greenschists in the hangingwall and phyllites in the footwall. The host rocks are overprinted by greenschist facies metamorphism. Locally, relics of an earlier high pressure metamorphic event can also be found. Particularly in the eastern part of the Schlaining mine, the ore follows mainly along five parallel, sub-vertical NW-SE trending faults. Elsewhere it can also occur as stratiform layers. The stibnite is deformed in a brittle style and thus clearly postdates the Tertiary late Alpine orogenic event.

Three stages of mineralization can be distinguished (Lehnert-Thiel, 1967): (i) firstly formation of arsenopyrite and gangue quartz, followed by (ii) stibnite with very small amounts of arsenopyrite, pyrite and gangue quartz, and lastly (iii) cinnabarite and gangue carbonate. The alteration haloes around the ore bodies are up to 10 cm wide and characterized by the dissolution of calcite and the precipitation of small quartz crystals. Fluid inclusion data from Belocky et al (1991) indicate that the Sb precipitated from an aqueous solution of low salinity at temperatures between 210 and 280°C at pressures below 1 kbar. Some vapour rich inclusions indicate boiling of the solution.

3) WHOLE ROCK COMPOSITION

Whole rock analyses of the hangingwall greenschists, alteration zone and the unaltered calcareous micaschists were carried out. The greenschists show the geochemical characteristics of N-type MORB and are, therefore, a highly unlikely source of the Sb. The alteration zones within the calcareous micaschists are enriched in SiO_2 and depleted in CaO relative to their unaltered equivalents (Fig. 1). This indicates that only calcite was replaced by quartz during alteration while the other constituents, i.e. the micas, remained stable.

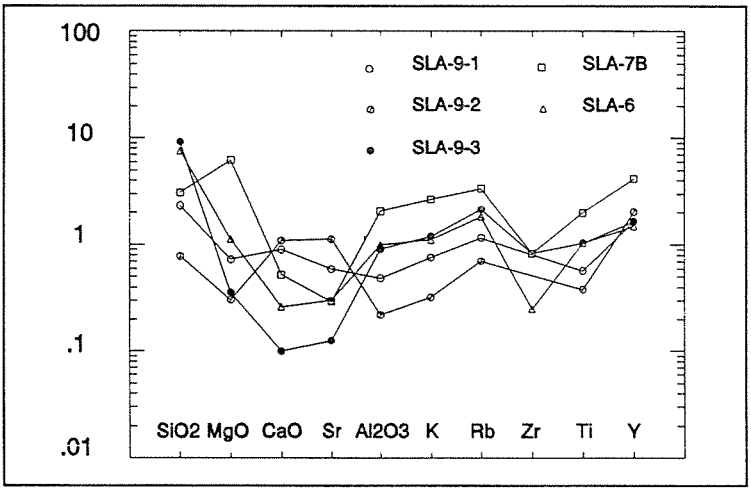

Fig. 1: Normalized element data for the investigated samples from the mining area. For normalizing values an average of calcareous micaschists from Koller (1985) are used. Sample legend: SLA-9-1 and SLA-9-2 calcareous micaschists; SLA-7B sligthly altered calcareous micaschist; SLA-6 and SLA-9-3 highly altered calcareous micaschists.

4) STRONTIUM ISOTOPES

The $^{87}Sr/^{86}Sr$ isotopic ratios of the greenschists (Fig. 2) are similar to those determined for equivalent rocks from the Tauern window (Höck & Scharbert, 1988). The values of unaltered calcareous micaschists vary between 0.707 to 0.711. The lower ratios around 0.707 are in good agreement with contemporaneous Upper Jurassic to Lower Cretaceous seawater. The higher ratios are explained by the exchange of Sr between calcite and mica during metamorphism. Calcite from the basal parts of the mineralized faults, believed to represent the isotopic composition of the mineralizing fluids, yielded $^{87}Sr/^{86}Sr$ ratios around 0.7125. These values are best explained by the interaction of metamorphic/hydrothermal fluids with the mica-rich sediments in the surroundings.

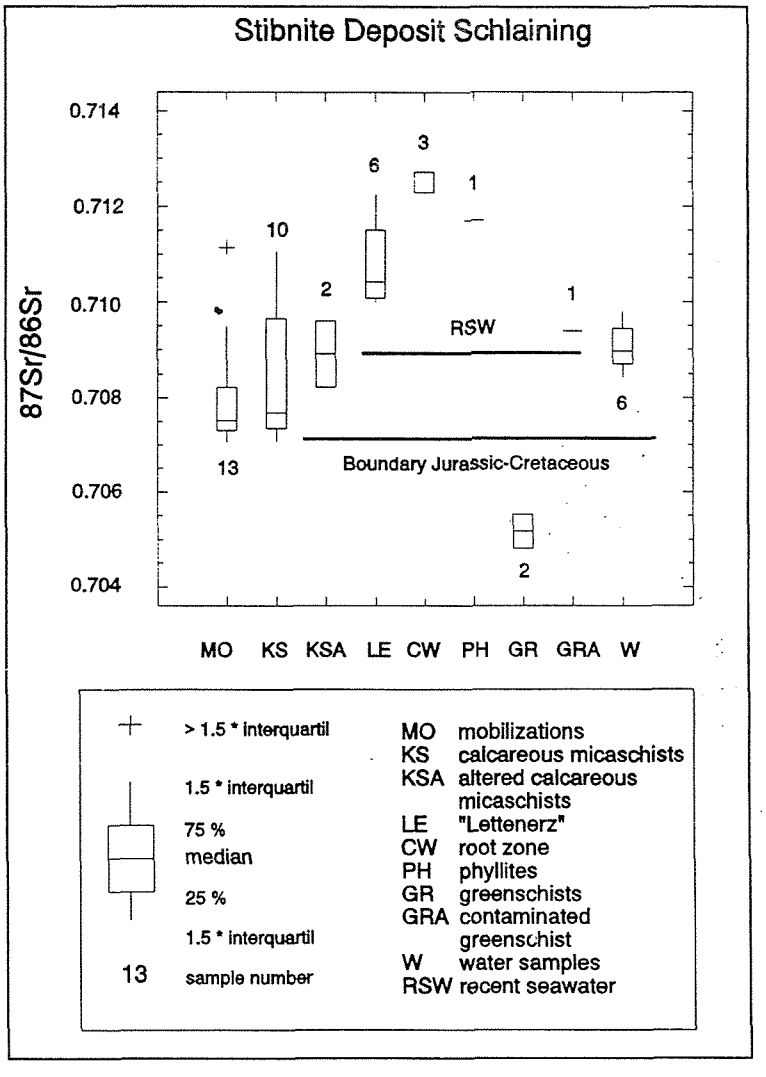

Fig. 2: Sr isotope relations of investigated samples from the stibnite mine Schlaining.

6) CONCLUSIONS

The Schlaining stibnite deposit was formed at temperatures between 210-280°C (Belocky et al., 1991) after the peak of the Tertiary metamorphic event. Cooling below 380°C after the peak of metamorphism happened between 19-22 Ma according to K/Ar ages of the micas (Koller, 1985).

Our data do not support a sedimentary Cretaceous ore formation, nor do they support any genetic link between the Sb mineralization and the Miocene andesitic volcanism in the wider region. The latter conclusion is confirmed by geophysical data which do not evidence the presence of any deep seated magmatic body in the Schlaining area (Schwendt, 1990).

In contrast, the results obtained in this study indicate that the Schlaining stibnite deposit was formed by hydrothermal convecting fluids circulating along postorogenic faults. Two genetic models are considered most likely: (i) Mobilization of a Sb mineralization of Kreuzeck or Rabant type, hosted in equivalents of the "Untere Schieferhülle" of the Tauern window, by ascending metamorphic fluids from deeper crustal levels during the waning stage of the late Alpine metamorphism. (ii) Convecting meteoric waters that have first descended into the Penninic unit after having scavenged Rb-bearing but also Sb-bearing crustal rocks from the overlying Lower Austroalpine unit, might have precipitated stibnite subsequent to cooling during their upwards path through calcareous schists of the Penninic unit.

7) REFERENCES

Belocky, R., Sachsenhofer, R.F. & Pohl, W. 1991. Neue Argumente für eine miozäne epithermale Genese der Antimonerzlagerstätte Schlaining (Burgenland/Österreich): Flüssigkeitseinschlußuntersuchungen und das Inkohlungsbild der benachbarten Tertiärbecken. Berg- u. hüttenm. Monatsh. 136:209-213

Hiessleitner, G. 1952. Serpentin- und Chromerzgeologie der Balkanhalbinsel und eines Teiles von Kleinasien. Jb. Geol. B.-A., Sb. 1, Vienna

Höck, V. & Scharbert, S. 1988. Metabasalts from the Central Part of the Hohe Tauern (Austria): Genetic implications from Sr-isotope and trace element studies. Mitt. österr. Geol. Ges., 88:151-165

Koller, F. 1985. Petrologie und Geochemie der Ophiolite des Penninikums am Alpenostrand. - Jb. Geol. B.-A. 128:83-155

Lehnert-Thiel, K. 1967. Ein Beitrag zur Paragenese und Generationenabfolge in der Antimon-Lagerstätte von Schlaining/Burgenland. - Arch. Lagerstforsch. Ostalp. 5:16-31

Nawaratne, M. 1989. Geochemical, petrological and isotopic studies related to the genesis of Antimony deposits in the Eastern Alps with special reference to the deposit of Schlaining. Unpub. thesis Vienna

Schwendt, A. 1990. Inkohlungsstudien im Tertiär des Alpenostrandes. Unpub. thesis, Leoben

Current Research in Geology Applied to Ore Deposits.Fenoll Hach-Alí, Torres-Ruiz & Gervilla(eds)(1993).ISBN 84-338-1772-8

MINERAL AND METAL ZONING OF THE LA PAZ DISTRICT, SAN LUIS POTOSI, MEXICO

Gunnesch, K.A.; Martínez, N. & Torres del Angel, C.
Universidad Autónoma de Nuevo León, Facultad Ciencias de la Tierra, Ap. Postal 104, 67700 Linares, N.L., Mexico

ABSTRACT: At La Paz two distinct zones of mineralization occur. In the western block a typical skarn mineralization is developed, consisting of Cu±Au associated to pyrite, arsenopyrite and pyrrhotite. Both endoskarn and exoskarn provide evidences of mineral zoning sequences. The eastern zone of the district is characterized by a Ag-Pb-Zn vein-type mineralization, showing vertical and horizontal metal zoning.

The La Paz district is located west of the city of Matehuala, in the State of San Luis Potosi, about 600 km north of Mexico City (fig.1). The district lies on the east flank of the Sierra del Fraile anteciine.

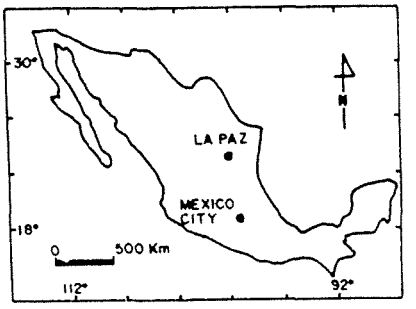

Fig.1. Location of La Paz with respect to Mexico City

The polymetallic skarn-vein deposits occur in a carbonate-dominant sedimentary sequence of Late Cretaceous. Ore related high level stocks of Oligocene age (35.7±1.0 m.y.; Tuta et al., 1988) range in composition from quartzdiorite to granodiorite, and tonalite porphyries.

Structural controls were of major importance in localizing mineralization. The Dolores- fault, which has formed later as the mineralization, divides the district in two zones, each of them showing very distinct mineralogical features (fig.2).

In the uplift Dolores-Cobriza block an endoskarn-exoskarn couplet is developed. The endoskarns are characterized by a mineral zoning toward limestone: (1) quartz + plagioclase + biotite + hornblende, (2) plagioclase + diopside ± sphene, (3) diopside + plagioclase ± calcic garnet ± calcite. The diagnostic assemblage is plagioclase + diopside, which is typical of most W skarn and

some Cu skarns (Einaudi & Burt, 1982) indicating relatively reducing conditions. Exoskarns most commonly also display a zoning sequence, consisting of: (1) calcic garnet + pyroxene + calcite, (2) calcite + wollastonite ± garnet ± pyroxene, (3) calcite + wollastonite + idocrase ± pyroxene ± garnet. These assemblages, which are characterized by the predominance of anhydrous calc-silicates, represent the initial high-temperature event of the skarn formation. Subsequently a retrograde metasomatic episode took place; the early skarn minerals were replaced by low-temperature assemblages consisting of dominantly hydrous silicates (epidote, tremolite/actinolite, clorite) and accessory calcite with ore minerals. The mineralization of Cu ± Au, associated to pyrite, arsenopyrite and pyrrhotite is generally restricted to the exoskarn. The earliest of the sulfides in the Dolores-Cobriza area, appears to be somewhat younger than the early calc-silicates of the exoskarn, e.g., grandite and diopside. On the basis of mineral paragenesis and experimental data (Barton & Skinner, 1979; Gamble, 1982) the upper temperature of deposition of earliest pyrite was of somewhere near 490° C or higher; earliest chalcopyrite was probably deposited at a temperature of at least 350° C, but possibly at 400° C or more. These data agree with our results from microthermometric studies. Primary fluid inclusions in early ore-stage quartz have homogenization temperatures of about 350° C and just over 450° C (fig.4A). All salinities reported from these inclusions have typically high values ranging from 28 to 40 equiv wt percent NaCl. Both the presence of vapor-rich inclusions and the varying liquid to vapor ratios in most of the samples suggest that trapping under boiling conditions occurred.

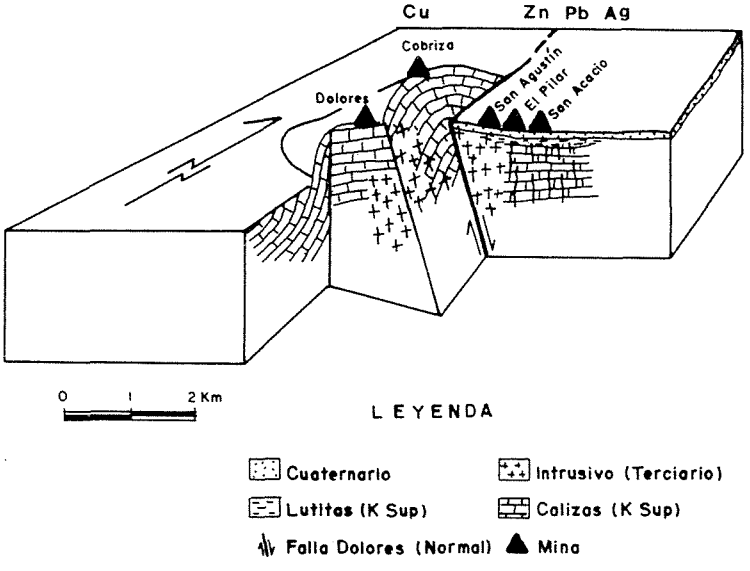

Fig.2. Blockdiagram of La Paz (modified after García Gutierrez, 1967) showing the metal zoning of the mining district

Unlike the skarn mineralization of the Dolores block, in the eastern structural zone of the district comprising the mines of San Agustín, El Pilar and San Acacio (fig.2), a Pb-Zn-Ag- vein type mineralization occurs. Metal distribution shows vertical and horizontal zonation trends. Directions of fluid movement of the mineralizing solutions were determined by combination of the data of field observations (ore mineral zoning), Ag/Pb, Ag/Zn and Zn/Pb assay metal ratios and fluid inclusion temperature zonation. Ore-bearing solutions flowed from the deeper portions in the west to the shallower levels in the east, with a remarkable lateral component. An example of metal zoning is depicted in Figure 3 showing the Ag/Zn assay metal ratio variation in a longitudinal section of the Hidalgo Vein, which is one of the main veins of the El Pilar mine.

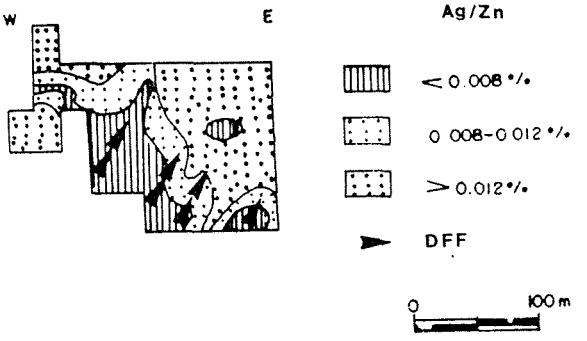

Fig.3. Longitudinal section of the Hidalgo Vein with the contours of variation of Ag/Zn assay metal ratio values (DFF = directions of fluid flow)

Fluid inclusion studies were carried out on ore-bearing quartz, calcite and fluorite. The results indicate that homogenization temperatures and salinities changed successively from west to east. In comparison with the west zone the El Pilar-San Agustín zone (fig.2) shows a decrease in both homogenization temperatures and salinities to 300° C and 20 equiv wt percent NaCl. This temperature is consistent with the sulfur isotope thermometric data of Castro (1990) who found that main-stage sphalerite and galena from El Pilar were deposited at temperatures ranging between 300° and 350° C. The lowest values are reported from San Acacio. Homogenization temperatures are below 340° C with maxima near 270° C (fig.4B), and salinities range from 5 to 20 equiv wt percent. Significantly, at San Acacio the Ag concentrations are the highest of the district. Mineralization consists of dominantly silver-bearing sulfosalts associated to galena, and with calcite as the main gangue mineral.

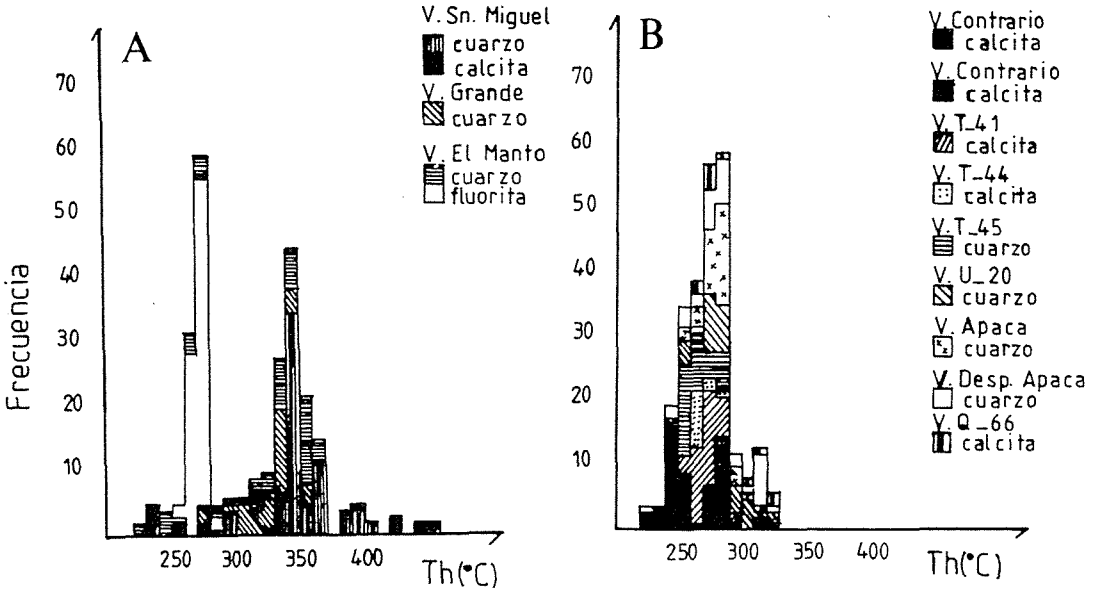

Fig.4. Summary of fluid inclusion homogenization data from ore-bearing quartz, calcite and fluorite (A, Dolores mine; B, San Acacio mine)

REFERENCES

Barton, P.B., Jr. & Skinner, B.J. 1979. Sulfide mineral stabilities. In: Barnes, H.L. (ed.) Geochemistry of hydrothermal ore deposits. Holt, Rinehart & Winston, New York, pp 278-403

Castro L., G.J. 1990. Erzpetrographische und geochemische Untersuchungen in der Ag-Pb-Zn-(Cu)- Lagerstätte von Santa María de la Paz, Matehuala, Mexiko. Dipl.-Arbeit, unpub., Univ. Karlsruhe, 85p

Einaudi, M.T. & Burt, D.M. 1982. Introduction - Terminology, Classification and Composition of Skarn Deposits. Econ. Geol. 77: 745-754

Gamble, R.P. 1982. An Experimental Study of Sulfidation Reactions Involving Andradite and Hedenbergite. Econ. Geol. 77: 784-797

García Gutierrez, C. 1967. Geología y Paragenesis del Distrito Minero de Matehuala, San Luis Potosí, México. Bol. Soc. Geol. Mex. 30: 29-62

Tuta, Z.H., Sutter, J.F., Kesler, S.E. & Ruiz, J. 1988. Geochronology of Mercury, Tin, and Fluorine Mineralization in Northern Mexico. Econ. Geol. 83: 1931-1942

Current Research in Geology Applied to Ore Deposits.Fenoll Hach-Alí, Torres-Ruiz & Gervilla(eds)(1993).ISBN 84-338-1772-8

ON THE AGE AND ORIGIN OF HYDROTHERMAL Pb-Zn-VEINS IN THE HARZ MOUNTAINS, GERMANY

Haack, U.; Leveque, J.; Friese, K.; Boness, M. & Lauterjung, J.
Inst. für Geowissenschaften und Lithosphärenforschung der Justus Liebig-Universität, Senckenbergstr. 3, D-6300 Giessen, Germany

Abstract
Isotopic studies of Pb and Sr on hydrothermal veins and possible source rocks in addition to U/Pb- and Rb/Sr-ratios as well as Rb/Sr age determinations by mixing lines showed that the veins were formed in the early Jurassic and are not connected with the intrusion of the Variscan, nearby Brocken granite. Their Pb and Sr was derived from the Paleozoic pile and not from the basement, the granite or nearby Bunter sandstone.

Introduction
The Harz Mts. are an isolated, uplifted block of the Rhenohercynian massif consisting mainly of Carboniferous and Devonian greywackes, sandstones, slates and diabases in a very low grade, almost unmetamorphic state. The Brocken granite intruded 295 Ma ago. (Schoell,1970, Eclogae Geol.Helv.63,229). Close to the northern boundary fault near Goslar the famous Devonian (Eifelian, 380Ma), syngenetic Rammelsberg deposit was mined for more than 1000 years for Pb, Ag, Cu and Zn. A great number of small, medium and large hydrothermal veins - often subparallel to the boundary fault - are mineralized with Pb, Zn and quartz and/or calcite as gafeld, Straßberg-Neudorf and the district of St.Andreasberg. Until about 10 years ago all these veins were considered as contemporaneous with the granite which was also taken as the source of the metals or at least as the heat engine which induced the circulation of the fluids. In this contribution we present evidence favouring a Jurassic age of the mineralization and an origin of Pb and Sr in the Paleozoic pile of sediments without any plutonic influence.

Pb-Isotopes
Two main groups of ore leads may be distinguished in the Harz Mts.: the lead of the 380Ma old Rammelsberg and the lead of the hydrothermal veins. Both are typical crustal leads. With only five exceptions out of 41 sampled occurrences (116 samples) all veins have the same lead with very little variation regardless of geographic position, depth, size of deposit, mineral assemblage, generation of mineral or temperature of formation. This remarkable uniformity is taken as indicating that the lead was either extracted from a very homogeneous and large source or that a hydrothermal process of regional scale homogenized the lead. This homogeneity also suggests that the various veins have about the same age.

Sr-Isotopes
It is remarkable that the Sr of the two largest deposits - Bad Grund and Lautenthal - is identical (0.713) and almost homogeneous, whereas the Sr of the smaller mineralizations differs from vein to vein and varies considerably within the same vein or district. The latter observation may indicate the influence of the different country rocks (mixing of Sr), whereas the homogeneous Sr in the large systems overwhelmed the Sr of local origin.

Source of the metals

In order to find the source of Sr and Pb it is necessary to compare the isotopic composition of these elements in the deposit with that in the presumptive source rocks at the time of deposition. In order to do this, one must measure the isotopic compositions in the veins, in the source rock and also their Rb/Sr and U/Pb-ratios as well as the age of mineralization. In Bad Grund this age is 183 Ma (see below). Recalculating the Pb and Sr of the Brocken granite, the Ecker gneiss (basement) and the Bunter sandstone from outside the Harz Mts. to this age excludes these rocks as sources of the metals. On the other hand, the isotopic composition of the Paleozoic sedimentary rocks is compatible with the hypothesis, that the Sr of the large deposits and the Pb were mobilized from the same formation which hosts the veins.

Rb/Sr- mixing age

Hydrothermally altered greywackes from the Bad Grund deposit contain inherited 2M- and newly formed 1M-illite. Grain size fractions which contain both varieties in varying proportions yield no good Rb/Sr- isochrons. If, however, the usual isochron model of interpretation is replaced by a two component mixing model, the points for the grain size fractions of two altered, former greywackes align well along two mixing lines in diagrams ($1/^{86}Sr$) vs. ($^{87}Sr/^{86}Sr$) recalculated to 182+/-12 and 184+/-10 Ma This mixing model accounts well for incomplete isotopic exchange during the hydrothermal event. The age of 183Ma is common for hydrothermal events in Europe and indicates that the time just before the final opening of the Atlantic Ocean was a time of major metallogenetic activity.

Summary

In all probability the Pb-Zn vein deposits in the Harz Mts. were formed during the early Jurassic without plutonic activity. They derived their metals from the Paleozoic sedimentary pile which hosts them. They are, therefore, intra-formational.

Current Research in Geology Applied to Ore Deposits.Fenoll Hach-Alí, Torres-Ruiz & Gervilla(eds)(1993).ISBN 84-338-1772-8

ALTERATION OF BASIC IGNEOUS ROCKS FROM THE ALMADEN MERCURY MINING DISTRICT

Higueras, P.
Dept. de Ingeniería, Geología y Mineralogía. Universidad Castilla-La Mancha, E.U.P. Almadén, 13400 Almadén, Ciudad Real, Spain

ABSTRACT: The Almaden mercury mineralizations are related to an alkaline suite of volcanic and subvolcanic rocks. All these are affected by an alteration process, characterized by the seudomorphic remplacement of the igneous minerales by: chlorite, talc, carbonates (ankerite, magnesite or siderite and calcite) and silica. In this paper, we try to sistematizate on a statistical basis this mineralogy, and to find a regional pattern of distribution of the minerals.

Almaden mercury mining district is the largest in the World, having produced one third of the total historic production of this metal. The main mines are Almaden, El Entredicho, and Las Cuevas.

The mineralizations in the District belong to several types, and have been clasified in several ways: SAUPE (1973), HERNANDEZ (1985), BORRERO & HIGUERAS (1990), ORTEGA & HERNANDEZ (1992), SAUPE (1990). All the types have in common the relationship with a magmatic suite of alkaline affinity (SAINZ DE BARANDA & LUNAR, 1989; HIGUERAS & MONTERRUBIO, 1992), which comprises basaltic pyroclastic rocks, basaltic-to-rhyolitic lavas, dolerites, and ultramafic xenoliths in the basaltic lavas, of different typologies. Figures 1 and 2 show the Nb/Y-Zr/TiO_2 diagram (WINCHESTER & FLOYD, 1977), and the REE chondrite normalizated spiderdiagram for these rocks.

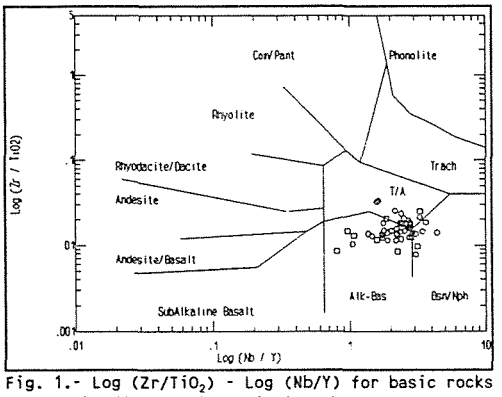

Fig. 1.- Log (Zr/TiO_2) - Log (Nb/Y) for basic rocks of the Almadén syncline. Circles: basalts. Squares: dolerites.

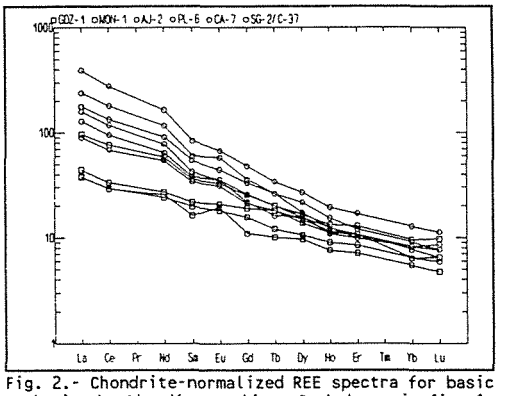

Fig. 2.- Chondrite-normalized REE spectra for basic rocks in the Almadén syncline. Symbols as in fig. 1.

Some of the basaltic lavas contain late-magmatic biotite or amphibole (brown hornblende?), suggesting a lamprophyre affinity (HIGUERAS & MUNHA, in prep.).

All the rocks in the area have suffered an alteration process, with important diferences in degree of evolution (HIGUERAS & ACOSTA, 1992). This process produces the seudomorphic reemplacement of the igneous minerals by carbonates (ankerite, calcite, magnesite and siderite), chlorite, silica, muscovite and talc. The textural characteristics of these minerals are the following:

Ankerite appears replacing all the igneous minerals, in all the

lithotypes, beenig specially common in basalts. Is also a common mineral in the filling of veinlets and vesicules.

Magnesite is only present in ultramafic xenoliths, and in one basaltic sample coming from El Entredicho mine. In both cases it is associated with ankerite in the reemplacement of olivine.

Siderite is present in the same rock types as magnesite, but they are incompatible minerals. So, for the semicuantitative study, they are considered together.

Calcite is as common as ankerite, and often appair together, as seudomorphic reeplacements, and veinlets and vesicules infillings.

Chlorite (clinocloro), like ankerite and calcite, is present in most rocks, in the same textural positions.

Silica is, in general, of micro- or cryptocristaline size. It is present in all the rock types, and in all the textural positions.

Muscovite is only present in the pyroclastic basic rocks, and it shows a characteristic green colour.

Talc is not a very common seudomorph of olivine, in the least alterated basalts.

A semicuantitative study of this mineralogy, on the basis of X Ray Diffractometry, has let an approach to the numerical characterization of the mineral secuences in the alteration process, and the setting of the main mineral associations. This has been made by Factor Analysis with Varimax rotarion, taking the semicuantitative abundances of the minerals in the mafic rocks (basalts and dolerites) as variables. The result are two rotated factors (RF), with the variables weigths graphically shown in Figure 3, and the factor scores for the samples shown in Figure 4.

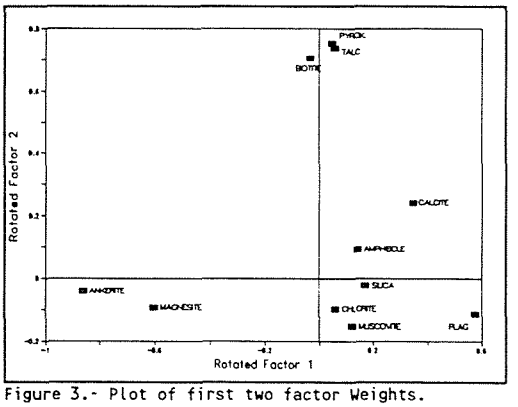

Figure 3.- Plot of first two factor Weights.

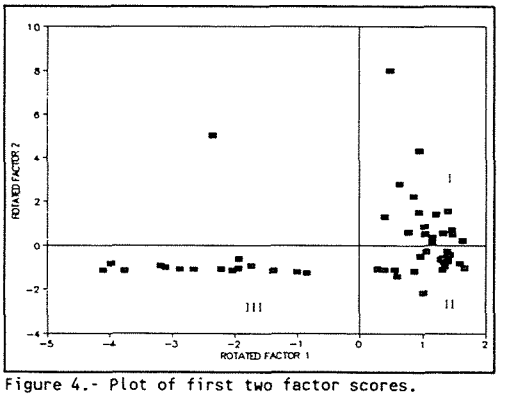

Figure 4.- Plot of first two factor scores.

Figure 3 displays the rotated factor loadings for the variables. It is clear an agrupation of them in three fields:

Field 1 clusters igneous pyroxene, talc and biotite, with high positive values for RF 2, and next-to-zero values for RF 1.

Field 2 clusters igneous plagioclase, silica, calcite, amphibole, chlorite and muscovite, with next-to-zero values for both RF.

Field 3 clusters the carbonates ankerite and magnesite (+ siderite), with high negative values for RF 1, and low negative values for RF 2.

Figure 4 shows the scores for the samples. They fall in three quadrants of the diagram: I, with positive RF 1 and 2, II, with positive RF 1 and negative RF 2, and III, with negative RF 1 and 2.

The interpretation of these data, supported by the petrographic studies, indicates that the samples in quadrant I are the least alterated, characterized by the persistence of pyroxene, the presence of talc on olivine seudomorphs, and biotite; samples in quadrant II display an intermediate degree of alteration, with plagioclase as the only relictic igneous mineral, and chlorite, calcite, silica, amphibole and muscovite as alteration products; and the samples in quadrant III are characterized by the total destruction of the igneous paragenesis, with magnesite or siderite, and/or ankerite as the main, sometimes the only, alteration products.

To study the regional distribution of the alteration, we have used the RF 1 and 2 scores for the samples to build the maps in figures 5 and 6.

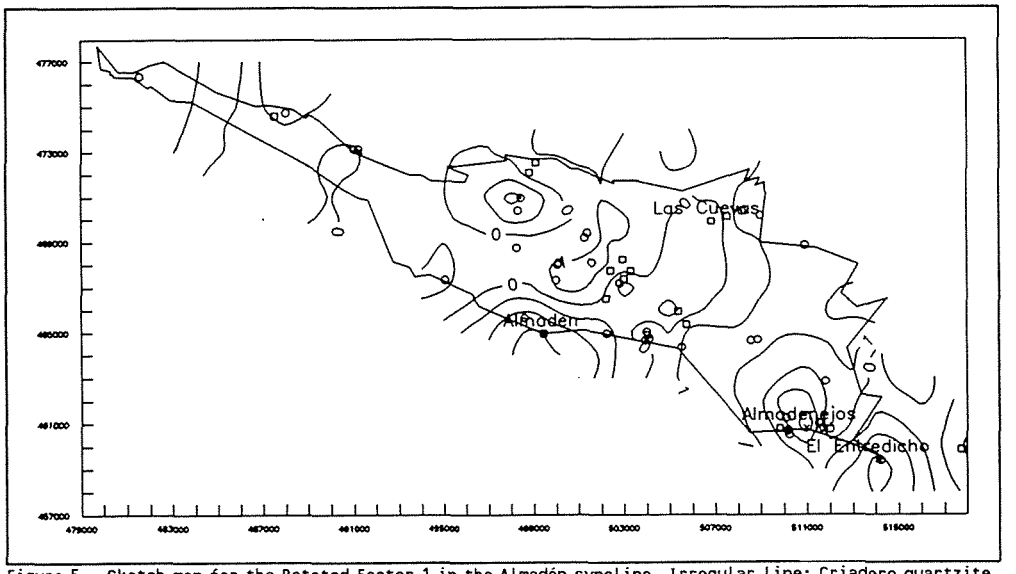

Figure 5.- Sketch map for the Rotated Factor 1 in the Almadén syncline. Irregular line: Criadero quartzite. Symbols for the samples, as in figures 1 and 2. Border: Lambert coordenates.

Figure 5 shows the map for RF1. The lowest values (i.e., the highest Fe-Mg carbonate contens) are clearly related with the main mines of the district: Almadén, Las Cuevas (both related by a NE-SW corridor of low values), El Entredicho, and Nueva and Vieja Concepción (Almadenejos). Another minimum is located north of Almadén, in an area with soils geochemistry mercury anomalys.

Figure 6 is the RF2 map. The Almadén syncline is divided by the values of this factor in three areas: Western half, with negative values; northeastern area, with high positive values, and El Entredicho area (SW corner), again with negative values.

On this basis, it can be stated a spatial relationship between the alteration and the mineralization on a regional scale. Studies on curse put forward also this relationship on a small-scale basis.

All this data support the generalization of the interpretation proposed by BORRERO & HIGUERAS (1991) for a mineralization in volcanic rocks (Corchuelo area): the alteration process is, in some way, related with the mercury mineralizations, and even can be used as a prospection guide to new mercury mineralizations in the district.

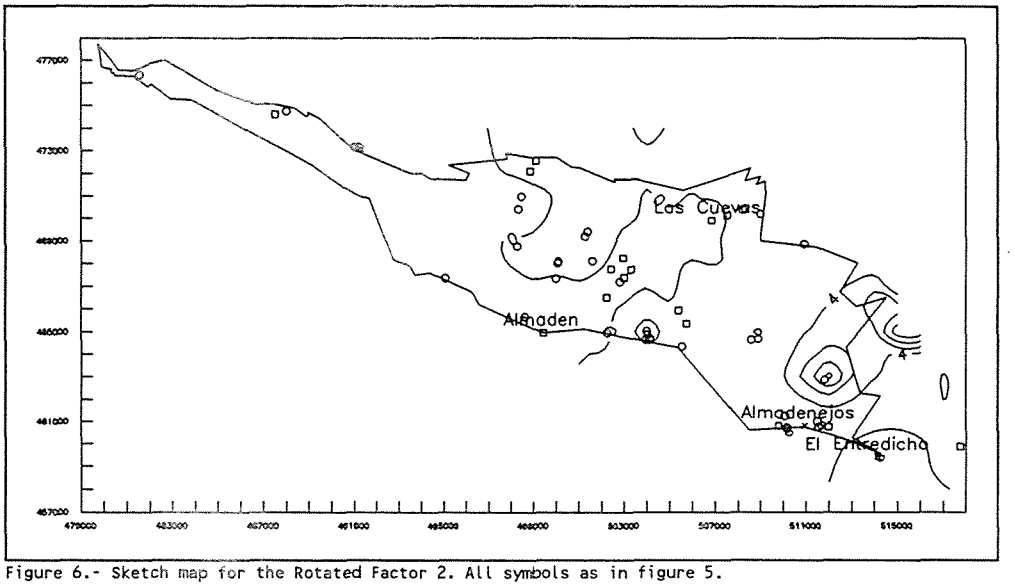

Figure 6.- Sketch map for the Rotated Factor 2. All symbols as in figure 5.

REFERENCES:

Borrero, J. & Higueras, P. 1990. Nuevos conocimientos sobre la geología y metalogénesis de los yacimientos de mercurio de Almadén (Ciudad Real). Bol. Geol. Min. 101: 872-890.

Borrero, J.; Higueras, P. 1991. Geología y génesis de las mineralizaciones de mercurio asociadas a volcanitas básicas en el sector de Corchuelo (Devónico superior del sinclinal de Almadén). Bol. Soc. Esp. Min. 14: 117-124.

Hernández, A. M. 1985. Estructura y génesis de los yacimientos de mercurio de la zona de Almadén. Ph.D. Abstract. Univ. Salamanca.

Higueras, P. & Monterrubio, S. 1992. Magmatismo y mineralizaciones de edad Silúrico en la Zona Centroibérica. In: Gutierrez-Marco, J.C., Saavedra, J., Rábano, I. (eds.) Paleozoico Inferior de Iberoamérica. C.S.I.C.-Univ. Extremadura. Madrid.

Sainz de Baranda, B. & Lunar, R. 1989. El volcanismo alcalino pre-hercínico del sinclinal de Almadén. Estudios Geol. 45: 337-348.

Saupé, F. 1973. La géologie du gisement de mercure d'Almadén (Province de Ciudad Real, Espagne). Sci. Terre, Mém 29.

Saupé, F. 1990. The geology of the Almadén mercury deposit. Econ. Geol. 85: 482-510.

Ortega, E. & Hernández, A.M. 1992. The mercury deposits of the Almadén syncline, Spain. Chron. rech. min. 506: 3-24.

Winchester, J.A. & Floyd, P.A. 1977. Geochemical discrimination of different magma series and their differenciation products using inmovile elements. Chem. Geol. 20: 325-332.

Current Research in Geology Applied to Ore Deposits.Fenoll Hach-Alí, Torres-Ruiz & Gervilla(eds)(1993).ISBN 84-338-1772-8

ORIGIN OF THE CIERCO Pb-Zn VEIN SYSTEM (CENTRAL PYRENEES, SPAIN): EVIDENCE FROM STABLE ISOTOPES, Sr ISOTOPES AND FLUID INCLUSIONS

Johnson, C.A. (1); Cardellach, E. (2); Tritlla, J. (3) & Hanan, B.B. (4)
(1) U.S. Geological Survey, MS963, Denver, CO 80225 U.S.A.
(2) Dept. de Geología, Universitat Autònona de Barcelona, Spain
(3) Dept. Cristal.lografía, Mineralogía i Depòsits Minerals. Universitat de Barcelona, Spain
(4) Dept. of Geological Sciences, San Diego State University, San Diego CA 92182 U.S.A.

ABSTRACT: The Cierco Pb-Zn vein system formed during Mesozoic time along a basin-margin fault zone. Mineral deposition took place at the interface between a shallow solution that carried marine sulfate and a brine that had scavenged base metals and Ba from Hercynian cristalline rocks at depth.

INTRODUCTION

The Cierco Pb-Zn deposits are about 10 km south of the Hercynian Maladeta Massif in the Central Pyrenees of Spain. The deposits comprise north- and east-trending veins contained within Devonian metasedimentary rocks, Permian-Triassic redbeds, and a granodiorite dike swarm termed the Bono Complex. The Bono granodiorite closely resembles and is probably related to the main Maladeta granodiorite. The Cierco district produced Pb and Zn until mining activity ceased in 1981.

The prevailing hypothesis on the origin of the Cierco deposits is that they were formed by hydrothermal activity that accompanied the emplacement of the Bono granodiorite in early Permian time (Castroviejo & Moreno, 1983). The basis for this hypothesis is the proximity of the deposits to the Bono Complex, and the orientation of the veins parallel and perpendicular to the margin of the Maladeta Massif, as if the original fractures were developed in the stress regime established by emplacement of the magma. Unfortunately, much of the genetic information that was contained in ore and host rock textures has been obscured by faulting and cataclasis that accompanied the Alpine Orogeny in Tertiary time.

In this study, we used stable isotope, strontium isotope, and fluid inclusion data to constrain both the source of the hydrothermal solutions that formed the deposits, and the source of the metals. We present a new genetic model for the deposits that may also apply to other similar deposits elsewhere in the central Pyrenees.

GEOLOGY AND MINERALOGY

The two most important veins, Solana and Rey, are a few centimeters to 3 m wide and are steeply-dipping. Sulfide mineralization is present for a strike length of 1-1.5km and extends to a depth of 300 m below the surface. The most common sulfides are galena and sphalerite (both dark- and honey-colored varieties); pyrite and chalcopyrite are less abundant. Trace amounts of bournonite, tetrahedrite, ullmanite, millerite, arsenopyrite, niccolite, magnetite, native silver, and lead

sulfosalts have also been observed (Castroviejo & Moreno, 1983). Gangue minerals are calcite, dolomite, quartz and barite. Barite is present only in the upper levels of the veins, whereas calcite is present at depth. The paragenesis is difficult to decipher because the ores have been sheared and brecciated by Alpine faulting. It is clear, however, that a period of galena+sphalerite+quartz precipitation preceeded calcite deposition. The minerals filled open spaces.

FLUID INCLUSION DATA

Fluid inclusions are <50 μm in size and are sparse, presumably due to the annealing effect of Alpine cataclasis. The inclusions contain both liquid and vapor phases. Homogenization temperatures for inclusions in sphalerite are 140-190°C (mean=170°C; n=40), and for inclusions in quartz are 140-180°C (mean=160°C; n=20). A few inclusions were found in calcite; they homogenized at 130-190°C. Eutectic temperatures for the inclusions as low as -40°C indicate that $CaCl_2$ may be present. Freezing measurements indicate that the fluids are brines with 23±3 equiv wt% NaCl.

ISOTOPE DATA

The sulfur isotopic compositions of sphalerite and galena span very small ranges and are indistinguishable in the two veins. The mean values are -0.8±0.6 permil (CDT) for sphalerite (n=24) and 4.3±0.9 permil for galena (n=25). The 3.5 permil difference between these two values corresponds to a sulfide deposition temperature of about 170°C. Pyrite averages -0.8 permil (n=2).

Sulfur isotopic compositions of barite are 13-21 permil (n=9) and oxygen isotopic compositions of the same samples are 10-15 permil (SMOW). Oxygen isotopic composition of quartz are 17-19 permil (SMOW) (n=3) and of calcite are 14-18‰ (SMOW) (n=20). Carbon isotopic composition of the same calcites are -5 to -1 permil (PDB).

Strontium isotope analyses were carried out on samples of barite and calcite. The $^{87}Sr/^{86}Sr$ values range from 0.71006 to 0.71229.

DISCUSSION AND CONCLUSIONS

The isotope and fluid inclusion data can be used to determine the composition of the hydrothermal solution(s) from which the Cierco ores precipitated. The fact that the $\delta^{34}S$ values of sphalerite and galena are (1) near zero, and (2) fairly uniform suggests that the $\delta^{34}S$ value of H_2S in the solution was itself near zero. This composition is characteristic of sulfur contained in magmas or magmatic rocks. The oxygen isotopic compositions of quartz are heavier than those typical of precipitates from magmatic fluids or from solutions that equilibrated with igneous rocks at high temperatures. The quartz compositions indicate that the $\delta^{18}O$ value of H_2O was 2-4 permil, which is several permil lighter than normal magmatic fluids and which suggests that the hydrothermal solution either (1) was a magmatic fluid that had undergone

retrograde oxygen exchange with rocks or (2) contained a meteoric water or seawater component. The strontium isotope data are incompatible with a simple magmatic origin for the ores. Cierco barites and calcites were less radiogenic at the time of magma emplacement than the Maladeta rocks (Michard-Vitrac et al., 1980). At least part of the strontium may have been derived from a less radiogenic reservoir. Candidates for this reservoir are sedimentary rocks, seawater, or connate waters.

The sulfur isotope fractionation observed between sulfides and barite is much smaller than the equilibrium fractionation at the inferred temperatures of ore formation. The barite $\delta^{34}S$ values resemble those of sulfates in Triassic marine evaporites that outcrop in northern Spain (Utrilla et al., 1992) and also extend to heavier values. The same is true of barite $\delta^{18}O$ values (Fig 1). A plausible source for the Cierco sulfate is either Triassic evaporites or connate waters contained in Triassic sediments. The barites having larger $\delta^{34}S$ and $\delta^{18}O$ values may have incorporated a small amount of sulfate produced by equilibrium oxidation of dissolved H_2S (Fig 1).

The location of the barite in the upper levels of the veins may be explained by the mixing of a downward-moving sulfate-rich solution and an upward-moving barium-rich solution. Barite precipitation occurred at the interface between the two solutions. A mixing model of this type is also consistent with the strontium isotope data. The strontium isotopic compositions of Cierco barite and calcite are intermediate between the compositions of Maladeta plutonic rocks in Triassic time and the composition of Permian-Triassic seawater-connate water (Fig. 2)

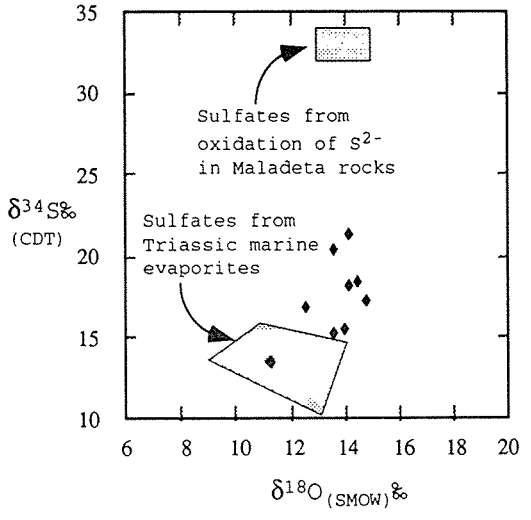

Fig. 1.- *S- and O- isotopic compositions of Cierco barites (diamonds). The data form a linear array which suggest that they are mixtures of sulfate derived from Triassic evaporites or Triassic seawater, and small amounts of sulfur scavenged from Hercynian crystalline rocks and oxidized by hydrothemal fluids.*

The $\delta^{13}C$ and $\delta^{18}O$ values of vein calcites record the waning stages of the hydrothermal system and the slowing of upward hydrothermal flow. Calcite near the intersections of veins has the heaviest compositions in both carbon and oxygen reflecting the descent of surficial waters along zones of high permeability. Temperatures probably decreased at this stage. The few fluid inclusion preserved in calcite indicate temperatures are slightly lower than for sphalerite and quartz.

We propose that ore deposition took place in Mesozoic time (probably Triassic) along a fault system of Hercynian age, reacti-

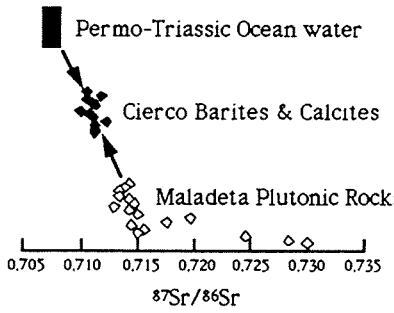

Fig.2.- *Sr-isotopic compositions of Cierco samples compared with the compositions of Maladeta rocks in Triassic time, and with the composition of Permo-Triassic seawater. The Cierco samples contain mixtures of Sr extracted from Maladeta rocks and Sr extracted from Permo-Triassic seawater/connate waters.*

vated during a period of extensional tectonism. Mineral precipitation occurred at the interface between a solution carrying marine sulfate that saturated the upper parts of a basin-margin fault zone, and a sulfide- and barium-rich brine that had scavenged sulfur and base metals from Hercynian crystalline rocks at depth. The brine was heated by an ambient, steep geothermal gradient that accompanied Mesozoic rifting. Our conclusions emphasize the importance of Mesozoic extension and basin development for Pb-Zn metallogenesis in the Pyrenees and, in combination with other studies (e.g. Cardellach et al., 1990; Canals et al., 1992), document an ore-forming process that may have operated over wide areas of southern Europe in Mesozoic time.

ACKNOWLEDGMENTS

This work was supported in part by NATO grant 910267 to C.J. and E.C. and by CICYT project PS88-0018 (Spanish Ministerio de Educación y Ciencia) to E.C.. We thank D.M. Rye for the use of his laboratory.

REFERENCES

Canals, A.,Cardellach, E., Rye, D.M. & Ayora, C. 1992. Origin of the Atrevida vein (Catalonian Coastal Ranges, Spain): mineralogic, fluid inclusion, and stable isotope study. Econ. Geol. 87:142-153

Castroviejo, R. and Moreno, F, 1983. Estructura y metalogenia del campo filoniano de Cierco (Pb-Zn-Ag) en el Pirineo de Lerida. Bol. Geologico y Minero XCIV-IV:291-320

Cardellach. E., Canals, A. & Tritlla, J. 1990. Late and posthercynian low temperature veins in the Catalonian coastal ranges. Acta Geol.Hispanica 25:75-81

Michard-Vitrac, A., Albarede, F., Dupuis, C. & Taylor, H.P., Jr. 1980. The genesis of Variscan (Hercynian) plutonic rock: inferences from Sr, Pb, and O studies on the Maladeta igneous complex, Central Pyrenees (Spain), Contrib. Mineral. Petrol. 72: 57 -72

Utrilla, R., Pierre, C., Orti, F. & Pueyo, J.J. 1992. Oxygen and sulphur isotope compositions as indicators of the origin of Mesozoic and Cenozoic evaporites from Spain. Chem. Geol. 102: 229-244

Current Research in Geology Applied to Ore Deposits. Fenoll Hach-Alí, Torres-Ruiz & Gervilla (eds) (1993). ISBN 84-338-1772-8

LEACHATE LEAD ISOTOPE STUDIES OF POTENTIAL SOURCES OF THE SOUTH PENNINE OREFIELD OF ENGLAND

Jones, D.G. (1) & Swainbank, I.G. (2)
(1) British Geological Survey, Keyworth, Nottingham, NG12 5GG, U.K.
(2) NERC Isotope Geosciences Lab., Keyworth, Nottingham, U.K.

ABSTRACT: Fluoritic MVT deposits occur in the the south Pennine Orefield in northern England. The source of the lead in the orefield has been investigated by lead isotopic studies of acid leachates from potential source rocks. HCl leachates of Viséan-Namurian shales from the basin just north of the orefield have the most appropriate Pb isotopic compositions. Leachates from the other rocks examined do not appear to be suitable sources of lead. HCl leachates of one Old Red sandstone and one Namurian sandstone have identical Pb isotopic values to the galenas, suggesting they have been mineralised by similar ore fluids. The results confirm the basin dewatering model of Plant and Jones (1989)

INTRODUCTION

The S Pennine Orefield comprises epigenetic vein, void infill and replacement Pb-Zn-Ba-F ores hosted in Viséan platform carbonates. The orefield has been classified as a fluoritic subtype of Mississippi Valley type ore deposits (Dunham, 1983).

Whole rock Pb isotopic studies (Jones et al, 1991) and a range of other evidence (summarised in Dunham, 1983; Halliday et al, 1990; Plant and Jones, 1989; Jones et al, 1991) suggest that Carboniferous basins were an important source of the mineralisation. The whole rock Pb data may not, however, be representative of the Pb available for leaching by mineralising fluids. Pb isotopic results from leaching experiments on a range of potential Pb source rocks are, therefore, reported here.

A two stage leaching process was carried out. Between 0.2 and 0.3 g of rock powder was shaken with 10 ml of 6 M HCl over a few days. The sample was centrifuged, the liquid decanted, and the lead separated from the leachate using a micro-anion exchange column in a hydrobromic acid medium. The residue was washed with milliQ water and then treated with 8M HNO_3. After centrifuging, the lead was separated as before and the residue washed. The clean residue was dissolved in HF/HNO_3 and the lead again separated.

Thirteen potential source rocks were examined, comprising Carboniferous (Viséan-Namurian) shales, Lower Palaeozoic argillites, Old Red (Devonian-Courceyan) and Namurian sandstones (Fig. 1).

RESULTS

Data for the different rock types are plotted as Fig. 2. Galena results from the south Pennines (Jones et al, 1991) are also shown.

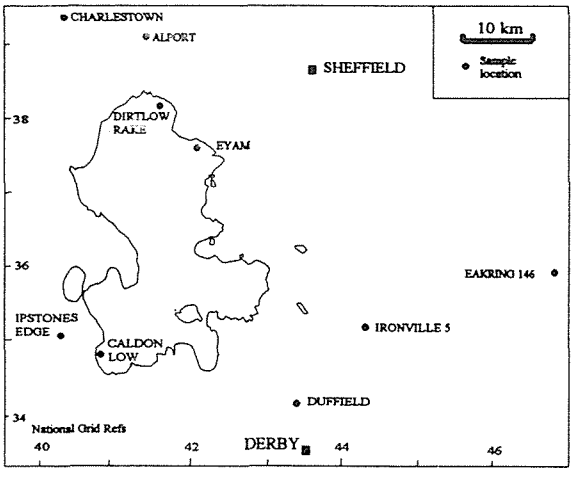

Namurian sandstones
Charlestown
Ipstones Edge

Visean-Namurian shales
Alport
Duffield

Old Red sandstones
Caldon Low
Eakring 146

L Palaeozoic shales
Eyam
Ironville 5

Line encloses outcrop of
Visean carbonate host rocks

Fig. 1 Location of samples around the S Pennine Orefield

The source rock data have been corrected to allow for the ingrowth of lead since extraction into ore fluids. A figure of 250 Ma BP was used for this correction. This lies within the age range between the host rock age (c335 Ma; Harland et al, 1989) and the youngest dates for the Pennine mineralisation based on Rb/Sr fluid inclusion ages and K/Ar and Ar/Ar altered wall rock dates (data summarised in Plant and Jones, 1989, Table 3.1). At the scale of the plots, altering this figure in the range 200-300 Ma has little effect on the uranogenic ($^{207}Pb/^{204}Pb$ v $^{206}Pb/^{204}Pb$) diagram and a negligible effect on the thorogenic ($^{208}Pb/^{204}Pb$ v $^{206}Pb/^{204}Pb$) diagram.

The choice of μ ($^{238}U/^{204}Pb$) and U/Th also affects the correction of the potential source rock data. The values used were based on the mean whole rock figures for each set of rocks and may not be valid for the leachates. The ratios in the whole rocks are fairly uniform for the Carboniferous and Lower Palaeozoic shales, but much more variable for the sandstones. Dixon et al (1990) found that most Pb in Lower Palaeozoic greywackes from Ireland was extracted using cold HCl. Assuming that much of the U would also be in easily leachable sites then μ for the whole rocks may at least be a reasonable estimate for the HCl leach. U/Th is more difficult to evaluate because of the strong chemical contrast between U and Th. The U, Th and Pb contents of the different leachates and the residues are currently being investigated.

Results for the Carboniferous shales show that the corrected HCl leachate data for the Alport samples plot very close to the early galena values. There is a decline in $^{207}Pb/^{204}Pb$ from the oldest to the youngest sample (227 to 230). A similar decline is seen in the nitric acid leachates and was observed in the whole rock data (Jones et al, 1991). The HNO_3 leachates do not match as well to the galena data. The Duffield samples do not map as closely onto the

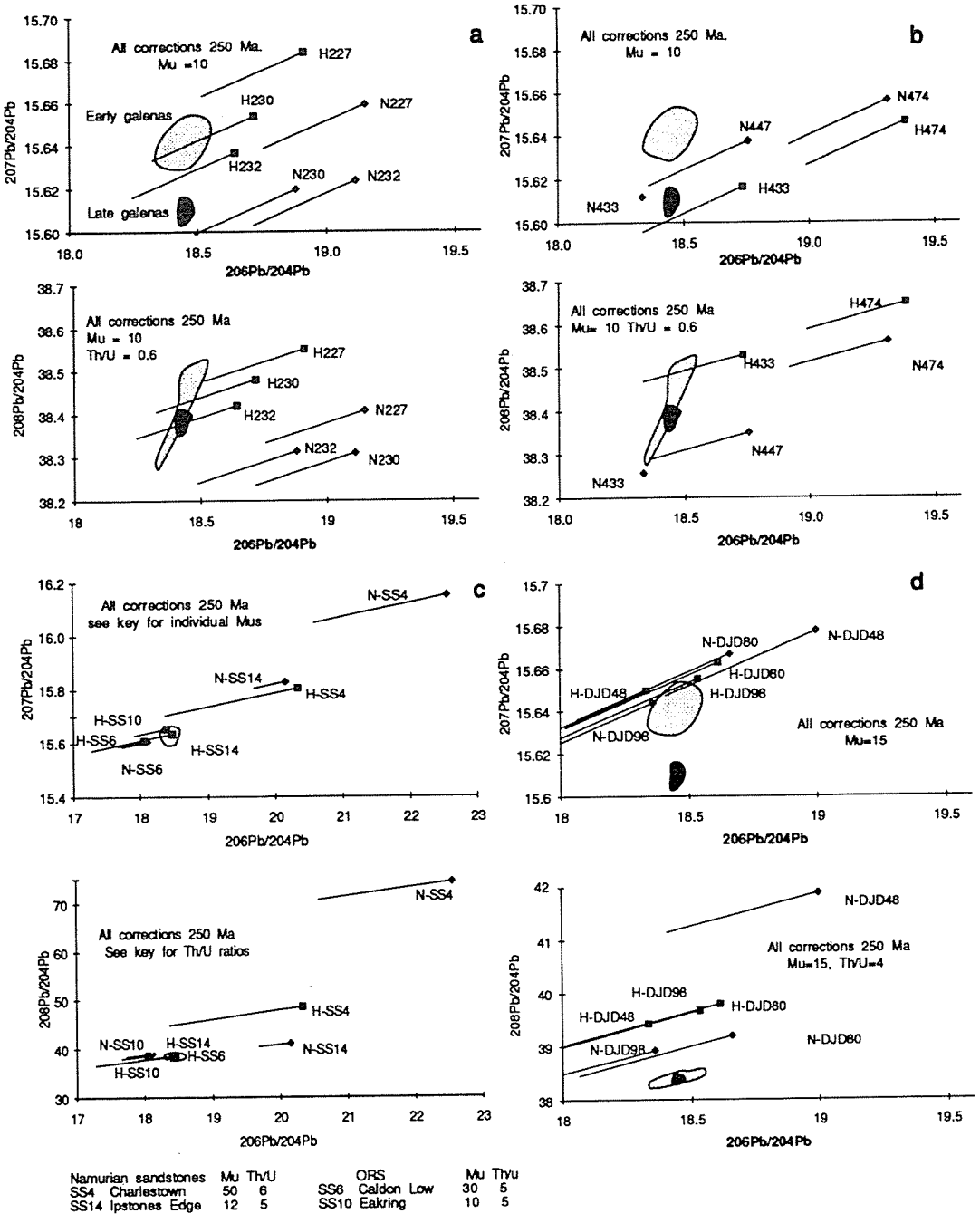

Figure 2 Pb isotope data for a) Carboniferous shales, Alport b) Carboniferous shales, Duffield c) Namurian and Old Red (ORS) sandstones d) L Palaeozoic shales. Correction lines allow for Pb ingrowth since 250 Ma. H = HCl leach, N = HNO_3 leach

galena results - one HCl and one HNO_3 leachate plot very close, the others do not. As the majority of the galena values are for samples from the north of the orefield, particularly from Dirtlow Rake, a local source of lead from the nearby Edale Basin is suggested. The trend towards lower $^{207}Pb/^{204}Pb$ with time, for both the Carboniferous shales and the galenas, indicates the possibility of the lead source becoming younger through time - consistent with progressive dewatering of higher stratigraphic units.

Only one HNO_3 leachate from the Lower Palaeozoic shales plots close to the galenas on the uranogenic diagram, whilst none of this sample group match on the thorogenic diagram, having much too high $^{208}Pb/^{204}Pb$ ratios.Hence these basement rocks do not seem, on present evidence, to be a credible source of Pb. This in contrast to the mineralisation in central Ireland, where the Lower Palaeozoic rocks are the most likely source (see for example, Dixon et al, 1990).

The Old Red sandstones mostly show lower $^{206}Pb/^{204}Pb$ than the galena and, therefore cannot be corrected to the galena compositions. An exception is the HCl leachate for SS-6 which has the same Pb signature as the galenas. One of the HCl leachates for the Namurian sandstones (SS-14) also plots within the galena field. The data suggest that the sandstones may contain traces of mineralisation comparable to that of the orefield, implying that mineralising fluids have passed through these rocks. This possibility is currently being investigated. The sandstones do not however, appear to have been significant Pb sources.

REFERENCES

Dixon P.R., LeHuray A.P., Rye D.M. 1990. Basement geology and tectonic evolution of Ireland as deduced from Pb isotopes. J Geol Soc, London, 147:121-132

Dunham K.C. 1983. Ore genesis in the English Pennines: a fluoritic subtype. In:Kisvarsanyi G, Grant SK, Pratt WP, Koenig JW (eds) International conference on Mississippi Valley type lead-zinc deposits, University of Missouri - Rolla Press, Rolla, 86-112

Halliday, A.N., Shepherd, T.J., Dickin, A.P. & Chesley, J.T. 1990. Sm-Nd evidence for the age and origin of a Mississippi Valley type deposit. Nature 344: 54-56.

Harland, W.B., Armstrong, R.L., Cox, A.V., Craig, L.E., Smith, A.G. & Smith, D.G. 1989. A geologic time scale 1989. Cambridge University press, Cambridge.

Jones D.G., Plant J.A., Colman T.B., Swainbank I.G. 1991. New evidence for Viséan-Namurian shales as the source of the Pennine mineralisation of England. In: Pagel M, Leroy JL (eds) Source, transport and deposition of metals. Procs 25 years SGA Anniversary meeting, Nancy, 30 Aug-3 Sept 1991, Balkema, Rotterdam: 309-312

Plant JA, Jones DG (eds) (1989) Metallogenic models and exploration criteria for buried carbonate-hosted ore deposits - a multidisciplinary study in eastern England. Brit Geol Surv, Keyworth, Inst Min Metall, London, 161p

Current Research in Geology Applied to Ore Deposits.Fenoll Hach-Alí, Torres-Ruiz & Gervilla(eds)(1993).ISBN 84-338-1772-8

ROLE OF RADIATION DEFECT IN MINERALS IN PROSPECTING FOR MINERAL DEPOSITS

Komov, I.L.
Inst. of Geochemistry & Physics of Minerals of Ukranian Ac. Sci. 34, Palladin Pr., Kiev, 252142, Ukraine

ABSTRACT: **Radiation mineralogy is a branch of mineralogy dealing with the problem of formation of minerals under the action of natural and artificial radiation.The investigation include:1.studies of minerals peculiarities arising around mineralization;2.effects of radiation in minerals.**

Radiation mineralogy offers considerable opportunity to search for a variety of mineral deposits viz. (a) sorting of quartz veins by ore content; (b) new methods of detecting concealed original ore bodies by color zonality; (c) determination of radioactive ore accumulations by the defects in surrounding minerals.

It is known that various deposits (rock crystal, gold, tungsten and tin) are spatially and genetically connected with quartz veins. Ionizing irradiation technique allows to sort quartz veins and surrounding blocks and to isolate ore-bearing varieties from the entire mass of quartz.

Two stages of forming productive mineralization are recognized for gold-bearing deposits and rock crystal manifestations. At the first stage quartz veins proper are developed from highly siliceous (silica-supersaturated) solutions in conditions of an abrupt equalization of thermodynamic potentials within a relatively short period of time. At the second stage ore bodies are formed.

In the second case the mineralization is related with the activity of special superposed silica-undersaturated solutions enriched with sodium, chlorine and lithium. The vein quartz from ore-bearing zones that was subjected to various changes under the action of superposed processes essentially differs from the non-ore-bearing qu-

artz. The non-ore-bearing quartz acquires a uniform smoky color under irradiation. The productive varieties show a sharp non-uniform variegated spotty and striated, usually smoky-citrine color.

Zones of metasomatic reworking accompanied by the development of a citrine color against a smoky background are pronounced in quartz. The superposition of rock crystal formation processes is recorded in the veins by the presence of solution cavities arranged along the cracks or quartz shatter zones, small quartz crystals being sometimes formed in the enclosing rocks.

Efficiency in investigations improves with a combined application of γ-irradiation and physical methods such as electron paramagnetic resonance (EPR) and thermoluminescence.

Gold- and tungsten-bearing quartz formations can be separated within the area of potential ore regions by the EPR spectra studies and γ-irradiation of quartz. This problem plays a special role in estimating gold ore deposits relative to gold evacuation from quartz ore bodies in the hypergenesis zone which distorts the estimation of their productivity. Observed in gold-bearing quartz veins is a high intensity of aluminum centers associated with the development of quartz formations under a higher activity of alkalis (sodium) in mineral-forming solutions. In these conditions Al^{3+} was concentrated in quartz substituting for Si^{4+}, the deficient charge being simultaneously compensated by sodium. In spite of O^{-}-Al centers concentration variation, observed in quartz is a distinct straight correlation between the gold and aluminum contents. The gold from hydrothermal solutions together with alkaline elements could be captured as a univalent cation Au^{+} into structural channels of quartz.

The gold content dependence of the IR absorption spectra inten-

sity responsible for the concentration of OH groups and water has been determined by applying the IR spectroscopy method for quartz studies. The water content grows as follows: non-gold-bearing quartz < slightly gold-bearing quartz < highly productive quartz. The above dependences can be used as appraising criteria for gold mineralization.

Under redeposition and migration of gold in hypergene zones, when traditional methods of analysis are ineffective, the determination of O^--Al centers concentration in quartz can be used for predictive evaluation of the deposits. The latter is of primary importance for analyzing drill cores of prospecting boreholes when single intersections of vein bodies characterized by a pronounced random gold distribution are seen.

Generally, gold-bearing quartz structures are marked by a higher intensity of O^--Al centes as compared with quartz from other formations which permits to apply this feature as a prospecting criterion in distinguishing gold-bearing quartz in areas combining gold-ore and copper-molybdenum mineralization.

Near-surface gold deposits are associated with quartz veins characterized by a diversity of morphological types, breccia textures, a wide interval of formation temperatures and spotty coloring. The spotty varieties of quartz recorded at irradiation as well as EPR data on Al-centers concentration in specimens of various genesis can serve as indicators of: (a) an additional information on conditions of quartz veins formation and of ore content thereof; (b) evaluation of vein quartz in an effort to disaggregate certain grades of quartz for production of transparent radiation-resistant quartz glass. This vein quartz is characterized by a lack of coloring under

irradiation (qualitative visual evaluation) and small concentrations of paramagnetic aluminum centers (semi-qualitative data).

The EPR method can be applied for an identification of radiation defects as rare-metal deposits are searched for. In naturally-irradiated quartz of one of the regions the concentration of radiation defects in mineralization zones is 5 to 10 times higher than the background value.

By irradiation data clearly specified is the zonality of objects, the prospects for persistence of the mineralization at depth. The estimated assessment of erosive shear depth can be conducted therewith.

A smoky color has been found to change for the smoky-cinrine and citrine one in homogeneous substratum rocks in the vertical direction while localizing veins (enclosing rocks - quartzites). These regularities can be utilized to determine the level of vein bodies erosive shear.

Current Research in Geology Applied to Ore Deposits.Fenoll Hach-Alí, Torres-Ruiz & Gervilla(eds)(1993).ISBN 84-338-1772-8

SIGNIFICANCE OF SULPHUR VALENCES IN METAL TRANSPORT AND PRECIPITATION OF MASSIVE SULPHIDES

Kucha, H.
University of Mining & Metallurgy, 30-059 Krakow, Mickiewicza 30, Poland

ABSTRACT.Compounds with mixed and intermediate sulfur valences form ubiquitous solid inclusions in banded ZnS and FeS_2.Banded sulfides grow from solutions carrying sulfur with mixed valences and euhedral sulfides precipitate from solutions having only S^{2-}. Direct intergrowths of native gold and Pd-arsenides with Fe-Pb-thiosulphates indicate a possible transport of noble metals by this sulfur ligand.

A role of sulfur in genesis of ore deposits is considered in very simplistic way.A popular notion says that only two sulfur valences occur in nature (-2) and (+6).Such a simplified approach is a result of difficulties in reliable determination of sulfur valence in microarea of ore samples.

Recent study of sulfur species diisolved in hot springs in New Zealand (Webster, 1987) indicates that more sulfur is present as thiosulphate complex than as sulfide or sulphate.Ubiquitous relics of compounds with mixed and intermediate sulfur valences were found in carbonate hosted Zn-Pb deposits in Ireland (Kucha, 1988). They appear during bacterial as well as during abiotic sulphate reduction.Similar phenomena are observed in Kupferschiefer (Kucha, 1990), where thiosulphates and minerals formed by their break-down and replacement appear in connection with banded sulfides and bacterial relics.In the last case bacterium wall is mineralized with pyrite and the inner part as well as matter cementing colony is composed of Ni-Co-As-Fe thiosulphates having an increased content of Ag and Pb.This phenomenon may document a step-wise reduction of sulfur by bacteria.Thiosulphates are also observed in carbonate-hosted Zn-Pb deposits in Belgium and Poland (Kucha & Viaene, 1993). The discussed presence of compounds with mixed and intermediate sulfur valences may explain a contradiction concerning formation of many major massive sulfide deposits at temperature range of 100 - 200°C (Roedder, 1976).At this temperature range neither bacterial nor abiotic reduction of sulphate to sulfide occurs at a

sufficient rate (Barnes, 1979; Ohmoto & Lasaga, 1982).To solve this problem and to obtain the observed sulfur isotopic signature of metal sulfides, a mechanism involving thiosulphates in solution with intermolecular exchange of S isotopes was proposed (Ohmoto & Lasaga, 1982).The ubiquitous presence of compounds with mixed and intermediate sulfur valences in the discussed deposits suggests a gradual sulfur reduction, in which each step of such reduction of S^{6+} to S^{2-} consumes only a fraction of energy required for a direct reduction of sulphate to sulfide.Therefore such abiotic reduction can take place efficiently at temperatures below 200°C.The step-wise sulfur reduction can be also responsible for isotopic fractionation of sulfur in sulfides precipitated this way.

The occurrence of intermediate sulfur valences may explain why some of the common minerals like sphalerite, pyrite and galena appear in binary mode - as euhedral crystals or as finely banded crusts overgrowing cavity walls as well as euhedral crystals (Kucha & Viaene, 1993).It is suggested that euhedral crystals are growing from the solutions where main dissolved sulfur has valence -2.Banded massive sulfides grow from the solutions where dissolved sulfur has mixed valences.In the last case ligands with mixed and intermediate valences may cause speciacion of Zn, Pb, Fe as well as trace elements being precipitated according to solubility index of given metal with given sulfur valence preveiling in the fluid.This way thick, monomineral crusts of banded sphalerite or pyrite etc. may be precipitated.Ubiquitous althogh usually small solid inclusions with intermediate and mixed sulfur valences preserved inside banded sulfides are replaced by the enclosing sulfide.Since these inclusions have finely banded structure the banding in ZnS, FeS_2 or PbS may be inherited also from a banded precursor composed of bands of thiosulphates, sulfites, sulfoxylanes etc (Kucha & Stumpfl, 1992; Kucha & Viaene, 1993).Sphalerite formed by replacement of such banded precursors has an increased content of chracteristic trace elements inheriter from the precursor phase: Ni, As, Pb, Tl and Ag (Kucha & Stumpfl, 1992; Kucha & Viaene, 1993).

Thiosulphates of heavy metals are weakly soluble or insoluble in water-eg., Pb, Ba etc (Valensi et al., 1963).However,

thiosulphates of Ag and Au (Mann, 1984) and Pt as well as Pd are soluble in water (Plimer & Williams, 1987).Threrefore this sulfur ligand can efficiently transport noble metalsat lower temperatures below 300-250°C as suggested by thermal stability of some of metal thiosulphates (Kucha & Viaene, 1993).Direct intergrowths of gold with thiosulphate occur in Comet mine,NSW, Australia, and Pd thiosulphate is present in Kupferschiefer intergrown with small specs of native gold.

Sulfur occurs in 7 major valence stages: -2 in monosulfides (ZnS), -1 in disulfides (FeS_2), 0 in native sulfur, +2 in sulfoxylanes ($CoSO_2$), +3 in subsulfites (CoS_2O_4), +4 in sulfites ($PbSO_3$; Paar et al., 1984) and pyrosulfites ($M^{2+}S_2O_5$; Latimer, 1952), and +6 in sulphates ($CaSO_4$ etc.).Sulfur valences intermediate between -1 and 0 are observed in polysulfides (Valensi et al., 1963). Sulfur also readily forms compounds with mixed valences such as thiosulphates having sulfur -2 and +6 (PbS_2O_3; Kucha, 1988).Also polythionates, $M^{2+}S_xO_6$, where x=2 to 6 have mixed sulfur valences, with average valence changing from +5 to +1.67 (Valensi et al., 1963).

Sulfur valence can be determined in the microarea of polished samples by electron microprobe because the SK_α and SK_β emission wavelength is valence dependent (Kucha et al., 1989).The SK_α wavelength difference between the sulfide S^{2-} and sulphate S^{6+} was found by microprobe to be 1.43 eV.The wavelength difference between the sulfide and sulphate for the SK_β line was measured by microprobe to be 1.78 eV (Kucha et al., 1989).The resolution of PET microprobe spectrometer of about 0.1eV is sufficient for relatively accurate determination of sulfur valences in polished sections.

The SK_β line reveals valence-related satellites on both sides of the sulfite K_β peak, and only one on the low energy side of the sulphate K_β peak.Thiosulphate shows a similar S^{6+} related satellite but half as intense as in sulphate (Kucha et al., 1989).
A fine scan of the SK_β peak top of thiosulphate reveals a double SK_β peak resolved by microprobe spectrometer and related to the presence of the sulfidic and sulphatic sulfuer.

RFERENCES

Barnes, H.L. 1979. Geochemistry of hydrothermal ore deposits.Wiley, New York, 798 pp.

Kucha, H.1988. Biogenic and non-biogenic concentration of sulphur and metals in the carbonate-hosted Ballinalack Zn-Pb deposit, Ireland.Mineral.Petrol., v 38, 171-187.

Kucha, H. 1990. Geochemistry of the Kupferschiefer, Poland.Geol. Rundschau, v 79, 387-399.

Kucha, H., Wouters, R. & Arkens, O. 1989. Determination of sulfur and iron valence by microprobe.Scanning Microscopy, v 3, 89-97.

Kucha, H. & Stumpfl, E.F. 1992. Thiosulphates as precursors of banded sphalerite and pyrite at Bleiberg, Austria.Min.Magazin, v 56, 165-172.

Kucha, H. & Viaene, W. 1993. Compounds with mixed and intermediate sulfur valences as precursors of banded sulfides in carbonate-hosted Zn-Pb deposits in Belgium and Poland.Mineral. Deposita, v 28, 13-21.

Latimer, W.M. 1952. Oxidation potentials.2nd edn., Prentice, New York.

Mann, A.W. 1984. Mobility of gold and silver in lateritic weathering profiles: some observations from Western Australia. Econ.Geol., v 79, 38-49.

Ohmoto, H. & Lasaga, A.C. 1982. Kinetics of reactions between aqueous sulphates and sulfides in hydrothermal systems.Geochim. Cosmochim.Acta, v 46, 1727-1745.

Paar, W.H., Braithwaite, R.S.W., Chen, T.T. & Keller, P. 1984. A new mineral, scotlandite ($PbSO_3$) from Leadhills, Scotland: the first naturally occurring sulfite.Min.Magazine 48, 283 -288.

Plimer, I.R. & Williams, P.A. 1987. New mechanism for the mobilization of the platinum-group elements in the supergene zone. 83-92.In: Prichard, H.M., Potts, P.J., Bowles, J.F.W., Cribb, S.J. (eds)Geoplatinum 87, Elsevier, Amsterdam, N.Y.

Valensi, G., Muylder Van, J., Pourbaix, M. 1963.Soufre.545-553.In: Pourbaix, M., Zoubov de, N., Muylder Van, J. (eds) Atlas d'Equilibres Electrochemiques a 25°C.Gauthier-Villars, Paris, 644 pp.

Current Research in Geology Applied to Ore Deposits. Fenoll Hach-Alí, Torres-Ruiz & Gervilla (eds) (1993). ISBN 84-338-1772-8

W-POLYMETALLIC SULPHIDE VEINS (SPANISH CENTRAL SYSTEM): DATA FROM FLUID INCLUSIONS AND MINERAL GEOTHERMOMETERS

López, J.A.(1); Vindel, E.(1); Boiron, M.C.(2); Cathelineau, M.(2); Sierra, J.(1) & Prieto, C. (3)
(1) Dept. Cristalografía y Mineralogía. Universidad Complutense, Madrid, Spain
(2) CREGU, BP 23, 54501 Vandoeuvre-les Nancy Cedex, France
(3) Dept. Cristalografía y Mineralogía. Universidad de Valladolid, Spain

ABSTRACT: This paper presents a multidisciplinary study, including detailed paragenetic reconstruction of the vein filling and host rock alterations, as well as P-T estimations using fluid inclusion and mineral geothermometers, of two representative W-polymetallic sulphide veins. The data document P-T-X evolution and the relationships between the sulphides and the early W stage.

The central domain of the Spanish Central System contains several W±(Sn,Mo) and Cu-Pb-Zn hydrothermal vein deposits. They present frequently multistage ore deposition which is characterized by the successive crystallization of W±(Sn,Mo) minerals and then Cu-Pb-Zn sulphides (Vindel, 1980; Quilez et al, 1990; Caballero et al., 1992). Very little is known on the condition of the sulphide deposition and their relationships with the early stage. Two representative veins, Cabeza Mediana and Collado, have been selected to depict the relationships between the different stages of fluid migration.

Fluid inclusion have been studied by microthermometry and Raman spectroscopy. Mineral geothermometry has been carried out on phengite and chlorite using crystal chemical data obtained by electron microprobe analysis.

1.- Ore and alteration stages

The W±(Sn)-polymetallic sulphide deposit from Cabeza Mediana is a vein type hosted by peraluminous leucogranites along N150° and subvertical fractures. W veins (wolframite-bearing quartz veins with minor amounts of sulphides) and S veins (sulphide-bearing quartz veins) are recognized. The Collado sulphides-quartz veins are W-free and formed along N-S extensional strike faults within monzogranites. Host rocks have been affected by the hydrothermal process in the vicinity of the lodes. Three different ore stages have been distinguished:

(1) During an early stage strong K-mica (phengite I) alteration affects the granite wall rock greisen , restricted to a narrow zone adjacent to the veins. The vein mineral assemblage is milky quartz (QI)- phengite (PhI) ± wolframite.
(2) A late crystallization of phengite (PhII) is associated with saccharoidal quartz (QII) and minor amounts of scheelite and fluorite.
(3) Chlorite-sulphide (pyrrhotite, sphalerite, chalcopyrite and galena) occur as late infillings of the early veins or veinlets 1) and 2).

2.- P-T reconstruction

Fluid inclusions in W-polymetallic sulphide veins result from successive trapping which corresponds to repeated stages of

quartz microfissuring. The same types of fluid inclusions are recognized in W and S veins:

- CO_2-H_2-NaCl-rich vapours (V_{C-W}) are scarce and present only in QI, as primary inclusions. They are characterized by a moderate density (0.5 to 0.7) and Th from 290° to 370°C (mode: 330°C (V)).
- CH_4-H_2O-NaCl-rich liquid inclusions (L_{W-m}) seem to be primary in QII and occur along healed fractures in QI. They display lower densities (0.25 to 0.70) and Th between 240° and 390°C (mode: 290°C(L)).
- L_{W-C} are (CO_2)-CH_4-H_2O-NaCl-rich liquid inclusions, displaying intermediate in ΣCH_4 contents and density (0.35 to 0.65) between V_{C-W} and L_{W-m}. CO_2 was detected only by Raman microprobe and Th are in the 290°-400°C range.Compositional observation by Raman spectroscopy indicates a progressive increase of the CH_4/CO_2 ratio from V_{C-W} to L_{W-m} fluid inclusions.
- L_{W1} and L_{W2} are aqueous inclusions and they occur along secondary healed fracture planes in QI and QII and postdate the other inclusion types. L_{W1} fluids are characterized by moderate salinities (3 to 9 wt%eq.NaCl) and Th (130° - 290°C). L_{W2} display low salinities (0.3 - 2.5 wt%eq.NaCl) and temperatures (Th= 90-210°C).

Sample	PhengiteI			PhengiteII		Chlorite			
FeO	1.96	1.41	2.21	2.15	2.27	30.14	30.63	30.75	39.28
Na_2O	0.42	0.48	0.41	0.38	0.41	---	0.04	---	0.07
K_2O	10.06	10.54	10.51	9.80	9.65	0.05	---	0.03	0.03
SiO_2	46.43	47.31	46.48	48.20	48.49	25.48	26.19	25.97	23.71
MnO	---	0.05	0.14	0.10	0.08	0.84	0.59	0.57	1.54
CaO	---	---	0.05	---	---	---	0.01	---	---
NiO	---	---	---	0.01	0.10	---	0.04	---	---
Al_2O_3	36.23	35.88	35.08	35.53	34.54	21.29	21.29	21.25	21.54
TiO_2	0.06	0.28	---	0.09	0.09	0.06	0.06	---	0.01
Cr_2O_3	---	---	---	0.05	---	0.06	---	---	---
MgO	0.57	0.84	0.77	0.80	1.15	10.39	7.84	9.51	2.27
Total	95.72	96.80	95.65	97.11	97.18	88.34	86.69	88.16	88.45
Si	3.07	3.09	3.09	3.13	3.16	2.74	2.86	2.80	2.70
Al^{IV}	0.93	0.91	0.91	0.87	0.84	1.26	1.13	1.20	1.30
Al^{VI}	1.89	1.86	1.85	1.85	1.79	1.44	1.61	1.49	1.59
Fe^{+2}	0.10	0.07	0.12	0.12	0.12	2.71	2.80	2.77	3.73
Mg	0.05	0.08	0.08	0.08	0.11	1.66	1.28	1.53	0.38
Mn	0.00	0.01	0.01	0.01	0.01	0.08	0.05	0.05	0.14
Oct	2.04	2.02	2.06	2.06	2.03	5.89	5.74	5.84	5.84
Ca	0.00	0.00	0.01	0.00	0.00	0.00	0.00	0.01	0.00
Na	0.05	0.06	0.05	0.05	0.05	0.00	0.01	0.00	0.01
K	0.85	0.88	0.89	0.81	0.79	0.01	0.00	0.00	0.02

Table 1.- Representative microprobe analyses (wt%) and structural formulae (half formulae) of phengite I, phengite II and chlorite from Cabeza Mediana and Collado

Mineral geothermometry has been carried out on phengites samples (phI and phII) from Cabeza Mediana and Collado, and on chlorites (ch) from Collado. Table 1 shows the results of selected microprobe analyses.

The structural formulae, calculated on the basis of 11 oxygens, display Si_{IV}=3.09 for phengite I and between 3.13 and 3.16

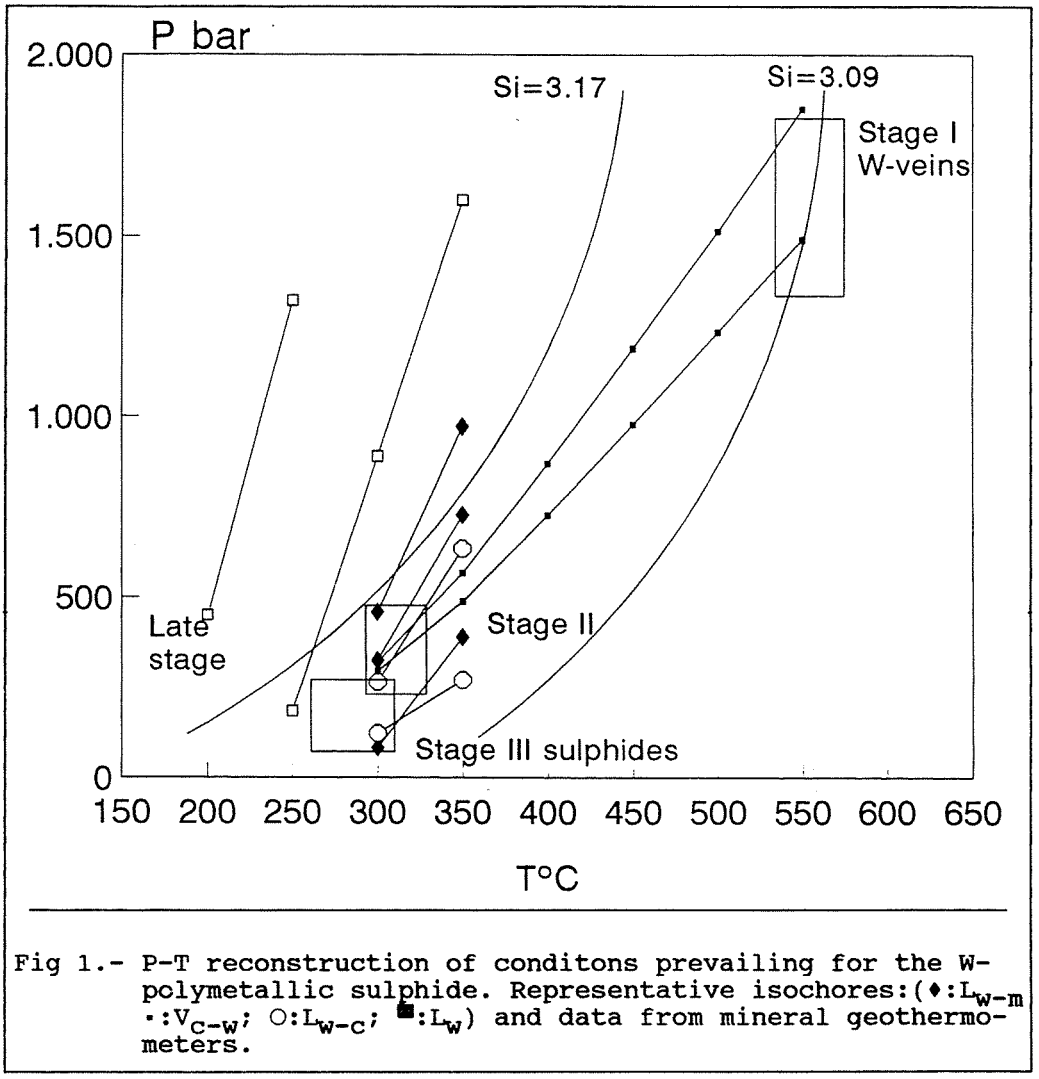

Fig 1.- P-T reconstruction of conditons prevailing for the W-polymetallic sulphide. Representative isochores:(♦:L_{w-m} •:V_{C-w}; ○:L_{w-c}; ■:L_w) and data from mineral geothermometers.

for phengite II. Combining V_{C-w} isochores with P-T curve calculate from Velde (1965) is shown that deposition of wolframite-QI, synchronous with phI, probably occurred around 500±50°C and 150±25 Mpa. In the same way, 300°±50°C and 25±5Mpa for the second stage are derived from phengite II geothermometry and L_{w-m} and L_{w-c} data (fig.1).

The structural formula of chlorites have been calculated on the basis of 14 oxigens (half formula). On basis of the classifi-

cation of chlorites (Fe/Fe+Mg vs. Si) proposed by Foster (1962), all of the samples from Collado fall in the field characterized by brunsvigite.

Using the Cathelineau and Nieva's (1985) chlorite geother mometer, 280±20°C is the estimated temperature for the chlorite-sulphide stage.

Conclusions

The P-T-X evolution of the studied veins involves a drop in pressure and temperature from the W to the sulphide stage during specific deformation events. Dilution and cooling characterize the whole evolution of the system in relation with a change in the fluid pressure regime from lithostactic to hydrostatic pres sure. A drop in PCO_2 and density correspond to the transition between type V_{C-W} and L_{W-m} fluid and to the later sulphide-chlo rite stage.

Acknowledgements: This work has benefited from a financial support of an "Action Intégrée France-Espagne" which involved CREGU (Vandoeuvre,Nancy) and the Universities of Madrid and Valladolid.

References:

Caballero,J.M.;Casquet,C.;Galindo,C.;Gonzalez Casado,J.M.; López Garcia,J.A.; Quilez,E.; Sierra,J.; Tornos,F. & Vindel,E.1992. La Sierra de Guadarrama: Un ejemplo de actividad hidrotermal recurrente en el tiempo y en el espacio. III Cong. Geol. de España,3:42-45

Cathelineau,M.& Nieva,D.1985.A chlorite solid solution geothermometer The Los Azufres (Mexico) geothermal system. Contrib. Mineral Petrol.91:235-244

Foster,M.D.(1962). Interpretation of the composition and a classification of the chlorites. US Geol.Surv.Prof.Pap.414A,27pp.

Quilez,E.;Sierra,J.& Vindel,E.1990. A fluid-inclusion study and genetic model of wolframite-bearing quartz veins, Garganta de los Montes, Spanish Central System. Mineral. Magazine, 54: 267-278

Velde,B.(1965). Phengites micas, synthesis, stability and natural occurrence. Am.Jour.Sci. 263:886-913

Vindel,E.(1980).Estudio mineralógico y metalogénico de las mineralizaciones de la Sierra de Guadarrama. P.D. Thesis.Univ. Complutense.Madrid.249pp.

Current Research in Geology Applied to Ore Deposits.Fenoll Hach-Alí, Torres-Ruiz & Gervilla(eds)(1993).ISBN 84-338-1772-8

UNUSUAL NUKUNDAMITE OCCURRENCE IN AN IRON DEPOSIT FROM ROMANIA AND ITS METALLOGENETIC IMPLICATIONS

Lupulescu, M. (1); Watson, E.B. (2) & Wark, D. (2)
(1) Dept. of Mineralogy. University of Bucharest, N. Balcescu 1, 70111 Bucharest, Romania
(2) R.P.I. Dept. of Geology, Troy., N.Y., U.S.A.

ABSTRACT. A nukundamite like mineral have been identified in an iron occurrence and it belongs to a sulfides-bearing hydrothermal association.The relations between the regionally metamorphosed paragenese and the hydrothermal one show the appearance of nukundamite leads to the breakdown of magnetite and the hematite formation.

The iron occurrences of Boutari (Poiana Rusca Mts.,Romania) are hosted by mesometamorphic rocks which appear on a small area in the southern part of the massif.The iron ore is lense-like and is located in an up-lifted tectonic block.

The mineralogical composition of the ore and the physiographic relations between minerals show two different genetic mineral parageneses:

(A) The magnetite-bearing iron oxides paragenesis which is regionally metamorphosed in almandine-amphibolite facies. The magnetite is partially oxidized to hematite in some ore bodies.

(B) The sulfide-bearing paragenese which is made up of pyrite,pyrrhotite,chalcopyrite,bornite,covellite and sphalerite. This is a hydrothermal mineral association and it superposes the magnetite-bearing paragenese in some ore bodies.

In the last association we have identified the rare mineral nukundamite which has been previous described only in copper deposits.

Mineralogical features

In the iron occurrences of Boutari,the nukundamite appears filling narrow veins which penetrate the magnetite grains or between them. It is associated and substitutes the bornite and the chalcopyrite.

The nukundamite grains have very small size, orange color, strong bireflectance and anisotropism in pale-green to grey.

The chemical composition made by electron microprobe analysis (Jeol 733 Superprobe) in the Rensselaer Polytechnic Institute, Troy, S.U.A., shows the following values (wt%): Cu-56.34; Fe-11.83; S 31.68; Bi-0.08; Au-0.15; Ag-0.01, which corresponds to the $Cu_{5.38}$ $Fe_{1.29}$ S_6calculated formula for 6 sulfur atoms.

The quantitative reflectance measurements show the folowing average values for 1000 measurements: (488 nm)-21.739;(553 nm)-25.134; (590 nm)-28.206; (650 nm)-28.071, using the magnetite as standard.

We have used monoreflecting values due to the very small size of the nukundamite grains. For the same reason we have used 10g and 25g loads for the microhardness identification. The aquired values are 88.2 kg/mm^2 for the former and 254 kg/mm^2 for the later load.

Mineralogenetic implications

The relations between the two mineral paragenesis and between the mineral components of the sulfides-bearing association show the nukundamite-bornite-chalcopyrite represents thermodinamically stable association and when the nukundamite is present the pyrite and the pyrrhotite disappear.

The experimental studies of Sugaki et al. (1975) showed the nukundamite --chalcopyrite tie line is stable up to 350^0 C and this is not compatible with the former accepted bornite-pyrite tie line. The pyrite-bornite assemblage is more common than the nukundamite-chalcopyrite assemblage in nature and this fact indicates at temperatures lesser than 300^0 C the phase-relations must change in the Cu-Fe-S system. The nukundamite hydrothermal synthesis (Sugaki et al., 1981) confirms the appearence of the nukundamite-chalcopyrite association in the 250^0-450^0 C temperature range and this is in good agreement with Rosemboom & Kullerud (1958) data which found the $Cu_{5.5}$ Fe $S_{6.5}$ composition is stable up to 510^0 C.

According to the thermodynamic data of Vaughan &Craig (1978) and Barton &Skinner (1979) the appearance of nukundamite takes place by bornite breakdown as in the following reaction:

$$Cu_5 Fe S_4 + 0.5\ Cu\ S + S_2 \text{---} Cu_{5.5} Fe S_{6.5} \quad (1)$$

This reaction is possibly in a 227^0-482^0 C temperature range in good agreement with the presented experimental data.

The fact that nukundamite and covellite are rare minerals in hypogene ore is due to the low sulphur pressure (Yund &Kullerud, 1966) and not to the thermal phases instability. The covellite nucleation takes place at low temperature and this means at temperature over 227^0-250^0 C when a suitable sulphur pressure is reached

the bornite breaksdown and due to the reaction (1)the nukundamite is generated and it is more abundent with higher temperature.

We have mentioned at the begining about the magnetite to hematite transition. We can connect this reaction with the moment of the sulfides-bearing hydrothermal phase. We have talked earlier that nukundamite appears in a temperature range as 250^0-450^0 C and this is in good agreement with the 200^0-600^0 C temperature range given for hematite (Ramdohr,1969). Then, we can consider there is an incompatibility between the magnetite stability and the sulfide-bearing hydrothermal phase which determines the oxidation of magnetite to hematite.

The magnetite can coexist with chalcopyrite-pyrite-pyrrhotite mineral association and it becomes instable when the pyrrhotite is substituted by pyrite-bornite-chalcopyrite and specially when idaite-nukundamite like minerals appear.

We can corroborate the abundence of hematite with the pyrrhotite breakdown and the presence of nukundamite in the light of the cited experimental data and the field and microscopical observationes.

If the genetic connection of the magnetite-bearing formation is accepted being related to a regionally metamorphic dalslandian event the magmatic connection of the sulfide-bearing hydrothermal association is not known.

In the nearby areas there are some Upper-Cretaceous-Paleogene magmatites which have copper and minor base-metal related mineralisations such as Tincova or Rusca Montana occurrences. This leads us to the consideration that some deeper magmatites intruded in the crystalline schists are the source for the hydrothermal solutions which generated the sulfides paragenesis in which nukundamite appears.

References

Barton, P.B. & Skinner, B.J. 1979. Sulfide mineral stabilities. In: Barnes, H.L., (ed.). Geochemistry of Hydrotermal Ore Deposits. John Wiley and Sons, 278-403.

Ramdohr, P. 1969. The ore minerals and their intergrowths. Pergamon Press.

Rosemboom,E.H. & Kullerud, G. 1958. The solidus in the system Cu-Fe-S system between 400^0-800^0 C. Carnegie Institution of Washington Year Book, 57, 222-227.

Sugaki, A, Shima, H., Kitakaze, A., Harada, H. 1975. Izothermal phase relations in the system Cu-Fe-S under hydrothermal conditions at 350^0 and 300^0 C. Econ. geol., 70, 806-823.

Sugaki, A., Shima, H., Kitakaze, A., Mizota, A. 1981. Hydrothermal synthesis of nukundamite and its crystal structure. Amer. Mineral., 66, 398-402.

Vaughan, D.J. & Craig,J.R. 1978. Mineral chemistry of metal sulfides. Cambridge University Press.

Yund, R.A. & Kullerud, G. 1966. Thermal stability of assemblages in the Cu-Fe-S system. J. of Petrology, 7, 454-488.

Current Research in Geology Applied to Ore Deposits. Fenoll Hach-Alí, Torres-Ruiz & Gervilla (eds) (1993). ISBN 84-338-1772-8

APPLICATION OF GRAPHITE GEOTHERMOMETRY TO THE RECOGNITION OF THE TEMPERATURE OF FORMATION IN SOME SPANISH GRAPHITE DEPOSITS

Luque, F.J. (1); Barrenechea, J.F. (1); Rodas, M. (1) & Galan, E. (2)

(1) Dept. Cristalografía y Mineralogía, Facultad de Geología, Universidad Complutense, 28040 Madrid, Spain

(2) Dept. Cristalografía y Mineralogía, Facultad de Química, Universidad de Sevilla, 41071 Sevilla, Spain

ABSTRACT: This paper examines the potential use of the variation of the c_o parameter of graphite with temperature for geothermometric estimations, in two Spanish deposits formed at low- and high-temperature conditions. At low-grade metamorphic conditions, the c_o parameter of graphite is affected by other factors besides the temperature, so graphite geothermometry (based on c_o) can only be used in such rocks for qualitative estimations. For temperatures above 500ºC, when the fully ordered graphite appears, there is a close correlation between the temperature estimations based on the structural ordering of graphite and from mineral-exchange geothermometry and, so, graphite thermometry can be a useful tool.

Introduction

The aim of the present paper is to test, geologically, the reliability of the XRD-derived c_o parameter as a geothermometer, specifically, to test the temperature-c_o calibration of Shengelia et al. (1979). Since there are no comparative studies dealing with the differences between graphite geothermometry and other geothermometers based on element partitioning between mineral phases, we present here two case studies emphasizing these comparisons. In order to test the temperature range of applicability of this graphite geothermometer, the study focused on graphites formed in contrasting temperature environments (i.e., under low- and high-temperature conditions). Although the geothermometer developed by Shengelia et al. (1979) is based, exclusively, on the progressive graphitization of carbonaceous material during regional metamorphism, this study intends to test the applicability of the geothermometer to graphites originating under two different genetic conditions (i.e., both to metamorphosed organic matter and "fluid-deposited" graphite).

For these purposes we have selected a graphite-rich horizon of Silurian slates located south of El Muyo (Segovia province, Central Spain) in the eastern part of the Spanish Central Range and a group of high-temperature graphite-bearing dikes located in the margins of the Ronda ultramafic Complex (Málaga province, Southern Spain).

Analytical procedures

Chemical compositions of minerals involved in geothermometric calculations based on exchange equilibria were obtained using a JEOL JXA-50A electron microprobe. Chlorite compositions were calculated by X-ray diffraction methods and the results were verified by electron probe.

Graphite parameters were calculated by means of X-ray diffraction (XRD). Graphite was removed from the host rock by acid treatment in an HF and H_2SO_4 solution heated at 70ºC. Graphite concentrates obtained in this way were washed thoroughly to remove free acid and then purified by flotation in distilled water. Samples were scanned from low to high angles, usually five times (but at least twice), using silicon powder as an internal standard. At these analytical conditions, the interplanar spacing (d_{002}) was determined and the c_o parameter calculated.

Mineralogy

a) Black shales

The study focused on a graphite-rich horizon (20 m thick) in the Early Silurian slates of the eastern part of the Spanish Central Range. On the basis of mineral associations, two different lithologies have been distinguished in the studied materials (Barrenechea et al., 1992): siliceous slates and carbonaceous slates. The former are composed of quartz, plagioclase, phengite and trioctahedral Fe-rich chlorite. The carbonaceous slates are composed of quartz, plagioclase, graphitised carbonaceous matter, illite, pyrite and apatite nodules. In both lithologies, graphite and chlorite are mutually exclusive. Graphite appears as very thin flakes interlaminated with quartz and micas defining the foliation in the slates.

Following the classification of Landis (1971), three graphite types (d_{1A}, d_2 and d_3), characterized by different values of $d_{(002)}$, symmetry and intensity of the (002) reflection, can be recognized in the studied samples. The most crystalline graphites were sampled in the levels of tight folding within the horizon. The results of the TEM study suggest that any quantitative interpretation of the XRD data is hindered because of sample inhomogeneity.

b) High-temperature dikes

The graphite-bearing acidic dikes studied are restricted to the serpentinized marginal zones of the ultramafic massifs of the Serranía de Ronda (Southern Spain). The dikes were formed by anatexis of the underlying sediments and graphite is thought to be deposited from CO_2- and CH_4-rich fluids generated during the partial melting of the carbonaceous sediments (Luque et al., 1987).

The mineral associations in the dikes permit the distinction between those dikes that contain the original mineralogy (untransformed dikes) from those in which this original assemblage has been partially or totally modified by late hydrothermal processes (transformed dikes). In both cases, the dikes are characterized by a high graphite content (up to 15% in weight).

Untransformed dikes consist of cordierite, quartz, garnet, biotite, graphite and ilmenite. Graphite is found as platy xenomorphous aggregates randomly distributed in the rock; these graphite flakes, in places, have been mechanically introduced in microfissures forming in nest-like aggregates. Graphite flakes range up to 250 μm in size, and textural relations indicate that it was formed almost synchronously with the other minerals. For the purposes of this study, only mineral compositions from untransformed dikes have been considered because, during hydrothermal alteration, the chemical compositions of minerals were changed and they did not attain equilibria (Luque et al., 1987). Diffraction patterns of graphite found in both transformed and untransformed dikes present all the reflections of this mineral (with sharp 004, 101, 100, and 103 peaks), indicating a high degree of structural ordering. TEM images showed an ordered arrangement of carbon layers in these graphites.

Geothermometry

a) Black shales

The substitution of Si for Al in the tetrahedral sites of chlorites is dependent upon the temperature of formation, and it is sensitive enough to be used as a geothermometer, as pointed out by Cathelineau & Nieva (1985) and Cathelineau (1988). These estimations have been used to determine the temperature of formation of the siliceous slates, which ranges from 300 ±20°C to 390 ±20°C (Table 1). On the basis of the observed mineral assemblages and illite crystallinity, the temperature range obtained by the first method seems to be more reasonable (Barrenechea et al., 1992).

The graphite c_o parameter in the carbonaceous slates is quite variable due to different degrees of structural ordering. These variations in such a thin horizon would indicate that temperature was not the only factor that influenced graphite crystallinity. The c_o parameter for the most crystalline graphites (d_{1A}) indicates a temperature of about 310°C (±15°C), by reference to the temperature-c_o calibration of Shengelia et al. (1979). This value is close to that obtained from chlorite Al^{IV} content by means of the equation proposed by Cathelineau & Nieva (1985).

b) High-temperature dikes

The temperature of formation of graphite-bearing dikes has been determined using Fe-Mg partitioning between the coexisting mineral pairs garnet-biotite and cordierite-garnet. The estimated temperatures range from 765°C to 830°C (Table 1).

Differences between $d_{(002)}$ reflection of graphite in transformed and untransformed dikes are negligible. Based on the c_o data of graphite from both types of dikes the estimated temperature of formation is 825 ±15°C. This temperature, obviously, represent the thermal conditions attained before the hydrothermal alteration.

TABLE 1: Temperature estimations for the Silurian black shales and for the high-temperature dikes by means of different geothermometers. Δ (T_a-T_{gr}) indicates the difference in temperature calculated using the given geothermometer and using graphite geothermometry.

	Geothermometer	Temperature	Δ (T_a-T_{gr})
Black shales	Chlorite (Cathelineau & Nieva, 1985)	300 ±20°C	+ 10°C
	Chlorite (Cathelineau, 1988)	390 ±20°C	+ 90°C
	Graphite (Shengelia et al., 1979)	310 ±15°C	---
High-Temperature Dikes	Biotite-garnet (Indares & Martignole, 1985)	765-805°C (P=0 kb) 800-830°C (P=5 kb)	- 40°C - 10°C
	Biotite-garnet (Ferry & Spear, 1978)	790 ±15°C	- 35°C
	*Biotite-garnet (Saxena, 1969)	775°C	- 50°C
	Garnet-cordierite (Bhattacharya et al., 1988)	785 ±20°C	- 40°C
	*Garnet-cordierite	625-775°C	- 190 to - 50°C
	Graphite (Shengelia et al., 1979)	825 ±15°C	---

* After Dickey & Obata (1974)

Discussion

In order to center the discussion we can summarize our observations in two points:

1) At low grade metamorphic conditions (chlorite zone), different graphite types, classified according to lattice perfection, have been recognized in a thin horizon.

2) At high temperature, only fully ordered graphite appears. Its structural ordering is not dependent on other factors, such as late hydrothermal alteration, confirming that graphitization is an irreversible process.

We have pointed out that, in the Silurian black shales, only the most crystalline graphitised matter gives a temperature estimate close to that calculated on the basis of Al^{IV} content in chlorite, a temperature compatible with other geological and mineralogical criteria. This fact suggests that although temperature is the major factor controlling graphite crystallinity, it is not the only important one. Among the different influences on graphite structural ordering, the most prominent are: 1) the pressure, 2) the role of lithology and, 3) the nature of the original carbonaceous matter. The available data on graphite crystallinity in the studied black shales suggest that some combination of the above mentioned factors operated (shear stresses being the most important). Therefore, graphite geothermometry can only be successfully used for qualititative aims rather than for a quantitative temperature estimation at temperatures below 500°C.

A different aspect of graphite geothermometry is represented by the high-temperature dikes associated with the ultramafic rocks of southern Spain. The crystallinity of graphite in the dikes appears to be unaffected by factors other than temperature. The difference in temperature estimations by graphite geothermometry and by exchange geothermometry ranges from 10°C to 40°C, a deviation explainable on the basis of the accuracy of both methods. Therefore, we can contend that, at temperatures above 500°C (i.e., from the appearance of ordered graphite), the lattice parameter c_o of fluid-deposited graphite seems to be influenced only by temperature and the roles of other factors would be meaningless, and graphite geothermometry accurate.

On the other hand, it is neccesary to address that graphite geothermometry at temperatures above 500°C is useful on both heat-treated organic matter (metamorphosed carbonaceous material) and fluid-deposited graphite. The first case is illustrated through the study of Shengelia et al. (1979) in which graphite geothermometry is verified by garnet-biotite geothermometry in graphitic schists. The applicability on fluid-deposited graphite is documented through the papers of Katz (1987) on graphite veins from Sri Lanka (which originated at granulite facies conditions, T=750°C, from a CO_2-rich fluid), Luque et al. (1992) on graphite veins generated from magmatic (mainly mantle-derived) melts, and the graphite-bearing dikes studied in this work.

Conclusions

The two case studies presented in this paper show that the relationship between the degree of structural ordering of graphite (represented by the c_o parameter) and its temperature of formation is a potential method to evaluate the temperatures reached by the rocks in which it appears. Although graphite geothermometry at low-grade metamorphic conditions has some restrictions relative to the influence of other factors on the graphite c_o parameter (mainly the effects of pressure, original composition of the carbonaceous matter, and lithology), it can be used for qualitative estimations, especially if one relies on data from the most-ordered graphites found in a particular lithology. At temperatures above 500°C it is not influenced by such factors and it can be a useful tool in determining peak temperatures.

Graphite geothermometry at high temperature is useful on both metamorphosed organic matter and fluid-deposited graphite, and it is independent of retrometamorphic or pressure effects, factors that clearly influence the exchange equilibria. In addition, graphite geothermometry can be successfully used in those cases in which no other thermometric indicators exist, such as some epigenetic graphite deposits (i.e., graphite veins), where good agreement with temperatures deduced from geological or field evidence is found.

References

BARRENECHEA, J.F., RODAS, M. & ARCHE, A. 1992. Relation between graphitization of organic matter and clay mineralogy, Silurian black shales in Central Spain. *Min. Mag.*, 56, 477-85.

BHATTACHARYA, A., MAZUMDAR, A.C. & SEN, S.K. 1988. Fe-Mg mixing in cordierite: Constraints from natural data and implications for cordierite-garnet geothermometry in granulites. *Am. Mineral.*, 73, 338-44.

CATHELINEAU, M. 1988. Cation site occupancy in chlorites and illites as a function of temperature. *Clay Min.*, 23, 471-85.

CATHELINEAU, M. & NIEVA, D. 1985. A chlorite solid solution geothermometer. The Los Azufres (Mexico) geothermal field. *Contrib. Mineral. Petrol.*, 91, 235-44.

DICKEY, J.S. & OBATA, M. 1974. Graphitic hornfels dikes in the Ronda high-temperature peridotite massif. *Am. Mineral.*, 59, 1183-89.

FERRY, J.M. & SPEAR, F.S. 1978. Experimental calibration of the partitioning of Fe and Mg between biotite and garnet. *Contrib. Mineral. Petrol.*, 66, 113-17.

INDARES, A. & MARTIGNOLE, J. 1985. Biotite-garnet geothermometry in the granulite facies: the influence of Ti and Al in biotite. *Am. Mineral.*, 70, 272-78.

KATZ, M.B. 1987. Graphite deposits of Sri Lanka: a consequence of granulite facies metamorphism. *Mineralium Deposita*, 22, 18-25.

LANDIS, C. A. 1971. Graphitization of dispersed carbonaceous material in metamorphic rocks. *Contrib. Mineral. Petrol.*, 30, 34-45.

LUQUE, F. J., RODAS, M., VELASCO, F. & GALAN, E. 1987. Mineralogía y geotermometría de los diques ácidos con grafito asociados a rocas ultramáficas de la Serranía de Ronda, Málaga. *Estudios Geológicos*, 43, 367-75.

LUQUE, F.J., RODAS, M. & GALAN, E. 1992. Graphite vein mineralization in the ultramafic rocks of southern Spain: Mineralogy and genetic relationships. *Mineralium Deposita*, 27, 226-233.

SAXENA, S.K. 1969. Silicate solid solution and geothermometry: 3. Distribution of Fe and Mg between coexisting garnet and biotite. *Contrib. Mineral. Petrol.*, 22, 259-67.

SHENGELIA, D.M., AKHVLEDIANI, R.A. & KETSKHOVELI, D.N. 1979. The graphite geothermometer. *Dokl. Acad. Nauk SSSR*, 235, 132-34.

Current Research in Geology Applied to Ore Deposits. Fenoll Hach-Alí, Torres-Ruiz & Gervilla (eds) (1993). ISBN 84-338-1772-8

Ni, Cu AND MAJOR ELEMENT REMOBILIZATION, VAMMALA MINE, FINLAND

Marshall, B. (1) & Mancini, F. (2)
(1) University of Technology, Sydney, Australia
(2) University of Turku, Turku, Finland

ABSTRACT: Granitic dykes derived from migmatitic hostrocks intruded a D_3-related fracture system in a 1.89 Ga peridotite bearing Ni-Cu-Fe sulphides. Alteration zones formed during metasomatic exchange between the dykes and sulphide-bearing peridotite. Gresens' equation is used to document the exchange relative to now-serpentinized peridotite, and provides a basis for evaluating the partially-masked metasomatism which included remobilization of sulphides. Remobilization has not affected grade at stope-scale.

1. INTRODUCTION

The Vammala mine is located in southwestern Finland, 175 km northwest of Helsinki. The Ni-Cu sulphide ore is hosted by the Stormi layered ultramafic body which has a sill-like form within migmatitic gneisses and a 1.89 Ga U-Pb age. This age typifies a group of synorogenic Svecokarelian mafic-ultramafic intrusions (Häkli et al. 1979); but although commonly classified as "bodies emplaced during orogenesis", the precise affinities of the intrusions and their magmatic nickel deposits are contentious.

Predominantly net-textured or matrix ore occupies the lowermost of the three layers comprising the ultramafite. Typical ore grades are 0.5-1.0% Cu, 1-2% Ni and 5-10% S; subeconomic mineralization contains < 1% Cu + Ni.

The ultramafite and orebodies are cut by a series of dykes which range from "gabbroic" (plagioclase, aphanitic serpentine and phlogopite) to "granitic" (plagioclase, potassium feldspar, biotite and quartz) in composition (Häkli et al. 1979). The dykes are parallelled by near monominerallic alteration zones comprising (from unaltered peridotite to the dyke) talc, actinolite, anthophyllite, chlorite (Papunen 1985).

We examine the nature of the alteration assemblages in the ultramafite adjacent to the feldspar-rich dykes. An attempt is made to evaluate element mobility, to effect mass-balance determinations, and to assess volume changes associated with the alteration. The influence of the alteration processes on the Vammala Ni-Cu ore is assessed.

2. PERTINENT GEOLOGY

2.1 *Hostrocks and ore*

The paragneisses hosting the ultramafite are migmatitic biotite-plagioclase-quartz gneisses with garnet, cordierite and sillimanite. Mineralogical assemblages are consistent with metamorphic conditions of the upper amphibolite/lower granulite facies (Peltonen 1990). Four periods of deformation are inferred. D_1 - D_2 produced the migmatitic layering, but the latter was not retrogressed by D_3, which also produced migmatitic leucosome. Thus, peak or near-peak metamorphism accompanied D_1-D_3. The east-trending upright F_3 folds control the regional distribution of the metasedimentary rocks (Kilpeläinen & Rastas 1992).

The lowermost layer of the Stormi ultramafite hosts the main economic concentrations of sulphide. It ranges from lherzolitic peridotite to dunite in composition and has a well-preserved cumulate texture, despite each olivine grain being substantially serpentinized. Monoclinic pyrrhotite-pentlandite-chalcopyrite $\pm$ cubanite $\pm$ mackinawite $\pm$ vallerite constitutes the ore-forming assemblage. The sulphides are an integral part of the primary igneous texture. Dykes affecting the silicate phases must inevitably influence the sulphide species.

2.2 *Fracture system*

The fracture system which controls the orientation of dykes and alteration assemblages, resolves into a conjugate set of fractures, of high dihedral angle, bracketing a N-S fracture set. The system is consistent with the proposed (Kilpeläinen & Rastas 1991) north-south direction of contraction during D_3. "T" and "X" relationships of dykes in the stope only require a dilational opening mode. Oblique extension is sufficient to explain most minor fault displacements. The few more substantial displacements are ascribed to reactivation either during D_4 or subsequent to serpentinization.

2.3 *Alteration assemblages and dykes*

The principal lithological characteristics of the alteration assemblages and dykes are summarized in Table 1. Although four zones separate the "parent" rock from the dyke, zone 1 is uncommon and zone 2 is not always present. The zones are typically symmetrical about the dyke with respect to both sequence and thickness. Uncommon cases of thickness-asymmetry are related to diffusion rates being higher above than below less steeply inclined dykes. There is no simple correlation between dyke-thickness and the thickness of the alteration zones. For example, 1.5cm of alteration abut a 5cm dyke, 3cm abut a 1cm dyke, and 0.5cm abut a fracture where no feldspar exists.

Mineralogical changes involve conversion of olivine and pyroxene/amphibole to varying proportions of amphibole, phlogopite and chlorite. In the "parent" rock, residual cores of clinopyroxene remain within poikiloblastic tremolitic hornblende, in turn overgrown with rims of magnesio-cummingtonite at the interface with now-serpentinized olivine. In zones 1 and 2, olivine converts to fine grained talc, phlogopite and interleaved chlorite, and all the amphibole recrystallizes to nematoblastic magnesio-cummingtonite. Apart from sparse amounts of stubby phlogopite and interleaved chlorite, zone 3 comprises fibrous magnesio-cummingtonite with a highly preferred orientation normal to the zone-boundary. Zone 4 comprises coarse euhedral phlogopite and interleaved chlorite with minor stubby magnesio-cummingtonite.

The dykes comprise plagioclase ($Na_2O/CaO \simeq 2$ to 5), magnesio-hornblende to magnesio-cummingtonite, minor phlogopite and interleaved chlorite, coarse apatite, and variable amounts of quartz and K-feldspar.

3. ALTERATION CHEMISTRY

3.1 *Analytical data and evaluation methods*

Wholerock analyses were obtained for the serpentinized "parent" rock, the discrete zones of alteration excluding the thin poorly developed zone 1, and the more equigranular dykes. It is likely that serpentinization occurred substantially later, and under conditions of lower temperature and pressure, than those producing the dykes of partial melt and the cummingtonite-phlogopite alteration assemblages.

The metasomatic changes have been evaluated: (a) in relation to the percentage-change in concentration of each element analysed; (b) by normalization against a presumed immobile component (Al_2O_3); and (c) by the application of Gresens' (1967) equation. The latter states that:

$$X_n\,(\%) = f_v\,(g_B / g_A)\,C_n^B - C_n^A$$
$$A \longrightarrow B$$

where X_n is the weight of component n, expressed as a percentage of the weight of rock A, added to or removed from rock A in order to form rock B; f_v is the volume factor obtained by dividing the volume of B by that of A; g_B and g_A are the respective specific gravities; and C_n^B and C_n^A are the respective concentrations of n in B and A.

3.2 *Results*

The percentage-changes in concentration of selected components involved in the assumed constant-volume alteration of the "parent" rock to zones 2, 3 and 4, exhibit three main trends; progressive enrichment (K_2O, Rb_2O, Al_2O_3, P_2O_5 and TiO_2); progressive depletion (Cr_2O_3, V_2O_3, LOI and MgO); and combinations of enrichment and depletion (Cu, MnO, SiO_2, FeO, Co, S and Ni). The least variable components are SiO_2, FeO and MgO, whereas Al_2O_3 and TiO_2 show substantial enrichment, and Rb_2O, K_2O and P_2O_5 show extreme enrichment.

The Al_2O_3-normalised data show that whereas K_2O, Rb_2O and P_2O_5 are relatively enriched, all other components are relatively depleted. The behaviour of Al_2O_3 is most closely approximated by TiO_2, K_2O and Rb_2O.

The Gresens equation for an assumed constant volume ($f_v = 0$) shows that over the 10 metasomatic changes investigated there is a net enrichment (excluding volatiles) of 23.4 kg per 1000 kg (2.3 wt %) of assumed source rocks. This involved mean additions of SiO_2, Al_2O_3 and K_2O (3.6, 3.4 and 1.3 wt %), mean losses of FeO, MgO, CaO, Cu, Ni and S (0.2, 3.0, 0.5, 0.2, 0.3 and 1.9 wt %) and negligible changes in TiO_2, P_2O_5 and Co.

Table 1. Hand-specimen characteristics of the "parent" rock, alteration assemblages and feldspar-rich median zones.

Material	Thickness (cm)	Colour	Mineralogy and texture	Sulphide distribution
"Parent" rock		dark grey to black, other than for sulphides.	serpentinized olivine subhedra (2.5mm) in a matrix of oikocrystic pyroxene-amphibole and/or Fe-Ni-Cu sulphides; an igneous, commonly cumulate texture, with a planar lamination (Jackson 1967) in places.	disseminated or net-textured po, pe and cp; primary distribution.
Zone 1[a]	0[b]-0.5	pale yellow-green to green-brown	iddingsite products after olivine - "iddingsite" enrichment is accompanied by blurring of the primary (igneous) texture.	disseminated and net textures become blurred.
Zone 2	0-2.5	pale grey	sheaf-like patches (up to 5mm) of prismatic amphibole; interlocking patches are disoriented; all primary texture lost.	ragged patches due to invasion by amphibole sheaves.
Zone 3	0.2-1.5	very pale grey with green -brown tints.	fibrous-looking prismatic amphibole showing a highly preferred orientation normal to the zone boundaries.	planar and wedge-shapped screens between prismatic amphiboles.
Zone 4	0.2-1.5	dark green-grey-black	chlorite, brown-black mica and minor amphibole; varies from disoriented to a planar preferred orientation sub-parallel to the zone boundaries.	sparse to irregular concentrations between the silicate phases.
Feldspar-rich median zone	0-100[c] (usually < 20)	ranges from a uniform pale to medium blue-grey, to grey patches(up to 3cm) in a dark green-black matrix	from equigranular medium grained feldspar (1-2mm), to coarse feldspar (up to 3cm) and brown mica (up to 1.5cm) in a finer grained (< 3mm), commonly serpentinized and foliated matrix of chlorite, brown mica and amphibole, ± quartz; where the matrix is foliated, the pegmatitic feldspar is porphyroclastic.	most variable; may lack sulphides, or contain discrete splashes in the matrix, or form a central zone of abundant, commonly durchbewegt (Marshall and Gilligan, 1989) sulphide.

[a] Numbered from the "parent rock" to the median zone.

[b] Zero implies that the zone is not always developed.

[c] Most uncertain due to extremely intermittent core recovery.

Best-fit volume factors were determined from composition-volume diagrams (Gresens 1967 fig. 3) for each of the 10 changes. They range between 0.85 and 1.2, but yield a mean of 0.97; an overall volume decrease of 3%. By applying these factors, best-fit gains and losses were obtained. This yielded a net loss (excluding volatiles) of 24.6 kg per 1000 kg (2.5 wt %) of assumed source rocks. It involved mean gains of SiO_2, Al_2O_3, K_2O and P_2O_5 (0.9, 3.2, 1.0 and 0.1 wt %), mean losses of FeO, MgO, CaO, Ni and S (0.7, 3.9, 0.6, 0.4 and 2.1 wt %), and negligible changes in TiO_2, Cu and Co.

For both constant-volume and best-fit volume factors, there is a net loss of volatiles (loss on ignition) of about 5 wt %. This is consistent with the presence of serpentinized olivine in the "parent" rock.

4. DISCUSSION AND CONCLUSIONS

Because serpentinization most probably post-dated the alteration zones, it follows that the latter derived from peridotite rather than serpentinised peridotite. The present alteration chemistry and "parent" rock therefore reflect: (a) alteration of peridotite to amphibole-phlogopite assemblages; and (b) alteration of peridotite to serpentinised peridotite (the "parent" rock). Nevertheless, the magmatic texture in the "parent" is perfectly preserved, the sulphide droplets have maintained their form, and only the olivine is serpentinized. We therefore suggest that, at constant volume, sufficient MgO and SiO_2 were removed from the rock to substantially lower the specific gravity, but that the relative concentrations of the other components (except LOI) were unaffected. Our interpretation of the transitions from *peridotite* to the alteration zones is that the majority of gains and losses would follow those of the transitions from serpentinised peridotite ("parent" rock) to the alteration zones, and that f_v would be zero to slightly positive rather than negative. Exceptions are that the SiO_2-gain would be less, the MgO-loss more and the LOI-loss very much less.

Following-on from the interpretation, although small gains in SiO_2 and P_2O_5 could reflect reconcentration of components in the peridotite, massive gains in Al_2O_3, K_2O and, most probably, BaO and Rb_2O require metasomatic enrichment. Similarly, reconcentration could explain small losses, but massive losses of MgO and CaO require metasomatic depletion. Phlogopite, Mg-rich amphibole and coarse apatite in the dykes, loss of quartz and K-feldspar from the dykes, and alteration zones mainly comprising amphibole and phlogopite, are mineralogical evidence of the metasomatic exchange.

Ni, Cu, Fe and S are mass-loss components. However, the loss is not progressive; they are redistributed but retained in zones 1 to 3, whereas major losses are incurred from zone 4. The existence of irregularly distributed Ni-Cu-Fe sulphide masses within the dykes are in keeping with external remobilization during the metasomatic exchange. However, at stope-scale, remobilization has neither enriched nor depleted the ore.

We conclude that the dykes were formed when granitic melt intruded the ultramafite under high amphibolite-facies conditions. Prior to crystallization, the alteration zones formed during metasomatic exchange. Remobilization of Ni-Cu-Fe sulphides was part of this exchange.

REFERENCES

Gresens, R.L. 1967. Composition-volume relationships of metasomatism. Chem. Geol. 2: 47-65.

Häkli, T.A., Vormisto, K. & Hänninen, E. 1979. Vammala, a nickel deposit in layered ultramafite, southwest Finland. Econ. Geol. 74: 1166-1182.

Kilpeläinen, T. & Rastas, J. 1992. Vammalan Stormin Ni-malmin ympäristön metamorfisista ja rakennegeologista tutkimuksista. Institute of Geology and Mineralogy, University of Turku, Finland, Publication No. 30: 1-18.

Marshall, B. & Gilligan, L.B. 1989. Durchbewegung structure, piercement cusps and piercement veins: formation and interpretation. Econ. Geol. 84: 2311-2319.

Papunen, H. & Vorma, A. 1985. Nickel deposits in Finland, a review. Geol. Surv. Finland, Bull. 333: 123-143.

Peltonen, P. 1990. Metamorphic olivine in picritic metavolcanics from southern Finland. Geol. Soc. Finland, Bull. 362: 99-114.

Current Research in Geology Applied to Ore Deposits.Fenoll Hach-Alí, Torres-Ruiz & Gervilla(eds)(1993).ISBN 84-338-1772-8

THE EVOLUTION OF COPPER MINERALIZATION IN THE OKIEP DISTRICT, SOUTH AFRICA

Meyer, F.M. (1); Boer, R.H. (2) & Cawthorn, R.G. (1)
(1) Dept. of Geology, University of the Witwatersrand Private Bag 3, Wits 2050, Johannesburg, South Africa
(2) Economic Geology Research Unit. University of the Witwatersrand Private Bag 3, Wits 2050, Johannesburg, South Africa

Abstract: The Okiep copper mineralization evolved in three distinct stages. During a magmatic stage the copper ore formed by immiscibility of sulphide from a basic, mantle-derived magma. Sulphide saturation was controled by assimilation of siliceous crustal material. Subsequent granulite facies metamorphism caused extensive oxidation of the ores and devolatilization of SO_2 which resulted in the conversion of pyrrhotite and chalcopyrite into magnetite and bornite. Remobilization of sulphides occurred during a late hydrothermal stage.

Introduction and Geological Setting: The Okiep District constitutes a major source of copper in South Africa. Sulphide mineralization was first reported here in 1685, but systematic mining commenced in 1850 only. During the more than 100 years of commercial exploitation, up to 15 mines produced ca. 2 million tons of Cu metal from 100 million tons of ore. Individual ore bodies range in size from 200000 tons to almost 40 million tons. The Okiep District is situated in the Proterozoic Namaqualand Metamorphic Complex, in the north-western Cape Province of South Africa (Fig. 1). The gneissic terrane has undergone granulite facies metamorphism and polyphase deformation and the inferred P-T conditions are 6 kbar and ≥ 800°C (Clifford et al., 1975). The dominant regional-scale deformation style is sub-horizontal, with large recumbent folds and flat-lying foliation.

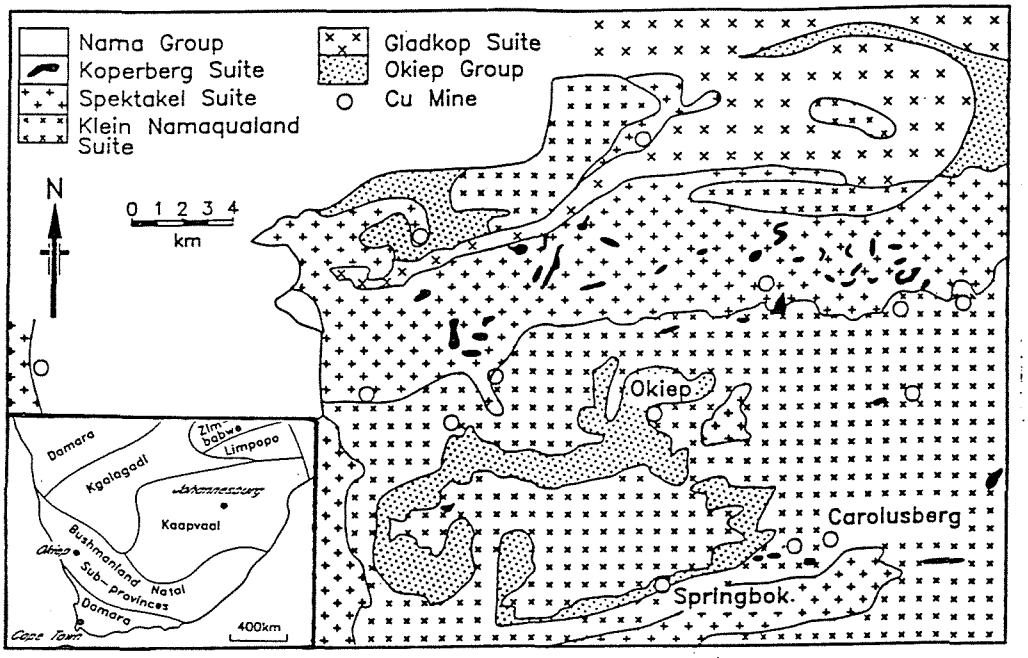

Figure 1: Simplified geological map of the Okiep Copper District

Copper mineralization is contained in the ca. 1100 Ma old Koperberg Suite, which occurs as a swarm of east-west trending dykes and pipe-like bodies, covering an area of 60 km by 50 km. These bodies intrude granite gneiss country rocks along discontinous zones characterized by steeply dipping foliations and associated folding. The intrusives range from old quartz andesinites, through diorite and norite, to younger hypersthenite and glimmerite. The more mafic rock types have the most potential for containing copper mineralization.

The general perception is that the copper ore formed by immiscibility of sulphide liquid from a basic magma. All studies into the genesis of the mineralization, therefore, invariably have also addressed questions related to the origin of the host rocks. More recently, Cawthorn and Meyer (1993) and Boer et al. (1993), however, questioned the magmatic model. They found that the Okiep ores display many features which are atypical for magmatic sulphides, that the style of mineralization is unique, and that the deposits cannot be simply classified in terms of well-known ore-deposit types.

In this paper we present new mineralogical, geochemical and stable isotope data which allows a reconstruction of the magmatic and metamorphic evolution of the Koperberg Suite and the associated copper ore.

Petrography and Mineral Chemistry: The mineralogy of the Koperberg Suite is dominated by variations in modal proportions of plagioclase, orthopyroxene and biotite. Accessory minerals include apatite, K-feldspar, zircon, quartz, anhydrite, various sulphides and Fe-Ti oxides. Amphibole and clinopyroxene are rare, while olivine is conspicous by its absence. Orthopyroxene compositions vary between En_{38} and En_{69} and plagioclase ranges from An_{31} to An_{69}. In contrast to many layered mafic intrusions, orthopyroxene and plagioclase compositions are not correlated which may be attributed to either contamination of the Koperberg magma by crustal material or equilibration under variable fO_2 conditions. Oxygen fugacities obtained from orthopyroxene oxybarometry are in excess of that of the NNO buffer and, in the case of Carolusberg, fall within the stability field of anhydrite (Fig. 2).

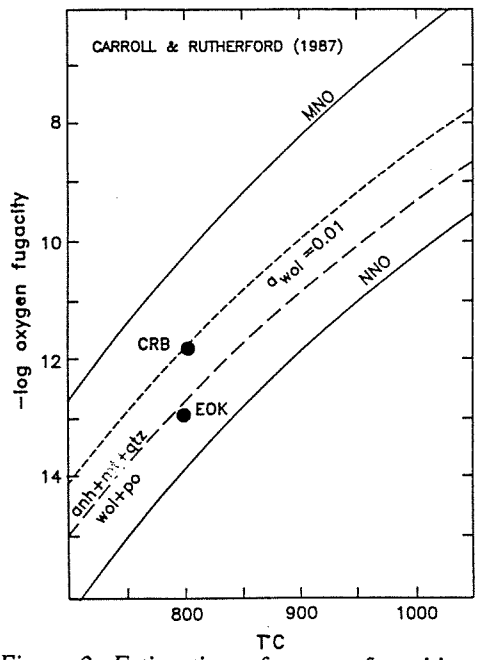

Figure 2: Estimation of oxygen fugacities for the East Okiep and Carolusberg ore bodies

Magnetite is the dominant ore mineral in the leucocratic rocks while sulphides predominate in the more mafic rock types. The latter may occur interstitial between silicates, along cleavage planes in biotite, in granoblastic-textured rocks with polygonal and straight boundaries against orthopyroxene and oxides and as massive ore. Some ore bodies also show a late-stage, low-temperature hydrothermal alteration of silicates and remobilization of sulphides (e.g. Hoits mine). Sulphide parageneses exhibit distinct differences between the various ore bodies. A Fe- and S-rich assemblage comprising chalcopyrite, pyrrhotite and minor pentlandite occurs at East

Okiep (Fig. 1) while the majority of the remaining ore bodies are characterized by an intermediate assemblage consisting of chalcopyrite and bornite. The Carolusberg West ore body (Fig. 1), however, contains a Fe- and S-poor paragenesis involving mainly bornite as well as chalcocite. Iron-titanium oxides are also characterized by three distinct assemblages signifying varying degrees of oxidation. Magnetite with ilmenite oxyexsolution lamellae occurs at East Okiep, magnetite together with discrete granular ilmenite forms part of the intermediate assemblage, and Ti-free magnetite together with discrete grains of titanohematite-ilmenite intergrowths make up the oxide assemblage at Carolusberg West.
Whole-rock analyses of the copper ores display high Fe_2O_3/TiO_3, Cu/Ni and Cu/S ratios, and low S/Se ratios. The oxidized Carolusberg ore is characterized by a mean Cu/S ratio of 2.7 and a S/Se ratio of 1000 while the non-oxidized East Okiep ore has Cu/S and S/Se ratios typical for magmatic sulphides, i.e. 0.8 and 20000, respectively.

Stable Isotopes: Whole-rock $^{18}O/^{16}O$ ratios for the Koperberg Suite rocks vary between 5.9 and 8.3‰ and are controlled by the modal mineralogy. Granite gneiss country rocks have normal whole-rock $\delta^{18}O$ values for granitic rocks being in the range 7.7-8.2‰. The order of decreasing ^{18}O-enrichment in the main host rock minerals is andesine (6.2-9.6‰), hypersthene (6.2-7.4‰), phlogopite (5.1-5.7‰) and magnetite (2.4-5.2‰). Accessory phases give $^{18}O/^{16}O$ ratios of 6.5-7.1‰ for zircon and 5.5-6.6‰ for apatite. The $\delta^{18}O$ andesine and hypersthene data indicate significant enrichment relative to mantle-derived rocks (Fig.3). This enrichment resulted from contamination of the magmas with crustal rocks. Mixing calculations based on a two-end-member model show that an ^{18}O increase of the Koperberg Suite by 1.7‰ requires ca 40% contamination by crustal material with a $\delta^{18}O$ value of 10‰. The $\Delta^{18}O$ andesine-hypersthene values display a wide range from -0.1 to +2.2‰. This is indicative of open-system, disequilibrium behavier and it is suggested that in addition to crustal contamination further modification took place due to subsolidus exchange with an isotopically heavy fluid of metamorphic origin.

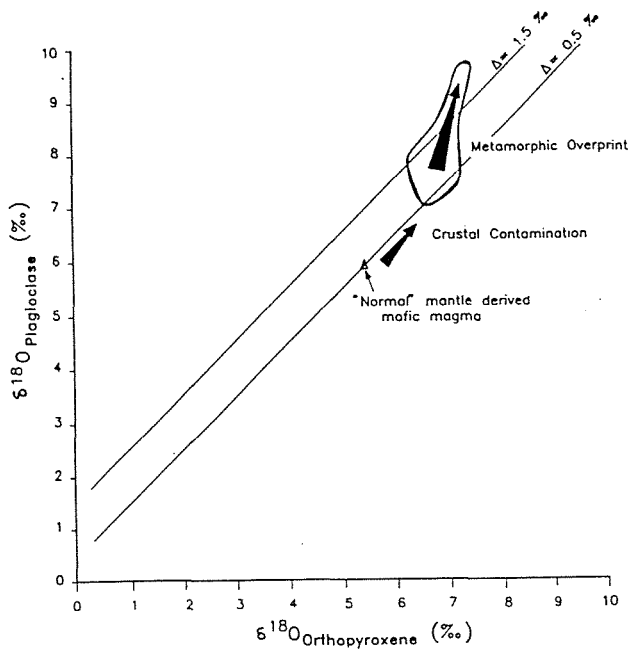

Figure 3: Plot of $\delta^{18}O_{plag}$ versus $\delta^{18}O_{opx}$

Sulphur isotope ratios in sulphides are light relative to mantle values. The $\delta^{34}S$ values for chalcopyrite vary from -1.5 to -3.8‰, for bornite from -1.9 to -4.1‰, and for pyrrhotite from -1.9 to -2.5‰. Reversed chalcopyrite-bornite fractionation and the lack of temperature concordancy indicate open system, disequilibrium behaviour. However, in bulk samples $\delta^{34}S$

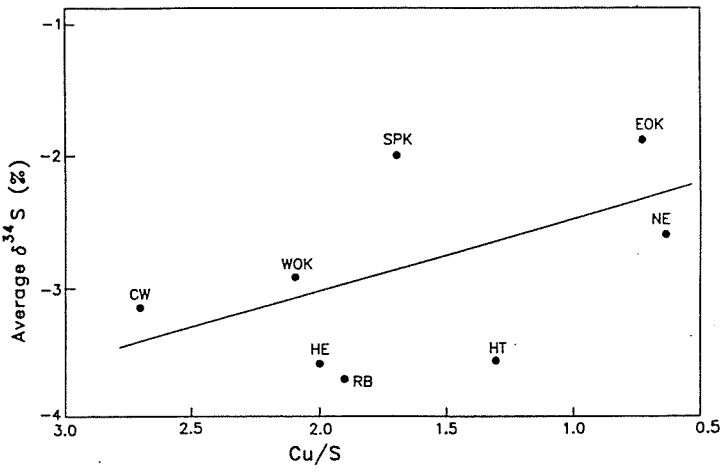

Figure 4: Plot of $\delta^{32}S$ versus Cu/S ratios for the major ore bodies

values decrease systematically with increasing Cu/S ratios of the ore (Fig. 4). This trend may be diagnostic for an oxidation process which resulted in the devolatilization of a SO_2-rich vapour phase.

Summary and Conclusions: The sulphide mineralogy of most of the Okiep ores is dominated by bornite, whereas immiscible magmatic sulphide ores contain pyrrhotite and chalcopyrite. Hence, it is difficult to envisage a primary magmatic origin for the Okiep sulphides. Geochemical and mineralogical evidence demonstrates that the ores have undergone an extensive oxidative event coupled with SO_2 devolatilization in which pyrrhotite and chalcopyrite were converted to Ti-free magnetite and bornite. The devolatilization event was also responcible for the high Cu/S and low S/Se ratios in the Carolusberg ore. It is envisaged that the Koperberg Suite originated from mantle-derived basaltic magmas which were enmplaced over a protracted period of time into a region undergoing deformation and granulite facies metamorphismm. Oxidation probably occurred as a result of the metamophic overprint. The original magma was further modified by assimilation of crustal material. The degree and localization of contamination with silica-rich rocks presumably controled the degree and localization of sulphide saturation. The present interpretation of the evolution of the Okiep copper ores recognizess three distinct stages. A primary magmatic event (e.g. East Okiep); this was almost completely obliterated during a second stage of high temperature oxidative metamorphism (i.e. Carolusberg), and final period of low-temperature hydrothermal remobilization (i.e. Hoits).

References:

Boer, R.H., Meyer, F.M. & Cawthorn, R.G. 1993. Stable isotope evidence for crustal contamination and desulphidation of the cupriferous Koperberg Suite, Namaqualand, South Africa. Geochim. Cosmochim. Acta (submitted).

Cawthorn, R.G. & Meyer, F.M. 1993. Petrochemistry of the Okiep Copper District basic intrusive bodies, northern Cape Province, South Africa. Econ. Geol. (in press).

Clifford, T.N., Gronow, L., Rex, D.C. & Burger, A.J. 1975. Geochronological and petrographical studies of high-grade metamorphic rocks and intrusives in Namaqualand, South Africa. J. Petrol. 16: 154-188.

Carroll, M.R. & Rutherford, M.J. 1987. The stability of igneous anhydrite: experimental results and implications for sulfur behaviour in the 1982 El Chinion trchyandesite and evolved magmas. J. Petrol. 28: 781-801.

Current Research in Geology Applied to Ore Deposits. Fenoll Hach-Alí, Torres-Ruiz & Gervilla (eds) (1993). ISBN 84-338-1772-8

PARAGENESIS AND REGIONAL ZONING OF THE POLYMETALLIC ORE DEPOSITS IN THE AGUILAS AND SIERRA ALMAGRERA-HERRERIAS AREAS, SOUTHEASTERN SPAIN

Morales Ruano, S. (1); Both, R.A. (2) & Fenoll Hach-Alí, P. (1)
(1) Dept. de Mineralogía y Petrología, Universidad de Granada-CSIC, Granada, Spain
(2) Dept. of Geology and Geophysics, University of Adelaide South Australia

ABSTRACT

The Aguilas and Sierra Almagrera-Herrerías mineral districts are located in the highly mineralized interior domain of the Betic Cordillera in southeastern Spain. Deposits in the Aguilas area are dominantly Fe-Pb-Zn veins, while those in the Sierra Almagrera-Herrerías area are Cu-Pb-Zn-Ba-Fe veins. Mineral assemblages present in both groups of deposits exhibit complex paragenetic sequences, with significant differences between the two groups. The Aguilas group is characterized by a high temperature (400º-450ºC) assemblage in the early stage of mineral deposition, whereas the late stage minerals are present only in the Sierra Almagrera-Herrerías deposits. The regional distribution of mineral assemblages, representing various stages of the paragenesis, shows a geographic distribution that suggests a regional zoning of deposits within each group.

1 INTRODUCTION

The base metal and precious metal deposits of south-eastern Spain were major sources of Pb, Zn and Ag during the 19th century and up to the middle of the 20th century. Some mining districts are still in operation (although at greatly reduced levels) after more than 2000 years of continuous production (Arribas et al., 1991). The metallogenetic importance of the region is demonstrated by the presence of more than 3000 known occurrences of mineralization between Cabo de Gata, Almería and Cartagena, Murcia. This contribution is concerned with the paragenesis and compositional variations of deposits in the central part of the region, in particular those in the vicinity of Aguilas (Sierra

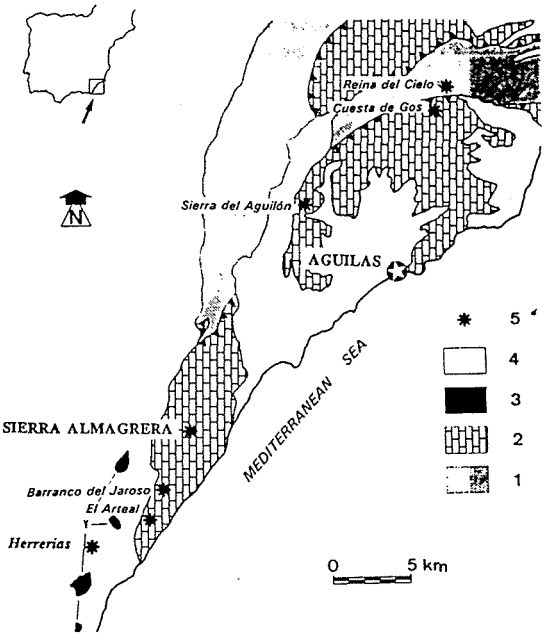

Figure 1. Geological map: 1 Nevado-Filabride Complex. 2 Alpujarride Complex. 3 Volcanic rocks. 4 Neogene sediments. 5 Outcrops.

del Aguilón, Ermita de la Cuesta de Gos and Reina del Cielo) and Sierra Almagrera-Herrerías (El Jaroso, El Arteal and Herrerías) (Fig. 1).

These consist of base metal vein deposits spatially related to volcanism in the region. In addition to these deposits other occurrences of mineralization, of lesser economic significance, include pyrite disseminations and Fe-Mn oxide veins (with relic sulphide minerals) in volcanic host rocks

2 GEOLOGICAL SETTING AND ORE DEPOSITS

The host rocks of the deposits under investigation belong to the interior domain of the Betic Cordillera, which resulted from the collision of Africa with Europe during the Cainozoic. This domain is characterized by a nappe structure comprised of a series of superposed tectonostratigraphic units of Palaeozoic and Mesozoic metasediments referred to as (from bottom to top) the Nevado-Filábride, Alpujárride and Maláguide complexes. Subsequently, Neogene sediments were deposited in intermontane basins.

The majority of the deposits in the Aguilas and Sierra Almagrera-Herrerías areas are hosted by rocks of the Loma de Bas unit of the Alpujárride complex or the Cantal unit of the Nevado-Filábride complex (Alvarez, 1987). The former consists of graphitic mica and quartz-mica schists and the latter of quartzites and mica schists with staurolite, garnet, kyanite and sillimanite. An exception is the Herrerías mine, where the host rock is hydrothermally altered marl of Tortonian age (Alvado, 1986).

Post-collision Neogene volcanism produced the Almería-Cartagena volcanic belt that, from south to north, shows a variation from calc-alkaline to high-potassium calc-alkaline to shoshonitic and to ultrapotassic composition, along with a trend in age from 18 to 2 Ma. In the Aguilas area the volcanic rocks mainly belong to the shoshonite series (Castroviejo, 1991), although some outcrops occur of hydrothermally altered microtonalites with relic phenocrysts of sanidine, indicating a correlation with the high potassium calc-alkaline series. Volcanic rocks in the Sierra Almagrera-Herrerías area are present as dacitic and rhyodacitic domes, of the shoshonitic series, related to the N-S Palomares fault. These rocks consist of explosive breccias rich in sanadine and biotite phenocrysts.

Although none of the economically important deposits in the Aguilas and Sierra Almagrera-Herrerías area is hosted by volcanic rocks (cf. Rodalquilar, Cunningham et al., 1990; Mazarron, Espinosa et al., 1974), there is a close spatial relationship between the distribution of the volcanism and mineralization, and volcanic rocks were encountered in some of the mine workings.

3 MINERAL ASSEMBLAGES AND TEXTURES

The main geological, mineralogical and textural features of the deposits included in this study are summarized in Table 1. From textural studies two generalized paragenetic sequences have been established, one for the deposits in the Aguilas area and the other for deposits in the Sierra Almagrera-Herrerías area. As shown in Table 1, the veins are polymetallic deposits of Fe-Pb-Zn-Cu-Ba-Ag, with minor amounts of Ni-Bi-As. However, two groups

of deposits can be distinguished, with significant differences in mineralogy, chemistry and textures.

Table 1. Mineral assemblages and textural features of Aguilas– Sierra Almagrera areas.

LOCALITY	MAJOR ELEMENTS	MINOR ELEMENTS	HOST ROCKS	MORPHO-LOGY	MAJOR ORE MINERALS	MINOR ORE MINERALS	GANGUE MINERALS	MAIN TEXTURAL FEATURES
SIERRA DEL AGUILON	Zn-Pb-Fe-Cu	As-Ag	Alpujarride Complex	veins, pseudo-stockworks	sp, gn, py	cp, apy, cbn, agpnt	qtz	cp disease; sp stars in cp; lamellar twinning in cp
ERMITA CUESTA DE GOS	Fe-Pb-Zn	Bi-As	Alpujarride Complex	veins	py,mc, gn, sp, po	cp,apy,bi	qtz, (bar)	mc–py lamellae; mc intergrowths / inclusions in py; porous patches in py (after mc?); sp stars in cp
REINA DEL CIELO	Fe-As-Zn	Cu-Pb-Bi	Nevado-Filabride Complex	veins	py,mc, gn,sp,po	cp,gn, po, bi	qtz, bar	lamellar py-mc with euhedral outlines, some ap overgrowths; "birds-eye" textures of py-mc (after po) within py crystals
EL JAROSO	Cu-Fe-Pb-Zn-Ba	Ni-Bi-Ag	Alpujarride Complex	veins, dissemina-tions	cp,gn,py,mc	sp, thd, bou, bi, ger	bar, sid, qtz	colloform & botryoidal py-mc; colloform sp; compositional zoning of apy
EL ARTEAL	Cu-Fe-Pb-Zn-Ba	Ag-Bi	Alpujarride Complex	veins	py,mc,gn, veen	sp, thd, bou, bi, ger	bar, sid, qtz	colloform & botryoidal py-mc; colloform sp; dendritic gn; fibrous & radial barite; compositional zoning of apy and thd; framboidal py; melnikovite-type py
HERRERIAS	Ba	Pb-Zn-Ag	Neogene sediments	stratiform, veins	bar,Fe-Mn ox.	gn,sp	bar	comb textured bar; dendritic gn; colloform sp.

Abbreviations: *apy: arsenopyrite; agpnt: argentopentlandite; bi: bismuthinite & native bismuth; bou: bournonite; cbn: cubanite; cp: chalcopyrite;ger: gersdorffite;gn: galena;mc: marcasite; po: pyrrhotite; py: pyrite; sp: sphalerite; thd: tetrahedrite; veen: veenite; bar: barite; qtz: quartz;sid: siderite.*

The Aguilas group consists of Fe-Pb-Zn deposits, the main ore minerals being pyrite, marcasite, sphalerite, and galena with quartz as the major gangue mineral. The mineral assemblage and textures of this group indicate high temperatures of formation (400º-450ºC, Morales & Fenoll, 1992) for the first stage of the paragenetic sequence (see below).

In the Sierra Almagrera-Herrerías area the deposits are characterized by Cu-Pb-Zn-Ba-Fe. The major ore minerals are chalcopyrite, galena, pyrite, marcasite, and veenite, with barite as the major gangue mineral. Textures observed in this group of deposits are characteristic of open space deposition at relatively low temperatures.

Differences are also observed in the paragenetic sequences for the two groups of deposits (Fig. 2). The first stage (argentopentlandite, cubanite, sphalerite, and chalcopyrite) is seen only in the Aguilas deposits and most minerals of the final stage (galena, veenite, bournonite, tetrahedrite) are present only in the Sierra Almagrera-Herrerías deposits. Minerals of the intermediate stages are found in both groups of deposits. In addition to the changes in mineral assemblages with time, some trends are also observed in mineral chemistry. For example, sphalerite was deposited throughout almost the entire paragenetic sequence and shows a gradual decrease in Fe content from about 10 wt. % in the initial stage to virtually 0 wt. % in the final stage.

4 CONCLUSIONS

Although four stages of mineral deposition can be recognized, textural features and trends in mineral chemistry (e.g. of

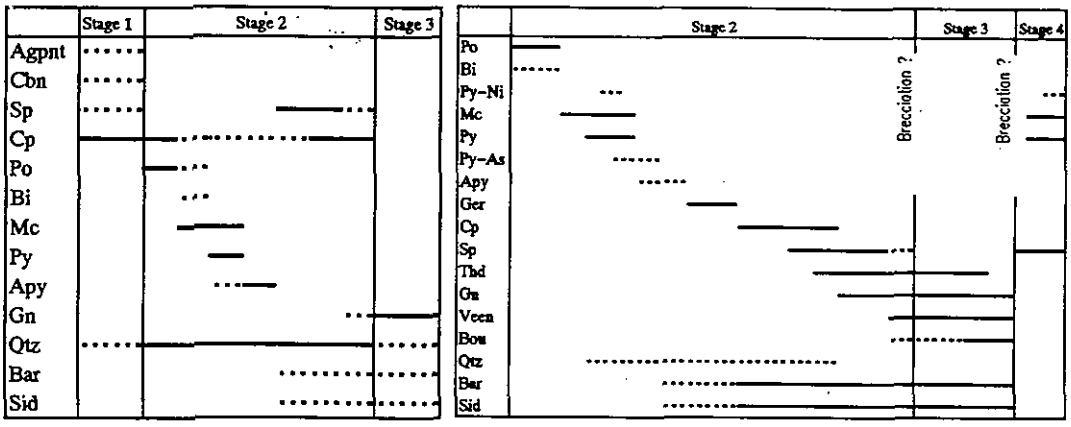

Figure 2. Paragenetic sequences for: (A) Aguilas area. (B) Sierra Almagrera area

sphalerite) indicate that the sequence of crystallization was more or less continuous.

The mineral assemblages corresponding to each stage, although more common in certain deposits, can also be present in others. This suggests a continuity of deposition that resulted in a zonation on a regional scale within each group. Accordingly, in the Aguilas group, mineral assemblages of the high temperature paragenetic stage are mainly found in the Sierra del Aguilón deposits, but rarely in the deposits of Ermita de la Cuesta de Gos and not at all in Reina del Cielo. Within the Sierra Almagrera-Herrerías group, the deposits of El Jaroso and El Arteal are characterized by intermediate and final stages of the paragenesis and those of Herrerías by the final stage only. This deposit differs from other veins described above, as the Ag, Pb, and Zn are associated with barite veins within a sequence of Fe-Mn oxides that appear to represent exhalites deposited in Tortonian marls.

REFERENCES

Alvado, A. 1986. Sédimentation, déformation, et manifestations magmatiques néogènes associées au couloir de décrochement de Palomares. Ph. D. Université P. et M. Curie, Paris. 240 pp.

Alvarez, F. 1987. La tectónica de la Zona Bética en la región de Aguilas. Ph. D. University of Salamanca (Spain). 371 pp.

Arribas, A. Jr; Tosdal, R.M. & Wooden, J.L.. 1991. Lead isotope constraints in the origin of base-and precious-metal deposits from southeastern Spain. In: Pagel, M. Leroy, J.L. (eds). Source, transport and deposition of metals. Balkema, Rotterdam. pp 241-244.

Castroviejo, R.; Nodal, T.; Podwysocki, M.H. & Insua, M. 1991. Mineralizaciones subvolcánicas (Au- Ag- Sn-Sulfuros polimetálicos) y hallazgo de afloramientos de pórfidos tonalíticos neógenos en la Sierra de Lomo de Bas (Murcia). Bol. Soc. Esp. Mineralogía. 14:183-200.

Cunningham, C.G.; Arribas, A. Jr.; Rytuba, J.J. & Arribas, A. 1990. Mineralized and unmineralized calderas in Spain; Part I, evolution of the Los Frailes; Caldera. Mineral. Deposita. 25 suppl.: s21-s28.

Espinosa, J.; Martín-Vivaldi, J.M. & Perez-Rojas, A. 1974. Mapa geológico de España 1:50000. Hoja 978, Llano. Instituto Geológico de España, Madrid.

Morales Ruano, S. & Fenoll Hach-Alí, P. 1992. Quimismo de las paragénesis asociadas al vulcanismo terciario del sector Aguilas-Sierra Almagrera (SE de España). Bol. Soc. Esp. Mineralogía. 15-1: 282-286.

ACKNOWLEDGEMENTS

This study has been supported by the Research Group 4028 of the Junta Andalucía and by DGICYT project PB-0107. R.A.B. acknowledges with gratitude the award of a Visiting Research Fellowship by the Dirección General de Investigación Científica y Técnica (DGICYT) de España.

Current Research in Geology Applied to Ore Deposits. Fenoll Hach-Alí, Torres-Ruiz & Gervilla (eds) (1993). ISBN 84-338-1772-8

CYMRITE IN THE STRATIFORM BARITE DEPOSITS OF ZAMORA PROVINCE (CENTRAL WEST SPAIN)

Moro Benito, M.C. (1); Cembranos Pérez, M.L. (1) & Pérez del Villar Guillen, L. (2)
(1) Dept. Geología. Facultad de Ciencias. Universidad de Salamanca. 37008 Salamanca, Spain
(2) Dept. Técnicas Geológicas del CIEMAT, 28008 Madrid, Spain

ABSTRACT: During the research carried out on the Late Silurian -Early Devonian stratiform barite deposits of the Zamora province, cymrite ($BaAl_2Si_2O_8.H_2O$) has been detected in the metamorphic siliceous and carbonate baritic rocks. The aim of this work is to report the mineralogical and chemical characteristics of this hydrated Ba-feldspar.

INTRODUCTION: Anhidrous and hydrated barium-feldspars, celsian, hyalophane and cymrite, associated with sedimentary and metamorphic rocks and metamorphosed barite deposits have been studied by several authors. Among them, Bjorlykke and Griffin (1973) reported hyalophane from Lower Devonian barium-rich shales in the Oslo region. Cymrite and celsian have been identified in manganese-rich metamorphic rocks from Andros island (Greece) by Reinecke (1982). Coats et al.(1980 and 1990), and Fortey and Beddoe-Stephens (1982) described celsian, hyalophane and cymrite in quartz-celsian rocks from the mineralized zone of the Aberfeldy stratabound barium zinc deposits (Scotland). Jakobsen (1990) described and discussed the genetic significance of an hydrous Ba-silicate similar to cymrite but with 4 molecules of H_2O present in unmetamorphosed black organic-rich cherts, together with hyalophane and barite, in central North Greenland. Russell (1988) suggested that authigenic Ba-feldspars or their hydrated precursors may precipitate from aluminosilicate gels in conditions of variable pH but where the activity of water is low.

GEOLOGY AND METALLOGENIC CHARACTERISTICS OF THE BARITE DEPOSITS.

The barite deposits studied (Ambiciosa, Mary Carmen and Astur mines) are located in the central-western zone of the Zamora province. All of them are hosted by the thick Late Silurian-Early Devonian volcano-sedimentary sequence of the Alcañices Synform (Iberian Massif). These materials were affected by four different Hercynian deformation phases and a low-grade dynamothermal metamorphic event, characterized by a low-medium pressure (New Hampshire type) and a temperature of about 350°C (Antona,1989).

The barite deposits have been studied from different points of view by Moro (1980), Moro and Arribas (1980), Poole et al. (1990), Moro and Arribas (1989), Hernández et al. (1991), Perez del Villar et al (1992) and Moro et al.(1992). Following the above mentioned authors, these barite deposits could have formed in restricted and partially anoxic marine basins, developed in a continental margin, by interaction between the barium-rich solutions, furnished to the basin through exhalative hydrothermal vents, and the SO_4^{2-} ions from seawater. Later, the diagenetic and above all the metamorphic events produced the texto-estructural features observed at present in the different types of barite distinguised.

SAMPLES AND RESULTS: The samples studied come from the barite-bearing siliceous, schistose and carbonate beds located above and below of the stratiphorm massive barite of the Ambiciosa, Mary Carmen and Astur mines.(Fig 1)

The barite-cymrite-bearing samples have been studied by polarizing and scanning electron microscopy, using a DSM-940 Zeiss equipment coupled to energy dispersive spectrometry. Backscattered electron images as well as Si, Al and Ba mapping have been taken. The X-ray diffraction patterns, DTA and TG diagrams and IR spectrum have been obtained from on a concentrate of cymrite obtained by electromagnetic and densymetric separation methods.

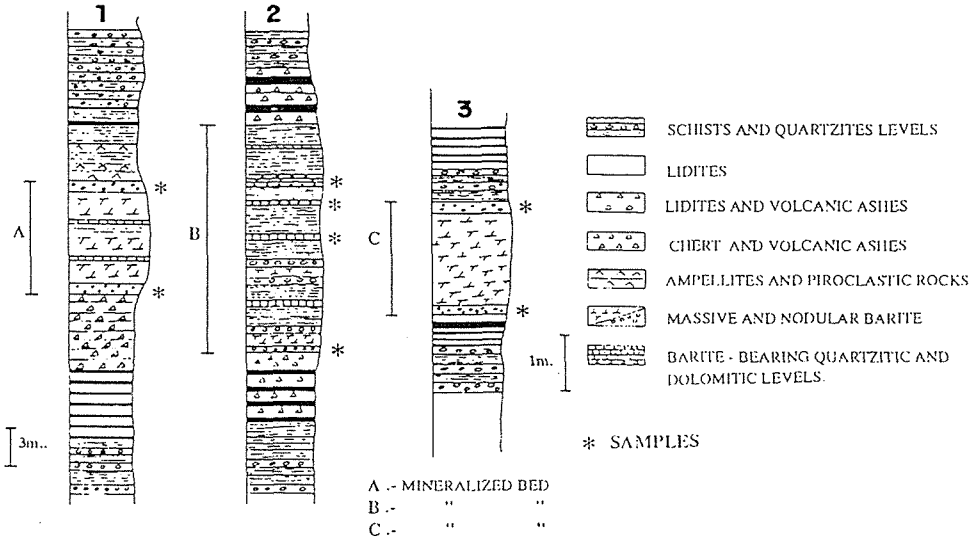

Fig 1.- Stratigraphic sequences of the Ambiciosa(1), Mary Carmen (2) and Astur(3) mines.

The chemical composition of cymrite has been determined using a CAMEBAX SX-50 electron microprobe at the analytical service of the University of Oviedo. Seexteen crystals of cymrite of samples from the three mines studied have been anlayzed.

All the samples are characterized by a compact and finely laminated structure, with very fine grain size. The diagenetic and/or metamorphic lenticles, nodules, rosettes and crystals of barite up to 3 cm in size and scattered in the rock matrix, can be observed. The laminated structures of samples, due to variations in the mineralogical composition and carbonaceous matter content, is frequently affected by slumping structures.(Fig 2a). The matrix of samples has a low oriented microcrystalline texture and it is mainly formed by sericite subeuhedral to euhedral crystals of cymrite, barite, Mg-calcite and quartz. The carbonaceous matter (vitrinite) and sulfides mainly pyrite, are accessory minerals and they are concentrated in very fine laminae.

Backscattered electron images and Si, Al and Ba mapping show the distribution of cymrite,in the rock matrix, as well as the euhedral-subeuhedral habit of the crystals.(Fig 3).

The X-ray diffraction patterns, ATD and TG diagrams as well as de IR spectrum have corroborated the existence of cymrite in the hostrocks of the barite deposits studied.

Table 1 shows the chemical composition and structural formulae of the cymrites analyzed.

Table 1.- Electron microprobe analyses of cymrite.

	Mary Carmen (n=10)		Astur (n=3)		Ambiciosa (n=3)	
	$\bar{x}$	σ	$\bar{x}$	σ	$\bar{x}$	σ
SiO_2	30,974	1,253	33,164	0,981	32,827	1,681
Al_2O_3	20,740	0,556	22,467	2,044	22,321	1,936
MgO	0,045	0,133	0,035	0,606	0,0187	0,032
CaO	0,039	0,030	0,024	0,021	0,02	0,035
BaO	37,725	0,0917	38,956	1,039	38,994	0,752
Na_2O	0,072	0,012	0,162	0,096	0,081	0,033
K_2O	0,492	0,194	0,391	0,127	0,276	0,065
Total	91,090	1,591	96,290	3,335	95,966	0,316
	STRUCTURAL FORMULA, BASED ON 8 OXYGENS					
Si	2,175	0,033	2,179	0,056	2,176	0,115
Al	1,718	0,027	1,737	0,087	1,744	0,149
Mg	0,005	0,014	0,003	0,006	0,002	0,003
Ca	0,003	0,002	0,002	0,002	0,001	0,002
Ba	1,040	0,038	1,004	0,041	1,013	0,018
Na	0,010	0,002	0,020	0,011	0,011	0,004
K	0,044	0,018	0,033	0,012	0,023	0,006

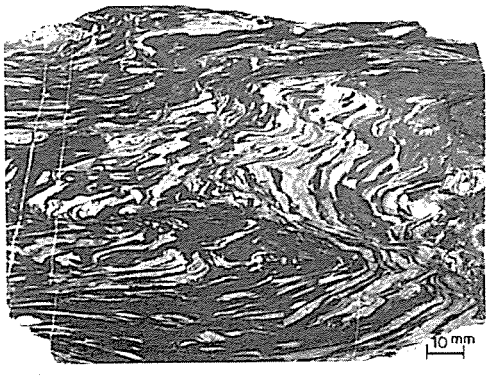

a

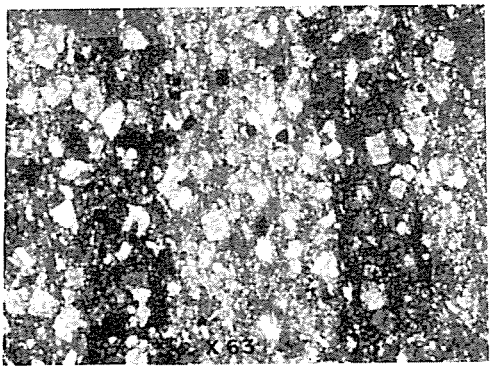

b

Fig 2.- Macroscopic aspect of the samples from the barite-cymrite-bearing siliceous and schistose rocks (a). Microscopic aspect of the euhedral to subeuhedral cymrite crystals (b).

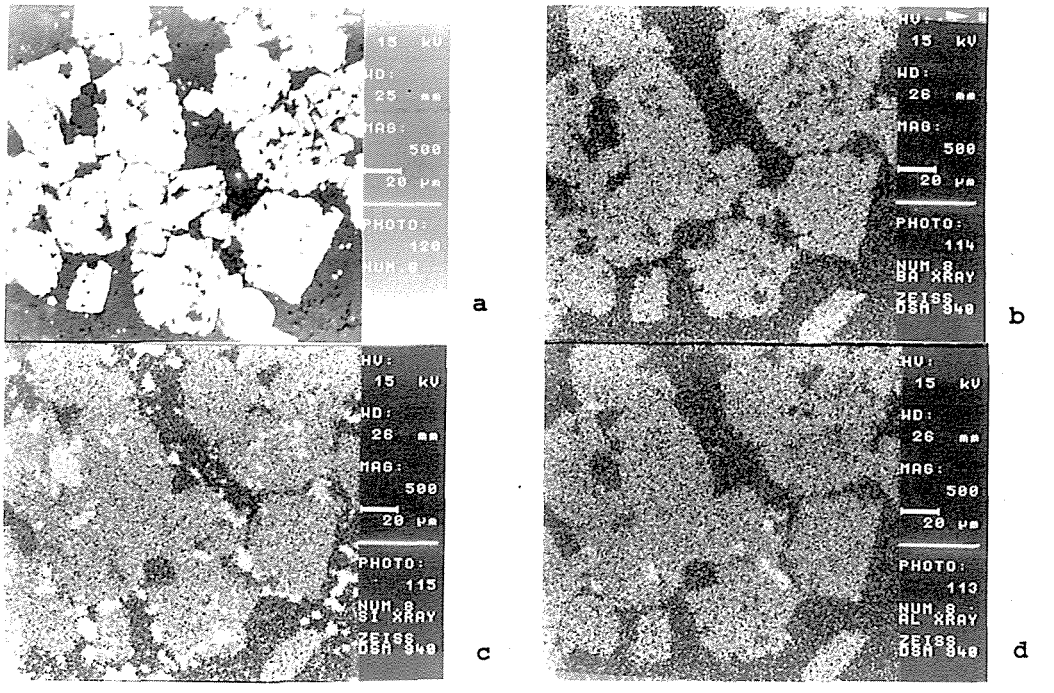

Fig 3.- (a) Backscattered electron image of cymrite. (b, c and d): Ba, Si and Al mapping of the same image.

ACKNOWLEDGEMENTS: Funding for this work was provided by the D.G.I.C.Y.T.(M.E.C. España; project: PS-88-0039) and Castilla-León Autonomous Government (project SA-15/09/92).

REFERENCES:

Antona, J.F.1989. Tesis de Licenciatura. University of Salamanca.
Bjorlykke,K.O.and Griffin,W.L. 1973. J. Sediment. Petrol. 43:461-5.
Coats,J.S, Smith,C.G, Fortey,N.J, Gallagher,M.J, May,F.& McCourt, W.J. 1980. Appl. Earth Sci., 89: B 110-22.
Coats,J.S.& Fortey,N.J. 1990. 8th IAGOD Symposium: Abstracts.
Fortey,N.J.& Beddoe-Stephens,B.1982. Mineral Mag. 46: 63-72.
Hernández,E,Moro,M.C. & Cembranos,M.L.1991. Plinius, nº 5, 102-103.
Jakobsen,U.H. 1990. Mineralogical Magazine. 54: 81-89.
Moro,M.C.1980. Tesis Doctoral. Universidad de Salamanca.
Moro,M.C.& Arribas,A.1980.I Symposium Diagenesis Rocas Sedimentarias . Barcelona. 325-338.
Moro,M.C.& Arribas,A.1989. Zamora ore field. In: Milka K. de Brodtkorb (ed). Nonmetalliferous stratabound ore fields. Van Nostrand Reinhold. New York.
Moro,M.C,Hernández,E,Cembranos,M.L. & Pérez del Villar,L. 1992. III Congreso Geológico de España y VIII Latinoamericano. Actas tomo 3:205-211.
Perez del Villar,L.,Moro,M.C. & Cembranos,M.L.1992. Clay Minerals, 27: 309-323.
Poole,F.G.,Moro,M.C.,Lopera,F.& Arribas,A. 1990. 8th IAGOD Symposium Otawa. Canada, A 21-A 22.
Reinecke, T. 1982. Contrib. Mineral. Petrol. 79:333-6.
Russell,J.1988. Proccedings seventh IAGOD Symposium (Nagele U.Obermiller).Stuttgart

Current Research in Geology Applied to Ore Deposits. Fenoll Hach-Ali, Torres-Ruiz & Gervilla (eds) (1993). ISBN 84-338-1772-8

MASS BALANCE, ELEMENT MOBILITY AND REACTION PATH IN MESOTHERMAL GOLD DEPOSITS: AN EXAMPLE FROM FLAMBEAU LAKE, ONTARIO

Mountain, B.W. & Williams-Jones, A.E.
Fluid-Rock Interaction Lab., Dept. of Earth and Planetary Sciences, McGill University, Montreal, Quebec, Canada

ABSTRACT: Gold-bearing, quartz-ankerite-albite veins associated with carbonatized, albitized and desilicated wallrock occur at Flambeau Lake, Ontario. A mass balance study indicates that SiO_2, Al_2O_3, Fe_2O_3, MgO and K_2O were removed from the wall rock and CaO, CO_2, S and Na_2O were added. Zr, Ti, LREE remained immobile during alteration. The behaviour of Li, V and Mo suggests that the fluid/rock ratio decreased away from the vein. It is proposed that the introduction of a quartz-undersaturated, CO_2-rich fluid into fractures caused carbonatization of chlorite and dissolution of quartz in the wallrock which provided new pathways which increased access of the infiltrating fluid to the rock and promoted reactions that led to preferential concentration of gold in felsic and intermediate quartz-rich rocks relative to the less reactive quartz-poor mafic volcanics.

Introduction

Most studies of wallrock alteration provide petrographic descriptions of the altered rocks, estimate the masses of components added to or lost from the rock, and interpret the physicochemical conditions that were active during the process. Rarely, however, are attempts made to actually determine the reaction path (e.g. Brimhall, 1979; Böhlke, 1989), i.e., reconstruct the spatial and temporal distribution of changes that occur in a rock during progressive interaction with a hydrothermal fluid. In this paper we report on an attempt to establish such a reaction path for a mesothermal gold deposit at Flambeau Lake, Ontario, based on a detailed analysis of bulk chemical and mineral compositions in the alteration halo of a single vein. The study showed that: 1) reaction progressed through spatially separate but temporally coincident steps of quartz dissolution, carbonatization, and albitization; 2) quartz dissolution provided the driving force for reaction by creating the pathways necessary to permit the infiltration of fresh aliquots of fluid; and 3) reaction terminated when changes in intensive parameters led to quartz saturation.

Geological Setting

Gold mineralization, in the Flambeau Lake area, is hosted by networks of extension veins in the Archean, greenschist facies, mafic to felsic Lower Wabigoon volcanics (Blackburn and Janes, 1983). Mineralized veins contain ankerite-albite adjacent to their margins and have cores of quartz. The textures of the albite crystals indicate that open-space filling dominated the ankerite-albite stage, which was followed by infilling of quartz. Intense wall rock alteration accompanied formation of veins which contain albite-ankerite while those which are composed only of quartz show little wallrock alteration. There is also evidence of blockage of fluid infiltration by pre-existing, quartz-only veins.

Alteration Mineralogy and Chemistry

In order to investigate the mass transfers which occurred during alteration, a single alteration halo developed in quartz diorite adjacent to a quartz-ankerite-albite vein was sectioned into 13 samples (about 12 g each). A least squared regression method, using sample major element composition and mineral compositions was used to calculate the abundance of the constituent minerals. Figure 1a shows the important characteristics of the alteration halo. In the chlorite zone (**Chl**), no distinct mineralogical changes are recognized. The zone is characterized by microveinlets of chlorite and associated disseminated pyrite. Significant mineralogical changes become apparent in the transitional zone (**Trans**), where

a progressive increase in ankerite and albite accompanied a gradual loss of chlorite. In the ankerite-albite zone (**Ank-Alb**), chlorite was completely removed. This is associated with a gradual increase and decrease, respectively, in the contents of albite and quartz. Immediately adjacent to the vein (the albite zone; **Alb**) there is a sharp rise in albite content and sharp decreases in ankerite and sericite content.

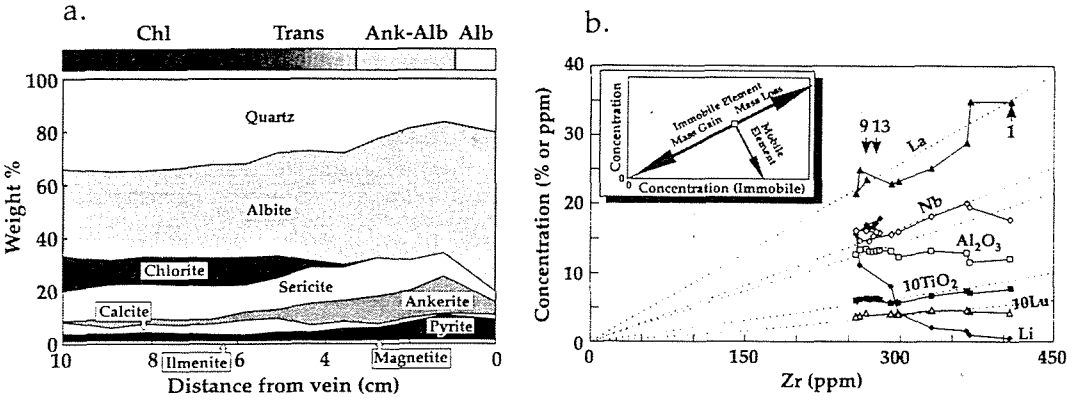

Figure 1. a. Calculated mineral abundances (weight %), plotted versus decreasing distance from vein, across the quartz diorite alteration halo. The grey scale at the top shows the position of each alteration zone. **b.** Concentration plot of Zr versus selected major element oxides and trace elements. The dotted lines are not regressions but simply lines which go from the origin through the precursor (Sample 13 for Nb, Li, Al_2O_3 and TiO_2; Sample 9 for La and Lu). Solid lines connect adjacent samples. Numbered arrows indicate the position of selected samples. The inset diagram shows the expected trend when two elements are immobile during mass loss or gain as well as the trend, when plotted against an immobile element, for an element which is lost during alteration (e.g. Li).

Mass Balance and Element Mobility

In order to obtain a reliable estimate of the chemical exchanges that have occurred between fluid and rock during alteration, it is necessary to determine how mass loss or gain has contributed to composition changes. Following the method of Maclean and Kranidiotis (1986), a diagram of Zr versus selected elements was constructed to test for immobility (Fig. 1b). Linear trends with approximately constant slope are evident between La-Zr, TiO_2-Zr and Nb-Zr (up to Sample 2). Similar trends were observed between Zr-U, Zr-Th and Zr-LREE. It was concluded that Zr, U, Th, TiO_2, LREE and, to some extent, Nb remained immobile during alteration. However, it is evident that Al_2O_3 did not remain immobile. Mass factors, used to correct for mass changes during alteration, were calculated using the ratio $Zr_{unaltered}/Zr_{altered}$. Mass transfers for selected major and trace elements are plotted against distance from the vein in Figure 2. In the chlorite zone there appears to have been little noticeable change and, except for perhaps Na_2O and V, all displayed elements show flat profiles. In the remaining alteration zones, major and minor elements exhibit two types of behaviours: 1) mass transfer profiles with gradual positive or negative slopes, such as those of SiO_2, Al_2O_3, S, Li, Mo, Pb and V (up to the Ank-Alb zone); 2) mass transfer profiles with distinct discontinuities such as those of Fe_2O_3, MgO, CaO, CO_2 and V (after the Trans zone). Of particular note are the mass transfer profiles for SiO_2 and Al_2O_3, which both show a 40% mass loss, K_2O, which shows little change up to the Ank-Alb zone and then a drop to a 80% loss, and Li, which shows a

gradual decline to a 98% loss adjacent to the vein wall.

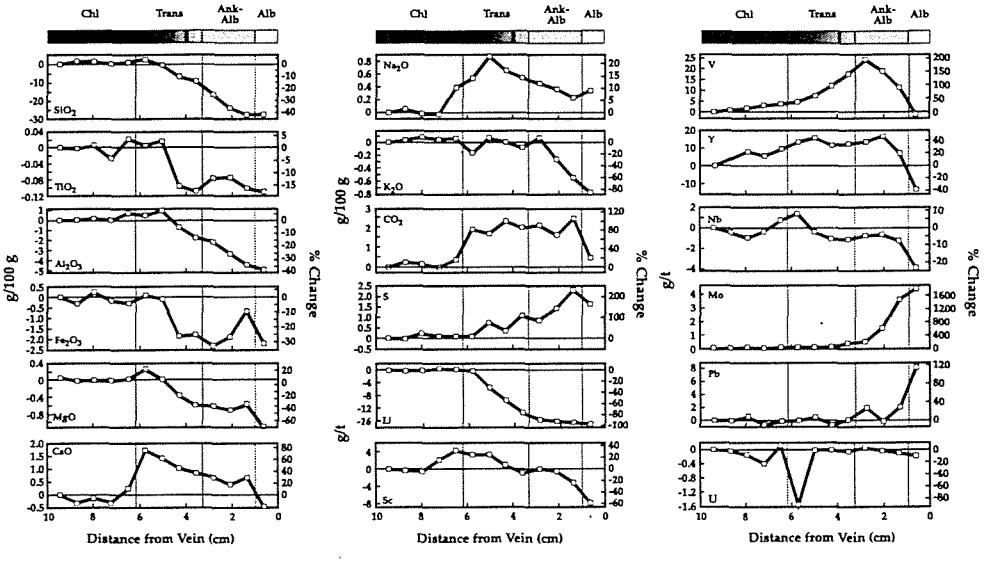

Figure 2. Mass transfer profiles, calculated assuming constant Zr, for selected major element oxides and trace elements, across the quartz diorite alteration halo. Scales on the left side of each plot show mass changes in absolute units (g/100 g precursor for SiO_2 to S and g/tonne precursor for Li to U). Those on the right side show percentage change from the precursor. The gray scales at the top show the position of each alteration zone. Dotted lines show the boundaries of each alteration zone.

Discussion

Textural relationships in the veins, the large amounts of SiO_2 removed from the host and the presence of quartz-only veins with no significant associated alteration all point to a source fluid which was initially undersaturated with quartz, remained undersaturated during the main part of the intense alteration, and eventually evolved to precipitate quartz. Although quartz in the quartz-ankerite-albite veins appears to have been deposited late, the blockage of fluid infiltration and thus alteration by pre-existing quartz-only veins, shows that the process was cyclical. Each cycle was characterized by the initiation of fracturing and the influx of pressured hydrothermal fluid (Sibson et al., 1988). Concurrent with this influx of fluid there was desilication, carbonatization and albitization in the alteration zones and the precipitation of ankerite and albite along the fracture margins. The dissolution of large amounts of quartz created extensive pathways into the wallrock. This ensured more widespread reaction than would have been the case if the fluid was saturated with respect to quartz on entry into the felsic or intermediate horizon. Fluid pressure eventually declined, resulting in the partial closure of the veins and the deposition of quartz (Fig. 3a). The onset of quartz deposition in the wallrock and the fractures terminated alteration. A single iteration of this process created veins which are lined with ankerite-albite and filled with quartz.

The shape of mass transfer profiles allows an interpretation of the sequence of events which occurred during alteration. Gradually increasing or decreasing mass changes (e.g. Li) suggest a progressive increase of fluid/rock ratio (F/R) towards the vein. Trends which show sharp discontinuities indicate reactions which went to completion before the maximum F/R ratio was reached. The two reactions which best exemplify these twoend members are the

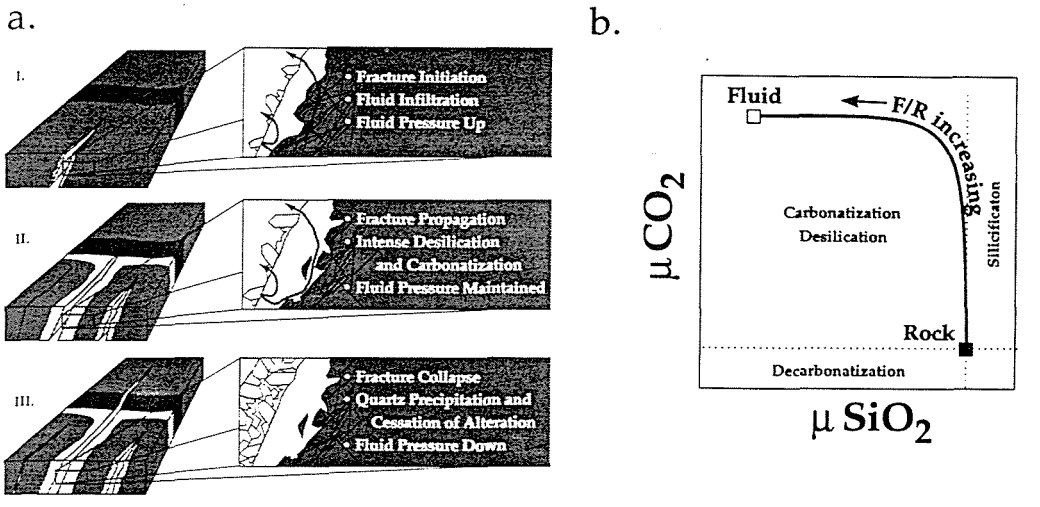

Figure 3. a. Schematic diagram showing the proposed sequence of events during one mineralizing cycle. I. influx of pressurized, quartz-undersaturated fluid which promoted vein propagation and opening. II. single-pass flow of this fluid through the fractures concurrent with vein propagation. III. pressure decrease causing vein collapse, quartz deposition and termination of alteration. **b.** Schematic diagram showing the relative positions of the fluid and rock in chemical potential space and the path of the rock as fluid/rock ratio (F/R) increased.

carbonatization of chlorite and the dissolution of quartz. The hydrothermal fluid entered the fracture undersaturated with respect to quartz but contained a high CO_2 component. It can be inferred, therefore, that the μSiO_2 of the fluid was lower, and the μCO_2 higher, than that of the rock. At low F/R, the lower μCO_2 of the rock required that carbonatization was the dominant reaction because only small amounts of quartz needed to dissolve to maintain the fluid at quartz saturation, and therefore the μSiO_2 of the rock was not significantly affected. As F/R increased, carbonatization went to completion while μSiO_2 of the rock was still unaffected. Further increases in F/R ratio caused continued desilication of the wallrock but no further carbonatization could have occurred.

REFERENCES

Blackburn, C.E. & Janes, D.A. 1983. Gold deposits in northwestern Ontario. Ontario Geol. Survey Misc. Paper 110:194-210.

Brimhall, G.H., Jr. 1979. Lithologic determination of mass transfer mechanisms of multiple-stage porphyry copper mineralization at Butte, Montana: Vein formation by hypogene leaching and enrichment of potassium-silicate protore. Econ. Geol. 74:556-589.

Böhlke, J.K. 1989. Comparison of metasomatic reactions between a common CO_2-rich vein fluid and diverse wall rocks: Intensive variables, mass transfers, and Au mineralization at Alleghany, California. Econ. Geol. 84:291-327.

Maclean, W.H. & Kranidiotis, P. 1987. Immobile elements as monitors of mass transfers in hydrothermal alteration: Phelps Dodge massive sulfide deposit, Matagami, Quebec. Econ. Geol. 82:951-962.

Sibson, R.H., Robert, R. & Poulsen, H. 1988. High angle faults, fluid pressure cycling and mesothermal gold-quartz deposition. Geology 16:551-555.

Current Research in Geology Applied to Ore Deposits. Fenoll Hach-Alí, Torres-Ruiz & Gervilla (eds) (1993). ISBN 84-338-1772-8

MULTI-STAGE GEOCHEMICAL SIGNATURES FROM THE VEIN SYSTEM OF THE SAINT SALVY Zn DEPOSITS, SW FRANCE: FLUID INCLUSION AND STABLE ISOTOPE EVIDENCE

Munoz, M.; Boyce, A.J.; Fallick, P.; Courjault-Radé, P. & Tollon, F.
C.N.R.S. URA n° 67, Toulouse, France and S.U.R.R.C. Isotope Geology Unit, Glasgow, Scotland

Abstract: Fluid inclusion and stable isotope investigation carried out on the Saint-Salvy Zn deposit give evidence of a succession of different fluids related to late Variscan and post-Variscan tectonic events. Fluids vary from metamorphic to basin-derived brines composition. The economic mineralisation was formed during an early Mesozoic tensional event.

Sphalerite-dominated mineralization of the Saint Salvy deposit is situated to the south of the late Variscan Sidobre batholith, and adjacent to the Mesozoic-Cenozoïc Aquitain Basin. It occurs within an E-W vein system that cross-cuts Cambrian black shales of the Paleozoic basement.

The current metallogenic hypothesis is that the economic Zn mineralization is Late Variscan in age, formed as the product of convective fluid circulation along the sheared southern margin of the cooling Sidobre batholith (Beziat, 1973 ; Foglierini et al., 1980 ; Cassard et al., 1988). It has been that the ore might have been derived from remobilization of a primary Cambrian stratiform Zn mineralization (Barbanson, 1979 ; Barbanson et Tollon, 1979 ; Foglierini et al., 1980 ; Kim, 1985).

A detailed fluid inclusion (Munoz et al., 1986) and stable isotope survey reveals a succession (E_0 to E_4) of late and post-Variscan hydrothermal mineralizing fluids. Fluids from the main mineralizing episode are pretty low in temperature and look like meteoric fluids derived from the Aquitain Basin - rather than granite-equilibrated fluids; $\delta^{34}S$ analysis are consistent with S being leached from the Cambrian succession.

Succession of mineralizing episodes

Episode E_0 corresponds to stratiform-schistoform mineralization composed of sphalerite (2-3 wt.% Fe) and pyrite, hosted in Cambrian black shales.

E_1 corresponds to a skarn formation synchronous with the emplacement of the late orogenic batholith. The paragenesis observed within the skarn comprises garnet, pyroxene, quartz, and scarce sulphides (iron-rich sphalerite, up to 14 wt.%, and subordinate pyrite and pyrrhotite).

E_2 coincides with a brittle extensional shear zone event, dominated by quartz veins with scarce sulfide (automorphic

arsenopyrite crystal patches associated with subordinate pyrite, cosalite and rare xenomorphic iron-rich, up to 10 wt% Fe, sphalerite).

E_3 and E_4 are related to tensional tectonics.
E_3 Episode is characterised by barren chalcedonic quartz veins and breccia cements.

E_4 coincides with deposition of the economic Zn mineralization. A dense network of fractures and cockade breccia were formed with siderite, alternating and with massive Fe-poor sphalerite (2-3 wt% Fe) with minor galena. Centimetric euhedral clear quartz crystals fill druses and occupy the centre of some fractures .

Fluid inclusions and stable isotopes data

E_0 sphalerite and pyrite $\delta^{34}S$ range from 4.7% to 9.4% ; E_4 sphalerite and galena $\delta^{34}S$ range from 1.8% to 8.8% ; These data suggest a possible derivation of the economic stage sulfur from Cambrian mineralization.

E_2 calculated $\delta^{18}O$ fluid and directly measured fluid inclusion δD plot within the magmatic/metamorphic fluid field (average values: +7.6% , -61%) (see figure). Taking into account the composition H_2O-CO_2-(NaCl) and the temperature (T_H=295-375°C), this could reflect derivation from late Variscan metamorphic fluids rather than from the Sidobre granite system.

E3 fluid isotopic data plot close to the meteoric water line (average $\delta^{18}O$ and δD values: -9.7% and -64%). The high salinity (25 wt.% NaCl eq.), the presence of $CaCl_2$ and low temperatures (monophase H2O inclusions) of these fluids, suggest that the fluid may have leached solutes from the adjacent Aquitain Basin, probably at the end of the early Mesozoic syn-rift phase (early Hettangian).

The E4 Zn-bearing fluids are H2O-NaCl-CaCl2 (22-25 wt.% NaCl eq.) brines with homogenization temperatures ranging between 80 and 140°C (mean 110°C). Calculated fluid $\delta^{18}O$ ranges from -4.0% to +6.0% and directly measured fluid inclusions δD ranges from -92% to -111% . These data enhance the interpretation that these fluids were derived from the Aquitain Basin. The low δD of these fluids suggest that "organic" fluids (H derived directly or indirectly from organic matter) may have been involved. However, carbon from E4 siderite has $\delta^{13}C$ from +2.6% to +4.4% , which is not a typical organic signature. We consider that carbon, as with sulphur of this stage, may have been derived from marine sediments in the basement. During the post-rift phase, the first major tectonic/thermal event is recorded at the Lias/Dogger transition (c. 180Ma) in the whole French Massif Central and nearby Aquitain Basin (). The

subsequent high geothermal gradient would allow warming of infiltrated basinal-derived brines, increasing their ability to leach zinc.

This study emphasizes i) the major role played by the repeated exploitation of the fault system by hydrothermal fluids associated with tectonic events in SW France from late Variscan to early Mesozoic: late Variscan extensional shear zone event, reactivated during the early Mesozoic tensional phases - linked to the very beginning of the Atlantic opening - at the Triassic/Hettangian and Lias/Dogger transitions. The latter phase appears to be responsible for the deposition of the economic Zn mineralisation, ii) the role played by the late Triassic - early Hettangian evaporitic reservoir of the Aquitain Basin with respect to the second largest Zn deposit formation in France.

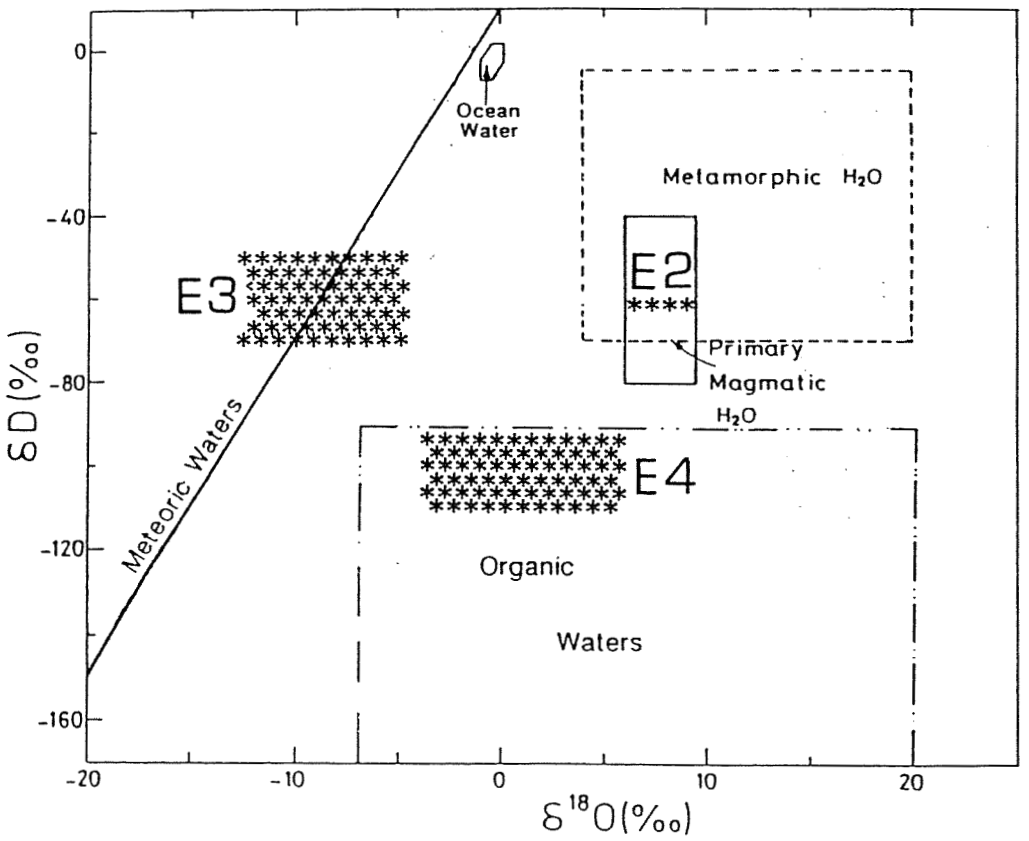

E2, E3 and E4 fluids composition plotted witin the δD versus δ18O diagram.

References

BARBANSON, L. (1979): Etude des minéralisations stratiformes du district zincifère de Saint-Salvy. Thèse Doct. 3e cycle, Univ. Toulouse-III, France.
BARBANSON,L. & TOLLON, F. (1980): Les minéralisations zincifères stratiformes associées au gisement filonien de Saint-Salvy (Tarn). C. R. Acad. Sci. Fr., 291, 9-12.
BEZIAT, P. (1973): Style des déformations et figures d'interférences sur la bordure Sud-Est du Sidobre. Bull. BRGM., France, 4, 161-183.
BONHOMME, M.G. (1982): Age triasique et jurassique des argiles associées aux minéralisations filoniennes et des phénomènes diagenètiques tardifs en Europe de l'Ouest - Contexte géodynamique et implications genètiques. C. R. Acad. Sci., 294, 521-524.
BONHOMME, M.G., BÜHMANN, D. & BESNUS, Y. (1982): Reliability of K-Ar dating of clays and silicifications associated with vein mineralization in western Europe. Geol. Rund., ,
FOGLIERINI, F.,BEZIAT, P., TOLLON, F. & CHABOD, J.C. (1980): Le gisement filonien de Noailhac-Saint-Salvy (Tarn). In: Gisements français. 26th Int. Geol. Congr, Paris, E6, 1-43.
KIM, Y.D. (1985): Etude gitologique et géochimique du gisement zincifère de Saint-Salvy, Montagne Noire, Massif Central français. Thèse Doct. 3e cycle, Université de Toulouse-III, France.
LANCELOT, J. & VELLA, V. (1989): Datation U-Pb liasique de la pechblende de Rabajac - Mise en évidence d'une préconcentration uranifère permienne dans le bassin de Lodève (Hérault). Bull. soc. Géol. Fr., 8, 309-315.
LEVEQUE, M.H., LANCELOT, J. & GEORGE, E. (1988): The Bertholène uranium deposit - Mineralogical characteristics and U-Pb dating of the primary U mineralization and its subsequent recrystallization - Consequences upon the evolution of the U deposits of the Massif Central. Chem. Geol., 69, 163-174.
MUNOZ, M., KIM, Y.D., VERRAES, G. & TOLLON F. (1986): Altérations hydrothermales et minéralisations zincifères filoniennes du gisement de Noailhac-Saint-Salvy (Tarn, France)- leurs successions et conditions de cristallisation. C.R. Acad. Sc. Paris, t. 302, Série II, n° 8.
SCHMITT, J.M., BAUBRON, J.C. & BONHOMME, M.G. (1984): Pétrographie et datations K-Ar des transformations minérales affectant le gîte uranifère de Bertholène (Aveyron, France). Miner. Dep., 19, 123-131.

Current Research in Geology Applied to Ore Deposits. Fenoll Hach-Ali, Torres-Ruiz & Gervilla (eds) (1993). ISBN 84-338-1772-8

$^{40}Ar/^{39}Ar$ GEOCHRONOLOGY OF GOLD MINERALIZATION AND ARCHAEAN TECTONICS IN THE YILGARN BLOCK, WESTERN AUSTRALIA

Napier, R.W.
Dept. of Earth Sciences, The University of Leeds, Leeds LS2 9JT, U.K.

ABSTRACT: Potassic alteration minerals associated with Archaean high temperature lode-gold mineralization in granitoid-greenstone terrains of the Yilgarn block of Western Australia have been dated by the $^{40}Ar/^{39}Ar$ method. The palaeotemperatures measured from a suite of minerals including hornblende and biotite in this method range from >500°C to <300°C. However, minerals dated yield identical ages within a small error (*ca.*2585±2Ma). This suggests either that ore-bearing fluids were emplaced into significantly cooler rocks, or that cooling following mineralization was extremely rapid.

INTRODUCTION

The Yilgarn block of Western Australia is an Archaean granitoid-greenstone terrain with dimensions of approximately 800km X 800km. Subsequent to their deposition at *ca.*2900Ma-2700Ma (eg. McNaughton *et al.*, 1990), greenstone belts of the Yilgarn block underwent a complex deformation history involving magmatism, metamorphism, mineralization and subsequent dyke emplacement. Despite the well-documented geological characteristics of Archaean lode-gold deposits (eg. Groves *et al.*, 1990), models for their *genesis* remain uncertain. Little emphasis has been placed on the timing of gold mineralization and relative uplift (exhumation) rates, even though an absolute time framework would be of considerable genetic significance. Gold is mono-isotopic and the precise determination of the age of associated sulphide ores has met with limited success because of the open system process responsible for concentrating epigenetic metals. The age of mineralization is generally determined by analysis of silicate minerals which occur in association with the sulphides, and are assumed to be cogenetic. However, the variation in closure temperatures of cogenetic silicates implies that some minerals may record post-mineralization cooling ages rather than true mineralization ages (eg. Clark, 1987). This phenomenon may be used to the geologist's advantage, as cooling rates of metamorphic terrains tend to be a reflection of their exhumation rates, which in turn are pivotal to constraining models for their genesis.

REGIONAL SAMPLING

The Coolgardie and Southern Cross regions in the central Yilgarn block of Western Australia contain amphibolite facies metabasites (which normally host hydrothermal gold mineralization) displaying assemblages containing suites of potassic minerals which should be eminently suitable for $^{40}Ar/^{39}Ar$ thermochronology. Stable mineral phases at amphibolite grade (including hornblende and biotite) occur in the alteration selvedges of gold bearing veins. Because of a marked contrast in the closure temperature (Tc) of Ar during cooling with respect to these minerals (hornblende *ca.*500°C,

biotite *ca*.300°C (McDougall & Harrison, 1988)), a cooling rate related to exhumation may be estimated by dating pure separates of hornblende and biotite from a single sample. It should also be possible to isolate this main hydrothermal event from younger thermal perturbations by dating minerals from outside the alteration halo and precluding those areas which record younger events.

Granitoids from high crustal levels hosting gold mineralization in the Eastern Goldfields region of the Yilgarn Block occasionally contain mafic minerals including hornblende and biotite that are suitable for $^{40}Ar/^{39}Ar$ geochronology in a similar fashion to the amphibolite facies to examine cooling relationships of igneous bodies to metamorphic terrains.

GOLD MINERALIZATION

A range of cooling ages has been obtained and analysed. Hydrothermal minerals yield average $^{40}Ar/^{39}Ar$ ages of *ca*.2585Ma, with highest precision errors of ±2Ma. Hornblende and biotite pairs from single samples yield identical mineralization ages within a relatively small error implying cooling rates of >>100°C/Ma; for example, at the Bayleys and Kings Cross mines in Coolgardie:

Sample: Bayleys.1.Ore	hornblende $^{40}Ar/^{39}Ar$ age	2585±4Ma
	biotite $^{40}Ar/^{39}Ar$ age	2586±4Ma
Sample: Kings.Cross.Ore	hornblende $^{40}Ar/^{39}Ar$ age	2583±3Ma
	biotite $^{40}Ar/^{39}Ar$ age	2587±2Ma

These data may be explained by one of two possible models;
(i) ore-bearing fluids were emplaced in a transient thermal pulse into a significantly cooler environment, or
(ii) exhumation following mineralization was extremely rapid with only rarely recorded modern analogues (eg. Hill *et al.*, 1992).
The almost ubiquitous correlation of regional metamorphic facies with gold depositional conditions (although mineralization is generally demonstrably post-peak of metamorphism) at all exposed crustal levels in the Yilgarn block strongly favours of model (ii), and syn-metamorphic gold mineralization at high temperatures is favoured by other workers in amphibolite facies deposits (Bloem *et al.*, this volume; Knight *et al.*, this volume). However, rapid exhumation of deeper crustal levels is extremely rare by modern standards, and similar $^{40}Ar/^{39}Ar$ studies in mines close to Kings Cross and Bayleys indicate significantly younger ages of mineralization (<2500Ma) but with comparably rapid cooling rates. The deposition of lode-gold mineralization 70Ma to 100Ma after peak regional metamorphic temperatures were attained has been recorded in the Abitibi Greenstone Belt of Canada (Hanes *et al.*, 1992). Thus, the timing of mineralization relative to peak metamorphism remains highly controversial in amphibolite facies terrains in the absence of detailed geochronology of regional metamorphism.

REGIONAL METAMORPHISM

Regionally metamorphosed hornblendes from the Coolgardie region yield average $^{40}Ar/^{39}Ar$ ages of *ca*.2650Ma, suggesting a post-peak metamorphism cooling rate of >5°C/Ma using regional metamorphic

data compiled by McNaughton *et al.*, 1990. Disparities between the ages recorded by metamorphic amphiboles and hydrothermally altered amphiboles may be due to differences in closure temperatures of the hornblendes (although compositional variation is subtle), or may be explained by model (i).

Regionally metamorphosed hornblendes from the Southern Cross region yield average $^{40}Ar/^{39}Ar$ ages of *ca.*2000Ma, suggesting either excess ^{40}Ar in the hydrothermal system, or a hornblende phase that is poorly retentive with respect to ^{40}Ar (ie. has a low Tc). Rb/Sr ages derived from hydrothermal hornblende-plagioclase isochrons confirm a 2585Ma hydrothermal cooling age and rule out excess ^{40}Ar effects. Furthermore, laser $^{40}Ar/^{39}Ar$ studies on a metamorphic biotite in a mafic amphibolite imply a higher ^{40}Ar Tc for some regionally metamorphosed biotites than for regionally metamorphosed amphiboles. This indicates that submicroscopic scale exsolution observed in regional amphiboles drastically reduce their Tc by in excess of 200°C (Harrison & Fitzgerald, 1986).

GRANITOIDS

Unmineralized samples from a number of mineralized granitoids in the greenschist facies of the Eastern Goldfields region of the Yilgarn block have been analysed by the $^{40}Ar/^{39}Ar$ method. Age spectra display plateau ages at *ca.*2580Ma. The difference in ages between hornblende and biotite pairs is within experimental error of the two analyses. Biotite ages, however, are predominantly younger by 10-20Ma. Initial crystallization has been measured at *ca.*2660Ma, contemporaneous with regional metamorphism (McNaughton & Cassidy, 1990; Cassidy, 1992). This cooling history implies heat loss by unroofing rather than simple conductive loss into cooler country rocks (Harrison & Clarke, 1979). Mineralization hosted by Eastern goldfields granitoids studied is thought to occur at *ca.*350-425°C (Lawlers deposit, Cassidy 1992), a temperature range bracketed by the closure temperatures of hornblende and biotite; therefore mineralization must have occurred at *ca.*2580Ma *if* it was part of the same tectonothermal event.

CONCLUSIONS

Tectonism and gold mineralization in the Coolgardie, Southern Cross and Eastern Goldfields regions of Western Australia are influenced by significant tectonothermal activity at *ca.*2580Ma to 2590Ma. The spatial diversity the regions, yet good geochronological correlation between them, implies a significant Yilgarn-scale event. Timing relationships determined in this work and others (eg. Clark 1987) indicate that gold mineralization may not have occurred as a single event, but may have been deposited in pulses from 2635Ma to <2500Ma. Mineralization at *ca.*2585Ma may be implicitly associated with contemporaneous rapid exhumation. It is concluded that if the rapid cooling associated with mineralisation is *not* due to transient thermal pulses within cooler lithologies, then the cooling path followed by granitoid bodies within greenstone belts, and possibly by higher temperature metamorphic terrains, represents

isothermal decompression (slow cooling above *ca*.500°C) followed by unroofing and rapid cooling below 500°C.

ACKNOWLEDGEMENTS
This work forms part of a Ph.D. study by the author. Funding from DENI and MERIWA, and cooperation from mining companies operating in Southern Cross and Coolgardie is gratefully acknowledged.

REFERENCES

Cassidy, K.F., 1992. Archaean granitoid-hosted gold-deposits in greenschist to amphibolite facies terrains: A high P-T to low P-T depositional continuum equivalent to greenstone-hosted deposits. Ph.D. thesis, the University of Western Australia, Nedlands, 296pp. (unpublished)

Clark, M.E., 1987. The geology of the Victory gold mine, Kambalda, Western Australia. Ph.D. thesis, Queen's University, Kingston, Ontario, 99pp. (unpublished)

Groves, D.I., Knox-Robinson, C.M., Ho, S.E. & Rock, N.M.S., 1990. An overview of Archaean lode-gold deposits. In: Ho, S.E., Groves, D.I. and Bennett, J.M. (eds), Gold deposits of the Yilgarn Block, Western Australia: Nature, Genesis and Exploration Guides. Geology Department of University Extension, The University of Western Australia, Publication 20: 1-18

Hanes, J.A., Archibald, D.A., Hodgson, C.J., Robert, F., 1992. Dating of auriferous quartz vein deposits in the Abitibi Greenstone belt, Canada: $^{40}Ar/^{39}Ar$ evidence for a 70- to 100-m.y.-time gap between plutonism-metamorphism and mineralization. Econ. Geol. 87: 1849-1861

Harrison, T.M. & Clarke G.K.C., 1979. A model of the thermal effects of igneous intrusion and uplift as applied to Quottoon pluton, British Columbia. Can. J. Earth Sci. 16:411-420

Harrison, T.M., & Fitzgerald, J.D., 1986. Exsolution in hornblende and its consequences for 40Ar/39Ar age spectra and closure temperature. Geochim. Cosmocim. Acta 50: 247-253

Hill, E.J., Baldwin, S.L. and Lister, G.S., 1992. Unroofing of active metamorphic core complexes in the D'Entrecasteaux Islands, Papua New Guinea. Geology 20: 907-910

McNaughton, N.J. & Cassidy, K.F., 1990. A reassessment of the age of the Liberty Granodiorite: Implications for a model of synchronous mesothermal gold mineralization within the Norseman-Wiluna belt, Western Australia. Aust. J. Earth Sci. 37: 373-376

McNaughton, N.J., Cassidy, K.F., Groves, D.I. & Perring, C.S., 1990. Timing of mineralization. In: Ho, S.E., Groves, D.I. & Bennett, J.M. (eds), Gold deposits of the Yilgarn Block, Western Australia: Nature, Genesis and Exploration Guides. Geology Department of University Extension, The University of Western Australia, Publication 20: 221-225

McDougall, I. & Harrison, T.M., 1988. Geochronology and thermochronology by the $^{40}Ar/^{39}Ar$ method. Oxford Monographs on Geology and Geophysics, Number 9, Oxford University Press, 212 pp.

Current Research in Geology Applied to Ore Deposits.Fenoll Hach-Ali, Torres-Ruiz & Gervilla(eds)(1993).ISBN 84-338-1772-8

TYPOMORPHISM AND GENESIS OF NATIVE GOLD OF HYPERGENESIS ZONE OF KAZAKHSTAN AND THE ENISEI RIDGE GOLD DEPOSITS

Nesterenko, G.V.(1); Vorotnicov, B.A.(1); Kulikov, A.A.(2) & Zhmodik, S.M.(1)
(1) Inst. of Geology SB AS Novosibirisk, Russia
(2) Inst. of Geology SB AS, Ulan-Ude, Russia

The results of the study of the typomorphic specific features and conditions of the native gold formation of the zone of gold deposits hupergenesis of Kazakhstan (Maikain, Kosmuren, Vasilkovskii, Suvenirand Alpus) and to a lesser extent of other regions of the Asian Part of the former USSR, are presented. A more detailed mineralogical-geochemical study is done in the first two deposits as well as in Olympiadinskoye deposit of the Yenisei ridge, and the whole section of hypergenesis zone is tested. The typomorphic specific features and the conditions of the formation of the basic varieties of hypergene gold are characterized in shorts. The geological situation and the specific features of the structure of studies deposits are elucidated in the preceding works (Nesterenko, 1991; Nesterenko et al.,1983).

The hypergenesis zones of Maikain (Fig.1) and Kosmurun deposits are much similar. They have their maximum depth of 65- and 40 m over continuous sulfide bodies characterized by low (first ppm) gold content occurring mainly in the form of invisible submicroscopic impurities. A thin horizon of pyrite sypuchka (fine-grained sand) is developed on the zones bottom. Available is the essential (5-10 multiple) secondary enrichment by noble metals with their maximum concentration in the lower parts of the zones where some enlargement of native zone is observed though the share of the visible gravitationally enriching metal is low and ranges from percentage parts to 4-13%. Among invisible gold forms there are sorbed and other easily mobile agents able to dissolve by distilled water.

Olympiadinskoye vein-impregnation gold sulfide deposit is situated in the area of development of metamorphosed carbonate-sand-shale rocks of Upper Riphean. Sulfide mineralization (2-7%) is laid on quarts-muscovite-carbonate and other metasomatites. Gold is mainly microscopical. Linear gold bearing crusts of weathering (crust ores) are widely developed in the deposit. Their thickness equals to 100 m but in separate wells it is 300-400 m. The crusts of weathering are built by sand-aleurite-clay porous rocks, the pelite component in which has a kaolinite-hydroshale composition, and the psammite-aleurite components - a quartz ore. The share of free "extracted" native gold in "crust" test ranges from 0,2 to 15,4% and that is more than in primary one.

Among visible particles of native gold from the studied zones of hypergenesis, relict endpgenic and new-formed hupergenic gold occurs. The content and character of the former mainly due to primary mineralization, though its homogenic transformation is observed: silver leaching and sometimes that of other impurities and development of fineness phases and rims (Fig.2). The relations between the genetic types of native gold are not stable and change to predominating hypergene ones during the transition from low sulfide gold mineralization to mainly sulfide one and from cold humid to hot semiarid climate. Three main varieties differing from one another in the peculiarities of composition and structure as well as the way of formation, are observed in hypergene native gold particles.

The first mostly spread variety is pure it occurs along the whole section of the oxidation zones (Fig 1) and crusts of weathering. The forms of its manifestation vary. The forms of free growth predominate: crystals, chains, brunches, films, sponge - druse like forms as well as those of looped colloform rounded and drop-like forms (Fig.3).

Besides, the forms of the creation of cavities and cracks formed due to removing water filled later with are established. Sometimes native gold forms edges on endogenous relict precious metal. Small visible, microscopical and submicrosckopic particles predominate in the native gold of this variety, but large nuggets occur gold purity of the characterized variety is very high: from 1000-995 to 980, and more seldom it is lower (Fig.1). Accordingly, the content of the basic impurity-silver ranges from "not discovered" to 1-2%, more seldom-more. This gold is formed to out mind, (Nesterenko et al., 1985) from gold-containing solution as the result of decay of halogen complexes, mainly, Au^{I} chloride (Au^{III} -$AuCl^{-}_{4}$ complex is formed only at oxidation-reduction potential of more then 1000mv not occurring in natural waters). The most possible reducing agents of gold are: Mn^{2+} - subzones of limonite in alkaline medium, Fe^{2+} - subzones of jarosites in acid waters and H_2S under acid reducing hydrogen sulfide conditions. Under these conditions Silver does not reduce but may precipitate from solutions in the form of poorly soluble halogenides. It may be supposed that, during the process of evolution of solutions and "gold" precipitations, they may come through colloidal (gel) stage, owing to which sponge-looped forms of native gold sometimes have microlayered structure (Fig.4,5).

The similar gold morphology can appear due to selective silver dissolution and diffusion (Fig.6,7). Porous, sponge-looped gold is formed during the experiments with the melting of sulfide concentrate with native gold put into it. Melting is carried out with pirosulphatic potassium at 600°C during 2 hours. Small gold particles are altered upon the whole (Fig.6) and in bigger ones the unaltered central part and porous gold in the peripheral part of the nuggets. Besides, gold purity alters in one nugget from the center to the edge from 770 to 900 °/oo and in the other from 680 to 830 °/oo. The structure of altered gold is similar to that of porous sponge gold of hypergenesis zone of gold deposits (Fig.7). Besides, the microlayered gold particles texture is not revealed. The mechanism of the silver removal from gold is not quite clear. The formation of microporous in gold may be related either to the presence of silver in the form of an independent phase (and this contradicts the information on the alteration of elementary cell parameters depending on the silver concentration) or is due to the diffusion silver redistribution in gold with altering physical-chemical parameters of the system.

The second hypergene variety is represented by silver containing gold with inhomogeneous composition (Fig.8). Purity of separate phases in such gold of Maikain deposit is within the ranges of 850-995 units. Here it occurs at the depth of about 60 m in the lower oxidation zone in the horizon of quartz-barite sypuchka with native sulphur (Fig. 1). The nuggets are rather large, of placer size, of lump long form, often in petrovskaite AuAgS(Se) cover. The close relation of this gold to the above sulfide allows to suppose that sulphur-containing complexes, among which thiosulphate complexes gold and silver of $(Au,Ag)(S_2O_3)^{3-}_{2}$

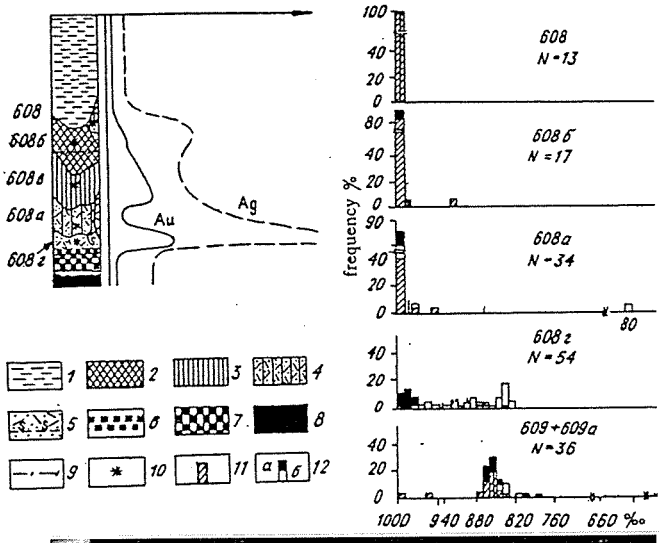

Fig. 1. The alteration of native gold fineness in the section of the oxidation zone of Maikain "C" deposit. 1–8 – subzones of the oxiidation zone with the prevailing development of: 1–clays of the funnel of collapse, 2–limonites, 3–jarosites, 4–quartz–barite–jarosites, 5–quartz–barit sypuchka, in the lower part with native sulphur and small layers of hypergene sulphides, 6–pyrite sypuchka, 7–zone of mixed primary and secondary sulphide ores, 8–zone of primary sulphide ores, 9–level of ground waters, 10–place of selection of native gold samples, 11–12 histograms of fineness of homogeneous (11) and heterogeneous (12) native gold.

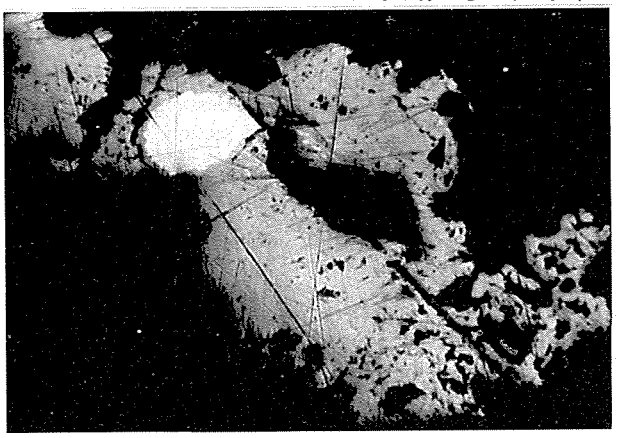

Fig.2 Two phase nugget: of low fineness endogenous relict (white) and pure pypergenic altered (grey. Yuzhny Bessapan deposit (Uzbekistan). Mounted polished section, magn. x300.

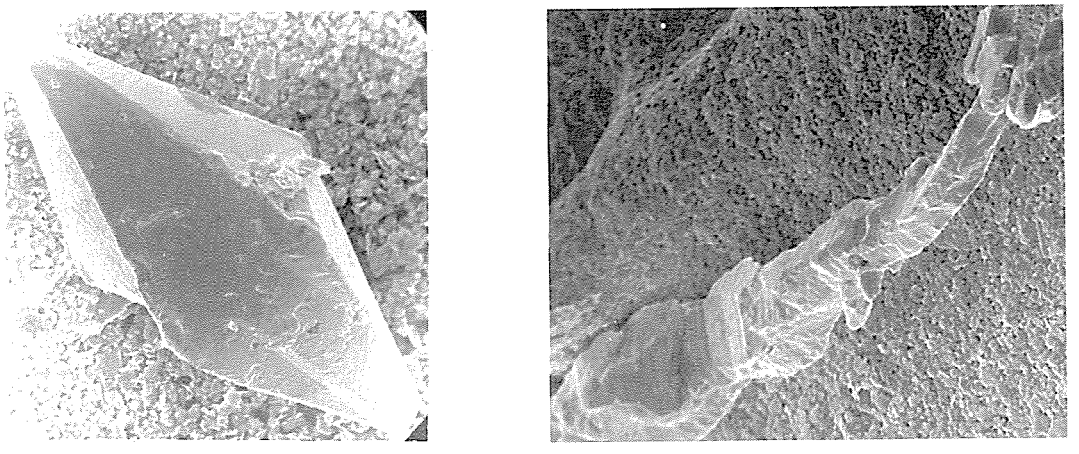

Fig. 3 New–formed hypergene nuggets: crystals and a "branch" of crystals, magn 440; 240. Maikain and Kosmurun deposits

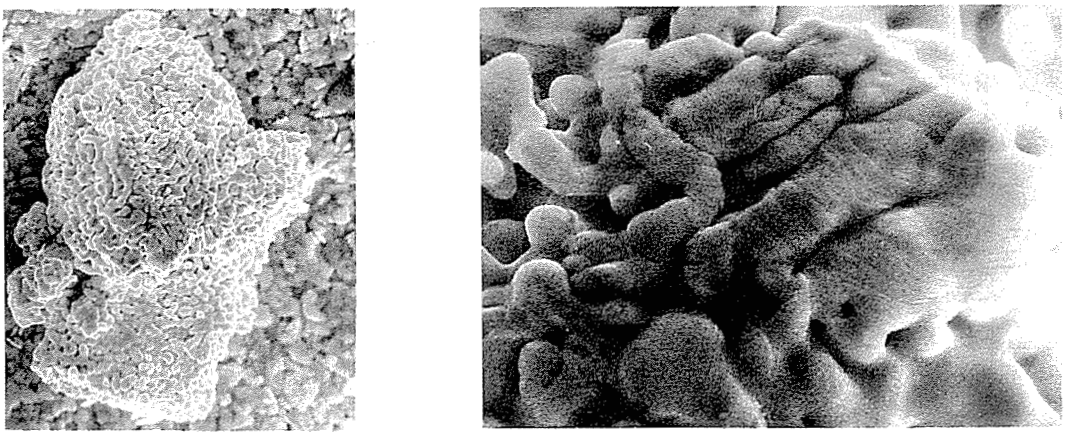

Fig. 4 Coloform–sponge nuggets, layered microstructure is seen, magn. 670;4300.

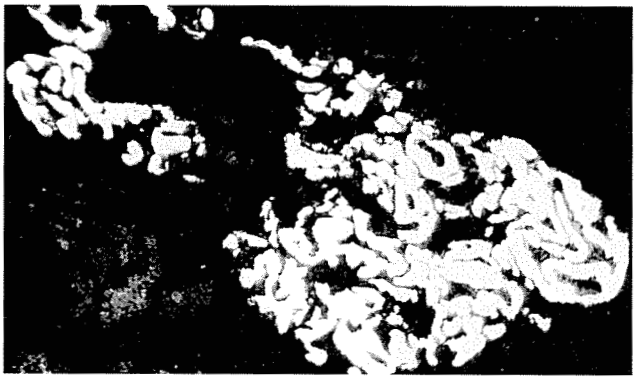

Fig. 5 Hypergene pure nuggets with looped ("brain–like") structure. Yuzhny Bessapan deposit. Mounted polished section, magn. 660

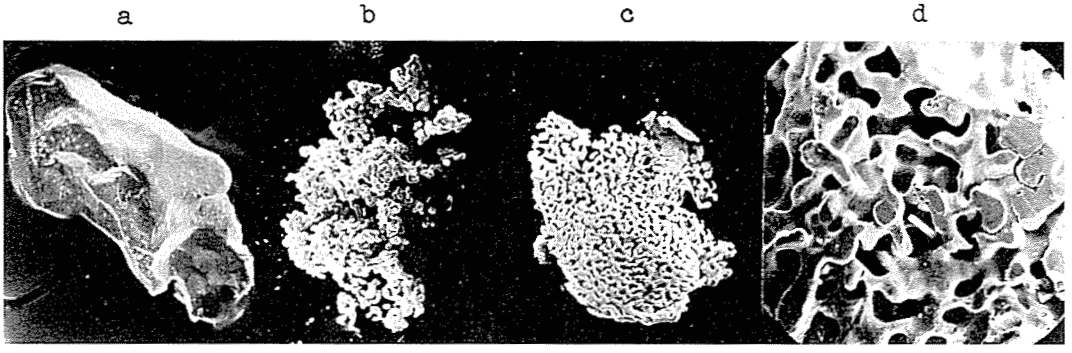

Fig.6 (a,b) Gold extracted from beresite (test 12–6–1): a–by gravitational method, magn. 360; b–d– by sulphide concentrate melting method with $K_2S_2O_7$. Magn. 300;270;1000.

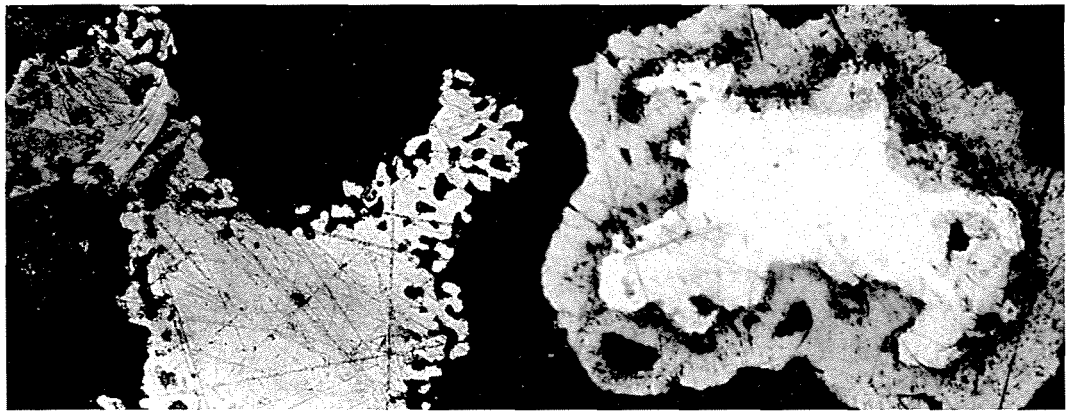

Fig. 7 Gold extracted by melting. Mounted polished section, magn. 800. The outer edge has a a sponge-porous structure and is of a golden-yellow colour; the center is homogeneous of white-yellow colour.

Fig. 8 Heterogeneous hypergene nugget (white and grey) in petrovskaite cover (dark grey). Maikain "C". Mounted polished section, mgn. 400.

type are the most likely, participate in its formation. It is from these solutions that the artificial petrovskaite analogue was synthesized. The thiosulphate complexes are very stable but they exist in a narrow range of pH and Eh values and accordingly in a relatively thin layer, transitional between "sulfide" and "sulfate-sulfide" subzones.

The third hypergene variety of native gold, the so-called mustard gold, is formed due to oxidation and decay of gold bearing minerals proper: tellurides of gold, aurostibnites and likely gold silver sulphides: jutenboogardtite, petrovskaite and penjenite. Mustard gold is usually represented by fine grained dusty microporous forms, often of a yellow-brown color. The Purity of the studied samples is close to 1000. According to S.V.Jablokova's data similar gold from Kuranakh deposit (Jakutiya) has not constant purity due to mottled distribution of silver. Mustard gold though being of a rather large size, is not resistant to the mechanical effect and easily turns to dust due to its microporous structure.

In conclusion it is noted that the processes of homogenic formation of native gold are largely revealed under specific conditions. The basic and most spread forms of gold migration in the waters of hypergenesis zone of gold mineralization is its chloride complex, and the most spread variety - very pure native gold, often building crustals, branches and also looped-sponge forms.

References

Nesterenko G.V.(1991): Forecasting of gold mineralization by placers (on the example of South Siberian regions). Novosibirsk, Nauka, Siberian Branch, 191 p.

Nesterenko G.V., Vorotnikov B.A., Nikolaeva N.M., Peshchevitsky B.I.(1985):New formation of gold-bearing minerals in oxidation zone of sulfide deposits of Central Kazakhstan. Proceedings of IMA, Issue 5, part 14, p.555-568.

Current Research in Geology Applied to Ore Deposits.Fenoll Hach-Alí, Torres-Ruiz & Gervilla(eds)(1993).ISBN 84-338-1772-8

OPHIOLITIC CHROMITITES FROM NAN-UTTARADIT, NORTHERN THAILAND: A RESULT OF BONINITIC-TYPE MELT AND PERIDOTITE INTERACTION

Orberger, B.; Girardeau, J.; Mercier, J.C.C.; Lorand, J.P. & Pitragool, S.
Lab. de Pétrologie Physique. Université Paris 7, Inst. de Physique du Globe de Paris, 2-Place Jussieu F-75251 Paris Cedex 05, France

Abstract NU ultramafics are subdivided into 1) peridotites and orthopyroxenites hosting chromitite lenses and layers, and 2) clinopyroxenites bearing chromitite xenoliths. The peridotites originated through partial melting and melt/rock interactions in a subduction zone environment. Chromitite lenses and clinopyroxenites are successive segregates from source melts with boninitic signatures, generated under low fO_2 from a depleted mantle and Ca-enriched during uprise through dissolution of wall-rock clinopyroxene. Chromitite layers crystallized from multiple tholeiitic injections. Chromitite xenoliths are but re-equilibrated and plastically deformed fragments of the other types.

Introduction

Chromitites in ophiolites usually envelopped in dunite, occur either as pods in the upper part of the depleted mantle sequence and as layers and bands in the zone forming transition from the upper mantle to the lower oceanic crust. Tholeiitic island-arc magmas are considered as the source for their constitutive Cr-spinels; among the different possibilities for spinel accumulation, the process of multiple magma injections into magma conduits is now usually suggested (e.g. Lago *et al.*, 1982).

The chromitites of the Nan-Uttaradit ophiolite also occur in the mantle sequence and transition zone, but are generally associated with orthopyroxenite. The mantle sequence is heterogeneous and comprises peridotites and orthopyroxenites forming intermingled bodies. However, some chromitite is also hosted in intrusive clinopyroxenites. Chromitites in the orthopyroxenites are extremely Cr-rich, with the highest concentrations ever observed in ophiolites. Based on field observations, petrography and geochemistry of whole rocks and minerals, a coherent model for the evolution of this peculiar ophiolite is proposed

Geological and tectonic setting

The Nan-Uttaradit (NU) ophiolite represents a 150 km NE-SW trending suture zone separating the Shan Thai craton to the west and the Indosinian chinese craton to the East. (Panjasawatwong, 1991 and papers therein; Fig. 1a). The time of the continent-continent collision is uncertain and ranges from pre-Late Permian to Late Triassic (*op. cit.*). Plate tectonic models differ from author to author including westward subduction beneath the Shan thai craton, eastward subduction under the Indochina craton, or, finally, a pair of subduction zones dipping one to the east, the other to the west (Cooper *et al.* 1989 and papers therein).

No continuous exposure of the complete sequence exists in the entire belt because of extensive faulting and thrusting during obduction. Mafic and ultramafic rocks appear as tectonized slices within sediments of variable ages, Permo-Triassic in the western part, Siluro-Devonian in the southeastern one and Jurassic in the East and north-Eastern ones (Baum *et al. 1970*). Chromitite occurrences were found all over the belt (Fig. 1b).

Petrography

The *ultramafic rocks* can be subdivided into two groups (Fig. 1c): 1) rock types including all peridotites and associated orthopyroxenite (group-A) and 2) the orthers pyroxenites comprising clinopyroxenites and websterites forming layers and a large sheet (group-B). These two groups show either tectonic or magmatic contact relationship. Group-A peridotites and orthopyroxenites are strongly serpentinized. Primary minerals, such as olivine and orthopyroxene, show no preferred crystal shape orientation. In some samples, large crystals of orthopyroxene or clinopyroxene are poikilitically intergrown with olivine. These orthopyroxenes contain inclusions of olivine, plagioclase and spinels. Clinopyroxene and orthopyroxene crystallization points to re-equilibration

related to circulation of magmas. The group-B pyroxenites may be fresh or amphibolitized. Fresh pyroxenites display magmatic textures with indication of high temperature deformation. Amphibolitization yielded tremolite and chlorite.

The *chromitites* (Fig. 1c) can be subdivided into three major types: *lenses* (type I), *layers and bands* (type II) 3), *xenoliths* (type III). Types I and II occur in group-A peridotites and orthopyroxenites, but are essentially found in association with orthopyroxenite, only minor occurrences being embedded in dunite. *Lenses* are of small to intermediate size (max. 20 m long and 10m wide); sometimes they suffered deformation during shearing. *Multiple layers and bands* (up to 30 cm thick) are hosted in orthopyroxenite and have been exploited in the northern and central parts of the belt (Fig. 1c). There, chromitite grades into disseminated chromitite; in places nodular type chromite also occurs. Type III *chromitites* are found in group-B pyroxenite: contrastingly, they represent sharp secant contacts to the host foliated pyroxenite, clearly not related to deformation. The largest bodies of metric scale look like similar fragments, but are folded parallel to the foliation and lineation. These observations strongly suggest that type III chromitites were deformed at high temperatures within the host pyroxenite.

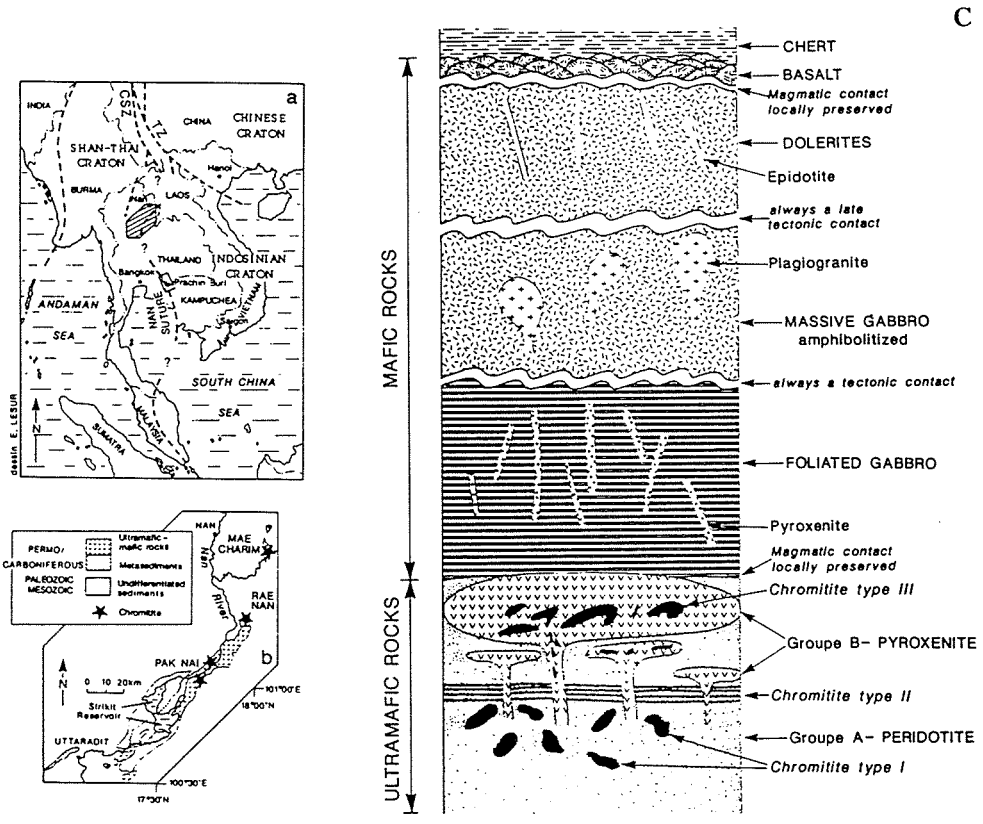

Fig. 1: a) Geotectonic setting of the Nan-Uttaradit ophiolite in south-east Asia b) location of the major chromitite deposits c) schematic cross-section through the ophiolite sequence.

Geochemistry of ultramafic rocks

Peridotites and pyroxenites have been analysed for major and minor oxides and a number of trace elements to obtain informations on the parental magma composition and indications on the geotectonic setting for the formation of the ophiolite. Their composition has been compared to reference peridotites and pyroxenites from the Lanzo and the Pyrenean massifs as well as the Leka ophiolite (Bodinier, 1988; Bodinier *et al.* 1988; Furnes *et al.* 1992).

Group-A peridotites: MgO-contents vary from 32.75 to 47.19 and in general decrease with increasing Al_2O_3, following the general trend for the reference peridotites. MgO-poor samples falling outside;theyare located close to shear zones or are clinopyroxene-bearing dunites. No correlation is observed between CaO, TiO_2 and Al_2O_3. CaO is strongly depleted in most of the peridotites (<< 0.6 wt.%), irrespective of Al_2O_3 which ranges from 0.56 to 3.13 wt.%. Some peridotites in the northern part plot at the high melting degree apex. TiO_2 contents generally do not exceed 0.03 wt.%. Thus some NU peridotites experienced a high degree of melting as indicated by low Al_2O_3, CaO, TiO_2 and Na_2O and high MgO contents which are comparable to those from the most depleted peridotites from the Lanzo and Pyrenean massifs. On the other hand, these depleted NU peridotites significantly differ from the Leka-peridotites in having lower MgO, CaO and MnO. The least Al_2O_3-depleted NU peridotites display uncorrelated and low TiO_2, Na_2O contents and are virtually CaO free, a feature not observed in any of the reference peridotites.

The trace elements V and Sc increase with increasing Al_2O_3, while Co decreases with the latter. The scatter is however much larger than for the reference peridotites. Transition elements (TE) normalised to SC1, a reference "primitive mantle" sample (Jagoutz *et al. 1979*), and presented in spider-diagrams, show a strong negative Ti-anomaly compared to the Lanzo and Pyrenean peridotites. The TE-patterns differ according to the modal compositions and are not as homogeneous as those for the Leka peridotite which represent a residuum of partial melting.

Group-B pyroxenites are rich in CaO (average: 17.13 wt.%) and MgO (average: 21.25 wt.%) and poor in Al_2O_3 (average: 2.69 wt.%;). TiO_2 and Al_2O_3 are positively correlated. Two types of pyroxenites may be distinguished, one with a high and constant Mg# (89 to 90) and high CaO/TiO_2 ratios (181-252), the other with a lower Mg# and lower CaO/TiO_2 ratios (43-126). Compared to the reference pyroxenites, the NU-pyroxenites are significantly lower in Al_2O_3. Transition element-patterns and Ti/V-and Ti/Sc-ratios reflect boninitic rather than island-arc or mid-ocean ridge basalt compositions.

Mineral Chemistry

Olivines have forsterite and NiO-contents which vary according to the mass ratio of spinel and olivine and to the extent of subsolidus re-equilibration between silicate and oxide phases during high plastic deformation: Fo and NiO increase from values of Fo_{81}, NiO: 0.13 wt.% in CaO-rich dunites, through intermediate values of Fo_{90}, NiO 0.43 wt.% in lherzolite, harzburgite and dunites, to the highest values of Fo_{98}, NiO: 0.76 wt.% from olivine inclusions in chromitite.

Clinopyroxenes in group-B pyroxenites are diopsides and reflect the bulk-rock composition, which varies as a function of the distance to the xenolithic chromitite. Clinopyroxenes, away from chromitites have an average composition of $En_{43.77}$ $Wo_{49.23}$ $Fs_{13.43}$ while those close to chromitite are poorer in Fe. Mg-numbers are higher close to chromitites (0.91-0.94 against 0.84 to 0.88) due to subsolidus re-equilibration. Clinopyroxenes away from the xenolithic chromitites are also low in Al_2O_3 as well as in Cr_2O_3 (0.32-4.61 and 0.06-0.11 wt.%, respectively). Close to the chromitites, more variable Cr contents are observed (0.04-0.37 wt.%) and reflect the complex exchange reaction between Cr and Al (Mercier, 1976).

Chromite composition differs according to the three chromitite types. Cr-spinels from type I in chromitite lenses show boninitic Cr- and Mg-numbers (0.9 and 0.7, respectively) and are very Cr-rich (58-68 wt.%). Cr-spinels from type II chromitite layers and bands have Cr# and Mg# similar to those for stratiform intrusions. Cr-spinels from type III xenolithic chromitites have variable Cr# (0.35 to 0.80), but an almost constant Mg# (0.5). They are richer in TiO_2 (0.3-0.8)wt.%) and in Fe^{3+} than type I and II chromites.

Concluding remarks

Petrographical and geochemical data for the NU-ultramafic rocks and associated chromitites show that they do represent the lower part of an ophiolite formed in an arc/subduction zone-environment. The group-A peridotites and orthopyroxenites characterize an upper mantle which has been very depleted and would result from an interaction with percolating magmas. Lens-shaped Cr-rich chromitites (type I) segregated as the early monomineralic endmember from a magma with boninitic signatures which, during its uprise, evolved through clinopyroxene dissolution, and segregated clinopyroxenites. Upwards-transported chromitite fragments later underwent subsolidus re-equilibration.

References:

Bodinier J.L. 1988: Geochemistry and petrogenesis of the Lanzo peridotite body, western Alps, *Tectonophysics 149:* 67-88.

Bodinier J.L., Dupuy C., Dostal J. 1988: Geochemistry and petrogenesis of eastern Pyrenean peridotites. *Geochim. Cosmochim Acta 52*: 2893-2907.

Furnes H., Pedersen R.B., Hertogen J., Albrektsen B.A. 1992: Magma development of the Leka ophiolite complex, central Norwegian Caledonides. *Lithos 27*, 259-277.

Jagoutz E., Palme H., Baddenhausen H., Blum K., Cendales M., Dreibus G., Spettel B., Lorenz V., Wänke H. (1979): The abundance of major, minot and trace elments in the earth mantle as derived from prinmitive ultramafic nodules. *Proc. Lunar. Sci. Conf. 10 th*, p. 2031-2050.

Lago, B.; Rabinowicz, M.; Nicolas, A. 1982: Podiform chromite ore-bodies: a genetic model. *Petrology 23*: 103-125

Mercier, J.C.C. (1976): Single pyroxene geothermometry and geobarometry. *Amer. Mineral.* 45, 603-615.

Panjasawatwong, Y. 1991: Petrology, geochemistry and tectonic implications of igneous rocks in the Nan Suture, Thailand, and an empirical study of the effects of Ca/Na, Al/Si and H_2O on plagioclase-melt equilibria at 5-10 kbar pressure. *Unpublished Ph.D. Thesis, University of Tasmania, Hobart*, Australia, 239 p.

Current Research in Geology Applied to Ore Deposits.Fenoll Hach-Alí, Torres-Ruiz & Gervilla(eds)(1993).ISBN 84-338-1772-8

TRANSPORT OF URANIUM BY SEDIMENTARY BRINES AT TEMPERATURES BETWEEN 80° AND 200°C

Pagel, M.
Centre de Recherches sur la Géologie des Matières Premières Minérales et Energétiques and GS CNRS-CREGU -BP 23, 54501 Vandoeuvre les Nancy, France

ABSTRACT : Fluid inclusion studies in gangue minerals from unconformity-type deposits in Saskatchewan (Canada) and North Territory (Australia) and from tectonolithologic-type deposits in France (Lodève), Niger (Akouta) and Gabon (Oklo) have shown that uranium was transported by brines at temperatures in the range 80 - 200°C. From oxygen and hydrogen isotope data, it is demonstrated that these brines have a sedimentary origin. Chloride and carbonate are probably the main anions capable to form stable complexes with dissolved U(VI).

Recent studies on fluid inclusions and stable isotopes in several uranium deposits have shown that brines are involved in the transport of uranium. This is especially the case for tectonolithologic and unconformity-type deposits. The tectonolithologic-type deposit is controlled by the tectonics (the mineralization is associated with a fracture zone) and the lithology (the mineralization is located in an organic-rich formation). The unconformity-type deposit is spatially associated with a major unconformity between a Lower Proterozoic metamorphic and granitic basement and a Middle Proterozoic unmetamorphosed sandstone cover. However, small deposits related to a post-Hercynian unconformity are also known in Aveyron, France (George et al, 1986).

This paper reviews the fluid inclusions data obtained on the tectonolithologic-type deposits, the Akouta deposit (Forbes, 1987), the Lodève deposits (Bonifas, 1992)), the Oklo deposit (Gauthier-Lafaye, 1986) and data on unconformity-type deposits (Pagel and Jaffrezic, 1975, Ypma and Fuzikawa, 1980, George et al., 1986). The most difficult task in studying fluid inclusions in uranium deposits is to find gangue minerals paragenetically associated with pitchblende deposition. If it is now evident that brines are responsible for the transportation of uranium, it remains difficult to prove the deposition mechanism in detail but the main factor is related to the change in oxygen fugacity.

The main characteristics of the mineralizing fluid (salinity, temperature, origin) are presented and a comparison is made with the basinal brines at the origin of the Pb-Zn MVT deposits in order to put more constraints on the formation of metals deposits in sedimentary basins.

Salinity

In the Lodève deposits, the temperature of last melting of ice is between -20 and -28°C indicating the presence of divalent cations in the brine.

In the Akouta deposit, the pre-ore dolomite has a salinity of 14-18% eq. weight NaCl, the ore stage sphalerite 8-22% and the post-ore dolomite and sphalerite from 22 to 24% eq. weight NaCl.

In the Oklo deposit, the melting temperatures for fluid inclusions in dolomite, barite and calcite associated with uranium mineralization are between -16 and -38°C, indicating the presence of divalent cations in the brine.

In the unconformity-type deposits, the fluid inclusions contain a brine saturated with NaCl at room temperature or are near saturation. Pagel and Jaffrezic (1977) have analysed the ionic composition of the mineralizing brine (Ca/Na at.= 0.17 to 0.34, Ca/Mg at. = 1.3 to 3.1 and Cl/Br at. = 55). In the Brousse-Broqiès deposit, the melting temperature is between -10 and -39°C.

All these data show that Na-Ca-Cl brines are especially observed as a mineralization fluid for the transportation of uranium.

Temperature

In the Lodève deposits, the homogenization temperatures (Th) of sphalerite and dolomite are about 90-100 and 110°C respectively.

In the Akouta deposit, the pre-ore dolomite has Th ranging from 105 to 120°C, the ore stage sphalerite from 85 to 175°C and the post-ore dolomite and sphalerite between 105 and 120°C.

In the Oklo deposit, the syntectonic fluid phase responsible for the mineralisation yielded average homogenisation temperatures between 105 and 120°C (dolomite, barite and calcite).

In the Precambrian unconformity-type uranium deposits from Saskatchewan and Australia, the temperature is variable between 150 and 200°C in general. In the Nabarlek and Jabiluka deposits in Australia, the temperatures recorded by Ypma and Fuzikawa (1980) range between 110 and 160°C. In the Brousse-Broquiès deposit, the Th ranges from 80 to 130°C in quartz and is 100±10°C in carbonates.

Source

In the Lodève deposits, the range of $\partial^{18}O$ data on dolomite crystals sampled in two uranium deposits (Mas Laveyre and Mares 4-5) is narrow and is between +18 and +20‰. The two calculated $\partial^{18}O$ for the brine at temperatures derived on the same crystals by fluid inclusions is +1.8 and +4.1‰SMOW. The $\partial^{13}C$ varies from 0 to -3.3 ‰PDB. These values are best explained by brine equilibrated with the Cambrian dolomitic formation. No organic signature appears despite an important amount of organic matter in the Autunian.

In the Akouta deposit, the brine related to the ore stage dolomite is characterized by calculated $\partial^{18}O$ between - 3 and +13‰SMOW and $\partial^{13}C$ about -21‰PDB. The brine has an oxygen isotopic composition compatible with a sedimentary formation water and the carbon isotopes originate from the organic matter.

In Saskatchewan, it was demonstrated that the oxygen and hydrogen isotopic composition of the mineralizing fluid is comparable with that of the brine equilibrated with the diagenetic illite in the Athabasca sandstone (∂D = -65 to -35‰SMOW and $\partial^{18}O$ = +2 to +8‰SMOW).

Nature of the uranium complexes

From presently known thermodynamic data, it is generally assumed that uranyl-carbonates predominate in near-neutral and alcaline conditions whereas uranyl- chlorides (UO_2Cl^+, $UO_2Cl_2^o$) are stable at acid pH. However, Nguyen et al. (1991) have recently shown that chloride mixed complexes of the type $(UO_2)_m(OH)_nCl_p^{(2m-n-p)}$ could play a major role in uranium transportation in near neutral and neutral solution. This dilemna could not be solved with the available thermodynamic data.

Oxydized versus reduced brines in sedimentary basins

The chemical and temperature data obtained on fluid inclusions from the considered uranium deposits are quite comparable to the data obtained on Pb-Zn Mississipi Valley-type deposits. It should be noted that no hydrocarbon inclusions are present in gangue minerals directly associated with pitchblende whereas they are often described in MVT deposits.

The mineralogy and geochemistry of the ores are very different. In the Pb-Zn deposits, there is no uranium associated with the mineralization. On the contrary, in tectonolithologic- type uranium deposits, Zn and Pb are present in significant amounts in the ore.

These two types of association could be explained considering the fO_2-pH of the mineralizing solution :

(1) - In oxydized near neutral conditions, Pb and Zn are transported in fluids with sulfate and uranium as uranyl-carbonates (Langmuir, 1978) or as mixed complex such as mixed chloride of general formula $(UO_2)_m(OH)_nCl_p^{(2m-n-p)}$ (Nguyen -Trung et al., 1991). If the mixed chloride complexes are the dominant species, uranium could be transported by the same Pb-Zn mineralizing solution. If carbonate is the ligand of uranium, the U transport would be possible depending of the carbonate content of the solution.

(2) - In reduced acid conditions, Pb and Zn are transported as chlorides whereas uranium occuring at the tetravalent state is not soluble.

Conclusions

(1) The mineralizing fluids in tectonolithologic- and unconformity-types uranium deposits are higly saline and are Ca-Na-Cl brines.
(2) The temperatures of deposition, derived from homogenization temperatures of fluid inclusions, range from 80 to 200°C.
(3) Uranium could be transported as uranyl-carbonate or mixed chloride complexes, however the thermodynamic data are not sufficient to decide.
(4) The difference in fO_2-pH could explain the presence of Pb-Zn in U deposits and the absence of U in Pb-Zn deposits considering mixed chloride complexes as the major ligands. If uranyl-carbonate is the dominant uranium-bearing complex, the carbonate content will also be a key factor.

References

Bonifas B. (1992) - Caractérisation minéralogique et géochimique de zones riches en uranium du bassin de Lodève (Hérault, France). Thèse de Diplôme doctoral de Recherche, Nancy, 168 p.

Forbes P. (1989) - Rôles des structures sédimentaires et tectoniques, du volcanisme alcalin régional et des fluides diagénétiques-hydrothermaux pour la formation des minéralisations à U-Zr-Zn-V-Mo d'Akouta (Niger). Géol. Géochim. Uranium, Mém. Nancy, 17, 376 p.

Gauthier-Lafaye F. (1986) - Les gisements d'uranium du Gabon et les réacteurs d'Oklo. Modèle métallogénique des gîtes à fortes teneurs du Protérozoique inférieur. Sciences Géologiques, Strasbourg, Mém 78, 206 p.

George E., Pagel M., Dusausoy Y. and Gauthier J.M. (1986) - Formation conditions of a tetragonal uranium oxide : αU_3O_7 in the Brousse-Broquiès basin (Aveyron, France). Uranium, 3, 69-89.

Nguyen-Trung C., Palmer D.A., Mesmer R.E. and Begun G.M. (1991) - Raman, UV-visible absorption spectral and potentiometric studies of complexation of uranyl (VI) ion in aqueous chloride solutions at 25°C, 0.1 MPa. In Source, Transport and Deposition of Metals, Pagel and Leroy (eds), Balkema, 99-102.

Pagel M. and Jaffrezic H. (1977) - Analyses chimiques de saumures des inclusions du quartz et de la dolomite du gisement de Rabbit Lake (Canada). Aspect méthodologique et importance génétique. Comptes Rendus à l'Académie des Sciences, Paris, 284, 113-116.

Ypma and Fuzikawa K. (1980) - Fluid inclusion and oxygen isotope studies of the Nabarlek and Jabiluka uranium deposits, Northern Territory, Australia. In Uranium in the Pine Creek Geosyncline, Ferguson and Goleby, eds, IAEA, 375-395.

Current Research in Geology Applied to Ore Deposits. Fenoll Hach-Alí, Torres-Ruiz & Gervilla (eds) (1993). ISBN 84-338-1772-8

FLUID-MINERAL INTERACTIONS AND THE ORIGIN OF THE TRIMOUNS TALC AND CHLORITE DEPOSIT (PYRENEES, FRANCE)

Parseval, Ph. de (1); Moine, B. (1); Fortune, J.P. (1) & Ferret, J. (2)
(1) Lab. Mineralogie, URA CNRS 67, 39 Allées J. Guesde 31000 Toulouse, France
(2) Talc de Luzenac, 2 Place Edouard Bouillières, 31100 Toulouse, France

ABSTRACT. The Trimouns talc and chlorite deposit originated from the intense hydrothermal alteration of dolostones into talc and micaschists or pegmatites into Mg-chlorite. The LREE were largely leached through the alteration. Highly saline fluids ± CO_2 were trapped at T ~ 320° C and P ~ 2.5 kb. Our data suggest that the CO_2-bearing and quartz undersaturated fluids at the origin of chlorite ore were produced by reaction of primary brines with dolomite.

With an annual production surpassing 300,000 metric tons, Trimouns in the French Pyrénées is one of the largest talc and chlorite deposits in the world.

PETROGRAPHY AND GEOCHEMISTRY

The deposit occurs in a zone of intense shearing between the Saint-Barthelemy gneissic dome and the overthrusted cover rocks consisting of epimetamorphic schists underlain by a thick dolomitic formation (HD) (Fig. 1). Talc and chlorite were produced by hydrothermal alteration of these rocks. A late Hercynian age was assumed for the deposit from structural evidences (Fortuné et al.,1980). However, a Pyrenean age (100.6 ± 1.1 m.y.) has been obtained by $^{40}Ar/^{39}Ar$ dating of hydrothermal phlogopite (Maluski and Monié, 1992, unpub. data)

The present paper is based on the detailed mineralogical and chemical investigation by de Parseval (1992) which greatly improved the former studies (Fortuné et al., 1980 ; Moine et al., 1982 and 1989). Two main types of ores were formed, depending on the composition of the primary rocks. Talc-dominant (tremolite-free) ores originated from dolostones which implies an addition of Si and the leaching of Ca and CO_2. Chlorite(clinochlore)-dominant ores result from the alteration of micaschists and pegmatites through two intermediate metasomatic zones composed of quartz-muscovite-chlorite ± phlogopite and quartz-chlorite ± phlogopite, respectively. The chemical data indicate a large addition of Mg, the almost complete leaching of Na, K and Ca, the partial leaching of SiO_2 and the relatively immobile behavior of Al, Fe, Ti and P. In these ores, Ti is present as neogenic titanite or rutile and P is contained in fluor-apatite.

The REE were dramatically leached in the course of the alteration of dolostones (Maestracci, 1987). Compared with the micaschists and pegmatites, the chlorite ores are strongly depleted in LREE while HREE are nearly inert because of the stability of zircon (Maestracci, 1987 ; de Parseval, 1992). However, the intermediate phlopopite-bearing zones show a systematic REE-enrichment (Fig. 2a and 2b). This behavior seems to be mainly governed by the stability of allanite. Neogenic Mg-rich allanite is present in the phlogopite zone from pegmatites. In the micaschists, primary Fe-rich allanite is the main REE-bearing mineral and it remains stable (maybe altered into the Mg-rich variety) in the

phlogopite zones. In the HD, geodic crystallisation of Mg-allanite and other REE minerals is frequent.

FLUID INCLUSIONS

No fluid was trapped in the talc ore. Fluid inclusions were studied in **(1)** neogenic apatite from the chlorite ore, **(2)** recrystallized quartz pods in the quartz-chlorite zone adjacent to the chlorite ore and **(3)** allanite crystals in the HD.

All the fluids are brines where $CaCl_2$ (+$MgCl_2$) often predominates over NaCl. Type A inclusions are characteristic of apatite. Their salinity is about 20 wt% eq. NaCl and they contain around 5 mol% CO_2 and small daughter crystals of Mg-rich calcite (Raman determination). Type B inclusions predominate in the quartz pods and are abundant in allanite. They are CO_2-free, halite-bearing brines with a salt content of 30-35 wt%. Allanite also contains fluid inclusions of type A, however with several unidentified (except for calcite) daughter minerals and with a gas phase composed of CH_4 instead of CO_2.

Fig. 3 exhibits isochores for the different fluids. All the isochores plot along the same P-T trend which suggests they were trapped under similar physical conditions. The CO_2-bearing inclusions were trapped at pressure > 1.5-2 kb. We assume P = 2.5 kb for T = 320° C as likely trapping conditions. The similarity between the P-T-X features of the fluids in allanite and in the deposit suggests that the same hydrothermal solutions leached REE from the primary rocks and then deposited them in the HD.

FLUID-MINERAL REACTIONS

As said, we have no direct evidence of the nature of the fluid at the origin of the alteration of dolomite into talc. However, some of its features can be inferred from thermochemical calculation. Fig. 4 displays an activity phase diagram for the system SiO_2-CaO-MgO-H_2O-CO_2 at T = 350°C and P = 2kb . The limits of saturation with respect with carbonates were calculated for fluids A (20 wt% NaCl; X_{CO_2} =.05) and B (30 wt% NaCl; X_{CO_2} arbitrarily fixed at 0.0033), respectively, for fugacity coefficients of CO_2 in the brines deduced from Bowers and Helgeson (1983). The infiltrating solution (I) must plot in the talc field and its composition must vary along a line of slope nearly unity in the course of its equilibration with dolomite (II). Evidently, this cannot be obtained from type A (CO_2-bearing) fluid but only from a nearly CO_2-free fluid as type B. The high salinity is another important factor to produce only talc. For the same CO_2 content but a lower salinity, the fugacity coefficient of CO_2 would be lower and the dolomite saturation limit would cross the talc-tremolite limit so that the latter mineral would crystallize too.

The speciation of the infiltrating solution was calculated taking into account the data on fluid inclusions ($\sum Cl$; $\sum Na/\sum Ca$; $\sum CO_2$), activity ratios from Fig.4 (I) and activity coefficients deduced from Helgeson et al.(1981). The appropriate system of heterogeneous equations was solved via the Newton-Raphson method. Then an algorithm of mass transfer evaluation for irreversible reactions involving minerals and aqueous solutions (Helgeson et al., 1970) was used to calculate the composition of the solution in equilibrium with talc and dolomite (II, Fig. 4). A water/rock ratio of about 1000 can be caculated for the overall alteration of dolomite. The following bulk mass balance equation was deduced :

$$\text{dolomite} + 1.71SiO_{2aq} + 0.26Mg_{tot} = 0.42\text{talc} + Ca_{tot} + 2CO_{2tot}$$

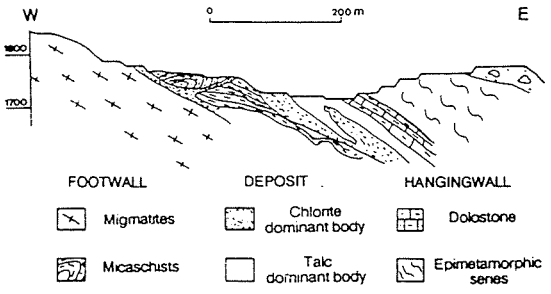

Fig.1 - A typical section across the Trimouns deposit.

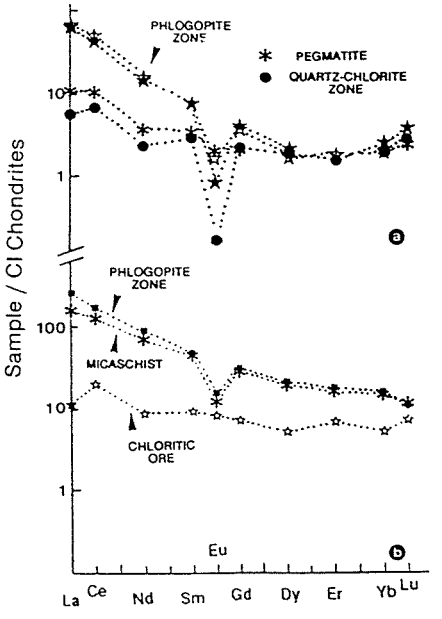

Fig.2 - Variations of REE patterns resulting from the alteration of a pegmatite (a) and a micaschist (b).

	Infiltrating solution I	Talc-Dolomite equil. solution II
SiO2	0,03037	0,01932
Ca tot	2,05195	2,0585
CO2 tot	0,18379	0,19689
Mg tot	7,939 E-2	7,617 E-2
Talc	0	2,76281 E-3
Dolomite	0	6,55 E-3

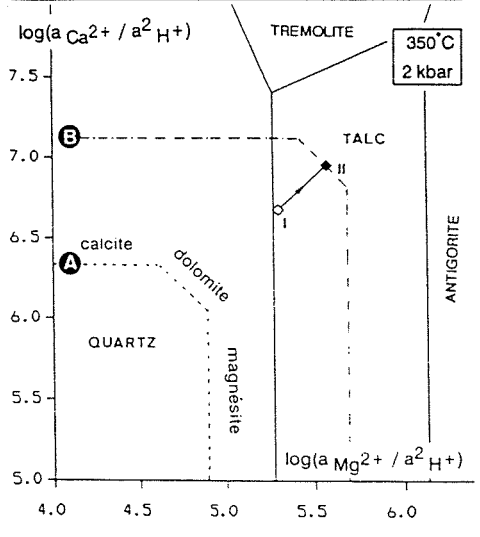

Fig.4 - Activity diagram for the system SiO_2-CaO-MgO-H_2O-CO_2 calculated at 350°C and 2kb after Brown & al. (1988) with carbonates saturation limits for fluids A and B (see text). Inset : calculated change of the composition of the hydrothermal fluid through the alteration of dolomite into talc.

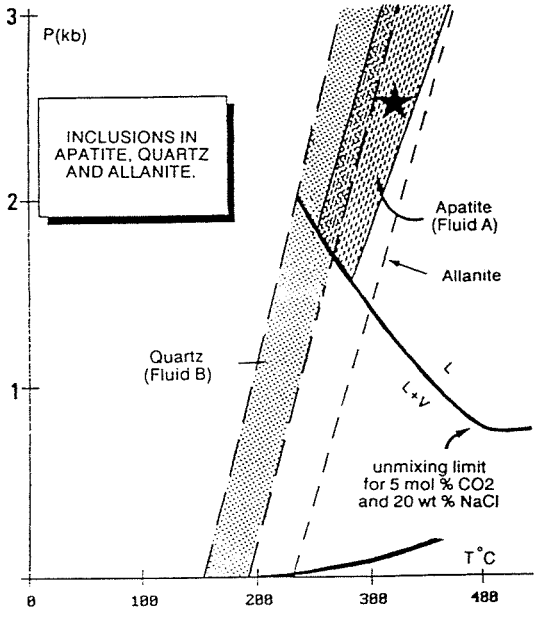

Fig.3 - Isochores of the different fluids calculated from Bowers & Helgeson (1983) and Zhang & Frantz (1987).

This relation implies a decrease by about 11% of the volume of the minerals. Such a moderate decrease is not incompatible with the preservation of the structures of the dolostones in the talc rocks.

DISCUSSION AND CONCLUSION

The above results broadly support the model proposed by Moine et al (1989) in order to explain the general connection between chlorite and talc ore. An initial fluid (here fluid B) would reacts with dolomite, thus becoming enriched in CO_2 and highly undersaturated with respect to quartz (here fluid A) before reacting with silicoaluminous rocks to produce chlorite. However, the large contrast in the CO_2 content of fluid A and B (about 3 moles) cannot be explained by a simple mass transfer model. The possibility of accumulation of CO_2 through repeated reaction with dolomite has to be considered as well as addition of CO_2 from an external source. A high salinity of the fluids with a high Ca(+Mg)/Na ratio is characteristic of this type of talc deposits and probably explains the lack of tremolite. If a Pyrenean age of the deposit was definitely proved, such compositions might well result from reaction with Triassic evaporites.

REFERENCES

Brown TH, Berman RG & Perkins EH 1989. PTA-SYSTEM: Geo-Calc software package for the calculation and display of activity-temperature-pressure phase diagrams. Am Mineral **74**:485-487.

Bowers TS & Helgeson HC 1983. Calculation of the thermodynamic and geochemical consequences of nonideal mixing in the system H_2O-CO_2-NaCl on phase relations in geologic systems: Equation of state for H_2O-CO_2-NaCl fluids at high pressures and temperatures. Geochim Cosmochim Acta **47**:1247-1275.

Helgeson HC, Kirkham DH & Flowers GC 1981. Theoretical prediction of the thermodynamic behavior of aqueous electrolytes at high pressures and temperatures: IV. Calculation of activity coefficients, osmotic coefficients and apparent molal and standard and relative partial properties to 600° C and 5 kb. Am J Sci **281**:1249-1516.

Helgeson HC, Brown TH, Nigrini A & Jones TA 1970. Calculation of mass transfer in geochemical processes involving aqueous solutions. Geochim Cosmochim Acta **34**:569-592.

Fortuné JP, Gavoille B & Thiébaut J 1980. Le gisement de talc de Trimouns près Luzenac (Ariège). Intern. Geol. Congr. 26, E10, 43 p.

Maestracci C 1987. Le gisement de talc-chlorite de Trimouns (Ariège): Etude géochimique des processus hydrothermaux. Unpub. DEA, Toulouse University, France.

Moine B, Fortuné JP, Moreau P & Viguier F 1989. Comparative mineralogy, geochemistry and conditions of formation of two metasomatic talc and chlorite deposits: Trimouns (Pyrénées, France) and Rabenwald (Eastern Alps, Austria). Econ Geol **84**:1398-1416.

Moine B, Gavoille B & Thiébaut J 1982. Géochimie des transformations à l'origine du gisement de talc et chlorite de Trimouns (Luzenac, Ariège, France). I-Mobilité des éléments et zonalités. Bull Minéral **105**: 62-75.

Parseval Ph de 1992. Etude minéralogique et géochimique du gisement de talc et chlorite de Trimouns (Pyrénées, France). Unpub PhD, Toulouse University, France.

Zhang YG & Frantz JD 1987. Determination temperatures and densities of supercritical fluids in the system NaCl-$CaCl_2$-H_2O using synthetic fluid inclusions. Chem Geol **64**: 335-350.

Current Research in Geology Applied to Ore Deposits. Fenoll Hach-Alí, Torres-Ruiz & Gervilla (eds) (1993). ISBN 84-338-1772-8

PROTEROZOIC NORMAL AND METAL-RICH BLACK SHALES FROM THE BOHEMIAN MASSIF, CZECH REPUBLIC: INDUSTRIAL AND ENVIRONMENTAL ASPECTS

Pašava, J. (1); Gabriel, Z. (2) & Kovalová, M. (3)
(1) Czech Geological Survey, Prague, Czech Republic
(2) Ministry for Economic Policy and Development of the Czech Republic, Prague, Czech Republic
(3) Příbram VII, Czech Republic

Black shales can be a source of metals, sulphur and carbon or appropriate host environment for industrial ore deposits. Sulphur and toxic heavy metal rich facies can however, cause a serious enviromental harm. Proterozoic black shales from the Bohemian Massif are given as an example.

INTRODUCTION

The Bohemian Massif has a long history of mining and is well known for its Variscan gold, uranium and base-metal deposits. Proterozoic black shales played an important role in the metallogeny of the Bohemian Massif. Pyritic black shales were intensively worked at many locations from the 16th through 19th centuries for the production of sulphuric acid. Black shales also served as sources of sulphur, metals and carbon or as an appropriate host rock for epigenetic ores (Kříbek, 1990).

However, metal-rich black shales can cause, by the release of acids, toxic metals and radioactive gas, serious environmental harm as already reported from Canada (Reichenbach 1992, Zentilli et al., 1992), Finland (Loukola-Ruskeeniemi 1990), U.S.A. (Harrel et al. 1991) and other areas of the world.

The results of the complex study of the Proterozoic black shales at selected localities (Hromnice near Pilsen and Kamenec near Radnice) from the Barrandian Upper Proterozoic, are summarized in the following text with the aim to display both their economic geological significance and potential environmental danger.

GEOLOGICAL SETTING

The Barrandian Upper Proterozoic belongs to the Moldanubicum of the Central European Variscan Belt and is composed of a complex of eugeosynclinal aleuropelitic and greywacke sediments and abundant products of submarine basic volcanism (Fig. 1). The Proterozoic exhibits a simple structure with interchanging anticlinorial and synclinorial belts trending NE-SW (Holubec, 1966). The formation of isolated and semi-isolated basins, resulting from volcanic and tectonic activities, with limited water circulation, played an important role in the deposition of black shales.

NORMAL AND METAL-RICH BLACK SHALES

Generally, two types of black shales can be distinguished based on geological position and geochemical characteristics (Pašava 1990).

NORMAL BLACK SHALES form, together with greywackes, thick flyshoid sequences (Fig. 1). They are poor in metals and sulphur (Table 1) with concentrations very close to normal black shale in sense of Vine and Tourtelot (1970).

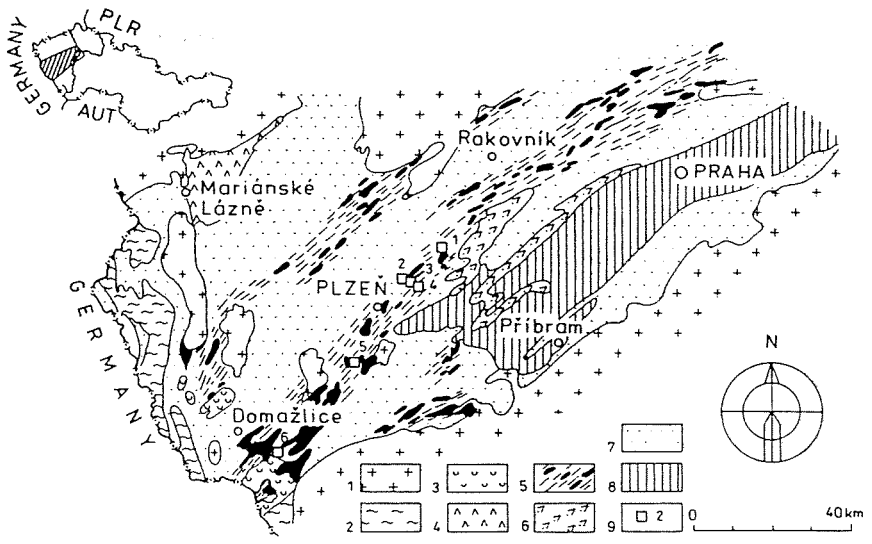

Fig. 1. Geology and location of the Proterozoic black shales in the Bohemian Massif.
1 - Granitoids, 2 - Gneiss and migmatites of Moldanubicum, 3 - Mafic rocks, 4 - Mafites of the divergent-margin type, 5 - Proterozoic spilite group with metal-rich black shales and tholeitic volcanites, 6 - Lower Paleozoic volcanites, 7 - Proterozoic flyschoid series (normal black shale and greywacke, 8 - Lower Paleozoic sedimentary series, 9 - Metal-rich black shales (1-Kamenec n. Radnice, KA-5 borehole; 2-Hromnice n. Pilsen, HRM-3 borehole)

METAL-RICH BLACK SHALES

Geological position	-	semi-isolated and isolated basins
	-	close association with basic volcanogenic rocks
Lithology	-	black metaaleurites with a laminated structure (irregular alternating of dark layers rich in C_{org} and framboidal pyrite, with lighter layers composed predominantly of a volcanogenic admixtures is typical)
Geochemistry	-	typical high metal and sulphur contents (Tab. 1)
Mineralogy	-	the most frequent sulphide is framboidal pyrite (Ni>Co) predominantly bound to C_{org}-rich layers
	-	sphalerite, chalcopyrite, millerite, pentlandite, molybdenite, galena, unnamed Mo-selenide and Mo-telluride occur in younger quartz and quartz-carbonate veinlets in close association with recrystallized pyrite (Co>Ni)
	-	REE phosphates, rutile, uraninite, berthierite, clausthalite, gold and otavite (Cd carbonate), known as accessories
Organic Geochemistry	-	Rock Eval pyrolysis and laser Ramman spectra confirm high maturity of organic matter, at

the stage prior to well-crystallized graphite

Sulphur Isotopes - wide range of $\delta^{34}S$ values (-31‰ - -2‰) in sulphides reflects bacterial reduction of the Upper Proterozoic marine sulphate

Carbon isotopes - $\delta^{13}C$ values of organic matter (-36‰ - -30‰) verify that autotrophic sulphur bacteria is the dominant organic material

TABLE 1. DISTRIBUTION OF SELECTED TRACE AND MAJOR ELEMENTS IN THE PROTEROZOIC NORMAL AND METAL-RICH BLACK SHALES FROM HROMNICE (HRM) AND KAMENEC (KA) LOCALITIES (data from Kovalová and Litochleb, 1992; Pašava, 1990 and Zimmerhakl, 1982).

Drill hole	HRM-1	KA-1	HRM-3		KA-5		Average black shale
	n=33	n=21	n=17		n=11		Vine & Tourtelot
Rock type	NBS	NBS	MBS		MBS		(1970)
Element	x	x	x	$x_{max.}$	x	$x_{max.}$	
Zn (ppm)	383	65	243	14170	960	1200	< 300
Cu	93	30	590	1180	299	398	70
Ni	88	32	600	1200	429	607	50
Mo	33	4	153	272	87	127	10
Pb	25	15	25	72	20	36	20
As	56	8	148	597	143	375	n.d.
Co	12	8	21	46	28	44	10
Cr	156	n.d.	317	1230	393	673	65
V	570	82	1109	2020	804	1991	100
C_{org} (wt.%)	0.68	n.d.	3.5		2.3		
S	1.61	n.d.	7.7		4.8		
Fe_{tot}	4.15	n.d.	8.27				

n = number of samples; x = arithmetic mean; $x_{max.}$ = maximum value; n.d. = not determined;
NBS = normal black shale; MBS = metal-rich black shale

Lead Isotopes - no correlation between the presence of radiogenic lead ($^{206}Pb/^{204}Pb$ ranges from 19.898 to 21.735) and the distance from Variscan plutons suggest that metal-rich black shales were most likely enriched by uranium during the Cadomian tectonomagmatic processes (Pašava & Amov, subm.)

Fluid Inclusions - low salinity (3-7 wt.% NaCl) water inclusions in calcite, from carbonate veinlets, with temperatures of homogenization (Th = 115 - 225°C) suggest diagenetic or late hydrothermal origin at the Kamenec locality

- H_2O-CO_2 inclusions (10-50 mole % of CO_2; dCO_2 = 0.605-0.807 g/cm^3) in quartz from quartz-sulphidic veinlets and H_2O-type inclusions in quartz and calcite (salinity up to 9 wt.% NaCl eq., Th = 100-280°C) suggest that they were probably trapped during the Cadomian metamorphic processes (Dobeš and Pašava, 1992)

ORIGIN OF METAL-RICH BLACK SHALES

I. Primary Metal Enrichment

- deposition of black shales in (semi-) isolated basins under the important role of submarine volcanism (mixturing of oxidation and reduction layers)
- volcanogenic-hydrothermal exhalation as the source of metals
- entrapment of metals by abundant organic matter (organometallic complexes, framboidal pyrite)

II. Diagenesis

- disintegration of unstable organometallic bonds and origin of sulphides
- formation of younger quartz, carbonate and quartz-carbonate veinlets (e.g. Kamenec locality)
- mobilization and recrystallization of sulphides

III. Metamorphism (T = up to 300°C, P = up to 220 MPa)

- formation of younger quartz, carbonate, and quartz-carbonate veinlets with mobilization and recrystallization of sulphides (e.g. Hromnice locality)

CONCLUSIONS

Sulphur- and toxic metal - rich black shales, widely outcropping in many locations of the central and western Bohemia often near populated areas [e.g. Plzeň (Pilsen)], represent not only the important source rock for Variscan epigenetic ore deposits but also a potential serious harm for humans and other living forms. Therefore, any help and support as well as an involvement of health, agricultural and other experts are needed for a proper evaluation of their environmental impact.

REFERENCES

Dobeš, P. & Pašava, J. 1992. Sulphidic vein mineralization in black shales of the Barrandian Upper Proterozoic, Czechoslovakia: a fluid inclusion study. In: B. Kříbek (ed.) Metallogeny of anoxic environments, Guliver s.r.o., Prague, 13-14.

Harrell, J.A., Belsito, M.E., Michael, E. & Kumar, A. 1991. Radon hazards associated with outcrops of Ohio Shale in Ohio. Env. Geol. Wat. Sci. 18:17-26.

Kovalová, M. & Litochleb, J. 1992. Geochemically anomalous black shales of the western Bohemian Upper Proterozoic. In: B. Kříbek (ed.) Metallogeny of anoxic environments, Guliver s.r.o., Prague, pp 8-9.

Kříbek, B. 1990. The role of organic matter rich formations in the metallogeny of the Bohemian Massif. Econ. Geol. 84:1525-1540.

Loukola-Ruskeeniemi, K. 1990. Metalliferous black shales - a probable source of mercury in pike in Lake Kolmisoppi, Sotkamo, Finland. Bull Geol. Soc. Finl. 62:167-175.

Pašava, J. 1990. Anomalous metal-rich black shales - a new type of mineralization in the Barrandian Proterozoic (Bohemian Massif). Ph.D. thesis, Geol. Surv. Prague, pp 1-145.

Pašava, J. & Amov, B.. Isotopic composition of lead in Proterozoic anoxic metasedimentary and volcanogenic rocks from the Bohemian Massif with metallogenetic implications. MS, Isot. Geosc., pp. 1-17 (submitted).

Reichenbach, I. 1992. Black shales as an environmental hazard: a database on black shales in Canada. Internal Report, Geol. Surv. Can., pp 69.

Vine, J.D. & Tourtelot, E.B. 1970. Geochemistry of black shales - a summary report. Econ. Geol. 65:253-272.

Zimmerhakl, P. 1982. Geology and geochemistry of metasedimentary and volcanogenic rocks from K-1 borehole at Kamenec near Radnice. M.Sc. thesis, Charles University, Prague. pp. 1-124 (in Czech).

Current Research in Geology Applied to Ore Deposits.Fenoll Hach-Ali, Torres-Ruiz & Gervilla(eds)(1993).ISBN 84-338-1772-8

COMBINED APPLICATION OF VARIOUS GEOCHEMICAL METHODS ON KUPFERSHIEFER OF THE NORTH-SUDETIC SYNCLINE, SW POLAND: EVIDENCE FOR POST-DEPOSITIONAL ACCUMULATION OF COPPER AND SILVER

Püttmann, W (1); Bechtel, A. (2); Speczik, S. (3) & Fermont, W.J.J. (4)
(1) Lehrstuhl für Geologie und Geochemie, RWTH Aachen, Germany
(2) Mineralogisch-Petrologisches Inst., Universität Bonn, Germany
(3) Geological Inst., University of Warszawa, Poland
(4) Rijks Geologische Dienst, Heerlen, The Netherlands

ABSTRACT:
The mechanism and the timing of base metal accumulation in the Permian Kupferschiefer of the Central European Zechstein basin has been discussed controversially in the past. Thereby, the possible role of organic matter in metal accumulation processes was considered primary with respect to a carbon source for sulfate reducing microorganisms.
The data presented here were obtained from Kupferschiefer profiles of Konrad mine in the North-Sudetic syncline of Southwest Poland. Several geochemical methods such as analyses of extractable organic matter by gas chromatography - mass spectrometry, analyses of solid organic matter by Rock-Eval and stable isotope measurements (C) were carried out. The results provide conclusive evidence for a participation of organic matter (hydrogen donor) in an abiological reduction of sulphate as supply of hydrogen sulphide. Concomitant maturation studies indicate an effective temperature of approximately 100°C in the present case.

SAMPLE PROVENANCE

20 samples from three Kupferschiefer profiles taken from Konrad mine in Southwest Poland have been analyzed in the present study. Figure 1 shows the geographical position of Konrad mine located at the northernmost edge of the North-Sudetic Syncline along a fault zone that separates it from the Fore-Sudetic Block. Due to the deposition of Kupferschiefer near to the former Zechstein sea

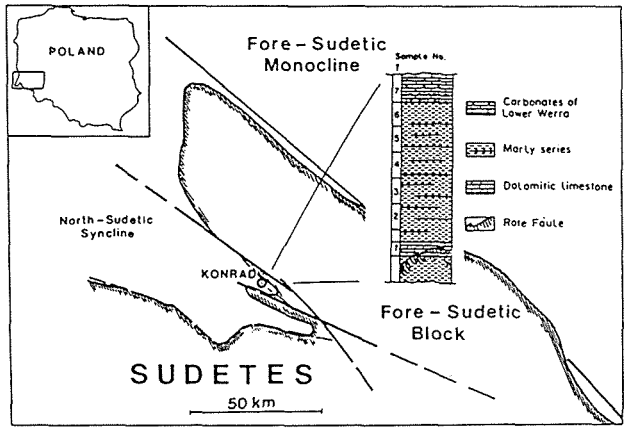

Figure 1: Geographical position of Konrad mine and a representative lithological profile (no. 1) of the 1.4 m thick Kupferschiefer section and the adjacent rocks (adopted from Püttmann et al., 1991).

shoreline the lithology of Kupferschiefer is dominated by marly series as indicated by relatively low organic carbon contents (<2%). Nevertheless, for simplicity the term Kupferschiefer is used further on. The three analyzed profiles have in common the appearance of the Rote Fäule zone directly at the bottom of the marls. Due to the deposition near the shoreline of Zechstein sea, the sedimentary conditions in the particular area of Konrad mine might have been less anoxic in comparison to most other areas of Kupferschiefer deposition.

RESULTS

In Figure 2 the results obtained from metal analyses and from organic geochemical investigations including Rock-Eval analyses carried out on profile no. 1 are shown.
The base metal contents are characterized by a strong copper predominance. Along the total profile, lead and zinc do not exceed amounts of more than 100 ppm each. Instead, the amount of copper rised to values of up to 4.19% in the marly series. The distribution profile of silver varies almost parallel with the copper profile. In the bottom part of the marls, near to the Rote Fäule, the concentration of both metals is very low. An explanation for this can bee seen in the high oxidizing potential of the Rote Fäule. Precipitation of copper and silver is inhibited under the Eh conditions of this zone. More distant from the Rote Fäule accumulation of copper and silver was possible in a less oxidizing environment.

Extract analysis and determination of the relative intensities of individual compounds have shown that the composition of the extracts varies significantly along the profile (Püttmann et al., 1988). The most remarkable observations are the depletion of saturated hydrocarbons in the bottom part of the section and the relative decrease of alkylated aromatic hydrocarbons in relation to the unsubstituted counterparts as measured by the ratio of phenanthrene versus the sum of methylphenanthrenes (Ph/ΣMePh). The ratio increases drastically in and near to the Rote Fäule (Fig. 2). Therefore, the ratio was used as a parameter for the measurement of the degree of oxidation of the organic matter (Püttmann et al., 1988). The highest degree of oxidation of organic matter in the bottom part of the section corresponds with low amounts of copper. Here, hydrogen equivalents were obviously used up without being able to drop the Eh to a level required for copper precipitation.
The redox conditions can be assumed to be governed by the availability of hydrogen equivalents contributed by organic matter present in the marly shale. An appropriate method for the study of the capacity of organic matter in redox processes is the determination of the hydrogen index (HI) by use of Rock-Eval analysis. This index is measured as mg hydrocarbons/g organic carbon (mg HC/g Corg). Figure 2 shows that the HI increases drastically from the bottom to the top of the marly shale. This means that the amount of hydrogen linked to organic carbon diminished together with an increase of the oxidizing potential governed by the Rote Fäule. This is opposite to the trend observed in Kupferschiefer profiles from the Lower Rhine basin, where the hydrogen index increases from the top to the bottom of the shale due to increasing anoxity (unpubl. results). The loss

of hydrogen is not accompanied by a simultaneous incorporation of oxygen into the organic matter. This is evidenced by the oxygen index (OI = mg CO_2/g Corg) determined in the same sample set (Fig. 2). The OI remains almost constant within the analyzed section. An explanation for this can be seen in an oxidation of part of the organic carbon and its transformation to CO_2. In order to proof this assumption the isotopic composition of the organic matter has been investigated.

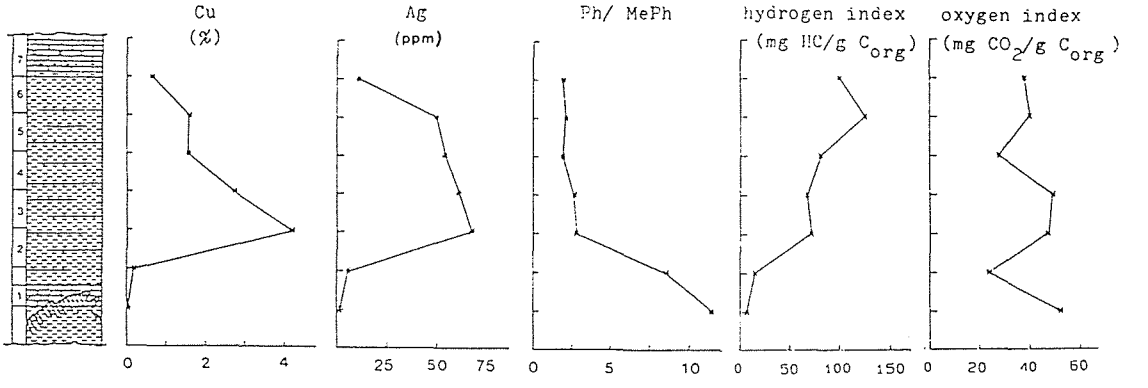

Figure 2: Variation of the copper content (%), the silver content (ppm), the hydrogen index (HI measured as mg HC/g Corg) and the ratio of phenanthrene/sum of methylphenanthrenes (Ph/ΣMePh) in the seven samples of profile no. 1 from Kupferschiefer and adjacent rocks (Konrad mine).

STABLE ISOTOPE ANALYSES

The samples from the Kupferschiefer profiles were additionally investigated with respect to carbon isotopic composition of both, extractable organic matter and the kerogen not soluble in organic solvents. Results obtained from profiles no. 2 and 3 are shown in Figure 3. The $\delta^{13}C$ values obtained from the kerogen as well as of the extractable organic matter (bitumen) are significantly higher (~3‰) in the bottom part compared to the upper part of each profile. A similar variance was also observed in base metal mineralized Kupferschiefer profils from the Richelsdorf Hills, Germany (Bechtel & Püttmann, 1991) and in one non-mineralized profile from the Lower Rhine Basin which was associated with the occurrence of red-coloured rocks in the underlying Zechstein conglomerate (Bechtel & Püttmann, 1992). Such a strong variation of the isotopic composition of organic carbon in a 1.4 m thick profile cannot be explained by a simultaneous facies variation, because the investigation of Kupferschiefer profiles in areas not influenced by the oxidizing potential of Rotliegend formation waters revealed only a small effect of a facies change during Kupferschiefer deposition on the $\delta^{13}C$-values of the organic matter. For this reason, the observed trends (Fig. 3) have to be discussed either in connection with the influence of oxidizing fluids or as a result of significantly higher thermal maturity affecting the Kupferschiefer primarily in the bottom part. The latter possibility can be neglected, because a substantial temperature decrease within a section of 1.4 m thickness is

unlikely. Therefore, the observed shift of organic matter towards heavier carbon isotopes with approximation to the Rote Fäule was induced most likely by oxidation of the inherent organic matter. This results in a shift of the carbon isotopic composition similar to the one observed by increasing maturation because oxidation affects preferentially the lighter aliphatic material. This explanation coincides with the results obtained from Rock-Eval analysis indicating a major loss of hydrogen equivalents from organic matter preferentially in the bottom section.

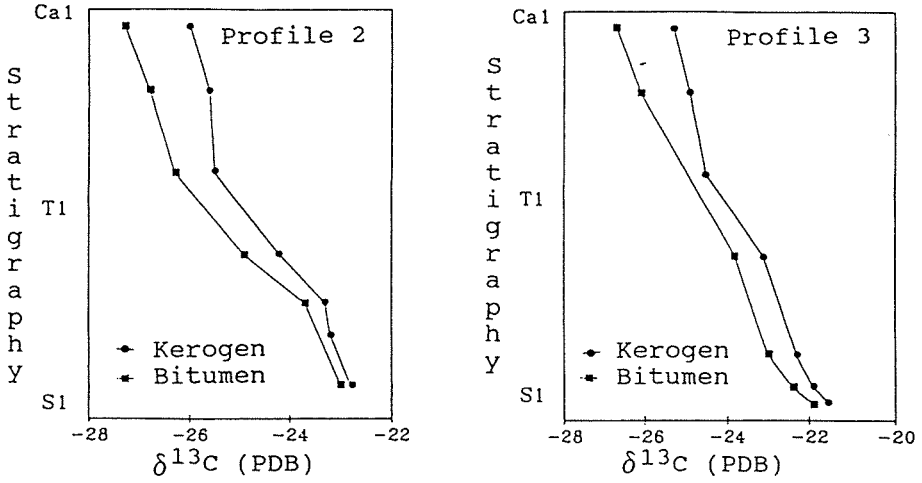

Figure 3: Variation of the $\delta^{13}C$-values determined in the kerogen and the extractable organic matter (bitumen) in samples from two Kupferschiefer profiles and adjacent rocks from Konrad mine. Ca1 = Carbonates of Lower Werra, T1 = Kupferschiefer and S1 = Zechstein conglomerate.

REFERENCES:

BECHTEL A. & PÜTTMANN W. (1991): The origin of the Kupferschiefer-type mineralization in the Richelsdorf Hills, Germany, as deduced from stable isotope and organic geochemical studies. Chem. Geol. 91, 1-18.

BECHTEL A. & PÜTTMANN W. (1992): Combined isotopic and biomarker investigations of temperature- and facies-dependent variations in the Kupferschiefer of the Lower Rhine Basin, NW Germany. Chem. Geol. 102, 23-40.

PÜTTMANN W., HAGEMANN H. W., MERZ C. & SPECZIK S. (1988): Influence of organic material on mineralization processes in the Permian Kupferschiefer Formation, Poland. Org. Geochem. 13, 357-363.

PÜTTMANN W., FERMONT W.J.J. & SPECZIK S. (1991): The possible role of organic matter in transport and accumulation of metals exemplified at the Permian Kupferschiefer formation. Ore Geol. Rev. 6, 563-579.

Current Research in Geology Applied to Ore Deposits. Fenoll Hach-Alí, Torres-Ruiz & Gervilla (eds) (1993). ISBN 84-338-1772-8

THE SUBVOLCANIC ROCKS OF THE CERRO NEGRO DISTRICT (FAMATINA, LA RIOJA, ARGENTINA): CHARACTERIZATION, HYDROTHERMAL ALTERATION AND ASSOCIATED MINERALIZATION.

Ríos Gómez, J. (1); Suárez, O. (2); García-Iglesias, J. (1) & Loredo, J. (1)
(1) Dept. de Explotación y Prospección de Minas, Universidad de Oviedo, Oviedo, Spain
(2) Dept. de Geología. Universidad de Oviedo, Oviedo, Spain

ABSTRACT

The vein mineralizations of Cerro Negro district, in the orogene known as Famatina System, are related to tertiary chalcoalkaline rocks of strong subvolcanic character and intermediate to acid nature.

They are constituted by a complex paragenesis of Zn, Pb, Ag and Cu sulphides of meso-epithermal type, with subordinate As-Co-Ni-Bi minerals and Cd, Ga and Ge traces.

These igneous rocks are affected by a complex hydrothermal alteration with phases between 320ºC and 150ºC, temperatures in agreement with the estimated values for the hydrothermal phases of mineralized veins.

REGIONAL AND LOCAL GEOLOGY

According to De Alba (1979), the Famatina System (fig.1) is constituted of:

- a great marine ordovician sedimentary sequence affected by a low-grade metamorphism (Negro Peinado Formation).
- Intrusions of devonian granitoids (Ñuñorco Formation).
- Discordant superposition of carboniferous and permian continental sediments (Patquía Formation)
- Dykes and stocks of subvolcanic and occasionaly volcanic rocks (Mogote Formation), which cuts across the whole.

Most outcrops in Cerro Negro district are constituted of limolites, shales and sandstones of Negro Peinado Formation. They show a low grade regional and contact metamorphism and N-S subvertical schistosity.

Frequent dykes and stocks of subvolcanic rocks of intermediate to acid nature cutting the sedimentary series, anyway scarce acid volcanic rocks, are present in the area. They belong to Mogote Formation of miocene-pliocene age (andean tectonic).

An hydrothermalism related to these magmatic phases originates mineralized veins, and produces alteration as much in igneous rocks as in the enclosing sedimentary rocks (Ríos Gómez, 1988/91).

SUBVOLCANIC ROCKS

a) General characteristics

They show a clear structural control in post-subductive extensive regime of the andean orogenian cycle (Schalamuk et al., 1990).

The stocks and dykes from the district follow the main structural lineaments of the area. They range from microdiorite to quartzdiorite and granitic porphyry, with strong subvolcanic nature. The porphyric texture with chalcosodic plagioclase feldspar crystals inside microgranular ground-mass of quartz, plagioclase feldspar and potassic feldspar, is dominant. In spite of alterations, primary textures and minerals can be recognized. Chemical analises (Table I) show that rocks range from intermediate to acid nature, and they can be considered as typical rocks of chalcoalkaline series with high k-content (Baker, 1984).

The presence of porphyric textures occasionaly accompanied of granophiric textures and data of major elements, suggests moderate pressures and relatively shallow emplacements.

b) Hydrothermal alterations

At the moment is not possible to indicate a detailed zonation of alterations, provided the grade of superposition and complexity they have. Six alteration types have been identified:

- Chloritic alteration

  It is represented by the association chlorite (essential) ± epidote ± ilmenite ± sphene ± carbonate, and limited to the subvolcanic rocks. It is

particularly visible in the eastern sector of the district.
Chlorite appears as replacing of ferromagnesian minerals or as filling of miarolitic cavities and small fractures.
According to petrographic characteristics, two well diferenciated chlorite types can be distinguished; and the use of chlorite geothermometer (Cathelineau, 1988) shows a first deposition stage between 350ºC and 300ºC (320ºC), represented by chlorites with high Al, Fe and Mg contents, and a late stage in the range of 150ºC, represented by a typical vermicular chlorite with normal Al, Fe and Mg contents.

- Sericitic alteration
  It preferably appears bording the silicified zones closed to veins and it is characterized by sericite ± white mica (muscovite) ± quartz ± pyrite ± rutile.
  This alteration which is particularly characteristic of the enclosing rocks, affects igneous rocks too.
- Potassic alteration
  This is an early alteration essentialy defined by biotite (neoformation) ± potassic feldspar ± quartz, which shows a poor development limited to subvolcanic rocks.
- Silicification
  This alteration is present in the whole of the sector, and it accompanies the another before mentioned. At least, it presents two episodes:
  1) Silicification of enclosing rocks by massive replacement and fracture filling after a fracturation stage. It is very strong in some sectors of the area.
  2) A second silicification phase which can be subdivided in several fracture filling stages, affecting both subvolcanic rocks and mineralized veins. In this phase, quartz is frequently accompanied by carbonates and sulphides.
- Argillitic alteration
  The subvolcanic rocks show argillitic alteration by an increasing transformation of potassic and plagioclase feldspars towards the dyke borders, where the friability of the rocks increases.
- Albitisation
  This is restricted to porphyries and appears as patches by replacement of plagioclase feldspars.

MINERALIZATION

More than twenty subvertical beaded vein mineralizations of WNW-ESE and NNW-SSE predominant trends are known in the district (Ríos et al., 1992). Texture are from banded and colloform to brecciated. The veins range from 0.5 to 3 m.thickness and the average run is 200 m. These mineralizations could correspond with the external phase of Nevados del Famatina Cu-Mo porphyry (fig.1).

The polymetallic mineralizations of the district show a pulsating genesis with gradual decreasing of temperature and mineral associations from mesothermal to epithermal. Main minerals of the paragenesis are: arsenopyrite, pyrite, pyrrhotite, magnetite, titanomagnetite, sphalerite, chalcopyrite, marcasite, bornite, galena, tetrahedrite; minor quantities of argentiferous minerals (argentite, argirodite, native silver), Ag-sulfosalts (proustite, pyrargyrite, miargyrite, freibergite) and Fe-Co-Ni sulfoarsenides (chloantite, rammelsbergite and safflorite) are present. Small particles of native gold and electrum occasionaly appear. In addition to the dominant Fe and Mn carbonates (siderite and rhodocrosite) and quartz, calcite and baryte are present as gangue minerals.

In the altered subvolcanic rocks a paragenesis constituted by magnetite, arsenopyrite, pyrrhotite, pyrite, marcasite, chalcopyrite, sphalerite and occasional small particles of native gold and electrum, is superposed.

In mineralized veins, fluid inclusion studies in quartz and crystallochemical studies of arsenopyrite in equilibrium with pyrite give ore-forming fluids temperature from 350ºC to 250ºC.

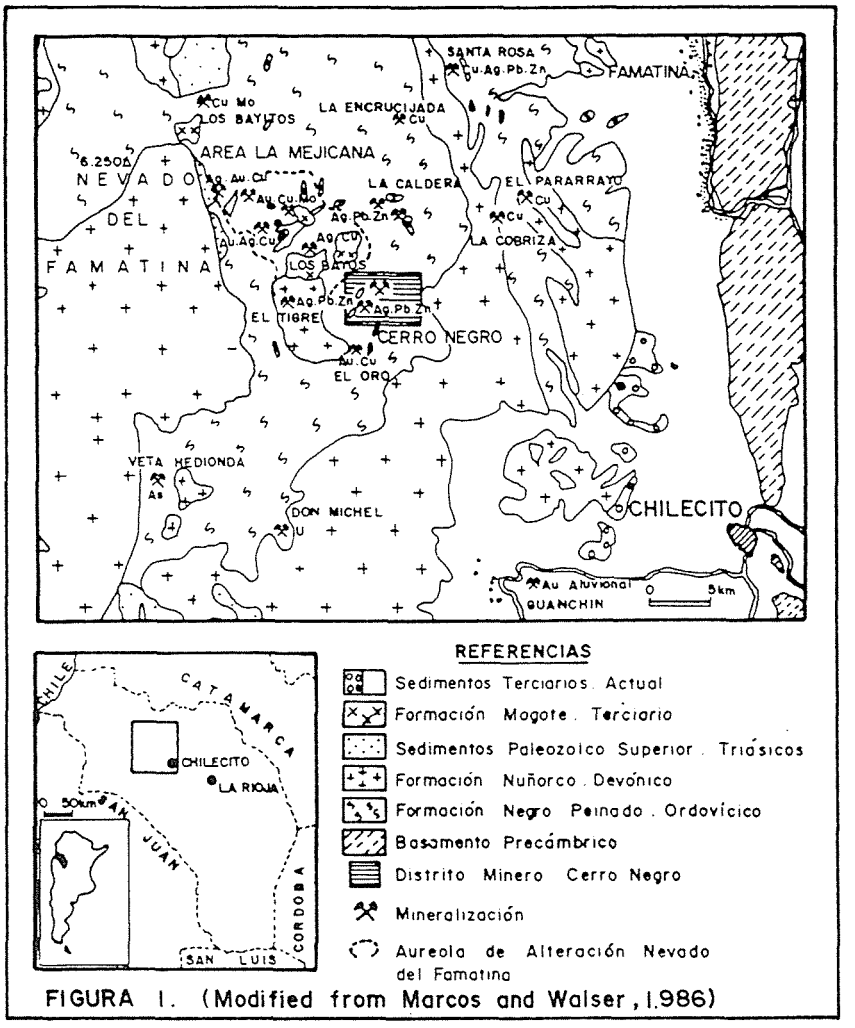

FIGURA 1. (Modified from Marcos and Walser, 1.986)

TABLE I: CHEMICAL ANALYSES OF SUBVOLCANIC ROCKS

SAMPLE		M 1	M 2	M 3	M 4	M 5
SiO2	%	56.96	66.89	68.11	76.68	77.36
TiO2	%	1.59	0.44	0.51	0.17	0.16
Al2O3	%	14.96	15.37	15.18	12.64	12.60
Fe2O3	%	11.24	5.53	5.25	1.48	1.40
MgO	%	2.39	1.63	1.45	0.20	0.22
MnO	%	0.49	0.28	0.19	0.01	0.04
CaO	%	3.64	1.63	2.19	0.21	0.56
Na2O	%	3.77	2.60	2.57	1.98	1.90
K2O	%	0.98	3.72	2.82	5.99	5.20
P2O5	%	0.54	0.09	0.09	0.04	0.02
LOI	%	4.08	2.09	2.37	0.97	1.38
TOTAL	%	100.65	100.26	100.73	100.37	100.84

CONCLUSIONS

Cerro Negro mineralizations are related to tertiary subvolcanic rocks affected by an hydrothermal alteration which shows several phases between 320ºC and 150ºC deduced from chlorite geotermometer data.

These phases and temperatures can be correlated to those correspondant to mineralized veins originated in a structuraly controlled open system. In mineralized veins, crystallochemical and fluid inclusion studies show phases comprised between 350ºC and 150ºC, and they are in agreement with data from chlorite of altered igneous rocks.

REFERENCES

Barker, P.E. (1984). Evolution and classification of orogenic volcanic rocks. Thorpe R.S.(ed): Orogenic andesite and relative rocks, 11-24. J.Whiley and Sons.

Cathelineau, M.(1988). Cation site occupancy in chlorites and illites as a function of temperature. Clay Minerals, 23, 471-485.

De Alba, E. (1979). Servicio Geológico Nacional. Hoja 16 d. Bol. 163. Buenos Aires, Argentina.

Marcos,O. y Walser G.(1986). Informe SVAB AR B6006-B6004. CLAR. DNMG.La Rioja, Argentina.

Rios Gómez, J.(1988-1991). Evaluaciones previas e informes geológicos inéditos. CLAR. DNMG.L.R.,Argentina.

Rios Gómez, J. et al. (1992) Características geológicas y mineralógicas del distrito de Cerro Negro (La Rioja, Argentina). Actas VIII Congreso Latinoamericano de Geologia, tomo IV, 242-246. Salamanca.

Schalamuk, A. et al. (1990). Polymetallic Ag-Te bearing paragenesis of the Cerro Negro District,Famatina Range, La Rioja, Argentina. I.A.G.O.D. Canadá.

Current Research in Geology Applied to Ore Deposits. Fenoll Hach-Alí, Torres-Ruiz & Gervilla (eds) (1993). ISBN 84-338-1772-8

THE TAGANANA ALKALINE INTRUSIONS (TENERIFE, CANARY ISLANDS): FIRST DATA ON THEIR ORE MINERALS

Rodríguez-Losada, J.A. (1); Martínez-Frías, J. (2) & Hernandez-Pacheco, A.(3)
(1) Dept. de Geología, Universidad de La Laguna, Islas Canarias, Spain
(2) IAGM (CSIC-Universidad de Granada), Granada, Spain
(3) Dept. de Petrología y Geoquímica, Universidad Complutense, Madrid, Spain

ABSTRACT: Two types of intrusive rocks occur in the Taganana area (NE Tenerife): nepheline syenites and alkali gabbros. Their petrology and geochemistry were established, with special attention to the characteristics of the ore mineral assemblage. This study suggests: 1) the existence of separation processes between oxides and sulphides during magmatic crystallization, and 2) temperatures of 640° to 700°C, and fO_2 values within the range $10^{-18.5}$-10^{-17}.

INTRODUCTION

The intrusive rocks of Taganana (NE Tenerife) occur, on the surface, as a small outcrop of about 2,500 m^2. It is located at 16°01'12''W and 28°34'26''N, close to Taganana, the most important village in the area. Its stratigraphic position corresponds to the bottom part of the Taganana Basal Unit, which is called "Arco de Taganana" because of its arc-like morphology (Carracedo, 1979; Bravo & Hernández Pacheco, 1980). García Talavera (1976) established a local stratigraphic sequence within which this outcrop is the oldest unit in the island. The author called it "Serie Basal" (of Miocene age), and placed it below the "Old Basaltic Series" from Fuster et al (1968). In this sense, the K/Ar dating carried out by Ancochea et al (1990) gives ages of 5.7 m.y.b.p for these rocks.

The present work offers new data about the petrological characterization and geochemistry of these alkaline intrusions. Attention has specially devoted to the study of the ore minerals and their textures, stressing both the equilibrium thermodynamic conditions and the fO_2 values.

THE TAGANANA ALKALINE INTRUSIONS: ORE MINERAL CHARACTERISTICS

As previously defined, two main types of intrusive rocks occur in the study area: nepheline syenites and alkali gabbros. In both cases, a dyke swarm cut these intrusions. Dykes are mainly of basaltic composition although salic dykes are also visible. They include syenites and alkali pyroxenite fragments and have been affected by brecciation and alteration processes.

Alkali feldspar and minor nepheline, apatite, sphene, chlorites, zeolites and augite (partially transformed into hornblende), are the main minerals which form part of the syenites. The alkali gabbros are mostly constituted by idiomorphic and subidiomorphic plagioclase (about 65% to 79% of the whole rock) and augite (about 20%); hornblende occurs as a consequence of the augite transformation, and minor biotite, apatite and sphene are also present.

Geochemical analysis of both types of rocks (syenites and alkali gabbros) (Table 1) show a moderate undersaturation and peralkaline

Table 1: Analyses of nepheline syenites (1-3) and alkali gabbros (4-6)

	1	2	3	4	5	6
SiO_2	55.60	55.75	55.85	52.10	52.05	52.10
Al_2O_3	19.50	19.60	19.55	18.75	18.90	
Fe_2O_3	1.10	1.08	1.06	3.80	3.85	18.80
FeO	1.35	1.45	1.40	2.85	2.80	3.90
MgO	1.15	1.25	1.10	2.10	2.15	2.80
CaO	3.40	3.55	3.50	6.10	6.05	2.15
Na_2O	6.45	6.40	6.40	5.95	5.90	5.95
K_2O	4.45	4.35	4.30	2.90	2.95	5.90
MnO	0.22	0.22	0.22	0.16	0.16	3.00
TiO_2	0.90	0.94	0.96	1.95	1.95	0.16
P_2O_5	0.22	0.19	0.20	0.66	0.66	1.95
H_2O+	2.25	1.95	2.26	1.27	1.18	0.64
H_2O-	1.15	1.10	1.13	0.82	0.97	0.94
Other	1.95	2.11	1.83	0.91	1.15	1.02
						1.20
TOTAL	99.69	99.94	99.76	100.32	100.72	100.51

character. Relatively high alumina contents must be interpreted as a later alteration effect.

In broad terms, the textural and compositional characteristics of the ore minerals are similar in both types of rocks. These minerals constitute a simple assemblage of magnetite, ilmenite, maghemite, pyrite, and pyrrhotite.

In the nepheline syenites, magnetite and ilmenite occur as subidiomorphic to allotriomorphic crystals (up to 500 µm), which are included so in the vitreous matrix as in the phenocrystals. There are also some crystals of maghemite resulting from the oxidation of the magnetite. Small crystals of pyrite (50-200 µm) are frequent in the matrix, although the presence of small drop-like inclusions of pyrite (< 50 µm) into the magnetite crystals could be interpreted as unmixing phenomena between oxides and sulphides. Pyrrhotite is very scarce, appearing as small tabular crystals (< 100 µm) within the matrix.

In the alkali gabbros, sulphides are more abundant, and magnetite, pyrite and pyrrhotite reach bigger sizes than in the syenites. From a textural point of view, two types of pyrite have been identified: 1) idiomorphous crystals, with clean surfaces and well developed faces, and 2) irregular crystals, with porous surfaces. Oxidation processes affecting to the magnetite, with the subsequent formation of maghemite, are also more evident. Microprobe analyses of magnetites and ilmenites are given in Table 2.

From the chemical composition of both coexisting oxide phases it has estimated, using the curves of Buddington and Lindsley (1964), that these alkaline intrusions crystallized at temperatures between 640° and 700°C and under oxygen fugacities of around $10^{-18.5}$ and 10^{-17} atm.

This study suggests that these metallic phases appear to have formed during magmatic crystallization process. This interpretation contrasts with the hydrothermal origin which has been proposed to explain the genesis of other compositionally similar assemblages in the Canary islands (e.g. syenites from La Gomera) (Rodríguez Losada et al, 1990).

	1	2	3	4	5	6
FeO	84.85	85.98	85.37	45.15	80.93	45.62
TiO_2	4.41	4.89	5.80	48.20	9.40	48.31
Cr_2O_3	0.00	0.02	0.00	0.03	0.03	0.02
Al_2O_3	0.40	0.23	0.83	0.05	1.23	0.04
MnO	3.29	2.34	1.18	3.45	1.21	3.14
MgO	0.03	0.04	0.11	0.96	0.17	0.69
ZnO	0.44	0.17	0.17	0.04	0.23	0.08
SiO_2	0.16	0.03	0.02	0.01	0.04	0.02
CaO	0.02	0.02	0.01	0.00	0.00	0.02
NiO	0.02	0.05	0.00	0.00	0.00	0.00
Ag_2O	0.01	0.00	0.01	0.00	0.00	0.04
CoO	0.12	0.10	0.12	0.01	0.07	0.06
As_2O_3	0.05	0.00	0.18	0.02	0.00	0.00
TOTAL	93.80	93.87	93.80	97.92	93.31	98.04

Recalculated analyses (after Carmichael, 1967)

FeO	31.42	32.93	34.76	38.11	37.72	38.96
Fe_2O_3	59.38	58.96	56.23	7.82	48.00	7.40
TOTAL	99.75	99.77	99.44	98.70	98.11	98.78
%UVS	12.77	14.17	16.84	---		---
$\%R_2O_3$				7.61	27.540	7.20
T°C				640		710
$logfO_2$				-18.50		-17.00

Table 2: Microprobe analyses of magnetites and ilmenites in the Taganana alkaline intrusions (1 and 2: nepheline syenite. 3-6: alkali gabbros). (CAMECA SX50 electron microprobe. Beam Energy: 20 Kv. Beam current: 25 nA. Beam Ø: 7 µm. Time of analysis: 100 s). Standard collection of the "Servicios Técnicos, Universidad de Granada).

ACKNOWLEDGEMENTS

This work forms part of the research project AMB92-0408 and it was completed in cooperation with IGCP Project 318 (IUGS/UNESCO) and with the Spanish Working Group on Geology and Metallogeny of Hydrothermal Seafloor Deposits.

REFERENCES

Ancochea, E., Fúster, J.M., Ibarrola, E., Cendrero, A., Coello, J., Hernán, F., Cantagrel, J.M. and Jamond, C. 1990. Volcanic evolution of the island of Tenerife (Canary Island) in the light of new K-Ar data. J. Volcan. Geoth. Res., 44:231-249.

Bravo, T. and Hernández Pacheco, A. 1980. Islas Canarias. Excursión 121 A-C: Tenerife. 26 Cong. Geol. Inter. Paris. Bol. ITGE, 91: 379-390.

Buddington, A.F. and Lindsley, D.H. 1964. Iron-titanium oxide minerals and synthetic equivalents. Jour. of Petrol., 5, 2: 310-357.

Carmichael, I.S.E. 1967. The iron-Titanium Oxides of Salic Volcanic Rocks and their Associated Ferromagnesian Silicates. Contr. Mineral. and Petrol., 14: 36-64.

Carracedo, J. C. 1979. Paleomagnetismo e historia volcánica de Tenerife. Aula de Cultura de Tenerife, 82 p.

Fuster, J.M., Araña, V., Brandle, J.L., Navarro, M., Alonso, U. and Aparicio, A. 1968. Geology and volcanology of the Canary Islands: Tenerife. I. Lucas Mallada, CSIC, 218 p.

García Talavera, F. 1976. Nota sobre el afloramiento de rocas granudas sieníticas en la serie basal de Tenerife (Canarias). Estudios Geol., 32: 41-46.

Rodríguez Losada, J.A., De la Nuez, J. and Martínez Frías, J. 1990. Minerales accesorios de Fe y Ti en las intrusiones alcalinas de Tamargada, La Gomera (Islas canarias). Rev. Soc. Geol. Esp., 3 (1-2): 161-166.

Current Research in Geology Applied to Ore Deposits. Fenoll Hach-Alí, Torres-Ruiz & Gervilla (eds) (1993). ISBN 84-338-1772-8

URANIUM AND MOLYBDENUM MINERALIZATION IN THE PERMIAN VOLCANO-SEDIMENTARY FORMATIONS OF THE WESTERN CARPATHIANS, SLOVAKIA

Rojkovič, I.
Geological Inst. of the Slovak Academy of Sciences, 84226 Bratislava, Slovakia

ABSTRACT: Uranium and molybdenum mineralization occurs in the Permian volcano-sedimentary formations. It is mostly stratiform and related to acid volcanism. Ore elements were accumalated by reduction and adsorbtion processes from 270±30 to 240±30 Ma. Due to their remobilization and concentration higher grade ores were formed during the Alpine orogeny from 130±20 to 100±20 Ma.

INTRODUCTION

The end of the Hercynian orogeny was accompanied by graben tectonics, continental volcanism and mineralizing processes at the southern edge of the Eurasian plate (Tischler and Finlow-Bates 1980). Many uranium deposits in the Alps show spatial relation to the Permian acid volcanism or they are found directly in the volcanites (Mittempergher 1972, Haditsch and Mostler 1982, Burkhard et al. 1985, Cadel et al. 1987, Pagel 1990). Uranium and molybdenum mineralization in the Permian continental volcano-sedimentary formations may also be observed in the Western Carpathians (Fig. 1) in Novoveská Huta (Rojkovič et al. 1993), Jahodná (Rojkovič and Mihál' 1991), Kálnica and Selec (Rojkovič 1980). Volcanism is represented by rhyolites accompanied by dacites, andesites and volcanoclastics (Fig. 2). Continental sediments are dominant but they are replaced by lagoonal lithofacies in the uppermost part of the Permian.

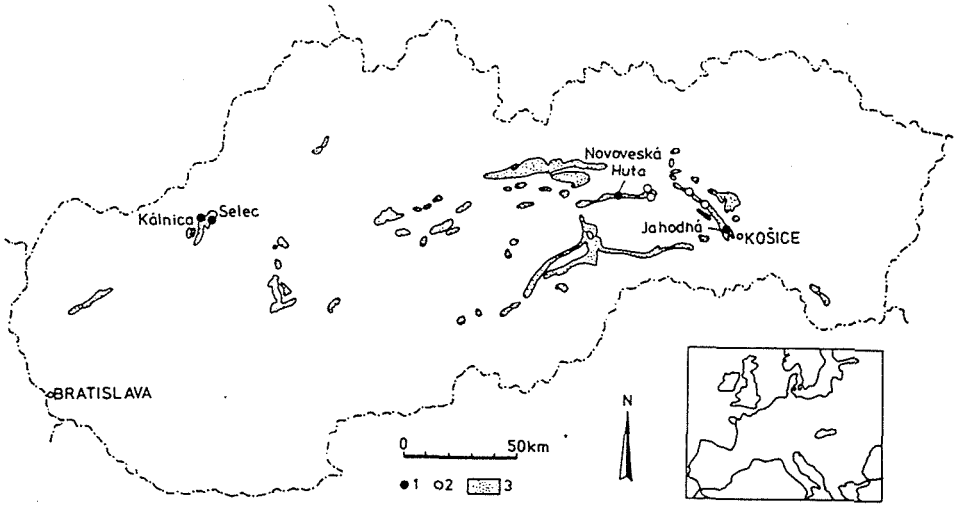

Fig. 1. Uranium and molybdenum deposits (1) and occurrences (2) in the Permian formations (3) of the Western Carpathians.

URANIUM AND MOLYBDENUM ORES

Uranium and molybdenum mineralization is spatially related to volcanic rocks in two ore-bearing horizons near Novoveská Huta (Fig. 2). The upper horizon in sandstones and conglomerates of volcanoclastic character overlies rhyolites and their tuffs. The lower one is bound to breccias in the upper part of the volcano-sedimentary complex with intermediate volcanism. The mineralized horizon is 4 km long, from 200 to 600 m wide and up to 80 m thick. Ore lenses range in thickness from several metres to tens of metres. Their extension varies from tens to tens of thousands of square metres. They are mostly concordant to the wall rocks but planes concordant to the Alpine cleavage are also locally mineralized. The mineralized rocks underwent intensive silicification, sericitization, carbonatization, pyritization and they are accompanied by increased contents of apatite and tourmaline. The dominant ore minerals are uraninite and molybdenite accompanied by U-Ti oxides and pyrite. The homogenization temperatures of fluid inclusions in carbonates accompanying mineralization is from 110 to 120°C (Rojkovič et al. 1993) . The high grade mineralization represented by uraninite, coffinite, molybdenite accompanied by pyrite, chalcopyrite, quartz, Fe-dolomite and other minerals also occurs in veins and near the faults cutting the mineralized horizons (Fig. 3). The homogenization temperatures of fluid inclusions in carbonates and quartz of the veins ranges from 95 to 190°C.

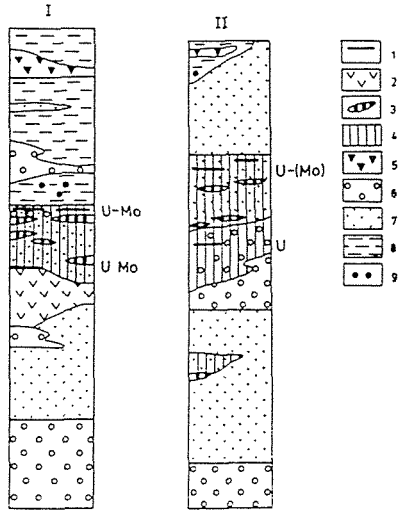

Fig. 2. Lithostratigraphic scheme of the Permian in Novoveská Huta and Jahodná (I) and Kálnica and Selec (II) adapted according to Novotný and Mihál' (1987 - I) and Novotný and Mihál' (in Štimmel et al. 1984 - II). 1 - mineralization, 2 - dacites and andesites, 3 - rhyolites, 4 - volcanoclastics, 5 - gypsum, anhydrites, 6 - conglomerates, 7 - sandstones, 8 - shales, 9 - carbonate concretions.

The contents of U (16 ppm),Mo (4 ppm), Cu (84 ppm) and Y (28 ppm) are from two to eight times higher in non-mineralized rhyolites and their tuffs than in sedimentary rocks. Fission track reprints show that uranium occurs mostly in the matrix of rhyolites and their tuffs. Due to their devitrification and alteration uranium was mobilized and concentrated in sericite and in Ti oxides. Uranium is bound mostly in Ti oxides in dacites and andesites.

U and Mo in ores are accompanied by Cu, Pb, Co and Y. Content of U and Mo in high grade ores exceeds 0.1 wt. %. The rocks are poor in organic matter (mostly below 0.2 wt. %). The isotopic

composition of $\delta^{34}S$ varies from -32.7 to +2.7 and $\delta^{13}C$ from -27.1 to -0.5 $‰$. A larger variability in the stratiform ores suggests mixing of meteoric solutions with fluids of volcanic origin and their complex history. U/Pb isotope dating gave two age groups of uranium mineralization (Kolektiv 1984): 240±30 Ma for low grade stratiform ore and 130±20 Ma for high grade ore near faults.

Uranium and molybdenum mineralization in Jahodná also occurs in two horizons of the same volcano-sedimentary formation as in Novoveská Huta. The upper horizon is in acid volcanoclastics and the lower one is near the contact between andesites and sandstones. High grade ores are bound to crossing of ore bodies by transversal reverse faults. Ore mineralization is represented by uraninite, brannerite, molybdenite and pyrite (Fig. 4). Rocks with uranium and molybdenum mineralization are cut by veis of Fe-dolomite with quartz and chalcopyrite.

There are several less significant occurrences of uranium and molybdenum mineralization associated with volcanites and pyroclastics in the Permian formations. Poor uranium and molybdenum mineralization occurs in rhyolites and their tuffs, as well as in dacites and andesites in the same lithostratigraphic position as in Novoveská Huta. U-Ti oxides (uranium-bearing leucoxene) are accompanied by molybdenite, pyrite, chalcopyrite, tennantite, arsenopyrite and xenotime. The supergene zone is characterized by torbernite accompanied by iron hydroxides.

The stratiform uranium mineralization occurs in the Považský Inovec Mts. in the ore field from Kálnica to Selec. It is located in rhyolite tuffs and in conglomerates and sandstones with volcanoclastic material. Uranium mineralization is absent in the peripheral evolution of the formation, where the products of volcanism are only rudimentary (Štimmel et al. 1984). Ore lenses are mostly from 100 to 150 m long and from 2 to 15 m thick. Uraninite accompanied by pyrite and locally by molybdenite is the main ore mineral in both horizons. The uranium and molybdenum ore is significantly enriched (U>0.1 wt. % and Mo>0.1 wt.%) in the zones of faulting, cuting ore-bearing horizons. This ore is accompanied by younger sulphides of copper. The ores with high uranium content display ages of 100±20 Ma, whereas the lower grade Permian ores show an age of 270± 30 Ma (Štimmel et al. 1984).

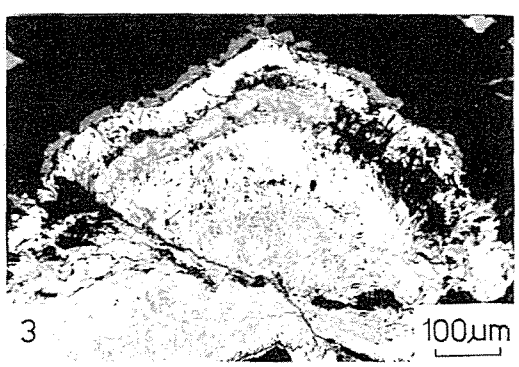

Fig. 3. Colloform uraninite (white) rimmed by molybdenite (grey). SEM-BEI

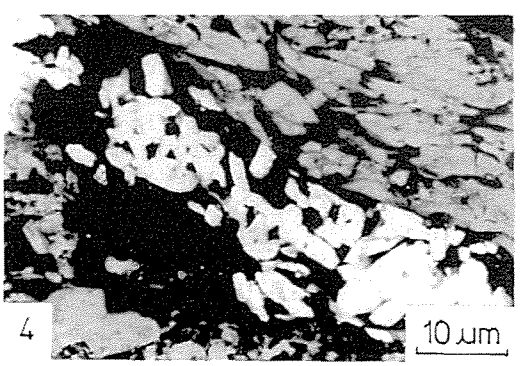

Fig. 4. Scales of molybdenite (grey) accompanied by brannerite (white). SEM-BEI

CONCLUSIONS

The Permian acid volcanites and their tuffs with increased contents of uranium and accompanying elements are potential source-rocks for ore mineralization. The distribution of uranium in the studied non-mineralized and mineralized rocks indicate its mobilization in aquiferous horizons and accumulation by reduction and adsorbtion processes due to mixing of oxic meteoric solutions with solutions derived from reducing hot springs. Uranium was also accumulated by adsorbtion of Ti oxides and Fe hydroxides. The original stratiform concentrations were formed during the Permian. The Alpine orogeny formed structures for circulation of hydrothermal fluids from preconcentrations in low-grade ores into structurally prepared places where high-grade ores were formed during the Creataceous.

REFERENCES

Burkhard, D.J.M. & Rybach, L. & Bächtiger, K. 1985. Uranium and copper ore minerals in a Lower Permian lapilli -agglomerate tuff in Eastern Switzerland (Weisstannental, Kanton St. Gallen). Schweiz. Mineral. Petrogr. Mitt. 65: 335-352

Cadel, G. & Fuchs, Y. & Meneghel, L. 1987: Uranium mineralization associated with the evolution of a Permo-Carboniferous volcanic field-Examples from Novazza and Val Vedello (northern Italy). Uranium, 3: 407-421

Haditsch, J.G. & Mostler, H. 1982. Late Variscan and Early Alpine mineralization in the Eastern Alps. Ore genesis: the state of the art, Springer, Berlin, Heidelberg, New York, pp. 585-589

Kolektiv 1984. Czechoslovak uranium deposits. SNTL, Praha: 365 pp. (in Czech)

Mittempergher, M. 1972. The paleogeographical, lithological and structural controls of uranium occurrences in the Alps. 2nd International symposium on the mineral deposits of the Alps, Ljubljana: 63-76

Novotný, L. & Mihál', F. 1987. New lithostratigraphical units in the Krompachy Group (Eastern Slovakia). Mineralia Slov., Bratislava 19: 97-113 (in Slovak)

Pagel, M. 1990. Le Permien et la métalogénie de l'uranium. Chron. Rech. Min. 499: 57-68

Rojkovič, I. 1980. Mineralogical characterization of uranium mineralization in the Permian of the Považský Inovec Mts. Permian of the West Carpathians. GÚDŠ Bratislava, pp. 137-145

Rojkovič, I. & Mihál', F. 1991. Geological structure and uranium mineralization in Permian of the north-eastern part of the Slovenské rudohorie Mts., Mineralia Slov., Bratislava, 23: 123-132 (in Slovak)

Rojkovič, I., Novotný L., Háber, M. 1993. Stratiform and vein U, Mo and Cu mineralization in the Novoveská Huta area, CSFR. Mineral. Deposita, 28: 58-65.

Štimmel, I. a kol., 1984. Final report of geological survey in Považský Inovec Mts.Manuscript, (Geofond, Bratislava), 236 (in Slovak)

Tischler, S.E., Finlow-Bates, T. 1980. Plate tectonic processes that governed the mineralization of the Eastern Alps. Mineral. Deposita, 15: 19-34.

Current Research in Geology Applied to Ore Deposits.Fenoll Hach-Ali, Torres-Ruiz & Gervilla(eds)(1993).ISBN 84-338-1772-8

PRELIMINARY $^{87}Sr/^{86}Sr$ SYSTEMATICS IN FLUORITE ORES FROM DIFFERENT DEPOSIT TYPES IN THE VALE DO RIBEIRA DISTRICT (SOUTHERN BRAZIL)

Ronchi, L.H.(1); Touray, J-C (1), Dardenne, M.A.(2) & Pimentel, M.M. (2)

(1) Université D'Orléans, ESEM, Rue Leonard de Vinci, 45072 Orléans Cedex 2, France. URA 1366 du CNRS et Gdr. "Métallogenie et Matériaux Minéraux".

(2) Universidade de Brasília, Inst. de Geoc. 70910 Brasília, DF, Brazil.

ABSTRACT: Different types of fluorite deposits (replacement, fracture filling and disseminated) with different ages have been studied in the Vale do Ribeira District. They have a complex history including recrystallisation at the contact with granitoid intrusions and remobilization by later hydrothermal fluid circulation as well as karstification. Preliminary Sr-isotopic data reveal crustal and mantelic sources and suggest a polyphase hydrothermal history with late imprint of the $^{87}Sr/^{86}Sr$ ratio in strata-bound fluorites.

Introduction: Previous studies in the area (Ronchi et al., submitted) deal with geological and mining data, fluid inclusions studies, REE patterns and Sm-Nd isotopes in fluorite. They have shown the existence of at least three different types of fluorite deposits in the Vale do Ribeira District. Fluorine and REE of these deposits are supposed to derive mainly from crustal sources, specially in the strata-bound and fracture filling deposits. However mantle contributions due to "carbonatite-related" hydrothermal fluids, are possible. In this note additional conclusions from Sr-isotopic ratio determinations in fluorite are reported.

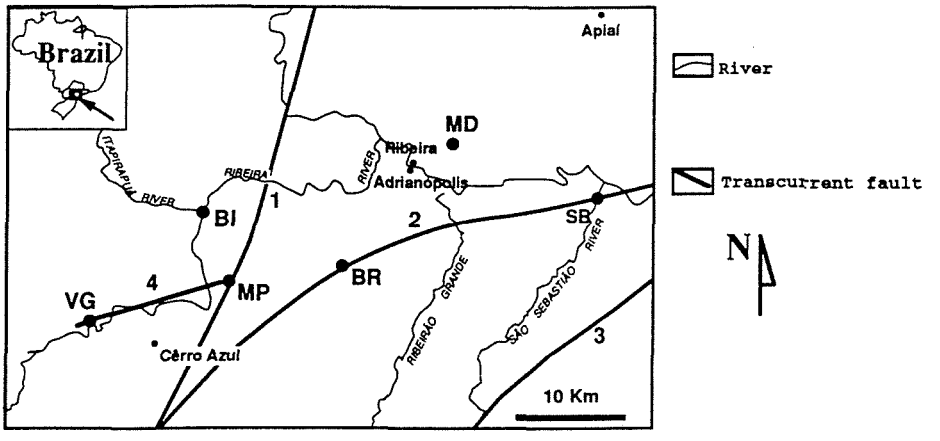

Figure 1- Location of the deposits. Faults: 1-Morro Agudo, 2-Ribeira Lineament 3-Lançinha, 4-Cêrro Azul. See text for abbreviations

Geology of fluorite deposits : Six fluorite deposits occurs in a roughly linear geographic trend in the Vale do Ribeira region, they are controlled by the great transcurrent fault known as the Ribeira Lineament and the Cêrro Azul fault, both with N60-70E directions (Fig. 1). Three of them are strata-bound, two others are associated to carbonatites and the latter is a fracture-filling deposit. These deposits have been characterized (Ronchi et al, submitted) by their morphology; contact relations with enclosing rocks; mineralogy; ore textures and structures; geochemical data (REE, Sm-Nd and fluid inclusions in fluorite).

The strata-bound Proterozoic deposits (Volta Grande, VG, 1.1MT, 35-40% CaF_2; Sete Barras, SB, 2.5MT, 50-60% CaF_2 and Mato Dentro, MD 1.5MT 40-50% CaF_2) were formed after replacement of calc-dolomitic marble (green-schist facies) and karstic collapse breccias or other internal sediments. The deposition of primary fluorite occurred after the culmination of the regional metamorphism, which included a phase of ductile deformation of marbles, and before the granitoids intrusions dated at around 500-650 Ma,(Brasiliano orogeny, Hasui et al, 1984). In the contact with the granitoids the primary microcrystalline or stratoid ore are locally associated to macrocrystalline "recrystallized" ore. Late hydrothermal fluid circulations added to the ore successive generations of quartz, calcite, adularia (VG,MD) and barite (VG,MP). Important late karstification reworking are observed.

Mato Preto, MP (2.65MT 60% CaF_2) and Barra do Itapirapuã, BI (non-economic), two Cretaceous carbonatite-associated deposits, are respectively the largest and the smallest occurrences known in the region. Both display carbonatite replacement by massive ore and disseminated fluorite. At Barra do Itapirapuã bodies of strata-bound Proterozoic fluorite occur near two carbonatitic plugs containing only disseminated uneconomic fluorite. Mato Preto is the unique economic fluorite deposit associated to carbonatites in Brazil, this mineral being always rare or absent in other Brazilian carbonatites (Mariano, 1989).

The last type, Braz, BR, 0.2MT 20% CaF_2, is a non-economic Proterozoic occurrence, characterized by minor replacement strata-bound microcrystalline ore with a commoner remobilized ore filling centimeter-scale fractures and displaying a fluorite + tourmaline + muscovite paragenesis.

Description of the analyzed fluorite samples: The $^{87}Sr/^{86}Sr$ ratios were determined in 13 fluorite ore samples chosen according to their different textural characteristics (Tab. 1). The microcrystalline and stratoid ores from the three strata-bound deposits have essentially the same mineralogy with some differences as the presence of adularia and yellowish dissolution residues (iron oxide/hydroxide?) in VG. Oxidized pyrite and black carbon-like dissolution residues are present in MD and SB. Macrocrystalline ore is made of pure fluorite.

Volta Grande : Two typical microcrystalline ores, respectively a stratified (VG87) and a homogeneous ore (VG38) were selected, both with the same mineralogical composition i.e. essentially fluorite and quartz with minor white mica, adularia and unidentified yellowish phases. In spite of their similarity they were collected in different ore bodies and Sm-Nd data suggest different sources for REE trapped by these samples.

Mato Dentro : Sample MD3 is made of two parts: A) microcrystalline ore made of impure fluorite, B) macrocrystalline pure fluorite. Samples MD17 and 41 are microcrystalline ores similar to MD3A, but MD41 contains non-replaced carbonate residues of marble.
Sete Barras : Sample SB34 also display two analyzed parts A) macrocrystalline pure fluorite and B) impure microcrystalline fluorite. SB66 is a stratified microcrystalline ore with a similar composition.
Braz : both samples (BR2 and BR5) are veinlets containing fluorite + tourmaline + muscovite with BR2 having a finer texture than BR5.
Mato Preto : MP sample is composed of fluorite with opaques and REE-rich phases. We analyzed A)the bulk ore and B)isolated colorless fluorite.

Table 1- Geochemical data and sample characteristics. *no available data; Fl=fluorite, Qz=quartz, Ad=Adularia, Ca=carbonate, Mu=muscovite, Py=Pyrite, R=dissolution residua, Tl=tourmaline, REE=rare earth rich-minerals. Errors quoted are 1σ.

Sample	$^{87}Sr/^{86}Sr$	Error	La/Sm	Ore type	Paragenesis
VG 87	0.71051	±0.00012	3.5	Stratoid	Fl + Qz >> Ad + Mu + R
VG 38	0.71091	±0.00015	4.9	Microcrystalline	Fl + Qz >> Ad + Mu + R
MD 3B	0.71516	±0.00010	2.4	Macrocrystalline	Pure Fl
MD 41	0.71534	±0.00013	5.5	Microcrystalline	Fl+ Qz >> Ca + Mu + Py + R
MD 17	0.71558	±0.00007	4.9	Microcrystalline	Fl + Qz >> Mu + Py + R
MD 3A	0.71560	±0.00015	2.8	Microcrystalline	Fl + Qz >> Mu + Py + R
SB 34B	0.72463	±0.00009	2.6	Microcrystalline	Fl + Qz >> Mu + Py + R
SB 34A	0.72645	±0.00027	3.4	Macrocrystalline	Pure Fl
SB 66	0.72803	±0.00010	2.9	Stratoid	Fl + Qz >> Mu + Py + R
BR 2	0.72728	±0.00008	*	Fracture filling	Fl + Tl + Mu
BR 5	0.77357	±0.00007	3.0	Fracture filling	Fl + Tl + Mu
MP A	0.70544	±0.00018	7.1	Colorless	Fl + REE + R
MP B	0.78394	±0.00007	4.4	Colorless	Pure Fl

Strontium-isotopic composition of the fluorite ores: Fluorite crystals were dissolved in HF and HCl and Sr was separated from the solution using conventional ion-exchange techniques at the Institute of Geosciences, University of Brasília. Isotopic analyses were carried out using a Varian-Mat TH-5 mass spectrometer at the University of São Paulo. When applied to minerals with very low Rb/Sr ratios, such as fluorite, Sr-isotopic studies may be used to characterize the sources of elements. In this respect, Kesler et al (1981) demonstrated a mixed source (limestone and volcanics) for replacement fluorites of Cohahuila, Mexico. Recent investigations of Jurassic vein fluorites from Santa Catarina, Brazil (Tassinari & Flores, 1992) indicated highly radiogenic Sr in hydrothermal fluids with higher ratio (0.7292 to 0.7402) than in the host altered granite (0.7215). Coupled studies of associated barite and fluorite may reveal similar or different ratios (Demaiffe & Dejonghe, 1991) which give some hints to the genetical relations between both phases. An interpretation of the results collected in table 1 leads to the following points: 1)Bulk sample MPA has a typical mantle signature, as usual for carbonatite (Faure, 1986) while MPB (pure fluorite) reveals a considerable contamination by radiogenic Sr.

2)The Sr-isotopic ratios are characteristic of each strata-bound deposit, with values more or less contaminated by radiogenic Sr. On the opposite, very variable data were obtained at Braz and Mato Preto. 3)In the strata-bound deposits, Sr-isotopic ratios are higher than 0.70906±0.00003, the inferred isotopic composition of marine water at the Phanerozoic (Faure, 1986). 4) In the strata-bound deposits REE patterns as illustrated by the La/Sm ratios, display variations within each deposit (Fig. 2), even if they are limited between associated microcrystalline and macrocrystalline fluorites from the same sample. 5)Previous studies (Ronchi et al., submitted) suggest, for strata-bound fluorites, significant exchanges of REE with Nd losses related to late hydrothermal circulations. A definite interpretation of Sr-isotopic results, would require additional results for host rocks at a regional scale. Presently our preferred hypothesis to explain the constant $^{87}Sr/^{86}Sr$ ratios in each strata-bound deposit, whatever the ore texture, is a late imprint of this signature, possibly in relation with post-granitoid hydrothermal circulations.

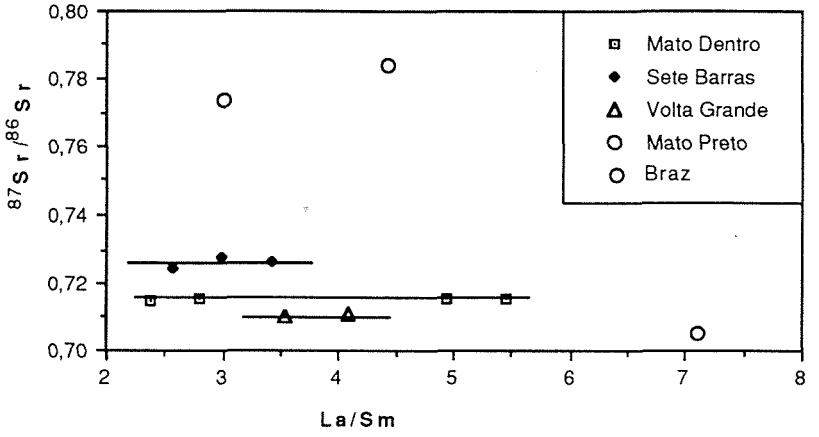

Figure 2 - $^{87}Sr/^{86}Sr$ versus La/Sm plot.

Acknowledgements: The authors thanks Dr. Wilson Teixeira (University of São Paulo, Brazil) for isotopic analysis. We also thanks Maria da Graça Viana for technical assistance.

REFERENCES

Demaiffe,D. & Dejonghe,L.1991. Geochimie isotopique du Sr des barites, anhydrites, calcites et fluorites de Belgique.An.Soc.Géo.Belg.113(2):231-240.

Faure,G. 1986. Principles of isotope geology. John Wiley & Sons, New York.

Kesler, S.E.; Ruiz, J. & Jones, L.M. 1983. Strontium-isotopic geochemistry of fluorite mineralization (Coahuila, Mexico) Isotope Geoscience, 1:65-75.

Hasui,Y.; Fonseca,M.J.G. & Ramalho,R. 1984. A parte central da região de dobramentos sudeste e o maciço mediano de Guaxupé. In: Schobbenhaus et al. (coord) "Geologia do Brasil" Chap.7:307-328.

Mariano,A.N. 1989. Nature of economic mineralization in carbonatites and related rocks.In: Bell; Carbonatites: genesis and evolution; pp. 149-176.

Tassinari,C.C.G. & Flores,J.A.A. 1992. Aplicação dos isótopos de Sr e Nd na mineralização de fluorita do Poço 5, Segunda Linha Torrens, Sudeste de Santa Catarina. In: 37° Cong. Bras. Geol.SBG São Paulo. Bol.Res.Exp. 1:259-260.

Current Research in Geology Applied to Ore Deposits. Fenoll Hach-Alí, Torres-Ruiz & Gervilla (eds) (1993). ISBN 84-338-1772-8

EVIDENCE FOR REDUCED HIGH-SALINITY ORE FLUIDS IN THE ARCHAEAN PORPHYRY-STYLE Cu-Au-Mo DEPOSIT AT BODDINGTON, WESTERN AUSTRALIA

Roth, E.(1) & Anderson, G.(2)

(1) Dept. of Geology, Key Centre for Strategic Mineral Deposits, University of Western Australia, Nedlands, W.A. 6009, Australia

(2) Boddington Gold Mine, Boddington, W.A. 6390, Australia

ABSTRACT: Primary Cu-Au-Mo mineralization at the Boddington Gold Mine is hosted in hydrothermally-altered Archaean intermediate intrusions and volcanic rocks with calcalkaline affinity. The intrusions form composite stocks, consisting of distinct generations of equigranular and porphyritic diorite and quartz diorite, and a strong spatial association exists between the distribution of mineralized veins, potassic alteration assemblages (hydrothermal biotite + quartz), and dioritic intrusions. Microthermometric data indicate that the ore fluids are best approximated in composition by the H_2O-$CaCl_2$-NaCl system, with maximum salinities estimated at 21-25wt% $CaCl_2$ and 10-15wt% NaCl. The Boddington deposit is an Archaean example of a gold-rich porphyry-ore system which formed under lower fO_2 and higher fS_2 conditions than in Phanerozoic analogues.

INTRODUCTION

The Boddington Gold Mine is situated approximately 120km SE of Perth, Western Australia, within the Saddleback greenstone belt, a NW-trending belt of Archaean metavolcanic and metasedimentary rocks within the Western Gneiss Terrain of the Yilgarn Block. The major ore resource within this deposit is laterite-hosted (reserves were 60Mt @ 1.6g Au/tonne at the commencement of mining in August, 1987). Diamond drilling has identified discrete bodies of economic and subeconomic porphyry-style Cu-Au-Mo mineralization within the late-Archaean (*ca* 2700Ma), hydrothermally-altered intermediate intrusions and volcanic/volcaniclastic rocks underlying the laterite orebody. This mineralization style contrasts significantly to the lode-gold deposits elsewhere in the Yilgarn Block.

HOST ROCKS TO MINERALIZATION

Primary mineralization at the Boddington Gold Mine is hosted within the andesitic volcanic/volcaniclastic rocks and cogenetic dioritic intrusions of the Wells Formation in the northern Saddleback greenstone belt (Fig. 1). The mineralized intrusions form complex composite stocks consisting of distinct generations of equigranular and porphyritic diorite and quartz diorite. The main central dioritic stock occupies an area of some 0.2km^2 and consists dominantly of an early stage, medium grained (2-3mm), equigranular diorite with minor porphyritic diorite. Later-stage, strongly-porphyritic quartz diorite occurs in metre-scale dykes, and consists of andesine plagioclase phenocrysts (up to 5mm) hosted within a fine grained (0.1mm) plagioclase-rich groundmass. Porphyritic diorite and quartz diorite are the dominant intermediate intrusions within peripheral bedrock prospects. Porphyritic and aphanitic andesite, dacite, and andesitic to dacitic volcaniclastic rocks constitute the host rocks. Whole-rock geochemical data indicate that unaltered regional equivalents of the intermediate igneous rocks within the

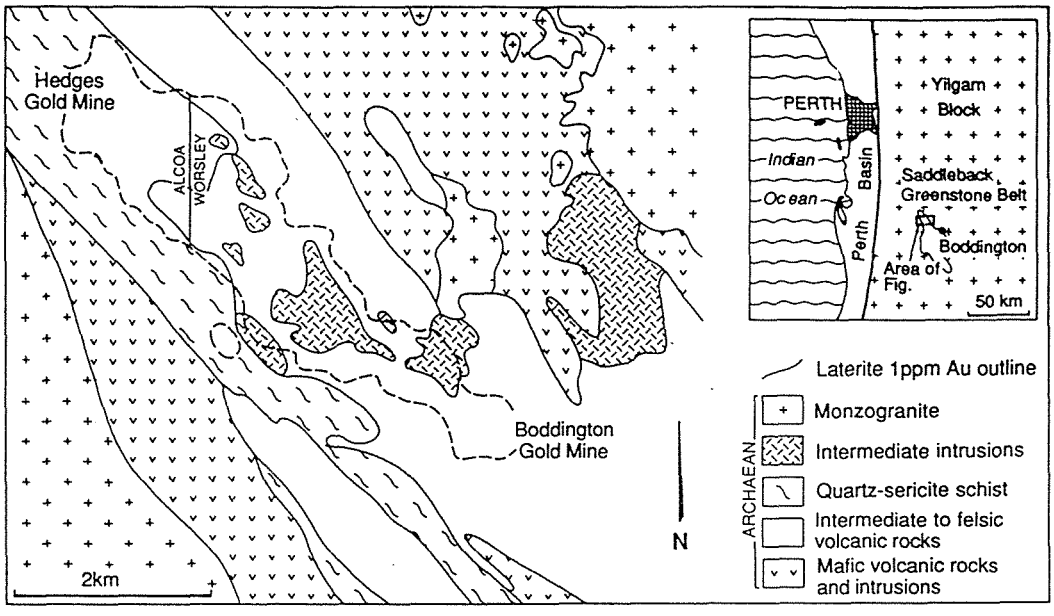

Figure 1. Geological setting of the Boddington Gold Mine.

minesite are comparable in composition to andesites and diorites in modern calcalkaline rock suites (Roth & Anderson, submitted).

HYDROTHERMAL ALTERATION

Pervasive potassic alteration assemblages, defined by hydrothermal biotite and quartz, are spatially and temporally related to dioritic intrusions. Hydrothermal biotite occurs in distinct groundmass-hosted aggregates containing fine grained (0.1mm), light brown to khaki green biotite flakes. Hydrothermal quartz is dominantly vein- and veinlet-hosted. Quartz-sericite±pyrite occur in late stage zones of moderate to high strain deformation. Detailed descriptions of all alteration assemblages are presented in Roth & Anderson (submitted).

MINERALIZATION

The important gold±copper-bearing vein assemblages include quartz-sulphide, quartz-epidote-sulphide, and actinolite-sulphide veins. Chalcopyrite, pyrrhotite, and pyrite are the dominant sulphide phases. Accessory opaque phases include cubanite, molybdenite, scheelite, sphalerite, galena, arsenopyrite, bismuthinite, native Au, native Bi, and Bi- and Ag-tellurides.

Quartz-sulphide veins adjacent to the central dioritic stock locally contain the highest abundances of chalcopyrite and cubanite within the deposit. Massive chalcopyrite aggregates within these veins commonly contain cubanite exsolution lamellae, and the associated whole-rock Cu concentrations and Cu:Au ratios may exceed 1wt% and 5000:1, respectively. Quartz-epidote-sulphide veins post-date the formation of quartz±sulphide veins, and are associated with moderate whole-rock Au concentrations (mostly 1-2ppm) and a wide range in Cu:Au ratios (300:1 to 7300:1). Actinolite-sulphide veins post-date both quartz±sulphide and quartz-epidote-sulphide veins. Actinolite veins with biotite-epidote selvedges consistently contain high Au-Cu concentrations (whole-rock values 5-10ppm, up to 60ppm,

Au; 0.1-0.2wt% Cu), and are associated with relatively low Cu:Au ratios (<450:1). In contrast, actinolite veins with quartz-albite selvedges are poorly-mineralized and characterized by high whole-rock Cu:Au ratios (up to 12800:1).

Gold mineralization in a peripheral bedrock prospect (Pit G) is hosted in subvertical and foliation-subparallel quartz veins which are locally laminated and contain the highest abundances of native Au within the deposit. Galena and sphalerite are common accessory phases. Whole-rock Cu:Au ratios are 20:1 for these quartz veins.

FLUID INCLUSION DATA

Moderate- and high-salinity aqueous inclusions are the dominant primary and pseudosecondary fluid inclusion types. Microthermometric data indicate that the composition of the ore fluid is best approximated by the H_2O-$CaCl_2$-NaCl system, although the actual fluid composition is complex and probably contains other divalent- and monovalent-cation chlorides (e.g., $MgCl_2$ and LiCl). Spatial and temporal relationships are evident on a deposit scale in both the total and relative salt contents of the ore fluid.

Low temperature data indicate that the maximum salinities for three-phase fluid inclusions (liquid+vapour+halite) in early-stage blue quartz±sulphide veins are 21-25wt% $CaCl_2$ and 10-15wt% NaCl, with the highest salinity calculated for an individual inclusion being 23wt% $CaCl_2$ and 14wt% NaCl (i.e., a total salt content of 37wt%). In contrast, fluid inclusions from native Au-bearing quartz veins within the Pit G prospect are dominantly two-phase (liquid+vapour), and contain the lowest $CaCl_2$ content (maximum salinities are estimated at 4-10wt% $CaCl_2$ and 2-7wt% NaCl) and the lowest total salinity of all mineralized vein assemblages within the deposit. No evidence for phase separation has been preserved in any vein type.

Homogenization temperatures for fluid inclusions in early-stage quartz-sulphide and quartz-epidote-sulphide veins dominantly range between 280°C and 340°C. In contrast, homogenization temperatures for inclusions within the Pit G quartz veins are slightly lower (dominantly range from 210°C to 300°C). Three-phase fluid inclusions in actinolite-sulphide veins are characterized by the highest homogenization temperatures (350°C to 440°C) of all inclusion types.

The Boddington ore fluids are closely allied in morphology and total salinity to early-stage ore fluids in Phanerozoic porphyry-copper systems (review by Roedder, 1984). However, the H_2O-$CaCl_2$-NaCl composition contrasts significantly with that of the H_2O-NaCl-KCl ore fluids commonly documented in the Phanerozoic porphyry-ore systems.

SULPHUR ISOTOPE DATA

$\delta^{34}S$ values for sulphides from the Boddington deposit are tightly constrained to the range +1.0‰ to +2.7‰ CDT (median value of +1.9‰; one standard deviation equals 0.5‰). Since hydrothermal sulphide $\delta^{34}S$ is primarily controlled by the sulphur isotope composition and SO_4^{2-}/H_2S ratio of the mineralizing fluid (Ohmoto and Rye, 1979), $\delta^{34}S_{fluid}$ values can be calculated and range between +1.0‰ and +3.0‰. The limited range in fluid $\delta^{34}S$ values indicates a uniformity in the sulphur source, whereas the absolute values indicate sulphur derivation from a either a magmatic source or by dissolution of primary magmatic sulphides. The spatial and temporal relationship of mineralized vein assemblages to dioritic stocks in the Boddington deposit indicates a probable magmatic origin for the sulphides.

IMPLICATIONS OF REDUCED FLUIDS IN ARCHAEAN PORPHYRY SYSTEMS

Equilibrium mineral assemblages and sulphur isotopic data indicate that sulphides in the Boddington deposit were precipitated from hydrothermal fluids with a redox state below that of the SO_4^{2-}/H_2S boundary: i.e., the deposit formed under conditions of higher fS_2 and lower fO_2 than in Phanerozoic porphyry-ore systems (see review by Titley and Beane, 1981). Mineralogical evidence for the lower fO_2 conditions includes the absence of magnetite and/or sulphates from wallrock alteration assemblages, the abundance of pyrrhotite in vein assemblages, and the absence of haematite as a trapped mineral phase in fluid inclusions.

Integrated petrological and geochemical studies (e.g., Candela, 1989) have shown that the fS_2 and fO_2 conditions during intrusion emplacement may partially control the development of porphyry-Cu-style mineralization. The more reduced nature of the Boddington hydrothermal system, if typical of Archaean examples, could therefore explain why Archaean porphyry-ore systems are consistently of lower ore grade and tonnage than their Phanerozoic analogues.

CONCLUSIONS

The calcalkaline affinity of the host rocks to mineralization, mineralogy of wallrock alteration assemblages, fluid inclusion data, and Au-rich nature of the primary Cu-Au-Mo mineralization all indicate that the Boddington deposit has affinities with Phanerozoic porphyry-ore systems associated with dioritic intrusions. Broadly similar genetic models are envisaged, although the high salinity ore fluids at Boddington were rich in $CaCl_2$ and NaCl rather than NaCl and KCl for modern analogues, and were also relatively reduced. This mineralization style contrasts to the lode-gold deposits from which the bulk of gold production in the Yilgarn Block has been derived.

ACKNOWLEDGEMENTS

This study forms part of a Ph.D. research project as completed by Eric Roth and supervised by Professor David Groves. Worsley Alumina Pty Ltd are acknowledged for their financial support of the research project and permission to publish this abstract. Eric Roth received financial support from an Australian Postgraduate Research Award.

REFERENCES

Barley, M.E. & Groves, D.I. 1992. Supercontinent cycles and the distribution of metal deposits through time. Geol. 20: 291-294.

Candela, P.A. 1989. Felsic magmas, volatiles, and metallogenesis. In: Whitney, J.A., Naldrett A.J. (eds.) Ore Deposition Associated with Magmas. Rev. in Econ. Geol. 4: 223-233.

Ohmoto, H. & Rye, R.O. 1979. Isotopes of sulfur and carbon. In: Barnes, H.L. (ed.) Geochemistry of Hydrothermal Ore Deposits, Second Edition, p. 509-567. Wiley and Sons, New York.

Roedder, E. 1984. Fluid Inclusions. Min. Soc. Am. Reviews in Mineralogy 12, 644p.

Roth, E. & Anderson, G. submitted. Petrology and geochemistry of wallrock alteration associated with Archaean porphyry-style Cu-Au-Mo mineralization at the Boddington Gold Mine, Western Australia. Mineralium Deposita.

Titley, S.R. & Beane, R.E. 1981. Porphyry copper deposits, Part I. Econ. Geol. 75th Anniversary Volume, 214-235.

Current Research in Geology Applied to Ore Deposits.Fenoll Hach-Alí, Torres-Ruiz & Gervilla(eds)(1993).ISBN 84-338-1772-8

MINERALOGICAL AND GEOCHEMICAL PECULIARITIES OF NATIVE GOLD IN WEATHERING CRUST OF DIORITE PORPHYRY (CENTRAL KAZAKHSTAN)

Sherbov, B.L.; Strakhovenko, V.D.; Malikov Yu.I. & Zhmodik, S.M.
Inst. of Geology SB AS, Novosibirsk, Russia

Abstract: The distribution,the composition and the morphology of native Au and associated elements in Mesozoic-Cenozoic weathering crust of the diorite porphyry of Pervomaisky district (Central Kazakhstan) were investigated by means of atomic absorption, neutron-activated beta-autoragiograhy, microprobe analysis and scanning electron microscopy. Zones of the secondary Au enrichment (up to 6 g/t Au) proceeded due to a weathering. Three types of Au: relic, transformed and newly formed can be distinguished in weathering crust according to several features: a morphology of deposits, gold minerals, composition and trace elements. Relation between Au types distinguished in weathering profile varies significantly with two latter predominating. Based on a calculation of the Au-balance in granulometric fractions, it was found that significant amount of Au in weathering products exist in light-moving forms. There are no mineral forms of Au in fractions 1 mkm.

Weathering crust of area type with a thickness up to 40m (80m in liner zones) is typical of Central Kazakhstan. Weathering crusts were formed in a wide range of age: from late Triassic to Paleogene-Oligocene. According to chemical composition and physical properties of rocks, three zones can be distinguished in weathering profiles: initial rocks, disintegration zone and clay structure eluvial. Extent, thickness and composition of weathering crusts are determinate by the type of initial rocks and their structure and tectonic positions. Exogenic minerals are present by kaolinite with middle degree of order, mica politype 1M, goethite, hydrogoethite, hematite, hydromica and montmorillonite. Volume weight of rocks in a profile ranges from 3.1 g/cm^3 (diorite porphyry) to 1.65 g/cm^3 in upper layers of clay eluvial. As this process takes place, rocks retain structural features of initial rocks.

The initial rocks of Au-bearing weathering crust are present by propylitizated a diorite porphyry with contents from 3.2 to 61 mg/t. Using autoradiogrraphy we found that characteristic feature of Au-distribution is its spatial correlation with sulfides and firstly with pyrite. Gold can: a) be situated in microcracks of pyrite; b) form the intergrowths; c) enrich by disperse deposits some parts of pyrite or; d) surround cataclastic crystals in as isometric formation. Variations in the composition of native Au is mainly determined by the relationship between Au and Ag. The composition of native gold changes within (82.6-91.6)% for Au and (8.3-17.2)% for Ag in 95% of measurements (n=16). The frequency of Hg in gold is 50% at the contents close to the boundary limit of microprobe analysis sensibility. In none of gold pieces from initial rocks Bi was found (Fig 1,2).

Conversions from analytical data to absolute masses (mg/cm^3) and calculation element's concentration coefficients indicate dynamics of their behavior during the weathering crust formation. According to degree of element's mobility an eluvial pofile can be split into three groups: accumulated, stable and mobile. The first group includes Cu,Ti,Cs; the secondary group: Al, Si, Li, Rb, Pb, V, Mo, Be, Ba, Au and the third group: Na, Mg, Ca, Sr, Co, Ni, Zn, Ag. Referring Au to the group of stable elements testifies only that the alteration of its concentrations in zones of weathering crust is small relatively initially rocks.

Nonuniform Au-distribution in a profile provides enough reason for its significant geochemical activity which is manifested in the redistribution and the formation of high concentrations in some layers of weathering crust (Fig. 3). Generally these layers are enriched by iron hydroxide and oxide. The distribution of silver unlike Au tends to have removal in to upper parts of profile. The

correlation analysis confirms the each of significant relationship between Au and main (as well as secondary) elements exclusive of Mo and V.

The obtained results allow us to draw a conclusion about complicated behavior and variety of shapes of Au existence in a weathering crust. Different events (mechanisms) can be recognized in native gold formation and its concentration in a weathering crust. 1. The native Au of initial rocks can be inherited without its essential change. 2. The idiomorfic octahedral crystals and their twins can be produced in fluids of hypergenesis zones. Idiomorphic crystals need for their growth enough free space. This is appropriate to upper layers of the weathering crust. 3. Co-precipitation of Au with iron hydroxide(oxide) results in formation of thin loop-like undergrowths. The existence of layers with high Au-contents in a weathering profile indicates on the possibility of this process. Gold in these layers is concentrated in the colloform worn the new formations (50 m) of goethite-hematite composition. The formation of such specimens can occur at places, where physical-chemical conditions change abruptly and precipitation Au and Fe goes on simultaneously. 4. The change of native gold of initial rocks is accounted for by leaching silver and other impurities from Au composition. Honeycombs, loop-like gold's structures indicates on such possibility. A similar structure of Au was obtained in experiments of the pyroleaching drawing Au out of the ore.An pieces with zone structure (initially uniform) has emerged from the alloying of gold bearing ore with pyrosulfate Na and translating all minerals (but Au) into hydrophilic water soluble. The composition of central parts in these Au pieces corresponds to initial ore, whereas the silver is removed from the boundary parts where a formation of porous, loop-like, honeycombs structures occurs. The mechanism of removing silver from Au is unclear. Evidently, in this case a diffusive redistribution of silver in solid phase should be suggested. The occurrence of similar structures is possible either if silver exist in Au as an own phase, or as a result of removing silver after its diffusive redistrubition in Au under changes of physical-chemical conditions in hypergenis's process. 5. Sorbtion forms of Au occur in clay minerals and in iron hydroxides. The share of such Au increases abruptly in weathering layers with small contents of gold and decreases in ore's layers where the native Au exist. The existence of Au in the sorbtion form was shown in experimental and natural systems. 6. Of special interest is mobile, light extracting by water fluids gold. When acted upon by NH_4OH water solution (pH=7-8) and chlorous acid (pH=4) to the material of the weathering crust the quantity of such gold can be 50% or more in the weathering crust under study. The nature of light-moving Au needs further investigations. Gold located in unstable minerals, or in the submicron size can easily go over into light-moving form(fig.4).

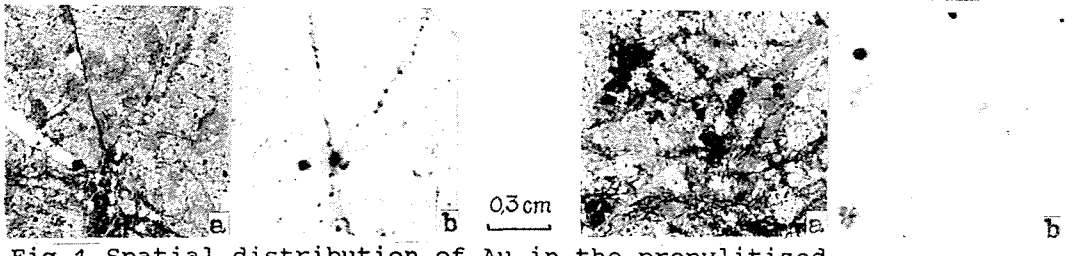

Fig.1. Spatial distribution of Au in the propylitized diorite porphyry. Gold concentrates in pyrite a) sample b) autoradiograhy records. Au distribution (black dots) and sulfur (in pyrite)-grey dotts.

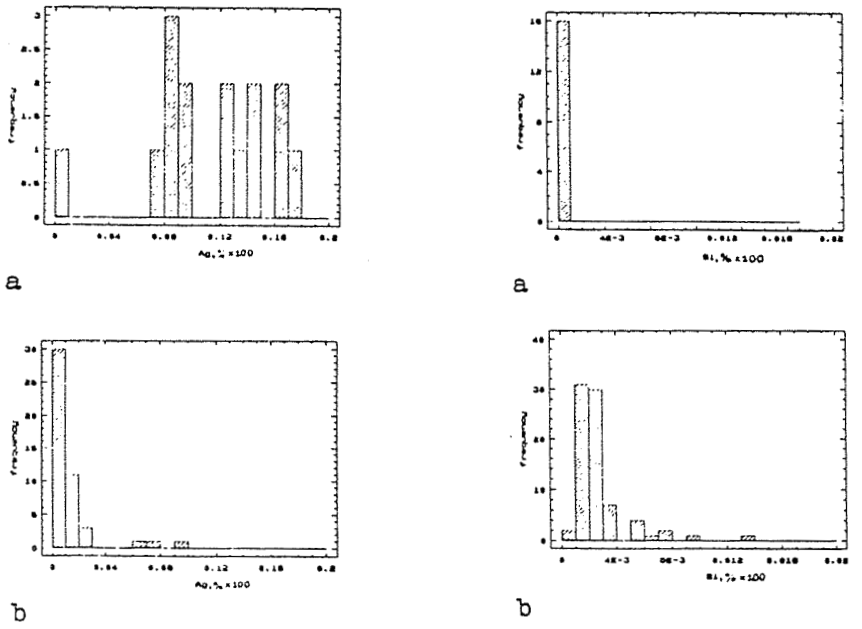

Fig.2 Histograms frequency and concentrations Ag (left) and Bi in native gold from rocks of Pervomaisky district. a) Au from the initially rock; b) Au from the weathering crust.

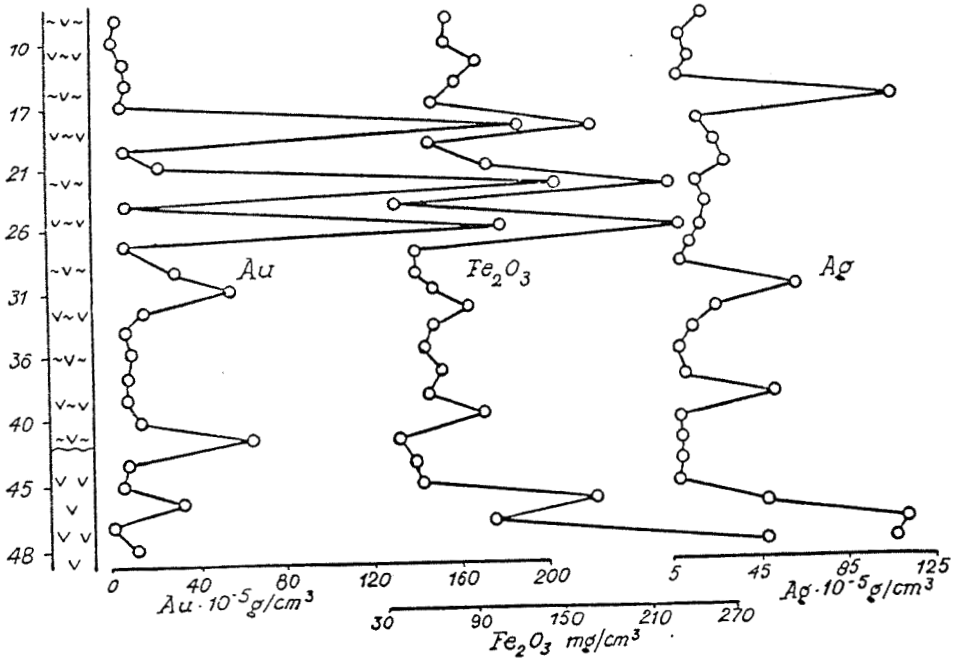

Fig.3 Distribution of Au, Ag, Fe in the weathering profile.

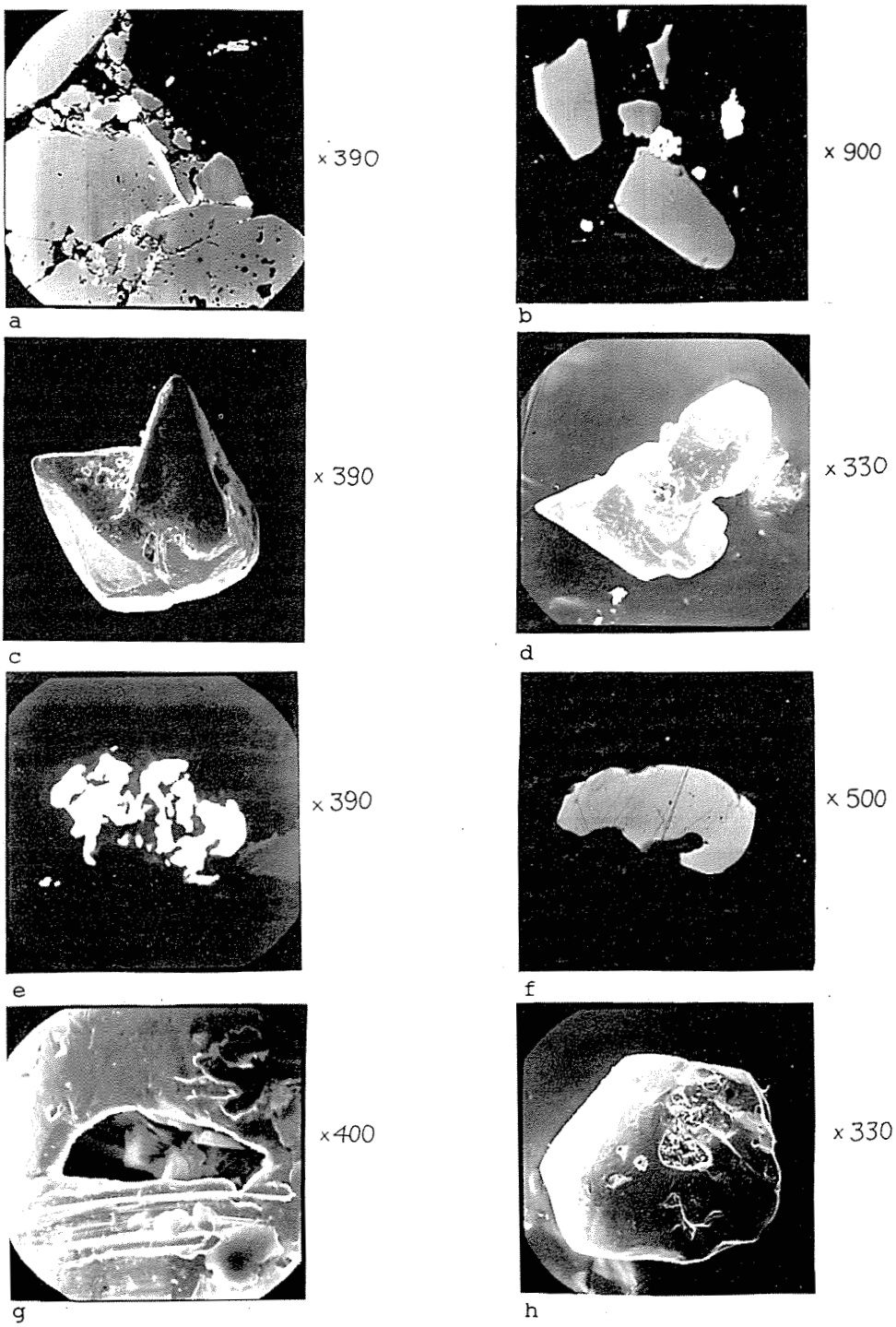

Fig.4. Morphology of native gold in initially rocks (a,b) and in weathering crust: crystals (c,d), spongy, porous Au(e,f,g,h)Scanning electron microscopy "Jeol".

Current Research in Geology Applied to Ore Deposits.Fenoll Hach-Ali, Torres-Ruiz & Gervilla(eds)(1993).ISBN 84-338-1772-8

APPARENT STABLE ISOTOPE HETEROGENEITIES IN CARBONATES DUE TO THE EFFECT OF ORGANIC MATTER AND SULPHIDES: CASE STUDY ON THE SAN VICENTE MVT ZINC-LEAD DEPOSIT, PERU

Spangenberg, J. (1); Sharp, Z.D. (2) & Fontboté, L. (1)

(1) Dept. de Minéralogie, Université de Genève, 13, rue des Maraîches, CH-1211, Genéve 4, Switzerland

(2) Inst. de Minéralogie, Université de Lausanne, CH-1015 Lausanne, Switzerland

ABSTRACT: The presence of organic matter and sulfides can be responsible for apparent stable isotopic heterogeneities in gangue minerals from carbonate-hosted base metal deposits. A combined sodium hypochlorite and silver phosphate pretreatment (Charef and Sheppard, 1984) is in most cases necessary for the precise isotopic analysis of such carbonate samples. This pretreatment allows the recognition of otherwise unnoticed slightly marked variations of the $\delta^{13}C$ and $\delta^{18}O$ values, that can be relevant for monitoring ore-bearing fluid flow.

1 INTRODUCTION

Changes in stable isotope composition of host and gangue carbonates of MVT deposits are mainly explained as an effect of changes in fluid composition, water/rock ratios, temperature, and a combination of them as the result of basinal brine migration.

In the course of a geochemical investigation of the gangue carbonates of the San Vicente MVT Zn-Pb deposit, Central Peru, we have observed within single hand specimens extreme isotopic variations, as large as 6‰ $\delta^{13}C$ and 4‰ $\delta^{18}O$, i.e., of the same order as those observed for the entire deposit. Ghazban et al., (1990) made a similar observation at the Nanisivik MVT Zn-Pb deposit of Canada, where large carbon and oxygen isotope variations were measured within a single carbonate generation at a millimeter scale. Is difficult to imagine that changes in the physicochemical conditions could be the primary factor accounting for such extreme isotopic variations.

The present work shows that: 1) some of the variations of the measured $\delta^{13}C$ and $\delta^{18}O$ are *apparent*, and due to interferences caused by the presence of sulfides and organic matter in the analyzed carbonates; 2) a combined sodium hypochlorite (NaOCl) and silver phosphate (Ag_3PO_4) pretreatment (Charef and Sheppard, 1984) of the carbonate samples virtually overcomes this analytical problem; 3) the isotopic variations at the centimeter to sub-millimeter scale, evaluated with a combination of conventional and *in situ* laser methods, are very small (± 0.1 to 0.4‰ $\delta^{13}C$ and 0.2 to 0.7‰ $\delta^{18}O$); 4) the pretreatment for organic matter and sulfides allows us the recognition of potential existing slight isotopic variations in carbonate gangue minerals, which otherwise might be overlooked.

2 SAMPLE MATERIAL AND ANALYTICAL PROCEDURES

An ore sample of the San Vicente mine showing a characteristic rhythmic banding, known as zebra rock or diagenetic crystallization rhythmites (Fontboté and Gorzawski, 1990) was submitted to detailed stable isotopic analyses (Fig. 1).The geology and genetic aspects of the San Vicente ore deposit are discussed in Fontboté and Gorzawski (1990) and Moritz et al. (1993).The main ore minerals, sphalerite and galena, are interbanded with white sparry dolomite and dark replacement dolomite.

Three distinct dolomite generations occur in the host rocks:

- early-stage dark grey replacement dolomite (generation I), is a fine- to medium- grained dolomite, with abundant inclusions of organic matter and occasionally sulfides;
- white sparry dolomite (generation II) intimately associated with sulfides;
- late-stage void-filling milky white dolomite (generation III).

All the stable isotope analyses were performed at the University of Lausanne. Four different analytical procedures have been compared: 1) the different carbonate generations were selectively sampled using a micro drilling dental device and conventionally dissolved in phosphoric acid following standard CO_2-extraction techniques; 2) conventional CO_2-extraction combined with the preoxidation of organic matter by NaOCl-solution and trapping of the acid evolved gas in a vessel containing Ag_3PO_4 as proposed by Charef and Sheppard (1984); 3) *in situ* laser microprobe CO_2-extraction without treatment, following the procedure of Sharp (1992) were use to study the isotopic zonation at sub-millimeter scale across a single 1 cm thick band of white sparry dolomite (Fig. 1); and 4) *in situ* laser extraction with Ag_3PO_4 treatment.

Tests performed on a laboratory standard dolomite slow that the Ag_3PO_4- or the combined NaOCl+Ag_3PO_4 pretreatment do not significantly change the analytical precision of ±0.05‰ for $\delta^{13}C$ and ±0.1‰ for $\delta^{18}O$.

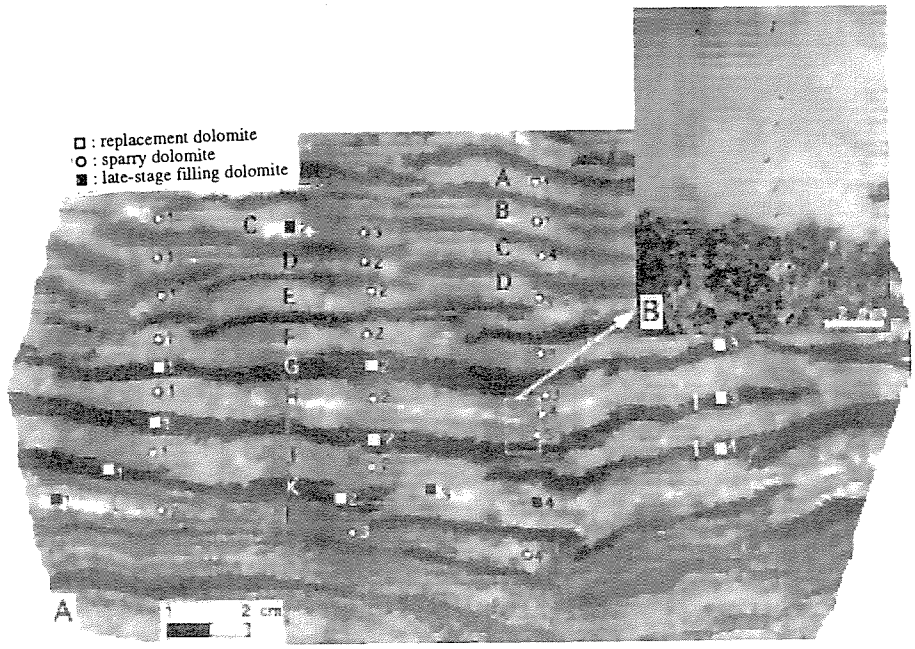

Fig. 1. A. Representative hand specimen of zebra ore showing the sampled sites. B. Detail of the *in situ* laser microsampled area. Individual bands (letters) and specific sample locations (numbers) correspond to independent analyses.

3 RESULTS AND DISCUSSION

A comparison between the results of the conventional isotopic analyses with and without pretreatment (Fig. 2 and Table 1) shows a dramatic difference. The use of the combined $NaOCl+Ag_3PO_4$ pretreatment for the replacement dolomite and of the Ag_3PO_4 trap for the sparry dolomite and late-stage filling dolomite eliminates most of the heterogeneities found in the non-treated samples. Without pretreatment, the dark replacement dolomite displays a strong variation of $\delta^{13}C$ (between 1.4 and 8.4‰) and $\delta^{18}O$ (between -8.4 and -6.3‰). The two most erratic $\delta^{13}C$ values (7.9‰ and 8.4‰) are probably mainly due to the presence of sulfur species as shown by the strong decrease of the values achieved with the Ag_3PO_4-only treatment. In these same two samples the oxygen isotope ratios are clearly lowered with the Ag_3PO_4 pre-treatment. The use of the combined pretreatment decreases slightly but consistently the $\delta^{13}C$ values and has no clear influence on the $\delta^{18}O$ values, suggesting that the main disturbing effects for the carbon isotopic ratios are due to the presence of organic matter and sulfur species whereas the oxygen isotope ratios are disturbed mainly by the presence of sulfides.

The sparry dolomite is virtually free of organic matter but bears variable amounts of sulfides. Accordingly, important differences are already achieved with the Ag_3PO_4-only treatment, with the help of which, for instance, instead of the erratically heavy $\delta^{13}C$ value of 18.7‰ a ratio of 0.7‰ is obtained. The results show that the treatment with NaOCl is not necessary for this dolomite generation.

The use of the above described pretreatment produces less important changes on the isotopic values of the very clean void-filling dolomite, but eliminates the still significant dispersion (see Fig. 1 and 2).

Variations in the $\delta^{13}C$ and $\delta^{18}O$ values at a sub-millimeter scale were evaluated with the *in situ* laser extraction technique. The range in the $\delta^{18}O$ values for the dark replacement dolomite and light grey sparry dolomite are small (-7.9 to -7.2‰). As expected, the $\delta^{18}O$ values for the late-stage dolomite are 3‰ lighter than the earlier dolomite generations. The $\delta^{13}C$ values for the sparry dolomite are in good agreement with the conventional pretreated analyses, while the $\delta^{13}C$ values for the replacement dolomite are closer to the unpretreated values. The late-stage filling dolomite is depleted in ^{13}C relative to the conventional analyses.

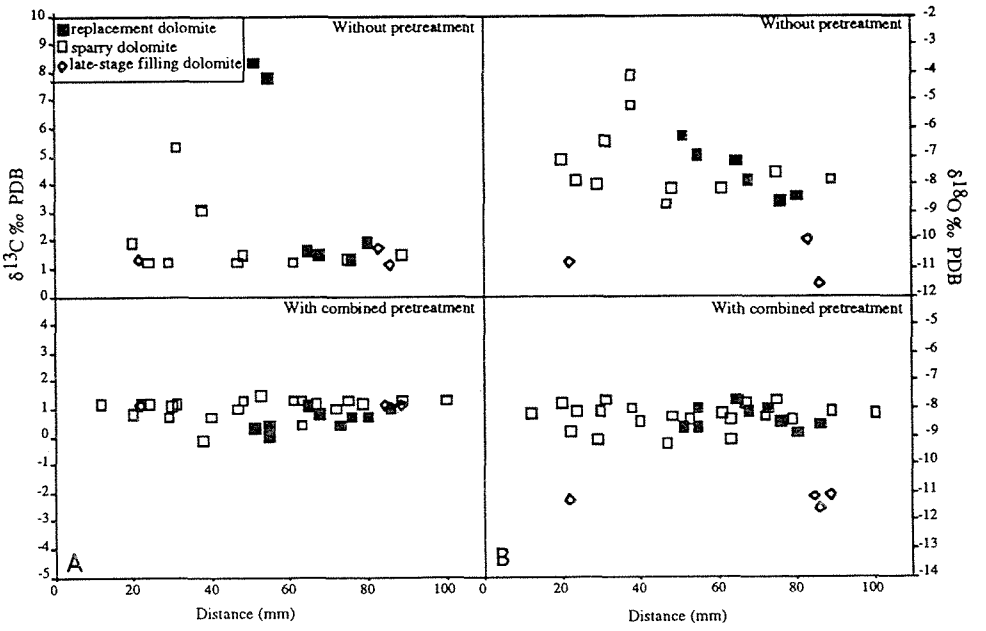

Fig. 2. Variations of $\delta^{13}C$ (A) and $\delta^{18}O$ (B) values in replacement dolomite, sparry dolomite and late-stage filling dolomite of a zebra ore hand specimen, using conventional acid extraction with and without pretreatment. Distances are referred to the lower edge.

Table 1: Summary of the average $\delta^{13}C$ and $\delta^{18}O$ values and 1σ of the gangue dolomites analysed by different procedures.

Dolomite generation	Analytical procedure (n)	$\delta^{13}C$ (‰)	$\delta^{18}O$ (‰)
Dark replacement dolomite	Conventional (6)	3.8 (3.4)	-7.5 (0.8)
	$NaOCl+Ag_3PO_4$ (9)	0.6 (0.4)	-8.4 (0.4)
	Ag_3PO_4 (3)	1.2 (0.3)	-8.5 (0.2)
	In situ (3)	1.4 (0.1)	-7.4 (0.1)
Light grey sparry dolomite	Conventional (11)	2.0 (1.3)	-7.2 (1.4)
	$NaOCl+Ag_3PO_4$ (9)	0.8 (0.2)	-8.3 (0.5)
	Ag_3PO_4 (22)	1.1 (0.3)	-8.3 (0.4)
	In situ (7)	1.0 (0.3)	-7.5 (0.6)
Late-stage filling dolomite	Conventional (3)	1.4 (0.3)	-10.8 (0.7)
	$NaOCl+Ag_3PO_4$	-	-
	Ag_3PO_4 (4)	1.1 (0.1)	-11.3 (0.2)
	In situ (3)	0.5 (0.2)	-10.7 (0.4)

The silver phosphate treatment could not be successfully applied to the *in situ* analyses, therefore the results are not summarized in Table 1.

The following conclusions can be drawn regarding the *in situ* laser analyses of sulfides- and organic matter-rich carbonates (Table 1): 1) In samples rich in organic matter (e.g. dark replacement dolomite) the $\delta^{13}C$ and $\delta^{18}O$ values are equivalent to conventional analyses, but different from samples pretreated to remove the disturbing effects of sulfur species and organic contaminants; 2) in samples rich only in sulfides (e.g. light grey sparry dolomite) the $\delta^{13}C$ values are correct, but the $\delta^{18}O$ values are elevated by ~1‰ to

those obtained with pretreatment; 3) the lower $\delta^{13}C$ values for the late-stage dolomite may reflect kinetic fractionation effects common to all laser analyses (Sharp, 1992) or may be explained by a more precise micro-sampling than can be obtained with conventional drilling. Furthermore, a simple Ag_3PO_4 trap was tested. This procedure does not alleviate the problem of sulfur contamination.

4 CONCLUSIONS

1. Our results show that *apparent* isotopic variations in the MVT gangue carbonates of San Vicente deposit are mainly due to the influence of the analytical disturbing presence of sulfides in the carbonate sample, and that the associated organic matter plays a minor role.
2. The combined sodium hypochlorite and silver phosphate pretreatment, proposed by Charef and Sheppard (1984) is necessary for the accurate isotopic analysis of organic matter and sulfides bearing carbonates, most gangue carbonates from sediment-hosted base metal deposits.
3. For the isotopic analyses of virtually organic matter free carbonates, i.e. white sparry and open space filling dolomite from MVT deposits, the treatment with silver phosphate is sufficient.
4. Using this analytical methodology the total variation of the $\delta^{13}C$ and $\delta^{18}O$ values of a defined carbonate generation in a hand specimen can be lowered to the global analytical and sampling error, i.e., not larger than ±0.1 to 0.4‰. Without this pretreatment an additional error in the range of +1 to +2‰, and occasionally up to +10‰ may be introduced.
5. There is an isotopic shift associated with the *in situ* laser technique. The $\delta^{13}C$ and $\delta^{18}O$ values are elevated relative to conventional *pretreated* samples by 0.5 to 1‰. The *in situ* method yields reproducible results. These data indicate that there is no appreciable isotopic variations at the sub-millimeter scale within any of the three carbonate generations.
6. The pretreatment methodology allows us to recognize subtle isotopic variations in the gangue carbonates that can be relevant for tracing basinal fluid pathways, and that would otherwise go unnoticed without pretreatment. For example in the samples studied in the present work, the variations of the stable isotope compositions within and between bands of a defined carbonate generation are very small (±0.1 to 0.4‰ $\delta^{13}C$ and 0.2 to 0.7 ‰ $\delta^{18}O$), suggesting uniform chemical and physicochemical conditions during precipitation of a given carbonate generation at least at a centimeter scale.
7. Stable isotopic results ($\delta^{13}C$ and $\delta^{18}O$) of other carbonate-hosted base metal deposits should be reviewed, taking in account the important disturbing influence of the almost ubiquitous presence of organic carbon and sulfides.

Acknowledgements: This study is supported by the Swiss National Science Foundation (Grant n° 21.30.309.90). This is a contribution to IGC Project n° 342 *Age and Isotopes of South American Ores.* Thanks are due to the staff of San Ignacio de Morococha S.A. Mining Company for their help during the field work. We also gratefully acknowledge J. Hunziker (University of Lausanne) and R. Moritz (University of Geneva) for their suggestions during this study, and M. Doppler and J. Metzger (University of Geneva) for their help in the preparation of the illustrations.

REFERENCES

Charef, A. and Sheppard, M.F. (1984) Carbon and oxygen isotope analysis of calcite or dolomite associated with organic matter. Isotope Geoscience, 2: 325-333.

Fontboté, L. and Gorzawski, H. (1990) Genesis of the Mississippi Valley-type Zn-Pb deposit of San Vicente, Central Peru: geologic and isotopic (Sr, O, C, S) evidence. Econ. Geol., 85: 1402-1437.

Ghazban, F., Schwarcz, H.P. and Ford, D.C. (1990) Carbon and sulfur isotope evidence for in situ reduction of sulfate, Nanisivik lead-zinc deposit, Northwest Territories, Baffin Island, Canada. Econ. Geol., 85: 360-375.

Moritz, R., Fontboté, L., Spangenberg, J. Fontignie, D., Sharp, Z.D., and Rosas, S. (1993) Brine evolution and formation of Mississippi Valley-type deposits in the Pucará Basin, central Peru: Sr, C, and O isotopic evidence. Geofluids. Abstract Volume (in press).

Sharp, Z.D. (1992) In situ laser microprobe techniques for stable isotope analysis. Chemical Geology (Isotope Geoscience Section), 101: 3-19.

Current Research in Geology Applied to Ore Deposits. Fenoll Hach-Alí, Torres-Ruiz & Gervilla (eds) (1993). ISBN 84-338-1772-8

CHEMICAL EVOLUTION OF THE CALABONA PORPHYRY COPPER SYSTEM (ITALY)

Stefanini, B.(1); Wiliams-Jones, A.E. (2) & Ghezzo, C. (1)
(1) Scienze della Terra. Universitá degli Studi di Siena. V. delle Cerchia 3, Siena, Italy
(2) Earth & Planetary Sciences. McGill University, 3450 University St., Montreal, QC, Canada, H3A 2A7

ABSTRACT: The calculated gains and losses of chemical species during hydrothermal alteration of the Calabona porphyry Cu deposit show that most of the major elements were essentially conserved during the early potassic and propylitic stages. By contrast, late-stage alteration produced significant chemical changes involving progressive leaching of Mg, Fe, Cu, Ca and Na with evolution from earlier sodic through phyllic to late argillic. The lack of major bulk chemical changes during the potassic stage is consistent with alteration by an orthomagmatic fluid not far from equilibrium with the rock. Fluids of external origin are considered to have been responsible for the development of the propylitic alteration; continued inflow of these fluids toward the inner parts of the pluton, along a heating path, initiated late-stage alteration. The strong leaching that accompanied this stage, is explained by combined effects of boiling and high fluid/rock ratio.

INTRODUCTION

The Calabona porphyry Cu system is located in NW Sardinia (Italy) and probably represents the best example of a porphyry-type system in the region. A previous study of the deposit (Frezzotti et al., 1992), led to a generalized descriptive model of alteration-mineralization zonation and to the recognition of high salinity-high temperature fluids of probable magmatic origin. In this paper we report on a quantitative analysis of mass transfer and progressive mineralogical alteration during the evolution of the hydrothermal system.

GEOLOGY

The deposit is spatially and genetically associated with an Oligocene calc-alkaline porphyritic stock of mainly dacitic composition. The stock was emplaced at shallow depth in mica schists and phyllites of the Paleozoic basement near the contact with overlying Mesozoic sediments that contain thick lenses of gypsum. Most of the stock has been affected by repeated episodes of hydrothermal alteration. However, some least altered rocks have been identified and their composition lies on a magmatic trend delineated by cogenetic volcanic rocks.

HYDROTHERMAL ALTERATION

On the basis of spatial and mineralogical relations, the hydrothermal alteration can be divided into early and late stages. The earlier stage consists of pervasive potassic and propylitic alteration which developed in the inner and peripheral zones of the intrusive complex, respectively. The later stage is represented by successive phases of sodic, phyllic and argillic alteration which largely overprinted the early alteration. Modal mineral abundances for the various alteration zones are presented in Figure 1.

The least altered rocks consist of quartz, plagioclase, amphibole, magnetite, biotite and minor K-feldspar; albite and chlorite are present as alteration products of K-feldspar and biotite, respectively.

Albite, chlorite, calcite and epidote are dominant in the propylitic alteration zone. Muscovite and kaolinite are included in the assemblage and increase significantly, together with calcite and pyrite, from the inner to the outer parts of the zone. Spotty propylitic assemblages, partially preserved from later alteration, has been recognized close to the potassic core.

In the deeper parts of the potassic alteration zone, the dominant assemblage consists

of quartz, plagioclase, biotite, K-feldspar, anhydrite, magnetite, and minor pyrite and chalcopyrite. At higher levels, anhydrite and K-feldspar increase in abundance while magnetite decreases sharply; here, pyrite, chalcopyrite and bornite comprise the main hypogene mineralization.

A transitional zone separates the potassic and the superimposed late stages of alteration. In this zone biotite is altered to sericite, plagioclase is altered to sericite and albite, K-feldspar is almost absent, and anhydrite is abundant. Chalcopyrite and bornite are absent, and pyrite is the only sulfide mineral.

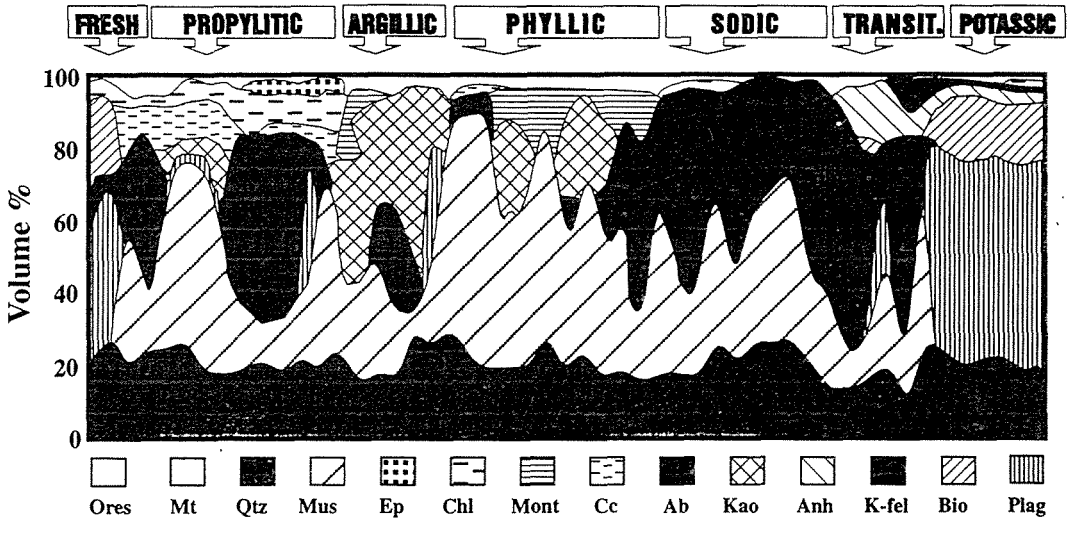

FIG. 1. An idealized section across the deposit showing the distribution of the major primary and secondary minerals. Mineral abundances were calculated using a linear least square regression method relating whole-rock chemical analyses to the products of the amount and composition of the constituent mineral phases (Böhlke, 1989).

During the late-stage sodic alteration, plagioclase and K-feldspar were almost completely replaced by equivalent amounts of albite and sericite. These minerals, together with quartz, represent up to 90% of the rock by volume, with the ratio of sericite/albite gradually increasing from the sodic to the phyllic zone. Chlorite is sporadically observed in the groundmass, but especially with the sodic alteration. Kaolinite and montmorillonite are commonly associated with sericite and become dominant (up to 50 vol%) in the argillic zone where Cu-sulfides like covellite and digenite occur together with pyrite.

MASS BALANCE CALCULATIONS

In order to reliably estimate the masses of chemical species added to or lost from the rock during the different alteration stages, it is necessary to compare equivalent volumes of rock. This was done using the isocon method of Grant (1986) and the volume factor method of Gresens (1967). The precursor rocks to the potassic and propylitic alteration zones were assumed to be represented by the composition of the least altered samples, whereas the average composition of potassically altered samples was used to represent the precursor to the sodic, phyllic and argillic alteration stages. Although Al, Ti, Zr, Th, Nb and REE displayed varying degrees of mobility in the different alteration zones, we were

able to identify at least two elements with immobile behaviour in each sample. Using these immobile pairs, volume factors (F_v) were graphically derived by the isocon technique, and were found to be within 5% of those obtained with Gresens' analytical approach. The range of volume changes is generally restricted from -5% to +10%. However, some propylitic rocks show volume increases as high as 50%.

Normalized mineral abundances were computed for a representative set of altered samples using these data and a regression method that related whole rock and mineral compositions. This permitted reactions between altered and unaltered rocks, to be written, and between early and late altered rocks that, when balanced, provide estimates of the masses of components added from, or lost to the fluid phase during alteration. Calculated gains and losses for the major elements are shown in Figure 2.

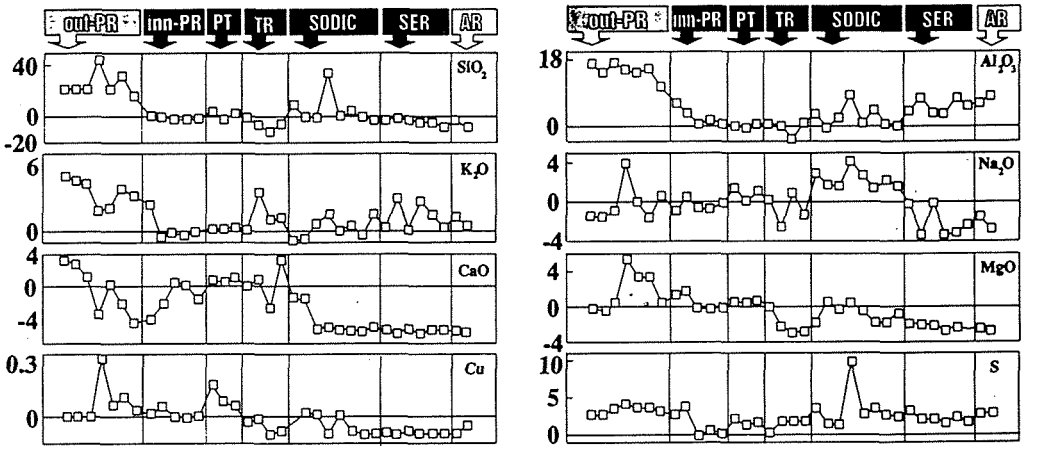

FIG. 2. Gains and losses (g/100g precursor) in the different alteration zones.

The propylitic zone shows distinct enrichment trends for Si, Al and K in passing from the inner to the outer part of the zone, due to increasing sericite and kaolinite abundances. Ca was leached in the inner propylitic zone and then redeposited, in similar amounts, in the outer propylitic zone. This trend is paralleled by that of CO_2 and reflects the outward increase in calcite abundance. There are only minor changes in the major elements in the potassic zone, with the exceptions of Cu and S which were added to the rock in significant amounts. Late-stage alteration of the potassic assemblage commenced with depletions in Mg, Fe and Cu as a result of the replacement of biotite by muscovite and the dissolution of Cu-sulfides. Sericite partially replaced plagioclase which accounts for the increase in K in the rock. Ca liberated by plagioclase was fixed as anhydrite, and an increase in Na indicates the onset of albitization. In the sodic alteration zone, silica generally remained constant, whereas Na, K and Al show significant gains. This chemical shift corresponded to extensive replacement of plagioclase by albite and muscovite, and of biotite and/or chlorite by sericite. Anhydrite was removed and Ca was strongly leached during sodic alteration, as it was during succeeding late alteration stages. Only K and Al increased during the phyllic and argillic alteration stages, whereas there was extensive leaching of all other elements.

DISCUSSION

The small changes in the proportions of major elements and the very minor mass and volume variations that characterize potassic alteration, are consistent with what might be expected during the early, rock-dominated stage of hydrothermal activity involving orthomagmatic fluid near equilibrium with the magmatic rocks. Furthermore, the predominance of biotite rather than K-feldspar as the major potassic mineral is consistent with a dacitic magma (Hollister, 1978).

Propylitic alteration in the outer parts of the intrusion is believed to have been caused by a moderate salinity fluid. This fluid may have been derivated from meteoric/formational water that acquired salinity by interacting with evaporites in the overlying sedimentary rocks (Stefanini et al., in prep.). Reaction of the propylitic fluid with the intrusion did not substantially change the chemistry of the rock, although it caused mineralogical re-equilibration of the igneous minerals to a lower temperature assemblage.

It is possible that this same fluid, on entering the intrusion further, increased in temperature and caused sodic alteration by exchanging Na^+ for K^+ and Ca^{2+}, thereby converting K-feldspar and plagioclase to albite. Heating of the hydrothermal fluid would also have tended to make it undersaturated with respect to quartz, and therefore have caused a loss of silica in the rock. The lack of evidence for this during sodic alteration, but strong silica leaching during the succeeding phyllic-argillic stage, may reflect low and high water/rock ratios, respectively. It is furthermore likely that Cu deposited during potassic alteration was leached during the sodic and phyllic stages, and transported in solution as a chloride complex.

Phyllic alteration was accompanied by boiling (Frezzotti et al., 1992), especially at higher levels in the system. This gave rise to a low pH vapour phase that probably caused the pervasive leaching documented for all major elements except K and Al (which were fixed as sericite). Boiling was also responsible for the extensive hydrofracturing and subsequent sharp decreases in pressure and temperature which lowered silica solubility in the liquid and precipitated quartz in fractures. Copper leached during sodic and phyllic alteration probably deposited as covellite and digenite.

The strong enrichment in Ca, K, Si and Al in the outermost part of the propylitic alteration zone contrasts strongly with the moderate metasomatic effects observed in the inner propylitic zone. These trends are believed to reflect an overprint of phyllic-argillic alteration which produced abundant sericite and clays from albite and plagioclase, and which may have precipitated the previously leached calcium as calcite during cooling.

REFERENCES

Böhlke, J.K. 1989. Comparison of metasomatic reactions between a common CO_2-rich vein fluid and diverse wall-rocks: intensive variables, mass transfers and Au mineralization at Alleghany, California. Econ. Geol. 84:291-327

Frezzotti, M.L., Ghezzo, C., Stefanini, B. 1992. The Calabona intrusive complex (Sardinia, Italy): evidence for a porphyry copper system. Econ. Geol. 87:425-436

Grant, J.A. 1986. The isocon diagram - a simple solution to Gresens' equation for metasomatic alteration. Econ. Geol. 81:1976-1982

Gresens, R.L. 1967. Composition-volume relationships of metasomatism. Chem. Geol. 2:47-65

Hollister, V.F. 1978. Geology of Porphyry Copper Deposits of the Western Hemisphere: New York, Soc. Min. Engi. AIME, 219 p.

Current Research in Geology Applied to Ore Deposits.Fenoll Hach-Alí, Torres-Ruiz & Gervilla(eds)(1993).ISBN 84-338-1772-8

REE FRACTIONATION AND FLUID INCLUSION STUDIES IN FLUORITES FROM THE VALLE DE TENA (SPANISH CENTRAL PYRENEES).

Subías, I. & Fernández-Nieto, C.
Dept. Cristalografía y Mineralogía, Universidad de Zaragoza, Zaragoza, Spain

Abstract: Results of the study of REE distribution and fluid inclusions indicate that all the fluorites have a common geochemical fingerprint and that leaching of the granite by the ore-forming fluids is the likely source of fluorine. On the other hand, fractionation and Tb/Ca-Tb/La confirm an hidrothermal origin for all fluorite deposits. Overall, it can be deduced a depositional sequence from the LREE-bearing fluorite to the HREE-bearing ones, forming the former by remobilization from the latter.

INTRODUCTION

The valle de Tena fluorite district is located in the north end of Huesca province, Spain, ca 80 Km North of Huesca. This zone belongs to the Axial Pyrenean Zone and its geology was essentially shaped during the Hercynian orogeny. The stratigraphic sequence is composed of pelitic, psamitic and carbonatic rocks belonging to Devonian, Carboniferous and Permian age. These rocks was folded and metamorphosed under very low grade (anchizone) conditions during Hercynian times. The late Hercynian times were marked by the emplacement of plutonic bodies producing a close halo of contact metamorphism and by great E-W overthrust.

Two main types of fluorite occurrences have been identified in these area:

type 1: E-W vein deposits hosted by devonian limestones.

type 2: a) pockets, b) nodules, c) E-W veins related to highly silicified carboniferous limestones which contain Li-donbassites.

Geochemical investigation of fluorite have been performed to determine the origin of the ore-forming fluids.

REE DISTRIBUTION PATTERNS

The chondrite normalized distribution patterns of fluorites from regional occurrences can be split into three groups (figure 1):

a) "normal" (Möller, 1991) REE spectra showing a decrease from the LREE to the HREE. These fluorite patterns represent the typical trend for the REE in hydrotermal solutions (Bilal & Langer, 1989) and are characteristic for the type 1 deposits (Subías & Fernández-Nieto, 1991). These fluorites are marked by positive Eu anomaly. These normalized curves are similar to those ones of the pyrenean granitoids (Arranz, 1991).

b) Some REE spectra of fluorites from either type 1 or type 2a show a horizontal trend to La to Lu.

c) "ligand-rich" (Möller, op. cit.) REE distribution spectra produced by an

enrichment in HREE. Type 2a, 2b and 2c fluorite ores display these patterns.

Both b) and c) patterns show a Eu and Ce negative anomalies.

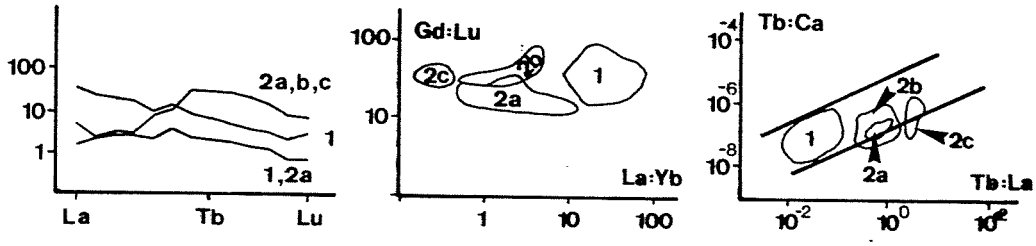

Figure 1: REE distribution patterns of fluorite. (1, 2a, 2b and 2c, see text for explanation).

On the other hand, the La/Yb vs Gd/Lu diagram allows one to observe that for a heavy lanthanoids content nearly invariable, a progressive impoverishment of the light lanthanoids exists (figure). Taking into account that complex stability increases from La to Lu (Möller & Morteani, 1983), this trend suggest that fluorites follow a depositional sequence, being the type 1 ores the first in be deposited while the type 2c deposits are the last. Moreover, the similarity of Gd/Lu ratio between all the ores described above seems to indicate that a common geochemical fingerprint exists.

The mean values of Tb/Ca and Tb/La ratios of each one of the fluorite deposits are plotted in the variation diagram of Möller et al. (1976). All these values are located within the hydrothermal field. All of the lodes display a trend parallel to the x-axis (Tb/La ratios increase while Tb/Ca ratios are quite homogeneous) what it can be interpreted as a remobilization trend.

FLUID INCLUSION STUDIES

All the fluorite samples contain two-phase fluid inclusions (liquid + vapour bubble). No evidence of CO_2 phases have been observed in the microthermometric analysis.

Fluid inclusions are abundant in all fluorite deposits. Nevertheless, there is a great number of fluid inclusions related to fractures and/or cleavage planes and, therefore these inclusions were assumed to be secundary. A smaller number of fluid inclusions occur as isolated group, sometimes confined within growth zones of fluorite crystals, and these inclusions were assumed to be prymary.

Inclusion shapes may vary from negative crystals to subspherical or irregular and their dimensions range from 5 to 30 μm, but most are in the range 10-15 μm.

During heating runs a number of inclusions were stretched. This phenomenon is revelaed by a marked increase of the bubble size upon cooling down to room temperature after homogenization. On the other hand, necking down is relatively common.

The fluid inclusions from the type 1 fluorites ores show eutectic temperatures, below -45°C, point out to the presence of several salts in solution. Total salinities of 17.5 ± 1.8 wt% NaCl eq. are deduced from last ice melting temperatures of -13.6 ± 1.9°C. They have homogenezation temperatures at about 155.1 ± 21°C (figure 2)

The fluid inclusions occur in fluorites from the types 2a, 2b and 2c mineralizations have slighty lower homogenization temperatures, between 157.3 to 133.8°C. Salinity is clearly lower and ranges between 7.3 to 7.9 wt% NaCl eq (figure 2).

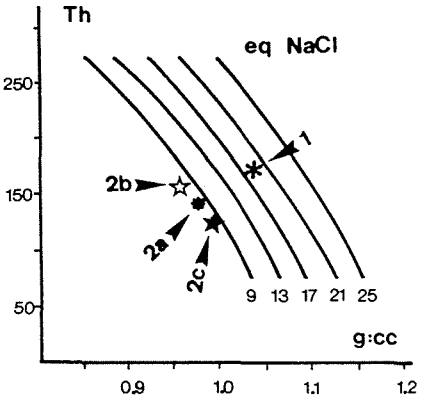

Figure 2: Data from fluid inclusion for each deposit from the Tena valley plotted in a homogenization temperature (Th) vs density diagram (see text for explanation).

The minimum depth of mineral deposition have been deduced by using the Haas's (1971) abacus, obtaining a depth range from 100 m (type 1) to 20 m for 2c fluorite deposits.

DISCUSSION

The similarity of the REE patterns between pyrenean granitic rocks and the fluorite in type 1 deposits, and the positive Eu anomaly of these fluorite ores, suggest that leaching of the granite by the fluids in the hydrothermal system is the likely source of fluorine.

The REE normalized curves of the type 2 ores indicate low Ca^{2+}/F^- ratios of the fluid because of the enrichment of the HREE. This means that the origin of the fluorite-forming fluid must be either from a F^- rich source or from mobilization of a previous fluorite deposit.

On the other hand, fractionation and Tb/Ca-Tb/La ratios confirm an hydrothermal origin for the fluorites in all sorts of the deposits from the valle de Tena and they suggest that the fluorite from the type 1 propect was deposited early and the fluorite in the type 2 deposits was deposited later from more evolved fluids.

In short, geochemical investigations of fluorite leads one to deduce that

type 1 fluorite deposits can be consider as a precursor for the type 2 ones which may be formed by mobilization of the latter ones.

REFERENCES

Arranz, E. (1991): Petrología, Estructura y Geoquímica de los granitoides del macizo de la Maladeta en su sector Tahüll-Lago Negro (provincia de Lérida). Tesis Licenciatura. Univ. Zaragoza (inédito), 173 p.

Bilal, B.A. & Langer, P. (1989): Complex formation of the lanthanides in fluorite-bearing hydrothermal solutions. Lanthanide a. Actn. Res., 3:141-150.

Möller, P. (1991): REE fractionation in hydrothermal fluorite and calcite. Pagel, M & Leroy, J.L. (eds.)Source, Transport and Deposition of metals, 91-94.

Möller, P. & Morteani, G. (1983): On the geochemical fractionation of REE during the formation of Ca-minerals and its application to problems of the genesis of ore deposits. In Augusthitis, S.S. (ed.) The significance of trace elements in solving petrogenetic problems and controversies. Theophrastus Pub., Athens, Greece, 747-791.

Möller, P.; Parekh, P.P.; Schneider, J. (1976): The application of Tb/Ca-Tb/La abundance ratios to problems of fluospar genesis. Min. Dep., 11:111-116.

Subías, I. & Fernández-Nieto, C. (1991): Geología y Geoquímica (REE y trazas) del filón de fluorita Ana Mary (Lanuza, Huesca). Bol. Soc. Esp. Min. 14:151-160.

Current Research in Geology Applied to Ore Deposits. Fenoll Hach-Alí, Torres-Ruiz & Gervilla (eds) (1993). ISBN 84-338-1772-8

ISOTOPIC CHARACTERIZATION OF THE VALLE DE TENA (SPANISH CENTRAL PYRENEES) SULPHIDE DEPOSITS: PRELIMINARY S, C , AND O RESULTS.

Subías, I.(1); Recio, C. (2) & Fernández-Nieto, C. (1)
(1) Dept. de Cristalografía y Mineralogía, Universidad de Zaragoza, Zaragoza, Spain
(2) Servicio General de Análisis de Isótopos Estables, Universidad de Salamanca, Salamanca, Spain.

Abstract: S, C and O isotopic data have been gathered from three from three ore deposits from the Valle de Tena. Sulphur isotopic results are consistent with a deep-seated source for the sulphur, and C and O isotopes measured in ore-stage calcites indicate equilibrium with meteoric waters. The existence of a meteoric-hydrothermal system leaching sulphur and metals from the igneous rocks is suggested.

INTRODUCTION

There are some ore deposits and occurrences located in the surroundings of Panticosa granite (Central Pyrenees, Spain); the more important ones are Yenefrito and Lanuza mines and the Tebarray veins. The aim of this paper is to characterize the sulfur isotopic signature of the ore-forming fluids as derived from the study of the stable isotope ratios measured in sulphides and calcites. The geological setting of these deposits is dealt with by Subías and Fernández-Nieto (this volume).

Isotopic analyses were performed at the SGAIE of University of Salamanca employing standard techniques as described by Robinson & Kusakabe (1975), McCrea (1950) and Craig (1957). Isotopic ratios were measured in two different SIRA-II mass spectometers, one of them equipped with an ISOCARB device. Average precision in our laboratory is ±0.27 ($\delta^{34}S_{CDT}$) and ±0.2($\delta^{18}O$,$\delta^{13}C$). Results are reported in the usual "delta" notation.

YENEFRITO Pb–Zn DEPOSIT

Yenefrito ore replaces an E-W diabase dyke cutting Lower Devonian marls. The bulk of the deposit consist of quartz which was latter mineralized by the sulphide association, irregularly distributed into it. The ore minerals are galena, sphalerite, pyrite, chalcopyrite, with minor pirrhotite and boulangerite. Microthermometric studies reveal a mean homogenization temperature of 167°C and salinity ranges between 5.4 to 17.6 %wt eq. NaCl.

LANUZA FLUORITE DEPOSIT

The Lanuza fluospar occurs as a vein within the Lower Devonian carbonates. The mineralization at Lanuza consists of chalcopyrite and pyrite, with later calcite and fluorite which is benefited. Both calcite and sulphides are scarce and randomly distributed near the wall rock (Subías & Fernández-Nieto, 1991). On the other hand, microthermometric studies on fluorite indicate a homogenization temperature of 140°C and salinity of 17.35 %wt eq. NaCl.

TEBARRAY F-Zn-Pb VEINS

The Tebarray veins are hosted by Upper Devonian marbles. The paragenetic succession of the ore is made up of pyrite, sphalerite-1, galena-1, sphalerite-2, galena-2, tetrahedrite and fluorite. The sulphides occur in the edge of the veins while fluorite appears in the center. From the log (Ga/Ge) ratio on sphalerites, it can be deduced that sphalerite-1 were formed at ≈ 255°C, while sphalerite-2 were deposited from a fluid at 275°C. Fluid inclusions data in fluorite indicate homogenization temperatures of 160°C and salinity value of 16 %wt eq. NaCl.

RESULTS

Sulphur isotopes

Sulphur isotope results are reported in Table 1 and Fig. 1. 44 analysis of the different paragenetic phases were obtained. In Fig. 2 the values corresponding to the different paragenetic stages in the three deposits studied have been plotted.

Samp	$\delta^{34}S_{CDT}$	Min	Samp	$\delta^{34}S_{CDT}$	Min	Samp	$\delta^{34}S_{CDT}$	Min	Samp	$\delta^{34}S_{CDT}$	Min
FY1	-4.4	gn	Y23	-2.1	py	T52	4.6	sph1	T33S	6.5	sph2
FY1	-1.3	sph	Y52	-3.0	gn	T16	5.3	sph1	T52B	6.5	sph1
YE1	-4.3	gn	T13	1.0	sph2	T67	5.5	gn1	T21	6.8	sph1
YE4	-3.9	gn	T34	1.5	sph1	T52	5.5	sph2	L10	7.0	cpy
YE4	-2.6	gn	T24	2.2	sph1	T34	5.7	sph2	T53	7.2	sph1
YE5	-4.3	gn	T11	2.5	sph1	M14	5.7	sph1	T33	7.2	sph2
Y21	-3.1	gn	T67	2.6	py	T67	5.8	gn1	T13	7.2	sph1
Y21	-2.2	py	T41	3.6	sph1	T26	5.9	sph1	T24	8.9	gn1
FY21	-0.3	py	T41	3.6	sph1	T33	6.1	gn2	L2	10.2	cpy
FY21	0.4	sph	T64	4.2	py	T16	6.1	gn1	T14B	11.4	py
Y23	-3.3	gn	T64	4.4	sph1	T34	6.3	gn2	T14	12.0	py
	$\delta^{13}C_{PDB}$			$\delta^{18}O_{PDB}$			$\delta^{18}O_{SMOW}$				
L16	1.51			-14.99			15.46	cta			
L17	0.76			-15.41			15.03	cta			
L28	1.62			-14.89			15.56	cta			

Table 1: Stable isotope ratios from the different deposits studied. (Y, FY: Yenefrito; T, M: Tebarray and L: Lanuza)

From Fig. 1 and Table 1 it follows that $\delta^{34}S_{CDT}$ values for the Yenefrito deposit are lighter, ranging from -4.4 to 0.4 per mil, than those corresponding to Tebarray that varie between 1 to 12 per mil. The two only results for chalcopyrite in the Lanuza deposit are indistinguishable from those of Tebarray. In Fig. 2 the data have been plotted separatedly for the different deposits and the different paragenetic phases. At Yenefrito, values corresponding to pyrite and sphalerite are undistinguishable, but the galenas are isotopically lighter. This is as expected considering the equilibrium fractionations between galena and the other minerals. At Tebarray two different mineralization stages have been identified by petrographic means. The pyrite and the first-stage sphalerite and galena are isotopically undistinguishable, and this prevents assuming equilibrium crystallization. Also, two very different pyrites can be identified on isotopic grounds, that are not obvious petrographically. With regard to second-stage sphalerite and galena, both the petrographic and isotopic study indicate that they resulted from the remobilization of the first stage phases. Too few data are available from the Lanuza deposit, although as a first approach, the data make it similar to Tebarray.

C and O isotopes

Three calcites from the Lanuza deposit were analyzed for C and O isotopes. $\delta^{13}C_{PDB}$ values range from 0.76 to 1.62 and $\delta^{18}O_{SMOW}$ from 15.03 to 15.56 (table 1). Although the ranges are very tight, C and O show a good correlation when plotted against each other (fig. 4). $\delta^{13}C_{PDB}$ values are consistent with derivation from regional marine carbonates, but the $\delta^{18}O_{SMOW}$ departs very markedly from normal marine values in the area (Wickham & Taylor, 1990). However, there is no other obvious derivation for the mineralized calcites, such that some sort of process must have modified the original values.

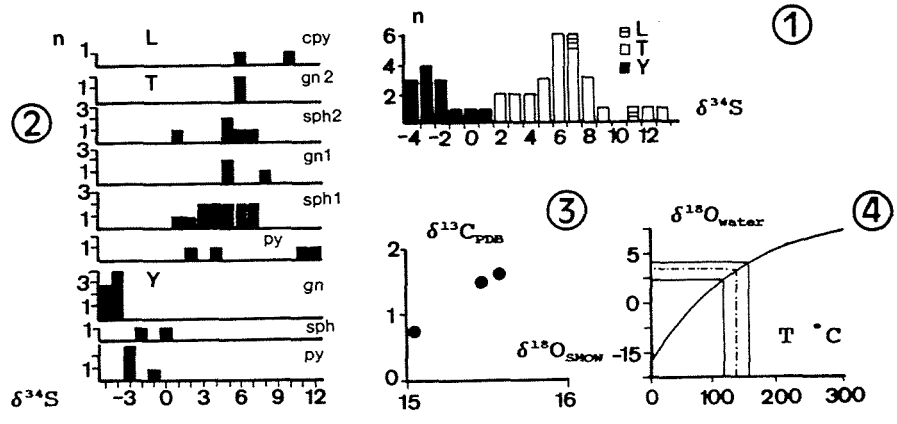

Fig. 1: Histogram of $\delta^{34}S_{CDT}$ values measured in the Valle de Tena deposists.

Fig. 2: Histogram of $\delta^{34}S_{CDT}$ values, separated by deposits and paragenetic stage (Y: Yenefrito, T: Tebarray, L: Lanuza).

Fig. 3 (left): $\delta^{18}O_{SMOW}$ vs $\delta^{13}C_{PDB}$ plot of ore-stage calcites from Lanuza.

Fig. 4 (right): Calculated $\delta^{18}O_{SMOW}$ values of waters in equilibrium with average ore-stage calcites from the Lanuza deposit. Discontinuous lines indicate ranges of fluid inclusion homogenization temperatures.

DISCUSSION

Overall, the sulphur data are indicative of a deep-seated (igneous?) derivation of the sulphur, although the lack of regional sulphur data to compare with our results prevent us from testing this possibility. However, the scarce data on sulphur isotopic ratios in granitoids and related rocks (see for example Ohmoto, 1986; Recio et al., 1991) are grossly compatible with the values determined in this study. The data reported in Recio et al. (1991) correspond to cordierite-bearing granites from the C.I.M. that are not unlike some facies of the Panticosa granite (Debon, 1975). Until further research provides additional data we will assume that the igneous rocks were the ultimate source of the sulphur, since sedimentary sulphates would have higher values and diagenetic sulphides would be lighter.

Attempts to calculate isotopic temperatures yield geologically meaningless values, and therefore it is concluded either that the pairs that on petrographic grounds seemed cogenetic were not so, or that if they were equillibrium has been modified by later processes. The grouping of the values in Fig. 1 points towards a common deep-seated origin for the sulphur, but the disequilibrium between minerals as evidenced by Fig. 2, indicates that conditions were changing during mineralization. This is consistent with the paragenetic sequence as well.

The nearest approach to a genetic model that can be attempted with the limited data set available would indicate the existence in the host-rocks of a hydrothermal convection syste. If it was induced by the nearby plutonics or is much later than them, remains to be solved. This hydrothermal system would leach sulphur and metals from the intrusives, depositing them as it cooled in the country rocks. Variations in the heat driving it, or in the availibilty and/or derivation of the water would induce differences during the time the deposit took to form, causing the differentiation of successive stages in the mineralization. Later batches partially leached the phases earlier formed, causing disequilibration, dissolution and reprecipitation alongside likely new deposition of sulphides. The origin of the water can only be speculated with the data available. Possible origins would be meteoric waters, although to relate this system with the one proposed by Wickham & Taylor (1990) poses some major problems. The movilization of metamorphic fluids

is unlike given the generally low-grade metamorphism (Subías et al., 1990) of the area. The possibility of a juvenile derivation of the water cannot be tested with the data available, although the isotopic composition of the water in equilibrium with the calcites at different temperatures, as represented in Fig. 4 could extrapolated to magmatic values at higher temperatures. However, the combined use of the C and O isotopes is more consistent with a meteoric derivation. The $\delta^{13}C_{PDB}$ values are consistent with the ore stage calcites being derived from the regional carbonates, and the interaction between light-O meteoric waters and heavy-O carbonates could give the range of values observed at the temperatures inferred from fluid inclusion studies (120-160°C).

Evidence for the activity of large convection systems of surficial origin affecting the plutonics and their host has given by Wickham & Taylor (1985, 1987, 1990) based on stable isotope systematics. Their model could explain the isotopic signature of the carbonates, but a more homogeneous, equilibrium sulphur isotope signature would be expected. Also, higher fluid inclusion homogenization temperatures would have been preserved. Until further data are available, the hypothesis of meteoric-hydrothermal system leaching sulphur and metals from the granites seems to us the most reasonable explanation for the origin of these deposits, but the timing and driving force for such system remains to be explained.

Clearly, a thorough isotopic characterization of the plutonics and the hosts of the mineralizations is required to test the above, and is currently under way.

REFERENCES

Craig, H. (1957): Isotopic standards for carbon and oxygen and correction factors for mass spectometric analysis of carbon dioxide. Geochim. Cosmochim. Acta, 12:133-149.

Debon, F. (1975): Les massifs granitoïdes á structure concentrique de Cauterets - Panticosa (Pyrénées occidentales) et leurs enclaves: une étude pétrographique et géoquimique. Thése Sc. Univ. Nancy I, 420 p.

McCrea, J.M. (1950): On the isotopic chemistry of carbonates and a palaeotemperature scale. J. Chem. Phys., 18:849-857.

Ohmoto, H. (1986): Stable isotope geochemistry of ore deposits. In: Valley, J.W.; Taylor, H.P., jr.; O'Neill, J.R. (eds.) Stable isotopes in high temperature geological processes. M.S.A. Reviews in mineralogy, 16:491-559.

Recio, C.; Fallick, A.E.; Ugidos, J.M. (1991): Sulphur isotope systematics of granitoids and associated rocks from the Avila-La Alberca Area (Western Sistema Central, Spain). Rev. Soc. Geol. Esp., 4 (3-4):371-381.

Robinson, B.W. & Kurasabe, M. (1975): Quantitative preparation of sulfur dioxide for $^{34}S/^{32}S$ analyses from sulfides by combustion with cuprous oxide. Anal. Chem. 47:1179-1181.

Subías, I.; Fernández-Nieto, C.; González López, J.M. (1990): Estudio mineralógico de la serie Devónica y Carbonífero inferior de Sallent de Gállego (Huesca). Bol. Soc. Esp. Min., 13:183-194.

Subías, I. & Fernández-Nieto (1991): Geología y geoquímica (REE y trazas) del filón de fluorita Ana Mary (Lanuza, Huesca). Bol Soc. Esp. Min., 14:151-160.

Wickham, S.M. & Taylor, H.P.jr. (1985): Stable isotopic evidence for large-scale seawater infiltration in a regional metamorphic terrane; the Trois Seigneurs, Pyrenees, France. Contr. Min. Petr., 91:122-137.

Wickham, S.M. & Taylor, H.P.jr. (1987): Stable isotope constraints on the origin and depth of penetration of hydrothermal fluids associated with Hercynian regional metamorphism and crustal anatexis in the Pyrenees. Contr. Min. Petr., 95:255-268.

Wickham, S.M. & Taylor, H.P.jr. (1990): Hydrothermal systems associated with regional metamorphism and crustal anatexis: Examples from the Pyrenees, France. In: Studies in Geophysics. The role of fluids in crustal processes. National Academic Press. Washington, 96-112 p.

Current Research in Geology Applied to Ore Deposits.Fenoll Hach-Alí, Torres-Ruiz & Gervilla(eds)(1993).ISBN 84-338-1772-8

FLUID ROCK INTERACTION IN THE CARRO DEL DIABLO W-Sn SKARN (SPANISH CENTRAL SYSTEM) AS DEDUCED BY C-O ISOTOPES

Tornos, F.
Inst. Tecnológico Geominero de España, Rios Rosas 23, 28003 Madrid, Spain

ABSTRACT: $\delta^{18}O$ and $\delta^{13}C$ depletion during metasomatic replacement of marbles by skarns in the Carro del Diablo skarn is interpretated here on the basis of unidimensional fluid flow models. Mineralogical and isotopic changes define the existence of infiltration, geochemical and reaction fronts. Isotopic variations in the marbles show that dispersion has played an important role in the genesis of skarn. The isotopic signatures of the skarn seem to be related with isotopic equilibration with the hydrothermal fluid; distillation effects look to be only important in the case of $\delta^{13}C$.

1. Introduction.-

Metasomatic replacement of marbles by skarns is usually related with an isotopic depletion in both $\delta^{18}O$ and $\delta^{13}C$ of carbonates. This feature has been interpretated by several authors (e.g., Bowman et al., 1985; Soler, 1990) as due to an adimensional infiltration process and, to a lesser extent, distillation mechanisms. The first one only produces an isotopic equilibration of minerals with the inflowing fluid while distillation is coupled with the progressive reaction of silica and carbonates giving rise to an assemblage of calcsilicates. However, these conventional models show several problems when they are applied to skarn deposits. Distillation ss. is a process of isochemical metamorphism were fluids and minerals are in isotopic equilibrium; this is not to case in skarns, where silica and other reactants are supplied by a fluid in isotopic disequilibrium. Also, adimensional infiltration models presume that isotopic changes are associated with the successive filling of porosity of an unaltered rock with the fluid; this mechanism seems to be against the metasomatic theory. Recently developed unidimensional models (e.g., Blattner & Lassey, 1989) are in better agreementwith metasomatic processes since they imply that successive batches of fluid cross a set of rock cells that have been equilibrated with previous batches of fluid.

2. General description and interpretation of the skarn.-

The skarn of El Carro del Diablo is a complex magnesic skarn located in the contact between adamellites 279+10 Ma (Casquet et al, in prep) and dolomitic marbles of unknown age. An early **laminar skarn** consists of calcite + condrodite + fluoborite + diopside + phlogopite + spinel. It is cut by the **vein skarn,** composed of up to decimetric crystals of diopside. Fluid inclusion studies, carbonate geothermometry and paragenetic considerations show that this major and

early stage took place at temperatures between 420 and 630°C at fluid pressures close to 2 kbars. Fluids responsible of this alteration were low-salinity (4.5-6.4 wt% NaCI eq.) H_20 rich (H_20=0.994) fluids. The early paragenesis are replaced by later ones that carry most of the cassiterite and scheelite mineralization (Casquet & Tornos, 1984).

Isotopic analysis have been performed on 4 samples of marbles away from the skarn (1.2 km.), 7 samples of marbles close to the skarn, 3 samples of the laminar skarn and one of a marble close to the vein skarn. Also, three whole rock samples of the granite have been analyzed for $\delta^{18}O$. Geochemical studies show that most of the isotopic signature is related to the early stage and isotopic overprints due to late alteration are minor. A mean temperature of 575°C and an XCO_2 = 0.001 were chosen for the isotopic modeling. A mean isotopic $\delta^{18}O$ signature of the granite of + 9.0‰ ($\delta^{18}O$ between + 7.4 and + 11.0‰) and a $\delta^{18}O_{fluid}$ of + 8.8‰. were used for further calculations. A $\delta^{13}C_{fluid}$ value of -11‰was used on the basis of signatures of similar hercynian granites (Sheppard, 1986).

3. The isotopic variation model for skarn alteration.-

Theoretically, isotopic zonation of skarns can be divided in three distinct zones separated by metasomatic fronts (Fig.1):

a) The **infiltration** front with the isotopic signature of the fluid controlled by the one of the rock (Blattner & Lassey, 1989); there is no evidence of alteration.

b) The **geochemical** front after which the isotopic composition of the rock is controlled by the one of the fluid. Retardation of the geochemical front respect the infiltration one is governed by the isotopic porosity.

c) The, so called here, **reaction** front that produce mineralogical changes and were distillation can be a factor for isotopic depletion. Retardation of the reaction front depends on the concentration of solutes in the fluid and kinetic restrictions.

4. Isotopic alteration in the skarn.-

Marbles away from the skarn ($\delta^{18}O$=+21.4‰and $\delta^{13}C$=-2.6‰were chosen for calculations) are thought to be unaffected by the metasomatic alteration. Marbles within the skarn outcrop are isotopically depleted and, thus, they must be affected by the geochemical front. Its distribution does not fit the predicted sharp signatures (Figs.1 to 3). This is interpreted by Blattner & Lassey (1989) as due to a degradation of the isotopic front related with degree of equilibrium and/or omnidirectional dispersion. At these temperatures and pressures, isotopic exchange can be assumed instantaneous (Frimmel, 1992) so this trend is interpreted as due to lateral dispersion (Peclet number = 3 to 30). This degradation of the geochemical front is consistent with the morphology of the skarn, developed in a deep setting and without any major structural control. The reaction front affect these rocks before they reach isotopic equilibrium with the advective fluid (Fig.2 and 3). Skarn samples can be interpretated as a product of both distillation and infllltration. In Fig.2 and 3 distillation curves are constructed on the basis of

the progressive reaction of dolomite with silica to produce diopside and forsterite plus calcite and diopside. In both cases, $SiO_{2,aq}$ is assumed to be in equilibrium with the fluid; in this part of the graphs the Xaxis has no geological meaning since its slope cannot be controlled. $\delta^{18}O$ seem not to change due to reaction and it follows the previous trend. This seems in coherence with the fact that the low proportion of $SiO_{2(aq)}$ and other solutes in the fluid are, in excess, much lower that the amount of oxygen carried as water and, thus, most of the $\delta^{18}O$ depletion after this front must be related to infiltration. $\delta^{13}C$ signatures of samples of the laminar skarn show similar, but lighter, values. However, the important depletion in $\delta^{13}C$ in the sample adjacent to the diopside suggest that distillation has been involved. The coincidence between the fractionation expected in the formation of pure diopside ($\delta^{13}C$ =-1 5.6‰ at F(O) =0.33) and the calculated $\delta^{13}C_{rock}$ in equilibrium with the fluid ($\delta^{13}C$=-13.4‰) does not allow to steady if the observed signature of the sample ($\delta^{13}C$=-13.1‰) is only controlled by distillation or if the infiltration process counteract the distillation depletion after it traverse its minimum values. This is in agreementwith the low amount of carbon in the fluid (ΣC=0.313%) that suggest that isotopic depletion due to distillation can be significative in advanced processes.

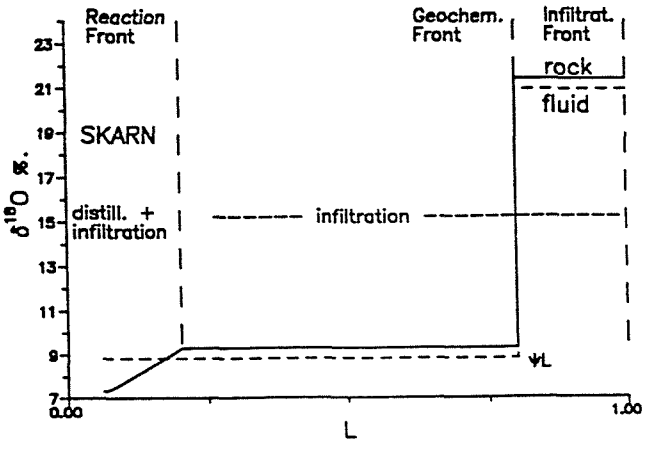

Fig.1.- Theoretical profiles in the formation of an skarn

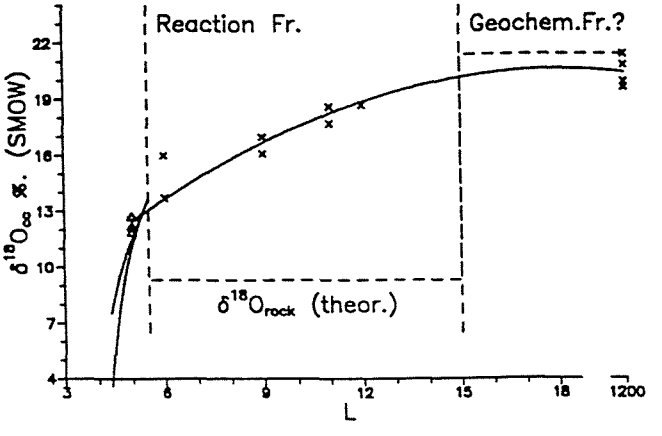

Fig.2.- $\delta^{18}O$ variation respect to distance. The situation of the geochemical front is speculative.

5. Conclusions.-

This study confirm that skarn formation can be likely interpretated on the basis of unidimensional fluid flow models and the existence of three different isotopic fronts, as has been modeled earlier for non-reactive metasomatism (Blattner & Lassey, 1989; Frimmel, 1992). $\delta^{18}O$ depletion inside the skarn seem to be associated with the isotopic equilibrium with the infiltration fluid more than with distillation processes. In the case of $\delta^{13}C$, distillation can have an important influence in the case of extreme ones.

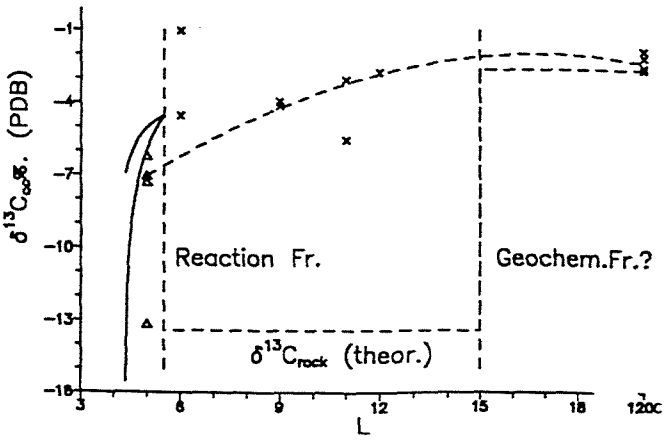

Fig.3.- $\delta^{13}C$ variation respect to distance.

Acknowledgements.-

I acknowledge the suggestions of C.Casquet, J.Delgado and P.Blattner. Isotopic analysis have been financiated by the CICYT project number PB88-124.

References.-

Blattner,P., Lassey,K.R. 1989: Stable-isotope exchange fronts, Damkohler numbers and fluid to rock ratios. Chem.Geol., 78, 381-392

Bowman,J.R., Covert,J.J., Clark,A.H., Mathieson,G.A. 1985. The Can Tung E zone scheelite skarn orebody, Tungsten, NW territories: O, H, C isotopic studies. Econ. Geol., 80, 1872-1895 Casquet,C., Tornos,F. 1984. El skarn de W-Sn del Carro del Diablo (Sistema Central Español). Bol.Geol.Min., 95-1, 58-79

Frimmel,H.E. 1992. Isotopic fronts in hydrothermally mineralized carbonate rocks. Miner. Deposita. 274, 257-267

Sheppard, S.M.F. 1986. Igneous rocks III.- Isotopic case studies of magmatism in Asia, Euroasia and oceanic islands. In Valley, Taylor, O'Neil eds., Stable isotopes in high temperature geological processes, Rev. Mineralogy 16, 319-423

Soler,A. 1990. Geologia i metalogenia del contacte sud del granit d'Andorra (Pirineu Central). Thesis Univ.Barcelona, 2 volumes, 886 pp.

Current Research in Geology Applied to Ore Deposits.Fenoll Hach-Alí, Torres-Ruiz & Gervilla(eds)(1993).ISBN 84-338-1772-8

THE ROLE OF FLUID MIXING IN THE GENESIS OF FLUORITE-BARITE-BASE METAL VEINS

Tornos, F. (1); Casquet, C. (2), Galindo, C. (2) & Caballero, J.M. (2)
(1) Inst. Tecnológico Geominero de España, Rios Rosas 23, 28003 Madrid, Spain
(2) Dept. Petrología, Facultad de Geología, 28040 Madrid, Spain

ABSTRACT: Numerical models predict that fluid mixing can be an important mechanism in the genesis of veins with barite, fluorite and sulphides. Mixing of supergene fluids of probable marine origin and ascending low-salinity ones with minor amounts of metals leached out from the host granites, accounts for the observed paragenesis in zoned fluorite-barite veins of the Sierra del Guadarrama, Spanish Central System. Here, the fluorite-rich zone can be explained by mixing of the ascending fluid with the supergene one in the deeper, reduced and hot section of the system. Upwards and/or later, the increased $\Sigma SO_4/\Sigma H_2S$ ratio of the fluid leads to the development of the barite zone. As found in nature, both zones are surrounded by two quartz-rich ones. Significative amounts of sulphides are found all along the fluorite-barite mixing zone. The relative location and proportion of the minerals depends on the amount of mixing, chemical changes due to fluid mixing and temperature of formation.

1. Introduction

Fluorite and barite-rich veins carrying significative amounts of Zn, Pb, Cu and Ag are common in the Hercynian Belt. Many of them share some common features such as the paragenesis, the presence of a vertical and lateral zonation, low temperature (<300°C) and pressure (<500 bars) of formation and a genesis related with the circulation of different types of water-rich brines. In many of them the relationship with granitoids has been proven to be spatial only , since the vein postdate by many Ma their time of emplacement.

The purpose of this work is to model the conditions of ore deposition in these type of veins. They are grounded on geological and geochemical studies of veins found in the Spanish Central System (SCS) (Tornos et al., 1991; Galindo et al., in press.).

2. Geological setting

In the central area of the SCS many lens-shaped veins with fluorite, barite and some sulphides are found trending N60-70°E and N110-125°E. Most of them are enclosed by Hercynian granitoids with ages between 320 and 284 Ma. Usually they display a gross vertical and lateral zonation with a deeper and outer fluorite-rich zone and an upper and external barite one. These zones pass downward and upward into quartz. Sulphides, mainly galena and sphalerite with minor amounts of pyrite and chalcopyrite, are found in all the zones. The

host granite is affected by a quartz-phengite-chlorite alteration. The ores have been interpretated as resulting from the mixing of a hot (>300°C), low-salinity (<0.6 molal) Na-K aqueous fluids (XH_2O>0.98) that rised along fractures in the granites with a more saline (>2.8 molal) Ca-Mg-Na-K brine (XH_2O>0.99) of supergene origin; fluorite formed at temperatures between 150 and 270°C whilst homogenization temperatures of fluid inclusions in barite range between 120 and 200°C (Tornos et al., 1991). Mixing of fluids is also confirmed by the $^{87}Sr/^{86}Sr$, ϵNd and $\delta^{34}S$ signatures of the hydrothermal minerals (Galindo et al., in press.). Sulphur in sulphides, with $\delta^{34}S$ close to 0‰, is interpreted as related to the hydrothermal leaching of granites whilst barite ($\delta^{34}S$ between +15.5 and +15.8‰) has a seawater signature. These veins have been dated by Sm/Nd at 145±18 Ma. As has been pointed out by Galindo et al. (op.ct.) and Rowan et al. (1993), the Late Jurassic seems to represent an important metallogenic epoch in Europe since it is a period of major tectonic activity leading to abnormal heat flow and development of convective hydrothermal cells.

3. Geochemical model

The formation of these veins has been modeled using the geochemical codes SOLVEQ and CHILLER (Spycher & Reed, 1992) by simulation of the processes of cooling and fluid mixing . The composition of the deep ascending fluid at 300°C has been based on fluid inclusion analysis ($m\Sigma Na=0.19$; $m\Sigma K=0.13$; $m\Sigma Ca=-0.26\times10^{-3}$) and the assumption that pH (=5.1), $m\Sigma Al$, $m\Sigma Mg$ and $mSiO_{2(aq)}$ are buffered by the enclosing altered granitoids consisting of quartz, K feldspar, phengite and chlorite s.s. A close-to-equilibrium state after fluid mixing is assumed. Original contents of metals and sulphur are kept at low values (200 ppm of Ba and F, 100 ppm of Cu, Zn and Pb and an $m\Sigma S$ of 10^{-3}) to emphatize the capability of the ore forming processes. The supergene fluid (25°C, pH=7) has the composition of seawater recalculated to a fluid inclusions $m\Sigma Cl$ of 2.91. Total salinities of both fluids have been estimated from salinity-enthalpy relationships in fluid mixing processes.

Different runs were performed changing fluid composition, type of fractionation of the hydrothermal minerals and interaction/buffering with the host rock. However, results were fairly constant. The most important consequences are:

Results

- Simple cooling of the ascending fluid gives rise an acidification up to pH values close to 3.3 at 100°C. The precipitation of sulphates is thus inhibited and important amounts of fluorite can be laid down (>70%weight) at very low temperatures only (60 to 25°C). Quartz with significative proportions of sulphides (1-6%) becomes the main mineral of the vein between 150 and 60°C. These results are consistent with those of Rowan et al. (1993) in the sense that formation of fluorite veins at high temperatures by simple cooling

requires huge quantities of fluorine in the system (4.72 molal for a mΣCa of 0.45 at 200°C).

- Fluid mixing inhibits the extreme acidification of the system, and pH is kept mildly acid to neutral (4.6 at 290°C to 6 at 100°C).
- The precipitation of sulphates is a process clearly related to the mixing with an oxidized fluid. Barite is precipitated due to fluid mixing even from extremely low (5 ppm) Ba-bearing ascending fluids.
- If the chemical composition of the supergene fluid doesn't change down to great depths, starting of fluid mixing at high temperatures (>200°C) leads to the precipitation of anhydrite, quartz and barite. Here, the formation of anhydrite inhibits the precipitation of fluorite even al high mΣF.
- Veins with barite, quartz and sulphides can be formed by mixing of the ascending and the oxidized supergene fluids at temperatures close to or below 180-200°C. At these conditions neither anhydrite nor fluorite are formed.
- Fluorite can only precipitate at high temperatures by the addition of Ca from the supergene fluid (F comes in the ascending fluid). The critical factor that leads to the precipitation of fluorite is that the supergene fluid be previously impoverished in ΣSO_4, by the extraction of sulphate due to precipitation of barite in the higher portions of the system. Fluorite can account for 90-99% of the mineral precipitate in the range 280 to 180°C.
- High supergene/ascending fluid mixing ratios lead to the precipitation of quartz + sulphides.
- Fluid mixing seems to be a quite effective mechanism for precipitating base metal sulphides. For concentrations in the deep fluid of 10 ppm ore grades of up to 3-12% weight can be reached in selected zones of the system.

4. Discussion

The calculations above support the formerly established hypothesis that fluid mixing played an important role in the genesis of fluorite-barite-base metal veins. Mixing of slightly modified seawater with low-salinity fluids involved in postmagmatic hydrothermal cells is a suitable mechanism for forming these kind of veins; metals are derived by the hydrothermal leaching of the enclosing granites, while sulphur is provided by the two fluids. Precipitation of major quantities of fluorite and barite (>90%) can take place from relatively low Ba-F concentrations in the fluid (200 ppm). Ore grades similar to those reported in the veins are predicted even at very low concentrations (10 ppm); however, increasing the metal content of the fluids rises dramatically the amount of precipitated sulphides.

The position of the ore zones in the vein, the vertical zonation and the presence/absence of fluorite, barite and quartz is controled by variables such as the maximum temperature of the beginning of fluid mixing, grade of interaction between the two fluids and vertical variations in the ΣSO_4 content of the fluid. The relative depth and temperature reached by the supergene

fluid, without chemical modifications, defines the location and composition of the sulphate zone. In mixing processes at high temperatures, anhydrite is the dominant sulphate, whilst under approximately 200°C, barite is the stable one. The absence of anhydrite in these veins is consistent with the low capability of the supergene fluid to preserve the original chemistry at depth, particularly the sulphate content. The calculations show that the supergene fluid is progressively impoverished in ΣSO_4 due to the precipitation of sulphates, mainly barite, in the shallower portions of the mixing zone. Mixing of the sulphate-depleted supergene fluid and the unmodified ascending one in the fracture below the barite zone, leads to the precipitation of fluorite due to the dramatic increase of the mCa^{2+} of the resulting system. Thus, the complete zoning can be explained on the basis of simple cooling in the deepest zones of the system leading to the precipitation of quartz ± sulphides. Furtherly mixing of the ascending fluid leads to the formation of fluorite in the deeper part of the mixing zone, whilst barite dominates in the shallower one; both can contain significative amounts of sulphides. Finally, theoretical models predict also the formation of a new quartz ± sulphides zone in the uppermost part of the hydrothermal system.

Acknowledgements: This work has been benefitted from the discussions and help of J.Locutura, M.Reed, E.Rowan and C.Ayora.

References:

- Galindo,C., Tornos,F., Darbyshire,F., Casquet,C. (in press): Sm/Nd Dating and Isotope Constraints for the Origin of the Barite-Fluorite (Pb-Zn) Veins of the Sierra del Guadarrama (Spanish Central System, Spain).
- Spycher,N.F., Reed,M.H. (1992): Microcomputer-based modeling of speciation and water-mineral-gas reactions using programs SOLVEQ and CHILLER. In Proc. 7th Int.Symp. on Water-Rock Interaction, Kharaka,Y., Maest,A.S. (eds.), Balkema, Rotterdam, 1087-1090
- Rowan,E.L., Thibieroz,J., King,G.C.P., Bethke,C.M., Marsily,G. (1993): Thermal and hydrologic conditions for fluorite mineralization in regions of continental extension: an example from the Albigeois dictrict, France. Abstracts Mississippi Valley Type Deposits Workshop. Paris, Feb.1993
- Tornos,F., Casquet,C., Locutura,J., Collado,R. (1991): Fluid inclusion and geochemical evidence for fluid mixing in the genesis of Ba-F (Pb-Zn) lodes of the Spanish Central System. Mineralog. Mag., 55, 225-234.

Current Research in Geology Applied to Ore Deposits. Fenoll Hach-Alí, Torres-Ruiz & Gervilla (eds) (1993). ISBN 84-338-1772-8

ORIGIN OF THE CARBONATE-HOSTED MERCURY VEINS FROM THE ESPADAN MOUNTAINS (IBERIAN RANGES, EASTERN SPAIN): EVIDENCE FROM FLUID INCLUSIONS AND STABLE ISOTOPES

Tritlla, J. (1) & Cardellach, E. (2)

(1) Dept. Cristal.lografia, Mineralogía i Depòsits Minerals, Universitat de Barcelona, Barcelona, Spain
(2) Dept. de Geología. Facultat de Ciències. Universitat Autònoma de Barcelona, 08193 Bellaterra, Spain

ABSTRACT: The carbonate-hosted mercury veins from the Espadán mountains formed as a consequence of an effervescence mechanism that caused the unmixing of a CO_2-rich phase. This separation led to the precipitation of xenotopic-c dolomite and a shift of $\delta^{13}C$ and $\delta^{18}O$ of hydrothermal carbonates to lighter values than those of the enclosing dolomites. The effervescence produced an enrichment of Hg in the gaseous phase. The most important Hg deposits are related to this event.

INTRODUCTION

The Sierra de Espadán area is located between the Castellón and Valencia Provinces (Eastern Spain). This area is a major anticlinal structure made up of Mesozoic materials, mostly Triassic in age (Buntsandstein, Muschelkalk and Keuper facies), constituting the eastern outcrops of the Iberian Ranges. The Eslida-Artana-Betxí mercury deposits are located near the axis of this anticline. They occur as small veins (up to 10 cm thick) crosscutting the lower levels of the Muschelkalk facies (black to grey dolomites).

MINERALOGY

The structure of the veins is simple. In the Betxí and Artana deposits, a first generation of brown cloudy calcite (CC1) is overgrown and partially corroded by clear euhedral centimetre-sized dolomite crystals, characterized by a xenotopic-c texture, and by the high number of primary fluid inclusions, especially around the CC1 relicts. Together with the xenotopic-c dolomite, minor amounts of quartz are deposited as euhedral crystals, with fluid inclusions similar to the dolomite crystals. In one locality (Eslida), the veins, although crosscutting the same enclosing rock, do not contain xenotopic-c dolomite crystals and are only made up of calcite (CC1) and quartz in variable amounts.

The main ore mineral is cinnabar. It occurs as a micron-size red powder, mixed with stibiconite, goethite and malachite, in pockets on the dolomite or quartz crystals. In some quartz-dolomite veins is the hypogene paragenesis, composed by a mercurian tetrahedrite ("schwatzite") and minor amounts of chalcopyrite and an unknown phase of Hg-Ag-Sb-S, partially preserved. The mercurian tetrahedrite is always corroded by a mixture of cuprite, powdered cinnabar, covellite, stibiconite and malachite. A late generation of euhedral calcite (CC2) fills the remaining open spaces.

FLUID INCLUSIONS

Primary fluid inclusions in xenotopic-c dolomite and in quartz range in size between 1 and 20 μm. At room temperature it is possible

to distinguish three different types: **(1)** inclusions filled by a saline aqueous liquid, a non-condensable gas bubble (mainly CO_2) and a halite crystal; **(2)** identical to type 1, but with a double CO_2 bubble (liquid + gas), and **(3)** liquid rich CO_2 ($\pm N_2$) fluid inclusions, with minor amounts of water riming the fluid inclusion walls. Fluid inclusions of types 1 and 2 are found predominantly in the dolomite-quartz veins.

The microthermometric measurements carried out on type 1 and 2 inclusions show the eutectic temperatures (Te), indicating a solution with calcium chloride (Te from -58 to -52°C). The high amount of $CaCl_2$ in the solution is also confirmed by the metastability of the hydrohalite (Tm_h from +8 to +12°C). CO_2 is detected by the melting of clathrate. Halite dissolves between +200 and +230°C, whilst the homogeneization temperatures by bubble shrinkage are between +210 and +240°C. Salinities are very constant, ranging from 32 to 33.3 wt% NaCl eq. calculated using the Flincor program (Brown, 1989). These fluid inclusions were analyzed by the Cryo-SEM-EDS method (Ayora y Fontarnau, 1990), confirming that they belong to the system NaCl-$CaCl_2$-KCl, with Na:Ca:K ratios from 0.79:0.15:0.07 to 0.88:0.07:0.06. The homogenization temperature versus salinity plot suggests a boiling system. Only a few inclusions of type 2 are found. These have the same salinity as type 1, but decrepitate above 180°C. The CO_2 can fill up to 30% of the volume of the fluid inclusions. Homogenization temperature of this CO_2 to the liquid phase ranges from 21.9 to 28.7°C. Just a few type 3 primary fluid inclusions have been found.

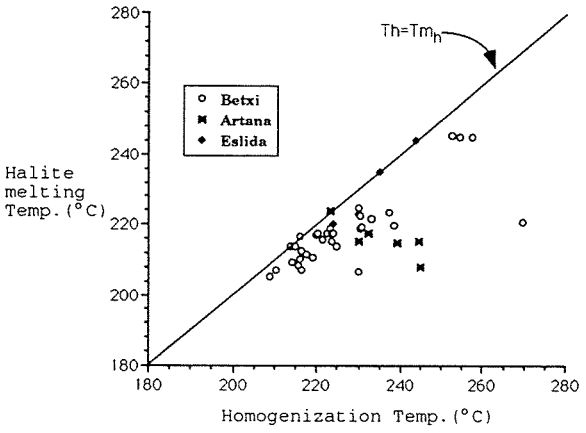

Fig.1.- *Homogenization (Th) vs halite melting temperatures (Tm_h) plot for type 1 fluid inclusions.*

The fluid inclusions in the quartz from the calcite(CC1)-quartz veins of Eslida, are mainly of type 3, ranging from 1 to 20 μm in size. Raman microprobe analyses gave compositions between 18.3 to 4.0 mol % of N_2 and homogenization temperatures around +25°C to the liquid phase. Isochores and densities were calculated with the Flincor program. Type 1 inclusions are sometimes found. Is significant that the nature and homogenization temperatures of these CO_2 inclusions are similar to type 2 inclusions (double CO_2 bubble).

The presence in these veins of two inmiscible fluids trapped simultanously may be used as a geobarometer (Guilhaumou et al, 1981). The intersection of the isocores calculated for both systems, which have very different slopes, allows to determine the pressure and to correct the trapping temperature. The intersection of maximum and minimum

isochores, calculated for the aqueous hypersaline and the CO_2-N_2 bearing fluid inclusions, corrects the trapping temperature from 230 to 265-275°C, and gives a pressure between 900 and 1050 bars.

STABLE ISOTOPES

C and O isotopes have been analyzed in carbonates (dolomites and calcites) from the Artana, Betxí and Eslida deposits. Results are shown in Fig.1. The samples of the unmineralized limestones of Triassic (Muschelkalk) age have a $\delta^{13}C$=+0.3‰ and $\delta^{18}O$=+25.2‰; dolomitized limestones around the mineralized areas have $\delta^{13}C$=-1 to +2.7‰, and $\delta^{18}O$=+21 to +23.5‰. The $\delta^{18}O$ composition is about 2‰ lighter than the regional limestones, suggesting that the dolomitization took place as a consequence of a hydrothermal event.

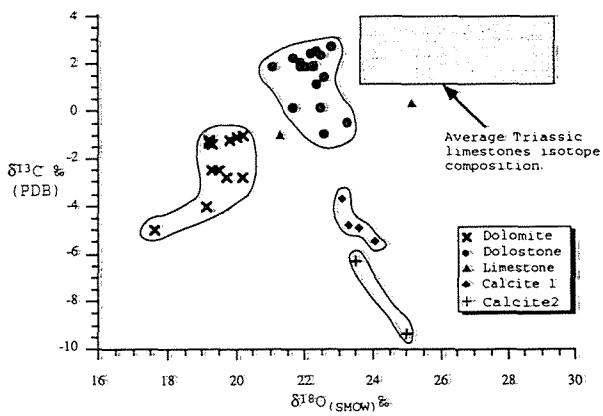

Fig. 3 - *Carbon and oxygen isotopic composition of the carbonates from veins and enclosing rocks.*

Vein xenotopic-c dolomite has $\delta^{18}O$ and $\delta^{13}C$ values depleted in ^{18}O and ^{13}C relative to the dolostones, with values as low as 17.5‰ and -5.1‰ respectively. The ^{13}C depletion can be explained by a loss of about 30% of CO_2 from the initial fluid during an event of effervescence. The CO_2 loss is also related to carbonate deposition, which can be represented by the following reaction:

$$Mg^{++} + Ca^{++} + 4\ HCO_3^- = CaMg(CO_3)_2 + 2H_2O + 2CO_2$$

The ^{18}O depletion can be explained by reactions that produce CO_2 during post-boiling equilibration of fluids and host rocks, having a strong fractionation effect on the $\delta^{18}O$ of water (Lynch et al; 1990). In this case, isotopic equilibrium between CO_2 and H_2O can be assumed (Bowers, 1991). When the original fluid intersects the H_2O-CO_2 miscibility gap (1000 bars, in this situation), a vapor phase of composition corresponding to the vapor-rich limb of this miscibility gap forms, and then the CO_2 gas becomes isotopically heavier than the liquid water. As the effervescence progresses, the $\delta^{18}O$ of the remnant fluid becomes lighter, as can be seen in the dolomite $\delta^{18}O$ composition. This is in contrast to boiling of pure water, where the lighter isotope partitions into the water vapor, and the liquid becomes progressively heavier.

The CC1 and CC2 calcites have very similar $\delta^{18}O$ values (from 23.1 to 24.1‰) to the dolostones, but show more negative $\delta^{13}C$ values, ranging from -3.7 to -9.0 ‰. The ^{13}C depletion suggests that these calcites precipitated from organic matter-rich surficial waters that dissolved

the preexisting dolostones.

CONCLUSIONS

The mineralizing fluids involved in the genesis of the veins belong to the $NaCl-CaCl_2-KCl-H_2O-CO_2-N_2$ system. The presence of primary aqueous and non-aqueous fluid inclusions in the same growth bands of a single crystal and the same homogeneization temperature of the CO_2-bearing inclusions suggest an effervescence mechanism that would trigger the deposition of the ore and non ore minerals of the veins. This effervescence could be related to a hydraulic fracturing event which originated the opening of the veins. As can be seen in the Th/salinity plot, boiling is very restricted, as there is not a significant salinity increase and temperature decrease in the fluid that would be produced produced by a high entalphy steam loss.

Stable isotopes of C and O of carbonates confirm the effervescence of CO_2 as the main process for the precipitation of the carbonate-hosted mercury veins. ^{13}C and ^{18}O depletion in carbonates is explained by the CO_2-bearing gas loss from the original fluid, which strongly fractionates the heavier isotopes.

According to Krupp (1988), an efficient mechanism to transport and concentrate mercury in hydrothermal systems is the evolution, from an homogeneous fluid, of a gas-rich phase (steam, CO_2, H_2S, etc), where mercury can easily be concentrated. The most important concentrations of mercury in these carbonate-hosted deposits are located in the Eslida veins, where no xenotopic-c dolomite is found and fluid incluions are predominantly of type 3 (CO_2-bearing inclusions) indicating that these veins formed above the effervescence horizon, and suggesting preconcentration of Hg in the CO_2-bearing phase.

ACKNOWLEDGMENTS: This work was supported by CICYT project PS88-0018 (Spanish Ministerio de Educación y Ciencia) and a CIRIT 1990 grant (Generalitat de Catalunya) to J.T..

REFERENCES

Ayora, C & Fontarnau, R. 1990, X-ray microanalysis of frozen fluid inclusions.. Chem. Geol., 89, 135-148.

Bowers, T.S., 1991, The deposition of gold and other metals: Pressure-induced fluid inmiscibility and associated stable isotope signatures. Geochim. Cosmochim. Acta, vol. 55, 2417-2434.

Brown, P.E.,1989, FLINCOR: a microcomputer program for the reduction and investigation of fluid inclusions data. Am. Min., Vol. 74, 1390-1393.

Guilhaumou, N., Dhamelincourt, P., Touray, J.C., & Touret, J., 1981, Etude des inclusions fluides du système N_2-CO_2 de dolomites et de quartz de Tunisie septentrionale. Données de la microcryoscopie et de l'analyse à la microsonde à effet Raman. Geochim.Cosmochim. Acta, vol. 45, 657-673

Lynch, J.V.G., Longstaffe, F.J. & Nesbitt, B.E., 1990, Stable isotope and fluid inclusion indications of large -scale hydrothermal paleoflow, boiling and fluid mixing in the keno Hill Ag-Pb-Zn district, Yukon territory, Canada. Geochim. Cosmochim. Acta, 54, 1045-1059.

Current Research in Geology Applied to Ore Deposits. Fenoll Hach-Alí, Torres-Ruiz & Gervilla (eds) (1993). ISBN 84-338-1772-8

ZINC-RICH CHROMITES FROM EARLY PROTEROZOIC CONGLOMERATES AT THE TARKWA GOLD MINE, GHANA

Weiser, Th. & Hirdes, W.

Federal Inst. for Geosciences and Natural Resources (BGR), P.O. Box 51 01 53, D-3000 Hannover 51, Germany

ABSTRACT: The early Proterozoic Tarkwaian Group of Ghana contains one of three known early Precambrian quartz-pebble conglomerates which are being mined for gold, the others being the Witwatersrand goldfields of South Africa and the Serra de Jacobina goldfields of Brazil. The paragenesis of the ore minerals mainly consists of hematite, magnetite, and gold. Very rare is chromite which contains up to 19.4 wt.% ZnO, the highest value ever reported.

INTRODUCTION:

Zinc-bearing chromites were first described from Norway (Donath, 1930). Using electron microprobe technique more and more world-wide occurrences of Zn-rich chromites were discovered, mainly associated with sulphide mineralization. The first observation of detrital Zn-rich chromites was made in the Witwatersrand conglomerate (Schidlowski, 1970). During an investigation on the gold-bearing conglomerates at Tarkwa gold mine, Ghana we found detrital chromites with contents of ZnO reaching up to 19.4 wt.%, the highest value ever reported.

GEOLOGICAL SETTING:

The sediments of the Tarkwaian group consist of conglomerates, sandstones and minor argillites metamorphosed to low grade. They are erosion products of Birimian supracrustal rocks and their comagmatic belt-type granitoid plutons.

The gold-bearing conglomerates which contain the chromites are a part of the Banket Series and occur in a 250 km long, NE-SW-trending strip of Tarkwaian rocks within the Ashanti volcanic belt. The Banket Series consists of four major conglomerate horizons, from which only two of them (Main Reef and West Reef) carry consistently economic gold grades. The chromites discussed here originate from heavy mineral foresets in quartzite between the Upper and Lower Band of the Main Reef.

MINERALOGY:

Unlike the Witwatersrand and Serra de Jacobina gold deposits which carry as major constituents heavy minerals which are stable under reducing, or at least oxygen-deficient, atmospheric conditions (pyrite, uraninite), the ores at Tarkwa comprise a gold-magnetite-hematite-(ilmenite) paragenesis which is largely comparable to the "black sand parageneses" encountered in present-day placers. Other minerals observed at Tarkwa - some of which occur only very sporadically - include zircon, rutile, quartz, carbonate, chlorite, tourmaline, garnet, chromite, epidote, diamond, pyrite, pyrrhotite, chalcopyrite or bornite. This is certainly a small number when compared to more than 80 ore minerals described from the Witwatersrand ores.

The minerals may be grouped into three categories, i.e. allogenic minerals (e.g. zircon, ilmenite), authigenic minerals (e.g. pyrite), and minerals which are present both as allogenic and authigenic constituents (e.g. hematite, magnetite).

Hematite is by far the most abundant opaque mineral in the Tarkwaian conglomerates. Magnetite is relatively seldom. Chromite is very rare and could be detected exclusively rimmed by magnetite.

The subidiomorphic to xenomorphic gold particles are mostly smaller than 10 µm. Microprobe analyses showed values of the fineness between 952 and 986 which are characteristic for the transportation of the gold.

ANALYTICAL RESULTS:
In total nine chromite grains were analyzed. Under the ore microscope they are all homogeneous, grey with a bluish tinge and strongly isotropic in oil immersion. The reflectivity lies between 17.0 and 14.6% (440 - 700 nm). This is distinctly higher compared with Zn-free chromites from the Stillwater Complex (Criddle & Stanley, 1986) and in good agreement with the observation on Zn-rich rims around chromites from the Witwatersrand by Schidlowski (1970).

Microprobe analyses showed a great variation in the chemical composition of the chromites in the six examined samples but also in a sample itself. On the other side the single grains are always homogeneous as to be seen from the backscattered electron images (Fig. 1a-c). The point analyses confirm this observation.

The Cr203 content lies between 37.2 and 60.5 wt.%, the content of Al203 between 2.7 and 16.2 wt.%, and the calculated Fe203 content differs between 3.6 and 16.7 wt.%. All analyzed chromites are free of magnesium. The most interesting features is the unusual high amount of ZnO. The average value of all analyzed grains is 13.3 wt.%. The maximum value of 19.4 wt.% in grain no. 6 (Table 1) is the highest Zn content in chromites (greater than 35 wt.% Cr203) ever reported except the new mineral zincochromite. A similar content of zinc (19.1 wt.% ZnO) show chromites from Sykesville, USA which are associated with sulphide mineralization (Wylie et al., 1987). The calculated FeO content lies between 15.7 and 24.3 wt.%. All analyses snow a nearly constant MnO value of 0.8 wt.%, whereas V and Ti could be detected in traces only once. The general formula of the Zn-rich chromites from Tarkwa corresponds to

$$(Fe_{0.64}Zn_{0.36})_{1.00}(Cr_{1.45}Al_{0.33}Fe_{0.22})_{2.00}O_4$$

Due to this the following proportions of spinel endmembers can be calculated

16.5 mol.% ZnAl2O4
11.0 mol.% ZnFe2O4
8.5 mol.% ZnCr2O4
64.0 mol.% FeCr2O4

DISCUSSION and CONCLUSION:
The source of zinc in chromite has been a matter of debate for a long time. Zinc-bearing chromites (>0.5 at.% Zn) from Alaska are explained as crystallization products from a sulphide melt seggregated from gabbroic magma (Czamanske et al., 1976). For the high Zn content of the chromites from the Sykesville district, USA metasomatism by Zn-rich fluids is assumed (Wylie et al., 1987). Schidlowski (1970) supposed circulating Zn-bearing solutions to be the source of the Zn-rich rims of the detrital chromites from the Witwatersrand conglomerate.

However it is not easy to understand that chromites with such high Zn contents as discussed here are of original magmatic origin or the result of secondary processes after deposition in the conglomerate. As to the formation and origin of the Zn-rich chromites in the Tarkwaian conglomerate there is no explanation at the moment. Neither an ultramafic complex nor any sulphide mineralization in the back country is known.

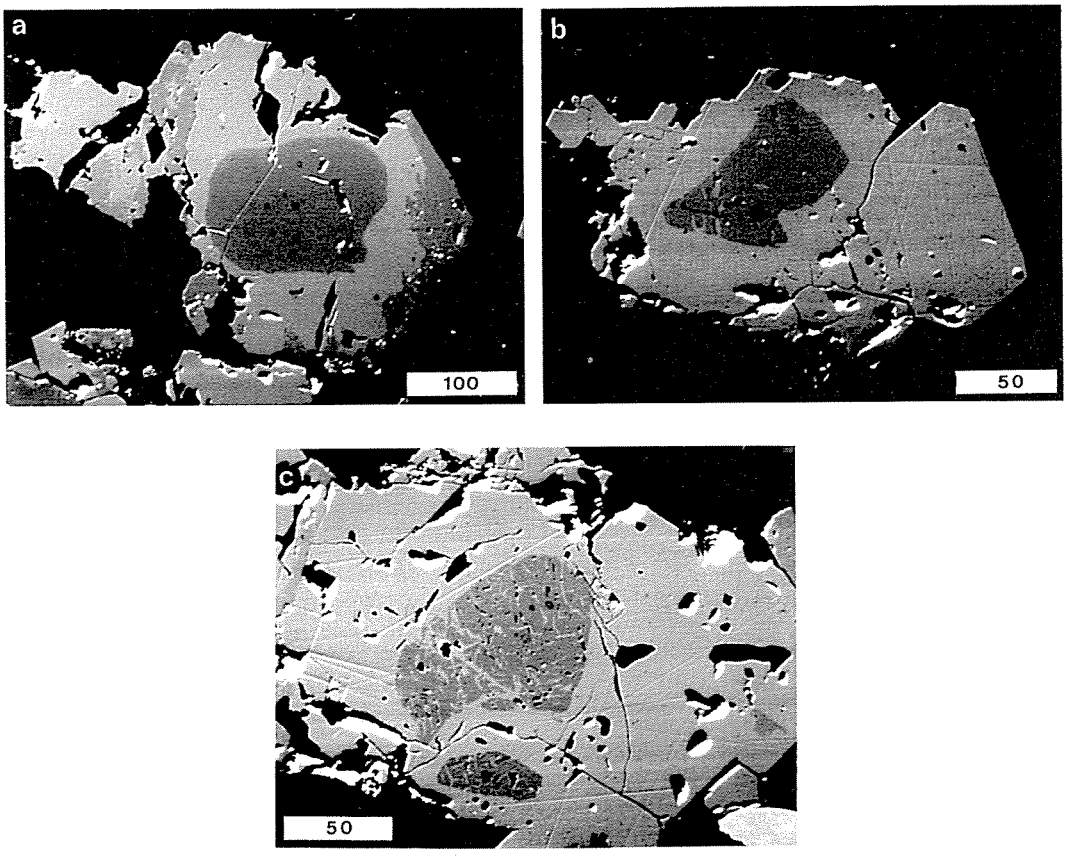

FIGURE 1

Backscattered electron images (BEI) of oxides in the Tarkwaian conglomerate

a - Magnetite with rounded core of detrital chromite (dark). Magnetite is partly replaced by hematite (grain no. 3)
scale bar: 100 µm

b - Idiomorphic chromite (dark) rimmed by magnetite (grain no. 9)
scale bar: 50 µm

c - Chromite (dark) myrmekitic-like replaced by magnetite (grain 7)
scale bar: 50 µm

TABLE 1. ELECTRON-MICROPROBE ANALYSES OF CHROMITE

grain no.*)	1(2)	2(4)	3(4)	4(3)	5(2)	6(2)	7(2)	8(5)	9(2)
					weight per cent				
Cr_2O_3	53.00	45.75	60.54	46.83	55.55	39.48	37.17	55.38	56.53
Al_2O_3	5.91	13.89	2.70	6.20	5.74	16.21	10.28	3.87	3.93
V_2O_3	-	-	-	-	-	-	0.30	-	-
Fe_2O_3	6.71	4.15	3.58	13.01	5.69	7.82	16.72	6.85	5.40
FeO	21.93	19.52	21.98	18.32	24.34	15.73	15.89	19.99	20.32
MgO	-	-	-	-	-	-	-	-	-
MnO	0.96	0.80	1.41	0.81	1.05	0.60	0.48	0.77	0.69
ZnO	10.36	14.44	9.78	14.66	8.32	19.42	18.09	12.61	12.27
TiO_2	0.19	0.20	-	0.31	-	-	-	-	-
Total	99.06	98.75	99.99	100.14	100.69	99.26	98.93	99.47	99.14
					atomic proportions				
Cr	1.554	1.300	1.781	1.368	1.598	1.116	1.082	1.636	1.674
Al	0.259	0.588	0.119	0.270	0.246	0.683	0.446	0.171	0.174
V	-	-	-	-	-	-	0.009	-	-
Fe^{3+}	0.187	0.122	0.100	0.362	0.156	0.201	0.463	0.193	0.152
Fe^{2+}	0.680	0.587	0.624	0.566	0.744	0.470	0.491	0.627	0.638
Mg	-	-	-	-	-	-	-	-	-
Mn	0.030	0.024	0.041	0.026	0.032	0.018	0.015	0.025	0.022
Zn	0.284	0.383	0.335	0.400	0.224	0.512	0.494	0.348	0.340
Ti	0.006	0.005	-	0.008	-	-	-	-	-
					endmember proportions				
gahnite	12.95	29.40	5.95	13.50	12.30	34.15	22.30	8.55	8.70
franklinite	9.35	5.60	5.00	18.10	7.80	10.05	23.60	9.65	7.60
zincochromite	6.10	3.30	22.55	8.40	2.30	7.00	3.50	16.60	17.70
chromite	71.60	61.70	66.50	60.00	77.60	48.80	50.60	65.20	66.00

*) number of analyses in parenthesis

for the calculation of the endmembers V was added to Fe^{3+} and Mn and Ti to Fe^{2+}

REFERENCES:

Criddle, A.J. & Stanley, C.J. (eds.) 1986. The Quantiative Data File for Ore. Brit. Mus. Nat. Hist., London

Czamanske, G.K., Himmelberg, G.R. & Goff, F.E. 1976. Zoned Cr,Fe-spinel from the Perouse layered Gabbro, Fairweather Range, Alaska. Earth Planet. Sci. Lett. 33:111-118

Donath, M. 1930. Geologisch-mineralogische Studien an serbischen Chromitlagerstätten.- Ph.D. thesis, Bergakademie Freiberg, Freiberg/Saxony

Schidlowski, M. 1970. Untersuchungen zur Metallogenese im südwestlichen Witwatersrand-Becken (Oranje-Freistaat-Goldfeld, Südafrika). Beih. geol. Jb. 85

Wylie A.G., Candela, P.A. & Burke, T.M. 1987. Compositional zoning in unusual Zn-rich chromite from the Sykesville district of Maryland and its bearing on the origin of "ferritchromit". Am. Mineral. 72:413-422

Current Research in Geology Applied to Ore Deposits.Fenoll Hach-Alí, Torres-Ruiz & Gervilla(eds)(1993).ISBN 84-338-1772-8

THE ALPINE Pb-Zn DEPOSITS OF THE DRAU RANGE (AUSTRIA/SLOVENIA): PARAGENESIS AND SPHALERITE GEOCHEMISTRY

Zeeb, S.; Kuhlemann, J. & Bechstädt, T.
Geol.-Pal. Inst. Universität Heidelberg, Inf 234, D-6900 Heidelberg, Germany

ABSTRACT: The ore deposits in the Drau Range consist of sphalerite, galena, iron sulfides, fluorite and barite. Two main mineralization phases can be divided by the succession of deep burial carbonate cements. Within the first phase a distinct succession of sphalerite types can be distingished by optical methods. Their trace element distribution is clearly related to cathodoluminescence and fluorescence characteristics.

The strata-bound Pb-Zn deposits of the Drau Range, including the mines of Bleiberg and Mezica (Fig.1), are hosted by platform carbonates (e.g. Wetterstein Formation) of Ladinian/Carnian age, sporadically also of Norian age.

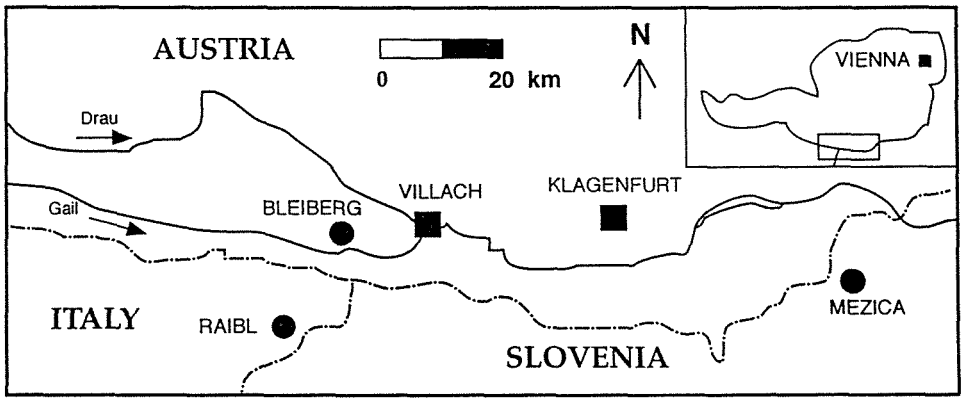

Fig.1: Investigated area.

Concordant and discordant ore bodies are connected with palaeogeographic structures, e.g. areas containing a microkarst of Triassic age, causing higher porosity. The sequence of carbonate cementation within the sedimentary carbonbate rocks (ZEEH 1990) forms the framework for the relative dating of the ore precipitation (Fig.2).

The near surface to shallow burial diagenesis from meteoric-vadose to marine phreatic environments was terminated by a dolomitization ("replacement dolomite" sensu HENRICH & ZANKL 1986) and/or a recrystallization by altered marine solutions. The carbonate cementation of deep burial diagenesis includes two types of saddle dolomite ("clear" and "cloudy" saddle dolomite) and three types of blocky calcite ("zoned", "corrosive" and "uniform" blocky calcite).

During near surface to shallow burial diagenesis barite, grey coloured anhydrite and pyrite framboides were formed. After recrystallization at the end of shallow burial diagenesis the ore formation started with disseminated grains of so-called "small" sphalerite and some coarse FeS_2 (pyrite, marcasite, melnikovite-pyrite).

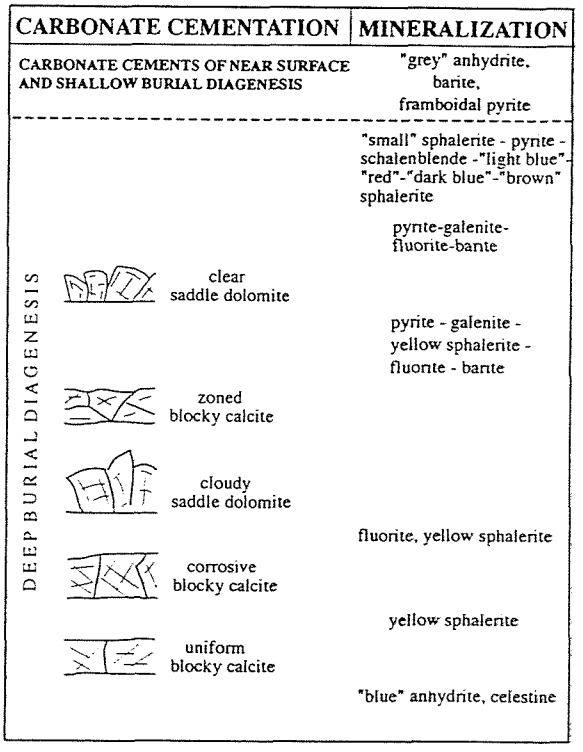

Fig.2: Relative succession of ore mineralization within the sequence of deep burial carbonate cements.

The following widespread distinct succession of sphalerite can be characterized under cathodoluminescence (CL) as follows: "schalenblende" - "light blue" - "red" - "dark blue" - dark yellow ("clear") - "brown". The ore formation phases ended with the mineralization of FeS_2, galena, barite and fluorite. Another ore formation phase is recognized after the precipitation of "clear" saddle dolo-mite and comprises major amounts of FeS_2, galena, some clear, yellow coloured sphalerite, fluorite and finaly barite.

Only very small amounts of FeS_2, galena, "yellow" sphalerite and fluorite mineralized during the later carbonate cementation. Latest diagenetic products like blue coloured anhydrite and celestine occur after the formation of the latest "uniform" blocky calcite. Finally oxidized ore minerals like smithsonite, hemimorphite, wulfenite, cerussite and hydrozincite were formed under meteoric conditions.

A comparison of the sphalerite types, including the early formed "small" disseminated type and the later formed "yellow" type, shows geochemical characteristics closely related to the CL and fluorescence observations. The "small" type, schalenblende and the "brown" type show dull CL and relative enrichment of Tl, As, Ge and partly Fe (except "small" sphalerite depleted of Fe). The elements Tl and Fe are known for quenching CL effects (MARSHALL 1988). "Light blue" sphalerite is relatively depleted of Cu, Tl, Ge and Fe and is slightly enriched with Ag. The reason for the bright CL is not clear.

The CL of "dark blue" sphalerite is closely related to the CL of the "light blue" type. The "dark blue" type is depleted of all trace elements. Since artificial pure ZnS shows blue CL with increasing intensity due to increasing irregularities in the structure of the crystal (GUMLICH & RIEHL 1971) it is suggested that the CL of the natural "dark blue" sphalerite is caused by the ZnS itself. According to this assumption the bright CL of "light blue" sphalerite could be caused by irregularities and the frequent submicroscopic inclusions.

The "red" sphalerite is strongly enriched with Cu and Ag. Since Cu as the only trace element in artificial ZnS causes pri-marily green CL (GUMLICH & RIEHL 1971) it is suggested that the combination of Cu with Ga, which was not measured, causes the orange to red CL (see MARSHALL 1988). A positive correlation of Cu and Ga can be assumed according to PIMMINGER et al.(1985a). "Red" sphalerite can also be found as a concentric zonation or a sector zonation within big crystals of the "dark blue" type.

A comparison of the trace element content in some sphalerite types with the Clarke value of the earth's crust (Fig.3) shows an increasing enrichment from Ag, Ge, Tl to As and a strong enrichment of Cd. Cu is only enriched in type "red" but depleted in all other sphalerite types. Fe is generally depleted.

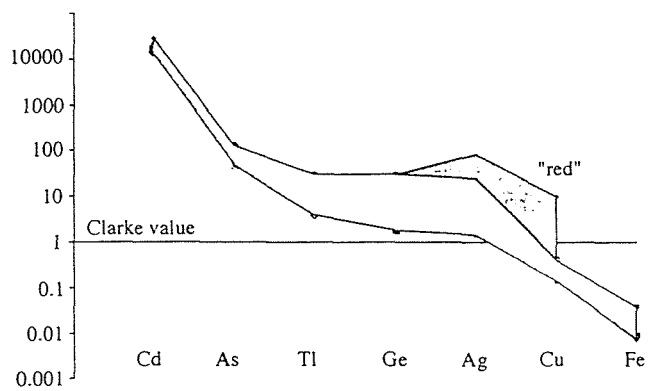

Fig.3: Envelope of the sphalerite types "light blue", "red", "dark blue" and "yellow" versus the Clarke value of earth's crust (offset of type "red" signed).

Relative changes of the trace element distribution in the sphalerite succession are characterized by high contents of Tl, As and Ge at the beginning and in the end of the first and main mineralization phase (Fig.4a). The positive correlation of these elements has been shown by PIMMINGER et al.(1985a) for Bleiberg and is also indicated in Fig.4a. The entire succession of "light blue", "red" and "dark blue" sphalerite shows a depletion of these elements but partly an enrichment of Ag and Cu followed by the "dark blue" type poor in all trace elements (Fig.4b).

The last, "yellow" sphalerite appears in several phases within the cement succession and is interpreted as a mobilization of older sphalerites. The trace element distribution shows that Fe, Tl, As, Ge and Cd cluster around the average content of all investigated samples while Ag and Cu are extremely depleted.

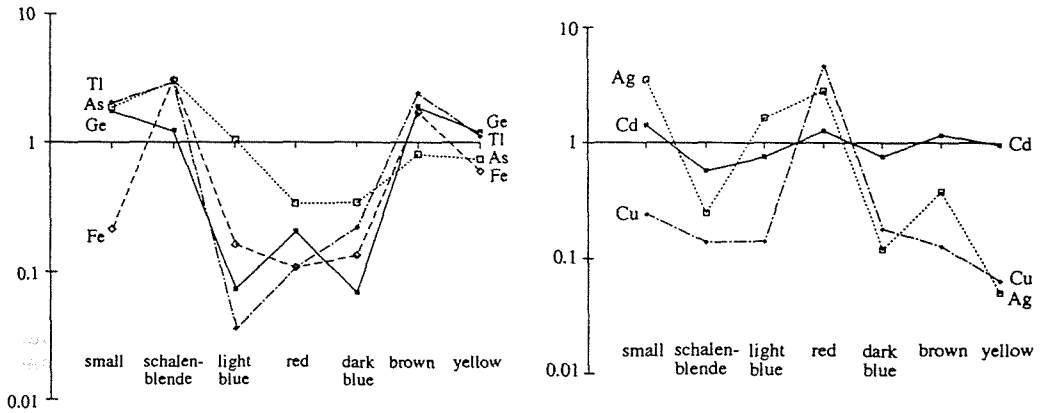

Fig.4a/4b: Relative abundance of the trace elements (4a) Fe, As, Tl, and Ge as well as (4b) Cd, Cu and Ag in the succession of sphalerite types of the Drau Range.

The abundance of the sphalerite types is very variable in regional and local size. Trace element contents of sphalerites based on whole rock analysis are strongly influenced by the dominating sphalerite type. Sporadic occurrences of every sphalerite type can be observed in most localities independently from the position of the orebody within Ladinian to middle Carnian strata. The sphalerite succession can better be explained by a single, rather than a multiple, pulsating formation process. The occurrence of "dark blue" sphalerite in Norian strata indicates a late Norian to post-Norian mineralization of the sphalerite and the following major part of the first ore formation phase.

References:

Gumlich, H.-E. & Riehl, N. 1971. Phosphore der ZnS-Gruppe (II-IV-Verbindungen). In: Riehl (eds.) Einführung in die Lumineszenz. Verlag Karl Thiemig KG München pp. 35-109

Henrich, R., Zankl, H. 1986. Diagenesis of Upper Triassic Wettersteinreefs of the Bavarian Alps. In: Schroeder, J.H., Purser, B.H. (eds.) Reef Diagenesis. Springer Berlin Heidelberg New York pp. 245-268

Marshall, D. J. 1988. Cathodoluminescence of geological materials. Unwin Hyman Boston London Sydney Wellington pp. 146

Pimminger, M., Grasserbauer, M., Schroll, E. & Cerny, I. 1985a. Trace element distribution in sphalerites from Pb Zn-ore occurrences of the Eastern Alps. Tschermaks Min. Petr. Mitt. 34: 131-141

Zeeh, S. 1990. Fazies und Diagenese des obersten Wettersteinkalkes der Gailtaler Alpen. Freiburger Geowiss. Beitr. 1 pp. 210+VI

Current Research in Geology Applied to Ore Deposits.Fenoll Hach-Alí, Torres-Ruiz & Gervilla(eds)(1993).ISBN 84-338-1772-8

POLYGENE OF GOLD ORE IN CARBONACEOUS SCHISTS OF OPHIOLITE BELTS. KHOLBA DEPOSIT, EASTERN SAYAN, RUSSIA

Zhmodik, S.M.(1); Dobretsov, N.L.(1);Mironov, A.G.(2); Roshchektaev, P.A.(3); Karmanov, N.S.(2); Kulikov, A.A.(2); Nemirovskaya, N.A.(1) & Ochirov, Y.Ch.(2)
(1) Inst. of Geology SB AS, Novosibirsk, Russia
(2) Inst. of Geology SB AS, Ulan-Ude, Russia
(3) Okinskaya Expedition, Mondy, Russia

Abstract: The spatial distribution, chemical and micro-component composition of gold ores of Kholba deposit have been studied using local analysis methods (autoradiography, microprobe) together with spark source mass-spectrometry. According to the data of complex study of Kholba deposit the gold mineralization has been established to be formed due to primary hydrothermal-sedimentary gold enrichment of black shales and following metal redistribution in processes of metamorphism and rock deformation. the additional portion of ore component has been brought or redistrinuted during granite melt interaction with ophiolite complex rocks and black shales.

Discovery of large gold ore deposit at Kholba is a bright example of application of the theories about possibility of a primary gold accumulation during the processes of volcanogenic and hydrothermal-sedimentary depositiong and secondary redistribution of gold. Prospecting of Kholba deposit of quartz--vein type resulted in discovery of thin quartz veins with irregular gold distribution and low gold volume. Having supposed the stratification nature of ore bodies and therefore having changed the prospecting thinking we succeeded to reveal the extended mineralized zones with rather stable content of ore component and increasihg of gold volume in ores.

Kholba deposit located in the south eastern part of the East Sayan within the Caledonids. Kholba ore field is composed with: 1) Archean-Lower Proterozoic rocks of Gargan block basement complex; 2) Riphean-Vendian schist-carbonate complex of the basement's cover; 3) Upper Proterozoic ophiolitic rock association of tectonic nappe; 4) Barungol volcano-plutonic complex of paleovolcanic structure; 5) Lower-Middle Paleozoic intrusions of Sumsunur plagiogranite complex; 6) Kholba fault zone.

The complicated polygenic and polychronous zoned metamorphic rock complex formed due to combination of regional, contact and dislocation metamorphism processes, was established within the ore field.

The morphology of Kholba ore bodies is defined by the structure of steep dislocated packages of Au-bearing sedimentary and volcanic-sedimentary rocks and sulphide horizons and their related zone of schistosity amd metasomatic alterations of Au-quartz ores. Combination of these types gives a complicated distribution picture of Au-ores and defines formation of the two main types of ore bodies: 1) mineralized zones and 2) vein-like ore bodies. Within mineralized zones there are: 1a- bedded-banded ores with interlayered sulphide mineralization; 1b- massive lense-like pyrite, pyrite-polymetal and lense-like-banded metasomatic ores; 1c- veinlet-impregnated ores presented by beresites, sulphidized quartz mylonites and Mu-Qu-Ab metasomatic rocks (so-called listvenites).

The spatial distribution of gold in Kholba ores has been studied by neutrone-activation beta-radiography method. Au may hav the various modes of occurrence inside sulphide minerals, within their fractures, over their surface or inside quartz and carbonate but immediately close to sulphides.

The banded Au-distribution in bedded-banded ores related to schists, sulphidized limestones and siliceous rocks is most typical. The banded structure is stipulated by both the rhythm alternating of sulphide and silicate minerals in ores and regularly oriented Au-distribution inside homogenous sulphide aggregates (Fig.1) Deformation of such ores and formation of different order folds result in re-distribution of gold with corresponding enrichment of saddle parts of folds and fractures parallel to axial surfaces of folds. More homogenous Au-distribution is typical of the massive pyrite and pyrite-polymetal ores related to metasomatic re-distribution of ore material. Moreover, the dependence of granulometric Au composition on dimensions of sulphides composing the ores of this structural-morphological type is clear. Veinlet-impregnated character of Au-distribution is established in metasomatically altered beresitized, sulphidized rocks and rocks with Qu-mineralization. In beresites the Au- enrichment of peripherical parts of sulphide veinlets was fixed. Rather large grains of native gold are usually related to the ends of quartz-sulphide microveinlets in beresites. The highest unregular Au-distribution is noted in quartz veins.

At a whole, homogenous Au-distribution is established for disperse pyrite, pyrrotine and polymetal ores. Unregularity was caused by micro-gold occurrence within the marginal parts of opal-like quartz, such phenomenon being fixed everywhere in disperse ores with ovoids of opal-like quartz. Au-association with periphery parts of rounded quartz grains can be explained by the primary opal enrichment in fine-disperse gold. Thermal affect, dynamometamorphism and following recrystallization of siliceous material have resulted in gold cleaning and moving away to the edge parts of opal-like quartz ovoids. Such enrichment is fixed in ores with sings of sulphide mass deformation and rotation of ovoids and without them.

Despite the correlation between Au and As their occurrences in ores do not always coincide. Arsenicum concentrates in the separate zones of pyrite, but gold can be oserved both in As-bearing parts of pyrite and outside them or on the boundary of zones. Correlation revealed is explained by more common causes. They are predominantly occurrence of Au and As and their connection with iron sulphides and polymetals (first of all - pyrite). Basing on autoradigraphy study the conclusion about Au-occurrence in ore deposits mainly in nativ form under its high dispersity was made.

Combination of autoradiography and microprobe techniques allowed evaluation of various chemical types of gold within deposit. Histogram of native gold composition compiled using 2322 microprobe analyses of individual gold grains (Fig.2) fixes concentrational range from 0.3-0.5 ro 99.6% of Au with the gap in area of 5-16% Au. Histogram's habit is polymodal with maximums C_{Au}=23-24%, 40-41%, 47-48%,, 54-55%, 93-95% and a series of superimposed peaks from 48 to 84%. Native gold composition estimated in thin-sections (8-15 cm^2) from the different mineral types is highly variable: Ag-content ranges from 40 to 79% of Au. The findings of native silver with 0.3-0.5% of Au in quartz metasomatic vein and with 53-83% of Au (in gold grains) in sphalerite-pyrite ores notes the extreme irregularity of gold.

Apart from the native form of gold and silver the following minerals of these elements were established on deposit by means of microprobe analyses: hessite, uytenbogaardite, akantite, argentite, pyrargirite, stromeyerite.

The study of native gold chemical composition, known to be the main typomorphic sign provided the dustinguishing of the six gold-bearing mineral assemblages: carbonate, quartz-pyrite (100-84% Au); carbonbate-quartz-pyrite with subordinate amount of minerals of polymetals (84-70% Au); quartz-carbonate-pyrite-polymetal (70-58% Au); carbonate-quartz-pyrite-pyrrotite-polymetal rarely with tellurides (57-43% Au); pyrite-chalcopyrite-quartz-galena (44-38% Au); quartz-carbonate-chalcopyrite-pyrite-galena (<42% Au). Silver minerals are observed in latter three assemblages. The quality composition of minerals in associations distinguished do not change, but their quantity interrelations do.

On the whole deposit the maximum abundances of gold were established in pyrite and quartz. In other minerals (carbonate, galena, chalcopyrite, sphalerite, pyrrotite) the gold frequency factor is lower. It confirms that the main amount of gold on deposit could not be formed by gold-bearing solutions superimposing on earlier existed sulphide mineralization.

The main peculiarity of native gold of Kholba deposit, revealed due to mass-spectrometry study, is high irregularity of micro-element composition of gold. So, sixty analysed gold grains were not enough to describe the main tendencies and to reveal causes of such irregularity. Concentrations change: $6*10^{-4}$ to $2550*10^{-4}$ for Cu, $(0.5-0.8)*10^{-4}$ to $601*10^{-4}$ for Sb, $26*10^{-4}$ to $2790*10^{-4}$ for Hg, 0.0 to $(0.7-33.4)*10^{-4}$ at.% for Pd. Content variations of othere elements: Te, Fe, S, Cl, K, Ca, Ti, Cr, Ni, Pb, Bi p first of all fix the mineral inclusions in native gold and, hence, conditions of their formation (Fig.3).

The gold mineralization has been established to be formed due to primary hydrothermal-sedimentary gold enrichment of carbonaceous deposits and following later metal redistribution in processes of metamorphism and rock deformation. The additional portion of ore component has been brought while granite melt interacting with ophiolite complex rocks and black shales. The signs of hydrothermal- sedimentary nature of such mineralization are following: 1-spatial relation of ore mineralization to carbonaceous deposits and ophiolites, as well as participation of ultramafic rocks in ore process; 2-wide spread of banded and bedded types of spatial ore distribution in ores; 3-occurrence of paradox mineral associations: pyrrotite, uytenbogaardtite, marcasite, pyrite; 4-isotopic composition of sulphide sulphur close to meteorite content; 5-abundance of disperse sulphide ores with ovoids of chalcedone-like quartz enriched in gold; 6-occurrence of silver minerals: akantite, argentite pyrargirite, stromeyerite, hessite; 7-high dispersity of gold: from 1 up to 10 mkm comprise 90%; 8-occurrence of low-standard gold and native silver.

The signs of polygene ore mineralization are following: 1-interaction of fluid-saturated granitoids with gold bearing black shale deposits and ophiolite complex rocks, with further formation of hybrid rocks and metasomatic rocks of berezite-listvenite type; 2-ore mineralization relation to dynamic metamorphism zone; 3-occurrence of minerals (sulphides) either with sings of a growth under dynamic metamorphism or (and) with signs of current or displacement of earlier existed sulphide materiel; 4-variety of spatial gold distribution types in ores. Besides bedded and banded types there are veinlet-impregnated spotted and homogeneous types of spatial gold distribution with gold enrichment of saddle parts of ore folds, fractures being parallel to axis surfaces of folds

and veinlet salbands; 5-native gold relation to various minerals; pyrite, quartz, carbonate, galena, sphalerite, pyrrotite, chalcopyrite, seldom graphite; 6-variety of native gold morphological types: drop-like, lens-like, sphere-shaped, angular, lump-like and film types, crystals and others; extremely heterogenic composition of native gold: from native silver and custelite up to rather high-standard gold (99,6% of Au); 7-variety of trace elements in the native gold: Cu, As, Hg, Te, Pd, C, U, Ni, Cr etc.

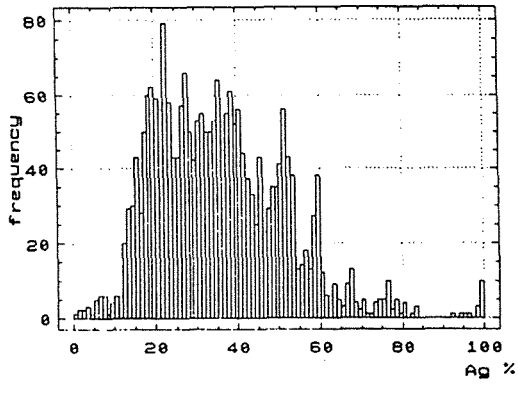

Fig.1. Frequency histogram of native gold chemical composition (Ag) of Kholba deposit.

Fig.2 Activation beta-autoradiogram, fixing gold distribution in banded pyrite ore with banded disperse gold distribution (1-10 mkm).

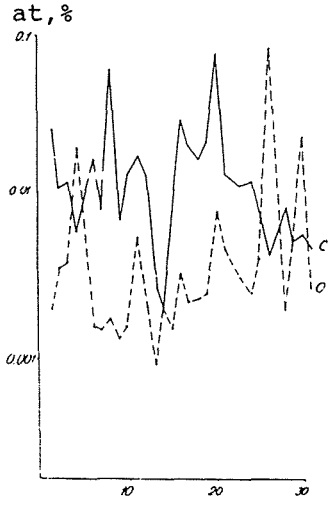

Fig.3. Distribution of C and O in gold grain (data of the layer after layer spark mass-spectrometry analyses. The sample is prepared as an electrode. Abscissa-number of analyzed layer gold; ordinate - the concentration of C and O.

2 Massive and stratabound sulphide deposits in volcanic and sedimentary sequences

Current Research in Geology Applied to Ore Deposits. Fenoll Hach-Ali, Torres-Ruiz & Gervilla (eds) (1993). ISBN 84-338-1772-8

ORE MINERALOGY OF THE ZECHSTEIN COPPER DEPOSITS, POLAND

Banas, M. & Salamon, W.
University of Mining and Metallurgy, Al. Mickiewicza 30, 30-059 Kraków, Poland

16 elements form respective ore minerals, another 6 metals occur as isomorphic substitutions or organometallic compounds. Textures and structures of the ores, mineral parageneses, vertical and horizontal distribution of ore minerals and elements and secondary alterations of ore mineralization are discribed.

Cu, Fe, Pb, Zn, Co, Ni, Ag, Au, Pd, Mo, Bi, Hg, Ge, U, As and Se form their respective minerals in copper ore deposits at the Fore-Sudetic Monocline. Such elements as V, Cd, Re, Pt, Sn and Sb are present as isomorphic substitutions or organometallic substances. Sulphides are the most common ore minerals. Sulphosalts and arsenides and sulphoarsenides are less abundant. Native metals and amalgams, however present in small quantities, are common minor constituents in the deposit. Selenides, organometallic compounds, arsenates and thiosulphates occur locally. Occasionally oxides and hydroxides are found.

Most of sulphides are cupriferous. They are always main minerals in the ore-zone of the Cu-bearing Permian of the Fore-Sudetic Monocline. Some of the Cu-sulphides are widely non-stoichiometric, particularly those of the bornite and chalcopyrite.
Galena and sphalerite are ubiquitous. They are present mainly in the carbonate rocks of the upper sections of the ore-horizon, but can also be found in Pb- and Zn-bearing shales.

Silver minerals are economically very important, with stromeyerite being the main mineral. Molibdenite and castaingite are also common. Sulphides of Ni, Co, Bi and Ge are less abundant.

In some parts of the deposit sulphosalts, namely tetrahedrite-tennantite and enargite-luzonite, are found very often. The first two usually carry Bi and Hg.

Arsenides and sulphoarsenides, common in the entire mineralized area, are usually present in smaller amounts or only as traces. The most common of the above mentioned are minerals of the cobaltite-gersdorffite series. Palladium arsenides are observed only locally.

Native metals are represented mainly by silver, electrum, plumbian gold and Ag-Hg amalgams. Native silver is present in all of the mineralized sections and is economically important in silver production. Also gold is recoverd during silver refining.

Selenides of Pb, Hg, Cu and Bi occur in trace amounts.

A more recent research (H. Kucha) indicates the presence of Co-Ag-As-Fe thiosulphates cementing framboidal pyrite and Cu-Fe thiosulphates intergrown with chalcopyrite. These compounds seems to be very common in the deposit, however their physical and chemical properties are poorly known.

Arsenides, mainly of Co and Ni, are rare. Also rare are chlorides. The organic substance contains refractory metals Cu, Fe, V, Mo, Ni, Hg as well as Pt, Pd and Au (H. Kucha, W. Salamon). Thucholite, rich in uraninite inclusions, is common in middle sections of the ore-horizon. The thucholite contains organic compounds of Pt and Pd (H.Kucha).

Oxides and hydroxides of Fe are observed mainly in these sections of the ore-horizon, which are intersected by faults and strongly sheared.

A majority of ore minerals is present in microscopic sizes. Sulphides seen in hand specimens are epigenetic and form a subordinate part of ore mineralization. Accumulations of ore minerals are polycrystalline. Ni-Co minerals have a strong tendency to occur as small inclusions in Cu-sulphides.

Cu-sulphides form infillings and cements in sandstones. Finely-dispersed impregnations, laminae of cloudy sulphides and sulphide streaks are most common structures in black shales. Nests, lenses and small veinlets are most typical sulphide structures in carbonates.

Sulphide minerals, exept of Ni, Co and sometimes Pb, Zn and U, are xenomorphous. Metacolloidal textures associated with pyrite, pitchblende and castaingite are rare. Replacements of rock-forming minerals by sulphides are common.

There are 3 main types of mineralization at the Fore-Sudetic Monocline: Cu-Fe-S, Cu-S, Pb-Zn-Fe-S. The Cu-As-S type of ore mineralization is less common.

Copper sulphides constitute a major portion of ore mineralization and are present in white sandstone, black shale and overlying calcitic-dolomite. The ore-horizon is discordant to stratigraphic bounda-

ries. Fe-sulphides have similar vertical distribution as Cu-sulphides. Pb and Zn occur in upper sections of the ore-horizon above Cu ores and in Pb- and Zn-bearing shales. Silver minerals are typical of the middle parts of the vertical profile. Co, Ni, Mo and Hg minerals are found only in Cu-bearing shale. Bi, Au and Pd minerals are present in the boundary dolomite and at the bottom part of the black shale. In similar manner minerals of U and selenides of Pb, Hg and Bi occur. In general, the occurrence of minerals of elements associated with copper are restricted to black shale, locally present boundary dolomite and the topmost part of the white sandstone.

Stratiform Permian mineralization at the Fore-Sudetic Monocline is characterized by a significant variability. The Cu-Fe-S mineralization occurs in the SE part of the Monocline, while the Cu-S type is observed in its central part, but it encompasses patchy areas of bornite-chalcopyrite mineralization. Often both types of Cu-sulphide mineralization can enclose tracts of tennantite rich ore. The latter extend up to several tens of meters appearing erratically through the ore-field or following faults. The horizontally extensive Pb-Zn-Fe-S areas are up to several hundred meters wide and occur mainly in the NE part of the Monocline. Silver is present mainly in the SE area of the Monocline. Similar pattern is shown by Ni and Co, Hg as well as Au, Pd, Bi, U and Mo.

Stratiform copper ores of the Fore-Sudetic Monocline show variable but significant alterations. The main changes can be refered to diagenesis and tectonics. Diagenesis brought about remobilization and reconcentration of many elements. It caused evolution of organic matter and disintegration of organometallic complexes, crystallization and recrystallization of sedimentary minerals, transformation of clay minerals, dissolution of some minerals and their precipitation, infiltration of diagenetic fluids and their reactions with ore minerals.

Subsequent tectonic deformations and associated fine fracturing were followed by formation of various veins and veinlets. No rock alterations have been found around them. Mineral assemblages of some of these veins are different from those present in the ore-zone, eg. barite, tennantite, Ni-Co arsenides.

Recrystallization of carbonates created very common nest-like sulphide fillings of intercrystalline spaces within the carbonates.

Diagenetic differentiation of black shales forced sulphides to concentrate mainly in carbonate laminae. In the uppermost part of white sandstone, infiltration sulphides replace earlier cements as well as locally terrigenous grains. The infiltration during diagenesis caused also replacements among sulphides: framboidal pyrite was partly replaced by other sulphides, polymetallic mineralization entered thucholite, and many diagenetic and katagenetic mineral assemblages were formed. Secondary alterations are expressed also by ubiquitous covellinization of copper sulphides.

Current Research in Geology Applied to Ore Deposits.Fenoll Hach-Alí, Torres-Ruiz & Gervilla(eds)(1993).ISBN 84-338-1772-8

METALLOGENESIS OF PARTS OF NORTH GONDWANA DURING THE CAMBRIAN TO EARLY ORDOVICIAN

Boni, M. (1); Bechstädt, T. (2) & Russo, A. (2)
(1) Dipto. Scienze della Terra. Universita` di Napoli, Largo S. Marcelino 10, I-80138 Napoli, Italia
(2) Geolog. Palãontolog. Inst. Universität Heidelberg, INF 234, D-6900 Heidelberg, Germany

Abstract: The Cambrian carbonate to terrigenous ore-hosting sequences in Sardinia, S France and N Spain show differences in the sedimentological evolution, for instance the type of the carbonate platforms. Important similarities exist, however, in respect to the tensional geodynamic setting as well as type and stratigraphic position (mainly Lower Cambrian) of the stratabound mineralizations. The Pb-isotope data of the galenas indicate a common origin (continental crust) of the mineralizations considered.

The Cambrian is a well known metallogenetic period in North-Gondwanan areas (Sardinia, Montagne Noire, N Spain), where stratabound ores occur in carbonate rocks of Early to early Middle Cambrian age. Strong synsedimentary tensional tectonics, associated with deep reaching faults, is very distinct. It is sometimes difficult to separate tectonic and eustatic signals. An example is the interval at the Early/Middle Cambrian boundary, where a distinct ("eustatic") sea level rise is evident, in some areas masked by clear tensional effects. The tectonic regime during the Early Cambrian can be related with an intracratonic rifting situation and/or with early stages of a passive margin setting. This can be deduced not only from the facies associations, but also from the types of ores (Sedex to MVT).

SW-Sardinia: The Cambrian sequence in Sardinia (Fig.1a) follows different evolutionary stages (Bechstädt & Boni, 1989). These are from base to top: Nebida Group: (1) Terrigenous-carbonate homoclinal ramp (Matoppa Fm.); (2) Carbonate-terrigenous ramp or rimmed shelf, prograding westwards and slowly aggrading to sea level (Punta Manna Fm.). Gonnesa Group: (3) Isolated carbonate platform, aggraded to sea level, rimmed by basinal areas in the west and east (Santa Barbara Fm.), marked by slumps, debris flows and local megabreccias; (4) Isolated, flooded platform (San Giovanni Fm.). Iglesias Group: (5) Segmentation and complete drowning, due to an "eustatic" sea level rise. This is indicated by the fossil-rich, calcareous shales to nodular limestones of the Campo Pisano Fm. (Middle Cambrian). (6) Deep water clastics (shales to sandstones) of the Cabitza Fm.(Middle Cambrian to Early Ordovician).
The mineralizations show a distinct relation with the above mentioned periods of platform instability. The ores consist of: (A) massive sulfides (Zn>Pb) and barite occurring in the upper Punta Manna to lower Santa Barbara Fms., in the transitional interval between stages 2 and 3. The mineral occurrences consist of mainly pyrite and sphalerite, with minor amounts of galena. The ores are syngenetic or early diagenetic (Sedex), as confirmed by field observations, petrographic data and both Sr and S isotopic data. The ores could have been deposited from solutions discharging to the sea through structurally controlled feeder zones. (B) significant concentrations of, sphalerite-galena, are contained in the upper parts of the San Giovanni and Campo Pisano Fms. within micritic limestones. Brecciated sediments of evolutionary stage 4, situated in marginal areas to the platform, host late diagenetic to epigenetic ores (possible MVT).

Montagne Noire: Cambro-Ordovician sediments occur on the northern and the southern side (Fig. 1b). In the south, sedimentation starts with a mainly terrigenous sequence (Orbiel Fm.)(Courjault-Radé and Gandin, 1988) containing limestones and, at its top, volcanic products. Tectonic instabilities caused the change to a typical Early Cambrian carbonate platform (La Clamoux Fm.), followed by carbonate-terrigenous sedimentation. Again the platform was drowned at the passage from Early to Middle Cambrian, as indicated by nodular fossiliferous limestones, followed by deep water terrigenous sediments (Barroubio Fm.). The ore-bearing horizons in the Lower Cambrian sequence never reach the economic values of Sardinia. In the alternances of the Orbiel Fm. disseminated pyrite with associated galena and sphalerite occur as well as some lenses of massive sulphides. The latter are sometimes associated with (possibly epigenetic) native gold and show spatial association with basic volcanites. The transition between Orbiel and La Clamoux Fms. is characterized by a Zn geochemical anomaly in the limestones and by small PbS occurrences in the black shales.

Northern Spain: Here two areas are of main metallogenetic interest: the Western Asturo-Leonesian (WALZ) and the Cantabrian zones. In the WALZ, Cambrian sedimentation (Fig. 1c1-1c2) starts with a shallow marine to continental terrigenous sequence containing carbonate intercalations in its lower part (Candana Group; Perez Estaun et al. 1990).

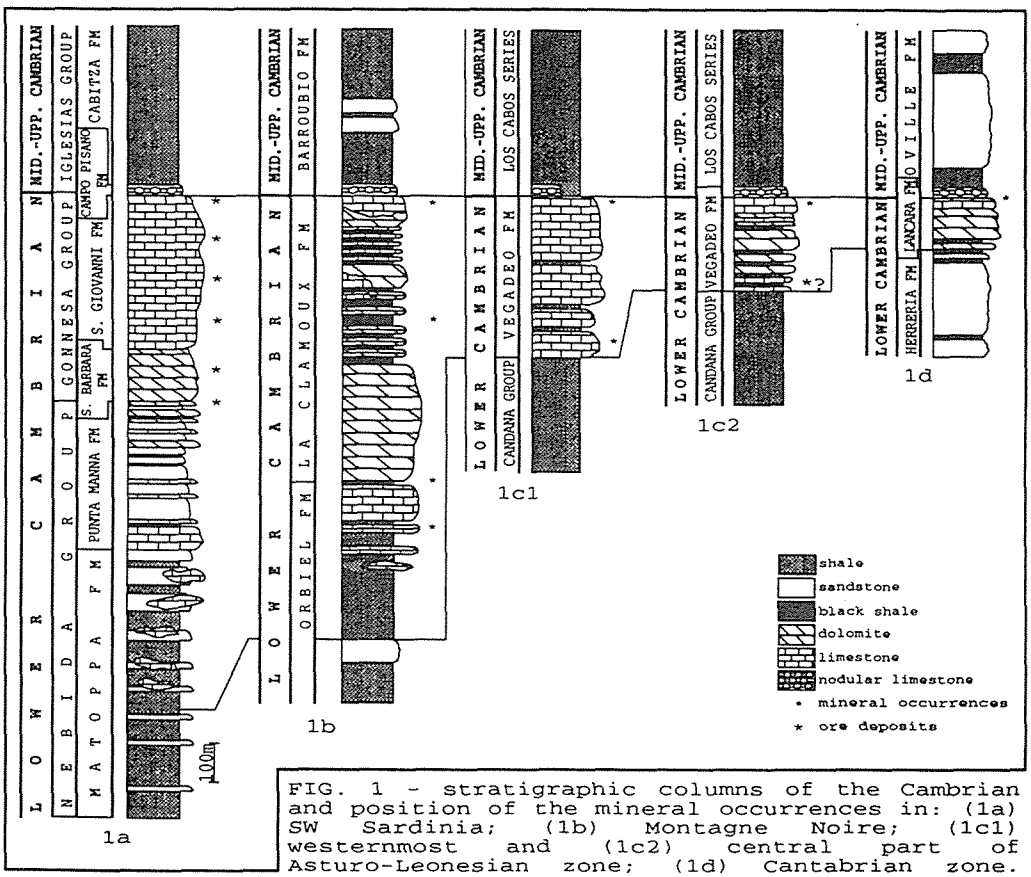

FIG. 1 - stratigraphic columns of the Cambrian and position of the mineral occurrences in: (1a) SW Sardinia; (1b) Montagne Noire; (1c1) westernmost and (1c2) central part of Asturo-Leonesian zone; (1d) Cantabrian zone.

The limestones of the Vegadeo Fm.follow, with a transitional interval (Capas de Transito) at its base. The carbonate sequence is drowned with the terrigenous Los Cabos Series (Middle Cambrian to Arenig).
The Vegadeo Fm.consists of two distinct facies belts: (a) In the western part of the WALZ, the lower Vegadeo Fm. is indicative of outer parts of a tidal homoclinal ramp where terrigenous input was low. In the upper Vegadeo Fm., this barrier prograded and the area shallowed. The western WALZ then corresponded to inter-supratidal inner parts of a carbonate platform. (b) In the central WALZ, the carbonates of already the lower Vegadeo Fm. are indicative of intertidal inner parts of a ramp. The upper part of the Fm., due to a relative sea level rise, consist of subtidal laminated dolomites, shallowing upward into intertidal limestones. Fossiliferous limestones at the top of the Vegadeo Fm.again indicate the Middle Cambrian drowning event. These beds are equivalent to the Campo Pisano Fm. in Sardinia, the upper part of the Lancara Fm in Cantabria (see below) and the lower part of the Barroubio Fm. in Montagne Noire.
The most important Zn-Pb orebody in the WALZ, the now worked out Rubiales deposit, related to the Hercynian metallogenesis (Arias & Tornos in press), occurred within the Lower Cambrian Transition Beds. Two other mineralized levels are important, although of lower economic interest: A stratiform horizon is situated in the lower part of the Vegadeo Fm.; the ore minerals consist of sphalerite, galena and pyrite. In the second horizon, situated at the top of the Vegadeo Fm., the ore minerals consist of galena, sphalerite, calcopyrite and pyrite, disseminated in a silicified lithotype, replacing the Lower- to Middle Cambrian carbonates. These mineralizations have been interpreted so far (Ribera et al., 1991) as ranging from synsedimentary or early diagenetic (sedimentary-exhalative) to late diagenetic.

In the western parts of the Cantabrian zone a complete Cambrian sequence (Fig. 1d) is present. It consists (from base to top) of: Terrigenous clastics and dolomites of the Herreria Fm., deposited in a deltaic environment (Perez Estaun et al. 1990), gradually pass into the Láncara Fm. Mainly tidal carbonates of its lower part (Zamarreño, 1975) are followed by nodular limestones. This is indicative of the Middle Cambrian drowning. Deep water terrigenous clastics (Oville and Barrios Fms., Middle Cambrian to Early Ordovician) follow.
Some small stratabound occurrences, consisting of sphalerite, galena and barite, are present in the upper part of the Lancara Fm. (Luque et al., 1990). Their stratigraphic position is the same as the ores at the top of the Vegadeo Fm. in the Asturo-Leonesian Zone.

Lead isotopic data: The Pb-isotopic ratios for the stratabound ores in the Cambrian carbonates have been compared between Sardinia (Boni and Köppel, 1985), Southern France (Brévart et al., 1982) and Spain (Arias and Tornos, in press; and own data). The concentration fields (Fig. 2), corresponding to low-radiogenic galenas, are almost perfectly overlapping in the three areas: This is indicative of the same origin (continental crust) for Pb. For the Sardic and French stratabound ores an Early Paleozoic ore-emplacement is considered, whereas some of the mineralizations of Northern Spain (among those Rubiales) are thought to be Hercynian in age. The Sardic or the French "Hercynian" galenas, however, show different concentration fields, indicating an external contribution of Hercynian Pb. This can be ruled out for the considered "Hercynian" deposits of Northern Spain, notwithstanding metamorphism and later circulation of hydrothermal fluids.

FIG.2 - Pb-isotope diagrams with the evolution curves of Stacey and Kramers (1975). The three fields correspond to the three mineralized districts: 1. SW Sardinia; 2. Northern Spain; 3. Montagne Noire

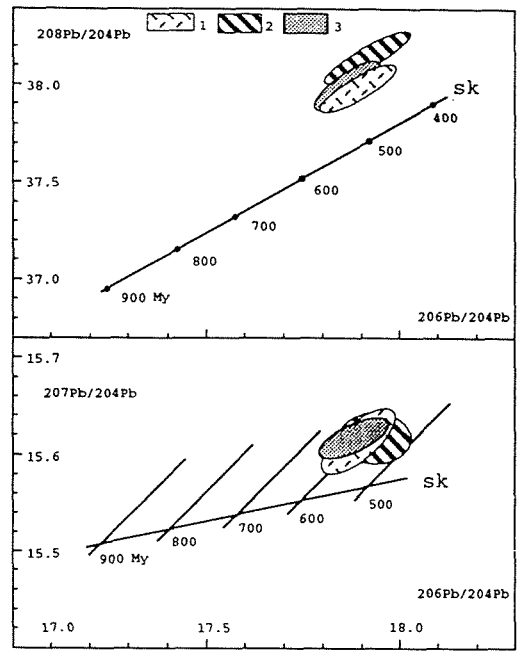

REFERENCES

Arias, D. & Tornos, F. in press. Sulphur and lead isotope geochemistry of the Rubiales Zn-Pb ore deposit (NW Spain). European Journal of Mineralogy.

Bechstädt, T. & Boni, M. 1989. Tectonic control on the formation of a carbonate platform: The Cambrian of south-western Sardinia. In Crevello, P.D. et al. (eds.) Controls on carbonate platform and basin development. Soc. Econ. Paleont. Miner., Spec. Publ. 44:107-122.

Boni, M. & Köppel, V. 1985. Ore lead isotope pattern from the Iglesiente-Sulcis area (SW Sardinia) and the problem of remobilization of metals. Miner. Deposita. 20:185-193.

Brévart, O., Dupré, B. & Allègre, C. J. 1982. Metallogenic provinces and the remobilization process studied by lead isotopes: lead-zinc ore deposits from the Southern Massif Central, France. Economic Geology. 77:564-575.

Courjault-Radé, P. & Gandin, A. 1988. Metallogenesis and geodynamic context in the Lower-Middle Cambrian of Montagne Noire (France) and Sardinia (Italy). In Boissonas, J. & Omenetto, P. (eds.) Mineral deposits within the European Community. Springer Berlin Heidelberg New York, pp. 428-442.

Luque, C., Martinez Garcia, E. & Ruiz, F. 1990. Part II: Cantabrian and Palentian zones, 5 Metallogenesis. In Dallmeyer, R. D. & Martinez Garcia, E. (eds.) Pre-Mesozoic geology of Iberia, Springer Berlin Heidelberg New York, pp. 80-87.

Perez Estaun, A., Bastida, F., Martinez Catalan, J. R., Gutierrez Marco, J. C., Marcos, A. & Pulgar, J. A. 1990. Part II: Cantabrian and Palentian zones, 2 Stratigraphy. In Dallmeyer, R. D. & Martinez Garcia, E. (eds.) Pre-Mesozoic geology of Iberia, Springer Berlin Heidelberg New York, pp. 92-102.

Ribera, F., Tornos, F. & Locutura, J. 1991. Las mineralizaciones estratoides de Zn-Pb de la serie de Vegadeo en la zona de Ponferrada (zona Astur Occidental Leonesa, NO de España). Geogaceta, 11.

Zamarreño, I. 1975. Peritidal origin of Cambrian Carbonates in Northwest Spain. In Ginsburg, R. N. (ed.) Tidal deposits: A casebook of recent examples and fossil counterparts. Springer Berlin Heidelberg New York, pp. 323-332.

Current Research in Geology Applied to Ore Deposits. Fenoll Hach-Alí, Torres-Ruiz & Gervilla (eds) (1993). ISBN 84-338-1772-8

RAPID SILL-SEDIMENT COMPLEX FORMATION: THE CAUSE OF SUPER-GIANT MINERALIZATION AT RIO TINTO?

Boulter, C.A.
Dept. of Geology. The University, Southampton, U.K. SO9 5NR

ABSTRACT: The volcanogenic sequence that hosts the Rio Tinto super-giant massive sulphide is a sill-sediment complex with a very high sill to sediment ratio. Ubiquitous evidence for magma wet-sediment interaction requires that the bulk of the sills were intruded contemporaneously under an unconsolidated cover of around 100m. Pronounced basin floor deformation resulted from thickness variations in the complex on the order of 400m which generated topography on a similar scale. Because the intrusive sheets placed a lid over high temperature hydrothermal circulation systems triggered by the intense magmatic pulse, discharge would have been considerably focused on a limited number of sites. Coincidence of these and troughs in the deforming sea floor created major stratiform sheets.

The Rio Tinto volcanogenic massive sulphide is unusual in the VMS class because the host sequence represents a very limited melt thickness. Despite this it is the biggest deposit in the class and the Iberian Pyrite Belt is the largest repository of massive sulphide in the world. Rio Tinto is also unusual in the extent of magma wet-sediment interaction that is evident in the mineralized environment. Much of the stratigraphic unit known as the Volcano-Sedimentary Complex that contains the deposits is a sill-sediment complex. The upper part of the complex is either a single quartz porphyry sheet up to 600m thick or a series of branching sheets each on the hectometric scale. Rafts of sedimentary rock within the acid porphyry show that it was emplaced as a series of finger-like intrusions. West of Rio Tinto the sense of asymmetry of these sedimentary screens means that the acid sheet cuts up section and is regionally slightly discordant. The lower part of the sill-complex is mainly dolerite intrusives with a very variable sill to sediment ratio ranging upwards from 5 to 1. In one section the basic portion is virtually a single dolerite sill 300m thick that includes very minor sedimentary screens.

Evidence for coeval magmatic intrusion and sedimentation (cf. Guaymas and other sedimented ridges) is abundant in the form of interaction between fluidised sediment and brecciated magma. About 70% of igneous/sedimentary contacts are characterised by peperites (Fig. 1) commonly only a few metres thick but, where contact relations involve rafting of country rock, peperite zones extend for many 10s of metres (e.g. Corta Atalaya). The majority of the peperites have the classic form of in situ mixtures of brecciated magmatic rock with jig-saw fit patterns and a sedimentary matrix. The slight regional discordance of the large acid sheet and some local more abrupt steps across the country rock, brought acid magma into contact with a variety of sediment types. Accordingly the peperite style is controlled by the nature of the host; interaction was greatest where magma injected mud and minimal against gravel. Globular peperite is very rare but several porphyry-mud contacts are characterised by dispersal of igneous fragments in the host sediment. Columnar cooling joints have been penetrated for 10s of metres but the extent of penetration of slurried mud is much greater in breccia dykes which are up to 200m in length in acid sheets. More coherent clastic dykes are rarely abundant but some form discordant sheeted intrusions into host igneous intrusions. Many of the sedimentary screens within the acid sheets are semi-continuous and internally are commonly cut by abundant

sub-concordant magmatic intrusions. Sharp truncation of sedimentary layering demonstrates replacement of fluidised sediment by magma. To fill the breccia dykes, peperite breccias, and cooling joints, requires considerable volumes of sediment and this leads to intrusion erosion of the muddy parts of the host rock.

Internal brecciation of the acid intrusions is widespread and the lateral change from peperite to a monomict porphyry breccia shows a genetic link. The monomict breccia is an intrusive hydroclastic breccia and was probably formed by steam generated in the peperite zone penetrating further into the intrusive than the slurried sediment. Alteration is clearly associated with this process as the matrix is typically strongly cleaved and chloritised relative to cores of little affected porphyry. The resultant rock has been interpreted as pyroclastic rather than hydroclastic in origin. Alteration along sill margins and around sheeted sedimentary dyke swarms is also attributed to processes associated with magma wet-sediment interaction. The chemical and mineralogical changes are currently being investigated.

Because this widespread magma wet-sediment interaction took place in a sill-sediment complex with very minor sediment, the large dolerite and QFP sills must be very closely related in time. DSDP drilling in the Guaymas shows that sills expel pore fluid from contact zones equivalent to sill thickness. A progressive build up of the Rio Tinto complex would have dewatered the sedimentary screens before the next intrusion preventing any further fluidisation of sediment. Immediately before the main phase of intrusive activity, distinctive acid intrusions outside the Rio Tinto area generated large volumes of hydroclastic detritus when they became extrusive. This event involved a microporphyritic QFP and a quartz poor, coarsely feldspar phyric, QFP. Very high-level intrusions commonly break down their cover of wet-sediment and by this means can form a major sediment source. This event produced a sedimentary sequence dominated by gravel-grade volcaniclastic rocks in largely disorganised beds between 10 and 30m in thickness (Fig. 2). These debris flow deposits mainly contain highly angular fracture-bound clasts of porphyry (hydroclasts) with some clasts of peperite, hydroclastic breccia, and silicified iron-rich mudrock. A small percentage of clasts are highly irregularly shaped as a result of plastic deformation suggesting they were transported whilst very hot.

There is considerable field evidence in the Rio Tinto district that acid and basic magmas coexisted in the same magmatic plumbing system. The major acid and basic sills that form more than 85% of the sill-sediment complex were emplaced essentially synchronously. One locality in the Odiel River WNW of Rio Tinto records back-veining of acid magma into basic along a QFP/dolerite contact showing that both phases were emplaced before either solidified. Several varieties of acid porphyry also coexisted as indicated by the mingling of these magmas commonly seen on the margins of the main phase acid sills. The major acid sills underlie the sequence of resedimented hydroclastic breccias east of Rio Tinto but regional discordance gradually transfers this volcaniclastic package to below the QFP sills. In the Odiel River dolerite intrudes these acid derived breccias and demonstrates that the main pulse of acid plus basic magma post-dated some acid magmatism. Such relations have been erroneously interpreted as cycles.

The combined field relations indicate an unusually high rate of magma supply to the near surface especially in the pulse that created the bulk of the sills. Cover thickness was probably less than 100m during the main intrusion event and may have been much less; quantification is difficult because of intrusion erosion of wet sediment. Aggregate thicknesses for the sill-sediment complex vary from 400 to 800m and in view of the thin cover most of this variability must have been

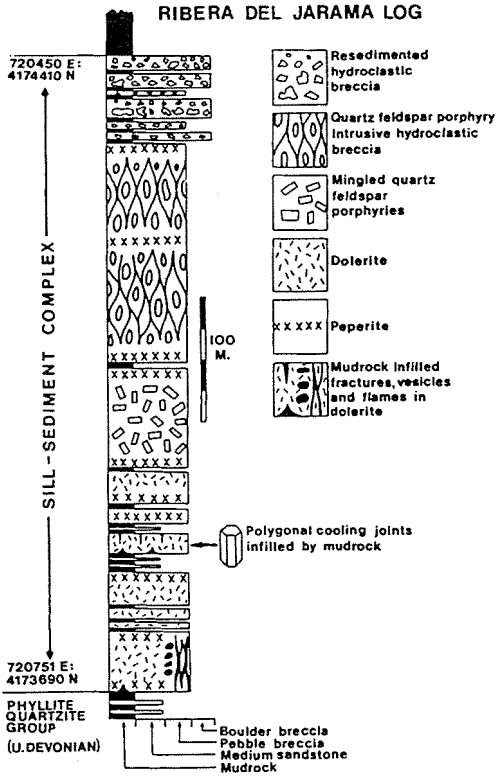

Figure 1 A simiplified graphic log of the most continuous exposure through the sill-sediment complex in the Jarama River east of Rio Tinto. Intrusions are shown at a uniform grain size.

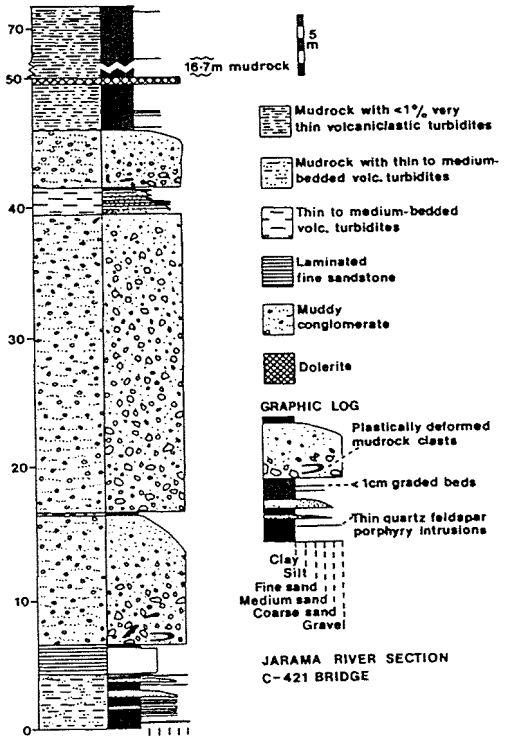

Figure 2 A measured section through an example of the resedimented hydro-clastic breccias to show the bed characteristics of these disorganised gravels.

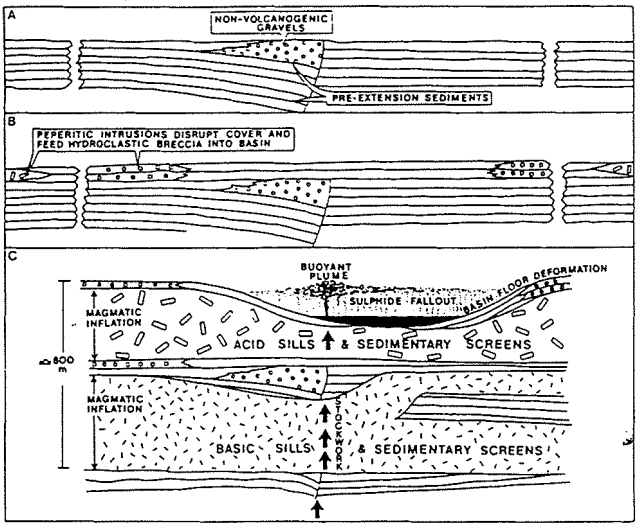

Figure 3 Schematic cross-sections illustrating the evolution of the Rio Tinto sill-sediment complex. Wedge shaped units of non-volcanogenic gravels possibly mark extension that led to the magmatic activity. Part (C) shows the major inflation of the sequence during the rapid formation of the main sills.

expressed as sea floor deformation (Fig. 3). Magmatic pulses in sedimented ridges (e.g. Escanaba Trough) have produced steep sided laccoliths and relief on the 100m scale. At Rio Tinto there is an inverse relation between sill complex thickness and mineralization. Basin floor deformation due to varying amounts of magmatic inflation appears to have created a topographic trap for exhalative hydrothermal plumes and played a major role in forming extensive stratiform sheets.

In the currently forming sill-sediment complex in the Guaymas there are two distinct hydrothermal systems, one low temperature driven by expulsion of fluids adjacent to sills; the second is a high temperature system driven by magma chambers or feeder dykes to the higher level sills. A key aspect of the latter is that the sills placed a lid over the hydrothermal convection cells and considerably restricted opportunities for discharge which tended to be focused on a limited number of sites. Because of the extensive nature of the Rio Tinto sill-sediment complex this interference with the expected pattern hydrothermal circulation would have been even more pronounced. The coincidence of highly focused discharge and an evolving topography to contain the plumes has created the world's greatest massive sulphide deposit.

Current Research in Geology Applied to Ore Deposits.Fenoll Hach-Alí, Torres-Ruiz & Gervilla(eds)(1993).ISBN 84-338-1772-8

ARE SEDEX LEAD-ZINC DEPOSITS AND SEDIMENT-HOSTED STRATIFORM COPPER DEPOSITS GENETICALLY RELATED?

Brown, A.C.
Dept. of Mineral Engineering, Ecole Polytechnique de Montréal, P.O. Box 6079, Sta. A., Montréal, Québec, Canada H3C 3A7

Abstract

Sediment-hosted sedex and stratiform copper deposits (SCDs) are commonly formed in rifted continental environments and their ore-forming fluids may be products of various types of basin sediment diagenesis. Dominantly marine basin fillings may produce dense reduced Pb-Zn-rich brines to form sedex deposits, and dominantly continental red-bed ± basalt rift fillings followed by marine or lacustrine grey-beds may generate oxidizing SCD-forming fluids.

Introduction:

Sediment-hosted stratiform exhalative lead-zinc (sedex) deposits and sediment-hosted stratiform copper deposits (SCDs) differ distinctly in their typical metal base-metal ratios, but by definition, both deposit types are hosted by predominantly sedimentary strata. Furthermore, most descriptions of sedex mineralization since Finlow-Bates (1980) and Large (1980) have related sedex deposits more specifically to sediment-filled cratonic rift basins, and similarly, there have been many recent suggestions that SCDs are hosted by continental rift basins (see, for example, the numerous deposit descriptions and summary articles in Boyle et al., 1989). In both cases, the mineralization is normally considered a normal product of sedimentary basin evolution during and following an extensional tectonic event in continental crust. Given that broadly similar tectonic environments have apparently given rise to two distinctively different deposit types, some basic similarities and differences between these two major mineral deposit types and their environments should be examined in order to reaffirm the separate identities of each deposit type.

Common characteristics of sedex deposits:

1) Known mainly for lead-zinc sulphide zones (commonly grading >10% combined lead-zinc); copper is exceptional; silver is commonly economic. Some deposits consist predominantly of barite with minor base-metal content.
2) Hosted predominantly by marine sedimentary strata: carbonates, carbonaceous shales, turbidites, evaporites, as well as coarse clastic basin-margin units. Coeval igneous activity is absent or minor. If volcanics are present, they are typically bimodal and dominantly mafic. Metamorphism is overprinted, if present.
3) Aside from stockwork zones, the mineralization is typically massive to well-banded, sheet-like, strictly stratiform and conformable to bedding, as in a chemical sediment. Total mineralization commonly consists of several stratigraphically stacked sulphide zones, with tonnages often >100 Mt.
4) A footwall stockwork zone (dominantly silicified, sometimes tourmalinized, chloritized) may underlie the tabular mineralization, especially where shallow depths allowed ore-fluid boiling and the formation of cross-cutting breccia zones. If copper is present, it is most common in this high-temperature zone.

5) At the hand-specimen scale, tabular sulphide zones typically consist of massive bands of fine-grained sulphides interbedded with chert-rich and/or barite-rich bands; thick massive beds (closer to vent) generally thin toward the extremities of ore zones.
6) Synsedimentary sulphides (mainly pyrite and/or pyrrhotite, galena, sphalerite, chalcopyrite) are typically very fine-grained and difficult to separate metallurgically; several large deposits remain unexploited in spite of good base-metal grades. Grain-size may be up-graded by overprinted regional or contact metamorphism.
7) Mineralization may be proximal to district-scale synsedimentary faults which delimit sedimentary basin margins and which probably acted as exhalative feeder channels. Many tabular deposits have no footwall feeder and are considered distal brine pool deposits.
8) Ages of known deposits are predominantly Middle Proterozoic and Early and Late Paleozoic.

From the above, the formation of sedex deposits may be summarized as follows, taken mainly from Large (1983), Lydon (1983) and Sangster (1990).
A tectonically extended epicratonic embayment or intracratonic rift is invaded by oceanic water and filled largely by coarse clastic debris adjacent to the tectonically active rift margins and by marine carbonates, shales, etc. in more distal basin positions. Under the extensional tectonic regime, the rise of asthenospheric material into the thinned crust results in an anomalously high geothermal gradient and an accelerated influx of mantle heat. Trapping of normal to abnormal heat beneath aquicludes (e.g., shale units) in the basin sediments, together with high salinitiies from sediment diagenesis, semi-permeable membrane phenomena, and/or leaching of evaporitic units, would lead to the formation of hot dense pore-fluid brines deep within the sedimentary basin. Temperatures of 200°C would be sufficient to form Pb- and/or Zn-rich brines; copper would accompany lead and zinc only if the brine temperature clearly surpassed 250°C. The brine would be sulphidic due to the predominance of marine sediments in the basin sequence. Generally, the high salinity of the metalliferous brine assures that the potential ore fluid cannot rise and exhale at surface. However, the aquiclude also results in over-pressuring of the pore fluids, as commonly observed in petroleum basins (Hanor, 1979), such that the hot metalliferous brine may escape abruptly to surface if the aquiclude barrier is ruptured, for example, by episodic movements on synsedimentary basin faults. The ascending hot metalliferous brine may boil in shallow marine basins to form brecciated feeders and plume accumulations of sulphides proximal to the vent. Or water depth may be sufficient to prevent boiling, and the ore-fluid density may be greater than seawater such that the fluid exhales and glides into topographic depressions; fine-grained sulphides and chert then precipitate largely by cooling of successive exhalative additions to distal brine pools.

Common characteristics of sediment-hosted stratiform copper deposits

1) A prominent cupriferous zone, commonly grading several percent copper; lead and zinc are rarely abundant; other metals such as silver and cobalt can be very significant economically;
2) Hosted by sedimentary rocks, without apparent need of coeval igneous activity or metamorphism. Immediate host-rock is typically sulfur-rich (pyrite- or gypsum/anhydrite-rich) carbonaceous "grey-beds" and evaporites of marine or lacustrine origin. Footwall strata are coarse-grained continental red-beds. If present, volcanics are bimodal and dominantly mafic. Lithologies are typical of continental rift basin fillings.

3) Cupriferous zone typically lies immediately above the redoxcline between grey-beds and red-beds, and may measure many metres in thickness; the remainder of the grey-beds are commonly sterile, unmineralized pyritic beds.
4) Complete cupriferous zone, including uneconomic mineralized portions, is peneconformable (demonstrably not conformable); ore zones are generally conformable.
5) Remarkably continuous laterally along bedding, giving tonnages commonly measured in 100s Mt, even 1000s Mt.
6) Sulphides are generally fine-grained and disseminated, typically distributed in well-bedded concentrations along the host-rock stratification.
7) Metals and ore minerals are often well zoned, extending from copper-rich sulphides next to the redoxcline, to iron-rich sulphides stratigraphically above. Lead and zinc sulphides may fringe the cupriferous zone.
8) Textures indicate that copper sulphides (mainly chalcocite, bornite, chalcopyrite) were emplaced by post-sedimentary replacement of original syndiagenetic sulphides (e.g., pyrite) and/or sulphates.
9) Deposits are temporally and spatially associated with strata formed in warm arid climates (evaporitic units, red-beds); prominent ages include Middle-Late Proterozoic and late Paleozoic.

The formation of SCDs with these characteristics has been summarized recently by Brown (1992). Most of these features are well-established in an overprint depositional model fundamentally related to the normal development and evolution of continental rift basins in which a dominant footwall continental (red-bed) sequence is overlain by a chemically reduced sulfur-rich (grey-bed) sediment. A low-temperature metalliferous chloride brine occupying the abundant pores of the coarse-grained red-beds migrates or diffuses across a redoxcline into largely carbonaceous sulfide-rich grey-beds and the metals are screened out to form a zoned array of cupriferous sulphides and generally minor amounts of other metal sulphides such as galena and sphalerite. However, the source of the red-bed ore-forming brine is not entirely clear. As in the case of the sedex brines, the high salinities could result from sediment/pore water diagenesis, leaching of associated evaporitic units, semi-permeable membrane effects across very fine-grained strata, etc., and elevated brine tempertures could also result from accumulations of anomalous heat beneath fine-grained aquicludes (e.g., the mineralized grey-bed itself), especially if the geothermal gradient were steep as would be expected in a thinned rifting continental crust. The warm brine could then leach metals from the footwall strata. Walker (1989) shows that labile red-beds could provide very significant amounts of copper; other sources could include the predominantly basaltic and/or metabasaltic units which underlie the red-beds in some cases. In all cases, the brine which mineralizes the grey-beds has been in intimate contact with red-beds before reaching the grey-beds and is expected to have equilibrated with hematite, i.e., to be oxidizing, rather than sulfidic as in the case of sedex brines.

Concluding Remarks:

In spite of the many contrasts between sedex- and SCD-forming environments as presented in the above descriptions, there are significant similarities, some of which have been mentioned elsewhere. Brown (1981) noted the common continental rift setting of SCDs and suggested that deep basin fluids could have "exhaled" into the footwall red-beds. McGoldrich and Keays (1990) propose that the copper and lead-zinc deposits of Mt. Isa are cogenetic, and resulted from a common oxidizing metalliferous basin fluid; copper was deposited in pyritic muds closer to the source than lead and zinc which, being more

soluble, were transported to more distal sites before deposition. They indicate that the synsedimentary exhalative deposition of the lead-zinc sulphide bodies may in fact be have been post-sedimentary, similar to the early diagenetic timing of much SCD mineralization according to the overprint model. If so, some sedex deposits may be converging on a SCD model as much as some SCDs may be converging toward an exhalative model.

However, according to the more generally accepted sedex model described earlier, the basin sediments are dominated by marine units, assuring a reduced basin-derived ore solutions. Even if both mineral deposit types form under similar extensional tectonics in continental crust, the redox character of basin-derived fluids could range from reducing to oxidizing. If rifting took place where the continent was previously submarine, as in an area of epi-continental submergence, the rift fillings could be expected to be dominated by marine units from which reducing basin fluid would arise. If rifting occurred in topographically high continental areas, basin fillings could be dominantly continental red-beds before an eventual marine incursion or lacustrine basin produced overlying grey-beds; deep basin-derived ore fluids would then be oxidizing and favourable for copper transport. With these clearly different types of ore fluids, sedex and SCD mineralization would form from divergently different processes within a common extensional tectonic environment.

References:

Boyle, R.W., Brown, A.C., Jefferson, C.W., Jowett, E.C. and Kirkham, R.V., eds. (1989) Sediment-Hosted Stratiform Copper Deposits: Geological Association of Canada, Special Paper 36, 710 p.

Brown, A.C. (1981) Stratiform copper deposits and pene-exhalative environments: Geological Soc. Amer., Abstracts with Programs, v. 13(7), p. 418.

Brown, A.C. (1992) Sediment-hosted stratiform copper deposits: Geoscience Canada, v. 19, no. 3, p. 125-141.

Finlow-Bates, T. (1980) The chemical and physical controls on the genesis of submarine exhalative orebodies and their implications for formulating exploration concepts. A review: Geol. Jahr., v. 40, p. 131-168.

Hanor, J.S. (1979) The sedimentary genesis of hydrothermal fluids, dans Geochemistry of Hydrothermal Ore Deposits, H.L. Barnes, ed.: John Wiley & Sons, p. 137-172.

Large, D.E. (1980) Geological parameters associated with sediment-hosted, submarine exhalative Pb-Zn deposits: an empirical model for mineral exploration: Geol. Jahr., v. 40, p. 59-129.

Large, D.E. (1983) Sediment-hosted massive sulphide lead-zinc deposits: an empirical model, in Sediment-Hosted Stratiform Lead-Zinc Deposits, D.F. Sangster, ed.: Mineral. Assoc. Can., Short Course Handbook, v. 8, p. 1-29.

Lydon, J.W. (1983) Chemical parameters controlling the origin and deposition of sediment-hosted stratiform lead-zinc deposits, in (see Large (1983) reference above), p. 175-250.

McGoldrick, P.J. and Keays, R.R. (1990) Mount Isa copper and lead-zinc-silver ores: Coincidence or cogenesis?: Economic Geology, v. 85, p. 641-650.

Sangster, D.F. ed. (1983) Short Course in Sediment-Hosted Stratiform Lead-Zinc Deposits: Mineralogical Assoc. of Canada, Short Course Handbook, v. 8, 309 p.

Sangster, D.F. (1990) Mississippi Valley-type and sedex lead-zinc deposits: a comparative examination: Trans. Inst. Min. Metall., Sec. B, p. B21-B42.

Walker, T.R. (1989) Application of diagenetic alterations in redbeds to the origin of copper in stratiform copper deposits, in Boyle, R.W., Brown, A.C., Jefferson, C.W., Jowett, E.C. and Kirkham, R.V., eds., Sediment-hosted Stratiform Copper Deposits: Geol. Assoc. Can., Special Paper 36, p. 85-96.

Current Research in Geology Applied to Ore Deposits.Fenoll Hach-Alí, Torres-Ruiz & Gervilla(eds)(1993).ISBN 84-338-1772-8

TYPES OF MASSIVE BASE METAL SULPHIDE DEPOSITS IN RUDNY ALTAI

Fedorov, D.T. & Montine, S.A.
Ecores Ltd., Domodedovskaia 24-3, Moscow 115582, Russia

ABSTRACT: Massive base metal sulfide deposits in the volcanic belt of Rudny Altai were formed together with Devonian rhyolitic volcanoes. The ore composition is similar with Kuroko deposits, there are cupper-zinc,pyrite-polymetallic and barite-polymetallic deposits. Orebodies are stratiform, stratabound, lens-like or stockwork-like and are dynamo-metamorphozed in various degrees.

The volcanic belt of Rudny Altai lies from the South-East to the North-West in Eastern Kazakhstan and Altaisky krai of Russia. It is about 500 kilometres long and 100 to 150 kilometres wide (Shcherba et al.,1984). This is one of the greatest massive sulfide ore belts in the world, containing over a billion tons of massive base and precious metals sulfide ores. It was formed in Devonian on the active margin of Siberian continental plate (Zonenshain et al.,1990). All major deposits lie within Devonian sedimentary and volcanic rocks. The volcanism was antidrome and essentially rhyolitic.

There are about forty deposits of more than two million tons in eight mining districts: Rubtsovsky, Zmeinogorsky, and Zolotushinsky in Russia and Priirtyshsky, Beriozovsko-Belousovsky, Snegirikhinsky, Leninogorsky and Zyrianovsky in Eastern Kazakhstan. Ridder-Sokolnoie, Zyrianovskoie and Tyshinskoie deposits are giants. Average content of base metals in sum is of 3 to 5% in disseminated ore deposits and of 6 to 13% (22% at most) in massive sulfide deposits. About twenty deposits are in production, some new ones are not because of a lack of investments.

Massive sulfide deposits of Rudny Altai differ in the ore composition, the position in volcanic structures, the orebody morphology and the degree of metamorphism. The ore composition of the deposits is similar with the Kuroko ones. They contain cupper, lead, zinc and precious metals. On the triangle diagram Cu-Pb-Zn dots of the average ore compositions are in the area of 3 to 52% of Cu, 3 to 39% of Pb and 35 to 79% of Zn (Figure). There are three major types of deposits: cupper-zinc (Pb less than 10%), pyrite-polymetallic (Pb of 10 to 20%) and polymetallic, mainly lead-zinc deposits (Cu less than 20%), often with the hight barite and precious metals content. The lead content in the deposits decreases toward Irtyshsky fault at the South-West of Rudny Altai, wich is considered as the main former subduction zone.

Most of the deposits lie in depressions on the tops or on the slopes of rhyolitic stratovolcanoes and extrusive domes and are overlied by sedimentary rocks, basalts and tuffs (Volcanogenic,1978). Some deposits were formed in sediments before volcanic eruptions and were overlied by rhyolitic lavas

(Orlovskoie and Zolotushinskoie deposits) or essentially in sedimentary rocks (Zyrianovskoie and Grekhovskoie deposits).

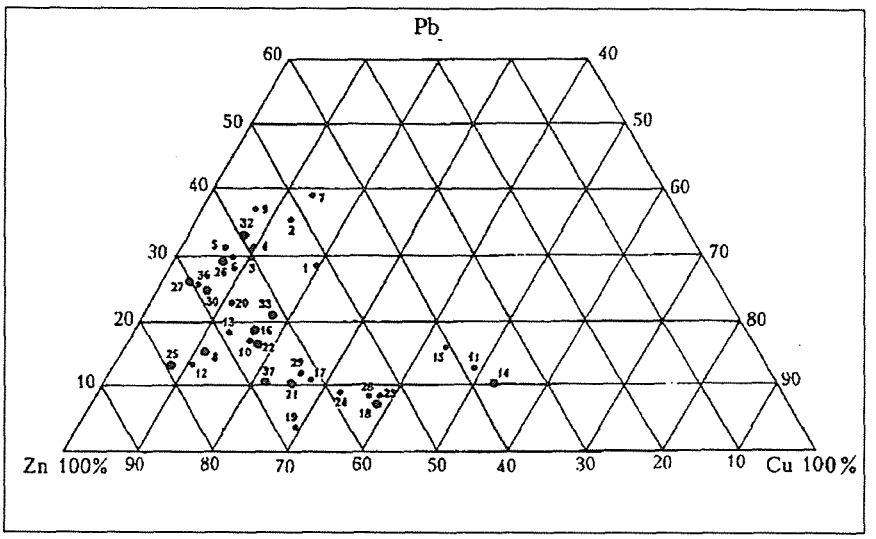

Figure. Average ore composition of massive sulfide deposits of Rudny Altai. Deposits:
1-Rubtsovskoie,4-Stepnoie,11-Zolotushinskoie,13-Yubileinoie,14-Orlovskoie,16-Artemievskoie,17-Shemonaikhinskoie,18-Nikolaievskoie,19-Novo-Beriozovskoie,21-Irtyshskoie,22-Belousovskoie,23-Yubileino-Snegirikhinskoie,25-Tishinskoie,26-Ridder-Sokolnoie,27-Novo-Leninogorskoie,28-Shubinskoie,30-Chekmar,32-Zyrianovskoie,33-Grekhovskoie,37-Maleevskoie

There are four types of orebodies in the Rudny Altai deposits. The first is formed by a series of small stratiform layers of 1 to 3 metres thick (10 m at most), composed of polymetallic massive and disseminated ores in siltstones (Zyrianovskoie, Stepnoie and Yubileinoie deposits). The second is presented by a large stratabound orebody of some hundred metres in plan and of 10 to 20 metres thick, sometimes to 50 metres. The pyrite-polymetallic Rubtsovskoie, Artemievskoie, Tishinskoie and Maleevskoie deposits are of this type. Orebodies of Nikolaievskoie and Orlovskoie massive cupper-zinc deposits are lens-like, they are about 50 to 100 metres thick and of 200 by 400 metres in plan. The fourth type is presented by lode and stockwork-like barite-polymetallic deposits, wich often have a small stratabound orebody on the top. These are Ridder-Sokolnoie, Novo-Leninogorskoie and Chekmar deposits in Leninogorsky mining district.

In spite of all deposits were formed in Devonian, the ores and rocks were dynamo-metamorphozed in different degrees. Nikolaievskoie and Artemievskoie deposits in Priirtyshsky mining district and Ridder-Sokolnoie deposit are non-metamorphozed and keep the subhorizontal bedding, the original orebody morphology and colloform and finegrained ore structures (Fedorov et al.,1987). Gently metamorphozed deposits

as Shemonaikhinskoie, Yubileino - Snegirikhinskoie and Shubinskoie, are inclined and slightly recrystallized, but sometimes keep colloform ore structures. Tishinskoie, Chekmar and Zyrianovskoie deposits are more metamorphozed, recrystallized, have a vertical bedding and deformed morphology. The deposits of Beriozovsko-Belousovsky mining district as Novo-Beriozovskoie, Irtyshskoie and Belousovskoie are situated in the Irtyshsky fault zone and are strongly dynamo-metamorphozed. They are of vertical or overturned bedding, completly recrystallized, orebodies are band-like and have metamorphic apophysis, the original ore zoning is never preserved.

References (all in Russian)

Fedorov,D.T.,Kuzhakhmetov,R.I.,Leonov,S.A. and Pozdniakova,N.V. 1987. Artemievskoie massive base metal sulfide deposit in Rudny Altai. Geol.Rudnykh Mestorozhdenii.4:35-43.

Shcherba,G.N., Diachkov,B.A. and Nakhtigal,G.P. 1984.Metallogeny of Rudny Altai and Kalba. Nauka, Alma-Ata.

Volcanogenic massive sulfide polymetallic deposits. 1978.Yakovlev,G.F.(ed).Ed.of Moscow University. Moscow.

Zonenshain,L.P.,Kuzmin,M.I. and Natapov,L.M. 1990. Tectonics of the lithosphere plates of the territory of the U.S.S.R. Nedra,Moscow.

Current Research in Geology Applied to Ore Deposits.Fenoll Hach-Alí, Torres-Ruiz & Gervilla(eds)(1993).ISBN 84-338-1772-8

PRESERVATION OF SYN-DEPOSITIONAL GEOCHEMICAL CHARACTERISTICS OF THE BROKEN HILL MASSIVE SULPHIDE DEPOSITS, SOUTH AFRICA, DURING UPPER AMPHIBOLITE FACIES METAMORPHISM

Frimmel, H.E. (1); Hoffmann, D. (1) & Moore, J.M.(2)
(1) Dept. of Geological Sciences, University of Cape Town, Rondebosch 7700, South Africa
(2) Dept. of Geology, Rhodes University, Grahamstown 6140, South Africa

ABSTRACT: Banded iron formation rocks associated with a massive sulphide ore body at the Broken Hill Pb–Zn–Cu–Ag deposit in the Namaqualand Metamorphic Complex, South Africa, were investigated with respect to their geochemistry and mineral compositions. The results reveal that no significant element transfer took place across lithological boundaries on a cm-scale, not even of volatile species such as HF, during medium- to high grade metamorphism. This permits conclusions to be drawn about the protoliths of the various mesobands, and a comparison to be made between this deposit and modern sedimentary exhalative base metal mineralization in the Red Sea.

1. INTRODUCTION

The Broken Hill deposit near Aggeneys in the northern Cape Province, South Africa, is a metamorphosed stratiform Pb–Zn–Cu–Ag sulphide deposit situated in the mid-Proterozoic supracrustal sequence of the Bushmanland Subprovince in the Namaqualand Metamorphic Complex. The deposit comprises two superposed ore bodies, each consisting mainly of massive sulphide lenses and banded iron formation which are hosted by metapelites associated with massive quartzite. Broken Hill has been compared with Sedex-type deposits (Ryan *et al.*, 1986). It was subjected to upper amphibolite facies metamorphism during the 1.1 Ga Namaqualand metamorphic event (Waters, 1989). This study concerns the affects metamorphism had on the geochemical characteristics of the precursor rocks, in particular the extent to which the ore bodies and sourrounding host rocks behaved as open or closed systems. Data was collected mainly from the tectonically lower ore body (LOB) which comprises, apart from massive Pb–Zn–Cu sulphide rock, magnetite-rich iron formation with a well preserved cm-thick banding of alternating amphibole- and garnet-rich mesobands.

2. EQUILIBRIUM ASSEMBLAGES AND MINERAL CHEMISTRY

The host metapelites are characterized by the equilibrium assemblage muscovite + biotite +sillimanite + garnet + quartz + magnetite ± K-feldspar ± graphite ± sulphides. Ferruginous quartzite (quartz + magnetite ± garnet) and garnetiferous quartzite (quartz + garnet ± biotite ± gahnite ± apatite ± staurolite) enclose the iron formation and massive sulphide lenses of the ore bodies. Silicate-rich bands with the following mineral assemblages can be distinguished within the banded iron formation, which both overlie and underlie the massive sulphide lens of the LOB. They comprise: (i) garnet-rich bands with quartz + magnetite + garnet + apatite ± biotite ± sillimanite ± gahnite ± barite ± sulphides, and quartz + magnetite + garnet + orthopyroxene; (ii) amphibole-rich bands with quartz + grunerite + olivine + magnetite ± garnet ± biotite ± pyroxferroite ± sillimanite ± apatite ± barite ± sulphides; (iii) quartz- magnetite-rich bands (quartz + magnetite + gahnite ± biotite ±

tourmaline); and (iv) garnet–magnetite–rich bands (garnet + magnetite + quartz). The massive sulphide rock consist of pyrrotite + galena + sphalerite + chalcopyrite + quartz ± biotite ± muscovite ± tourmaline ± garnet ± gahnite.

The garnets in and around the LOB are essentially solid solutions between almandine and spessartine. Individual garnet grains are generally homogeneous but significant differences exists in X_{Spes} between the various rock types but also within the garnet–rich iron formation bands. There is a strong gradient from high X_{Spes} in the iron formation bands near the massive sulphide bodies (62 mole%) to low X_{Spes} in the ferruginous quartzites and pelites further away from the ore lenses.

Similar variations were found in the composition of the clinoamphiboles. They are Fe–rich grunerites with variable amounts of Mn and Mg. X_{Mn} varies from an average of 0.22 in the west to 0.13 in the eastern part of the LOB. X_{Mg} varies between 0.19 and 0.23. Both X_{Mn} and X_{Mg} decrease slightly with distance from the ore lenses. On a cm scale, there is considerable variation in X_{Fe} and X_{Mg} between individual mesobands.

Olivine can be described as knebelite, a solid solution between fayalite and tephroite. It is confined to the iron formation bands and does not show significant compositional variations. Orthopyroxene is very rare and is of manganoan ferrosilite composition. Pyroxferroite is more common and occurs in varying proportions within the amphibole–rich bands. Compositionally, it can be also described as essentially a solid solution between an Fe– and a Mn–end member. The Mn–bearing minerals can be listed in order of decreasing X_{Mn} as follows:
pyroxferroite > garnet > olivine > orthopyroxene > amphibole.

The micas are of particular interest because they occur, in variable proportion, in almost all rock types and show a variety of partly unusual compositions. Biotite in the silicate–rich bands within the iron formation is similar to the Ba–rich variety kinoshitalite. BaO contents in biotite are highest in the garnet–rich bands (up to 15 wt%) and decrease away from the iron formation toward the quartzites and pelites. A similar trend was noted for muscovite. Biotite in the massive sulphide horizons is relatively enriched in phlogopite with X_{Mg} (=Mg/Mg+Fe) reaching up to 0.75. Generally, X_{Mg} decreases with increasing distance from the ore lenses (down to 0.23 in the pelites). This trend is, in accordance with the 'Fe–F avoidance rule', positively correlated to the F content in the biotite (decrease from 6 to 1 wt%).

The gahnite can be described as ferooan with X_{gahn} = 0.46 – 0.69, X_{herc} = 0.19 – 0.49, X_{spin} = 0.02 – 0.05 and insignificant galaxite component. The variation is largely due to differences in the host rock type. The Zn content in gahnite decreases rapidly with increasing distance away from the ore bodies.

Tourmaline within massive magnetite iron formation bands is strongly enriched in Fe but depleted in F compared to tourmaline in the massive sulphide lenses. Staurolite found in a garnet quartzite is of a zincian variety with 6.7 wt% ZnO. The oxides in the iron formation comprise magnetite of almost ideal composition, ilmenite with around 5 wt% MnO in massive sulphide rock as opposed to 2 wt% MnO for ilmenite in garnet quartzite, and rutile.

3. METAMORPHIC P–T–FLUID CONDITIONS

Two reactions derived from the mineral assemblages in the pelites permit an estimation of the peak metamorphic P–T conditions to be made. The intersection of the reaction curves for Ms + Qtz = Kfs + Sil + H_2O and Alm + Ms = Ann + Sill + Qtz indicates a temperature around 670°C at a pressure of around 4 Kbar. Similar temperatures were calculated from garnet–biotite thermometry for the surrounding pelites by using Ganguly & Saxena's (1984) calibration. Other calibrations yielded considerably lower temperatures. Application of the same calibrations to garnet–biotite pairs in the silicate–rich iron formation bands and quartzites gave geologically meaningless low temperatures, which is attributed to the high Mn contents in these rocks. The univariant assemblage grunerite + fayalite + quartz is in good agreement with the P–T conditions estimated.

The composition of the fluid in the system C–H–O–S–F–Cl in equilibrium with iron formation can be constrained by coexisting silicate, carbonate and sulphide phases.The carbonic species are nor further considered because of the general lack of any carbonate phases in the sequence studied. In the amphibole –rich bands, the ambient oxygen fugacity was close to the quartz–magnetite–fayalite buffer. For the massive sulphide lenses, $f(O_2)$ and $f(S_2)$ can be constrained by the assemblage pyrrhotite–pyrite–magnetite, by the coexistence of ilmenite and rutile, and by the desulphurization of sphalerite to gahnite: log $f(O_2)$ −15 to −18, log $f(S_2)$ −1 to −3. The fugacities of F and Cl were estimated from the respective activities in biotite, muscovite, apatite and tourmaline. Cl is virtually absent, but there is strong evidence for a high F–content in the metamorphic fluid in equilibrium with the iron formation. The maximun HF fugacities were calculated for the amphibole–rich mesobands (10 bars), the garnet–rich bands (5 bars) and in the massive sulphide lenses (4 bars), whereas f(HF) decreases to about 2 bars in the garnet quartzite and 0.5 bars in the pelites.

4. GEOCHEMISTRY OF THE SILICATE–RICH MESOBANDS

The geochemistry of the silicate–rich mesobands is not consistent with that of ironstones but compares reasonably well with that of iron formations. Poor correlation exist between the composition of the silicate–rich bands and that of both 'Algoma–' and 'Lake Superior–type' iron formations. Rather the major element contents of the amphibole– and garnet–rich bands are respectively comparable with Mn–rich and Mn–poor iron formations from Satnuru, India (Bhattacharya *et al.*, 1990).

5. GENETIC MODEL

The preservation of compositional banding on a mm–scale, which is believed to represent bedding, of distinct gradients in X_{Mn} in both garnet and amphibole, and of X_{Ba} and X_F in both biotite and muscovite are interpreted to be primary features. They indicate the absence of significant element transfer during metamorphism, not even of volatile species such as HF, across lithological boundaries. Hence, the geochemical characteristics of today's metamorphic rocks can be considered representative of the original sediments. This permit

conclusions to be made about the origin of the iron formation on the basis of their geochemistry.

The silicate–rich iron formation mesobands are interpreted to have formed as chemical precipitates from metalliferous brines and thus to be of submarine exhalative origin.The relative enrichment of the garnet–rich bands in Mn compared to the amphibole–rich bands is evidence for the precursor of the garnet–rich bands having been deposited in a more oxidizing (distal) environment compared to the amphibole–rich bands which originate from a more anaerobic proximal environment. The garnets can be derived from a Mn–rich precursor such as chamosite, whereas the amphiboles probably reflect originally Fe–montmorillonite–rich precipitates.

The result obtained in this study indicate strong similarities between the Broken Hill massive sulphide deposit and base metal mineralization in the Red Sea where massive sulphide horizons are also enclosed by oxide and silicate facies iron formation (Hackett & Bishoff, 1973).

REFERENCES

Bhattacharya, A., Spiring, B., Zen, S.K., Natarjan, R. & Mazumdar, A.C., 1990. Compositional characteristics and phase equilibria in manganiferous iron formations from a high–grade terrain near Satnuru, Karnataka, India. J. metam. Geol., 8: 525–538

Ganguly, J. & Saxena, S.K., 1984. Mixing properties of aluminosilicate garnets: constraints from natural and experimental data, and applications to geothermobarometry. Am. Mineral., 69: 88–97.

Hackett, J.P. & Bishoff, J.L., 1973. New data on the stratigraphy, extent and geological history of the Res Sea geothermal deposits. Econ. Geol., 68: 553–564.

Ryan, P.J., Lawrence, A.L., Lipson, R.D., Moore, J.M., Paterson, A., Stedman, D.P. & Van Zyl, D., 1982. The Aggeneys base metal sulphide deposits, Namaqualand district. In: Anhaeusser, C.R. & Maske, S. (eds.), *Mineral Deposits of Southern Africa*, vol.II, Geol. Soc. S. Afr., p.1447–1474.

Waters, D.J., 1989. Metamorphic evidence for the heating and cooling path of Namaqualand granulites. In: Daly, J.S., Cliff, R.A. & Yardley, B.W.D. (eds.), *Evolution of Metamorphic Belts*, Geol. Soc. Spec. Publ. No.43, 357–363.

Current Research in Geology Applied to Ore Deposits. Fenoll Hach-Ali, Torres-Ruiz & Gervilla (eds) (1993). ISBN 84-338-1772-8

RELATIONSHIPS BETWEEN SHALLOW MAGMA CHAMBERS AND SEA-FLOOR HYDROTHERMAL SYSTEMS IN THE LØKKEN OPHIOLITE, NORWEGIAN CALEDONIDES

Grenne T.
Geological Survey of Norway, P.B. 3006 Lade, N-7002 Trondheim, Norway

ABSTRACT: The Ordovician Løkken VMS deposit is very large for ophiolite terranes. The Fe-Cu-Zn sulphides were deposited in a period of vigorous volcanism and replenishment of a very shallow magma reservoir by new mafic magma. Correlatable ophiolite fragments elsewhere in the region do not have equivalent shallow intrusions, and sea-floor sulphide deposits are sparse and very small. The increased volcanism and hydrothermal activity at Løkken is thought to result from the short distance from the sea floor down to the magma chamber.

The Early Ordovician ophiolites of the western Trondheim region, including their dominantly sedimentary covers, are considered as remnants of an Ordovician marginal basin, deformed and emplaced in its present position during the Caledonian orogeny (Roberts et al. 1984). The Løkken ophiolite is the most densely mineralized among the many ophiolite fragments in the region. In addition to a number of small VMS deposits with related stockwork-type mineralization, it contains the Løkken Cu-Zn-pyrite ore body (Grenne et al. 1980, Grenne 1989a,b, Grenne and Vokes 1990). With its original 25-30 million tonnes of ore, this is the largest known ophiolite-hosted massive sulphide deposit in the world.

The Løkken ophiolite shows a tripartite subdivision of its 1-2 km thick volcanic sequence (Fig. 1). The massive sulphides are situated in the middle volcanic member (MVM), closely associated with thick jasper beds, both signifying a strong increase in hydrothermal activity. The MVM is volumetrically subordinate to the lower and upper volcanic members, but marks a period of more vigorous volcanic activity with voluminous eruptions of fluid magma forming thick sheet flows in contrast to the, generally, normal pillowed basalts of the lower and upper volcanic members. This was accompanied by intense sea-floor faulting activity giving rise to abundant thick talus breccias.

The MVM lavas had their source in exceptionally shallow (0.5 km) reservoirs of basaltic magma which had intruded the underlying basaltic sequence and a subjacent sheeted dyke complex. Lava flows which were penecontemporaneous with deposition of the Løkken ore body show anomalous chemical compositions, with evidence of hybridization between mafic and intermediate phases prior to eruption, and possibly melting of intermediate cumulus assemblages. Furthermore, a 'reverse' magmatic development, from early, fractionated compositions (mafic to intermediate) towards late, more primitive basaltic melts of a different parentage, is found in both the MVM and the shallow plutonic complex. This is interpreted to indicate that the peak of hydrothermal activity was reached during a period of replenishment of the shallow reservoir by new mafic magma.

Correlatable ophiolite fragments elsewhere in the region (Fig. 1) do not have equivalent shallow gabbro intrusions (Grenne et al. 1980,

Heim et al. 1987). Massive sulphide deposits are very small and scarce, or are completely lacking, and hydrothermal activity must have been significantly weaker than in the Løkken area. A slight analogy with Løkken is seen in the Vassfjell ophiolite, where hydrothermal activity and sulphide deposition was related to a shift from highly fractionated ferrobasalts towards more primitive basaltic volcanism.

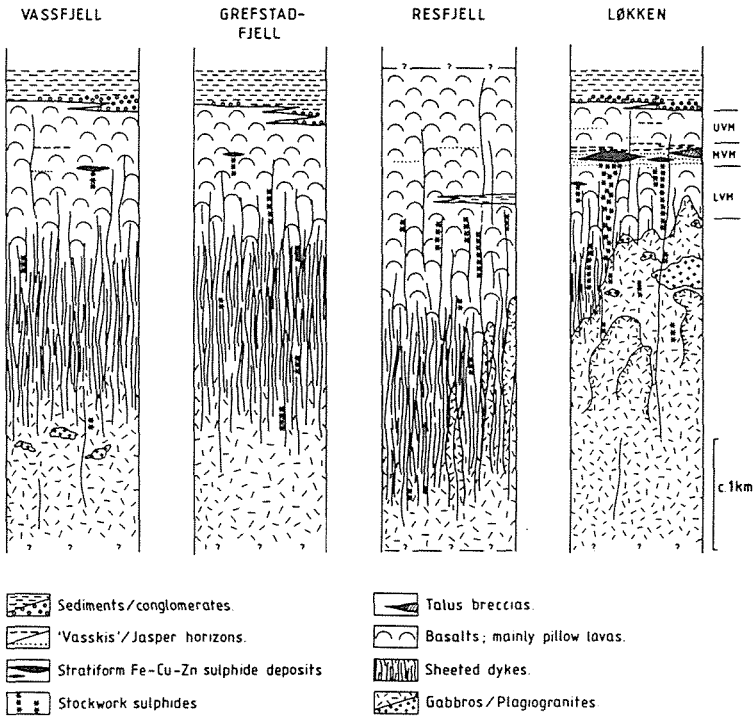

Fig. 1. Generalized sections of the Vassfjell, Grefstadfjell, Resfjell and Løkken ophiolite fragments. Question marks denote unexposed bases or tectonic boundaries.

The following points arise from the relationships observed in the ophiolites of the western Trondheim region:

1) The most vigorous hydrothermal activity was induced in regions where the magma reservoir was very shallow.
2) The peak of hydrothermal activity, with large-scale sulphide deposition, was reached *within* a period of increased volcanic activity;
3) The lavas erupted during this period had their source in the shallow magma reservoirs;
4) The peak of hydrothermal activity was contemporaneous with introduction of more primitive melts to the shallow magma chamber.

This is in accordance with observations from active geothermal fields where contemporaneity between hydrothermal activity, volcanism and magma chamber replenishment is demonstrable (Ballard & Francheteau

1983, Bjørnsson et al. 1977). However, it is partly at variance with common models for sea-floor sulphide deposition, which postulate a hiatus (Franklin et al. 1980), rather than an increase in volcanic activity; or alternatively, that the largest deposits form just before or just after a period of intense volcanism because the time interval between eruptions is supposedly not great enough to allow a very large deposit to accumulate (Scott 1987). The latter may, admittedly, be important in certain settings, but is not necessarily relevant if one presupposes a sufficient sea-floor relief such as at Løkken, where sulphides and lavas could be deposited contemporaneously with, and adjacent to each other, but not necessarily overlapping.

At Løkken, both the increased volcanic activity and the increased hydrothermal activity resulted from the unusually short distance from the sea floor down to the magma chamber. The intense hydrothermal activity is ascribed to the significant compression of the isogeotherms above shallow heat sources, and hence a greater opportunity of formation of large, high-temperature, sea-water convection systems within the oceanic crust.

REFERENCES:

Ballard, R.D. & Francheteau, J. 1983. Geologic processes of the mid-ocean ridge and their relation to sulphide deposition. In: Rona, P.A., Boström, K., Laubier, L., Smith, K.L. (eds.) Hydrothermal processes at seafloor spreading centers. Plenum Press, New York and London, pp 17-26

Bjørnsson, A., Sæmundsson, K., Einarsson, P., Tryggvasson, E., Grønvold, K. 1977. Current rifting episode in north Iceland. Nature 266:318-323

Franklin, J.M., Lydon, J.W., Sangster, D.M. 1980. Volcanic-associated massive sulfide deposits. Econ. Geol. 75th Anniv. Vol.:485-627

Grenne, T., Grammeltvedt, G., Vokes, F.M. 1980. Cyprus-type sulphide deposits in the western Trondheim district, central Norwegian Caledonides. In: Panayiotou, A. (ed.) Ophiolites, Proc. Int. Ophiolite Symp. Cyprus 1979, pp. 727-743

Grenne, T. 1989a. Magmatic evolution of the Løkken SSZ ophiolite, Norwegian Caledonides: Relationships between anomalous lavas and high-level intrusions. Geol. Journ. 24:251-274

Grenne, T. 1989b. The feeder zone to the Løkken ophiolite-hosted massive sulfide deposit and related mineralizations in the central Norwegian Caledonides. Econ. Geol. 84:2173-2195

Grenne, T. & Vokes, F.M. 1990: Sea-floor sulfides at the Høydal volcanogenic deposit, central Norwegian Caledonides. Econ. Geol. 85:344-359

Heim, M., Grenne, T., Prestvik, T. 1987. The Resfjell ophiolite fragment, southwest Trondheim Region, Central Norwegian Caledonides. Norges Geol. Unders. Bull. 409:49-71

Roberts, D., Grenne, T., Ryan, P.D. 1984. Ordovician marginal basin development in the central Norwegian Caledonides. In: Kokelaar, B.P. & Howells, M.F. (eds.) Marginal basin geology. Geol. Soc. London Spec. Publ. 16:233-244

Scott, S.D. 1987. Seafloor polymetallic sulfides: Scientific curosities or mines of the future? In: Teleki, P.G. et al. (eds.). Marine Minerals. D. Reidel Publishing Company, pp 277-300

Current Research in Geology Applied to Ore Deposits.Fenoll Hach-Alí, Torres-Ruiz & Gervilla(eds)(1993).ISBN 84-338-1772-8

Pb-ISOTOPE SYSTEMATICS OF ORES, SEDIMENTS AND VOLCANIC ROCKS FROM THE JADE HYDROTHERMAL FIELD IN THE OKINAWA BACK-ARC TROUGH

Halbach, P. (1); Pracejus, B. (1); Hansmann, W. (2) & Köppel, V. (2)
(1) FU Berlin, Fachbereich Geowissenschaften, Malteserstr. 74-100, 1000 Berlin 46, Germany
(2) Inst. for Crystallography and Petrography, ETH-Zentrum, CH-8092 Zürich, Switzerland

The hydrothermal JADE-field is located in the central Okinawa trough which is a tectonically active back-arc basin related to the subduction of the Philippine plate under the Eurasian continent. The Okinawa trough extends from Taiwan to the island of Kyushu and is accompanied to the SE by the Ryukyu island chain which is the outer non-volcanic arc of the back-arc system and represents an elongated piece of the Asian continental margin. Felsic volcanism occurs presently in the northeastern part of the inner arc. Geophysical data indicate crustal thinning below the through to 15 km in the SW and 25 km in the NE. In the central part, the trough consists of five E-W to ENE-WSW trending segments which are aligned en echeleon and obliquely to the general NE to NNE strike of the back-arc system. Its central part represents a transition zone from present-day arc volcanism to more mafic volcanism associated with spreading. The local ridges in the troughs are composed of a bimodal assemblage of volcanic rocks ranging from basalts to rhyolites.

The Izena depression in which the JADE-field is located lies is the middle Okinawa trough where the continental crust is about 20 km thick. Hemipelagic unconsolidated silty clays of Holocene age cover the sea floor and have a maximum thickness of 20-30 m, for example in the deepest part of the Izena depression. Below these sediments late Pleistocene felsic volcanics of dacitic to rhyolitic composition occur and contain intercalated mud sediments and acid tuff layers which can both reach several meters of thickness. Well stratified Pleistocene to Miocene shallow marine mudstones, in places rich in foraminifera, reach in the in the central Okinawa trough a thickness of several thousand meters. Within this sedimentary sequence basaltic sills and dykes occur. Miocene rocks also include green tuff layers. Several unconformities were recognized in the Neogene strata. Pre-Tertiary sedimentary rocks of the continental crust include sandstones, phyllites and dark shales, and occasionally interbedded limestones.

The JADE-field with extensions of 1800 m by 600 m is located at a water depth of 1250 to 1610 m on the NE slope of the Izena depression, which has a diameter of 5 km, and lies at the eastern end of a rift graben segment. The Zn-Pb-Cu(-Ag-Au) mineralization consists mainly of sphalerite, galena, pyrite, marcasite, chalcopyrite and Sb-, respectively As-dominated fahlore and barite, anglesite and amorphous silica and resembles in many aspects the Kuroko-type deposits of Japan. Based on textural and paragenetic differences several ore types can be distinguished: massive, Zn-Pb-rich "black ore" and fine grained, porous friable Ba-Zn-Pb-rich "black ore", Zn-Cu-rich massive "green ore", Fe-rich "replacement ore", and "impregnation ore" in hydrother-mally altered felsic volcanics.

Lead isotope analyses were performed on fresh and altered volcanic rocks, sediments and on the different ore types. Within the 2σ reproducibility the data define in both, the uranogenic and thorogenic evolution diagrams a linear array of which the different lithologies occupy distinct or partially overlapping segments (Fig.1a,b). The ore-lead defines a tight cluster at the less radiogenic end of the sedimentary data field. The altered volcanics partly overlap with the data of sediments and ores and also extend to less radiogenic Pb whereas fresh volcanics define the least radiogenic portion of the array. It remains an open question whether the lead in the fresh volcanic rocks really represents an end member or whether it was also contaminated by lead with a composition such as observed in the recent sediments. It is noteworthy that the linear arrays of both diagrams extrapolates to a MORB-type lead at 206Pb/204Pb of about 18.1. which suggests that the volcanic rocks may partly derive from a depleted mantle source.

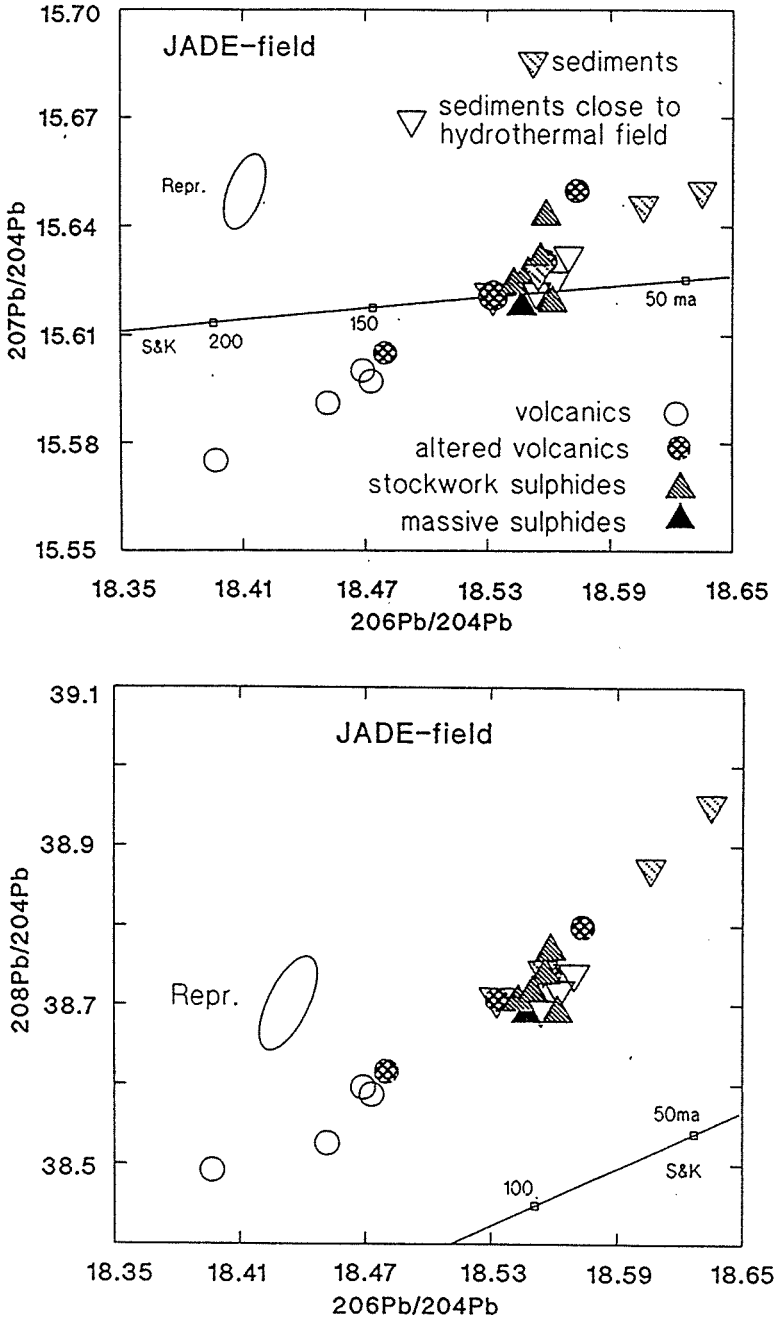

Fig.1a,b: Pb-evolution diagram with growth curve by Stacey and Kramers. Repr. denotes the 2σ reproducibility

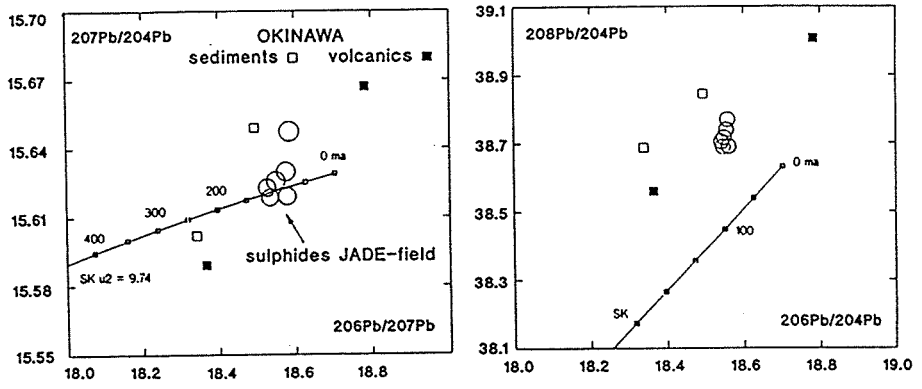

Fib. 2a,b: Comparison of sulphides from the JADE-field with sediments and volcanics from Okinawa

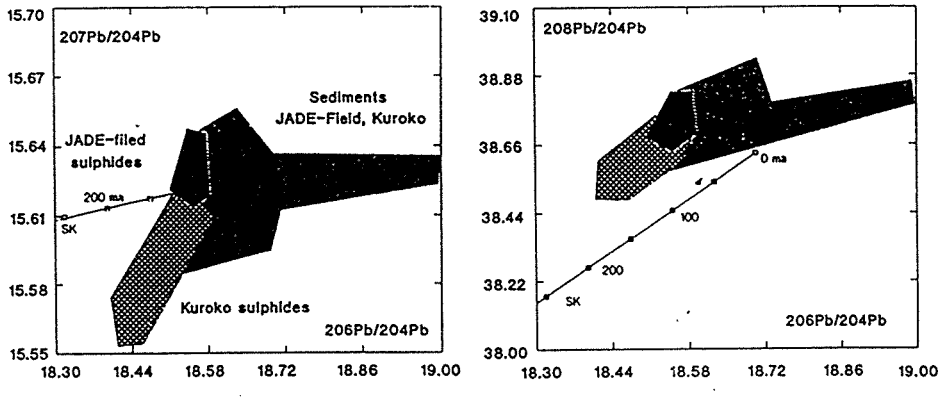

Fig.3a,b: Comparison of sulphides from the JADE-field with Kuroko sulphides

Black and green ores are isotopically homogeneous whereas sulfides from the stockwork zone exhibit some variations which are, however, barely significant. The ore-lead is isotopically similar to the least radiogenic lead observed in sediments collected within the chauldron close to the ore field (4 samples with 390 to 3000 ppm Pb) as well from outside the caldera with no hydrothermal activity (1 sample, 50 ppm Pb). Two samples (27 and 243 ppm Pb) from areas with no known hydrothermal activities and located 100 km and 300 km away from the JADE-field contain a somewhat more radiogenic Pb.

The ore-lead is dominated by a sedimentary component, but its position at the less radiogenic end of the sedimentary array indicates the presence of a component from magmatic rocks. We therefore conclude that the ore lead is essentially a two component mixture of lead derived from magmatic rocks and from sediments. However, the thickness of the sedimentary cover of the chauldron apparently does not exceed a few centimeters and therefore could not have contributed significant amounts of metals to the deposit. However, it seems likely that hemipelagic mudstones which are intercalated within recent volcanic rocks and probably also Pleistocene and Neogene hemipelagic sediments which underly the volcanics constitute in important metal source. Although direct isotopic evidence from these sediments is lacking, they probably were exposed to the hydrothermal alteration processes which led to the mineralization in the chauldron. The back-arc region is underlain by continental crust of about 20 km thickness and therefore other sources may have also contributed lead to the deposit. However, the data of two cretaceous phyllite samples and two volcanic rocks, including a green tuff, from the near-by Okianawa island do not follow the observed linear trend. Their data field barely encompasses the ore-lead of the JADE-field (Fig.2a,b).

The ore-lead of the massive ore of the JADE-field is isotopically very similar to the lead of the Kuroko-type deposits of Japan; only the lead of the stockwork-ore has slightly higher $^{207}Pb/^{204}Pb$ and $^{208}Pb/^{204}Pb$ ratios (Fig.3a,b). Similar to the Jade field, the lead of the Kuroko ores is slightly more radiogenic than the lead of the accompanying volcanics. The presence of a lead component derived from basement sediments is thus indicated.

References:

Fehn, U., Doe B.R. and Delevaux M.H. (1983): The distribution of lead isotopes and the origin of Kuroko ore deposits in the Hokuroku district, Japan. Econ.Geol. Monogr. 5, 488-506

Halbach, P. Pracejus,B. and Märten, A. (1993): Geology and Mineralogy of Massive Sulfide Ores from the Central Okinawa Trough, Japan. Special Issue Econ. Geol., in press.

Halbach P.E., Märten A., and Schwanold G. (1991): Present-day Kuroko-type ore formation - Results from the central Okinawa Trough. in: Source, Transport and Deposition of Metals, edts. M. Pagel, J.L.Leroy, A.A.Kalkema, Rotterdam, 623-626.

Kimura, M. (1985): Back-arc rifting in the Okinawa Trough. Marine and Petr. Geol. 2 222-240.

Sibuet, J.-C., Letouzey,J., Barbier, F., Charvet, J., Foucher, J.-P., Hilde, T.W.C., Kimura, M., Ling-Yun, C., Marsset, B., Muller, C., and Stephan J.-F. (1987): Back-arc extension in the Okinawa Trough: J.Geophys.Res. 92, B13, 14041-14063.

Current Research in Geology Applied to Ore Deposits. Fenoll Hach-Alí, Torres-Ruiz & Gervilla (eds) (1993). ISBN 84-338-1772-8

THE SOURCE OF SULPHUR FOR THE STRATABOUND SULPHIDE DEPOSIT HORNI BENEŠOV (CZECH REPUBLIC)

Hladíková, J. (1); Fojt, B. (2); Kříbek, B. (3) & Mixa, P. (1)
(1) Czech Geological Survey, Prague, Czech Republic
(2) Faculty of Sciences, Masaryk University, Brno, Czech Republic
(3) CREGU, Nancy, France

ABSTRACT: Results of sulphur isotope analyses of sulphides from ore accumulations, content of trace elements in pyrites, carbon isotope analyses of mineralized carbonates and gas chromatographic analyses of extractable organic compounds show the important role of anoxic sediments for the formation of submarine exhalative Pb-Zn deposit of Horní Benešov.

The Pb-Zn deposit Horní Benešov is bound to the Devonian volcanic and sedimentary complex of the Šternberk-Horní Benešov belt, tectonically modified by horizontal strike-slip, within the eastern part of the Rhenohercynian zone. The en echellon oriented ore bodies are located in the dragged-out and sheared, steeply declined slice of Devonian rocks, surrounded by the Lower Carboniferous flysch sediments. The Devonian sequence consists of basic and felsic volcanic rocks, their tuffs, marbles and shallow water black shales. Pyrite, sphalerite and galena are the main ore minerals, barite was common in upper part of the deposit. The disseminated and stockwork ores in brecciated massive quartzose rocks and silicified marbles and streaky and banded ores in the sericitic schists can be distinguished. The mineralization is considered to be of a submarine exhalative origin and was partly metamorphically remobilized (Havelka et al. 1963). On the basis of the texture, ore breccias, banded ores, ore disseminations and veins (veinlets) can be distinguished. The veins and veinlets propbably represent younger metamorphic mobilizates. The ore breccias were interpreted by Urbánek (1988) as slump or explosive breccias which are older than the ores with banded texture. The origin of the Horní Benešov deposit was complex and very intensively affected by alteration processes and by Variscan polyphase tectonics.

To discuss the source of sulphur at this base metal deposit the sulphur isotope composition of ore minerals as well as pyrites from non-mineralized host rocks (metavolcanics and metasediments) were determined. The sulphur isotope composition of barites from the Horní Benešov stratabound deposit is consistent with that of barites from the Meggen and Rammelsberg deposits, which are also located in the Rhenohercynian zone, and all barites are in the range of δ^{34}S values postulated for the Devonian seawater sulphate. However, in contrast to the positive δ^{34}S values of base metal sulphides from Rammelsberg and Meggen, the sulphur isotopic composition of galenas and sphalerites from the Horní Benešov deposit varies from 0 to -10 per mil and indicates that the hydrothermal solution contained sulphur with low δ^{34}S values (Hladíková et al. 1992). It was found in a study of the isotopic of sulphur in the Devonian rocks that only black shales and their metamorphic equivalents contain sulphides with very low δ^{34}S values (Hladíková & Kříbek, 1988). Thus, it can be assumed that at least part of sulphur in the hydrothermal system was derived from the sediments of an anoxic environment. It is known that sulphur isotope composition of pyrites can characterize the conditions of anoxic environment. Therefore we have paid attention to pyrites from ore accummulations. In contrast to sphalerite and galena, whose sulphur is isotopically relatively homogeneous, the sulphur isotopic composition of pyrites in this deposit varies in a wide range from -20 to +20 per mil. For better understanding of pyrite origin, its sulphur isotopic composition has been compared with its trace element contents.

Ni, Ag, Mn and Mo contents and sulphur isotopic composition were determined in a set of 26 samples of pyrites collected from a horizontal drill core in the central part of the deposit

between level 9 and 10. On the basis of sulphur isotope composition, the data set can be divided into three subsets. Subset I (Table 1) is characterized by very negative δ34 S values, while subset III (Table 1) has positive δ34 S values. The greatest number of samples lie in the intermediate subset II, which shows the δ34 S values from -6.3 to +1.9 per mil. When the δ34 S values were compared with the average quantitative contents of microelements in the individual subsets, the following relations were found. Subset I: negative δ34 S values, relatively high contents of Ag, Ni and Mo, relatively low contents of Mn. Subset II: δ34 S values close to O per mil, medium contents of Ag, Mo and Mn, relatively high content of Ni. Subset III: positive δ34 S values, low contents of Ag, Ni and Mo, high Mn content. Textural, structural and mineralogical analyses lead to the conclusion that pyrites of subset I belong to the breccia ores, while those of subset III to ores of the banded types according to the classification of Urbánek (1988). The most numerous subset II can be evaluated as pyrites of the ore-bearing rocks of a transition character, with no sharp inclination to either group. We assume that pyritic sulphur and microelements were derived from sea water which contains a sufficient amount of sulphate, Ag, Ni and Mo, while the Mn content is low (Stumm & Morgan, 1970). In the framework of this interpretation, the pyrites of the ore-bearing breccias (subset I) were formed in the period of unlimited communication between the partial anoxic basin, in which the pyritic black shales were deposited, and the oxic ocean. This combination ensured a sufficient influx of sulphate and trace elements from the oxic ocean to the anoxic environment. The pyrites of the banded sulphidic ores (subset III), whose δ34 S values are positive and which contain low amounts of Ni, Mo and Ag, were apparently formed under conditions of limited supply of seawater sulphate to the system where the sulphate reduction took place. It could be the period when anoxic basin was separated from the oxic environment. The elevated Mn contents in this subset can be explained on the basis of hydrothermal supply of this element, which forms the most extensive elemental aureole in a number of submarine exhalative deposits.

Sulphur isotopes of sulphides from the Horní Benešov deposit provide evidence of an interaction of the anoxic sediments with the hydrothermal system. This interaction has also been demonstrated by data on the isotopic composition of the carbonate carbon. While carbon isotopic composition of the non-mineralized carbonates in the deposit varies from -1 to +3 per mil, in the vicinity of the sulphidic ore minerals, carbonates with δ13 C values between -3 and -12 per mil have been found (Hladíková et al. 1990). These lower δ13 C values could be explained by the fact that in addition to marine carbonate the hydrothermal solution contained also carbon dioxide with low δ13 C value. Such carbon dioxide was probably formed through oxidation of the sedimentary organic matter whose δ13 C values vary from -23 to -29 per mil. The results of analysis of the extractable organic molecules from the non-mineralized black shales and those from the ore deposit also support the concept of interaction between anoxic sediments and hydrothermal system. In the former case, only aliphatic hydrocarbons were found, however, the ores were found to contain also oxidation derivatives, ketones, quinones and the derivatives of higher carboxylic acids (Kříbek 1990). The oxidation of organic matter to carbon dioxide in the hydrothermal fluid should be coupled with sulphate reduction (Peter & Shanks III, 1992) and in analogy to the deposits of Guaymas Basin it is possible to assume that organic compounds of sediments were sulphate reducing agents.

It follows that the anoxic sediments in the Horní Benešov deposit were not simply a passive host environment of the sulphidic ore deposit. In addition, they were the source of at least part of the sulphur essential for the formation of sulphides and a number of trace elements. Interaction between black shales and the hydrothermal system is reflected in the negative δ34 S values for the ore-bearing sulphides, negative δ13 C values of the carbonates accompanying the ore deposit and the presence of organic molecules in the ores.

Table 1
Sulphur isotope composition and contents of Ag, Ni, Mn and Mo of pyrites from the Horní Benešov deposit

Sample Number	$\delta^{34}S$ (‰)	Ag (ppm)	Ni (ppm)	Mn (ppm)	Mo (ppm)
Subset I					
2	-19.0	130	940	7600	170
3	-17.9	170	960	1200	120
4	-13.9	270	750	450	95
5	-14.1	120	320	300	50
26	-17.3	35	890	560	25
24	-19.3	70	30	350	620
1	-9.5	120	340	470	60
Subset II					
11	-5.2	30	95	300	20
6	-0.7	140	970	650	15
13	1.9	40	1600	630	10
7	-3.3	130	1500	100	30
14	-3.2	60	1700	100	20
15	-6.3	15	140	330	15
16	-4.8	40	630	1330	25
19	-1.9	75	340	1200	90
20	1.5	35	30	1060	340
8	-3.5	230	130	750	45
25	-0.6	100	840	500	25
Subset III					
9	17.3	13	35	2460	10
10	16.0	20	25	990	10
12	12.6	55	150	5000	30
17	7.8	30	40	1000	35
18	15.2	20	50	1400	40
21	9.7	20	20	770	25
22	14.0	40	40	2200	35
23	12.9	40	25	1200	30

References:

Havelka,J. & Palas, M. & Scharm B. 1963. A new conception of the base-metal metallogeny in Jeseníky Province and its consequence for the geological exploration. Geologický průzkum. 8:225-227. (In Czech).

Hladíková, J. & Kříbek, B.1988. Distribution and isotopic composition of sulphidic sulphur on NE part of the Bohemian Massif. Čas.Mineral.Geol.33:113-129.

Hladíková, J. & Šmejkal, V. & Fojt,B. & Pertold, Z.& Aichler,J. 1990. Isotopic composition of sulphur, carbon and oxygen from selected localities in Jeseníky Mts.Sbor.Geol.Věd, Ložisková geologie a mineralogie. 29: 141-165. (In Czech).

Hladíková,J.& Aichler,J.& Mixa, P.1992.Source of sulphur of base metalal sulphide deposits at the NE margin of the Bohemian Massif (Czechoslovakia). Abstracts, 29th International Geological Congres, Kyoto, 3:757.

Kříbek,B. 1990. The carbonaceous formations and their role in metallogeny of the Bohemian Massif. MS-Doctor of Science Thesis.Faculty of Science, Charles University. Prague. (In Czech)

Peter, J.M & Shanks III, W.C. 1992. Sulfur, carbon and oxygen isotope variations in submarine hydrothermal deposits of Guaymas Basin, Gulf of California, USA. Geochim. Cosmochim. Acta. 56:2025-2040.

Stumm, W.& Morgan, J.J. 1970. Aquatic Chemistry. Wiley, New York. Urbánek, J. 1988. New findings from the revision exploration on Horní Benešov base-metal deposit. Geologický průzkum 30: 193-198. (In Czech)

Current Research in Geology Applied to Ore Deposits. Fenoll Hach-Alí, Torres-Ruiz & Gervilla (eds) (1993). ISBN 84-338-1772-8

METAMORPHISM AND POLYGENESIS OF THE ROŽNA BARITE-HYALOPHANE-SULPHIDE DEPOSIT (THE BOHEMIAN MASSIF, CZECH REPUBLIC)

Hladíková, J. (1); Kříbek, B. (2); Uhlík, Z. (3) & Žák (1)
(1) Czech Geological Survey, Malostranské náměstí 19, 11821 Prague, Czech Republic
(2) CNRS-CREGU, B.P. 23, 54501 Vandoeuvre, Cedex, France
(3) GEAM, 59251 Dolní Rožínka, Czech Republic

ABSTRACT: The Rožná stratiform deposit originated by mixing of the hydrothermal solutios carrying Ba, Zn, Pb and Si with seawater on the bottom of isolated oceanic trough filled with terrigenous sediments derived mostly from contemporaneous volcanics. The high productivity and restricted nature of the trough resulted in a low oxygen concentration in the bottom waters and low recycling rates for the organic matter. During the Variscan thermal event, the ore and its host rocks were metamorphosed to the upper amphibolite grade. Post-orogenic intrusions generated heat and magmatic fluid that produced skarn ore by replacement of calc-silicate and marble.

The Rožná ore deposit of the Moldanubian zone is hosted within the Gföhl unit, a high-grade metamorphic complex composed of migmatitic biotite- and sillimanite-biotite gneiss intercalated with marble, calc-silicate gneiss and amphibolite. The area has undergone several metamorphic events: regional high-temperature and high to moderate pressure metamorphism in the upper amphibolite facies up to granite melting; medium grade, low-pressure metamorphism associated with granite intrusions; and retrograde metamorphism in the greenschist facies probably related to a burial metamorphic event. The age of the Gföhl unit is problematic. Radiometric data point to a ~2.6 Ga crystalline basement but the age of sedimentation is probably not older than the Upper Proterozoic (Kröner at al., 1988). According to the findings of microfosils in some marbles, at least part of the rock complex can be of Lower Paleozoic age (Andrusov & Čorná, 1976).

Based on ore mineralogy and textures, the stratiform ores which occur within the Rožná uranium mine field can be characterized as (1) massive barite ore, (2) disseminated sulphide ore in marble, and (3) calc-silicate ores.

The massive barite-hyalophane ore with disseminated sulphides form strata-bound lenticular ore bodies trend in the general north-south direction and dip 40°-50° W, with vertical extention of about 500 m. (Fig.1). The thickness is very variable and can reach up to 8 m. The present footwall of the ore consists of banded calc-silicate gneiss and marbles, whereas the hanging wall is made up of biotite gneiss; minor barite ore is found in the gneiss. The relatively simple mineral assemblage includes barite (15 6 - 86.7%), hyalophane (5,2 - 19%), calcite, quartz, pyrite, pyrrhotite, sphalerite, galena and minor amounts of pyrargyrite, Ag-tetraedrite, fluorite, pyrotitanite and rutile. The ore average 3,2% Zn, 1,8% Pb and 120 ppm Ag. The hanging wall rocks are enriched in Fe, Co and Cr, footwal rocks in Pb, Zn and Ag. Well-developed metamorphic structures and textures indicate the ore has been metamorphosed to the upper amphibolite grade. The texture include pressure solution seam and sheared zone formation, cataclastic deformation of pyrite

and hyalophane and granoblastic annealing-recrystallization of sphalerite and galenite.

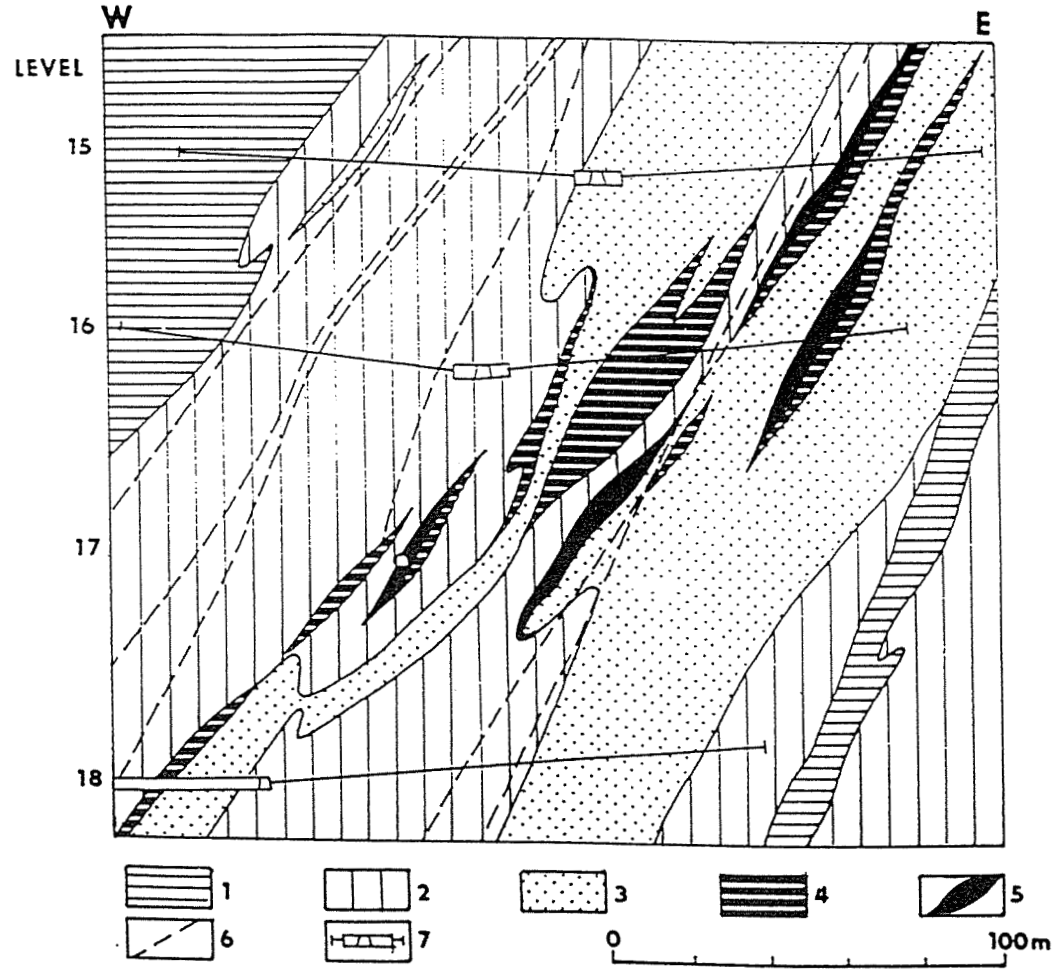

Fig.1. Vertical section cross the Rožná uranium mine field showing the relationship between massive barite-hyalophane-sulphidic ore and the host rock complex. Explanation: 1/ amphibolite, 2:fine-grained biotite- and sillimanite-biotite gneiss, 3:medium-grained biotite and sillimanite-biotite gneiss, 4:marble and calc silicate gneiss, 5:barite-hyalophane-sulphidic ore, 6:fault, 7:levels and drillings

The ore contains rounded clasts of the wall rocks (amphibolite, gneiss) up to 30 centimetres in diametr.

Disseminated Pb-Zn mineralization is limited to the contact of massive barite ore with calc-silicate gneiss or marble. Galena is recrystallized and coarse grained, the crystals are elongated and foliated in one plane and exhibit an equiliblium granoblastic texture. Sphalerite is similarly recrystallized, and sphalerite-sphalerite grain boundaries are commonly subgranoblastic.

Calc-silicate ores can be subdivided into two subtypes: ore-bearing calc-silicate gneiss and post-metamorphic calc-silicates

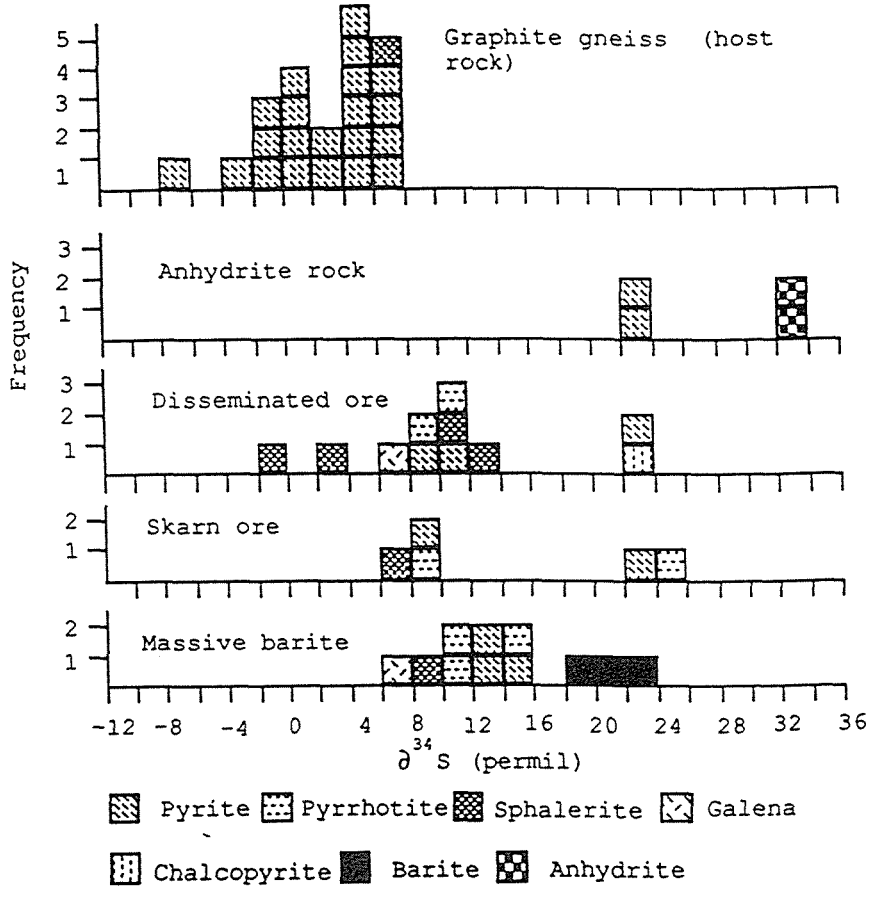

Fig.2. Isotopic composition of sulphides, barite and anhydrite from the Rožná host-rock graphitic gneiss, anhydrite lens, massive barite ore, disseminated and skarn ore

(skarns). Calc-silicate gneiss occurs adjacent to massive barite ore. It consists mainly of pyroxene, anthophyllite and serpentinite, with minor calcite, olivine, humite minerals and sulphides. Both plagioclase and hyalophane are frequently replaced by sphalerite, galenite and pyrrhotite along the cleavage planes.

The post-metamorphic skarn ore contains pyrite and minor amounts of sphalerite and galenite in calc-silicate assemblage of gangue minerals that includes andradite-grossularite garnet, diopside, calcite, quartz, epidote, and minor chlorite and actinolite.

The results of isotope study show the heavy $\partial^{34}S$ ratios for sulphide in all the ore types (Fig.2), indicating either an advanced stage of the high-temperature seawater sulphate reduction or low-temperature sulphide formation in an anoxic, restricted marine environment where sulphate and sulphide isotopic composition gradually shifted to the more positive values due to continuous bacterial removal of the ^{32}S isotope (Ohmoto & Ray, 1979). The restricted character of the sedimentary environment of the barite

ore seems to be supported by an elevated content of the organic carbon in the host rock (0.2 - 2.1%) and by heavy isotopic composition of pyrite and anhydrite sulphur in anhydrite lens, which occur in the footwall of the barite ore.

The $^{87}Sr/^{86}Sr$ ratios in ore (0.7077 - 0.7079) are close to but slightly lower than that for anhydrite (0.7080). This invokes an involvement of strontium from the surrounding rocks to a sea-water dominated hydrothermal system.

The isotopic composition of lead in galenas from massive barite and skarn ore is very homogeneous ($^{206}Pb/^{204}Pb$ = 17.65 - 17.66, $^{207}Pb/^{204}Pb$ = 15.47 - 15.51, $^{208}Pb/^{204}Pb$ = 37.36 - 37.45) and point to a lower crust or upper mantle source, the isotopic age being 640 Ma based on the model of Stancey and Kramers (1975).

It is proposed that massive barite-hyalophane-sulphidic ore was deposited in relatively deep water trough where the extensively fractured oceanic crust provided conduits for ascending barium, silica and metal bearing hydrothermal solutions that discharged on the sea floor. The presence of the oceanic crust is supported by the chemical composition of an associated metavolcanic rocks which correspond to oceanic tholeiites (Klápová,1977; Šichtařová, 1977). The isotopic composition of galena indicates that the source of the metals was probably subsea volcanites or volcanite-derived sedimentary rocks. The high organic carbon contents in the host rocks and occurence of metaevaporites points to an anoxic sedimentary environment with increased seawater salinity. The ore and its host rocks were metamorphosed during the Variscan thermal event, and the carbonate enriched part of the ore body was transformed to calc-silicate gneiss. A part of Pb and Zn was remobilized to form dissemination in marble. However, the possibility of pre-metamorphic enrichement cannot be ruled out. Coregional, post-tectonic intrusions generated heat and magmatic fluids during theVariscan thermal event than produced skarn ore by replacement of marble. All types of ore were finally affected by retrograde metamorphism in the greenschist facies.

Literature used:

Andrusov,D.& Čorna, O. 1976. Über das Alter des Moldanubikums nach mikrofloristichen Forschungen. Geologicke Prace, Spravy. 85:81-89 (Bratislava)

Klápová, H. 1977. Petrochemistry and metamorphism of amphibolites frpm Straz part of the Moldanubicum. M.S.,Diploma thesis. Carles University, Prague (in Czech)

Kröner, A., Wendt, I., Liew, T.C., Compson, W., Todt, W., Fiala, J., Vaňková, V. & Vaňek, J. 1988. U-Pb zirkon and Sm-Nd model ages of high-grade Moldanubian metasediments, the Bohemian Massif, Czechoslovakia. Contrib. Mineral. Petrolog. 99: 257-266.

Ohmoto, H. & Rye, R.O. 1979. Isotopes of sulphur and carbon.- In: Barnes, H.L. (ed;) Geochemistry of hydrothermal deposits. J. Wiley, New York, pp. 509-561.

Šichtařová, I. 1877. Petrochemistry of amphibolites of the eastern part of the Moldanubicum. M.S., Diploma thesis. Charles University, Prague (in Czezch)

Stacey, J.S. & Kramers, J. D. 1975. Approximation of terrestrial lead isotope evolution by a two-stage model. Earth Planet. Sci; Letters, 26: 207-221.

Current Research in Geology Applied to Ore Deposits. Fenoll Hach-Alí, Torres-Ruiz & Gervilla(eds)(1993). ISBN 84-338-1772-8

TECTONIC MOBILIZATION OF MERCURY IN THE ALMADEN DISTRICT, LAS CUEVAS DEPOSIT, CIUDAD REAL, SPAIN

Jebrak, M. (1) & Hernández, A.(2)

(1) Dépt. des Sciences de la Terre, Université du Quebec à Montreal, Géoterap, CP 8888, Succ. A, Montréal (QUE) H3C 3P8, Canada.

(2) Minas de Almadén y Arrayanes, S.A., 13400 Almadén, Ciudad Real, Spain

ABSTRACT: The Las Cuevas mercury mine is the only deposit located on the northern flank of the Almadèn syncline. It displays epigenetic features (hydraulic breccia, tension cracks)with cinnabar and realgar within quartz-arenite, black shale and volcanoclastics rocks. The ore is controlled by the nose of a drag-fold associated with a transcurrent fault. It appears as a remobilization during the Hercynian phase of folding of an early stratabound concentration of mercury.

The Las Cuevas mercury deposit is one of the main deposits of the Almadén district. It is located 7.5 km to the Northeast of the city and the old deposit of Almadén. This mineralization has been mined since the antiquity. However, it was subsequently lost and was only rediscovered in 1774. Modern production began in 1988. Reserves are estimated from 120 000 to 150 000 flasks of mercury, with a grade of approximately 5%.

Las Cuevas is very different from the classical type of mercury deposit of the Almadèn district (Saupé, 1990): (1) it is the only deposit located on the northern flank of the Almadèn syncline (fig. 1); (2) it is hosted by shale, quartzite and volcanics formerly considered to the upper Silurian to Devonian in age (Soler et al., 1970), therefore distinctly younger than the lower Silurian Criadero quartzite which contains most of the ore on the southern flank of the syncline. Moreover, the ore zone is nearly vertical and crosscuts the stratigraphy. Rytuba et al. (1989) suggested an association with a caldera due to the presence of some brecciation. However, Saupé (1990) interpreted the deposits as an hydrothermal stockwerk. Ortega and Hernandez (1992) suggested an association with a late hydrothermal vent.

A detailed geological and structural study has led to a reassessment of the regional context and the significance of the mineralisation. Three stratigraphic sequences may be distinguished: at the base, a first sedimentary unit consisting of quartz-arenites and black shales, with a characteristic black quartzite horizon; a volcano- sedimentary sequence, called Frailesca, which is 150 m thick, with basaltic ash fall tuffs, lavas and pyroclastics, locally crosscutting the black shale; at the top, a second sedimentary unit, containing grey quartzites and shales. These series are similar to those of the Almadén area and should be related to the Silurian formation. The ore is situated in the core of a tight anticlinal dragfold, which is associated with a major sinistral WNW-ESE fault. Only one quartzite horizon within the shale which may be related to the San Francisco quartzite in the Almadén mine, has been observed. Tectonic movement and variation in the regional paleogeography (Gallardo-Millàn et al., 1993) may explain the disappearance of the other horizons.

Five episodes of deformation may be distinguished: the first two correspond to NW-SE to E-W folding, synchronous with the development of folds overturned to the north, followed by NE-SW folding. The deposit is located in the hinge zone of the anticline. Deformation increases near the contact between the black quartzite and volcanic tuffs. Near the southern fault, folds of phase 1 are tilted to the vertical and therefore control the geometry of the primary ore horizon. Preliminary quantitative analysis of the faults shows that it is possible to distinguish two main episodes of brittle to ductile deformation displayed by reverse faults. Late normal faults crosscut the whole deposit.

Mercury appears in different facies, always near the contact between the black quartzite and the volcanites. The vertical column geometry results from the early folding of the quartzite and the location of most of the ore in the nose of the fold (fig. 2). Four facies may be distinguished (1) hydraulic veins of cinnabar within the black quartzite; (2) tension gashes with cinnabar and pyrite, developing a white mica bearing metasomatic rocks within the volcanics and the black shale; (3) N-S cinnabar veinlets; (4) native mercury within permeable zones, especially brittle structures and late dolomitic tension gashes. Such a spatial distribution is similar to some descriptions of smaller deposits in the former USSR (Nikitovka; Akhakhcha; West Paliansk; Fedorchuk, 1974).

The Las Cuevas deposits therefore prove that a part of the cinnabar mineralization in the Almadén district may be related to the remobilization during the Hercynian phase of folding of an early concentration of mercury.

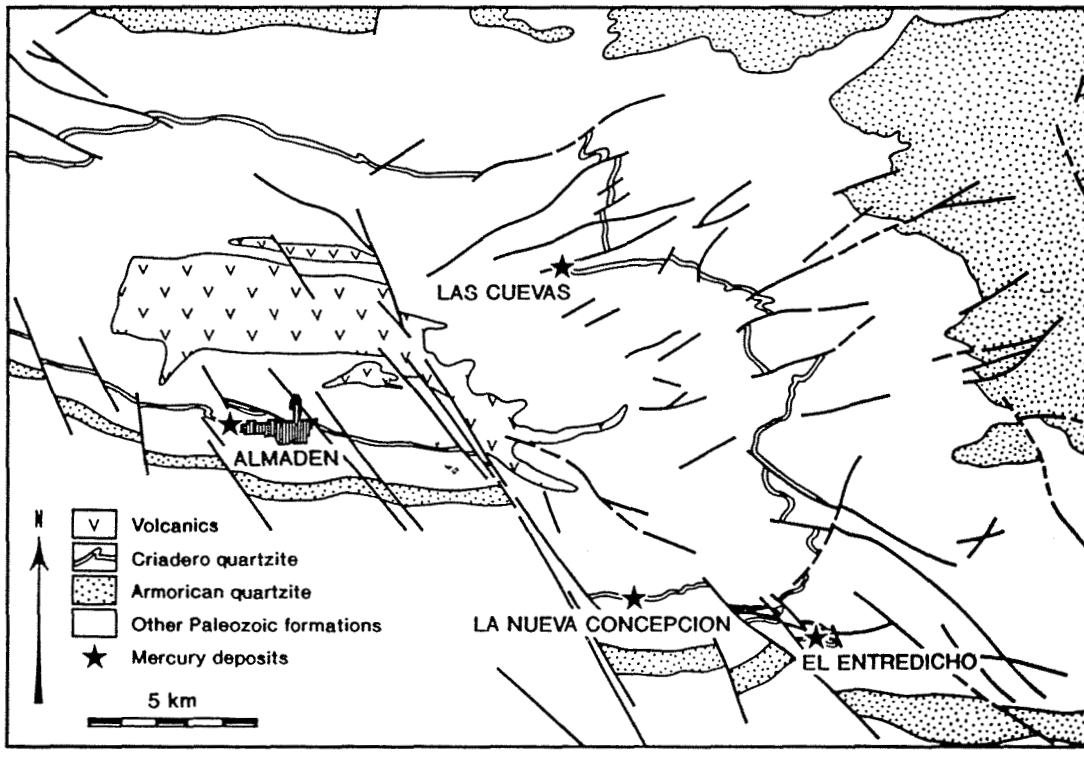

Fig. 1 Location map

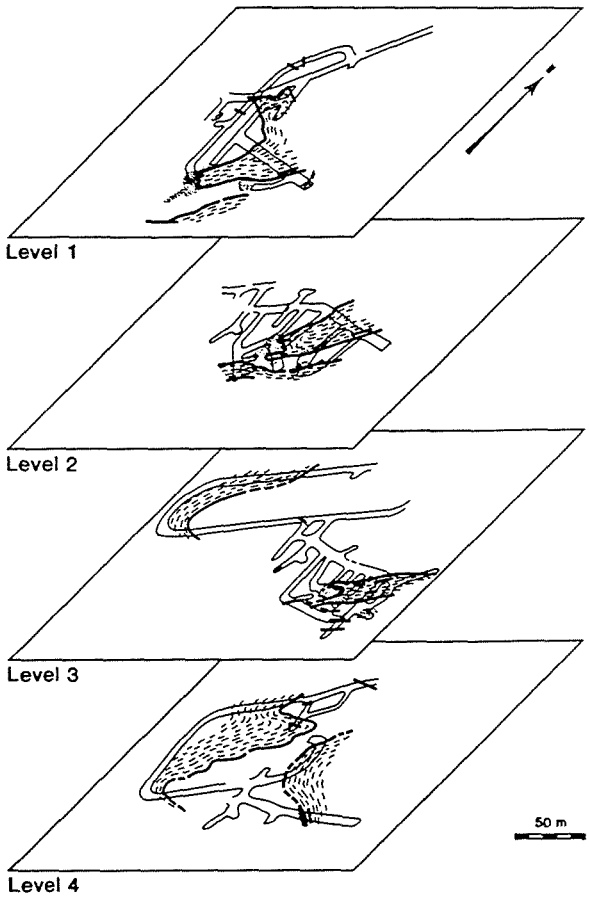

Fig. 2. Projection of level plans of the Las Cuevas mine; dashed pattern = shale and quartzite; stiple = mercury ore

References

Fedorchuk, V.P. 1974. Genetic and commercial types of Mercury Deposits, in Congreso Internacional del Mercurio, tomo I, Barcelone, Mai 1974, pp. 117-143

Gallardo-Millàn, J.L., Higueras, P., & Molina, J.M. 1993. Anàlysis estratigràfico de la "Cuarcita de Criadero" en el sinclinal de Almadén. *in* C. Quesada, J.T. Oliveira, P. Fonseca et A. Castro (eds) Contribuciones al conocimiento geologico del Macizo Ibérico.

Ortega E. & Hernandez, A. 1992. The mercury deposits of the Almadén syncline, Spain. Chronique de la recherche minière, 506: 3-24

Rytuba, J.J., Rye, R.O., Hernandez, A.M, Dean, J.A., & Arribas, A. Sr. 1989. Genesis of Almaden type mercury deposits, Almaden, Spain. Int. Geol. Congr., Washington, vol. 2, p. 2741

Saupé, F. 1990. Geology of the Almadén mercury deposit, Province of Ciudad Real, Spain. Economic Geology, 85: 482-510

Soler, M., Felgueroso, C. & Aguilar, M. 1970. Un ejemplo de la aplication de tecnicas petrograficas y microtectonicas a la geologia minera: el Yacimiento de mercurio de Las Cuevas (Almadén). Acta Jornadas Minero-Metalurgicas, Bilbao, 2: 313-330

Current Research in Geology Applied to Ore Deposits.Fenoll Hach-Ali, Torres-Ruiz & Gervilla(eds)(1993).ISBN 84-338-1772-8

LEAD ISOTOPE COMPOSITION OF STRATABOUND Cu-Pb-Zn-Ba OCCURRENCES IN UPPER PALAEOZOIC-MESOZOIC SEDIMENTS IN EAST GREENLAND

Jensen, S.M.
Dept. of Geology, University of Aarhus, 8000 Århus C, Denmark

ABSTRACT: Upper Carboniferous-Triassic sediments in the Jameson Land basin in central East Greenland host important base metal occurrences. Lead isotope evidence suggests that deeply buried Upper Palaeozoic clastics or their crystalline basement sources have supplied the lead in Pb-Zn vein deposits, whereas in Triassic stratiform Cu-Pb-Zn mineralisation the lead was mobilised from sediments at shallower levels. Stratabound Ba-Pb-Zn replacement ores in Upper Permian carbonates with suspected underlying feeder veins may represent mixing of lead remobilised from sediments at shallow and deeper basinal levels, respectively.

1. INTRODUCTION

Of the more than 150 known ore mineral occurrences in central East Greenland several Ba-Pb-Zn and Cu-Pb-Zn deposits are hosted in Upper Palaeozoic-Mesozoic sediments in the Jameson Land basin (Fig. 1). However, only the Blyklippen Pb-Zn deposit has been exploited. The mine produced 544,600 t of ore averaging 9.3% Pb and 9.9% Zn in the years 1956 to 1962 (Harpøth *et al.*, 1986).

Further exploration has revealed several other prospects in the region, for example the Tertiary Malmbjerg porphyry-molybdenum deposit with 150 Mt of 0.23% MoS_2 ore (Fig. 1) and W-Sb-Au mineralised veins in Upper Proterozoic metasediments *c.* 130 km north of Blyklippen (Harpøth *et al.*, 1986).

2. GEOLOGIC SETTING

The fault-bounded Jameson Land basin is filled by a 16-18 km thick sequence of Devonian to Cretaceous sediments (Larsen & Marcussen, 1992). Formation of the basin began in Late Caledonian time with left-lateral strike-slip tensional tectonics and deposition of Devonian red-beds and volcanics.

In the Late Carboniferous-Early Permian the stress regime changed to E-W tension (incipient rifting in the North Atlantic region) and clastic sediments were laid down in the resulting graben structures. Uplift and peneplanation preceded Late Permian transgression and deposition of basal conglomerates and marine carbonates, black shales and evaporites. Following a Late Permian regression and an Early Triassic transgression continental clastic sedimentation dominated for the remainder of the Triassic (Surlyk *et al.*, 1986). Jurassic-Cretaceous sedimentation was mainly marine.

Extensive magmatic activity was associated with the Tertiary continental break-up: intrusion of basaltic dykes and sills in the Jameson Land basin, flood basalt volcanism in East and West Greenland and intrusion of layered gabbros and alkaline complexes (*e.g.* the Skaergaard intrusion).

The stratabound occurrences in western Jameson Land may represent different levels of exposure of a fault-controlled mineralising

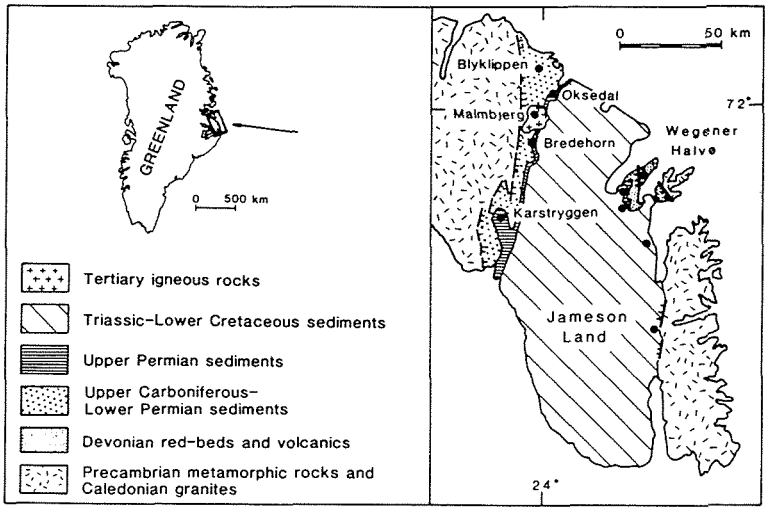

Fig. 1. Simplified geological map of the Jameson Land basin in central East Greenland. Filled circles show locations of some major base metal occurrences.

system that formed vein ores in coarse clastic sediments at lower stratigraphic levels and replacement ores in carbonate rocks at higher levels. Styles of mineralisation for the major deposits and exposed stratigraphic levels gradually change from north to south (Fig. 1): Pb-Zn-Ba veins in Upper Carboniferous and Lower Permian sandstones at Blyklippen, laminated replacement Ba-Pb-Zn ores with suspected underlying feeder veins in Upper Permian carbonates at Oksedal and Bredehorn (Harpøth *et al.* 1986), and celestite ($SrSO_4$) and minor Pb-Zn replacement in Upper Permian carbonates at Karstryggen (Scholle *et al.*, 1990).

On Wegener Halvø Pb-Zn occurrences are found in Upper Permian carbonate reef structures and thin carbonaceous black shales that resemble the Permian Kupferschiefer bed of north-western Europe (Thomassen *et al.*, 1982).

Widespread syn-diagenetic stratiform Cu-Pb-Zn mineralisation occurs in Triassic fluvial and lacustrine sediments along the eastern margin of the Jameson Land basin (Thomassen *et al.*, 1982).

3. LEAD ISOTOPE DATA

Lead isotope analyses on *c.* 65 galena and copper sulphide samples are graphically outlined in Fig. 2.

Geographical position of occurrences and age and type of host rock can be used to describe the variation in lead isotope ratios: vein and replacement Ba-Pb-Zn deposits hosted in Upper Carboniferous-Upper Permian rocks along the western margin of the Jameson Land basin have the least radiogenic ratios and distinctly low $^{207}Pb/^{204}Pb$ ratios; more radiogenic lead and higher $^{207}Pb/^{204}Pb$ ratios are found for syn-diagenetic Triassic stratiform occurrences along the eastern margin of the Jameson Land basin and Pb-Zn occurrences hosted in Upper Permian carbonates and shales on Wegener Halvø (Fig. 1).

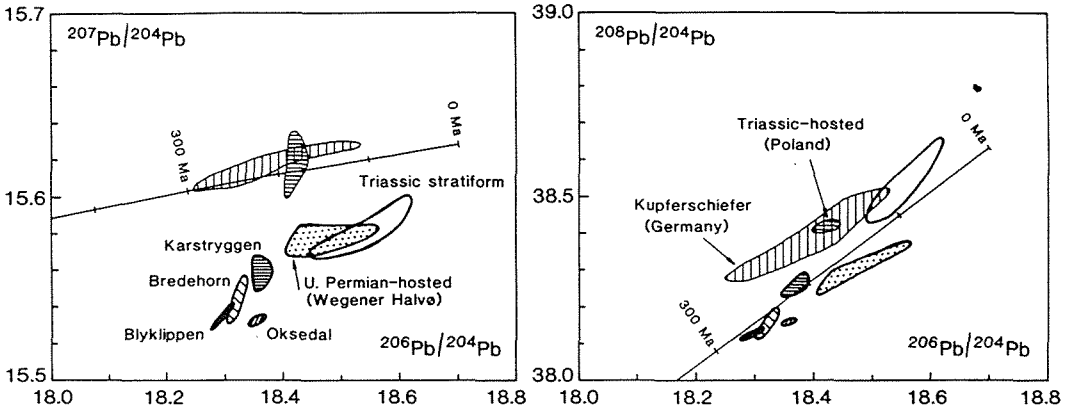

Fig. 2. Lead isotope compositional fields for sediment-hosted base metal occurrences in the Jameson Land basin compared to data for the Permian Kupferschiefer in Germany (Wedepohl *et al.*, 1978) and Pb-Zn ores in the Triassic Muschelkalk in Poland (Zartman *et al.*, 1979). Terrestrial lead isotope growth curves from Stacey & Kramers (1975).

In coordinates of $^{208}Pb/^{204}Pb$ and $^{206}Pb/^{204}Pb$ the occurrences in Upper Carboniferous-Upper Permian rocks closely follow the growth curve of Stacey & Kramers (1975), whereas the Triassic stratiform Cu-Pb-Zn occurrences plot above the thorogenic lead growth curve.

A comparison with lead isotope data for the Kupferschiefer in Germany and Pb-Zn ores in the Triassic Muschelkalk of the Silesia-Cracow region in Poland shows broad linear trends of compositions for both north-western Europe and eastern Jameson Land (Fig. 2). The Silesia-Cracow ores define a steep array comparable to the trend for vein and replacement mineralisation in western Jameson Land. All analysed ore leads in the Jameson Land basin have been derived from reservoirs with lower μ-values than those in the European deposits.

4. DISCUSSION

Triassic stratiform mineralisation is considered synsedimentary-diagenetic (Thomassen *et al.*, 1982). Upper Permian-hosted occurrences on Wegener Halvø appear to represent both syngenetic and epigenetic mineralisation (Harpøth *et al.*, 1986) and have similar, but slightly less radiogenic lead isotope compositions.

A model for vein and replacement mineralisation that invokes circulation of basinal fluids is preferred. Connate waters may have been expelled during compaction of the thick sediment pile. The conspicuous alignment of the deposits along the faulted basin margin suggests that faulting was important as ground preparation or for triggering mineralisation. Tertiary basaltic sills and dykes constitute as much as 10% of the rock volume (Larsen & Marcussen, 1992) and may have augmented circulation by heating fluids.

Ranges of lead isotope compositions for mineralisation in western Jameson Land show broadly linear trends in both the uranogenic and thorogenic lead isotope diagrams (Fig. 2). The trends may have been produced by progressive dilution of low-μ lead mineralising fluids derived at depth (comparable to Blyklippen vein lead) as they reached

higher stratigraphic levels and reacted with the Upper Permian marine carbonate rocks to form replacement ores. Bredehorn samples occupy intermediate positions on these postulated mixing trends.

The lower-μ lead component in vein galenas is considered derived from Palaeozoic conglomerates and sandstones in deeper parts of the basin. The source of the clastic sediments is the Middle Proterozoic gneisses, Upper Proterozoic sediments and Caledonian granites to the west of the basin fault margin. Mineralised samples from Middle Proterozoic gneisses in this region suggest a lead source age of *c.* 930 Ma and a first stage μ value of 8.1 (Jensen, in review).

Strontium isotope data for the Karstryggen celestite deposit in Upper Permian carbonates indicate that the Sr is derived from continental clastic sediments rather than marine brines (Scholle *et al.*, 1990), and this further supports the notion that metals in the vein and replacement sulphide ores may have been mobilised from sediments within the Jameson Land basin.

5. ACKNOWLEDGEMENTS

The Danish Natural Science Research Council and the Danish Research Academy granted funds for analytical work. Published by permission of the Director of the Geological Survey of Greenland.

6. REFERENCES

Harpøth, O., Pedersen, J. L., Schønwandt, H. K. & Thomassen, B. 1986. The mineral occurrences of central East Greenland. Meddr Grønland, Geosci. 17, 139 pp.

Jensen, S. M. in review. Lead isotope studies on mineralisations and ore deposits in East Greenland. Rapp. Grønlands geol. Unders.

Larsen, H. C. & Marcussen, C. 1992. Sill-intrusion, flood basalt emplacement and deep crustal structure of the Scoresby Sund region, East Greenland. In: Storey, B. C., Alabaster, T. & Pankhurst, R. J. (eds.) Magmatism and the causes of continental break-up. Geological Society Special Publication 68, pp 365-386.

Scholle, P. A., Stemmerik, L. & Harpøth, O. 1990. Origin of major karst-associated celestite mineralization in Karstryggen, central East Greenland. Jour. Sed. Petrology 60:397-410.

Stacey, J. S. & Kramers, J. D. 1975. Approximation of terrestrial lead isotope evolution by a two-stage model. Earth Planet. Sci. Lett. 26:207-221.

Surlyk, F., Hurst, J. M., Piasecki, S., Rolle, F., Scholle, P. A., Stemmerik, L. & Thomsen, E. 1986. The Permian of the western margin of the Greenland Sea—a future exploration target. In: Halbouty, M. T. (edit.) Future petroleum provinces in the world. Amer. Assoc. Petrol. Geol. Memoir 40, pp 629-659.

Thomassen, B., Clemmensen, L. B. & Schønwandt, H. K. 1982. Stratabound copper-lead-zinc mineralisation in the Permo-Triassic of central East Greenland. Bull. Grønlands geol. Unders. 143, 42 pp.

Wedepohl, K. H., Delevaux, M. H. & Doe, B. R. 1978. The potential source of lead in the Permian Kupferschiefer bed of Europe and some selected Paleozoic mineral deposits in the Federal Republic of Germany. Contrib. Mineral. Petrol. 65:273-281.

Zartman, R. E., Pawlowska, J. & Rubinowski, Z. 1979. Lead isotopic composition of ore deposits from the Silesia-Cracow mining district. Praise Inst. Geol. 95:133-151.

Current Research in Geology Applied to Ore Deposits. Fenoll Hach-Alí, Torres-Ruiz & Gervilla (eds) (1993). ISBN 84-338-1772-8

A MASSIVE SULPHIDE DEPOSIT FORMED BELOW THE SEA FLOOR AND ASSOCIATED WITH FELSIC SILLS (HAJAR, MOROCCO)

Leblanc, M.
CNRS, Centre Géol. Géophysique, Université de Montpellier II, 34095 Montpellier, France

ABSTRACT : The massive sulfide deposit of Hajar (15 Mt), Marrakech, Morocco, lies conformably within Visean sediments which were slightly metamorphised during the Variscan orogeny in lower greenschist facies conditions. The Hajar sulfide orebody is surrounded by biotite hornfels (350-400°C) and K-feldspar rocks (>600°C) ; the massive and banded sulfide ore (pyrrhotite, sphalerite) comprises rhyolitic horizons and abundant xenolithes of felsitic material, angular or lenticular and fluidal. This close association of sulfides, felsic magma and metamorphic aureole can be explain by the intrusion *within the sediments* of a phreato-magmatic sill, depositing or/and carrying sulfides.

INTRODUCTION

It is generally accepted that massive sulfide deposits formed as hydrothermal precipitates and sediments *on* the sea floor, at the discharge sites of hydrothermal convective systems (Hutchinson, 1973). This model was strengthened by the discovery of active hydrothermal vents and associated sulfide deposits along mid oceanic ridges (Francheteau *et al* , 1979). Nevertheless, the corresponding sulfide bodies are substantially smaller, from 2 to 3 orders of magnitude, except in sediment-covered ridges, near active margins (Davis, 1987) or in back-arc basins (Fouquet *et al* , 1991). One of the main problem dealing with the genesis of massive sulfide deposits is to explain how a 400°C-fluid reaching a cold sea water (4°C) can deposit a huge volume of sulfides covering a wide surface around the discharge site. In the case of sediment-covered ridges, sediments probably acted as thermal screens for mineralizing hydrothermal fluids allowing efficient sulfide deposition *beneath* the sea floor (Einsele, 1982 ; Davis, 1987). The massive sulfide deposit of Hajar (Visean terranes of Marrakech, Morocco) is surrounded by a biotite metamorphic halo and is closely associated with rhyolitic material. The aim of this paper is to describe the relationships between sulfides, rhyolite and enclosing sediments in the Hajar orebody and to discuss a possible genetic model (Leblanc, 1993).

THE HAJAR OREBODY

The massive sulfide deposit of Hajar is located in the Visean terranes of Marrakech (Bernard *et al* , 1988) which belong to the western external basin of the Variscan orogenic domain of Morocco. This external basin is characterized by moving thrusts and by syntectonic turbiditic sedimentation and associated felsic and basic magmatism ; massive sulfide deposits are present and correlations with the South-Iberic Pyritic Belt are possible (Bordonaro *et al* , 1979).

Discovered in 1984, below a thick quaternary cover (Felenc *et al* , 1985), this important orebody (15 Mt of workable ore) lies conformably within Upper Visean turbidites which only suffered low grade greenschist facies metamorphic conditions during Variscan tectonics. It corresponds to a 70 m thick lense, up to 500 m in length, of massive and banded sulfide layers gradding laterally to interbanded sulfide and sediment layers ; accessory lenses, a few meters thick, are present both in the footwall and in the hangingwall. The sulfide beds (pyrrhotite-sphalerite-galena-chalcopyrite with biotite-muscovite-chlorite) display a very fine mineral banding and always contain abundant angular or flexuous fragments of chloritite ; the banding can be discordant wih flow textures and wallrock fragments can be included ; chloritite-rich sulfide beds are more abundant along the borders of the orebody. Small sulfide injections, in the form of glove fingers or of fractures filling, locally cut the stratification plane, either upwards or downwards. Sphalerite-(galena)-rich ores are mainly developped along the margins of the massive sulfide lense as well along the footwall than along the hangingwall ; primary pyrite is locally present instead of pyrrhotite. Stockwork facies are poorly extended and there is no jasper bed at the top.

From mineralogical and textural evidences, the sulfide association crystallized at temperatures over 300°C ; pyrrhotite and sphalerite (8-9 mol% FeS) display no compositional

variation through the orebody. Preliminary lead isotopic data reveal no variation in fluid source (Fariss, 1992) and sulfur isotopic data (Ouiguir, 1987) should indicate a magmatic source for sulfur ($\partial^{34}S$ about 1‰).

THE METAMORPHIC HALO

The Hajar deposit is surrounded by a metamorphic zone characterized by the progressive developpement of biotite and pyrrhotite up to constitute biotite-labrador-pyrrhotite hornfelds (with accessory calcite-sericite-quartz-apatite-ilmenite) ; K-feldspar is present near the contacts. This biotite metamorphic zone is wider at the footwall (40 m) than at the hangingwall (20 m). The metamorphic association is also present along the wallrocks of small sulfide injection structures, at a millimeter scale, or along isolated sulfide beds. Within the orebody, interbedded sediments are strongly sericitised and impregnated by biotite and sulfides (up to 15 vol% and 20 vol% respectively), along intergranular pores and along the more permeable stratification planes.

The developpement of the metamorphic halo corresponds to a prograde continuous reaction : quartz+muscovite+carbonate+pyrite+Ti-oxides ----> biotite+Ca-plagioclase+pyrrhotite+ilmenite from carbonated shales in presence of fluids between 350 and 400°C (Ferry, 1984 ; Goujou *et al*, 1988) ; sanidine indicates temperatures above 600°C along the contacts. Biotite was later chloritized ; biotite and chlorite generally are iron-rich.

RHYOLITE MATERIAL

Rhyolite sills, a few meters in thickness, are present laterally (eastwards) or about 50 m below the orebody ; they include massive, breccia and hyaloclastite facies and are sulfide (up to 15 vol%)- and biotite-rich ; they are surrounded by biotitic hornfelds.

The massive sulfide lense is flanked, along its footwall as along its hangingwall, by lenticular horizons of rhyolitic material strongly transformed in a biotite-pyrrhotite-plagioclase assemblage which then was chloritized. There, narrow sills are still recognizable : they locally cut the enclosing sediments, which by place may be melted, and are surrounded by a biotite-sanidine metamorphic halo ; they are sulfide-rich (up to 30 vol%) and exhibit flow and breccia structures.

Within the massive sulfide orebody there are also scarce rhyolitic horizons whith small apophysis cutting and metamorphosing the interbedded sediments (biotite-labrador-pyrrhotite-sericite-ilmenite assemblage). More important is the fact that most of the chloritite fragments appear to be rhyolitic material : they display flexuous flow structures and can be vesicular ; scarce rhyolitic quartz, apatite crystals and relatively abundant zircon crystals with typical shapes of late rhyolitic zircons are present. They include abundant pyrrhotite blades, concordant with respect to the flow structure, and a sulfide-biotite assemblage filling vesicules and fractures.

The intimate sulfide-rhyolite association, their mutual relationships (sulfide-bearing rhyolite sills, rhyolitic fragments within massive sulfide) and the developpement of a similar thermal metamorphic halo, along the wallrocks both of rhyolite sills and of sulfide bodies, show that sulfide ore and rhyolite were together emplaced.

DISCUSSION

From the above descriptions and data and refering to the sediment-covered oceanic ridges and the associated magmatic and hydrothermal intrusions within sediments (Kelts, 1982 ; Einsele, 1982), it is suggested that the Hajar orebody was emplaced as a phreatomagmatic intrusion within soft sediments. The hot intrusion of rhyolite sills within water-rich sediments allows the formation of supercritic fluids flowing with rhyolitic material along stratification plane. The estimated temperatures (350-450°C) and the thickness of the biotite halo (40 m downwards, 20 m upwards) are consistent with the estimated cooling temperatures (900-600°C) of a rhyolite sill. Soft deformation structures accompanying small injections of sulfide or rhyolite show that enclosing sediments were not fully lithified and consequently that sill emplacement occured les than 300 m below seafloor. Then, the metamorphosed sediments, becoming harder and less permeable, acted as a thermal screen allowing a more efficient deposition of sulfides from the flowing hydrothermal fluids. There was probably a kind of sulfide mush flowing and carrying rhyolitic elements as well as fragments of the enclosing metamorphosed sediments ; these structures were overprinted by Variscan tectonics.

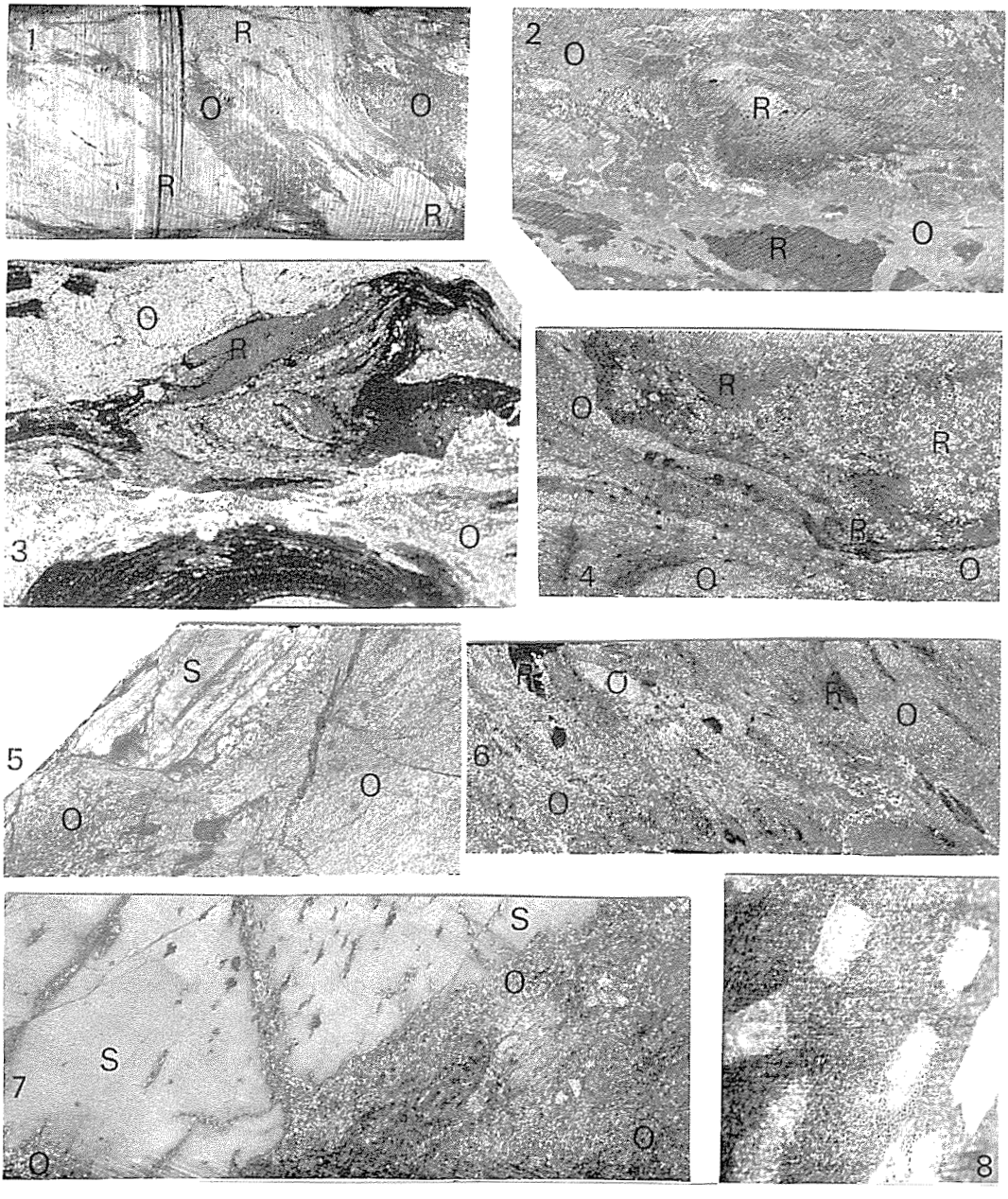

1. Sulfide-rich rhyolite sill (East of the orebody) ; 2. Sulfide-rhyolite flow breccia (top) ; 3. Sulfide-rhyolite flow breccia (floor) ; 4. Sulfide-rich rhyolite fragment in ore (upper part) ; 5. Zn-rich ore with angular metasilt fragment (upper part) ; 6. Zn-rich ore with flow structures and rhyolite fragments (lower part) ;
7. Discordant contact ore/ metasilt layer ; 8. Spotted (spots=calcite+seric.chl.sulf.Q.) biotitite (footwall).

R : rhyolite material ; **O** : sulfide ore ; **S** : metasilts.

With regard to the source zone of the ore forming elements, it is obvious that they cannot come from the surrounding rocks which, furthermore, were rather enriched in sulfides. The mineralizing fluids probably came from a deeper source zone and accompanied upwelling felsic magmas. A convective hydrothermal system initiated by felsic magma reservoirs can be proposed.

CONCLUSIONS

(1) - Massive sulfide deposits can be formed *beneath* the sea floor, by phreatomagmatic sills intruding soft sediments ;

(2) - Some characteristics of other massive sulfide deposits can be explained following this genetic model (metamorphic alteration of hangingwall, sulfide mineralogical zoning, flow and breccia structures in sulfide ore, lateral gradation to rhyolite body, no stockwork, etc...) ;

(3) - Mass balance calculations concerning metals transfer from oceanic crust to sea water, by convective hydrothermal systems, must take into account the possibility of metal deposition *beneath* the sea floor.

Acknowledgments : The Guemassa Mining Company (ONA holding), Casablanca, is gratefully acknowledged for supplying technical and financial support and giving permission for this investigation to be published.

REFERENCES

Bernard, A.J., Maier, O.W. & Mellal, A. 1988. Aperçu sur les amas sulfurés massifs des hercynides marocaines. Mineral. Deposita 23 : 104-114

Bordonaro, M., Gaillet, J.L. & Michard, A. 1979. Le géosynclinal carbonifère sud-mésétien dans les Jebilets (Maroc). Une corrélation avec la province pyriteuse du Sud de l'Espagne. C.R.Acad.Sci., Paris. 288 : 1371-1374

Davis, E.E. 1987. Massive sulfides in a sedimented rift valley, northern Juan de Fuca Ridge. Earth.Planet.Sci.Letters 82 : 49-61

Einsele, G. 1982. Mechanisms of sill intrusion into soft sediments and expulsion of pore water. Init.Rep.Deep Sea Drill.Proj. 64 : 1169-1176

Fariss, K. 1992. Composition isotopique en plomb et genèse des gisements Pb-Zn à encaissant paléozoïque de l'Anti-Atlas et Haut-Atlas marocains. Diplôme Etudes. Approfondies, Univ. Montpellier 2, 48 p.

Felenc, J., Aldi, M., Bellot, A., Fournier, M., Heurras, M. & Didori S. 1985. Découverte d'un amas caché à pyrrhotite et métaux de base à Hajar (massif des Guemassa, Maroc). Chron.Rech.Min. 478 : 61-66

Ferry, J.M. 1984. A biotite isograde in South-Central Maine, USA : mineral reactions, fluid transfer and heat transfer. J.Petrol. 25 : 871-893

Fouquet, Y. 1991. Hydrothermal activity and metallogenesis in the Lau back-arc basin. Nature 349 : 778-781

Francheteau, J. 1978. Massive deep sea sulfide ore deposits discovered by submersible on the East Pacific Ridge. Nature 277 : 523-528

Goujou, J.C., Goldberg, J.M. & Leyreloup, A. 1988. Réaction de décarbonatation dans les roches calcaréo-pélitiques de la Ballongue (zone nord-pyrénéenne) : formation de biotite et de plagioclase. C.R.Acad.Sci., Paris, 307 : 39-44

Hutchinson, R.W. 1973. Volcanogenic sulfide deposits and their metallogenic significance. Econ.Geol. 68 : 1223-1246

Kelts, K. 1982. Petrology of hydrothermally metamorphosed sediments at deep sea drilling site 477, southern Guaymas basin rift, Gulf of California. Init.Rep.Deep Sea Drill.Proj. 64 : 1123-1136

Leblanc, M. 1993. Amas sulfuré formé par injection de sills dans des sédiments : exemple d'Hajar (Marrakech, Maroc). C. R. Acad. Sci. Paris, 316 : 499-503

Ouiguir, H. 1987. Etude métallographique et géochimie isotopique du soufre de la minéralisation de Douar Lahjar (Maroc). Dipl. Et. Approf., Inst. Nat. Polyt. Lorraine, Nancy, 44p.

FIGURE : Photographies of drill cores (scale : the smaller side is about 4 cm wide)

Current Research in Geology Applied to Ore Deposits. Fenoll Hach-Ali, Torres-Ruiz & Gervilla (eds) (1993). ISBN 84-338-1772-8

PALAEOSTRUCTURAL MARKERS IN THE SOUTHERN IBERIAN PYRITE BELT: STOCKWORKS AND FEEDER ZONES OF VOLCANO-MASSIVE SULPHIDE DEPOSITS

Leistel, J-M.; Bonijoly, D. & Marcoux, E.
BRGM - BP 6009 - 45060 Orleans Cedex 2, France

Abstract: The VMS deposits of the Late Devonian-Early Carboniferous South Iberian Belt are commonly rooted in their feeder stockworks. Many other sulphide occurrences, show no obvious relationship with the VMS, although they are certainly contemporaneous with the massive deposits from the structural standpoint; they also show the same chemico-mineralogical and isotopic signatures. It is probable that these occurrences mark palaeostructural channels leading to the massive sulphide emplacement.

INTRODUCTION: The geometry of volcano-massive sulphide deposits is now well established and extensively described: a stockwork cutting the country rock passes upward, more or less progressively, into stratiform massive sulphides. The stockwork marks the subsurface path of the mineralizing fluids that deposited the massive sulphides on the floor of a basin. The importance of structural control on the emplacement of the massive mineralization has been shown by the discovery of deposits such as Corbett in Canada and by the alignments of pipes and massive sulphide bodies along active faults on present-day ocean floors.

In the South Iberian Pyrite Belt, some very spectacular stockworks such as Rio Tinto (Garcia Palomero, 1990) and San Miguel leave no doubt as to their nature and their link with the stratiform massive sulphides. For many other vein sulphide occurrences, however, it is not easy to determine whether they represent feeder stockworks to massive sulphides or whether they are later, independent vein manifestations. Detailed mineralogical, isotopic and structural studies carried out on numerous massive sulphide bodies and vein occurrences of the South Iberian Pyrite Belt have now enabled this problem to be resolved and have provided criteria for characterizing the roots of the massive sulphide deposits in this region.

GEOLOGICAL SETTING: The South Iberian Pyrite Belt is one of the largest massive sulphide provinces in the world, with probably more than 80 deposits containing in excess of 1000 Mt of sulphide ore. The belt comprises rocks ranging in age from Late Devonian to Early Carboniferous with, in particular, a thick volcano-sedimentary formation (VS) hosting the sulphide deposits. This formation is intercalated between a Late Devonian phyllitic quartzite formation (PQ) and Dinantian detrital Culm deposits (Schermerhorn, 1971; Routhier et al., 1980; Oliveira, 1990). The whole of the belt was deformed into synclines and anticlines, and strongly affected by thrust planes during Middle Westphalian tectonism.

The massive sulphide deposits of this Pyrite Belt are well described (Schermerhorn, 1970; Routhier et al., 1980; Strauss and Gray, 1984; Garcia Palomero, 1990; Barriga, 1990; Leca, 1990), but the vein mineralization is much less well known due to the absence

of economic interest. The 1:50,000-scale geological maps of Spain show some 100 occurrences representing vein mineralization hosted by the PQ, VS and Culm formations and comprising predominantly quartz-pyrite-chalcopyrite (La Ratera, Los Sililos, Las Viñas), in places quartz-galena-sphalerite (La Aurora) and more rarely quartz-stibnite (La Esmeralda, Nerón) or quartz-cassiterite-scheelite (Bajo Corumbel - La Palma del Condado; Sáez *et al.*, 1988). Vein mineralization with fluorite-galena-sphalerite-chalcopyrite (Los Angeles) and quartz-pyrite ± chalcopyrite-grey copper (Lomochaparro, Valdeflores, Magalejo) is also hosted by the granite and granodiorite intrusions at the northeastern edge of the Belt.

Although some of the mineralization is clearly later than the stratiform massive sulphides (Bajo Corumbel, Sáez *et al.*, 1988; Nerón), the interpretation for most of these quartz-sulphide vein occurrences is still open to question. The La Ratera - Los Sililos group is without doubt the most important of the occurrences, forming an E-W vein swarm about 5 km long to the east of Valverde del Camino; the Las Viñas (or Los Hundimientos, near Sotiel) mineralization belongs to this group. The veins are hosted by the PQ formations and are in places very close to the transition zone with the overlying VS formations.

HOMOGENEITY OF MINERAL PARAGENESIS: Compared to the massive sulphides, the feeder stockworks show a specific paragenesis with pyrrhotite-pyrite and Bi and Co minerals. This association is also found in the mineralization of the La Ratera - Los Sililos group (Marcoux and Moelo, 1993).

HOMOGENEITY OF LEAD ISOTOPIC SIGNATURE: The massive sulphides and their feeder stockworks show a very characteristic lead isotopic signature ($^{206}Pb/^{204}Pb$ = 18.187 ± 0.050, $^{207}Pb/^{204}Pb$ = 15.620 ± 0.025, Marcoux *et al.*, 1992) that is clearly less radiogenic than that of the later veins ($^{206}Pb/^{204}Pb$ >18.30). The sulphide mineralization of the La Ratera-Los Sililos group shows an identical isotopic signature to that of the massive sulphides and their underlying stockworks.

HOMOGENEITY OF STRUCTURAL PATTERNS: The feeder stockworks of the volcano-massive sulphides represent one of the more visible traces of the structure that controlled the emplacement of the mineralization. A statistical analysis of the distribution of the sulphide veins in the spectacular Rio Tinto stockwork has made it possible to determine the primary structure, after unfolding the Hercynian deformation (Bonijoly, 1993). The fractures fall into three families (N 120°E, N 5°E and N 70°E) all of which could result from a N 120°E sinistral shear tectonism contemporaneous with the emplacement of the orebodies. The structures in the La Ratera-Los Sililos-Las Viñas vein corridor strike N 100°E; here the vein mineralization appears to predate the first phase of Hercynian deformation and to have been transposed along the major foliation plane (Bonijoly, 1993). The original orientation of this vein corridor was probably similar to the main structural direction of the Rio Tinto stockwork.

CONCLUSION: The feeder zones of the massive sulphide deposits in the South Iberian Province show analogous mineralogical, lead

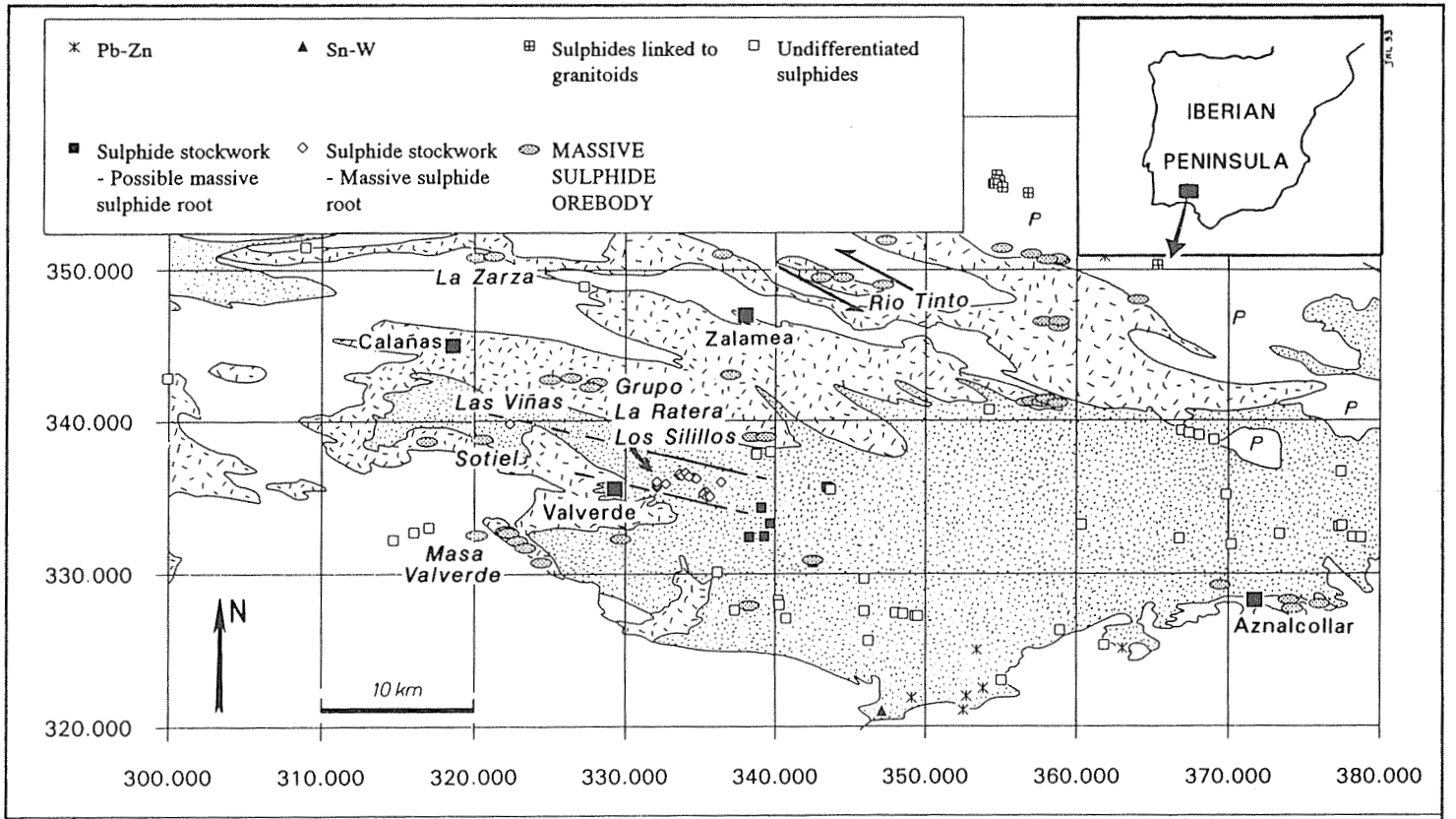

SOUTH IBERIAN PYRITE BELT: Mineralized occurrences and deposits
Area of Valverde - Rio Tinto (Spain)

isotopic and structural traits. Therefore, quartz-sulphide vein mineralization that shows the same traits can be considered as belonging to them. This will make it possible to map the palaeostructures that could have controlled the emplacement of the massive sulphide mineralization, which should provide a practical exploration guideline.

This work was financially supported by a BRGM research project and partly by the Commission of European Communities (contract MA2M-CT90-0029).

REFERENCES

Barriga F.J.A.S. 1990. Metallogenesis in the Iberian pyrite belt. in Pre-Mesozoic Geology of Iberia, R.D. Dallmeyer et E. Martínez García Ed., Springer-Verlag, pp.369-379.

Bonijoly D. 1993. Structural context of volcano-massive sulphide deposits in the South Iberian Pyrite Belt. C.E.C. Final Report of Contract MA2M-CT90-0029, in press.

Garcia Palomero F. 1990. Rio Tinto deposits. Geology and geological models for their exploration and ore reserves evaluation. In: Sulphide Deposits - Their Origin and Processing, Inst. Min. Metal., pp.17-35.

Leca X. 1990. Discovery of concealed massive-sulphide bodies at Neves- Corvo, southern Portugal - a case history. Trans. Instn. Min. Metall., Sect.B, 99, pp.B139-B152.

Marcoux E., Leistel J.M., Sobol F., Milési J.P., Lescuyer J.L., Leca X. 1992. Signature isotopique du plomb des amas sulfurés de la province de Huelva, Espagne. Conséquences métallogéniques et géodynamiques. C. R. Acad. Sci. Paris, Série II, 314, pp.1469-1476.

Marcoux E., Moello Y. 1993. Comparative mineralogy of massive and stringer sulphide ore deposits in Southern Spain. 2nd Biennal SGA Meeting, Granada, Spain, Sept. 1993.

Oliveira J.T. 1990. South Portuguese Zone: 1) Introduction, 2) Stratigraphy and synsedimentary tectonism. In: R.D. Dallmeyer and E. Martínez Garcia (Eds.), Pre-Mesozoic geology of Iberia, Springer-Verlag, pp.333-347.

Routhier P., Aye F., Boyer C., Lecolle M., Molière P., Picot P., Roger G. 1980. La ceinture sud-ibérique à amas sulfurés dans sa partie espagnole médiane. Tableau géologique et métallogénique. Synthèse sur le type amas sulfurés volcano-sédimentaires. 26th Inter. Geol. Congr., Paris; BRGM Mem. 94, 265 p.

Saez R., Ruiz de Almodovar, Pascual E. 1988. Mineralizaciones estratoligadas de scheelita en la faja piritica del suroeste iberico. Bol. Soc. Esp. Mineral., 11-1, pp.135-141.

Schermerhorn L.J.G. 1970. The deposition of volcanics and pyrite in the Iberian pyrite belt. Mineral. Deposita., 5, pp.273-279.

Schermerhorn L.J.G. 1971. An outline stratigraphy of the Iberian pyrite belt. Bol. Geol. Min., Spain, v.82, pp.238-268.

Strauss G.K., Gray K.G. 1984. Base metal deposits in the Iberian pyrite belt. in Geology and metallogeny of copper deposits, Ed. Friedrich et al., Springer Verlag, pp.304-324.

Current Research in Geology Applied to Ore Deposits.Fenoll Hach-Alí, Torres-Ruiz & Gervilla(eds)(1993).ISBN 84-338-1772-8

BLACK SHALE-HOSTED, LOW GRADE Ni-Cu-Zn DEPOSIT AT TALVIVAARA, FINLAND

Loukola-Ruskeeniemi, K. (1) & Heino, T. (2)
(1) Geological Survey of Finland. SF-02150 Espoo, Finland
(2) Geological Survey of Finland. P.B. Box 1237, SF-70701, Kuopio, Finland

ABSTRACT: The Talvivaara deposit contains 300 Mt ore averaging 0,26% Ni, 0,14% Cu and 0,53% Zn. It is hosted by metasediments rich in graphitic carbon (median value 8%). Trace element concentration (B, F, Hg, Se, etc) point to hydrothermal influx. Sulphur isotope $\delta^{34}S$ values of Ni-Cu-Zn-rich black schists (average for 100 pyrite samples -0,84‰ and for 120 pyrrhotite samples -0,61‰) indicate that hydrothermal sulphur was mixed with seawater. Sulphides are syndiagenetic in origin and, in part, have been recrystallized and mobilized.

INTRODUCTION

Thick beds of argillaceous sediments containing abundant organic matter and sulphur were deposited at the sea bottom in eastern Finland 1.96-1.97 billion years ago. Concurrently, hydrothermal processes connected with seafloor spreading occurred in these sedimentation basins. In the Outokumpu area, Cu, Co, Zn, and occasionally also Ni, were deposited, and at Talvivaara, some 150 km northwest of Outokumpu, Ni, Cu, and Zn (see Figs. 1 and 13 in Loukola-Ruskeeniemi 1992).

In the *Outokumpu* district, 11 Cu-Zn-Co massive sulphide deposits originally had combined reserves of 50 Mt ore grading 2.8% Cu, 1 % Zn, 0,2% Co and 0.1% Ni (Gaál and Parkkinen, in press). Three deposits were mined during 1913-1989. Ores are hosted by cherty quarzite and calc-silicate rocks associated with serpentinite. Sedimentary structures are found in the upper parts of the ore.

The occurrences of *Talvivaara* were discovered in 1977, and the ore estimate completed two years later indicated more than 300 Mt averaging 0.14% Cu, 0.26% Ni, 0.02% Co, 0.53% Zn, 0,35% Mn, 10% Fe, 7% C, 630 ppm V, 102 ppm Mo and 2.6 ppm Ag (Ervamaa and Heino 1980). The Outokumpu company owns the deposit at present, but has not yet begun mining activities.

RESULTS

Geological setting. In the Talvivaara area, Early Proterozoic arkosites and quartzites rest on late Archaean basement, usually with a tectonic contact in between (see Fig. 4 in Loukola-Ruskeeniemi et al. 1991). The arkosites and quartzites are in turn overlain by thin layers of calc-silicate rocks derived from dolomites. These sediments are overlain by mica schists and black schists (=metamorphosed black shales). Black schist contains layers with Ni > 0.2% (Fig. 1). In places, the horizon with Ni+Cu+Zn > 0.8% is up to 330 m thick. The Talvivaara schists containing > 1% C_{graf} and > 1% S are classified into four groups (Fig. 2). Ni-Cu-Zn-rich black schists differ from other black schists in their greater electrical conductivity. Resistivity is less than 0.01 Ωm, compared with values of 0.01-10 Ωm for normal black schists.

Mineral composition. 'Normal' black schist (Fig. 2) has quartz, micas, graphite and sulphides as main minerals, while accessories include rutile, apatite, zircon, feldspar and garnet. Ni-Cu-Zn-rich black schist contains quartz phlogopite, graphite and sulphides. Mn-rich black schist (Mn > 0.8%) contains quartz, micas, graphite, iron sulphides and alabandite (MnS). The black calc-silicate rock consists of tremolite, graphite and sulphides (including alabandite), and sometimes it also contains Mn-bearing garnet.

Sulphides. Pyrite occurs as spheroidal grains (<0.01 mm), which have gradually coalesced and recrystallized into coarser grains. Pyrrhotite is present in the fine-grained sulphide dissemination and as coarser grains, and sometimes enclose fine-grained spheroidal pyrite. Sphalerite occurs as rounded small (<0.01 mm) grains and coarser grains. In addition Ni-Cu-Zn-rich black schist (Fig. 2) contains chalcopyrite and pentlandite, while Mn-rich black schist contains alabandite.

Geochemistry. Median concentration of graphitic carbon is 8% (range 1.5-18%, 278 samples) and that of sulphur 9% (range 1.8-26%, 278 samples). Average Ni, Cu, Zn, Co and Mn concentrations are shown in table 2 in Loukola-Ruskeeniemi *et al.* (1991). In addition to elements determined by ICP-AES alnalysis, numerous trace elements were determined by various methods. Rare earth element patterns (Fig. 7e in Loukola-Ruskeeniemi 1991) show cerium depletion indicating a marine origin, and a positive europium anomaly indicating hydrothermal influx.

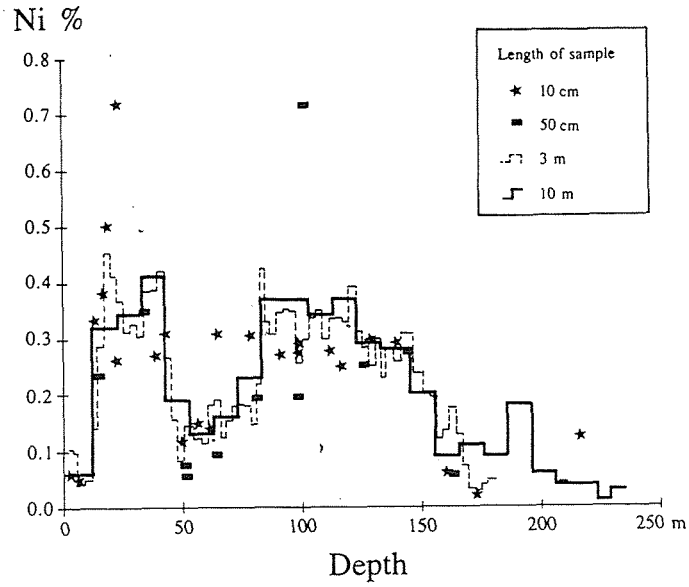

Fig. 1. Nickel values in drill core 3344: 308. Already a 10-m-long sample provides enough information for the ore estimate.

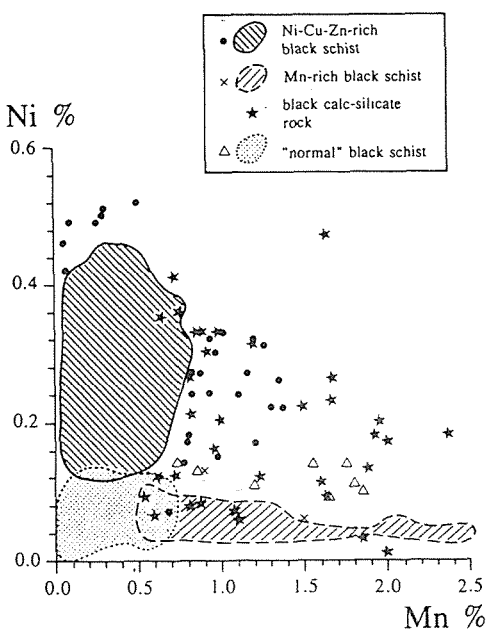

Fig. 2. Nickel and manganese concentrations of altogether 1505 black schist samples (average length 10 m, see Fig. 1) and 43 samples of black calc–silicate rock (length 0.5–3.0 m).

The hydrothermal influx is confirmed by other trace element data. Even the limited results reported in Table 1 provide strong evidence for hydrothermal addition. A detailed description and interpretation of the major and trace element data will be published elsewhere (Loukola–Ruskeeniemi and Heino, in prep.). Gold correlates with Sb (0.9), Hg (0.7) and S (0.5). Uranium concentrations are low compared with those of the Scandinavian alum shales. Uranium correlates with thorium in 13 samples, but not in 7 other samples. This might be due to redistribution of uranium. Thorium correlates with cerium (r=0.9).

Degree of pyritization (DOP) is a measure of the ratio pyrite iron/(pyrite iron + reactive iron) which is considered to be indicative of the depositional environment of a sediment (e.g. Leventhal and Taylor 1990). DOP values for the Talvivaara black schists range from 55.9% to 89.8% with an average of 75.2% (11 determinations). Results point to euxinic conditions.

Sulphur isotope $\delta^{34}S$ *values* of the 'normal' black schists (Ni+Cu+Zn $\leq$ 0.8% and Mn $\leq$ 0.8%) exhibit a bimodal frecuency distribution in drill core 3344:329 (85 samples). Heavier sulphur occurs in the beds of normal black schist lying between

Table 1. Trace element concentrations in black schists and black calc–silicate rocks, determined by DCP (Ag, Pb, B), FA-DCP (Au, Pd, Pt), ICP-MS (Bi, Ce, Nb, Sb, Sn, Th, Tl, U, W), GFAA (Se) etc., at X-Ray Assay Laboratories. Average sample size 50 cm in drill core. *d.l.*= detection limit ; *n*= number of samples

	median	*max*	*(d.l.)*	*n*
Ag ppm	1.5	49	(0.5)	132
Au ppb	13	150	(1)	125
B ppm	22	300	(10)	132
Bi ppm	0.5	1.8	(0.1)	24
Ce ppm	39	76	(0.5)	26
Cl ppm	70	160	(20)	125
F ppm	915	10000	(20)	144
Hg ppb	1160	7470	(5)	102
Nb ppm	2	9	(1)	20
Pb ppm	39	1600	(2)	132
Pd ppb	21	91	(1)	125
Pt ppb	10	50	(10)	125
Sb ppm	3	63	(1)	20
Se ppm	18	67	(0.1)	132
Sn ppm	2	5	(1)	20
Th ppm	6	12	(0.1)	20
Tl ppm	11	19	(1)	26
U ppm	17	47	(0.1)	20
W ppm	4	25	(1)	20

Table 2. Average sulphur isotope $\delta^{34}S$ values (‰) of pyrite and pyrrhotite in 'normal' black schist (Ni+Cu+Zn ≤ 0.8% and Mn ≤ 0.8%) and Ni–Cu–Zn-rich black schist. *n*= number of samples

	pyrite	*pyrrhotite*
'Normal' black schist	-3.38 *n*=102	-4.40 *n*=57
Ni–Cu–Zn-rich black schist	-0.84 *n*=100	-0.61 *n*=120

Ni–Cu–Zn–rich black schist horizons, whereas a fairly constant level of –5‰ characterizes the normal black schists farther away. The S–isotope values for the Ni–Cu–Zn–rich black schists exhibit regular fluctuations between some 2‰ and –3‰. No correlation exists between the nickel and S–isotope values. The average S–isotope values differ for the normal and metal–rich black schists at Talvivaara (Table 2). The heavier sulphur in the Ni–Cu–Zn–rich black schists (max 12.19‰) is due to sulphur of hydrothermal origin mixing with sea–water.

Carbon isotope $\delta^{13}C$ (PDB) values, ranging from –24.70 to –27.42 (4 samples), are comparable to the average isotopic composition of organic carbon in sedimentary rocks.

CONCLUSIONS

The Talvivaara black schists were deposited in euxinic conditions and their relatively high carbon concentrations (median 8%) point not only to a vigorous organic production but to the relatively good preservation of organic material in the sediments. Organic matter may be better preserved in euxinic than in oxidizing conditions, since in euxinic conditions there are fewer bacterial grazers (Lee, 1992).

The Outokumpu rock assemblage that host the Outokumpu ore deposits consists of serpentinite, Cr–bearing calc–silicate rocks, cherty quartz rocks and black schist and is considered ophiolitic. Cr–bearing calc–silicate rocks and altered serpentinites (talc–carbonate rocks) are also encountered at Talvivaara. Looked at world–wide, the composition of ophiolites and associated ores has changed significantly over time. When ophiolites appeared about 2.0–1.9 Ga ago, Cr, Ni and Cu were concentrated within them. According to Dobretsov *et al.* (1992), a change in upper mantle convection may be the key to the magmatic and

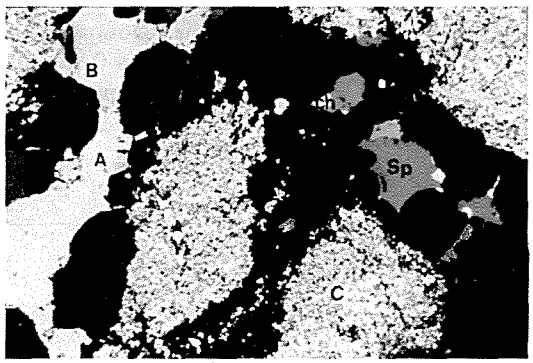

Fig. 3. Nickel and cobalt concentrations in **A**) coarse-grained pyrite: 0.05% Ni and 0.13% Co; **B**) coarse-grained pyrrhotite: 0.36% Ni and 0.05% Co; **C**) spheroidal pyrite (<0.01 mm): 0.33–0.49% Ni and 0.06–0.08% Co. **sp** = sphalerite, **ch** = chalcopyrite. Drill core 3344: 329, 145.65 m.

metallogenic evolution. The analogues for Outokumpu-type deposits are the Cu-Zn and Zn sulphide ores deposited from 'black smokers' at the bottom of modern mid-ocean ridges.

The precursors to the Talvivaara black schists were metalliferous organic-rich muds deposited in rift basin associated with seafloor spreading. The hydrothermal processes operative during thir deposition and diagenesis were similar to those encountered in recent ocean ridge environments. Spheroidal pyrite with grain size < 0.01 mm contains nickel and other metals (Fig. 3), which suggest a syngenetic origin for the mineralization. The S-isotope $\delta^{34}S$ values indicate that the sulphides are syndiagenetic and to some extent have later been recrystallized and mobilized. During the recrystallization phase, most of the Ni in the fine-grained pyrite became bound in pyrrhotite and pentlandite.

REFERENCES

Dobretsov, N.L., Konnikov, E.G. & Dobretsov, N.N. (1992). Precambrian ophiolite belts of southern Siberia, Russia, and their metallogeny. *Precambrian Res.* 58: 427–446.

Ervamaa, P. & Heino, T. (1980). A progress report on ore prospecting in the Kainuu – North Savo black schist-serpentinite formations in 1977–1979 (in Finnish). *Unpubl. Rep. M19/3344/–80/1/10, Geol, Surv. Finl.*

Gaál, G. & Parkkinen, J. (in press). Ophiolite-hosted Cu-Zn-Co deposits of the Outokumpu type and Proterozoic to Phanerozoic analogues. *Proc. of the 8th IAGOD symp., August 12–18, 1990, Ottawa, Canada.*

Lee, C. (1992) Controls on organic carbon preservation: The use of stratified water bodies to compare intrinsic rates of decomposition in oxic and anoxic systems. *Geochim. Cosmochim. Acta* 56: 3323–3335.

Leventhl J. & Taylor, C. (1990). Comparison of methods to determine degree of pyritization. *Geochim. Cosmochim. Acta* 54: 2621–2625.

Loukola-Ruskeeniemi, K. (1991). Geochemical evidence for hydrothermal origin of sulphur, base metals and gold in Proterozoic metamorphosed black shales, Kainuu and Outokumpu areas, Finland. *Mineral. Deposita* 26: 152–164.

Loukola-Ruskeeniemi, K. (1992). Geochemistry of Proterozoic metamorphosed black shales in eastern Finland, with implications for exploration and environmental studies. *Geol. Surv. Finl.,* 86 pp.

Loukola-Ruskeeniemi, K., Heino, T., Talvitie, J. & Vanne, J. (1991). Base-metal-rich metamorphosed black shales associated with Early Proterozoic ophiolites in the Kainuu schist belt, Finland: A genetic link with the Outokumpu rock assemblage. *Mineral. Deposita* 26: 143–151.

Current Research in Geology Applied to Ore Deposits.Fenoll Hach-Alí, Torres-Ruiz & Gervilla(eds)(1993).ISBN 84-338-1772-8

COMPARATIVE MINERALOGY OF MASSIVE AND STRINGER SULPHIDE ORE DEPOSITS IN SOUTHERN SPAIN

Marcoux, E. (1) & Moelo, Y (2)
(1) BRGM - SGN/GEO, BP 6009, 45060 Orleans Cedex, France
(2) CNRS - CRSCM, Rue de la Férollerie, 45100 Orleans, France

The stringers of the massive sulphide deposits in the South Iberian Pyrite Belt of southern Spain show a particular bismuth, telluride and cobalt paragenesis that is not seen in the overlying massive deposits; i.e. bismuthinite, nuffieldite and hammarite, and joseite and tetradymite. This paragenesis also makes it possible to distinguish the stringers from other quartz-sulphide veinlets.

Most massive sulphide deposits are located above feeder channels along which the ore fluids ascended to form the massive sulphide bodies; these are known as pipes, stringers or, more generally, stockworks and feeder zones,. These stringers are commonly well expressed in Iberian Pyrite Belt of southern Spain, particularly in Rio Tinto, San Miguel, Aznalcóllar, Tharsis, Concepción, etc.

The CEC research project into the factors of base- and precious metal enrichment of the South Iberian massive sulphides, carried out jointly since 1990 by BRGM, RTM and SEISMA with the collaboration of APIRSA, has led BRGM to undertake a multidisciplinary programme on more than 20 massive sulphide deposits and their immediate vicinities.

The results of the mineralogical studies show that the mineralogy of the stringers beneath the massive sulphide bodies is varied and original. It includes several rare minerals that are not seen in the overlying massive sulphides and that, for the most part, have not before been reported in the South Iberian Pyrite Belt.

The mineralogy of the Spanish massive sulphide deposits has been well studied (Strauss and Madel, 1974; Strauss *et al.*, 1980, 1981; Garcia-Palomero, 1980; Routhier *et al.*, 1980; Sierra, 1984; Garcia de Miguel, 1990, to cite only a few). The paragenesis invariably consists of dominant pyrite, sphalerite, galena and chalcopyrite, generally with accessory grey copper, cassiterite and pyrrhotite, and numerous trace minerals including electrum; bismuth, cobalt and telluride minerals are absent.

The mineralogy of the stringers is to a great extent similar to that of the massive sulphides. The paragenesis includes pyrite, galena, sphalerite, chalcopyrite, arsenopyrite and grey copper which are not significantly different in their mineralogical compositions from those in the massive sulphides. The discriminating mineralogical differences between the two ore types occur in the accessory and trace minerals; the stockworks contain three mineral associations that are unknown in the massive deposits, i.e. bismuth, cobalt and telluride parageneses.

The bismuth paragenesis is found in the chalcopyrite veinlets cutting fractured pyrite crystals, and is fairly common in the stringers (Rio Tinto, Tharsis, Concepción, Aznalcóllar) where they can be as large as 200 μm. It comprises native bismuth, bismuthinite, Bi_2S_3-PbS minerals (galenobismuthite, cosalite), Bi_2S_3-Cu_2S minerals (emplectite, wittichenite) and complex Bi-Pb-Cu-Sb sulphosalts (hammarite, krupkaite, nuffieldite, giessenite, etc.). The mineral associations indicate a syncrystallization of most of these species in equilibrium with chalcopyrite and tetrahedrite.

The cobalt paragenesis, which is known at Tharsis and Rio Tinto and has been reported at Sotiel (Garcia de Miguel, 1990), is composed commonly-fractured euhedral crystals (1-2 mm) of cobaltite, alloclasite and glaucodot, associated with pyrite, arsenopyrite and löllingite.

The telluride paragenesis, associated with the cobalt-bismuth minerals at Tharsis, is composed of bismuth tellurides (joseite A, tetradymite and tellurobismuthite).

Mineralogical studies of Kuroko deposits (Urabe, 1974) have shown a similar distribution, with bismuth minerals (wittichenite, emplectite, bismuthinite, aikinite) restricted to the "keiko ore" of the stringers. The same pattern has been recorded at Jabal Sayid in Saudi Arabia (Sabir, 1979) where bismuth tellurides are restricted to the stockwork zone underlying the massive ore. Most of the studies of stratabound sulphide deposits (see Franklin *et al*, 1981; Craig and Vokes, 1992) have not, or only just, dealt with this aspect of mineralogical zoning between the massive and stringer ores.

Chemical analyses being carried out tend to show that Bi, Co and Te concentrations are identical in the massive sulphides and their underlying stringers; in the massive sulphides, however, the three metals occur as trace elements in the major minerals. The mineralogical expression of these metals in the stringer zone must thus be attributed to different physico-chemical conditions of deposition, probably characterized by higher temperatures and pressures. This aspect is in the process of being studied.

The discovery of these rare minerals adds to the mineralogical data on the South Iberian massive sulphide deposits. It will also help increase our understanding of the complex dissolution-precipitation mechanisms that operated in these transit zones crossed by the hydrothermal fluids. Finally, from the standpoint of mineral exploration, the identification of these minerals in a mineralized veinlet within a drill core or a surface occurrence will be a positive indicator of a massive sulphide stringer.

References

Craig, J.R. & Vokes, F.M., 1992. Ore mineralogy of the Appalachian-Caledonian stratabound sulfide deposits. Ore Geology Reviews, 7: 77-123.

Franklin, J.M., Lydon, J.W. & Sangster D.F., 1981. Volcanic-associated massive sulfide deposits. Econ. Geol.: 75th Anniversary Volume: 485-627.

Garcia-Palomero, F., 1980. Caracteres geológicos y relaciones morfológicas y genéticas de las mineralizaciones del anticlinal de Rio Tinto. Arquivos de la provincia de Huelva, Huelva.

Garcia de Miguel, J.M., 1990. Mineralogía, paragénesis y sucesión de los sulfuros masivos de la Faja Pirítica en el suroeste de la península Ibérica. Bol. Geol. Min., 101-1: 73-105.

Routhier, P., Aye, F., Boyer, C, Lecolle, M., Molière, P., Picot, P. & Roger, G., 1980. La ceinture sud-ibérique à amas sulfurés dans sa partie espagnole médiane. Mém. Bur. Rech. Géol. Min. 94: 265 p.

Sabir, H. 1979. Etude géologique et minéralogique de la minéralisation sulfurée polymétallique de Jabal Sayid (Arable Saoudite). Thesis, Univ. d'Orléans (France), 174 p.

Sierra, J., 1984. Geología, mineralogía y metalogenía del yacimiento de Aznalcóllar. Bol. Geol. Min. 95: 553-568.

Strauss, G.K. & Madel. J., 1974. Geology of massive sulphide deposits in the Spanish-Portuguese Pyrite belt. Geol. Rundschau 63 (1): 191-211.

Strauss, G.K., Roger, G., Lécolle, M. & Lopéra, E., 1981. Geochemical and geological study of the volcano-sedimentary sulfide orebody of La Zarza, Huelva Province, Spain. Econ. Geol., 76: 1975-2000.

Urabe, T., 1974. Mineralogical aspects of the Kuroko deposits in Japan and their implications. Mineral. Deposita, 9: 309-324.

Current Research in Geology Applied to Ore Deposits.Fenoll Hach-Alí, Torres-Ruiz & Gervilla(eds)(1993).ISBN 84-338-1772-8

CONCEPTUALIZED REMOBILIZATION AND SYN-TECTONIC ORE EMPLACEMENT

Marshall, B. (1) & Gilligan, L.B. (2)
(1) University of Technology, Sydney, Australia
(2) Dept. of Mineral Resources and Energy, Sydney, Australia

ABSTRACT: Remobilization of pre-tectonic deposits and syn-tectonic ore emplacement are genetic models which have been controversially applied to many Pb-Zn and Cu-Zn-Pb ± Au deposits on the basis of meso- and microstructural data. A conceptual approach is used to evaluate the gross effects and fabric evolution in parent deposits remobilized during metamorphism and deformation. A comparable approach is adopted for syn-tectonic emplacement of vein systems and massive replacement mineralization. Remobilization and syn-tectonic emplacement are not mutually exclusive and, to a limited degree, each is an integral part of the other. Conceptualization shows that each process inevitably yields complex meso- and microstructural relations and complex heterogeneous parageneses. Successful discrimination between the models requires structural analysis at all scales of observation, logical and objective evaluation of all other data, and a conceptual grasp of the processes involved in remobilization and syn-tectonic emplacement.

1. INTRODUCTION

Sulphides which precipitate from hydrothermal or metahydrothermal solution, or crystallize from a melt, may subsequently undergo basin dewatering and diagenesis, and regional metamorphism and deformation. This is of concern, because these processes modify the textures and distributions of the sulphides and their alteration assemblages. They therefore extend the genetic picture, potentially mask the processes of initial formation, impact upon exploration, and substantially influence exploitation.

Metamorphic mobilization involves increasing the concentration of metallic constituents originally dispersed or disseminated in ordinary rocks; whereas remobilization involves modifying the concentration and distribution of preexisting massive and semi-massive mineralization (Marshall & Gilligan 1987, 1993). A syngenetic deposit can form from mobilization during basin dewatering; when metamorphosed and/or deformed, the deposit is *remobilized.* Depending upon the *degree* and *extent* of remobilization and whether the remobilization is *internal* or *external* (op. cit.) the resulting deposit could be classified as metamorphosed or, for the products of extensive external remobilization, metamorphogenic (Marshall & Gilligan 1987; Pohl 1992).

Syn-tectonic refers to metamorphogenic mineralization arising through advective transfer (e.g. Bell et al. 1988). Its use should be refined by placing mineralization within a structural-event sequence (e.g. syn-S_1, post-S_1/pre-S_2). The syn-tectonic concept reflects beliefs that: large fluid volumes, such as those deriving from diagenetic/metamorphic devolatilization, are needed to form vein-type deposits; appropriate levels of permeability in brittle and ductile crust are favoured by active deformation; large-scale replacements, as envisaged for some base-metal deposits (e.g. de Roo 1989), are facilitated by active deformation.

The prograde-metamorphic devolatilization model (e.g. Fyfe et al. 1978; Pohl 1992) are the favoured explanation for many shearzone- and turbidite-hosted gold deposits. It has been more controversially applied, by invoking massive replacement, to a range of Pb-Zn and Cu-Zn-Pb ± Au deposits, many of which are alternatively interpreted as either weakly or strongly remobilized VMS or SEDEX types (for examples see Marshall 1991, Pohl 1992, Marshall & Gilligan 1993). Much of the evidence adduced in support of syn-tectonic emplacement derives from the interpretation of micro-structural relations between ore-mineral species, alteration-mineral species, and microfabric elements such as cleavage and elongation lineation (e.g. Bell et al. 1988; de Roo 1989; Aerden 1991).

Much of the microstructural evidence is equally compatible with complex mechanical and chemical remobilization of pre-tectonic mineralization (Marshall 1991; Marshall & Gilligan 1993), and is seemingly at variance with other evidence (Phillips 1993). Interpretations rather than observations are at fault. In an attempt to aid better interpretation of observations, the processes involved are conceptualized.

2. REMOBILIZATION CONCEPTUALIZED

The geometry, distribution and nature of physically and chemically remobilized mineralization must be influenced by those of the parent body. This has resulted in the use of enveloping-surface principles to reveal parent geometry and of supposed primary zonation to aid structural interpretation (e.g. Sangster 1979; Aerden 1991). The approach embodies the notion that the parent had the "classical" geometry and zonation of VMS or SEDEX systems (but see Large 1992).

To improve on this too simple approach, we shall consider basin development and regional metamorphic inversion from the viewpoints of: the possible forms of pre-cleavage (pre-S_1) mineralization; and the potential for remobilization of these pre-S_1 deposits. We shall then examine the response of massive-sulphide lenses as they undergo diagenesis, metamorphism and deformation.

2.1 *Basin formation and inversion*

An extension-contraction cycle (basin formation and regional metamorphic inversion) is tracked in temperature-time space as a diagenesis-metamorphism curve (Fig. 1). Numbers along this curve correspond with those in Table 1 and equate with ore formation and remobilization. Two cleavage-producing events are recognized.

The relationship between pre-S_1 mineralization and hostrock layering are conveyed by exhalative, subhalative and inhalative oretypes (Table 1 - types 1a,b,c), and by epi-diagenetic and epigenetic replacements and vein systems (Table 1 - types 2 and 3). A particular body of mineralization can be concordant or discordant, syngenetic or epigenetic, or formed during the extensional or early contractional history of the basin. But in all cases, the mineralization and its alteration assemblages will be overprinted (and thereby remobilized) by the cleavage-producing event (Fig. 1).

Depending upon the *degree* and *extent* of remobilization, on whether it is *internal* or *external*, and particularly upon the mechanism, the S_1-event at peak metamorphism will yield metamorphosed or metamorphogenic deposits (Table 1 - type 4). Misinterpretation of the inherited relationship (Table 1 - types 1,2,3) could eventuate, even for simple mechanical remobilization, when one considers the distortions induced by folding and cleavage development. For more complex chemical and mixed remobilizations, the potential for misinterpreting original and newly formed ore-host relationships is enormous. A metamorphogenic deposit would be syn-S_1 and strictly involve syn-tectonic emplacement!

Pregnant fluids arising from chemical remobilization could form vein systems with demonstrably different kinematics from the S_1 strain axes. Where also unrelated to the S_2-event, the vein systems are inter-S (Fig. 1; Table 2 - type 5) and reflect strains which failed to produce a ductile fabric.

The remaining stages (Fig. 1 - 6, 7) are on the waning part of the metamorphic cycle. Stage 6 is likely to be retrogressive, involve the introduction of external fluids, and chemically conform with the retrograde-leaching model of Pohl (1992). The potential for remobilization (Table 1 - types 6,7) will be influenced by the nature of the introduced fluids.

Finally, hydrothermal emplacements of magmatic source, or from metamorphic *mobilization*, could form syn-cleavage (i.e syn-tectonically). Remobilization and externally sourced syn-tectonism are compatible.

2.2 *Responses of sulphide lenses and hostrocks*

A feeder-linked system of sediment-hosted sulphide lenses, is subjected to diagenesis and cleavage-producing regional metamorphism (Fig. 1). The various processes, which are here assumed to progressively yield folded and foliated greenschist-facies rocks, are substantially overlapping.

Stage 1 (Fig. 1 - 1 and 2). Physical dewatering under compaction; development of compaction fabrics through pressure solution (sulphides, quartz, CO_3) and recrystallization (e.g. galena - Broadbent & McKnight 1993); negligible change in ore-hostrock angular relations.

Stage 2 (Fig. 1 - 3). Horizontal shortening and thrusting with ongoing dewatering; incipient cleavage development through pressure solution and recrystallization; sulphides and

hostrocks have similar ductilities (for exceptions see Marshall & Gilligan 1987) - little potential for external remobilization; massive sulphide lenses rotate toward the plane of maximum shortening.

Stage 3 (Fig. 1 - 3 to 4). Increasing temperature and pressure cause recrystallization and chemical dewatering of silicates; increasing grainsize reduces the efficiency of pressure solution - strainrate accommodated by efficient dislocation flow in sulphides but less so in silicates - the increasing ductility contrast favours mechanical remobilization; cleavage/schistosity substantially enhanced; selective dissolution of sulphides yields pregnant metahydrothermal fluids for chemical remobilization.

Stage 4 (Fig. 1 - 4). With bulk shortening and extention, foliation development peaks and the angles between sulphide lenses, feeder system and maximum shortening plane are minimized; ongoing deformation partitions into high-strain zones; chemical dewatering peaks - high fluid pressures generate syn-foliation vein systems through hydraulic fracture in low-strain zones - focussed fluids emplace replacive mineralization in high-strain zones; further mechanical remobilization, including distortion of sulphide-lens/hostrock relationships, particularly in the high-strain zones.

Stage 5 (Fig. 1 - 4 to 5). A flat peak allows complex interplays between pulsed fluid release, vein and replacement mineralization, and deformation - early veins are deformed, later veins undeformed - replacement sulphides are overprinted by foliation, yet also overprint it - complex parageneses are characteristic; strain discontinuities marginal to high-strain zones and at ore-hostrock interfaces become shear zones as deformation partitioning intensifies - ore-hostrock relationships become further offset and distorted.

Stage 6 (Fig. 1 - 5). Waning temperatures inhibit deformation, but residual fluids form post-S_1, vein systems.

3. SYN-TECTONIC EMPLACEMENT CONCEPTUALIZED

Syn-tectonic emplacement can involve dilational vein systems or replacement through substantial mass exchange. Large fluid volumes must pass through the incrementally opening fracture, or pervasively through the replaced rock, concurrent with deformation and metamorphism. Folds and related fabrics develop over substantial time-frames. The notion of a period of deformation marking a sharp time-line is not tenable on a time-scale of ore-forming processes. Stages 2 to 5 (above) constitute the period of deformation, although folding, cleavage-development and extension mainly characterise late stage 3 to early stage 5.

Consider metamorphic mobilization (commencing Fig. 1 - 3) producing pregnant fluids which focus into evolving antiformal traps within a sedimentary sequence; cleavage is weak to absent and folds are gentle to open. High fluid pressures facilitate: sulphide-vein formation in competent low permeability units, grain-scale dilatancy and sulphide dissemination in high-permeability but low-reactivity units, and massive replacements in high-reactivity units. With ongoing deformation (moving from 3 to 4 - Fig. 1), the veins become folded or boudinaged, disseminated mineralization becomes flattened and stretched within cleavage, and massive sulphides develop deformation fabrics and could undergo *external* remobilization.

Further metamorphism and deformation (Fig. 1 - 4) and reestablishment of high fluid pressures, conceivably at higher temperature, could cause the next wave of vein formation and disseminative and massive replacements. The metal ratios could be different and previously deposited phases could undergo dissolution; both due to the higher fluid temperature. Until overtaken by cleavage intensification, this phase of mineralization would overprint the foliation.

Without needing to proceed further (e.g. to stage 5 above), an evolving system of metamorphogenic mobilization and deformation is able to create early, syn- and late systems of veins, disseminations and replacements. And remobilization is an integral part of the process! Complex parageneses and relationships to fabric elements are inevitable; they are unlikely to be consistent throughout the deposit.

4. CONCLUSIONS

Conceptualization shows that remobilization is an integral part of syn-tectonic emplacement. Although the converse is less applicable, the two processes could proceed concurrently yet

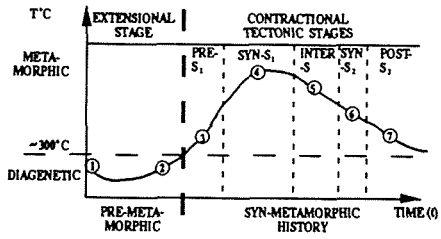

Fig. 1. Schematic framework for ore formation and remobilization during diagenesis and regional metamorphism (after Marshall & Gilligan 1993)

Table 1. Interaction of ore genesis and remobilization (modified from Marshall & Gilligan 1993)

Initial Formation	Metamorphosed/ metamorphogenic	Metamorphogenic	Metamorphosed/ metamorphogenic	Metamorphogenic
(1) (2) (3)	(4)	(5)	(6)	(7)
(1a) exhalative, concordant, syngenetic.	(4a) mechanical internal/external remobilization of 1, 2, 3.	(5a) metahydrothermal as for 4b but post-S_1	(6a) remobilization as for 4a, b, c, of 1, 2, 3, 4; syn-S_2	(7a) as for 5a but post-S_2
(1b) subhalative, discordant, epigenetic.	(4b) chemical internal/external remobilization of 1, 2, 3; syn-S_3 vein systems.	(5b) metahydrothermal portion of 4c but emplaced post-S_2	(6b) remobilization as for 4a, b, c, of 5; syn-S_3	(7b) as for 5b but post-S_3
(1c) inhalative, concordant/discordant, epigenic	(4c) mixed internal / external remobilization of 1, 2, 3.			
(2) hydrothermal emplacement/replacement, discordant/concordant, epi-diagenetic.				
(3) hydrothermal, emplacement/replacement, discordant/concordant, epigenetic				

separately. The processes yield similarly complex meso- and micro-structural relationships and complex heterogenous parageneses. They are unlikely to have distinctively different fluid-inclusion populations, fluid chemistry, isotopics, and metal sources. Discriminating between the models for a given deposite will be impeded by overconfident interpretations of inconclusive data, irrespective of its type. Successful discrimination is likely to involve thorough geometric and kinematic analyses of ore and hostrocks on all scales of observation, a logical evaluation of interpretations in the context of all other available evidence (see Phillips 1993), impeccable objectivity and a conceptual grasp of the processes.

REFERENCES

Aerden, D.G. 1991. Foliation-boudinage control on the formation of the Rosebery Pb-Zn orebody, Tasmania. J. Struct. Geol. 13: 759-775.

Bell, T.H., Perkins, W.G. & Swager, C.P. 1988. Structural controls on development and localization of syntectonic copper mineralization at Mount Isa, Queensland. Econ. Geol. 83: 69-85.

Broadbent, G. & McKight, S. 1993. Microstructures of ore minerals form the Century deposit, northern Queensland. Geol. Soc. Aust. Abs. 34: 11.

Fyfe, W.A., Price, N.J. & Thompson, A.B. 1978. Fluids in the Earth's Crust. Elsevier, Amsterdam.

Marshall, B. 1991. Remobilization and massive sulphide deposits. Geol. Dept. & Univ. Extension, University of Western Australia. 25: 84-89.

Marshall, B. & Gilligan, L.B. 1987. An introduction to remobilization: Information from ore-body geometry and experimental considerations. Ore Geol. Rev. 2: 87-131.

Marshall, B. & Gilligan, L.B. 1993. Remobilization, syn-tectonic processes and massive sulphide deposits. Ore Geol. Rev. in press.

Phillips, N. 1993. Microstructures for timing ore introduction: caution. Geol. Soc. Aust. Abs. 34: 62-63.

Pohl, W. 1992. Defining metamorphogenic mineral deposits - an introduction. Min. & Pet. 45: 145-152.

de Roo, J.A. 1989. The Elura Ag-Pb-Zn mine in Australia - ore genesis in a slate belt by syndeformational metasomatism along hydrothermal fluid conduits, Econ. Geol. 84: 256-278.

Sangster, D.F. 1979. Evidence of an exhalative origin for deposits of the Cobar district, New South Wales. BMR J. Aust. Geol. Geophys. 4: 15-27.

Current Research in Geology Applied to Ore Deposits. Fenoll Hach-Ali, Torres-Ruiz & Gervilla (eds) (1993). ISBN 84-338-1772-8

MIOCENE VOLCANOGENIC MASSIVE SULPHIDE Pb-Zn-Cu-Au-BEARING DEPOSITS IN THE CONTINENTAL MARGIN OF THE MAGHREBIDES

Mendousse, Cl.
Lab. d'Etude des Systèmes Hydrothermaux, J.E.D.R.E.D. "Magmas et Métaux", Université Nancy I, BP 239, 54506 Vandoeuvre les Nancy, France

ABSTRACT : The VMS deposits of Oued El Kebir and Bou Soufa (Algeria) are hosted in dacitic rocks of a fractionned calc-alkaline sequence, linked to the Burdigalian-Langhian distensive deformation, connected to the continental crustal spreading of internal Maghrebides. They belong to the group "Pb-Zn-Cu-Au", one of the numerous varieties of Kuroko-type deposits. Ore-forming processes occurred in shallow-water depth . New mineralogical and geochemical data, in relation with the main extensive Burdigalian deformations, indicate that they are controlled by the evolution of magmatic hydrothermal fluids under increasing influence of sea-water.Their specificities would be related to their mediterranean original geodynamic setting.

INTRODUCTION

While basic ore-forming processes of volcanogenic massive sulphides (VMS) are similar in most geodynamic settings, specific characteristics of hydrothermal fluids, geochemical and mineralogical composition of ores, in relation with properties of the crust, indicate the difference between mid-ocean ridge, back-arc basin, and less usual continental crustal environments. The genesis models of Archean, Paleozoic, Cyprus and Kuroko VMS types widely studied (Ohmoto and Skinner, 1983) were improved by the results obtained on the actual submarine deep-water sulphide mineralizations (Stolze and Large, 1992).This paper will refer to the genesis of Miocene northern algerian Pb, Zn, Cu, Au, Ag VMS deposits in order to outline their common characteristics with Kuroko-type deposits, recently better defined by Urabe and Marumo (1991), but also their geochemical specifications related to their mediterranean geodynamic setting.The ore deposits are hosted in dacitic rocks of a fractionned calc-alkaline sequence, linked to the Burdigalian-Langhian distensive deformation, connected to the crustal spreading on continental margins, post-collisionnal events of European-African plates. New mineralogical and geochemical data, in relation with the main tectonic events indicate that the ore-forming processes are controlled by the evolution of magmatic hydrothermal fluids under increasing influence of sea-water.

1 MIOCENE MAGMATIC ROCKS AND GEOLOGICAL SETTING

The volcanic massif of El Aouana is located on the limit of internal-external zones of Maghrebides chain, the first ones would have the value of the south border of European continental crust (Bouillin, 1986).The emission of continental lava flows and air fall pyroclastic rock is followed by the intrusion of dacitic domes . An transtension deformation, with E-W dextral strike-slip and NW-SE normal faults (Villemaire, 1987), is contemporary with the formation of a collapse caldera structure, about 7 kms in diameter, spread over by shallow-sea water.This tectonic event, well-defined in Northern Tunisia by Philipp et al., (1986), has just been dated Burdigalian-Langhien in Eastern Algeria (Monié et al., 1992).The deposition of the Oued El Kebir stratiform ore bodies and thin lenses of pyroclastic and epiclastic rocks occurred during a volcanic quiescence. Upper marine andesitic and dacitic lava flows, interbedded in numerous pyroclastic flow sheets, filled the caldera and microdiorites set up along the caldera faults. A transpression deformation with strike-slip faults, reverse faults and folds, occurred during Tortonian - Serravallian .
The volcanic sequence is characterized by the volumic importance of dacites and the lack of basalts. The major and trace elements of representative samples of fresh and less altered rocks are given in the table 1.Thanks to their mineralogical characteristics, their major and trace elements, the upper andesites appear to be typical continental orogenic rocks .The less altered calc-alkaline volcanic rocks have similar chondrites normalized REE patterns, with a slight LREE-enrichment and a relatively flat pattern for M-HREE with a negative europium anomaly .They indicate usual enrichment from microdiorites to dacites, except for the upper dacites .According to Campbell et

al.(1982), the chondrite normalized REE patterns of the lower dacitic, host rocks of VMS, rank among the acid magmatic rocks with high-metallogenic potentiality (figure 1a) ; when the upper dacitic lava have patterns of barren volcanic rocks (figure 1b) .The higher La/Yb ratios of the lower dacites sets apart from Kuroko mature back-arc basin volcanic sequence.

Table 1: Chemical composition of the main volcanic units

	Lower dacites		Upper andesites	Upper dacites		Microdiorites
	C67	D156	JJ1	VIL65b	VIL 61b	Bm5
SiO2	69,92	72,64	63,37	63,29	65,74	60,30
TiO2	0,29	0,38	0,48	0,48	0,22	0,26
Al2O3	15,43	14,33	14,92	17,04	16,07	17,54
Fe2O3	1,29	1,87	5,89	5,08	3,39	5,50
MgO	0,05	0,43	2,84	0,86	0,40	2,52
MnO	0,02	-	-	0,01	0,02	0,02
CaO	2,52	1,38	5,50	3,83	4,00	4,40
Na2O	2,54	0,24	3,12	4,12	4,05	5,41
K2O	2,66	1,26	1,37	2,56	2,61	1,83
P2O5	0,34	0,17	0,19	0,20	0,11	0,26
LOI	5,13	7,62	2,05	2,32	3,23	1,83
Rb*	68	67	85	65	105	53
Sr*	814	357	242	372	216	548
Ba*	1004	83	210	214	215	180
Zr*	100	166	102	87	76	65
Co*	<5	<5	12	10	6	14
Ni*	7	32	25	17	11	16
Cr*	12	52	62	20	6	7
V*	52	195	141	146	63	163
Cu*	15	128	25	22	10	17
Zn*	21	63	81	29	21	77
Pb*	62	397	38	10	9	13

*µg/g

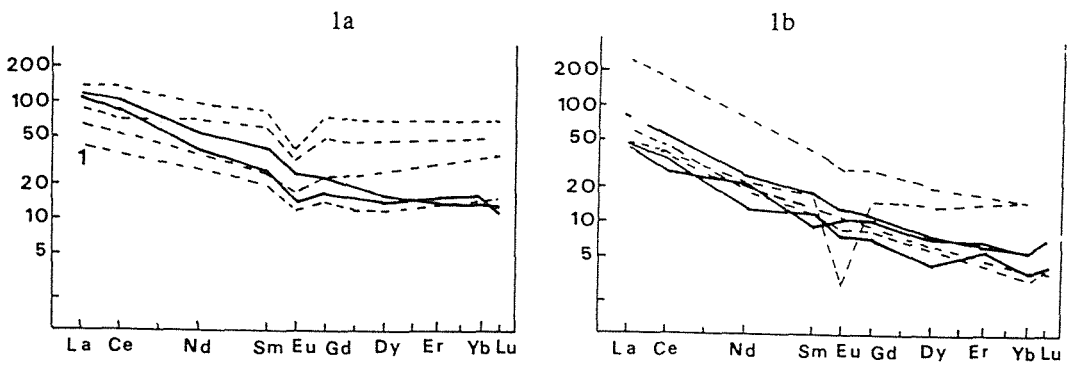

Figure 1- Chondrite normalized REE patterns : 1a for ore-bearing felsic volcanic rocks, 1b for barren felsic volcanic rocks (Dashed lines from Campbell et al.(1982), full lines : samples from table 1 ; 1 Kuroko host-rocks).

This magmatism is contemporary of an extensive deformation, with strike-slip faults and opening of miocene sedimentary pull-apart basins . It would be related to a crustal post-collisionnal extension, in relation with the collapse of alboran-block and the opening of the oceanic Southern Balear Basin.

2 THE ORE DEPOSITS

The ore deposit of Oued El Kebir, in the central part of the volcanic massif, consists of five main stratiform massive sulphide ore bodies, underlying by stockworks of veins linked to NW-SE normal dextral faults and N-S strike-slip faults. Lodes are associated to them. Mineralizations are

strictly localized at the border, between altered intrusive dacites and highly altered marine pyroclastic and epiclastic rocks . In the ore deposit of Bou Soufa, located at 2,5 kms to the north, the ore bodies, mainly stockworks and lodes, developed in dacitic domes and their brecciated pipes. A sulphide show laid also at 2,5 kms towards the south. Doming and ore deposition were roughly contemporaneous events, with continued upward movement of the dome postore.

2 . 1 The ore paragenetic data

The massive and stratiform ore bodies, several meter thickness, are characterized by typical syngenetic textures, reworked by dissolution and filling textures. From structural and textural studies three main stages of mineralization are defined (table 2).The genesis of caldera structure occurrs in the first stages.The beginning of the stage III corresponds to deformation event, followed by the progressive stopping up of the stockworks. The thick ore bodies are characterized by typical Kuroko distribution of yellow and black ores, relayed laterally and upward by barytic ores (Villemaire, 1987) .The lodes are rich in galena and baryte. The ore deposit has higher Pb/Zn ratio than Kuroko type (about 1,34 -Touahri, 1987) .The primary paragenetic sequence for one complete ore system is slightly different from Kuroko one (table 2).Several ore systems could run together, or successively .

Table 2 : Paragenetic sequence in massive sulphide ore deposit (Oued El Kebir)

Ore bodies	Lower massive and stratiform ores		Upper stratiform ores wallrock of lodes	Lodes, veins, stockworks
Main textures	framboids disseminated replacement ores	massive,framboids,collo-form.crust.laminated reworked.brecciated ores	striped, laminated geodic ores smoker products	banding,crustification structures disseminated ores.
Mineralization	Stage I		Stage II	Stage III
Pyrite Marcasite Sphalerite				
Galena Chalcopyrite Tennantite/tetraedrite Enargite Boulangerite				
Quartz Baryte Calcite Siderite				
Hydrothermal Alteration	argillic advanced argillic			propylitic

The compositions of sulphides and sulfosalts of the different ores were analysed by electron microprobe .The studies of the trace element contents, of their distributions according to the mineral species and their localization in the ore bodies, indicate an evolution of average grades through the stages of mineralizations . The pyrites from stratiform bodies, and particularly those of black-ores are characterized by their relatively high and evenly distributed As and Au contents ; while the pyrites of lodes are barren. Pyrites contain also Ag, with less constant distributions .The other Ag- bearing sulphides are galena and tennantite-tetraedrite of the stage I and II .The content of moles % FeS in sphalerites (stage I and II) is low, and increases (0,4 to 5,3 %) from the bottom to the top of the stratiform bodies, it's lower in sphalerites (stage III). So, thanks to the trace element contents of sphalerites and pyrites, their Au-average grade production, these ores belong to Au-bearing VMS, and indicate numerous similarities with Kuroko ores (Hannington and Scott, 1989).

2.2 Fluid inclusions data

As the geothermometer Cd/Mn in galena and sphalerite (Bethke and Barton, 1971), gave unrealistic temperatures, because a non-equilibrium syncristallisation; fluid inclusions were studied by microthermometry . The conditions of fluid-trapping were defined in quartz and baryte of the three mineralized stages. Different types of aqueous inclusions are identified.The minimal temperatures of trapping conditions, without pressure correction in this shallow-depth water environnment, and the corresponding salinities are the following : the stage I- more than 340°C, 14 wt % eq. NaCl ;

the stage II developps from 320°C-14 wt % to 180°C-5% ; the stage III is characterized by lower temperatures 140°to 120°C-12 to 14 wt% eq.NaCl. If the range of temperatures is in good agreement with those of Kuroko VMS, the salinities are typically higher (to three times).

3 GENESIS MODEL : DISCUSSION

In relation with mineralizations, three main types of mineral alteration assemblages have been identified, they graded from kaolinite core to propylitic margins and relayed also in the time (table 2). Discharge area correspond to advanced argillic zones, with leaching of alkali in the footwall rocks and deposition above of sulphide ores.Recharge area are characterized by addition of Mg from sea water.The progressive influence of sea water was well-registred by chemical balance of major, traces and by fractionment of REE (Mendousse 1991).So, the clear decrease of salinity may be related to introduction of sea-water in the hydrothermal system, favoured by the active deformation during ore deposition. Chemical environment of alterations defined from the report of equilibrium curves in isothermal pH- f O2, indicate a lateral, but also a timing increasing of pH from core to the extern zones, under a fugacity f O2 :10^{-33} to 10^{-34}.The massive and stratiform ore deposition occurred in the range of temperature 340°C to 180°C, with evolutions of the fugacity of sulfur from f S2 :10^{-6} to <10^{-14} .Chemical balances for major, trace elements, particularly the Pb, and REE during fluid-rock interaction, would favour a leaching model of dacitic host-rock sequence in a magmatic hydrothermal system, progressively enriched by sea-water.
In conclusion, these mediterranean Au-bearing VMS deposits are linked to a particular basal dacitic unit of a cal-alkaline sequence. In the spectrum of Kuroko deposits style , they belong to Pb-Zn-Cu -Au VMS type and represent one reference with salinity about 12-14 wt% eqNaCl, no much frequent in the genetic models according to Stolze and Large (1992). Their specificity would be reliable to their shallow-water depth formation and to their original geodynamic setting in spreading continental crust, during an post-collisionnal extensive deformation.

Acknowledgements : I thank J. Leroy and P. Barbey for their advices.(J.E. DRED- Magmas et Métaux). The manuscript benefitted from a review by J. Leroy.

REFERENCES

Bouillin, J.P. 1986. Le "bassin maghrébin" : une ancienne limite entre l'Europe et l'Afrique à l'ouest des Alpes. Bull. Soc.géol. France 8, 4: 547-558.

Bethke, P.M. & Barton, P. 1971 . Distribution of some minor elements b'etween coexisting sulfide minerals. Econ. geol. 66: 140-163.

Campbell, I.H., Coad, P., Franklin, J.M., Gorton, M.P., Scott, D, Sowa, J. &Thurston, P.C. 1982. Rare earth elements in volcanic rocks associated with Cu-Zn massive sulphide mineralization : a preliminary report. Can. J. Earth Sci.19: 619-623.

Hannington, M.D. &Scott, S.D. 1989. Sulfidation equilibria as guides to gold mineralization in volcanogenic massive sulfides : evidence from sulfide mineralogy and the composition of sphalerite.

Horikoshi, E.1990. Opening of the sea of japan and Kuroko deposit formation. Mineral.Deposita 25: 140-145.

Mendousse, Cl.1991. Mass-transfer during fluid-rock interactions in massive sulfide deposits (rare earth, trace and major elements). In: Pagel,M. and Leroy,J. (eds) Source,transport and deposition of metals. A.A.BALKEMA, 73-76.

Monié, P., Montigny, R. & Maluski, H. 1992. Age Burdigalien de la tectonique ductile extensive dans le massif de l'Edough (Kabylies, Algérie). Données radiomètriques 39 Ar-40 Ar.. Bull. Soc.géol. France, 5:571-584.

Ohmoto, H.& Skinner, BJ. 1983.The kuroko and related volcanogenic massive sulfide deposits. Econ.Geol. monograph 5. 604p.

Philip, H. , Andrieux, J., Dlada, M., Chidi, L., &Ben Ayed, N. 1986. Evolution tectonique mio-plio-quaternaire du fossé de Kasserine (Tunisie centrale) : implications sur l'évolution géodynamique récente de la Tunisie Bull.Soc.géol.France, 4: 559-568.

Stolze, J.& Large, R.R. 1992. Evaluation of the source-rock control on precious metal grades in volcanic-hosted massive sulfide deposits from Western Tasmania. Econ. Geol. 87: 720-738.

Touahri, B. 1987. Géochimie et métallogénie des minéralisations à Pb et Zn du Nord de l'Algérie. Th.Dr Etat, Paris VI, 348p.

Urabe, T.& Marumo, K.1991. A new model for Kuroko-type deposits of Japan . Episodes 14,3 : 246-251.

Villemaire,Cl. 1987. Les amas sulfurés du massif miocène d'El Aouana (Algérie)- I.Dynamisme de mise en place des roches volcaniques et implications métallogéniques. Journ.of Afr. Earth Sci 1: 133-148.

Current Research in Geology Applied to Ore Deposits.Fenoll Hach-Alí, Torres-Ruiz & Gervilla(eds)(1993).ISBN 84-338-1772-8

EVALUATION OF FLUID MIXING AND FLUID-ROCK INTERACTION PROCESSES DURING GENESIS OF THE SAN VICENTE Zn-Pb MVT DEPOSIT, CENTRAL PERU, BASED ON Sr, O AND C ISOTOPIC COVARIATIONS

Moritz, R. (1); Spangenberg, J. (1,2) & Fontboté, L. (1)
(1) Dépt. de Minéralogie, rue des Maraîchers 13, 1211 Geneva 4, Switzerland
(2) Inst. de Minéralogie, UNIL BFSH-2, 1015 Lausanne, Switzerland

ABSTRACT: The Sr, O and C isotopic compositions of replacement and sparry dolomite from the San Vicente Zn-Pb Mississippi Valley-type deposit, Peru, are contrasted with those of carbonates from the remainder of the host Pucará basin. Covariation of $\delta^{13}C$ and $\delta^{18}O$ values of the different carbonate generations at San Vicente suggest fluid mixing during ore formation. 1/Sr-$^{87}Sr/^{86}Sr$ covariations indicate that one fluid involved in ore genesis is likely derived from detrital rocks underlying the carbonate rock sequence at San Vicente. The source of the other fluid(s) remains equivocal. Quantitative geochemical calculations allow us to model the covariations between Sr, O and C isotopes, and also indicate that fluid mixing coupled with fluid-rock interaction was an important process during genesis of the San Vicente deposit.

INTRODUCTION

Sr isotope geochemistry, along with O and C isotopes, provides useful information about the nature of the fluids from which carbonates were precipitated in Mississippi Valley-type (MVT) deposits. Simultaneous changes in elemental abundances and radiogenic and stable isotope values may also reveal diagnostic trends on covariations diagrams which, together with quantitative modeling, place limitations on the geochemical mixing processes involved in carbonate diagenesis and ore-formation in sedimentary basins, including water-rock interaction and fluid mixing (Banner and Hanson, 1990; Farr, 1992; Zheng and Hoefs, 1993). The Zn-Pb mine at San Vicente is a typical MVT deposit located in central Peru (Fontboté and Gorzawski, 1990). It is presently one of the major Zn producers of Peru with an accumulated production of about 14 million metric tons, reserves exceeding 4 million tons, and Zn and Pb grades of 11% and 0.8%, respectively. In this study, we combine Sr, O and C isotopic data and Sr abundances from the San Vicente Zn-Pb deposit obtained by Fontboté and Gorzawski (1990) with similar data obtained on a regional basis from the host sedimentary basin. The aim is to add further constraints on the nature of the fluids present during ore-formation, and to evaluate the importance of fluid mixing and/or fluid-rock interaction during the genesis of this deposit.

The San Vicente Zn-Pb deposit is located in the eastern part of the Pucará basin, central Peru (Fig.1). Regional geological and metallogenic aspects of this basin are discussed in Fontboté (1990), and the geologic setting and genetic aspects of the San Vicente Zn-Pb MVT deposit can be found in Fontboté and Gorzawski (1990). The Pucará basin is an extensive Triassic-Jurassic carbonate plateform on the western margin of the Brazilian Shield. The Pucará Group, composed of the Chambará, Aramachay, and Condorsinga Formations, was deposited at the beginning of the Andean cycle during marine transgression over clastic sedimentary rocks, volcaniclastic rocks and alkaline to sub-alkaline volcanic rocks of the Late Permian to Early Triassic Mitu Group (Fig.1). Shallow water sedimentary rock facies, including abundant evaporites and oolithical barriers, predominate across the entire basin, except in the Aramachay Formation characterized by deeper anoxic facies.

Carbonates from ore-bearing (Shalipayco and San Vicente) and barren areas (Tingocancha, Malpaso and Tarma, Fig.1), and from different positions in the stratigraphic column have been analyzed for their Sr, C and O isotopic composition. The carbonates represent different subsequent evolution stages of the Pucará basin, spanning sedimentary to late diagenetic events. They can be subdivided in two groups: (1) original and moderately diagenetically modified sedimentary rocks, including limestones, replacement dolomites and evaporites, and (2) late diagenetic carbonates, including ore-stage replacement dolomite, white sparry dolomite and coarse-crystalline calcite.

RESULTS AND DISCUSSION

Sr isotopes and concentrations

Most of the limestone and replacement dolomite from the Pucará basin yield $^{87}Sr/^{86}Sr$ ratios that fall within or very close to the range of seawater $^{87}Sr/^{86}Sr$ values published by Koepnick et al. (1990) for the Upper Triassic to Lower Jurassic (Fig.2A). Two groups of carbonates yield distinctively different Sr isotopic compositions. (1) At the San Vicente Zn-Pb mine, sparry dolomite and part of the replacement dolomite from the ore-bearing areas are slightly enriched in ^{87}Sr with respect to Upper Triassic to Lower Jurassic seawater, with sparry dolomite being more enriched in ^{87}Sr than replacement dolomite. (2) Carbonates near the basal contact with the detrital rocks of the

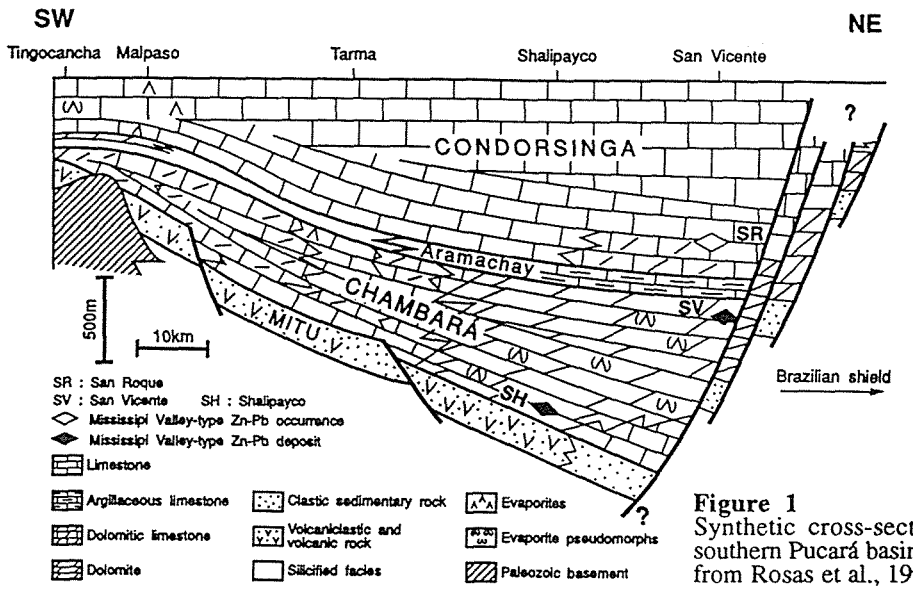

Figure 1
Synthetic cross-section of the southern Pucará basin (Modified from Rosas et al., 1992).

Mitu Group show a progressive increase in $^{87}Sr/^{86}Sr$ ratios towards the base of the carbonate sequence (based on sampling at Tingocancha, Malpaso and Shalipayco, Fig.1). The ^{87}Sr-enrichment is more important in the later case than for replacement and sparry dolomites from the San Vicente deposit which lies between 500 and 1100 m above the contact with the detrital rocks (Fig.2A). Both trends indicate that carbonate rocks at the San Vicente deposit and at the base of the Pucará basin interacted with ^{87}Sr-enriched brines.

Mixing between various Sr-bearing endmembers is also indicated by Figure 2B which shows the covariation between $^{87}Sr/^{86}Sr$ ratios and 1/Sr values. Two trends can be recognized. The upper endmember of trend I is the ^{87}Sr-enriched replacement dolomites from the base of the Pucará sequence with $^{87}Sr/^{86}Sr$ values near 0.7086 and Sr abundances around 100 ppm ($1/Sr \times 1000 \approx 10$, Y in Fig.2B). The second endmember is the replacement dolomites with low $^{87}Sr/^{86}Sr$ Upper Triassic-Lower Jurassic seawater-like values and Sr abundances in the 50 to 80 ppm range ($1/Sr \times 1000 \approx 12.5$ to 20, X in Fig.2B). Trend I is most likely explained by interaction of the lowermost replacement dolomites of the Pucará basin at Tingocancha, Malpaso and Shalipayco with a brine enriched in radiogenic Sr derived from alkaline to sub-alkaline volcanic rocks and detrital minerals of the immediately underlying Mitu Group. Pb isotopic compositions of galenas from Shalipayco are in agreement with this interpretation (Fontboté and Gorzawski, 1990). The widening of trend I towards the lower right X endmember in Figure 2B appears to be a function of sample location, in other words the initial Sr concentration and isotopic composition of the non-mineralized carbonate rock interacting with the ^{87}Sr-enriched brine. The left part of trend I (x' in Fig.2B) is composed of samples from the Malpaso profil in the western part of the basin (Fig.1), while the right part (x" in Fig.2B) consists of samples from Shalipayco and San Vicente, thus the eastern part of the basin (Fig.1).

By contrast, the ore-bearing replacement and sparry dolomites from the San Vicente deposit display a nearly horizontal trend, ranging from low Sr abundances ($1/Sr \times 1000 \approx 20$) to high Sr abundances ($1/Sr \times 1000 \approx 2$, trend II in Fig.2B). Sparry dolomite is systematically enriched in Sr compared to immediately adjacent replacement dolomite. The right endmember of the horizontal trend II lies in-between endmembers x" and Y of trend I (Fig.2B), with the sparry dolomite having higher $^{87}Sr/^{86}Sr$ ratios than the ore-bearing replacement dolomite. There is a concomitant increase in $^{87}Sr/^{86}Sr$ ratios and Sr contents of the ore-bearing replacement dolomite and subsequently of the sparry dolomite relative to non-mineralized replacement dolomite (x" in Fig.2B) that parallels trend I decribed above. This strongly suggests that, during mineralization, the host rocks at the San Vicente MVT deposit interacted with a fluid that was derived from detrital rocks below the carbonate rock sequence (Fig.1), and that had similar Sr isotopic composition and Sr concentration characteristics as the one that produced the enrichment in ^{87}Sr and Sr abundances in non-mineralized replacement

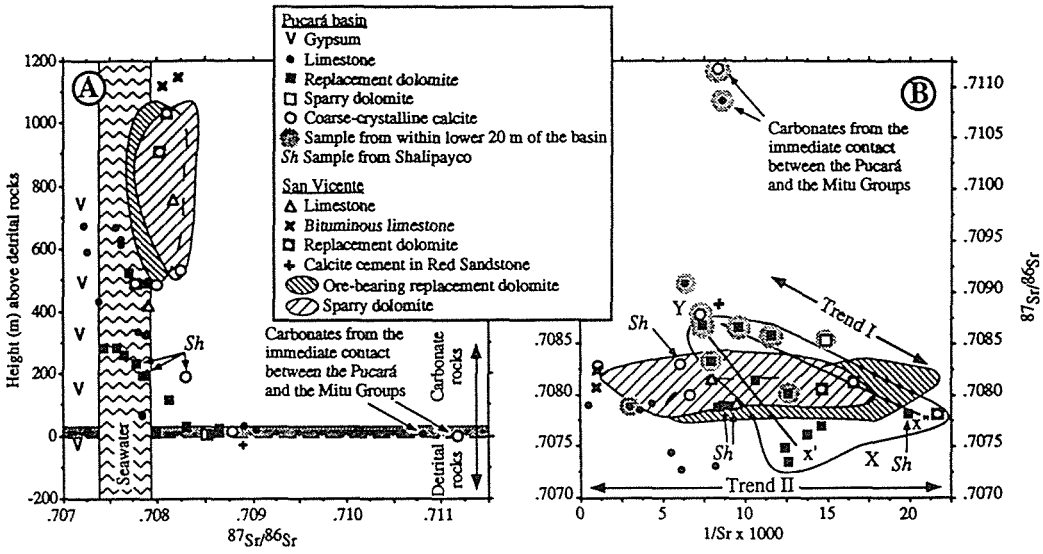

Figure 2 - Height vs. $^{87}Sr/^{86}Sr$ ratios and $^{87}Sr/^{86}Sr$ ratios vs. 1/Sr x 1000 (ppm^{-1}). San Vicente data is from Fontboté and Gorzawski (1990) and Upper Triassic to Lower Jurassic seawater Sr range is from Koepnick et al. (1990).

dolomite in the lower Pucará sequence at Tingocancha, Malpaso and Shalipayco (Fig.1). Steeply dipping faults in the eastern Pucará basin (Fig.1) are conceivable channelways for fluid migration from depth, whereby the highly radiogenic nature of such a fluid near its source would have been progressively buffered by interaction with carbonate rocks encountered along its path. The horizontal spread in 1/Sr values (Fig.2B) can be attributed to a variety of factors. A second, non- to slightly radiogenic fluid, might be responsible for the horizontal spread. Such a scenario implies a combination of fluid mixing and fluid-rock interaction at San Vicente during mineralization. Possible sources for such a fluid are the Aramachay Formation, located immediately above the main San Vicente ore bodies (Fig.1), in which bituminous silty limestone is characterized by high Sr abundances (Fig.2B) and a high illite content (Fontboté and Gorzawski, 1990), and the Upper Precambrian rocks located below and to the east of San Vicente (Fig.1). Independently to the presence or the absence of a second fluid at San Vicente, the large spread parallel to the 1/Sr axis can be related to variations of the fluid-dolomite distribution coefficient of Sr. Sr concentration in dolomites are a function of host mineral stoichiometry and variations of the Sr/Ca ratio of the precipitating fluid (Vahrenkamp and Swart, 1990), as well as of kinetic effects such as precipitation rate (Lorens, 1981). The relative importance of these different parameters is unclear at this stage of the study, and still requires further investigations.

Covariations between Sr, O and C isotopic compositions of the carbonates

Additional evidence for the nature of the fluids and the type of mixing processes is provided by the stable isotopes. Covariance between $^{87}Sr/^{86}Sr$ ratios and $\delta^{18}O$ values, and between $\delta^{13}C$ and $\delta^{18}O$ values of the various carbonates from the Pucará basin are shown in Figure 3. The marked increase in $^{87}Sr/^{86}Sr$ ratios of the carbonates towards the lower part of the basin at Tingocancha, Malpaso and Shalipayco is only accompanied by a slight shift towards lighter $\delta^{18}O$ values (trend I in Fig.3A), whereas the slight ^{87}Sr-enrichment in the various carbonate generations at San Vicente is accompanied by a more important depletion in ^{18}O (trend II in Fig.3A). Covariance between $\delta^{13}C$ and $\delta^{18}O$ values (Fig.3B) shows no significant difference between both trends, except for a limestone and a coarse-crystalline calcite from the immediate contact between the Pucará and the Mitu Groups which have low $\delta^{13}C$ values around -4‰. Trend I has a roughly inverted L-shape in the $\delta^{13}C$-$\delta^{18}O$ diagram, and trend II that includes the replacement and sparry dolomites from San Vicente and the replacement dolomites sampled regionally displays a broadly linear correlation with a positive slope (Fig.3B).

Calculations based on the approach suggested by Banner and Hanson (1990) for trend I, with the inverted L-shape in $\delta^{13}C$-$\delta^{18}O$ space, show that the shift towards higher $^{87}Sr/^{86}Sr$ ratios accompanied by a slight depletion in $\delta^{18}O$ values and essentially no changes in $\delta^{13}C$ values for most

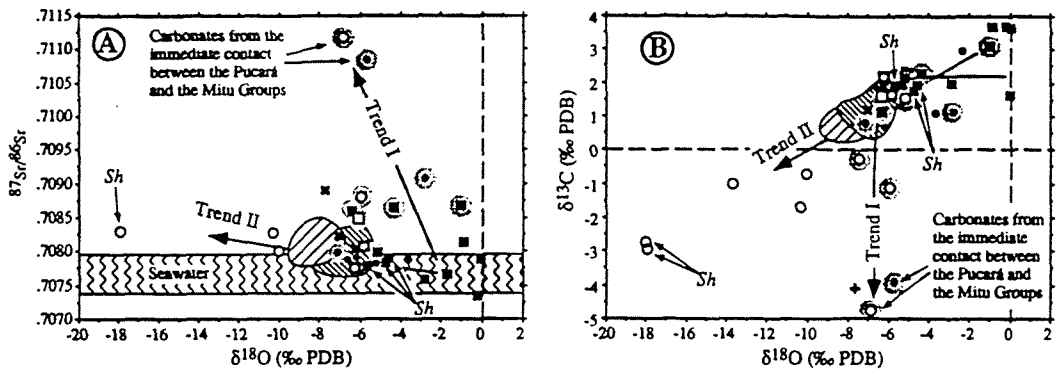

Figure 3 - $^{87}Sr/^{86}Sr$ vs. $\delta^{18}O$ and $\delta^{13}C$ vs. $\delta^{18}O$ covariations. See Figure 2 for symbols.

of the samples can be explained by a simple brine-carbonate rock interaction model. For instance, interaction of the carbonate rocks at the base of the Pucará Group with a saline fluid with 20,000 ppm Ca, 300 ppm Sr, 50 ppm total dissolved carbon (TDC), $^{87}Sr/^{86}Sr$ = 0.71125, $\delta^{13}C$ (PDB) = -5‰ and $\delta^{18}O$ (SMOW) = 4‰ at a temperature of 80°C allows us to reproduce the covariations of trend I in Figure 3. Such a fluid composition is compatible with the one expected for deep formation waters.

In contrast, the linear correlation with the positive slope shown by the regional replacement dolomites, and the replacement and sparry dolomites from San Vicente in $\delta^{13}C$-$\delta^{18}O$ space (Fig.3B) is diagnostic of fluid mixing (Banner and Hanson, 1990; Farr, 1992) assuming that HCO_3^- is the dominant dissolved carbon species. Together with the Sr isotopic data (Fig.2B), this is evidence of combined fluid mixing and fluid-rock interaction at the San Vicente MVT deposit. A model based on variable mixing ratios between a hot ^{87}Sr-enriched saline brine with a warm dilute brine enriched in TDC, various degrees of water/rock ratios and slight temperature shifts reproduces the trend of the ore-bearing replacement and sparry dolomite at San Vicente. The characteristics of the two fluids used in our calculations are the following: (1) the hot ^{87}Sr-enriched saline brine has 20,000 ppm Ca, 300 ppm Sr, 50 ppm TDC, $^{87}Sr/^{86}Sr$ = 0.70875, $\delta^{13}C$ (PDB) = -5‰ and $\delta^{18}O$ (SMOW) = 4‰ at a temperature of 140°C, and (2) the warm dilute C-rich brine has 2000 ppm Ca, 100 ppm Sr, 2500 ppm TDC, $^{87}Sr/^{86}Sr$ = 0.7078, $\delta^{13}C$ (PDB) = -15‰ and $\delta^{18}O$ (SMOW) = 0‰ at a temperature of 70°C. Although speculative, the different fluid parameters were selected based on the assumption that the hot ^{87}Sr-enriched saline brine is derived from detrital rocks at the base of the Pucará Group, and volcanic and volcaniclastic rocks of the Mitu Group, whereas the warm dilute C-enriched brine is locally derived from bituminous limestone of the Aramachay Formation directly overlying the San Vicente deposit (Fig.1). Initial wallrock compositions were estimated from replacement dolomites sampled regionally, remote from the Mitu-Pucará contact and from any ore deposit or mineralization. To account for the trend towards lighter $\delta^{13}C$ and $\delta^{18}O$ values and higher $^{87}Sr/^{86}Sr$ ratios of the late stage sparry dolomite, the temperature of both fluids were increased by 20°C and the ore-bearing replacement dolomites produced previously were used to set the initial wallrock compositions for the fluid-rock interaction calculations. The modeling requires that the proportion of the hot ^{87}Sr-enriched saline brine involved in the mixing process and the brine/wallrock ratios are increasing as one progresses from the replacement dolomite towards the late stage sparry dolomite.

However, other parameters need also to be taken into account before a final conclusion can be reached as to whether fluid mixing combined with fluid-rock interaction is the main factor governing the covariation displayed by the Sr, O and C isotopic data, and is responsible for ore genesis at San Vicente. As discussed by Zheng and Hoefs (1993), if H_2CO_3 is the main dissolved carbon species instead of HCO_3^-, then the covariation with the positive slope does not necessarily require fluid mixing, but can be explained by temperature variations of a single fluid coupled with fluid-rock interaction. Further isotopic studies at a fine scale (Spangenberg et al., submitted) and fluid inclusion microthermometry may resolve these uncertainties. Unfortunately, covariation between Sr isotopic compositions and $\delta^{18}O$ values does not permit to distinguish between fluid mixing and fluid-rock interaction processes (Farr, 1992). Finally, some late-stage coarse crystalline calcites, also present in San Vicente and Shalipayco, yield very low $\delta^{18}O$ values (PDB) between -10‰ to -18‰ combined with low $\delta^{13}C$ values (PDB) of -1‰ to -3‰ (Fig.3). The O isotopic values of these calcites require

fluids with very low $\delta^{18}O$ values between -22‰ to -32‰ (SMOW) depending on the equilibration temperature. Such ^{18}O-depleted fluids have most likely a meteoric origin. The depleted $\delta^{13}C$ values are in line with such a meteoric origin of the fluids. This last data set shows that after, or possibly during late stages of ore deposition, a fluid distinctly different in its composition and its origin relative to the fluids postulated above migrated through the Pucará basin, notably in ore-bearing areas at San Vicente and Shalipayco. In brief, the importance of this ^{18}O-depleted fluid needs also to be evaluated critically when modeling the covariation of the Sr, O and C isotopic compositions. Preliminary modeling shows that mixing between a dilute, nonradiogenic meteoric fluid with the hot ^{87}Sr-enriched saline brine with the abovementioned characteristics cannot account for the covariations of the San Vicente carbonates displayed in Figure 3.

CONCLUSIONS

Covariation in $\delta^{13}C$-$\delta^{18}O$ diagram suggests fluid mixing during ore formation at San Vicente, assuming that HCO_3^- is the dominant dissolved carbon species. Covariations between $\delta^{18}O$ and $^{87}Sr/^{86}Sr$ ratios, and between 1/Sr values and $^{87}Sr/^{86}Sr$ ratios are compatible with such a scenario. Based on 1/Sr-$^{87}Sr/^{86}Sr$ covariations, one fluid involved in ore genesis is likely derived from detrital rocks underlying the carbonate rock sequence at San Vicente. The source of the other fluid(s) remains equivocal at this stage of the study. Quantitative geochemical calculations, based on fluid compositions compatible with derivation from the different possible source rocks in and adjacent to the Pucará basin, allow us to model the covariations between Sr, O and C isotopes, and also indicate fluid mixing coupled with fluid-rock interaction during genesis of the San Vicente deposit. Our conclusion is in line with several studies carried out in other MVT deposits that also invoke fluid mixing as an important factor during ore genesis.

ACKNOWLEDGEMENTS

This study is supported by the Swiss National Science Foundation (Grant n° 21.30.309.90), and it is a contribution to IGCP project n° 342 (Age and Isotopes of South American Ores). Stable isotope analyses were performed in the laboratory of J. Hunziker at the University of Lausanne. J. Hunziker, Z. Sharp, M. Bill (all University of Lausanne), D. Fontignie, M. Falcheri and D.M. Yu (all University of Geneva) are thanked for assistance and advice during the analytical part of this study. Thanks are also due J. Metzger (University of Geneva) for drafting Figure 1, and S. Rosas for providing many samples and for discussions on geological aspects of the Pucará basin.

REFERENCES

Banner, J.L. & Hanson, G.N. 1990. Calculation of simultaneous isotopic and trace element variations during water-rock interaction with applications to carbonate diagenesis. Geochim. Cosmochim. Acta, 54: 3123-3137.

Farr, M.R. 1992. Geochemical variation of dolomite cement within the Cambrian Bonneterre Formation, Missouri: Evidence for fluid mixing. J. Sediment. Petrology, 62: 636-651.

Fontboté, L. 1990. Stratabound ore deposits in the Pucará basin. An overview. In: Fontboté, L., Amstutz, G.C., Cardozo, M., Cedillo, E. & Frutos, J. (eds.) Stratabound ore deposits in the Andes. Springer, Heidelberg, 253-266.

Fontboté, L. & Gorzawski, H. 1990. Genesis of the Mississippi Valley-type Zn-Pb deposit of San Vicente, Central Peru: Geologic and isotopic (Sr, O, C, S, Pb) evidence. Econ. Geol., 85: 1402-1437.

Koepnick, R.B., Denison, R.E., Burke, W.H., Hetherington, E.A. & Dahl, D.A. 1990. Construction of the Triassic and Jurassic portion of the Phanerozoic curve of seawater $^{87}Sr/^{86}Sr$. Chem. Geol., 80: 327-349.

Lorens, R.B. 1981. Sr, Cd, Mn and Co distribution coefficients in calcite as a function of calcite precipitation rate. Geochim. Cosmochim. Acta, 45: 553-561.

Rosas, S., Fontboté, L., Moritz, R. & Spangenberg, J. 1992. Sedimentological and diagenetic evolution of the Pucará basin (central Peru). Facies, lithogeochemistry, and isotope data (Sr, C, O). 13.Geowissenschaftliches Lateinamerika-Kolloquium, Münster, Germany, Abstracts.

Spangenberg, J., Sharp, Z.D. & Fontboté, L. Submitted. Apparent carbon and oxygen isotope variations of carbonate gangue minerals in the MVT Zn-Pb San Vicente deposit, Central Peru: the effect of organic matter and sulfides. Econ. Geol.

Vahrenkamp, V.C. & Swart, P.K. 1990. New distribution coefficient for the incorporation of strontium into dolomite and its implications for the formation of ancient dolomites. Geology, 18: 387-391.

Zheng, Y.-F. & Hoefs, J. 1993. Carbon and oxygen isotopic covariations in hydrothermal calcites. Theoretical modeling on mixing processes and application to Pb-Zn deposits in the Harz Mountains, Germany. Mineral. Deposita, 28: 79-89.

Current Research in Geology Applied to Ore Deposits. Fenoll Hach-Alí, Torres-Ruiz & Gervilla (eds) (1993). ISBN 84-338-1772-8

MASSIVE SULPHIDE DEPOSITS IN THE EASTERN PONTIC METALLOGENIC PROVINCE, N.E. TURKEY

Özgür, N.
Inst. für Geologie, Geophysik und Geoinformatik der Freien Universität Berlin, Malteserstr. 74-100, W-1000 Berlin 46, Germany

ABSTRACT: The massive sulfide deposits in the East Pontic metallogenic province are linked to a 150 to 300 m thick strongly altered Upper Cretaceous pyroclastics. The deposits (i.e. Murgul) in the eastern part is assigned to a subvolcanic-hydrothermal formation and might be interpreted as a transitional type tending to porphyry copper deposits (Murgul type) whereas the deposits in the western part (i.e. Lahanos and Madenköy) are of a submarine hydrothermal activity sequence related to island arc volcanism. The deposits of the Lahanos and Madenköy represent Kuroko-type deposits exactly.

1 INTRODUCTION

The East Pontic metallogenic province extends over an area of more than 350 km E-W and 60 km N-S representing an island arc system of Jurassic throughout Miocene age hosting a great number of base metal deposits (Fig. 1). The ratio of important deposits changes along the general strike from the E (Cu>> Pb+Zn) to W (Pb+Zn>>Cu) progressively. The biggest deposits are Murgul, Madenköy, and Lahanos which have been investigated because of different genetically interpretations. The aim of this paper is to give an genetically overview and to elucidate the formation of these different deposits in the area.

2 GEOLOGIC SETTING

The metallogenic province consists of about 3.000 m thick volcanic sequence with relatively thin intercalations and lenses of marine sediments which can be divided into three cycles (Schneider et al. 1988):

(1) The first cycle comprises a volcanic pile deposited between Jurassic and Upper Cretaceous which is represented by initial basaltic activity and changes progressively to felsic lava flows.

(2) The second cycle starts transgressively with volcanic breccias, tuffs, and marine sediments overlain by andesitic and rhyolitic flows and followed by limestone of Maastrichtian age.

(3) The last cycle is introduced by marine sediments of Paleocene age which are overlain by andesitic and basaltic lava flows constituting Tertiary volcanic activity.

In the entire metallogenic province, the important deposits are linked to a 150 to 300 m thick altered dacitic pyroclastics revealing very turbulent and repeated volcanic activity (Tugal 1969; Cagatay & Boyle 1980; Özgür 1985).

3 THE ORE DEPOSITS

The ore mineral paragenesis of the Murgul, Madenköy, and Lahanos consists of pyrite, chalcopyrite, sphalerite, galena, fahlore, arsenopyrite, covellite, gold, ± bornite, and minor quantities of aikinite, hessite, tetradymite, and clausthalite.

The deposits consist of (1) disseminated ore, (2) stockwork ore, and (3) small ore lodes. The first ore type shows varying Cu contents ranging from 0,2 to 0,8 percent which can be considered as the oldest mineralization. The second ore type with Cu contents of 1.0 to 3.0 percent indicates a younger phase of hydrothermal remobilization. Cu contents of the third ore

type range up to 10.0 percent and are developed mainly as relatively short veins. The deposits of the Lahanos and Madenköy in the western part indicate massive ore comparable with Kuroko-type deposits (type 4).

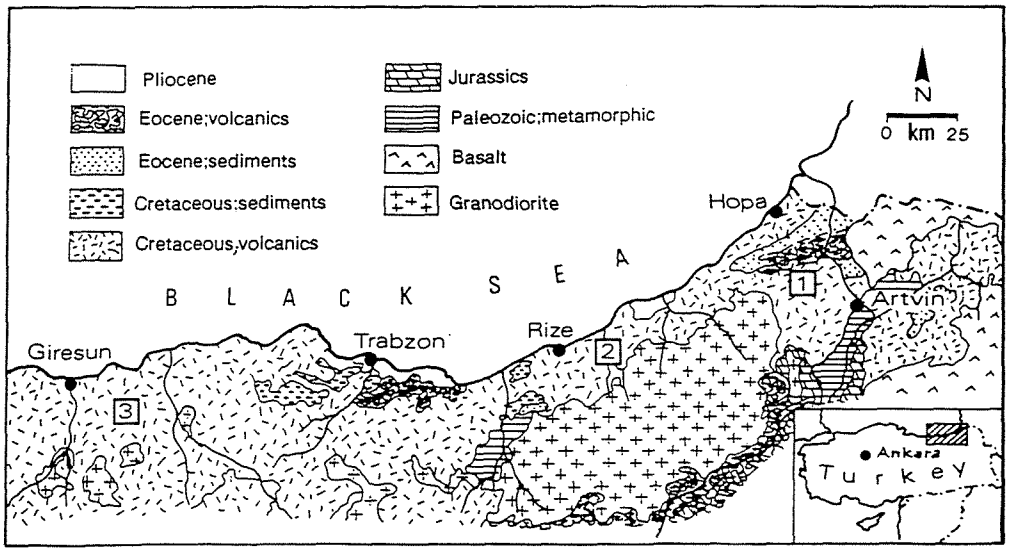

Fig. 1: Geologic setting and location map of the East Pontic metallogenic province; 1: Murgul, 2: Madenköy, 3: Lahanos.

The recoverable ore reserves are estimated at about 40 million metric tons with an average content of 1,25 percent Cu, 0,1 percent Zn, 0,05 percent Pb, 25 ppm Ag, and 0,2 ppm Au (Murgul), 30 million metric tons with an average content of 2,9 percent Cu and 4,3 percent Zn (Madenköy), and 8 million metric tons with an average content of 1,6 percent Cu and 2,3 percent Zn (Lahanos).

4 HYDROTHERMAL ALTERATION AND MINERALIZATION

The deposits in the metallogenic province are confined to a distinct phase of altered dacitic and rhyolitic eruptives. Intense host rock alteration might be divided into (i) an initial stage representing a phyllic and argillic zone and (ii) a late stage of silicic alteration in the central part (Cagatay & Boyle 1980; Schneider et al. 1988). Initial stage of alteration is attributed to the destruction of the primary paragenesis of the pyroclastic series and to the replacement of the rock by quartz and sericite. An extensive but poor mineralization (type 1) took place during the first stage. As a late stage of hydrothermal alteration the silicic alteration is intimately related to economic mineralization of the second and third ore types.

The rare earth element patterns of the pyroclastic host rocks of the above mentioned deposits in the metallogenic province indicate a progressive REE depletion with an increase of intensity in phyllic, argillic, and silicic alteration (Schneider et al., 1988). Due to ascending hydrothermal fluids the dacitic and rhyolitic host rocks of these three deposits are strongly altered and exhibit therefore dispersion patterns by the depletion of Na, Ca, K, Mn, Ti, Rb, Cs, and REE as well as by the enrichment of Cu, Zn, Pb, As, Ba, F, Ag, and Au (Tugal 1969; Cagatay & Boyle 1980; Özgür 1985). In connection with hydrothermal alteration Cu is enriched within phyllic and silicic alteration zones. Therefore, Özgür (1985) proposed the use of the elements F, Ti, and Mn as pathfinder elements for the exploration of blind deposits of the same type in the metallogenic province.

The pyrites of the deposits of the Murgul, Madenköy, and Lahanos indicate a volcanogenic origin in respect to ratio of Co/Ni and differ from the Lahanos and Madenköy pyrites obviously. On the other hand, the Lahanos pyrites indicate volcanogenic as well as sedimentary formation while the Madenköy pyrites establish a transition between Murgul and Lahanos pyrites. In the geochemical ratio of Cu/As and Ag/As of Pyrites and chalcopyrites the deposits of the Murgul, Madenköy, and Lahanos indicate a geochemical similarity with respect to a genetic comparison with the Fiji deposits (Colley & Rice 1975; Özgür 1985).

5 DISCUSSION AND CONCLUSIONS

The deposits of the Murgul, Madenköy, and Lahanos are linked to the strongly altered pyroclastics. The host rocks exhibit in the western part of the metallotect immense intercalations of marine sediments whereas in the eastern part the sparsely and locally intercalated marine sediments indicate a shallow water depositional environment. Geochemical and isotopic data indicate that the pyroclastics have derived from magmas generated by partial melting of distinct sources in the upper mantle. The mineralization of the deposits of the Lahanos and Madenköy is predominantly stratiform whereas the Murgul deposit in the eastern part indicates strata-bound stockworks, short veins, and disseminations.

The hydrothermal mineralization in the metallogenic province consists of (i) an early distal one of phyllic and argillic alteration zones and (ii) a late stage of silicic alteration. The first ore type occurs with the first stage of alteration. The second and third ore types correspond with the second stage of alteration. The deposits of the Lahanos and Madenköy in the metallogenic province might be compared with the ore Kuroko-deposits, Japan (Cathles et al. 1983) and Undu, Fiji (Colley & Rice 1975). The δ34S values of sulfides in Murgul and Lahanos range from 2.33 to 4.83 per mil and are comparable with the values of the Kuroko-type deposits (Ohmoto et al. 1983) additionally.

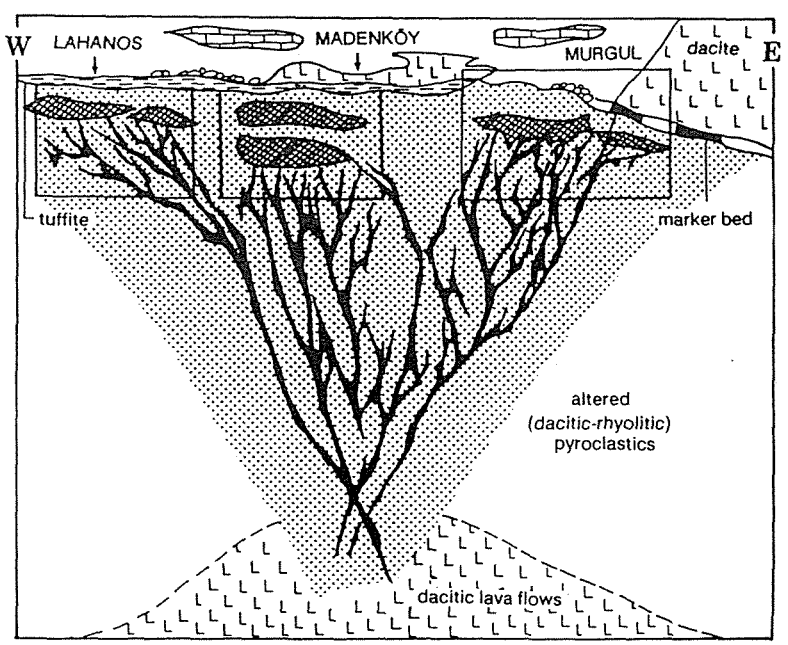

Fig. 2: Schematic presentation of the investigated ore deposits of the Murgul, Madenköy, and Lahanos in the East Pontic metallogenic province

According to the geological, microscopical, geochemical, and isotopic data the copper deposit Murgul in the eastern part of the metallogenic province can be assigned to a subvolcanic-hydrothermal formation with an Upper Cretaceous island arc volcanism under subaerial conditions. The host rock of the Murgul deposits shows feauteres similar to the "ore related breccias" suggesting a subsurface brecciation generated by volcanoplutonic activity contemporaneous with tuff sedimentation. On the other hand, the copper ore deposits of the Lahanos and Madenköy in the eastern part are related to a submarine-hydrothermal activity in a volcano-sedimentary sequence under temporally subaquatic conditions (Fig. 2). Subsequently, the Murgul copper ore deposit might be interpreted as a transitional type tending to copper porphyries (Murgul type) whereas the deposits of Lahanos and Madenköy represent Kuroko-type deposits exactly.

REFERENCES

Cagatay, M.N. & Boyle, D.R. 1980. Geology, geochemistry and hydrothermal alteration of the Madenköy massive sulphide deposit, eastern Black Sea region, Turkey. Proc. 5th Quadrennial IAGOD Symp., pp. 653-677.

Colley, H. & Rice, C.M. 1975. A Kuroko-type ore deposit in Fiji. Econ. Geol. 70: 1373-1386.

Cathles, L.M., Guber, A.L., Lenagh, T.C., & Dudas, F.Ö. 1983. Kuroko-type massive sulfide deposits of Japan. Econ. Geol. Mon. 5:96-114.

Ohmoto, H., Mizukami, M., Drummond, S.E., Eldridge, C.S., Pisutha-Arnond, V., & Lenagh, T.C. 1983. Chemical processes of Kuroko formation. Econ. Geol. Mon. 5:570-604.

Özgür, N. 1985. Zur Geochemie und Genese der Kupferlagerstätte Murgul, E-Pontiden/Türkei. Ph.D. thesis, Freie Universität Berlin, 139 p.

Schneider, H.-J., Özgür, N., & Palacios, C.M. 1988. Relationship between alteration, rare earth element distribution, and mineralization of the Murgul copper deposit, northeastern Turkey. Econ. Geol. 83:1238-1246.

Tugal, H.T. 1969. Pyrite sulphide deposits of the Lahanos mine area, eastern Black Sea region, Turkey. Ph.D.thesis, Dunham University, 182 p.

Current Research in Geology Applied to Ore Deposits. Fenoll Hach-Alí, Torres-Ruiz & Gervilla (eds) (1993). ISBN 84-338-1772-8

DISTRIBUTION OF SELECTED MAJOR AND TRACE ELEMENTS IN THE VOLCANIC HOST ROCKS OF THE RIO TINTO MASSIVE SULPHIDE DEPOSITS

Piantone, P. (1); Freyssinet, Ph. (1); Sobol, F. (2) & Leistel, J.M. (1)
(1) BRGM, BP 6009, 45060 Orléans Cedex 02, France
(2) Rio Tinto Minera, S.A. Minas de Riotinto, Huelva, Spain

Abstract: A study has been made of the distribution of several elements in the basal volcanic rocks of the Rio Tinto district (South Spain), where the hydrothermal alteration halo extends to 2.5 km from the mineralization. The inner zone of this halo (0-500 m) shows intense leaching of Na in favour of K and Mg, and is characterized by anomalous Tl-Rb-Ba values; the Rb/Tl ratio has been modified and Tl appears to be related to the alteration micas. The outer zone (1000-2500 m) shows chloritization of the volcanic rocks, and contains traces of sulphides enriched in Sb-Se, which are the pathfinders of the mineralization.

INTRODUCTION: Available data on the study of hydrothermal haloes shows that numerous indications can serve as mineral exploration guidelines. For example, many authors (Möller *et al.*, 1983; Ikramuddin *et al.*, 1983; Smith and Huston, 1992) have shown that the redistribution of elements such as K-Na-Rb-As-Sb-Tl during hydrothermal processes depends on the proximity of these elements to the hydrothermal hot springs. Other authors (Hauff *et al.*, 1989; Offler and Whitford, 1992) show that the crystallography and/or the crystallochemistry of the micas are generally modified by the hydrothermal alteration at regional scale . This article presents the first results of a lithogeochemical study carried out on the mineralogical and geochemical signatures of the basal volcanic formations in the vicinity of the Rio Tinto massive sulphide deposit (VMS)(South Spain). The behaviour of K, Mg, Ba, Tl, Sb, Se and Rb in the proximal and distal host formations of the VMS body are briefly described and discussed.

GEOLOGICAL SETTING: The Rio Tinto massive sulphide deposit are situated in the Huelva Province of South Spain, 90 km northwest of Sevilla and 70 km northeast of Huelva. They form part of the Paleozoic South Iberian Pyrite Belt, which is composed of numerous volcanic centres genetically associated with the VMS, and covered by a monotonous and diachronous Culm sedimentary series. The VMS mined at Rio Tinto bodies are hosted by the basal (V1) acidic volcanic formations (rhyolite to dacite) made up of pyroclastite, breccia and lava flows and domes (Garcia Palomero, 1990) that crop out in an E-W anticline. Different Middle to Late Carboniferous tectono-metamorphic phases (Routhier *et al.*, 1978) developed a schistosity and neogenic minerals. In spite of this, the hydrothermal alterations related to the deposition of the sulphides (chloritization and phyllitization) remain perfectly identifiable.

LITHOGEOCHEMICAL STUDY: Samples, solely from the hanging wall of the massive sulphide bodies in the basal acidic volcanic rocks (V1) were collected from the mineralized zone outward for several kilometres. The rocks of this acidic volcanic complex are relatively homogeneous with a chemical composition that, with very few exceptions, from rhyolite *s.s.* to rhyodacite.

Alteration mineralogy: The neogenic minerals formed after the deposition and emplacement of the volcanic rocks result from two successive events (Routhier *et al.*, 1978): a hydrothermal alteration related to the massive sulphide emplacement, and a greenschist-type metamorphic alteration.

Three major alteration facies are distinguished on the basis of petrographic studies and whole-rock chemical analyses: 1) a feldspathic facies (albite and/or K-feldspar) with subordinate white mica; 2) a mica-chlorite facies, and; 3) a mica-abundant facies corresponding to the inner haloes of hydrothermal alteration around the massive sulphide body. The volcanic textures are well preserved in all three facies, apart from in a few samples from the mica-abundant facies.

The feldspathic facies shows a redistribution of the alkaline ions, which is marked by a sodic or potassic metasomatism; the facies contains green epidote, some rare mica and calcite. The mica-chlorite facies shows a development of white mica distributed preferentially in the deformation planes (shear foliation, deformed areas around phenocrysts); chlorite, green epidote and carbonates are common but have an irregular distribution. The mica-abundant facies generally shows the same paragenesis as the mica-chlorite facies, although epidote is exceptional and the carbonates are better represented (dolomite); the chlorite is also exceptional, having developed with the neogenic mica in the pressure shadows.

Geochemical haloes: Many elements in the basal V1 volcanic rocks show significant anomalies related to the hydrothermal alteration and sulphide deposition. The highest concentrations of the chalcophile elements (Mo, As, Cu, etc.) are in the inner part of the halo, close (0-500 m) to the massive sulphide body; their distribution is very erratic and shows a "nugget effect". The elements in the aluminosilicates and carbonates (Mg, Rb, K, Sr, Na, etc.) show more regular anomalies (positive or negative) extending over several kilometres. To illustrate the size of the geochemical haloes, the distributions of Na, K, Sb, Se, Ba and Tl are presented as a function of their distance from the mineralized zone (fig. A).

DISCUSSION:

Outer anomalies (1000-2500 m): The Na, Mg and K distribution anomalies are explained by a leaching of the volcanic rocks in the hydrothermal zones with a partial redistribution due to mineral neogenesis. The outer halo (1000 to 3000 m) shows facies enriched in chlorite with respect to the average composition of the volcanic rocks. The Mg anomalies in the outer zone of the hydrothermal halo can be explained by an exchange system similar to that established by Mottl (1983) for the mid-ocean ridges: a trapping of sea-water magnesium and neogenesis of chlorites in the little altered facies of the volcanic rocks.

The outer halo also shows Sb and Se anomalies superposed on the Mg anomalies (fig. A), which demonstrates the presence of neogenic sulphides several kilometres distant from the massive sulphide bodies, contrary to the classically presented picture (Smith and Huston, 1992).

Inner anomalies (1-500 m): Hydrothermal alteration in the mineralized zone follows a classic pattern: Na is intensely leached to the benefit of K and Mg (fig. A). Analysis of the correlations between Tl and Rb reveals two groups of samples distinguished by their Tl/Rb ratios (fig. B): the one, with Tl/Rb = 0.25 and the other with Tl/Rb = 0.6×10^{-2}. The thallium distribution therefore probably resulted from two distinct geochemical processes. The first group was obtained from rock that had been strongly altered under high-temperature conditions with high water/rock ratios; here the alteration micas would be the main Tl carriers. The second group comes from rock showing little or no alteration; here the low Tl/Rb ratio would be representative of the geochemical background and the Tl would be distributed between the K-feldspar and the micas.

Ba, like Tl, shows in a correlation with Rb in the inner zone (fig. B). An electron microprobe analysis of the inner zone micas has shown the Ba localization to be in the interfoliate site of the white micas ($Na^+ + K^+ \Leftrightarrow \frac{1}{2}[Ba^{2+} + Ca^{2+}]$). This localization of Ba in the white micas and the good correlation of Rb-Ba-Tl support the hypothesis that Tl was trapped in the white micas of the inner zones.

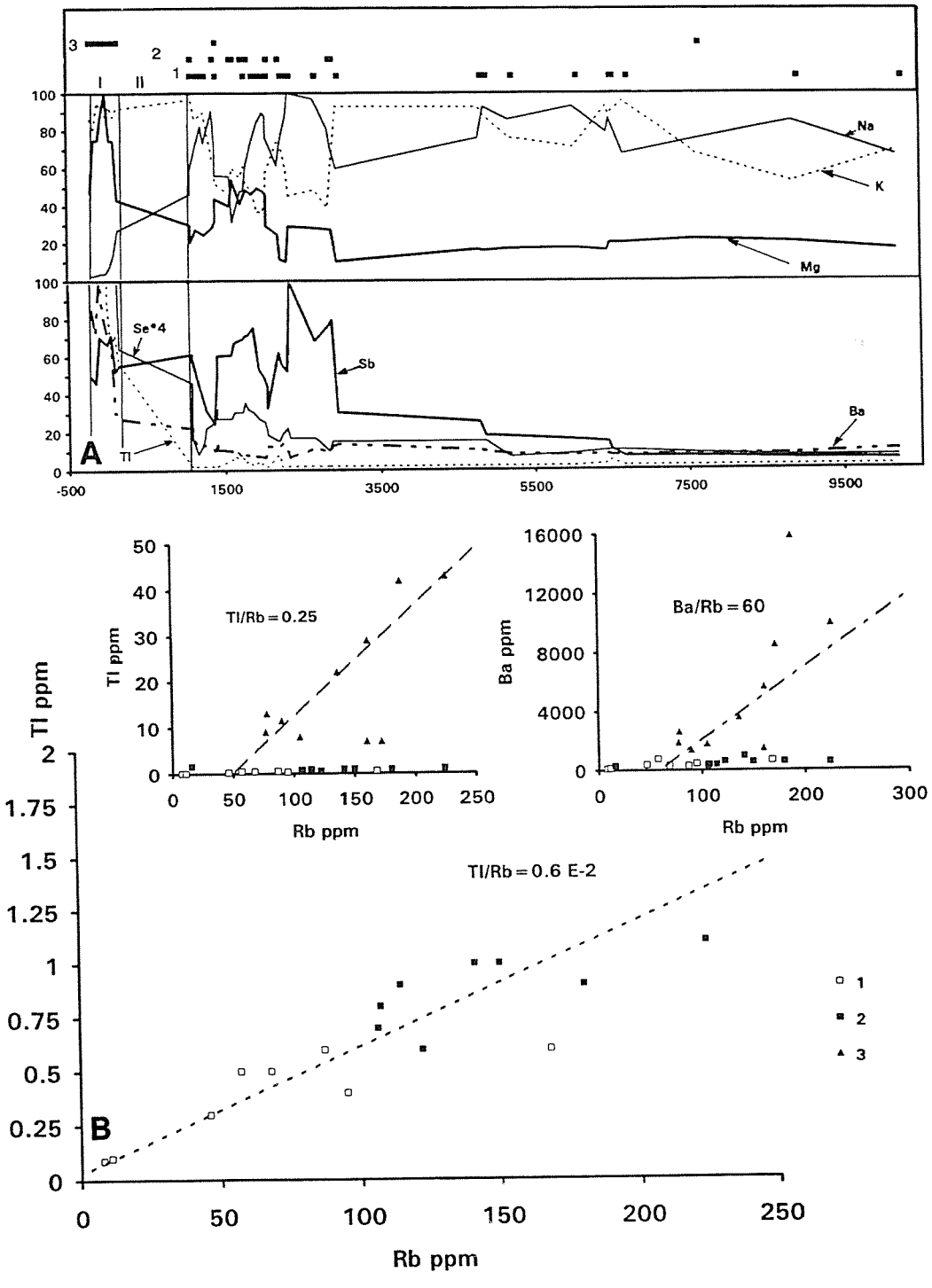
3
2
1
I
II
Na
K
Mg
Se*4
Sb
Ba
Tl
A
-500
1500
3500
5500
7500
9500
Tl/Rb = 0.25
Tl ppm
Rb ppm
Ba/Rb = 60
Ba ppm
Rb ppm
Tl/Rb = 0.6 E-2
Tl ppm
Rb ppm
B
1
2
3

CONCLUSIONS: The lithogeochemical study has revealed several potential hydrothermal-alteration pathfinders that resisted later metamorphic events:

1) In a homogeneous lithological background, the positive (Mg, Sb, Se, Tl) and negative (Na) anomalies resulting from hydrothermal alteration around the Rio Tinto massive sulphide deposit are sufficiently strong to be used as tracers of hydrothermalism in the basal volcanic formations. The halo shows an inner zone (0-500 m) in the rhyodacite has been leached of Na in favour of K and Mg, and an outer zone (1000-2500 m) characterized by a more marked chloritization of the volcanic rocks, as well as the presence of Sb and Se enriched sulphides.
2) Both thallium and barium are reliable pathfinders of proximal hydrothermal alteration (0-500 m). They are contained in the micas and thus have a relatively regular distribution.
3) Analysis of the Tl and Rb distribution over the whole of the Rio Tinto area shows that two processes controlled their distribution in the rocks; one is characteristic of the hydrothermal alteration, the other appears to be regional.

REFERENCES

Garcia Palomero G. 1990. Rio-Tinto deposits-geology and geological models for their exploration and ore-reserve evaluation. In: Sulphide deposits: their origin and processing. ed. P.M.J. Gray et al. Inst. Mining Metall, London, 310 p.

Hauff P.L., Kruse F.A., Bakken B.M. and Madrid R. 1989. Using illite polytipe and illite crystallinity to characterize gold deposit - from megascopic to microscopic perspective. 9th International Clay Conference, Strasbourg, France, Abstract No. 358.

Ikramuddin M., Asmeron Y., Nordstrom P., Kinart K., Martin W., Digby S., Elder D., Nijak W. and Afemari A. 1983. Thallium: a potential guide to mineral deposits. Journal of Geoch. Expl., 19, pp. 465-490.

Möller P., Dieterle M.A., Dulski P., Germann K., Schneider H.J. and Shutz W. 1983. Geochemical proximity indicators of massive sulfide mineralization in the Iberian Pyrite Belt and the East Pontic Metallotect. Mineral. Deposita, 18, pp. 387-398.

Mottl M.J. 1983. Metabasalts, axial hot springs, and the structure of hydrothermal systems at mid-ocena ridges. Geol. Soc. Amer. Bull., 94, pp. 161-180

Offler R. and Whitford D.J. 1992. Wall-rock alteration and metamorphism of volcanic-hosted massive sulfide deposit at Que River, Tasmania: petrology and mineralogy. Econ. Geol., 87, pp. 686-705.

Routhier P., Aye F., Boyer C., Lécolle M., Molière P., Picot P. and Roger G. 1978. La ceinture sud-ibérique à amas sulfurés dans sa partie espagnole médiane. BRGM Mémoire, 94, 265 p.

Smith R. and Huston D. 1992. Distribution and association of selected trace elements at the Rosebery Deposit, Tasmania. Econ. Geol., 87, pp. 707-719.

FIGURES

A.- Distribution of tenors of chosen elements in relation to distance from the massive sulphide body. (I) San Dionisio deposit, (II) zone covered by waste. (1) feldspathic facies, (2) mica-chlorite facies, (3) mica-abundant facies. The values used to trace the Xi_n/Xi_{max} or Xi curves corresponds to the moving average of four samples.

B-Rb/Tl et Rb/Ba correlations.

Current Research in Geology Applied to Ore Deposits. Fenoll Hach-Alí, Torres-Ruiz & Gervilla (eds) (1993). ISBN 84-338-1772-8

UPPER PROTEROZOIC, MARGINAL POLYMETALLIC ORE BELT OF THE SIBERIAN PLATFORM (STRATIFORM Pb-Zn DEPOSITS: TYPES, MODELS FOR ORIGIN AND LAWS OF DISTRIBUTION)

Ponomarev, V.
Inst. of Geology, Siberian Branch of Russian Academy of Sciences, Novosibirsk, Russia

ABSTRACT: The margins structures of Siberian Platform contains an important metallogenic districts characterized by stratiform Pb-Zn deposits associated with thick sequence of terrigene-carbonate rocks having Riphean age. Hot rock lithologies can be used as a basis for empirical classification of base metal deposits in three major groups. These deposits are chemical precipitates from exhalative hydrothermal solutions on the sea floor (hydrothermal-sedimentary model).

1 INTRODUCTION

The area investigated is situated in the East Siberia. The problem in question is based on the results of geologic-geochemical analysis of the stratiform Pb-Zn deposits in the peri-craton miogeosynclinal depression of marginal parts of the Siberian (Yenisei Mountain Ridge, Presayan'e, West Baikalian, Patom Highland and South-East Yakut) Platform. These deposits form linear elongated zone known as "Upper proterozoic marginal polymetallic ore belt of Siberian Platform". The term "stratiform" is used to describe the Pb-Zn deposits, that are paragenetic related to the metasedimentary formations and characterized by specific conditions of origin and laws of distribution in the earth's crust.

In peri-craton areas of Siberian Platform sedimentation took place in shallow-water basins. The primary formations were formed by flysch-like, terrigenous, terrigenous-carbonaceous sediments of mixed composition, less siliceous and carbonaceous. The peri-craton areas are characterized by the absence or weak display of the volcanism. The type and tectonic peculiarities of development in Upper Precambrian of peri-craton areas clear synchronization of tectonic processes insufficiently. Essentially granitoidal magmatism and peculiarities of sedimentation (sedimentation was marked by the miogeosynclinal character with essential role of carbonate and terrigenous arkosic formation) allow to compare the geodynamic conditions of the Upper Precambrian peri-craton areas of the Siberian platform with Recent margin-continental marine basin conditions.

In the above structures the stratiform deposits are confined to terrigenous-carbonaceous and to carbonate formations, namely the mid-Riphean, and form metallogenic belts of hundreds kilometers in length along the strike. The deposits differ in their size, morphology and composition according to variations of structure and composition of ore-bearing complexes that accumulated not far from various stable paleotectonic uplifts.

2 MAJOR TYPES OF STRATIFORM PB-ZN DEPOSITS

As an example, polymetallic ores in the stratiform deposits of Yenisei Mountain Ridge are described. Yenisei Ridge is located in the south-western part of Siberian Platform. There are three large rock cycles in Rifhean deposit section of Yenisei Ridge. Each cycle is represented by essentially terrigenous and carbonate deposits in its lower and upper parts, respectively. Terrigenous sedimentation was replaced by carbonate one in each of these cycles due to the regional tectonic reconstruction, followed by the general tendency to downwarping and deepening of the sedimentation basin. The stratiform lead-zinc ores are related to the terrigenous-carbonate cycle. On the basis of lithological-formation and facies analysis and using geological-genetic modelling, three following typical geological situations of Pb-Zn ores location were distinguished. These typical situations are considered to reflect a favorable geological environment in which a submarine deposit could form and could be preserved. Thus they can be used as an exploration parameters.

F i r s t typical situation is characteristic of Pb-Zn ores formed in the vicinity of the ore-incurrent canals in the local depressions under the conditions of shallow-water basin on the slopes of paleonplefts which controlled the development of reefogenous and biogermal facies. The ore-bearing strata is characterized by the large variety of rocks and facial variability. For its lower part chemogenic dolomites and limestones, algal ferruginous dolomites and calcareous intraclasts are characteristic. Within the upper part of the ore-bearing section carbonaceus consedimental breccias composed by dolomite and limestone fragments cedimented by clayey and carbonate-aleurolite-clayey matrix. These deposits are usually Pb-Zn rich. Prevail ore minerals are represented by galena, sphalerite, pyrite, quartz, ankekite and dolomite. Chalcopyrite, various sulphosalts and pyrrhotite are marked as secondary minerals. Isotopic composition of S in the sulphide ores varies from +14.4 to +21.1 permill. Average isotopic composition of ^{13}C and ^{18}O is -0.75 and +17.4 permill, respectively. Analysis of deposition temperatures for the polymetallic ores by S - isotopic geathermometry showed narrow interval of the process from 160 to 220°C.

S e c o n d typical situation characterizes polymetallic mineralization in carbonaceous shale strata at certain distance from the ore-incurrent canals. The ore-bearing strata produces local troughs in the most sagged parts of paleodepressions. It is made of phyllitoid-graphitic shales and aleurolites, carbonaceous-quartz-micaceous shales with intercalations of sericitic quarzites. The ores occur as lenticular bodies that are conformable with bedding at the scale of deposits. A significant part of the ore occurs as diagenetic crystallization rhythmites. The deposit consists of the fine-grained pyrite, marcasite, galena, shalerite and minor minerals: arsenopyrite, bournonite, chalcopyrite, pyrrhotite. Framboidal pyrite is widely spread. The silver is associated with the galena. The Zn:Pb ratio is 10:1 on the average.

In contrast with the 1-st typical situation, isotopic composition of S in ores is characterized by the wide $\delta^{34}S$ variations from +18.2 to -22.2 permill. Isotopic composition analysis of the ore-bearing strata carbonates demonstrates rather stable ^{18}O composition (15.7-18.6 permill). The ^{13}C is consistently enriched by light isotope from -2.13 to -7.17 permill. Deposition temperature of the ore substance over isotopic pairs is up to 100°C.

T h i r d typical situation represents a variant of Pb-Zn deposits occurring in small but deep depression troughs composed of slow-water shale-carbonate sediments. This is large stratiform Pb-Zn deposits of high tonnage. "Gorevskoye" deposit can be an example of such situation.

The ore-bearing strata is shale-carbonate and consists of limestones with subordinate quantity of clay, carbonaceous-quarts-clayey shales and dolomites. The ores occur chiefly as lens-shaped bodies generally to the bedding. The most important sulfides are galena, sphalerite and pyrrotite. Pyrite, murcasite, magnetite and arsenopyrite are found in minor amounts, bournonite, boulangerite, natite silver occur sporadically. The Zn:Pb ratio is 1:4 on the average. The following types of structures are established: banded and stratified, massive, intervein-impregnated, foliated and folicited-banded, breccia, veined structures in massive ores.

Isotopic composition of sulfur of ore sulfides (200 samples) as well as of total sulfur of sedimentary and olivine dolerite dikes (50 samples) in "Gorevskoye" deposits was determined. Ore sulfides are enriched in S up to 17.6±3.2 permill, on the average varying from 10.5 to 23.8 permill. With the approaching the country rock progressive depletion on ^{34}S from early to later associations of sulfides and enrichment in this isotope (up to 2-4 permill) is observed. Isotopic differences in pairs sphalerite-galena and pyrrhotite-arsenopyrite give evidence on deposition of these minerals in the environment near to isotope equilibrium at temperatures 100-250° C (syngenetic ores) and 300-400° C (metamorphogenetic-transformed). The $\delta^{34}S$ values of the sedimentary rocks vary from -4.1 to +18 permill, most of samples are enriched in ^{34}S. The $\delta^{34}S$ values of dikes vary from 1.6 to 3.8 permill. Isotopic composition of C and O in inclosing limestones is close to normal pelagic limestones and, on the average, is -2 and +17 permill, respectively. In sideroplesites of ore bodies lightening of C isotopes to -7.1 permill and O isotopes to +15 permill takes place.

Twenty four galenas from 12 ore deposits of Yenisei Ridge show a narrow range of isotopic ratios (Pb(206)/Pb(204) = 17.06 - 17,40; Pb(207)/Pb(204) = 15.31 - 15.59; Pb(208)/Pb(204) = 37.01 - 37.29). Variation of isotopic composition of lead in galenas and ore-bearing formation shows that the source of ore material in the investigated deposits is predominantly crustal-typical for orogenic zones. The average model ages of ores (about 9x10 years) coincide with the age of host sedimentary beds.

3 CONCLUDING REMARKS

Syngenetic and epigenetic models were used to explain the genesis of this type of Siberian stratiform Pb-Zn deposits. Most

of the earlier workers favored a epigenetic origin. Later, syngenetic model appears to have gained favor.

The genetic model for these Pb-Zn deposits of East Siberia must consider the following geologic features: 1) deposits concentrate within a thick terrigenous-carbonate and carbonate sequence; 2) the stratiform orebodies are controlled by the stratigraphical, geotectonical and litological-facies factors of sedimentation; 3) lack of intrusive bodies directly connected to the deposits; 4) lack of important regional and local structures clearly control the location of orebodies; 5) deposition and formation of the orebodies parallel to the bedding; 6) the lamination and bedding of fine-grained sulphide minerals is concordant with the bedding in the host sediments (carbonates and shales); 7) very fine grained chert is commonly found interbedded with stratiform sulphide; 8) ores are characterized by relative simplicity and stability of composition and are usually composed of framboidal aggregate pyrite or pyrrhotite with sphalerite and galena; 9) ore has many variation of textures of atectonic deformation and diagenetic transformation; 10) both the ore and the rock-forming leads are of the same isochronous age and lead isotope investigations indicate that metals were probably leached from crustal; 11) ore sulfides are enriched in S to 25 permill; 12) the temperatures indicated by sulfur isotope geothermometry give evidence on deposition of sulfides minerals at temperatures 100 - 250 C; 13) considerable proportion of crustal (including organic) carbon found in deposits; 14) the ores and the rocks were metamorphosed under green-schist facies; 15) all metamorphic transformations occur within the limits of primary ore bodies; 16) the discordance of ore mineralization in the ores within stratigraphic unit formed after or during metamorphism are considered as remobilisation.

The ore deposition may be explained by hydrotermal-sedimentary model. The first stratiform sulfide bodies formed during by mixing of a hot ore solution with surrounding sea water as a rule in sea-floor depressions. Hydrothermal-sedimentary polymetallic bodies are formed in two stages. During sedimentogenesis the deposition is controlled by the brine/sea water contact, where the sulphate-reduction process takes place (model of the Red Sea). The velocity of sulphide accumulation exceeds many times a host rock sedimentation rate. During dyagenesis sea-floor sediment becomes crystallized.

Current Research in Geology Applied to Ore Deposits. Fenoll Hach-Alí, Torres-Ruiz & Gervilla (eds) (1993). ISBN 84-338-1772-8

DISTRIBUTION AND ORIGIN OF GOLD AND SILVER IN HOST ROCKS OF VOLCANOGENIC MASSIVE SULPHIDE AND MANGANESE DEPOSITS IN THE PYRITE BELT OF SOUTHERN SPAIN

Rahders, E. (1) & Germann, K. (2)

(1) Freie Universität Berlin, FR Rohstoff und Umweltgeologie, Malteserstr. 74, D-1000 Berlin 46, Germany

(2) Technische Universität Berlin, FG Lagerstättenforschung, Ernst Reuter-Platz 1, D-1000, Berlin 12, Germany

ABSTRACT:

In the Pyrite Belt of Southern Spain, massive sulfide and stratiform manganese deposits are hosted by a volcanic-sedimentary complex of Lower Carboniferous age. Both can be related to hydrothermal events during the waning phase of the volcanic activity, producing exhalitic sediments and alteration phenomena. The sulfide ores and their gossan equivalents are important producers of gold. Average gold grades in sulfide ores are 0.7 ppm, but the distribution in the different ore types is inhomogeneous. Relatively unknown are the gold and silver contents of the host rocks. These exhalitic and altered rocks were examined to determine the respective distribution of the two precious metals. Higher Au and Ag concentrations of more than 0.1 ppm were only analysed in the immediate host rocks (up to some tens of meters away from the orebodies) of both hydrothermal mineralizations. Considerable gold enrichments of up to 1.6 ppm were detected in the low-pyrite quartz-bearing lateral equivalents of massive sulfide orebodies (the "azufrones" of the spanish miners). For the first time gold anomalies were discovered in a bleached jasper-type within the manganese formation. Au concentrations of up to 1 ppm occur in these exhalitic host rocks.

1. INTRODUCTION

The Pyrite Belt represents the central part of the South Portuguese Zone, including more than 70 large stratiform massive sulfide and some 360 small-sized manganese ore deposits. They are hosted by a volcanic-sedimentary complex of Lower Carboniferous age (Barriga 1990). Both can be related to hydrothermal events during the waning phase of the volcanic activity, producing exhalitic sediments and alteration phenomena (Schütz et al. 1988).

The sulfide ores in a lower stratigraphic position are mainly linked to quartz-keratophyric volcanics, and the overlying manganese-jasper mineralization ("manganese formation") occur on top of an intermediate to mafic volcanic pile.

Rocks, such as tuffs, shales, black shales and cherts, which are in direct contact to the orebodies, show alteration (pyritization, chloritization, sericitization, silification, and carbonatization), and element dispersion phenomena (halos of As, Sb, Tl).

The sulfide ores and their gossan equivalents are important producers of gold. Average gold grades in sulfide ores are 0.7 ppm, but the distribution in the different ore types is inhomogeneous (Strauss & Beck 1990). Relatively unknown are the gold and silver contents of the host rocks.

To analyse Au contents and to determine the distribution, three mines, "Tharsis", "La Zarza" and "Sotiel" were explored in more detail. For this proposel exhalitic and altered host rocks were examined. As equivalent to recent sulfide genesis at the seafloor some Au-rich mineralisation are described, with comparable ore-minerals and hydrothermal alteration products.

After dissolution with aqua regia, gold was concentrated in an organic MIBK-phase and detected by furnace atomic absorption spectrometry (GF-AAS) down to a detection limit of 1 ppb. Silver was determined in nitric acid solutions by AAS, without preconcentration (d.l. 50 ppb).

2. RESULTS

As the basis for the metallogenetic interpretation of the Au-distribution we used the geochemical composition of the volcanic-sedimentary rocks. Exhalitic and altered rocks were characterized by their element contents of Au, Ag, Al, Fe, Ti, Mn, Mg, Ca, Na, K, Corg., Ccar., Li, Ba, Sr, Zr, Sc, Y, Nb, Cu, Pb, Zn, Cd, As, Sb, Tl, Ni, Co, Cr, and partly W (Rahders 1992).

Background values of 1.2 and 2 ppb Au are typical for host rocks in a greater distance. Gold enrichments of more than 0.1 ppm are detected in a distance of up to some tens of meters away from the orebodies.

The host rocks of pyrite ores show median values of 0.5 ppm Au/ 4.4 ppm Ag in quartz-rich sulfide ores ("azufrones") and 0.11 ppm Au / 1.9 ppm Ag in chloritites (Fig. 1). These horizons are either in the footwall of the orebodies or represent lateral extensions of the orebodies. They are characterized by silification, pyritization, and chloritization. Hydrothermally altered rocks are enriched in Na and K, while Fe, Mg, Pb, Zn, Cu, As, Sb decrease. Occasionally, higher Ba- and Ca-concentrations occur.

The host rocks of manganese ores show mean values between 5 and 83 ppb Au. Anomalously high gold concentrations of up to 1 ppm are found in jasperoid rocks. Jasperoid rocks are exhalitic products occurring in close association with the manganese mineralization. The gold-rich jasper appears bleached and is geochemically different to the gold-poor type with respect to As, Ni, Co, Ba, Sr, and Li. Silver enrichment up to 3 ppm occurs, within the manganese ores.

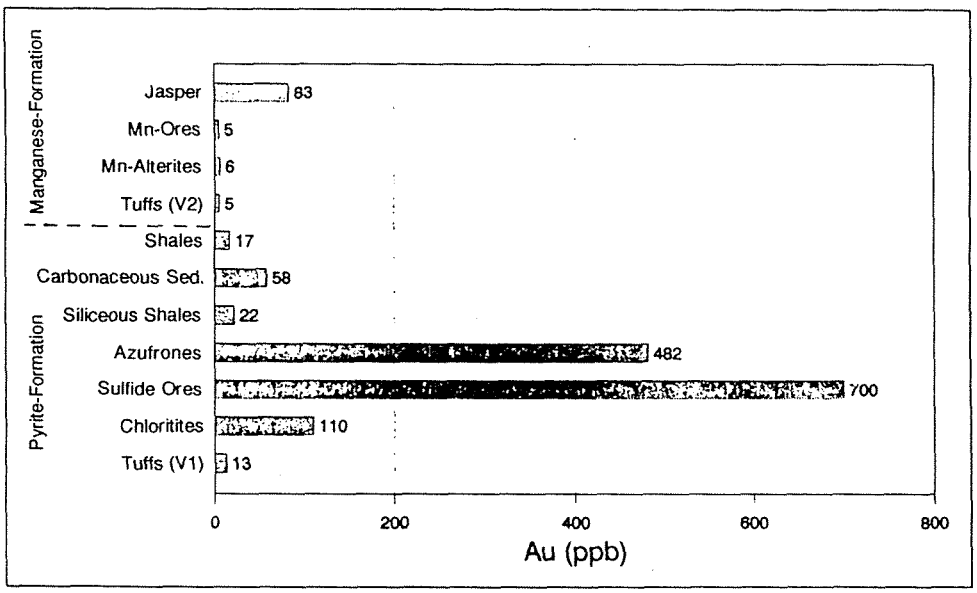

Fig. 1: Mean Au-contents of host rock types.

3. CONCLUSIONS

A different source of gold can be expected for the two mineralizations and their host rocks. Gold and silver in rocks of the first hydrothermal event are remobilized from footwall or stockwork ores during a late stage of sulfide-producing hydrothermal events. Gold anomalies in jasperoid rocks of the second manganese producing hydrothermal stage are related to mafic rocks (Fig. 2.). The Ni/Co-ratio (< 0.5) of these rocks with anomalous Au-values are quite different to those of the pyrite ores (> 1). For the second Au anomaly there is no evidence for any gold remobilization from footwall ores or any rocks of the preceding pyrite-formation.

Anomalous Au concentrations within the Pyrite Belt deposits are generally linked to environments of strong silification, comparable to recent hydrothermal systems. Occasionally, there are tectonic parallels to deposits found in back-arc positions

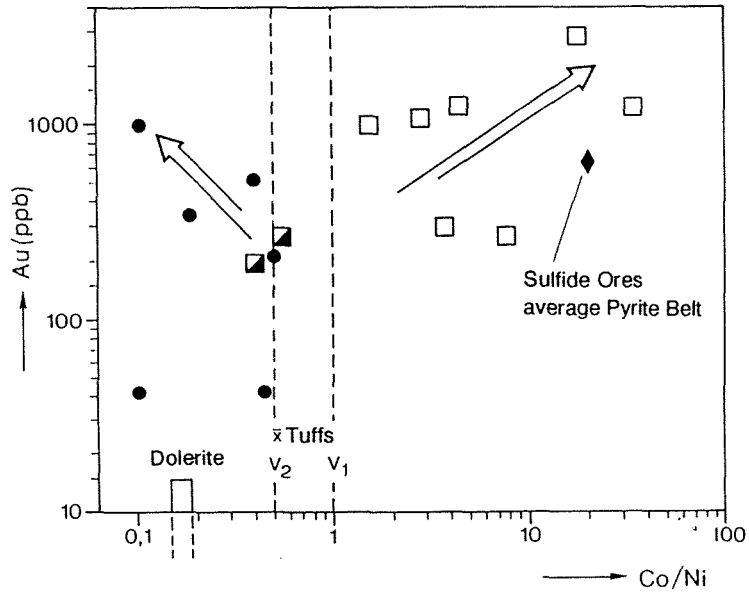

Fig.2: The Ni/Co-ratio of the gold anomalies in the Pyrite-Formation □ related to V_1: felsic tuffs and the Manganese-Formation ● related to V_2: intermediate tuffs.

above the continental crust. Recent gold-rich sulfide mineralizations from the Okinawa Trough are closely related to a bimodal volcanism (Halbach et al. 1989). These gold-rich mineralizations show the same enrichment mechanisms, but they possess higher Pb and Zn contents than the Paleozoic Pyrite Belt deposits. Generally, gold enrichment occurs in the last stage of hydrothermalism as a function of convecting ore-carrying solutions underneath the orebodies, with seawater mixing and lateral precipitation in a mainly siliceous facies.

4. REFERENCES

Barriga, F.J.A.S. 1990: Metallogenesis in the Iberian Pyrite Belt. In: Dallmeyer, R.D. & Martinez Garcia, E. (eds.) Pre-mesozoic geology of Iberia. Springer Berlin Heidelberg New York, pp 369-379

Halbach, P., Nakamura, K., Washner, M. et al. 1989: Probable modern analogue of Kuroko-type massive sulphide deposits in the Okinawa Trough back-arc basin. Nature, 338: 496-499

Rahders, E. 1992: Verteilung von Gold und Silber in den Nebengesteinen der vulkanisch-sedimentären Sulfid- und Manganerzlagerstätten des SW-Iberischen Pyritgürtels, Provinz Huelva, Spanien. Berliner Geowiss. Abh. A 143:1-117

Schütz, W., Dulski, P. & Germann, K. 1988 : Geochemical feature of magmatic evolution and ore deposition in the Pyrite Belt of Southern Spain.- In: Friedrich, G.H. & Herzig, P.M. (eds.) Base Metal Sulfide Deposits, Springer Berlin Heidelberg New York, pp 241-254

Strauss, G.K. & Beck, J.S. 1990: Gold mineralisation in the SW Iberian Pyrite Belt. Mineral. Deposita. 25: 237-245

Current Research in Geology Applied to Ore Deposits.Fenoll Hach-Alí, Torres-Ruiz & Gervilla(eds)(1993).ISBN 84-338-1772-8

TYPES OF MINERALIZATION IN THE BLIND MASSIVE SULPHIDE DEPOSIT OF THE "MASA VALVERDE" (HUELVA, SPAIN), IN THE IBERIAN PYRITE BELT

Ruiz, C. & Arribas, A.
Escuela Técnica Superior de Ingenieros de Minas de Madrid, Rios Rosas 21, 28003 Madrid, Spain

ABSTRACT

The **Masa Valverde** deposit is one of the most recent geophysical discoveries in the **Iberian Pyrite Belt (IPB)**. It is a blind deposit, situated at an average depth of 600 m, and whose investigation has been carried out on drill-core only. The lithoestratigraphy is similar to that of the other IPB deposits, and only the main characteristics of the four types of mineralisation occuring in the deposit will be described here: exhalite, massive sulphide, chloritic and stockwork types.

INTRODUCTION

The **Masa Valverde** deposit is situated in the southern part of the IPB, 14 Km SW of Valverde del Camino, in the Province of Huelva. The deposit, which does not outcrop, lies at a depth of 400 - 825 m and was discovered by the State exploration Company **ADARO** in 1986 (1), using geophysical techniques, chiefly gravity (fig.1).The study of the mineralization has been based entirely on core samples from 18 boreholes made by ADARO, and is part of a research project of the Dirección General de Minas.

GEOLOGY

In the vicinity of the deposit the lithostratigraphic column consists of the following rock formations (from footwall to hangingwall):
Phyllites and Quartzites (PQ) of the Upper Devonian.

Volcano-Sedimentary Complex (CVS) of Tournaisean-Visean age and including **Initial Volcanism (V1)**, where the sulphide mineralization is found, formed mainly of acid tuffs and tuffaceous slates; **Basic Volcanism (V2)** with spilites; **Manganese Formation** with tuffs, tuffites and slates with jasper lenses; **Purple Slates**, which is a marker horizon of great extent; **Final Volcanism (V3)** formed by acid pyroclastics.

Culm (Upper Visean) consisting of a great thickness of slates and graywakes.

Miocene, formed by conglomerates and sandstones.

Quaternary, consisting of gossans and sandstones.

TYPES OF MINERALIZATION

The following mineralization types can be distinguished in the **Masa** Valverde deposit: exhalites, massive sulphides, stockworks and chloritites.

1.-EXHALITES

Two types of exhalites have been recognised: of quartz and sulphide, and of quartz-magnetite and/or carbonate-haematite with possible chlorite.

1.1.- Exhalites of quartz and sulphide

These occur in two clearly different levels. The lower is located in the transition zone of stockwork to massive sulphide, and the upper is found in the hangingwall of the massive sulphides. The exhalites of the first type are formed of white,

microcrystalline quartz, much of which has been recrystallised giving rise to mosaic or plumose quarzt. Sulphides occur in irregular fashion within the quartz, mainly pyrite and low-iron sphalerite, along with small quantities of galena, bournonite, tetrahedrite, arsenopyrite and chalcopyrite. Ocassionally, traces of sericite and chlorite and small quantities of ankerite are observed.

1.2.- Exhalites of quartz-magnetite and/or carbonate-haematite with chlorite

These rocks correspond to the red jaspers of the IPB. Quartz is microcrystalline and cotains fine grain haematite with colloform textures, wich shows that they were recrystallised silica gels. There are abundant idiomorphs of ankerite and twinned calcite distributed in the chert, wich sometimes form plates, also spotted calcite. In some of these rocks radiolaria and haematised radiolaria are seen. The chert is strongly fractured and the fractures are filled with quartz, chlorite and magnetite, which enclose chert fragments. The magnetite, sometimes abundant, generally appears as idiomorphic crystals. Accessory apatite, sericite, pyrite and chalcopyrite are found, together with some martite.

2.- MASSIVE SULPHIDES

The massive sulphides form lenses immediately above the stockwork, or intercalated with pyroclastic rocks. Two principal types occur: massive sulphides sensu strictu, and massive banded sulphides. Both types can be brecciated locally, and generally have a low rare earth element content, with pronounced negative anomalies in Eu (2).

2.1.- Massive Sulphides s.s.

These consist principally of pyrite, and in order of decreasing abundance, sphalerite, galena, tetrahedrite, arsenopyrite, bournonite, cassiterite, stannite, cubanite, pyrrhotite and electrum. In some samples the pyrite is practically the sole component (90-99%), while in the so-called complex sulphide the pyrite accounts for 50-65% by volume, followed by sphalerite and galena. The gangue comprises 0.5 - 12 % by volume of the mineralization and is formed principally of quarzt and carbonate accompanied by small quantities of sericite and chlorite.

Pyrite occurs principally as idiomorphic crystals, occasionally zoned when overgrown on sphalerite, galena or chalcopyrite. The colloform textures are relatively frequent as are oolites formed about a nucleus of pyrite and alternating cocentric bands of chalcopyrite and tetrahedrite. **Sphalerite** appears between the crystals of pyrite, filling microcavities, and in veinlets. Occasionally it occurs as individual crystals, sometimes zoned, or banded with other sulphides within the massive pyrite. Frequently the sphalerite contains exsolved chalcopyrite, rarely stannite. The microprobe analysis shows that the Fe content of the sphalerite in the same drillhole increases with depth, the converse of the behaviour of Zn. **Galena** and **Chalcopyrite** occurs within or in between the pyrite crystals, in veinlets of alternating composition. Occasionally they show colloform textures with pyrite. **Tetrahedrite** occurs in veinlets within the chalcopyrite, galena and gangue, or interstitially between the pyrite crystals. **Arsenopyrite** appears in idiomorphic crystals, either isolated, or forming irregular clusters within the pyrite. **Bournonite** occurs in veinlets, associated with tetrahedrite. **Cassiterite** (Fig. 2) forms crystals of 5 to 15 microns within the sphalerite, and occasionally within the pyrite or gangue minerals. **Stannine** is scarce, occuring in small grains associated with chalcopyrite, sphalerite or galena, and exolved in low-iron sphalerite. **Cubanite** always appears as pink-gray grains in the pyrite, chalcopyrite and galena. **Electrum** is exceptional, as is native **Au** (3). **Pyrrhotite** is very rare and forms small rounded grains within the pyrite.

The principal gangue minerals are **quartz and carbonate**, occuring together or separately, forming veinlets or filling microcavities. The quartz began to be deposited before the carbonate, the latter being of ankeritic and sideritic composition. Sometimes they are replaced by low-iron sphalerite along the cleavage planes. Some **sericite** and **chlorite** also occur, the former, though rare, is widely distributed and appears in scales or radiating fibrous strands within the sulphides.

2.2.- Banded Massive Sulphides

The banded sulphides are formed by the intercalation within the massive pyrite of bands of mainly sphalerite and galena (+/- gangue) more or less parallel to the stratification. Otherwise, the mineralogical characteristics of the banded sulphides are analogous to the massive sulphides s.s.

3.- CHLORITITES AND STOCKWORK

3.1.- Chloritites

Chloritic chimneys occur in the Valverde deposit below the massive sulphide, generally asociated with a stockwork and cross-cut by it, or they can occur as masses intercalated with tuffs. Those chloritites, whose development is usually prior to the formation of the stockwork, probably represent the feeder channels of the mineralising fluids. It is worth noting the frequency and relative abundance within the chloritites of tiny **zircons** with radioactive haloes (fig.3), together with accesory quantities of **rutile** and **apatite** in small idiomorphic crystals. The chlorititc chimneys are strongly tectonised, which affects both the chloritites and the veins of sulphide in the stockwork.

The electron microprobe analysis of the chloritites from the chloritite chimneys, and those from the stockwork, has shown that the chloritites from the upper parts are richer in Fe and Mn, these elements decreasing with depth. The converse occurs with the Mg content which decreases upwards.

3.2.- Stockwork

The stockwork zones are formed in general by cross-cuting well-defined veins of a few millimetres to 5 cm thickness. They are usually found in the chloritite chimneys immediately below the massive sulphides, except in the cases where tectonism has changed the original position. The stockworks are generally hosted by tuffs, rhyolitic lavas and tuffaceous slates, where they form networks of variable density. The veins are formed of sulphide, principally pyrite and chalcopyrite, chlorite and/or carbonate and quartz, as well as minor quantities of sphalerite, arsenopyrite, tetrahedrite, bornite and cubanite. The complete absence of galena is noteworthy.
Pyrite is the dominant metallic mineral, occuring as idiomorphic or subidiomorphic crystals, either independently or forming more or less compact masses. Only occasionally does it give rise to geliform textures, largely recrystallised. **Chalcopyrite** is omnipresent, being either an accesory mineral or the principal component of the vein. The chalcopyrite appears under the following forms: fine criss-crossing veinlets within the pyrite; interstitial plates between the pyrite crystals, with idiomorphic pyrite inclusions; as crystals or irregular associations with the gangue; and within the sphalerite where it gives rise to exsolutions in the form of droplets or laminae, the latter occuring along the cleavage (111). **Sphalerite** is generally found between the pyrite crystals or included in the pyrite and chalcopyrite, occasionally giving rise to colloform textures. **Tetrahedrite** is scarce and is associated with the chalcopyrite, sometimes appearing as small grains within pyrite. **Bornite** is rare and forms grains in the pyrite and chalcopyrite.

Of the gangue minerals, **chlorite** forms micro to cryptocrystalline aggregates with frayed edges and occacionally well-developed tabular crystals. Microprobe analysis shows that the stockwork chloritites have the same vertical zonation as previously described for the chloritite chimneys. The stockwork **carbonates** occur interstitially among the sulphides, which they sometimes cross-cut in veins, and correspond compositionally to ankerite and siderite, never calcite. In agreement with the mineralogical studies, ankerite is more abundant at depth, while siderite is more abundant in the upper parts. This vertical zonation of the carbonates follows that of the chlorite, showing an impoverishment in Mg and an enrichment in Fe in the upper parts of the stockwork. The quartz is frequenttly plumose, and sometimes forms crystallization pressure shadows over the sulphides, occasionally bent as a consequence of tectonic stresses.
The formation of the stockwork, whose development was controlled by fractures, was brought about in two fundamental stages: the first gave rise to the chloritisation, incipient carbonitisation and deposition of sulphides; the second took place after fragmentation of the already-formed stockwork, and gave rise to the development of new veins with quartz, chlorite and carbonate.

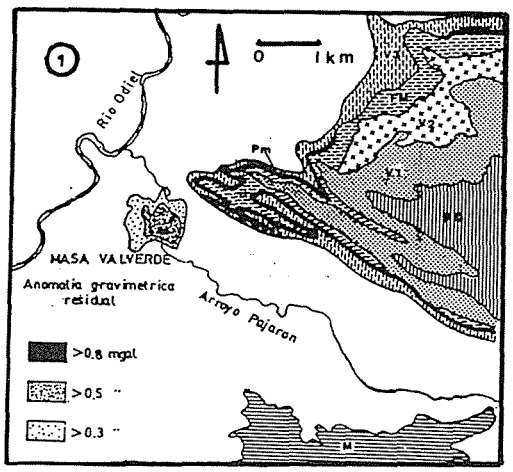

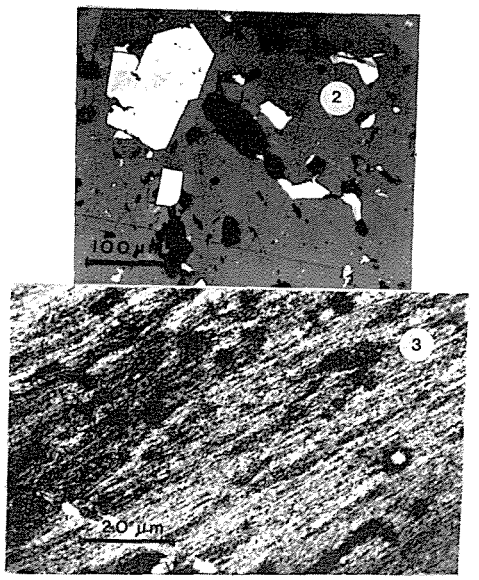

Fig 1.- Location of the gravity anomaly of **Masa Valverde** deposit (Huelva, Spain). **Fig 2.**- Cassiterite (dark grey, center) and pyrite (white) crystals in sphalerite (PPL, =N). **Fig 3.**- Two types of fine grain zircon crystals in chloritite (PPL, +N).

BIBLIOGRAFIA

(1) **Faura, J., Ramirez-Copeiro, J., Rosales, F. (1991).** Una experiencia de investigación de yacimientos ocultos bajo el Culm. Simposium: Los Sulfuros Complejos del Suroeste de España. Club Español de la Minería. 35-53.

(2) **Ruiz, C. & Espi, J.A. (1992).** Mineralogía y Geoquímica de Tierras Raras en el Cinturón Pirítico Español. III Congreso Geología de España. Salamanca. 3: 324-328.

(3) **Vázquez, F., Ruiz, C., Espí, J.A., Navarro, J.A. (1992).** Applications of the geochemical and mineralogical characterization of noble metals in massive sulphides in the SW of Spain. XV World Mining Congress, Madrid, Proccedings II:927-936.

Current Research in Geology Applied to Ore Deposits.Fenoll Hach-Alí, Torres-Ruiz & Gervilla(eds)(1993).ISBN 84-338-1772-8

PRESENTLY-FORMING HYDROTHERMAL SEAFLOOR DEPOSITS OF MANUS AND WOOLARK BASINS, S.W. PACIFIC, AS MODELS FOR ANCIENT ORES

Scott, S.D. (1) & Binns, R.A. (2)

(1) Marine Geology Research Lab., Dept. of Geology, University of Toronto, Toronto, Ontario M5S 3B1, Canada

(2) CSIRO Division of Exploration Geoscience, P.O. Box 136, North Ryde, New South Wales 2113, Australia

ABSTRACT: Since 1986, an international research team has been exploring offshore eastern Papua New Guinea for actively forming hydrothermal deposits that may provide models for ancient ore deposits on land. Extensive Fe-Si-Mn oxide deposits and precious metal-rich (Ag to 545 ppm, Au to 21 ppm) barite-silica spires occur on Franklin Seamount, a young submarine basaltic andesite volcano located near the western propagating tip of a seafloor spreading axis in the Woodlark Basin. In the eastern Manus back-arc basin, a very large (800 x 350 m) actively forming polymetallic sulfide deposit was found along the flank of a dacite lava dome. The deposit has close similarities to ancient massive sulfides ores in Canada and Australia.

Introduction

Since 1986, the authors have been leading an Australian-Canadian research team exploring offshore eastern Papua New Guinea with Russian and Papua New Guinean partners for actively forming hydrothermal deposits that may represent resources for the future and provide models for ancient ore deposits on land. Our main objective has been to study the origins and geological environments of modern seafloor hydrothermal deposits, preferentially in felsic volcanic rocks, as a means of improving exploration models for ancient volcanogenic massive sulfide and related ore types on land. To date, we have conducted six PACLARK and PACMANUS expeditions in the western Woodlark Basin and eastern Manus Basin. The locations and regional tectonic settings of these two sites are in Figure 1. Seagoing activities have included detailed bathymetric mapping, magnetic surveys, deep-tow camera/video traverses, water column measurements and sampling, dredging, sediment coring and, in western Woodlark, a series of dives with the Russian Mir submersibles. The work in western Woodlark Basin has been rewarded by the discovery of large Fe-Si-Mn oxide deposits, that are perhaps equivalent to ancient iron formations, and what appears to be a little recognized type of gold mineralization associated with barite, silica and minor sulfides. The more recent work in the eastern Manus Basin has discovered a very large, actively forming, polymetallic sulfide deposit with many characteristics of ancient volcanogenic massive sulfide ores.

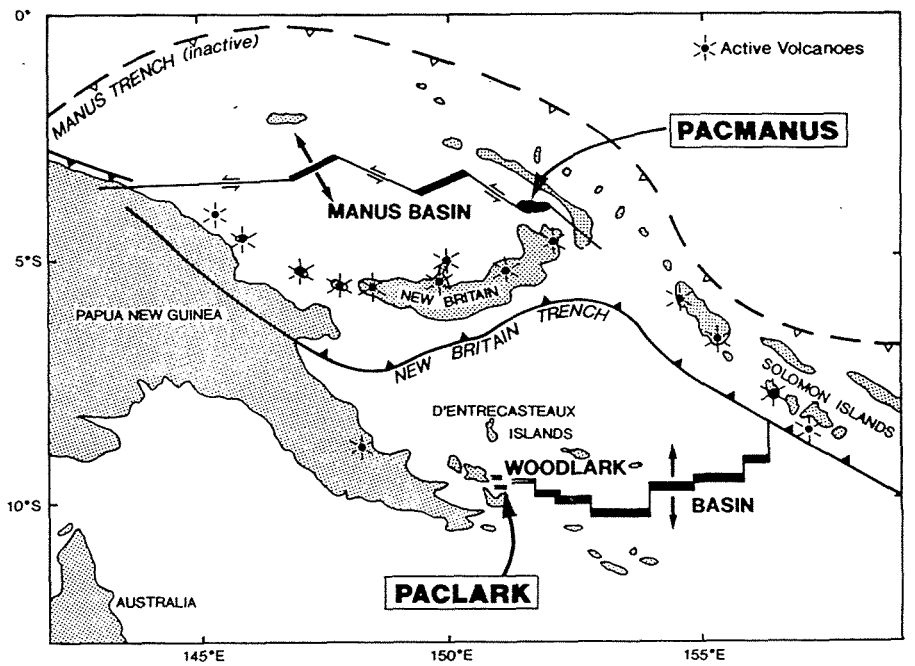

Figure 1. Location of PACLARK operations in the western Woodlark Basin and PACMANUS operations in the eastern Manus Basin, Papua New Guinea (Wheller et al., 1992). Extension occurs within a transpressional regime caused by the oblique convergence of the Pacific and Indo-Australian Plates.

Fe-Si-Mn Oxide and Baritic Gold Deposits of Western Woodlark Basin

Woodlark is a young oceanic basin that for the past 5 Myr has been propagating westward into the Cretaceous - Tertiary continental crust of Papua New Guinea (Benes et al., submitted). Ahead of the seafloor spreading, submarine volcanism ranging in composition from high-Mg andesite to mildly peralkaline rhyolite is emplaced on thinned continental crust. Hot springs occur in these same rocks on nearby islands but only weak indications of hydrothermal activity were found on the seafloor. However, near the western propagating tip of the seafloor spreading axis, complexly-shaped hydrothermal spires and mounds of Fe-Si-Mn oxide up to several meters thick and 100-200 meters in extent are widely distributed at 2143-2366 m depth on and near Franklin Seamount (Binns et al., 1993). Franklin is a young submarine basaltic andesite volcano with a pronounced collapsed summit caldera and with rare occurrences of sodic rhyolite. Some chimneys are venting a 20-30°C, mildly acid, base metal-containing clear fluid which is a mixture of sea water and a

270-350°C hydrothermal end-member. The composition of the end member fluid is similar to that of black smokers on mid-ocean ridges, but lacks reduced sulfur. Inactive gold-rich barite-silica chimneys with sparsely disseminated sulfides occur in the summit caldera and similar material may underlie Fe-Si-Mn deposits.

The yellow-orange to red-brown Fe-Si-Mn deposits consist mainly of a Si-bearing Fe-oxyhydroxide phase, much of it in the form of filaments of probable microbial origin. Bright green nontronite crystallized in internal patches and veinlets. The deposits contain anomalous As, Sb, and Hg. Rare earth element patterns and Sr isotope ratios confirm the importance of seawater components in their formation.

The baritic deposits are particularly rich in Ag (to 545 ppm) and Au (to 21 ppm), and contain significant Zn, Cu, and also Pb both as galena and rare cerussite (first seafloor discovery of this mineral). The silver occurs within disseminated pyrite spheroids and anhedra of colloidal origin, partly as submicron-sized Sb sulfosalt inclusions. The site of Au has not been determined. Fluid inclusions suggest formation from a fluid of moderate temperature (184-244°C) slightly more saline than sea water (3.4-5.8 wt % equiv. NaCl).

No massive sulfide deposits have been found, but vent fluid chemistry suggests that sulfide stockworks probably occur within the underlying volcanic pile. The Franklin Seamount occurrences confirm that seafloor hydrothermal activity may be associated with submarine volcanism where accretional spreading propagates into a continental margin environment, a setting that may have numerous ancient analogs. They support an exhalative origin for iron formations associated with ancient volcanic sequences, the chemistry of which may constitute a useful pathfinder to base metal and precious metal ores. The discovery of ore-grade Au and Ag in baritic chimneys at Franklin Seamount suggests targets for land-based exploration.

Polymetallic Sulfide Deposits of Eastern Manus Back-arc Basin

In eastern Manus Basin, where spreading is occurring in the arc itself in close proximity to continental rocks, a 60 km wide zone of subparallel volcanic ridges with intervening sediments occurs within a pull-apart basin between two transform faults (Taylor et al., 1991). The apparent neo-volcanic zone is a 30-km long, high standing, NE-SW striking, Y-shaped edifice, informally named Pual Ridge ("Pual" means "fork" in a local PNG dialect). Pual Ridge consists predominantly of dacite/rhyodacite with andesite and displays two prominent, 40 m high, dacite lava domes. Nearby ridges are built of basalt and andesite. The area was deemed to be prospective for polymetallic sulfides because of the presence of pronounced methane and Mn anomalies detected in the water column on earlier expeditions (Sakai, 1991).

In 1991, we found by deep-tow video on Pual Ridge a very large (800 x 350 m), actively forming, polymetallic sulfide deposit, named PACMANUS, along the flank and intervening valley of one of the lava domes at 1650-1675 m water depth (Binns and Scott, 1993). Another actively forming deposit of unknown size and hosted by altered andesite lies 10 km to the northeast and there are several inactive

hydrothermal deposits scattered along the ridge. All of these deposits lie within a hydrothermal field that extends discontinuously for about 2.5 km. Videos of the PACMANUS deposit show large spires and chimneys up to 4 m high, and mounds up to 100 m across. Fauna (crabs, clams, mussels, snails, shrimp, small fish, and some tube worms) are abundant in the hydrothermal areas. A cauldron in a basalt ridge, 23 km to the east of Pual, contains another small hydrothermal vent field.

Only two small samples from an active PACMANUS chimney were recovered. Their mineralogy is a high temperature assemblage of chalcopyrite, bornite, tennantite, sphalerite or wurtzite and anhydrite. The bornite and tennantite are silver rich. Gold values for the two samples are 2 and 10 ppm. Alteration of the dacite is primarily to white mica and displays 40% HREE depletion relative to LREE.

A pronounced methane and particulate plume was detected in the water column for at least 14 km to the northeast of the PACMANUS vent field. Zinc values of 130 to 8700 ppm in the sediments beneath the plume offer an insight into the primary dispersion pattern of lithogeochemical tracers for massive sulfide exploration on land.

The PACMANUS deposit and its surrounding volcanic rocks have close similarities to ancient massive sulfides of Archean to Phanerozoic age in Canada and Australia which make important contributions to the mineral wealth of these countries. Similarities to the Archean-age Millenbach massive sulfide deposit of Noranda, Quebec, are particularly impressive.

References

V. Benes, S.D. Scott and R.A. Binns (submitted) Tectonics of rift propagation into a continental margin: Western Woodlark Basin, Papua New Guinea: Jour. Geophys. Res.

R.A. Binns and S.D. Scott (1993) Actively-forming polymetallic sulfide deposits associated with felsic volcanic rocks in the eastern Manus Basin, Papua New Guinea: Econ. Geol., v. 88, in press.

R.A. Binns, S.D. Scott and 9 others (1993) Hydrothermal oxide and gold-rich sulfate deposits of Franklin Seamount, western Woodlark Basin, Papua New Guinea: Econ. Geol., v. 88, in press.

H.Sakai (1991) Expedition: East Manus Basin hydrothermal field, Hakuro-Maru cruise KH90-3, Leg 2, A brief summary report for SOPAC: SOPAC Cruise Report 138, 3 pp.

B. Taylor, K.A.W. Crook, J.M.Sinton and L. Petersen (1991) Manus Basin, Papua New Guinea, SeaMARC II sidescan sonar imagery and bathymetry: Pacific Seafloor Atlas, Hawaii Inst. Geophys., Honolulu, Sheets 4-6.

G. Wheller, R. Binns and S. Scott (1992) The PACMANUS/PACLARK program: Search for modern "Kuroko-type" analogues in the SW Pacific: InterRidge News, v. 1, no. 1, p. 7-9.

Current Research in Geology Applied to Ore Deposits.Fenoll Hach-Alí, Torres-Ruiz & Gervilla(eds)(1993).ISBN 84-338-1772-8

REE GEOCHEMISTRY OF THE BAIYINCHANG Cu-POLYMETALLIC OREFIELD, N.W. CHINA

Song, X.; Zhang, J. & Xu, Q.
Institute of Mineral Deposits, Chinese Academy of Geological Sciences, 26 Baianzhuang Road, Beijing 100037, China

ABSTRACT: Massive sulphide deposits of the Baiyinchang Orefield occur in a spilite-keratophyre series of the early Paleozoic Era.REE have been determined for rocks and associated ores from the orefield. REE parameters and REE patterns have been calculated and plotted. The results indicate that ores from the Zheyaoshan Cu-Zn deposit of the orefield have flat to slightly steep patterns with well-developed Eu anomalies similar to those for felsic rocks including quartz keratophyre, quartz keratophyre tuff and quartz albitite porphyre whereas ores from the Huoyanshan Cu-Zn deposit of the orefield have steeper,negative-sloping REE patterns(sometimes with positive Eu anomalies)similar to those for spilite and K-rich spilite. This suggests that the Zheyaoshan deposit and the Huoyanshan deposit are genetically related to felsic and alkaline-basic rocks,respectively. Sm/Nd ratios for all the rocks and ores from the orefield are analogical and lower than the Sm/Nd average for chondrites. This implicates that the rocks and ores in the orefield principally derived from the same crust-mantle mixed source.

INTRODUCTION

Research on REE as tracers during the formation and evolution of mineral deposits(Graf,1977;Whit-ford et al. 1988)and indicators of mineral exploration(Thurston,1981; Campbell et al.1982; Strong, 1984) and for ore genesis and petrogenesis(Cullers and Graf, 1984; Plimer et al. 1991; Song, 1991) increases and more and more new data of REE are published with advance and improvement of analytical methods and instruments.In order to reveal genesis of volcanic-hosted massive sulphide(VHMS) deposits in China,REE for rocks and ores from a few VHMS deposits in NW China have been determined. Their REE parameters and REE patterns have been calculated and plotted. This paper reflects partial results of the above-mentioned study and only deals with the Baiyinchang Cu-polymetallic Orefield, the largest VHMS orefield in China.

GEOLOGICAL SETTING AND ORE GEOLOGY

The Baiyinchang Cu-polymetallic Orefield consists of Zheyaoshan, and Huoyanshan Cu-Zn deposits, Tongchanggou Cu deposit, Xiaotieshan, Sigejuan, and Lapaigou Zn-Pb-Cu deposits. The orefield is situated in the eastern part of the Northern Qilian Mountains arc-volcanic rock belt belonging to a trench-arc-basis system of the early Paleozoic Era at the active continental margin of the Northern China Craton(L.Xia and Z.Xia,1991). The arc-volcanic rock belt is composed of continuous differential spilite-keratophyre sequence,including spilite,K-rich spilite,keratophyre, quartz keratophyre, tuff, tuff breccia and tufflava. A number of quartz albitite porphyre, and diabase intrusives occur in the volcanic rock sequence.

The dominant host rock of these deposits is quartz keratophyre tuff. In some parts of the orefield, orebodies can be found in metadiabase (e.g. at Huoyanshan). At Xiaotieshan,quartz albitite porphyre commonly occurs as bottem wall of Zn-Pb-Cu orebody. Most orebodies of the orefield are lenticular and bed-like. Length along strike of the biggest ore lens of the orefield is 600 m. Its thickness varies from 10 m to n.10 m. Down dip it can be traced over 300 m. The biggest bed-like orebody at Xiaotieshan has length of 1000 m and dip extension up to 500 m.

Ore structures are principally massive and disseminated, partly banded, rhythmic and net-veined, rarely brecciated. In addition, wrinkled structure and pressure shadow texture can be found in the orefield.

Principal ore minerals are pyrite,chalcopyrite,sphalerite and galena.Minor ore minerals are tetra-

hedrite, covelline, magnetite, pyrrhotite and arsenopyrite. Principal gangue minerals are quartz, sericite, clinochlore and carbonate minerals. Minor gangue minerals are barite and chloritoid.Proportion of these ore, and gangue minerals vary with different deposits.
Alterations, such as silification,sericitization,chloritization and carbonatization are well developed in the orefield.

REE PARAMETERS AND REE PATTERNS FOR ROCKS

Basic Rocks

Basic rocks from the Baiyinchang Orefield are characterized by enrichment in LREE (LREE/HREE>1). Of them, K-rich spilite(No.1) and spilite(No.2) have higher $\sum$REE (94.77-139.95 ppm), δ Eu (0.81-1.06), δ Ce(0.95-2.32) and Eu/$\sum$REE (0.009-0.017) values whereas metadiabase(No.3) has lower $\sum$REE (79.17 ppm), δ Eu(0.40) and Eu/$\sum$REE(0.008) values (Table 1). All of them have low Sm/Nd ratio, 0.21, 0.27 and 0.23, respectively.
K-rich spilite and spilite have steeper, negative-sloping REE patterns without Eu anomalies(Fig.1). But the metadiabase has well-developed Eu anomaly. This may be attributable to mobilization of Eu during alteration of the diabase.

Felsic Rocks

Quartz keratophyre(No.4) and quartz keratophyre(No.5) tuff in the Baiyinchang Orefield have lower $\sum$REE(18.76-61.15 ppm), very low δ Eu(0.11-0.31), and Sm/Nd(0.18-0.22) values, but they have higher δ Ce(0.93-1.09), and Y/$\sum$REE(0.20-0.21) values.The inaltered and unmineralized quartz albitite porphyre(No.6) as bottem wall of orebody at Xiaotieshan has higher $\sum$REE(110.44 ppm) and LREE/HREE (2.63) value, but lower δ Eu(0.61), and δ Ce(0.89) values(Table 1).
All felsic rocks from the orefield have flat REE patterns with negative Eu anomalies and their REE patterns are very similar.Of them,quartz keratophyre tuff,the dominant host rock of these deposits has very evident negative Eu anomaly(Fig.2).

REE PARAMETERS AND REE PATTERNS FOR ORES

Zheyaoshan Cu-Zn deposit

REE patterns for the three types of ore (No.11-13) from Zheyaoshan deposit are characterized by lower δ Eu(0.29-0.41), and Eu/$\sum$REE (0.003-0.004)values and are similar to those for quartz keratophyre tuff and quartz keratophyre from the same deposit.The massive pyrite ore(No.12)has evident enrichment in HREE (LREE/HREE=0.55), very low δ Ce (0.48) and very high Y/$\sum$REE (0.396) values and is quite different from other two types of ore.
REE patterns for the three types of ore from the Zheyaoshan deposit are slightly steep or flat with evident negative Eu anomalies and very similar to that for their host rock. However the massive pyrite ore (No.12) has negative Ce anomaly(δ Ce=0.48) and is different from other two ore types and their host rock(Fig.2).

Huoyanshan Cu-Zn deposit

REE parameters for ores from Huoyanshan are also listed in Table 1. Except for fine-grained bedded-massive pyrite ore(No.9), other selected ores(No.7,8,10) from the Huoyanshan deposit have very low $\sum$REE (2.657-6.701 ppm) and higher LREE/HREE (4.13-8.30) values. Their δ Eu, and δ Ce values are quite high and principally similar to those for the basic rocks in the orefield.
REE patterns for these ores from Huoyanshan are similar to those for the basic rocks of the orefield. However, the ores have much lower $\sum$REE values and steeper REE patterns (sometimes with positive Eu anomalies) than the basic rocks(Fig.1).

Table 1. REE parameters for rocks and ores of the Baiyinchang Orefield

No.	∑REE	LREE	HREE	LREE/HREE	δ Eu	δ Ce	Sm/Nd	Eu/∑REE	Y/∑REE
1	139.95	108.02	31.93	3.38	0.81	0.95	0.21	0.009	0.129
2	94.77	57.94	36.83	1.57	1.06	2.32	0.27	0.017	0.222
3	79.17	6.07	23.10	2.43	0.40	1.00	0.23	0.008	0.134
4	18.76	11.17	7.59	1.47	0.31	1.09	0.18	0.003	0.20
5	61.15	37.62	23.53	1.60	0.11	0.93	0.22	0.002	0.21
6	110.44	79.98	30.46	2.63	0.61	0.89	0.20	0.006	0.16
7	6.701	5.478	1.223	4.48	0.88	1.21	0.22	0.006	0.096
8	2.657	2.139	0.158	4.13	1.73	0.78	0.22	0.017	0.100
9	69.891	62.533	4.358	14.35	0.96	0.87	0.17	0.006	0.026
10	2.716	2.424	0.292	8.30	2.09	0.86	0.13	0.013	0.059
11	79.00	56.103	22.896	2.45	0.29	0.88	0.21	0.003	0.181
12	7.713	2.747	4.966	0.55	0.31	0.48	0.30	0.003	0.396
13	11.389	8.273	3.116	2.66	0.41	0.86	0.21	0.004	0.157

1-K-rich spilite;2-Spilite;3-Metadiabase; 4-Quartz keratophyre;5-Quartz keratophyre tuff; 6-Quartz albitite porphyre;7-Meso-coarse-grained rhythmic pyrite ore;8-Fine-grained rhythmic cupereous pyrite ore;9-Fine-grained bedded-massive pyrite ore; 10-Massive pyrite ore; 11-Densely disseminated pyrite ore;12-Massive pyrite ore;13-Massive cupereous pyrite ore

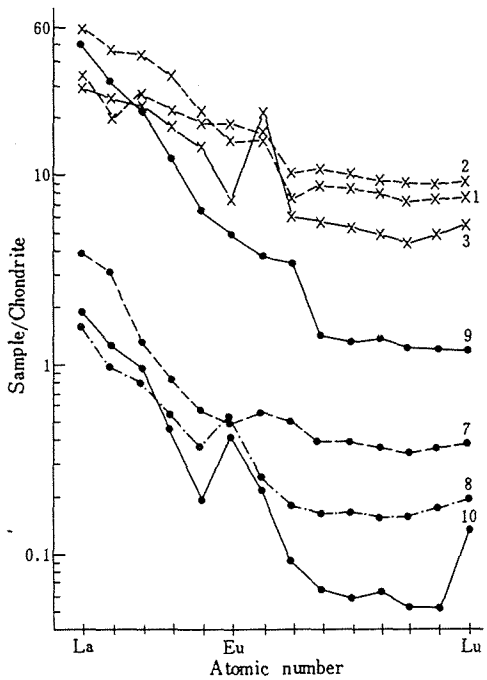

Fig. 1. Chondrite-normalized REE patterns for sulphide ores from Huoyanshan deposit and basic rocks from the Baiyinchang Orefield, NW China

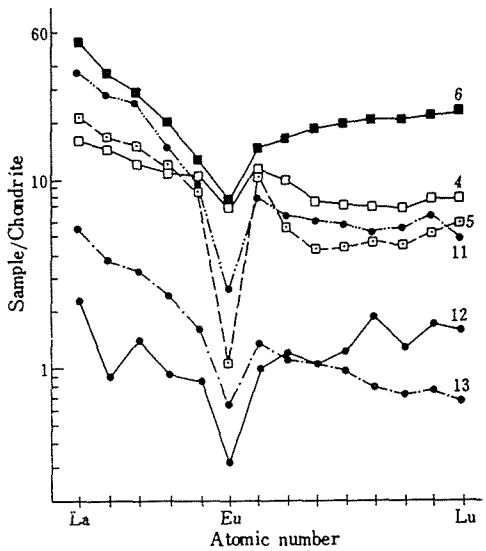

Fig. 2. Chondrite-normalized REE patterns for sulphide ores from Zheyaoshan deposit and felsic rocks from the Baiyinchang Orefield, NW China

CONCLUSIONS

All basic rocks, felsic rocks and associated ores from the Baiyinchang Orefield have enrichment in LREE and lower Sm/Nd (0.18–0.30) ratios than the Sm/Nd average (0.321) for chondrites calculated from Masuda et al.(1973). This implicates they have affinity and derived from a crust–mantle mixed source,but not a pure mantle source. REE patterns for ores from the Zheyaoshan Cu–Zn deposit are very similar to those for the felsic rocks in the Baiyinchang Orefield whereas REE patterns for ores from the Huoyanshan Cu–Zn deposit are similar to those for the basic rocks in the orefield. This suggests that the deposits in same orefield derived from different sources,i.e.the Zheyaoshan ores and the Huoyanshan ores derived from felsic rocks and basic rocks,respectively.The difference of rock source between the two deposits has been proved by the follwing geological observation i.e. some orebodies of the Huoyanshan deposit occur in the basic rocks. The negative Ce anomaly for the massive pyrite ore from Zheyaoshan indicates that there was some mixture of seawater in the ore-forming fluid. The basis for this conclusion is that the chondrite–normalized REE patterns for sea-water shows a large Ce depletion compared with the other rare earth elements(Humphris,1984).

Acknowledgements. This paper forms part of a research project funded by National Natural Science Foundation of China. We grateful to Ms. Xinyu WU for performing ICP–MS analyses.

REFERENCES

Campbell,I.H.,Coad,P.,Franklin,J.M.,Gorton,M.P.,Scott,S.D.,Sowa,J.,Thurston,P.C. 1982. Rare earth elements in volcanic rocks associated with Cu–Zn massive sulphide mineralization:a preliminary report. Cana. J. Earth Sci. 19:619–623

Cullers,R.L. & Graf,J.L. 1984.Rare earth elements in igneous rocks of the continental crust:intermediate and silicic rocks–ore petrogenesis.In:Henderson,P.(ed) Rare earth element geochemistry. Elsevier, Amsterdam, pp.275–316

Grafr,J.L. 1977. Rare earth elements as hydrothermal tracers during the formation of massive sulphide deposits in volcanic rocks. Econ. Geol. 72:527–54

Humphris,S.E. 1984. The mobility of the rare earth elements in the crust.In: Henderson,P.(ed) Rare earth element geochemistry. Elsevier, Amsterdam, pp. 317–342

Jiang,X. & Cong, G. 1989. Petrogenesis of spilite–keratophyre series in Baiyinchang district. J. Changchun Uni. Earth Sci. 19:157–164(in Chinese)

Masuda,A., Nakamura,N.,Tamaka,T. 1973. Fine structures of multually normalized rare–earth patterns of chondrites. Geochim. Cosmchim. Acta 37:239–248

Plimer, I.R.,Lu, J.,Kleeman, J.D. 1991. Trace and rare earth elements in cassiterite— sources of components for the tin deposit of the Mole granite, Australia. Mineral. Deposita. 26:267–724

Song,X. 1991. Geochemical characteristics of volcanogenic massive sulphide deposits in China. In: Pagel,M. & Leroy, J.L.(eds) Source, transport and deposition of metals. A.A.Balkema,Rotterdam, pp.367–370

Strong, D.F. 1984.Rare earth elements in volcanic rocks of the Buchans area,Newfoundland.Cana. J. Earth Sci. 21:757–780

Thurston,P.C. 1981.Economic evaluation of Archean volcanic rocks using REE geochemistry.Geol. Society of Australia, Special Publication 7 pp.435–490

Whitford,D.J., Korsch,M.J.,Porritt,P.M.,Craven,S.J. 1988. Rare earth element mobility around the volcanogenic polymetallic massive sulphide deposit at Que River,Tasmania,Australia. Chem.Geol. 68:105–119

Xia,L. & Xia, Z. 1991. Marine volcanic rocks from Qilian and Qinling Mountains. China Uni. Geosciences Press, Wuhan (in Chinese)

Current Research in Geology Applied to Ore Deposits.Fenoll Hach-Alí, Torres-Ruiz & Gervilla(eds)(1993).ISBN 84-338-1772-8

HYDROTHERMAL ALTERATION RELATED TO THE "MASA VALVERDE" MASSIVE SULPHIDE DEPOSIT, IBERIAN PYRITE BELT, SPAIN

Toscano, M. (1); Ruiz de Almodóvar, G. (1); Pascual, E. (2) & Sáez, R. (1)

(1) Dept. Cristalografía y Mineralogía, Facultad de Ciencias, Universidad de Sevilla, 21819 La Rábida, Huelva, Spain

(2) Dept. Geología y Minería, Facultad de Ciencias, Universidad de Sevilla, 21819 La Rábida, Huelva, Spain

ABSTRACT: Footwall alteration related to the Masa Valverde orebody consists of an inner chloritic zone with Fe-chlorite + siderite + Ba-muscovite surrounded by a sericitic one in which Ba-K-Na micas occur. A stockwork mineralization, made of pyrite and minor base metal sulphides is associated to both described zones. Hydrothermal fluids, with significant participation of CO_2, cause a Fe(Mg) metasomatism in inner zones with extreme leaching of Na and lesser complete loss of K, and substantial loss of LREE and Eu as alteration progresses. This model differs from current ones for IPB, such as for Riotinto.

INTRODUCTION

The Iberian Pyirite Belt (IPB) is a major metallogenic province, generally characterized by massive sulphide deposits. These ore deposits, show important variations in metallic contents, relative positions of sulfide masses and feeder areas or type and mineralization of associated stockworks (Ruiz de Almodóvar & Sáez, 1992).

The best known regional reference model is related to the Riotinto ores, characterized by a Cu-rich stockwork with an inner alteration zone made of quartz + Mg-chlorite + pyrite and two phases of sericitic alteration (García Palomero, 1980). However, other mineralizations, such as Salgadinho (Plimer & Carvalho, 1982) can differ in features so substantial as the absence of massive sulphide and geometry, mineralogy and geochemistry of the alteration zone.

The Masa Valverde, recently discovered by E.N. Adaro, exhibit alteration peculiarities similar to those founds in Salgadinho, but contrarily to this one, consists of a massive sulphide deposit underlain by an stockwork zone. In this note we show preliminary mineralogical and geochemical results which denote some of the peculiarities of the Masa Valverde orebody, some of which could be potentially useful as metallogenetic indicators at a regional scale.

REGIONAL GEOLOGY

The lithostratigraphic column of the Iberian Pyrite Belt is divided after Schermerhorn (1971) in three main units: The PQ Group (Upper Devonian), composed by slates and sandstones with some limestone lenses near the top of the sequence; the Volcano-Sedimentary Complex (VSC), made of felsic and mafic volcanics interbedded in a lower Carboniferous detritic sequence including massive sulfide deposits associated to felsic volcanic rocks and the Culm Group, composed by turbiditic sucesions of slate and sandstones of midle Carboniferous age, which represents the top of the stratigraphic sequence. All these rocks were folded and metamorphosed under low-grade conditions (Munhà, 1983) during the hercynian orogeny.

The Masa Valverde mineralization is located under the Culm sequence and there is not direct geological information. The mineralized horizon outcrops in the southern flank of the Valverde del Camino Anticline, 1.5 Km to the north of the drilled area, where is represented by several small mineralizations of polymetallic complex ore and/or pyrite (Cibeles, Cruz Infante, Campanario, Descamisada). The footwall rocks in the Masa Valverde and related mineralization consist of felsic tuffs and tuffites related to the first local volcanic episode (Fig. 1). The rocks appear strongly altered, making difficult to identify original texture and composition in many instances. In spite of this

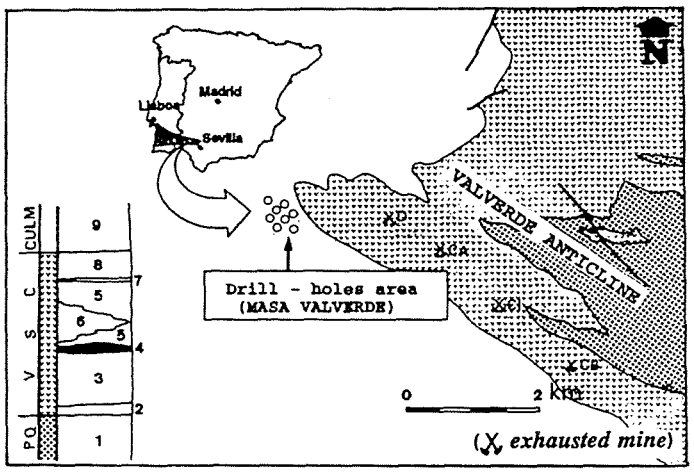

Fig. 1. Geological map and stratigrafic sequence of Valverde area. 1.- Slates and sandstones. 2.- Mafic sill. 3.- Felsic tuffs and tuffites. 4.- Massive sulphides. 5.- Pyro- and epiclastic felsic tuffites and tuffs. 6.- Mafic flows and breccias. 7.- Purple slates. 8.- Felsic epiclastites. 9.- Slates and sandstones.

difficulty it is possible to recognize lateral facies changes between fine tuffite material, crystal tuffs and vitric tuffs interbedded with epiclastic sandstones.

The hanging-wall sequence in the Masa Valverde area comprises gray-brown slates, well-bedded felsic tuffs, purple slates and a epiclastic sequence transitional to the Culm group.

The original stratigraphic sequence is complicated by folding, faulting and local sedimentary recurrences whose geometry is impossible to establish with the available drill core information.

HYDROTHERMAL ALTERATION

Hydrothermal alteration underlies the massive sulphide deposit below the deepest studied drill cores, which in turn reach 170 m. below the ore masses. This alteration produces several mineral assemblages which change continuously in space: quartz + sericite ± pyrite, quartz + chlorite + sericite ± pyrite ± sphalerite ± galena and Fe-chlorite + carbonates ± quartz ± sericite ± pyrite ± chalcopyrite. This diversity indicates several mineralogical processes to operate during alteration, which are difficult to distinguish in time and space and are all related to sulphide genesis. However, the first of the assemblages described predominates in the peripheral zones of the hydrothermal system, whereas Fe-chlorite + carbonate-rich alteration products are dominants in the inner parts.

Alteration increase towards the inner zones in the system, in which chloritization predominates, the lateral and vertical distribution of alteration types is *grosso modo* controlled by the previous bulk composition of country rocks.

Mineralogy

Sericites are commonly muscovites, although some of them have very low K/Na ratios corresponding to paragonites. Except these latter, all sericites studied have high Ba contents with atomic K/Ba substitutions ranging from 0.05 to 0.23 (fig. 2). Phengite content is invariably low, atomic Fe+Mg ranging from 0.11 to 0.55 for 22 oxygens. Other chemical changes, such as in Fe/Fe+Mg ratios, also appear to be related to Ba abundance in sericite.

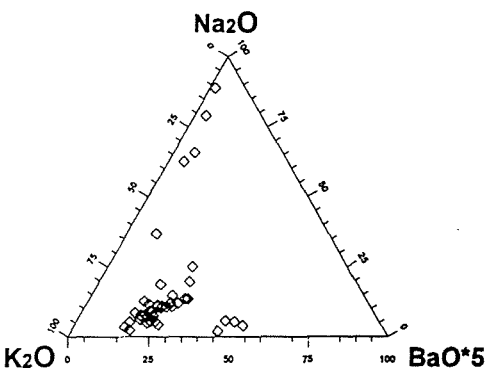

Fig. 2. EMP sericite compositions.

Chlorites include both triochtahedral and diochtahedral subgroups. Triochtahedral chlorites are by far the commonests. According to the classification by Hey (fig.3), they are ripidolites with Fe/Fe+Mg ratios ranging from 0.6 to 0.85, which decrease with depth. Chlorite geothermometry (Walshe, 1986; Tornos, 1990) yields a temperature interval from 217 to 248 ºC for chlorite crystallization. Diochtahedral chlorites exist only in places, are Al-rich and can be classified as donbassites. They are apparently unrelated to the massive sulphide deposit formation.

Carbonates are siderites with low contents in Mg, Mn and Ca. Siderites paragenetic with ripidolites have Fe/Fe+Mg ratios ranging from 0.80 to 0.97 with a variation trend similar to that found for chlorites. Carbonatization affecting especially to a zone comprised between 30 and 60 m below the massive sulphide footwall.

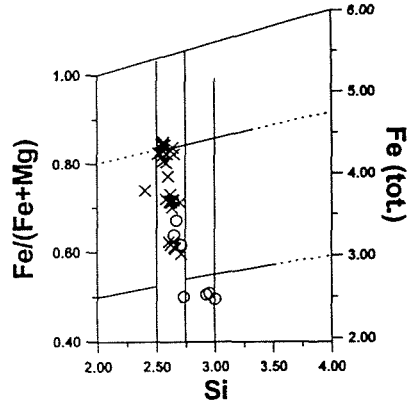

Fig. 3. EMP triochtaedral Chlorite compositions in Hey's diagram. Crosses: Masa Valverde footwall chlorites. Circles: Riotinto stocwork chlorites.

Most of sulphides occurring in the stockwork zone are pyrite, with minor chalcopyrite, sphalerite and galena. Pyrrothite appears as inclusion in pyrite. Other more scarce accesory ore phases are boulangerite, fahlore and arsenopyrite.

Geochemistry

The most conspicuous chemical changes produced during hydrothermal alteration are concentration of Fe and Mg in the inner zones of the system and extreme leaching of sodium. Although potassium moves also towards the outer zones, it is not completely leached from the inner zones.

All alterated rocks have high Ba contents (0.2-2.5 % Ba), which are greater than those found in other rocks with chloritic alteration in the IPB (fig. 4). Barium concentration is more evident in sericitized samples, in which Ba is concentrated with regard to potassium.

REE behaviour is characterized by LREE mobility, with a marked La depletion related to chloritization. Some chlorite-rich samples, however, are among the richest in La, which could be related to a previous concentration of LREE in accesory minerals such as zircon. Selective depletion in Eu related to chloritization is also shown, especially if Eu/Eu* values are correlated with mobile/immobile elemental ratios (*e.g.*, Mg/Ti).

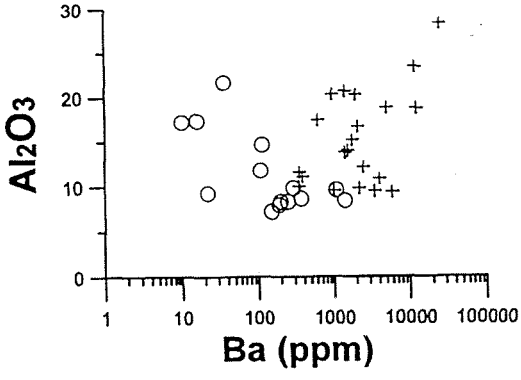

Fig. 4. Al_2O_3 vs Ba variation diagram for altered rocks of Masa Valverde (+) and other chloritic altered rocks of IPB (o) (partially after Bernard, *et al.*,1982) .

CONCLUSIONS

Footwall alteration in the Masa Valverde orebody differs from current alteration models in the IPB both in mineralogy and chemistry. The inner chloritic zone is characterized by Fe-chlorite and siderite, and neoformation of Ba-muscovites occur together with a moderate, non-intensive potassium leaching. This is in contrast with other models, such as those for Riotinto, in which the inner alteration zone is characterized by Mg-chlorite crystallization and an extreme leaching of alkalies, Ba and Ca. Temperature ranges obtained for Valverde (217-248 ºC) are well within previously obtained temperature intervals deduced by stable isotope analysis (Munhà *et al.*, 1986). Therefore, alteration processes should be controlled by other factors, apart from temperature.

Mineralogic and geochemical features found in Valverde are more similar to the Salgadinho stockwork, which is also hidden. Topographic restriction of siderite between 30 and 60 m below the massive sulphide lens suggests that CO_2-rich fluids had an important role, which could be related to mixing/unmixing of CO_2- and H_2O-rich fluids that would control carbonate precipitation.

It is possible that an innest Mg-chlorite alteration zone in Valverde could not have been cut by drilling, in which case further mineralogical and chemical studies could be used as prospection tools of a Cu-rich stockwork. These studies would be based on the above referred role of CO_2-rich fluids and should relate it in a more precise way to the observed geochemical behaviour of Ba, Mg (and Fe-Mg partition between chlorite and carbonates), LREE (mobilized as carbonate complexes?) and Eu, all which are shown to be related to progressive hydrothermal alteration in a qualitative form.

ACKNOWLEDGMENTS

This research has been possible by facilities given by E.N. Adaro, especially by staff members Dr. Jesús Ramírez Copeiro del Villar and Mr. Sebastián Maroto. Financial support has been obtained from CYCIT project PB 87-0931 and 4076 Investigation Group of Andalusian Regional Governement.

REFERENCES

Bernard, A.J., Dagallier, G. & Soler, E. 1982. The exhalative sediments linked to the volcanic exhalative massive sulphide deposits: a case study of European occurrences. In: G.C. Amstutz, A. El Goresy, G. Frenzel, C. Klutz, G. Moh, A. Wauschkuhn & R.A. Zimmermann (eds.) Ore Genesis: the state of the art. Springer Verlag, Berlin, pp. 553-562.

García Palomero, F. 1980. Caracteres geológicos y relaciones morfológicas y genéticas de los yacimientos del Anticlinal de Riotinto. Excma. Diputación Provincial de Huelva

Munhà, J. 1983. Low-grade regional metamorphism in the Iberian Pyrite Belt. Com. Serv. Geol. Port. 29:3-35

Munhà, J., Barriga, F. & Kerrich, R. 1986. High ^{18}O ore-forming fluids in volcanic-hosted base metal massive sulphide deposits: Geologic, $^{18}O/^{16}O$, and D/H evidence from the Iberian Pyrite Belt; Cradon, Wisconsin; and Blue Hill, Maine. Econ. Geol. 81:530-552

Plimer, I.R. & Carvalho, D. 1982. The geochemistry of hydrothermal alteration at the Salgadinho copper deposit, Portugal. Mineral. Deposita. 17:193-211

Ruiz de Almodóvar, G. & Sáez, R. 1992. Yacimientos de sulfuros masivos de la Faja Pirítica Suribérica. In: García Guinea J., Martínez Frías, J. (eds.) Recursos Minerales de España. C.S.I.C. pp 1309-1324

Schermerhorn, L.J.G. 1971. An outline stratigraphy of the Iberian Pyrite Belt. Bol. Geol. Min. 82-84:239-268

Tornos, F. 1990. Los skarns y mineralizaciones asociadas del Sistema Central español. Tesis doctoral, edit. Universidad Complutense, Madrid.

Walshe, J.L. 1986. A six-component chlorite solid solution model and the conditions of chlorite formation in hidrothermal and geothermal systems. Econ. Geol. 81:681-703.

Current Research in Geology Applied to Ore Deposits.Fenoll Hach-Alí, Torres-Ruiz & Gervilla(eds)(1993).ISBN 84-338-1772-8

THEORETICAL CALCULATION OF THE SOLUBILITY OF MONAZITE IN HYDROTHERMAL SOLUTIONS: APPLICATIONS TO REE MOBILITY DURING MASSIVE SULPHIDE FORMATION

Wood, S.A. (1) & Williams-Jones, A.E. (2)

(1) Dept. Geology and Geological Engineering, University of Idaho, Moscow, ID, 83843, U.S.A.

(2) Dept. Earth and Planetary Sciences, McGill University, Montreal, Quebec, H3A 2A7, Canada

ABSTRACT: We have used published thermodynamic data for monazite and aqueous REE species to calculate the solubility of monazite up to 300°C in hydrothermal solutions with compositions derived from data on seafloor hydrothermal vents. Based on these data, we find that chloride and hydroxide REE complexes, as well as the simple REE ions, are the most important REE-transporting species in massive sulfide-forming fluids. Our calculated values of La, Ce and Nd concentrations in equilibrium with monazite are in good agreement with those actually measured in seafloor hydrothermal vent fluids, suggesting that monazite, which has been identified in alteration zones of ancient massive sulfide deposits, may control REE concentrations in such fluids. However, better analytical data for phosphate and fluoride in seafloor vent fluids and accurate experimental data on REE complexation at high temperatures are required in order to verify this conclusion.

INTRODUCTION

A number of authors have concluded that the REE were mobile during the formation of massive sulfide ores (Graf, 1977; Baker and DeGroot, 1983; Campbell et al., 1984; MacLean, 1988; Dergachev et al., 1989). Measurements on modern seafloor hydrothermal vent fluids, thought to represent analogues of ancient massive sulfide-forming fluids, show that the REE content of the former is enriched by 10 to more than 1000 times ambient seawater (Michard et al., 1983; Piepgras and Wasserburg, 1985; Michard and Albarède, 1986; Campbell et al., 1988a). Hydrothermal monazite has been reported from the alteration zones of ancient exhalative massive sulfide deposits (Dergachev et al., 1989; Schandl and Gorton, 1991). The possibility therefore exists that monazite solubility plays a role in controlling REE contents of both modern seafloor hydrothermal vent fluids and ancient massive sulfide-forming fluids. We therefore have carried out calculations of monazite solubility to place constraints on the mobility of the light REE in such hydrothermal systems. We have performed these calculations for a temperature of 300°C and the pressure of saturated vapor, using thermodynamic data from a variety of published sources.

METHODOLOGY

We obtained the thermodynamic properties (ΔG_f, C_p, ΔH_f) of end member (La, Ce, Nd) monazites from the comprehensive review of Vieillard and Tardy (1984). However, we estimated S_{298} values for these phases from the entropies of the component oxides given in Robie et al. (1978), using the relation:

$$S_{298}(LnPO_4) = 1/2[S_{298}(Ln_2O_3) + S_{298}(P_2O_5)].$$

Molar volume data were calculated from lattice parameters for natural monazite given by Nriagu (1984). The activities of the solids were assumed to be unity in the initial calculations owing to a lack of knowledge of activity relations in monazite.

The thermodynamic properties of the simple aqueous REE ions were obtained using data and equations from Shock and Helgeson (1988) and Tanger and Helgeson (1988), with two exceptions. The standard partial molal entropies were taken from David (1986) to maintain consistency with the calculations of Wood (1990). The free energies of formation of the simple aqueous ions at 298 K were those of Vieillard and Tardy (1984). Stability constants for REE complexes were those estimated by Wood (1990). Thermodynamic properties of the aqueous phosphate species (PO_4^{3-}, HPO_4^{2-}, etc.) were calculated using the computer code, SUPCRT92 (Johnson et al., 1992). Those of all other aqueous species, except as otherwise noted later in the text, were also calculated using SUPCRT92. Free energy data

for water were taken from Helgeson and Kirkham (1974).

The extended Debye-Hückel equation of Helgeson (1969) and parameters given in Henley (1984), with the exception of å for REE species, which we set to 6.0 Å, were used to calculate activity coefficients for the various charged species. We assumed the activity coefficient of neutral species to be unity (cf. Helgeson, 1969).

We have employed published data for modern seafloor vent fluids (Michard et al., 1984; von Damm et al., 1985; von Damm and Bischoff, 1987; Bowers et al., 1988; Campbell et al. 1988a,b; Massoth et al., 1989) to guide our selection of the physicochemical parameters of ancient massive sulfide ore-depositing systems. We have employed a representative fluid composition (Table 1) for our initial monazite solubility calculations. We then explored the effect of varying several key parameters in turn.

TABLE 1: Representative physicochemical properties of seafloor hydrothermal vent fluids.

ΣNa	0.56 molal
ΣCl	0.60 molal
ΣPO_4	3×10^{-7} molal
ΣCa	3.7×10^{-2} molal
T	300°C
P	84 bars (SVP)
pH_{300}	4.5

In our model we have employed a temperature of 300°C, the highest temperature for which predictions of stability constants for REE - complexes are likely to be reliable (Wood, 1990), and pressure was, of necessity, assumed to be that of saturated vapor, as data are not available for the partial molar volumes of most of the relevant REE complexes. We make the standard assumption that the concentrations of sulfate and magnesium are effectively zero in the endmember vent fluid (Edmond et al., 1979; Michard et al., 1984; von Damm and Bischoff, 1987; Massoth et al., 1989; Campbell et al., 1988a,b). The pH and other compositional parameters were varied within the ranges for vent fluids associated with sediment-starved systems reported in the literature.

Monazite solubility was calculated by solving the relevant mass balance and mass action equations for the system using an algorithm modified from Crerar (1975). An iterative procedure was applied to incorporate activity coefficients. Our model includes only the major ions normally present in seawater hydrothermal vent fluids (Na^+, Ca^{2+}, Cl^-), and the REE and phosphate, which are required to calculate monazite solubility. Owing to a lack of knowledge of the temperature dependence of their thermodynamic properties, we have omitted REE-phosphate complexes. The data of Edmond et al. (1979) from some hotsprings from the Galapagos Spreading Center suggest that F^- concentrations in the hydrothermal endmember vent fluid are no higher than 10^{-5} M, and that F^- may be completely removed before the fluid is debauched onto the seafloor. To our knowledge, F^- concentrations have not been reported for any other vent system. We therefore do not consider REE-fluoride complexes in our model.

RESULTS

Under the conditions shown in Table 1, $LnOH^{2+}$ is the predominant species of La, Ce and Nd in solution. For Ce and Nd, the simple Ln^{3+} ion is next in importance, followed by the $LnCl^{2+}$ complex. In the case of La, the simple ion and the hydroxide and chloride complexes are approximately subequal in concentration. With a decrease in pH, the $LnOH^{2+}$ complex becomes relatively less important, but the concentrations of $LnCl^{2+}$ and Ln^{3+} relative to each other don't change. As expected, $LnOH^{2+}$ becomes more important with an increase of pH above 4.5. An increase in ΣCa above that shown in Table 1 results in a slight decrease in the importance of the chloride complex owing to Ca-chloride ion-pairing. An increase or decrease in ΣCl has little effect on the speciation as long as the change in Cl is matched by a change in ΣNa or ΣCa.

The solubility of each of the REE under the conditions shown in Table 1 is ΣCe = 0.2 μg/L, ΣLa = 0.3 μg/L and ΣNd = 0.1 μg/L. Concentrations measured in seafloor hydrothermal vent fluids are: ΣNd = 0.02-0.336 μg/L (East Pacific Rise;

Piepgras and Wasserburg, 1985), ΣCe = 0.2-1.9 μg/L and ΣNd = 0.1-1.1 μg/L (East Pacific Rise; Michard and Albarède, 1986) and ΣLa = 125-375 μg/L (Mid-Atlantic Ridge; Campbell et al., 1988a). The calculated solubilities are in good agreement with the measured values in some cases, but considerably lower in other cases. The solubility is strongly dependent on pH and at the lower pH of 3.5, we obtain ΣCe = 13 μg/L, ΣLa = 33 μg/L and ΣNd = 5 μg/L. Furthermore, there are several reasons to expect that the calculated monazite solubility represents a minimum estimate. First, the temperature of seafloor hydrothermal vents can reach 400°C, and it is reasonable to expect that the solubility will increase with increased temperature owing to increased REE complexation. Second, we have no data for higher REE-Cl and -OH complexes (e.g., $Ln(OH)_2^+$ and $LnCl_2^+$) or REE-phosphate complexes at high temperatures; these complexes may increase the solubility of monazite in hydrothermal solutions. Finally, although we have neglected fluoride complexes owing to a lack of knowledge of fluoride concentrations, even small amounts of this ligand could greatly increase monazite solubility as a result of the great stability of REE-fluoride complexes at elevated temperatures (Wood, 1990). We therefore conclude that seafloor hydrothermal vent fluids, and by analogy, ancient massive sulfide-forming fluids, are close to saturation with respect to monazite. These calculations can be further improved upon the arrival of more precise data on phosphate and fluoride concentrations in natural hydrothermal solutions and experimentally-derived data for REE complexes at elevated temperatures.

REFERENCES

Baker, J.H. and de Groot, P.A., 1983. Proterozoic seawater-felsic volcanics interaction W. Bergslagen, Sweden. Evidence for high REE mobility and implications for 1.8 Ga seawater compositions. Contrib. Mineral. Petrol., 82: 119-130.

Bowers, T.S., Campbell, A.C., Measures, C.I., Spivack, A.J., Khadem, M. and Edmond, J.M., 1988. Chemical controls on the composition of vent fluids at 13°-11°N and 21°N, East Pacific Rise. J. Geophys. Res., 93: 4522-4536.

Campbell, A.C., Palmer, M.R., Klinkhammer, G.P., Bowers, T.S., Edmond, J.M., Lawrence, J.R., Casey, J.F., Thompson, G., Humphris, S., Rona, P., and Karson, J.A., 1988a. Chemistry of hot springs on the mid-Atlantic Ridge. Nature, 335: 514-518.

Campbell, A.C., Bowers, T.S., Measures, C.I., Falkner, K.K., Khadem, M., and Edmond, J.M., 1988b. A time series of vent fluid compositions from 21°N, East Pacific Rise (1979, 1981, 1985), and the Guaymas Basin, Gulf of California (1982, 1985). J. Geophys. Res., 93: 4537-4549.

Campbell, I.H., Lesher, C.M., Coad, P., Franklyn, J.M., Gorton, M.P. and Thurston, P.C., 1984. Rare earth element mobility in alteration pipes below massive Cu-Zn-sulfide deposits. Chem. Geol., 45: 181-202.

Crerar, D.A., 1975. A method for computing multi-component chemical equilibria based on equilibrium constants. Geochim. Cosmochim. Acta, 39: 1375-1384.

David, F., 1986. Thermodynamic properties of lanthanide and actinide ions in aqeuous solution. J. Less-Comm. Met., 121: 27-42.

Dergachev, A.L., Sergeyeva, N.Y., and Dergacheva, A.A., 1989. Possibility of rare earth mineral formation during hydrothermal sedimentary massive sulfide deposition. Dokl. Akad. Nauk. SSR, 304: 1213-1217.

Edmond, J.M., Measures, C.I., McDuff, R.E., Chan, L.H., Collier, R., Grant, B., Gordon, L.I., and Corliss, J.B., 1979. Ridge crest hydrothermal activity and the balances of the major and minor elements in the ocean: The Galapagos data. Earth Planet. Sci. Let., 46: 1-18.

Graf, J.L., Jr., 1977. Rare earth elements as hydrothermal tracers during the formation of massive sulfide deposits in volcanic rocks. Econ. Geol., 72: 527-548.

Helgeson, H.C., 1969. Thermodynamics of hydrothermal systems at elevated temperatures and pressures. Am. J. Sci., 267: 729-804.

Helgeson, H.C. and Kirkham, D.H., 1974. Theoretical prediction of the thermodynamic behavior of aqueous electrolytes at high pressures and temperatures. I. Summary of the thermodynamic/electrostatic properties of the solvent. Am. J. Sci., 274: 1089-1198.

Henley, R.W., Truesdell, A.H. and Barton, P.B., Jr., 1984. Fluid-mineral equilibria in hydrothermal systems. Rev. Econ. Geol., 1: 267 p.

Johnson, J.W, Oelkers, E.H. and Helgeson, H.C., 1992. SUPCRT92: A software package for calculating the standard molal thermodynamic properties of minerals, gases, aqueous species and reactions from 1 to 5000 bars and 0° to 1000°C.

MacLean, W.H., 1988. Rare earth mobility at constant inter-REE ratios in the alteration zone at the Phelps Dodge Massive Sulfide Deposit, Mattagami, Quebec. Mineral. Deposita, 23: 231-238.

Massoth, G.J., Butterfield, D.A., Lupton, J.E., McDuff, R.E., Lilley, M.D., and Jonasson, I.R., 1989. Submarine venting of phase-separated hydrothermal fluids at Axial Volcano, Juan de Fuca Ridge. Nature, 340: 702-705.

Michard, A., Albarède, F., Michard, G., Minster, J.F., and Charlou, J.L., 1983. Rare earth elements and uranium in high-temperature solutions from East Pacific Rise hydrothermal vent fluid (13°N). Nature, 303: 795-797.

Michard, G., Albarède, F., Michard, A., Minster, J.-F., Charlou, J.-L., and Tan, N., 1984. Chemistry of solutions from the 13°N East Pacific Rise hydrothermal site. Earth Planet. Sci. Let., 67: 297-307.

Michard, A. and Albarède, F., 1986. The REE content of some hydrothermal fluids. Chem. Geol., 55: 51-60.

Nriagu, J.O., 1984. Phosphate minerals: Their properties and general modes of occurrence. In Nriagu, J.O. and Moore, P.B., eds., Phosphate Minerals, Springer-Verlag, New York, 1-136.

Piepgras, D.J. and Wasserburg, G.J., 1985. Strontium and neodymium isotopes in hot springs on the East Pacific Rise and Guaymas Basin. Earth Planet. Sci. Let., 72: 341-356.

Robie, R.A., Hemingway, B.S. and Fisher, J.R., 1978. Thermodynamic properties of minerals and related substances at 298.15 K and 1 bar (10^5 Pascals) pressure and at higher temperatures. U.S. Geol. Surv. Bull., 1452: 456 p.

Schandl, E.S. and Gorton, M.P., 1991. Postore mobilization of rare earth elements at Kidd Creek and other Archean massive sulfide deposits. Econ. Geol., 86: 1546-1553.

Shock, E.L. and Helgeson, H.C., 1988. Calculation of the thermodynamic and transport properties of aqueous species at high pressures and temperatures: correlation algorithms for ionic species and equation of state predictions to 5 kb and 1000°C. Geochim. Cosmochim. Acta, 52: 2009-2036.

Tanger, J.C., IV, and Helgeson, H.C., 1988. Calculation of the thermodynamic and transport properties of aqueous species at high pressures and temperatures: Revised equation of state for the standard partial molal properties of ions and electrolytes. Amer. J. Sci., 288: 19-98.

Vieillard, P. and Tardy, Y., 1984. Thermochemical properties of phosphates. In Nriagu, J.O. and Moore, P.B., eds., Phosphate Minerals, Springer-Verlag, New York, 171-198.

Von Damm, K.L., Edmond, J.M., Grant, B., Measures, C.I., Walden, B., and Weiss, R.F., 1985. Chemistry of submarine hydrothermal solutions at 21°N, East Pacific Rise. Geochim. Cosmochim. Acta, 49: 2197-2220.

Von Damm, K.L. and Bischoff, J.L., 1987. Chemistry of hydrothermal solutions from the southern Juan de Fuca Ridge. J. Geophys. Res., 92: 11334-11346.

Wood, S.A., 1990. The aqueous geochemistry of the rare earth elements and yttrium. Part II. Theoretical predictions of speciation in hydrothermal solutions to 350°C at saturated water vapor pressure. Chem. Geol., 88: 99-125.

3 Gold and other precious metals

Current Research in Geology Applied to Ore Deposits. Fenoll Hach-Alí, Torres-Ruiz & Gervilla (eds) (1993). ISBN 84-338-1772-8

PRECIOUS METAL DISTRIBUTION IN THE AKOLUK EPITHERMAL SYSTEM, N.E. TURKEY

Agdemir, N. (1); Lehmann, B. (1) Sönmez Sayili, I. (2) & Türkmen, H. (3)

(1) Inst. für Mineralogie und Mineralische Rohstoffe, Technische Universität Clausthal, Adolph-Roemer-Str. 2a, 3392 Clausthal-Zellerfeld, Germany

(2) Ankara Üniversitesi, Fen Fakültesi, Besevler., Turkey

(3) Maden Tetkik ve Arama Genel Müdürlügü, Ankara/Turkey

Abstract: Akoluk is an epithermal system in which precious metals (Au and Ag), Sb, As, Pb, Zn, Cu and Ba are enriched.

An investigation of precious metal contents in core samples defines three populations for gold with specific maxima: (1) regional background in dacitic tuff (5 ppb Au), (2) argillic altered dacitic tuff (220 ppb Au), and (3) barite veinlets (4000 ppb); and four populations for silver: (1) regional background (1 ppm Ag), (2) argillic altered dacitic tuff (10 ppm Ag), (3) barite veinlets without a silver mineral phase (56 ppm Ag), and (4) barite veinlets with a silver mineral phase (290 ppm Ag).

Gold occurs as "invisible gold" in pyrite and native gold; silver occurs in sulfides, native silver, and pyrargyrite.

Boiling and change of redox state are probably important processes for precious metal deposition in the Akoluk epithermal system.

Introduction and Geological Setting

Exploration activity on epithermal precious-metal systems in Turkey has begun extensively in the last ten years. There are some successes, for example Dikkili near Pergamon or Arapdag near Karsiyaka, Izmir region, in W-Turkey (Larson, 1989; Erler and Larson 1990; Sayili et al. 1990; Agdemir et al. 1991).

The study area of Akoluk is situated about 35 km SW of the city of Ordu in the Pontides tectonic zone of Turkey which is believed to have been part of a Mesozoic-Paleogene island arc running from the Carpathians and Balkans in Europe along the Black Sea coast and into the Minor Caucasus. The Pontides are characterized by extensive block-faulting along NE-SW, N-S and E-W directions which is a very important control for the mineralization in this region.

The local geology in the Akoluk area consists of Upper Cretaceous and Eocene volcanic and sedimentary sequences. From bottom to top, the lithostratigraphic section is composed of sandy carbonate rocks, a volcanic sequence that develops from andesitic to dacitic composition towards the top, overlain by shallow-water sediments and andesitic-basaltic lavas and tuffs.

The precious metal mineralization is controlled by NE-SW - trending fractures and occurs as low-angle and vertical veins, as microveinlets and disseminations in strongly altered Upper Cretaceous dacitic tuff.

Core samples from two drillholes with a total length of 202 m have been studied petrographically (microscopy and diffractometry) and geochemically (AAS). The drillcores have been provided by the UNDP project "Epithermal precious metal mineralization in NE-Turkey".

Alteration and Mineralization

The rock fabric of host rock dacitic tuff is vitrophyric. The primary magmatic mineral components are corroded quartz, zoned plagioclase, biotite, hornblende and augite. A main argillic alteration zone can be distinguished which is divided into two subzones.

The characteristic hydrothermal mineral assemblage is quartz (equigranular and amorphous), kaolinite (subzone Ia), illite and smectite (subzone Ib), ankerite, calcite and disseminated pyrite. Gypsum, some barite and sulfides (base metals) occur in

the small veinlets of this alteration zone. The thickness of this alteration zone is very variable and reaches a maximum of 40 m.
In the argillic alteration zone barite veinlets and veins occur with a maximum thickness of 20 m which are mineralized. The barite veinlets consist of barite, quartz, kaolinite, ankerite, gypsum and ore minerals.
Ore microscopy defines three different ore stages: (i) *the pyrite stage* is the earliest stage and occurs disseminated in the argillic alteration zone and in the barite veinlets. Pyrite is fine-grained, idiomorphic and is accompanied by Fe-poor sphalerite; (ii) the mineral assemblage of *the base metal stage* consists of pyrite, chalcopyrite, galena, sphalerite with chalcopyrite inclusions, tennantite, sulphosalts (bournonite with typical twin lamellation). Galena is replaced by bournonite and tennantite. Gangue is quartz. The base metal stage occurs in the small veinlets of the argillic alteration zone.
(iii) The *Sb-As-Au-Ag-Ba stage* occurs in the barite veinlets and consists of stibnite, zinkenite, melnikovite-pyrite, sphalerite (Fe-poor), realgar, native gold (mostly in barite and zinkenite), native silver, and pyrargyrite (replacing native silver). Gangue minerals are barite, quartz, opal, ankerite, kaolinite and gypsum.

Precious Metal Distribution

The core samples were analyzed in 1 m intervals for Au by graphite furnace AAS (detection limit 2 ppb) and for Ag by flame AAS (detection limit 1 ppm). The gold and silver data are plotted in the probability graphs of Figure 1 and define three populations for gold and four populations for silver. These are for gold: (1) regional background population ($x = 5$ ppb with 1s variation range of 1 - 20 ppb) for 46 samples of host rock dacitic tuff; (2) argillic altered dacitic tuff ($x = 220$ ppb with 1s variation range of 80 - 500 ppb) for 69 samples, and (3) barite veinlets ($x = 4000$ ppb with 1s variation range of 2500 - 6200 ppb) for 18 samples (Fig. 1a).
There are four populations for silver: (1) regional background population ($x = 1$ ppm with 1s variation range of 0.8 - 2 ppm) for 72 samples of host rock dacitic tuff; (2) argillic altered dacitic tuff ($x = 10$ ppm with 1s variation range of 6 - 18 ppm) for 46 samples; (3) barite veinlets without a silver mineral phase ($x = 56$ ppm with 1s variation range of 40 - 80 ppm) for eleven samples; and (4) barite veinlets with a silver mineral phase ($x = 290$ ppm with 1s variation range 210 - 420 ppm) for five samples (Fig. 1b).

Discussion and Conclusions

Studies of active hydrothermal systems and experimental data indicate that thio-sulfide- and chloride-complexing are the dominant hydrothermal transport mechanisms for gold and silver, respectively (Seward, 1973; Henley, 1986). The solubility of precious metals is controlled by: (1) temperature; (2) Cl^--concentration; (3) pH; (4) ΣH_2S, and (5) $\Sigma H_2S/\Sigma SO_4$ (Cole & Drummond, 1986). Gold and silver can be transported together as chloride-complexes under highly saline conditions and at higher temperatures, for example in the porphyry environment (Henley, 1986).
There is a number of factors which induce precipitation of precious metals : (1) temperature decrease, (2) pressure loss and/or boiling, (3) changes in the redox state of the system, (4) reduced activity of complexing ions (i.e. S or Cl).
The mineral assemblage of gold and silver together with the gangue minerals of barite and kaolinite points to a genetic relationship between precious metal deposition and gangue minerals. Concomitant deposition of these minerals can be produced by oxidation during mixing with cool groundwater or by boiling (exsolution of CO_2 and H_2S). Changes in the redox state are accompanied by a decrease in pH which leads to acid leaching (formation of kaolinite), formation of barite ($BaSO_4$), and redox-controlled precious metal deposition.

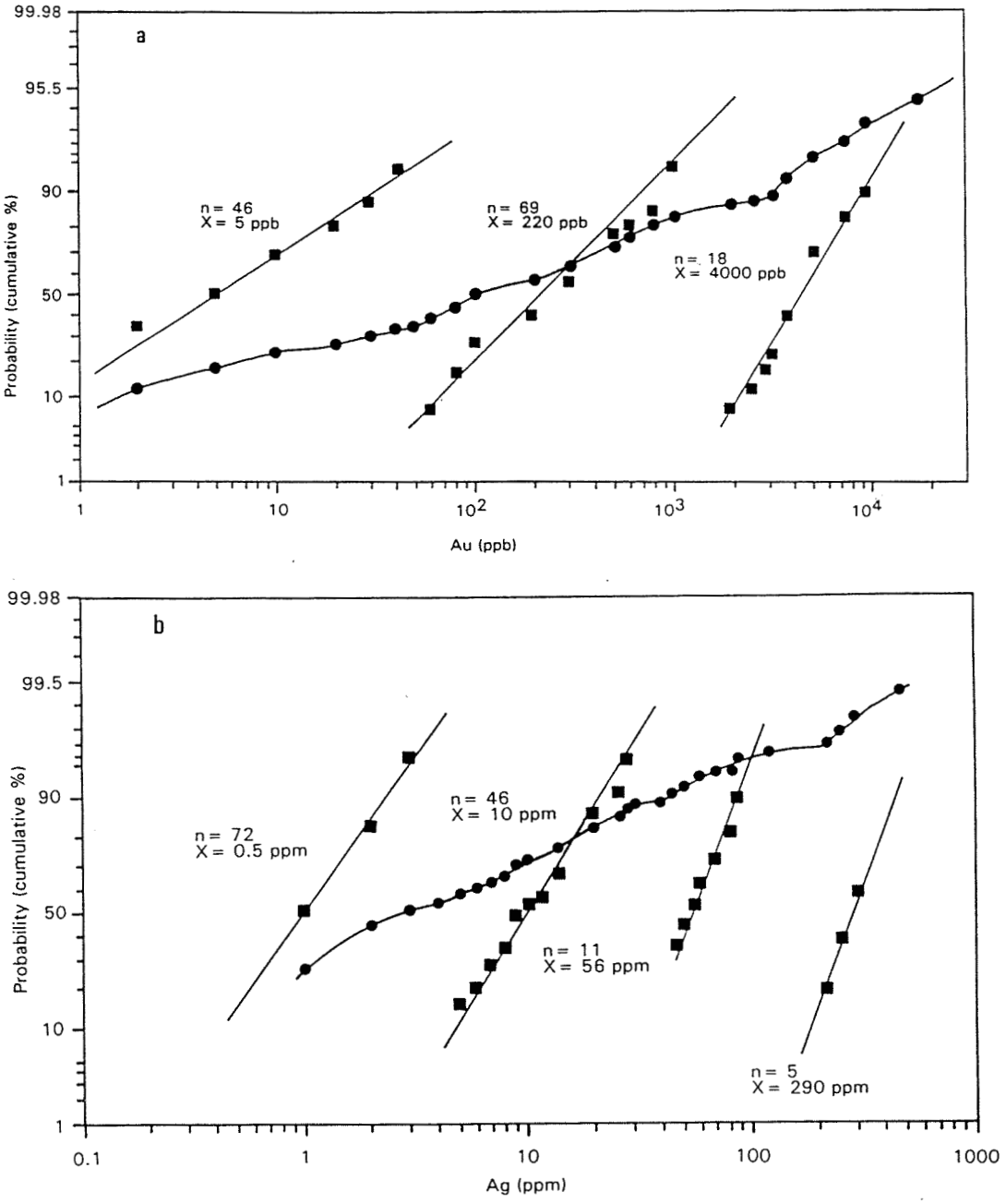

Fig. 1. Probability graphs for Au contents in 133 drillcore samples (a) and for Ag contents in 134 samples (b). Full circles define composite populations, successively broken up into three individual populations for gold and four populations for silver with log-normal characteristics (full squares). Detection limit is 2 ppb for gold and 1 ppm for silver.

References

Agdemir, N., Lehmann, B., Tietze, J. & Sayili, I.S., 1991, Alteration-mineralization pattern of the epithermal system of Sayaca/NE-Turkey: Preliminary results. Source, Transport and Deposition of Metals; eds., Pagel, M. and Leroy, J.L., Proceedings of the 25 Years SGA Anniversary Meeting Nancy, p. 157-159, Balkema, Rotterdam.

Cole, D.R. & Drummond, S.E., 1986, The effect of transport and boiling on Au/Ag ratios in hydrothermal solutions: A preliminary assessment and possible implications for the formation of epithermal precious-metal ore deposits. Journal of Geochemical Exploration, 25: 45-79.

Erler, A., Larson, L.T. 1990, Genetic classification of gold occurrences of the Aegean Region of Turkey. Intern. Earth-Sci. Congr. Aegean regions, Izmir/Turkey, p. 8-9.

Henley, R.W., 1986, Ore transport and deposition in epithermal environments. Stable Isotopes and Fluid Processes in Mineralization; eds., Hubert, H., Golding, S. and Ho, S.E., Geol. Dept. and Univ. Extension, Univ. of Western Australia Publ. 23: 51-69.

Larson, L.T., 1989, Geology and gold mineralization in Western Turkey. Mining Engineering, Nov. 1989, p. 1099-1102.

Sayili, I.S., Gonca, S., Gevrek, A.I., 1990, Gold mineralization at Arapdag. Karsiyaka, Izmir. Abstr. Intern. Earth-Sci. Cong. Aegean regions, Izmir, p. 29-30.

Seward, T.M., 1973, Thio complexes of gold and the transport of gold in hydrothermal ore solutions: Geochim. Cosmochim. Acta 37: 379-399.

Current Research in Geology Applied to Ore Deposits.Fenoll Hach-Ali, Torres-Ruiz & Gervilla(eds)(1993).ISBN 84-338-1772-8

FLUID INCLUSION CHEMISTRY OF HERCYNIAN, GRANITE-HOSTED VEIN Au-MINERALIZATION

Banks, D.A. (1); Yardley, B.W.D.(1); Miller, M.F. (2): Shepherd, T.J.(2); Cathelineau, M. (3); Boiron, M.C.(3); Urbano, R. (4); Florida, P. (4); Palomero, F.G. (5); Pereira, E.S. (6); Noronha, F. (7) & Barriga, F. (8).

(1) Earth Sciences, University of Leeds, Leeds LS2 9JT, U.K.; (2) BGS, U.K.; (3) CREGU, France; (4) ITGE, Spain; (5) Riotinto Minera, Spain; (6) DGGM, Portugal; (7) Porto University, Portugal; (8) Lisboa University, Portugal

ABSTRACT. Although spread over several hundred kilometres, Iberian granite-hosted quartz veins with Au mineralisation have fairly uniform fluid characteristics. In common with many Au deposits worldwide these veins contain large concentrations of CO_2-CH_4-N_2-H_2O fluids, but these were not involved in the enrichment of Au. Instead Au transport is associated with late stage, low salinity, low temperature H_2O-salt fluids. The carbonic fluids may be metamorphic in origin, whereas the H_2O-salt component was probably surface derived originally. The fluid characteristics are clearly different from the magmatic fluids responsible for Sn-W mineralisation and are therefore not linked with magmatic activity.

INTRODUCTION.

In the Iberian massif, Au is frequently found in or spatially associated with Hercynian granites and is borne in quartz veins containing sulphides, predominantly arsenopyrite locally accompanied by pyrite, stibnite and galena. The deposits display a multistage metallogenesis, a multistage and complex deformation of the vein structures which host the ores, with each deformational stage being characterised by specific metal deposition and wall rock alteration. The fluid characteristics of four Au occurrences, three in granites and one in metasediments, have been studied. Quartz veins in the granites at Corcoesto, Tomino and Penedono have all suffered intense microfracturing and fluid injection. Au is usually associated with arsenopyrite but is later than the sulphide precipitation. At Tomino the Au is also associated with chalcopyrite, bismuthinite and native bismuth. At Vila Pouca de Aguiar the quartz veins are in metasediments and the Au mineralisation is again a late event. It is usually found in intergranular spaces between pyrite and arsenopyrite and with galena which cuts these two minerals.

In addition to Au mineralisation Iberian, Hercynian, granites and those of SW-England are also host to Sn-W mineralisation which is magmatic in origin. The object of this study is to describe some of the bulk characteristics of the fluids in the Au-veins and to compare them to quartz veins containing Sn and W from other Hercynian granites.

FLUID INCLUSIONS.

In keeping with the complex deformation and fracturing history of the veins the nature and temporal evolution of the fluids is also complicated but is somewhat similar at each of the locations. In general the earliest fluids belong to the N_2-CH_4-CO_2-H_2O system followed by the fluids associated with the first mineralising event

(quartz-arsenopyrite): first CO_2-H_2O rich fluids and then CH_4-H_2O rich fluids, dominated by H_2O with a low density volatile phase enriched in CH_4. These fluids are typical of the inclusions within euhedral quartz crystals which formed after the main crystallisation of late euhedral arsenopyrite. The last fluids are H_2O-salt with a low salinity of c. 5 Wt.% and homogenisation temperatures of c. 200°C. At Corcoesto a more saline (c. 20Wt%) fluid has been observed. The low salinity fluids are probably related to the late stage of Au enrichment and the deposition of the Cu-Bi-Pb sulphide assemblage.

BULK VOLATILE COMPOSITION.

The major volatile component is H_2O (c. 80-95 mol%) followed by CO_2 (c. 1-20 mol%), CH_4 (c. 0.03-2 mol%), N_2 (c. 0-0.7 mol%) and H_2S (0-0.5 mol%). N_2 is mainly only detected at Tomino. Shepherd and Miller (1988) used fluid inclusion volatiles as a guide to Sn-W mineralisation in the Hercynian Granites of western Europe, in particular the relation between mol% N_2 and CO_2. As shown in Fig.1 the fluids are either rich or poor in N_2 with fluids associated with W-mineralisation having enhanced levels of CO_2 and N_2 (>0.5mol%) and fluids associated with Sn-mineralisation being depleted in dissolved gas. The fluids associated with the Au-mineralised quartz veins are distinctly different with most of the veins having substantially enhanced levels of CO_2 but little or no N_2 compared with those from the Sn-W veins.

ELECTROLYTE COMPOSITION.

The major components of the fluid are Na, K, Ca, Cl and SO_4 along with significant amounts of Mg, Li, B, Mn, Cu and Bi. Fe is absent from almost all samples, probably as a result of precipitation of sulphides or by the fO_2 being too high to allow its transport in solution. The Na/K ratios are variable and often K is the major fluid component. The high Cu, Bi and the absence of Fe is consistent with Au being associated with precipitation of chalcopyrite, bismuthinite and native bismuth and not with arsenopyrite. Again distinct differences exist between these granite-hosted veins and those from SW-England (Fig.2). There is some overlap of the Na-K-Ca ratios but the fluids in the Au-veins have a larger range of Na/K ratios and more variability. Whereas Sn-W veins are rich in Fe and Mn but have little Cu however, the Au-quartz veins are Mn-rich with Cu and essentially no Fe.

The value of the halogens, Cl, Br and to a lesser degree I, as conservative tracers of fluids has been recognised for some time in studies of near surface waters. Fluids from a wide range of hydrothermal settings can be distinguished based on Br/Cl and I/Cl ratios (Bolke and Irwin, 1992) with these halogens continuing to behave in a conservative manner to temperatures of at least 300°C (Banks et al, 1991). The data for the Sn-W veins (Fig.3) clusters around a Br/Cl ratio approximately half that of seawater and is consistent with a magmatic origin based on the compilation of magmatic Br/Cl ratios (Bolke & Irwin,1992). The much larger variation in I/Cl is almost entirely due to water-rock interaction and veins hosted by graphitic slates around the intrusions have the highest I values. However the Au veins are quite different having substantially enhanced Br concentrations relative to Cl and a much larger range of I/Cl values. Although covering a distance of several hundred kilometres the anion content of the fluids from these deposits is remarkably consistent. At Penedono, Tomino and

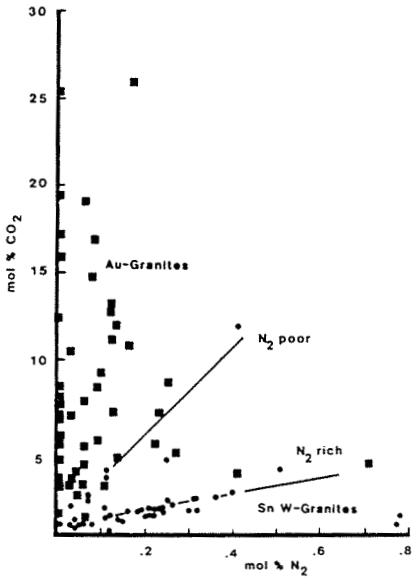

Figure 1. CO_2-N_2 covariance plot of inclusion volatiles.

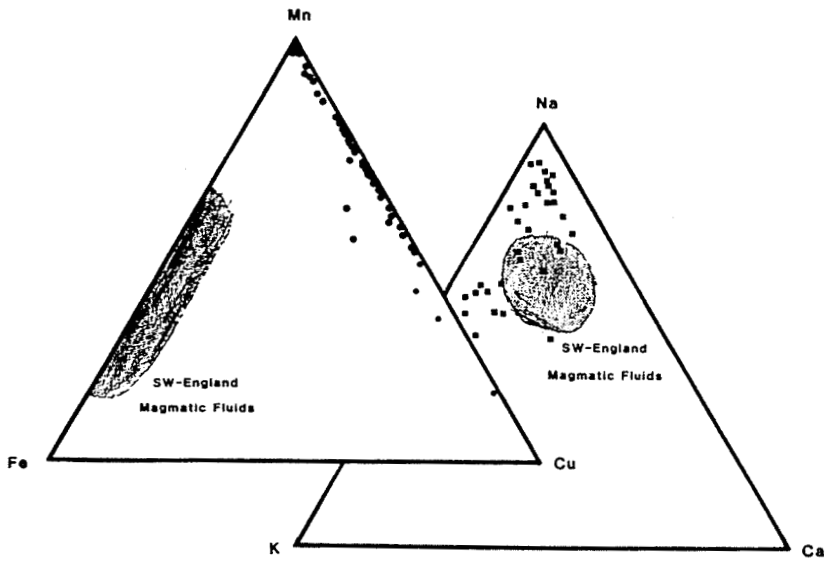

Figure 2. Na-K-Ca & Mn-Fe-Cu covariance plots of inclusion fluids.

Vila Pouca Br/Cl are tightly grouped unlike I/Cl, but at Corcoesto the situation is reversed. The large variation in Br/Cl is evidence of mixing of more than one saline fluid. One fluid is similar to that recorded from the other localities, the other must have a much lower Br/Cl and combined with the higher salinity (c. 20Wt%) may be derived from dissolution of evaporites.

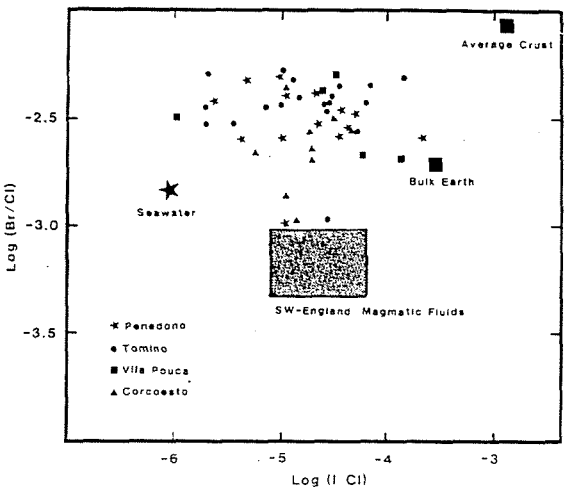

Figure 3. Br/Cl & I/Cl of inclusion fluids.

CONCLUSION.

There are distinct differences in the volatile and electrolyte composition of Hercynian granite-hosted quartz veins mineralised by Au and by Sn,W. Using the N_2, CO_2 and Fe, Mn, Cu content and the Br/Cl ratio it would be possible distinguish between the 2 types of mineralisation. Although the enrichment of Au appears to be related only to the late H_2O-salt fluids, the early precursor carbonic fluids were important in the precipitation of arsenopyrite which acts as the host for the Au. It is therefore still valid to use the volatile content of these fluids as an exploration tool for the type of fluid system associated with Au deposition. The fluids associated with Sn-W mineralisation are magmatic in origin whereas fluids associated with Au mineralisation are not. The CO_2-CH_4-N_2 components are likely to be of metamorphic origin, however the H_2O-salt component may not be. The Br/Cl ratio in particular is more consistent with a surface-derived fluid.

ACKNOWLEDGEMENTS.

This study was funded through C.E.C project MA2M-CT90-0033

REFERENCES.

Banks, D.A. Davies, G.R. Yardley, B.W.D. McCaig, A.M. & grant, N.T. 1991. The chemistry of brines from an Alpine thrust system in the central Pyrenees: An application of fluid inclusion analysis to the study of fluid behaviour in orogenesis. Geochim. Cosmochim. Acta. 55, 1021-1030.

Bolke, J.K. & Irwin, J.J. 1992. Laser microprobe analysis of Cl, Br, I and K in fluid inclusions: Implications for sources of salinity in some ancient hydrothermal fluids. Geochim. Cosmochim. Acta. 56, 203-226.

Shepherd, T.J. & Miller, M.F. 1988. Fluid inclusion volatiles as a guide to Tungsten deposits, Southwest England: Application to other Sn-W provinces in Western Europe. In: Boissonnas, J. & Omenetto, P. (eds) Mineral deposits within the European Community. Springer-Verlag, pp 29-52.

Current Research in Geology Applied to Ore Deposits. Fenoll Hach-Ali, Torres-Ruiz & Gervilla (eds) (1993). ISBN 84-338-1772-8

SOURCE AND TIMING OF GOLD DEPOSITION IN VOLCANIC AND INTRUSIVE SETTINGS IN THE SKELLEFTE DISTRICT, NORTHERN SWEDEN

Billström, K. (1) & Grensman, F. (2)
(1) LIG, P.O. Box 50 007, S-104 05 Stockholm, Sweden
(2) Terra Mining AB, Björkdalsgruvan, S-934 34 Kåge, Sweden

ABSTRACT: The nature of gold deposition in the Proterozoic Skellefte district is reviewed. It is suggested that two main stages of gold deposition occurred. The first stage was synchronous with, and part of, the deposition of the massive ores (1.89-1.88 Ga). The second stage, which probably was related to a stronger mobilization, took place shortly thereafter during a short time span (at c. 1.88-1.87 Ga). This stage, which possibly was related to uplift and rifting processes, involved an over-printing of previously formed VMS systems and a simultaneous input of gold to epigenetic quartz vein systems.

1 GEOLOGICAL SETTING

The Early Proterozoic Skellefte district in northern Sweden is known for its stratabound complex, massive sulphide ores carrying gold and other precious metals. Most tectonic reconstructions consider the area as an island arc environment, where massive sulphide ore deposition occurred during a vaning stage of volcanism.

The supracrustals have been intruded by a number of granitoids, ranging in age between c. 1.89 and 1.79 Ga, cf. Weihed et al., (1992). In this context, two presumably pre-metamorphic intrusive phases, the Jörn granitoid-forming event at c. 1.89 Ga and a magmatic pulse at c. 1.88-1.87 Ga generating rocks in the Gallejaur structure, are of interest. During the last decade several new Au mineralizations in epigenetic quartz vein systems, and spatially associated with intrusives, have been found. Evidently, significant Au enrichments are found in both volcanic terrains (VMS systems) and in intrusive settings and it is of considerable interest to find out whether or not a temporal and/or genetic relationship exists between the two gold environments.

2 STYLES OF MINERALIZATION

2.1 Au in epigenetic quartz vein systems

Except for the Barsele prospect, the other mineralizations are described in Weihed et al.(1992). The quartz veins apparently occur in rocks of different chemistries, but are generally structurally controlled. Detailed studies of epigenetic systems (e.g. Broman et al., 1993) have revealed that veins have been repeatedly fractured, gold may thus have been mobilized at different stages. The Barsele mineralization is found about 40 km west of the westernmost (Vindelgransele VMS ore), hitherto known, Skellefte massive ore but it shares several geological features with typical Skellefte ores and its presence may indicate a continuation of the Skellefte district. The Barsele mineralization is found in a

metavolcanic environment, with spilitic pillow lavas, porphyries and metasediments. A zone rich in gold, arsenopyrite and sulfosalts occurs associated with quartz veins in the area and at present its genetic relation to the massive ore lenses, carrying mainly arsenopyrite, sphalerite and chalcopyrite, is not clear. It is interesting to note that the epigenetic systems mentioned below are found in marginal parts of the Skellefte district, and also the Boliden and Holmtjärn VMS ores discussed below, examplifying highly gold-enriched massive ores, are situated in extreme ends of the massive ore-bearing zone in the Skellefte district.

2.2 Au in VMS systems

In particular two massive sulphide ores, Holmtjärn (8g Au/ton ore) and Boliden (15.5g/ton), have elevated gold concentrations. The common presence of mafic dykes (lamprophyres at Boliden and Holmtjärn) in numerous gold-enriched VMS ores may suggest that post-volcanic intrusive activity was crucial for reaching high gold grades in VMS ores. Another factor which may govern high gold grades is the presence of arsenic as both the VMS ores at Boliden and Holmtjärn and several epigenetic quartz systems are rich in arsenopyrite. In the following, the nature of gold deposition in the Skellefte district will be discussed with emphasis on new and earlier published Pb isotope data.

3 A Pb ISOTOPIC FRAME-WORK FOR THE SKELLEFTE ORE DISTRICT

Published high-precision lead isotope results from massive ores in the Skellefte district are summarized in Billström and Vivallo (1993), while Sundblad et al. (1993) reported data from some intrusive-hosted Au-mineralizations. When results are plotted in conventional Pb-Pb diagrams, ore leads can be grouped on basis of their geographic locations suggesting the presence of specific Pb isotopic domains (cf. Fig. 1).

In Fig. 1 galena isotope data for selected massive ore systems are compared with results for galenas from Au systems in VMS settings at Holmtjärn (north-central area), Boliden (eastern) and from epigenetic settings at Vindelgransele (westernmost area), Tallberg (north-central), Björkdal (eastern) and Barsele. In their evaluation of galena data from Vindelgransele, Tallberg and the Finnish Kangaskylä Au deposit, Sundblad et al. (1993) noted that Pb isotope data were aligned along one linear trend. This was interpreted as indicating a mixture of a comparitively unradiogenic endmember (a volcanic source reflected by data from the Vindelgransele VMS deposit) and an intrusive source (with an isotopic composition similar to that of the Tallberg porhyry-type deposit). When plotted, the preliminary data from Barsele (jamesonite from the Au paragenesis, arsenopyrite from the VMS assemblage) form an extension of the linear Au trend. On the contrary, the new galena data from Björkdal and quartz-tourmaline lodes in the Boliden Au ore appear to indicate a more complex pattern (Fig. 1). An apparent feature is that galena data for these Au-rich zones are similar to that of nearby VMS ore bodies, occurring either in the immediate surroundings to the Au zone or found in the same Pb isotopic province.

4 SOURCE AND TIMING OF Au DEPOSITION IN THE SKELLEFTE DISTRICT

In Tab. 1 evidences are presented which are relevant when adressing questions related to source and timing of gold deposition. It seems that significant gold mobilization occurred, on the one hand during a primary synvolcanic stage when the base metals were deposited and, on the other hand, at a subsequent stage when both felsic and mafic magmatism prevailed.

Table 1. Evidences in favour of early (pre-metamorphic) stages of gold deposition.

OBSERVATION	IMPLICATION
Paragenesis	
*certain VMS systems carry sheelite, Bi-Te minerals and tourmaline in gold-rich zones. The same mineralogy typifies epigenetic Au ores	genetical coupling between high-grade Au zones in intrusive and extrusive settings.
* gold appears to be part of the base metal paragenesis in VMS ores	Au was deposited simultaneously with the base metals
Stable isotopes	
*influence of a surface-derived (probably sea water) fluid at Tallberg and Björkdal.	if sea water was available during gold deposition, then this must have taken place during a pre- or syn-uplift stage.
Pb isotope evidence	
* data for ores at Tallberg, Björkdal and Middagsberget are similar to those of nearby VMS deposits found in the same Pb isotopic domain	the time span between deposition of gold in epigenetic and VMS settings must have been very short and a similar source of Pb (and gold) is indicated.
* In VMS ores at Boliden and Holmtjärn where isotopic data exist for both qz vein settings and the base metal ore, such data are very similar	Au deposition was a more or less continuous process in these environments.
* vein Pb at Näsliden and Pb extracted from gold at Holmtjärn are more primitive than data typifying the respective VMS ore.	a deep source of Pb (and gold?) exists

The second major stage was probably linked to a period of rifting and bimodal magmatism and tentatively this occurred close in time to the Gallejaur magmatism (c. 1873 Ma, Skiöld, 1988). This hypothesis finds some support from the proximity between the Gallejaur structure and the gold-enriched Holmtjärn VMS ore. With respect to the source of gold, this is less well constrained. A primitive, deeply situated source is anticipated from certain Pb isotope data. This is consistent with gold-bearing solutions penetrating deep rift structures and possibly such fluids travelled partly along the same structures as were utilized by ascending magmas. Presumably, the second stage of gold mobilization involved both material from the previously formed crust (1.89-1.88 Ga) as well as from a juvenile source.

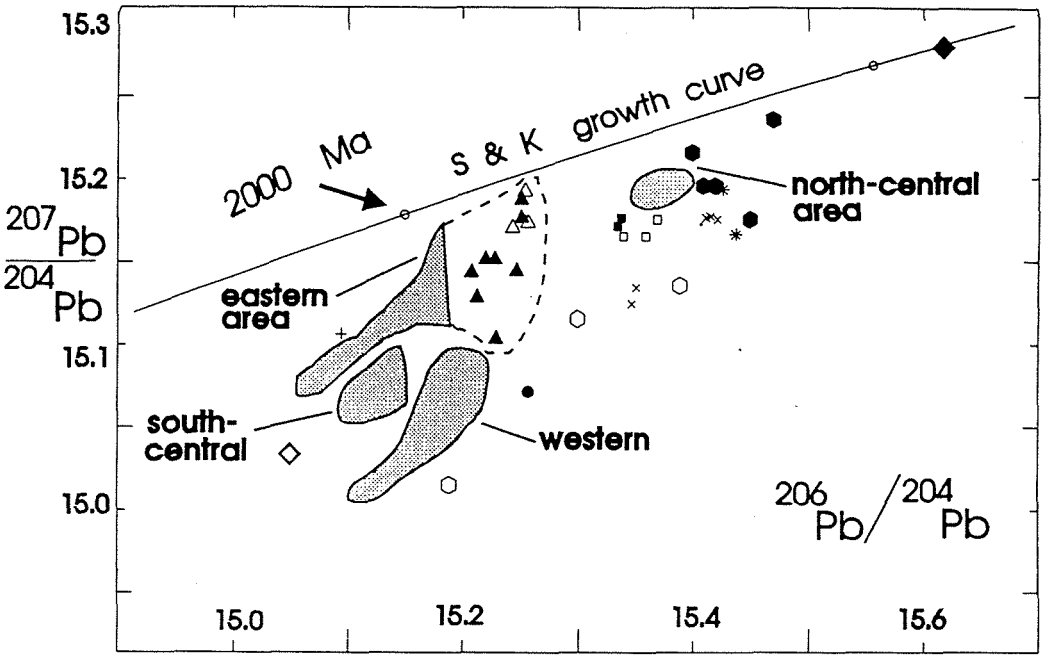

Fig. 1. Pb isotope data for epigenetic and VMS settings. + = Björkdal (Au), * = Tallberg(Au), x = Vindelgransele(Au), filled circle = Vindelgransele(VMS), open squares = Holmtjärn(Qz veins), filled squares= Holmtjärn(VMS), open polygons = Näsliden(veins), filled polygons= Näsliden(VMS), open triangles = Boliden(Au), filled triangles = Boliden(VMS), open rhomboeder = Barsele-arsenopyrite, filled rhomboeder = Barsele-jamesonite (Pb-sulfosalt).

REFERENCES

Billström, K. & Vivallo, W. 1993. Synvolcanic mixing of ore Pb and the development of lead isotopic provinces in the Skellefte district, Sweden. Submitted to Min. Dep.

Broman, C., Billström, K., Gustavsson, K. & Fallick, A.E. 1993. Fluid inclusions, stable isotopes and gold deposition at Björkdal, in northern Sweden. Submitted to Min. Dep.

Sundblad, K., Weihed, P., Billström, K., Markkula, H. & Mäkele, M. et al. 1993. Source of metals and age constraints for epigenetic gold deposits in the Skellefte and Pohjanmaa districts, central part of the Fennoscandian shield. Accepted for publication in Min. Dep.

Skiöld, T. 1988. Implications of new U-Pb zircon chronology to early Proterozoic crustal accretion in northern Sweden. Prec. Res. 38:147-164.

Weihed, P., Bergman, J. & Bergström, U. 1992. Metallogeny and tectonic evolution of the early Proterozoic Skellefte district, northern Sweden. Prec. Res. 58:143-167.

Current Research in Geology Applied to Ore Deposits.Fenoll Hach-Ali, Torres-Ruiz & Gervilla(eds)(1993).ISBN 84-338-1772-8

RELATED MINE-SCALE FAULT AND FOLD CONTROLS ON ARCHAEAN GOLD MINERALIZATION IN THE AMPHIBOLITE FACIES SOUTHERN CROSS GREENSTONE BELT, WESTERN AUSTRALIA

Bloem, E.J.M.; Groves, D.I. & Ridley, J.R.
Key Centre for Strategic Mineral Deposits, Dept. of Geology, University of Western Australia, Nedlands WA 6009, Australia

ABSTRACT: The lode-gold deposits and associated alteration envelopes in the Southern Cross greenstone belt are located in both folds and in shear zones. At fold hinges, gold mineralization occurs within tensional quartz veins, whereas in shear zones, gold concentrations are related to subtle variations in the strike of the shear zone, with individual ore-shoots generally related to extensional features. Ore-shoots parallel extensional crenulation cleavages, which developed throughout deformation.

INTRODUCTION

The Southern Cross greenstone belt occurs within a complex Archaean granitoid-greenstone terrain affected by overlapping metamorphism, deformation, and granitoid emplacement (Bloem et al., 1993). Lode-gold deposits in this belt occur predominantly within metamorphosed, volcanic-dominated greenstone sequences (Ahmat, 1986; Bloem & Ridley, 1991). The lode-gold deposits and associated alteration envelopes are located in different structural settings, these being either fold (e.g. Copperhead and Golden Pig deposits) or shear-zone dominated (e.g. Polaris South, Fraser's, Hopes Hill and Corinthia).

LITHOLOGY, METAMORPHISM AND ALTERATION

Lithology and Metamorphism

The lithostratigraphic sequence in the Southern Cross greenstone belt comprises tholeiitic and high-Mg basalts plus komatiites, together with banded iron formation (BIF) and minor interflow sedimentary rocks, overlain by younger sequences of terrigenous sedimentary rocks (Gee, 1982). Fold-controlled gold deposits are predominantly hosted by BIF, whereas shear zone related deposits are mostly hosted by mafic and ultramafic rocks and micaceous schists. Most deposits are located at or near lithological contacts. The rocks in the Southern Cross greenstone belt underwent low- to mid-amphibolite facies metamorphism (Ahmat, 1986). Syn-kinematic mineral assemblages suggest that peak metamorphism occurred during deformation (Bloem et al., 1993).

Alteration and mineralization assemblages

Proximal alteration assemblages of diopside-calcite, apatite, or fibrous tremolite-chlorite rims and distal biotite - pyrrhotite ± tschermakitic amphibole ± chlorite alteration envelopes surround sulphidic gold-bearing quartz veins in mafic and ultramafic rocks. In micaceous schists, sulphidic gold-bearing, quartz ± plagioclase veins are associated with biotite enrichment in the wallrock. Mineralization in BIF is characterized by quartz-veining and strong sulphidation (normally pyrrhotite). Veining occurring throughout the deformation event (Barnicoat et al., 1991), and the characteristic alteration assemblages, particularly diopside, calcite and tschermakitic amphiboles, indicate gold precipitation during deformation at near-peak metamorphic conditions (Bloem et al.,

1993). Sulphidation of Fe-rich (or high Fe/Mg) rocks was most likely the most efficient gold-depositing mechanism (Groves et al., 1988).

STRUCTURAL CONTROLS ON GOLD MINERALIZATION

Gold associated with fold hinges
Competent BIF units are normally deformed into buckle folds in contrast to plastically deformed mafic and ultramafic rocks. Gold mineralization associated with folds of competent BIF units is generally concentrated in synforms or near fold hinges of antiforms and within secondary shear zones developed near fold limbs. Sulphides in the host-rock and tensional quartz veins contain gold at fold hinges. At one deposit, gold is sited in a relatively low-strain area in a synformal buckle fold defined by BIF. At another, gold mineralization occurs on drag fold-closures within BIF, with ore-shoots sub-parallel to fold axes and along secondary shears (Bloem et al., 1993).

Gold associated with subtle differences in shear zone trend
Gold mineralization in the Southern Cross greenstone belt also occurs within several ductile shear zones, such as the NW-trending Fraser's-Corinthia shear zone (Bloem & Ridley, 1991). Economic gold mineralization is predominantly present in areas where the shear zone changes in strike and width (e.g. Polaris South, Fraser's, Hopes Hill, and Corinthia). With decreasing width gold grades increase. When the shear zone changes orientation, it is often intersected by km-scale ductile-brittle shear bands, offsetting the shear zone and disrupting gold mineralization. Generally, the shear zone was dominated by strike-slip movement. North of Southern Cross, where the greenstone belt is only a few kilometres wide and surrounded by granitoid domes, reverse movement prevailed, especially in narrow, more northerly trending areas, as indicated by the geometry of *en echelon* quartz veins.

Gold distribution related to extension within shear zones
One deposit is located in the neck of a boudinaged BIF unit, indicating that boudinage locally controlled fluid infiltration and mineralization. There is a clear relationship between gold mineralization, alteration, shear zone and main foliation trends, and the plunge of the mineral lineation. On a regional scale, ore-bodies are parallel to shear zone boundaries and main foliation. On a smaller scale, individual gold lodes and mineral lineations have similar plunge. Mineralization is also related to small-scale accommodating structures such as extensional crenulation cleavages (ECC's, e.g. Platt & Vissers, 1980) as individual ore-shoots have the same strike as ECC's. This creates an *en echelon* pattern of gold lodes on the mine scale. Relatively late ECC's offset earlier ECC controlled ore-shoots, indicating ongoing ECC creation both during and after the mineralizing event. This progressive ECC development caused rotation of the ore-shoots towards parallelism with the strike of the shear zone (Fig. 1).

DISCUSSION
In the Southern Cross greenstone belt, buckle folding occurred mostly in competent BIF. Large-scale shear zones, such as the Fraser's-Corinthia shear zone, developed preferentially in plastically deforming mafic and ultramafic rocks. These large scale

primary shear zones are generally located along extensively sheared fold limbs, locally causing boudinage of competent BIF units. Ore-bearing fluids were probably channelled through first-order shear zones, such as the Fraser's-Corinthia shear zone, into second-order shear zones, as indicated by the existence of extensive veining and alteration assemblages within the first-order shear

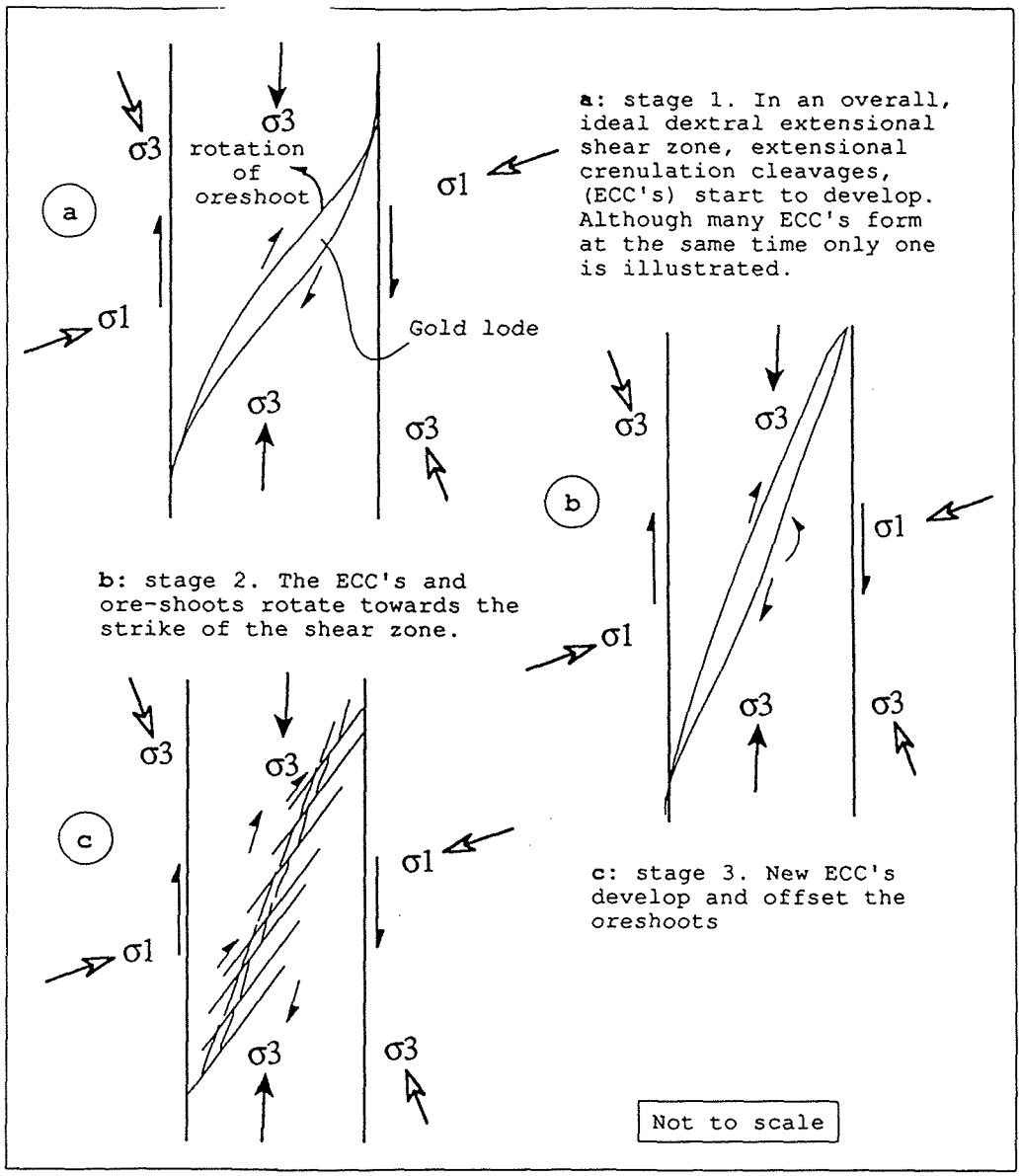

Figure 1. Schematic diagram illustrating the development and relationship between extensional crenulation cleavages (ECC's) and gold mineralization in extensional shear zones in the Southern Cross greenstone belt.

zones. Gold precipitation reflects the passage of excessive amounts of fluids through chemically suitable rocks (high Fe/Mg ratio) and the presence of structurally favourable sites. Second-order shear zones cross-cut folded BIF in places, introducing gold-bearing fluids into tensional quartz vein arrays within folded, chemically favourable, Fe-rich BIF. This provided ideal conditions for fold-related lode-gold deposits.

CONCLUSIONS

Gold deposition is commonly developed near lithological boundaries, at fold hinges and in shear zones. The deposition of gold along the Fraser's-Corinthia shear zone on a regional scale is favoured in areas where the shear zone was: 1) under horizontal extension (i.e. boudinage, ECC's (Fig. 1) and *en echelon* veins in plan view) or 2) under vertical extension (i.e. vertical *en echelon* veins).
Gold mineralization is related to a progressive deformation event accompanied by amphibolite facies metamorphism, in which the contrasting competency of adjacent lithological units caused structural heterogeneities that focussed ore-fluids from which gold was deposited via fluid-rock reactions with chemically suitable host rocks.

ACKNOWLEDGEMENTS

The financial support of Broken Hill Metals N.L., Burmine Ltd. and MERIWA is gratefully acknowledged. This paper is part of a Ph.D. study by E.B., who is the recipient of University of Western Australia and Overseas Postgraduate Research scholarships. H.J. Dalstra and J. Beeson are thanked for their comments.

REFERENCES

Ahmat, A.L., 1986. Metamorphic patterns in the greenstone belts of the Southern Cross Province, Western Australia. Geol. Surv. West. Aust., Prof. Paper 19: 1-21.

Barnicoat, A.C., Fare, R.J., Groves, D.I. & McNaughton N.J., 1991. Synmetamorphic lode-gold deposits in high-grade Archean settings. Geology, Vol. 19: 921-924.

Bloem, E.J.M. & Ridley, J.R., 1991. Structural Controls on a gold-hosted deformation zone at Hopes Hill (Southern Cross Province, Western Australia): Mineralization in a zone of flattening or of simple shear? Extended Abstract. Geol. Dept. & Univ. Extension, Univ. West. Aust., Publ. 25: 120-123.

Bloem, E.J.M., Dalstra, H.J., Groves, D.I. & Ridley, J.R., 1993. Metamorphic and structural setting of amphibolite-hosted gold deposits between Southern Cross and Bullfinch, Southern Cross Province, Yilgarn Block, Western Australia. Mineralium Deposita, submitted.

Gee, R.D., 1982. Explanatory Notes on the Southern Cross 1:250.000 Geological Sheet (SH 50-16), Western Australia. Geol. Survey. West. Aust., 25 p.

Groves, D.I., Ho, S.E., McNaughton, N.J,, Mueller, A.G., Perring, C.S., Rock, N.M.S. & Swarnecki, S., 1988. Genetic models for Archaean lode-gold deposits in Western Australia. Geol. Dept. & Univ. Extension, Univ. West. Aust., Publ. 12: 1-22.

Platt, J.P. & Vissers, R.L.M., 1980. Extensional structures in anisotropic rocks. J. Struct. Geol., Vol. 2: 394-410.

Current Research in Geology Applied to Ore Deposits. Fenoll Hach-Alí, Torres-Ruiz & Gervilla (eds) (1993). ISBN 84-338-1772-8

EPIGENETIC, BIF-HOSTED Au MINERALIZATION AT GEITA, TANZANIA, EVIDENCE FROM STRUCTURAL GEOLOGY, ORE PETROGRAPHY AND GEOCHEMISTRY

Borg, G.
Inst. für Geologie und Paläontologie, Universität Heidelberg, INF 234, 69120 Heidelberg, Germany

Abstract: Pyrite-gold-mineralization at Geita Mine is hosted by Archean BIF but cross-cuts both sedimentary strata and a prominent D_2-fold. The mineralization is of the gold-only type (+ Ag) with base metal values at background levels. Mineralization and associated actinolite/tremolite-carbonate alteration are spatially and probabaly genetically related to lamprophyre dykes which were emplaced probabaly during a late phase of the deformational history.

Geita Mine (closed 1962) is situated south of Lake Victoria in NW-Tanzania, within the Archean (2.84 Ga-old) Sukumaland Greenstone Belt. The greenstones comprise mafic volcanics, oxide BIF with interbedded trachyandesite and felsic pyroclastics. A coarse clastic sequence tops the Archean stratigraphy (Borg, 1992). Pre-(?), syn-, and post-orogenic granitoids can be distinguished and several gene-

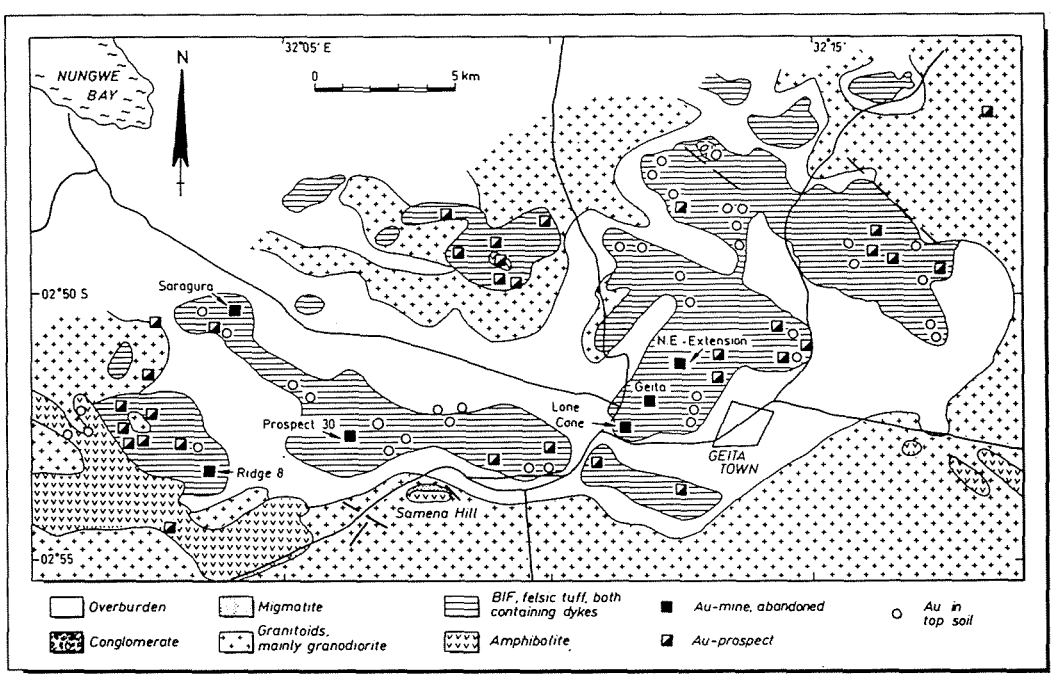

Fig.1 Geological map of the Geita area (after Naylor, 1961).

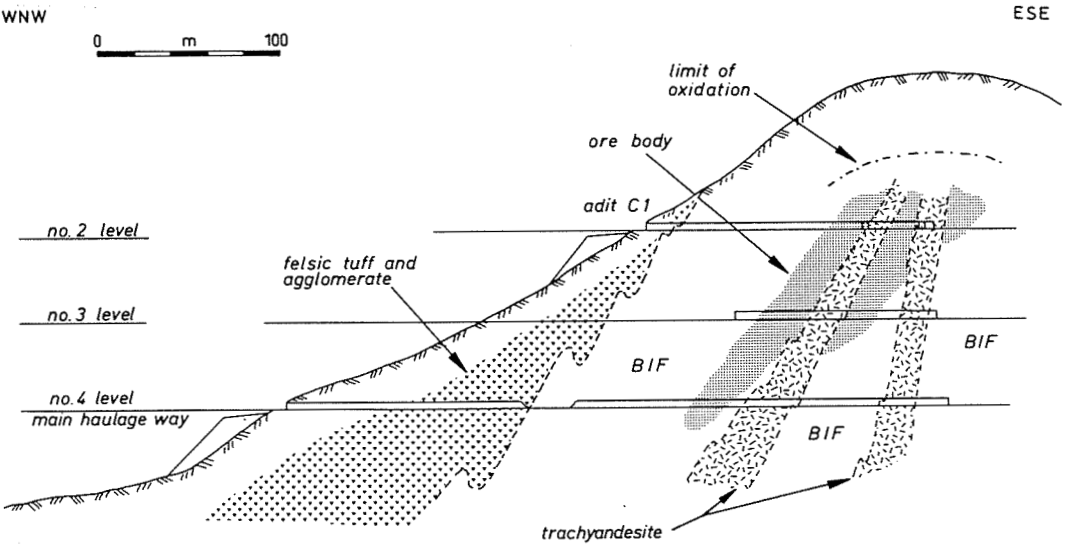

Fig.2 Cross-section through SW-part of Geita Mine, orientated normal to the axial plane of the reclined, northerly plunging fold in BIF and trachyandesite.

rations of lamprophyric, trachytic and basaltic dykes have been identified. Metamorphism (M_1 2.7 Ga?, M_2 2.55 Ga) has been generally of greenschist facies grade and at least three folding events can be distinguished. All lithostratigraphic units of the greenstone belt host significant (economic) gold mineralization (Fig.1), varying only in tonnage, grade and style, according to the physico-chemical properties of the host rocks. However, the granitoids are barren of gold mineralization.

The ore bodies transgress an isoclinal, reclined D_2-fold (axial plane 305°/70°; f.axis 45°/350°) in BIF and trachyandesite which has been subsequently offset by normal faults (Fig.2 and 3). The ore bodies occur in and adjacent to mineralized mylonites, breccias, shear zones and

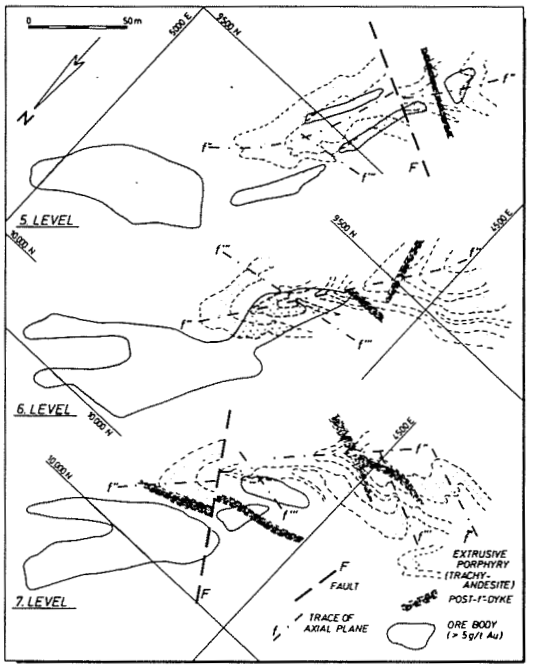

Fig.3 Relationship between BIF (white), trachyandesite (stippled), dykes (dark shading), folds, faults and ore bodies (grey shading).

quartz veins in the vicinity of lamprophyre dykes and appear to be unaffected by D_2-folding and faulting events (Fig.3).

The rocks contain an early (pre-ore) assemblage of fine-grained magnetite-quartzite (plus carbonate?). Early, poicilitic pyrite I can be distinguished from a later, inclusion-free type (IIa) and both have replaced magnetite I (Fig.4). Locally "accretionary" recrystallization affected magnetite I and here it contains rare inclusions of pyrite IIb. Minor mineralization in late quartz-carbonate-veins is characterized by traces of pyrite, chalcopyrite, native gold and possibly some molybdenite. The main portion of the gold is probably contained submicroscopically within pyrite, as indicated by a strong correlation between pyrite and gold contents. The gold-related alteration assemblage consists of actinolite/tremolite-biotite-stilpnomelane-carbonate and has locally replaced chert layers.

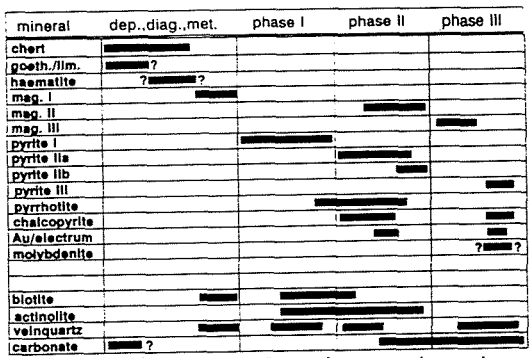

Fig.4 Primary and epigenetic mineral parageneses at Geita Mine.

At Geita, the ore is of the gold-only type, enriched in Au, Ag, S, LILE (Rb, Sr, K, Ba), Ca and Mg. Base metals occur only in background concentrations, common for barren Archean oxide BIF (Cu+Pb+Zn<300ppm) and plot clearly away from the field of typical VMS-deposits (Fig.5). Other groups of elements such as (HFSE, FTSM and REE) remained immobile during the mineralizing process (e.g. REE; Fig.6). K/Rb and K/Ba ratios point to a magmatic fluid source, excluding a seafloor hydrothermal environment.

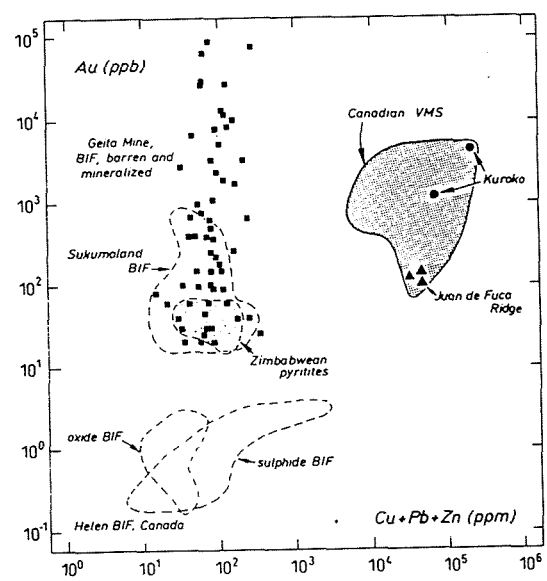

Fig.5 Au and base metals in ore and barren BIF from Geita (squares), BIF from Sukumaland, BIF from Canada and Zimbabwe compared with VMS deposits (data from Foster, 1989).

The metallogenetic process affected the Archean supracrustal succession as a whole and was not an isolated event, genetically related to the deposition of one particular stra-

tigraphic unit. The spatial, geochemical and probably temporal association of the gold-pyrite mineralization with lamprophyre dykes at Geita suggest an epigenetic origin from a late-magmatic hydrothermal fluid phase, succeeding lamprophyre emplacement. The lamprophyres are envisaged to have acted mainly as fluid source since they seem volumetrically unlikely to be the main source of gold. An association with VMS-type mineralization or intraformational redistribution of VMS, as suggested by Kuehn et al. (1990) and Kühn and Germann (1991), is unlikely. An extraformational source, e.g. the thick mafic volcanic pile of the Lower Nyanzian, might have provided a more favourable source.

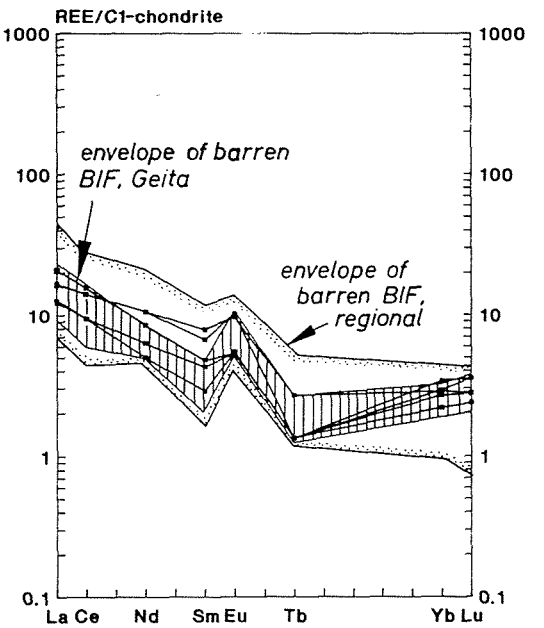

Fig.6 REE patterns of mineralized BIF and barren BIF (normalized to values of Evensen et al. 1978).

REFERENCES

Borg, G. 1992. New aspects on the Lithostratigraphy and Evolution of the Siga Hills, an Archaean Granite-Greenstone Terrain in NW-Tanzania. Z.angew.Geol.. 38/2:89-93.

Evensen, N.M., Hamilton, P.J. and O'Nions, R.K. 1978. Rare-earth abundances in chondritic meteorites. Geochim.Cosmochim.Acta. 42:1199-1212.

Foster, R.P. 1989. Archean gold mineralization in Zimbabwe: Implications for metallogenesis and Exploration. Econ.Geol. Monograph 6: 54-70.

Kuehn, S., Ogola, J., Sango, P. 1990. Regional setting and nature of gold mineralization in Tanzania and southwest Kenya. Precambrian Research. 46:71-82.

Kühn, S. and Germann, K. 1991. Metallgenetisches Modell für die an eine archaische Eisenformation gebundene Gold-Sulfid-Vererzung von Geita, Tanzania. Berichte zur Lagerstätten- und Rohstofforschung, Hannover. 3:60p.

Naylor, W.I. 1961. The geology of the Geita District: QDS 20 and 32 (9 NW. and SW.). Rec.Geol.Surv.Tanganyika. 9:13-18.

Current Research in Geology Applied to Ore Deposits.Fenoll Hach-Alí, Torres-Ruiz & Gervilla(eds)(1993).ISBN 84-338-1772-8

THE NEZHDANINSKOYE MESOTHERMAL GOLD DEPOSIT, RUSSIA: ORE-FORMING FLUID AND DEPOSITION ENVIRONMENT

Bortnikov, N.S.; Gamyanin, G.N.; Naumov, V.B. & Nosik, L.P.
I.G.E.M., Russia Acad. Sci., 35 Staromonetny per., Moscow 109017, Russia

ABSTRACT: Fluid inclusion study indicates that fluid responsible for ore formation has moderate salinity and consists of $H_2O>CO_2>CH_4=N_2>H_2S$. TP conditions are estimated to have ranged from 285 to 315°C and 1.5-1.7 kb. Stable isotopes indicate multiple sources of fluid.

1 INTRODUCTION

The Nezhdaninskoye deposit is a vein- and veinlet-disseminated gold deposit in low Permian black shales in Sakha-Yakutia, Russian Federation. The gold reserves are estimated to be 475 metric tons at an average grade of 5 g per tone. A fluid inclusion and sulfur, carbon and oxygen isotope investigation was undertaken to obtain information on the temperature, pressure and composition of the mineralizing fluid and its origin.

2 GEOLOGICAL SETTING

The Nezhdaninskoye deposit is located in South-Verkhoyansk synclinorium. It is hosted by a 400-m-thick sequence aleurolites and a 800-m-thick sequence of carbonaceous argillites. These rocks contain up to 2 wt. per cent of organic matter. Host rocks have been metamorphosed to low greenschist facies. The ore bodies are controlled by the tectonic zone which includes the foliation, brecciation, shear zones. The sedimentary sequence are intruded by small stocks of gabbro-diorite and numerous dykes of aplite, spessartite, kersantite and diorite porphyrites.

3 MINERALIZATION

Three episodes in the mineralization have been presumed. Numerous barren quartz veins and veinlets were originated during earliest events. Auriferous quartz veins and disseminated zones were formed during the second episode. Several mineral paragenetic assemblages have been recognized. They are: (1) scheelite+pyrite+arsenopyrite+quartz with native gold; (2) chalcopyrite+galena+sphalerite; (3) tetrahedrite+lead sulfantimonites with native gold; (4) stibnite. Numerous quartz veinlets containing owyheeite, pyrargyrite, freibergite were formed during the third episode.

4 FLUID INCLUSIONS

4.1 Microthermometric study

Fluid inclusions in quartz and sphalerite have been studied. They are considered to be primary and primary-secondary in origin and have been grouped into two types: (1) CO_2-rich inclusions consisting of single or of two CO_2-dominated phases and (2) H_2O-rich inclusions consisting of two or three phases at room temperature. CO_2-rich inclusions show the homogenization temperatures of CO_2 to liquid phase ranging from 14.2 to 25.5°C. H_2O-rich inclusions homogenized to liquid water from 285 to 315°C. The CO_2 densities are estimated to range from 0.75 to 0.85 g/cc.

4.2 Leachate and gas analyses

Leachate and gases released from thermally decrepitated inclusions in crushed vein quartz samples were analyzed by ion and gas chromatography. Ion chromatography revealed the presence of Cl^- and SO_4^- ranging from 1.2 to 10.3 g/kg H_2O and from 0.1 to 3.1 g/kg H_2O; respectively. The F^- contents are below detection limit. NO_2^+, NO_3^-, PO_4^{3-} and Br^- have not been detected. The released gases contain between 4.5 and 85.5 mole percent H_2O and between 14 and 94 mole percent CO_2; CH_4 and N_2 content falls within the range of 0.03 to 0.4 mole percent and 0.2 to 0.3 mole percent, respectively.

5 STABLE ISOTOPES

5.1 Sulfur isotopes

The sulfur isotope composition of sulfides (170 analyses) in igneous and sedimentary rocks and in auriferous ore bodies have been investigated. Marcasite in sedimentary rocks has a $\delta^{34}S$ value (vs CDT) range from -1.9 to 10.3 per mil, pyrrhotite and pyrite in igneous rocks display from -4.0 to -1.6 per mil and from -2.4 to 0.7 per mil, respectively. The overall range of $\delta^{34}S$ values in sulfides in ore bodies (155 analyses) is from -18.0 to 6.0 per mil. The most sulfides (125 analyses) has a $\delta^{34}S$ value range from -6.0 to 1.0 per mil. The $\delta^{34}S$ values (per mil) are from -11.0 to 6.0 for pyrite, from -6.7 to -1.6 for pyrrhotite, from -9.0 to 2.2 for arsenopyrite, from -6.2 to 0.7 for sphalerite, from -8.2 to -1.4 for galena.

5.2 Carbon and oxygen isotopes

The 19 calcite analyses have a $\delta^{13}C$ value (vs PDB) range from -14.7 to 1.0 per mil, with a mean of -7.5 per mil. The oxygen isotopic

compositions of igneous, host and alteration rocks and calcite and quartz have been investigated (80 analyses). The $\delta^{18}O$ values (vs SMOW) of calcite in the 19 samples analyzed range from 15.0 to 22.5 per mil. The auriferous quartz analyses revealed a $\delta^{18}O$ value ranging from 5.1 to 15.2 per mil. The $\delta^{18}O$ values of minerals in igneous rocks (quartz, feldspars, biotite) vary from -6.6 to 14.2 per mil. The bulk isotopic composition of host and alteration rocks lies between 1.5 to 12.3 per mil and 8.4 to 11.9 per mil, respectively.

6 ORE-FORMING FLUID AND DEPOSITION ENVIRONMENT

Fluid inclusion data indicate that ore-forming fluid have moderate salinity and consist of $H_2O+CO_2>N_2=CH_4$. Fluid inclusions trapped in a two-phase field are evidence that there were two coexisting immiscible fluids circulating in the fractures during mineral deposition. The occurrence of syngenetic CO_2-liquid rich and CO_2-vapor rich inclusions indicates boiling of fluid. The data obtained may suggest the hypothesis that fluid unmixing have been induced by a decrease in pressure and/or temperature. The CO_2 pressures ranging from 1.2 to 1.7kb are assumed to be minimal values of total fluid pressure as the contribution of other volatile components has remained unknown. Since homogenization temperature of fluid inclusions trapped boiling fluids need minimum pressure correction value the deposition temperature is considered to have been ranged of 285-315^{o}C.

Fluid carrying H_2S of $\delta^{34}S$ values of -6.0 to 1.0 per mil may be responsible for the $\delta^{34}S$ value (-6.5 to 0.7 per mil) of pyrite precipitated at 300^{o}C. The most likely candidates of a sulfur source are host sedimentary rocks, sulfide minerals disseminated in host rocks and granitoid magma. Values of $\delta^{34}S$ ranging from -30 to 10.0 per mil are common in argillites (Nielsen,1979). The $\delta^{34}S$ value of H_2S resulted from the pyrite hydratation should range approximately from -1.0 to 13.0 per mil in the case under consideration. The $\delta^{34}S$ values of fluid related to granite magma lie within -3.0 to 7.0 per mil (Ohmoto & Rye,1979). The data obtained can be interpreted to suggest the mixing between mostly magmatic sulfur of 0±3 per mil and sulfur remobilized from sedimentary rocks. If the dominant carbon species in the ore fluid was H_2CO_3 and the temperature of carbonate deposition was higher than 200^{o}C, then $\delta^{13}C_{calcite}=\delta^{13}C_{H2CO3}=\delta^{13}C_f$ (Ohmoto & Rye,1979). The wide variation of $\delta^{13}C$ values in the Nezdaninskoye deposit may reflect the multiple source of carbon. It may be generated by the decarbonation (-8.0 to 4.0 per mil), hydrolysis of reduced C in sedimentary rocks (-10.0 to -35.0 per mil) and may be derived from purely magmatic source (-3.0 to -7.5 per mil) (Ohmoto,1986). Oxygen isotope composition of the ore fluid calculated from isotopic analyses, trapping temperatures and the quartz-waper and calcite-waper (Field & Fifarek,1985) appear to have been

variable from -6.0 to 17.0 per mil. These results may indicate the involment in vein formation of water from different sources, probably meteoric and magmatic in origin.
Thermodynamic calculations of mineral stability fields in the range of 1kbar and 300 to 325°C indicate neitral pH conditions of 5.5 to 6.0, a_{O2} and a_{S2} of the mineralizing fluids were in the range about 10^{-31} to 10^{-36} and 10^{-11} to 10^{-7}, respectively.

REFERENCES

Field,C.W. & Fifarek,R.H. 1985. Light stable isotope systematics in the epithermal environment. In: B.R.Berger & P.M.Bethke (eds.). Geology and geochemistry of epithermal systems. Rev.Econ.Geol.2, p.99-128.
Nielsen,J. 1979. Sulfur isotopes. In: Jaeger,E. & Hunziker,J. (ed.). Lectures in isotope geology. Springer, Berlin, pp.283-312.
Ohmoto,H. 1986. Stable isotope geochemistry of ore deposits. In: J.W.Valley, H.P.Taylor & J.R.O.O'Neil (eds.). Stable isotopes in high temperature geological processes. Rev. in Mineralogy,16, p.491-560.
Ohmoto,H. & Rye,R.O. 1979. Isotopes of sulfur and carbon. In: Barnes,H.L.(ed.). Geochemistry of hydrothermal ore deposition,2 nd ed. Wiley Interci. New-York, pp.509-567.

Current Research in Geology Applied to Ore Deposits.Fenoll Hach-Alí, Torres-Ruiz & Gervilla(eds)(1993).ISBN 84-338-1772-8

PHASED OR CYCLIC EMPLACEMENT FOR THE LATE-HERCYNIAN GOLD DEPOSITS

Bouchot, V.
BRGM, BP 6009, 45060 Orleans Cedex 02, France

ABSTRACT: A synthesis of textural studies on Variscan auriferous-vein-bearing shear zones shows that the gold emplacement possibly occurred according to two models: a cyclic development with early precipitation of Au-arsenopyrite or phased development with the trapping of native gold during late shear.

INTRODUCTION

All the vein-gold deposits of the French Hercynian basement were emplaced during a mineralizing event towards the end of the Variscan orogeny (Bouchot *et al.*, 1989; Boiron *et al.*, 1989; Bouchot and Gros, 1991; Lescuyer *et al.*, 1993). The deposits are located within or close to major ductile shear zones (100 km long by 1 km wide) of the basement and in the vicinity of Late-Hercynian granite intrusions. The gold structures are related to small (1-10 km long by 1-20 m wide) ductile-brittle or brittle shear zones enclosing gold-bearing veins with a quartz ± sulphide gangue; arsenopyrite is everywhere present in the mineralization.

The French deposits can be divided into those (the most common) in which the gold is free (cf. La Bellière, Salsigne, Le Bourneix, Lauriéras) and those in which the gold is camouflaged by arsenopyrite (cf. Châtelet, Villeranges, Viges); each type reveals specific textural features. Our textural studies of the ores, coupled with those of other authors (Hubert, 1986; Bouchot, 1990; Bouchot and Gros, 1991; Bouchot, 1992; Boiron *et al.*, 1992; Essarraj, 1992; Lescuyer *et al.*, 1993) show that development of the two types of gold mineralization results from different dynamics: a phased development for the quartz veins with free gold and a cyclic development for the quartz veins with Au-arsenopyrite In spite of the two dynamic models being radically different, their paragenetic evolution was chemically and mineralogically similar: a first paragenesis (P1) with As-Fe-S, followed by a second paragenesis (P2) with Cu-Sb-Pb-Zn-Bi-Ag. The aim of this paper is to detail the specific characteristics of each model and then discuss those that differentiate the two models. The textural studies were carried out using optical microscopy (Le Bourneix, Salsigne, La Bellière, Châtelet) or cathodoluminescence (Le Bourneix, Lauriéras).

1. PHASED DYNAMICS FOR THE VEINS WITH FREE GOLD

The dynamic model common to Hercynian deposits with free gold has been defined in the La Bellière, Le Bourneix, Lauriéras and Salsigne deposits (Table 1). The gold, in its native state, is contained in variably deformed quartz veins in which the quartz gangue encloses sulphides ranging from a few per cent (La Bellière, Le Bourneix) to more than 50% (2X ore at Salsigne). The emplacement of the mineralization occurred in three successive stages: a first stage of vein quartz infill, a second stage of vein deformation, and a final stage of gold entrapment. This phased evolution reflects a continuum of deformation along the mylonitic shear zones within the ductile-brittle domain of the basement synchronous with hydrothermal fluid circulation under pressure.

Stage 1 - Major quartz infill: During development of the mylonitic zones, the impregnating fluids lowered the resistance of the country rocks and accelerated non-coaxial deformation. Shear movements thus caused transtensional openings that trapped quartz veins with pyrrhotite-arsenopyrite-pyrite ± chalcopyrite (Paragenesis 1) but no gold. These openings can occur in the centre (La Bellière), at the top (Salsigne 2X) or at the bottom of the mylonitic zone. The veins

comprise an infill of white quartz (Q1) that was generally deposited in several phases; the quartz gangue is either massive (Salsigne 2X) or it encompasses fragments of variably silicified country rock to form quartz breccias (Le Bourneix, Lauriéras). This quartz deposition was accompanied by crystallization of the first P1 sulphides in which the arsenopyrite is free of gold (except locally at Lauriéras; Essarraj, 1992). In the veins, these P1 sulphides form euhedral crystals, isolated or aggregated into small patches between the macrocrystalline (x1 mm) Q1 quartz grains. In the hydrothermalized mylonites, the same sulphides form elongate arsenopyrite-pyrite bodies and pyrrhotite veinlets with the crystals being respectively granular and stretched along the shear planes (La Bellière, Salsigne, Le Bourneix). The infill crystallization was slow, forming macrocrystalline patches of Q1 quartz and squat crystals of arsenopyrite and associated pyrite.

Stage 2 - Vein deformation and syntectonic sulphide deposition: After deposition of the Q1 vein quartz, continued shear deformation became concentrated along the lenticular quartz veins, which acted as rheologically resistant bodies isolated in the hydrothermalized mylonites. The stage is reflected by folded veinlets (La Bellière, Salsigne 2X) and by intra-vein shear (Salsigne 2X) or vein-edge shear (Lauriéras). The macrocrystalline Q1 quartz within these preferential deformation zones became cataclased (brittle domain at Le Bourneix, Lauriéras and Salsigne 2X vein) or polygonized (ductile domain at La Bellière, Salsigne 2X stockwork) with a concomitant reduction in grain size from macrocrystalline to microcrystalline (5-100 μm). Depending on the type of deformation, ductile or brittle, this microcrystalline quartz (MCQ) either forms the cement of a tectonic breccia with clasts of little cataclased Q1 quartz, or forms centimetre-wide mylonitic bands. Cataclasis of the veins aided the modest (Le Bourneix, Lauriéras) or abundant (Salsigne) deposition of syntectonic sulphides (pyrrhotite, pyrite, arsenopyrite) which crystallized in bands along the shear planes or were disseminated (seeds) in the cataclased facies (MCQ); these sulphides belong to the P1 paragenesis, deposition of which began during stage 1. By the end of stage 2, almost 90% of the total volume of the veins had been filled by Q1 quartz and P1 sulphides.

Stage 3 - Gold entrapment: After the peak vein deformation, the final shear-zone movements were accompanied by the entrapment of gold, of a small amount of hyalin or fibrous quartz (Q2), and of paragenesis P2 minerals. Although variable from one district to another, if not from one deposit to another, the more common P2 minerals are galena, chalcopyrite, sphalerite, sulphosalts (Pb, Pb-Ag) and Bi minerals (abundant at Salsigne). At microscope scale, these final movements are reflected by a microfracturing of the Q1 quartz-P1 sulphide assemblage (Lauriéras, Le Bourneix, Salsigne) deposited during stage 1 or by microflows between the quartz grains deformed during stage 2. These events generated micro-openings which aided the percolation of residual fluids through the veins with the deposition of gold and associated minerals (Q2, P2), until the tectono-hydrothermal system became blocked. Thus two types of gold trap have been identified relative to the texture of the deformed assemblage:

1. Traps generated during stage 3: these are sinuous gashes containing fibrous quartz and P2 sulphides cutting the P1 sulphide bands (Salsigne 2X; Lescuyer *et al.*, 1993) and hyalin quartz veinlets and filled cracks cutting the Q1 macrocrystalline quartz (Le Bourneix and Lauriéras; Hubert, 1986; Essarraj, 1992).
2. Traps generated during stage 2, but active during stage 3: these comprise cataclased MCQ quartz (+ P1 sulphides) (Le Bourneix: Hubert, 1986; Bonnemaison, 1986. Lauriéras: Essarraj, 1992) in which particles of gold and P2 sulphides are disseminated. These facies, with a high permeability of tectonic origin, were late sites of gold mineralization.

2. CYCLIC DYNAMICS FOR THE VEINS WITH Au-ARSENOPYRITE

This dynamic model, common to the Au-arsenopyrite mineralization of the La Marche district, has been defined at Châtelet (Table 1). The gold veins line fault zones, generated at shallow depth, and are composed of zoned breccias with clasts of country rock and of vein quartz surrounded by a commonly banded quartz cement. The repetition of multiple generations of quartz reflects a cyclic deposition with each sequence comprising two successive phases (Bouchot and Gros, 1991): a pre-rupture phase with comb quartz (CQ), followed by a syn-rupture phase with microcrystalline quartz (MCQ) forming the main host to the Au-arsenopyrite.

Pre-rupture phase: The deformation gave rise to minimum displacements along the fault and to tensional stress phenomena. The movements were accompanied by a material transfer from zones of dissolution (stress areas) towards zones of openings (protected areas). The small voids generated during this pre-rupture phase were thus lined with comb quartz (CQ) barren of sulphides and gold.

Syn-rupture phase: With the fault-plane irregularities having been weakened by the material transfer, any abrupt displacement caused by the operating stress field would have caused seismic-type rupture. The existing voids would thus have been abruptly widened and linked. The resultant drop in fluid pressure, inherent with such abrupt opening, gave rise successively to fluid suction towards the jog through a pumping effect (Sibson, 1990), and to oversaturation of the solution with concomitant precipitation of microcrystalline quartz (MCQ) and pyrrhotite, pyrite and Au-arsenopyrite (paragenesis 1). The precipitation is reflected by the presence of multiple microcrystalline quartz grains which, on deposition, moulded the euhedral facies of the earlier comb quartz (CQ). Gold was trapped in the crystal lattice of the arsenopyrite which forms small euhedral rods between the MCQ grains. The infill of microcrystalline quartz (MCQ) closed the drain and stopped fluid circulation: the residual voids then became sites for the growth of ever coarser quartz. The fault zone thus rediscovered its original resistance and passed back from a rupture-type regime to a dissolution-crystallization regime until the rupture point was again reached. This chain of events then enabled the successive development of new quartz sequences.

Following the cyclic genesis of the Au-Arsenopyrite-bearing veins, the mineralization was cut by non-gold-bearing veinlets of ankerite, quartz, chlorite, jamesonite, tetrahedrite, chalcostibnite, sphalerite, and chalcopyrite (paragenesis 2).

3. DISCUSSION

The paragenetic evolution, characterized by a first paragenesis of As-Fe-S and then a second paragenesis of Cu-Sb-Pb-Zn-Ag-Bi is common to the Late-Hercynian mineralization, whatever its emplacement dynamics (Table 1). This suggests that all the mineralization derived from similar hydrothermal fluids circulating during a single mineralizing event. On the other hand, the entrapment of the gold was heterochronous between the two models: in the cyclic model the Au atoms are trapped early in the lattice of paragenesis 1 arsenopyrite, whereas in the phased model the gold is deposited later as free gold with paragenesis 2. From a comparative analysis of the emplacement models and the textural studies of the ores, it is considered that the early entrapment of gold in the arsenopyrite was due largely to specific depositional kinetics of the cyclic model (Table 1); a sudden drop in pressure associated with seismic rupture resulting in the rapid crystallization of microcrystalline quartz and fine rods of Au-arsenopyrite. The very rapid growth of arsenopyrite would have been one of the principal causes of gold becoming trapped in the lattice.Such kinetic conditions did not occur in the phased model where the macrocrystalline

Table 1 - Comparison between the phased and cyclic emplacement models for Variscan gold mineralization.

Paragenesis 1 with As-Fe-S; Paragenesis 2 with Cu-Pb-Sb-Zn-Ag-Bi;
MCQ: microcrystalline quartz; Q1: macrocrystalline quartz; CQ: comb quartz.

PHASED MODEL	Stage 1	Stage 2	Stage 3
Mylonitic zone *Ductile-brittle domain*	 Quartz vein emplacement	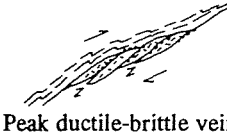 Peak ductile-brittle vein deformation	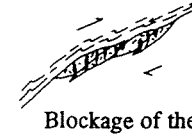 Blockage of the hydrothermal system
Quartz gangue	Slow growth of Q1	Granulation of Q1 to MCQ	Crystallization of Q2 and trapping of **native gold**
Paragenesis 1 Paragenesis 2-Gold			
Paragenesis 1-Au Paragenesis 2			
Quartz gangue	Slow growth of CQ	Precipitation of MCQ with **Au-arsenopyrite**	Crystallization of veinlets without gold
Cataclastic zone *Brittle domain*	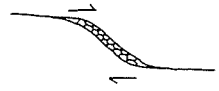 Opening of gashes	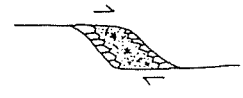 Abrupt opening and vein emplacement (jog)	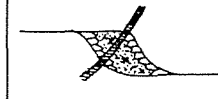 Late veinlet emplacement
	1 sequence repeated **n** times		
CYCLIC MODEL	Pre-rupture phase	Syn-rupture phase	Post-ore stage

quartz (Q1) and the squat non-auriferous arsenopyrite patches of paragenesis 1 crystallized very slowly. It was only later, notably following a progressive drop in temperature (Bourneix: Touray *et al.*, 1989; Salsigne: Lescuyer *et al.*, 1993) after the peak deformation (stage 2), that the physico-chemical conditions became suitable for the deposition of (native) gold along with paragenesis 2. The two types of gold entrapment strongly suggest that gold was already present in the fluid at the beginning of the hydrothermal system.

The particular reasons as to why a cyclic evolution should develop rather than a phased evolution, which is more common in the Variscan basement, are still not clearly understood. Nevertheless, it is known that the cyclic dynamics developed at shallow depth and consequently under superficial P-T conditions that allowed seismic pumping (Sibson, 1990). On the other hand, with the greater depth of the ductile-brittle domain, the seismic events with a cyclic character were followed by a polyphase and continuous tectono-hydrothermal development leading to the entrapment of free gold; such dynamics were clearly different from the seismic-valve-type cyclic dynamics of the Archaean mesothermal veins in Canada (Sibson, 1990) and thus constitute a particular feature of the Variscan mesothermal mineralization.

REFERENCES

Boiron, Cathelineau M. & Trescases J.J. 1989. Condition of gold-bearing arsenopyrite crystallization in the Villeranges Basin, Marche-Combrailles shear zone, France; a mineralogy and fluid inclusion study. Econ. Geol., vol. 84, pp. 1340-1362

Boiron M.C., Essarraj S., Sellier S., Cathelineau M., Lespinasse M. & Poty B. 1992. Identification of fluid inclusions in relation to their host microstructural domains in quartz by cathodoluminescence. Geochimi. Cosmochimi. Acta, vol.56, pp. 175-185

Bonnemaison M. 1986. Les "filons de quartz aurifère" : un cas particulier de shear zone aurifère. Chron. rech. min., n° 482, pp. 55-66

Bouchot V., Gros Y. & Bonnemaison M. 1989. Structural controls of the auriferous shear zones of the Saint-Yrieix district, Massif central, France : evidences from the Le Bourneix and Lauriéras gold deposits. Econ. Geol., vol. 84, pp. 1315-1327

Bouchot V. 1990. Les quartz du gîte aurifère du Châtelet (Creuse, France) : texture, chronologie séquentielle et mécanisme de formation. BRGM Report R31539, 45 p.

Bouchot V. & Gros Y. 1991. Dynamics of the Châtelet gold mineralization (France). 25 years SGA Anniversary Meeting, Nancy, Extended Abstract, Balkema ed., Rotterdam, pp. 427-430

Bouchot V. 1992. Les veines quartzeuses aurifères associées aux zones de cisaillement du gisement de La Bellière (France) : texture du minerai, mécanisme de formation, chronologie de mise en place. BRGM report R35667, 76 p.

Essarraj. S. 1992. Migrations des fluides, microfissuration et conditions de dépôt de l'or dans les veines de quartz aurifères. Doctorat Thesis, Inst. Nation. Polytech. Lorraine, France

Hubert P. 1986. Textures et inclusions fluides des quartz aurifères. Application au gîte de Cros-Gallet (France) et au prospect de Sanoukou (district de Kéniéba, Mali). Doctorat Thesis, Univ. Orléans. (France), BRGM Doc.n°114, 249 p.

Lescuyer J.L., Bouchot V., Cassard D., Feybesse J.L., Marcoux E., Moine B., Piantone P., Tegyey M. & Tollon F. 1993. Le gisement aurifère de Salsigne (Aude, France) : contexte lithostructural et modèle génétique d'une concentration syntectonique tardi-carbonifère. Submitted to Chron. rech. min.

Sibson R.H. 1990. Faulting and fluid flow. MAC Short Course on 'Crustal Fluids', Hand book vol.18,B.E Nesbit ed., pp.93-132

Touray J.C., Marcoux E., Hubert P. & Proust D. 1989. Hydrothermal processes and ore-forming fluids in the Le Bourneix gold deposit, France. Econ. Geol., vol. 84, pp.1328-1339

Current Research in Geology Applied to Ore Deposits.Fenoll Hach-Alí, Torres-Ruiz & Gervilla(eds)(1993).ISBN 84-338-1772-8

CONSTRAINTS OF BRITTLE TECTONICS IN THE GENESIS OF GOLD DEPOSIT OF THE LAURIERAS GOLD MINE (LIMOUSIN, FRENCH MASSIF CENTRAL): STATISTICAL ANALYSIS OF GOLD CONTENTS LINKED WITH A STUDY OF FRACTURATION CONTRIBUTION

Chalier, M. (1); Lenain, J.F. (1); Bril, H. (1) & Auriol, M. (2)

(1) Lab. de Geologie, Unite D'Analyse Sructurale et Metalogenie, 123 Av. A. Thomas, 87060 Limoges Cedex, France

(2) Societe des Mines du Bourneix, B.P. 36, 87500 St-Yrieix-La-Perche, France

Using intensive numerical technics in gold deposit of Laurieras mine reveals :
a- the presence of two populations of gold,
b- a significant correlation between the means and standard deviations of these populations, and the levels of competency and sulfides content of the different facies of gold quartz vein and its surrounding.
Cartography and structural analysis of gold contents on both populations show :
a- that gold concentration is related to secant structural directions, relative to general strike of the quartz vein and,
b- That gold deposit has occured late relative to the major phases of quartz vein emplacement.

Geological setting

The Laurieras gold deposit is located in an anatectic metamorphic series, composed mainly by aluminous sillimanite paragneiss and orthogneiss intruded by many metric to decametric granitic sills.

The mineralization is located on a N 60°E fault, dipping 60°NW and occurs in polyphased quartz lenses containing early sulfides (pyrite and arsenopyrite).

Statistical analysis

Statistical analysis has been performed on more than 10000 geochemical data (Au contents), coming from the front of two exploited lenses (East and West lenses). It shows that Au content is due to the superimposition of two distinct gold populations : a population A with low average content and low standard deviation and a population B characterized by high average content and high standard deviation.

Statistical decomposition of the mixed populations, was made applying non linear regression analysis. It is based on criteria such as :

- petrographic facies of the quartz structure as well as of its surrounding rocks
- East and West lenses
- relative enrichment of each lens

This analysis confirms the assumption of the occurence of mixed populations.

The results show that the whole site has been affected by two major metallogenetic events. Their efficiency depends on physico-mineralogic characteristics of the host : competency and sulfides content.

Randomization technics have shown a qualitative link between the early sulfides contents of the mineralized structure and its host rocks, and the gold content of population A : the facies with high sulfides contents are significantly enriched in A gold.

No direct relation between B gold enrichment and the different criteria was pointed out, but the gold content difference between both populations as well as standard deviation of population B increase significantly with competency of rocks. This fact suggests that population B results of remobilization processes controlled by facies competency.

These two populations are found in a late milky quartz facies, gently deformed, with geodic tendency, early sulfides being absent. Their presence leads to think on late deposition of the mineralization, eventually contemporaneous with the crystallization of this quartz. It certainly occurs later than the major phases of crystallization of the quartz mass.

Cartography of the gold contents in the auriferous structure

Isocontent curves are drawed from the projection of geochemical results (coming from fronts) on slice and vein maps (fighure).

Morphology of the mineralized bodies was very finely determined applying this method. It shows a great analogy with the two lenses where three column types cut each other.

Two of them are sub vertical with EW and NS directions. They cross-cut the main direction of the mineralized structure. The third one is characterized by a very low dip but its orientation is not precisely determined.

Graphically EW oriented columns are cross-cut by the two others.

Study of fracturation

- In the quartz vein
  structural synthesis of front surveys shows three main directions of fracturation :
  - N 60°E
  - EW
  - NS

- In the surrounding rocks
  analysis of microfracturation shows the three previous directions and a later N 120°E one.

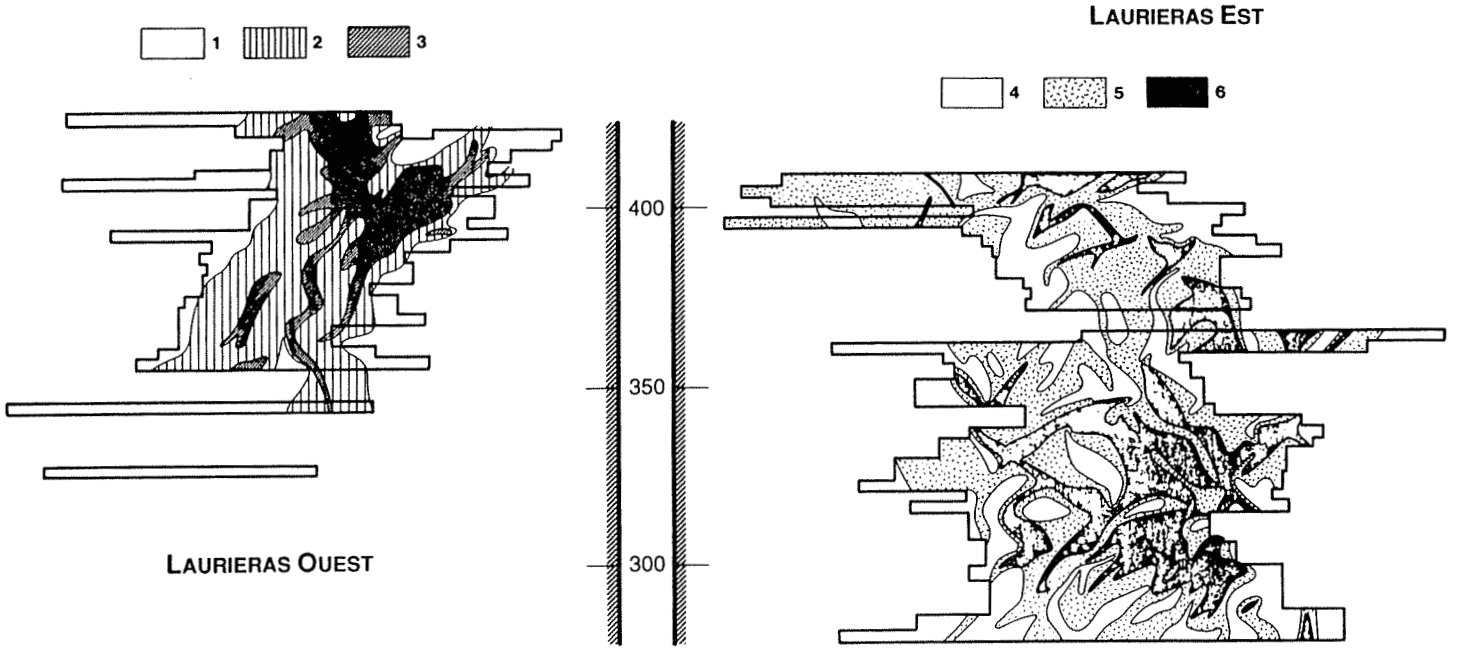

LE GISEMENT DE LAURIERAS, LENTILLE OUEST ET LENTILLE EST . COUPE LONGITUDINALE.

TENEURS MOYENNES EN OR DES FRONTS :

LAURIERAS OUEST	LAURIERAS EST
1 : 0 - 2 g/t	**4** : 0 - 4 g/t
2 : 2 - 25 g/t	**5** : 4 - 17 g/t
3 : > 25 g/t	**6** : > 17 g/t

0 50 100 m

Intersection of directions EW and NS with the direction of the vein was projected on stereographic net. It shows exactly the dip of high Au content bearing columns which were defined by graphical analysis.

Petrology of alteration

Direction N 60°E is found from millimetric to decametric scale. It is followed by white or grey quartz veinlets. The earliest phase shows ductile quartz deformation evidences. Later fractures occur in fragile field. It is characterized by late illitisation which sometimes envades the vein wallrock on several decimeters (large structures). In such zones primary minerals exist only as relics.

EW micro fractures are characterized by :

- phengitic alterations which develop on a few centimeters in wallrock. Phengite occurs as small automorphous minerals organized in a regular network in plagioclase
- this phase is crosscuted by sub horizontal veinlets containing inframillimetric phengite, but pre-existing phengites however, are not destabilized.

NS direction is characterized by millimetric to centimetric hyaline geodic quartz microveinlets. They have not developed specific alteration.

N 120°E direction corresponds to millimetric to centimetric geodic carbonates microveinlets. This important phase opens preexisting NS quartz microveinlets but does not develop specific alteration.

Conclusions

This works confirms by an independent way previous results by S. ESSARRAJ : the economic auriferous mineralization occurs as a late event.

Statistical treatment combined with a study of gold repartition in the auriferous structure and with the analysis of fracturation is of great interest for prediction of exploitation. It is a guide for prospecting economic sites.

S. ESSARRAJ, Migration des fluides, microfissuration et conditions de dépôt de l'or dans les veines de quartz aurifères, Thèse Doct. Inst. Nat. Polytech. Lorraine, 399p, 1992.

Current Research in Geology Applied to Ore Deposits. Fenoll Hach-Ali, Torres-Ruiz & Gervilla (eds) (1993). ISBN 84-338-1772-8

MINERALOGY OF PLATINUM AND PALLADIUM IN THE LAC SHEEN Ni-Cu-PGE SHOWING, ABITIBI-TEMISCAMINQUE, QUEBEC, CANADA

Cook, N.J. (1); Wood, S.A. (2); Bernhardt, H.J. (3) & Medenbach, O. (3)
(1) Mineralogisches Inst., 8700 Würzburg, Germany
(2) Dept. of Geology, University of Idaho, Moscow, Idaho, U.S.A.
(3) Inst. für Mineralogie, Ruhr-Universität Bochum, 4630 Bochum, Germany

ABSTRACT

Moncheite and michinerite are the main Pt and Pd phases within the small subeconomic Ni-Cu-PGE deposit at Lac Sheen. They are typically enclosed within silicates rather than sulphides. Textural evidence supports a hydrothermal genesis for the deposit, or at least substantial PGE remobilisation, which may have been syn-metamorphic. Within nearby boulders, which may be unrelated to the showing, an unnamed Pt-Pb-Bi-S-bearing phase has been identified. Analytical and optical data are given in this paper.

INTRODUCTION AND GEOLOGICAL SETTING

The subeconomic Lac Sheen showing is located near the village of Belleterre in the Abitibi-Temiscaminque region of Quebec (Fig. 1), immediately north of the Grenville Front; the tectonic contact between the Superior and Grenville provinces. The mineralisation is restricted to narrow lenticular bodies of metagabbro, intruded parallel to the regional schistosity of the Archean metasediments of the Pontiac Group. Intense deformation has accompanied the metamorphism. A series of quartz veins and pegmatites crosscut the sequence, with the sulphide content being highest close to the contact with these features.

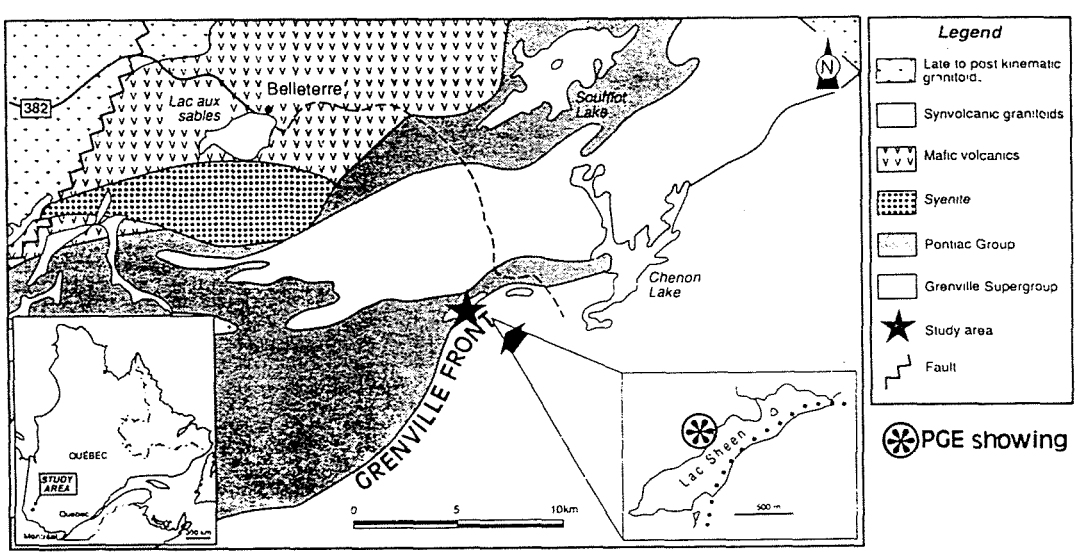

Figure 1 Geological map of the Belleterre area, Abitibi-Temiscaminque, Quebec, Canada, showing the location of the Lac Sheen Ni-Cu-PGE showing.

Concentrations of PGE, ranging up to 1 g/t (Pt+Pd) have been determined, with a Pt/Pd ratio seldom varying far from 1:1. The contents of the other PGE are extremely low. Amphibolite boulders lying some 200 m from the *in situ* mineralisation also contain 0.5 - 1 g/t (Pt+Pd) but differ by also containing up to several g/t Au, as electrum. Cook *et al.* (1992) have speculated upon the origin of these boulders, based on their appreciably different Au/(Au+PGE) signatures. They could have been transported southwestwards over considerable distances from their source during the glacial episode which has affected the region, and may be unrelated to the Lac Sheen deposit itself.

Our previous studies of the deposit (Wood and Vlassoupoulos, 1990; Cook *et al.*, 1992) have concentrated on the behaviour of the PGE when mobilised into the secondary environment. The present paper addresses the primary mineralogy of the deposit.

MINERALOGY

The mineralogy of the metagabbro units is dominated by tremolitic amphibole, with lesser chlorite, plagioclase, quartz, epidote, oxides of Fe and Ti and sulphides; chalcopyrite, pyrrhotite, pentlandite, pyrite, marcasite, galena, violarite, tetrahedrite, arsenopyrite; native bismuth, tellurobismuthinite, altaite and various bismuthotelluride minerals. In both the *in situ* and boulder samples, coarse-grained chalcopyrite and pentlandite occur as anhedral granular aggregates within the tremolite (Mg/(Mg+Fe = 0.93) - quartz gangue. Both sulphides display textural evidence of having undergone metamorphism. The rarer pyrite occurs as small porphyroblasts, commonly fractured, with the fractures infilled by chalcopyrite.

Extremely small (generally <10μm in diameter) grains of the platinum and palladium tellurides and bismuthotellurides moncheite ($Pt(Bi,Te)_2$) and michinerite (PdBiTe) occur at grain boundaries between chalcopyrite and amphibole and totally enclosed within the amphibole (Fig. 2a). None of the 24 grains observed was totally enclosed within the sulphides. The majority of the PGM grains were found in samples carrying abundant quartz veins.

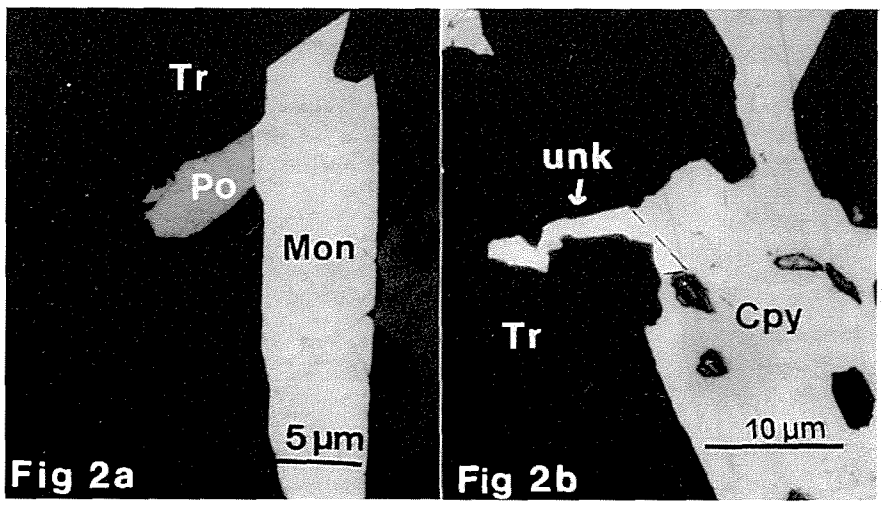

Figure 2 a. Photomicrograph of a large moncheite grain (Mon) combined with pyrrhotite (Po) in a tremolite (Tr) matrix. b. Grain of unknown Pt-mineral (unk) combined with chalcopyrite (Cpy) in tremolite (Tr) matrix.

Electron probe microanalysis of moncheite revealed a range in compositions between close to end member moncheite ($PtTe_2$) with 5 percent Bi, up to compositions with more than 20% Bi (Fig. 3). A partial solid solution

exists between moncheite and insiswaite ($PtBi_2$) according to Tarkian (1987). Moncheite contains less than 1 wt. % Pd. The michinerite contains 2.5 to 3.0 wt. % Pt and is otherwise close to ideal stoichiometric composition, PdBiTe (Table 1; see also Fig. 3). No metal alloys, sulphides or arsenides of the PGE were observed in the samples. A telluride and/or bismuthotelluride dominated PGM mineralogy is typical of comparable mafic-hosted deposits (Cabri, 1981). We noted that the Pt-bearing phase moncheite was more abundant than the Pd-bearing michinerite, thus presenting the possibility that significant Pd could be in solid solution within the abundant pentlandite, as it is in many other deposits (e.g. Paktunc et al., 1990).

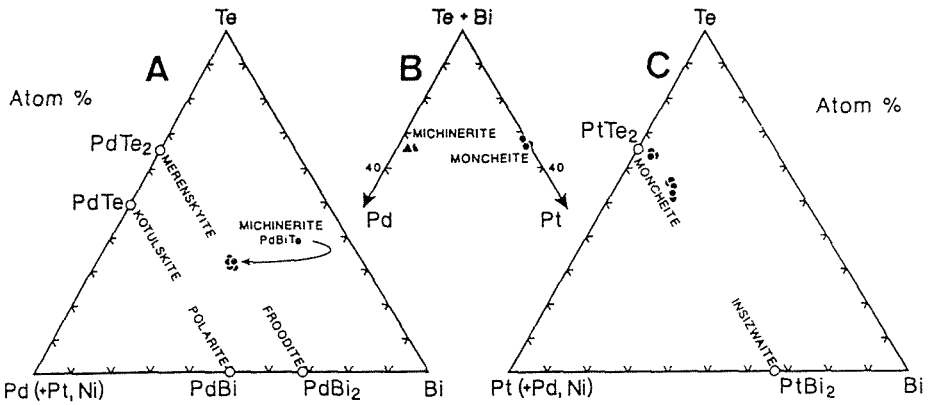

Figure 3 Composition of PGM phases in terms of A. Te-Pd(+Pt+Ni)-Bi, B. Te+Bi-Pd-Pt, and C. Te-Pt(+Pd+Ni)-Bi. Open circles are ideal stoichiometric compositions, closed circles our analyses.

Within the boulders, a Pt-bearing phase was identified, whose composition (Table 1) does not match up to any currently known phase. Twenty-two grains of the phase, the largest of which is 18 μm in diameter were observed. The phase is white-grey in colour, non-pleochroic and anisotropic without internal reflections and is located totally enclosed within the amphibole or at the chalcopyrite-amphibole grain contacts (Fig. 2b). The formula of this mineral phase conforms closely to $PtBi_2.PbS.2Bi_2(S,Se)_3$. Optical and scanning electron microscopy of the phase shows it not to be an intergrowth of two or more phases. Reflectance spectra of the phase in air and immersion oil are also unique. Ongoing work is focussing on obtaining full X-Ray spectra on this phase, in order to determine the structure.

Table 1 Representative electron probe microanalyses of selected PGM phases.

	Michinerite	Bi-poor Moncheite	Bi-rich Moncheite	Unnamed Phase
Pd	22.12	0.78	0.23	0
Pt	2.85	37.85	39.78	10.51
Ni	0	0.30	0	0.12
Te	28.46	53.56	40.38	0
Bi	46.61	5.75	20.38	66.11
Pb	0	0	0	10.18
Fe	0.24	0.08	0.87	0.87
Cu	0	0	0	0.30
S	0	0	0	10.04
Se	0	0	0	1.79
TOTAL	100.28	98.32	101.64	99.92

DISCUSSION

Although the PGM occur in the same rock units as the sulphides, they do not appear to be intimately related to one another. The PGM chiefly occur within the metamorphic silicate minerals. That some of the PGM are combined with chalcopyrite is probably more due to that mineral acting as a nucleation surface rather than impying a genetic relationship. The textural association of the PGM at the Lac Sheen showing, with tremolite rather than sulphides support a hydrothermal event at some stage in the history of the deposit. This was possibly part of the regional upper greenschist - lower amphibolite grade metamorphic event and played a significant role in the distribution of PGE in the showing as they are seen today. Evidence for the hydrothermal genesis or redistribution of PGE in various deposits has been presented by a number of authors (e.g. McCallum *et al.*, 1976; Rowell and Edgar, 1986; Nyman *et al.*, 1990; Mogessie *et al.*, 1991), thus proving the pioneering ideas of Stumpfl (1974) and Stumpfl and Tarkian (1976) that late hydrothermal fluids could indeed play a very significant role. Mountain and Wood (1987), Wood et al. (1989, 1991) and many others have, in recent years, demonstrated by experiment, not insignificant solubilities of the PGE in hydrothermal solutions.

REFERENCES

Cabri, L.J. 1981. Platinum Group Elements: Mineralogy, Geology, Recovery. Can. Inst. Min Metall., Spec. Vol. 23, 267p.

Cook, N.J, Wood, S.A. & Zhang, Y. 1992. Transport and fixation of Au, Pt and Pd around the Lac Sheen Cu-Ni-PGE occurrence in Quebec, Canada. J. Geochem. Expl. 46, 187-228.

McCallum, M.E., Loucks, R.R., Carlson, R.R., Cooley, E.F. & Doerge, T.A. 1976. Platinum metals associated with the hydrothermal copper ores of the New Rambler Mine, Medicine Bow Mountain, Wyoming. Econ. Geol. 71,1429-1450.

Mogessie, A., Stumpfl, E., & Weiblen, P.W. 1991. The role of fluids in the formation of platinum group minerals, Duluth Complex, Minnesota: Mineralogic, textural and chemical evidence. Econ. Geol. 86, 1506-1518.

Mountain, B.W. & Wood, S.A. 1988. Chemical controls on the solubility, transport and deposition of platinum and palladium in hydrothermal solutions: A thermodynamic approach. Econ. Geol. 81, 492-510.

Nyman, M.W., Sheets, R.W. & Bodnar, R.J. 1990. Fluid-inclusion evidence for the physical and chemical conditions associated with intermediate temperature PGE mineralisation at the New Rambler deposit, Southeastern Wyoming. Can. Mineral. 28, 629-638.

Paktunc, A.D., Hulbert, L.J. & Harris, D.C. 1990. Partitioning of the platinum- group and other trace elements in sulfides from the Bushveld Complex and Canadian occurrences of nickel-copper sulfides. Can. Mineral. 28, 475-488.

Rowell, W.F. & Edgar, A.D. 1986. Platinum-group element mineralization in a hydrothermal Cu-Ni-sulfide occurrence, Rathbun Lake, Northeastern Ontario. Econ. Geol. 81, 1272-1277.

Stumpfl, E.F. 1974. The genesis of platinum deposits: further thoughts. Minerals Science Engineering 6, 120-141.

Stumpfl, E.F., & Tarkian, M. 1976. Platinum genesis: New mineralogical evidence. Econ. Geol. 71, 1451-1460.

Tarkian, M. 1987. Compositional variations and reflectance of the common platinum-group minerals. Mineral. & Petrol. 36, 169-190.

Wood, S.A. & Vlassoupoulos, D. 1990. The dispersion of Pt, Pd and Au in surficial media about two PGE-Cu-Ni prospects in Quebec. Can. Mineral. 28, 649-663.

Wood, S.A., Mountain, B.W., Fenlon, B.J. 1989. Thermodynamic constraints on the solubility of platinum and palladium in hydrothermal solutions, reassessment of hydroxide, bisulfide and ammonia complexes. Econ. Geol. 84, 2020-2028.

Wood, S.A., Mountain, B.W., & Pan, P. 1992. Recent advances in the aqueous geochemistry of platinum, palladium and gold. Can. Mineral.

Current Research in Geology Applied to Ore Deposits.Fenoll Hach-Alí, Torres-Ruiz & Gervilla(eds)(1993).ISBN 84-338-1772-8

TIMING OF GOLD MINERALIZATION IN CONTRASTING METAMORPHIC TERRAINS: EVIDENCE FOR HETEROGENEOUS DEFORMATION AND DIACHRONOUS METAMORPHISM, SOUTHERN CROSS PROVINCE, WESTERN AUSTRALIA

Dalstra, H.J. & Ridley, J.R.
Key Centre for Strategic Mineral Deposits, Dept. of Geology, The University of Western Australia, Nedlands, WA 6009, Australia

ABSTRACT: Gold mineralisation in amphibolite facies terrains of the Southern Cross greenstone belt occured syn-peak metamorphism and early in the structural history. In contrast, mineralisation in sub-greenschist facies terrains in the Marda greenstone belt was post metamorphism and relatively late in the structural history. Assuming that gold mineralisation was a discrete event in the Archean Yilgarn Block, as indicated by reconnaissance geochronology, this suggests that metamorphism and deformation were both heterogeneous and diachronous in the Southern Cross Province.

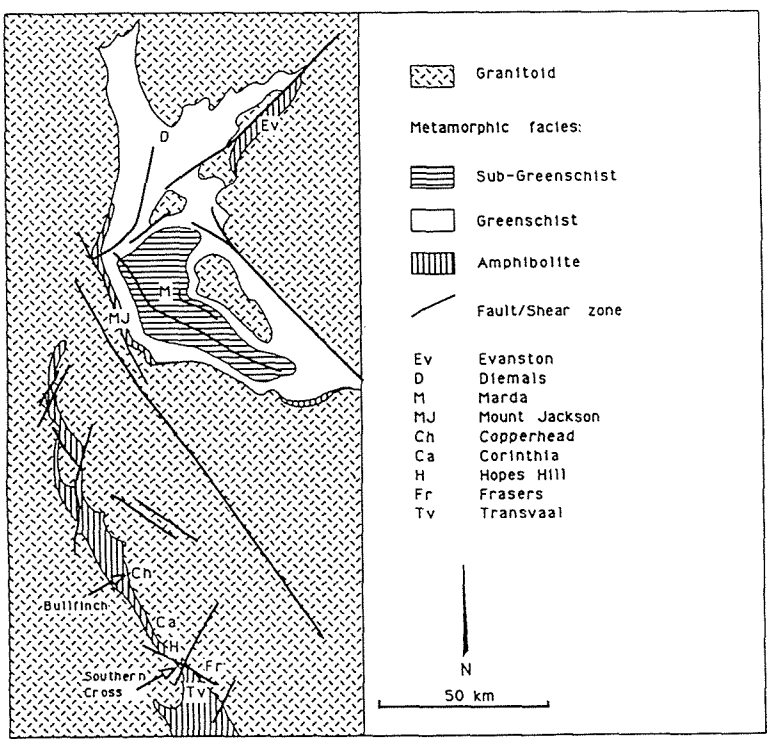

Figure 1: Simplified geological map outlining the major metamorphic terrains and showing the locations of the deposits referred to in the text.

INTRODUCTION

Archean lode-gold deposits are generally structurally controlled gold-only deposits in which gold occurs both as native gold in

quartz veins and as an integral part of wallrock alteration. In general, the timing of gold mineralisation is late in the structural history of the Archean terrains, and wallrock alteration and associated gold mineralisation occured broadly within a regional metamorphic event (Groves et al. 1990). Lead model ages on gold-related sulphides from all provinces of the Yilgarn Block (Browning et al. 1987) and high precision geochronological data on mineralisation are consistent with a broadly synchronous gold mineralisation event late in the Archean evolution (McNaughton et al. 1990).

The Southern Cross and Marda greenstone belts are adjacent Archean greenstone belts located in the Southern Cross Province in the Central Yilgarn Block, Western Australia. In terms of their intensity of deformation and metamorphic grade, they form two contrasting belts in the granitoid-dominated terrain (Figure 1). The Southern Cross belt is a narrow and intensely deformed greenstone belt of predominantly amphibolite metamorphic grade, and the Marda belt has an overall basin-shape geometry with less intense deformation and generally lower (sub-greenschist) metamorphic grade (Ahmat 1986, Mueller 1988).

MINERALISATION IN AMPHIBOLITE FACIES METAMORPHIC TERRAINS.

The structural history of the Southern Cross belt can be summarised into: **D1** isoclinal folding, **D2** shearing and tightening of D1 folds, **D3** conjugate strike-slip faulting and **D4** reactivation of D1-D3 structures (Mueller, 1988, Barnicoat et al., 1991, Bloem & Ridley, 1991). At Southern Cross, economic gold mineralisation occurs in D2 shear zones in the Transvaal deposit and in the Frasers, Hopes Hill, and Corinthia deposits (Bloem & Ridley 1991) with major ore shoots plunging parallel to mineral and stretching lineations. Near Bullfinch, mineralisation occurs in D1 drag folds and D2 shears in the Copperhead deposit with major ore shoots plunging parallel to D1 fold axes.

Proximal alteration assemblages and ore textures (sulphides enclosed by syn-kinematic metamorphic porphyroblasts) suggest syn-peak metamorphic timing of gold mineralisation. Temperature conditions during mineralisation and metamorphism, as determined by garnet-biotite, garnet-cordierite and arsenopyrite geothermometry, were in the order of 500-580°C at metamorphic pressures below 3.5 kbars. (Table 1)

MINERALISATION IN SUB-GREENSCHIST FACIES METAMORPHIC TERRAINS.

The structural history of the central Marda belt can be summarised as:

D1 tight to isoclinal folding, resulting in E-W trending map-scale upright folds.

D2 buckle folding, resulting in smaller scale N-S trending upright folds with an S2 axial planar fabric.

D3 Brittle to brittle-ductile faulting with fault zones following E-W trending stratigraphic contacts characterised by strong chlorite-muscovite fabrics. Offset on the faults is in the order of a few meters.

D4 Conjugate brittle faulting.

Gold mineralisation in the core of the Marda belt is hosted by (ultra)mafic volcanics, BIF, and acid volcanics which were only weakly affected by regional metamorphism (Prehnite-Pumpellyite metamorphic grade). Scattered mineralisation occurs for

approximately 6 km along strike in a sinistral D3 fault which follows subvertical E-W trending stratigraphic contacts, but curves into a N-S trending thrust fault before it terminates.
Proximal alteration assemblages in wallrock adjacent to the fault indicate similar temperature conditions during alteration and gold mineralisation to those during regional metamorphism. More specifically, chlorite geothermometry yields temperatures of 260°C-300°C. Alteration minerals clearly overprint regional metamorphic assemblages (Table 1).

Table 1: Summary of characteristics of some gold deposits in the Southern Cross Province with emphasis on those within the amphibolite facies terrains of the Southern Cross Belt and the prehnite-pumpellyite facies terrains of the Marda Belt.

Deposit	Host Rock	Mineralised Structure	Regional Metamorphic Assemblages	Proximal Wallrock Alteration
Southern Cross Belt				
Transvaal	meta-sedimentary & ultramafic rocks	D2 shear zone	biotite-muscovite-andalusite-cordierite-garnet (staurolite) tremolite-chlorite	biotite-pyrrhotite-loellingite-arsenopyrite -chalcopyrite-tellurides -native gold/silver
Hopes Hill, Corinthia, Frasers : Bloem & Ridley (1991)	mafic/ ultramafic volcanics	D2 shear zone	(act.)hornblende-An. rich plagioclase-ilmenite tremolite-chlorite-olivine	diopside-calcite-biotite -scheelite-pyrrhotite-pyrite-chalcopyrite-galena-native gold
Copperhead (Bullfinch)	mafic volcanics, BIF	D1 drag folds, D2 shears	actinolite-hornblende-An. rich plagioclase -ilmenite grunerite biotite-cordierite-musc	dolomite-calcite-biotite tremolite-actinolite pyrite-pyrrhotite-chalcopyrite-galena-native gold
Marda Belt				
Great Unknown (Marda)	high-Mg basalts, BIF	D3 sinistral fault	chlorite-albite-epidote prehnite-calcite (pumpellyite)	chlorite-muscovite-siderite-ankerite pyrite-arsenopyrite-gersdorffite-galena native gold
Allens Find (Marda)	acid volcanics	D3 fault (thrust)	sericite-chlorite-albite-epidote	chlorite-muscovite-siderite-ankerite pyrite native gold

DISCUSSION

Structural schemes for the Southern Cross and Marda greenstone belts are different, with the Marda belt preserving an early phase of E-W folding. D1-D3 in the Southern Cross belt and D2-D4 in the Marda belt were roughly contemporaneous, and present progressive deformation in an E-W compressive regime.
Timing of gold mineralisation in the amphibolite facies Southern Cross greenstone belt is late-D1, syn-D2, and syn-peak metamorphism, whereas timing of mineralisation in the prehnite-pumpellyite facies

Marda belt is syn-D3 and late-post-peak metamorphism. Mineralisation in the Southern Cross belt is synchronous with a major phase of deformation whereas mineralisation in the Marda belt is related to a minor deformation phase.
If gold mineralisation was a craton-scale, relatively short lived event in the Yilgarn Block (Groves et al. 1990), this suggests that both early deformation and metamorphism were heterogeneous and diachronous in low- and high-grade metamorphic terrains in greenstone belts of the Southern Cross Province.
The central Marda belt possibly preserves ocean-floor metamorphism, while metamorphism in the Southern Cross belt is better characterised as regional metamorphism or regional-scale contact metamorphism related to the vast amount of granitoids intruded into the region.

ACKNOWLEDGEMENTS
HJD is indebted to Prof. David Groves and Erik Bloem for suggestions and comments on this paper. HJD is the recipient of OPRS, URS, and AGSO Research Awards. Burmine Ltd and Reynolds Australia Mines Pty Ltd are gratefully acknowledged for their support of research on the Copperhead and Transvaal deposits.

REFERENCES
Ahmat A L. 1986. Metamorphic patterns in the greenstone belts of the Southern Cross Province, Western Australia. Geol. Survey West.Aust. Prof. Papers: 1-21

Barnicoat A C, Fare R I, Groves D I, McNaughton N J. 1991. Syn-metamorphic lode-gold deposits in high grade Archean Settings. Geology 19: 921-924

Bloem E M, Ridley J R. 1991. Structural controls on a gold deposit within a deformation zone at Hopes Hill, Southern Cross Province, Western Australia. Mineralisation in a zone of flattening or of simple shear? In Extended Abstracts, Structural Geology in Mining and Exploration, Geology Department (Key Centre) & Univ. Extension, Univ. West. Aust. publication no 25: 120-122

Browning P, Groves D I, Blockley J G, Rosman K J R. 1987. Lead isotope constraints on the age and source of gold mineralization in the Archean Yilgarn Block, Western Australia. Economic Geology 82: 971-986

Groves D I, Knox Robinson C M, Ho S E, Rock N M S. 1990. An overview of Archean lode-gold deposits. In Gold Deposits of the Archean Yilgarn Block, Western Australia: Nature, Genesis and Exploration Guides. Geology Department (Key Centre) & Univ. Extension, Univ. West. Aust. Publication, No 20: 2-18

McNaughton N J, Cassidy, K F, Groves D I, Perring C S. 1990. Timing of Mineralization. In Gold Deposits of the Archean Yilgarn Block, Western Australia: Nature, Genesis and Exploration Guides. Geology Department (Key Centre) & Univ. Extension, Univ. West. Aust. Publication, No 20: 221-226

Mueller A G, 1988. Archean Gold-Silver deposits with prominent calc-silicate alteration in the Southern Cross greenstone belt, Western Australia. Analogues of Phanerozoic skarn deposits. In: Advances in Understanding Precambrian Gold Deposits, Geology Department & Univ. Extension, Univ. West. Aust. Publication, No 12: 141-163.

Current Research in Geology Applied to Ore Deposits.Fenoll Hach-Alí, Torres-Ruiz & Gervilla(eds)(1993).ISBN 84-338-1772-8

THE MOBILIZATION OF PGE IN LOW-TEMPERATURE ENVIRONMENTS: IMPLICATIONS FOR SEDIMENT-HOSTED STRATABOUND COPPER DEPOSITS

Dowling, K.(1); Bierlein, F.P.(1); Walshe, J.L.(2); Wallace, M.W.(1); Gostin, V.A.(3) & Keays, R.R. (4)

(1) School of Earth Sciences, University of Melbourne, Australia
(2) Dept. of Geology, Australian National University, Canberra, Australia
(3) Dept. of Geology and Geophysics, University of Adelaide, Australia
(4) Geology Dept., Laurentian University, Sudbury, Canada

The economic significance of sediment-hosted stratabound copper deposits ('Kupferschiefer-type') is not only related to consistent copper grades of considerable lateral extent but also to the presence of ancillary metals such as cobalt and silver which are won in variable amounts (e.g. The Zambian Copper Belt and White Pine, Michigan). Research has identified a Platinum Group Element (PGE) association in this style of deposit (Mountain and Wood, 1988). Due to the paucity of information relating to PGE mobility in low-temperature environments, the potential gain from PGE exploitation in such environments has not been actualised.

With this in mind, a study was launched to assess the chemical association between PGE and copper in low-temperature sedimentary environments. The widely dispersed Late Proterozoic Acraman impact ejecta horizon and its host marine shales in the Adelaide Geosyncline provides an environment where metal signatures are easily traceable and where the source of the metals is known. The ejecta horizon was formed when the Middle Proterozoic dacitic volcanics in the Gawler Ranges, central South Australia, were impacted by a very large meteorite (ca. 4km in diameter). The resulting structure, now represented by Lake Acraman, is Australia's largest meteorite impact structure. Debris from the impact was strewn over many hundreds of kilometres, some falling into the shallow sea of the Adelaide Geosyncline, some 300km to the east of the impact site (Fig. 1).

The Bunyeroo Formation (~600Ma) which hosts the ejecta horizon consists of monotonous deep-shelf red and pyritic shales, with minor interbedded concretionary carbonates. The ejecta horizon is typically 0 to 40cm in thickness and is composed of a basal clastic layer of poorly-sorted, angular fragments which locally reach boulder size. It is in turn overlain by a thin shale layer containing abundant coarse sand-size fragments and a graded layer which fines up from coarse-medium sand to a fine muddy sand. All clasts and most sand-sized fragments have been derived from a pink to red porphyritic volcanic rock, similar to that currently exposed at the Lake Acraman impact site. The ejecta horizon is almost invariably enveloped by a green shale alteration halo which ranges in thickness from a few millimetres to several metres.

The ejecta horizon and the green shale alteration envelope exhibit strong, but variable PGE enrichment with Ir (up to 100 times) and Pt (up to 300 times) enriched relative to the hosting red shale background values (Wallace *et al.*,1990; Fig. 2). Where the green shale envelope is most narrow, metal enrichment is moderate and the PGE exhibit chondritic ratios. In contrast, a wider green alteration envelope yields significantly greater PGE, Cu and Au enrichments. In this case, Cu and Pt are well correlated and the PGE exhibit strong non-chondritic ratios.

Thin green shale layers and isolated green reduction spots occur stratigraphically above and below the Acraman impact ejecta horizon within the red shale sequence. These do not show non-chemical evidence of meteoritic contribution, though are similarly enriched in Ir and Pt, as well as Cu, V, Zn, and Ni. Their stratigraphic position relative to the ejecta horizon appears to have no influence on the degree of PGE enrichment.

The green shale halo associated with the ejecta horizon and the green shales at other stratigraphic levels have a similar chemical signature, suggesting a similarity in the enrichment process. The very high Pd/Ir, Pt/Ir and Au/Ir ratios of all the green shales, together with the Cu-PGE correlation are not satisfactorily explained by a single source extraterrestrial origin. The ejecta horizon, thin green shale horizons, and reduction spots all contain a meteoritic PGE component such that mobilization of the PGE, presumably by low-temperature fluids, contributed to its enrichment.

The Acraman ejecta horizon reveals many features which are relevant to a depositional model for a sediment-hosted stratabound copper deposit. Both are characterized by an abrupt or diffusional chemical transition boundary, which in our case study is identified as an anoxic, sulphur-rich green bed adjacent to an oxic red bed. The depositional model proposed to account for this phenomena is a two-fold process:

•**Within the thick red bed sedimentary pile, particular beds are metal-enriched by primary basinal processes**. Reducing or low Eh-fluids, derived from deep within the sedimentary basin, are preferentially channelled along zones of enhanced porosity and permeability. These fluids reduce the ferric iron in the red shales to ferrous iron which is then removed in solution, leaving the shales with their distinctive green colour. The Acraman ejecta horizon and the isolated green beds and reduction spots are good examples of this.

•**The circulation of oxidising fluids within the sedimentary pile results in the development of a redox interaction front.** Low-temperature (160 to 220°C) saline fluids, saturated with atmospheric oxygen (Jaireth, 1992), are capable of mobilising significant amounts of PGE and Au as chloro-complexes. Metal movement is by both infiltration (in zones of higher permeability) and diffusion (in fine grained compact sediments). Pre-existing green beds act as chemical traps where metal

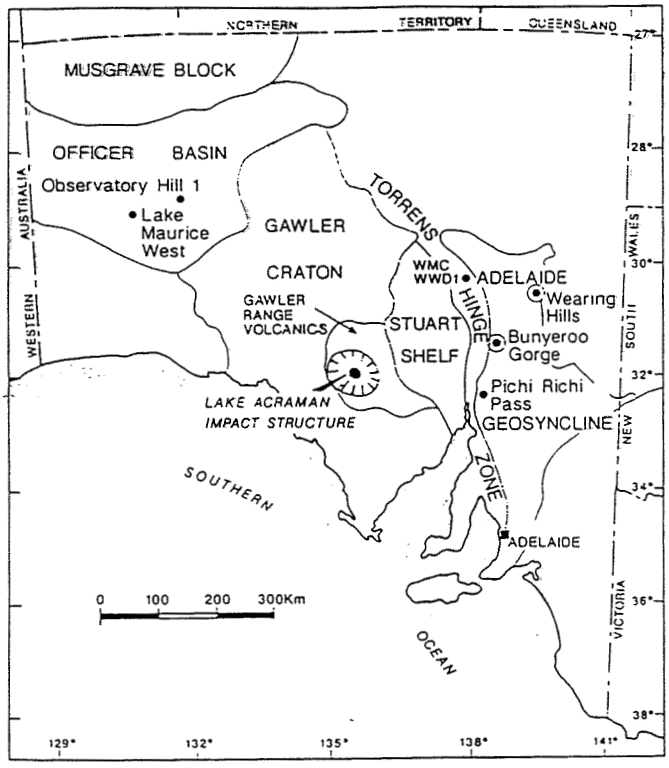

Figure 1: Location map the Adelaide Geosyncline and the meteorite impact site at Lake Acraman.

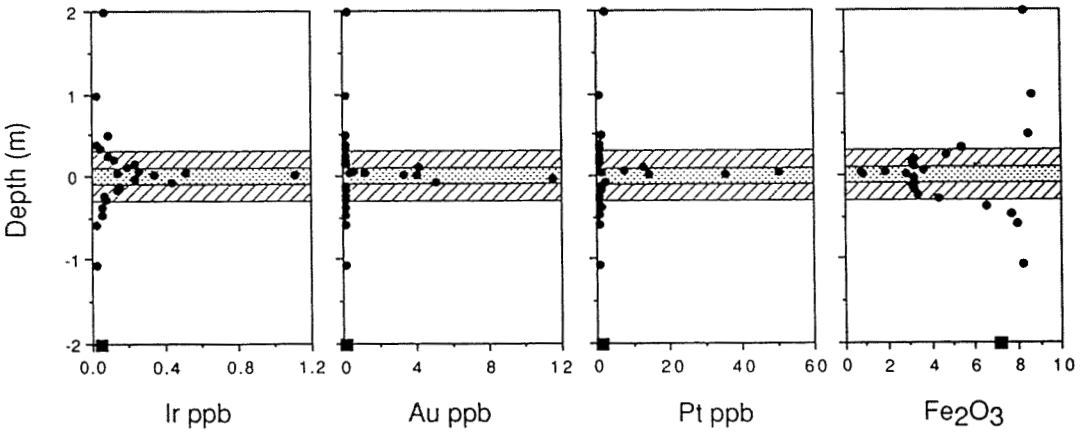

Figure 2: Element abundance profiles across the ejecta horizon: Ejecta horizon is speckled; Green shale envelope is stripped; Red shale has no pattern. Depth is recorded as distance above and below the Ejecta horizon.

deposition is induced. Earlier precipitated metals are redissolved in response to oxidation state and fluctuations in fluid-rock ratio resulting in spatially restricted, though ore-grade quantities of PGE being precipitated.

Additional features identified as significant in the generation of sediment-hosted stratabound copper deposits and identified in the Acraman ejecta horizon include:

1. Development is probably restricted to sedimentary basins which were active after the oxygenation of the planet.

2. A thick red bed basin sequence which permits a bimodal metal source. The mental source may be the sediments themselves in addition to a meteoritic or igneous component.

3. Its formation occurred in low paleolatitudes.

4. The unit in question is well defined and zoned.

5. Abundant original sulphur is available in the precursor strata.

The recognition of significant PGE mobility in low-temperature environments has several important genetic and exploration implications. Economically important accumulations of the PGE and metals might be anticipated in environments in which such solutions entered redox environments, e.g. sediment-hosted stratabound copper deposits. An exploration rationale should be formulated with this in mind.

References:

Jaireth, S., 1992. The calculated solubility of platinum and gold in oxygen-saturated fluids and the genesis of platinum-palladium and gold mineralization in the unconformity-related uranium deposit. Mineralium Deposita 27 (1): 42-54.

Mountain, B. W. and Wood, S.A. 1988. Chemical Controls On the Solubility, transport and deposition of platinum and palladium in hydrothermal solutions: A thermodynamic approach. *Economic Geology,* 83:492-510.

Wallace, M.W., Gostin, V.A. and Keays, R.R., 1990, Acraman impact ejecta and host shales: Evidence for low-temperature mobilisation of iridium and other platinoids: Geology, v. 18, p. 132-135.

Current Research in Geology Applied to Ore Deposits.Fenoll Hach-Alí, Torres-Ruiz & Gervilla(eds)(1993).ISBN 84-338-1772-8

GOLD-BEARING QUARTZ VEINS IN A LITHOSPHERIC SHEAR ZONE (S.W. HOGGAR, ALGERIA)

Ferkous, K. (1) & Leblanc, M. (2)
(1) EREM, PB 102 Boumerdes, Algerie
(2) CNRS, CGG, 34095 Montpellier, France

ABSTRACT : The Amesmessa-Tirek gold district is located along a vertical and N-S trending crustal-scale ductile shear zone which corresponds to a late Proterozoïc dextral strike-slip fault. In Amesmessa, most of the ultramylonites proceeds from felsic dikes emplaced during shearing. Gold-rich quartz veins are laminated parallel to foliation (native gold is associated with pyrite and galena along late shear planes) and they are surrounded by a carbonate-sericite hydrothermal alteration halo ; late undeformed E-W quartz veins are gold-poor. Shear-related fluids are parental H_2O-CO_2-rich fluids for gold mineralization and associated alteration ; a deep-seated source for the CO_2 supply is suggested by the presence of scarce carbonatite dikes within the shear zone.

INTRODUCTION

Shear zone hosted gold deposits are economically important features mainly in Archean and Proterozoic shields ; gold bearing shear zones are generally small, 10-50 km long and 0.1-1 km wide, and gold mineralization is typically restricted to narrow sets of third-order shear veins (Poulsen and Robert, 1989). One of the main shear zones of the Tuareg shield trends N-S over 900 km and includes several gold occurences of vein-type along a 100 km long segment ; among them, the Amesmessa prospect exhibits both gold-rich shear veins and gold-poor extensional veins. The aim of this work is to describe the relationships of the different types of gold veins with the shear structures and to discuss the origin of the mineralizing fluids.

GEOLOGICAL SETTING AND STRUCTURE OF THE HOST SHEAR ZONE

The N-S framework of the Tuareg shield (Algeria) was built during Pan African tectonics (around 600 Ma) which produced N-S trending folds with associated metamorphism grading from greenschist to amphibolite facies (Bertrand and Caby, 1978). The contact between the central Archean In Ouzzal block (metamorphosed in granulite facies conditions during the Eburnean orogeny, 2000 Ma) and the eastern part of the Pan African belt corresponds to a major shear zone, N-S trending and outcropping over 900 km long. This late Pan African structure is overprinted by the Ordovician cover, North and South of the Tuareg shield. Several gold occurences have been discovered and investigated in the southernmost part of this shear zone by the Mining and Exploration Research Algerian National Office (SONAREM then EREM) ; among them, the most important are the Tirek prospect (Attoum, 1983 ; Kouadri, 1983) and the Amesmessa prospect (Kouadri, 1983 ; Ferkous, 1991), 14 and 9 km long respectively.

In Amesmessa, the shear zone is from 1 to 2 km in width and exhibits an asymetrical structure : from West to East, there is a progressive gradation from ultramylonites to mylonites then, through protomylonites, to the Proterozoic gneisses of the Pan African eastern compartment which are nealy parallel ; whereas the western contact of the ultramylonite unit (300 m in width) with the Archean block is sharp and discordant. The ultramylonite foliation is roughly N-S trending and subvertical, stretching lineations are subhorizontal and mylonite structures indicate a dextral transcurrent movement.

The ultramylonite unit mainly consists of black phyllonites comprising quartz, K-feldspar and brown biotite with accessory pyrite, calcite, pistacite, Ti-oxides, zircon and apatite. The development of brown biotite along foliation plane and in pressure shadow zones indicates that shearing occured in biotite subfacies metamorphic conditions (350-400°C) ; green biotite then Fe-chlorite crystallized during last shear movements. Ultramylonites include light layers and lenses of still recognizable felsic material which progressively grades to dark ultramylonites by increasing development of biotite. Felsic rocks with granophyric textures are locally very abundant forming swarms of N-S trending lenticular dikes emplaced during shearing ; they may constitute up to 80 vol.% of the shear zone. Dikes and bodies of mafic rocks (diabase, gabbro, pyroxenite) are subordonate and show a metamorphic assemblage characterized by the presence of zoisite and

amphibole. There are also scarce foliated dikes of phlogopite-olivine-bearing carbonatite similar to those which crosscut the granulitic foliation of the Archean In Ouzzal block.

Proterozoic rocks of the eastern compartment were folded during Pan African tectonics in lower amphibolite facies metamorphic conditions ; up to 2 km away from the shear zone, foliation and lineation are parallel to those of ultramylonites, then the foliation progressively becomes flat. The western Archean block escaped penetrative deformation during shearing and shows only a 50 m thick cataclastic zone along its border.

QUARTZ VEINS, GOLD MINERALIZATION AND HYDROTHERMAL ALTERATION

In Amesmessa, the economic gold-bearing quartz veins are N-S trending and are located in the narrow ultramylonite band. They constitute swarms of veins with horsetail endings and oblique veinlets which may cut across the ultramylonite foliation ; they clearly correspond to the opening of oblique-extension veins in a dextral shear system. The main veins are, on average, less than 1 m in thickness and from 150 to 300 m long ; their vertical extension seems to be more important. They exhibit a lenticular ribboned structure of alternatively white and dark grey quartz ribbons, separated by late shear planes which are underlined by ferruginous coatings and punctuated by small solution voids. The N-S quartz veins display porphyroclastic textures with a N-S stretching direction ; plastic deformation and secondary granulation are more developed in the dark grey ribbons. Local cross-cutting relationships between the two types of quartz, as well as stylolite-like indented contacts, suggest a multistaged evolution including a succession of crystallization and pressure-dissolution stages. Several generations of heterogeneous CO_2-H_2O-rich fluid inclusions are present in the quartz porphyroclasts. At last, euhedral quartz crystals are covered with aragonite and chalcedony in solution cavities developed along late shear planes.

Ore minerals (pyrite, galena, native gold, sphalerite) are no abundant, they reach up to 3 vol. % in the fine-grained dark grey quartz ribbons where they are located along the intergranular joints. Sulfides are undeformed. Small gold flakes are generally present around or in the vicinity of the galena grains, but most of gold occures in late solution cavities as irregular leaves covering quartz crystals ; both gold types display similar silver contents (8-10 wt% Ag). Small dots of gold are also present on limonitized pyrite crystals suggesting that pyrite is a gold carrier mineral.

The E-W quartz veins are located in the mylonite zone, eastward from the ultramylonite band, they cross-cut the mylonite foliation. They correspond to banded veins of white quartz, about 1 m thick, and show open-space filling textures (quartz comb texture, vugs, wallrock fragments) which indicate a N-S opening vector ; quartz is undeformed. These E-W veins display low gold contents which are bound to a primary sulfide association (chalcopyrite, galena, pyrite, sphalerite), no native gold has still been observed.

The N-S quartz veins are always enveloped by a light coloured hydrothermal halo, 2 to 7 m in thickness, whereas the E-W quartz veins show no marked alteration in the enclosing rocks. The hydrothermal mineral assemblage (carbonate-sericite-albite-quartz-pyrite) overprints the ultramylonite foliation and corresponds to a retrogressive stage which postdates peak metamorphism of the main shearing episode. This hydrothermal alteration mineral assemblage corresponds to a low grade greenschist facies and to temperatures about 250°C (Sander and Enaudi, 1990). Pyrite is more abundant (up to 5 wt%) along the borders of the quartz veins and low gold contents are found there ; carbonate composition changes from Fe-dolomite to ankerite, then Mg-siderite, away from the quartz veins.

GEOCHEMICAL DATA

Following the hypothesis of a felsic rock derivation for the ultramylonites, there are apparent Fe-K-Ti enrichments and SiO_2 losses during the formation of the biotite-rich ultramylonites. Assuming that Ti is an immobile element (TiO_2/P_2O_5 is unvariant), a mass balance calculation mainly shows a strong loss of silica which implies an important mass reduction from rhyolite to ultramylonite during shearing (about 55 %). Most of the investigated rocks show enrichments in LREE, Au (>10 ppb) and S (100 to 1100 ppm), suggesting a pervasive hydrothermal alteration in the shear zone.

During the hydrothermal alteration related to the mineralization, the metasomatic changes are characterized by a strong supply of CO_2, up to 20 wt%, SiO_2 and CaO. Although important mass and volume changes may be calculated, there is no structural evidence of significant inflation structures in the alteration zones, except for the presence of a discrete network of fractures along which the carbonate-sericite-pyrite alteration is more important. Ultramylonites, hydrothermally altered rocks and quartz veins show similar REE patterns, characterized by a LREE enrichment (CN La/Er = 15 to 40) with a progressive dilution of REE contents from ultramylonite to quartz vein.

Barium is the unique notable trace element related to the mineralization (150-250 ppm) ; Au-Pb-Ag are positively correlated and there are only very low As contents (<10 ppm). The E-W veins are distinct from the N-S veins by their low Ba and high Cu contents.

DISCUSSION

The shear zone acted as pathway for magmas originated either from crustal (felsic magmas), upper mantle (mafic magmas) or deeper source zone (carbonatite). Thermal dissipation of sheared rocks and of associated magmatic intrusions can heat a large volume of fluids along this major lithospheric structure. The development of brown biotite during shearing indicates that high temperature (350-400°C) hydrous fluids were present, allowing the metasomatic transformation of felsic rocks into ultramylonites. Gold mineralization, in Amesmessa, is located within the western ultra mylonite band which is in contact with the colder and more rigid Archean In Ouzzal block ; this western border which is characterized by strong rheological and thermal gradients probably played an important role in channeling fluids.

The N-S quartz veins formed late in the structural evolution of their host shear zone : they locally cut the ultramylonite foliation and postdate peak metamorphism, as the hydrothermal mineral assemblage (lower grade greenschist facies) replace the metamorphic assemblage of the ultramylonite (upper grade greenschist facies) ; nevertheles quartz suffered plastic deformation, shearing, dynamic dissolution and recristallisation. They probably correspond to dilational jogs, approximatively parallel to the foliation, formed during the late increments of dextral shearing and promoted by structural inhomogeneities and competency contrasts within the ultramylonite foliation. Fluids were drawn in these dilatant structures and triggered the opening of the veins ; from structural evidence, the N-S quartz vein were formed by repeated opening and shearing stages. The formation of shear veins during the transition from ductile to brittle deformation is a common feature in most shear zone related gold districts (Poulsen and Robert, 1989).

The E-W quartz veins may correspond to coeval transverse structures opened, perpendicular to foliation, in the less ductile mylonite zone ; nevertheless, their undeformed quartz textures and their particular ore mineral assemblage, including copper sulfides and without native gold, suggest a later formation, in the same deformational regime, and differences in fluid composition.

From geochemical data, the most obvious fluid source for the formation of the quartz veins lies in the fluids which accompayied ductile deformation in ultramylonites ; they were efficiently channelled in these late brittle structures (Guha *et al*, 1983). Along the borders of the veins, porosity increased in response to microcrack propagation during the phase of rising hydraulic pressure ; fluid/rock interactions promoted carbonate alteration in the enclosing rocks. The formation of carbonate is indicative of CO_2-rich fluids as attested by the presence of heterogeneous CO_2-H_2O fluid inclusions in quartz. Mineral changes correspond to the breakdown of biotite and alkali feldspar as shown in the following reaction :

Quartz + Sodic Plagioclase + Biotite + CO_2 + H_2S = Fe-Mg Carbonate + Sericite + Albite + Pyrite + Ti-oxide

This metasomatic reaction implies a strong supply of CO_2 which could be generated from a deep seated mantle source (Colvine *et al,* 1988), as suggested by the presence of carbonatite dikes in the shear zone. Preliminary isotopic investigations on galena show an extremely poor radiogenic lead composition, strengthening the hypothesis of a mantle source.

In these conditions, and considering its association with sulfides, gold was probably transported as thio-complexes which can precipitate, at constant temperature, if fO_2 or fS_2 decrase or pH increases (Seward, 1981). Thus gold precipitation can occur in response to interactions of the mineralizing fluid with the carbonate-rich wall rocks (Fyfe, 1987).

CONCLUSIONS

(A)- The deep ductile shear zone of Amesmessa is a crustal-scale Pan African de strike-slip fault which acted as a path-way for mantle and crustal magmas ; it is characterized by the existence of a mylonitized *dike complex of felsic rocks* emplaced within the shear zone, these felsic rocks being the main parent material of ultramylonites. Ductile deformation occurred around 400°C in upper greenschist metamorphic conditions (biotite subfacies).

(B)- The gold-bearing quartz veins are preferentially developed *in a narrow ultramylonite band* along the Western part of this major ductile shear zone which is characterized by strong thermal and deformational gradients. They correspond to shear-veins (dilational jogs) opened approximately parallel to the foliation. These laminated quartz veins were formed by repeated hydraulic fracturing, during the late increments of shearing (from ductile to brittle regime), and quartz suffered intracrystalline deformation. Late banded quartz veins, which are poorly auriferous, developped orthogonally to the foliation within *mylonites* and remained undeformed.

(C)- Hydrothermal alteration accompanying the gold-bearing quartz veins corresponds to a metasomatic transformation of ultramylonites to a carbonate-sericite-albite-pyrite mineral assemblage which postdates the main shearing episode and peak metamorphism. This metasomatic reaction implies *a strong CO_2 supply probably from a deep-seated mantle source* as suggested by the presence of *carbonatite dikes* in the shear zone and by the existence of abundant inclusions of CO_2-H_2O-rich fluids in quartz. Similar REE patterns in ultramylonites, hydrothermally altered rocks and quartz veins show that the hydrothermal fluids which accompanied the ultramylonite formation were driven in dilational zones during the ductile-brittle transition.

(D)- The ore mineral association (pyrite, galena, native gold, sphalerite) crystallized along late shear planes within the quartz veins ; gold precipitation could be caused by reactions between hydrothermal fluids and carbonate-pyrite-rich wallrocks (decrease of sulfur and oxygen fugacities). There is no evidence of gold preconcentration or of a particular source-rock and the ultimate source of gold remains unknown.

ACKNOWLEDGMENTS : This work was supported by an Algerian-French grant. We thank the E.RE.M. team in Tamanrasset for helpfull assistance on field.

REFERENCES

Attoum, A. 1983. Etude géologique et structurale des mylonites pan-africaines et des minéralisations aurifères associées dans le secteur de Tirec (Hoggar, Algérie). Thèse de 3e cycle, uni. Montpellier II, 98 p

Bertrand, J.M.L., Caby, R. 1978. Geodynamic evolution of the pan-africain orogenic belt: a new interpretation of the Hoggar shield (Algerian Sahara). Geol. Rundschau, 67, 2, pp 357-388

Colvine, A.C., Fyon, J.A., Heather, K.B., Marmont, S., Soussan, Smith, P.M., Troop, D.G. .1988. Archean lode gold deposits in Ontario. Ontario Geol. Surv., Misc. Pap. 139 ; 136 p

Ferkous, K. 1991. Altération hydrothermale dans une zone de cisaillement : exemple du gisement aurifére d'Amesmessa (Hoggar, Algérie). Dipl. Etudes Approf. Univ. Montpellier 2, 50p

Ferkous, K., Leblanc, M. 1993. Gold mineralization and associated hydrothermal alteration in a late proterozoic shear zone (Hoggar, Algeria). Min. Deposita (submited)

Fyfe, W.S. 1987. Tectonics, fluids and ore deposits: mobilization and remobilization. Ore Geol. Rev.: 2, pp 21-36

Guha, J., Archambault, G., Leroy, J. 1983. A correlation between the evolution of mineralizing fluids and the geomechanical development of a shear zone as illustrated by the Henderson 2 Mine, Quebec : Economic Geology, v. 78, pp 1605-1618

Kouadri, M. 1983. Etude des minéralisations aurifères du district d'In Ouzzal sur l'exemple de Tirek et d'Amesmesa (SW Hoggar, Algérie). Thesis Doct. Ing., Univ. Paris 6, 168 p

Poulsen, K.H., Robert, F. 1989. A comparison of structural style and gold endowment of three Archean gold districts, Superior Province, Canada, in Extended Abstracts Poster Programme, v. 1, Bicentennial Gold 88, Melbourne, pp 36-38

Sander, M.V., Einaudi, A.M. 1990. Epithermal deposition of gold during transition from propylitic to potassic alteration at Round Mountain, Nevada. Econ. Geol. v. 85, pp 285-311

Seward, T.M. 1984. The transport and deposition of gold in hydrothermal systems. *In* Gold'82, Univ Univ. Zimbabwe, Foster R.P. Edit., pp 165-181

Current Research in Geology Applied to Ore Deposits.Fenoll Hach-Alí, Torres-Ruiz & Gervilla(eds)(1993).ISBN 84-338-1772-8

SOURCES OF THE DETRITAL GOLD MINERALIZATIONS IN THE BOLIVIAN ALTIPLANO

Fornari, M. & Herail G.
ORSTOM (UR1H - TOA), Casilla 9214, La Paz, Bolivia & Casilla 53390 Correo Central 1, Santiago de Chile, Chile

ABSTRACT: The study of the gold placers located in the southern part of the Bolivian Altiplano allows to define two main types of primary mineralizations. One is the free gold mineralizations in quartz vein ocurring in Lower Paleozoic rocks whereas the other derive from the erosion of explosive products of the calc-alcaline volcanism related to the Andean magmatic arc. This last source appears to be a new one by the fact that gold is not derived from classical epithermal occurrences but is dispersed within ignimbritic layers.

The Southern Altiplano of Bolivia presents a general flat topography with a main altitude of about 3900 m; above this surface stand up volcanic apparatus of lower Miocene (e.g. C° Bonete, C° Morokho, C° Lipez), Middle to upper Miocene (e.g. C° Panizo on the Argentina border), and Plio-Quaternary ages.

The area presents a semi-arid climate and many temporary streams have running water only during the rainfall season (from December to March). These conditions make that in the area only placers of reduced size are present which are worked occasionally. Only along the main rivers (rio San Juan de Oro) and in part along the rio Guadalupe, rio Viluyo, rio Pedrenal, fluvial sediments crop out in voluminous terraces.

The studied area is about 80 x 60 km and is located between the border with Argentina at the eastern side and the C° Lipez at the Western side (21°30'-22°15'S/66°15'-67°W).

The local geology consists mainly of outcrops of strongly folded (Ocloyic Orogeny, ca.435 Ma) lower Paleozoic shales and quartzites (probably Ordovician).

The lower Paleozoic beds were later implicated in complex thrust structures during the Andean Orogeny. The erosion of these structures furnished material of the detrital deposits of the San Vicente Formation (Oligocene) and was followed by the main volcanic activity. This activity began with the emission of lavas flows, sills, dykes of mainly basic composition and of alcaline affinity (Formation Rondal, ± 23 Ma, Fornari et al., 1989, Kussmaul et al., 1975), followed by the main calc-alcaline activity which spans to actual time.

The calc-alcaline activity produced great volumes of pyroclastic rocks (ignimbrites and tuffs), domes and sub-volcanic intrusives and lava flows; these rocks are generally of dacitic composition. Several paleovolcanoes and calderas have been identified (e.g. C° Bonete, C° Morokho); the pyroclastic tuffs and the ignimbritics deposits form extended outcrops which in many places are preserved as flat plateaus (mesetas).

Sampling with gold pan of the numerous headwaters in the drainage red cutting these plateaus and also of the soils and proximal colluvial deposits formed on the ignimbrites allowed to recover numerous gold grains. Gold grains were also recovered from the main rivers (Rio Guadalupe, Pedrenal), and from the Vilader placer.

The placer of Vilader which is located near C° Lipez, at an altitude of 4190 m, consists of an alluvial fan made of slope material eroded from Lower Paleozoic outcrops (Ramos, 1993, Fornari et al., 1991).

The gold grains recovered in the placer are small; the mean length is about 0.94 mm with a range of 0.1 to 6 mm and their distribution has a skewness to the small dimensions. The mean flatness index (Length + breadth / 2*thickness) is about 2.6, corresponding to grains that are not flattened. The grains have morphoscopic features (irregular shapes, inclusion of quartz) that indicate a very short distance of transportation. In fact, the gold is derived from the erosion of gold-quartz veins located in the Ordovician rocks.

The analyses of the chemical composition of the gold grains made by electron microprobe indicate silver contents of about 4%, 7-9% and 14%.

Furthermore some grains show change in composition, with silver-depleted external rims; the presence of a low Ag rim is interpreted as a preferential leaching of silver developed in weathering profile.

So the gold recovered from the Vilader placer provides the identity of the Lower Paleozoic source, as confirmed by the composition of some gold particles recovered from small quartz vein, although they show a narrow range in their silver contents.

The gold grains recovered from the main rivers show morphoscopic features such as folded border, smoothed outlines, striation marks, which are characteristic of transport in permanent streams of water. These characteristics are acquired in a relatively short distance of transport (less than 10 km).

The gold grains recovered from samples of the soils on ignimbrites and from the small headwaters that cut the ignimbritic plateaus, show a particular morphology with globular forms and consequently small values of the flatness index (between 1 and 4); crystalline shapes are preserved, not only in the hollows of the grain but also in the border of the grain (figure). These facts indicate that the gold grains are of local origin and come from the erosion of the ignimbrites.(Pozzo, 1990, Fornari et al., 1991).

These "volcanic" gold grains show also a characteristic composition: the gold is very pure (0 to 3% Ag, generally less than 1%, with the same content in the centers and in the rims of the grains).

This volcanic gold appear to be dispersed with very low grade within the ignimbrites: preliminary analysis of whole rocks gave Au-content around the clarke of felsic rocks (2-3ppb) and in any case lower than 10 ppb.

Figure:
A Gold grain from the Co Pabellon area: characteristic globular form, SEM photography, scale bar 100µm
B: globular gold grain (SEM photography, scale bar 50µm)
C: Detail of B: primary crystalline outlines conserved on the surface of the gold grain (scale bar 10µm).

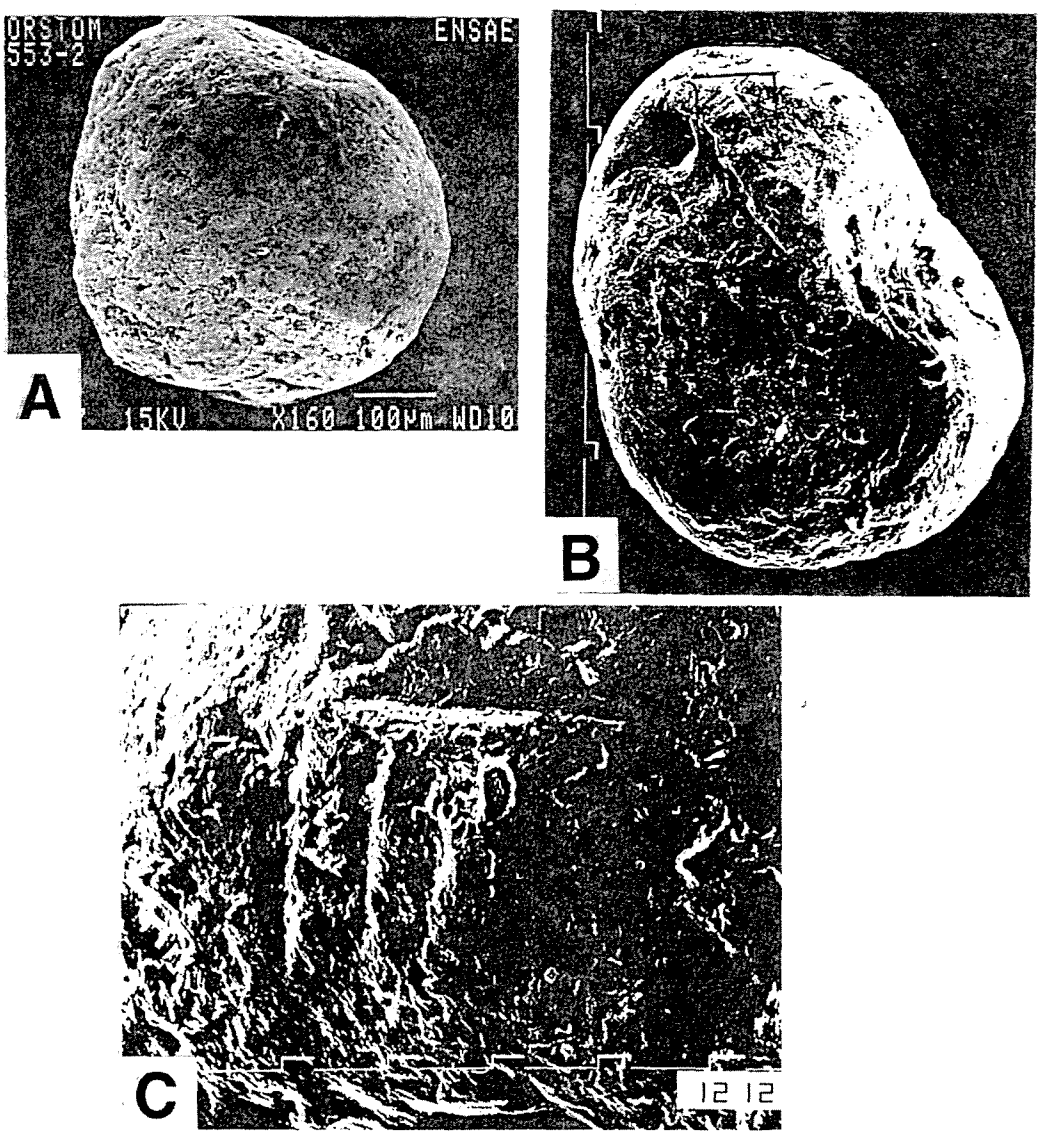

The distribution of these volcanic gold grains, although widely present in many places in tuffs and ignimbrites of the Southern Altiplano is not homogeneous and some ignimbritic levels of the area of the Cerro Pabellon near Guadalupe which were emitted from the Cerro Bonete center appear to be richer in gold than those of the same type emitted from the Cerro Morokho center.

This "volcanic" gold is not related to the Bi, Ag, (Zn, Pb) vein mineralizations present in the area. The study of the mineral paragenesis of the Mina Bolivar located in dacitic resurgent domes of the C° Bonete, no revealed the presence of gold, (Ahlfeld & Scheider-scherbina, 1964, Baily et al., 1992).

The reconstitution of the successive volcanic events for the C° Morokho and the C° Bonete centers shows that there is an early stage of explosive type during which are deposited pyroclastic tuffs and ignimbrites followed by a stage of emplacement of resurgent domes, with breccias and lava flows; a late stage of alteration and sometimes of vein mineralization concludes this evolution.

The gold appear to be exhaled with the pyroclastic deposits, at the early stage, probably in a manner analogous to the case of the Mount Erebus volcano where the presence of gold grains in the eruptive products has been recently documented (Meeker et al., 1991)

The fact that gold can be emitted with the volatile phase implies particular magmatic conditions and can be an unfavorable factor for the further presence of epithermal Au-mineralizations.

REFERENCES

Ahlfeld & Scheider-Scherbina, 1964. Los yacimientos minerales y de hidrocarburos de Bolivia. Bol. Dept. Nac. Geol., 5, 388p.

Bailly L., Leroy J., Fornari M., Hérail G. 1992. El distrito minero de Los Lipez: estudio de las alteraciones ligadas a las mineralizaciones hidrotermales (Pb,Zn,Ag,Bi) del Cerro Bonete. Soc. Geol. Boliviana, Bull. 27, 28:35.

Fornari M., Herail G., Pozzo I.L., Viscarra G. 1989. Los yacimientos de oro de los Lipez (Bolivia) Tomo I: Estratigrafia y dinamica de emplazamiento de los volcanitas del area de Guadalupe. Orstom en Bolivie N° 19.27p La Paz.

Fornari M., Hérail G., Ramos W. 1991. Le placer de Vilader, modèle génétique. Gisements alluviaux d'or, Alluvial gold placer, :159-173. Ed Orstom Paris.

KUSSMAUL, S., JORDAN, L., PLOSKONKA, E., 1975. Isotopic ages of Tertiary volcanic rocks of SW Bolivia. Geol Jb., Hannover, :111-117.

Meeker K. A.,Chuan R. L.,Kyle P.R.& Palais J. M. 1991. Emission of elemental gold particles from Mount Erebus, Ross Island, Antartica. Geoph. Research Letter, 18, 8 :1405-1408.

Pozzo, I. L., 1991.Geologia y caracteristicas del oro aluvial en ambiente volcanico, region de Guadalupe, Prov. Sud lipez, departamento de Potosi. Un metodo para localisar posibles mineralizaciones primarias. *Thesis* 98p, Univ. Mayor San Andres. La Paz Bolivia.

Ramos C. W. El placer de Vilader y sus fuentes primarias *Thesis de grado*, 151p + annexes. Univ. Mayor San Andres. La Paz Bolivia.

U.S. Geological Survey & Servicio Geologico de Bolivia, 1991. Geology and mineral resources of the Altiplano and Cordillera Occidental, Bolivia. U.S. Geol. Surv. Bull.1975, 365p.

Current Research in Geology Applied to Ore Deposits. Fenoll Hach-Alí, Torres-Ruiz & Gervilla (eds) (1993). ISBN 84-338-1772-8

MULTIPLE FLUID SOURCES AND DEPOSITIONAL MECHANISM AT THE ARCHAEAN MESOZONAL-EPIZONAL GOLDEN KILOMETRE GOLD MINE, WESTERN AUSTRALIA

Gebre-Mariam, M.; Groves, D.I.; McNaughton, N.J. & Mikucki, E.J.
Key Centre, Dept. of Geology, University of Western Australia, Nedlands, 6009, Australia

ABSTRACT

The Archaean mesozonal-epizonal Golden Kilometre gold deposit is hosted by an Fe-rich granophyre in a layered gabbro sill. Gold occurs in both altered wallrock and in quartz veins. Three types of fluid inclusion occur in gold-bearing quartz veins: Type-1, H_2O-CO_2-CH_4-NaCl, Type-2, $CH_4 \pm CO_2$, and Type-3, H_2O-salt. Type-1 inclusions satisfy the requirements of immiscibility, and are trapped on the solvus in the relevant system. Type-2 inclusions are interpreted to be a product of deposit-scale processes whereas, aqueous Type-3 inclusions represent an aqueous fluid which mixed with the carbonic fluids. Calculated ore-fluid $\delta^{18}O_{H2O}$ values of 1.6±1.9 ‰ implicate incursion of surface water, whereas the carbonic fluid inclusions imply the involvement of either a deeply sourced metamorphic or magmatic fluid. Lead isotope data suggest a deep crustal to mantle Pb source. Gold deposition in the wallrocks occurred via fluid-wallrock interaction, whereas phase separation and possibly fluid mixing were the major gold-depositional processes in the veins.

REGIONAL SETTING

The Golden Kilometre deposit (Fig. 1), in the Mt Pleasant area of the Norseman-Wiluna belt, 40 km NW of Kalgoorlie, Western Australia, is hosted by a quartz-gabbro zone of the Mt Pleasant sill, a layered and differentiated mafic to ultramafic sill. The supracrustal succession of the area, dated at 2,689±2 Ma (Pidgeon, 1986), has undergone up to greenschist facies metamorphism. In general, the rocks are unstrained with no pervasive or spaced fabric. Late-stage granitoids and porphyries intrude the greenstone succession.

MINERALIZATION AND ALTERATION

Gold mineralization at Golden Kilometre is controlled by lower-order brittle-ductile strike-slip faults associated with regional strike-slip faults. The deposit comprises a system of laminated quartz veins and related altered wallrock. Metasomatic alteration shows distinct color zonation, related to sequential wallrock alteration around the veins. Two major alteration zones can be defined: a distal chlorite-calcite and a proximal muscovite-ankerite zone. The muscovite-ankerite zone can, itself, be subdivided into distal pyrrhotite and proximal pyrite subzones. Progressive hydrothermal alteration has resulted in actinolite-chlorite assemblages of the wallrock being replaced by chlorite-albite-biotite±epidote-calcite assemblages within the chlorite-calcite zone. Intense alteration adjacent to veins led to replacement of these phases by muscovite-ankerite-sulphide assemblages. Chlorite [Mg/(Mg+Fe)] systematically increases with proximity to vein margins, while ilmenite and magnetite are replaced as the dominant opaque mineral phases by leucoxene, pyrite, pyrrhotite and minor arsenopyrite. The above mineralogical zonation can best be explained by metasomatism of the surrounding wallrocks via K-, CO_2- and H_2S-rich ore fluids infiltrating outward from vein conduits.

In the wallrock, gold occurs as discrete, ≤100 μm-sized particles included in gangue and sulphide minerals. Gold grade is always higher in the pyrite subzone than in the pyrrhotite subzone of the muscovite-ankerite zone. In the veins, gold occurs as coarse grains (commonly 1 to 2 mm), shows evidence of occurring late in the vein paragenesis, and is commonly associated with zones of recrystallized quartz or deposited along with sericite, chlorite and ankerite within late, cross-cutting fractures and 'spider' veinlets. Minor galena, sphalerite, pyrite, pyrrhotite, chalcopyrite, and scheelite also occur within gold-bearing veins.

Sulphides in the wallrock formed by the sulphidation of earlier-formed chlorite, ilmenite, and magnetite. The zonation of the ore-minerals, pyrrhotite and pyrite, the close spatial association of gold grade with proximal pyrite subzone, and the systematic changes in chlorite composition clearly indicate that deposition of wallrock-hosted gold is related to fluid-wallrock interaction (cf. Phillips & Groves, 1983). The cause of gold deposition in the veins is discussed below.

FLUID INCLUSIONS

Three compositional types of inclusions occur in gold-bearing quartz veins. These are: Type-1, H_2O-CO_2-CH_4-NaCl, Type-2, $CH_4 \pm CO_2$, and Type-3, H_2O-salt. The textural relationship between inclusions suggest contemporaneous trapping. Type-1 inclusions satisfy the requirements of immiscibility in the system H_2O-CO_2-CH_4-NaCl, and are interpreted to have been trapped on the solvus in that system. Inclusion fluids of this type range in composition from 0.01 to 0.99 X_{CO2} equiv. and from 0 to 8.7 equiv. wt% NaCl (mean of 3.7 wt% NaCl equiv.). Measurements of Tm_{CO2} suggest appreciable CH_4 in most Type-1 inclusion fluids, with calculated CO_2/CH_4 ratios of between 3 and 99 (most ≤10). Equivalent CO_2 densities vary from 0.50 to 0.89 g/cc. Th_{total} ranges from 160 to 325 °C, with the majority of values in the range 225 to 280 °C. Type-2 inclusions are monophase, supercritical CH_4 fluids. Th_{CH4} of -110.9 to -72.2 °C corresponds to densities of 0.19 to 0.33 g/cc. Type-3 inclusions are subdivided into Type-3A, low to moderate salinity (0.82 to 10.0 equiv. wt % NaCl) with Th_{total} 91.6 to 259 °C, and Type-3B, high salinity (19.42 to 22.82 equiv. wt % NaCl) with Th_{total} 79 to 181 °C. During freezing-point depression measurement, no CO_2 phases were detected nor was clathrate formed. Assuming Th_{total} of Type-1 inclusions represent true trapping temperature and that Type-2 inclusions were trapped at the same temperature as Type-1 inclusions, intersecting isochores for Type-1 inclusions yield pressures of 1 to 1.5 kb, and for Type-2 0.65 to 1.9 kb. Application of pressure corrections for Type-3 inclusions yield Th_{total} of 200 to 370 °C, broadly overlapping with those of Type-1 inclusions.

The above data indicate that a number of different fluids of roughly similar temperature and pressure but of markedly different bulk composition were present during vein formation at the Golden Kilometre deposit. The composition of the Type-1 inclusions is similar to that of other Archaean mesozonal gold deposits interpreted to be deposited from deeply sourced fluids. The origin of Type-2 inclusions, at present, is equivocal. Available experimental and thermodynamic data suggest that pure CH_4 fluids cannot be produced by unmixing of Type-1 fluids. It is suggested that a combination of deposit-scale processes, including one or more of differential partitioning, disequilibrium CO_2 depletion, and

fluctuating oxidation state, produced these inclusions from Type-1 fluids. Likewise, the absence of CO_2 in Type-3 inclusions suggests that those inclusions are not a product of unmixing of Type-1 fluids. Solvus relationships for H_2O-CO_2-CH_4-NaCl fluids indicate that even the most H_2O-rich fluids existing along the solvus should form clathrate during freezing. This was not observed in any Type-3 inclusions. In light of oxygen isotope data, discussed below, they are interpreted to represent an external fluid, possibly surface water, that mixed with the deeply sourced ore fluids.

Unmixing of fluids has been inferred as the major cause of gold deposition in many vein-hosted Archaean deposit (Robert & Kelly, 1987), and this process and possibly the mixing of surface water with deeply sourced fluids is considered responsible for the precipitation of coarse grained gold in the quartz veins of the Golden Kilometre deposit.

STABLE ISOTOPES

Carbon and oxygen isotopic determinations were performed on a suite of 19 ankerite samples. $\delta^{13}C$ values range from -6.8 to -4.6‰ (mean -5.8‰), and $\delta^{18}O$ from 8.0 to 9.7‰ (mean 8.8‰). For a formation temperature of 275±50 °C, and assuming a CO_2/CH_4 ratio of 10 and equilibrium isotopic fractionation between CO_2 and CH_4, the $\delta^{13}C$ of the total ore-fluid carbon ($\delta^{13}C_{\Sigma C}$) is -7.4±1.2‰. This broadly overlaps with $\delta^{13}C_{\Sigma C}$ of other deposits from the Norseman-Wiluna Belt, and may therefore indicate a similar carbon source. In contrast, calculated $\delta^{18}O_{H2O}$ values of 1.6±1.9‰ differ markedly from other mesozonal deposits, and are best explained by a seawater or meteoric water influx into the ore fluids. Simple mass balance considerations indicate that such decoupling of the fluid $\delta^{13}C$ and $\delta^{18}O$ is to be expected during mixing between low-CO_2 surface waters and ascending CO_2-rich ore solutions. The $\delta^{13}C$ of the ascending fluid would dominate the carbon budget whereas the $\delta^{18}O$ of the fluid might be largely derived from the surface water.

RADIOGENIC ISOTOPES

The initial Pb-isotopic composition of the Golden Kilometre ore-fluid, estimated from gold-related galena, is similar to the Pb-isotopic composition of lode-gold deposits elsewhere in the Mt Pleasant-Kalgoorlie-Kambalda region, implying a homogeneous Pb-source region over a strike length of >100 km. Comparison of lead isotopic composition of the deposits with the Pb-isotopic composition of country rocks and mantle - crust Pb reservoirs suggest that the source of Pb in the gold deposits is best modelled as a mixture of Pb from the mantle or mantle-derived greenstone rocks and/or their sedimentary derivatives, and Pb from older felsic crust or derived granitoids.

DISCUSSION AND CONCLUSION

Recent genetic models for Archaean lode-gold deposits generally favour either fluid-rock interaction or phase separation as the predominant controls on gold deposition. Petrographic, mineralogic and fluid inclusion studies suggest that both these processes were important at the Golden Kilometre deposit. In particular, the zonation of ore minerals, pyrite and pyrrhotite, the associated gold grade distribution, and the systematic changes in chlorite composition clearly indicate that deposition of wallrock gold is

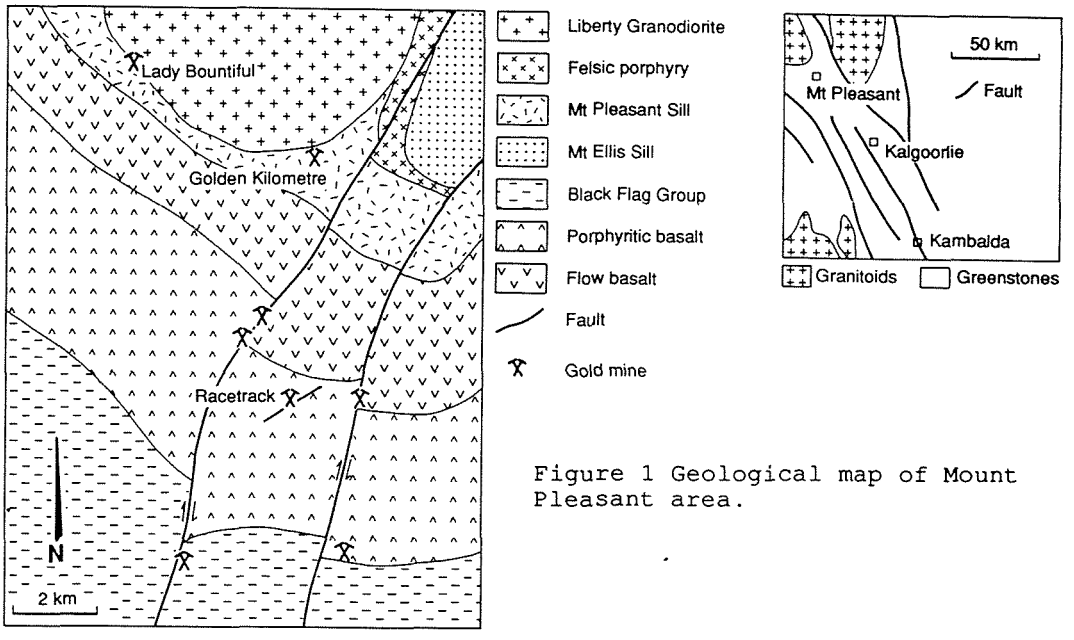

Figure 1 Geological map of Mount Pleasant area.

related to fluid-wallrock interaction. Deposition of paragenetically late gold in veins occurred due to the unmixing of deeply derived Type-1 H_2O-CO_2-CH_4-NaCl fluids, and possibly due to the mixing of these fluids with surface water. This mixing of deeply derived fluids and surface water is supported by fluid inclusion and oxygen isotopic data. In addition to the carbonic-aqueous Type-1 fluids which indicate either a metamorphic or magmatic derivation, lead isotope data suggest a deep crustal to mantle lead source, consistent with transport in the deeply sourced metamorphic or magmatic fluids.

In conclusion, this case study has demonstrated that at the Archaean Golden Kilometre gold deposit multiple fluids, either metamorphic or magmatic and surface water (meteoric or sea water), were involved in ore deposition, and deposition of gold took place through a variety of mechanisms: fluid-wallrock interaction, phase separation and possibly mixing of fluids.

ACKNOWLEDGMENTS

This study forms part of a PhD project carried out by MGM, who acknowledges the support of the Black Flag Consolidated Limited and the Key Centre, and the receipt of UWA and UNDP scholarships.

REFERENCES

Phillips, G.N. & Groves, D.I. 1983. The nature of Archaean gold-bearing fluids as deduced from gold deposits of Western Australia. J. Geol. Soc. Aust. 30: 25-39

Pidgeon, R.T. 1986.Correlation of acid volcanics in the Archaean Western Australia. West. Aust. Mineral & Petrol. Research Instit. Report 27

Robert, F. & Kelly, W.C. 1987. Ore-forming fluids in Archean gold-bearing quartz veins at the Sigma Mine, Abitibi Greenstone, Quebec, Canada. Econ. Geol. 82: 1464-1482

Current Research in Geology Applied to Ore Deposits.Fenoll Hach-Alí, Torres-Ruiz & Gervilla(eds)(1993).ISBN 84-338-1772-8

MINERALOGY OF COPPER-GOLD FROM PLACERS OF WEST SAYAN, (TUVA, RUSSIA)

Generalov, M.E.
Inst. Geology of Ore Deposits (IGEM), Moscow 109017, Staromonetny 35, Russia.

ABSTRACT: Cu-Au alloys with compositions close to AuCu, Cu3Au and Au3Cu were founded in placer gold from alluvial deposits of W.Sayan which are connected with gabbro-ultrabasic rocks of the Kurtushibinsky ridge. Mineralogy of Cu-Au-phases - bearing gold (copper gold) from this occurence was characterized and some conditions of their formation was evaluated. Supposed source rocks of the copper gold are rodingite-like metasomatites.

Copper-bearing gold (copper gold, CG) was founded in placer gold (collection of Krupnik V.M., Konovod A.A.) from several alluvial deposits which are connected mainly with gabbro-ultrabasitic complex of the Kurtushibinsky ridge of W.Sayan (Republic of Tuva, Russian Federation). Geologically it is a zone of the ophiolitic belt of caledonian age. Several types of gold deposits of quartz-vein type were known here but none of them contain CG.

CG grains vary from 0.1 to 3 mm in size.Most of CG grains are heterogenous. Usually they contain high-purity gold (purity 995-940), gold of intermediate purity (900 - 800), electrum (480 - 720) and Cu - Au alloys.

High-purity gold (Tab.2,an.19-22) mainly forms irregular mantles around CG grains which are connected with diffusion-related bearing-out of Cu and Ag from outher zones of CG grains.

Intermediate purity gold (Tab.2,an.29-30) commonly occures as intergrows with lamellar AuCu-phases (fig.1).

Electrum (Tab.2,an.24-28) also may fill spaces between AuCu-plates but small rounded inclusions of the electrum within AuCu and its intergrows with curvilinear borders are more common. Some isolations of electrum are enriched in Hg (up to 3.5 mass %).

It may be supposed that gold with higher purity usually forms as a result of postcrystallization processes in CG (decomposition of Au-Cu-Ag - solid solutions or diffusion-related processes), while electrum often crystallize together with initial Au-Cu-phases and may be considered as a concentrator of Ag and Hg which can not be included into structures of Au-Cu alloys in appreciably contents.

Cu-Au phases known in nature [2,3,4,5,6] have compositions close to Cu3Au, AuCu, Au3Cu. These alloys together primary were described by Novgorodova et al. in deposit from Urals [3,4] were founded in studied placer gold from W.Sayan.

The most widespread phase in studied CG is AuCu. Its composition is (mol.%): 44.9 - 51.2 Cu, 48.3 - 54.4 Au, up to 0.6 % Ag (examples in Tab.2, an.5-10). AuCu-phase may occure as individual grains or as lamells (thickness 0.5-50 m) in (Au,Ag)-matrix. In some CG grains several stages of AuCu crystallization (decomposition of Au-Cu-Ag - solid solutions) can be observed. It looks as lamellar AuCu - (Au,Ag) systems between more thick AuCu lamells of the preceding lamellar system. Some CG grains have up to 3 of such AuCu generations.

Etching of visually homogenous AuCu grains by HCl-HNO3 - solutions shows polycrystal structure some of them and leads to the appearing of pseudoanisotropic effects. Possible reason of this effects is a system of orientated (Au,Ag)-microinclusions in AuCu-matrix. This effects allows to distinguish several generation of AuCu within some grains. The older generation looks as parallele-pipedal crystals (up to 0.2 mm) with greater pseudoanisotropy within the AuCu matrix with smaller pseudoanisotropy (fig.2).

X-ray diffraction data (tab.1) show that AuCu phase is tetra-auricupride (AuCuI), P4/mmm, a=3.96, c=3.69±0.01 Å. The reflection (001) was not obserwed. It may point on the disordering of Cu and Au and the value of the parameter a of P4/mmmcell

may be evaluated as 2.80 A. Reflections of cubic AuCu (a≈3.88 Å [5]) and orthorombic AuCuII were not observed. The AuCu phase have clear pinkish tint. Reflection data are in the tab.3. Microhardness of the AuCu-phase is 210-260 kG/mm^2 (P=20g).

Phases with compositions close to Cu3Au (auricupride) were found only in 2 of 8 studied placers containing CG. They occure as individual grains with size up to 0.5 mm and as irregular subgrains (0.03-0.1 mm) in outher zones of CG grains with predominant AuCu in the center. Sometimes orientated system of fine AuCu-lamells can be observed after acid etching in central parts of Cu3Au grains (fig.3). The composition of auricupride is (mol.%): 27.3-32.1 Cu, 67.8-72.5 Au, < 0.2 % Ag, tab.2, an.1-4). The deviation from ideal formula may be connected with fine-grained inclusions of AuCu-phase which are results of decomposition of nonstoichiometric initial solid solutions in the Cu-Au system. An other possible reason of the deviation may be disordering of the crystal structure of this phase.

According to X-ray diffraction data this phase is cubic, Pm3m, a=3.76±0.01 Å (tab.1). Optical properties of Cu3Au and AuCu phases are very close (tab.3). The microhardness of Cu3Au is 170-190 kG/mm^2 .

Phases which are compositionally close to Au3Cu differs from high-purity gold by orange tint and better polishing. Acid ethcing allows to observe heterogeneity of CG grains containing "Au3Cu"- phases. In some grains veriform, ovoidal areas with content of Cu > 7 mas.% are surrounded by high-purity gold with Cu < 3 % . Latticed systems were also observed. "Au3Cu"-phases may form also individual grains or relicts surrounded by high-purity gold mantles.Their compositions are (mol.%): 19.7-31.8 Cu, 67.0-78.8 Au,0.5-2.8 Ag (Tab.2,an.11-16). Their stoichiometry vary approximately from Au4Cu to Au2Cu. The excess of Au is connected with (Au,Ag)-phase inclusions, but X-ray diffraction data point on the presence of (Au,Ag)-phases even in microscopically homogenous grains with the composition close to Au2Cu while reflections of AuCu-, Cu3Au-phases were not observed here. It point on the possibility of the real deviations of the composition of "Cu3Au"-phase to compositions with greater content of Cu in the result of the disordering of crystal structure of this compound.

X-ray diffraction data for this phase are: Fm3m, a = 4.01±0.01 Å. Reflection data are in the tab.3. Microhardness value is 140-165 kG/mm^2 .

Besides Cu-Au and Au-Ag phases CG grains often contains mineral inclusions which were entrapped during CG growth. Many of CG grains contains small (5-50 m) rounded sulphide inclusions. Visually they are composed of brown- and bluish-grey-coloured sulphides. The first sulphide is bornite(Cu-60.2, Fe-11.3, S-26.9 mas.%) and the second (Cu-71.2, S-25.8 mas.%, Cu1.4S) obviousely is a mixture of Cu-sulphides. The uniformity of sulphide inclusions point on its origin as a result of the decomposition of homogenous Fe-Cu-S - phases which have been stable at the temperature of their entrapment. Among silicate inclusions idiomorphic grains of garnets (andradite-grossulare), pyroxene (salite-diopside), rounded inclusions of chlorite, and intersticions of serpentine between some CG subgrains were estimated. Inclusions of quartz which are typical for other varieties of placer gold were not observed in CG.

Known occurences of CG are connected with basic-ultrabasic intrusions [5,6]. The complex of estimated mineral inclusions in studied CG show that the source of this CG may be rodingite-like metasomatites (garnet-pyroxene-clorite rocks). Rodingites were described as an host rock on the wellknown occurence of CG "Zolotaya Gora" (Urals) [1,5]. The origin of rodingites is connected with last stages of the formation of basic-ultrabasic intrusions.

The decomposition of solid solutions which leads to the formation of intergrows similar to intergrows of Cu-Au- and (Au,Ag)- phases within studied CG grains take place at T below 400-200 C. These temperatures may be considered as lower limits of the formation of initial Cu-Au-Ag-phases.

Some of microscopically homogenous phases of CG (an.11-19) have compositions close to mean compositions of theoretical solid solutions which were transformed into lamellar intergrows of Cu-Au- and (Au,Ag)-phases. Such phases may be

considered as examples of metastable initial phases.The possible reason of their conservation may be tempering as a result of a sharp fall of T. In contrast to AuCu-compounds from deposit "Zolotaya Gora" which are composed of tetragonal and orthorombic phases [2], X-ray difraction data for studied AuCu show only P4/mmm-phase.This fact may point on very slow cooling after AuCu-crystallization. Thus the thermal history of the CG mineralization may be described as sharp variations of T at early stages and slow cooling at late stages.

Very small portion of sulphidic Cu in CG microparagenesises point on very small activity of S in the ore-forming fluid. It is difficult to expect here appreciable migration of Cu, Au, Ag in a form of S-bearing compounds.

The general trend of the zoning of CG grains from the core to the mantle is: (Au,Ag)=>(Au,Ag)+AuCu=>AuCu=>AuCu+Cu3Au=>Cu3Au. On the basis of the zoning the increasing of Cu activity during CG growth can be expected.

Tab.1 XRD-data for studied Cu-Au-phases.

d/n	I	hkl
Cu3Au		
2.66	2	110
2.19	6	111
1.89	4	200
1.69	3	210
1.54	2	211
1.33	8	220
1.25	4	300
1.13	10	311
1.08	7	222
1.04	2	320
AuCu		
2.80	2	110
2.23	10	111
1.99	5	200
1.84	1	002
1.74	2	201
1.40	3	220
1.35	7	022
1.19	10	131
1.13	5	113
1.11	6	222
1.034	5	132
1.007	3	123
Au3Cu		
2.32	8	111
2.01	10	200
1.42	6	220
1.21	8	311
1.15	5	222
1.006	5	400

Tab.2 Microprobe data for main phases of studied CG.

N	Cu	Au	Ag	Hg	totals	Cu	Au	Ag	Hg
	mas.%					at.%			
1	45.14	52.77	0.20	0.00	98.11	72.5	27.3	0.2	0.0
2	42.39	56.40	0.00	0.00	98.79	70.0	30.0	0.0	0.0
3	38.92	57.06	0.07	0.00	96.05	67.8	32.1	0.1	0.0
4	39.68	58.20	0.10	0.00	97.98	67.8	32.1	0.1	0.0
5	24.45	77.28	0.13	0.00	101.86	49.4	50.4	0.2	0.0
6	25.00	75.56	0.08	0.00	100.64	50.6	49.3	0.1	0.0
7	25.35	75.19	0.00	0.00	100.54	51.1	48.9	0.0	0.0
8	24.67	74.12	0.24	0.00	99.03	50.6	49.1	0.3	0.0
9	24.63	77.04	0.11	0.00	101.78	49.7	50.2	0.1	0.0
10	25.26	73.79	0.43	0.00	99.48	51.2	48.3	0.5	0.0
11	7.96	89.35	1.78	0.00	99.09	21.0	76.2	2.8	0.0
12	7.25	89.94	0.98	0.00	98.17	19.7	78.8	1.6	0.0
13	11.68	85.68	1.83	0.35	99.54	28.8	68.2	2.7	0.3
14	13.23	86.46	0.84	0.00	100.50	31.8	67.0	1.2	0.0
15	9.76	90.18	0.90	0.00	100.84	24.8	73.9	1.3	0.0
16	9.87	90.59	0.52	0.00	100.98	25.1	74.2	0.8	0.0
17	2.35	92.06	4.35	0.21	98.97	6.8	85.7	7.4	0.2
18	1.25	99.30	0.81	0.17	101.53	3.7	94.7	1.4	0.2
19	1.31	94.28	2.99	0.00	98.58	3.9	90.8	5.3	0.0
20	1.25	99.14	0.25	0.15	100.75	3.6	95.9	0.4	0.1
21	2.09	95.80	0.00	0.45	98.34	6.3	93.3	0.0	0.4
22	1.38	97.75	0.00	0.66	99.89	4.2	95.2	0.0	0.6
23	0.00	47.30	52.79	0.00	100.09	0.0	32.9	67.1	0.0
24	0.23	58.46	38.96	0.00	97.65	0.5	54.6	44.9	0.0
25	0.97	66.26	32.55	0.69	100.47	2.3	51.2	45.9	0.5
26	1.20	70.50	27.23	0.00	98.93	3.0	56.9	40.1	0.0
27	0.13	72.66	26.41	1.36	100.56	0.3	59.3	39.1	1.1
28	0.48	62.44	31.36	3.51	97.79	1.1	53.8	42.5	2.6
29	2.48	85.88	11.31	0.00	99.67	6.7	75.2	18.1	0.0
30	2.32	85.47	10.54	0.68	99.01	6.4	75.9	17.1	0.6

Microprobe "Cameca MS-46", 20 kV, beam diameter 1-2 μm, standarts: Au, Ag, Cu, HgS. Analyst: Golovanova T.I.(IGEM)

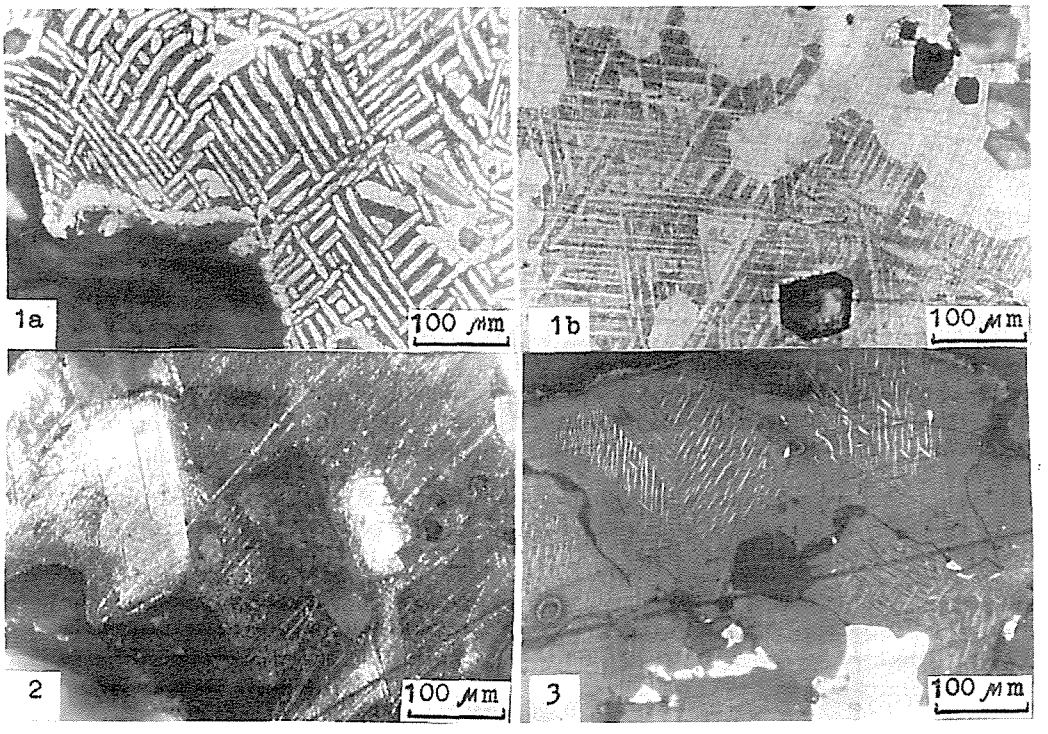

Fig 1. Lamellar systems of AuCu- (white) and Au,Ag (grey) - phases.
Fig 2. Pseudoanisotropic effects in crystals of the older AuCu generation within AuCu matrix.
Fig 3. AuCu lamells (white) within Cu3Au subgrains (grey).

λ,nm	R,(%) Cu3Au	AuCu	Au3Cu	λ,nm	R,(%) Cu3Au	AuCu	Au3Cu
420	29.0	28.0	29.5	580	60.5	60.0	67.5
440	31.0	29.5	28.0	600	70.0	67.5	74.5
460	33.5	32.0	30.0	620	77.0	74.0	80.5
480	36.0	34.5	32.5	640	82.0	78.5	85.5
500	38.5	37.0	35.5	660	85.5	82.5	89.0
520	41.0	40.0	40.5	680	88.0	84.5	91.0
540	45.0	45.0	48.0	700	88.0	85.0	88.0
560	51.0	51.5	59.0	720	87.5	84.5	84.5

Tab.3 Reflection data for studied Cu-Au phases.

MSFP-2
Standart-Al

Analyst:
Krinov D.I.
(IGEM)

REFERENCES:

1. Murzin V.V. et al. Copper gold in zones of rodingitization. Geologya rudnich mestorojdenii (Geology of Ore Deposits) 1987, N.5, 96-99 (in russian).

2. Murzin V.V., Sustavov S.G. Solid-phase transformations in the natural copper gold. Izvestia AN SSSR, Ser. geol. 1989, N.11, 94-104 (in russian).

3. Novgorogova M.I.,Tsepin A.I.On the phase composition of copper gold. Doklady AN SSSR, 1976, 227, N.1 (in russian).

4. Novgorodova M.I. et al. New data on the crystallochemistry and properties of natural alloys in the system Cu-Au. Zapisky VMO (All-union Mineralogical Soc.) 1977, 106, N 5, 540-551 (in russian).

5. Novgorodova M.I. Native metals in hydrothermal ores. Nauka,1983 (in russian).

6. Ramdohr P. On the widespread paragenesis of ore minerals connected with serpentinization. Geol. rudn. mestorojdenii. 1967, N.2, 32-43 (in russian).

Current Research in Geology Applied to Ore Deposits.Fenoll Hach-Alí, Torres-Ruiz & Gervilla(eds)(1993).ISBN 84-338-1772-8

MINERALOGY AND MINERAL CHEMISTRY OF THE LAS AGUILAS Ni-Cu DEPOSIT (PROVINCE OF SAN LUIS, ARGENTINA)

Gervilla, F. (1); Sabalúa, J.C. (2); Carrillo, R. (3); Fenoll Hach-Alí, P. (1) & Acevedo, R.D. (4)
(1) Dept. de Mineralogía y Petrología, Universidad de Granada, Spain.
(2) Dirección General de Fabricaciones Militares. C.E.G.M., Mendoza, Argentina.
(3) Centro de Investigación en Recursos Geológicos, CONICET, Buenos Aires, Argentina
(4) Dept. de Geología, Universidad de Oviedo, Spain

ABSTRACT

The Ni-Cu deposit at Las Aguilas includes two ore bodies made up of pyrrhotite, pentlandite and chalcopyrite with minor ilmenite, rutile, pyrite, Ni-rich, Fe-bearing cobaltite, Pt-rich, Ni-bearing merenskyite, gold and electrum. The ore bodies are hosted by dunites, harzburgites and bronzitites. Chemical and textural features of both the ore minerals and the silicates and spinels from the enclosing rocks show that the mineralization was formed from an immiscible sulfide melt generated during crystal fractionation of a mafic melt. Later, folding and metamorfism movilizated the sulfides.

INTRODUCTION

The Las Aguilas mining district is located 40 km to the north of San Luis city, the capital of San Luis Province (Argentina). It comprises two Ni-Cu ore bodies hosted by mafic-ultramafic rocks including dunites, harzburgites, bronzitites, norites and amphibolites. These mafic-ultramafic rocks crop out as small lenticular bodies (500x300m and 400x150m) elongated in the direction NNE-SSW and dipping 80°-85° E, parallel to the main foliation of the country rocks (granulites and gneisses). They belong to a set of occurrences of mafic-ultramafic rocks distributed in a narrow (100x15km), NNE-SSW-oriented belt on the eastern side of the Sierra Grande de San Luis. The probably age of these rocks is Upper Precambrian-Cambrian (Sabalúa, 1983).

The ore bodies consist of Fe-Ni-Cu sulfides, mainly pyrrhotite, pentlandite and chalcopyrite. They are exclusively hosted by dunites, harzburgites and bronzitites and are discordant to the contacts between such rocks. Exploration by the Dirección General de Fabricaciones Militares (Argentina) has shown the existence of more than 2 million tons of ores with average grades of 0.51%Ni, 0.50%Cu and 0.035%Co.

In this paper we present new data on the mineralogy and mineral chemistry of both the sulfide ores and the enclosing mafic-ultramafic rocks. Special attention will be paid to the fractionation trends recorded by the chemical compositions of both orthopyroxene and chromian spinel, and to the abundance and distribution of platinum-group minerals in the ore association.

THE HOST MAFIC-ULTRAMAFIC ROCKS

These occur as two pseudo-tabular, highly folded bodies, having the ultramafic rocks in the cores of very asymmetrical antiform structures. Thus, from the cores to the flanks of the structures

there are interlayered harzburgites and dunites, bronzitites, norites and amphibolites.

Dunites consist of cumulus olivine relatively rich in Fe (Fo_{81-79}) and disseminated chromian spinel, locally with intercumulus bronzite (En_{84-82}). This orthopyroxene contains up to 1.37%Al_2O_3 (Fig. 1B). Chromian spinel shows a very unusual Al- and Fe-rich composition, having Y_{Cr} values (Y_{Cr}=Cr/ R^{3+}) between 0.45 and 0.25, and X_{Mg} values (X_{Mg}=Mg/ R^{2+}) between 0.45 and 0.20 (Fig. 1A). Mineralized dunites exhibit rounded olivine crystals cemented by the sulfide mass.

Olivine, bronzite and chromian spinels in the harzburgites show similar chemical composition to those in the orthopyroxe-bearing dunites. However, both olivine and bronzite are cumulus minerals, and the latter usually displays rounded or tabular inclusions of sulfides.

Barren bronzitites are made up of cumulus crystals of bronzite with disseminated chromian spinels and sulfides. Where mineralized, bronzitites can contain up to 90 vol% sulfides. These sulfides may occur as inclusions in the orthopyroxene but mainly intergranularly corroding the bronzite crystals. Locally, deformed bronzite crystals are cut by sulfide veins preserving the former orientation of the deformed crystals. Bronzite is Fe- and Al-richer than that from the ultramafic rocks, having enstatite percentages between 83 and 79, and Al_2O_3 contents between 1.7 and 2.6wt% (Fig. 1B). It generally exhibits lamellar exsolutions of clinopyroxene of augitic composition but

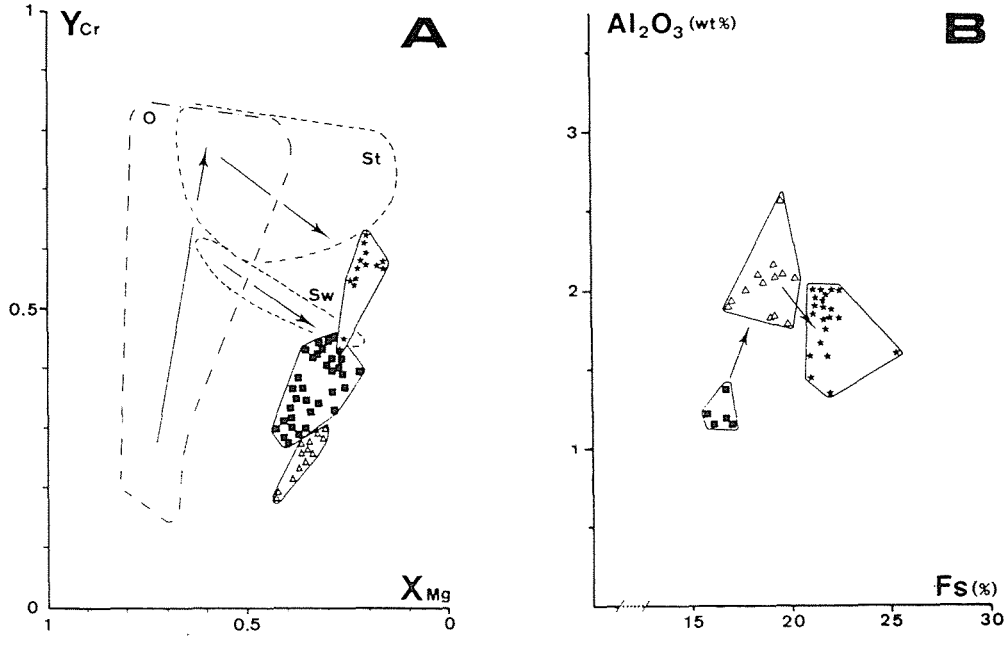

Figure 1. A. Y_{Cr} vs X_{Mg} diagram of the analyzed chromites in dunites (black squares), in bronzitites (open triangles) and in plagioclase-bearing bronzitites (black stars). The compositional fields of chromites from ophiolitic complexes (O) (Leblanc, 1985), from magmatic stratiform complexes (St) (Irvine, 1967) and from the Stillwater Complex (Sw) (Jackson, 1968) have also been plotted for comparison. In the field (O) field arrow indicates the compositional variation of chromites from lherzolite to dunite while in the (St) and (Sw) fields arrows show the magmatic fractionation trends of the Bushveld and Stillwater Complexes, respectively. **B.** Al_2O_3 content of the orthopyroxenenes versus their ferrosilite content. Arrows show the evolutionary trend from dunites (black squares) to bronzitites (open triangles) and from bronzitites to plagioclase-bearing bronzitites (black stars).

extremely rich in Al_2O_3 (up to 10.25 wt%). Chromian spinels are also Al-richer, but with similar FeO contents to those from the ultramafic rocks (Fig. 1A).

Some bronzitites are transitional to norites, containing a small amount of calcic plagioclase (An_{88-86}) which occurs as intercumulus crystals. These rocks are also mineralogically characterized by the existence of Fe-rich bronzites (En_{79-74}) with 1.3-2.1 wt% Al_2O_3, scarce Cr- and Fe-rich chromian spinel (Fig. 1) and up to 20 vol% sulfides.

In the different mafic-ultramafic rocks there exist secondary amphibole and brown mica. These minerals mainly replace the orthopyroxene. The amphibole is a magnesian hornblende always having the same composition, independent of the composition of the enclosing rocks. On the contrary, the Mg/Fe ratio of the brown mica decreases from the ultramafic to mafic rocks.

Fe-Ni-Cu SULFIDE ORES

The sulfide association consists mainly of hexagonal pyrrhotite with flame exsolutions of pentlandite, granular aggregates of pentlandite locally showing a slight alteration to bravoite, and chalcopyrite filling the intergranular spaces. No variation is observed, either in the relative proportions of sulfides or in their texture, in ores hosted by different silicate rocks.

In addition to the described sulfides, the ore association also contains minor amounts of ilmenite, rutile, Co-Ni-Fe sulfarsenides, pyrite, Pd-Pt-Ni tellurides, native gold and electrum (AuAg). Ilmenite and rutile are partly oxidized and associated with chromian spinel, and all occur intergranular with respect to bronzite crystals. Pyrite is very scarce, occuring only as minute crystals (<50 μm) included in pyrrhotite. Co-Ni-Fe sulfarsenides are relatively more abundant than pyrite, having greater grain size (up to 200 μm) and a chemical composition that corresponds to a Ni-rich, Fe-bearing cobaltite. However, the most interesting feature is that they often exhibit very small inclusions (<5 μm) of gold, electrum and merenskyite ($PdTe_2$).

Apart from the above occurrence of merenskyite, Pd-Pt-Ni tellurides are ubiquitous minerals in the ore association; between 2 and 6 grains have been observed in each of the different ore samples studied. The grain sizes are very variable, from submicroscopic up to a crystal with 80 μm across (Fig. 2A). These minerals occur as rounded to subhedral inclusions in pentlandite (Fig. 2A),

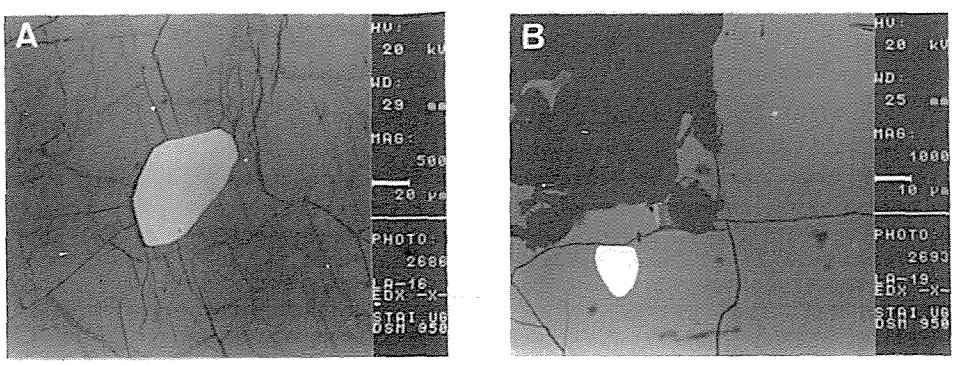

Figure 2. Back scattered images of Pt-rich, Ni-bearing merenskyite grains included in pentlandite (A) and in pyrrhotite (B).

pyrrhotite (Fig. 2B) and sulfarsenides, but they have not been observed in chalcopyrite. On the basis of semiquantitative analyses made with a scanning electron microscope, the chemical composition of the tellurides can be expresed as $(Pd,Pt,Ni)(Te,Bi)_2$, with Bi very subordinate to Te and being Pd the more abundant metal. This composition corresponds to a Pt-rich, Ni-bearing merenskyite. No tellurides richer in Pt or Ni have been found.

CONCLUDING REMARKS

The chemical composition of orthopyroxene defines a very clear fractionation trend marked by a progresive enrichment in their FeO contents from dunites to norites. Al_2O_3 follows FeO, but when plagioclase begins to crystallize orthopyroxene become impoverished in Al_2O_3. Chromian spinel shows the same chemical variations which correspond to spinels that crystallize from fractionating basaltic melts (Irvine, 1976).

The above chemical trends and the mineralogical and textural characteristics of the mafic-ultramafic rocks support the hypothesis that they have been formed by crystal fractionation of a mafic melt. During this process an immiscible sulfide melt was formed collecting Ni, Cu, Co, As, Te, Au, Ag and PGE. The fact that only bronzite exhibits sulfide inclusions suggests that the sulfide melt was formed after the crystallization of olivine and part of it settled to form mineralized dunites.

Sulfide mineralogy and textures agree with a magmatic origin from the breakdown of a Cu-bearing monosulfide solid solution (mss) on cooling. However, the discordance between the ore body and the lithologic contacts of the host rocks, as well as the existence of sulfide veins cutting previously deformed orthopyroxenes, suggest that during folding and metamorphism the sulfide mass was plastically moved to low pressure zones of the fold. The present textures shows that this process occured without any change in fO_2 and fS_2, at temperatures at least as high as that of exsolution of pentlandite from mss (615°C; Naldrett et al. 1967).

AKNOWLEDGMENTS

The authors are very grateful to the Dirección General de Fabricaciones Militares (Argentina) and specially to Colonel J.C. Delucchi for the facilities given for the realization of this researh. This work has been financially supported by the Junta de Andalucía (Research Group nº 4028) and the I.C.I. throught a Project for the Cooperation with Iberoamerica. We thank Prof. R.A. Both who kindly improved the English text.

REFERENCES

Irvine, T.N. (1967). Chromian spinel as petrogenetic indicator. Part II: Petrologic applications. *Canadian Jour. Earth Sci.*, v.4, p.71-703.

Irvine, T.N. (1976). Chromite crystallization in the join Mg_2SiO_4-$CaAl_2Si_2O_8$-$MgCr_2O_4$-SiO_2. *Carnagie Inst. Washington Year Book*, 76, p.465-472.

Jackson, E.D. (1968). Chemical variations in co-existing chromite and olivine in chromitite zones of the Stillwater Complex. In: Magmatic ore deposits. *Econ. Geol., Monogr., 4.* p.41-75.

Leblanc, M. (1985). Les gisements de spinelles chromifères. *Bull. Mineral.* v.108, p.587-602.

Naldrett, A.J., Craig, J.R., Kullerud, G. (1967). The central portion of the Fe-Ni-S system and its bearing on pentlandite exsolution in iron-nickel sulfide ores. *Econ. Geol.*, v.62, p.826-847.

Sabalúa, J.C. (1983). Prospección rocas básicas-Provincia de San Luis. *report C.E.G.M. 25/83*, Mendoza.

Current Research in Geology Applied to Ore Deposits.Fenoll Hach-Alí, Torres-Ruiz & Gervilla(eds)(1993).ISBN 84-338-1772-8

AURIFEROUS MINERALIZATION IN THE YALI-LOICA MINING DISTRICT IN THE CENTRAL LITORAL IN CHILE

Gonzalez Muñoz, I.
Dept. de Geología, Facultad de Ciencias Físicas y Matemáticas, Universidad de Chile, Casilla 13518, correo 21, Santiago de Chile, Chile

ABSTRACT: At the Yali-Loica mining district (Región Metropolitan), numerous gold deposits can be found either as vein or as placers. The vein deposits are structurally controlled by the main fault systems striking: N50°E, N75°W and E-W, with nearly vertical dips. These structures have been used as the access for mineralizing fluids precipitating quartz, pirite, native gold and in some placers lead zinc and silver. The vein systems are located in a large intrusive body made up principally of tonalitic-adamelite compounds, corresponding to the paleozoic coast range batholith. Emphasis is placed on the mineralogical determination and morphology of the residual sediments and on the relation with gold content of the original rock.

INTRODUCTION: This work forms part of the program in Project 7556 and E-1700-9255 of DTI of the University of Chile "Preliminary study of gold placer deposits", developed together with ORSTOM. The study reported here is located, between 33°50' and 33°59' South latitude in the Central Coastal area of Chile (Fig. 1). In this area there are numerous auriferous deposits that are found as hydrothermal deposits or as secondary deposits where the relationship vein-placer can be established. Mining and geological reports of auriferous placers in this area are quoted in Peebles, F., González, I. (1991) and González, I. (1991).

GEOLOGY AND SEDIMENTOLOGY: The field studies and the analysis of structure alignmet an using LANDSAT imagery, have revealed the existence of numerous faults, which to is a large extent control the auriferous mineralization in the mining district Yali-Loica. These faults are grouped in three principal striking systems: N55°E; N75°W y E-O (Fig. 2) and they have served as ascending means for the mineralizing solutions that have deposited quartz as gangue with pirite, hematite, calcopirite. Gold content is found free or forming part of pirites in the quartz. In some places minerals with galena sphalerite and silver are found. The range of these veins varies between 20 cm and 2 m, with extensions from 50 m to 10 km, the depth is 40 m, with changeable percentages in the surface of 40 g/t to 0.1 g/t in deeper places. Exceptionally contents of 340 g/t of gold, have been reported in "Mina El Nono", where the samples have been obtained from rubble. The parent rock presents 0.7 g/t. The others gold percentages obtained from veins in other mines in the district under study are the following: Rosita, 2.2 g/t; Caracol, 0.08 g/t; Loica Alta, 0.024 g/t; Mansa Veta with content of 0.060 g/t and Caledonia 4 g/t. These veins are located in the Paleozoic Coasted Batholith defined by Muñoz Cristi (1962), Corvalán y Dávila (1964); Corvalán y Munizaga (1972) Vergara and Drake (1979), etc.. The Central Batholith intrudes into the mesozoic formations producing phenomena of contact, metamorphism and

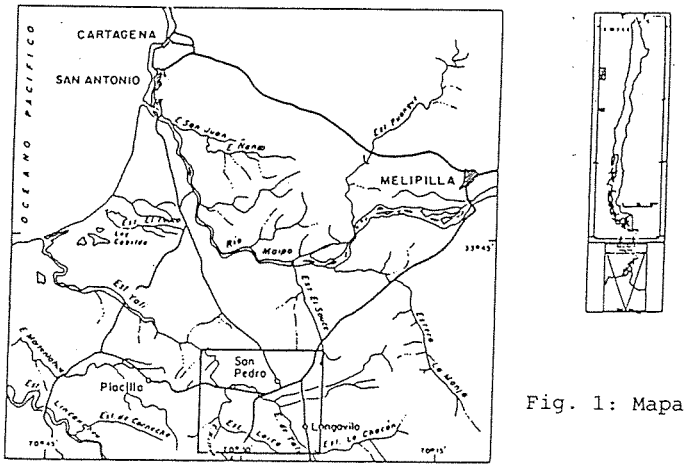

Fig. 1: Mapa de ubicación

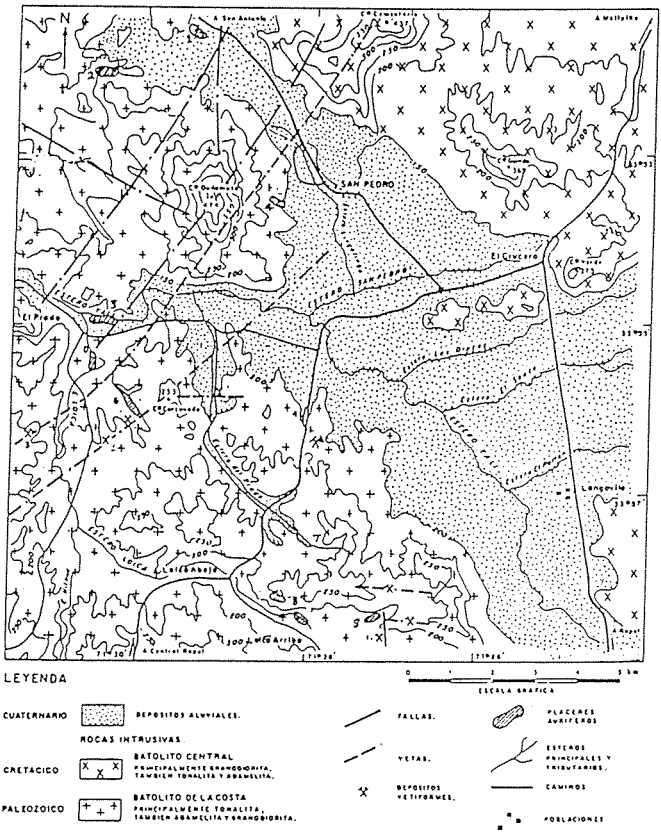

Fig. 2: Mapa Geológico Distrito Minero Yali-Loica

hydrothermal alteration, the latter being resposible for the metallic and non metallic generation in the Eastern sector of the Cordillera de la Costa (Peebles, F.; Gajardo, A.; González, I., 1987). The main metallic mineralization is auriferous. The relief is moderate, the highest extensions reach above sea level, e.g. Quilamuta hill. The present hydrografic basin is formed by the Yali and its affluents among which the Loica, El Prado, San Pedro, Lingo-Lingo are more noticeable. The rivulet flow of these is intermittent staying dry for about 7 months in a year. These sediments would be the transportation and depositary means of the coluvios coming from the primary sources, concentrating the heavy sediments in levels of terraces, and gullies, sometimes very near the place of origin. The gold-placers that have been studied are: (1) Lo Engañado, (2) Quilamuta, (3) El Yali, (4) San Pedro, (5) El Prado Verde, (6) El Alamo Huacho, (7) Loica Bajo, (8) Loica Alto y (9) El Litre (Fig. 2). The majority of these gold-placers were put in operation on the 80's using local equipement by ENAMI. On studing the stratified profiles of the different gold-placers we can conclude that in the past the river flow was larger and stronger considering the type of clasts that are found. It can be observed that the aurifeours mantle has an overcharge varying from a panning site to another, it ranges from 1.80 m to 8 m. The sedimentologic studies in the aurifeous heavy sediments reveal a short transport whose mineralogical composition is made up of piroxene, anphibole, magnetite, ilmenite, zircon, epidote and gold, (González, I. 1984). Many of these minerals which have a low resistance to erosion maintain their euhedral forms upon observation by SEM. The gold grains show high sphericity, low roundness, worn surfaces, molds and some of them retain quartz and other detritic minerals. The mineralogical composition of the heavy sediments forming the auriferous mantle is similar to the heavy forming minerals in the rocks of primary mines (Herail, 1991).

CONCLUSION: The geological and geochemical study of the primary sources in addition to gold placer sediments lead to the establishment of the relationship between vein and placer. The analysis of microtextures by SEM of gold particles and heavy minerals, also supports this conclusion.

REFERENCES:

Corvalán, J. and Dávila, A., 1964. Mapa Geológico de la Hoja Valparaíso - San Antonio. Instituto de Investigaciones Geológicas, Chile. Bol. N°28, 40 p.

González, I., 1984. Estudio sedimentológico y mineralógico del Litoral Central de Chile, Tesis de Doctorado, Universidad Autónoma de Madrid, España, 171 p.

González, I., 1991. Sedimentología y Mineralogía de placeres auríferos y su relación con Yacimientos hidrotermales, Actas del Symposium international. Alluvial gold Placers. 1991, 13 pág.

Herail, G. et col., 1991. The glacial gold placer of Suches Antaquilla and its exploration/ El placer glacial de Suches Antaquilla y su exploración. Field guidebook/ Libreta guia de la excursion de campo. Symp. Int. sur les Gis. Alluv. d'or, La Paz, juin 1991, 70 p.

Muñoz Cristi, J. 1962. Estudios petrográficos y petrológicos sobre el Batolito de la Costa de las provincias de Santiago y Valparaíso. Public. Inst. Geología. Santiago de Chile, 93 p.

Peebles, F., González, I., 1991. Placeres auríferos del Litoral Central de Chile. Resúmenes "Simposio Internacional sobre Yacimientos Aluviales de Oro", 5 p.

Vergara, M. and Drake, R., 1979. Evidencias de periodicidad en el volcanismo cenozoico de los Andes Centrales. Actas Primer Congreso Geológico Chileno, 10 p.

Current Research in Geology Applied to Ore Deposits.Fenoll Hach-Alí, Torres-Ruiz & Gervilla(eds)(1993).ISBN 84-338-1772-8

THE WILUNA LODE-GOLD DEPOSITS, WESTERN AUSTRALIA: AN EXAMPLE OF A HIGH CRUSTAL-LEVEL ARCHAEAN LODE-GOLD SYSTEM

Hagemann, S.G.; Groves, D.I. & Ridley, J.R.
Key Centre for Strategic Mineral Deposits, Dept. of Geology. University of Western Australia, Nedlands, WA 6009, Australia

ABSTRACT: The Archean Wiluna lode-gold deposits in the north of the Norseman-Wiluna Belt, Western Australia, are controlled by the Wiluna strike-slip fault system. Mineralization-related hydrothermal alteration is spatially and temporally related to the fault system, and gold occurs in two distinct mineralization (metal) associations: (1) gold-arsenopyrite (As)-pyrite, and (2) gold-stibnite (Sb). The fluid evolution of the fossil hydrothermal system is complex with five fluid regimes identified, controlled by three major processes: fluid-rock interaction, retrograde boiling, and fluid mixing. A combination of fluid-inclusion and stable- and Pb-isotope data indicate, at least at the higher levels of the hydrothermal system, an incursion of surface waters into the fault system during mineralization.

INTRODUCTION

Recent genetic models for Archean granitoid-greenstone gold mineralization discuss the contribution of magmatic, mantle, metamorphic, and meteoric fluid-source reservoirs. The last has been firmly rejected by various researchers for the hydrothermal systems that deposited the so-called mesothermal lode-gold deposits (Kerrich, 1987; Groves & Phillips, 1987), although it may be important in hydrothermal systems in similar Mesozoic and Cenozoic deposits (Böhlke et al., 1989).

However, recent studies on the Archean Wiluna lode-gold deposits (Hagemann, 1992) have shown that these deposits formed at a relatively high crustal level and that surface waters (seawater and/or meteoric waters) played a role in some ore-forming processes. This contribution characterizes the nature of the ore fluids, and presents a fluid evolution model of the fossil hydrothermal system at Wiluna.

REGIONAL AND MINE GEOLOGY

The Wiluna lode-gold deposits are located in the Wiluna domain of the Wiluna greenstone belt, which is the northernmost extension of the Norseman-Wiluna Belt. The Wiluna domain is a very-low-grade metamorphosed (prehnite-pumpellyite facies) supracrustal terrain with dominantly brittle deformation.

The deposits were discovered in 1901, comprise eight major mines that have produced approximately 2.4 million ounces Au, with resources of 1.2 million ounces Au at a grade of 3.8 g/t Au (Hagemann et al., 1992). In addition 38.3 t of As and 3.5 t of Sb were produced. Collectively, the Wiluna deposits are the fifth largest gold producer in the Yilgarn Block (Groves et al., 1989).

Structural setting

The Wiluna lode-gold deposits are hosted in a succession of low- and high-MgO basalts, komatiitic basalts, dolerites, and felsic intrusive rocks. The lithologies strike N-NNW and face SW. Gold mineralization is controlled by the Wiluna strike-slip fault system which consists of N- and NE-trending, steeply dipping sets of

principal displacement faults and associated subsidiary structures. The movement on all faults was dextral, with minor oblique-reverse and/or oblique normal motion and maximum displacement of 1350 m. On a deposit scale, mineralization is controlled by structural inhomogeneities on the principal displacement faults and/or subsidiary structures, whereas on an ore shoot-scale, the control is by the intersection of planar structural elements.

Hydrothermal alteration and mineralization

Gold mineralization occurs in two distinct mineralogical (metal) associations: (1) gold-arsenopyrite (As)-pyrite, Ore Association 1, and (2) gold-stibnite (Sb), Ore Association 2. The former is accompanied by distinct (sericite - carbonate - quartz ± albite) hydrothermal alteration extending up to 150 m from gold lodes, most strongly and extensively in the hanging wall of each lode. Gold-stibnite mineralization occurs within the area mineralized by gold-pyrite-arsenopyrite, but has a restricted vertical (and lateral) extent, being only developed in the uppermost 200 m ('625ft level') of some of the gold lodes. Alteration halos around gold-stibnite mineralization are of restricted extent (< 5 m), comprising quartz and minor carbonate.

NATURE OF ORE FLUIDS

Fluid inclusion data

Three types of fluid inclusion are genetically related to Ore Association 1: (1) aqueous inclusions with apparent salinities between 1 and 22 equiv. wt % NaCl, (2) H_2O-CO_2±NaCl inclusions with variable (10 - 20 mole %) CO_2 contents and low (4 equiv. wt % NaCl) salinities, and (3) CO_2-rich inclusions with rare thin water rims. Homogenization temperatures of aqueous inclusions are 100-375°C (peak 200-250°C); those of H_2O-CO_2 inclusions are 250-375°C (mean 295°C).

Fluid inclusions related to Ore Association 2 are of two types: (1) aqueous inclusions of low salinity (< 9 equiv. wt % NaCl), and (2) H_2O-CO_2 inclusions of low salinity (mean 5 equiv. wt % NaCl) and low XCO_2 contents (average 0.17). Average homogenization temperatures of both types of inclusion are 230±50°C.

The fluid inclusion petrography, microthermometry, compositions, and densities allow the identification of five fluid regimes. Regime 1 is associated only with early graphite-bearing quartz veins and has no direct relationship with mineralization. Regimes 2 and 3 are associated with Ore Association 1, Regime 4 with quartz-stibnite mineralization, while Regime 5 reflects lower-temperature processes in Ore Association 1.

Stable- and Pb-isotope data

Calculated $\delta^{34}S(H_2S)$ values for fluids in equilibrium with pyrite (0.2 to 1.5 ‰) and stibnite (-2.1 to -2.6 ‰) are not diagnostic of fluid source. The difference in $\delta^{34}S(H_2S)$ values, however, suggests slightly more oxidizing conditions during stibnite precipitation.

Reduced carbon and carbonate carbon- and oxygen-isotope values indicate that, during the evolution of the hydrothermal system, the carbon isotope signature changed significantly. The inferred light $\delta^{18}O$ values (to -4.3 ‰) of some of the fluid regimes suggests that ore fluids contained a surface water component.

Delta^{18}O and δD data confirm that the hydrothermal system at Wiluna contained more than one fluid. The light δD_{fluid} (-6 to 9 ‰) and $\delta^{18}O_{fluid}$ (3.2 to 5.4 ‰) inferred to be in equilibrium with sheet silicates (close to SMOW) suggest involvement of surface water (seawater?) during Ore Association 1 mineralization.

Lead from sulfides is characterized by a pronounced heterogeneity in least-radiogenic Pb-isotope compositions, in contrast to other lode-gold deposits in the Norseman-Wiluna Belt. The Pb-source is likely to be heterogeneous, with Pb contributions from both mantle-derived and older crustal rocks.

FLUID EVOLUTION OF THE HYDROTHERMAL SYSTEM

The available data show that the fluid evolution of the hydrothermal system was controlled by three major processes: fluid-rock interaction, retrograde boiling, and fluid mixing.

Fluid-rock interaction: Ore Association 1 sulfides dominantly occur finely disseminated in wallrocks adjacent to shear veins and in fragments of implosion breccias (Hagemann et al., 1992), indicating that gold-pyrite-arsenopyrite precipitation was primarily controlled by fluid-wallrock reactions (sulfidation) rather than by processes such as phase separation. The temperature during mineralization is estimated from the arsenopyrite geothermometer as 350±50°C.

Retrograde boiling: The following evidence indicates retrograde boiling (c.f. Ramboz et al., 1982): (1) pervasive contemporaneity of aqueous, H_2O-CO_2±NaCl, and CO_2-rich fluid inclusions; (2) vapor- and liquid-rich H_2O-CO_2±NaCl fluid inclusions that homogenize in the vapor and liquid phases, respectively; (3) salt partitioning in favor of the liquid phase in cogenetic liquid/vapor pairs.

The coexistance of weakly- to moderately-saline aqueous fluids, containing minor CO_2, and CO_2-rich fluids with minor weakly-saline H_2O can be explained by boiling of a single, homogeneous, low-salinity H_2O-CO_2 fluid. Retrograde boiling is suggested to occur at approximately 270±50°C (Hagemann, 1992). As retrograde boiling caused at most minor sulfide precipitation (Ore Association 1), its magnitude (extent) was evidently insufficient for vapor separation to compete with fluid-wallrock reactions in influencing gold solubilities (c.f. Seward, 1989).

Fluid mixing: Evidence for surface water infiltration into the strike-slip fault zone, at least in the shallow parts of the system, and mixing with ascending deep-seated fluids from the mantle and/or low-mid crust (Hagemann et al., 1992) includes: (1) differences in salinity and abundance of complex cations in different fluid inclusion populations; (2) isotopic signatures ($\delta^{13}C$, $\delta^{18}O$ to -4 ‰) of surface fluids in equilibrium with gangue carbonates; (3) evolution in both fluid inclusion composition and P-T conditions of mineralization between gold-pyrite-arsenopyrite and gold-stibnite associations; (4) the lack of high-XCO_2 fluid inclusions in quartz in gold-stibnite mineralization, which could be explained by dilution of CO_2 by surface waters; (5) the large range of total homogenization temperatures (180 - 350°C) of primary inclusions in quartz associated with gold-stibnite mineralization.

Aqueous and low-XCO_2 fluid inclusions, primarily those related to Ore Association 2, but locally to the gold-arsenopyrite-pyrite association, are thus suggested to result from fluid mixing.

Stibnite precipitation, in particular, may have resulted from cooling of deep-seated fluids on mixing with surface waters.

SUMMARY AND CONCLUSIONS

At Wiluna, the very-low metamorphic grade host rocks, their brittle deformation, the style of mineralization, the vertical zonation with respect to stibnite, and the evidence for fluid mixing between deeply derived fluids and surface waters, in combination, indicate that the fault- and mineralizing-systems formed at a high-level, 'epizonal' (< 5 km), crustal level. The depth restriction of the gold-stibnite association from the 625 ft level to the current surface could represent a transition zone in a complex hydrothermal system showing vertical zonation.

ACKNOWLEDGEMENTS

The support given by Asarco Australia Ltd and their permission to publish is gratefully acknowledged. This study forms part of a Ph.D project, carried out by S.G.H. at UWA. S.G.H. is supported by Asarco Australia Ltd and funded by a University Research Scholarship and the Key Centre for Strategic Mineral Deposits.

REFERENCES

Böhlke, J.K., Kirschbaum, C. & Irwin, J. 1989. Simultaneous analyses of noble-gas isotopes and halogens in fluid inclusions in neutron-irradiated quartz veins by use of a laser-microprobe noble-gas mass spectrometer. In: Shanks III, W.C., Criss, R.E. (eds.) New frontiers in stable isotopic research: laser probes, ionprobes, and small-sample analyses. U.S. Geological Survey Bulletin 1890: 61-88.

Groves, D.I. & Phillips, G.N. 1987. The genesis and tectonic controls on Archean gold deposits of the Western Australian Shield: a metamorphic-replacement model. Ore Geol. Rev. 2: 287-322.

Groves, D.I., Barley, M.E. & Ho, S.E. 1989. The nature, genesis and tectonic setting of mesothermal gold mineralization in the Yilgarn Block, Western Australia. Econ. Geol. Monograph 6: 71-85.

Hagemann, S.G., Groves, D.I., Ridley, J.R. & Vearncombe, J.R. 1992. The Archean lode-gold deposits at Wiluna, Western Australia: high-level brittle-style mineralization in a strike-slip regime. Econ. Geol. 87: 1022-1053.

Hagemann, S.G. 1992. The Wiluna lode-gold deposits, Western Australia: A case study of a high crustal level Archean lode-gold system. Ph.D thesis, Univ. West. Australia, 181p. (unpublished).

Kerrich, R. 1987. The stable isotope geochemistry of Au-Ag vein deposits in metamorphic rocks. In: Kyser, T.K.(ed.) Stable isotope geochemistry of low-temperature fluids. Min. Assoc. Canada Short Course 13: 287-336.

Ramboz, C., Pichavant, M. & Weisbrod, A. 1982. Fluid immiscibility in natural processes: use and misuse of fluid inclusion data: II Interpretation of fluid inclusion data in terms of immiscibility. Chemical Geology 37: 29-48.

Seward, T.M. 1989. The hydrothermal chemistry of gold and its implications for ore formation: boiling and conductive cooling as examples. Econ. Geol. Monograph 6: 398-404.

Current Research in Geology Applied to Ore Deposits. Fenoll Hach-Alí, Torres-Ruiz & Gervilla (eds) (1993). ISBN 84-338-1772-8

FLUID INCLUSION EVIDENCE FOR THE ORIGIN OF EPITHERMAL GOLD QUARTZ VEINS IN THE CHORTIS BLOCK, NICARAGUA

Högelsberger, H. (1) & Sundblad, K. (2)

(1) Inst. für Geochemie der Universität Wien, Dr. Karl-Lueger-Ring 1, A-1010 Wien, Austria

(2) Institutionen för Geologi och Geokemi, Stockholms Universitet, S-106 91 Stockholm, Sweden

ABSTRACT: New fluid inclusion data are presented for auriferous quartz veins representing three Nicaraguan ore districts (Matagalpa, Limón and Chorreadero). Most inclusions are liquid-rich and consist of low saline water. In addition, vapour inclusions in a few samples indicate evidence for boiling. The data presented in this paper form, together with previously published results on structures, mineralogy and lead isotope systematics, a base for a division of the Nicaraguan quartz veins into at least two groups. The Highland group is characterized by a unimodal T_h distribution, whereas the Nicaraguan Depression group shows a bimodal distribution pattern. This pattern is interpreted to reflect repeated pulses or fluid influx, which is consistent with available information on the lead isotopic systematics.

INTRODUCTION

Nicaragua has been the leading producer of gold ore in Central America during the 20th century. About half a dozen ore districts, located all over the country, have been exploited on industrial scale. Most of the production stems from auriferous epithermal quartz veins, which are genetically associated with Cenozoic subduction-related volcanism.

Fluid inclusion studies often reveal two different fluid regimes in auriferous quartz veins: 1. fluids containing carbon dioxide and water with moderate to high salt content in mesothermal mineralizations and 2. low saline aqueous fluid in epithermal veins. In order to check the validity of this general rule and to clarify the evolution history of the ore-bearing fluids, a fluid inclusion study of three key districts in Nicaragua was initiated.

GEOLOGY

The auriferous quartz veins of Nicaragua are hosted by a belt of Cenozoic continental margin basalts and basaltic andesites. These calcalkaline volcanic rocks were formed as a result of the subduction of the Cocos Plate oceanic crust under the continental crust of the Chortis Block. The Chortis Block is part of the Caribbean Plate and consists of phyllites and mica schists which are unconformably overlain by Mesozoic sediments. Numerous gold bearing quartz veins have been mined in Nicaragua. Based on the metal content, structural trends and lead isotope composition, Sundblad et al. (1991) distinguished between three populations of gold-bearing quartz veins: the Atlantic Coast group, the Highland group, and the Nicaraguan Depression group. The veins in the

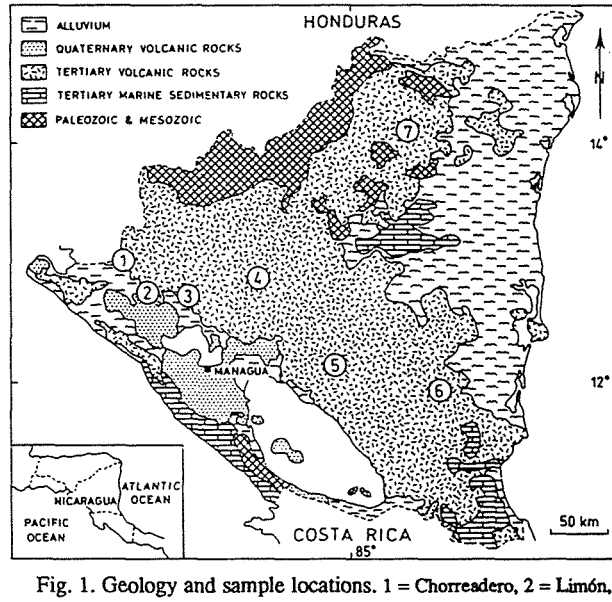

Fig. 1. Geology and sample locations. 1 = Chorreadero, 2 = Limón, 3 = India, 4 = Matagalpa, 5 = Libertad, 6 = Topacio and 7 = Bonanza.

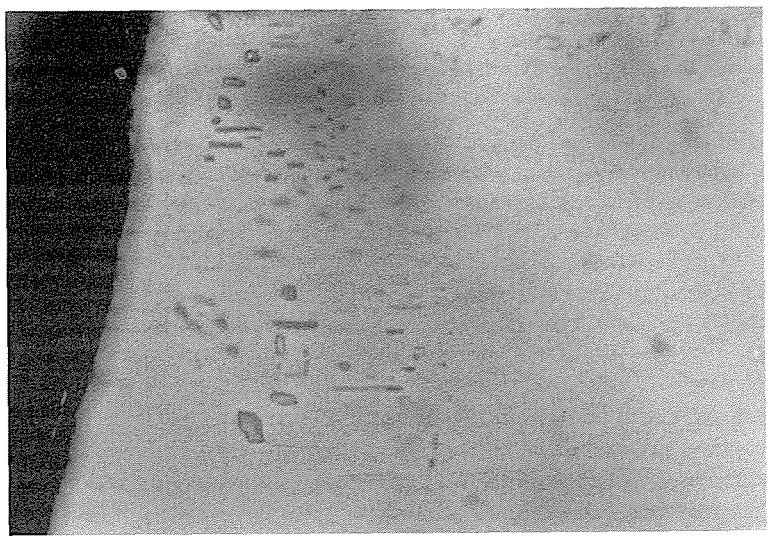

a. Low temperature inclusions (T_h: 101 + 121°C) hosted by calcite in sample 76 (Las Palomas vein, Chorreadero District).

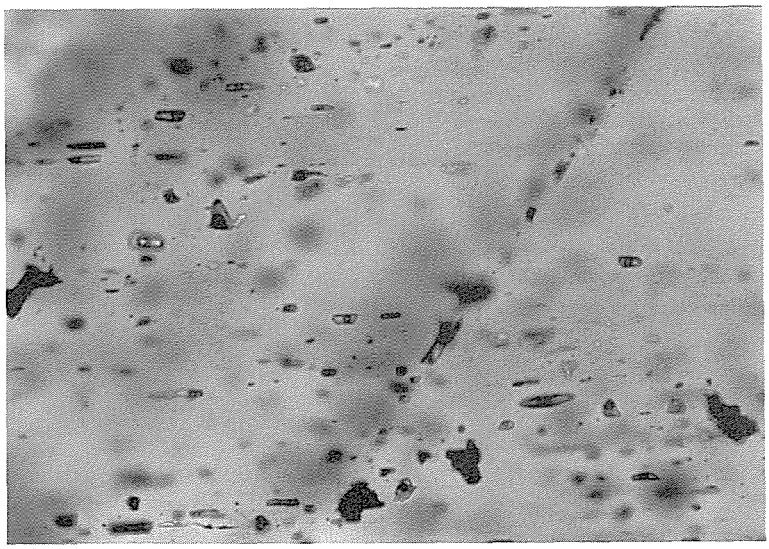

b. Primary inclusions of sample 78 (Mina Verde vein, Matagalpa District).

Fig. 2. Photomicrographs of fluid inclusions. Width = 250 μm.

Atlantic Coast group are polymetallic with abundant galena, sphalerite and chalcopyrite. No fluid inclusion studies have yet been carried out there. The veins in the *Highland group* (La Libertad, Matagalpa and Topacio mining districts) contain considerably less sulphide minerals and are controlled by NE-SW-trending structures. The *Nicaraguan Depression group* include the most important mining camp of Nicaragua, the El Limón district, as well as other significant disticts (La India and Chorreadero). The veins are controlled by a major NW-SE-trending basin referred to as the Nicaraguan Depression. This structure extends for 600 kilometres along the Pacific coast and is related to Pliocene-Pleistocene extension.

A heterogenous lead isotopic pattern was recognized for the veins belonging to the Nicaraguan Depression group indicating a complex metal derivation (Sundblad et al., 1991). This is in marked contrast to the veins of the Highland and Atlantic Coast groups, which display very homogeneous lead isotopic signatures indicating metal derivation from large homogenized metal reservoirs.

Several features of the veins in the Nicaraguan Depression group, indicate that they were formed in a lower pressure regime (i.e. at more shallow depths) compared to the veins in the Highland group. Metamorphic mineral assemblages including chlorite, epidote and wairakite are documented in the La Libertad mining district (Darce, 1990). This indicates higher metamorphic conditions and/or a higher thermal gradient compared with the El Limón district (Nicaraguan Depression group), where no such mineral assemblages have been recorded. Furthermore, a siliceous cap (interpreted as the preserved original top of the vein system) has been identified immediately above some of the veins in the El Limón district indicating a very shallow emplacement of the veins in the Nicaraguan Depression (Lilljequist, 1984).

FLUID INCLUSION STUDIES

PREVIOUS INVESTIGATIONS

Several fluid inclusion investigations have been carried out on various veins in Nicaragua (Table 1). Gleason (1977) investigated the Panteon vein system of the El Limón district. He obtained T_h-values between 73 and 319 °C with a distinct peak at around 200 °C. Salt contents were always below 0.5 eq.wt. % NaCl. Morales (1988) studied various veins of the Libertad District (Highland Group). The homogenization temperatures vary between 172 and 316°C with a mode around 230-240°C. The salinity is in a range of 1-2.1 eq.wt. % NaCl. None of these authors found daughter crystals, detectable carbon dioxide or evidence for boiling. Hålenius (1985) studied and compared primary inclusions at different levels of the Panteon vein. Again he found low saline fluids (<2.4 eq.wt.% NaCl). In samples derived from the lower levels, most T_h-values cluster between 200 and 220°C. In the upper parts, he observed a bimodal distribution of homogenization temperatures. Hålenius (1985) explained this phenomenon as well as the presence of vapour-rich inclusions by the effect of boiling.

Table 1. Available fluid inclusion data on the epithermal auriferous quartz veins, Nicaragua.

Group	District	Vein	Reference
Highland	La Libertad	San Juan, Zopilote, Tres Amigos, Mojon and Azul	Morales (1988)
Highland	Topacio	Topacio	Morales (1988)
Highland	Matagalpa	La Reina	This paper
Highland	Matagalpa	Mina Verde	This paper
Nicaraguan Depression	El Limón	Panteon	Gleason (1977), Hålenius (1985)
Nicaraguan Depression	El Limón	Talavera II	This paper
Nicaraguan Depression	Chorreadero	Las Palomas	This paper

THIS INVESTIGATION

In this study, six samples representing three ore districts were selected (Table 1 & 2). To obtain temperatures of homogenization (T_h) and of last ice melting (T_m), fluid inclusions were measured by microthermometry using a LINKAM TM-600 cooling/ heating stage. The results are summarized in Table 2.

The size of the investigated fluid inclusions ranges from <5 to 50 µm. They are hosted by vein quartz. Sample 76 (Las Palomas vein, Chorreadero District) is, however, an exception as two inclusions were found in calcite (Fig. 2a). The shapes of the inclusions vary from irregular to subrounded or elongated. Negative crystal shapes are rare. Most of the inclusions are arranged in clusters or planes. The distinction between primary and secondary origin is often ambiguous. Nevertheless, sample 78 (Mina Verde vein, Matagalpa District) contains tubular shaped inclusions which are arranged in three dimensions parallel to each other (Fig 2b). Therefore, they are regarded as primary. All measured inclusions are liquid-rich and consist of two phases (liquid and vapour). Homogenization takes place into the liquid state. The inclusions are aqueous with no detectable traces of CO_2. The salinities derived from the T_m-data (Bodnar, 1992) are very low (in 90% of the measurements below 2.1 eq. wt.% NaCl). Homogenization temperatures vary in general over a wide range (Tab. 2). Distribution histograms of T_h-values display in most cases, however, a maximum of frequency at around 250°C (Fig. 3). Sample 2 (Las Palomas vein, Chorreadero District) shows an additional peak at around 180°C (Fig. 3c). In several samples vapour inclusions occur as well. They consist of only one visible phase; it is impossible to observe any phase transitions.

DISCUSSION

The outlined inclusion data are similar to such reported from previous work on the Nicaraguan gold mineralizations. T_h-histograms derived from samples of the Highland group display a clear frequency maximum at around 250°C (Fig. 3a & b). This is in good accordance with results obtained by Morales (1985). Sample 78 (Mina Verde vein, Matagalpa District) contain vapour inclusions, which seem to be cogenetic with liquid-rich ones (Fig. 2b). This feature indicates boiling. Boiling can be an important mechanism to change pH of a hydrothermal solution and thus trigger gold precipitation. Drummond & Ohmoto (1985) demonstrated that, up to a temperature of 250°C, boiling is a very effective way to cause gold mineralizations. On the other hand, Bodnar et al. (1985) have stressed that, in epithermal systems, necking down is a wide-spread phenomenon, which can lead to similar features as boiling. As vapour inclusions do not occur in all samples, boiling can not be the only way of gold precipitation.

Table 2. Summary of characteristics of investigated quartz vein samples. Salinity calculation after Bodnar (1992). Sample numbers identical with those reported by Sundblad et al. (1991).

Group	District	Vein	Sample	Description	Au content	T_h range	Salinity
Highland	Matagalpa	La Reina	26	white vein quartz	27 ppm	83-307°C	0.3-1.6 %
Highland	Matagalpa	La Reina	79	white filling in breccia	---	137-320°C	0.7-1.6 %
Highland	Matagalpa	Mina Verde	78	vuggy vein quartz	---	211-285°C	1.2-2.1 %
Nicaraguan Depr.	Chorreadero	Las Palomas	2	white massive vein	16 ppm	98-304°C	0.5-2.6 %
Nicaraguan Depr.	Chorreadero	Las Palomas	76	white massive vein	24 ppm	95-306°C	0.2-2.9 %
Nicaraguan Depr.	Limón	Talavera II	16	banded milky quartz	15 ppm	170-281°C	0.5-3.7 %

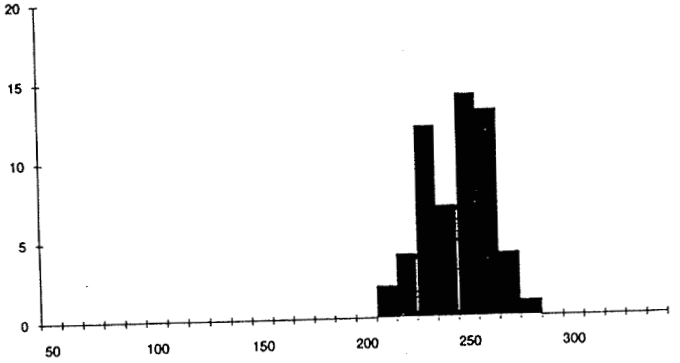

a. samples 26 & 79 (La Reina vein, Matagalpa District).

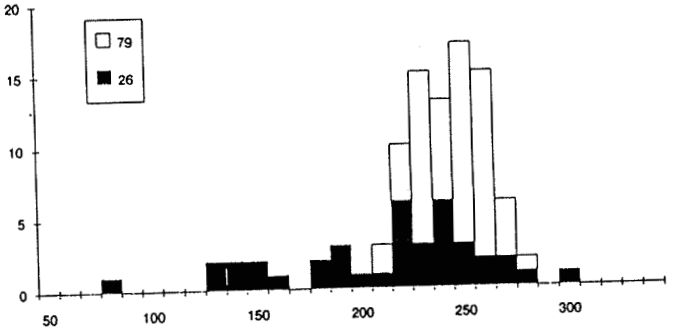

b. sample 78 (Mina Verde vein, Matagalpa District).

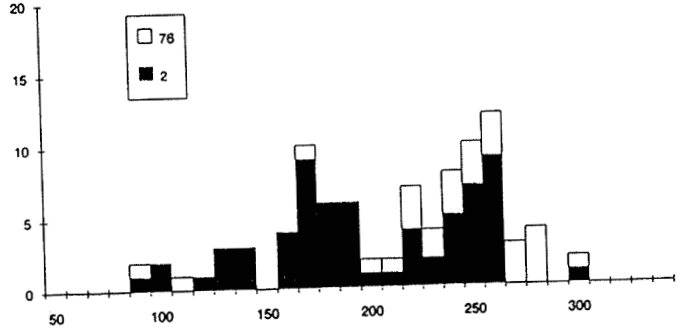

c. samples 2 & 76 (Las Palomas vein, Chorreadero District).

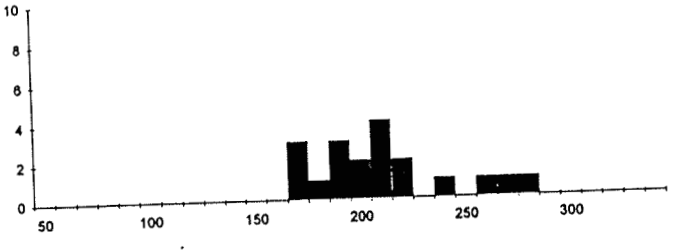

d. sample 16 (Talavera II vein, Limón District).

Fig. 3. Distribution histograms of homogenization temperatures of all fluid inclusions.

In samples originating from the Nicaraguan Depression group, unimodal frequency plots as well as bimodal distribution patterns (with peaks at 180°C and 270°C) occur (Fig. 3c). The latter are similar to those observed and interpreted as due to boiling by Hålenius (1985). Boiling is however not a satisfactory explanation for the observed bimodality, since the temperature difference between the two peaks would have required a pressure decrease of more than 1kb. An alternative explanation for the bimodality is that it results from more than one single fluid input. This has only been recognized in the Nicaraguan Depression group and is consistent with the heterogenous lead isotopic pattern recognized in these veins. The present fluid inclusion data provide therefore another argument for a fundamental genetic distinction between veins associated with the Nicaraguan Depression from those in the Nicaraguan Highland.

CONCLUSIONS

The new obtained data of fluid inclusions are in accordance with results from previous work. All these papers indicate a low salinity fluid and most T_h-histograms show a distinct unimodal frequency maximum. Bimodal distribution recognized in the Nicaraguan Depression group seems to be caused by repeated pulses or fluid influx. Evidence of boiling has been noted in a few samples. Gold precipitation appears also to be caused by cooling and fluid mixing between hydrothermal and meteoric waters.

ACKNOWLEDGEMENTS

Thanks are due to Michael Götzinger (Vienna) for making the cooling/heating stage (FWF Project No. P6072-GEO) available and to Ulf Hålenius (Stockholm) for constructive criticism. Financial support from NFR (Swedish Natural Science Research Council) and SAREC (Swedish Agency for Reseach in Developing Countries) to KS is acknowledged.

REFERENCES

Bodnar, R.J. 1992: Revised equation and table for freezing-point depressions of H_2O-salt fluid inclusions. PACROFI IV Abstract volume.

Bodnar, R.J., Reynolds, T.J. & Kuehn, C.A. 1985: Fluid inclusion systematics in epithermal systems. In BERGER, B.R. & BETHKE. P.M. (eds.): Geology and geochemistry of epithermal systems. -Rev. in Econ. Geol., 2: 73-97.

Darce, M. 1990: Mineralogic alteration patterns in volcanic rocks of the La Libertad gold mining district and its surroundings, Nicaragua. Economic Geology, 85: 1059-1071.

Drummond, S.E. & Ohmoto, H. 1985: Chemical evolution and mineral deposition in boiling hydrothermal systems. Chem. Geol., 80: 126-147.

Gleason, R.J. 1977: Wall-rock alteration, fluid inclusion, and mine water analyses of the Panteon vein system, Limón, Nicaragua. - Unpublished M.Sci. thesis Dartmouth College, New Hampshire, 105 pp.

Hålenius, U. 1985: Fluid inclusion microthermometry on quartz from the Panteon vein, El Limón area, Nicaragua. Unpublished report NICA 84007, Swedish Geological Company, Luleå, Sweden, 30 pp.

Lilljequist, R. 1984: Investigations of hydrothermal alteration zones in the Limón district, Nicaragua. Unpublished report, Swedish Geological Company, Luleå, Sweden, 22 pp.

Morales, A. 1988: Fluid inclusion studies of gold-bearing quartz veins in La Libertad mining district, Nicaragua. Unpublished undergraduate thesis, Stockholm University, 34 pp.

Sundblad, K., Cumming, G.L. & Krstic, D. 1991: Lead isotopic evidence for the formation of epithermal gold quartz veins in the Chortis Block, Nicaragua. Economic Geology 86, 944-959.

Current Research in Geology Applied to Ore Deposits.Fenoll Hach-Ali, Torres-Ruiz & Gervilla(eds)(1993).ISBN 84-338-1772-8

THE EUREKA GOLD DEPOSIT, GURUVE GREENSTONE BELT, ZIMBABWE: GEOLOGY, GEOCHEMISTRY, STABLE ISOTOPE AND FLUID INCLUSION STUDIES

Höppner, M.
Bundesanstalt für Geowissenschaften und Rohstoffe, Hannover, Germany

ABSTRACT: Eureka is an Archean shear zone hosted gold deposit situated on the eastern margin of the Guruve greenstone belt in northern Zimbabwe. The host rocks are mainly foliated granitoids and subordinate schists. The ore paragenesis consists of quartz, scheelite, molybdenite and native gold. Wall rock alteration is nearly absent. Isotope analyses indicate ore forming fluids predominantly of magmatic origin. As a consequence of alternating episodes of vein growth and syngenetic to postgenetic deformations the fluid inclusions were highly deformed and reequilibrated after trapping. Fluid inclusions are generally aqueous and of high salinity. A "fluid fault valve model" is proposed as genetic model for Eureka.

Introduction

The Eureka Mine is the northernmost operating gold mine on the Archean Zimbabwe craton. Eureka is situated on the eastern border of the Guruve greenstone belt at the contact of a foliated, coarse- to medium-grained hornblende-biotite-granitoid with meta-sediments and meta-volcanics of the Shamvaian group. The gold bearing quartz veins at Eureka are lodged in several south dipping discrete shear zones, orientated parallel to the host rock foliation.

Geological Setting

The studied area is situated on the northern margin of the Archean Zimbabwe Craton. In the area around Eureka Mine the Guruve greenstone belt comprises rocks of the volcanics-dominated `Western Succession` of the `Upper Greenstones´ of the Bulawayan Group (2.8 Ga) and of the sediment-dominated Shamvaian Group (2.7 Ga). The Bulawayan Group consists of conspicuous bands of completely serpentinized ultramafics of komatiitic composition and associated talc schists and banded ironstones. In addition, metabasalts of tholeiitic composition and interflow-sediments are present. The rocks of the Shamvaian Group cover large parts of the study area, comprising meta-greywackes and meta-grits, intercalated with small occurrences of amphibolite schists, which are interpreted as metamorphosed volcanics. The foliated Eureka granitoid is of granitic-granodioritic composition. According to the classification of CHAPPELL & WHITE (1974) it plots with the I-type granites, and in the diagrams after PEARCE et al. (1984) it falls into the fields of 'volcanic arc granites´. The mineralogical and chemical composition indicates an origin by partial melting of deep parts of the surrounding greenstone series. Genetically the Eureka granitoid is correlated

with the 'Younger Granites' (2.65 Ga) of the Chilimanzi Suite. A set of pegmatitic and aplitic dykes was injected in the mine area during a late phase of formation of the gold quartz veins.

Regional Deformation and Metamorphism

The structural and metamorphic evolution of the area is dominated by three orogenic phases:

- The Archean Orogeny (2.6 Ga) is correlated with an upper greenschist to epidote-amphibolite-facies metamorphism. Structural analysis shows that the formation of the gold quartz veins at Eureka was associated with this period.
- The Magondi Orogeny (1.8 - 2.0 Ga) which had a subordinate influence on structures and mineral paragenesis in the studied area.
- The Pan-African Orogeny (450 - 1000 Ma), connected to a retrograde greenschist-facies regional metamorphism and an overprinting of Archean structures in the northern part of the investigated area.

Furthermore, the area is influenced by deformations resulting from granite diapirism, especially near the granite-greenstone contacts.

Mineralization

In the Eureka deposit several gold-bearing quartz veins are lodged in discrete shear zones parallel to the foliation of the host rocks, dipping south with approx. 50°. The average gold contents of the ore vary from 2 to 10 ppm, but exceptionally may reach 65 ppm.

The paragenesis consists mainly of quartz, scheelite, molybdenite and native gold. Chalcopyrite and covellite occur in the primary paragenesis and some pyrrhotite fills small late cracks in the quartz veins. Generally, the sulfide contents of the quartz veins are very low and may reach about 0.5% at maximum. Gold always occurs as free gold in the quartz veins with maximum grainsizes of approx. 0.1 mm at an average fineness of 996. Inside the gold grains, tiny dendrites of bismuth and minute grains of tellurium-bismuthite occur.

Wall Rock Alterations

Caused by interactions of the mineralizing fluids with the host rocks, slight changes of chemistry, including hydrolysis of feldspars and potassic alteration, took place. The latter produced a thin biotite-halo (mm size range) in the contact zone to the quartz veins within the granodioritic host rocks. With regard to the high contents of potassium, a magmatic origin of the mineralizing fluids is probable. The precipitation of gold obviously was not essentially controlled by alteration processes.

Structural Setting

Macroscopically, the gold quartz veins of Eureka consist of banded, thin, lenticular bodies some tens of metres in length and up to 1 m wide (pinch and swell structure). The quartz bodies are dipping parallel to a prominent SW-plunging transport-lineation. According to relative age relationships, the emplacement of the gold quartz veins took place during a syn- to late kinematic stage of a late magmatic activity. The majority of the quartz veins was intersected and displaced by aplitic dykes, which in some places again were displaced by quartz veins.

The emplacement of the gold quartz veins is related to deformation in the brittle/ductile transition during simple shear. This deformation was caused by the building up of supra hydrostatic fluid pressures and an anisotropic thrust-stress regime, leading to fault valve behaviour (SIBSON et al., 1988; SIBSON, 1989, 1992). The layered structure of the gold quartz veins is related to cyclic processes of veining following repetitive variations in shear-stress and fluid pressures. Caused by increasing stress due to re-consolidation of the rock after vein mineralization, quartz veins generated during the previous cycle were deformed under regional stress regime conditions.

Stable Isotopes

H/D- and $^{18}O/^{16}O$- investigations were carried out for identification of the source of the ore-forming fluids. The isotopic composition of oxygen for the mineralizing fluids was calculated using $\delta^{18}O$ values from vein quartzes, temperatures of vein formation and the quartz-water oxygen isotope calibrations of MATSUHISA et al. (1979). The δD-values of extracted fluid inclusion waters (-58 to -87 ‰) and $\delta^{18}O$ values calculated from quartz (6.40 to 7.05 ‰) show a significant overlap with the primary magmatic water compositions. The results of isotopic analyses are very uniform and suggest that magmatic water was a significant component of the mineralizing fluids.

Fluid Inclusions

As a consequence of alternating episodes of vein growth and syngenetic to postgenetic deformations, fluid inclusions in quartz are highly deformed and reequilibrated after trapping due to strong cyclic variations of pressure. For this reason the fluid inclusions were classified with respect to genetic criteria. All early formed inclusions are aqueous and of high salinity. Microthermometric and Raman microprobe techniques failed to detect CO_2, CH_4, H_2S and N_2. Homogenization temperatures range from 111 to 225°C (mode:120 - 150°C), and salinities vary from 9.3 to 31.5 wt.% NaCl equivalent, with a mean at approx. 22 wt.% NaCl equivalent. Low eutectic temperatures (-38.9 - -67.3°C, mode: ~ -56°C) and melting temperatures of the salt hydrates (down to -50.4°C) indicate contents of $CaCl_2$,

LiCl or other chlorides in addition to NaCl in the inclusion-brines. Later formed inclusions are always two phase aqueous (L +V) and homogenize into liquid at temperatures in the 90° to 120°C range. The salinities are lower (~ 6 wt.% NaCl equivalent) than those of the earlier formed types.

Estimations of vein formation-conditions based on fluid inclusion characteristics point to temperatures of approx. 450°C and pressures of approx. 1-3 Kbar for veining and 4-6 Kbar for reequilibration.

Genetic Model

A 'fluid fault valve model' (SIBSON et al., 1988; SIBSON, 1992), influenced by processes of late magmatism and deformation and prograde regional metamorphism during the Archean consolidation of the Zimbabwe Craton (approx. 2.6 Ga) is proposed. Magmatic and possibly subordinate metamorphic fluids are suggested as the media of gold transport. At an impermeable barrier, possibly developed at the base of the seismogenic zone, supra-hydrostatic fluid pressures (P_{FLUID} against P_{LITH}) were generated. Under these conditions (T approx. 550 - 600°C, P approx. 2 - 7 kbar), gold can be transported in the form of chloride complexes. Shear faults were generated due to rising tectonic activity and/or fluid pressures ($P_{FLUID} > P_{LITH}$). In these rupture zones, fluids were rapidly drained upwards. Caused by the sudden decrease in temperature (< 450°C) and pressure (P_{FLUID} against $P_{HYDR.}$) the faults were sealed by precipitation of the solutes from the fluids. Cyclic repetition of this earlier process due to persistent activity of fluids and strain after sealing of the faults led to the typical banded character of the gold-bearing quartz veins at Eureka. Rapid crystallization and a low 'geochemical gradient' between main host rocks and mineralizing fluids permitted only very weak alteration of country rocks. In the late stage of these seismo-hydrothermal activities, pegmatitic and aplitic dykes intruded and were partly cut by the latest quartz veins.

References

MATSUHISA, Y., GOLDSMITH, J.R. & CLAYTON, R.N. (1979): Oxygen isotopic fractionation in the system quartz-albite-anorthite-water.- Geochim. et Cosmochim. Acta, **43**, pp 1131-1140.

SIBSON, R.H. (1992): Fault-valve behavior and the hydrostatic-lithostatic fluid pressure interface.- Earth Science Rev., **32**, pp. 141-144.

SIBSON, R.H., ROBERT, F. & POULSEN, K.H. (1988): High-angle reverse faults, fluid-pressure cycling, and mesothermal gold-quartz deposits.- Geology, **16**, pp. 551-555.

Current Research in Geology Applied to Ore Deposits. Fenoll Hach-Alí, Torres-Ruiz & Gervilla (eds) (1993). ISBN 84-338-1772-8

METAMORPHIC AND OXYGEN ISOTOPE ZONATION OF DEPOSITS IN THE AMPHIBOLITE FACIES COOLGARDIE GOLDFIELD, WESTERN AUSTRALIA

Knight, J.T.; Groves, D.I. & Ridley, J.R.
Key Centre for Strategic Minerals, Dept. of Geology, University of Western Australia, Nedlands, Perth, W.A. 6009, Australia

ABSTRACT: Archaean lode-gold deposits in the Coolgardie Goldfield occur in amphibolite-facies mafic and ultramafic rocks. Two different styles of gold-related wallrock alteration in the Goldfield, a high-temperature group (520-590 ±25°C) consisting of garnet-hornblende-plagioclase-pyrrhotite, and a medium-temperature group (480-520 ±50°C, 2-4kb) of amphibole-plagioclase-calcite-biotite-arsenopyrite, are spatially controlled by plan-view distance from the syntectonic Calooli Monzogranite, with the high-temperature group located more proximal to the contact. Delta ^{18}O values of co-existing hydrothermal calcite, quartz, and scheelite indicate mineralisation in an open-system at amphibolite facies conditions, and suggest that gold deposition in the high-temperature deposits was from a fluid which was in isotopic equilibrium with the Calooli Monzogranite. In the low-temperature group of deposits, ore-fluid $\delta^{18}O$ values are buffered by interaction with greenstones in fluid conduits.

INTRODUCTION

The Coolgardie Goldfield is located at the eastern margin of the ca. 2700-2690Ma volcano-sedimentary sequence of the Norseman-Wiluna Belt, 560km east of Perth and <40km southwest of the giant Kalgoorlie deposits. The Goldfield covers about 900km^2, was discovered in 1892, and has since produced >50t Au and 0.25t Ag. The regional geology consists of an arcuate series of complexly deformed mafic-ultramafic rocks, minor interflow sedimentary rocks, and felsic volcaniclastic rocks. The sequence has been intruded by a suite of felsic and mafic porphyries, and is bounded to the west by the syntectonic Calooli and Bali Monzogranites, to the east by the post-tectonic Mungari Granite, and to the south by unnamed granitoids.

METAMORPHIC AND STRUCTURAL SETTING

Country rocks at Coolgardie have been metamorphosed to the low- to mid-amphibolite facies. In mafic rocks, the typical equilibrium assemblage consists of hornblende-plagioclase (An>35)-ilmenite± titanite ±quartz ±epidote, and in ultramafic rocks the assemblage is tremolite-chlorite ±forsterite ±talc ±carbonate ±anthophyllite. Silicate geothermobarometry indicates that, in the east of the Goldfield, peak metamorphic temperatures reached 480±50°C. Metamorphic grade increases westwards towards the Calooli Monzogranite with temperatures of 525±50°C attained in the centre of the Goldfield, and peak metamorphic conditions of 545±50°C and 2.8-3.4kb proximal to the granitoid-greenstone contact (Figure 1).

Archaean lode-gold deposits in the Coolgardie camp, which occur as laminated quartz reefs, along sheared felsic porphyry-ultramafic rock contacts, and in quartz vein sets, are located in four different sets of post-D_1-thrusting structures (designated D_{2A}-D_{2D}). The structural style, associated fabrics defined by peak metamorphic amphiboles, and domainal distribution of the structures with respect to the western granitoid-greenstone contact, suggest that they formed in a heterogeneous stress field that developed in response to

either the anomalous geometry of the syntectonic granitoids, or the mechanics of their intrusion into the greenstones.

WALLROCK ALTERATION

Two different styles of gold-related wallrock alteration can be recognised at Coolgardie. These can be classified (using the scheme of Mueller and Groves, 1991) into (i) a high-temperature group characterised by the presence of almandine garnet-hornblende-plagioclase-calcite-chlorite±biotite±K-feldspar, with pyrrhotite and minor sphalerite, and (ii) a medium-temperature group characterised by calcic amphibole-biotite-plagioclase-calcite, with abundant arsenopyrite and pyrrhotite. Silicate and sulphide geothermobarometry indicates that the medium-temperature group formed at 480±50°C, and 3-4kb in the east, increasing to 510-520±50°C and 2-4kb in the central and western parts of the Coolgardie Goldfield (Figure 1). In contrast, the high-temperature group formed at 520-590±50°C at the western margin of the Goldfield.

The spatial distribution of the two styles of gold-related alteration is broadly controlled by distance from the western, syntectonic granitoids, with the high-temperature group more proximal to the contact than the medium-temperature group. An isograd (the garnet-in isograd), which divides the occurrence of the two alteration styles, closely parallels the plan-view contact between the greenstones and the Calooli Monzogranite (Figure 1).

RELATIVE TIMING OF MINERALISATION

Both styles of alteration are characterised by mono-or bimineralic alteration assemblages. These high thermodynamic variance equilibrium assemblages indicate that mineralisation occurred in an open-system at, or near to peak metamorphic conditions (c.f. Barnicoat et al., 1991). In addition, the equilibrium textural relationships between sulphides, native gold, and silicates, combined with (i) the similarity of the P-T conditions indicated by wallrock alteration and peak-metamorphic assemblages, and (ii) the correlation between higher temperature metasomatic and metamorphic assemblages and the western granitoid contact suggest that gold mineralisation was broadly synchronous with regional metamorphism and granitoid emplacement (c.f. Witt, 1991).

OXYGEN ISOTOPIC ZONATION

The oxygen isotopic composition of hydrothermal, gold-related quartz, calcite, and scheelite has been determined for several deposits of the Coolgardie Goldfield. The $\delta^{18}O$ value of the H_2O in equilibrium with these minerals is broadly correlated with metamorphic grade and plan-view distance from the Calooli Monzogranite (Figure 2). Ore-fluid $\delta^{18}O$ values for deposits proximal to this pluton are in the range 8 to 10‰. Distal deposits have lower $\delta^{18}O_{H2O}$, with the lowest value (4.2±1.6‰) obtained from Barbara-Surprise located >7km from the contact. A δ-δ plot of co-existing hydrothermal quartz and calcite indicates that these minerals were deposited in equilibrium at about 500°C (Figure 3), and suggests that the trend in ore-fluid $\delta^{18}O$ values is probably reflecting open-system hydrothermal behaviour. In this case, the variation in ore-fluid values from relatively oxygen-enriched proximal to the Calooli Monzogranite to oxygen-depleted distal to this pluton can potentially be explained by gold deposition at high temperatures from a hydrothermal fluid which was initially in isotopic equilibrium with magmatic rocks but underwent progressive

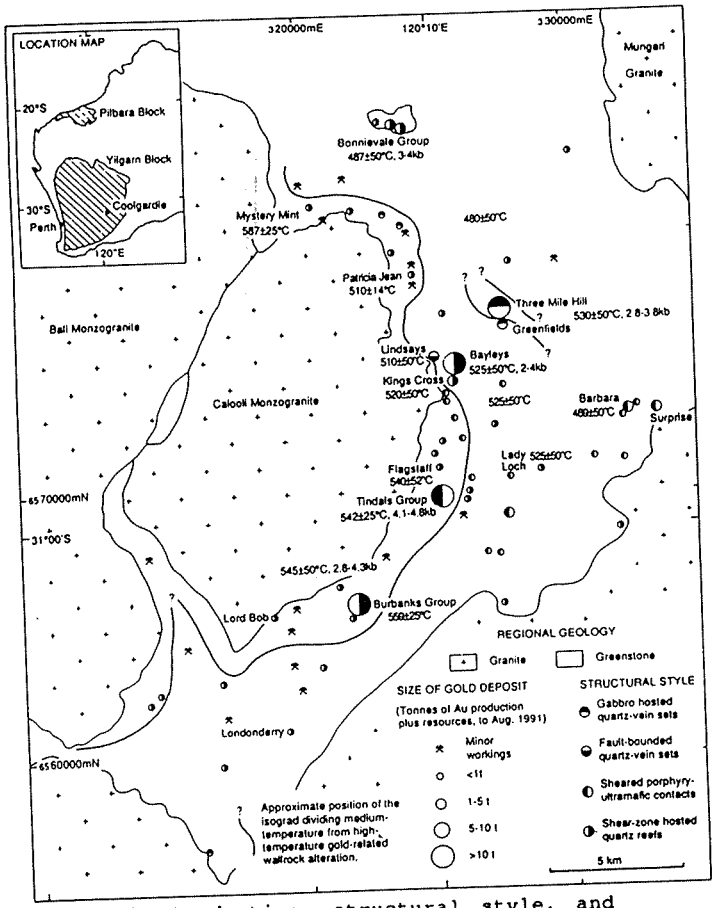

Figure 1. Production, structural style, and metamorphic grade for significant deposits in the Coolgardie Goldfield, W.A. Also shown is the isograd which divides high- and medium-temperature wallrock alteration assemblages

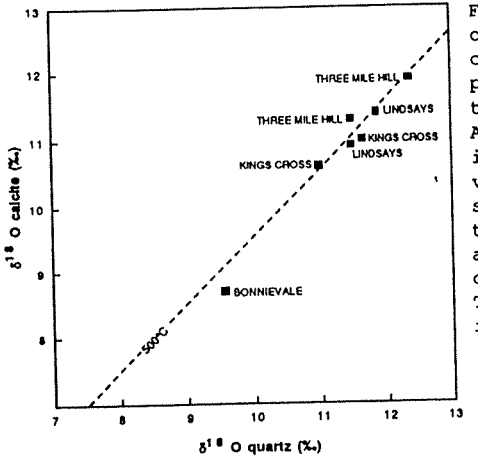

Figure 2. δ-δ plot of $\delta^{18}O$ compositions of coexisting quartz-calcite pairs from deposits in the Coolgardie Goldfield. Also shown is the 500°C isotherm. The isotopic variability of the samples, and their tendency to conform to an equilibrium slope are characteristics of high T-P, open system fluid infiltration.

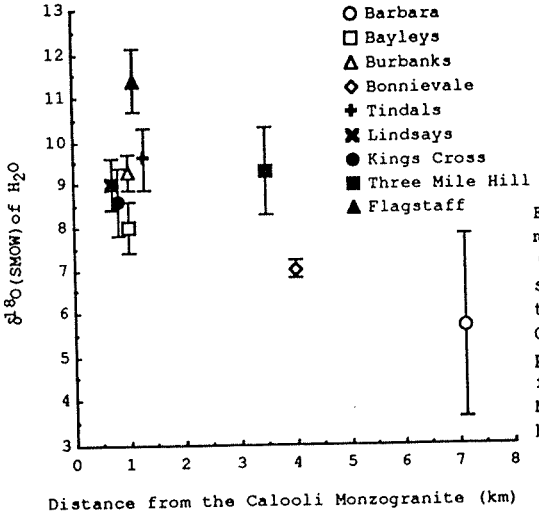

Figure 3. Plot of mean values of $\delta^{18}O$ (SMOW) of H_2O for selected deposits in the Coolgardie Goldfield versus plan-view distance from the Calooli Monzogranite. Error bars are ±1σ.

isotopic exchange with greenstone lithologies at lower temperatures during migration from source regions.

In contrast to the oxygen isotopic data, reconnaissance fluid inclusion and carbon- and hydrogen-isotope studies indicate that gold mineralisation was deposited from a homogeneous H_2O-CO_2-CH_4-NaCl fluid, characterised by a narrow range of ore-fluid $\delta^{13}C$ values (-2 to -4‰), and δD values characteristic of magmatic or metamorphic waters (i.e. -40 to -60‰). In addition, Pb- and Sr-isotope studies of gold-related galena and scheelite from deposits in the Goldfield indicate camp-scale homogeneity of the Pb- and Sr- source to the fluid. The data from this study and others (Mueller et al., 1991; McNaughton et al., 1992) suggest that gold mineralisation in the >150km district from Mt. Pleasant to Kambalda, including Coolgardie and Kalgoorlie, was deposited from a fluid with a homogeneous Pb- and Sr-isotopic composition, characteristic of a large-scale hydrothermal system.

CONCLUSIONS

The syntectonic granitoids at Coolgardie, through the mechanics of their intrusion and/or anomalous geometry with respect to regional stress fields, have played a role in the development of heterogeneous D_2 structures that host gold mineralisation in the Goldfield. The distribution of wallrock alteration types in the Coolgardie camp is also broadly controlled by distance from the granitoids and regional metamorphic grade, parameters which appear interrelated. In addition, oxygen isotopic values of gold-related minerals suggest that the ore-fluids either equilibrated with these or similar plutons, or that the Calooli Monzogranite contributed oxygen to the ore-fluid. The goldfield-scale and regional-scale homogeneity of the Pb- and Sr- source to the fluid appears to argue against a local source, such as the granitoids actually exposed at Coolgardie, unless all the granitoids, over a considerable cratonic segment formed from the same source. The most likely source is a deep granitoid below the exposed plutons.

ACKNOWLEDGEMENTS

This study forms part of a Ph.D. study by J.T.K. funded by MERIWA. UWA, OPRS, and MERIWA scholarships are gratefully acknowledged, as is the support of the companies operating in the Coolgardie area.

REFERENCES

Barnicoat, A.C., Fare, R.J., Groves, D.I., McNaughton, N.J. 1991. Synmetamorphic lode-gold deposits in high-grade Archean settings. Geology 19: 921-924

McNaughton, N.J., Groves, D.I., Witt, W.K. 1993. The source of lead in Archean lode-gold deposits of the Menzies-Kalgoorlie-Kambalda region, Yilgarn Block, Western Australia. Mineral. Deposita, submitted

Mueller, A.G. & Groves, D.I. 1991. The classification of Western Australian greenstone-hosted gold deposits according to wallrock alteration assemblages. Ore Geol. Rev. 6: 291-331

Mueller, A.G., De Laeter, J., Groves, D.I. 1991. Strontium isotope systematics of hydrothermal minerals from epigenetic Archean gold deposits in the Yilgarn Block, Western Australia. Econ. Geol. 86: 780-809

Witt, W.K. 1993. Lithological and structural controls on gold mineralization in the Archaean Menzies-Kambalda area, Western Australia. Aust. J. Earth Sci. 40: 65-86

Current Research in Geology Applied to Ore Deposits. Fenoll Hach-Alí, Torres-Ruiz & Gervilla (eds) (1993). ISBN 84-338-1772-8

A THERMODYNAMIC MODEL OF THE EFFICIENCY OF CO_2-H_2O-CHLORIDE HIGH TEMPERATURE FLUIDS IN THE FORMATION OF Au-BEARING QUARTZ VEINS

Kolonin, G.R.; Pal'yanova, G.A. & Shironosova, G.P.
United Inst. of Geology, Geophysics and Mineralogy, Siberian Branch of the Russian Academy of Sciences, 630090, Novosibirsk, Russia

Abstract: The model of exsolution of the initial fluid into a vapor CO_2-enriched phase and chloride solution restricted in CO_2 content is proposed to explain gold ore genesis at the Sovetskoye and Eldorado deposits situated in the Yenisei mountain ridge in Central Siberia. Possible conditions of gold transport and precipitation as a result of the activity of denser and CO_2-depleted fluid phase within the temperature range 400-25°C and pressure from 1kbar to saturated vapor pressure were calculated. Gold mineralization is considered to be formed during cooling of the fluid from 400°C temperature when the initial Au concentration exceeds 1-2ppm up to .01ppm at 200-150°C.

INTRODUCTION

During the past decade the important role of CO_2 in high-temperature fluids producing gold-bearing quartz veins has been emphasized repeatedly by many geochemists in Russia and other countries. For example, Yu.Ljachov(1988) discussed it in connection with the genesis of different types of gold deposits in Russia and Kazakhstan. The same conclusions were drawn in the papers describing many Canadian (Robert,Kelly,1987), Australian(Phillips, Groves,1983) and France Hercinian gold deposits(Boiron et al,1990). F.Robert and W.Kelly(1987) consider that at least Archean gold mineralization was derived after activity of CO_2-bearing fluids exsolved from a single homogenious parent fluid. The same idea was used by the authors in connection with the genesis of the Sovetskoye and Eldorado gold deposits, because the abundance of fluid inclusions namely in quartz of gold-bearing zones as well as wide variations in CO_2 content in different inclusions for these deposits were found by Yu.Dolgov, et.al.(1990), A.Vernikovskaya and A.Tomilenko (1992). The essential role of CO_2-H_2O-chloride fluid at Au-bearing bodies formation was substantiated in the above cited and other papers. The chemical aspect of transport and precipitation ability relative to gold remains beyond serious discussion. This made us to carry out the thermodynamic computations of possible gold solubility in these fluids and have estimated different types of its precipitation mechanism.

THERMODYNAMICAL DATA AND COMPOSITIONS OF MODEL SOLUTIONS

The calculation in the Au-CO_2-NaCl-H_2O systems for temperature range from 100 to 400°C and 1kbar - saturated vapor pressure were made with the help of the programme "GIBBS"(Shvarov,1976). The possibility of formation of 16 dissolved particles, including a gold complex $AuCl_2^-$ and $AuOH^o$, was taken into account. Since the acidity is one of the factors influencing the gold solubility , calculations of gold content for solutions with different carbonic acid concentrations were made which allowed to identificate of the effect of the carbonic acid as the acid component on the gold content of solutions. 1, 2, 4.3m NaCl solutions and pure water saturated in CO_2 were taken as a model. Data on CO_2-solubility in chloride solutions and water for the temperature and pressure interval studied were taken from papers by Takenouchi, Kennedy(1964) and Bowers, Helgeson(1983). The CO_2 and NaCl concentrations in calculations correspond to those in gas-liquid inclusions determined by thermobarogeochemical methods.

ESSENCE OF GOLD TRANSPORT AND PRECIPITATION MODEL

The results of fluid inclusion studies of Proterozoic gold-bearing veins of Sovetskoye and Eldorado mines show possible coexistence of the inclusions with different CO_2:H_2O ratio (Dolgov et. al.,1990; Vernikovskaya et.al.,1992), especially for productive quartz. It is one of the reasons why we have used the general idea of the parent fluid exsolution into a more saline aqueous fluid containing restricted amounts of CO_2 and CO_2-rich gas fluid with low salinity and H_2O content.
Fig.1(a,b) demonstrates possible CO_2 contents and calculated pH in NaCl-H_2O high density fluid after its separation from the parent phase and cooling along two-phase curve for some typical chloride

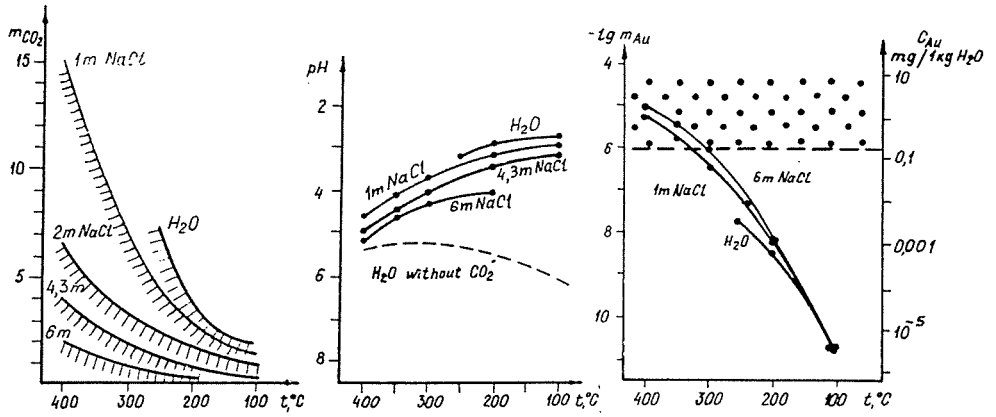

Fig.1.Solubility of CO_2 in pure water and solutions with different NaCL concentrations(a), pH(b) and gold solubility(c) of these solutions depending on temperatures(p=1kbar).

concentrations. Fig.1c shows the gold content represented in the form of $AuCl_2^-$ with insignificant additions of $AuOH^o$. Two important conclusions follow from this figure: 1)it is the temperature decrease which precipitates virtually the whole gold upto 200°C; 2)because fluid is acidified distincly during its cooling, especially at low NaCl content, CO_2 losses through effervescence do not favor the gold precipitation.
Fig.2 illustrates the influence of CO_2 loss at pH and Au concentrations when NaCl content equals 2m and temperature is constant. In both cases temperature decrease causes sharper pH decrease in comparison with CO_2 concentrations. We showed as an example the prevalent contribution of chloride complex in gold speciation for 300°C because its hydroxide form dominates at lg m_{CO_2}=-2 only when according to Fig.2a the pH fluid changes to 5.
The results above follow from the assumption about the absence of sulfide in solutions. At the same time the appreciable amounts of pyrite, arsenopyrite and some other sulfides are common of the Yenisei mointain ridge deposits and gold-bearing quartz veins in other places. Due to this it is necessary to provide the possibility of gold hydrosulfide complex formation in a more complete physical-chemical model. Fig.3a demonstrates the principal changes of gold speciation in the presence of pyrite. It is obvious

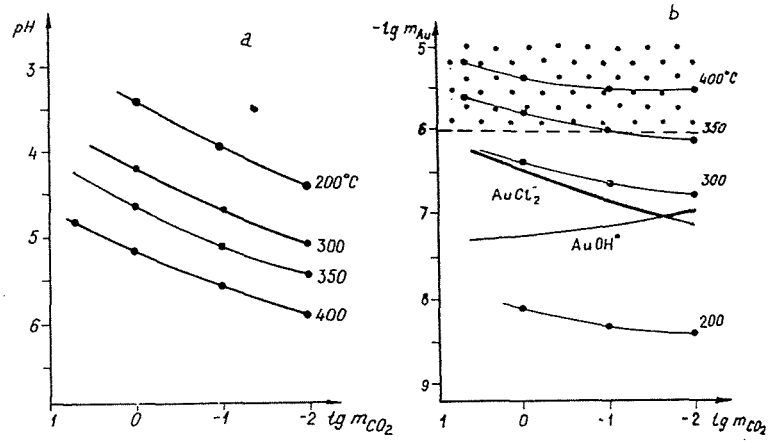

Fig.2.Influence of carbonic acid concentrations on pH(a) and possible gold concentrations in 2mNaCL solutions at different temperatures and 1kbar.

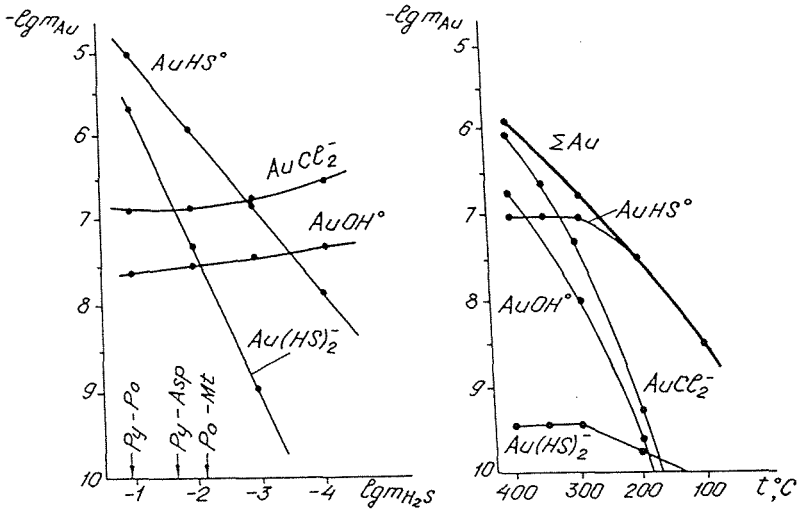

Fig.3.Gold solubility in chloride-carbonic acid-sulfide solutions: a)depending on sulfide concentrations at the temperature 350°C and 1kbar;b)depending on temperature at the 10^{-3}mH_2S.

that at 350°C as well as at other temperatures $AuHS^{\circ}$ and $Au(HS)_2^-$ predominate in the solutions when H_2S concentration exceeds 10^{-3}m level (points corresponding to pyrite-magnetite and other sulfide buffers are shown at the abscissa). But according to Fig.3b the temperature decrease remains the main reason of gold precipitation. At the same time the comparison with Fig.1c illustrates more smooth character of the gold concentration curve. At last the estimation of free HCl accurance in the fluid have been carry out as possible cause to favor gold solubility. The addition 0.01m HCl increases the gold concentration at 400°C upto 10ppm as a result of pH decrease.

CONCLUSIONS

1.Exsolution of gold-bearing carbonic dioxide-sodium chloride fluid into near neutral liquid phase and gaseous CO_2-riched phase is a general idea of thermodynamic model developed.
2.Solutions with restricted CO_2 concentrations(up to 10m/1kg H_2O) and NaCl(up to 2m/kg H_2O) formed after exsolution are considered as chemical environment transported the gold to the place of deposit.
3.Complex species $AuCl_2^-$ and additionally AuOH can provide gold concentration of CO_2-NaCl-H_2O fluid about 10^{-5}mol/kg H_2O,i.e. precipitation of 1-2ppm.
4.Decrease of temperature is the main reason of gold ore-forming process within the framework of this model.
5.When the fluid contains sulfide concentrations corresponding at least to conditions of the existance of magnetite-pyrite buffer(0.001m/kg H_2O), the main form of gold transport is presented by a hydrosulfide complex $AuHS^o$ the content of which may reach 10ppm at 400°C.

REFERENCES

Boiron,M.C.,Cathelineau,M.,Dubessy,J. and Bastoul,A.M. 1990 Fluids in Hercynian Au veins from the French variscan belt. Min. Magazin. 54:231-243

Bowers,T.S.,Helgeson,H.C. 1983. Calculation of the thermodynamic and geochemical consequences of nonideal mixing in the system H_2O-CO_2-NaCL on phase relations in geologic systems. Geochim.Cosmochim.Acta. 47:1247-1275

Dolgov,Yu.A.,Tomilenko,A.A.,Gibsher,N.A. 1990. Fluid regime and thermobarogeochemical criterions of quartz veins gold-bearity in metamorphic rocks.In: Thermobarogeochemistry of mineral formation processes,p.1,Novosibirsk:7-19

Ljachov,Yu.V. 1987. The thermobarogeochemical zoning and regime of formation of gold different depth depositions .DAN SSSR,297,N2:437-441

Phillips,G.N.,Groves D.J. 1983. The nature of Archean gold-bearing fluids as deduced from gold deposits of Western Australia. Journ.Geol.Soc.Australia 30:25-39

Robert,F.,Kelly,W.C. 1987. Ore-forming fluids in archean gold-bearing quartz veines at the Sigme mine, Abrtibi greenstone belt, Quebec, Canada. Ec.Geol.82:1464-1482

Shvarov,Yu.V. 1976. Calculation of equilibrium composition in the multi-component heterogenous system. DAN SSSR 229: 1224-1227

Takenouchi,S.,Kennedy,G.C. 1965. The solubility of carbon dioxide in NaCL solutions at high temperatures and pressures. Am.J.Sci. 263, N5:445-454

Vernikovskaya,A.E.,Tomilenko,A.A. 1990. Physical-chemical features of the gold deposit Eldorado(Yeniseisky Kriaszh) forming at conditions of the epidote-amphibolite facies of metamorfism. In: Thermobarogeochemistry of mineral formation processes,p.2, Novosibirsk:95-102

Current Research in Geology Applied to Ore Deposits.Fenoll Hach-Alí, Torres-Ruiz & Gervilla(eds)(1993).ISBN 84-338-1772-8

NEW TYPES OF GOLD MINERALIZATION

Komov, I.L.
Inst. of Geochemistry and Physics of Minerals of Ukranian Ac. Sci., Palladin Pr. 34, Kiev, 252680, Ukraine

ABSTRACT. Possibilities for revealing new types of gold deposits as associated with ultrabasites, carbonaceous, ferruginous and carboniferous formations are discussed.

An important dependence was revealed: a transition of the strictly determined part of the matter (gold) in some areas of the Earth's crust in the migration process from the state of dispersion to that of concentration. Values of such transition in terms of Ca for rock units of various ranks have been determined.

New data of field and experimental works have been used to consider association of elements from gold deposits of different genetic types. The general geochemical peculiarities of gold and Pt, V, W, Sb, Ag, As, Hg are noted. These elements are associated with gold ores and their concentrations are found in the deposits of Cu, Mo, Ag, Pl, Zn. The application of geological-genetic models of gold deposits and of ore-forming processes will prompt the local forecasts to be well-grounded.

Quite probable is a possibility to discover new and non-standard types of gold mineralization in ultrabasites, carbonaceous formations, rocks of iron-ore formations, carbonate (dolomite) formations. In the first case high concentrations of gold may be expected in ultrabasites (gabbro-pyroxene-dunite and hyperbasite formations) enriched by sulphides. Phanerozoic carbonaceous metasomatites and terrigenous complexes with high metal content may be of certain interest. The Carlin deposit (USA), for example, is characterized by

gold-arsenic mineralization along tectonic zones accompanied by carbonaceous metasomatic alterations of rocks. The basic minerals of the ore zones are pyrite and arsenopyrite containing fine-disperse gold. Vein-impregnated gold mineralization is typical of carbon-bearing terrigenous strata.

The most ancient deposits are attributed to the Riphean, the young ones - to the Paleogen. Gold-sulphide mineralization is characteristic of orogenic zones with intensive volcanism, synchronous with formation of ore-embedding sedimentary rocks. It is noteworthy that gold-sulphide deposits are preferably confined to carbonaceous rock mass metamorphosed under conditions of the greenschist facies. It is important to stress a great absorbing role of organic matter and anisotropy of terrigenous strata in localization of gold mineralization.

The iron-ore formation within which one can expect a hypogenic sulphide mineralization with secondary sulphidization along the linear crusts of weathering is a favourable object in search for gold mineralization. In this case the presence of horizons of iron ores rich in gold is quite probable. Ukrainian deposits occur in greenstone belts associated with the northern granitic complex and supracrustal rocks in greenstone belts; gold deposits are hosted in the quartz-carbonate veins with hydrothermally altered rocks. Pyrite veins contain inclusions of metasomatic albite, quartz, muscovite and ankerite. Gold is contained together with pyrite as an inclusion in pyrite. A late calcite replaces ankerite in veins and contact zones between the quartz veins.

Carbonate and dolomite bituminiferous rocks commonly containing pyrite and Au, Ag, Bi tellurides are promising in search for gold.

The OKhotsK median mass has been revealed to contain gold-silver deposits in carbonate (dolomite) rocks, basic minerals: quartz, calcite, epidote, garnet, tourmaline, pyroxene, sulphosalts, galenite, sphalerite, arsenopyrite, pyrite.

The Baikalian epoch presents some interest from the standpoint of complex gold and antimony deposits originating from that time. Ore zones are incorporated into quartzites and carbonate rocks having a contact with carbonaceous shales. Quartz-carbonate rocks are silicificated, ground, leached (as marshallites); they contain gold (coarse), antimonite, berthierite, Jamesonite, arsenopyrite, pyrite, pyrrhotite, chalcopyrite, sphalerite, native silver. Gold-enriched crusts of weathering are widely spread in altered rock zones. The zonal structure of deposits with a regular change of weathering products is observed from the centre of fractured zones with siliceous-ferruginous formations in the centre.

Ores of Chinese deposits diverse in the mineralogical aspect such as gold-antimony-tungsten (Vuoshchi), gold-antimony (LunShan), antimony-tungsten, tungsten-tin-antimony refer to the complex type. Besides antimonite, the ores contain scheelite, native gold, pyrite, arsenopyrite, sphalerite, galenite, chalcopyrite.

New complex gold-silver deposits have been discovered in Australia (Gibson) to extract gold, silver, lead and zinc from ores. High concentrations of gold are observed in deposits with a thick (20 m as much) laterite crust of weathering.

Brasil is known for its gold deposit (Tonco-Socco) in the sedimentary iron-ore formation where pyrite is responsible for gold occurrence.

Quite probable is revealing of Quarternary stratiform gold de-

posits where gold can concentrate in clay-sandy formations in the intermountain area and in near-shore marine troughs.

Current Research in Geology Applied to Ore Deposits. Fenoll Hach-Ali, Torres-Ruiz & Gervilla (eds) (1993). ISBN 84-338-1772-8

PRECIOUS AND BASE METAL MINERALIZATION AT THE POST-VARISCAN UNCONFORMITY OF CENTRAL EUROPE - A RECONSIDERATION

Large, D.E.
Paracelsusstr. 40, W3300 Braunschweig, Germany

ABSTRACT: Copper, gold and platinum-palladium mineralisation occurs within Palaeozoic shales and carbonates at several locations in central and western Europe. In the past, these occurrences have been difficult to classify and complex genetic theories have been proposed to explain them. This paper compares these occurrences to the gold and platinum-palladium mineralisation in the unconformity-related uranium deposits of the Proterozoic in northern Canada and Australia.

Precious metal (gold, platinum and palladium) mineralisation is known from the unconformity-related uranium deposits in the Proterozoic of Australia and Canada (Marmont 1987). These deposits are spatially related to unconformities between underlying folded and fractured „basement" and an overlying, thick succession of continental clastics. Occurrences of uranium and precious metal mineralisation at the post-Variscan unconformity in central and western Europe are examined to these deposits.

In western and central Europe, thick Permian successions of terrestrial redbeds and locally developed bimodal volcanics were deposited in fault-controlled basins between Variscan basement massifs. In areas affected by the Zechstein transgression, the post-Variscan unconformity is marked by transgressive carbonates. Renewed redbed deposition in the early Triassic extended further over the Variscan basement.

Examples of unconformity-related copper-bearing, precious metal mineralisation, as well as the classical unconformity-related uranium deposits, are associated with the post-Variscan unconformity in central and western Europe. These examples include:

1) Ronneburg uranium district in Thuringia, Germany, – uranium mineralisation hosted by faulted and fractured Lower Palaeozoic shales beneath the unconformably overlying Permian red beds (Lange & Freyhoff 1991)
2) Marsberg copper and Korbach-Goldhausen gold deposits, Germany, are hosted by Lower Carboniferous pyritic black shales and cherts, with thinly interlaminated tuffs, immediately underlying the post-Variscan unconformity. Complex selenide paragenesis is present in both deposits (Stribrny et al.1988).
3) Gold and PGE-bearing selenide mineralisation at several localities in the Lower Palaeozoic of the Harz Mountains, Germany, where the relationship to the unconformity is inferred from the geological relationships of the area as well as comparisons with the other unconformity-related deposits (Tischendorf 1959).
4) Hope's Nose-complex Pb-Ag-Au-Hg-Ni-Co-Cu-selenide paragenesis in Devonian carbonates beneath the unconformably overlying Permian red beds (Scrivenor 1982)

The similarities between the geological setting and style of the mineralisation at the post-Variscan unconformity in central and western Europe with the unconformity-related gold, PGE and uranium mineralisation in the Pine Creek Inlier, Australia, and Athabasca Basin, Canada, can be summarised as follows:

- Spatial relationship with an unconformity between basement and an overlying, thick sequence dominated by redbed clastics
- Close spatial association with carbonaceous pelites in the sub-unconformity basement
- Unconformity marks a period of arid weathering and erosion
- Mineralisation is located in zones of structural preparation (brecciation, fractures) in the sub-unconformity basement but also extends into the post-unconformity sequence
- Precious metal mineralisation invariably associated with selenides
- Mineralisation associated with hematitisation and bleaching
- Carbonate is the dominant gangue mineral

These features can be explained in terms of a genetic model that

includes the following characteristics:

- generation of saline, low-temperature and oxidising solutions in thick sequences of redbed clastics and evaporites,
- release/leaching of metals from this succession during diagenesis by this solution,
- precipitation of the metals within a structurally prepared, natural reductant trap, from oxidised, acid chloride solutions derived from the Permian and/or Triassic post-unconformity redbed and evaporite successions.

The necessity of a primary metal enrichment of the mineralised basement strata is questioned.

Unconformity-related precious metal deposits do not form obvious targets, and recent discoveries in southwest England (Leake et al. 1991) were only made after very detailed work. In view of the regional extent of the known occurrences throughout central Europe, further discoveries can be expected.

References

Lange, G. & Freyhoff, G. (1991) Geologie und Bergbau in der Uranlagerstätte Ronneburg/Thüringen. Erzmetall 44: 264 - 269.

Leake, R.C., Bland, D.J., Styles, M.T. & Cameron, D.G. (1991) Internal structure of Au-Pd-Pt grains from South Devon, England, in relation to low-temperature transport and deposition. Trans. Instn. Min. Metall. (Sect. B: Appl. earth sci.) 100: 159 - 178.

Marmont, S. (1987) Ore deposit models #13. Unconformity-type uranium deposits. Geoscience Canada 14: 219 - 229.

Scrivenor, R.C., Cooper, B.V., George, M.C. & Shepherd, T.J. (1982) Gold-bearing carbonate veins in the Middle Devonian limestone of Hope's Nose, Torquay (Abstract). Proc. Ussher. Soc. 5: 393.

Stribrny, B., Urban, H. & Weber, H. (1988) The Lower Carboniferous black shale formation, a possible source for noble and base metal deposits in the NE Rhenish Massif, Federal Republic of Germany. Mineral. Petrol. 39: 129 - 143.

Tischendorf, G. (1959) Zur Genesis einiger Selenidvorkommen, insbesondere von Tilkerode im Harz. Freiberger Forschungshefte C69, 168 p.

Current Research in Geology Applied to Ore Deposits. Fenoll Hach-Alí, Torres-Ruiz & Gervilla (eds) (1993). ISBN 84-338-1772-8

GEOLOGY AND MINERALOGY OF THE CARLES GOLD-BEARING SKARN, CANTABRIAN CORDILLERA, SPAIN

Martín-Izard, A.(1); Boixet, L.(2) & Maldonado, C.(2)
(1) Dept. de Geología, Universidad de Oviedo, 33005, Oviedo, Spain
(2) Minas de Carlés S.A., Entrerios 4, 33860 Salas Asturias, Spain

Abstract. This study presents a description of the Carlés gold-bearing skarn deposit in northwestern Spain with sections on the geometry and distribution of the pyrometasomatic facies. Emphasis is given to the relationship existing between calc-silicates and associated ore minerals, and to the paragenetic setting of the Au-bearing assemblages.

Introduction

The Carlés skarn deposit in the Cantabrian Cordillera, northwestern Spain, was mined for gold during the Roman times and for base metals during late 1800s and early 1900s. The deposit was investigated recently (1985-1991) by Anglo American Company (AAC) for potential production of gold and copper. This paper is based mainly on studies conducted by AAC.

Regional Setting

The Carlés deposit is located within the Cantabrian Zone of the Iberian Hercynian Massif which consists chiefly of Lower to Middle Paleozoic sedimentary rocks. The mineralized area occurs within the Somiedo-Correcilla tectonostratigraphic unit that was affected during the Hercynian Orogeny by epidermic-style deformation, with development of overlapping thrusts, folds and faults. Metallic ore deposit in the area, such as the Carlés gold-bearing skarn occur in association with post-orogenic igneous intrusions that range in composition from granite to mafic microporphyries.

Local Geology

Formation of the Carlés skarn involved three main lithologic units: Late Silurian clastic metasedimentary rocks of the Furada Formation, Early Devonian carbonate rocks of the Rañeces Group, and a stock of post-orogenic granodiorite. The Furada Formation consists of interbedded shale, phyllite, and sandstone, which occasionally is very rich in Fe-oxides (Sanchez et al, 1984). These rocks are covered by Lower Devonian limestone and marlstone of the Calizas de Nieva Formation (Zamarreño, 1976), but the contact between them is transitional. The granodiorite stock is similar to the other post-tectonic intrusives in the Salas-Belmonte region (Corretgé et al, 1970) and is characterized by the presence of basic-intermediate plagioclase (An 50-52%), augite-ferroaugite, hypersthene-ferrohyperthene, hornblende, biotite, K-feldspar and interstitial quartz. As accessory minerals there are zircon, apatite and sphene, and as secondary minerals chlorite and actinolite.

Hercynian deformation of the sedimentary rocks resulted in NE-SE folds with approx. 3 km wavelength and at least two sets of right-lateral fault systems, which trend E-W and NE-SW respectively. The emplacement of the granodiorite body was apparently constrained by structural and stratigraphic factors. The structural factors include preferential intrusion along NE-SW fractures (Corretgé et al, 1970), particularly at their intersection along E-W fractures (Jahoda et al, 1989). Evidence for a stratigraphic control is

provided by the increased thickness of the Carlés granodiorite at the boundary between the Furada and Calizas de Nieva formations.

Preferential emplacement of the granodiorite along faults resulted in longitudinal projections of granodiorite that subsequently intruded the host rock along bedding planes. The intrusion style varies according to the nature of the host rock. For example, within the clastic sediments sills are the most common. In contrast, within limestone, and at the boundary between the clastic and carbonate units, the magma uplifted the upper layers, forming a dome of up to 800 m in diameter. From this dome, wedges of granodiorite up to 200 m long and 40 m thick, extend into the surrounding rock. The result is a fir-type geometry due in part to emplacement along layers which were already folded (Fig. 1).

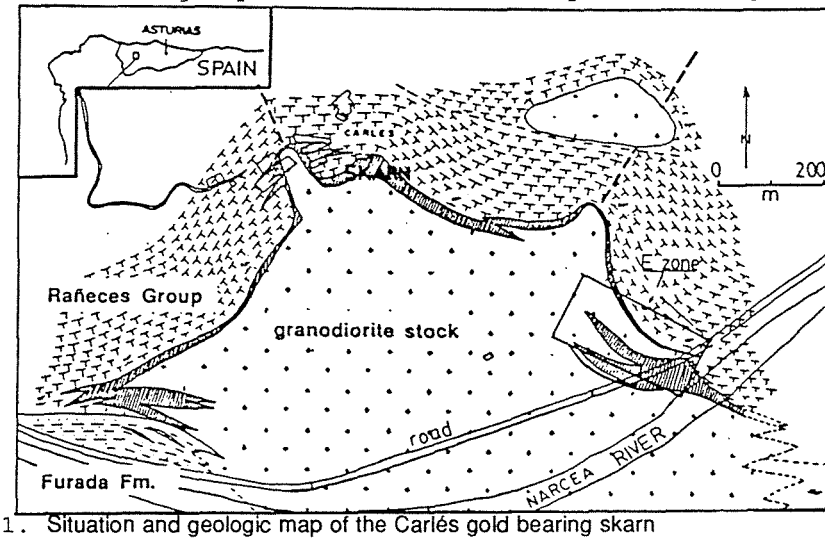

Fig 1. Situation and geologic map of the Carlés gold bearing skarn

The Carlés skarn deposit

The study of the Carlés skarn deposit was concentrated on the eastern sector of the district where two separate tongues of granodiorite provided excellent exposures of the ores and host rocks (Fig. 1). The larger of the two granodiorite tongues reached 200 m towards the SE of the main stock with a 60° NE dip. Longitudinally, the tongues show a mineralogical and textural gradient which is characterized by increasing silicification and development of secondary microcline, away from the main body.

The Carlés skarn occurs preferentially at the contact between granodiorite and carbonate rock and generally forms an irregular envelope around the igneous rock. Variations in skarn thickness are related to the morphology of the intrusive bodies. For example, the skarn is best developed in the regions between tongues of granodiorite and the main granodiorite stock and between granodiorite tongues. The maximum observed thickness is 50 m, but this may decrease sharply along the elongated granodiorite intrusions, being replaced by unmineralized marble. Locally, skarn bodies are found far from the intrusive rock and are associated to permeable structures such as bedding, joints, or faults (Fig. 1). Ore mineralization within the skarn includes Cu and Fe sulfides, magnetite, and Au-enriched zones.

Mineralogy

The following mineral assemblages (Fig. 2) have been identified at the Carlés skarn:

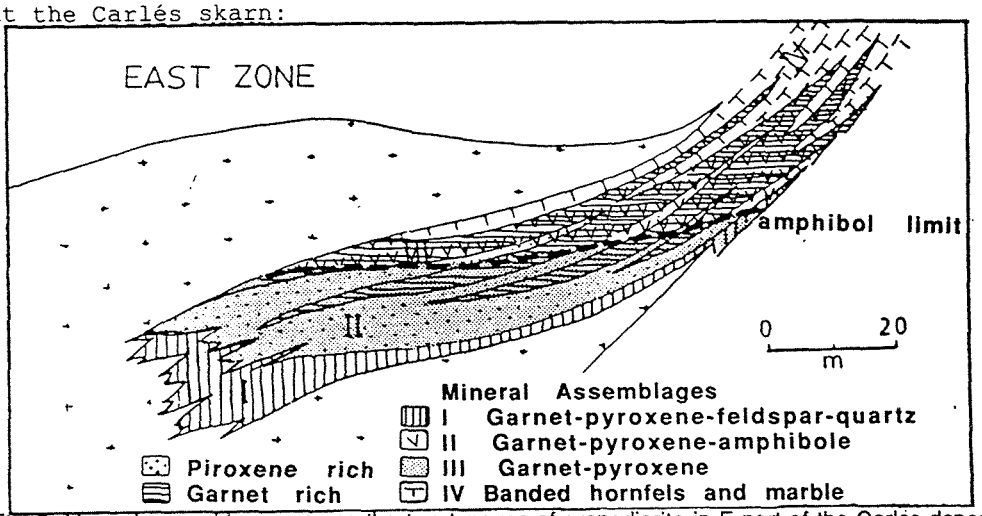

Fig. 2- Mineral assemblages among the two tongues of granodiorite in E part of the Carlés deposit.

I. Garnet-pyroxene-feldspar-quartz. This is the innermost assemblage and is characterized by abundant quartz and secondary microcline. Garnet(Gr-And) is scarce and replaced by pyroxene (Di-Hed) and pink microcline along crystal rims. Pyroxene forms cm to m wide layers and fine-grained crystalline aggregates. Together with quartz and secondary microcline pyroxene is also found within cross-cutting veinlets. Other minerals include apatite and sphene. Arsenopyrite, with minor associated löllingite and chalcopyrite, occurs as veins and lenses several cm long. The Au content in this assemblage is low (up to 1 ppm). Closer to the outer sections, amphibole is present and microcline and quartz decreases sharply.

II. Garnet-pyroxene-amphibole. Previously described by Williams (1989), this is the main skarn assemblage and host to the principal Au mineralization. Garnet appears as massive microcrystalline masses and is commonly replaced by pyroxene and amphibole. Both garnet and pyroxene are similar to those described in assemblage I. Amphibole is present at the boundary between garnet and pyroxene and filling veins and open spaces with quartz, sulfide, and calcite. Other minerals include apatite and chlorite, which is associated to late hydrothermal activity along major fractures. Calculated temperature of formation for chlorite based on microprobe analysis of Al^{VI} (Catalineau, 1988) is 205-237 ºC. Ore minerals in assemblage II have been divided into internal and external zones, according to their relative distance to the granodiorite stock. The internal zone contains chalcopyrite, arsenopirite, and löllingite, and is important economically (Au grade, up to 6 ppm). The ore in the internal zone appears as stratiform lenses up to 2 m wide and several tens of m long, and subordinately as quartz-rich veins. The external zone is high grade, stratiform, contains magnetite, chalcopyrite, and minor bornite and löllingite, and marks the boundary with assemblage III. Higher Au grades (up to 25 ppm. Au as electrum, 30-70% Ag) are found with löllingite-bornite association and with bismuth, bismuthinite, and hessite. Magnetite in assemblage II is always older than sulfides.

III. Garnet-pyroxene. This outermost assemblage has sharp boundaries and is characterized by lack of amphibole. Red garnet is euhedral, has anisotropic rims, and is replaced by pyroxene and microcline (in internal zones) and calcite (in external zones).Arsenopyrite and minor pyrrhotite are the most abundant sulfides. Cavity filling minerals include microcline, calcite, quartz, minor scapolite, arsenopyrite, and pyrrhotite. No significant Au values have been observed.
IV. Banded hornfels and marble. Grey banded hornfels layers, up to 3 m thick, are found at the footwall of some of the granodiorite tongues. The grey color is due to variable concentrations of biotite due to the contact metamorphism.

Other ore assemblages at Carlés include late, cross-cutting veins containing arsenopyrite, pyrite, chalcopyrite, molibdenite, and Pb and Sb sulfosalts.

Hydrothermal metallic mineralization in the Carlés deposit appears to be younger but directly related to the formation of the silicate skarn. This is suggested by the following observations: (1) the association between calc-silicates and ore minerals is very clear, particularly in assemblage II; and (2) the large-scale morphology of the ore deposit is similar to that of the skarn, both being controlled by the granodiorite.

Minerals Elements	Garn inner	Garn rim	Pyr Diop	Pyrx Hedb	Amp Hasti	Amp Parg	Amp Acti	Chlo rite1	Chlo rite2	Mine Elem	Asp Exte	Asp inter	Asp inner
SiO_2	37.04	38.55	53.65	49.54	38.59	36.20	50.25	26.05	27.44	Fe	34.68	34.68	34.36
TiO_2	0.45	o.93	0.03	0.01	0.56	0.61	0.05	0.014	0.033	S	34.14	31.77	29.90
Al_2O_3	10.37	18.48	0.395	0.18	10.35	13.32	1.20	13.38	15.10	As	30.51	33.52	35.62
FeO	16.26	4.67	8.56	25.58	32.15	29.89	30.34	45.77	40.54	Mine	Elect	Elect	Elect
MnO	0.26	0.17	0.24	0.52	0.21	0.17	0.51	0.366	0.384	Au	25.21	41.90	54.61
MgO	0.05	0.31	13.67	1.86	2.04	3.37	5.23	2.551	4.633	Ag	74.13	57.38	42.70
CaO	35.36	36.89	22.84	22.23	11.54	11.81	11.31	0.201	0.599	Mine	Löllin	Löllin	Löllin
Na_2O	0	0	0.06	0.07	1.41	1.24	0.19	0.09	0.10	Fe	33.45	27.78	28.01
K_2O	0	0	0.01	0.16	1.79	2.37	0.12	0.259	0.012	As	62.13	64.12	64.02
Total	99.85	100.0	99.45	100.0	98.65	98.99	99.24	88.68	88.84	Co	1.67	5.37	5.22

Table 1. Average of microprobe analysis results.

Overall, metallic mineralization at Carlés is most important in lenses within pyroxene layers, in contrast, ore in garnet layers is normally restricted to narrow veins and small pockets. The measured decrease in As concentration in arsenopyrite, intergrown or replacing löllingite, is interpreted as evidence for a temperature decline from the inner zone, near the granodiorite, to the outer zones, closer to the marble layers. Temperatures varying among 525 and 400 ºC and Log S fugacities are comprised between -6 and -10.

BIBLIOGRAPHICAL REFERENCES

Corretgé, L; Luque, C; Suarez, O (1970) Los stocks de la zona de Salas-Belmonte (Asturias). Bol. Geol. Min. España, LXXXI: 143-145.

Catalineau, M (1988) Cation site occupancy in chlorites and illites as a function of temperature. Clay Minerals 23: 471-485

Sanchez de la Torre, L; Vera Puente, C; Suarez Centi, C; Agueda, J (1984) Facies y ambientes sedimentarios del Silúrico y Devónico en la región central de Asturias. T. hom. Sanchez de la Torre. Pub. Geo. Uni. Aut. Barc. 20: 57-71

Zamarreño, I(1976) Depositos carbonatados de tipo "Tidal Flat" en el Devónico Inferior del NO de España. Trab. Geol. Univ. Oviedo, 8:59-85

Jahoda C. Andrews, J. Foster R. (1989) Structurals controls of Monte Roso and other gold deposits in NW Spain fractures jogs and hot-jogs. Institution of Mining and Metallugy Secction B 98- 1-6

Williams, MJ (1989).A preliminary investigation of calc-silicate assemblanges in E sector of Carles gold deposit Spain. Tes. Lic. Imperial College. London.

The autors are grateful to Dr. A. Arribas J.R. for help with the paper and to the Minas de Carlés staf. This paper was partially supported by the grants of the CICYT GEO 89/0832.

Current Research in Geology Applied to Ore Deposits.Fenoll Hach-Alí, Torres-Ruiz & Gervilla(eds)(1993).ISBN 84-338-1772-8

WHY IS GOLD ACCUMULATED IN PYRITE- AND ARSENOPYRITE-RICH MINERALIZATIONS? AN ELECTROCHEMICAL APPROACH

Möller, P.
GeoForschungsZentrum Potsdam, Telegrafenberg A50, 0-1561 Potsdam, Germany

Abstract
Combination of p- and n-type sulfides build up self-driving galvanic cells with cell potentials of >20 mV. p-n junctions mostly result from chemical zonation which becomes electrochemically active after fracturing of the zoned crystals. Au accumulates at p-type conducting arrays.

Introduction:

Pyrite and arsenopyrites occur as n- and p-type semiconductors that are largely controlled by their As/S molar ratio. In general, the type of conductivity depends on the concentrations of specific elements that substitute for the main elements and act either as electron donors or acceptors.

Results and discussion:

Linked sulfide minerals in contact with a common fluid were employed in studies of gold deposition at combinations of p- and n-type sulfides (simulating p-n junctions). High level doping of sulfides lead to rather uniform conductivity of the semiconductors and combinations of paragenetic semiconducting sulfides yield cell potentials as high as 120 mV, but decreasing with time to 20 mV.
If "doped" at low levels, differently conducting arrays of the electrode (mixed-type) can be exposed to solution. Partial or total dissolution of exposed anodically reacting domains might explain the observed changes of the sign of the potential difference of mixed-type sulfides.
In H_2S-saturated solutions gold is preferentially accumulated at the cathode (p-type sulfide), a process which is compensated by oxidizing dissolution of anodic sulfides. Each combination of crystals shows slightly different cell potentials probably due to varied contents of impurities that are controlled by the fluids from which the sulfides formed. For example, cogenetic arsenopyrite and pyrite linked to a galvanic cell leads to n-type arsenopyrite (As/S molar ratio <1; anode) and p-type pyrite (cathode). In such an arrangement the noble metal ions are predominantly reduced at the pyrite surface. The reverse should be observed in sulfidization reactions where the remaining arsenic-rich component could easily become p-type conducting. Minerals of varying conductivity types are formed if the sulfides are precipitated from chemically different fluids or are metasomatically overprinted to different extents.
It seems that linked sulfide minerals are a good experimental device to study the electrochemical consequences of chemical zonation of sulfide minerals. Zonation of sulfide crystals, e.g. by variation of arsenic contents, is without doubt (Marion et al., 1991) an excellent base for np-junctions which become accessible to fluids after

fracturing of the crystals. The observation that gold frequently heals microfractures in pyrite and arsenopyrite or precipitates at surfaces is consistent with the necessary pre-conditions of electrochemical precipitation.
Electron flow is not only possible at p-n junctions, but is also established where sulfide minerals are hosted in an electron-conducting matix such as graphite-bearing carbonaceous shear bands (Xavier and Forster, 1991).
Is the accumulation of gold caused by specific adsorption at sulfide surfaces (Jean and Bancroft, 1985; Hyland and Bancroft, 1989; Knipe et al., 1991; 1992) or by electrochemical deposition? Adsorption cannot be the only reason because (i) in linked sulfides assemblages gold is preferably collected at the cathode and (ii) other sulfides with enhanced energy gaps (ZnS and PbS; Shuey, 1975) are of minor importance in accumulating Au in nature.
Electrochemical nucleation of native gold (involving physical adsorption) is bound to potential differences at surfaces along which Au, once reduced to the metal state, clusters to form nuclei for further electrochemical deposition even with gold concentrations in the fluids beeing extremely low (i.e., $<10^{-12}$ mol/kg-solution). Pyrite is about three orders of magnitude more effective in sorbing gold from solutions than goethite (Schoonen et al., 1992). Combinations of n- and p-type sulfides are common in nature. The uneven distribution of gold deposited on sulfides indicates that the elctrochemical processes must dominate physical and/or chemical adsorption.
In contrast, chemical precipitation depends on supersaturation of the species that are involved in Au deposition. Since the complexing agents that transport Au are still present in excess in the fluid, chemical precipitation processes are very unlikely to be efficient, excepting decrease of sulfur activity due to sulfidization processes.
The experimental results (Möller and Kersten, subm.) show that externally and internally controlled electrochemical processes lead to Au accumulation on sulfides. The necessary conditions are common to all sulfide deposits. Typical examples selected from recent literature might unroll that the observations are consistent with the result of this experimental study.
Gold grains often occur close to grain boundaries of sulfides, i.e. between pyrite and chalcopyrite (Melling et al., 1990; Phillips, 1987), within fractured pyrite (Starling et al. 1989; Schreiber at al., 1990; Piekarz et al., 1991) or as coatings and along cracks of arsenopyrite (Marion et al., 1991). Therefore, gold accumulation was always later than the formation of the sulfides. Primary inclusions of Au flakes could form provided that growth of sulfide minerals was slow enough to allow sufficient amounts of gold to be reduced.
Pyrite often displays chemical zoning in Ni, Co or As contents (Marion et al., 1991). If such crystals are fractured the sample expose a great number of p-n junctions to infiltrating fluids
The potential difference at p-n junctions in single crystals are low, probably less than 100 mV and similar to those in experiments with cogenetic sulfides. Such potentials are still sufficient for gold accumulation from solutions with extremely low concentrations.
Pyrite and arsenopyrite with dispersed gold accumulation are described by Marcoux et al. (1989) and Wu et al. (1990) in samples form Le Chatelet gold deposit (Creuse, France) where gold is positively correlated with excess of arsenic (p-type).

Experimental examinations by Wu et al. (1990) showed that As-rich zones of arsenopyrite crystals are indeed enriched in Au.
Gold accumulation associated with massive sulfide and continuous sulfide veins is abundant. Often the sulfide mineralizations are steeply dipping lodes or veins, as for example, in Archeaen and Proterozoic greenstone belts and iron formations (Boyle, 1979). With cell potential of about 0.6 V Au could be mobilized at depth and re-deposited at higher levels.
The small self-driving galvanic cells between and within sulfide minerals with their tendency to electrochemical deposition of gold might be a great barrier in gold migration. Since these sulfides are ubiquitous, they could "filter" gold even from highly undersaturated Au solutions. This behaviour might explain why gold accumulation is abundant in the crust and particularly bound to occurrences of arsenic which is very efficient in controlling p-type conductivity of sulfide minerals. Sulfidization of arsenic minerals lead to very favourable conditions. Because of the incomplete sulfidization the newly formed arsenopyrite is enriched in As resulting in p-type conductivity. Thus gold is electrochemically accumulated on arsenopyrite and remaining löllingite is anodically dissolved (Möller and Kersten, subm.).

Conclusion

Electrochemical enrichment of gold at sulfide minerals might occur as a primary or secondary event. Au inclusions in the p-type zones are formed during growth of sulfides whereas native gold at grain boundaries precipitated from either late hydrothermal or supergene gold-bearing solutions. It might further be concluded that massive sulfides as well as dispersed sulfides in sediments or veins act as a barrier for gold migration. Even from extremely undersaturated solutions it is highly possible that Au is accumulated electrochemically from these fluids.
The presence of pyrite and arsenopyrite play a distinctive electrochemical role due to which Au accumulation can take place: (i) fluids that form these sulfide minerals also transport Au and (ii) arsenic is one of the most important elements determining the type of conductivity of these minerals. This is the main reason why gold is so tightly associated with arsenic. In the end both aspect are controlled by the source of migrating fluids.

References:

Boyle R.W. (1979) The geochemistry of gold and its deposits. Geol. Surv. Canada Bull. 280, 584p.

Hyland M.M., Bancroft G.M. (1989) An XPS study of gold deposition at low temperatures on sulphide minerals: reducing agents. Geochim. Cosmochim. Acta 53, 367-372.

Jean G.E., Bancroft G.M.(1985) An XPS and SEM study of gold deposition at low temperatures on sulfide mineral surfaces: concentration of gold by adsorption/reduction. Geochim. Cosmochim. Acta 49, 979-987.

Knipe S.W., Foster R.P., Stanley C.J. (1991) Hydrothermal precipitation of precious metals on sulfide substrates. In E.A. Ladeira (ed) Brazil Gold`91, 431-435

Knipe S.W., Foster R.P., Stanley C.J. (1992) The role of sulphide surfaces in the sorption of precious metals from hydrothermal fluids. Trans. Inst. Min. Metall., 101, B83-B88.

Marcoux E., Bonnemaison M., Braux Ch., Johan Z. (1989) Distribution of Au, Sb, As and Fe in gold-bearing arsenopyrite from Le Chatelet and Villerange deposits, Creuse, French Massif Central. C. R. Acad. Sci. Paris, t. 308, 293-300.

Marion P., Holliger P., Boiron M.C., Cathelineau M., Wagner F.E. (1991) New improvements in the characterization of refractory gold in pyrites: An electron microprobe, Mössbauer spectrometry and ion microprobe study. In E.A. Ladeira (ed): Brazil Gold`91, 889-395

Melling D.R., Watkinson D.H., Fox P.E., Cameron R.S. (1990) Carbonatization and propylic alteration of fragmental basaltic rocks, Quesnel River gold deposit, central British Columbia. Mineral. Deposita 25, 115-124

Möller P., Kersten G. (subm.) Electrochemical accumulation of gold on pyrite and arsenopyrite surfaces. Mineral. Deposita

Phillips P. (1987) Scotian gold: Beaver Dam deposit.-The N. Min. Mag. 1987, 82-83.

Piekarz G.F., Schrank A., Choudhouri A., Figueiredo B. Xavier R. (1991) A porphyry-type gold deposit in the Passa Tres granite, South Brazil. BRAZIL GOLD`91, 541-546

Schoonen M.A.A., Fisher N.S., Wente M. (1992) Gold sorption onto pyrite and goethite: a radiotracer study. Geochim. Cosmochim. Acta 56, 1801-1814.

Schreiber D.W., Amstutz G.C., Fontbote L. (1990) The formation of auriferous quartz-sulfide veins in the Pataz region, northern Peru: a synthesis of geological, mineralogical and geochemical data. Mineral. Deposita 25, 136-140

Shuey R.T. (1975) Semiconducting ore minerals. Elsevier, Amsterdam, Oxford, New York. 415p.

Starling A., Gilligan J.M., Carter A.H.C., Foster R.P., Saunder R.A. (1989) High-temperature hydrothermal precipitation of precious metals on the surface of pyrite. Nature, 340, 298-300

Wu X., Delbove F., Touray J.C. (1990) Conditions of formation of gold-bearing arsenopyrite: a comparison of synthetic crystals with samples from Le Chatelet gold deposit, Creuse, France. Mineral. Deposita 25, 8-12.

Xavier R.P., Foster R.P. (1991) The role of carbonaceous shear bands in fluid-flow and gold-precipitation in the Fazenda Maria Preta mine, Bahia, north-east Brazil. BRAZIL GOLD'91, 269-277

Current Research in Geology Applied to Ore Deposits.Fenoll Hach-Alí, Torres-Ruiz & Gervilla(eds)(1993).ISBN 84-338-1772-8

THE SEDIMENTARY ROCK-HOSTED GOLD DEPOSIT AT ZARSHURAN, IRAN: A PRELIMINARY FLUID INCLUSION AND SULPHUR ISOTOPE STUDY

Moritz, R. (1); Lotfi, M. (2)) & Saupé, F. (3)
(1) Dépt. de Minéralogie, Rue des Maraîchers 13, 1211 Geneva 4, Switzerland
(2) Geological Survey of Iran, P.O. Box 13185-1494, Teheran, Iran
(3) CRPG, BP 20, 54501 Vandoeuvre-lès-Nancy, France

ABSTRACT: The Zarshuran mine is a sedimentary rock-hosted gold deposit spatially associated with the Tertiary Central Iranian Volcanic Belt. Fluid inclusion microthermometry of quartz, fluorite and sphalerite indicates that the fluid during ore-deposition was a boiling CO_2-bearing aqueous solution with apparent salinities ranging between 2.6 and 8.5 wt % NaCl equivalent (not corrected for the presence of dissolved CO_2). Temperature of ore-deposition was in the range of 180°C to 220°C, and a minimum depth of ore-formation of 155 m is indicated by the fluid inclusion data. A limited number of $\delta^{34}S$ values from sphalerite (5.4‰ and 5.6‰), stibnite (3.6‰) and baryte (19.6‰ and 24.1‰) suggest that the Oligo-Miocene sedimentary host rocks are the most likely source of sulfur in sulfides and barytes at the Zarshuran gold deposit, although other source rocks cannot be ruled out at the present stage of the study.

INTRODUCTION

The northwest-trending Tertiary Central Iranian Volcanic Belt (CIVB) is a major segment of the Thethyan Eurasian metallogenic belt, linking the European Alpine and the Pacific metallogenic systems (Jankovic, 1977). The CIVB is mainly known for its porphyry copper and skarn deposits (Förster, 1978). Although epithermal gold deposits are generally associated with this type of metallogenic system (Sillitoe and Bonham, 1990; Mitchell, 1992), little attention has been given to epithermal gold deposits in the CIVB. In this contribution, we report and discuss preliminary microthermometric fluid inclusion and sulfur isotope data from the sedimentary rock-hosted gold deposit at Zarshuran, which is spatially associated with the CIVB.

GEOLOGICAL SETTING

The gold deposits and occurrences of the Zarshuran area are located in the Western Azerbaidjan province, northwestern Iran, about 60 km north of the town of Takab, at an altitude of 2500 m. The main tectonic feature of this area is a NNW-running reverse fault that brings into contact volcanic and Oligo-Miocene sedimentary rocks in the west with amphibolite to lower greenschist facies metamorphic rocks, considered to be of Precambrian age, on the eastern side of the fault (Alavi et al., 1982). The major Zarshuran gold mine lies about 5 km west of the regional NNW-running fault, and is hosted by Oligo-Miocene formations composed of limestone, calcareous mudstone and shale. It is located along the western limb of a NW-oriented anticline with a core consisting of mafic to ultramafic rocks inferred to be of Precambrian age. The main volcanic activity in the vicinity of the Zarshuran area is formed by Oligo-Miocene andesitic lavas, with subsidiary dacitic-rhyolitic lavas and related tuffs. The nearest intrusion to the gold center is the Precambrian (?) Doran granite located about 10 km to the west. A Tertiary porphyritic granite and a Tertiary tonalite occur about 40 km to the southwest and to the southeast, respectively, of the gold mine.

The sedimentary host rocks are silicified and are locally brecciated. This alteration and brecciation is recognized around the Zarshuran mine up to 2 km to the northwest near Balderghani, and occurs also 10 km west to the Zarshuran mine in the Agh Darreh area near the Doran granite. The present major gold productive zone in the Zarshuran mine is in a brecciated shale unit. The mineral association includes orpiment, quartz, cinnabar, sphalerite, realgar, stibnite and purple to colourless fluorite. Some baryte veins are present in some places. In addition, Bariand (1963) and Nicolini (1990, p.349-350) describe the presence of boulangerite, melnicovite, lorandite, getchellite, pyrite and galena. At this stage of the study, no unequivocal detailed paragenetic sequence can be given for the Zarshuran mine due to the general lack of mutual textural relationships between the different minerals,

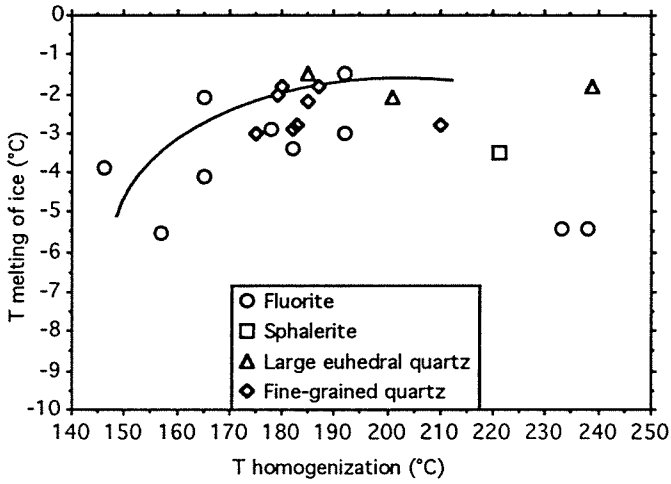

Figure 1 - Homogenization and final ice melting temperatures of the liquid-rich fluid inclusions

in particular between baryte and sulfide minerals. Preliminary observations indicate an initial silicification of the host rocks with formation of jasperoid. Sphalerite occurs later in the paragenesis, and is in turn crosscut by a subsequent fine-grained quartz generation. Fluorite appears to be one of the latest phases, since it growths into vugs. The geological setting, the mineral association and the alteration of the Zarshuran deposit are comparable to those of other sedimentary rock-hosted gold deposits such as described in the Western United States (Bagby and Berger, 1985) or in China (Cunningham et al., 1988), which are typically classified as Carlin-type deposits.

FLUID INCLUSION MICROTHERMOMETRY

Fluid inclusions were studied in large euhedral quartz crystals, late fine-grained quartz, sphalerite and fluorite spatially associated with the gold-bearings areas. In fluorite, the inclusions occur along trails that end at growth zones or that crosscut grain boundaries. In quartz and sphalerite, the inclusions occur as intragranular clusters and trails, or are locally isolated. Thus, the inclusions are of the secondary and pseudosecondary type. Some of the isolated inclusions might be of primary origin, but this cannot be proven unequivocally. Nevertheless, the type of occurrence of the inclusions indicates that they trapped fluids present during and following growth of sphalerite, quartz and fluorite. Two types of fluid inclusions were recognized. The most widespread fluid inclusion type is two phase at room temperature with the vapour phase occupying about 10 vol. %. The second fluid inclusion type is vapour-rich with a thin rim of liquid occupying less than 15 vol. % at room temperature. The latter fluid inclusion type has only been recognized in fluorite, either in trails containing only vapour-rich inclusions, or, more rarely, in trails containing both vapour-rich and liquid-rich inclusions. This leads us to the conclusion that both fluid types were coexisting during and following fluorite precipitation.

Microthermometric data obtained on the liquid-rich fluid inclusions are shown in Figure 1. Heating runs were performed before freezing measurements in order to avoid stretching of the inclusions. Homogenization temperatures to the liquid range between 146°C and 238°C. Melting of ice is completed between -1.5°C and -5.5°C. Apparent salinities calculated from the ice-melting temperatures range between 2.6 and 8.5 wt % NaCl equivalent. Some inclusions show ice-melting starting-temperatures below -33°C, which indicates that additional cations besides Na^+ are in solution. Given that the gold deposit is hosted by carbonate sedimentary rocks, these additional cations are likely Ca^{++} and, possibly, Mg^{++}. Neither clathrate melting, nor any additional phase changes were observed during the freezing runs. No phase changes were observed in the vapour-rich fluid inclusions during the freezing-heating runs apart from melting of a solid at -56.6°C in a few inclusions. Such phase behaviour indicates the presence of nearly pure CO_2 in the vapour-rich inclusions.

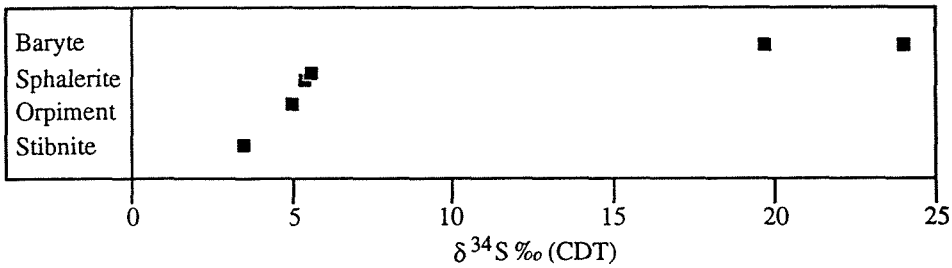

Figure 2 - Sulfur isotope data of sulfides and barytes from the Zarshuran gold deposit

The fluid inclusion data in Figure 1 show a covariant trend between a slight lowering of the ice-melting temperatures and decreasing homogenization temperatures. According to Hedenquist and Henley (1985) such a trend can be ascribed to boiling and steam loss of a gas-poor fluid which results in a slight enrichment of the dissolved salts with cooling. The vapour-rich inclusions coexisting with liquid-rich inclusions in the late-stage fluorite are supporting evidence that boiling occurred at the Zarshuran gold deposit. Thus, the homogenization temperatures represent trapping temperature conditions. The presence of CO_2 in the vapour-rich inclusions suggests the presence of dissolved CO_2 in the boiling fluid. Hedenquist and Henley (1985) have described how CO_2 can significantly contribute to the lowering of the ice-melting temperature in aqueous fluids without formation of liquid CO_2 or a CO_2-hydrate. Thus, the salinities between 2.6 and 8.5 wt % NaCl equivalent calculated above for the liquid-rich inclusions are only apparent and overestimate the real salinities of the fluids involved in the formation of the gold deposit. In addition, the presence of dissolved CO_2 can significantly increase the depth at which an aqueous fluid starts to boil. A salinity of 4 wt % NaCl equivalent (mode of apparent salinities in Fig. 1) and a boiling temperature of 200°C would indicate a depth of trapping of 155 m (Haas, 1971) if the presence of dissolved CO_2 is ignored. Thus, the depth of 155 m is only a minimum estimate of the real fluid trapping conditions and ore formation at Zarshuran.

SULFUR ISOTOPES

Sulfur isotope compositions of different minerals from the Zarshuran area are given in Figure 2. $\delta^{34}S$ values are 5.4 ‰ and 5.6 ‰ for sphalerites, 3.6 ‰ for stibnite, 5.0 ‰ for orpiment, and 19.6 ‰ and 24.1 ‰ for barytes. Temperatures cannot be calculated because no coexisting minerals could be analyzed. However, the temperature of mineralization is constrained by the homogenization temperatures of the fluid inclusions. Thus, the $\delta^{34}S$ values of H_2S in equilibrium with sphalerite and stibnite can be estimated in the Zarshuran gold deposit. At a temperature of 220°C, the two sphalerites yield $\delta^{34}S$ values for H_2S of 5.0 ‰ and 5.2 ‰, and the stibnite a $\delta^{34}S$ value of 6.7 ‰ according to equilibrium isotopic fractionation factors in Ohmoto and Rye (1979). At a temperature of 180°C the $\delta^{34}S$ values do not change significantly and are 4.9 ‰, 5.1 ‰ and 7.2 ‰. These values could reflect reduced sulfur obtained from diagenetic sulfide or organic matter, or reduction of evaporite derived sulfate, or a combination of the three (Ohmoto and Rye, 1979). The $\delta^{34}S$ values of baryte lie within the range of Upper Tertiary marine sulfate (Claypool et al., 1980), so that the sulfur in baryte could be derived from evaporites present in the Miocene sedimentary rocks of the area (Alavi et al., 1982). In conclusion, the sulfur isotope composition of sulfides and barytes associated with the Zarshuran gold deposit suggest that the host sedimentary rocks are the most likely source reservoir of sulfur. However, because of the small data set and in the absence of a correct characterization of the sulfur isotope composition of the postulated source rocks, we cannot rule out other sulfur sources at the present stage of the study.

CONCLUSIONS

1) The geological and structural settings, the mineral association and the alteration of the Zarshuran gold deposit are comparable to those of other sedimentary rock-hosted gold deposits typically classified as Carlin-type deposits.
2) The fluid present during ore-deposition was a boiling CO_2-bearing saline (Na^+-Ca^{++}) aqueous fluid with apparent salinities between 2.6 and 8.5 wt % NaCl equivalent (not corrected for the presence of dissolved CO_2).
3) Temperature of ore-deposition is inferred to be in the 180°C-220°C range, and a minimum ore-formation depth of 155 m is indicated by the fluid inclusion data.
4) The most likely source of sulfur in sulfides and barytes of the Zarshuran gold deposit are the host sedimentary rocks of Oligo-Miocene age. However, other sulfur sources cannot be ruled out at this stage of the study because of the limited data set and in the absence of sulfur isotope data of the different possible source rocks in the Zarshuran area.

ACKNOWLEDGEMENTS

This investigation is part of the research project "Treatise on the Geology of Iran" carried out under the supervision of A. Hushmandzadeh. We would like to thank the support of the Geological Survey of Iran for this study. Funding from the Swiss National Science Foundation (Grant n° 21.33789.92) to L. Fontboté and G. Stampfli is gratefully acknowledged.

REFERENCES

Alavi, M., Hajian, J., Amidi, M. & Bolourchi, H. 1982. Geology of Takab—Saein–Qal'eh. Geol. Surv. Iran, Report No. 50, 99 pp. with map at 1:250,000.

Bagby, W.C. & Berger, B.R. 1985. Geologic characteristics of sediment-hosted, disseminated precious-metal deposits in the Western United States. In Berger, B.R. and Bethke, P.M., eds., Geology and geochemistry of epithermal systems, Reviews in Economic Geology, v. 2, p. 169-202.

Bariand, P. 1963. Contribution à la minéralogie de l'Iran. Bull. Soc. franç. Minér. Crist., 86:17-64.

Claypool, G.E., Holser, W.T., Kaplan, I.R., Sakai, H. & Zak, I. 1980. The age curves of sulfur and oxygen isotopes in marine sulfate and their mutual interpretations. Chem. Geol., 28: 199-260.

Cunningham, C.G., Ashley, R.P., Chou, I-M., Zushu, H., Chaoyuan, W., & Wenkang, L. 1988. Newly discovered sedimentary rock-hosted disseminated gold deposits in the People's Republic of China. Econ. Geol., 83:1462-1467.

Förster, H. 1978. Mesozoic-Cenozoic metallogenesis in Iran. J. Geol. Soc. London, 135: 443-455.

Haas Jr., J.L. 1971. The effect of salinity on the maximum thermal gradient of a hydrothermal system at hydrostatic pressure. Econ. Geol., 66: 940-946.

Hedenquist, J.W. & Henley, R.W. 1985. The importance of CO_2 on freezing point measurements of fluid inclusions: evidence from active geothermal systems and implications for epithermal ore deposition. Econ. Geol., 80: 1379-1406.

Jankovic, S. 1977. The copper deposits and geotectonic setting of the Thethyan Eurasian metallogenic belt. Mineral. Deposita, 12: 37-47.

Mitchell, A.H.G. 1992. Andesitic arcs, epithermal gold and porphyry-type mineralization in the western Pacific and eastern Europe. Trans. Instn Min. Metall., 101: B125-B138.

Nicolini, P. 1990. Gîtologie et exploration minière. Paris, Lavoisier, 589 p.

Ohmoto, H. & Rye, R.O. 1979. Isotopes of sulfur and carbon. In Barnes, H.L., ed., Geochemistry of hydrothermal ore deposits: New York, Wiley Interscience, p. 509-567.

Sillitoe, R.H., & Bonham Jr., H.F. 1990. Sediment-hosted gold deposits: distal products of magmatic-hydrothermal systems. Geology, 18: 157-161.

Current Research in Geology Applied to Ore Deposits. Fenoll Hach-Alí, Torres-Ruiz & Gervilla (eds) (1993). ISBN 84-338-1772-8

SYN-METAMORPHIC AMPHIBOLITE-FACIES GOLD MINERALIZATION AND ALTERATION IN THE MT. YORK DISTRICT, PILBARA CRATON, WESTERN AUSTRALIA

Neumayr, P.(1); Groves, D.I. (1); Cabri, L.J. (2) & Koning, C.D. (3)

(1) Key Centre for Strategic Mineral Deposits, The University of Western Australia, Nedlands, W.A. 6009, Australia

(2) Canada Centre for Mineral & Energy Technology, Ottawa, Canada

(3) MIM-Exploration, West Perth, W.A., Australia

ABSTRACT: Gold mineralization in the Mt. York District was broadly synchronous with the regional metamorphic peak at 540±30° C and 3±1 kb. As a consequence, wallrock alteration comprises calc-silicate assemblages and biotite in place of the carbonate-white mica assemblages in lower metamorphic-grade gold mineralization. Zakanaka has rather conventional pyrrhotite-pyrite assemblages and at Main Hill the anomalous assemblage auriferous löllingite-arsenopyrite-pyrrhotite is developed as a result of the high temperature depositional conditions.

INTRODUCTION

The Mt. York District is located in an Archaean greenstone belt on the northeastern limb of the Pilgangoora syncline, Pilbara Craton, Western Australia, about 110km south of Port Hedland. Gold mineralization is hosted by mafic and ultramafic rocks of the *ca.* 3.46 Ga Warrawoona Group (Thorpe et al., 1990) at the Zakanaka prospect, and metamorphosed banded iron formation (BIF) of the *ca.* 3.33 Ga Gorge Creek Group at the Main Hill/Breccia Hill prospects. The Mt. York District was selected for detailed studies because of its anomalous amphibolite-facies metamorphic-grade setting and the contrasting host rocks for gold mineralization. In addition, the Archaean gold deposits of the Pilbara Craton, unlike those of the Yilgarn Block (Ho et al., 1990), are poorly documented, and this paper represents one of the few modern documentations of such prospects.

STRUCTURAL AND METAMORPHIC SETTING

Structure

Deformation in the Mt. York District is represented by two progressive stages of folding. Earlier N-trending, isoclinal and partly doubly-plunging F_{2A} folds (Neumayr et al., 1993) have been refolded by open to tight, steeply W-plunging F_{2B} folds (Fig. 1). Both, the S_{2A} and the locally developed S_{2B} foliations are defined by hornblende, implicating amphibolite-facies metamorphic conditions during both deformational events. Strain was heterogeneously distributed during both phases of deformation, and shear zones developed dominantly parallel to the limbs of F_{2A} folds.

Gold mineralization at the Main Hill/Breccia Hill prospect is controlled by competency contrast between the BIF sequence and the hangingwall- and footwall-quartzites during D_{2B} deformation, and is located along the limbs of F_{2B} buckle folds, along a D_{2B} reverse fault, and at the BIF-quartzite contact (Fig. 1). Erratic mineralization is spatially associated with quartz veins within foliated grunerite rock of the BIF unit.

Gold mineralization at Zakanaka occurs along a D_{2B} shear zone within amphibolites and at its intersection with an amphibolite-

ultramafic schist contact, similarly emphasising the competency-contrast control.

Metamorphism

Critical mineral assemblages, such as calcic plagioclase (An=30-40)+magnesio-hornblende in amphibolites, biotite+garnet and biotite+muscovite+andalusite in mica schists, and grunerite in the BIF are indicative of amphibolite-facies metamorphism in the district. Peak metamorphic temperatures and pressures are estimated as 540±30° C and 3±1 kb using biotite-garnet and plagioclase-amphibole thermometry and phengite barometry.

HYDROTHERMAL ALTERATION

Main Hill/Breccia Hill prospect

Gold mineralization at Main Hill/Breccia Hill is hosted in: i) quartz-breccias with a sulphide matrix, and ii) wallrock adjacent to quartz-biotite-amphibole±diopside veins. Alteration associated with the latter is zoned, from the vein edge to the wallrock, with biotite and pyrrhotite followed by calcic actinolite, which hosts composite arsenopyrite/löllingite grains and minor pyrrhotite. Breccias contain mainly pyrrhotite, composite arsenopyrite/löllingite grains and traces of chalcopyrite.

Composite ore grains, typically hosted in pyrrhotite, are zoned with a core of löllingite rimmed by arsenopyrite (Neumayr et al., 1993). Although microscopically visible gold occurs preferentially at the grain boundary between arsenopyrite and löllingite, isotopic imaging, line-scans across the grain boundaries, and spot analyses for Au with Secondary-Ion-Mass Spectrometry (SIMS) show that invisible gold is hosted by löllingite (20-33 ppm Au) whereas arsenopyrite (0.16-1.04 ppm Au) is essentially barren.

Ore textures suggest that löllingite and pyrrhotite precipitated together synchronous with wallrock alteration. Thus the auriferous löllingite represents syn-metamorphic gold mineralization. Löllingite was then replaced by arsenopyrite, possibly by a slightly retrograde solid-solid reaction between löllingite and pyrrhotite, although arsenopyrite could also have replaced löllingite under high-temperature hydrothermal conditions as a result of increasing a_{H2S°, decreasing a_{H3AsO3° or $a_{H2(g)}$ (oxidation) of the ore fluid. In either case, gold originally precipitated with löllingite at high temperatures, probably in solid solution, and was liberated and concentrated at the arsenopyrite-löllingite grain boundary during the replacement of löllingite by arsenopyrite. Arsenopyrite thermometry constrains the lower temperature limit for this reaction to 460°-540° C.

Zakanaka prospect

Alteration at Zakanaka occurs with quartz veining. Individual veins show characteristic, almost monomineralic zones, from vein centre to edge, of diopside-calcite-quartz-calcic plagioclase-microcline-amphibole in the most complete sequences. The wallrock adjacent to the quartz veins is intensely altered to biotite and minor amphibole. Gold mineralization is closely associated with pyrrhotite and pyrite in the wallrock adjacent to quartz veins.

Alteration zonation can be explained by: i) K-metasomatism in the distal (to mineralization) sections; and ii) K- and Ca-metasomatism in proximal sections. Balanced mineral reactions, using mineral compositions determined from microanalysis, suggest that K was added

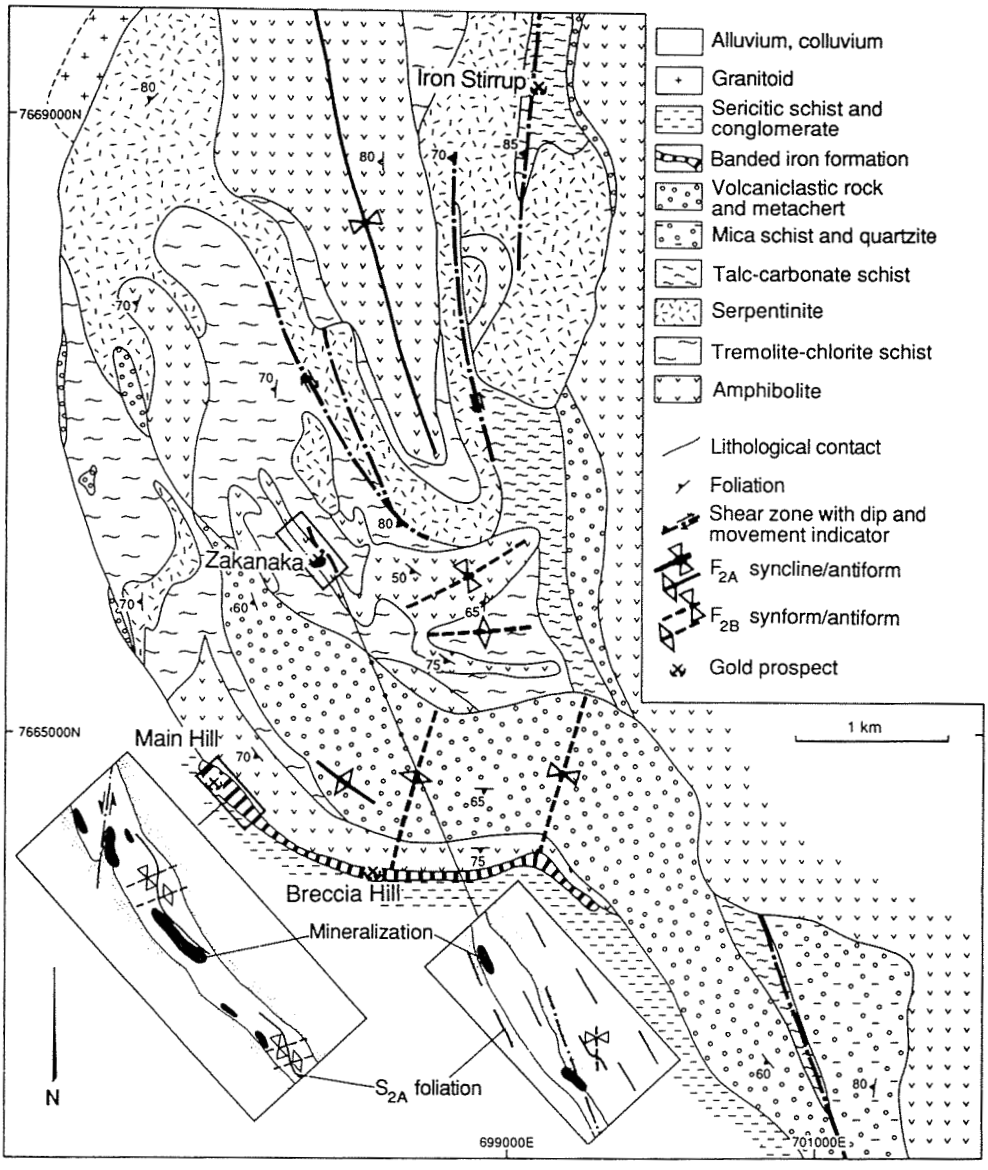

Fig. 1: Geological map of the Mt. York District showing lithologies, main structures and the location of gold prospects. Insets illustrate schematically structural controls on gold mineralization at the Main Hill and Zakanaka prospects. S_{2A} foliation is outlined by heavy black lines, mineralization is indicated by black pattern. Hanging and footwall are indicated by stippled area. Note that most of the mineralization in the BIF at Main Hill is controlled by competency contrast between the BIF and the hangingwall-quartzite, by F_{2B} buckle folds and a D_{2B} fault. Mineralization at Zakanaka is controlled by a D_{2B} fault and by competency contrast between amphibolites and ultramafic schists.

and Na, Ca, Mg and Fe lost into the hydrothermal fluid during the replacement of distal hornblende by biotite. In proximal portions, K, Ca, Mg, Fe and Ti were added to form calcic plagioclase, microcline, diopside, amphibole and titanite. Mass balance calculations (Gresens, 1967), using whole-rock chemical analyses, confirm gains and losses predicted from mineral reactions. Metasomatic amphibole contains higher K and lower Na concentrations than metamorphic amphibole. Hydrothermal biotite and amphibole have higher Mg/(Mg+Fe) ratios in distal than in proximal sections. Gold mineralization probably formed by wallrock sulphidation of biotite and amphibole adjacent to the quartz veins. Plots of mineral reactions with respect to T and X_{CO2} indicate minimum temperatures for quartz-clinopyroxene veins, and hence for gold mineralization of 510° at X_{CO2}=0.05.

CONCLUSIONS

Gold mineralization in the Mt. York District was broadly synchronous with the peak of amphibolite-facies metamorphism, and is mainly controlled by F_{2B} folds and D_{2B} shear zones. Hydrothermal alteration in both deposits is characterized by monomineralic or bimineralic (high thermodynamic variance) calc-silicate and biotite assemblages. At Main Hill gold precipitated in solid solution in löllingite and was subsequently released as native gold during the replacement of löllingite by arsenopyrite. Sulphidation of biotite wallrock was the main gold precipitation mechanism at Zakanaka. At both deposits, available evidence overwhelmingly implicates that open high-temperature (syn-peak metamorphic) hydrothermal systems were involved in gold mineralization. Such systems were clearly hotter and deeper than most of the well-documented "mesothermal" systems documented for Archaean lode-gold deposits in the literature.

ACKNOWLEDGEMENTS

The studies are part of a Ph.D. study by PN, who acknowledges the financial support of MIM Exploration, and the receipt of OPRS and UWA Postgraduate Scholarships. The authors are indebted to J.R. Ridley for critical comments on an earlier version of this abstract.

REFERENCES

Ho, S.E., Groves, D.I. & Bennett, J.M.1990. Gold deposits of the Archaean Yilgarn Block, Western Australia: nature, genesis and exploration guides. Geology Department (Key Centre) & University Extension, The University of Western Australia, Publ.No.20, 407p

Gresens, R.L. 1967. Composition-volume relationships of metasomatism. Chemical Geology 2: 47-65

Neumayr, P., Cabri, L.J., Groves, D.I., Mikucki, E.J. & Jackman, J.A. 1993.The mineralogical distribution of gold and relative timing of gold mineralization in two Archaean settings of high metamorphic grade in Australia. Canadian Mineralogist 31: (in press)

Thorpe, R.I., Hickman, A.H., Davis, D.W., Mortenson, J.K. & Trendall, A.F. 1990. Application of recent zircon U-Pb geochronology to the Marble Bar region, Pilbara Craton, to modelling Archaean lead evolution. In: Third International Archaean Symposium-Extended Abstract Volume. Geoconferences (W.A.), Perth, pp 11-13

Current Research in Geology Applied to Ore Deposits.Fenoll Hach-Ali, Torres-Ruiz & Gervilla(eds)(1993).ISBN 84-338-1772-8

LEAD ISOTOPE VARIATIONS IN LATE PROTEROZOIC GOLD-SILVER DEPOSITS IN THE WEISHANCHENG DISTRICT, CENTRAL CHINA, P.R.

Nie, F. (1); Bjørlykke, A. (1); Ge, B. (2) & Chengyu, W. (2)
(1) Dept. of Geology, University of Oslo, P.O. Box 1047, Blindern, Oslo, Norway
(2) Inst. of Mineral Deposits, Chinese Academy of Geological Sciences, Baiwanzhuang Road 26, Beijing 100037, China.

ABSTRACT: Poshan and Yingdongpo Au-Ag deposits in the Weishancheng district, Central China, occur entirely within Late Proterozoic carbonaceous sericite-quartz schist as layers and lenses. Lead isotope analyses of these two gold-silver deposits show that gold and silver were probably derived from a lower crust source. Comared to the Poshan deposit, the relatively high Th/U ratios and low ^{207}Pb content of the Yindongpo deposit indicates that its source material has undergone a more intensive U depletion. The high Au/Ag ratios of the Yindongpo deposit may also related to the same depletion process.

INTRODUCTION

The Poshan and Yingdongpo Au-Ag deposits in the Weishancheng district, located approximately 200 km north-northwest of Wuhan city, Central China, are the most important producers of Au and Ag in China. Other precious metals (Cd, Pt,Pd,Rh,Ir,Ru and Os) are recovered as by-products. In the present study, lead isotopic systematics of the Au-Ag ores have been examined with the aim of constraining possible sources of metals and ore fluids.

GEOLOGICAL SETTING

Weishancheng district belongs to the southeast sector of Qinling tectonic belt in China. Five mainformations of Late Proterozoic age were recognized in the district. These are, in stratigraphic order: Weitoushan, Dalishou, Liushanya, Dahe and Hushantou formations. Among these five formations, the Dalishou and Liushanya formations are made up of dominantly Late Proterozoic meta-mafic volcanics, whereas the remaining three formations comprise Late Proterozoic volcano-clastic, clastic sedimentary and carbonate rocks.

Gold and silver mineralization in the district occur within the Weitoushan Formation, which can be divided into three members. The lower member is composed of leptinite, marble, mica schist and plagioclase (Pl)-amphibole (Amp) schist. The middle member comprises granulitite, meta-silt stone, carbonaceous-sericite (Ser)-quartz (Q) schist and Pl -Amp schist. The upper member consists of leptinite, dolomite (Dol)-Q schist and Pl-Amp schist, which is overlain unconformable by a suite of biotite (Bi)-Pl gneisses and the Dalishou Formation. The Dalishou Formation is

mainly composed of Pl-Amp schist with K-Ar amphibole age of 391 ± 3 Ma, and leptinite.

Both the Poshan and Yindongpu deposits are located in the upper and middle members of the Weitoushan Formation. The most important host rock for the banded and disseminated-veinlet Au- and Ag- ore is carbonaceous-Ser-Q schist. The longth of each individual ore body ranges from 300 m to 1300 m and with thicknesses of 2 m to 25 m. Generally, the ore bodies are controlled by the occurrence of the carbonaceous-Ser-Q schist. The two deposits have a similar mineral assemblage and ore texture, although the Poshan deposit is characterized by the enrichment of Ag-bearing minerals and the Yindongpo by Au-bearing minerals. More than 40 species of Au- and Ag-bearing ore minerals have been identified. Gold is associated with electrum, calaverite and pyrite. In contrast, silver is associated with sylvane, argentite, stromeryerite, kustelite, proustite, miargyrite, jalpaite and cerargyrite. Associated gangue minerals are quartz, sericite, calcite, dolomite, florite, garnet, and amphibole. The sulfide ore has an average ore grade of 7-12 g/t Au and 330-388 g/t Ag, whereas sulfide oxidized ore has 0.5-1g/t Au and 210 g/t Ag. It was suggested that the banded and disseminated-veinlet ores were formed around 390-410 Ma by regional metamorphism (Chen and Zhou, 1984).

The Taoyuan biotite plagiogranite with K-Ar biotite age of 370 ± 10 Ma outcrops to the north, northwest and northeast of the two deposits. Some dioritic intrusions located in between the Weitoushan Formation and the Taoyuan biotite plagiogranite, have also been recognized. Chen and Zhou (1984) suggested these dioritic intrusions are older than 370 Ma. Various quartz veins, lamprophyres and syenitic dikes can also be found in the district.

LEAD ISOTOPE RESULTS

The methods are described by Nie and Bjørlykke (1992). The results are summarized in Figure 1A and 1B. Based on $^{207}Pb/^{204}Pb$ and $^{206}Pb/^{204}Pb$ ratios, all the analyzed samples can be roughly divided into two groups: (1) isotope compositions of gold-silver ores and sulfide minerals from the Poshan deposit are homogeneous and group closely together near the lower crust curve of the plumbotectonics II model (Zartman and Doe, 1981); and (2) whole ore samples and sulfide separates from the Yindongpopo deposit show a much lower 207Pb/204Pb ratios (Fig.1A) when compared with lower crust curve and lead isotope data of the Poshan deposit. On $^{208}Pb/^{204}Pb$-$^{206}Pb/^{204}Pb$ plot, ^{208}Pb content of the samples both from the Poshan and Yingdongpo deposits conforms to the lower crust lead or lie above lower crust curve (1B). The trace leads in pyrite and whole ore samples from these two deposits are indistinguishable in isotopic composition from the galena leads.

DISCUSSION

As noted above, both ^{207}Pb and ^{208}Pb content of ore and sulfide from the Poshan deposit conform to the lower crust lead. In contrast, ore and sulfide samples from the Yindong po deposit show a relatively low ^{207}Pb contents (Fig.1A). As the $^{208}Pb/^{204}Pb$ ratio is not as sensitive as the $^{207}Pb/^{204}Pb$, the $^{208}Pb/^{204}Pb$ ratios for all the ores and sulfide from the two deposits may indicated their lead derived from a lower crust source. The widespread $^{207}Pb/^{204}Pb$ ratios suggest that the two deposits have a somewhat different evolutionary history.

Lead from the Poshan and Yindongpo deposits are definitely enriched in ^{208}Pb, as most of data points plot above or close to the lower crust lead curve (Fig.1B). No mixing trend of mantle- and lower crust-related lead has been observed on the $^{208}Pb/^{204}Pb$ vs $^{206}Pb/^{204}Pb$ and $^{207}Pb/^{204}Pb$ vs $^{206}Pb/^{204}Pb206$ diagrams (Fig.1A and 1B). Th/U ratios for the host rock of gold-silver ores are well constrained, in the range of 8 to 12 for the Poshan deposit and 16 to 24 for the Yindongpo deposit. For Yindongpo deposit, high Th/U ratios and low ^{207}Pb content as well as near concordance of model Pb-age of gold-silver ores and stratigraphic age (945 Ma) could be interpreted as extensive loss of U prior to Au-Ag ore deposition. The U depletion process for the Yindongpo deposit may be divided into two stages: (1) The lower crust-related materials have mixed with some components with less radiogenic than even lower crust on the plubotectonics II model. Most likely candidate is U strongly depleted carbonaceous Ser-Q schist (Th/U = 18). Neodymium isotopic data from the gold-silver ores generally show negative eNd(945) values(-2.61 - -3.26) and older crustal residence age (2.0 Ga), suggesting that old crustal material (carbonaceous Ser-Q schist) was incorporated into the ores (Nie et al., 1993, this volume); (2) The mixed materials have undergone an intensive metasomatism and metamorphism, which resulted in U and Ag depletion. Previously studies showed that Archean and Proterozoic rocks metamorphosed in granulite facies are low in uranium content and thus have relative low $^{207}Pb/^{204}Pb$ or high $^{208}Pb/^{204}Pb$ ratios (Gray and Oversby, 1972). Thus, although the Pb-isotopic compositions of Proterozoic lower crust and mantle are poorly constrainted, we favour lower crust derivation for the Poshan and Yingdongpo deposits. The high Th/U ratios and low 207Pb content for the Yindongpo deposit may ascribe to U depletion by hydrothermal event.

CONCLUSION

From the present data, it is obvious that most of the lead within the Poshan and Yindongpo gold-silver deposits were indeed derived from Proterozoic lower crust source. Pb-isotopic variation encountered in the Yindongpo deposits indicate that it has somwhat different evolutionary history to the Poshan deposit. The high Th/U ratios, Au/Ag ratios

and low ^{207}Pb content of the Yindongpo deposit can be interpreted as U depletion caused by intensive metasomatism and metamorphism. Distinct $^{207}Pb/^{204}Pb$ ratios for the two deposits might help illustrate difference of gold and silver concentration in the two deposits.

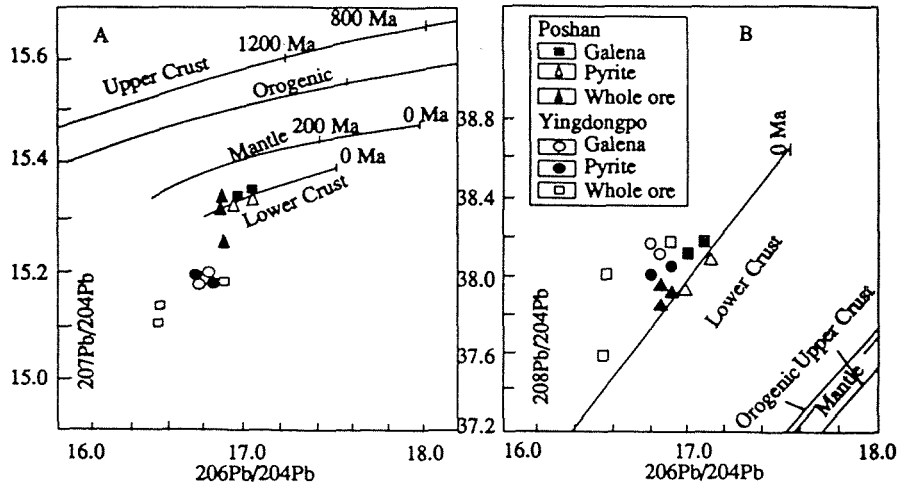

Fig.1 $^{207}Pb/^{204}Pb$ and $^{208}Pb/^{204}Pb$ vs $^{206}Pb/^{204}Pb$ ratios of galena, pyrite and whole gold-silver ore from the Poshan and Yindongpo deposits in the Weishancheng district. Pb-isotope evolution curves of the Upper crust, Orogene, Mantle and Lower Crust from Zartman and Doe(1981)

REFERENCES

Chen, D. K., and Zhou, D.S.,1984. Stratabound features and mineralization process of the Weishancheng gold-silver deposit. Mineral Deposits.3:37-46(In Chinese with English abstract).

Fengjun Nie and Arne Bjørlykke, 1993, Lead and sulfur isotopic studies of the Wulashan K-feldspar and quartz vein gold deposit, Southwest Inner Mongolia, P.R.China (submitted to Economic Geology)

Gray,C. M., and Oversby, V.M., 1972. The behaviour of lead isotopes during granulite facies metamorphism. Geochim. Cosmochim.Acta.36:936-952

Zartman,R.E.and Doe,B.R.,1981,Plumbotectonics-the model. Tectonophysics.75:135-162.

Current Research in Geology Applied to Ore Deposits.Fenoll Hach-Alí, Torres-Ruiz & Gervilla(eds)(1993).ISBN 84-338-1772-8

Nd-Sr ISOTOPE CONSTRAINTS ON THE ORIGIN OF LATE PROTEROZOIC GOLD-SILVER DEPOSITS IN THE WEISHANCHENG DISTRICT, CENTRAL CHINA, P.R.

Nie, F. (1); Bjørlykke, A. (1); Ge, B. (2) & Chengyu, W. (2)

(1) Dept. of Geology, University of Oslo, P.O. Box 1047, Blindern, Oslo, Norway

(2) Inst. of Mineral Deposits, Chinese Academy of Geological Sciences, Baiwanzhuang Road 26, Beijing 100037, China

ABSTRACT: Nd- and Sr-isotopic analyses of ores and related meta-volcano-sedimentary rocks of the Poshan and Yingdongpo Au-Ag-deposits in Weishancheng district show that Au and Ag were derived from two main sources. Most metals in the banded Au-Ag-ores formed during an earlier event around 945 Ma, and originated from a mantle-related mafic volcanic source. The metals in the disseminated-veinlet ores were produced by a late event around 390 to 410 Ma from the reaction between the banded ores and metamorphic fluid with a crustal signature.

INTRODUCTION

The Poshan and Yingdongpo Au-Ag deposits in the Weishancheng district, located approximately 200 km north-northwest of Wuhan city, Central China, are the most important producers of Au and Ag in China. Other precious metals (Cd, Pt,Pd,Rh,Ir,Ru and Os) are recovered as by-products.The Nd- and Sr-isotope systematics of Late Proterozoic metavolcano-sedimentary rocks and Au-Ag ores have been examined with the aim of constraining possible sources of metals and ore fluids.

GEOLOGICAL SETTING

Weishancheng district belongs to the southeast sector of Qinling tectonic belt in China. Five mainformations of Late Proterozoic age were recognized in the district. These are, in stratigraphic order: Weitoushan, Dalishou, Liushanya, Dahe and Hushantou formations. Among these five formations, the Dalishou and Liushanya formations are made up of dominantly Late Proterozoic meta-mafic volcanics, whereas the remaining three formations comprise Late Proterozoic volcano-clastic, clastic sedimentary and carbonate rocks. Gold and silver mineralization in the district occur within the Weitoushan Formation, which can be divided into three members. The lower member is composed of leptinite, marble, mica schist and plagioclase (Pl)-amphibole (Amp) schist. The middle member comprises granulitite, meta-silt stone, carbonaceous-sericite (Ser)-quartz (Q) schist and Pl -Amp schist. The upper member consists of leptinite, dolomite (Dol)-Q schist and Pl-Amp schist, which is overlain unconformable by a suite of biotite (Bi)-Pl gneisses and the Dalishou Formation. The Dalishou Formation is mainly composed of Pl-Amp schist with K-Ar amphibole age of 391 ± 3 Ma, and leptinite.

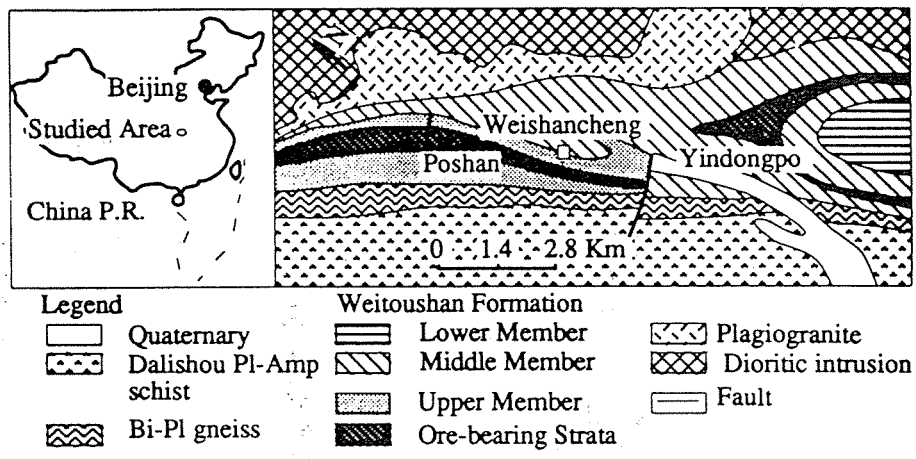

Fig.1 Diagrammatic geological map of the Weishancheng gold-silver mineralized district(modified from Chen and Zhou, 1984)

Both the Poshan and Yindongpu deposits are located in the upper and middle members of the Weitoushan Formation. The most important host rock for the banded and disseminated-veinlet Au- and Ag- ore is carbonaceous-Ser-Q schist. The longth of each individual ore body ranges from 300 m to 1300 m and with thicknesses of 2 m to 25 m. Generally, the ore bodies are controlled by the occurrence of the carbonaceous-Ser-Q schist. The two deposits have a similar mineral assemblage and ore texture, although the Poshan deposit is characterized by the enrichment of Ag-bearing minerals and the Yindongpo by Au-bearing minerals.More than 40 species of Au- and Ag-bearing ore minerals have been identified. Gold is associated with electrum, calaverite and pyrite. In contrast, silver is associated with sylvane, argentite, stromeryerite, kustelite, proustite, miargyrite, jalpaite and cerargyrite. Associated gangue minerals are quartz, sericite, calcite, dolomite, florite, garnet, and amphibole. The sulfide ore has an average ore grade of 7-12 g/t Au and 330-388 g/t Ag, whereas sulfide oxidized ore has 0.5-1g/t Au and 210 g/t Ag. It was suggested that the banded and disseminated-veinlet ores were formed around 390-410 Ma by regional metamorphism (Chen and Zhou, 1984).

The Taoyuan biotite plagiogranite with K-Ar biotite age of 370 ± 10 Ma outcrops to the north, northwest and northeast of the two deposits. Some dioritic intrusions located in between the Weitoushan Formation and the Taoyuan biotite plagiogranite, have also been recognized. Chen and Zhou (1984) suggested these dioritic intrusions are older than 370 Ma. Various quartz veins, lamprophyres and syenitic dikes can also be found in the district (Fig. 1).

SAMPLING AND ANALYTICAL RESULTS

The ore material used in the analyses were hand picked to

avoid any contamination by wall rocks with the help of binocular microscope. A number of wall rocks were also analyzed in order to identify Nd- and Sr-sources of the ore fluids. The detailed chemistry is described by Mearns (1986). The εNd(T) values and initial $^{87}Sr/^{86}Sr$ ratios of the samples were calculated using 945 Ma and 390 Ma.

Based on the εNd(T) values and initial $^{87}Sr/^{86}Sr$ ratios at 945 Ma, the ores and rocks can be roughly divided into three groups: (1) Banded ore/Pl-Amp schist showing high εNd(T) and low initial $^{87}Sr/^{86}Sr$ ratios; (2) disseminated-veinlet ore/Bi-Pl gneiss showing low εNd(T) values and high $^{87}Sr/^{86}Sr$ ratios; and (3) carbonaceous ser-Q schist and leptinite, which lie in between the fields of the banded ore/Pl-Amp schist and the disseminated-veinlet ore/Bi-Pl gneiss. Two Pl-Amp schist samples with igneous mineralogy, show the highest εNd(T) values of all the analyzed whole rock samples, which indicates they were derived from mafic igneous source. At 390 Ma, the disseminated-veinlet ores are plotted in between the fields of the banded ore and meta-sediments.

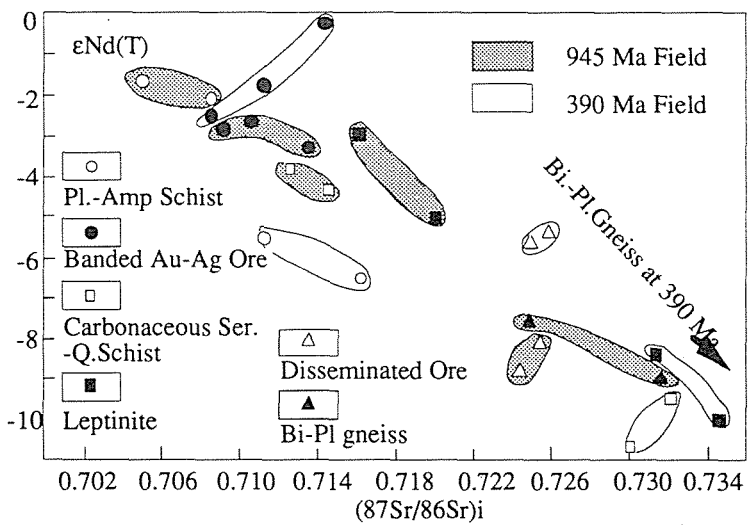

Fig.2 εNd(T) values and initial Sr isotope ratios of gold-silver ore samples at 945 Ma and 390 Ma. All the analyzed whole rock samples were also calculated at 945 Ma and 390 Ma.

DISCUSSIONS

The εNd(T) values and initial Sr-isotope ratios of all the ore samples at both 945 Ma and 390 Ma plot in Figure 2 and compared with Pl-Amp schist and other meta-sediments at Weishancheng district. The data points for the banded ore samples at 945 Ma lie close to the field of Pl-Amp schist, which suggests that the ore fluid acquired their Nd- and Sr-isotope composition mainly from mafic igneous source,but some contributions from the leptinite and carbonaceous Ser -Q schist can not be ruled out.

The εNd(T) and initial $^{87}Sr/^{86}Sr$ values of the disseminated -veinlet Au-Ag ore samples at 390 Ma plot between the field of banded ore and carbonaceous Ser-Q schist. The low εNd(T) values and high initial $^{87}Sr/^{86}Sr$ ratios of the the ore can be explained by mixing of wall rock-derived Nd and Sr, with highly radiogenic Nd and Sr of the banded ores. The data are consistent with local derivation of Nd and Sr in the ore fluids from the host schist and previously formed ores. The Bi-Pl gneiss has considerably lower εNd(T) values and much higher initial $^{87}Sr/^{86}Sr$ ratios than all the banded and disseminated-veinlet ores, indicating the Bi-Pl gneiss was not a source of metals in the ore fluid.

CONCLUSION

Metals in the banded ores were mainly derived from mafic volcanics-related fluid and were deposited around 945 Ma. In contrast, the disseminated-veinlet ores were produced by the reaction between the primary banded ores and hydro-thermal fluids with crustal signatures. Field observations also show that the banded ores are obviously cut by Au-Ag-bearing veinlet or/and veins.

REFERENCES

Chen, D. K., and Zhou, D.S.,1984. Stratabound features and mineralization process of the Weishancheng gold-silver deposit. Mineral Deposits.3:37-46(In Chinese with English abstract).

Mearns, E. W., 1986. Sm-Nd ages for Norwegian garnet peridotite. Lithos 19:269-278.

Current Research in Geology Applied to Ore Deposits.Fenoll Hach-Alí, Torres-Ruiz & Gervilla(eds)(1993).ISBN 84-338-1772-8

THE ASHANTI GOLDFIELDS MINE, OBUASI, GHANA: MINERALOGICAL CHARACTERISTICS, LIGHT STABLE ISOTOPES AND FLUID PROPERTIES

Oberthür, T. (1); Schmidt Mumm, A. (1); Vetter, U. (1); Weiser, Th.(1); Amanor, J.A. (2); Gyapong, W.A. (2); Kumi, R. (2), Blenkinsop, T.G. (3) & Chryssoulis, S. (4)

(1) Bundesanstalt für Geowissenschaften und Rohstoffe, Hannover, Germany

(2) Ashanti Goldfields Corp., Obuasi, Ghana

(3) Geology Dept., University of Zimbabwe, Harare

(4) London, Ontario, Canada

ABSTRACT:

The Ashanti mine is the largest gold producer in West Africa. Mineralization is structurally controlled and consists of refractory sulfide ores with arsenopyrite as the principal gold-carrier, and quartz veins with free-milling gold. Structural, geochemical, mineralogical, stable isotope and fluid inclusion studies combined support a metamorphic fluid model for the genesis of the deposit.

INTRODUCTION:

The Ashanti mine at Obuasi in Ghana is a giant gold deposit on world scale, its past gold production exceeding 700 t at a current target of 30 t annual output.

The deposit and numerous other gold occurrences are located close to and in a NE-SW trending transcrustal shear zone, some 250 km long, superimposed and transecting early Proterozoic rocks of the Birimian Supergroup (ca. 2.2-2.1 Ga). At Ashanti, gold mineralization is exposed ca. 8 km along strike and 1650 m down dip. It consists of two major primary ore types: (i) refractory sulfide ores, confined to the wall rocks, with auriferous arsenopyrite as the dominant sulfide, and (ii) quartz veins with minor sulfides but often spectacular showings of visible gold.

Our investigations were performed within the project "Metallogenesis of Gold in Africa" on behalf of the German Ministry for Technical Cooperation. It is the aim of this project to jointly investigate gold targets with counterpart geologists from African countries and thereby promote cooperation and scientific exchange. This paper presents some key studies towards metallogenetic modelling of the deposit.

REGIONAL AND MINE GEOLOGY:

Large areas of southern Ghana consist of Proterozoic rocks of the West African Craton. The supercrustal sequence is dominated by sedimentary and volcanic rocks of the Birimian Supergroup, which were folded, metamorphosed and intruded by various granitoids during the ca. 2.1 Ga Eburnean tectonothermal event (LEUBE et al. 1990). Deformation is attributed to a single progressive event involving NW-SE directed compression (EISENLOHR & HIRDES 1992), a concept that also applies to the local situation at Ashanti where further evidence was found for a sub-vertical extension direction. Host rocks of the ores are prodominantly metasediments (schists and feldspathic sandstones with turbidite affinities) with rare intercalated volcanic flow rocks. The rock sequence trends NE-SW with a steep westerly dip and was metamorphosed under greenschist facies conditions. Locally, intense metasomatic alteration (carbonatization), probably related to mineralization has affected the metasediments. The deposit is constituted by a number of individual orebodies, up to ca. 30 metres wide and some hundred metres long, which pinch and swell both along strike and dip. Sulfide ores and quartz veins are present in variable proportions in different mine sections. Both types of mineralization are syn-kinematic and structure-controlled, related to prolonged multistage episodes of tectonic activity and hydrothermal fluid flow.

MINERALOGY OF THE ORES:
Sulfide ores in the wall rocks and quartz veins transecting the latter constitute different entities in regard of mineral contents, mineralogical siting of gold and geochemistry and are thus treated separately.

The sulfide ores are dominated by arsenopyrite (60-95 % of the ore minerals), followed by pyrite, pyrrhotite, marcasite, subordinate chalcopyrite and sphalerite and rare microscopic gold. The sulfides occur disseminated or concentrated in stringers in the host rocks. The orientation of especially arsenopyrite needles parallel to foliation points to synkinematic emplacement of the sulfides. Analyses of sulfide concentrates revealed gold contents between 55 and 396 ppm, indicating that most of the gold is submicroscopic, hosted in sulfides. Secondary Ion Mass Spectrometry (SIMS) investigations proved that >99 % of the gold is concentrated in arsenopyrite (x=190 ppm, maxima=2500 ppm), whereas the Fe-sulfides show insignificant gold contents (ca. X. ppm). Gold concentration mapping revealed low contents in the centres of arsenopyrite crystals and elevated contents along distinct crystal growth zones towards their rims. An outermost crystal layer is usually gold-poor. Notably, gold contents appear to be independent of specific As/S ratios of the host arsenopyrite.

The quartz veins contain free-milling gold, which occurs in the form of irregular, individual grains, or mutually intergrown with a number of Cu-Pb-Zn-Sb-sulfides (galena, chalcopyrite, sphalerite, bournonite, boulangerite, tetrahedrite). Rare aurostibite, unspecified Bi-tellurides and auriferous loellingite were also detected, whereas occasional pyrite and arsenopyrite are usually bound to wall rock fragments in the veins. Notable are constant contents of Se in galena.

The two ore types are clearly distinguished by their mineralogies and consequently their geochemical signatures (Fe-As-S and apparent fineness values above 910 for sulfide ores, versus Cu-Pb-Zn-Sb-S and true fineness values ranging between 730 and 930 in the quartz veins). Sulfide mineralization texturally appears to predate the quartz veins. However, this ralationship might equally define a distinct temporal sequence of mineralization or could express overlapping events (vein emplacement and wall rock alteration) due to repetitive fluctuations in fluid flow.

STABLE ISOTOPES:
Peculiar stable isotope compositions characterize the deposit and its host rocks.
Carbonaceous matter (graphite) from schists and gouge is isotopically light (range -11.4 to -28.4, with two probable maxima at -16 and -25 per mil PDB), pointing to an organic derivation of the graphite. Carbonates are depleted in ^{13}C with values covering a tight range from -9.9 to -17.0 per mil. Relationships between carbon isotope compositions of graphite and carbonate carbon are twofold:

The organic carbon which is most depleted in ^{13}C shows no obvious relation to associated carbonates, whereas the subgroup of organic carbon with values between -10 and -20 per mil correlates excellently with the values of respective carbonate carbon, pointing to extensive isotopic homogenization between organic and carbonate carbon.

Oxygen isotope compositions of carbonates and quartz range from 12.9 to 22.2 (median 15.5 per mil SMOW) and 12.8 to 15.6 (median 14.7 per mil), resp..

$\delta^{18}O$ of the fluids, recalculated from $\delta^{18}O$ of quartz, is 9.4 and 11.6 per mil for the median values at 350 and 450°C, respectively, indicating a deep-seated fluid of magmatic/metamorphic origin.

Sulfur isotope compositions of pyrite from Birimian sediments range from -16.8 to +7.3 per mil CDT. A tendency towards ^{34}S-depletion and the wide spread of data testify on (biological) sulfate reduction. Arsenopyrite from the sulfide ores at Ashanti is isotopically light (range -5.3 to -8.9 per mil). The data display a tight unimodal distribution indicative of a large, homogeneous source. Notably, galena from the quartz veins is further depleted in ^{34}S (ca. -12 per mil).

Sulfides in most Archean hydrothermal gold deposits display $\delta^{34}S$ values ranging between +7 and -3 per mil (e.g. COLVINE et al. 1988). Exceptions with light isotopic compositions are the Golden Mile, Australia (PHILLIPS 1986) and the Hemlo deposit in Canada (CAMERON & HATTORI 1987), where the presence of sulfates and/or hematite points to the involvement of oxidized fluids responsible for the depletion in ^{34}S.

Mineralogical constraints at Ashanti (absence of sulfates and hematite, presence of Fe-sulfides coexisting with graphite), however, indicate an oxidation state of the fluid below the SO_2/H_2S boundary. It is proposed that the depleted $\delta^{34}S$ values of sulfides at Ashanti largely reflect a fractionated source, i.e. sulfides in Birimian sediments.

FLUID INCLUSION STUDIES:

Our investigations revealed peculiar inclusions in quartz:
(1) >99 % of the inclusions are monophase or rarely two-phase at room temperature and contain predominantly CO_2-rich gas mixtures, the other components being N_2 and minor CH_4. Initial melting after freezing is observed between -83 and -76°C (-146 to -123°C for N_2-rich inclusions), and final melting (Tm) occurs between -61.3 and -56.4°C. Temperatures of final homogenization (Th) are as low as -33.8°C, with the majority of Th falling into the range -15 to -9.8°C.
(2a) Low-saline aqueous inclusions with eutectic temperatures (Te) of -22.4 to -9.8°C and ice melting temperatures between -10.3 and -0.7°C. Final homogenization to liquid took place between 128 and 280°C.
(2b) High-saline aqueous inclusions with Te of -57.3 to -38.3°C and Tm(ice) of -24.6 to -18.4°C. Hydrate melting temperatures range between -18.3 and -10.6 in some inclusions, whereas Th to liquid occurred between 72 and 165°C.

Maximum densities obtained from CO_2-rich inclusions range up to 1.06 g/cm³, with most values ranging from 0.89 to 0.95 g/cm³. For aqueous inclusions, densities lie between 1.145 and 1.12 g/cm³ (high saline) and 1.07 to 0.84 g/cm³ (low saline). The predominance of CO_2-rich inclusions and near-absence of aqueous inclusions raises some questions in regard of original characteristics of the fluids and their later re-equilibration, e.g. are supercritical CO_2-rich fluids capable of transporting gold?

The measured fluid inclusion characteristics are proposed to result from (i) initial formation at elevated temperatures (500-550°C) and fluctuating pressures (2.8 - 5.2 Kbar), and (ii) extensive re-equilibration following a quasi-isobaric retrograde path during which mineralization proceeded in the active shear zone.

GEOCHRONOLOGY:
Various methods are currently employed in order to constrain the age of mineralization in the context of geochronological evolution of the terrane. Work in progress includes U/Pb on hydrothermal rutile, Pb/Pb on Pb-sulfides, arsenopyrite and gold (HÖHNDORF et al. 1993), and K/Ar on muscovite. Results of these studies will be presented at the meeting.

CONCLUSIONS:
Gold mineralization forms part of the crustal evolution of the early Proterozoic terrane in Ghana. Structural and petrographic investigations combined reveal that hydrothermal mineralization at Ashanti is largely syn-metamorphic and syn-kinematic, contemporaneous with the Eburnean tectonothermal event at ca. 2.1 Ga. Fluid flow was focussed in shear zones which were active late in the deformation history. Stable isotope compositions reflect large, homogeneous fluid sources of deep-seated, magmatic/metamorphic origin, and at the same time display signatures pointing to significant fluid/wall rock reactions taking place during the fluids' passage through the rock sequence. Fluid inclusions are predominantly CO_2-rich; their genesis still appears somewhat enigmatic but may be explained by initial formation at fluctuating pressures and subsequent re-equilibration during prolonged multistage episodes of tectonic activity and hydrothermal fluid flow. A (possibly synchronous) two-stage model for the mineralization is preferred which embraces sulfidization of country rocks ("wall-rock alteration") with a distinct mineralogical and geochemical signature (As-S-Au) and emplacement of gold quartz veins characterized by Ag-rich gold and Pb-Cu-Sb-Zn-sulfides.

Gold mineralization at Ashanti has many features in common with Archean mesothermal lode- and vein-type gold deposits. However, in contrast to these, Ashanti displays unique characteristics and distinct differences including its enormous size, structural position rather within than alongside a major transcrustal shear zone, certain stable isotope compositions unequivocally reflecting extensive fluid/wall rock interaction, and unusual fluid inclusion characteristics with CO_2 as the predominant species.

REFERENCES:
CAMERON, E.M. & HATTORI, K. (1987): Econ. Geol., 82, 1177-1191.
COLVINE, A.C. et al. (1988): Ontario Geol. Survey, Misc. Paper 139.
EISENLOHR, B.N. & HIRDES, W. (1992): Jour. African Earth Sciences, 14, 313-325.
HÖHNDORF, A. et al. (1993): Conf. on Sub-Saharan Geology '93, Harare, Zimbabwe.
LEUBE, A. et al. (1990): Precambrian Res., 46, 139-165.
PHILLIPS, G.N. (1986): Econ. Geol., 81, 779-808.

Current Research in Geology Applied to Ore Deposits. Fenoll Hach-Alí, Torres-Ruiz & Gervilla (eds) (1993). ISBN 84-338-1772-8

AN EXPERIMENTAL STUDY OF GOLD MOBILITY IN SULPHUR-SATURATED SOLUTIONS (IN CONNECTION WITH CONDITIONS OF GOLD-CONTAINING SULPHIDE-RICH ASSEMBLAGES)

Pal'yanova, G.A.; Laptev, Yu.V. & Kolonin, G.R.
United Inst. of Geology, Geophysics and Mineralogy, Siberian 630090, Novosibirsk, Russia

ABSTRACT: Based on new experimental data, possible gold speciation in solutions during formation of rather common sulfide-rich productive assamblages are discussed. The experiments show very high solubility of gold (up to 1.6g/1kgH_2O) in alkaline solutions (pH=7.3-8.5) at high sulfur contents (0.1-1.0m/kgH_2O), moderate temperature (200° C) and intermediate redox conditions. Peculiar features of physical-chemical conditions, corresponding to the interval of sulfide-sulfate equilibrium close to weakly alkaline pH values, provides a possibility for creating maximum solubility in the form of $Au(HS)_2^-$. This is assumed to be the main reason why late and pyrite-containing sulfide assamblages become enriched in gold during their deposition from solutions at moderate temperatures (<200° C). This fact was rather strongly supported with the help of cheking experiments when Au- and Ag-containing sulfide concentrate from Dzhida W-sulfide deposits (Buryatia, East Siberia) were leached by S-rich solutions at 200°C. The following series of metal mobility was established: Au(80%) > Ag(30%) > Cu(20%) > Bi(n%) > Pb, Zn(0).

INTRODUCTION

Participation of gold and silver polysulfide and thiosulfate and, later, hydrosulfide complexes in geochemical transport and deposition of gold and nonferrous metals is quite an old idea having been discussed for many years (Clocke, 1962; Turin, 1963; Seward, 1973; Webster, 1986; Shenberger, Barnes, 1989). Despite a rather limited temperature range of their stability, restricted up to 200-250° C, and desirability of high S-concentrations, sufficient alkalinity and intermediate redox conditions in ore-forming solutions, similar situation is expected to occur at the last stages of ore-formation when gold and silver-containing sulfide ores are formed. On the one hand Shenberger, Barnes (1989) reported the experimental evidences to explain extremely high gold solubility in weakly alkaline solutions (up to 7 - 8g/kg) due to formation hydrosulfide complex Au . This is the main reason why the authors of this paper decided to check gold mobility under specific S-saturated hydrothermal conditions.

EXPERIMENTS

The results of the experiments on gold solubility carried out in titanium autoclaves with strong sulfur solutions at the temperature 200°C and 50MPa are given in the Table. The working solutions were prepared by previously dissolving sulfur in NaOH of the required concentrations providing S:NaOH ratio about 1.3 and ensuring realization of the next possible schematic reaction:

$$16\ S + 14\ NaOH \rightarrow 3Na_2S + 2Na_2S_5 + Na_2S_2O_3 + Na_2SO_4 + 7H_2O.$$

All the concentration values of various sulfur forms indicated in the Table have been obtained by iodinemetric analysis of solutions cooled after the experiment. Only fractions of the undissociated H_2S and HS^--ion were separated from the total sulfide sulfur, based on the estimated pH and H_2S dissociation constant. Besides, sulfate sulfur, the amount of which didn't exceed 8% of the total concentration of the dissolved sulfur, was determined by a weight method. Gold content in this solution was also determined by iodinemetric method (after its complete oxidation into Au^{3+}). The data presented for alkaline solutions (Table, N 1-3) show about one-half of sulfur established in them is in the form of pentasulfide, then comes

Table

N	$m_i$mol/kg H_2O					pH_{25}	C_{Au}	
	$S_{el.}$	H_2S_{aq}	HS^-	S_5^{2-}	$S_2O_3^{2-}$		mx10^3	ppm
1	1.40	0.013	0.269	0.112	0.063	8.5	8.84	1740
2	0.70	0.010	0.155	0.043	0.034	8.2	4.00	788
3	0.35	0.008	0.081	0.015	0.032	8.0	1.66	327
4	0.175	0.006	0.040	0.007	0.017	7.8	0.73	144
5	0.088	0.020	0.010	-	-	7.3	0.31	61

hydrosulfide-ion, and the third is thiosulfate sulfur. For rather diluted solution (N 4) with pH < 8, the first three varieties of the dissolved sulfur occur in approximately comparable amounts. As for the estimated gold concentrations in the solution, which even for solutions 4 and 5, approaching in the total sulfur concentrations to those occuring in natural ones, they make up about hundred ppm and by 2-3 orders exceeds those reported usually both in experimental and calculated works. These data significantly change our understanding of the scales of gold mobility in reasonably S-concentrated solutions.

COMPARISION OF THE EXPERIMENTAL AND THERMODYNAMICAL DATA

Free energy minimization programme "Gibbs" was used to compare the experimental data obtained. We have the calculated possible gold concentrations, which should have been formed under experimental conditions according to a reliably studied reaction:

$$Au + 2\ HS^- + H^+ \rightarrow Au(HS)_{2^-} + 0.5\ H_2.$$

H_2 fugacity was determined with the help of two methods, based on the estimated concentrations of various forms of sulfur relative to: 1) mSO_4^{2-}/mH_2S+mHS^-; 2) $mS_2O_3^{2-}/mH_2S+mHS^-+mS_5^{2-}$. Both of these methods resulted in close f_{H2} values distinguished within one order (10^{-5} : 10^{-4}MPa). The comparison of the experimental Au concentrations and computed $mAu(HS)_{2^-}$ values versus the total S-concentration in the

solution, shown in Fig.1, indicate gold convergence at high S-concentrations, where as at low sulfur concentrations notable divergence of the experimental and calculated values occurs.
Fig.2 shows the dependence of gold concentrations in solutions on versus the total value $mH_2S \cdot mHS^-$. Distinctly seen are the differences associated with two methods of evaluating hydrogen fugacity, closer to the experimental line are the estimated points obtained by means

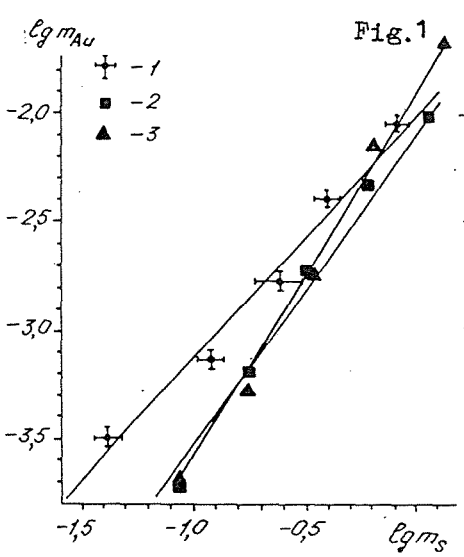

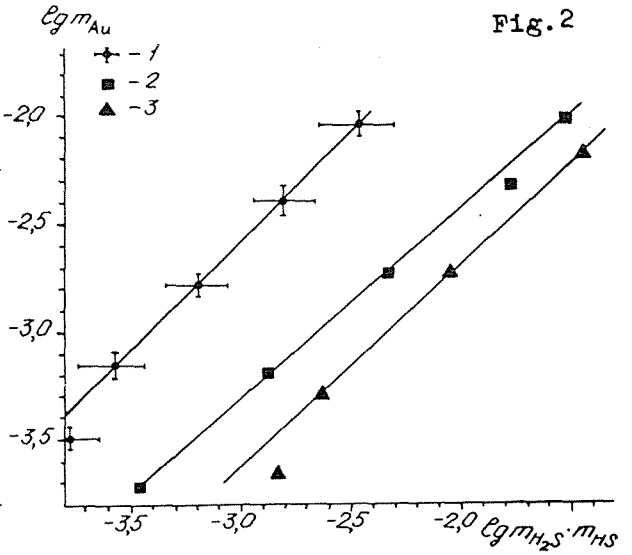

Fig.1.The gold solubility as a function of the total sulfur concentrations 1)experimental data, 2)results of calculations modeling sulfide-thiosulfate-polysulfide equilibrium, 3)results of calculations modeling sulfide-sulfate equilibrium.

Fig.2.The gold solubility as a function of the total value lg mH_2S mHS^-. The conventional symbols are the same in Fig.1.

of sulfide-thiosulfate-polysulfide equilibrium (curve 1). The preserved excess experimental solubility reaching nearly one order can be explained by four very different reasons: 1).additional formation of thiosulfate or polysulfide gold complexes; 2).formation of the following complexes possible just in alkaline solutions: $Au_2(HS)_2^{2-}$ (Seward, 1973), AuS^- (Belevantsev,et.al., 1982) or $Au(HS)_2S^{2-}$ and
AuS^- (Kolonin, et.al, 1982); 3)overestimation of the calculated value m_{H2} by 2log units; 4)the same of the solution pH by 1lg unit. Additional discussion of the most apparent reasons of the divergency of experimental and calculated data will be given in the report.

DISCUSSION

The data obtained support high gold solubility in S-rich solutions when the major portion of sulfur is found in an oxidized state (in the form of sulfides, thiosulfates and polysulfides). They are rather close to the results obtained earlier by Shenberger, Barnes (1989) which showed a possibility of formation of sulfide solutions with Au content higher than 1g/kg H_2O just under reasonably oxidized conditions approachihg to the line of sulfate-sulfide equilibrium. The additional support of the high gold mobility in S-saturated sulfide solutions are the results of checking experiments on gold (and silver) leaching from the sulfide concentrate of the Dzhida hubnerite-sulfide deposits situated in Buryatia (East Siberia). Charge by 95% was composed of pyrite. It also contained galenite, sphalerite, chalcopyrite, negligible mixture of Bi and Ag sulfides and 4ppm of gold. Its treatment at 200 C during only 1 hour led to leaching of 80% of Au and 30% of Ag, whereas only 20% of Cu and several % of Bi passed into solution (notable dissolution of Pb and Zn was not observed). Thus while modeling physical-chemical conditions of formation of Au-rich sulfide ores of the late stages of hydrothermal process very high Au mobility must be taken into account.

REFERENCES

Belevantsev,V.I., Kolonin,G.R., Vasil'eva,N.G., Shironosova,G.P., Shamovskay,G.I., Peshevitsky,B.I. 1982. Possible forms and gold solubility in ore-forming solutions. Pr. IGG SO AN USSR 505: 83-117

Cloke, P.L. 1963. The geologic role of polysulfides. Geochim. et Cosmochim. Acta 27:1265-1319

Kolonin,G.R., Sem'ekhin,G.N., Belevantsev V.I., Peshevitsky,B.I. 1982. The gold solubility in sulfidesolutions at 200 C. In: Chemistry, technology, analysis of gold and silver(in Russian). Nauka, Novosibirsk: 8

Laptev,Yu.V.1989. On the stability of polysulfides and thiosulfides in hydrotermal solutions. In: Third International Symposium on hydrothermal reactions (Abstracts). Frunze: 94

Renders,P.J. and Seward,T.M.1989. The stability of hydrosulfido- and sulfido-complexes of Au(1) and Ag(1) at 25 C. Geochim. et Cosmochim. Acta 53: 245-253

Seward,T.M. 1973. Thio complex of gold and the transport of gold in hydrothermal ore solutions. Geochim. et Cosmochim. Acta 37: 379-400

Shenberger,D.M., Barnes, H.L. 1989. Solubility of gold in aqueous sulfide solutions from 150-350 C. Geochim. et Cosmochim. Acta 53: 269-278

Tyurin,N.G.1963. On the question about a composition of hydrothermal solutions. Geology of ore deposits 4: 24-73

Webster, J.G.1986. The solubility of gold and silver in the system Au-Ag-S-O_2-H_2O at 25 C and 1 atm. Geochim. et Cosmochim. Acta 50: 1837-1845

Current Research in Geology Applied to Ore Deposits. Fenoll Hach-Alí, Torres-Ruiz & Gervilla (eds) (1993). ISBN 84-338-1772-8

TECTONIC SETTING, MINERALOGICAL CHARACTERISTICS, GEOCHEMICAL SIGNATURES AND AGE DATING OF A NEW TYPE OF EPITHERMAL CARBONATE-HOSTED, PRECIOUS METAL-FIVE ELEMENT DEPOSITS: THE VILLAMANIN AREA (CANTABRIAN ZONE, NORTHERN SPAIN)

Paniagua, A. (1); Fontboté, L. (2); Fenoll Hach-Alí, P. (3); Fallick, A.E. (4); Moreiras, D.B. (1) & Corretgé, L.G. (1)

(1) Dept. Geología, Univ. Oviedo, Spain (2) Dépt. Mineralogie, Univ. Géneve, Switzerland (3) Dept. Minera-logía-Petrología, Univ. Granada, Spain (4) Scottish Univ. Research & Reactor Centre, Glasgow, U.K.

ABSTRACT: The Providencia and Profunda mines (Villamanin, Spain) constitute an unusual carbonate-hosted epithermal gold deposit, connected to Late-Variscan deep faults. The ore is composed by Cu-Ni-Co-Fe sulfides, sulfarsenides and selenides, hematite and uraninite in quarzt-carbonate gangue, occurring as veins and pods located at the intersection of E-W and NE-SW high-angle faults. Significant Au concentrations with subordinate Ag-EGP anomalies have been detected. Au is present in a chemically bound state, but also as native gold or electrum. The deposition temperature ranges from 100º to 200ºC, in a low-pressure environment. Sulfur isotopic data show high $^{34}\delta$ ratios, suggesting an evaporitic source. Age dating of uraninite grains by the U-Th-Pb method give 273 ± 11 M. Y., in agreement with an age of 270 ± 12 M. Y. from Pb isotopic ratios in sulfides. Lead isotopic data show high Pb-Pb ratios, according with a radiogenic source of metals. This deposit represents a transition between carbonate-hosted epithermal gold deposits and Cobalt-type deposits formed in relation with late events of the Variscan orogeny.

INTRODUCTION.

The Cantabrian Zone (CZ) is the outermost part of the Variscan belt in the NW of the Iberian Peninsula. In the CZ the post-Variscan geodynamic processes have been of little effect on its tectonostratigraphic whole, giving rise to a preservation level in which the actual surface is often close to the paleotopographic surface at the end of the Variscan orogeny. This fact has contributed to keep a wide spectrum of hydrothermal deposits related to late-Variscan structures, from gold-bearing skarn deposits as the deeper ones, to epithermal mercury deposits as the shallower ones, offering the possibility of an almost complete study of this fossil hydrothermal system. A number of these deposits could be regarded as carbonate-hosted epithermal Au deposits. Into them, the Providencia and Profunda mines, type-locality of villamaninite, $(Cu,Ni,Co,Fe)(S,Se)_2$, display an uncommon high Ni, Co, Se and U content, remembering some aspects of five-elements and Mississippi Valley type deposits. The aim of this paper is to synthesize the results of an study developed along the last ten years, allowing to present a new model of epithermal gold deposit related to late-Variscan deep faults.

REGIONAL GEOLOGY.

The CZ constitutes the foreland thrust and fold belt of the Variscan collisional orogen in the northwestern Spain, being located in the central part of an arc described by the structures of the orogen (Asturian or Iberoarmorican arc). Stratigraphically it is formed by a roughly complete Paleozoic succession, from Cambrian to Stephanian age, up to 8000 m thick. This sequence can be subdivided in a lower fraction, constituted by a preorogenic series of alternative siliciclastic and carbonate sediments, lower Cambrian to Devonian, and an upper synorogenic one, formed by a thick carbonate series grading up and laterally to deeper siliciclastic sediments and finally to coastal-continental sediments in paralic facies. Structurally, the CZ has a thin-skinned geometry. The deformation took place under shallow crustal conditions, without regional metamorphism. The tectonic identity of the CZ is mostly defined by the geometric distribution of the thrust fault units, but several other factors are of geologic and metallogenic interest in their structural evolution. In a general way, the thrust faulting migrated from the hinterland towards the foreland, in a forward-type sequence. This fact, combined with the arcuate evolution of the orogen in the Ibero-Armorican massif, leaves the thrust sheets to a vergency toward the core of the Asturian Arc, as a centripetal orocline, displaying curving wedge shapes similar to that of the leaves in a photographic camera iris (Pérez-Estaún and Bastida 1990, into others, see figure 1). The core (called Palentian Zone or Pisuerga-Carrion Unit), assumed to be their relative autochthonous, has in addition some outstanding facts, as a higher metamorphic gradient (up to greenschist facies), the local presence of cleavage (Rodríguez-Fernández y Heredia 1990) and the existence of a large amount of small late-Variscan granitoids (Corretgé y Suárez 1990), usually located along large faults, the same ones controlling the location of most ore deposits. These faults traverse the allochthonous units as well as the synorogenic foreland basins along three main trends: a former NE-SW, an intermediate E-W and a late NW-SE direction. The ore deposits, located showing a clear hydrothermal zoning in and around the major faults, are generally hosted by limestones of any age, also by late-Variscan igneous rocks when present. The late-Variscan faults depict the transition of the former, dominant thin-skinned tectonic, to a later thick-skinned tectonic. This tectonic was firstly developed in the basement and become the result of spatial problems generated by crustal thickening at the end of the thrust sheets centripetal emplacement. The intrusion of igneous rocks, of significant mantle connection (Gallastegui *et al.* in press), was related to transtensive and transpressive episodes of the late-Variscan thick-skinned evolution of the CZ. It is reasonable to assume the presence of a large number of metal deposits and occurrences recognized at the moment in the CZ as a consequence of the development of a large hydrothermal system on and nearby the major late-Variscan faults, favoured by the increase of thermal gradient in relation to the igneous activity.

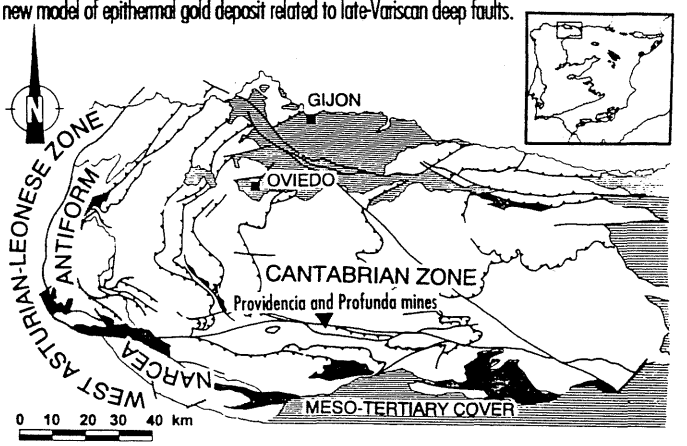

Figure 1. Geological sketch of the Cantabrian Zone showing the location of the studied area.

GEOLOGICAL SETTING, HOST ROCKS, ALTERATION AND INTERNAL ZONING.

The Providencia and Profunda mines are situated in the Bodon Unit. This unit constitutes a thrust sheet in which a sequence of materials from lower Cambrian to Namurian age are emplaced on the relative autochthonous of the Central Coal Basin, running toward the north along a thrust fault front of some 80 km from E to W. This fault front is interfered by the most important E-W late-Variscan fault of the CZ, the Leon Fault, running along about 150 km before to be hidden under the Meso-Tertiary cover. The interference between the Leon Fault and the Bodon Unit gives raise to a brittle shear zone of about 100 km from E to W, formed by a sequence of several shear duplexes, accompanied by some lateral dead faults. Respective to this shear zone, two different mineralization zones can be singled out. Into the shear duplexes a number of Cu deposits (sometimes with significant Ni-Co-U-As-Se-Au contents) are located, constituting a first, inner mineralized zone. Away of this zone, at the front of the next allochthonous units to the south, several Pb-Zn and Hg-As-Sb deposits are present, constituting the outer mineralized zone. The deposits are always located in or in contact with limestones of any age. The Providencia and Profunda mines are located at the central part of the principal duplex, the Providencia mine being the closest to the Leon fault (fig. 2). Both mines are connected toward a NE-SW high-angle fault which traverses the Bodon unit and dead to the south in a fold which also hosts the main Pb-Zn deposit of this area, called Fontun mine. The Providencia and Profunda mines are subvertical breccia pipes formed by several lenses at the intersection between E-W high-angle faults and the above mentioned NE-SW fault. The worked area in Profunda mine is 40 m wide in diameter, some 200 m deep, whereas Providencia mine was worked up to 110 m deep, both during the second half of the past century and the first third of this one. The Providencia and Profunda mines are hosted by limestones from the Barcaliente and Valdeteja Formations. Barcaliente Fm. (Ansbergian-Kinderskoutian) consists of dark grey micritic laminated limestones, very bituminous and foul, with some intraformational breccias and evaporitic levels, some 200 m thick. It hosts Providencia mine. Valdeteja Fm. (Marsdenian-Lower Moscovian) is deposited generally sharply, sometimes gradually on Barcaliente Fm., and consists of light to medium grey bioclastic, massive limestones, occasionally interbedded with carbonaceous shales, sharply disconic at the top, some 400 m thick, hosting the Profunda mine. Strong dolomitization and silicification along and around late-Variscan faults, specially at the location of ore deposits has been developed, constituting good criteria for high-scale exploration and research. In addition, high grades of Fe_2O_3 are present at the contact between ore veins and host-rocks. From wall to core, the ore is formed by: 1) an outer rim of hematitic jasperoid, grading to a colloidal assemblage of hematite plus dolomite; b) a thin sheet of barren dolomite and c) a dissemination of generally fine, rarely coarser sulfide grains in matrix of dolomite or magnesian calcite, with local presence of colorless, milky or smoky quartz, this later in U-rich samples. The ores have increasing contents in Ni, Co and Se at deeper levels. Au increases with increasing grades of Ni, Cu, As and Se in hypogenic veins of Providencia mine, but the higher concentrations are observed at the level of maximum supergenic enrichment together with U, As and Cu in Profunda mine. The PGE content is of some hundred ppb to some ppm in samples of primary ore at the Providencia mine, increasing with Ni, Cu, Au and Se contents. U in primary ores is correlated with As and Ni.

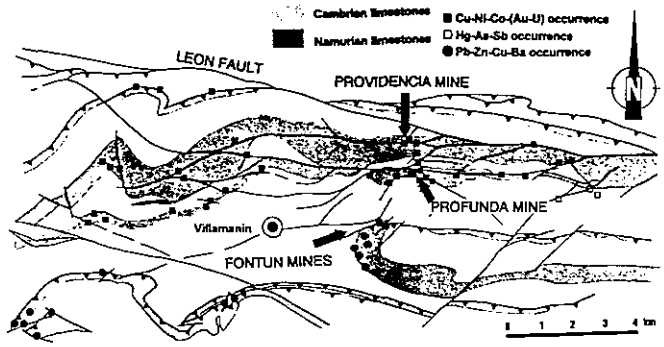

Figure 2.- Geological setting of Providencia and Profunda mines.

MINERALOGICAL EVOLUTION.

The paragenetic sequence in Providencia and Profunda mines is qualitatively similar, but quantitatively different. The mineral succession can be divided in three hypogenic stages plus a supergenic one, being the two first hypogenic stages dominant in samples from Providencia mine, the intermediate one dominant in Profunda mine, the late hypogenic one only locally present and the supergenic one richer in Profunda mine.

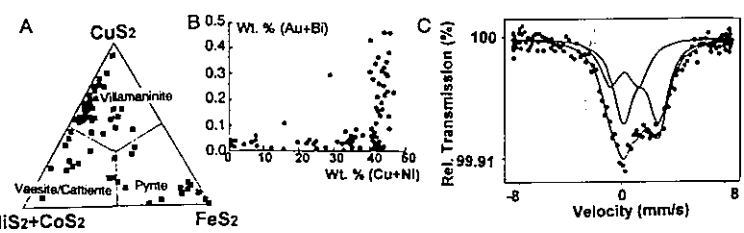

Figure 3.- Chemical characteristics of Providencia mine disulfides: A/ Plot of analysed points in the pseudoternary system CuS_2-FeS_2-(NiS_2+CoS_2). B/ Correlation Au+Bi versus Cu+Ni. C/ Mössbauer spectra of ^{197}Au in villamaninite. A and B from Paniagua 1991, C from Friedl *et al.* 1991.

The **early stage** can be subdivided in two episodes, concerning the first one the precipitation of an assemblage of colloidal silica, hematite and fine-grained pyrite, and the second one the precipitation of Cu-Ni-Co sulfides. This second episode is constituted by two main assemblages, the former one made by complex pyrite-type disulfides and the later one formed by Ni-Co-sulfarsenides and thiospinels, with local presence of uraninite, in dolomite matrix. The chemical composition of the disulfides cover the range of an almost complete FeS_2-CoS_2-NiS_2-CuS_2 solid solution (Paniagua 1989, 1991), being of far the widest known at this moment over the world. They include pyrite, vaesite, bravoite and villamaninite, this later discovered as mineral species at this locality (Schoeller & Powell 1920), and, after the results of Paniagua (1989) and Oudin *et al.* (1990), assumed to include the end-member CuS_2 (fig. 3A)by the IMA commission of new minerals and new mineral names. Villamaninite is monoclinic, pseudo cubic (Moreiras *et al.* 1991), and show a wide range of minor and trace elements, including Se (up to 8 wt%), As (up to 0.5 wt%), and Au (up to 3700 ppm). Au in villamaninite is present in a non-metallic, chemically bounded state (Friedl *et al.* 1991, fig. 3C). In addition, Co-Ni-sulfarsenides are gold-bearing.

Disulfides and sulfarsenides are sectorially and oscillatory zoned, curve-shaped, botroidal and colloform, suggesting precipitation from a diffusing-reacting system (colloidal gel). This shapes are also present in hematite, quartz (chalcedony) and dolomite of this assemblage. Furthermore, thiospinels (cuprian siegenite) and associated Co-gersdorffite have sometimes dendritic to skeletal growth, suggesting high supersaturation rate. Uraninite is growth in alternation with gersdorffite, being Th-poor (Th < 0.05 at. %) and carrying up to 3 wt. % REE.

The **intermediate stage** is formed by a first low-temperature Cu-Fe-S solid-solution (mostly decomposed to a chalcopyrite-bornite intergrowth) followed by an assemblage of chalcopyrite and talnakhite as major ore minerals. In addition, sphalerite, bravoite, pyrite, tetrahedrite-tennantite (Sb:As $\cong$ 1:2), native gold and a number of selenides, including clausthalite, tiemannite, krutaite, klockmannite, athabascaite, berzelianite, umangite, tyrellite and selenobismutite-guanajuatite are present. Chalcopyrite and talnakhite content Ni, Co and Se as minor elements (sometimes wt. % Ni+Co > 1 in talnakhite), but the Se content in chalcopyrite decrease dramatically when selenides are present in the sample. Sphalerite is also Se-rich (up to 1 wt. % Se), Cd-rich (m. a. 0,7 wt% Cd) and Fe-poor (m. a. 0,1 wt% Fe). Native gold is very pure (up to 4 at. % Ag) and sometimes PGE-bearing (up to 1 at. % Pt + Pd), whereas silver is strongly fractionated as minor element to the sulfides. The selenides are S-rich, except for clausthalite and tiemannite (S < 0,15 at. % in both), showing strong fractionation of Se to heavy metal chalcogenides. This stage is dominant in Profunda mine.

Later, but previous to the supergenic stage, an assemblage of idiomorphic chalcocite in gangue of fine-grained quartz-calcite has been locally observed, sometimes associated to pyrite and S-rich bornite. It constitutes the **late stage** of the hypogenic succession.

The **supergenic stage** is formed by Fe-Co-Ni-Cu oxides and hydroxides, carbonates and arsenates of Cu-Ni-Co-UO_2 (tirolite, annabergite, erythrite and zeunerite as the most common ones), supergenic sulfides (bornite, covellite, chalcocite, digenite, pyrite) and electrum (restricted to a thin level at the bottom of the supergenic zone in Profunda mine). Anomalous contents of REE ($\leq$ 0.30 wt. % La, 0.25 wt. % Nd) is detected in U-rich samples.

PTX-DETERMINATION AND SULFUR ISOTOPIC DATA.

Although fluid inclusion analysis is difficult because the small size of inclusions, and only a limited number (90 inclusions on 9 samples) has been measured, the presence of a complex paragenesis make possible a multimethod approach to the P-T-X conditions. The results are synthesized in figure 4. Equilibria for curves Vi and Bv were calculated by the method of Craig & Barton (1973), obtained by sulfidation of stoichiometric amounts of Cu, Fe monosulfides and Ni, Co thiospinels. Upper stability limits for estimated disulfide equilibria from DTG analyses. ΔH for CuS_2 calculated from crystalchemical data for pyrite-type disulfides, ΔS for CuS_2 was estimated by the sulfide sum method.

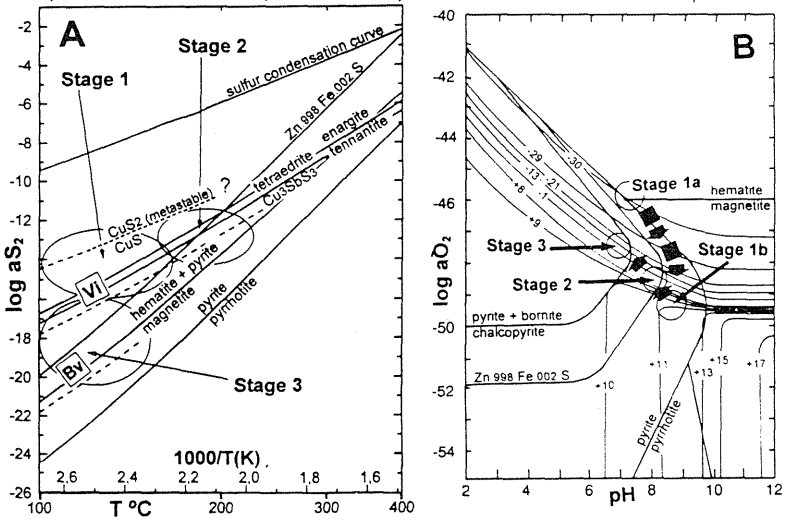

Figure 4.- A/ log fS_2-T diagram showing sulfidation reactions for this study. Dashed lines represent equilibria for natural disulfides from these localities. Vi=villamaninite $Cu_5Ni_3Co_1Fe_1S_2$. Bv=bravoite $Cu_1Ni_3Co_1Fe_5S_2$. **B/** log fO_2-pH diagram at T=150 ºC, I=3 and ΣS=0,01 showing the Fe-O-S boundaries and $\delta^{34}S$ contours for H_2S equiv. (Ohmoto1972). $\delta^{34}S$ values from this work (H_2S at $\delta^{34}S_{\Sigma S}$=+9 ‰).

Stage 1. Primary fluid inclusions from early quartz and dolomite associated with hematite have T_h ranging from 100 ºC to 140 ºC (m. a. 120 ºC) and salinities higher than 20 wt. % NaCl equiv. TG-DTG data on samples from Providencia mine show that Cu-rich villamaninite and Cu-bravoite are not stable above 220 ºC and 144 ºC respectively. Synthetic bravoite has an upper stability limit of 137 $\pm$ 6 ºC (Clark & Kullerud 1963, Craig 1973), and members of the CuS_2-FeS_2 binary system have been synthesized only below 250 ºC reaching a maximum content of 82 wt. % CuS_2 at 100 ºC, in each case at pH $\cong$ 8-9. The assumption of an upper temperature of 140 ºC yields a pressure of about 200 bars for this stage, giving a maximum deep of 2 km under hydrostatic conditions. The minimum deep, deduced from difference between the topographic level of the upper adit (1485 m altitude) and the tops of the closest mountains (some 2200 m altitude) is of roughly 700 m. Sulfur isotope analyses on disulfides of this stage give $\delta^{34}S$ values of 11.5-14.6 ‰ (9.3-12.4 ‰ H_2S equiv.).

Stage 2. Primary fluid inclusions from late quartz associated to chalcopyrite + sphalerite and secondary fluid inclusions from early quartz have Th from 135 to 204 ºC (m. a. 158 ºC) and a mean salinity of roughly 18 wt. % NaCl equiv. Talnakhite in samples from deep levels of Providencia mine shows inversion twinning, whereas at shallower levels it is untwinned. Inversion to talnakhite from its intermediate solid-solution is achieved at 186 ºC (Barton & Skinner 1979), suggesting for this stage thermal variations around this temperature. Fractionation of Se between coexisting Se-bearing chalcopyrite and sphalerite yields T $\cong$ 148 ºC, and between sphalerite and clausthalite (the Se-bearing equivalent of galena) gives T $\cong$ 156 ºC (according to Bethke & Barton 1971). Inversion twinning in berzelianite indicates T > 138 ºC (Barton & Skinner 1979). Equilibrium between coexisting tetrahedrite-tennantite and sphalerite (0.2 % FeS in ZnS) gives a temperature range of 183-200 ºC. Assuming a mean temperature of 175 ºC, Pressure correction versus a mean T_h of 158 ºC yields $\cong$ 150 bars, indicating a maximum deep of about 1.5 km under hydrostatic conditions. Sulfur isotope analyses on pyrite and sphalerite of this stage give $\delta^{34}S$ values of 6.8 to -2.1 ‰ (5.0 to -2.6 ‰ H_2S equiv.).

Stage 3. Secondary fluid inclusions on late quartz yield Th of 98-105 ºC and salinity of ≅ 9 wt. % NaCl equiv. Inversion twinning in idiomorphic chalcocite indicates T > 103.5 ºC, while associated, unaltered S-bornite suggests T < 125 ºC (Barton & Skinner 1979), indicating very shallow conditions. Sulfur isotope analysis on chalcocite gives $\delta^{34}S$ = -20.6 ‰ (-16.4 ‰ H_2S equiv.).

AGE DATING: U-TH-PB RELATION AND PB-PB ISOTOPIC DATA.

In order to evaluate the age of the deposits, single uraninite grains on samples from Profunda mine were analyzed by EPMA. According to Bowles (1990), the resulting age is 273 ± 11 million years. This data agrees with previous works related to the age of Variscan granitoids of the area. Suárez *et al.* (1978) report a Rb-Sr age of 284 ± 8 and 287 ± 8 m. y. for two Variscan granitoids located to the NW of the studied area and related to E-W and NE-SW late-Variscan faults. Gallastegui *et al.* (in press) report also a Rb-Sr age of 277 ± 1 m. y. for the most significant granodioritic stock of the CZ. The U-Pb age obtained in Profunda mine is also supported by Pb-Pb dating on samples of Providencia mine, yielding a mean age of 270 ± 12 m. y.

CONCLUSIONS.

The above mentioned data show that these mineralizations are formed by the deposition of a metal stock intermediate in character between a typical five-element one plus a typical gold-bearing epithermal one. This deposition took place as result of the interaction in epithermal P-T conditions between slightly acidic fluids and S-rich, bituminous carbonate rocks. At the contact with host rocks, fluids are strongly reduced and alkalinized, leaving to the precipitation of hematite and later Cu-Co-Ni disulfides, with chemically bounded Au. From this point the fluid evolved to more neutral and oxidant conditions. An increase of T at roughly constant αS_2 from stage 1 to stage 2 results in the partial destabilisation of early Cu-rich disulfides, leaving to the presence of native Au and selenides as result of the liberation of minor elements from the disulfide solid solution. A third stage is locally developed in conditions of lower P-T, pH and αS_2, higher αO_2. This three-stages evolution model agrees with the sequence of tectonic activity of the three late-Variscan fault systems recorded in the area. The high fluid salinity agrees with previous data in other Cu-Ni-Co deposits of the Cantabrian Zone (Paniagua *et al.* 1988), and show resemblances with MVTD (Roedder 1980, among others) and related breccia pipe uranium deposits (Wenrich 1985). Although the age of the ore deposition is very close to late-Variscan intrusion timing, $\delta^{34}S$ values are very high for a magmatic source, but congruent with a model of fluid-rock interaction in which organic-reduced sulfur from an evaporitic source could have been dominant.

REFERENCES.

Barton , P. B. Jr. & Skinner, B. J. 1979. Sulfide mineral stabilities. In: Barnes, H. L. (Ed) Geochemistry of hydrothermal ore deposits. 2nd ed. John Wiley & Sons, New York. pp 278-403.

Bethke, P. M. & Barton, P. B. 1971. Distribution of some minor elements between coexisting sulfide minerals. Econ. Geology, 66, pp 140-163.

Bowles, J. F. W. 1990. Age dating of individual grains of uraninite in rocks from electron microprobe analyses. Chemical Geology, 83, pp 47-53.

Clark, L. A. & Kullerud, G. 1963. The sulfur-rich portion of the Fe-Ni-S system. Econ. Geology, 58, pp 853-885.

Corretgé, L. G. & Suárez, O. 1990. Cantabrian and Palentian Zones: Igneous rocks. In: Dallmeyer, R. D., Martínez-García, E. (eds.) Pre-Mesozoic Geology of Iberia. Springer Berlin Heidelberg New York, pp 72-79.

Craig, J. R. 1973. Pyrite-pentlandite and other low temperature relations in the Fe-Ni-S system. Am. J. Sci. 273A, pp 496-510.

Craig, J. R. & Barton, P. B. Jr. 1973. Thermochemical approximations for sulfosalts. Econ. Geology, 68, pp 493-506.

Friedl, J., Paniagua, A. & Wagner, F. E. 1991. Mössbauer study of gold-bearing villamaninite. Neues Jahrb. Miner. Abh., 163 (2/3), pp 247-254.

Gallastegui, G., Heredia, N., Lasala, M. J., Reyes, J. & Rodríguez-Fernández, L. R. (in press). Rb-Sr dating of late-Variscan calc-alkaline magmatism in the Cantabrian Zone: the Peña Prieta stock, northern Spain. Rev. Soc. Geol. España, 7, pp 000-000.

Moreiras, D. B., Marcos, C., Paniagua, A., Díaz-Fernández, M. R. & García-Granda, S. 1991. Preliminary data about symmetry and structure of villamaninite. Neues Jahrb. Miner. Abh., 163 (2/3), pp 254-256.

Ohmoto, H. 1972. Systematics of sulfur and carbon isotopes in hydrothermal ore deposits. Econ. Geology, 67, pp 551-578.

Oudin, E., Marchig, V., Rösch, H., Lalou, C. & Brichet, E. 1990. Observation de CuS_2 à l'état naturel dans une cheminée hydrothermale du Pacifique Sud. C. R. Acad. Sci. Paris, 310-II, pp 221-226.

Paniagua, A. 1989. The pyrite-type Cu-rich disulfides in the Providencia mine, Leon, NW Spain. Neues Jahrb. Miner. Abh., 160 (1), pp 8-11.

Paniagua, A. 1991. Trace elements in villamaninite and other pyrite-type disulfides of the Providencia mine, Leon, NW Spain. Neues Jahrb. Miner. Abh., 163 (2/3), pp 241-247.

Paniagua, A., Loredo, J. & García-Iglesias, J. 1988. Epithermal Cu-Co-Ni mineralization in the Aramo mine (Cantabrian mountains, Spain): correlation between paragenetic and fluid inclusion data. Bull. Mineral. 111, pp 383-391.

Pérez-Estaún, A. & Bastida, F. 1990. Cantabrian and Palentian Zones: Structure of the CZ. In: Dallmeyer, R. D., Martínez-García, E. (eds.) Pre-Mesozoic Geology of Iberia. Springer Berlin Heidelberg New York, pp 55-69.

Rodríguez-Fernández, L. R. & Heredia, N. 1990. Cantabrian and Palentian Zones: Structure of the Palentian Zone. In: Dallmeyer, R. D., Martínez-García, E. (eds.) Pre-Mesozoic Geology of Iberia. Springer Berlin Heidelberg New York, pp 69-71.

Roedder, E. 1984. Fluid inclusions. Rev. Mineral., vol. 12, 644 pp.

Schoeller, W. R. & Powell, A. R. 1920. Villamaninite, a new mineral. Mineral. Mag., 19, pp 14-18.

Stacey, J. S. & Kramers, J. D. 1975. Approximation of terrestrial lead isotope evolution by a two-stage model. Earth Plan. Sci. Lett., 26, pp 207-221.

Suárez, O., Ruiz, F., Galán, J. & Vargas, I. 1978. Edades Rb-Sr de granitoides del Occidente de Asturias. Trab. Geol. Univ. Oviedo, 10, pp 437-442.

Vaughan, D. J. & Craig, J. R. 1978. Mineral chemistry of metal sulfides. Cambridge University Press, 493 pp.

Wenrich, K. J. 1985. Mineralization of breccia pipes in northern Arizona. Econ. Geology, 80, pp 1722-1735.

This paper was partly supported by two grants of research of the spanish Junta de Castilla-Leon and Ministerio de Educacion y Ciencia and a research assistance of the Oviedo University in the person of one of the authors (A. P.). It was also benefited of a Spanish-German Integrate Action of Research.

Current Research in Geology Applied to Ore Deposits.Fenoll Hach-Alí, Torres-Ruiz & Gervilla(eds)(1993).ISBN 84-338-1772-8

RIFT-RELATED MARINE BLACK SHALES, AN IMPORTANT SOURCE OF PGE

Pašava, J.
Czech Geological Survey, Malostranské nám. 19, 118 21 Praha 1, Czech Republic

Economically important *PGE accumulations are hosted in rift-related metal-rich black shales (without any tectonomagmatic activity) of different geological ages (Canada, China, Poland), while the metalliferous black shales in rift-volcanic-related settings (Czech Republic, Finland) are characterized by generally lower PGE values. While there are similarities, the differences are more numerous when comparing PGE-metal-rich black shales in both environments.

INTRODUCTION

Most unconventional PGE anomalies in metal-rich black shales, recently reported from various parts of the world, basically occur in two types of environments:

1. Intracontinental rifts and alucacogens in the continental crust without any intrusive rocks, as in the case of the Polish, Chinese and Canadian PGE-metal-rich black shales (for the remained of this text, this shall be noted as rift-related).
2. Intracontinental rifts associated with basic volcanism in the oceanic crust as in case of the Czech and Finnish PGE-metal-rich facies (for the remainder of this text, this shall be noted as rift-volcanic-related).

RIFT-RELATED OCCURRENCES

PGE in Copper Shales of the Kupferschiefer Type from Poland

The highest PGE concentrations within anoxic sediments, have been reported from the Polish Kupferschiefer by Kucha (1982). Kupferschiefer was deposited in a shallow, mud-dominated, stratified shelf sea, and its mineralization is related to the high post-Variscan heat flux and thermal events connected with intracontinental Permian rifting (Oszczepalski, 1989). Neither volcanic nor magmatic activities have been recognized within this period. Kucha (1982) reported the concentrations of up to 3000 ppm Au, 10 - 370 ppm Pt and 10 - 120 ppm (locally up to 1000 ppm) Pd. These anomalous concentrations were reported from a very thin (from a few mm up to 10 cm thick) layer at the bottom of the marine black shale when this shale is overlain by phosphates, borates, and thucholite-bearing shale. However, such extreme PGE values have not been confirmed either in the Polish (Jowett, pers. comm.) or the German Kupferschiefer (Tarkian, Stribrny, pers. comm.).

Kucha (1982) noted that PGE are associated with gold, As-sulfides and As-sulfoarsenides and has proposed that percolating basement brines were a source of platinoids and other metals that were concentrated at the border between oxic and anoxic environments (kerogen-calcite; thucholite-calcite black shale - white sandstone; etc.).

---

*The abreviation PGE used throughout the text denotes platinum group elements.

Relatively low reflectances of autochtonous organic matter, as well as sulfide mineral association and stable isotopes, indicate paleotemperatures of Na-Ca-Cl brines not higher than 90 - 120°C - most likely <105°C (Oszczepalski, 1989).

PGE in Metal-Rich Black Shales from China

The Early Cambrian marine black shales of south China host Ni-Mo deposits that outcrop discontinuously in an belt approximately 1600 km long (Coveney and Chen, 1991, Coveney et al., 1992). The evolution of numerous local sedimentary basins, developed within the shallow shelf, and the introduction of warm metal-bearing fluids during deposition or diagenesis, along with the important concentration role of abundant organics, could have been the major mechanisms of the formation of the deposits (Murowchick et al., 1992). Post-depositional hydrothermal activity is indicated in quartz-barite veins by low to moderate tempearture (109 - 143°C) fluid inclusions with salinity from 12% to 14% (Coveney et al., 1992). But here has been no volcanic activity associated with these deposits.

Ore occurs as thin (from few cm up to 35 cm) sulfide lenses and beds in nearly flat-laying black shales of the Lower Cambrian Niutitang Formation, a few meters above its contact with the Proterozoic (Sinian) Doushantuo Formation.

The Zunii Mo deposits are located near Songlin in the Guizhou Province, and represent the only anoxic sediments worldwide from which molybdenum is recovered. Fan (1983) says that he ore-bearing horizon varies from 5-15 cm and besides the economic concentrations of Mo (2-4 wt.%), contains also up to 4 wt% Ni, 2 wt.% Zn, 50 ppm Ag, 0.7 ppm Au, and anomalous concentrations of Pt (80 - 300 ppb), Pd (110 - 380 ppb), Ir (11 - 20 ppb), Os (50 - 150 ppb) and Ru (up to 4 ppb), Fan (1983). New analytical results revealed an average Pt - 295 ppb, Pd - 184 ppb, Rh - 25 ppb, Ru - 23 ppb, Ir - 1.7 ppb, Os - 118 ppb and Au - 334 ppb, with Pd/Pt rations varying from 0.85 to 1.3 (avg. 1.19), (Coveney et al. 1992).

It should be stressed, that the possible existence of the analogous ore type in the U.S.A. has been discussed by Coveney and Chen (1991).

PGE in Metal-Rich Black Shales from Canada

Abnormal PGE accumulations (Pt 149 - 618 ppb, Pd 91 - 319 ppb, Os <15 -60 ppb, Ir 0.8 - 3 ppb, Rh 5 - 14 ppb and Re 9.6 - 61 ppm) have been recently reported by Hulbert et al. (1992) from the Ni-Zn stratiform mineralization (Nick deposit). It is hosted by the Middle to Upper Devonian marine black shales in the Selwyn Basin, Yukon, Canada, which is an example of an epicratonic marine basin formed due to rifting of the continental margin of North America, during the early Paleozoic. No intrusive rocks are present in the mineralized area, which is greater than 80 km^2.

A thin (2-7 cm) ore bed lies at the base of the Phosphatic Chert Member, and contains 2.3 - 7.8 wt.% Ni, 0.14 - 1.3 wt.% Zn, 0.141 - 0.392 wt.% Mo, 0.19 - 0.42 wt.% As, 0.19 - 0.49 wt.% Ba, 0.06 - 0.24 wt.% Se, 0.017 - 0.041 wt.% Cu, with the C_{org} content varying between 1.3 - 2.5 wt.%. Pd/Pt ratios range from 0.47 to 0.61 (avg. 0.52). Besides pyrite and vaesite, a Ni-Fe-As sulfide (probably gersdorffite), a Cu-Sb sulfide (probably tetrahedrite), a U-phase (probably uraninite) as well as a Mo-sulfide (probably jordisite) have been reported by Grauch et al. (1991).

Discharge of dense organic-rich, metalliferous, hydrothermal fluids from extensive fissures through unconsolidated bottom sediments was proposed to explain the wide lateral distribution of mineralization. The sources of the metals were underlying organic-rich Silurian and Devonian strata. Hulbert et al. (1992) inferred a sulfide crystallization

temperature of about 138°C.

RIFT-VOLCANIC-RELATED OCCURRENCES

PGE in Metal-Rich Black Shales from the Czech Republic

Anomalous PGE contents have been reported in marine black shales of the Barrandian Upper Proterozoic from the Czech Republic (Pašava, 1991). They have been deposited in a number of (semi)isolated basins, accompanied by contemporaneous submarine basic volcanism, related to the evolution of the Proterozoic rift. Submarine volcanogenic - hydrothermal processes are presumed to be the principal sources of metals which have been accumulated by the abundant organics in the vicinity of volcanic centres (Pašava, 1991).

The metal-rich black shales from the Kamenec locality (avg. C_{org} - 2.3 wt.%) are characterized by concentrations of Zn up to 0.12 wt.%, Ni up to 0.06 wt.%, Cu up to 0.0398 wt.%, Mo up to 0.0127 wt.%, Cr up to 0.067 wt.%. Pd values are up to 42 ppb, Pt 12 ppb and Rh 1.7 ppb (Pašava, 1991).

Metalliferous facies from the Hromnice locality, are also significantly enriched in Zn (up to 0.41 wt.%), Ni (up to 0.12 wt.%), Cu (up to 0.104 wt.%), Mo (up to 0.02 wt.%), Au (up to 132 ppb), and contain up to 102 ppb Pd and 25 ppb Pt. Both the occurrences are found in close association with products of submarine volcanic activity. Tuffs and metabasalts alternate with finely laminated metal-rich black shales. Pyrite (framboidal and grainy), millerite, pentlandite, chalcopyrite, sphalerite, galena, molybdenite, native gold, and two new molybdenum minerals - telluride and selenide have been identified. Pd/Pt ratios vary from 2.76 to 12.77 (avg. 4.73).

The fluid inclusions in quartz and calcite from Kamenec can be a result of diagenetic processes or of later hydrothermal events, characterized by a temperature interval between 120 and 230°C. The H_2O-CO_2 inclusions from Hromnice resulted from the heterogenous trappings of immiscible CO_2-rich and H_2O-rich fluids during metamorphism (T about 300°C, P not exceeding 220 MPa).

PGE in Metal-Rich Black Shales from Finland

New PGE data from the Finnish Precambrian metal-rich black shales have been published by Loukola-Ruskeeniemi (1991). Metamorphosed marine Proterozoic (2.1 - 1.96 Ga) black shale formations from the rift structure of the Kainuu schist belt are 120 -150 m thick with the average C_{org} (7 wt.%) and S (6 - 8 wt.%). The average Pt and Pd values 10 ppb and 20 ppb, respectively, have been found in the low-mineralized (Ni+Cu+Zn < 0.8 wt.%) Talivaara black shales and are the same as those of the black shales from the Jormua ophiolite complex (Loukola-Ruskeeniemi in prep.). The average Pd/Pt ratio in the Talvivaara low-mineralized black shales is 1.4 and there are no available PGE data from high-mineralized black shale facies at Talvivaara Cu-Ni-Zn deposit. The following average PGE concentrations have been reported, based on 265 black shale sample set, from the Outokumpu area: 10 ppb of Pt, 19 ppb Pd, with the average Pd/Pt ratio 1.4 (Loukola-Ruskeeniemi in prep.). The highest values of Pt (70 ppb) and Pd (69 ppb) in Finnish metal-rich black shales have been reported from the Aalen and Jormua localities, respectively and Loukola-Ruskeeniemi (1991) suggested that hydrothermal processes associated with volcanic activity were mostly responsible for the metal enrichment.

DISCUSSION

The studied PGE-anomalous marine black shales have only a few features in common. They were deposited in marine environments of

intracontinental rifts and aulacogens of the different geologic ages (from Precambrian to Permo-Triassic), with organics participating in the precipitation and entrapment of metals. They also share the low-grade metamorphism as well as a close mineral association. The mineralization fluids range from low to medium-temperatures.

However, there are several important differences in the extent of mineralized horizons, geochemistry of trace elements, distribution of PGE, mineralogical assemblage, and the geochemistry and temperature of ore-bearing fluids, comparing both rift and rift-volcanic related occurrences.

The rift-related mineralized horizons are usually very thin (ranging from a few mm to 35 cm), and are closely associated with P-rich layers and carbonates or REE-phosphates with uranium (mostly overlying). Sometimes they can have a larger lateral extent, as reported by Hulbert et al. (1992) from the Selwyn Basin. Conversely, ore-layers from the rift-volcanic-related black shales have a greater vertical extent (X-XO m), developed only around basic volcanic centres and controlled by the alternating of metalliferous black shales with metatuffs.

The differences are also apparent in geochemistry. Generally, the rift-volcanic-related black shales are lower in almost all minor elements except Cu and Cr. The average Ni/Cu ratio (1.2) is practically the same as these values of the classical PGE deposits linked with mafic and ultramafic rocks (Sudbury - 1.18, Platreef - 1.5, Merensky Reef - 1.6; data from Hulbert et al., 1988) and differs from that of the rift-related PGE-rich black shales in China (34.4) and Canada (173.6). Cr values are higher in rift-volcanic black shale facies. The highest average Ni contents in rift-related metalliferous black shales (5.5 wt.% and 3.4 wt.% in Chinese and Canadian samples, respectively), are in excess of those known from the famous Sudbury (Canada), Great Dyke (Zimbabwe), Bushveld (South Africa) and Stillwater (U.S.A.) PGE-bearing igneous complexes, and are only comparable with nickel concentrations (1.5 - 3.6 wt.%) at Norilsk-Talnakh deposits (the former USSR). The high Ni-contents in the rift-related black shales show the two important Ni-metallogenetical events, the Lower Cambrian in South China and the Middle to Upper Devonian in Selwyn Basin, Canada. Moreover, the rift-related PGE-metal-rich black shales are also extremely rich in Mo. The Chinese deposits contain the highest average Mo content 3.9 wt.%, which is more than 10x higher than that of classical and relatively rich Climax-type Mo-deposits (0.2 - 0.3 wt.% Mo).

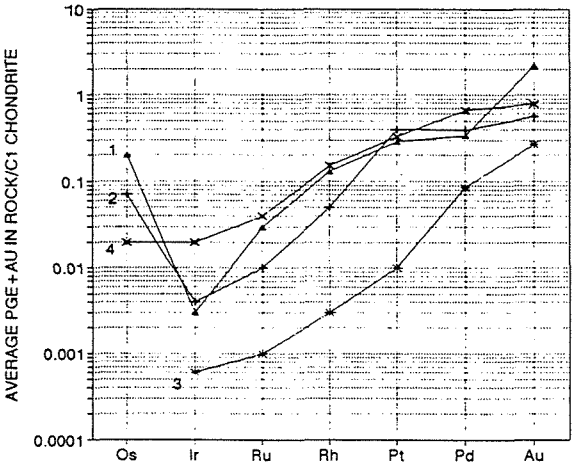

Fig. 1. Average chondrite-normalized PGE and Au data for rift- and rift-volcanic-related metal-rich black shales. 1 - Rift-related Cambrian black shales, south China (data from Coveney et al., 1992); 2 - Rift-related Devonian black shales, Selwyn basin, Yukon, Canada (data from Hulbert et al., 1992); 3 - Rift-volcanic-related Proterozoic black shales, Bohemian Massif, Czech Republic (data from Pašava, 1991); 4 - Typical PGE ore from Sudbury, Ontario, Canada (data from Hulbert et al., 1988).

The both types of world PGE - anomalous black shales also differ in distribution of the platinoids (Fig. 1). Economically important PGE accumulations are typical for rift-related occurrences, while the rift-volcanic-related localities show only anomalous PGE values. The average Pd/Pt ratios differ even within the rift-related ores (Chinese, 1.19; Canadian, 0.57) and are close to those of the Platreef deposit in Bushveld complex (1.1) and Sudbury ores, Canada (0.69), respectively (data from Hulbert et al., 1988). The Proterozoic rift-volcanic-related metal-rich black shales from the Czech Republic and Finland have the average Pd/Pt ratio 4.73 and 1.4, respectively, thus showing Pd enrichment. The similarly high average value of this ratio (5.0) was reported from low-temperature (160-300°C) PGE mineralizations in Precambrian metasediments at Messina, South Africa and from the Cu-Pd-Au-Ag mineralization hosted by Mississippian limestone at the Boss mine in Nevada (Lecher and Hsu, 1989). Pd/Pt ratios generally vary in hydrothermal PGE deposits due to the greater solubility and mobility of Pd in hydrothermal solutions (Cousins and Vermaak, 1976).

PGE and Au normalized data of rift-volcanic-related metal-rich black shales from the Czech Republic show, despite a significant difference in absolute concentrations, similar patterns as those of PGE ores hosted by mafic and ultramafic rocks from Sudbury. Relatively low Os and Ir values and high Pt, Pd and Au concentrations are typical for such, almost linear PGE patterns (Fig. 1). The rift-related Chinese and Canadian metal-rich black shales are on the other hand, characterized by a slightly different PGE + Au pattern shape, caused by strong Os enrichment and relative depletion of Ir and Rh (Fig. 1).

The major ore mineral assemblage in both rift and rift-volcanic-related occurrences is generally close (framboidal and disseminated pyrite, Ni, Zn, Mo, and Cu sulfides), only with a different proportion of individual minerals (Fe-Ni-Mo sulfides prevail in rift-related metal-rich black shales with the exception of the Polish Kupferschiefer where Cu-Pb-Zn sulfides are dominant, while Fe-Zn-Cu sulfides predominate in rift-volcanic-related facies). All of these associations have already been described from various hydrothermal PGE mineralizations.

The available temperature data based on fluid inclusions and mineral paragenesis point to low-temperature mineralization processes, with the temperatures ranging from 90 to 143°C and from 120 to 300°C in rift-related and rift-volcanic-related metal-rich black shales, respectively.

It seems relevant in case of rift-related PGE metal-rich black shales that thermal anomalies caused by a burial of sediments in connection with the formation of rifts, initiated movements of basinal brines, with subsequent leaching and precipitation of metals by the important reduction role of organics (Jowett, 1986, recently supported by the experimental studies by Gammons et al., 1992) and possibly also phosphates (Kucha, 1982). However, direct input of metals into the basins, through hydrothermal fluids along the faults, cannot also be ruled out (Hulbert et al., 1992, Murowchick et al., 1992). An extraterrestrial source for PGE in Chinese rift-related black shales, suggested by Fan et al. (1984) based on high Ir values, does not seem probable, because chondrite-normalized values for Ir are much less enriched that those for other PGE (Coveney et al., 1992).

The anomalous PGE concentrations, developed around volcanic centres in rift-volcanic-related Proterozoic metalliferous black shales, were most likely controlled by the geochemistry of hydrothermal-volcanogenic exhalations, again under the important participation of organic matter as proposed by Pasava (1991) and Loukola-Ruskeeniemi (1991).

OPEN QUESTIONS

Despite anomalous PGE accumulations, no discrete PGE or any other type of PGE-carriers have been identified within metal-rich black shales. The only exception is the Polish Kupferschiefer in which PGE are associated with gold, As-sulfides and As-sulfoarsenides (Kucha, 1982). This question is of key importance, considering that this new PGE ore type could be utilized in the future.

New statistical evaluations of the available geochemical data covering rift-related PGE-metal-rich black shales (Pasava, submitted) has revealed a significant relationship of Pd and Pt with Ni, Bi, Se, Y, Sb, Cu, Co, Au, U and F, pointing to a complex PGE association. The rift-volcanic-related metalliferous black shales from the Czech Republic have shown, besides very important links between Pd and Ni, similarly significant relationship of Pd with Au and between Pd/Zn and Pd/V.

It is very likely that organic matter played an important role in the origin of PGE accumulations in metal-rich black shales (Pasava, submitted). However, more mineralogical, organic geochemical, and isotopic investigations are necessary to clarify the role of organics. In particular, it is uncertain whether organics concentrated platinoids during deposition, so that they were mobilized into thin ore layers during late diagenesis or by metamorphic brines, or if black shales acted only as a geochemical reduction barrier, for epigenetic metal-rich hydrothermal fluids.

CONCLUSIONS

Rift-related metal-rich black shales bear economically important PGE concentrations (up to 818 ppb Pt and 1255 ppb Pd, with the average Pd/Pt = 0.71), mostly accompanied by giant Mo (up to 18.28 wt.%) and Ni (up to 7.8 wt.%) values but are low in Cu (Ni/Cu ranges from 34.4 to 173.6) and Cr (avg. 0.0016 wt%). Ore horizons are characterized by an extremely restricted vertical extent (few mm - 35 cm) in the strata. Complex PGE associations are indicated by significant relationships of Pd and Pt with Ni, Bi, Se, Y, Sb, Cu, Co, Au, U and F. Their chondrite normalized PGE+Au patterns show relatively a strong enrichment in Os and depletions of Ir and Ru.

Rift-volcanic-related metal-rich black shales carry the anomalous PGE accumulations (up to 60 ppb Pt and 102.2 ppb Pd, with the average Pd/Pt = 3.0), showing Pd enrichment and are mostly accompanied by higher Cr values (avg. 0.066 wt.%). Mineralized horizons have a much greater vertical extent (X-XO m). Pd shows strong correlations with Ni, Zn, Au and V while Pt exhibits highly significant links with Cu and Mo phases. Typically a low average Ni/Cu ratio (1.25) and the shape of the PGE and Au normalized pattern, are similar to that of hydrothermal PGE deposits in mafic and ultramafic rocks. The PGE concentrations, developed mostly around volcanic centres are probably controlled by volcanogenic-hydrothermal events.

As shown, metal-rich black shales in both types of environment represent an important host environment for PGE, sharing characteristics with both hydrothermal and magmatic PGE deposits.

REFERENCES

Cousins, C.A. & Vermaak, C.F. 1976. The Contribution of Southern African Ore Deposits to the Geochemistry of the Platinum-Group Metals. Econ. Geol. 71:287-305.

Coveney, R.M.Jr. & Chen, N. 1991. Ni-Mo-PGE-Au-rich ores in Chinese black shales and speculations on possible analogues in the United States. Mineral. Depos. 26:83-88.

Coveney, R.M.Jr., Murowchick, J.B., Grauch, R.I., Glascock, M.D. & Denison, J.R., 1992. Gold and platinum in shales with evidence against extraterrestrial sources of metals. Chem. Geol. 99:101-114.

Fan, D. 1983. Polyelements in the Lower Cambrian black shale series in southern China. In: S.S. Augustithis (ed.) The significance of trace metals in solving petrogenetic problems and controversies. Theophrastus Publications S.A., Athens, pp 447-474.

Fan, D., Yang, R. & Huang, Z. 1984. The Lower Cambrian black shales series and iridium anomaly in south China. In: Academia Sinica, Developments in Geoscience, Contributions to the 27th IGC (Moscow), Beijing, pp 215-224.

Gammons, C.H., Bloom, M.S. & Yu, Y. 1992. Experimental investigation of the hydrothermal geochemistry of platinum and palladium sulfide minerals in NaCl/H2SO4 solutions at 300°C. Geochim. Cosmochim. Acta, 56:3881-3894.

Grauch, R.I., Murowchick, J.B., Coveney, R.M.Jr.& Chen, N. 1991. Extreme concentration of Mo, Ni, PGE and Au in anoxic marine basins, China and Canada. In: M. Pagel, J.L. Leroy (eds.) Source, Transport and Deposition of Metals, A.A.Balkema, Rotterdam, pp 531-534.

Hulbert, L.J., Duke, M., Eckstrand, O.R., Lydon, J.W. & Scoates, R.F. 1988. Geological environments of platinum group elements. Geol. Surv. Can. Open File Report 1440, pp 1-148.

Hulbert, L.J., Gregoire, C.D. & Paktunc, D. 1992. Sedimentary nickel, zinc, and platinum-group-element mineralization in Devonian black shales at the Nick property, Yukon, Canada: A new deposit type. Explor. Min. Geol. 1:39-62.

Jowett, E.C. 1986. Genesis of Kupferschiefer Cu-Ag deposits by convective flow of Rotliegendes brines during Triassic rifting. Econ. Geol. 81:1823-1837.

Kucha, H. 1982. Platinum-group metals in the Zechstein copper deposits, Poland. Econ. Geol. 77:1587-1591.

Lechler, P.J. & Hsu, L.C. 1989. Review of hydrothermal platinum-group deposits with new data from Nevada. In: Proceedings, 1989 SME Meeting, Littleton, Nevada, preprint 89-55:7, pp 1-7.

Loukola-Ruskeeniemi, K. 1991. Geochemical evidence for the hydrothermal origin of sulphur, base metals and gold in Proterozoic metamorphosed black shales, Kainuu and Outokumpu areas, Finland. Miner. Depos. 26:143-152.

Loukola-Ruskeeniemi, K.. Geochemistry of metamorphosed black shales associated with early Proterozoic rift basins in the Kainuu and Outokumpu areas, Finland. Geol. Surv., Finl. Bull. (in prep.).

Oszczepalski, S. 1989. Kupferschiefer in southwestern Poland: Sedimentary environments, metal zoning, and ore controls. In: R.W. Boyle, A.C. Brown, G.F. Jefferson, E.C. Jowett, R.V. Kirkham (eds.) Sediment-hosted stratiform copper deposits. Geol. Ass. Can., Spec. Paper 36, pp 571-600.

Pašava, J. 1991. Comparison between the distribution of PGE in black shales from the Bohemian Massif (CSFR) and other black shale occurrences. Mineral. Depos. 26:99-103.

Pašava, J.. Anoxic sediments, an important environment for PGE; an overview. Ore Geology Review (submitted).

Current Research in Geology Applied to Ore Deposits.Fenoll Hach-Ali, Torres-Ruiz & Gervilla(eds)(1993).ISBN 84-338-1772-8

PGE AND GOLD IN THE ELACITE PORPHYRY COPPER DEPOSIT, BULGARIA

Petrunov, R. & Dragov, P.
Geological Inst., Bulgarian Academy of Sciences. Acad. G. Bonchev Str. 24, 1113 Sofia, Bulgaria

ABSTRACT: In the Elacite deposit, primary Au- and PGE-mineralization occurs in an early ore paragenesis which forms a linear stockwork in the isometric porphyry copper ore body. Characteristic minerals are magnetite, bornite and Co-Ni-thiospinels, as well as biotite and K-feldspar. The physico-chemical features of the environment were: neutral pH, low oxidation potential, low sulphur activity, elevated temperature and increased content of Te and Se in the hydrothermal fluids. Rocks of the basaltic layer are suggested as a source of the siderophile elemental association.

Introduction. The porphyry copper type of deposits are known to have similar, up to identical genetic, structural and textural features and metal and mineral compositions. However, some authors have defined classificational subtypes. Thus, Bonham, Jr. (1989) considered the so called alkalic porphyry copper-precious metal deposits showing increased contents of gold and platinum group elements (PGE), mostly Pd and Pt. Nevertheless, PGE minerals in them have not been described until a short time ago and researchers believed that PGE are included in the crystal structure of the main ore minerals. The first information on merenskyite, visotskite and stibiopalladinite in the Philippines Philex-Sto Tomas II deposit was provided by Piestrzinski et al. (1991). The next report on mineral forms of PGE concerns the Elacite deposit, where we have found an assemblage of Pd-, Pt-Pd-, Ni-, Cu-, Ag-, Bi-, Co-Ni- and other tellurides, selenides, arsenides and sulphides, as well as native gold, tellurium and bismuth (Petrunov et al., 1992). In the same paper we have given a geologic map and data on the methods and electron-probe analyses. The geochemical association of this mineralization is practically the same as that in the Cu-Ni magmatic deposits, the main primary source of PGE. Actually, the quantitative proportions of the elements differ, and we do not overestimate the above similarity. However, taking into account the recent finds of hydrothermal PGE deposits (Van der Flier-Keller, 1991; Kucha & Piestrzinski, 1991), as well as the concentrations of PGE in some contemporaneous ore-forming fluids (McKibben et al., 1990), we regard the occurrence of PGE-mineralization in the Elacite porphyry copper deposit as an evidence of the real possibility for a considerable PGE-enrichment and deposition in a hydrothermal environment.

Geology. The Elacite porphyry copper deposit is located in the northernmost part of the Panagyurishte ore zone, in the middle of the Sredna Gora Metallogenic Zone. Host rocks are Early Paleozoic greenschists, Paleozoic granodiorite and Late Cretaceous medium-acid subvolcanic dikes. The ore mineralization is medium- to low-temperature (>300-140°C), of the stockwork type, genetically related to a Late Cretaceous intermediate magmatism.

Mineral-paragenetic analysis. After analysing the structural-textural features of the ores, the mineral relationships and suc-

cessions, we have defined five successive mineral parageneses, named after part of the main minerals, as follows: quartz-feldspar (Qz-Fsp), magnetite-bornite-chalcopyrite (Mt-Bn-Cp), pyrite-chalcopyrite (Py-Cp), carbonate-quartz and pyrite (the last one is of the vein type).

The mineral aggregates of feldspars, variable quantities of quartz and biotite from the Qz-Fsp paragenesis are formed mostly metasomatically, to some extent as veinlets, among the dikes, granodiorite and schists. Their occurrence incsreases close to the rock contacts and at depth.

The Mt-Bn-Cp paragenesis forms a linear stockwork extending N-NW. It contains the richest variety of subordinate and rare minerals (except As- and Sb ones), which is the main feature distinguishing the Elacite deposit from the "standard" ones. Its characteristic sign is the absence of pyrite and the presence of pyrrhotite (turned into marcasite at a later stage); that, as well as the occurrence of magnetite, indicates deposition at low activity of sulphur. Such an environment favours the formation of Co-Ni-thiospinels, too. Rock alteration processes are characteristically manifested by chloritization, epidotization and biotitization. Local metasomatism of the earlier feldspar masses has produced biotite and redeposited K-feldspar.

The main ore minerals were formed in a close succession: magnetite - chalcopyrite+bornite+magnetite - quartz. The subordinate and rare minerals found in this paragenesis are (in the order of diminishing abundance): chlorite, epidote, molybdenite, native gold, merenskyite (platinoan and nickeloan included), carrolite, nickeloan linnaeite, sphalerite, pyrrhotite, hessite, clausthalite, kawazulite, naumannite, eucairite, bohdanowiczite, weissite, michenerite, Se-michenerite (?), three unnamed phases of probable formulae (Pd,Cu)2Te3, (Pd,Ag)3Te4 and PdNiTe3 (?), native tellurium and bismuth. They form fine, up to 100 μm (except the native gold which reaches up to a few mm in size) inclusions of one to three minerals (in some cases the observed picture resembles exsolution) mostly in chalcopyrite.

The Py-Cp paragenesis forms the isometric body of the deposit. Mineralogically, it is uniform but shows evidence of increased activity of the As-components, including primary as well as reactionary arsenides and sulpharsenides. Tetrahedrite has been found, too. Due to the penetration of the fluids amid the aggregates of the earlier paragenesis, part of the magnetite has turned into pyrite and chalcopyrite, and part of the iron has been redeposited as hematite. Cases of transformation of Pd-tellurides into arsenides (palladoarsenite and unnamed phases Pd4As3 and (Pd,Ni)2As) near tennantite-rammelsbergite veinlets have been observed. The same processes produced Co-Ni-sulpharsenides of the gersdorffite-cobaltite series. Gold occurs mostly as electrum.

The last two parageneses are not abundant in minerals but include base-metal sulphides, and the pyrite paragenesis shows increased contents of gold, too.

Ore-forming history. The spatial distribution of mineral parageneses is mainly controlled by tectonic events. We have distinguished the following successive ore-forming stages in the Elacite deposit (Fig. 1):

1. At the end of the Late Cretaceous, dike rocks were intru-

ded into a fault system extending mostly to NW. Faults were an important factor controlling the area of the supervening feldspathization, too. Later, at the stage of ore deposition, the dike faults were closed but the heterogeneities near the dike contacts played an ore-localizing role.

2. Next followed a deep faulting extending N-NW. At the boundary of the deposit it is vertical, up to 400-500 m wide and controls the area of the Mt-Bn-Cp paragenesis (A in fig. 1). Thus, at the beginning of ore deposition a linear stockwork was formed containing a considerable amount of gold and PGE, as well as a variety of metals (mostly with siderophile behaviour) and minerals (native metals, PGE-tellurides, Cu-, Bi-, Ag- and Pb-tellurides and selenides, Co-Ni-thiospinels etc.) alien to the "standard" type of porphyry copper deposits.

3. Emplacement of the isometric porphyry copper ore body. It was product of the simultaneous action of a continuous cataclasis of the rock massif in the space of intersection of three active fault systems (two diagonal and one slanting) and an abundant penetration of fluids forming the Py-Cp paragenesis. The linear stockwork was dislocated (B in fig. 1). Due to the fluid action on the earlier mineral deposits, there appeared reactional products (PGE-arsenides, Co-Ni-sulpharsenides, pyrite, chalcopyrite, hematite, wittichenite). Part of the gold was redeposited as electrum.

4. At the end of the tectonic and hydrothermal activities separate faults were still active forming Au-bearing pyrite veins above and around the ore body (C in fig. 1).

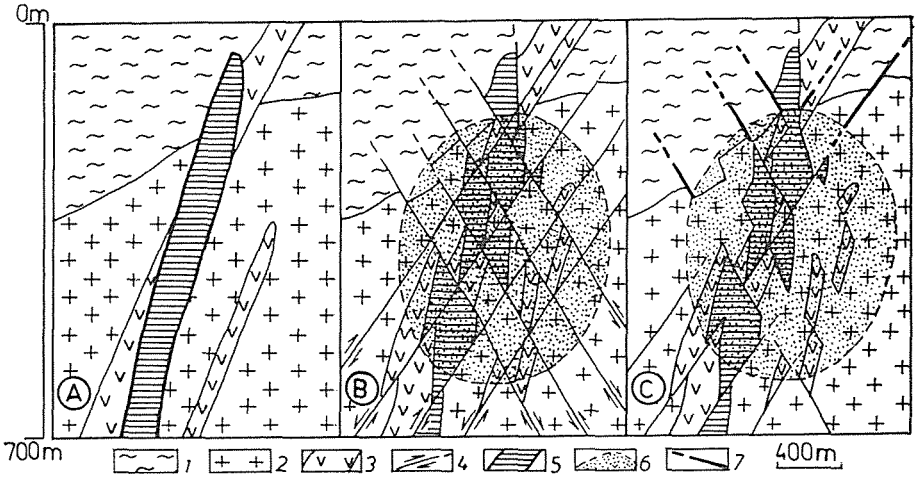

Fig. 1. Ore-forming sequences in the Elacite deposit (see text). 1, greenschist metamorphites (Cambrian); 2, granodiorite (Paleozoic); 3, quartz syenodiorite and granodiorite porphyries (Late Cretaceous); 4, faults; 5, linear stockwork with Mt-Bn-Cp paragenesis; 6, boundary of the isometric porphyry copper ore body (Py-Cp paragenesis); 7, pyrite veins (pyrite paragenesis).

On the basis of the mineral compositions of the successive parageneses, we suggest the following physico-chemical evolution

of the ore-forming environment: alkalic conditions - neutral pH-conditions with low oxidation potential and low activity of sulphur - high activities of sulphur and oxygene - final alkalization with variable, mostly high, sulphur activity and low copper activity.

Discussion on the genesis of the PGE-mineralization.

1. Source and transport. In the easternmost part of the Sredna Gora Metallogenic Zone (at the western Black Sea coast) there are placers containing gold and PGE-minerals. Their genesis is associated with the evolution of a K-subalkaline basalt magma (Late Cretaceous). In the Elacite area, the basaltic layer lies at a depth exceeding 20 km. Rocks of the above mentioned type in this layer are a likely endogenic source of the Au- and PGE-bearing mineral paragenesis at Elacite. We suggest that deep faulting promoted the penetration of fluids enriched in siderophile elements.

2. Deposition. Neutrality, low oxidation potential, low potential of sulphur and relatively high temperatures were the predominating physico-chemical conditions. Typical major minerals in such an environment are magnetite, bornite and Co-Ni-thiospinels. Characteristic features are also the absence of pyrite and the metasomatic development of biotite and K-felspar amid the ores.

According to Mountain & Wood (1988), the presence of increased contents of Te and Se in the fluids (manifested by the occurrence of tellurides and selenides) lowers the solubility of Pd and Pt. This may have caused their deposition as separate minerals.

References

Bonham, H. F., Jr. 1989. Bulk mineable gold deposits of the Western United States. - Econ. Geol. Monograph 6; 193-207.

Kucha, H., Piestrzinski, A. 1991. Gold-bearing sulfides from the Lubin copper deposit (Kupferschiefer-type, Poland). In: Moh, G. H. (ed.). Thalium and gold: observations and experimental contributions to mineralogy, geochemistry and crystal chemistry. N. Jb. Min. Abh. 163; 2/3; 197-270.

McKibben, M. A., A. E. Williams, G. E. M. Hall. 1990. Solubility and transport of platinum-group elements and Au in saline hydrothermal fluids: constraints from geothermal brine data. - Econ. Geol. 85, 8; 1926-1934.

Mountain, B. W., S. A. Wood. 1988. Chemical controls on the solubility, transport, and deposition of platinum and paladium in hydrothermal solution: A thermodynamic approach. - Econ. Geol. 83; 492-510.

Petrunov, R., P. Dragov, G. Ignatov, H. Neykov, Ts. Iliev, N. Vasileva, V. Tzatzov, S. Djunakov, K. Doncheva. 1992. Hydrothermal PGE-mineralization in the Elacite porphyry copper deposit (the Sredna Gora Metallogenic Zone, Bulgaria). - Comp. rend. Bulg. Acad. Sci., 45, 4; 37-40.

Piestrzinski, A., Schmidt, S. T., Franco, H. 1991. Gold-bearing chalcopyrite from the Philex- Sto, Tomas II porphyry copper deposit, Tuba, Benguet, Philippines. In: Moh, G. H. (ed.). Thalium and gold: observations and experimental contributins to mineralogy, geochemistry and crystal chemistry. N. Jb. Min. Abh. 163; 2/3; 197-270.

Van der Flier-Keller. 1991. Platinum-group elements in Tulamen coal, British Columbia, Canada. - Econ. Geol. 86, 2; 387-395.

Current Research in Geology Applied to Ore Deposits.Fenoll Hach-Alí, Torres-Ruiz & Gervilla(eds)(1993).ISBN 84-338-1772-8

PLATINUM-GROUP ELEMENTS (PGE) IN ORE-BEARING SEDIMENTS OF THE ZECHSTEIN FROM HUCKELHEIM (SPESSART, GERMANY)

Pfeiffer, Th.; Zereini, F. & Urban, H.
Inst. für Geochemie, J.W. Goethe-Universität, 6000 Frankfurt/Main, Germany

ABSTRACT: Drill core profiles of ore-bearing (Cu, Pb, Zn) Zechstein sediments from Huckelheim (Spessart, Germany) showed elevated PGE concentrations. Total PGE values average in the Zechsteinkonglomerat 1234 ppb, in the Kupferschiefer 43 ppb and in the Zechsteinkalk 1253 ppb. No correlations with the Cu-, Pb- and Zn-mineralisations were observed.

INTRODUCTION: Stratabound Cu-Pb-Zn-(Ag) ore deposits in the basal Zechstein (Kupferschiefer) in Germany have been mined in places like Mansfeld, Sangerhausen, Richelsdorf and in the Spessart. In the Spessart (Fig. 1) former mining took place in the Kupferschiefer at Bieber and Huckelheim. Shales from the Kupferschiefer in Poland exhibit anomalously high amounts of Pt and Pd (KUCHA, 1982), which are strongly bound to organic matter.

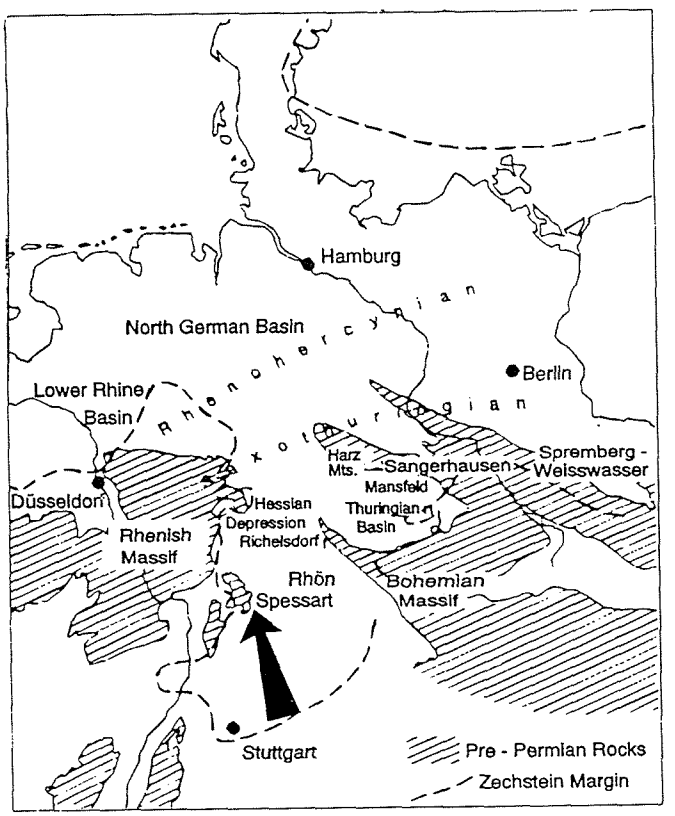

Fig. 1. Location of German Kupferschiefer occurrences in relation to major geologic features (after VAUGHAN et al., 1989)

The aim of the present investigation was to confine if such PGE enrichment can also be detected in the German part of the Lower Zechstein, which is in the Spessart devided into Zechsteinkonglomerat (Cl), Kupferschiefer (T1) and Zechsteinkalk (Ca1) with varying thicknesses.

METHODS: 88 samples of Zechstein sediments from the western Spessart were collected and analyzed for PGE`s, comprising 44 samples from four drill core profiles, containing the stratigraphic units Zechsteinkonglomerat (Cl), Kupferschiefer (T1) and Zechsteinkalk (Ca1) from Huckelheim, 23 samples from a profile near Bieber (2.3 m thickness) and 11 randomly picked samples from different locations of Huckelheim. Only the four drill cores showed base metal mineralizations. PGE`s (without Os) were analyzed by graphite furnace atomic absorption spectrometry (GFAAS), after preconcentration by nickel sulphide fire assay (ZEREINI & URBAN, 1992). The modal mineral composition of all rock samples was determined.

RESULTS: The highest PGE values are found in the 4 drill core profiles, with an average of 1234 ppb PGE`s in the Zechsteinkonglomerat, 43 ppb PGE`s in the Kupferschiefer and 1253 ppb PGE`s in the Zechsteinkalk.(Tab. 1).

Tab. 1. Range and average of PGE concentrations (ppb) in the basal Zechstein-sediments from 4 drill cores in the area of Huckelheim ((#) = number of samples).

	Zechsteinkonglomerat (8)		Kupferschiefer (25)		Zechsteinkalk (11)	
platinum	<2 - 267	85	<2 - 75	12	<2 - 227	80
palladium	<2 - 177	56	<2 - 7	2	<2 - 177	49
iridium	<2 - 361	108	<2 - 32	4	<2 - 363	133
rhodium	<2 - 2404	757	<2 - 106	17	<2 - 2353	759
ruthenium	<2 - 806	228	<2 - 45	9	<2 - 800	232
$\sum$ PGE	<2 - 3921	1234	<2 - 165	43	<2 - 3887	1253

The distribution of the PGE`s between the individual drill cores is inhomogenous. Maximum PGE values occur in drill core 2 (Fig. 2), where the Kupferschiefer is missing. Compared with the other cores, core 2 has the most pronounced Cu concentrations in the Zechsteinkonglomerat (0.13 - 3.7 %) and in the Zechsteinkalk (0.01 - 0.15 %). PGE concentrations in drill core 5 (Fig. 3) are distinctly lower. Here, total PGE`s are in the Zechsteinkonglomerat 72 ppb, in the Kupferschiefer 141 ppb and in the Zechsteinkalk 151 ppb. Characteristically high Zn (0.01 - 1.33 %) and Pb values (0.1 - 1.3 %) are observed, while Cu is very low (10 ppb - 241 ppb). The other drill cores exhibit PGE values resembling those in the normal crust (0.1 ppb - 10 ppb), although Cu-, Pb- and Zn-mineralizations are found. The samples containing no base metal mineralizations have PGE values ranging from 0.8 ppb - 2.2 ppb.

DISCUSSION: Possible explanations for the geochemical behaviour of PGE are obtained by correlating these with major and trace elements. No statistically significant linear relationships can be observed in the

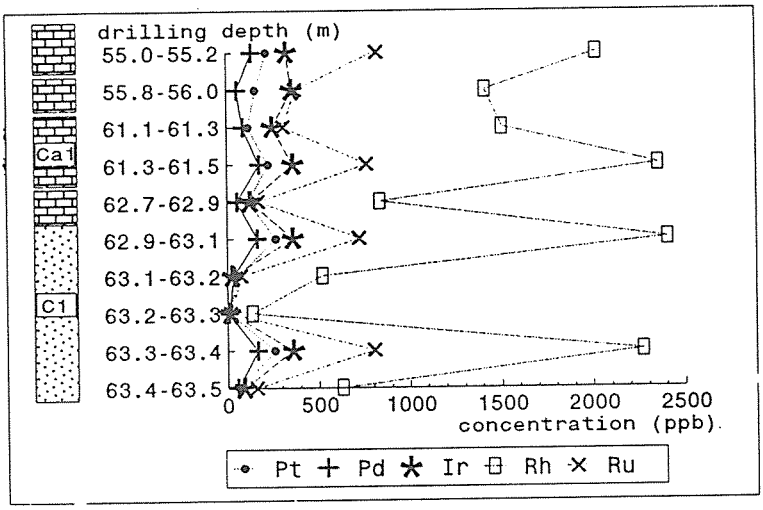

Fig. 2. Concentrations (ppb) and distribution of PGE in drill core 2 (Zechsteinkonglomerat (C1), Zechsteinkalk (Ca1)),N = 10.

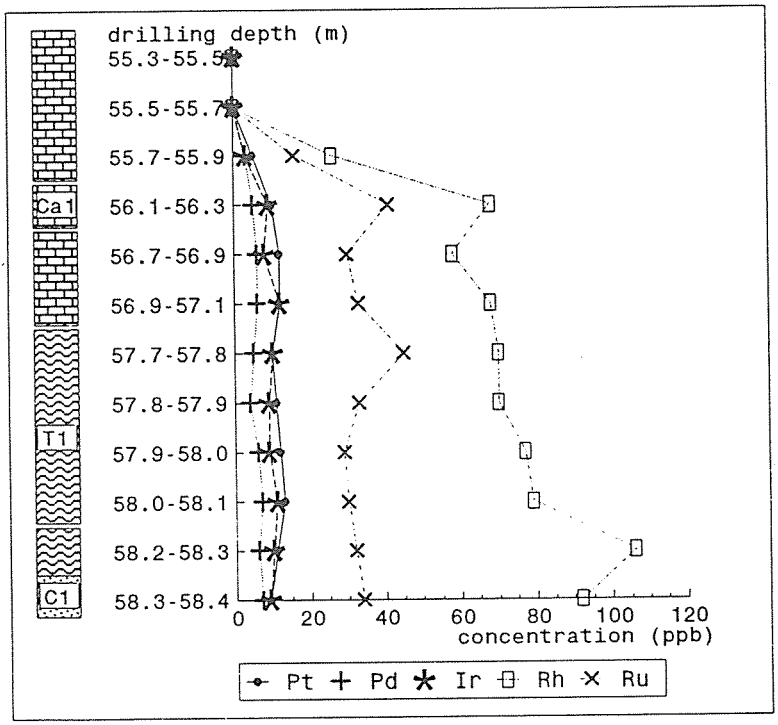

Fig. 3. Concentrations (ppb) and distribution of PGE in drill core 5 (Zechsteinkonglomerat (C1), Kupferschiefer (T1), Zechsteinkalk (Ca1)), N = 12.

Zechsteinkonglomerat between PGE`s and major as well as trace elements nor between PGE`s and mineral composition of the rocks. On the contrary, strong positive correlations (r = 0.98 - 0.99; significance = 0.05 %) exist only between the individual PGE`s. Correlations with C(org), Co and Fe are slightly positive.
In the Kupferschiefer a linear positive correlation is recognizable on the one hand between Pt and Sr, Ba, S, Co, Ni, Fe and on the other hand between Ir and P, Pd. Pt shows no or negative correlations to other elements. Pd, Rh and Ru are characterized by a linear positive relation. The Zechsteinkalk shows a positive correlation between Pd, Rh and C(org), Fe, Mn, V, Co, Cu, U. PGE`s exhibit against each other strong positive correlations (r = 0.89; significance level = 0.001 %). The samples without any base metal mineralization reveal a positive linear correlation only between PGE`s and C(org).

CONCLUSIONS: According to analytical results the stratigraphic units show strong lateral variations in the PGE`s. A look at the PGE values in the Zechsteinkonglomerat, ranging from < 2 ppb in drill core 9, over 9 ppb in core 5, to 1942 ppb in core 2, stresses this fact. No primary informations or trends connecting anormal PGE concentrations with stratigraphical units can be seen. A continous increase in PGE`s throughout the profiles is not present. Changes appear abruptly. No correlations between base metals and PGE`s can be observed. One has to conclude, that only the apparent correlation between PGE`s and C(org) can provide a tool for further investigations on the geochemical behaviour of PGE`s in such sedimentary environments. Ongoing work is concentrated on the determination of distinct platin-group minerals (PGM) in the sediments.

LITERATURE

Kucha, H. 1982. Platinum-group metals in the Zechstein copper deposits, Poland.Econ. Geol. 77: 1578-1591

Vaughan, D.J. et al. 1989. The Kupferschiefer: an overview with an appraisal of the different types of mineralization. Econ. Geol. 84: 1003-1027

Zereini, F. & Urban, H. 1992: Zur Bestimmung von Platingruppenelementen (PGE) in geologischen Proben nach der Nickelsulfid-Dokimasie: Inst. für Geochemie, Frankfurt/Main. Open file-Report 1992-1: 1-19

Current Research in Geology Applied to Ore Deposits.Fenoll Hach-Alí, Torres-Ruiz & Gervilla(eds)(1993).ISBN 84-338-1772-8

CARBONATE-HOSTED EPITHERMAL GOLD MINERALIZATION IN SOUTHERN TUSCANY (ITALY): THE EXAMPLES OF FRASSINE AND LA CAMPIGLIOLA

Ruggieri, G. (1); Lattanzai, P. (2) & Tanelli, G. (3)
(1) International Inst. for Geothermal Research, Pisa, Italy
(2) Dip.to di Scienze della Terra, Università di Firenze, Italy
(3) Dip.to di Scienze della Terra, Università Federico III, Napoli, Italy

ABSTRACT: At Frassine and La Campigliola, epithermal gold mineralization is associated with silicified masses replacing carbonatic rocks. Their genesis is related to shallow hydrothermal circulation associated with Pliocene-Quaternary magmatism. Fluid inclusion data indicate that at Frassine a temperature decrease of the hydrothermal fluids may have caused ore deposition, while at La Campiglola mixing phenomena and temperature increase may have played an important role in the evolution of the hydrothermal fluids.

INTRODUCTION

Southern Tuscany belong to the northern Appennines chain which was essentially built during the Tertiary tectonic Alpine event (e.g. Boccaletti et al., 1987). The geology of southern Tuscany can be represented by several tectono-stratigraphic units constituted by sedimentary, metamorphic and magmatic rocks of Paleozoic-Quaternary age.

Fron Pliocene to Quaternary southern Tuscany was interested by crustal extension and by late- to post-orogenic intrusive and effusive magmatism of both crustal anatectic and subcrustal origin (Peccerillo et al., 1987). The high heat flow linked to the emplacement of granitic stoks, belonging to this magmatism, is believed to be responsable for the development the present-day geothermal fields of Larderello and Monte Amiata.

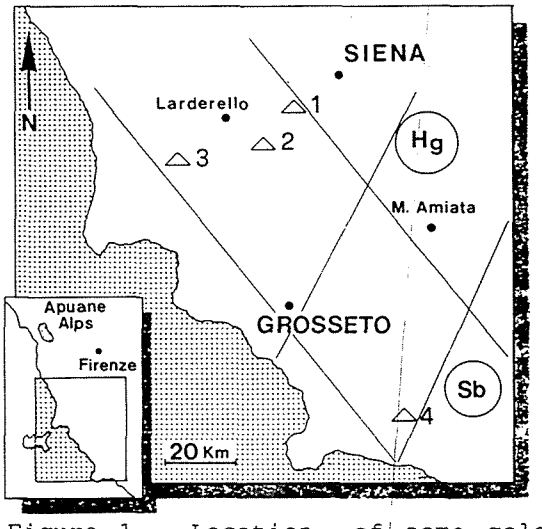

Figure 1 - Location of some gold epithermal occurrences and of the Sb and Hg metallogenic domains of southern Tuscany; 1.Cetine, 2.Ciciano, 3.Frassine, 4.La Campigliola.

In the last decade, several showings of carbonate-hosted disseminated gold mineralization have been recognized in southern Tuscany. The main characteristics of these showings have been described e.g. by Tanelli & Scarsella (1990) and Tanelli et al. (1991). The epithermal gold mineralization of southern Tuscany mostly occurs in the peripheral parts of the Larderello and Monte Amiata geothermal fields, over an area long known for Sb deposits (figure 1).

The mineralization consists of silicified masses replacing carbonatic rocks (usually the "Calcare Cavernoso" formation of the Tuscan Nappe) at the contact with overlying impervious

cover (commonly constituted by flysch terrains of the Liguridi allochtonous cover). Hydrothermal alteration of "Calcare Cavernoso" may produce the so called "Cenerone" which is formed essentially by pulverized dolomite. Argillic alteration (known as "losima") may also affect the flysch cover. Late-hydrothermal and/or supergene alteration is also sometimes present.
Gold is usually sub-microscopic, but rare occurrences of 10-15 micrometer grains have been reported (Tanelli & Scarsella, 1990).
The epithermal gold mineralization appears to be related to shallow hydrothermal activities associated with the Pliocene-Quaternary magmatism and the development of geothermal anomalies. Tanelli et al. (1991) proposed two general genetic environments for the epithermal gold mineralization of southern Tuscany: a) closed systems, where impounding phenomena predominate; b) open systems, characterized by boiling of the hydrothermal fluids.
This work presents preliminary data, with major emphasis on fluid inclusions, on two of these epithermal gold occurences of southern Tuscany.

FRASSINE MINERALIZATION

The Frassine Au-Sb mineralization is associated with siliceous bodies replacing the "Calcare Cavernoso" formation which is overlain by flysch terrains. At the surface the silicified masses are mostly formed by micro-crystalline quartz; in some thin sections, the micro-crystalline quartz displays the typical jigsaw-puzzle and/or reticulated textures of jasperoids. At depth silicification decreases, and gradually grades into unaltered carbonatic rocks. The siliceous bodies are often crosscut by fractures filled by euhedral quartz, barite and stibnite crystals. Calcite veins, which appears to predate the formation of silica bodies, are common at depth. Minor amounts of pyrite, kaolinite, illite, jarosite and iron hydroxides are also found. The highest gold grades (about 1 ppm) are related to the most silicified zones; locally, surficial high-grade supergene gold enrichments (up to 10 ppm) also occur.
Microthermometric studies were carried out on fluid inclusions in calcite, quartz and barite vein crystals. All these minerals contain two-phase aqueous liquid-rich inclusions. No evidence of boiling was found in fluid inclusions. Primary and pseudoseconday inclusions are present in calcite and quartz crystals, while in barite all inclusions appear to be pseudosecondary or secondary. Salinities, calculated from final ice melting temperature, and homogenization temperatures are shown in table 1, where are also reported microthermometric data for other epithermal occurrences of southern Tuscany. From table 1, it can be observed that all inclusions are characterized by low salinity fluids (<3 wt% NaCl eq.), with inclusions in quartz displaying the highest salinities. Homogenization temperatures (Th) are relatively low for all the studied inclusions (<182°C), and are believed to be close to the trapping temperatures of the fluids. Inclusions in quartz and barite show similar Th range and average, while inclusions in calcite have higher Th range and average. This fact may be interpreted to be the evidence of a cooling process which affects the hydrothermal fluids from the time of early calcite deposition to the time of late quartz and barite fracture filling. In this context the main silicification stage (which occurred between calcite and quartz-barite formation), and perhaps gold deposition, may be characterized by an intermediate temperature. A decrease of fluid temperatures may explain the

carbonate dissolution and silica deposition, and the formation of gold mineralization (Ruggieri, 1993).

TABLE 1 - Fluid inclusion data of Frassine and La Campigliola and of other epithermal Sb and/or Au occurrences of southern Tuscany; from Ruggieri (1993) modified. In parentheses average values for the studied localities.

LOCALITY	MINERAL	SALINITY (wt% NaCl eq.)	HOMOGENIZATION TEMPERATURE (°C)
Frassine	quartz	1,4-2,9 (2,1)	126-166 (146)
	barite	0,7-1,1 (0,8)	131-163 (145)
	calcite	0,5-1,2 (0,9)	140-182 (161)
La Campigliola	quartzI	2,7-6,1 (4,5)	194-234 (218)
	quartzII	1,9-6,0 (4,2)	165-185 (178)
Poggio Fuoco	quartz		125
Pereta	quartz		165-232
Monteauto	quartz	0,7-1,7	220
Selvena	quartz		189
San Martino sul Fiora	fluorite	4,2	116
La Sassa	quartz	2,1-4,0	196-210
	calcite	4,2	135-148
Campo di Sasso	sphalerite	4,6	178-185
Micciano	barite	4,2	178-203

LA CAMPIGLIOLA MINERALIZATION

This Sb-Au mineralization is predominanlty hosted within siliceous masses replacing the "Calcare Cavernoso". The latter is tectonically overlain by the "*Macigno*" sandstones, which are partially silicified near the contact with the "Calcare Cavernoso" and are affected by kaolinitization above the contact. The siliceous body predominanlty consists of micro-crystalline quartz and chalcedony; veins of subhedral centimetric quartz crystals may occur within the micro-crystalline bodies. These quartz veins are interpreted to result from the recrystallisation of the chalcedony masses and/or microcrystalline quartz. Quartz-chalcedony veins crosscutting the "Macigno" also occur. In these veins, chalcedony preceds quartz deposition, and the quartz crystals display the typical open-space filling textures. At depth, the silicified masses passes to the "Cenerone". Barite and stibnite are sometimes found in the micro-crystalline quartz.

Recrystallised quartz (quartz I) from the siliceous masses and quartz crystals (quartz II) from veins crosscutting the "Macigno" have been selected for fluid inclusion studies. Fluid inclusions in quartz I

are mostly two-phase aqueous liquid-rich but inclusions with variable liquid/vapour ratio, possibly indicating necking-down phenomena, also occur. The origin of inclusions in quartz I is probably related to the recrystallization phenomena that formed the host mineral. Quartz II contains only two-phase aqueous liquid-rich primary and pseudsecondary inclusions.
Microthermometric results (table 1) show that salinities values of quartz I and II are similar, while Th range and average of quartz I are higher than those of quartz II. Evidence of boiling processes from fluid inclusions was never observed.
Salinities and Th of inclusions in quartz II are representative of the fluids responsible for the deposition of the host minerals, and they are believed to be close to the physico-chemical conditions during the silicification event. The somewhat variable salinities of inclusions in quartz II may indicate a nearly isothermal mixing process. Inclusions in quartz I testify to a temperature increase, from the time of silicification, which produced the recrystallisation of chalcedony.

CONCLUSIONS

The general features and, specifically, the fluid inclusion data of the epithermal gold showings at Frassine and La Campigliola are similar to other Sb/Au occurrences in southern Tuscany. Fluid salinities are typically low; local higher values such as at La Campigliola may result from interaction with evaporitic horizons of the "Calcare Cavernoso" formation. Because of the shallow depth of formation, fluid inclusion Th are close to trapping temperatures. The low salinities and relatively low temperatures are compatible with a largely meteoric origin of the fluids, which circulated at moderate depths in an area characterized by high geothermal gradient. The absence of evidences of boiling of the hydrothermal fluids suggests that Frassine and La Campigliola belong to the type of environment of gold mineralization in southern Tuscany described by Tanelli et al. (1991) as "closed systems".

REFERENCES

Boccaletti, M., Decandia, F.A., Gasperi, G., Gelmini, R., Lazzarotto, A. & Zanzucchi, G. (eds.) 1987. Carta strutturale dell'Appennino Settentrionale. Note Illustrative. CNR Prog. Finalizz. Geodinamica. Siena: Tipografia Senese.

Peccerillo, A., Conticelli, S. & Manetti P. 1987. Petrological characteristics and the genesis of the recent magmatism of south Tuscany and north Latium: a review. Perid. Mineral., 56:157-172.

Ruggieri, G. 1993. Minerogenesi in ambiente epitermale: gli esempi delle mineralizzazioni aurifere di Furtei (Sardegna), Frassine e La Campiglola (Toscana meridionale). Unpubl. phD Thesis.

Tanelli, G. & Scarsella, A. 1990. Tipologia e modellizzazione genetica delle mineralizzazioni aurifere epitermali della Toscana meridionale. Ind. Min., 2:1-9.

Tanelli, G., Lattanzi, P., Ruggieri, G. & Corsini, F.1991. Metallogeny of gold in Tuscany, Italy. In: Ladeira E.A.(ed.) Brazil Gold'91. A.A. Balkema, Rotterdam, pp.109-114.

Current Research in Geology Applied to Ore Deposits. Fenoll Hach-Ali, Torres-Ruiz & Gervilla (eds) (1993). ISBN 84-338-1772-8

CONTROLS ON PGE MINERALIZATION IN THE EARLY PALEOPROTEROZOIC KEMI-KOILLISMAA-OULANKA MAFIC INTRUSION BELT, FENNOSCANDIAN SHIELD

Saini-Eidukat, B. (1); Thalhammer, O.A.R. (1); Alapieti, T. (2); Halkoaho, T.(2) & Iljina, M. (1,2)
(1) Inst. of Geological Sciences. Mining University of Leoben, A-8700 Leoben, Austria
(2) Dept. of Geology, University of Oulu, P.O. Box 400, SF-90571 Oulu, Finland

ABSTRACT: A number of processes operate to concentrate PGE's in mafic intrusions, including pre-magmatic mantle enrichment, intermediate staging chambers during partial melting with crustal contamination, and exsolution of an immiscible sulfide or magmatic volatile phases which mobilize and concentrate PGE's in the intrusion itself. When more than one of these processes occurs, the possibility of ore deposit formation increases. Some parent magmas of the early Paleoproterozoic intrusion belt of the Fennoscandian Shield have chemistries similar to modern boninites, which implies a previous mantle melting event. Slightly negative Nd isotopes indicate crustal contamination occurred before or during emplacement. The varied types of rich PGE concentrations were formed by the superposition of different concentration processes, including magma chamber and metamorphic processes.

1. Introduction

Understanding of the major PGE-bearing mafic intrusions of the world is maturing rapidly with the application of a variety of petrological and geochemical tools. The PGE-rich early Paleoproterozoic Kemi-Koillismaa-Oulanka mafic intrusion belt, Fennoscandian Shield provides an excellent opportunity to investigate the different processes responsible for PGE concentration. Here we will describe the intrusion belt's geologic setting, its geochemical characteristics, our concepts for metallogenesis of the large types of PGE mineralizations, and will compare them to similar deposits.

2. General Geology

The belt comprises approximately two dozen intrusion fragments stretching across the center of the Fennoscandian shield from the Finnish-Swedish border into Russian Karelia. Although subsequent tectonic processes have obscured evidence of the original tectonic setting, most workers infer from the presence of overlying sediments and coeval volcanics found in some parts of the belt that the intrusions were emplaced into a continental rifting environment (Alapieti et al., 1979; Brewer and Pharoah, 1990; Turchenko, 1992). Their age has been dated to the range 2.44 Ga (Koillismaa and Penikat Complexes, Alapieti, 1982; Huhma et al., 1990) to 2.34 Ga (Tsipringa intrusion, Oulanka Complex, Turchenko, 1992).

Lower contacts of the intrusions are generally intrusive into the Archean basement granite-gneisses. Upper contacts can be in erosional contact with approximately 2.3 Ga conglomerate, or in some cases in intrusive contact with the Archean basement. In cases, as in Russia, the upper contact is with overlying volcanics (the Sumi-Sariolan

group and the Imandra-Varzuga series on the Kola Peninsula) with tholeiitic chemistries (Brewer and Pharoah, 1990).

Descriptions of individual intrusions and mineralizations can be found in (Alapieti et al., 1990; Halkoaho et al., 1990a,b; Iljina et al., 1989, 1992) and references therein. The intrusions are usually made up of a number of cyclic repetitions of ultramafic-mafic packages, referred to as megacyclic units.

3. Geochemical characteristics

Two magma types have been recognized by examining the megacyclic units and basal dikes associated with the intrusions (Alapieti et al., 1990; Iljina et al., 1992). The first is enriched in MgO and Cr and depleted in Ti, Ta, Nb, and HREE's compared to tholeiites, while the second is less enriched in MgO and Cr. The chemical characteristics of the first type are similar to those referred to by different authors as modern boninites, contaminated komatiites, siliceous high magnesium basalts, and high magnesium andesites. They are also very similar to parental magmas proposed for the Bushveld and Stillwater Complexes. Regardless of the nomenclature used, these chemistries require special formation conditions to generate these very specific major and trace element characteristics.

In Finland, the overlying Juottiaapa volcanics (2.09 Ga) have an ε_{Nd} of +4.2, which indicates that the mantle source had been depleted for a long time (Huhma et al., 1990). The previous depletion may have been the formation of Archean crust during the Saamian (3.1-2.9) and Lopian (2.9-2.6) Ma orogenies. In contrast, Nd isotopic ratios for all the intrusions measured to date are between ε_{Nd} 0 to -2 (Penikat ε_{Nd} = -1.6, Huhma et al., 1990; Oulanka Complex ε_{Nd} = -0.7 to -1.7, Turchenko et al., 1991). This indicates crustal contamination may have played an important role at some time in the intrusions' history.

4. Genesis of Platinum Group Element Mineralization

The intrusions host a number of PGE mineralization types (Halkoaho et al., 1990a,b; Iljina et al., 1989, 1992; Lahtinen et al., 1989). These range from basal sulfide accumulations to stratiform layers within the layered series to basement-hosted concentrations. The layered series mineralizations occur with and without chromite, and with and without sulfides. PGE grades up to 100's of ppm have been recorded (Halkoaho et al., 1990a). Taken as a whole, the magmas of the intrusion belt must have been extraordinarily enriched in PGE to have formed such a large number of individual concentrations of different types.

In comparison to the Fennoscandian intrusions, the Bushveld and Stillwater Complexes have similar parent magma chemistries and negative ε_{Nd} values. Os isotopes

of the Stillwater (Lambert et al., 1989; Martin, 1989) Complex also indicate addition of a crustal component. The tholeiitic Noril'sk-Talnakh deposits and the Duluth Complex share similar tectonic settings, although different geochemistries than the Fennoscandian intrusions, but again, trace element and S isotopic evidence indicates some sort of crustal input.

The combined geologic, geochemical, and isotopic evidence to date indicates that the PGE concentrations in the Finnish intrusions are the result of a combination of several processes. These may include some or all of the following:

- a pre-magmatic mantle PGE enrichment event due to depletion
- a high degree of melting during the partial melting event with the addition of LILE-enriched fluid phase to form the boninitic chemistries
- crustal contamination, either in a lower crustal staging chamber or during emplacement
- thermochemical interaction at the interface between two magmas
- during crystallization, exsolution of an immiscible sulfide melt (Naldrett, 1989) and/or magmatic volatiles (Ballhaus and Stumpfl, 1986; Boudreau and McCallum, 1992) which may mobilize and concentrate the PGE's. This process may be aided by the presence of an interface between magma types. The final PGE mineralization may be emplaced outside the intrusion itself (basement-hosted mineralization?).
- subsequent metamorphic events may modify the PGE mineralogy, and remobilize and upgrade the PGE's (Thalhammer et al., 1993).

We propose that any one of the processes mentioned above independently may result in concentration of PGE's, but that the coincidence of two of more of them increases the possibility for formation of an economic ore deposit. In the Fennoscandian intrusions, boninite-type magma types are not the only attribute responsible for the formation of PGE concentrations. We suggest that, as in the Noril'sk, Sudbury, and Bushveld intrusions, crustal contamination played an important role.

References:

Alapieti, T., 1982, The Koillismaa layered igneous complex, Finland — its structure, mineralogy and geochemistry, with emphasis on the distribution of chromium: Geol. Surv. Finland, Bull. 319, 116 p.

Alapieti, T.T., Filén, B.A., Lahtinen, J.J., Lavrov, M.M., Smolkin, V.F., and Voitsekhovsky, S.N., 1990, Early Proterozoic layered intrusions in the northeastern part of the Fennoscandian shield: Min. Pet., v. 42, p. 1-22.

Alapieti, T.T., Hugg, R., Piirainen, T., and Ruotsalainen, A., 1979, The ultramafic and mafic intrusion at Näränkävaara, northeastern Finland: Geol. Surv. Finland, Rep. Invest. 35, 31 p.

Ballhaus, C.F., and Stumpfl, E.F., 1986, Sulfide and platinum mineralization in the Merensky Reef: Evidence from hydrous silicates and fluid inclusions: Contr. Min. Petr., v. 94, p. 193-204.

Boudreau, A.E., and McCallum, I.S., 1992, Concentration of platinum-group elements by magmatic fluids in layered intrusions: Econ. Geol., v. 87, p. 1830-1848.
Brewer, T.S., and Pharoah, T.C., 1990, Early Precambrian basic rocks of the Baltic Shield, *in* Hall, R. P., and Hughes, D. J., eds., Early Precambrian Basic Magmatism: London, Blackie, p. 273-293.
Halkoaho, T.A.A., Alapieti, T.T., and Lahtinen, J.J., 1990a, The Sompujärvi PGE reef in the Penikat layered intrusion, northern Finland: Min. Pet., v. 42, p. 39-55.
Halkoaho, T.A.A., Alapieti, T.T., Lahtinen, J.J., and Lerssi, J.M., 1990b, The Ala-Penikka PGE reefs in the Penikat layered intrusion, northern Finland: Min. Pet., v. 42, p. 23-38.
Huhma, H., Cliff, R.A., and Perttunen, V., 1990, Sm-Nd and Pb isotopic study of mafic rocks associated with early Proterozoic continental rifting: the Perapohja schist belt in northern Finland: Contrib. Mineral. Petrol., v. 104, p. 369.
Iljina, M.J., Alapieti, T.T., Lahtinen, J.J., and Lerssi, J.M., 1989, The Suhanko-Konttijärvi intrusion and related sulphide and PGE mineralizations, *in* ALapieti, T., eds., 5th International Platinum Symposium - Guide to the Post-Symposium Field Trip: Espoo, Geological Survey of FInland, p. 163-187.
Iljina, M.J., McElduff, B.M., and Alapieti, T.T., 1992, PGE mineralization in the Suhanko-Konttijärvi intrusion, Finland: Austral. J. Earth Sci., v. 39, p. 303-313.
Lahtinen, J.J., Alapieti, T.T., Halkoaho, T.A.A., Huhtelin, T.A., and Iljina, M.J., 1989, PGE mineralization in the Tornio-Näränkävaara layered intrusion belt, *in* Alapieti, T., eds., 5th International Platinum Symposium Guide to the post-symposium field trip: Espoo, Geological Survey of Finland, p. 43-58.
Lambert, D.D., Morgan, J.W., Walker, R.J., Shirey, S.B., Carlson, R.W., Zientek, M.L., and Koski, M.S., 1989, Rhenium-osmium and samarium-neodymium isotopic systematics of the Stillwater Complex: Science, v. 244, p. 1169-1174.
Martin, C.E., 1989, Re-Os isotopic investigation of the Stillwater Complex, Montana: Earth Planet. Sci. Lett., v. 93, p. 336-344.
Naldrett, A.J., 1989, Stratiform PGE deposits in layered intrusions, *in* eds., Ore Deposition Associated with Magmas: Reviews in Economic Geology, p. 135-165.
Thalhammer, O.A.R., Saini-Eidukat, B., and Iljina, M.J., 1993, PGE mineralization associated with silicates in the Portimo Layered Complex, Fennoscandian Shield, Finland: Signficance of an unusual deposit type, *in eds.:* this volume, p.
Turchenko, S.I., 1992, Precambrian metallogeny related to tectonics in the eastern part of the Baltic Shield: Prec. Res., v. 58, p. 121-141.
Turchenko, S.I., Semenov, V.S., Amelin, Y.V., Levchenkov, O.A., Neymark, L.A., Buiko, A.K., and Koptev-Dvornikov, J.V., 1991, Early Proterozoic riftogenic belt of northern Karelia and types of the Cu-Ni, PGE and Cu-Au mineralization [abstr.]: Geol. Fören. Stockholm Förh., v. 113, p. 70-72.

Current Research in Geology Applied to Ore Deposits. Fenoll Hach-Alí, Torres-Ruiz & Gervilla (eds) (1993). ISBN 84-338-1772-8

PLATINUM-GROUP ELEMENTS (PGE) IN ULTRABASIC AND BASIC ROCKS FROM THE FRANKENSTEIN GABBROIC COMPLEX (ODENWALD, GERMANY)

Skerstupp, B.; Zereini, F. & Urban, H.
Inst. für Geochimie, J.W. Goethe-Universität, 6000 Frankfurt/Main, Germany

ABSTRACT: Serpentinites, gabbros and diorites from the Frankenstein Gabbroic Complex (Odenwald, Germany) were geochemically investigated and analyzed for major, trace and platinum-group elements (PGE). Educts of the serpentinites were dunites, probably derived from an S-undersaturated magma. PGE abundances are generally low (0,4 - 7,2 ppb) and uniformly distributed within the complex. The ultramafic rocks seem to belong to a mantle-near regime.

GEOLOGICAL SETTING: The Frankenstein Gabbroic Complex (FGC) is situated in the southern part of Hessia, Germany, 35 km south of Frankfurt/Main (Fig. 1). It belongs to the northwestern part of the variscan orogen of the Bergsträsser Odenwald. This crystalline area numbers among the outcrops of the Saxothuringian Belt in Central Europe. The FGC covers an area about 10 km long and 5 km wide. Its longitudinal axis follows the general strike direction SW-NE within the Bergsträsser Odenwald. Isotopic ages, evidenced by $^{40}Ar/^{39}Ar$ measurements, date the synorogenic intrusion to the border Devonian/Carboniferous (ca. 360 Ma). The $^{87}Sr/^{86}Sr$ initial ratio of the gabbro indicates an uncontaminated mantle-derived magma, which intruded into a shallow crustal level (KIRSCH et al., 1988). The FGC consists mainly of gabbroic rocks. In addition, dioritic rocks, and mafic and felsic dikes are found. Petrographic and geochemical investigations indicated the existence of three gabbro types: a) massive gabbro; b) "mottled" gabbro; c) "thin-layered" gabbro. No zoning or regular distribution of these types is observed within the complex. Magma fractionation seems to be a more favourable explanation for the different types than magma mixing (KREHER et al., 1992). Ultramafic rocks (serpentinites) occur only locally in the core and the southwestern part of the complex. They form clearly separated, probably lenticular shaped bodies within the gabbro, and are supposed to be serpentinized pyroxene-hornblende-peridotites.

ANALYSES: 20 unmineralized rock samples (13 serpentinites, 4 diorites, and 3 gabbros) were collected from quarries. Pressed powder pellets were analyzed for 10 major and 13 trace elements using an wavelength-dispersive X-ray fluorescence spectrometer. Concentrations of PGE were measured by graphite furnace atomic absorption spectrometry, after preconcentration by nickel sulphide fire assay (ZEREINI & URBAN, 1992). Polished thin sections were microscopically examined. All analyses were carried out at the Institute of Geochemistry, University of Frankfurt/Main.

RESULTS AND DISCUSSION: Microscopic observations of the serpentinites revealed a typical mesh texture of chrysotile replacing olivine and orthopyroxene. No primary chromite or chromespinels could be detected. Fine grained interstitial secondary magnetite is the main ore mineral (1 - 4 vol.%). Diorites contain pyrite, and gabbros additional "hydrothermal" ore minerals (sphalerite, galenite), but both only in minor amounts.

Whole-rock geochemical data show for each of the three rock types (serpentinites, gabbros and diorites) uniformity. Concentrations of major elements (Tab. 1), trace elements (Tab. 2), and PGE (Tab. 3), including discriminant element ratios, are listed.

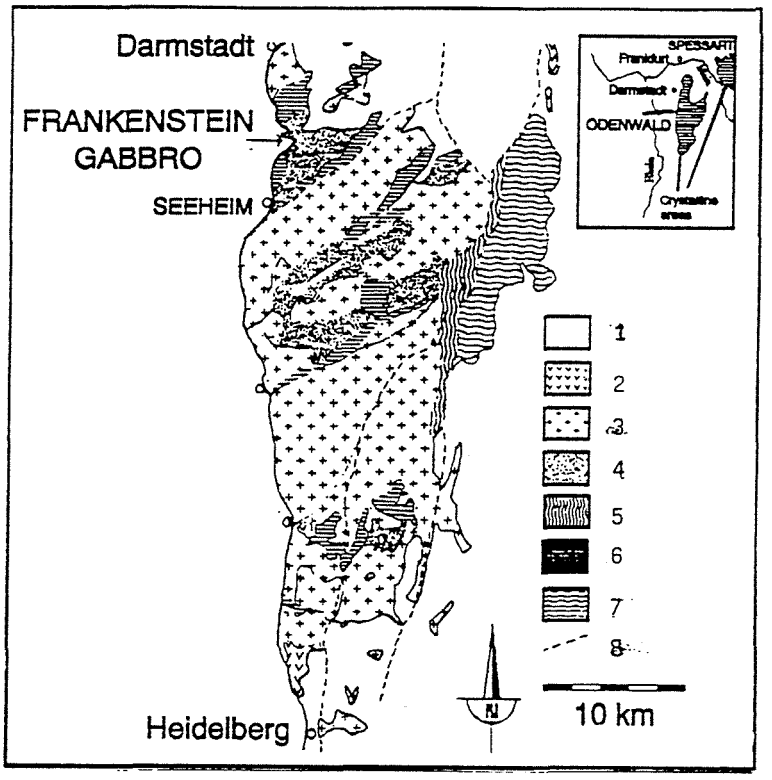

Fig. 1. Geological map of the Odenwald, Germany (after KIRSCH et al., 1988)
Symbols: 1 = Postvariscan Cover; 2 = Rhyolite; 3 = Granite, Granodiorite;
4 = Serpentinite, Gabbro, Diorite; 5 = Hornblende Gneisses;
6 = Metamorphic Schists; 7 = Gneissic Area (Böllstein-Odenwald); 8 = Faults.

Tab. 1. Mean average values of major elements [%]
(ma = massive; la = layered).

ROCK	SiO_2	TiO_2	Al_2O_3	Fe_2O_3	MnO	MgO	CaO	Na_2O	K_2O	P_2O_5	LOI
SERP	36.27	0.21	3.77	16.43	0.24	28.91	2.65	0.09	0.04	0.03	10.47
GAB(ma)	42.23	0.36	17.97	4.59	0.10	5.64	11.10	2.21	0.73	0.04	4.66
GAB(la)	43.31	0.38	18.86	4.55	0.08	5.51	11.64	2,07	0.34	0.08	4.53
DIOR	51.92	1.10	16.84	6.46	0.17	3.92	6.26	4.45	1.11	0.44	2.44

Tab. 2. Mean average values of trace elements [ppm].

ROCK	Sc	V	Cr	Co	Ni	Cu	Zn	Ga	La	W	Pb	S	F
SERP	17	63	1360	130	914	10	127	6	< 5	2	4	135	<400
GAB(ma)	21	84	94	26	36	37	83	17	< 5	< 2	16	312	<400
GAB(la)	19	88	108	23	38	34	35	18	< 5	< 2	5	543	<400
DIOR	20	133	17	17	16	11	107	22	30	3	13	327	<400

Tab. 3. Noble elements [ppb] and elemental ratios in 20 analyzed samples (* = below detection limit).

ROCK-#	Au	Pt	Pd	Ru	Rh	Ir	ΣPGE	Ni/Co	Co/(Co+Sc)	Pt/(Pt+Pd)
SERP-1	< 1	0.5	0.2	0.1	0.2	<0.1	1.1	6.8	0.89	0.71
SERP-2	< 1	0.1	*	0.1	0.1	<0.1	0.4	6.0	0.89	> 0.90
SERP-3	< 1	*	0.1	0.1	0.1	<0.1	0.4	7.5	0.90	< 0.20
SERP-4	< 1	3.0	0.2	0.1	0.1	<0.1	3.5	7.2	0.89	0.94
SERP-5	< 2	2.0	0.1	0.1	0.1	<0.1	2.4	7.2	0.90	0.95
SERP-6	< 2	4.0	0.3	0.2	0.1	<0.1	4.7	7.8	0.88	0.93
SERP-7	< 2	2.0	0.5	0.1	0.2	<0.1	2.9	6.7	0.89	0.80
SERP-8	< 2	*	0.4	*	0.1	<0.1	0.6	7.3	0.88	< 0.20
SERP-9	< 2	*	0.4	*	0.1	<0.1	0.6	7.3	0.88	< 0.20
SERP-10	< 2	0.5	0.4	0.2	0.2	<0.1	1.4	7.0	0.86	0.56
SERP-15	< 3	5.0	1.0	0.6	0.5	<0.1	7.2	6.9	0.87	0.83
SERP-16	< 2	3.0	0.4	0.2	0.2	<0.1	3.9	3.3	0.79	0.88
SERP-17	< 2	0.5	0.3	0.4	0.2	<0.1	1.5	7.0	0.88	0.63
GAB(ma)-18	< 2	1.0	0.4	0.4	0.4	<0.1	2.3	1.4	0.55	0.71
GAB(ma)-20	< 2	0.5	0.1	0.3	0.2	<0.1	1.2	2.6	0.48	0.83
GAB(la)-19	< 2	1.7	0.4	0.8	0.3	<0.1	3.3	1.7	0.55	0.81
DIOR-11	< 2	3.0	0.5	0.2	0.4	<0.1	4.2	1.0	0.42	0.86
DIOR-12	< 2	0.1	0.4	0.5	0.1	<0.1	1.2	0.7	0.44	0.20
DIOR-13	< 2	0.4	0.4	1.0	0.2	<0.1	2.1	1.5	0.36	0.50
DIOR-14	< 2	1.5	0.6	0.7	0.2	<0.1	3.1	0.9	0.53	0.71

The abundances of S are low (< 100 - 214 ppm) in the serpentinized peridotites. This, and the rare existence of sulfides seem to be indicators that the ultramafic rocks were probably derived from S-undersaturated magmas. Values > 0,80 (mean 0,88) and only limited variation of the ratio Co/(Co+Sc) lead to the conclusion that primary rocks were dunites, originating from the same magma. This view is supported by the little variation of the ratio Ni/Co. PGE (and Au) abundances are low in all rocks: serpentinites (0,4 -7,2 ppb), gabbros (1,2 - 3,3 ppb) and diorites (1,2 - 4,2 ppb).

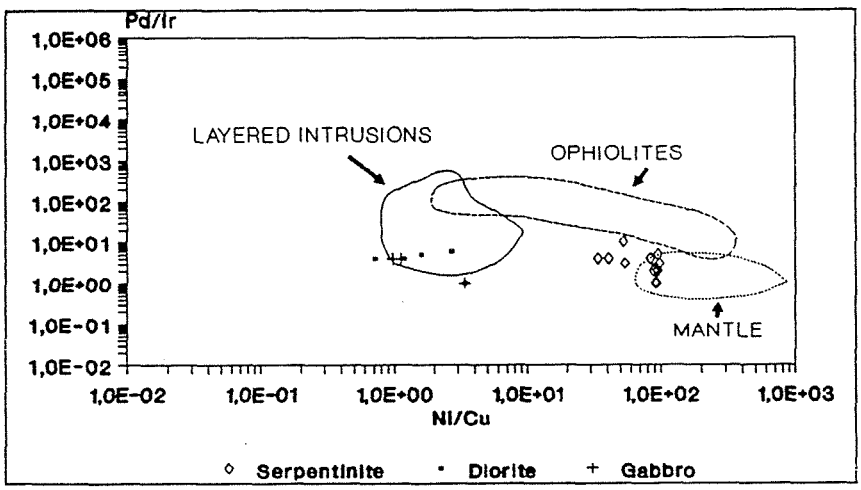

Fig. 2. Mantle-normalized PGE/Ni abundances.

Strongly altered rocks (SERP-15, -16) show no obvious depletion of PGEs. This stresses the assumption that PGEs behave immobile during serpentinization. No consistent lowering of the ratio Pt/Pt+Pd for more evolved rock types can be observed. A relatively uniform distribution of PGEs within the FGC might exist, due to the low S values. A diagram of PGEs and Ni in rock normalized to mantle values (Fig. 2) reveals flat patterns and no absolute enrichment. A relative enrichment of Pt and depletion of Ir in the serpentinites and gabbros is exposed and leads to a slightly positive slope between Ir and Pt. The Pd/Ir versus Ni/Cu metal ratio diagram (simplified after BARNES, 1990) provides a useful discriminant of the tectonic association of ultramafic rocks. The diagram (Fig. 3) highlights the primitive nature of the serpentinites which plot all within or near the mantle field. The gabbros and diorites plot within the layered intrusions field. The removal of olivine during fractional crystallization might link the ultramafic and mafic rocks cogenetically.

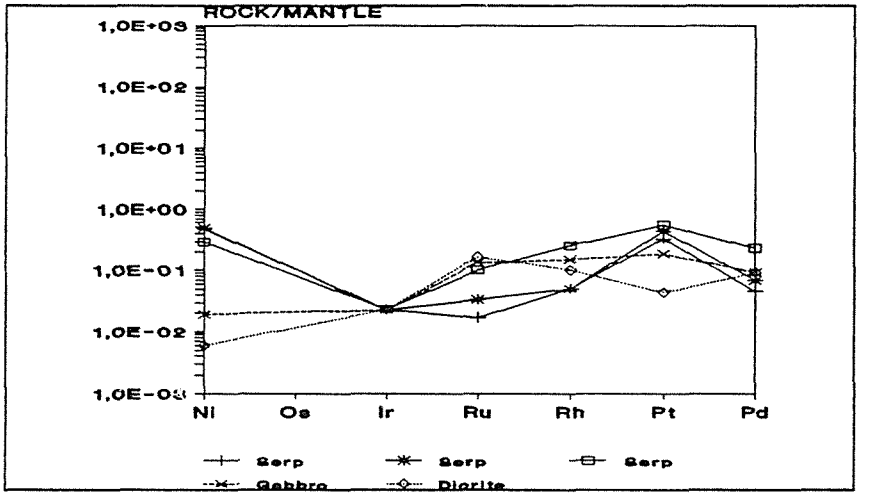

Fig. 3. Pd/Ir versus Ni/Cu metal ratio diagram.

LITERATURE

Barnes, S.-J. 1990. The use of metal ratios in prospecting for platinum-group element deposits in mafic and ultramafic intrusions. J. Geochem. Expl. 37:91-99

Kirsch, H., Kober, B. & Lippolt, H.J. 1988. Age of Intrusion and rapid cooling of the Frankenstein Gabbro (Odenwald, SW-Germany) evidenced by $^{40}Ar/^{39}Ar$ and single-zircon $^{207}Pb/^{206}Pb$ measurements. Geol. Runds. 77: 693-711

Kreher, B., Okrusch, M. & Schubert, W. 1992. Die Gabbrointrusion des Frankensteins (Odenwald): Petrographische und geochemische Betrachtungen zur magmatischen Entwicklung. In: Frankfurter geowiss. Arb., Ser. A, Bd.11, Frankfurt/M., pp. 99-101

Zereini, F. & Urban, H. 1992. Zur Bestimmung von Platingruppenelementen (PGE) in geologischen Proben nach der Nickelsulfid-Dokimasie. Inst. für Geochemie, Frankfurt/M. Open File-Report 1992-1:1-19

Current Research in Geology Applied to Ore Deposits. Fenoll Hach-Ali, Torres-Ruiz & Gervilla (eds) (1993). ISBN 84-338-1772-8

PGM AND ARSENIC Au-RICH MINERALIZATIONS IN SERPENTINITES OF ŚLĘZA OPHIOLITE, S.W. POLAND.

Speczik, S. & Olszy'nski, W.
Faculty of Geology, University of Warsaw, 02-089 Warsaw, al. Zwirki i Wigury 93, Poland

ABSTRACT: Pd-Sb dominated inclusions of PGM alloys were found in millerite associated with the serpentinites of Gogołów-Jordanów massif, Ślęża ophiolite. PGM occurrence in millerites is related to remobilization and fractionation of PGE due to serpentinization of parent rocks. Arsenic Au-rich mineralization is connected with post-collisional ophiolite complex evolution and with migration of secondary fluids.

GENERAL OVERVIEW

The major structure within the area is the gneissic block of Sowie Góry Mts., which is considered to be a massif uprised from the depth or an island that was brought to its position during the closure of Moravo-Silesian basin. Several fragments of oceanic crust e.g. Braszowice, Szklary, Ślęża ophiolites, occur in the surrounding of the Sowie Mts. block (Fig. 1). The largest of them is Ślęża ophiolite complex that represent nearly complete ophiolite suite (Majerowicz 1989). The Sowie Mts. block is thrusted westwards over the obducted Ślęża ophiolite. In Ślęża ophiolite, the older member - metamorphic peridotites is represented by serpentinites of Gogołów-Jordanów followed by ultramafic cumulates of different composition, metagabbros (mafic cumulates), and metabasalts (volcanic member). The degree of serpentinization of metamorphic peridotites is considered to be variable, with domination of intense serpentinized rocks like antigorite serpentinites, chrysolite-antigorite serpentinites with talc, carbonates, chromite, magnetite and scarce relicts of olivine and clinopyroxene.

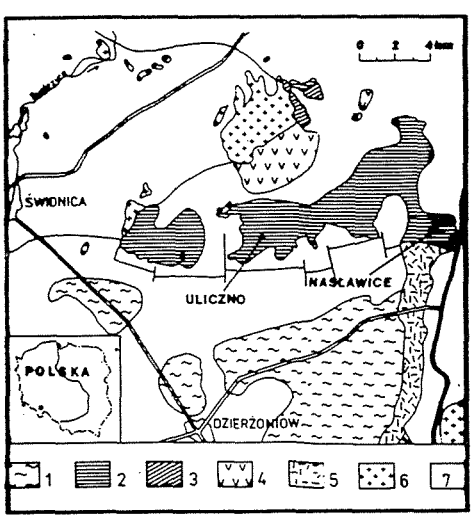

In early 70-ties gold particles were found during routine examinations of heavy mineral fraction of Uliczno stream. This investigation is the first attempt to clear the problem of mother rocks of mentioned alluvial gold. Two concepts were taken under consideration. First, with gold related to processes of serpentinization i.e. asbestos gold veins, and second with gold related to collisional etape of ophiolite evolution i.e. listvenite type mineralization. Therefore, in field works special attention was paid to those locations that were recognized of intense serpentinization, carbonatization, silicification that bear sympthoms of sulphide mineralization. Samples used in this study derived mostly from huge quarry of Nasławice.

Fig. 1. Geologic sketch map of the study area. Precambrian: 1-gneisses of the Sowie Mts. block; Paleozoic: 2-serpentinites, 3-amphibolites, 4-gabbros, 5-mylonites of Niemcza zone, 6-granitoids; 7-Tertiary and Quaternary deposits

Ore mineralization

Several zones up to 5m thick with intense sympthoms of serpentinization or carbonatization with silification were encountered in Nasławice. Gangue minerals are represented by calcite, antigorite, tremolite, talc, quartz and lizardite. Ore minerals consist both of oxides and sulphides. Oxides – magnetite and chromite are nearly unevenly dispersed throughout the rock. Sulphides show more complicated distribution pattern. Millerite forms small droplets, spots that often form larger clusters or patchy distributed agglomerations that cover an area of several square meters. They are connected mostly with strongly serpentinized host rocks.

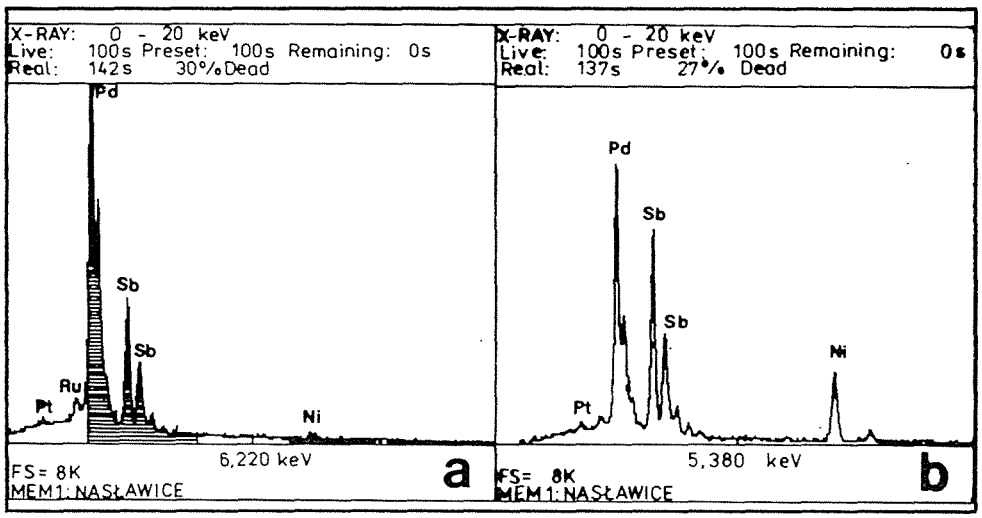

Fig. 2. EDS spectrum of sadburyite (A), and a Pd-Sb-Ni phase (B).

Arsenic minerals i.e. arsenopyrite, loellingite and gersdorffite tend to occur in small veinlets, elongated encrustations or impregnations parallel to zones of silicification. Magnetite is mostly elongated, hypidiomorphic or skeletal, with predominantly fresh appearence while chromite is strongly corroded and replaced, partly by gangue minerals. Chromite grains often show textural and compositional zonation, that is connected with serpentinization (Sałaciński 1992). In reflected light oval with irregular but sharp borders millerite aggregates are composed of millerite microcrystals showing at places changes in colour, reflectivity, anisotropy and other optical properties. By optical means it was found that at places millerite is intergrown by small inclusions of vaesite. Millerite occurs in association with chromite and magnetite but never with arsenic minerals. Some relict textures in millerite may suggest that it may be to some extent a pseudomorph after pentlandite.

Among arsenic minerals dominate hypidiomorphic arsenopyrite over loellingite and gersdorffite. Loellingite and arsenopyrite tend to occur together while gersdorffite forms more individual crystals. Contacts of arsenic minerals do not reveal sympthoms of corrosion and replacement by gangue minerals. The amount of arsenic minerals in some places reaches up to 10%/vol.

MICROPROBE INVESTIGATIONS

Microprobe investigations were performed with a use of Jeol microprobe,

a sample current of 15 nA with an accelerating potential 15 and 20 kV were applied. Back-scattered images and single element scans were used to identify the sourface outline of the compositional differences of PGM phases. Microprobe revealed that the observed changes in optical properties of some millerite aggregates are related to changes in mineral composition, mostly to different molecuar relations between sulphur and nickel. The occurence of a mineral that corresponds to stoichiometric vaesite was confirmed by microprobe as well as other minerals of Ni-S system were found. Some of their compositional varieties correspond to stoichiometric heazlewoodite and godlewskite.

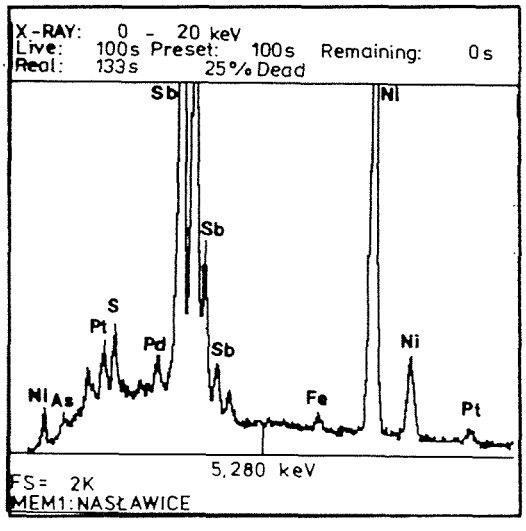

During millerite aggregates investigations (in magnifications higher than 10000X) it was found that on borders of some millerite crystals minute inclusions of very high reflectivity mineral occur. These oval, irregular inclusions show often sector type texture with generally lighter inner zones. Lighter parts are composed of Pd and Sb with minor admixture of Ni. Composition of lighter phase is close to stoichiometric sadburyite (Fig. 2A). Darker parts reveal increased content of Ni relative to Pd and Sb and common but small admixture of Pt and Ru (Fig. 2b). The Ni content may be partly related to matrix effect.

Fig. 3. EDS spectrum of breithauptite.

During the microprobe investigations of millerite also small intergrowths of mineral phases corresponding compositionaly to breithauptite (Fig. 3) and nisbite were encountered. The occurence of breithauptite was later confirmed also by optical means.

Back-scattered and x-ray images suggest increased amount of Au in all arsenic minerals. It is illustrated on single element scans for S (A) and Au (B) of loellingite and arsenopyrite aggregate (Fot. 1 - scale bar 0.5 mm). To the contrary millerite aggregates are devoid of Au. As suggested by single element scans Au is nearly unevenly dispersed in arsenic minerals. Chemical analysis of arsenic minerals (ASA) suggest that amount of Au in investigated arsenic minerals reaches up to 100 pms.

DISCUSSION

The association of PGM inclusions with ophiolitic chromite have been recently reported from several locations, however the occurrence of PGM in ophiolitic sulphides is reported extremaly rare (Mc Elduff & Stumpfl 1990, Thalhammer & al. 1990). PGM have not been yet found in chromites of Gogołów-Jordanów massif, and reported PGE alloys in millerite represent first finding of PGM in Ślęża ophiolite. Two generations of PGM have been recognized in the Troodos ophiolite. The first composed of Ru-Os-Ir sulphides has been formed during chromite formation, the second composed mostly of alloys during serpentinization (Mc Elduff & Stumpfl 1990). Parallely to in Hochgrössen and Kraubath ultramafic massifs alloys are thought to be formed after chromite (Thalhammer & al. 1990).

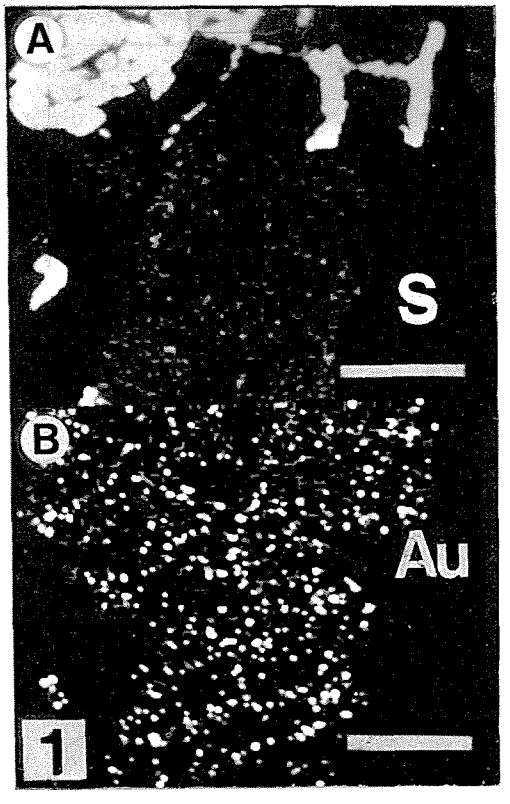

The Pd-Sb dominated composition of investigated PGE alloys is similar to those reported from Hochgrössen and Kraubach. The amount of PGE in matrix pentlandites is generally low, too low to account separately for PGE content in studied millerites of Gogołów-Jordanów. Therefore, the process that may led to Pd-Sb enrichment in millerites ought to be suggested. This process was credibly similar to that proposed by Thalhammer & al.(1990) with hydrothermal remobilisation of Pd, Pt and Ru from chromites and magmatic sulphides during serpentinization. They may have been transported together with Ni as bisulfide or chloride complexes of neutral and alkaline pH and deposited due to drop of temperature. The role of serpentinization processes in PGE remobilization and fractionation is challenged by some authors (Barnes & al. 1985).

Preliminary data, collected so far, suggest no links between millerite and arsenic Au-rich mineralizations It seems that arsenic mineralization is related to post-collisional events rather than to serpentinization, as millerite aggregates are recognized of low Au content.

CONCLUSIONS

Basing on presented preliminary data it is suggested that PGM mineralization is connected with primary content of these metals in sulphide phase of metamorphic peridotites. They were later due to processes of serpentinization locally redistributed and included in secondary minerals of Ni-S system. Arsenic and related Au mineralizations are connected with collisional events and migration of secondary fluids of mostly intraformational origin. They may have leached arsenic and gold from mother ophiolite rocks.

REFERENCES

Barnes, S.J., Naldrett, A.J. & Gorton, M.T. 1985. The origin of the fractionation of platinium-group elements in terrestrial magmas. Chem. Geol. 53:303-323

Majerowicz, A. & Pin, C. 1989. Recent progress in petrologic study of the Ślęża Mts. ophiolite complex. In: Int. Conf. Lower and Upper Paleozoic metabasites and ophiolites of the polish Sudetes. Wrocław, pp 34-72

McElduff, B. & Stumpfl, E.F. 1990. Platinium-group minerals from the Troodos ophiolite, Cyprus. Min. and Petrology. 42:211-232

Sałaciński, R. 1992. Origin of ore mineralization in mafic and ultramafic rocks of the Sowie Mts. block surrounding. Geol. Sudetica. 26:1-34

Thalhammer, O.A.R., Prochaska, W. & Mühlhans, H.W. 1990. Solid inclusions in chrome spinels and platinium group element concentrations from the Hochgrössen and Kraubath ultramafic massif (Austria). Contrib. Mineral. Petrol. 105:66-80

Current Research in Geology Applied to Ore Deposits. Fenoll Hach-Ali, Torres-Ruiz & Gervilla (eds) (1993). ISBN 84-338-1772-8

Au-Fe ASSOCIATIONS IN SILICATE PHASES AS EVIDENCE OF GOLD TRANSPORTATION IN AQUA-COMPLEXES

Stenina, N.G. (1); Distanova, A.N. (1); Berezin, Y.A. (2)
(1) Inst. of Geology SB RAN, Novosibirsk, Russia
(2) Inst. of Pure and Applied Mechanics, Novosibirsk, Russia

ABSTRACT. Au-Fe impurity inhomogeneities of submicron-micron size predicted on the basis of the mechanism of silicate substance redeposition via aqua-complexes $2SiO_3-H_2O-2Me^{+}Me^{3+}O_4$ are established by means of TEM and X-ray microanalysis in the minerals of granites. Quantum-chemical bases of the Au-Fe association are given. The investigation proves that the complex $2SiO_3-H_2O-2AuFeO_4$ is responsible for gold migration and concentration in the processes of rocks transformations from country gabbro to granites.

1 INTRODUCTION

Transition of gold from invisible state in mineral phases to the native metal in quartz loads is the principal problem of the formation of mining gold deposits. The known approaches to its solution are based on the data of petrological-mineralogical, geochemical and experimental studies. In two first cases these observations give only indirect information because they register the consequence of the mineral forming process. The experiments can not reproduce all complexities of natural systems.

Defects of crystal structure of minerals are caused by the conditions of minerals and rocks formation and transformation. Therefore they may be considered as the genetic code carrying the primary information on the laws of evolution of ore forming systems. The methods of transmission electron microscopy (TEM) is the single direct way to study microstructural features of minerals. The approach based on TEM combined with other methods data is used to investigate the mechanism of gold concentration in the processes of rocks transformations from wall gabbro to granites.

2 PETROLOGY AND GEOCHEMISTRY

The Paleozoic Kaakhem pluton rocks (Tuva, Altai-Sajan folded region, Russia) are the object of investigation. Pluton is emplaced in the sedimentary-volcanogenic rocks; gabbroid bodies of earlier mafic complex intrude them. The enclosing altered gabbroids and pluton rocks are ranged from quartz diorites and tonalites to high sodic granites and dyke leucocratic granites that indicate the principal role of transmagmatic fluides in this evolution (Distanova, 1981). The Kaakhem pluton belongs to the specific type of gold bearing granitoid plutons known in Altai-Sajan, Ural, North Kazakhstan regions. They are emplaced in the femic volcanogenic rocks having hightened clark of gold. Both this fact and the numerous evidences of interaction of granitoids with country mafic rocks allowed to Scherbakov (1967) and other explorers to conclude that they are the initial source of gold. The gold mineralization in scarns, quartz loads and stockworks in Kaakhem pluton are always related to relict gabbroid bodies. Gold bearing quartz loads and stockworks are often located in dyke granite bodies of granitoid complex. The increasing concentration of gold from the clark contents invisible in the minerals of wall

gabbroids up to the native gold in leucocratic granites shows that the process of granitization played the role of "mobilization" of gold.

There exists a lot of mineralogical-geochemical evidences of the positive Au-Fe correlation in the processes of rocks transformations with the participation of water. The siderophile gold behavior may be traced from the geological processes of the early history of the Earth (Brimhall, 1991) up to the formation of Au-Fe quartz loads (Naschwitz & Van Moort, 1991).

3 NEW DATA ON THE MECHANISM OF SILICATE SUBSTANCE TRANSFORMATIONS

The previous studies (Stenina & Distanova, 1991[1]) have shown that redeposition of silicate substance in rocks of Kaakhem pluton occurs via aqua-complexes $2SiO_3 - H_2O - 2MeO_4$ in which the position of Me may be occupied by Me^{3+}; Me^{+} is out of place ion-compensator. A model of granitic melt was proposed, whereby a "granitic magma" is a macroscopically extended network of water-, silica- and metal-oxide tetrahedra (Stenina & Distanova, 1991[2]). Basing on these data a new conception of quartz as an open system of natural chemical compound has been formulated (Stenina, 1991). According to it quartz incorporates water with various metal-oxide radicals and due to this its crystallchemical state changes. The known mineral forms of silica: citrine, amethyst, smoke quartz, opal, etc. record only the specific moments of the evolution of the fluid-silicate systems.

Basing on this mechanism we proposed that the form of complex responsible for gold migration and concentration in the processes of silicate substance redeposition is $2SiO_3 - H_2O - 2Au^{+}Me^{3+}$. The break of weak bonds in this complex explains the location of native gold in reef quartz. This hypothesis was experimentally confirmed by TEM and X-ray observations of Au-rich impurity defects (see Fig. 2 a, b in Stenina and Distanova, 1991[2]) interpreted as the segregations of aqua-complexes.

4 DISCUSSION AND EXPERIMENTAL EVIDENCES OF AU-FE WATER COMPLEXES

The geological data on the parallel Au and Fe migration in the processes of rocks transformations can not be the reliable basis for the determination of Me^{3+} as Fe^{3+} within aqua-complex $2SiO_3 - H_2O - 2Au^{+}Me^{3+}O_4$. The direct evidences may be received only during the studies of real structure of minerals. Quartz behavior under electron irradiation is an indicator of the chemical nature of elements occupying interstitial positions Me^{+} and tetrahedral ones Me^{3+} located at the defective domains of its framework. Quartz of granites changes its crystallchemical state under electron irradiation but doesn't amorphise. Contrary to this quartz of pegmatites having $Al^{3+} \rightarrow Si^{4+}$ and Na^{+} as an interstitial ion-compensator, transits to amorphous state in some minutes of irradiation (Stenina et al., 1984). These data allow us suppose that Au-partner within aqua-complex is Fe^{3+}. There are the following theoretical bases.

The chemical inertness of Au is caused by the structure of outer electron orbitals $5d^{10}6s^{1}$. The energy of the single electron removal from the 6s-orbital (the first ionization potential) is high (9.2 ev) as the previous 5d orbital, completely filled with electrons, has a configuration of two crossing dumb-bells with a minimum of electron density near the

domain of crossing. Therefore the 6s electron having the spherical symmetry can be represented as locating in the wells of an electron density distribution of 5d-electrons. The eventual Au-partner candidate within aqua-complex has to decrease maximally its first ionization potential. This follows from the requiments of the free energy minimum, i.e. from the condition of complex stability. Quantum mechanical arguments indicate that this metal is sure to have the similar structure of outerelectron orbitals (ds) but with a lower principal quantum number. This directs the search for the eventual candidate among the transition metals of the VIII-th group of the Mendeleev's Table. The analysis of their outer ds orbitals shows that Fe ($3d^6 4s^2$) is the most suitable element. There are two arguments for this: 1) Fe has two s-electrons that reduce the energy of exchange interaction between the electrons of d- and s-orbitals to the minimum; 2) it has the most number of vacancies on the d-orbitals among the transition metals of the fourth period.

Au-Fe association within aqua-complex is proved as a result of studies of granites thin sections by X-ray microanalysis. The photos of Fig. 1, representing the images of the same part of the granite surface, made in X-rays of Au and Fe, show, firstly, their coincidence in minerals of granite and, secondly, which is the most important, the close coincidence of Au and Fe in the impurity inhomogeneities in plagioclase and sphen. Basing on the electron microscopical data (Fig. 2) these impurity inhomogeneities are interpreted as the segregations of aqua-complexes, captured from the mineral-forming medium during the crystallization of mineral phases. Simultaneous presence of Fe and Au in impurity inhomogeneities of nonferrous minerals (plagioclase, sphen, quartz, and others) may be considered firstly as an experimental evidence of the metals transport by aqua-complexes and secondly as they are responsible for the Au-Fe association.

5 CONCLUSIONS

It may be concluded that iron plays the principal role in the formation of mining gold deposits. This conclusion is confirmed on the all levels of observations of the natural

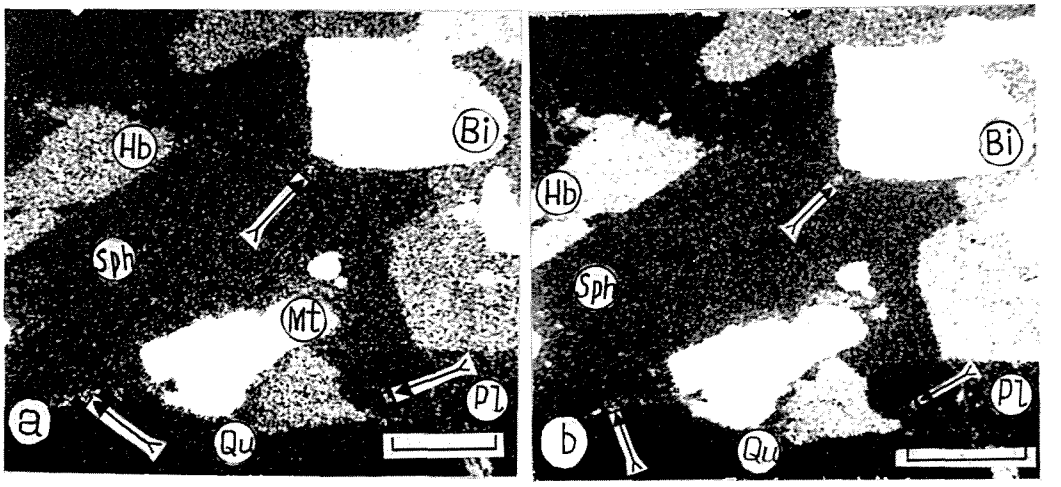

Fig. 1. X-ray images of the granite thin section. Mineral grains are marked: Mt – magnetite, Bi – biotite, Hb – hornblende, Sph – sphen, Qu – quartz, Pl – plagioclase. Au-Fe impurity inhomogeneities are pointed. a – FeK_α, exposure – 20 min, b – AuK_α, exposure – 72 min; scale bar = 20 μm.

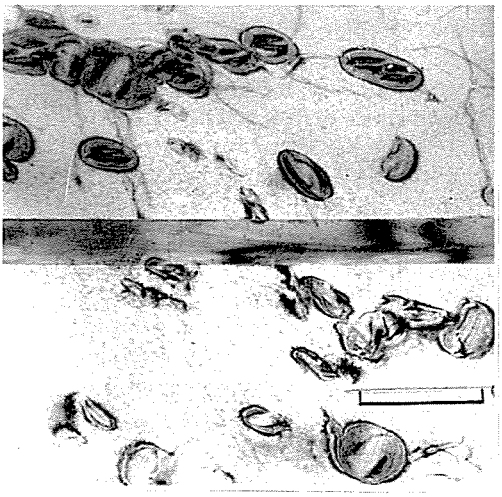

Fig. 2. TEM image of impurity defects, interpreted as the segregations of aqua-complexes $2SiO_3 - H_2O - 2Au^{+}Fe^{3+}O_4$ captured from the mineral-forming medium during crystallization. The defects known as "voids" are amorphous ("glass-like"), scale bar = 1 μm.

matter: magmatic associations, rocks, minerals and finally – on the level of fine peculiarities of the minerals inner structure. The results of this investigation may be considered on the one hand, as one more argument of the idea, that the defects of minerals structure are their genetical code; on the other hand, the experimental evidence of the existence of aqua-complexes. Quantum-chemical approach in the analysis of metal pairs within aqua-complexes manifest itself as a perspective way for determination of the nature of geochemical association.

REFERENCES

Brimhall, G. 1991. The genesis of ores. Scientific America. 5: 84-91.

Distanova, A.N. The structure of plutons and composition peculiarities of the early paleozoic granitoids (Kaakhem region, East Tuva). In: Poljakov, G.V. (ed.). Magmatic complexes of folded regions of South Siberia [in Russian]. Nauka, Novosibirsk, pp. 24-62.

Naschwitz, W. & Van Moort, J.C. 1992. Geochemistry of wall rock alteration, Rosebery Tasmania, Australia. Applied Geochemistry. 6: 267-278.

Scherbakov, Yu.G. 1967. Distribution and concentration conditions of gold in ore regions [in Russian]. Nauka, Moscow.

Stenina, N.G. 1991. Quartz as an indicator of the structure of a mineral-forming medium containing ore elements. In: Pagel, M. & Leroy, J. (eds.). Source, Transport and Deposition of Metals. Balkema Rotterdam, pp. 227-229.

Stenina, N.G. & Distanova, A.N. 1991[1]. Structural-chemical transformations of silicate minerals as the indicator or their genesis (on the example of Kaakhem pluton rocks, Tuva) [in Russian]. AIGG & M RAN Novosibirsk.

Stenina, N.G. & Distanova, A.N. 1991[2]. The nature of granitic melt and its ore potential. In: Pagel. M. & Leroy, J. (eds.). Source, Transport and Deposition of Metals. Balkema Rotterdam, pp. 821-824.

Stenina, N.G. et al. 1984. Structural state and diffusion of impurities in natural quartz of different genesis. Phys. & Chem. Minerals 10: 180-186.

Current Research in Geology Applied to Ore Deposits. Fenoll Hach-Alí, Torres-Ruiz & Gervilla (eds) (1993). ISBN 84-338-1772-8

PGE MINERALIZATION ASSOCIATED WITH SILICATES WITHIN THE SIIKA-KÄMÄ PGE REEF, PORTIMO LAYERED COMPLEX, FENNOSCANDIAN SHIELD, FINLAND: AN UNUSUAL MINERALIZATION TYPE

Thalhammer, O.A.R. (1); Saini-Eidukat, B. (1); Iljina, M.J. (1,2) & Alapieti, T.T. (2)
(1) Inst. of Geological Sciences. Mining University Leoben, A-8700 Leoben, Austria
(2) Dept. of Geology. University of Oulu, P.O. Box 400, SF-90571 Oulu, Finland

ABSTRACT: PGM's associated with silicates occur as a specific type of PGE mineralization in early Paleoproterozoic layered intrusions in northeastern Finland. This mineralization type occurs in a zone close to the boundary between a Cr-rich and a Cr-poor parental magma-type. PGM's occur as inclusions within hornblende rims of zoned amphiboles, or in chlorite schists of unusual geochemistry. Apart from a late and post-magmatic pre-concentration of PGE in this zone, we attribute the pervasive alteration of this zone and re-concentration of PGE's to metamorphic and deformational processes which occurred during the Svecofennian orogeny, some 600 my after the magmatic event.

Introduction and General Geology:

Paleoproterozoic (≈ 2440 my) layered intrusions occur scattered over a large area of the northeastern part of the Fennoscandian Shield from the Swedish/Finnish border in the southwest to the Kola peninsula, Russia in the northeast (Fig. 1; Alapieti et al. 1989;

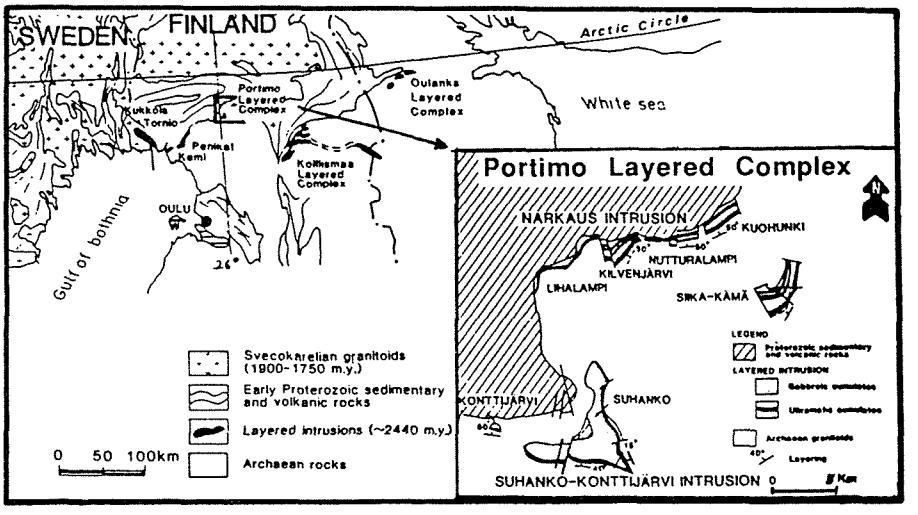

Fig. 1 General geological sketch map of the northeastern part of the Fennoscandian Shield showing the location of the Paleoproterozoic layered intrusions. Inset shows a magnification of the Portimo Complex with its intrusion blocks. Map taken from Alapieti et al. (1990).

1990). The layered intrusions are located within the late Archean basement complex or at the contact between that and overlying Proterozoic volcanics and sedimentary

sequences. The intrusions generally comprise a basal marginal series, followed by a layered series in which several megacyclic units (MCU) can be distinguished. Each MCU is formed by ultramafic rocks at the bottom and a series of gabbroic rocks above. The Koillismaa Complex (Fig. 1) is additionally characterized by a thick cap of granophyres. The intrusions have undergone a complex history of deformation and metamorphism after their emplacement and crystallization. Metamorphic and deformational overprint resulted in alteration of the primary magmatic mineralogy to greatly varying extents, and in breaking up of the intrusions into several tilted blocks (Alapieti et al. 1990). On the basis of geochemical investigations, two different parental magma types can be distinguished: one type shows boninitic affinities (Cr-rich type) and the second type is Cr- and MgO-poorer (further details about the geochemistry and its significance are given by Saini-Eidukat et al., 1993, this volume).

PGE mineralization types in the Kemi-Koillismaa-Oulanka intrusion belt

An unusually great variety of PGE mineralization types has been found in these intrusions. The following types have been studied in detail during extensive exploration activities of Outokumpu Finnmines Oy and Lapin Malmi, and have been described in several papers from the research group of Oulu University (Alapieti, 1989; Mineral. Petrol., v. 42, 1990):

(a) PGE-mineralization in association with chromite

PGE-enrichment occurs either in massive chromitites or associated with disseminated Cr-spinels.

(b) The offset mineralization

The offset mineralization is restricted to the Narkaus Intrusion (Portimo Complex, Fig. 1) and hosted by the basement complex close to the basal contact of the intrusion. The offset type is characterized by varying amounts of mainly Cu-sulfides with PGM's. The highest published PGE-contents are up to 24 ppm for Pd and up to 14 ppm for Pt.

(c) PGE mineralization in association with disseminated sulfides

This type shows erratic distribution mainly within the marginal series of the intrusion complexes and has been also found in the pre-intrusion dykes of the Suhanko-Konttijärvi intrusions (Portimo Complex, Fig. 1; Iljina et al. 1992), and may extend downwards into the basement granitoids. PGE-contents up to approximately 50 ppm, but mostly lower, have been encountered in association with Cu-Ni-sulfides.

(d) Massive pyrrhotite-PGE mineralization

The mineralization is formed by massive pyrrhotite lenses or slabs of 20 cm to 15 m in thickness within the marginal series of the Suhanko-Konttijärvi intrusion (Portimo Complex, Fig. 1). PGE-content is in the range of a few 100 ppb to 4 ppm, but reaches 20 ppm in one location .

(e) 'Reef'-type mineralization in the layered series

'Reef'-type PGE concentrations, normally base metal sulfide- or chromite-bearing, are occasionally characterized by abundant PGM associated with silicates and without BMS or chromite. This mode of PGE mineralization is found in the Penikat intrusion, where the SJ Reef contains up to 156 ppm Pd and 52 ppm Pt (Halkoaho et al., 1990a); the AP Reef, up to 11 ppm Pd and 3 ppm Pt (Halkoaho et al., 1990b); and the PV Reef, up to 2 ppm Pd and 4 ppm Pt (Huhtelin et al., 1990). It also occurs in the Suhanko-Konttijärvi intrusion (Rytikangas Reef, up to 20 ppm Pd+Pt, Iljina et al., 1992) and in the Siika-Kämä Reef of the Narkaus intrusion; the latter is described in more detail below.

PGM's associated with silicates in the Siika-Kämä Reef

PGM's associated with silicates are one of the peculiar mineralization types in the layered intrusion belt. One of the best examples of this mineralization and focus of this paper are certain parts of the Siika-Kämä Reef (Huhtelin et al., 1989) in the Narkaus intrusion (Fig. 1). The reef occurs in the contact zone of the Cr-rich and Cr-poor magma types which is also a lithological boundary with gabbros below and ultramafics above the contact. However, this type of PGE-mineralization occurs not only in the Narkaus intrusion but also in the Suhanko-Konttijärvi and in the Penikat intrusions, and is there, most significantly, positioned in the same contact zone.

The mineralization is hosted either by pyroxene-plagioclase, ultramafic or gabbro pegmatoids, or by chlorite schists. The cumulates are strongly altered which is displayed by an almost complete replacement of the primary magmatic mineralogy. The rocks are composed of zoned amphibole grains and altered plagioclase in an amphibole (hornblende) and chlorite matrix. The zonation of the big amphibole grains is defined by an actinolite core and a hornblende rim.

The chlorite schists form stratiform bodies broadly concordant to the magmatic stratigraphy, or may be dyke-like bodies cross-cutting the magmatic stratigraphy. Both types occur within the ultramafic metacumulates mentioned above. They are composed of >90% chlorite and of subordinate white mica, euhedral magnetite and accessory Cr-spinel. Their geochemistry, characterized by high MgO, Al_2O_3 and Cr, and low SiO_2 contents, is considerably depleted in most of the trace elements and REE (Fig. 2a).

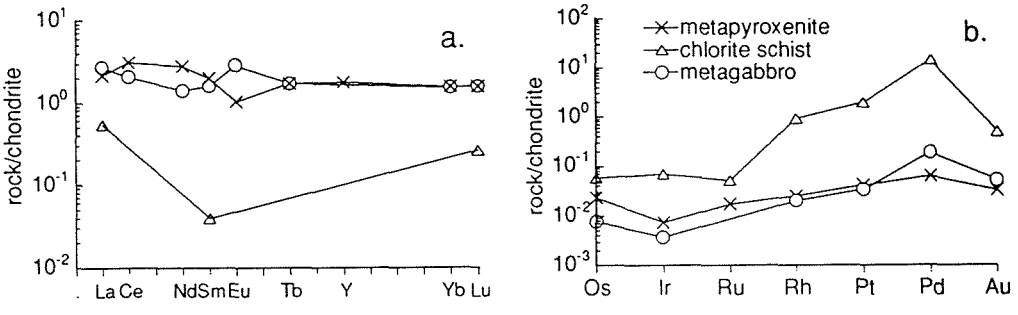

Fig. 2 a - Chondrite-normalized REE patterns of a metapyroxenite (host rock of the chlorite schist), a metagabbro (underlying the chlorite schist) and a chlorite schist. Symbols are as on Fig. 2b.
b - Chondrite-normalized PGE patterns of the same rock types as in Fig 2a.

When observed on a broad scale the Siika-Kämä Reef is sulfide associated (Huhtelin et al., 1989). In detail, however, two types of PGM–silicate associations can be distinguished:

i) In the strongly altered cumulates the PGM's, mainly Pd-Bi-Te-phases, are predominantly included in hornblende rims surrounding actinolite cores. The actinolite cores, however, are characterized by abundant mainly Cu-sulfide inclusions.
ii) In the chlorite schists the PGM's consist of sperrylite and Pd-As-Sb-phases, and occur between the silicate minerals. Total PGE-contents are up to 11 ppm, and can be considerably higher than those from the surrounding host rocks (Fig. 2b).

Discussion

The silicate-associated PGE mineralizations in the Siika-Kämä Reef display two striking features:

a) the obvious separation between sulfide and PGM inclusions in amphiboles of the altered cumulates. The former occur in actinolite cores, whereas the PGM inclusions are concentrated in hornblende rims or groundmass hornblendes,
b) the unusual mineralogical and chemical composition of the chlorite schists hosting high-grade PGE-mineralization, which resemble those of the SJ Reef (Penikat intrusion).

Sulfide- and PGM-inclusions in amphiboles

The zoned nature of the amphiboles is interpreted as the result of a prograde metamorphic evolution, possibly due to the 1.9–1.7 Ma Svecofennian orogeny. This conclusion is made by analogy to the strong effects this orogeny had on nearby metakomatiites (Gruau et al., 1992). We further propose that Fe, Ni, Cu and PGE were remobilized and precipitated from a metamorphic fluid. The separation of sulfides and PGM could be explained by a change in redox conditions during prograde metamorphic evolution. At lower Fe^{2+}/Fe^{3+} ratios, sulfides were included in actinolite cores, and an increase of the redox potential may have led to entrapment of PGM in hornblende rims.

The chlorite schists

The peculiar geochemistry of the chlorite schists can not be explained by magmatic processes alone. Therefore we suggest a complex history for the origin of this rock type. The ultramafic lithology at the contact between the two MCU's may have been a zone of weakness that was used as a pathway for fluids. We tentatively propose that the precursor rock type of these chlorite schists was initially affected by late- or post-magmatic metasomatism leading to a pre-concentration of PGE. In the course of metamorphism and deformation this "weak" zone was re-activated and suffered intensive metamorphic fluid circulation. As a result the rock was strongly chemically altered leading to its present chemical composition and to the redistribution and re-concentration of PGE. This scenario may also have been responsible for the formation of similar rock types and mineralization in the SJ Reef of the Penikat intrusion.

References

Alapieti, T.T., ed., 1989. 5th International Platinum Symposium: Guide to the post-symposium field trip, August 4-11, 1989. 29, Geological Survey of Finland, Espoo.

Alapieti T.T., Filen B.A., Lahtinen J.J., Lavrov M.M., Smolkin V.F. & Voitsekhovsky S.N. 1990. Early Proterozoic layered intrusions in the northeastern part of the Fennoscandian Shield. Mineralogy & Petrology 42: 1-22.

Gruau, G., Tourpin, S., Fourcade, S. & Blais, S. 1992. Loss of isotopic (Nd, O) and chemical (REE) memory during metamorphism of komatiites: New evidence from eastern Finland. Contrib. Mineral. Petrol. 122:66-82.

Halkoaho, T.A.A., Alapieti, T.T., and Lahtinen, J.J. 1990a. The Sompujärvi PGE Reef in the Penikat layered intrusion, northern Finland: Mineralogy & Petrology 42: 39-55.

Halkoaho, T.A.A., Alapieti, T.T., Lahtinen, J.J., and Lerssi, J.M. 1990b. The Ala-Penikka PGE Reefs in the Penikat layered intrusion, northern Finland: Mineralogy & Petrology 42: 23-38.

Huhtelin, T.A., Lahtinen, J.J., Alapieti, T.T., Korvuo, E., and Sotka, P., 1989. The Narkaus intrusion and related PGE and sulphide mineralizations. In Alapieti, T. (eds.) 5th International Platinum Symposium - Guide to the Post-Symposium Field Trip. Geological Survey of Finland, Espoo, pp. 145-161.

Iljina M.J., Alapieti T.T. & McElduff, B. M. 1992. Platinum-group element mineralization in the Suhanko-Konttijärvi intrusion, Finland. Austral. J. Earth Sci. 39: 303-313.

Saini-Eidukat B., Thalhammer O.A.R., Alapieti T.T., Halkoaho T.A.A. & Iljina M.J. 1993. Controls on PGE mineralization in the early Paleoproterozoic Kemi-Koillismaa Oulanka mafic intrusion belt, Fennoscandian Shield (this volume).

Current Research in Geology Applied to Ore Deposits. Fenoll Hach-Alí, Torres-Ruiz & Gervilla (eds) (1993). ISBN 84-338-1772-8

THE FRACTIONATION OF PGE IN ZONED ULTRAMAFIC COMPLEXES: THE CONDOTO COMPLEX, N.W. COLOMBIA

Tistl, M.
Ostpreussendamm 182 B, D-1000 Berlin 45, Germany

ABSTRACT: Zoned ultramafic complexes ("Alaskan Type Complexes") and related peridotites within Mg-rich basalts are the sources of placer platinum in NW-South America (NW-Ecuador to NW-Colombia). One of the richest alluvial platinum deposit occurs along the Condoto river which has its source in a zoned ultramafic complex (Alto Condoto Complex). The zonal arrangement of this 20 Ma-old zoned intrusion includes a magmatic rock sequence ranging from dunite to hornblendite. The different petrographic units are cumulates formed by fractional crystallization of a Mg-rich basaltic magma.

Parts of the central dunite are anomalously enriched in PtFe- and in minor degree in IrOs-alloys. The platinum-group elements (PGE) in all other lithologic units of the complex display a fractionation trend with a general increase of total PGEs from wehrlite to hornblendite. This "normal" trend is best described by increasing Pd and decreasing Ir abundances.

The controlling factor for PGE mineralization in zoned ultramafic complexes seems to be PtFe-alloy precipitation during olivine crystallization. This may be initiated by rapid tectonic movements causing pressure decrease and overheating of the magma, with PGE-alloy formation as a result of the fO_2 shift during olivine crystallization.

THE ZONED ULTRAMAFIC CONDOTO COMPLEX

The zoned ultramafic Condoto complex is one of a series of Tertiary complexes that occur along the Colombian Western Cordillera. It has an elliptical form (8 x 5 km) with concentrical shells of dunite in the core, wehrlite, olivine clinopyroxenite, hornblende-(magnetite) clinopyroxenite, and hornblendite towards the margin. A very heterogeneous unit occurs between clinopyroxenite and contact metamorphic hornfelses which includes metasomatically altered clinopyroxenites, contact anatectic and metamorphic rocks of the pyroxene hornfels facies. Typically, this unit is intruded by hornblende-plagioclase dykes.

A 200 x 300 m area of the central dunite is mineralized with PtFe-alloys ($\approx Pt_3Fe$) that occur as accessory minerals (Burgath & Tistl, 1993). The PtFe-alloys are euhedral (cubic) single crystals up to 1 mm in diameter, frequently with skeletal growth and growth defects. Crystal aggregates of PtFe greater than 13 mm in size are found sporadically. Some Os-lamellae are intergrown with PtFe, but other PGMs are very rare (Weiser et al. 1993). PGM/chromite intergrowths occur but are not common. Within this central zone chromite occurs in the form of disseminated grains as well as in form of irregular nodules (< 5 cm in diameter) and schlieren; however, larger or continuous chromitite lenses are not typical.

PGE's IN CUMULATE ROCKS OF THE ZONED ULTRAMAFIC COMPLEX

The total PGE contents average 43 ppb in dunites and olivine clinopyroxenites, and 136 ppb in magnetite-hornblende clinopyroxenites. The average PGE contents of the different lithologic units is shown in Fig. 1. Pt is clearly enriched in dunites. From wehrlites to hornblendites Pt correlates positively with Pd.

The strongly increasing Pd/Ir ratios from dunite to hornblende-magnetite clinopyroxenites (Fig. 2) shows the strong depletion of the magma in Ir which is incorporated into early crystallizing mineral phases (IrOs alloys). In contrast, Pd does not partition into early mineral phases, and is enriched during fractional crystallization. Pt, generally regarded to behave similar to Pd, or even to be more incompatible, is clearly enriched in dunites, but follows the "normal trend" parallel with Pd in all other rock types. This trend with increasing Pd/Ir ratios reflects the normal fractional crystallization of a Mg-rich basaltic magma.

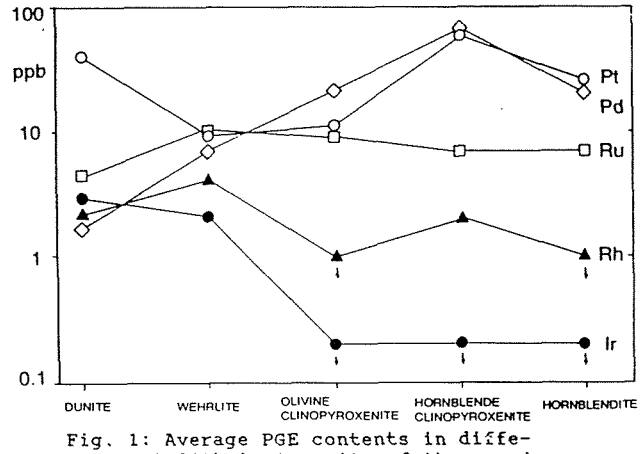

Fig. 1: Average PGE contents in different lithologic units of the zoned ultramafic complex of Condoto.

The precipitation of PGM in the zoned complex occurred contemporaneous, but independent to that of chromite (Burgath & Tistl, 1993). However, there is no positive correlation between PGE and Cr

in the PGE mineralized dunites as known in other PGM-bearing ultramafic units. The principal factors controlling the precipitation of both chromite and Pt are the fO_2 and fS_2 conditions within the magma (Von Gruenewaldt et al., 1989).

Therefore, the cogenetic assemblage of chromite and PGMs should have rather mechanical causes like the occasional trapping of PGM-crystals by simultaneously crystallizing and settling chromite grains than geochemical ones.

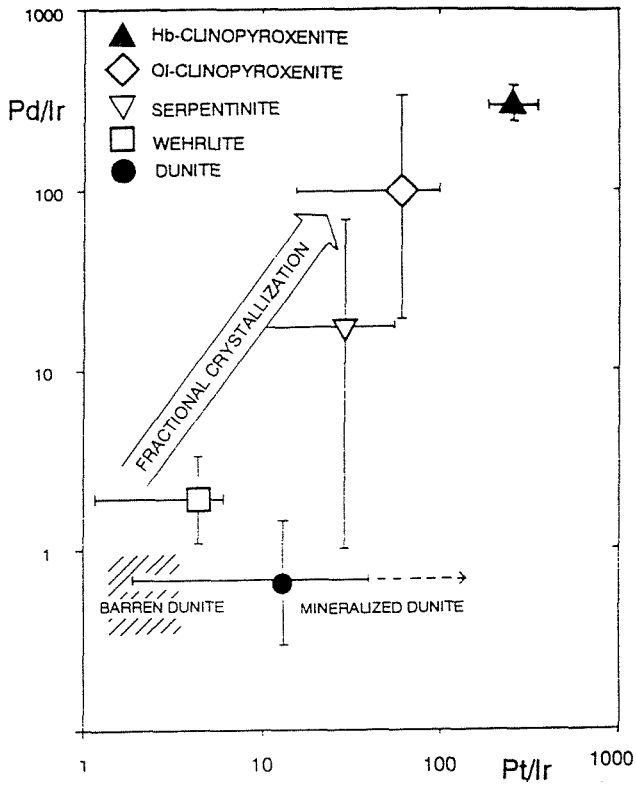

Fig. 2: Pd/Ir versus Pt/Ir diagram of different lithologic units of the zoned ultramafic complex of Condoto.

The PtFe-alloys are high-temperature segregations that have formed in an early phase of crystallization directly from a silicate melt. In an early stage of fractional crystallization Ir and Os form alloys while Ru crystallizes as a sulfide (RuS_2). However, the distribution patterns of Ru with constant contents in all rock types, and the rare occurrence of laurite, suggest that the Condoto magma never reached sufficiently high fS_2 for effective laurite crystallization. Such rarity of Ru-sulfide is known from other zoned ultramafic complexes (Nizhnii Tagil; Razin, 1976, and Tulameen; St. Louis et al., 1986). In this respect the evolution of zoned ultramafic intrusions clearly differs from that in ophiolites or layered mafic intrusions.

Although the degree of partial melting may influence the total availability of PGEs, with increasing Ir, Os, and Ru contents at higher melting rates, the formation of PtFe-mineralizations in zoned ultramafic complexes requires no Pt-enriched parental source. The more important factor is effective PtFe precipitation during the olivine crystallization stage, which can be initiated by changes of the physical conditions of the magma. Rapid pressure drop displaces

the melt solidus towards lower temperatures with concomitant overheating of the melt followed by rapid crystallization of IrOs-, PtFe-alloys, chromite, and olivine. The crystallization of olivine leads to an increase in fO_2 of the melt which lowers the solubility of Pt and Ir (Amossé et al., 1987). The light PGEs (Ru, Rh, Pd) can not form stable minerals at these pT conditions. This possibly very short episode of effective PtFe-alloy, chromite, and olivine crystallization essentially determines the mineralization potential of zoned ultramafic complexes. Differences in Pt-mineralization between individual zoned ultramafic complexes from Alaska and the Ural Mountains may thus be explained by their individual tectonic or thermal evolution. After the "dunitic event", the history of zoned ultramafic complexes follows normal fractionation trends which are principally controlled by fS_2 and the precipitation of PGEs as sulfides, with the main PGE enrichment in hornblende dominated rocks.

The cooperation in field work and sampling by R. Salinas, R. Muñoz (Ingeomias Medellín), and K.P. Burgath (BGR Hannover), is greatly appreciated.

REFERENCES

Amossé, J., Allibert, M., Fischer, W., Piboule, M. (1987) Etude de l'influence des fugacitées d'oxigène et de soufre sur la différenciation des platinoides des magmas ultramafiques. Résultats préliminaires. C.R.Acad. Sc. Paris, 304: Sér. II, No. 19, 1183-1185.

Burgath, K.P., Tistl, M. (1993) Accessory-type ferroplatinum mineralization in the dunitic core of the Condoto zoned ultramafic complex, Chocó, Colombia. in prep.

Razin, L.V. (1976) Geologic and genetic features of forsterite dunites and their platinum-group mineralization. Econ. Geol., 71:1371-1376.

Salinas, R., Tistl, M. (1992) A Tertiary zoned ultramafic complex and komatiitic basalts from Condoto, Chocó, NW Colombia. Zbl. Geol. Paläont. Teil I, 1991 (6):1659-1678.

St. Louis, R.M., Nesbitt, B.E., Morton, R.D. (1986) Geochemistry of platinum-group elements in the Tullameen ultramafic complex, Southern British Columbia. Econ. Geol., 81:961-973.

Tistl, M. (1993) Geochemistry of platinum-group elements of the zoned ultramafic Alto Condoto complex, NW Colombia. Econ. Geol., in print.

Von Gruenewaldt, G., Hulbert, L.J., Naldrett, A.J. (1989) Contrasting platinum-group element concentration patterns in cumulates of the Bushveld Complex. Mineral. Deposita, 24:219-229.

Weiser, Th., Tistl, M., Burgath, K.P. (1993) Mineralogy of dunite-hosted and placer PGM of the Condoto area. in prep.

Current Research in Geology Applied to Ore Deposits.Fenoll Hach-Alí, Torres-Ruiz & Gervilla(eds)(1993).ISBN 84-338-1772-8

FLUID INCLUSION STUDY AND THE GENETIC MODEL OF THE GOLD-QUARTZ DEPOSIT IN BLACK SHALES (ENISEY RIDGE, SIBERIA)

Tomilenko, A.A. & Gibsher, N.A.
Inst. of Mineralogy and Petrography Universitetskii Pr., 3, 630090, Novosibirsk, Russia

ABSTRACT: Investigation of fluid inclusions in ore and gangue quartz and native gold from the Sovetskoye deposit showed that crystallization of gold occurred from homogeneous and heterogeneous heated (up to 340°C),concentrated (up to 25 wt.% NaCl-equivalents), carbonaceous (up to 50 mole %) fluids.

Geological setting of the gold deposit

Sovetskoye gold-ore deposit is situated within the Central gold-bearing band on the eastern slope of the Yenisei ridge. Ore-enclosing rocks of the deposit are represented by phyllites, quartz-sericite-chlorite and quartz-muscovite-biotite shales of the Upper Proterozoic. The shales are enriched in carbon (up to 0.17%, Bogdanovich,1962) and gold (0,1-0,2 g/t, Petrov,1974). The deposit is confined to the limb of a large anticlinal fold complicated by a smaller folding and is divided into blocks by rupture dislocations. It consists of a series of vein-stringer zones having a high dip and concordance with the host rocks.

Vein-stringer zones are a group of contiguous, merging and newly branching veins, stringers and ore 'columns'. The veins and stringers are by 97% and more composed of quartz. Ore minerals are represented by pyrite, arsenopyrite, less often by pyrrhotite, galenite, sphalerite, chalcopyrite and marcasite. Gold occurs mainly in the native form, its distribution in orebodies is irregular. Direct correlation between the gold content and sulfides is absent.

Analytical procedure

Microthermometric measurements were performed on a heating-freezing stage (Dolgov and Bazarov, 1965). Salt concentration is expressed as wt.% NaCl equivalents. In gas-rich fluid inclusions CO_2 was identified by melting of a solid below - 56,6°C. Molar fractions of CO_2, CH_4, and N_2 were determined in individual inclusions by micro-Raman analysis on a U-1000 'Jobin Yvon' monochannel Raman spectrometer. The bulk composition of fluid inclusions in quartz and gold was determined by gas-chromatographic analysis (Osorgin,1990). From one sample

(50-100 mg) simultaneously CO_2, H_2O, CO, H_2, N_2, H_2S and hydrocarbons from C_1 (CH_4) to C_5 were analyzed.

Types of fluid inclusions

Based on phase proportions in the fluid inclusions at room temperature, three principal types may be recognized in quartz samples from the Sovetskoye gold deposit.

Type 1: aqueous, two-phase inclusions (L_{H2O} + V_{H2O}), gas:liquid rations range from essentially gaseous to essentially liquid inclusions.

Type 2: two and three-phase CO_2-rich inclusions (L_{H2O} + L_{CO2}; L_{H2O} + L_{CO2} + V_{CO2}).

CO2 content varies from 15 to 90%.

Type 3: single-phase inclusions with CO_2 or CH_4

(L_{CO2}; V_{CO2}; L_{CH4}; V_{CH4})

Negligible amounts of H_2O are found on the inclusion walls.

Analytical date on fluid inclusions.

In the quartz of the deposit ore zones all three types of fluid inclusions were found.Aqueous inclusions (type 1).Homogenization temperature ranges between 120-630$_0$C. Homogenization is observed both into liquid and gaseous phases. Salt concentration, according to freezing investigations, reaches 15-25 wt.%, NaCl equivalents. Generally, CO_2 content in these inclusions is very low.

Two-and three-phase CO_2-rich inclusions (type 2). Abundance of these inclusions in the ore zone sometimes amounts to 50% and more of all fluid inclusions. CO_2 homogenization into a liquid phase is measured between -4 - +31°C.Melting of solid CO_2 usually takes place at temperatures below the triple point of pure CO_2 (from -57 to -65°C). This deviation suggests the presence of various amounts of CH_4 and/or N_2 in the inclusions. According to the Raman-spectroscopy analysis of individual inclusions CO2 content makes up from 64 to 94 mol.%, CH_4-from 0.5 to 19 mole % and N_2-from 4 to 23 mole %, H_2S was not found. Complete homogenization of the inclusions occur in the range of temperatures from 250 to 340°C.Single-phase CO_2 and CH_4 inclusions (type 3). These liquid or gaseous CO_2 and CH_4 and hardly distinguishable amounts of H_2O. Melting temperature of CO_2 varies from -60.0 to -78 °C. The

Raman-spectroscopy analysis revealed 50-86 mole % CO_2, 3.0-32 mole % CH_4 and 6-35 mole % N_2. CO_2 homogenization into a liquid phase occurs in the range of -2 - 22°C.

Single-phase CH_4-rich inclusions homogenize into a liquid phase within the range from -82 to -94°C. According to Raman-spectroscopy investigations, there are 50-84 mole % CH_4, 11-38 mole % N_2 and 6.0-21 mole % CO_2.

Gas-chromatographic analysis showed that the main components of the fluid inclusions in quartz are H_2O (40-80 mole %) and CO_2 (15-56 mole %). Contents of CH_4 and N_2 vary in the range 0.6-7.6 mole % and 0.3-0.9 mole %, respectively

For native gold the fluid of the following composition is determined CO_2 - from 29 to 64 mole %, H_2O - from 31 to 68 mole %, CH_4 - from 0.0 to 2.4 mole % and N_2 - from 2,6 to 5.3 mole %.

Statistical reduction of the gas-chromatographic analyses of quartzes with particular gold content showed positive correlation between gold content in quartz and hydrocarbon content in the fluid (correlation coefficient is 0.79).

Quartz in the deposit ore zone formed both from homogeneous and heterogeneous fluids. The heterophase state of fluids is indicated by simultaneous presence of all the three types of fluid inclusions recognized in quartz among primary inclusions. The relationship of quartzes formed by homogeneous and heterogeneous fluids within separate quartz-vein zones is not constant.

In quartz from the ore-free zones of the deposit most are aqueous, two-phase inclusions (tape 1). Their homogenization occurs at temperatures from 125 to 360°C. Based on freezing investigations, total concentration of salts is 2 - 15 wt.%, NaCl-equivalents. Abundance of two- and three-phase CO_2-rich inclusions (type 2) is considerably less (less than 10%). According to Raman-spectroscopy analysis, in these rare inclusions CO_2 prevails (90 - 92 mole %),in considerable amounts N_2 (7 - 9 mole %) and negligible amounts CH_4 (0.n - 0.6 mole %) are found. Single-phase inclusions of liquid CO_2 and CH_4 (type 3) were not observed. Extremely rare are single-phase inclusions of gaseous methane. According to gas-chromatographic analysis of the gange quartz the fluid composition is represented by H_2O (86 - 98 mole %), CO_2 (1.6 - 12.5 mole %),negligible amounts of CH_4 (0.0 - 0.5 mole %) and N_2 (0.0 - 0.05 mole %).

Discussion and conclusions

Gold is extracted from quartz veins which are part of the complicated history of the Sovetskoye deposit formation. Study of fluid inclusions in ore and gange quartzes of the deposit and native gold showed that golddeposition occurred from heated (to 340°C), concentrated(up to 25 wt.%, NaCl equivalents) and carbon dioxide-rich (up to 56 mole %) fluids. Fluids of ore quartzes are characterized by homogeneous and heterogeneous state as well (separation of fluid into brine and carbon dioxide components).

Heterogenization may have been caused either by crack formation in metamorphous carbon- and gold-containing ore-enclosing shales, or by introduction of additional CO_2, CH_4 and N_2 - rich fluid portions into metamorphogenic fluid and to be the reason of gold deposition (Naden and Sheperd,1988).

References:

Bogdanovich V.A.,1969, 'Geologiya i Geofizika' (Geology and Geophysics). no 7,p.87-96.

Dolgov Yu.A., Bazarov L.Sh. Mineralogic thermometry and barometry (in Russian), Moscow, Nauka, p.118-122.

Osorgin N.Yu., 1990, Chromatographic analysis of a gaseous phase in minerals (procedure, apparatus, metrology) (in Russian). Institute of Geology and Geophysics, 32 p.

Petrov V.G.,1974. Studies of the Institute of Geology and Geophysics (in Russian), issue 60. 135p.

Naden J.,and Shepherd T.J.,1989, 'Nature',v.342,p.793-795.

Current Research in Geology Applied to Ore Deposits.Fenoll Hach-Alí, Torres-Ruiz & Gervilla(eds)(1993).ISBN 84-338-1772-8

PLATINUM-GROUP-MINERAL AND OTHER SOLID INCLUSIONS IN CHROMITE FROM THE "CHROMITE-ORES" OF THE SERRANIA DE RONDA LHERZOLITE MASSIFS (BETIC CORDILLERA), SOUTHERN SPAIN).

Torres-Ruiz, J. (1); Garuti, G. (2); Fenoll Hach-Alí, P. (1) & Gervilla, F. (1)
(1) Dept. de Mineralogía y Petrología & IAGM. Universidad de Granada-CSIC, Granada, Spain.
(2) Ist. di Mineralogia e Petrologia. Università di Modena, Italy

ABSTRACT

Platinum-group minerals (laurite, erlichmanite, irarsite, osarsite), base-metal sulfides (chalcopyrite, bornite, pentlandite, millerite), unidentified PGE-bearing phases (Ir-Rh-Cu, Ir-Rh-Ni, and Rh-Ir-Ni-Cu-Fe sulfides), Ni-arsenides (niccolite, maucherite), and silicates (Na-phlogopite, pargasite and pyroxenes) are present as inclusions in chromite of "Cr ores" of the Serrania de Ronda. Distinctive association and composition of the inclusions define three different groups of chromitites, which also are characterized by variations of the chondritic-normalized pattern of PGE. The character of the chromite inclusions is different when compared with ophiolitic and stratiform chromitites, and is probably related with peculiar chromite-forming systems in the subcontinental mantle.

INTRODUCTION

The lherzolite massifs of Serrania de Ronda (Ronda, Ojen, and Carratraca) are located in the so called internal zone of Betic Cordillera and constitute the base of the Los Reales Unit belonging to the Alpujarride Complex (Navarro-Vila and Tubia, 1983). These massifs are thought to represent slices of the upper mantle emplaced into the continental crust during alpine-age orogeny. A distinctive feature of the Serrania de Ronda mantle massifs is the coexistence of the four P-T mineral facies as defined by O'Hara (1967) within a relatively restricted mantle portion. From the contact with overlaying metapelitic sequence inwards the following zones occur succesively: garnet lherzolite, spinel lherzolite (ariegite and seiland subfacies) and plagioclase lherzolite. The origin of this zonation is still debated. Remaidi et al., (1991) and Garrido et al. (1992) put forward the existence of a large scale percolation system of silicate melts through the lithospheric mantle generating residual mantle and pyroxenitic dikes.

The mantle massifs contain three types of mineralization: 1) chromite (Cr ores), 2) chromite-Ni arsenides (Cr-Ni ores), and 3) Ni-Cu-Fe sulfide-graphite (S-G ores), all of which have variable contents of PGE and Au. These ores are believed to be genetically-related having segregated by differentiation of magmas that migrated from the core to the border of the mantle bodies under decreasing P-T conditions (Gervilla et al., 1988, Gervilla and Leblanc, 1990). The mineralogy and composition of the solid inclusions in chromite have been studied in chromitite samples from five different occurrences of the Cr ores: Cerro del Aguila, Arroyo de Los Caballos, Cañada del Lentisco and Mina Baeza (Ojén massif), and Arroyo de La Cala (Ronda massif). The investigated chromitites display field characters which are common to all the Cr ores. They have small size (the largest outcrops cover a few square meters), podiform or vein-like morphology, and are located within the limits of the plagioclase lherzolite facies, the chromitites usually bearing spatial relations with dunite pods.

SOLID INCLUSIONS IN CHROMITE

The solid inclusions in the investigated chromites are platinum-group minerals (PGM), base-metal sulfides (BMS) and arsenides (BMAS), and silicates. On the basis of the mineralogical assemblage of the inclusions, the investigated Cr ores can be divided into three groups:

Group 1 is constituted of chromitites from Cerro del Aguila (CDA) and Arroyo de los Caballos (CAB). They are characterized by the greatest variety of single- and/or polyphasic inclusions consisting of PGM, BMS, and silicates. PGM usually are less than 10μm across. Sulfides of the Laurite-Erlichmanite series are the most common (figure 1). They correspond to the formula $(Ru,Os,Ir)S_2$ with remarkable substitution of

Rh and As up to 2.55 and 3.02 wt% respectively. In the Ru-Os-(Ir+Rh) triangle laurite compositions cover the range of Ru_{36}-Os_{64} to Ru_{85}-Os_{15}, while the Ir+Rh content is as high as in laurite from ophiolitic chromitites reaching up to 16%. The great bulk of the laurite occurs as single-phase, automorphic crystals included in unaltered chromite (figure 2A), although some grains were found exceptionally in the silicate matrix of the chromite or along cracks. More rarely, laurite forms composite inclusions with one or more of the other PGE-bearing sulfides and/or BMS and silicates (figures 2B, 2C and 2D). In addition, strongly subordinate Ni arsenides (niccolite, maucherite) may be part of these composite inclusions. The sulfarsenide Irarsite (IrAsS) is comparatively rare, and usually occur in composite inclusions (figures 2B and 2C). Other PGE-bearing sulfides with variable metal associations (Ir-Rh-Cu, Ir-Rh-Ni, and Rh-Ir-Ni-Cu-Fe) have also been observed (figure 2B), but they could not be quantitatively analyzed because of their small size (<5μm). BMS are dominated by Cu-Ni phases forming various assemblages: chalcopyrite-pentlandite-millerite-bornite, chalcopyrite-bornite, pentlandite-niccolite. The silicate inclusions are modally more abundant and

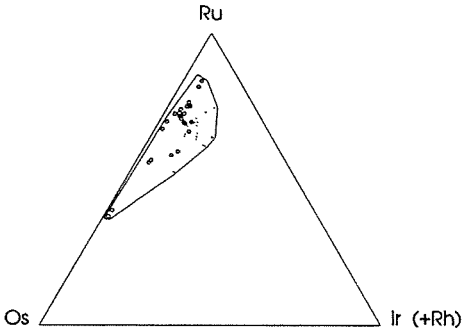

Figure 1.- Compositions of Laurite from Serrania de Ronda plotted on the Ru-Os-Ir(+Rh) triangle (atomic proportions). O = Cerro de El Aguila, • = Arroyo de Los Caballos.

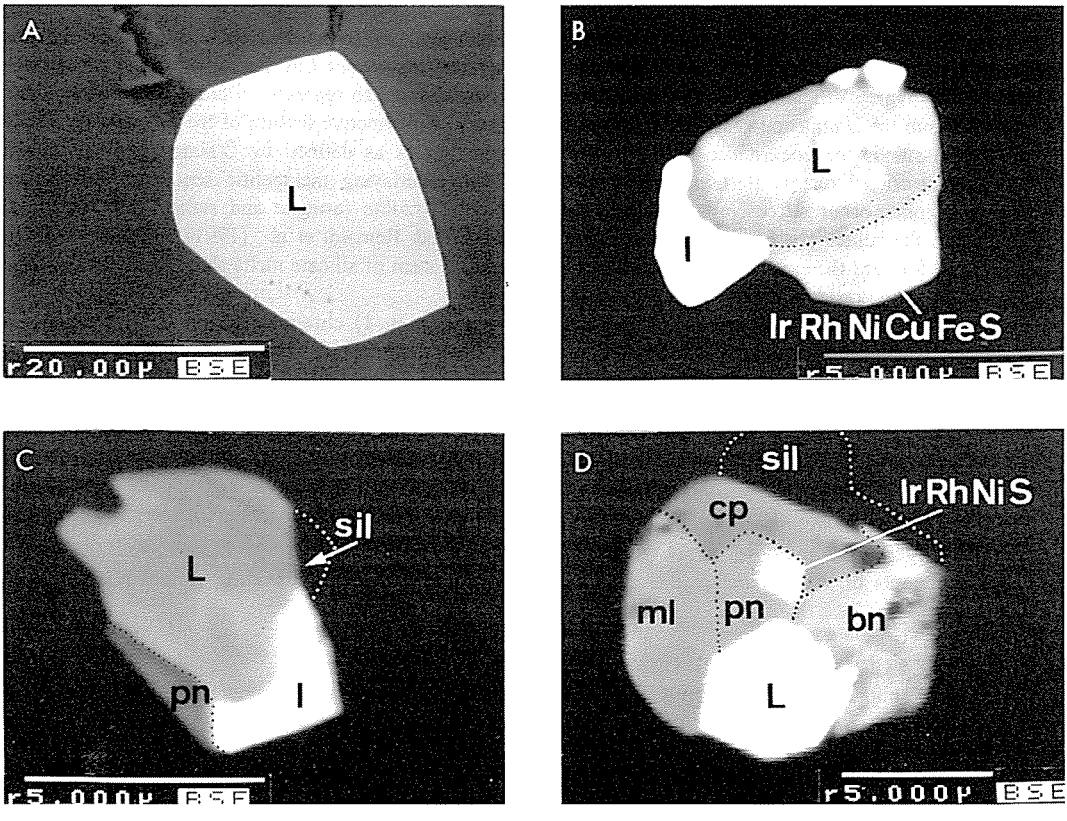

Figure 2.- Back-scattered images of single- and polyphasic inclusions in chromite. L = laurite, I = irarsite, cp = chalcopyrite, pn = pentlandite, bn = bornite, ml = millerite, sil = silicate.

reach up to some hundred microns across. They consist of phlogopite, pargasite, and pyroxenes in decreasing order of abundance. Phlogopite is remarkably rich in Na with Na_2O/K_2O ranging from 4.1 to 9.1.

Group 2 is composed of cromitites from La Cañada del Lentisco. In this occurrence PGM are rare and consist of the sulfarsenides osarsite (OsAsS) and irarsite (IrAsS). The PGM grains are euhedral to subhedral, and as large as 25μm and may be associated with Ni arsenides (niccolite, maucherite) that also occur as isolated inclusions independent from PGM. Pentlandite and chalcopyrite are very accessory phases occurring either as interstitial aggregates or chromite-included grains. One small grain of Au was found in one crack crossing a chromite grain. Silicate inclusions in chromite are similar but less abundant than in Group 1.

Group 3 comprises chromitites from Arroyo de la Cala and Mina Baeza. PGM and base metal sulfides are conspicuously absent. Only Ni arsenides (niccolite, maucherite) were found in these chromitites occurring as both interstitial grains among chromite crystals, and small to large (up to some hundred micrometers across) inclusions in unaltered chromite. Included silicates are similar to those of groups 1 and 2, although the Na_2O/KO_2 ratio of phlogopite is remarkably lower ranging from 0.49 to 0.71.

In all the investigated chromitites inclusions of secondary hydrous silicates such as serpentine and chlorite are common.

PGE CONTENTS OF THE CHROMITITES

In Group 1 chromitites, the observed abundance of Ru-Os-Ir PGM reflect the results of PGE analyses from the literature (Leblanc et al. ,1990) (figure 3) showing high contents of these refractory PGE, and a negative slope of the Rh-Pt-Pd condritic pattern characterized by relatively high ratios Pt/Pd (chondritic abundances). The Au chondritic ratios are variable but always below 1. Chromitites of Group 3 (analyses for group 2 are not available so far) display low overall concentration of PGE, specially of Os, Ir, Ru, and Rh, that is consistent with scarcity of specific PGM. They, however, have positive slope Rh-Pt-Pd of the condritic profile showing the inversion of the ratios Pt/Pd (chondritic abundances). Both chondritic ratios for Pd and Au are much higher than in group 1. The chondritic-normalized abundance of Au can reach up to 10 in samples where interstitial grains of gold had been observed. On the contrary, the relatively high Pd is not confirmed by the finding of specific minerals, leading to the conclusion that Pd could be present in solid solution within the Ni arsenides.

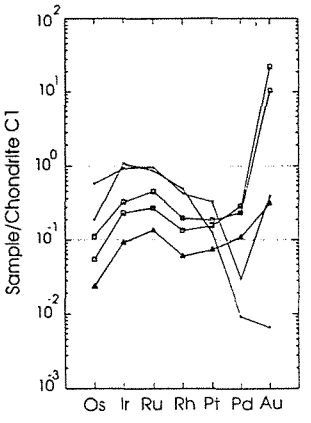

Figure 3.- Chondrite normalized PGE and Au of chromites. □ = Arroyo de La Cala, • = Arroyo de Los Caballos, Δ = Mina Baeza.

CHROMITE COMPOSITION

Compositional fields in Cr/(Cr+Al) vs Fe/(Fe+Mg) diagram of chromites from the five investigated occurrences are summarized in Figure 4. When relationships among Al, Fe", Mg, and Cr are considered, most of the samples are within the podiform field, although in the diagrams Cr/(Cr+Al) versus Fe/(Fe+Mg) and Al_2O_3 versus Cr_2O_3 samples from Arroyo de la Cala and Mina Baeza plot in the overlap area of the podiform and stratiform fields. On the other hand, the Ti content appears to be higher than normal (>0.25 wt% TiO_2) for ophiolitic chromitites in all the occurrences except for Cañada del Lentisco. These compositional features do not display any obvious correlation with the subdivision into three groups based on paragenetical characters of the inclusions, and the three groups largely overlap in most diagrams.

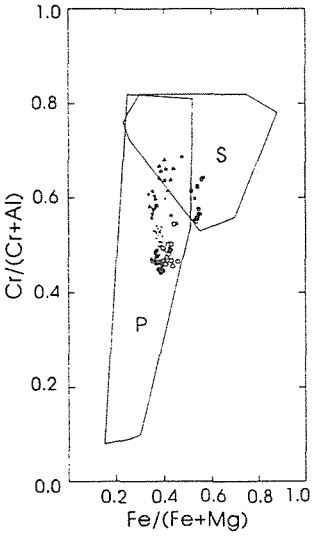

Figure 4.- Compositional field of chromites in Cr/(Cr+Al) vs Fe/(Fe+Mg) diagram. Symbols: O = Cerro del Aguila, • = Arroyo de Los Caballos, * = Cañada del Lentisco, □ = Arroyo de La Cala, Δ = Mina Baeza. S = compositional field of stratiform chromites, P = compositional field of podiform chromites.

CONCLUDING REMARKS

The comparative study of mineralogy, paragenesis, and composition of solid inclusions in the chromite suggests that the Cr ores of the Serrania de Ronda were formed in compositionally-distinct magmatic systems within the mantle lherzolite massifs. Chromitites of Group 1 probably crystallized in the presence of a hydrous-fluid phase characterized by relatively high S fugacity and concentration of Na. The relatively high S fugacity is responsible for the early formation of PGM-sulfides of the more refractory PGE Os, Ir, and Ru, and of the BMS featured by relatively high Cu/Ni ratios. In contrast, Pd and Au are low in the chromite-forming system. The magmatic system where chromitites of groups 2 and 3 were formed is characterized by a relatively Na-poor and k-rich fluid phase, with low S fugacity, whereas As is a major component of the volatile suite, and is responsible for the precipitation of large amounts of Ni-rich arsenide minerals occurring included in and interstitial to the chromite. The refractory PGE are strongly depleted with respect to group 1, whereas Pd and Au are relatively enriched. These features indicate that the Cr ores cannot be considered as a strictly homogeneous group of ores, and possibly were they originated under changing chemical conditions, in relation to upwelling and crustal evolution of the mantle.

Mineralogy of inclusions in the investigated chromitites is peculiar when compared with inclusions in chromitites from ophiolitic and stratiform complexes (Talkington et al., 1986) because of the absence of Os-Ru-Ir alloys, native metals, and the abundance of sulfarsenides and arsenides. The PGE chondritic patterns of the chromitites are also unusual ranging from podiform-type to profile with relatively higher Pt- and Pd-chondritic ratios. This feature has never been reported before for chromitites from the same rock unit (the plagioclase lherzolite), with the only exception of the Finero Complex in the Western Alps (Ferrario and Garuti, 1990), that similarly to the Serrania de Ronda is considered as subcontinental mantle.

ACKNOWLEDGEMENTS

This research has been supported by DGICYT (project n° PB87/0274) and by the Italien-Spanish Integrated Action (n° 25-A).

REFERENCES

Ferrario A & Garuti G (1990). Platinum-Group Mineral Inclusions in Chromitites of the Finero Mafic-Ultramafic Complex (Ivrea-Zone, Italy). Mineral. Petrol., 41, 125-143.

Garrido CJ, Remaïdi M, Bodinier JL, Gervilla F, Torres-Ruiz J & Fenoll Hach-Alí P (1992). Composite piroxenite layers from the Ronda Orogenic Lherzolite: evidence from Km-scale magma percolation in sub-continental mantle. III Congreso Geológico de España y VIII Congreso Latinoamericano, (1), 347-349.

Gervilla F, Leblanc M & Torres-Ruíz J (1988). Relaciones entre la zonalidad petrológica y metalogénica de los macizos lherzolíticos de las cadenas alpinas del Mediterráneo Occidental (Cordillera Bético-Rifeña y Kabylias). Estudios Geol., 44, 375-383.

Gervilla F & Leblanc M (1990). Magmatic ores in high-temperature alpine-type lherzolite massifs (Ronda, Spain, and Beni Bousera, Morocco). Econ. Geol., 85, 112-132

Leblanc M, Gervilla F & Jedwad J (1990). Noble metals segregation and fractionation in magmatic ores from Ronda and Beni Bousera lherzolite massifs (Spain, Morocco). Mineral. Petrol. 42, 233-248.

Navarro-Vila F & Tubía JM (1983). Essai d'une nouvelle differentiation des Nappes Alpujárrides dans le secteur occidental des Cordillères Bétiques (Andalousie, Espagne). C.R. Acad. Sc. Paris, 296 (II), 111-114.

O'Hara MJ (1967). Mineral facies in ultrabasic rocks. In: Ultramafic and related Rocks. P J Wyllie ed. New York, 7-17.

Remaïdi M,. Gervilla F, Bodinier JL, Leblanc M & Torres-Ruíz J (1991). Harzburgite, dunite and pyroxenite association in the Ronda ultramafic bodies- Geochemical evidence of percolation-reaction processes in sub-continental Mantle. In: meeting of the working group of IGCP Project n° 256. Ophiolite genesis and the evolution of oceanic Lithosphere. Granada, 15-15.

Current Research in Geology Applied to Ore Deposits.Fenoll Hach-Alí, Torres-Ruiz & Gervilla(eds)(1993).ISBN 84-338-1772-8

MAGNETITE-APATITE TYPE IRON ORE AND GOLD MINERALIZATION IN THE CERRO NEGRO NORTE DISTRICT, CHILE

Vivallo, W. (1); Espinoza, S. (2) & Henríquez, F. (3)
(1) Dept. de Geología. Universidad de Chile, Chile
(2) Dept. de Ciencias Geológicas. Universidad Católica del Norte, Chile
(3) Dept. de Ing. de Minas. Universidad de Santiago, Chile

ABSTRACT. The Cerro Negro Norte district, located in the Coastal Cordillera of northern Chile, consists of massive magnetite-apatite ores formed by the emplacement of an ore-magma. The orebodies are hosted by altered Cretaceous andesites, and when compared with less altered volcanics the ore shows gold enrichment. The emplacement of the ore-magma was followed by wall rock alteration produced by slightly alkaline, Ca, Mg, Fe and volatile-rich hydrothermal solutions. The relative gold enrichment found in the iron-ore and the subsequent development of slightly alkaline, volatile-rich hydrothermal solutions, point out the high potential of these volcanic environments in the generation of gold mineralization.

Introduction

The iron district Cerro Negro Norte is located in northern Chile, about 42 km to the NW of the town of Copiapó. It belongs to the Chilean Cretaceous Iron Belt (CIB), a metallogenic province, c 600 km x 50 km , striking in a NS-direction along Chile's Coastal Cordillera. The iron deposits of the CIB consist of massive magnetite-apatite ores ("Kiruna type") hosted by altered andesitic rocks of Cretaceous age. Based on the close temporal and spatial relationships between the ore, volcanic and plutonic rocks in the CIB, the origin of the iron ores has been explained by magmatic related processes, such as deuteric-hydrothermal activity, metamorphic processes and emplacement of a magnetite-apatite ore magma (Nyström & Henríquez 1993 and references therein). It is known that associated with these deposits there is uneconomical concentration of Au. The purpose of this work is to asses the potential of these magmatic environments in the generation of gold ores.

The Cerro Negro Norte district

The Cerro Negro Norte district consists of several massive magnetite orebodies, distributed along a NS striking belt of about 3 km long x 0.5 km wide. The geology of the district is dominated by a subhorizontal volcanic pile, which is intruded by plutonic rocks and dikes.

A NS striking belt of amphibolitic rocks, hosting the iron ores, dominates the central part of the district, where it displays gradual contact with volcanic rocks. The amphibolitic rocks consist mainly of actinolite with minor amounts of plagioclase, quartz and K-feldspar. Epidote, chlorite, titanite, pyrite and magnetite are common accessories. Veinlets of quartz ± scapolite, coarse-grained actinolite and quartz-tourmaline are cutting these amphibole-bearing rocks. When compared with the composition of the less altered volcanic rocks (andesitic in composition), the

amphibolitic rocks display a strong enrichment in Ca, Mg, Fe, P, F, Cl, Au, and are depleted in Na, K, Ti, Sr, Zr, Cu, Zn, Y and light rare earth elements (LREE) .

Volcanic rocks, with different degrees of alteration, are surrounding the amphibolitic rocks. The less altered relict of the volcanic rocks have a chemical composition consistent with an andesitic composition. These andesites are fine-grained porphyritic rocks, dark-gray in color, with plagioclase and amphibole phenocrysts, included in an aphanitic feldspar-quartz-rich groundmass. Silicified andesites display abundant quartz in the groundmass and quartz-bearing veinlets cutting the rocks, in someplaces silicification can be followed by albitization of plagioclase. Andesitic rocks affected by albitization-silicification display an irregular areal distribution, but they are always located outside of the amphibole-rich central lithologic unit. Moreover, the andesitic rocks may be affected by tourmalinization ± silicification, this process produces veinlets and dissemination of tourmaline. Rocks affected by strong tourmaline replacement are altered into a fine-grained, black tourmaline-quartz±garnet rock. Tourmaline, disseminated and in veinlets, is present in all lithologic units of the district, including the iron ores and amphibole-rich rocks. In comparison with the andesitic rocks, albitized rocks are characterized by a high Na/K ratio, and a general depletion of major elements (with exception of Si and Na) and most of the trace elements, including the REE. However, they show a relative enrichment in S, Zn and Au. The tourmalinization process has produced a strong B-enrichment, and general depletion of most of the other components, only Au, Cu and S display some enrichment in the tourmaline rich rock (mostly as a tourmaline breccia).

Irregularly shaped hydrothermal breccias are present in the eastern and western side of the district, around the iron ores. In the eastern side, the breccias are spatially related to hypabisal felsic rocks which are brecciated and cemented with tourmaline; but, brecciation is also affecting the volcanics. In the western part, the hydrothermal brecciation is developed in the volcanic rocks, consisting of monolithologic breccias cemented mainly by actinolite.

Mineralization

The mineralization of the district includes massive iron ores and small (<0.5 m wide and a few m long) magnetite-hematite-calcite bearing quartz-veins, which may contain Cu and Au mineralization. Compared with the andesitic rocks, the Au content of the iron ore is enriched by a factor of ten.

The iron ores are dominated by the magnetite-apatite-actinolite assemblage and minor amounts of pyrite, either disseminated or in veinlets.

Based on textural features and mode of emplacement, the iron ores can be grouped into (a) massive orebodies, tabular shaped (dike-shaped), vertical to subvertical, 1-2 m thick and several tenth of meters long; (b) irregular shaped massive ore bodies, with variable dimensions, the largest one being dome-like. (c) Disseminated mineralization is commonly located at the contact between the massive ores and the amphibole-rich wallrocks; it consists of veinlets and dissemination of magnetite in the amphibole-rich rock; (d) Massive orebodies, subhorizontal, 1-2 m thick, partly interlayered with the volcanic host rocks, and with intercalation of well-banded calcite-rich beds.

Quartz-veins are restricted to the margin of the district where they cut all lithologic units present in the studied area.

Discussion

The volcanic-intrusive environment of the Cerro Negro Norte district indicates a genetic relationship between the iron ores and the Cretaceous magmatism. This relationship, which is valid for the whole CIB ore province, has induced to explain the origin of the iron ores by deuteric-hydrothermal processes or metamorphic events related to the intrusion of the plutonic rocks, or by the emplacement of an "iron-ore-magma", originated during the general evolution of the Cretaceous magmatic arc (Nyström & Henríquez 1993 and references therein). Field evidences, such as mode of occurrence and emplacement patterns of the iron ore in the Cerro Negro Norte district, are consistent with an origin related to the emplacement of an iron-ore-magma which directly resulted in massive intrusive orebodies (dikes and domes) and efusives represented by subhorizontal massive ores interlayered with the altered volcanic rocks. Magnetite flows, and intrusive bodies of massive magnetite, similar to those observed in Cerro Negro Norte, have been recently identified within the CIB in the Pleito and Melón districts (V. Travissany 1992, oral comunication). The geochemical signature of the iron ore at Cerro Negro Norte is similar to that present in other districts of the CIB, e.g. El Algarrobo, Cerro Imán, Pleito, Cristales (Espinoza 1985), in which textural and geochemical evidences indicate a magmatic origin for the iron ores (González 1990, Lorca 1990, Nyström & Henríquez 1993).

The gradual contact between the different units of altered rocks, the existance of unaltered andesitic rocks within the altered units, and the zoned distribution of these around the iron ores, indicate a common andesitic protolith for all the altered volcanics. The hydrothermal breccias around the orebodies, the presence of silicified rocks, either albitized or tourmalinized, and intercalation of well-banded calcite rich deposits in the iron ores, are consistent with an intense hydrothermal activity centered on the iron ores. The field relationships among the altered rocks suggest that the emplacement of the iron ores was followed by hydrothermal activity, with fluids initially rich in Ca, Mg, Fe and volatiles, responsible for the actinolitization of the andesites and development of hydrothermal breccias with actinolite-dominated matrix. This fluid evolved to Si-Na-rich solutions producing a more external halo of albitized rocks. This first stage was probably a high-temperature event, where the fluid was dominated by a magmatic-hydrothermal component of slightly alkaline character, as indicated by the presence of feldspar in the amphibolitized rocks. A second stage of hydrothermal activity resulted in silicification ± tourmalinization and formation of a second generation of hydrothermal breccias (tourmaline breccias), overprinting the altered rocks formed at the first stage.

The relative enrichment of gold in the iron-ores suggests that the generation of a magma dominated by the magnetite-apatite assemblage, may favor a primary gold concentration during the magmatic stage. Hydrothermal activity related to the emplacement at a high crustal level of this ore-magma, along with the generation of slightly alkaline solutions rich in volatile, mainly Cl, represents an additional factor enhancing remobilization and concentration of Au originally contained in the magnetite ore body.

Conclusions

The iron ore in the Cerro Negro district was formed by the emplacement, at a high crustal level, of a magnetite-apatite magma ("ore-magma"). This ore-magma is tought to be formed during the evolution of a Cretaceous magmatic arc documented by extensive andesitic volcanism and emplacement of plutonic rocks. Compared with the andesitic volcanic rocks, the iron ore is enriched in gold, suggesting a primary Au concentration in the ore-magma. Its emplacement was followed by hydrothermal activity. A first alteration stage, characterized by high temperature, slightly alkaline solutions rich in Cl and other volatiles, produced both the amphibolitization (actinolite) of the volcanics close to the ores and an external halo of silicified ± albitized rocks. A late process of silicification ± tourmalinization overprinted the above described early alteration.

The primary concentration of gold in the iron ore-magma and the hydrothermal activity following its emplacement enhance the importance of these volcanic environments as potential sources for gold ores.

Acknowledgements. This work was financed by FONDECYT (Grant N° 91-1218) and the Swedish Agency for Research Cooperation with Developing Countries (Grant N° SWE-89-101). The support and information given by Compañía Minera del Pacífico (CMP) is acknowledged. J. Cembrano and B. Townley critically read the initial draft of manuscript and suggested valuable improvements.

References

Espinoza, S. 1985. Distribución de los elementos de transición en magnetitas de yacimientos de hierro chilenos y su significado en la tipología y génesis probable de los yacimientos. IV Congreso Geol. Chileno, Vol. 4: 836-853.

González, E. S. 1990. Geoquímica de las rocas de caja y de los cuerpos mineralizados del yacimiento Algarrobo, III Región. Thesis Univ. Chile, 121pp.

Lorca, G.F., 1990. Caracterización geoquímica de las piritas de los yacimientos de hierroEl Algarrobo y El Romeral. Thesis Univ. Chile, 138 pp.

Nyström, J.O. & Henríquez, F. 1993. magmatic features of the iron ores of Kiruna type in Chile and Sweden: ore textures and magmatic geochemistry. Accepted for publication in Econ. Geol.

4 Rare elements and other mineralizations associated with granitic rocks

Current Research in Geology Applied to Ore Deposits. Fenoll Hach-Alí, Torres-Ruiz & Gervilla (eds) (1993). ISBN 84-338-1772-8

REE CONTENTS OF FELDSPAR, MICA, TOURMALINE AND BERYL FROM GRANITIC PEGMATITES OF THE SIERRA ALBARRANA (CORDOBA, S.W. SPAIN)

Abad-Ortega, M.M. (1); Fenoll Hach-Alí, P. (1); Oddone, M. (2) & Ortega-Huertas, M. (1)
(1) Dept. de Mineralogía y Petrología & I.A.G.M. (Universidad de Granada-C.S.I.C.) Granada, Spain
(2) Dept. Quimica Generale, Universitá di Pavia, Via Taramelli 12, 27100 Pavia, Italy

ABSTRACT

The REE contents of feldspar, mica, tourmaline and beryl of quartzo-feldspathic pegmatites from Sierra Albarrana have been analyzed by neutron activation. Feldspar and tourmaline REE contents have been used to establish that the crystallization sequence of the pegmatitic bodies was from the border zone to the central zone, and that they formed from a melt in presence of an additional aqueous phase.

INTRODUCTION AND GEOLOGICAL CONTEXT

More than 60 pegmatite bodies occur in the Sierra Albarrana area. Their distribution is controlled by the regional metamorphic zonation (Garrote *et al.*, 1980), and their chemical composition varies according to the lithology of the host rocks. From a mineralogical point of view, three groups of pegmatites are distinguished: pegmatites with amphibole and/or epidote, pegmatites with aluminium silicates and quartzo-feldspathic pegmatites. This last group has been the main objective of this study.

The quartzo-feldspathic pegmatites crop out only in the sillimanite - K-feldspar and sillimanite-muscovite zones. The host rocks consist of gneisses, schists and quartzites of the Peña Grajera, Sierra Albarrana, Cabril and Montesina Formations (Garrote *et al.*, 1980). Some pegmatite bodies display a simple internal structure, while others have a clearly visible zonation, consisting of: (a) a border zone characterized by granitoid texture and medium grain size, with quartz and perthitic K-feldspar and rich in tourmaline, garnet, chlorite, muscovite and arborescent biotite; (b) an intermediate zone with coarse grain size and graphic texture, containing quartz, K-feldspar, albite and minor muscovite; and (c) a central zone with very coarse grain size (crystals from 1 to 2 m) and giant pegmatitic texture, and consisting predominantly of quartz and K-feldspar. Also present in the pegmatite bodies of all zones are lesser amounts of berthierine, beryl, chrysoberyl, zircon, pyrite, chalcopyrite, magnetite, Fe-Ti oxides, columbotantalite, fluorapatite, magniotriplite and several uranium minerals.

ANALYTICAL METHOD

REE analyses were made by neutron activation, using a 250 kw Triga Mark II reactor at the Pavia University. 0.3 g mineral samples were mixed with 0.3 g of international standard rocks (GSP1 and BCR1) of the United States Geological Survey (Oddone *et al.*, 1984). The REE abundances in chondritic meteorites used for the normalization have been taken from Haskin *et al.* (1968). In order to quantify the Eu anomalies in the samples, Eu/Eu* ratio were calculated, where Eu* represents the interpolated value between Sm and Gd.

RESULTS AND INTERPRETATION

The large size of the minerals in the Sierra Albarrana pegmatites required the analysis of individual minerals rather than whole rock analysis of the pegmatite zones. The REE composition of these minerals can explain the REE composition of the melt from which these pegmatites crystallized (Walker *et al.*, 1986).

Feldspars: Feldspar samples in border, intermediate and central zones of the pegmatites in several outcrops have been analyzed. The total REE contents are low [0.25 to 19.36 ppm for K-feldspars (Fig.1a) and 6.16 to 10.88 ppm for plagioclase (Fig.1b)]. The REE chondrite normalized patterns are similar for K- feldspar and plagioclase, with weak slopes for LREE, low concentrations for HREE and high positive anomalies for Eu (Eu/Eu* = 9.29 to 2.33 for K-feldspar and 8.22 to 2.89 for plagioclase). This tendency is the opposite to that reported by Buma *et al.* (1971). The Eu anomalies in K-feldspar and plagioclase decrease to the centre of the pegmatite bodies for all of the outcrops studied. According to Walker *et al.*(1986), trends of Eu anomalies can be used to interpret the crystallization sequence, because early crystallized (i.e. external) zones show larger Eu anomalies compared to late crystallized (i.e. central) zones.

Micas: The total REE contents are low [37.81 to 38.11 ppm for muscovite (Fig.1c) and 11.51 to 15.41 ppm for biotite (Fig.1d)]. The low contents of REE in these minerals can be explained by the presence of apatite and/or columbotantalite that are more selective for the REE than muscovite and biotite. The chondrite normalized patterns are different for each of the micas: muscovites show low slopes and lack of Eu anomalies, while biotites have high slopes with strong Eu anomalies. The difference between the REE content in Sierra Albarrana muscovites and biotites is due to the dioctahedral micas being more favourable to entrance of REE because of the size and number of vacancies in the octahedral positions (Roaldset, 1975); in the trioctahedral micas these positions are completely occupied and, consequently, less favourable to the entrance of REE. The Eu anomalies in biotites could be due to selective separation of Eu from the melt and its incorporation in the feldspar structure. These observations are in accordance with those of Haskin *et al.* (1966) and Buma *et al.* (1971).

Tourmalines: The total REE contents are low (23.15 to 10.78 ppm, Fig.1e). The REE chondrite normalized patterns do not have any consistent shape, but show strong differences between samples from different outcrops, or even from the same outcrop. This tendency indicates that tourmalines do not show any specific preference for REE (Gromet and Silver, 1983), because the crystallographic positions for entrance of REE have intermediate coordination numbers. For this reason, the distribution patterns of REE in tourmalines are very complex (Clark, 1984). The pattern may show positive, negative or no Eu anomalies. As observed by King *et al.* (1988), this could be due to the Eu being mainly in the trivalent state. Some of the tourmalines do not have Eu anomalies, due to the presence of minerals which host REE (uraninite and secondary uranium minerals, Fe-Ti oxide intergrowths, columbotantalite, etc). A decrease of both total REE and LREE contents of the tourmalines is observed towards the centre of the pegmatites. This trend is similar to that in the feldspars and, therefore, the REE contents in tourmalines are also indicative of a crystallization sequence from border to centre of the pegmatite body. On the other hand, the HREE contents of the Sierra Albarrana samples are lower than those granites (Neiva, 1974), and indicate that the tourmalines have been derived from a melt and an additional aqueous phase (Joliff *et al.*, 1987).

Beryls: The total REE contents are low (1.74 to 16.44 ppm, Fig.1f). The chondrite normalized patterns are consistent, with weak slopes for LREE, high Eu anomalies and low HREE contents. The strong Eu anomalies present in all the samples are due, as for the micas, to the selective separation of Eu from the melt and incorporation in the K-feldspar and plagioclase (Haskin *et al.*, 1966). A higher Eu anomaly observed in one sample may be due to the presence of REE host minerals (apatite and/or columbotantalite).

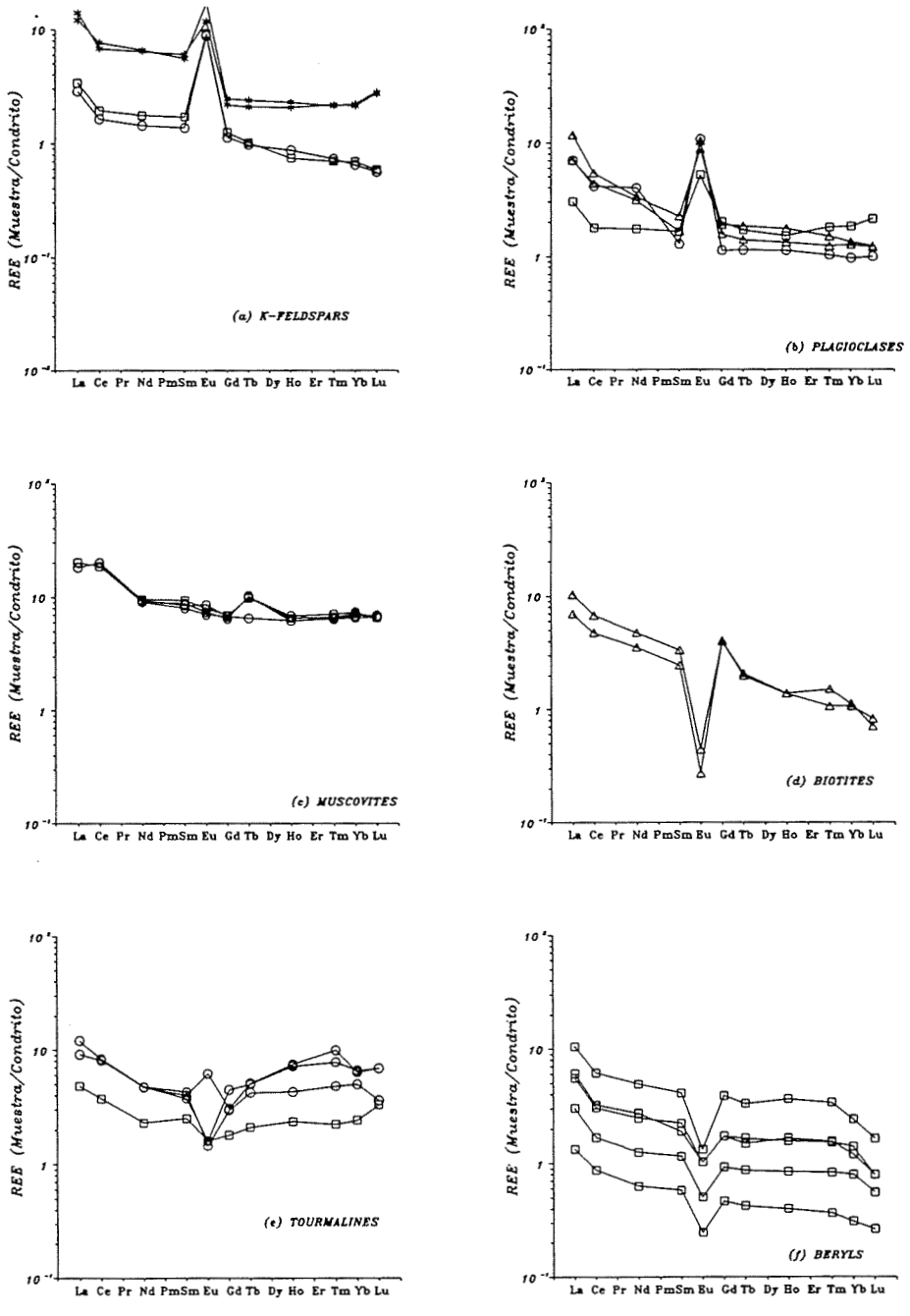

Fig.1. Diagrams of chondrite normalized REE patterns of minerals from different outcrops of the Sierra Albarrana granitic pegmatites: (a) K-feldspar, (b) plagioclase, (c) muscovite, (d) biotite, (e) tourmaline, (f) beryl. Legend of the samples: circles = border zone, squares = intermediate zone, asterisks = central zone, not zonation = triangles.

CONCLUSIONS

The REE contents in the different mineral phases studied (feldspars, micas, tourmalines and beryls) in the Sierra Albarrana granitic pegmatites are very low. The impoverishment of HREE in tourmalines indicates that crystallization proceeded in the presence of a melt and an additional aqueous phase.

The Eu content and the Eu/Eu* ratio in feldspars and tourmalines are indicative of the crystallization sequence of the diferent pegmatitic zones. Minerals from the early crystallized (external) zones have higher Eu anomalies than minerals from the late crystallized (internal) zones. The REE data, indicate a crystallization sequence from border to centre of the pegmatite bodies.

REFERENCES

Buma, G.; Frey, F.A. & Wones, D.R. 1971. New England granites: trace element evidence regarding their origin and differentiation. **Contrib. Mineral. Petrol.** 31:300-320.

Clark, A.M. 1984. Mineralogy of the rare earth elements. In: **Rare earth element geochemistry** (P. Henderson, Ed.), Elsevier 33-61.

Garrote, A; Ortega-Huertas, M. & Romero, J. 1980). Los yacimientos de pegmatitas de Sierra Albarrana (Prov. de Córdoba). Sierra Morena. **Temas Geol. Min. IGME** 145-168.

Gromet, L.P. & Silver, L.T.1983. Rare earth element distribution among minerals in a granodiorite and their petrogenetic implications. **Geoch. Cosmoch. Acta** 47:925-939.

Haskin, L.A.; Frey, F.A.; Schmitt, R.A. & Smith, R.H. 1966. Meteoritic, solar and terrestrial rare-earth distribution. In: L.J. Ahrens, F. Press, S.K. Rucorn y H.C. Urey, (Eds), **Physics and chemistry of the earth**, Pergamon 7:167-321.

Haskin, L.A.; Haskin, M.A.; Frey, F.A. & Wildeman, T.R. 1968. Relative and absolute terrestial abundances of the rare earths". In: L.H. Ahrens (Ed). **Origin and Distribution of the elements**, Pergamon 1:889-911.

Joliff, B.L.; Papike, J.J. & Laul, J.C. 1987. Mineral recorders of pegmatite internal evolution: REE content of tourmaline from the Bob Ingersoll Pegmatite, South Dakota. **Geoch. Cosmoch. Acta** 51:2225-2232.

King, R.W.; Kerrich, R.W. & Daddar, R. 1988. REE distribution in tourmaline: An INAA technique involving pretreatment by B volatilization. **Amer. Mineral.** 73:424-431.

Neiva, A.M.R. 1974. Geochemistry of tourmaline (schorlite from granites, aplites and pegmatites from northern Portugal. **Geoch. Cosmoch. Acta** 38:1307-1317.

Oddone, M.; Meloni, S. & Genova, N. 1984). Neutron activation analysis: A powerful tool for assay of rare-earth elements in terrestial materials. **Inorg. Chim. Acta** 94:283-290.

Pride, C. & Muecke, G.K. 1981). Rare earth element distributions among coexisting granulite facies minerals, Scourian Complex, NW Scotland. **Contrib. Mineral. Petrol.** 76:463-471.

Roaldset, E. 1975. Rare earth element distributions in some Precambrian rocks and their phyllosilicates, Numedal, Norway. **Geoch. Cosmoch. Acta** 39:455-469.

Walker, R.J.; Hanson, G.N. Papike, J.J.; O'Neil, J.R. & Laul, J.C. 1986. Internal evolution of the Tin Mountain pegmatite, Black Hills, South Dakota. **Amer. Mineral.** 71:440-349.

(This study has been supported by the "Grupos de Investigación n° 4065 y 4028 de la Junta de Andalucía" and by the "Acción Integrada Hispano-Italiana 9A/1992)".

We are grateful to Dr. Ross A. Both (University of Adelaida, Australia) for his assistence in translating the original text.

Current Research in Geology Applied to Ore Deposits.Fenoll Hach-Alí, Torres-Ruiz & Gervilla(eds)(1993).ISBN 84-338-1772-8

PETROGRAPHY, GEOCHEMISTRY, MINERALOGY AND GENESIS OF THE REE-Y-Nb-Zr ORES OF THE SIERRA DEL GALIÑEIRO, GALICIA, NORTHWESTERN SPAIN

Arribas, A. (1); Martín-Izard, A. (2); Arribas Jr A. (3) & Fontenla, V. (2)
(1) Escuela de Minas. Rios Rosas, 21, 28003 Madrid, Spain
(2) Dept. de Geología. Universidad de Oviedo, 33005 Oviedo, Spain
(3) Geological Survey of Japan, 1-1-3 Higashi, Tsukuba 305, Japan

INTRODUCTION

The REE-Y-Nb-Zr ores of the Sierra del Galiñeiro are located in the northwestern margin of the **Porriño Peralkaline Complex (PPC)**, about 7 Km west of Porriño and near the town of Zamanes. The ores were discovered in 1962 by the Junta de Energía Nuclear during exploration for radioactive minerals in northwestern Spain. Results of two drill holes carried out then established that high concentrations of zircon and allanite in a biotite orthogneiss of the **PPC** were responsible for the radioactivity. The area was then discarded as a source of uranium, but Arribas (1963) found anomalous concentrations of elements such as Y, Nb, and REE elements, particularly HREE, with a potential economic value. In 1976, **Altos Hornos de Vizcaya** briefly evaluated the area and **ERCROS** started in 1987 an exploration program with geophysics and geochemical studies (Rambaud et al, 1992). Recently, Rio Tinto Minera completed viability studies of the deposits. This report presents the results of geologic and metallogenic studies carried out on outcrop and drill-hole samples of the mineralized biotite orthogneiss and associated igneous rocks of the **PPC**.

GEOLOGICAL SETTING

The **Porriño Peralkaline Complex** is located in the southern section of the Malpica-Tuy Band, a structural unit which was thrusted on the Precambrian-Lower Cambrian basement and then folded during the second and third Variscan phases, respectively. The Complex occurs within metasedimentary rocks, mainly graywackes, of the Iberian Massif and is crosscut, together with the country rocks, by younger Variscan granitoids. Although the main petrological and structural features of the **PPC** were established by Floor (1964), new data related to the chemical composition and boundaries of the various facies which form the **PPC** were reported recently by Arribas et al.(1993). These data allowed the definition of new petrological facies and reinterpretation of the origin and evolution of the peralkaline rocks.

PETROGRAPHY

The Porriño Peralkaline Complex consists of up to 8 ring-shaped intrusive bodies which later were intensely deformed during the Variscan Orogeny. From the oldest to the youngest, the **PPC** consists of the following ten intrusive rock facies (Fig. 1):

1. **AMPHIBOLE facies (hornblende orthogneiss).**
2. **BIOTITE-AMPHIBOLE facies (Biotite-hornblende orthogneiss)** Floor (1964) considered it a metasomatized paragneiss, but the foliation and the petrological and geochemical features prove this rock was originally igneous.
3. **ZORRO facies (Coarse-grained riebeckite orthogneiss).**
4. **SARAMAGAL facies (Coarse-grained riebeckite-aegirine orthogneiss)**
5. **BANDA facies (Fine-grained riebeckite orthogneiss).**
6. **ERMITA facies (Fine-grained riebeckite-astrophyllite orthogneiss)**
7. **BANDED facies (Riebeckite-aegirine orthogneiss).**
8. **GALIÑEIRO facies (Riebeckite-aegirine orthogneiss).**
9. **MAGNETITE facies (Aegirine-riebeckite orthogneiss).**
10. **RADIOACTIVE facies (Fine-grained biotite orthogneiss)** This is the youngest petrologic facies in the complex and hosts the REE-Y-Nb-Zr deposits.

GEOCHEMISTRY

Results of major, trace, and rare-earths elements from samples of the **PPC** and country rocks (**paragneiss, older biotite orthogneiss** and **amphibolite**) within the Malpica-Tuy Band are summarized in table 1 and plotted in Figs.3 to 7. A gradient towards chemically more evolved rocks is observed in both the REE diagrams (Fig.7) and the bimodal diagrams of **Pearce et al.** (1984) and **Wallen et al.** (1987)(Figs.3 to 6), in which analyses of the La Guía and Piñeiro

Table 1. Average values of major (wt%), trace, and rare-earth element analyses (ppm) for whole-rock samples related to the Porriño Alkaline Complex. The maximun and minimun values are indicated for samples of radioactive gneiss from the Zamames deposit.

UNIT	FACIES	SiO_2	Al_2O_3	Fe_2O_3	MgO	CaO	Na_2O	K_2O	TiO_2	P_2O_5	MnO	Cr_2O_3
Country rock	Paragneiss	59.87	19.43	7.27	2.64	1.21	2.78	3.89	0.77	0.14	0.11	0.023
	Amphibolite	50.46	14.91	11.26	7.36	10.26	2.63	0.47	1.46	0.18	0.23	0.040
	Orthogneiss	74.33	12.68	2.30	0.34	1.26	3.41	4.45	0.16	0.04	0.04	0.013
Porriño Peralkaline Complex	Hornbl-biotite	65.8	13.8	6.26	1.28	1.61	3.41	3.84	1.11	0.32	0.11	0.012
	Piñeiro	75.49	11.34	2.76	0.01	0.10	4.29	5.04	0.16	0.02	0.05	0.018
	Zorro	73.44	13.39	3.59	0.01	0.08	3.97	4.65	0.26	0.01	0.05	0.027
	Saramagal	74.25	10.65	5.71	0.02	0.01	3.80	3.93	0.18	0.01	0.07	0.025
	Banda	75.54	11.68	4.95	0.02	0.04	3.77	4.73	0.26	0.01	0.03	0.016
	Ermita	76.98	9.55	3.97	0.09	0.09	4.27	3.83	0.23	0.04	0.08	0.019
	Guia	74.02	11.33	3.86	0.04	0.09	4.64	4.87	0.22	0.01	0.03	0.012
	Bandeada	74.16	10.66	5.71	0.01	0.01	3.96	4.09	0.18	0.02	0.11	0.019
	Galiñeiro	76.88	9.20	5.55	0.11	0.05	3.27	3.71	0.28	0.01	0.08	0.026
ZAMAMES DEPOSIT	Radioactive	79.36	10.1	4.02	0.1	0.77	4.41	1.52	0.62	0.14	0.44	0.018
	Radioactive	75.94	7.09	2.92	0.03	0.02	3.62	0.27	0.34	0.04	0.16	0.034

UNIT	FACIES	Rb	Sn	Ga	Zn	U	Th	Sr	La	Ba	Zr	Y	Ta	Nb	Be
Country rock	Paragneiss	135	5	25	130	5	8	240	34	1150	164	34	1	5	3
	Amphibolite	19	8	19	24	5	1	140	2	87	104	35	11	29	0.2
	Orthogneiss	140	2	18	30	5	14	132	26	811	101	37	1	20	0.4
Porriño Peralkaline Complex	Hornbl-biotite	170	7	26	70	5	14	268	69	758	306	46	4	20	6
	Piñeiro	165	4	37	41	5	28	11	53	160	452	43	5	47	0.3
	Zorro	190	14	36	125	8	21	10	53	20	752	55	9	125	5
	Saramagal	343	30	37	250	7	30	10	40	12	1846	35	13	261	10
	Banda	221	15	37	42	8	36	10	180	34	1279	71	19	147	0.5
	Ermita	210	16	48	47	14	53	10	129	25	1943	82	26	254	1
	Guia	290	4	37	97	8	31	12	126	89	1892	101	18	165	2.9
	Bandeada	285	60	43	194	5	43	10	156	28	2322	124	45	245	7
	Galiñeiro	317	17	32	149	7	46	10	161	6	2128	141	17	219	7
ZAMAMES DEPOSIT	Radioactive	130	290	45	2428	84	2310	86	1853	76	18616	5556	150	3426	41
	Radioactive	30	32	28	1887	5	14	20	787	5	13490	1229	470	1185	8

UNIT	FACIES	Ce	Pr	Nd	Sm	Eu	Gd	Tb	Dy	Ho	Er	Tm	Yb	Lu
Country rock	Paragneiss	70	<1	30	6	1.5	<2	1	<3	<1	<2	<1	4	0.5
	Amphibolite	23	2	18	5	1	4	1	5	1	3	1	3	1
	Orthogneiss	86	9	36	7	1.5	7	1.5	6	1.5	3	1	5	1
Porriño Peralkaline Complex	Hornbl-biotite	100	9	51	9	1.5	6	1	8	1	4	1	7	1.5
	Piñeiro	55	12	50	12	1	8	1	8	1	3	1	6	1
	Zorro	110	8	47	7	1	5	1	7	1	4	1	7	1
	Saramagal	70	<1	35	8	1	<2	2	<3	<1	<2	<1	12	1.5
	Banda	210	18	91	20	1	10	2	14	3	7	1	10	1
	Ermita	180	15	79	18	1	8	2	14	2	7	1	10	1
	Guia	250	20	110	17	1	11	2	13	2	8	1	10	1
	Bandeada	210	21	132	25	1	15	3	17	3	8	1	13	2
	Galiñeiro	460	36	230	36	1.5	25	3	25	4	13	2	15	2
ZAMAMES DEPOSIT	Radioactive	4100	300	1800	312	9	252	60	546	120	420	48	340	35
	Radioactive	2500	204	1210	299	11	208	30	264	48	110	11	89	10

peralkaline complexes,also located in the Malpica-Tuy Band, have been included. This geochemical trend is consistent with field observations and is characterized by the following sequence from less to more evolved facies: AMPHIBOLE-BIOTITE AMPHIBOLE-ZORRO-SARAMAGAL-BANDA-ERMITA-BANDED-GALIÑEIRO-MAGNETITE-RADIOACTIVE.

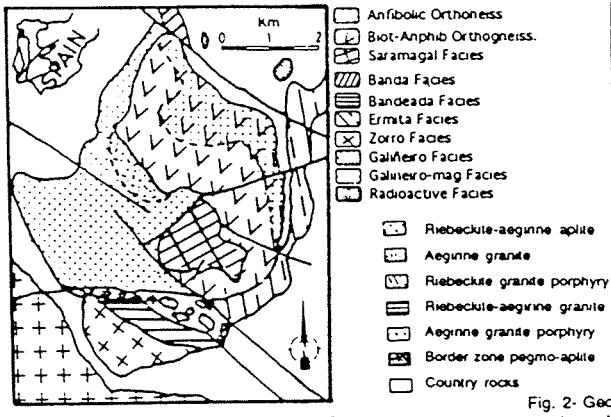

Fig. 1- Generalized geologic map of the Porriño Peralkaline Complex, northwestern Spain.

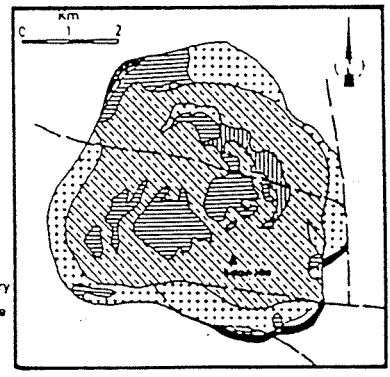

Fig. 2- Geological map of the Bokan Granite Complex, southern Alaska (adapted from Thompson et al., 1982).

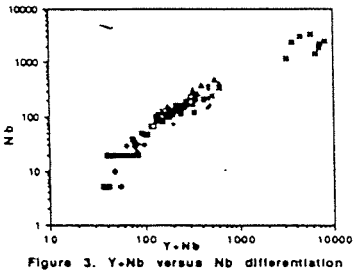

Figure 3. Y+Nb versus Nb differentiation trend for the Porriño Peralkaline Complex

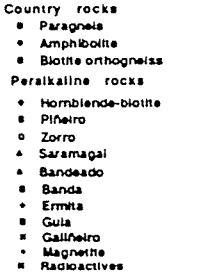

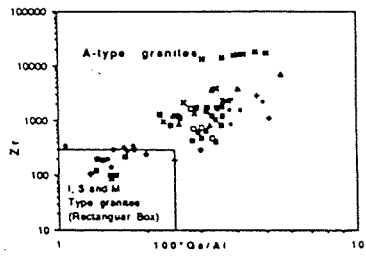

Figure 4. 1000*Ga/Al versus Zr tectonic discrimination diagram of Whalen et al. (1987) for the Porriño Peralkaline Complex

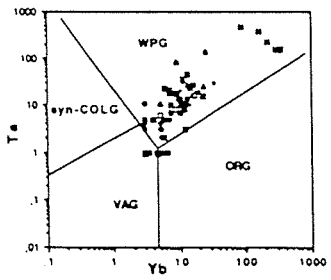

Figure 5. Yb-Ta tectonic discrimination diagram of Pearce et al. (1984) for the Porriño Peralkaline Complex

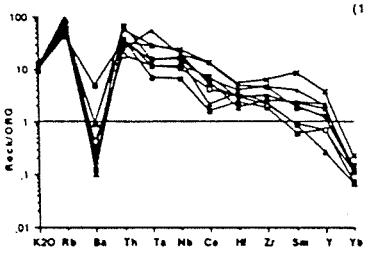

Figure 6. Normalized values for representative elements from peralkaline rocks

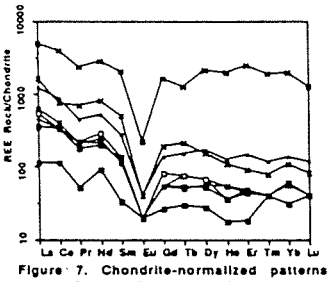

Figure 7. Chondrite-normalized patterns of the Porriño Peralkaline Complex.

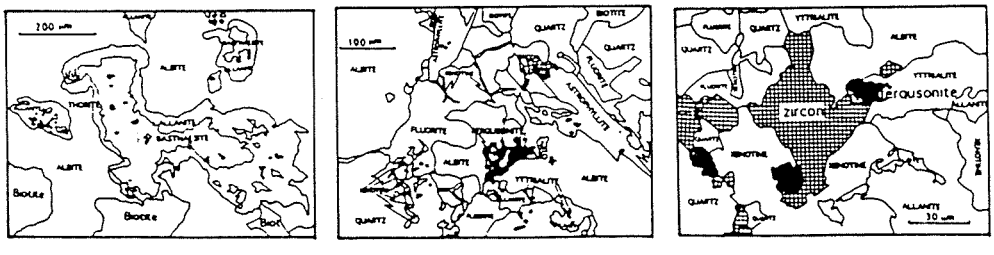

Figs. 8, 9, 10 - SEM backscatter images of extremely fine-grain REE minerals forming intergrowns in the radioactive orthogneiss of the Porriño Peralkaline Complex.

MINERALOGY

The **REE-Y-Nb-Zr** ores occur in a biotite orthogneiss located about 1 km east of the town of Zamanes. The study of the Zamanes deposit has been carried out mainly on drill-hole samples collected by the **Junta de Energía Nuclear (J.E.N.)** and **Rio Tinto Minera (R.T.M.)**. The ore body occurs to a depth of 50 m within a cupola of radioactive biotite orthogneiss which underlies an area of about 200x150 m and is slightly tilted towards the northeast. The host rocks show a strong preferred orientation and minor banding due to variable amounts of **quartz, albite, microcline, and biotite**. Accessory minerals are very abundant and include **zircon, grünnerite** (var. Mn-dannemorite), **astrophyllite**, and occasionally **riebeckite, aegirine** and **hornblende**. The REE-Y-Nb-Zr minerals form extremely fine grained intergrowths and aggregates (Figs. 8 to 10), and include **allanite, fergusonite, xenotime, monacite, thorite, thorianite, bastnaesite, yttrialite, ilmenorutile, apatite, zircon**, and possibly **gadolinite**. Associated minerals include **cassiterite, pyrrhotite, sphalerite, galena, pyrite**, and **chalcopyrite**. The presence of astrophyllite and fergusonite in the Zamames orebody was previously cited (Floor, 1961; Vergara et al 1991). The existence of pyrochlore has not been confirmed.

GENESIS OF THE ORE DEPOSIT

The **Zamanes REE-Y-Nb-Zr deposit** is similar to the deposits found in anorogenic granites in Nigeria (Matheis, 1979) and Thor Lake in Canada (Pollard an Taylor, 1993; Sinclair et al, 1993). However, the greatest similarities may be found with the Bokan Granite Complex of southern Alaska (Fig. 2). At Bokan (Thompson et al., 1982), the main lithology is also an aegirine granite which is crosscut successively by riebeckite porphyry, fine grained riebeckite porphyry, aegirine granite, and a late riebeckite-aegirine aplite. In Zamanes, both the deposit and the radioactive orthogneiss which hosts the REE-Y-Nb-Zr ores were originated by a late event during the magmatic evolution of the **PPC**. The geochemical data (Table 1) show that most of the samples from the **PPC** fall in the field of **WPG** (Within Plate Granites), perhaps with attenuated continental lithosphere (Figs.4 to 6). The **PPC** therefore may be considered as being made up of A-type granites, which intruded in an intracontinental rift environment associated with the opening of the Iapetus ocean during the Ordovician. Later, when the ocean closed in Devonian times, the **PPC** rocks were folded and overthrust on the Precambrian-Lower Cambrian basement during the first and second phases of Variscan deformation.

BIBLIOGRAPHICAL REFERENCES

Arribas, A(1963) Mineralogia y metalogenia del yacimiento Porriño. Bol Soc His Nat 61:51-57

Arribas,A; Martin-Izard, A; Arribas Jr, A(1993) The Zamanes REE-Y-Nb-Zr deposit in the Porriño Peralcaline Complex. Rare Earth Minerals Meeting. London: 1-3.

Floor, P(1966) Petrology of the Galiñeiro egirine-riebeckite gneiss. Leid Geol Med 36: 1-203

Matheis, G(1979) Exploration of Nb-Ta mineralization in Nigeria. Geo Soc Mal Bul 11:333-351

Pearce, J; Harris, B; Tindle, A(1984). Trace element discrimination diagrams for the tectonis interpretation of granitic rocks. Jo. of Petro. 25, 956-983.

Pollard, P; Taylor,R(1993) Be-Y-REE mineralisation in Thor Lake. REE Meeting Lond: 110-113

Rambaud, F; Alvarez, R; Bonilla, A(1992) El Complejo Igneo Peralkalino Del Monte Galiñeiro, y sus mineralizaciones. XV Cong Mun Miner III: 789-798

Sinclair, W; Jambor, J; Birkett, T(1993) REE Deposits in Canada: Alkaline Complexes as source of REE. Rare Earth Minerals Meeting. London: 110-113.

Vergara, A; Fernandez, M; Alvarez, R; Valle, F(1991) Determinación de lantanidos y otros elementos en fergusonitas. IV cong Espñ Geoqui, Soria: 56.

Thompson, T; Pierson, J; Lyttle, T(1982) Petrology and petrogenesis of the Bokan Granite Complex. Geol Soc American Bull, 93: 898-908.

Whalen, J; Currie, K; Chappell, B(1987) A-Type granites: Geochemical characteristics, discrimination and petrogenesis. Contr Min Petr, 95: 407-419

This paper was supported by grants from CICYT GEO 89/0832

Current Research in Geology Applied to Ore Deposits. Fenoll Hach-Alí, Torres-Ruiz & Gervilla (eds) (1993). ISBN 84-338-1772-8

PORPHYRY Cu AND Cu-Mo MINERALIZATION IN THE NORTHERN U.S. APPALACHIAN MOUNTAINS

Ayuso, R.A. & Foley, N.K.
U.S. Geological Survey, 954 National Center, Reston, VA 22092, U.S.A.

ABSTRACT: Regional petrographic and geochemical studies (major- and trace-element and isotopic compositions) in the northern U.S. Appalachians have identified tectonic blocks and suitable sources possibly associated with significant porphyry Cu-Mo deposits. Detailed studies of deposits such as Catheart Mountain provided important insights into fluid evolution models, isotopic (Rb-Sr, Pb-Pb, and O) systematics, and mineral reaction paths.

Although few porphyry Cu and Cu-Mo type systems are known in the northern U.S. Appalachian Mountains, on the basis of petrographic studies, bulk and isotope geochemistry, fluid inclusion determinations, reaction path modeling of alteration assemblages, and tectonic reconstructions, many favorable, but poorly exposed, granitic stocks are known to be present. The largest and best exposed porphyry Cu-Mo system in New England is associated with the Catheart Mountain granodiorite in the Chain Lakes massif, an area contained within the Boundary Mountains anticlinorium in northern Maine. The anticlinorium is thought to be underlain by Grenville-type crust (Laurentian) (Stewart, 1989), a feature that we think is critical to controlling the occurrence of source regions likely to be associated with significant porphyry-type mineralization. The Early Silurian Catheart Mountain granodiorite has been explored by surface geochemical surveys and diamond drilling programs, although detailed petrographic and geochemical information on the mineralized system is relatively new. The predominantly gray, fine-grained Catheart Mountain stock intruded the barren Ordovician Attean granodiorite; biotite and perhaps hornblende were originally present. Textural relations suggest that porphyritic granodioritic dikes, associated with the mineralization events, evolved in a shallow environment.

The Catheart Mountain porphyry Cu-Mo deposit is composed of hydrothermally altered equigranular granodiorite and porphyritic dikes having up to 4 wt.% pyrite, molybdenite, chalcopyrite, galena, and sphalerite. Hydrothermal alteration at Catheart Mountain is extensive and complex despite an overall, systematic, concentric zonation (Schmidt, 1974; Ayuso, 1989). Detailed studies have shown that much of the alteration is concentric about, and closely related to, numerous irregularly shaped and variously trending granodiorite porphyry dikes and to the mineralized veins. Zones of alteration vary from centimeters to many meters in thickness. Four main zones of hydrothermal alteration were found: potassic, to quartz-sericitic, argillic, and propylitic. In addition, several intermediate or transitional types occur. A succession of mineral assemblages formed during propylitic to potassic alteration reflect reaction path processes: biotite was replaced by chlorite and then by muscovite, plagioclase by albite + epidote, chlorite by muscovite, K-feldspar by muscovite, and sphene by rutile. All

rocks in the hydrothermal system can be systematically arranged in terms of an alteration index based on the abundances of K-feldspar, muscovite, and quartz. Rocks with high alteration indices have lower contents of CaO and Na_2O, higher values of Fe^{3+}/Fe^{2+} and K/Na, and higher abundances of Cu and Mo relative to rocks with lower alteration indices.

Infiltration of fluids at the onset of mineralization produced coarse-grained muscovite during the first stage of mineralization (pyrite + molybdenite). This first influx of sulfides was overprinted by an assemblage that included fine-grained muscovite, quartz, calcite, and a second influx of sulfide minerals (chalcopyrite + sphalerite + galena ± pyrite). Fluids associated with mineralization at Catheart Mountain had moderate temperatures (T=<305°C) (Molling and Ayuso, 1990), generally low salinities (<5% equiv. wt.% NaCl), and low-to-moderate CO_2 contents (Foley and Ayuso, 1992). In fact, CO_2 effervescence may have been an important process contributing to the deposition of the second stage of sulfide minerals during sericitic alteration. The occurrence of low-to-moderate CO_2 contents can be used to distinguish Catheart Mountain from classic porphyry Cu-Mo deposits elsewhere (Foley and Ayuso, 1992; Ayuso and Foley, 1992). Variations in trace element compositions and Pb-Sr-O isotopic variations indicate that magmas for the Catheart Mountain granodiorite were derived in the subcontinental lithosphere from a source that consisted of crustal basement rocks (Grenville-type), including those with mafic to intermediate compositions (Ayuso, 1989).

Other stocks in the Boundary Mountains area also contain porphyry Cu-Mo mineralization, for example in plutons at Sally Mountain and Priestly Lake, and in the composite Deboullie stock; however, in all of these systems, regional alteration zones are not well developed. The composite Devonian Deboullie stock is unique in this group because it ranges from mafic syenite to alkaline granodiorite and thus constitutes a distinct group of porphyry-type mineralization relative to the calc-alkaline Catheart Mountain granodiorite. In contrast to Catheart Mountain, porphyry Cu-Mo mineralization at Deboullie is associated with clinopyroxene + hornblende + biotite + quartz syenite, in the northern half of the Deboullie pluton. A younger hornblende+biotite granodiorite occurs only in the southern half of the pluton and is barren. Halogen contents and ratios in biotite and apatite in the syenite suggest that the type of mineralization shares many attributes found in syenitic porphyry Cu systems elsewhere, as distinct from those associated with porphyry Mo systems (Loferski and Ayuso, 1992). The Deboullie pluton, as in the case of the Catheart Mountain granodiorite, has a substantial mantle-derived component in its source region and was also affected by complex and protracted interactions with crustal rocks.

Plutonic rocks in the Boundary Mountains anticlinorium have a discrete range in major- and trace-element and isotopic compositions relative to plutonic rocks in more outboard tectonic zones of the northern U.S. Appalachians (Ayuso, 1989). In fact, plutonic rocks in northern Maine also share many geochemical attributes with plutonic rocks in the Matapedia zone in New Brunswick, Canada (broadly equivalent to the Boundary Mountains

anticlinorium) (Ruitenberg and Fyffe, 1982). More importantly, all of these rocks in northern Maine (Ayuso, 1989) and New Brunswick (Ruitenberg and Fyffe, 1982) have been linked genetically to magmatic source regions having affinities to porphyry Cu-Mo mineralization.

Devonian mafic syenitic rocks similar to the Deboullie stock are not abundant in this sector of the U.S. Appalachians (Ayuso and Loferski, 1992), and their scarcity suggests that the potential for undiscovered and economically important systems of this kind is not great. In contrast, Silurian and Devonian hornblende-bearing, calcic granodiorites exhibiting calc-alkaline affinities that resemble those in granitic rocks formed near active continental margins predominate in the Boundary Mountains anticlinorium and Connecticut Valley-Gaspe synclinorium in northern New England. Although our preliminary petrographic studies of other plutons in the Boundary Mountains anticlinorium have not identified extensive hydrothermal systems similar to that in the Catheart Mountain granodiorite, we think that granitic plutons in northern Vermont, New Hampshire, and northern and central Maine constitute the best potential hosts for undiscovered porphyry Cu-Mo systems.

Ayuso, R.A. 1989. Geochemistry of the Catheart Mountain porphyry copper deposit, Maine. Maine Geol. Survey 4:139-162

Ayuso, R.A. & Foley, N.K. 1992. Rb-Sr isotopic redistribution and character of hydrothermal fluids of the Catheart Mountain Cu-Mo deposit, Maine. U.S. Geol. Survey Bull. 2039, in press

Ayuso, R.A. & Loferski, P.J. 1992. Trace element geochemistry of syenite and granodiorite in the Deboullie pluton, northern Maine. Geol. Assoc. Canada 17:A5.

Foley, N.K. & Ayuso, R.A. 1992. Character of hydrothermal fluids in the Catheart Mountain Cu-Mo deposit, Maine: Constraints on modelling a mineralizing system. Geol. Assoc. Canada 17:A34

Loferski, P.J. & Ayuso, R.A. 1992. Mineral chemistry of biotite and apatite from syenitic rocks in the Deboullie pluton, northern Maine. Geol. Assoc. Canada 17:A67.

Molling, P.A. & Ayuso, R.A. 1990. Mineral paragenesis and hydrothermal alteration in the Catheart Mountain porphyry Cu-Mo deposit, Maine. Geol. Soc. America 22:57-58.

Ruitenberg, A.A. & Fyffe, L.R. 1982. Mineral deposits associated with granitoid intrusions and related subvolcanic stocks in New Brunswick and their relationship to Appalachian tectonic evolution. Canadian Min. Met. Bull. 1-15.

Schmidt, R.G. 1974. Preliminary study of rock alteration in the Catheart Mountain molybdenum-copper deposit, Maine. U.S. Geol. Survey J. Res. 2:189-194.

Stewart, D.B. 1989. Crustal processes in Maine. American Min. 74:698-714.

Current Research in Geology Applied to Ore Deposits.Fenoll Hach-Alí, Torres-Ruiz & Gervilla(eds)(1993).ISBN 84-338-1772-8

P-V-T-X CHANGES THROUGHOUT THE FORMATION OF INTRAGRANITIC Au CONCENTRATIONS IN THE NORTHWESTERN IBERIAN MASSIF (SPAIN-PORTUGAL): AN INTEGRATED FLUID INCLUSION STUDY

Boiron, M.C. (1); Essarraj, S. (1); Barakat, A. (1); Castroviejo, R. (1); Cathelineau, M. (1); Noronha, F. (2); Nogueira, P. (2); Yardley, B. (3); Banks, D. (3); Marignac, C. (4); Pereira, E. (5); Urbano, R. (6); Florido, P. (6) & García Palomero, F. (7)

(1) CREGU, BP 23, 54501 Vandoeuvre-les-Nancy Cedex, France; (2) Porto University, 877 Campo Alegre, Porto 4100, Portugal; (3) Leeds University, Woodhouse Lane, Leeds, LS2 9JT, U.K.; (4) ENM, Parc de Saurupt, Nancy, France; (5) DGGM, Ap. 89, 4466 S Mamede de Infesta Codex, Portugal; (6) ITGE, Rios Rosas 23, 28003 Madrid, Spain; (7) Rio Tinto Minera S.A., Zurbano 76, Madrid, Spain

The study of fluids associated with Au vein formation in granites from the north-western Iberian massif shows two major evolutions : i) a progressive change in the bulk chemical composition of the fluids from the early C-H-O-(N) fluids probably equilibrated with metamorphic host rocks to the late aqueous fluids probably related to the general meteoric fluid influx affecting the basement at the end of the Variscan orogenesis, and ii) changes in the P-T conditions from the early stage of sulphide deposition within quartz veins, under high P-T conditions (relatively deep structural levels), towards hydrothermal conditions typical of geothermal systems favourable to the Au concentration.

This paper presents an attempt to model the chemical evolution of fluids associated with the Au-bearing vein formation, and to define the processes of Au-enrichments in areas characterized by fairly good mining potential from the north-western Iberian massif (Galicia, Spain, Portugal). Proposed studies belong to a programme supported by the EC (Brite Euram program, contract MA2M-003) which is based on detailed multiscale and multidisciplinary approaches. They include the characterization of ore features, especially how gold distribute within the minerals, at what content, and under which state (combined or metallic), geochemical characterization of ore processes (typical mineral assemblages and associated elements) and ore forming processes (geochemical and structural traps, role of microfissural permeability on the control of ore fluid migration, and the effects of changes in the physical chemical conditions on gold deposition. Such studies are required to compare ores formed during similar geological events, and located within same metallogenic province. The area chosen is the north-western Iberian massif, which was one of the most actively prospected areas for gold, in Europe, in the last years. Data presented concern the results obtained using a multidisciplinary approach involving microstructural studies of fluid migration, and physical-chemical reconstruction based on mineral assemblages and fluid inclusion studies on one hand and thermodynamical calculations (P, T, fO2, fS2, pH) on the other hand .

1- METHODOLOGY

Fluids have been systematically studied as a function of the quartz sequences and their relationships with deformation (chronology of fluid inclusion planes) in the mineralized veins and their host rocks.Microthermometric characterization of the fluid inclusions was performed on wafers (300µm thick) using a heating-freezing Chaixmeca stage. Molar fractions of CO_2, CH_4, H_2S and N_2 were determined in individual inclusions by micro-Raman analysis performed on a DILOR X-Y multichannel modular Raman spectrometer. Bulk composition and molar volume were computed from the P-V-T-X properties of individual inclusions in the C-O-H-S system (Dubessy et al., 1989, 1992).

2-DATA ON P-T-V-X CONDITIONS

Three successive stages are recorded in the formation of the studied Late Hercynian gold-bearing quartz veins, each characterized by its own set of P-T conditions, mineral assemblage, fluid composition and fluid flow regime. Most stages have been found in all the deposits. The presentation focusses on the results obtained on granites especially the fluid evolution in the Corcoesto area (Malpica-Tuy shear band), with comparisons with other mineralized districts (Tomino (La Guardia province), Pino (Zamora province) in Spain and Penedono in Portugal).

The example of the Corcoesto deep drill hole

Fluid inclusions from Corcoesto drill core samples have been studied in mineralized quartz (MQ) and barren quartz in twelve samples from the surface to 540 m depth at CREGU (levels : surface, 66.5m, 70.85m, 147m, 189m, 256m, 346m, 365m, and 414m) and Porto University (levels 67m, 91m, 540m).Different types of quartz have been distinguished in mineralized zones :

- *early veins*: quartz lenses in metamorphic schists, and quartz associated with deformed pegmatoïds, and early quartz vein parallel to the granite foliation (generally barren);
- *quartz veinlets mineralized in arsenopyrite composed of* : Q1 quartz enriched in abundant small sized fluid inclusions ; clear overgrowths Q2 preceding the arsenopyrite deposition; and clear euhedral quartz or clear quartz cementing arsenopyrite crystals (Q3).
- *late barren quartz veinlets* : quartz comb veinlets Q4 associated with fluorite.

In mineralized quartz Q2-Q3, three major types of fluids have been recognized depending on the microthermometric and Raman data :

Q1-Q2 : Aquo-carbonic fluids with dominant CO2 (Vc-w and rare Lc-w)

Most of these fluids are observed as three fluid phase inclusions at room temperature. They have been observed as fluid inclusion plane in MQ I and MQ II-1 or as primary or pseudo-secondary fluid inclusions in MQ II-2. TmCO2 are ranging from -57.1 to -60.5°C but most of the data are in the range -59.0; -57.5°C. Tm cl are observed beetween 4 and 11°C with a mode around 8°C. Homogenization temperature of CO2 occur in the liquid phase between 9° and 30.3°C. ThCO2 in the vapor phase is ranging from 9° to 30.5°C with two modes at 24°C and 31°C. Global homogenization have been recorded in the range 280-390°C either to the liquid or to the vapour phase, and the salinity has been estimated in the range 7-8.5 % eq. wt.%NaCl considering the available data..

Inclusions with ThCO2 in the liquid phase have a rather dense volatile phase (0.5 to 1 g/cm3) slightly higher than inclusions with ThCO2 (V). Composition of the volatile phase is dominated by CO2 (80-100 mol %) , CH4 (0-18 mol.%) and display variable amounts of N2 (0-8 mol.%).

Latest arsenopyrite-Q3 : Aquo-carbonic fluids with dominant H2O (Lw-c) :

Fluid inclusions are scattered in euhedral quartz crystals crystallized around arsenopyrites. Liquid CO2 content is very low and is only detected by the presence of clathrates. Tm CO2 when visible is in the range -63 ; -57°C. Tm cl is in the range 6-15°C with a mode at 8°C. Global Th occur either in the liquid phase or in the vapor phase in the range 280-400°C either to the liquid or the vapour phase. These Lw-c inclusions (with no observed ThCO2 indicating a low homogenization of the CO2 phase to the vapour phase) are H2O dominated and contain a vapour phase displaying the following composition : CO2 : 50-100 mol % ; CH4 : 5-45 mol.% ; N2 : 0-8 mol.%. Fluid density are relatively constant with depth and are in the 0.4-0.8 g/cm3 range.

Au ore stage : Aqueous fluids (Lw)

They are always observed as fluid inclusion planes in Q2 or Q3 crosscutting aquo-carbonic fluid inclusion planes. Depending on melting temperature of ice two groups have been distinguished:
- low salinity fluid inclusions (Lw1) displaying TmH2O in the range -6 ; -1°C (salinity : 2-9 eq. wt.%NaCl). Such fluid inclusions are very abundant and very small. Global homogenization temperatures are in the range 150-350°C with a mode at 240°C and 300°C.
-higher salinity fluid inclusions (Lw2) in planes croscutting the Lw1 fluid inclusion planes. TmH2O is in the range -24 ; -12 °C and salinity is estimated between 16 and 24 eq. wt.%NaCl). Homogenization temperatures are in the range 100-150°C with a mode around 120°C. They are similar to those observed in the clear quartz from clear euhedral crystals in comb structures (Q 4).

Bulk chemical evolution

Early stages : The CO2-CH4-N2 ternary plot and the CH4/CO2 vs H2O binary plot show a rather clear evolution which is characterized by an increasing H2O content, and a CH4 content increase in the latest fluids (Q3) (Fig. 1). This evolution is recorded from the densest and earliest fluids Lc-w displaying a rather pure CO2 rich volatile phase towards Vc-w fluids in Q2, and then Lw-c fluids in Q3, of the fluids. During this evolution, the N2 content does not exhibit any clear evolution.

The data show that the changes in composition from c-w fluids with ThCO2 (L), to c-w fluids with ThCO2 (V), and Lw-c fluids are mostly characterized by an increase in water content, the w-c inclusions being enriched in water up to 80-90 mole % H2O.

For the Q1-Q2 stage, CO2/CH4 ratio for Lw-c is subconstant in the range 1-20 and is homogeneous at the sample scale. CO2/N2 do not exhibit strong variation (12 to 45). The volatile

phase of such type of fluid is thus relatively homogeneous. In Q3, Lc-w and Vc-w inclusions display variable CO2/CH4 and CO2/N2 ratios, especially for the inclusions displaying rather high CO2 contents,which are characcterized by CO2/CH4 ratio in the range 1-125.

In the case of the Corcoesto drilling, no clear differences appear with depth. The three types of fluids have been recognized in the different studied samples. There is thus no clear relationships between composition, density and gold content, probably due to the fact that gold is not related to this major fluid stage, but only arsenopyrite. However, it is clear that arsenopyrite crystallized during a major physical-chemical change of the system, characterized by dilution of dense carbonic fluids by dilute waters, correlatively to a change in the CO2-CH4 ratio in favour to CH4 (Fig. 1) probaly in relation with the unbuffering of the fluids by graphite.

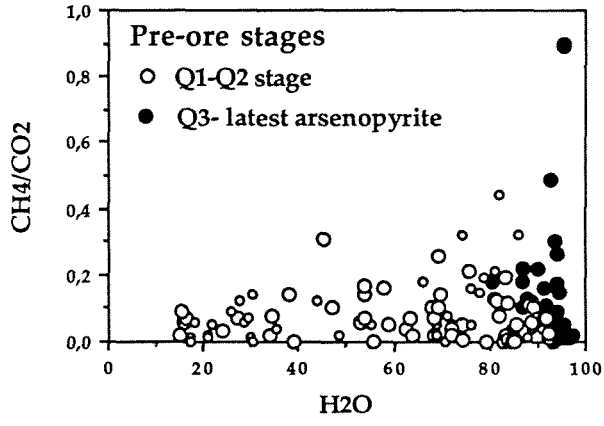

Fig. 1 : CH4/CO2 vs H2O diagram applied to individual fluid inclusion compositions issued from microthermometric and Raman analyses (Corcoesto, Pino, Penedono, Tomino deposits).

Late stages (Sulphide-Au stage) : The evolution of the Lw fluids is shown by the Tm H2O-Th plots . Series of fluids are trapped as fluid inclusion in microfissures (FIP) and document a cooling of the system from the Lw-c stage (Q3) towards relatively low temperatures. Fluid circulation ends with relatively dilute fluids (2- 9 wt%eq.NaCl) at temperatures of 200 to 250°C (Fig. 2). This stage is related to end of the intense microfissural activity in most mineralized samples.

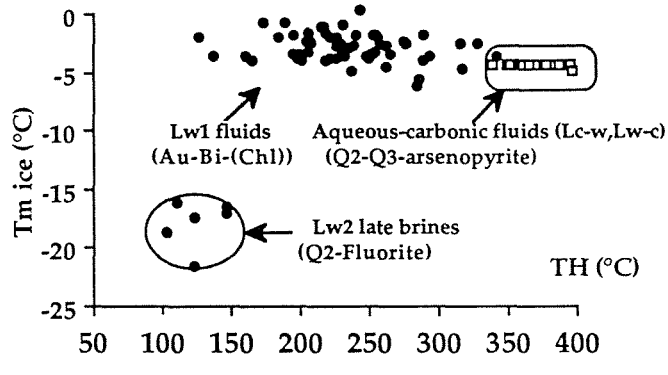

Fig. 2 : Tmice-Th diagram applied to the main fluid inclusion types found in the quartz-arsenopyrite veinlets from the Corcoesto granite.

General trends observed in the studied deposits

1 Early stage: formation of milky quartz veins. : milky quartz veins and veinlets formed mostly after the emplacement of late peraluminous granites (probably Westphalian); they also post-date some subsolidus alteration affecting these granites (albitization, quartz dissolution at Pino, greisenization at Tomino and Penedono). Early C-H-O-(N) fluids of metamorphic derivation are found in the surroundings of the early milky quartz veins, and as rare relics within the quartz itself. These are dense fluids trapped under pressures above 1Kb (frequently in the 2-4 kb range) and temperatures of 350° to 450°C. They may extremely enriched in CH4 and N2, indicating mixing with fluids produced by the devolatilization of C-rich units (Tomino, for instance).
2 Intermediate stage: early gold deposition : due to repeated tectonic reactivation, early milky quartz veins were strongly reworked Fluids involved in the formation of hyaline quartz veinlets belong to the C-H-O-(N) system and are essentially similar to those of the early stage. But at that stage, temperatures range from 250° to 350°C and pressures from 0.5 to 2.0 Kb depending on the localities.
3. Late stage: main gold deposition/enrichment : a renewal of tectonic reactivation (frequently a compressive regime characterized by new specific directions of major stresses) under quite different P-T conditions resulted in the main stage of gold ore deposits formation. The reactivation of early quartz veins (stages 1-2), results in microcracks which were now healed but not sealed by quartz. Native gold deposition took place, together with sulphides and sulphosalts (Pb-Ag dominated), along these cracks, especially when they crosscut earlier sulphides. In that case, it is difficult to determine wether the native gold deposited results entirely from a new gold input in the structure, or from a partial reworking of early concentrations into new mineral assemblages, although new input is in any case obvious.

Fluids associated with gold deposition are generally aqueous, have relatively low salinities, and were trapped under low temperatures in the 150-250°C range, at nearly hydrostatic pressures (ca. 0.5 kb). They are ubiquitous, were found in all the deposits, but their importance has been largely underestimated in the past as pointed out by Boiron et al.(1990) on the example of the french deposits.

CONCLUSION

As a whole, the successive appearance of the three stages just described reflect a series of major changes which are in turn correlated to the evolution of the Variscan belt. Thus are :

- changes in the bulk chemical composition of the fluids from the early C-H-O-(N) fluids probably equilibrated with metamorphic host rocks to the late aqueous fluids probably related to the general meteoric fluid influx affecting the basement at the end of the Variscan orogenesis. It is important to note that transition between each stage is relatively progressive and that dilution trends are frequently recorded.
- changes in the P-T conditions from the early stage of sulphide deposition within quartz veins, under lithostatic pressures and relatively high temperatures (relatively deep structural levels), towards hydrothermal conditions typical of geothermal system, with lower temperatures in the range 150-300°C and hydrostatic pressures (shallow levels).

These confirm the general evolution already described in the french part of the Variscan orogen (Boiron et al, 1989, 1990), where similar successsion of fluids have been demonstrated. It is shown in addition the lack of genetic relationships between the ore process and the D3 aluminous magmatism, and that most processes occured in between this latter stage and the late post tectonic granite magmatism.

References

Boiron, M.C., Cathelineau, M. & Trescases, J.J. 1989. Conditions of gold-bearing arsenopyrite crystallization in the Villeranges basin, Marche-Combrailles shear zone, France. A mineralogical and fluid inclusion study. Econ. Geol. 84: 1340-1362.
Boiron, M.C., Cathelineau,M., Dubessy, J. & Bastoul, A. 1990. Fluids in hercynian Au-veins from the french variscan belt. Min. Magazin. 54: 231-243.
Dubessy, J., Poty, B., & Ramboz, C. 1989. Advances in the C-O-H-N-S fluid geochemistry based on micro-Raman spectroscopic analysis of fluid inclusions. Eur J. Mineral. 1: 517-534
Dubessy, J., Thiery, R. & Canals, M. 1992. Modelling of phase equilibria involving mixed gas clathrates : Application to the determination of molar volume of the vapour phase and salinity of the aqueous solution in fluid inclusions. Eur J. Mineral. 4: 873-884.

Current Research in Geology Applied to Ore Deposits. Fenoll Hach-Alí, Torres-Ruiz & Gervilla (eds) (1993). ISBN 84-338-1772-8

THE BEHAVIOUR OF REE IN EPISYENITES (DEQUARTZIFIED AND ALKALINIZED GRANITES) FROM THE SIERRA DEL GUADARRAMA. SPANISH CENTRAL SYSTEM.

Caballero, J.M. (1); Casquet, C. (1); Galindo, C. (1) & Tornos, F. (2)
(1) Dept. Petrología y Geoquímica, U.C.M., 28040 Madrid, Spain
(2) ITGE, Rios Rosas 23, 28003 Madrid, Spain

Abstract: Episyenites are dequartzified and alkalinized granites arising by fluid/rock interaction during pervasive microfracturing of rocks at temperatures between ca. 650° and 350°C and fluid pressures lesser than 1 Kb. On the light of textural evidence, mass balance can be modelled on a constant volume basis. Protolith-normalized REE patterns show neat increases of the REE with REE_{Ep}/REE_{Gr} between 2.84 and 0.99. Ce and Eu often display negative anomalies matching those of the protolith . These changes are interpreted as reflecting the imposition by the part of the fluid, of the equilibrium pattern inherited from the source area slightly modified by changes of temperature, fluid pressure and pH along the fluid path. The absence of common REE patterns in the episyenites reflects local lithological controls, and suggests that a unique regional fluid was not involved in the alterations. REE were probably largely transported as PO_4^{3-} and OH^- complexes. Fixation of PO_4^{3-} as apatite led to the precipitation of the REE (at least the LREE) largely as allanite on account of the relatively high Ca activity in the fluid, proceeding in most of the cases from monzogranitic areas.

Introduction.

Episyenites from the Sierra del Guadarrama (SG; Spanish Central System), are peculiar rocks because, in spite of fitting the definition given by the french authors, i.e. dequartzified and alkalinized granites (Cathelineau, 1987a), they display a petrographic diversity not observed in the French Central Massif and other classic areas.

On the basis of the dominant feldspar, the SG episyenites have been classified as albite- or microcline-episyenites (Caballero et al., 1991). Moreover the first can be subdivided on the basis of the dominant ferromagnesian mineral into pyroxene-, amphibole- and biotite-episyenites. In turn, the pyroxene-episyenites consists of two varieties. The first contains hedembergite more or less transformed to hastingsite. The latter marks the transition towards the amphibole types. Chemically and petrographically, hedembergite-, amphibole- and biotite-episyenites form a continuum which is called the normal series. The second variety is peralcaline, with aegirine that evolves towards a complex amphibole identified as a fluor-sodian-ferri-clinoholmquinstite. On the other hand, the microcline-episyenites contain biotite as the only ferromagnesian mineral.

The normal series seems to correspond to a T-controlled evolution, ranging from ca. 650°C for the pyroxene-episyenites, down to 350°C for the biotite types. Finally the chlorite-episyenites, that represent most of the outcropping types, are interpreted as retrograded episyenites, either of the albitic or microclinic type, with temperatures of formation of the chlorite and part of the feldspar, lower than 350°C.

The analysis of fluid inclusions reveals the participation of moderate to low salinity fluids (< 12% wt NaCl equiv.) with CO2 below the detection limit. Fluorine is only detected in the pyroxene types, either as fluorite or contained in the amphibole. On the other hand neoformation of apatite is a characteristic feature of all the episyenite types.

Formation of episyenites can be considered an isochronous process on the basis of Rb-Sr dating (Casquet et al., 1992; Caballero et al., 1993).

Episyenites are important economic rocks as they can host important ore concentrations, e.g. U in vuggy types as in the French Central Massif or Cu-Zn-Sn-W mineralizations linked to superimposed younger alterations (Caballero et al., 1991).

The behavior of REE in these rocks, and particularly the mass balance, is essential to the understanding of the metasomatism leading to this peculiar group

of hydrothermal rocks. Also the economic potentiality of episyenites for REE makes these rocks attractive for a detailed geochemical survey.

Mass balance. Reference frame.

The absence of clustering on Gressens (1967) Xi-Fv diagrams, in all the studied samples, as well as the evidence of mobility of classically "inert" components, as evidenced by the increase of Al and Ti-minerals, prevents the use of a compositional reference frame.

Metasomatism in episyenites has taken place along a complex network of microfractures, accompanied by recrystallization-replacement processes of the igneous minerals. The preservation of the overall texture of the protoliths, i.e. average macroscopic grain size and porphirism including size and distribution of megacrysts, along with the absence of significant secondary porosity, lead us to conclude that a volume factor of one (constant volume) is the most realistic reference frame for mass balance considerations.

The total REE content of the episyenites analyzed varies between 118 (CEC1) and 248 ppm (JM150). Normalized to the granitic protoliths, all the samples show an increase of the total REE content with $\Sigma REE_{Ep}/\Sigma REE_{Gr}$ between 2.84 and 0.99. Fractionations vary between 1.26 and 0.66 and Ce and Eu often display negative anomalies (Table 1; Fig. 1).

OUTCROP	SAMPLE/TYPE	$(La/Yb)_{GN}$	$(Ce/Ce^*)_{GN}$	$(Eu/Eu^*)_{GN}$	$\Sigma REE_{ep}/\Sigma REE_{gr}$	$(La/Yb)_{CN,gr}$
J37	J37A, px J37j, px J37h2, mic	1.03 1.08 1.14	0.77 0.84 0.79	1.05 1.00 0.91	1.52 1.35 1.46	6.00
CEC	CEC1, px CEC3, px CEC4, px	0.89 0.99 0.92	0.98 0.99 0.92	0.93 0.84 0.92	1.28 1.36 1.49	7.18
J83	J83b, amph J84a, chlor	1.26 0.92	0.97 0.91	0.78 0.85	1.95 1.56	5.79
J34	J34f2, amph	1.12	0.99	0.95	1.32	4.58
JM114	JM114, bt	0.95	1.00	0.95	1.22	10.87
JM154	JM150, bt JM37, chlor	1.01 0.88	0.96 0.95	0.98 0.93	1.14 1.06	14.93
J25	J25b2, chlor	0.94	0.93	0.96	1.35	8.75
V6	V6, chlor	1.20	0.73	1.31	2.84	3.64
J39	J39g, chlor J39h, chlor	0.70 0.66	0.97 0.91	0.90 0.79	1.23 1.09	17.10
JM131	JM131, chlor	0.86	1.10	0.97	0.99	10.80

Table 1.- Several parameters (Fractionations, Ce and Eu anomalies and enrichment factors) of REE in episyenites. Keys: (px) piroxene-, (amph) amphibole-, (bt) biotite-, (chlor) chlorite- and (mic) microcline-episyenites. GN.- Protolith normalized (Granite). CN.- Chondrite normalized.

Mineralogical features.

The group of accesory minerals that control most of the content of REE in these episyenites is simple and similar to that found in other unmineralized types (Cathelineau, 1987). It consists of monacite, allanite, sphene, apatite and zircon, except in the peralkaline varieties where monacite and allanite are absent. Of these minerals, only monacite is an igneous relict whilst zircon grains consist always of igneous cores and hydrothermal overgrowths. The other minerals are all hydrothermal. Significatively, monacite often shows disequilibrium textures, consisting of a corona of apatite that match the previous grain, and an outer overgrowth of allanite. The transformation can be modelled by the following constant volume reaction:

$$1.59REE(PO_4) + 1.41(PO_4)^{3-} + 5Ca^{2+} + OH^- = Ca_5(PO_4)_3(OH) + 1.59REE^{3+}$$

The REE given out by the transformation of monacite into apatite are fixed in the

allanite shell ($(La/Dy)_{Mon,CN} \approx (La/Dy)_{Allan,CN}$; $Ca^*_{Mon} = Ce^*_{Allan}$), suggesting that the fluid was REE satured.

The REE contents in sphene, apatite and zircon are below the microprobe detection limit. However in the peralkaline types the sphene show a strong deficit in Ca (Ca = 0.86 p.f.u.) suggesting that REE could be present through the exchange vector:

$$(2REE^{3+})^{VII} + (R^{2+})^{VI} = (2Ca)^{VII} + (Ti)^{VI} \text{ (Exley, 1980)}$$

Discussion and conclusions.

REE have traditionally been considered close to inert during the episyenitization and they are only modified by younger mineralization processes (Cathelinau, 1987b; Leroy & Turpin, 1988; Maruejol, 1989). However this is probably a consequence of the reference frame employed by the above authors, i.e constant Al_2O_3. In fact, if this reference frame is applied to our case the ($\Sigma REE_{Ep}/\Sigma REE_{Gr}$) would be lowered. In any case, and because the REE patterns normalized to the protoliths show fractionation ($(La/Yb)_{GN} \neq 1$), an amount of mobility is evidenced in any case. Also, the mobility is not restricted to the high temperature types, which in fact show a strong REE enrichment, but also to the low temperature types. In fact the chlorite-episyenites show a depletion of REE with regard to the protoliths. Moreover this is associated with a decrease of the $(La/Yb)_{GN}$ ratio (samples J84a, JM37; Table 1; Fig.1C,F).

As fluids are simple and no evidence of fluorine is seen, with the exception of the high temperature types, the complexing of REE with ligands like PO_4^{3-} and OH^- is strongly suggested. The first has been inferred also by Cathelineau (1987b) or Gieré & Williams (1992), and its importance is strengthened by the abundance of apatite in all the samples and its participation in the left member of the monacite $\leftrightarrows$ apatite reaction (see above). OH-complexes migth have been important particularly at high temperature, on account of the high values of the pH inferred for the fluid (Casquet et al., 1992; Wood, 1990). The participation of Cl^- complexes at high temperatures can be rejected (Wood, 1990), however they could have played a significant role during the retrograde depletions where a diferential mobility of LREE is inferred, probably as a consequence of the increased stability of the LREE$[Cl_3]$ complexes vs. the HREE$[Cl_3]$ ones.

Taken into account the similarity of the granitic protoliths in the area, the REE pattern of the episyenites will be dependent upon the nature of the fluid source and the relative stability of REE in the solution. With regard to the latter, and at the inferred temperatures of the process (T>350°C), no significative differences can be expected, REE forming complexes being neutral (Wood, 1990; Bau & Möller, 1991). As a consequence, it is envisaged that the fluid will tend to impose a REE pattern on the episyenites, somewhat similar to that of the rocks found in the source area, with some minor differences due to changes in variables as temperature, fluid pressure or pH along the fluid path. This will also be enhanced by the increasing fluid/rock ratio. Likewise, the Eu anomalies of the protoliths will be largely reproduced in the alteration patterns because of the tendency for this element to be in the divalent form at T>350°C (Sverjensky, 1984; Wood, 1990; Bau, 1991). The importance of the REE changes during alteration will thus be strongly dependent on the differences among the source rocks and the protoliths. Extreme cases are represented by samples V6 and J83b (see Table 1, Figs. 1C,H). The first is a chloritized episyenite developed on a leucogranite ($(La/Yb)_{CN}$=3.64; Ce^*_{CN}=1.71; Eu^*_{CN}=0.24) that forms a small body inside a large massif of monzogranites ($(La/Yb)_{CN}$=6.04; Eu^*_{CN}=0.42). Thus, the protolith-episyenite differences probably reflect to a large extent, the disequilibrium between the fluid, formerly equilibrated with the regional monzogranites (higher total REE content, higher $(La/Yb)_{CN}$ ratio and a positive Eu^*_{CN}) and the leucogranitic body. This also holds true for sample J83b. In the other cases differences are minor, probably reflecting similarities between the source areas and the protoliths. Thus, local controls seem to have played an important role in the formation of episyenites as evidenced by the absence of a common REE pattern, in spite of the larger $(La/Yb)_{CN}$ ratios of the protoliths (between 3.64 and 17.1; Table I). A unique regional fluid common to all the episyenites in the Sierra del Guadarrama,

can thus be ruled out.

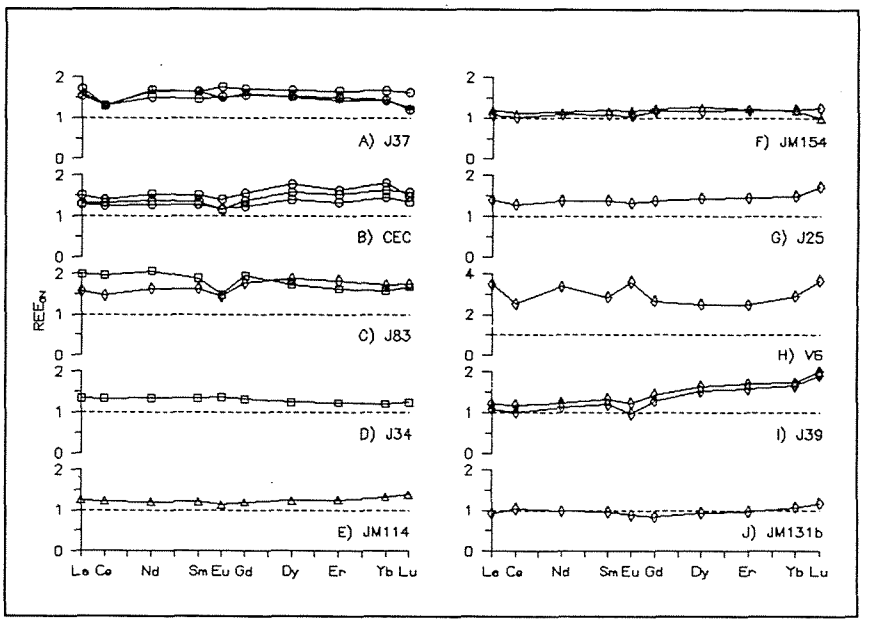

Figure 1.- Protolith normalized (GN) patterns of episyenites. Keys: (O) piroxene-, (□) amphibole-, (△) biotite-, (◇) chlorite- and (*) microcline-episyenites.

Acknowledgements.- Financial support were provided by DGICYT project number PB88-0124.

References.

Bau, M. (1991). Rare-Earth element mobility during hydrothermal and metamorphic fluid-rock interaction and the significance of the oxidation state of europium. Chem. Geol., 93: 219-230.

Bau, M.; Möller, P. (1991). REE systematics as source of information on mineralogenesis. Source, Transport and Deposition of Metals. Pagel & Leroy Eds.: 17-21.

Caballero, J.M.; Casquet, C.; Tornos, F.; Pellicer, M.J. (1991). Caracterización petrográfica de las episienitas de la Sierra del Guadarrama, Sistema Central Español (S.C.E.) Bol. Soc. Esp. Miner., 14: 273-284

Caballero, J.M.; Casquet, C.; Galindo, C.; Gonzalez-Casado, J.M.; Pankhurst, R.; Tornos, F. (1993). Geocronología por el método Rb-Sr de las episienitas de la Sierra del Guadarrama, S.C.E., España. Geogaceta. (in press).

Cathelineau, M. (1987a). Les interactions entre fluides et minéraux: themométrie et modèlization. PhD Thesis, I.N.P.L., Nancy, France.

Cathelineau, M. (1987b). U-Th-REE mobility during albitization and quartz dissolution in granitoids. Bull. Mineral., 110: 249-259.

Casquet, J.M.; Caballero, J.M.; Galindo, C.; Tornos, F. (1992). A revised model for the formation of dequartzified and alkalinized granites (episyenites). Water Rock Interactions. Kharaka & Maest eds.:1481-1484.

Exley, R.A. (1980). Microprobe studies of REE-rich accesory minerals. Earth Planet. Sc. Lett., 48: 97-110.

Gieré, R.; Williams, C.T. (1992). REE-bearing minerals in a Ti-rich vein from the Adamello contact aureole (Italy). Contrib. Mineral. Petrol., 112: 83-100.

Gressens, R. (1967). Composition-volume relationships of metasomatism. Chem. Geol., 2: 47-65.

Leroy, J.; Turpin, L. (1988). REE, Th and U behaviour during hydrothermal and supergene processes in an granitic environment. Chem. Geol., 68: 239-251.

Maruejol, P. (1989). Metasomatose alcaline et mineralization uraniféres: Les albitites du gisement de Lagoa Real (Bresil). Mém. Geol. Geochim. Mat. Prèmiér. Energ., 18, France.

Sverjensky, D. (1984). Europium redox equilibria in aqueous solution. Earth Planet. Sc. Lett., 49: 853-864.

Wood, S. (1991). The aqueous chemistry of the rare-earth elements and yttrium. 2. Theorical predictions of speciation in hydrothermal solutions to 350ºC at saturation water vapor-pressure. Chem. Geol., 88: 99-125.

Current Research in Geology Applied to Ore Deposits.Fenoll Hach-Alí, Torres-Ruiz & Gervilla(eds)(1993).ISBN 84-338-1772-8

MAJOR STRUCTURAL FACTORS OF Au CONCENTRATIONS IN THE NORTHWESTERN IBERIAN MASSIF (SPAIN-PORTUGAL): A MULTIDISCIPLINARY AND MULTISCALE STUDY

Cathelineau, M. (1); Boiron, M.C. (1); Essarraj, S. (1); Barakat, A. (1); García Palomero, F. (2); Urbano, R. (3); Toyos, J.M. (3), Florido, P. (3); Pereira, E.S. (4); Meireles, C. (4); Ferreira, N. (4); Castro, P. (4); Noronha, F. (5); Doria, A. (5); Ribeiro, M.A. (5); Barriga, F. (6); Mateus, A. (6); Yardley, B. (7) & Banks, D. (7)

(1) CREGU, BP 23, 54501 Vandoeuvre-les-Nancy Cedex, France; (2) Rio Tinto Minera, S.A., Zurbano 76, Madrid, Spain; (3) ITGE, Rios Rosas 23, 28003 Madrid, Spain; (4) DGGM, Ap. 89, 4466 S Mamede de Infesta Codex, Portugal; (5) Porto University, 877 Campo Alegre, Porto 4100, Portugal; (6) Lisboa University, Lisboa 1700, Portugal; (7) Leeds University, Woodhouse Lane, Leeds, LS2 9JT, U.K.

Au ore genesis in late Hercynian vein type deposits from the Iberian massif is mostly controlled by structural factors, especially : i) a long-lived tectonic activity affecting the crystalline basement during the progressive uplift of the Hercynian belt, ii) strong microfracturing stages of the previous quartz lenses due to latest brittle deformational stages, iii) rheological heterogeneities.

Au-vein type deposits from Western Europe display a multistage metallogenesis, a multistage and complex deformation of the vein structures which host the ores, each deformational stage being characterized by specific metal deposition and wall rock alteration. The time-space relationships between deformational events, the percolating fluid types and the specific resulting fluid-rock interactions and metal deposition, the exact timing of gold introduction within the veins are generally unknown. This work is an attempt to model Au-bearing vein formation, and to define the processes of Au-enrichments in areas characterized by fairly good mining potential, comparing ores formed during similar geological events, and located within same metallogenic province. It has been supported by EC (Brite Euram programme, contract MA2M 0033).The area chosen is the north-wester Iberian province, which was one of the most actively prospected areas for gold, in Europe, in the last years.

The Au-mineralizations from the Hisperic zone

A large number of gold occurrences is known in the Iberian massif. Some were known (and mined) in Roman and pre-Roman times, others were found in more or less recent times, mostly as a result of the efforts of national mining bureaus and geological surveys, and exploration companies, sometimes with involvement of universities. These Au-concentrations occurs in many situations and rocks, often in granites (Corcoesto,Tomino along the Malpica-Tuy shear zone, Penedono, Pino), or in Paleozoic sediments (anchi- to epizonal metamorphic series displaying enrichments in organic matter presenting rather low maturation index, quartzites, metavolcanites metasediments and greenschist/lower amphibolite facies metasedimentary sequences) in the case of Franca , Tres Minas, Vila Pouca de Aguiar deposits in Portugal.

The careful characterization of geological and structural environments of Au-veins is essential for a correct understanding of the role played by surrounding rocks, and is of prime importance in exploration. Thus, the nature of host rocks (type of granite, chemistry and physical characteristics of metasediments and volcanics), and the degree and style of deformation, are key factors for the understanding of ore forming processes. The role of pre-concentrations, the effects of contrasted rheological properties of rock units on the propagation of deformation, and the fluid-rock interactions controlling redox processes have to be especially investigated.

Conditions of ore formation have been estimated through a multidisciplinary characterization of wall-rocks, paleofluids (P-T-X-V conditions), paleopathways (microfracturing patterns), traps, deformation and ores, and multiscale characterization of the enclosing formations (regional, field and mine studies of the host formations, soil geochemical studies, low and deep drillings, and structural studies).

RESULTS

Au veins in granites: the examples of Corcoesto, Tomino, Pino and Penedono

The Corcoesto area (North Western Galicia, Spain; *Rio Tinto Minera s.a. prospection zone*), belongs to the northern part of the major deformation zone , so-called Malpica-Tui shear band in Galicia (Spain). This major shear zone is underlineated by series of syntectonic granite intrusions formed during the D3 deformational stage. Field works at Corcoesto have consisted in the complete drilling of a deep drill hole (746.5 m depth). The mineralized zone is characterized by an intense

VPA this phase is not well marked in A autochtonous unit, prevailing a S1 foliation while in the other units D2 developed a S2 foliation that transposes the S1, mainly in the most pelitic lithologies.Some quartz veins occur related to this deformation stage; 3) the D3 event is responsible for a large subvertical kilometric folds and for the uplifting of the former structures. These ones are reactivated with dextral shearing sense. At França D3 does not produce any penetrative cleavage, besides important shears, it was observed large subvertical folds near these shear bands and the quartz veins are affected by dextral shearing sense, these shears are filled up by iron oxides and quartz. In VPA, D3 deformation affects all the units with subvertical crenulation-cleavage (S3), stricking N120°E; a late D3 brittle ductile deformation is expressed mainly by a tensional fracture system N40° to N50°E. The rotation of the greatest principal stress (s1) from NE to NNE induces a sinistral shear sense in this tensional fractures and in some cases the earlier subvertical foliation N120(S0//S1//S2) is reactivated with dextral shear sense. In same places this shear deformation is accompained by intense hydrothermal alteration with silicification and chloritization (Tres Minas); 4) the D4 event affects all the former structures . D4 is a brittle phase with two conjugated fracture system stricking N10W to N20E, conditionned by a strain field that is consistent with a dextral shearing prevailing in the previous shear planes N120 Vilariça fault (N10E) in França area and Regua - Verin fault (N15-to N20E) in VPA area are D4 events.

In VPA area Au-mineralizations occur in different structures associted either in quartz veins predominatly subvertical and stricking N30E to N50E (Vale de Campo, Vale de Egua and Velhaquinhas) corresponding to sinistral fractures related to D3 or with silicified zones in metasediments which are related to dextral shear zones N120E Tres Minas mineralization is controlled by the latter one.

Studies of textural and chronological relationships between the differents ore minerals have shown that arsenopyrite, pyrite and galena are the main sulphide minerals in mineralized structures from França and VPA areas and appears associated with late quartz infilling of D3 to D4 structures. At França gold occurs at a combined state within arsenopyrite II as well as electrum during a relatively late stage (quartz II - siderite - sericite -chlorite) of the vein fillings; in VPA mineralized structures electrum / or gold occur predominantly, as a latter phase in intragranular spaces between pyrite and arsenopyrite, or in microcracks inside arsenopyrite/ pyrite generally associated with galena and sulphosalts. The latter gold is associated with aqueous fluid migration.

MAIN STAGES OF FLUID MIGRATION IN RELATION WITH DEFORMATION

Three successive stages are recorded in the formation of most studied gold-bearing quartz veins. They are each characterized by its own set of P-T conditions, mineral assemblage, fluid composition and deformational state (closely related to fluid flow regime). The order of succession knows no exception.

Quartz matrix formation : Milky quartz veins and veinlets formed mostly after the emplacement of late peraluminous granites (probably Westphalian); they also post-date some subsolidus alteration affecting these granites (albitization-tourmalinisation at Penedono, quartz dissolution at Pino, greisenisation at Tomino). Diffuse alteration, and sulphide crystallization in some instances (pyrite, then barren arsenopyrite) in the surrounding rocks seem to preceed the deposition of massive milky quartz in open space (tension gashes at Corcoesto and Tomino, filling of earlier structures at Penedono). No true mylonites were developed in the surroundings of the quartz veins. These features are at variance with those of typical Late Variscan shear-zones which are generally observed nearby at a regional scale.

High P-T conditions (pressures above 1Kb and temperatures of 350° to 550°C) are recorded and are roughly the same as those which prevailed during the late metamorphic stage in the Variscan terranes during or just after the hyper-collision event.There is no clear evidence of gold deposition at that stage, even at low concentrations in sulphides (pyrite, pyrrhotite, arsenopyrite) (see below).

Quartz vein reactivation : Due to repeated tectonic reactivation, early milky quartz veins were strongly reworked and were repeatedly subjected to intense fracturation; there were several alternances of micro-crack formation and healing or sealing by hyaline or clear quartz. Sulphide deposition (barren arsenopyrite) locally took place in the microcrystalline quartz, but was never massive. The alternances of increasing and decreasing permeabilities recorded by the quartz veinlets formation are reflected in strong pressure variations in one and the same vein, as demonstrated by the extreme range of calculated fluid densities from one inclusion to the other even within a small quartz grain (see later).Some gold intrduction could be related to this stage in some instances. In both cases, early carbonic fluids percolating granite are assumed equilibrated with the metamorphic host rocks,

subparallel faulting and microfracturing of sandwiches of granite bands and metamorphic series, but coïncide strictly with the presence of dense networks of quartz-arsenopyrite veinlets (tension gashes) within the foliated granites. In most mineralized areas (the two granite sills), the dominant structures are thin quartz-arsenopyrite veinlets oriented from surface two to 500 meters depth : i) N30° E, nearly parallel to the foliation plane (dip : 50±10°W) , ii) N90° to N110°E (dipping 50-70°N), the E-W direction being dominant , iii) N150°, less frequent.

A great variety of fluids linked to long lived heat anomalies within the same shear zone which affected the metamorphic surrounding rocks. Quartz preceding arsenopyrite in the dominant N90-110°E veinlets are CO_2-H_2O rich fluids and are followed by H2O-(CH4-CO2) fluids having a low density volatile phase. Aqueous fluids have been recognized in most samples in fluid inclusion planes, especially in the mineralized areas, and are associated with the assemblage chlorite-phengite-Au-Bi/Bism. They are followed by one late generation of low temperature brine.

Similar geometric and chronologic features have been found at Tomino (South Galicia, Spain, *ITGE prospection zone*) where the granite is affected by an intense microfracturing accompanied by strong water-rock interactions of relatively high temperature (greisens). Field and laboratory works demonstrate a rather unusual geometric feature of the fluid migration . The highest density of quartz veins occurs in the central part of the granite dyke (Alto de Pozas), within a segment of 2 km lengh. The sets of quartz veins (1 to 10 cm thick) are limited to granitic dyke and oriented N70°-80°W, steeply dipping Northwards. The quartz veins are often spaced about 1 m, with thickness ranging from simple fissures, with occasional filling sulfides to few dm. Structurally, quartz veins are filling extension gash fractures developped in the last stage of the third phase of deformation. The foliation in the Pedrada granite is parallel to the schistosity and corresponds to the third phase of the hercynian deformation.(N 160°-170°E dipping around 50° NE) .

Oriented samples have been taken along a profile vein/fresh granite of the Urgal zone. Microfissuring is only represented as fluid inclusion planes either in the granite or in the major quartz tension gashes, oriented N80±10° direction. In the vein itself, the geometry of the late microfracturing is dominated by fissures parallel or sub-perpendicular to the (N150°E) to the vein direction. The number of cracks decreases from the vein towards the granite, indicating a chanellized fluid (CO2-CH4 rich fluids) migration through cracks. New reactivation produces the arsenopyrite crystallization, but a late brittle event is needed to get new microfissuring and mineralization (dilute aqueous fluids associated with gold-chlorite, and chalcopyrite, sphalerite, bismuthinite, nauve bismuth) associated with aqueous fluids of relatively low temperature.

At each stage there is a constant orientation of the microcrack network indicating a probable permanence of the major stress direction all along the hydrothermal history of the granite.

Au concentrations in metamorphic series : the Vilariça fault zone and the Vila Pouca de Aguiar area

Important structural studies have been carried out in North-Eastern Portugal (Vilariça fault zone -França deposit and Vila Pouca de Aguiar area VPA) in order to reconstruct the evolution in the different deformational stages and their relationships with metallogeny. These two areas also are considered to be better for giving a good image of relation between metasedimentary host rocks with mineralized structures.

Vila Pouca de Aguiar (VPA) is a vast area characterized by several occurrences of auriferous mineralizations namely Tres Minas (were the Romans have exploited 16Mt on two open pits) and the northeasternmost sector (Curros) woth several occurrences of gold mineralizations.

In the França and VPA areas, the admitted regional structural models for the Central Iberian Zone appear to be valid. França is situated on autochtonous "Douro inferior Group" involving host rocks of lower Devonian and VPA on the parautochtonous "Peritransmontano Group" involving host rocks of lower Silurian (Landoverian) to lower Devonian (Ribeiro, 1974). Cartography and lithostratigraphic studies on VPA area allowed the individualization of four lithostratigraphic units (A, B, C, D), predominantly constituted by quartzites , chlorites phyllites, black shales interbedded with acid metavolcanic and dalc silicate rocks. The A unit represents an autochtonous basement and B, C, and D units the parautochtonous (Peritransmontano Group).

At least, four Hercynian deformational phases are recognized : 1) The D1 characterized by axial planar slaty cleaveage (S1) with vergence to the north (domain of the recumbent folds). There is a continous deformation process between D1 and D2 giving place to important thrust nappes, responsible for the parautochton character of the "Peritransmontano Group"; 2) the well marked subhorizontal S2 cleavage. At França, it is overturned to south , with reverse sense of the thrusts ; at

and are very similar to those described in the metamorphic environments such as in Vila Pouca area. However, these fluids which are important for the formation of chemical traps for gold (sulphides and early quartz deposition), seem to have less impact on the transport and deposition of the economic concentration of gold.

Intense microfissuring and main gold deposition/enrichment stage: A renewal of tectonic reactivation (frequently a compressive regime characterized by new specific directions of major stresses) under quite different P-T conditions resulted in the main stage of gold ore deposits formation. The reactivation of early quartz veins (stages 1-2), resulting in microcracks which were now healed but not sealed by quartz. Native gold deposition took place, together with sulphides (galena, chalcopyrite-Bi/Bismuthinite) and sulphosalts (Pb-Ag dominated)in frequent association with calcite (or siderite at França)- (Fe) chlorite, (± sericite) , along these cracks, especially when they crosscut earlier sulphides (arsenopyrite). The economic ores do not result from a reworking of preconcentrations. Although at the root of the concept of maturation of gold bearing shear-zones (Bonnemaison and Marcoux, 1989), the very fact of gold preconcentration in early sulphides could not be assessed in our studies. There is no evidence for a remobilization of early concentrated gold in the arsenopyrite lattice, again at variance with the maturation concept.

CONCLUSIONS

The interactions between regional studies, industrial research and laboratory approaches have helped to get a definition of the factors controlling economic ore formation (deformation, lithology, time-space relationships between ore deposition and major geological events , ...) and the modelling of metallogenic processes. They yield to the following conclusions :

- as a whole, the successive appearance of the three stages just described reflect a series of major changes which are in turn correlated to the evolution of the Variscan belt : changes in P-T-X conditions (see Boiron et al, this abstract volume), and changes in the factors controlling the fluid migration. The nature of the fluid migration and the geometry of the thermal anomalies has changed from stage to stage. It appears that the successive events recorded in the more long lived mineralized areas reflect progressive uplift of a segment of the Variscan belt at the end of its hyper-collision stage, while long lived thermal anomalies (315-285 Ma) evolved at depth.

-the main factors controlling the enrichments are linked to the :

1- formation of the main channels : the complex superimposition of early deformations from D1 to D4 are responsible for specific structures which have evolved from ductile to britlle regime and are associated with the main shear zones affecting the Gallicia area. The earliest quartz deposition, which creates the specific potential trap for later mineralizations are formed at that stage (D3 to D4).Contrary to the "gold bearing shear zone" model (Bonnemaison and Marcoux, 1987, 1989), it is shown that mineralized faulted areas are not typical ductile shear zones : major shear zones are barren, and the evidence of early ductile deformation due to shears is generally minor along the mineralized faults.

2- the formation of the most efficient trap for ores at the stage of Au mobility, which is favoured by:

- strong microfracturing stages of the previous quartz lenses due to late brittle deformational stages . Such microfracturing is extremely complex in detail, and results from the superimposition of each brittle stage on the early quartz matrix (milky quartz cemented by microcrystalline quartz).
- strong rheological heterogeneities, such as those produced by the presence of metric quartz lenses within micaschist, or granite bands in metamorphic rocks (Corcoesto, Tomino) show that stress intensities are higher in the quartz vein, in the center and near its boundaries, this explaining a more intense fracturing of the vein than the host rock, and the lack of mineralization outside the quartz vein. Therefore, the early quartz matrix (milky quartz cemented by microcristalline quartz) acquires its permeability thanks to further stress reactivations, which yield higher fluid flows within the veins than in the surroundings. This process explains that only quartz veins are mineralized although the gold inputs are late compared to the quartz matrix formation.

References

Bonnemaison, M. & Marcoux, E. 1987. Les zones de cisaillement aurifères du socle hercynien français. Chron. Rech. Min. 488: 29-42

Bonnemaison, M. & Marcoux, E. 1989. Auriferous mineralization in some shear zones : A three stage model of metallogenesis. Min. Deposita 25: 96-104.

Current Research in Geology Applied to Ore Deposits.Fenoll Hach-Alí, Torres-Ruiz & Gervilla(eds)(1993).ISBN 84-338-1772-8

URANIFEROUS MINERALIZATIONS AROUND THE MALADETA GRANITIC MASSIF (CENTRAL PYRENEES, SPAIN)

Charlet, J.M.
Faculté Polytechnique de Mons, 9 Rue de Houdain, 7000 Mons (Belgium)

ABSTRACT. Uraniferous stratiform anomalies in the Silurian black shales of the Central Pyrenees have been studied up to contact with the Maladeta granite. More pronouced anomalies occur in the Lower Devonian hornfels and lead to the development of uraniferous minerals. The genesis of these U mineralizations is discussed.

Uraniferous stratiform anomalies in the Silurian black shales have been described by the author in the south part of the Central Pyrenees from the "Sierra Negra" zone to the "Pallaresa" zone (fig. 1.) An objectif of this research has been the behaviour of the radioelements from the unmetamorphosed shales up to the granite contact.

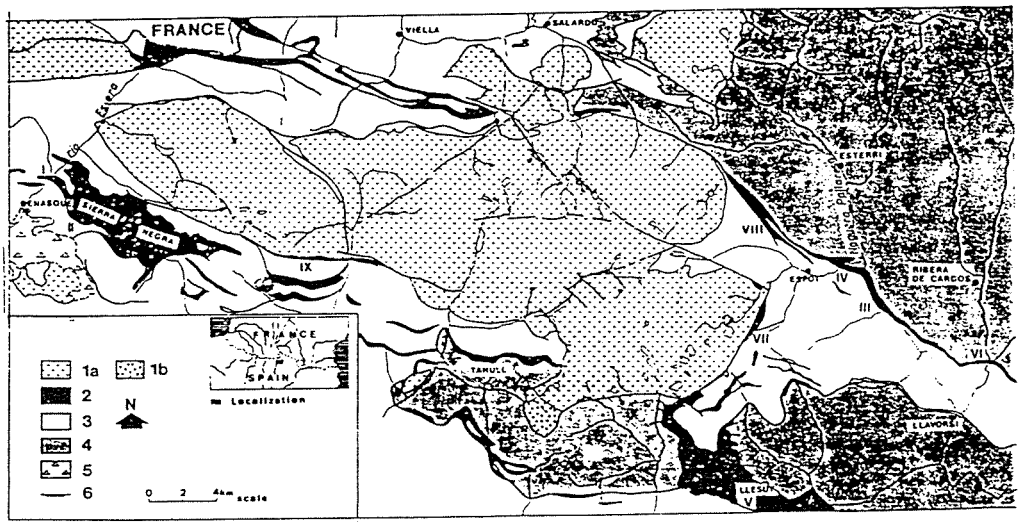

Fig. 1. Geological situation of the studied zone (I-IX)
1. Granitoïds with different petrographical facies (1a granitic rocks - 1b basic rocks).
2. Silurian - 3. Post Silurian - 4. Cambro-ordovician.
5. Glacial drift - 6. Principal faults. Geological map from Zwart (1972) and Charlet (1979).

In the eastern extremity of the Maladeta granite massif uraniferous occurences have been discovered (Charlet 1992) and a more extensive study of these occurences has been continued during 1992-1993. The geological and metallogenic context of the uraniferous mineralizations is specified in this paper.
Since some twenty years the author studies the Maladeta granite massif and the contact metamorphism (Charlet 1977, 1983). The metamorphism appears to be polyphasic. During a first phase, the Silurian black shales are transformed into sillimanite hornfels where actual granite contact exists, but into andalusite schists more distant from this point. Similary, the

Lower Devonian limy and silty formations give rise to skarn of grossular and vesuvianite near the point of granite contact, but farther away to a paragenesis typical of epidote-albite hornfels facies. The second metamorphic phase is characterized by a lower temperature retrograde metamorphism of the preceding parageneses and undergoes development at the point of granite contact resulting from the association of actinolite (asbestos) with epidote.
The anomalies discovered by a radiometric survey have been studied by gamma-ray spectrometry.

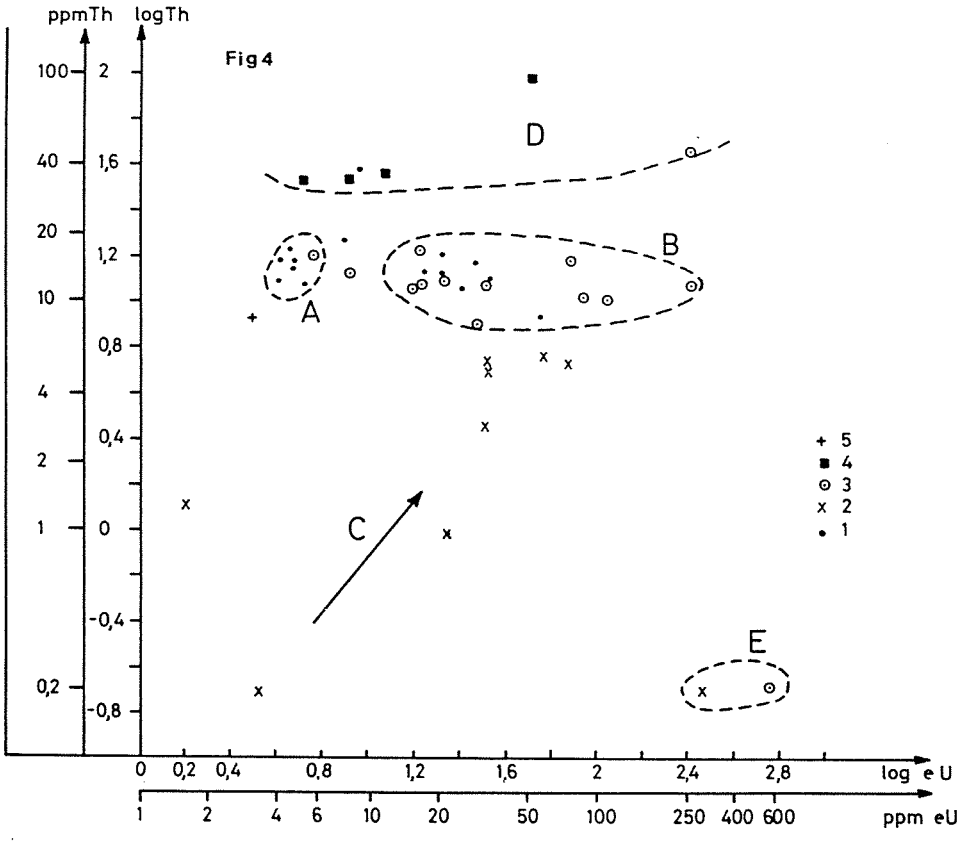

Fig. 2. Uranium and thorium distribution.
1. Black shales (Silurian). 2. Lower Devonian limy and silty formations.
3. Andalousite schists (Silurian). 4. Leucogranitic veins.
5. Granodiorite of the Maladeta massif.

The figure 2 summaries the distribution of uranium and thorium. Domain A include the "normal" shales of the Silurian. The trend to the domain B characterizes the stratiform anomalies in the black shales and include unmetamorphised shales and andalousite hornfels located at the point of granite contact. Domain D enclose thorium-uranium anomalies in leucogranitic veins or sometimes in Silurian black shales. The trend of the domain C is a feature of the limestones and silstones of Lower Devonian, thorium concentrations going with the lithology (negative correlation thorium-carbonates, $r^2 = 0,86$). The trend C goes to the domain B including uraniferous anomalies which can exceed 70 ppm in pyritous limestones

with 55 % of $CaCO_3$. The domain E with very low thorium values shows high uraniferous concentrations (500-600 ppm U) in the lower part of Devonian with the development of apatite skarn. These anomalies has been studied by microscopic analysis and qualitative microprobe analysis. Fig. 4 shows a parageneses pyrite-hematite-brannerite (U-Ti oxyde) observed at the point 3002 (fig. 3).

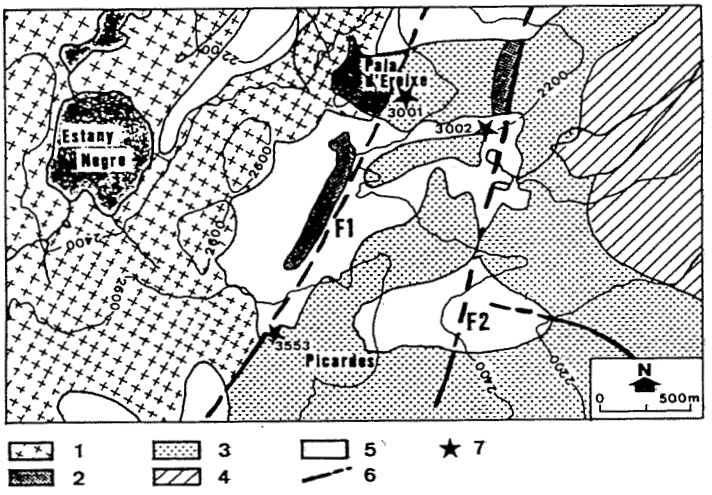

Fig. 3. Geological sketch of the uraniferous occurences (Eastern part of the Maladeta Massif, zone VII, fig. 1).
1. Granite - 2. Silurian - 3. Lower Devonian - 4. Middle Devonian - 5. Glacial drift - 6. faults - 7. Uraniferous occurences.

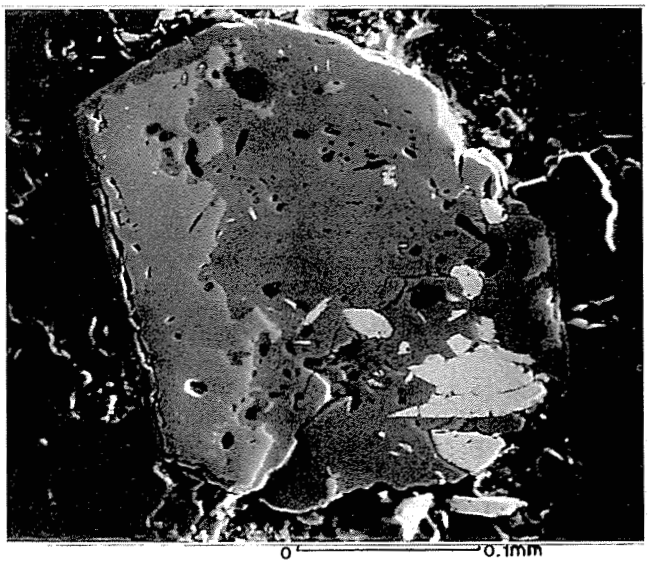

Fig. 4. Microphotograph of a polished surface.
Py : Pyrite - H : Hematite - U-Ti : Brannerite.

Conclusions.

The stratiform uraniferous anomalies of the Silurian black shales subsist in the metamorphic aureole up to contact with Maladeta granite and allow lithostratigraphic correlations at the regional scale. They belong at the domain B (Fig. 2.).
The magmatic feature appears determined by thorium anomalies (domain D) in the leucogranitic veins but also in some beds of the Silurian (possibly with volcanic origin).
The uranium mineralizations (domain E) can be considered typical of skarn and hornfels deposits already described by various authors (Booyle, 1982). They occur in a paragenetic sequence of low temperature with epidote, chlorite and actinolite and in a fault set F1 - F2 (Fig. 3.). One can consider that solutions bearing uranyl ion have migrated until they encouter oxyding-reducing interface (hematite - pyrite). Uranium has precipitated into a titaniferous phase, titanium being probably in relation with a process of primary sulphidation of a Fe-Ti oxyde as described by Clemmey (1981).
The high ratio Th/U in leucogranitic veins might suggest a uranium source is to found in the early crystallization of thorium minerals (monazites). However, the spatial distribution of the occurences at the base of the Devonian, overlying the Silurian uraniferous black shales tends to suggest a remobilization of uranium from the black shales, facilitated by the fault system along the Maladeta massif border (Fig. 3.).

References.

BOOYLE, RW. **1992** - Geochemical prospecting for uranium and thorium deposits. Elsevier, Amsterdam.CHARLET J.-M. 1992.

CHARLET J.-M. **1977** - Le métamorphisme au contact des granitoïdes entre les vallées de l'Esera et de la Noguera Ribagorzana (Pyrénées centrales espagnoles). Ann. Soc. géol. Nord : 165-177.

CHARLET J.-M. **1983** - Los granitos intrusivos ligados a la orogenesis hercinica. In Carbonifero y Permico de Espagna : 315-328.

CHARLET J.-M. **1990** - Découverte d'anomalies uranifères dans le Silurien des Pyrénées centrales espagnoles. Ann. Soc. géol. Nord, 58 : 187-194.

CHARLET J.-M. **1992** - Découverte d'indices uranifères à l'extrémité orientale du massif granitique de la Maladeta (Pyrénées centrales espagnoles) : contexte géologique et métallogénique. C.R. Acad. Sci. Paris, 314 : 683-690.

CLEMMEY H. **1981** - Some aspects of the genesis of heavy mineral assemblages in Lower Proterozoic uranium - gold conglomerates. Min. Magazine., 44 : 399-408.

Current Research in Geology Applied to Ore Deposits.Fenoll Hach-Alí, Torres-Ruiz & Gervilla(eds)(1993).ISBN 84-338-1772-8

NIGERITE IN RARE-ELEMENT PEGMATITES AND ASSOCIATED GRANITES OF THE SEIXOSO AREA (NORTHERN PORTUGAL)

Helal, B. (1); Bilal, E. (1) & Pereira E. (2)
(1) Ecole des Mines de Saint-Etienne, France
(2) Serviços Geologicos de Portugal, Portugal

ABSTRACT: Nigerite is a peraluminous mineral always associated with aluminium silicate and/or muscovite in which Sn, Zn and Fe are essential constituents. In Seixoso area, nigerite occurs along pegmatites contacts with pelitic wallrocks and in pelitic xenoliths found in top of the highly evolved Outeiro granite. Nigerite is a secondary mineral formed during the interaction of the a Sn, Zn-rich and S-poor fluid, initially in equilibrium with pegmatitic or granitic magma, and pelitic rocks. Nigerite occasionally crystallize at a late-magmatic stage in samples of the GSP facies contaminated by pelitic xenoliths. Compared to nigerite from the other known occurrences, Seixoso nigerite have a high content of Ti and a variable Sn/Zn ratio due to the Sn substitution by two Zn in B sites. On account of this substitution, we propose a new nigerite structural formula: $(Zn,Mg,Fe^{2+})\ [Zn_{4-2x},(Sn,Ti)_x,[]_x](Al,Fe^{3+})_{12}O_{22}(OH)_2$.

I. INTRODUCTION

Nigerite was first discovered in quartz-sillimanite rocks associated with cassiterite-bearing pegmatites of central Nigeria, in 1944, by Jacobson and Weeb (1947). It is the first mineral to be discovered in which tin, zinc and aluminium are essential constituents. Only few papers now exist describing nigerite occurrences. Ginzburg et al. (1961) found nigerite as a common accessory mineral in pegmatite of Eastern Siberia. Maijer (1965) describes nigerite in cassiterite-bearing pegmatites of the Seixoso area (Northern Portugal) and in a andalousite-rich sample taken in the margin of a small intrusion of tourmaline-bearing granite. Van Tassel (1965) reports an occurrence of nigerite in a cassiterite-bearing pegmatite near Lixa (Douro Litoral province, Portugal). Kloosterman (1974) found nigerite in tin-tantalum pegmatites of Amapa (Brazil) and in quartz-muscovite marginal facies associated with these pegmatites. Bannister et al. (1947) showed that nigerite has the approximate formula: $(Zn,Mg,Fe^{2+})(Sn,Zn)_2(Al,Fe^{3+})_{12}O_{22}(OH)_2$.
They reported that it is trigonal with symmetry $\bar{3}m$ and determined the following crystallographic parameters: *a* and *c* are equal respectively, to 5.72 and 13.86 Å. This paper presents new data on nigerite of Seixoso area, first discovered by Maijer (1965), and on its mode of occurrence. The Seixoso nigerite is compared with that of the other known occurrences and a new nigerite structural formula is proposed. The chemical conditions for nigerite formation are discussed.

II. GEOLOGICAL SETTING

The Seixoso area corresponds to the SE margin of the Hercynian Celorico de Basto batholith (sheet 10-A of the geological map of Portugal in the 1/50000 scale) and is located in the NW sector of Minho province (Northern Portugal). The SE margin of the Celorico de Basto batholith consists mainly of a coarse-grained porphyritic biotite granite intruding metasedimentary rocks which belongs to the allocthonous Vila Nune unit (Pereira, 1987). This batholith is surrounded by a well developed aureole of contact metamorphism. Post-tectonic peraluminous granites form rather small bodies intrusive both in the Celorico de Basto batholith and in its aureole of contact metamorphism. In Seixoso area, a granite intrusion outcrops in form of two main apices (Seixoso granite and Outeiro granite) and of numerous and small apices or dikes-like bodies. Seixoso granite and Outeiro granite are heterogeneous and characterized by a horizontal magmatic layering which was accentuated by post-magmatic pervasive albitization and greisenization which become more intense upwards: their are grading from biotite-bearing facies at depth, through two-mica or muscovite-tourmaline facies into roof of apex (Helal, 1992). Apical facies (apogranites) are highly evolved and sometimes (in Seixoso granite) poorly mineralized in cassiterite. Biotite-bearing facies, apogranites of Seixoso granite or Outeiro granite and Seixoso pegmatite (the most evolved terms) are considered as belonging to a single differentiation serie (Helal, 1992). The apogranites-pegmatites transition is characterized by a sodolithic-type evolution: there is a decrease in SiO_2 and K_2O accompanied by increasing Al_2O_3, Na_2O, Li, F (P_2O_5, Sn, Ta, Nb, Be).

III. NIGERITE IN SEIXISO PEGMATITE

The Seixoso Sn-Ta-Nb-Li-Be-bearing pegmatite field consists in a main concordant and subhorizontal (the dip varies from 10 to 30°E) pegmatite which laterally take root in top of Seixoso granite, two minor concordant pegmatites and about ten dike-like veins. All these pegmatites strike about N-S and have a thickness which varies from 5 to 10 m. Internal structure of each pegmatite is weakly developed but a stocksheider-like marginal facies characterized by coarse grained cleavelandite (albite) which radiates upward from the footwall and downward from the hanging wall is

systematically observed. Seixoso pegmatites consists mainly of a facies (GSP facies) the texture of which is typically granitic but extremely porphyritic: K-feldspar megacrysts (may be up to 30 cm in size) are enclosed in a fine-grained matrix which consists in elongated weakly zoned albite lath, quartz and minor muscovite. Cassiterite, Li-phosphates of the amblygonite-montebrasite serie, Ti, Sn-rich chrysoberyl and pseudo-ixiolite (Ti-rich columbite-tantalite) are the characteristic accessory minerals. These pegmatites had been affected, like Seixoso granite and Outeiro granite, by late-stage albitization and greisenization.

-Nigerite along pegmatites contacts: Nigerite generally occurs in close association with the margins of Seixoso pegmatites, near the pegmatite-host rock contact. Pelitic wallrocks along the pegmatite contact have been affected by a recrystallisation apparently due to heat loss from the pegmatite. The recrystallisation apparently due to heat loss from the pegmatite. The crystallised zone (2 to 3cm wide) is characterized by coarsening of biotite and quartz crysts and disappearance of the foliation. Pelitic wallroks around each pegmatite of the Seixoso pegmatite field have recorded three episodes of hydrothermal alteration deduced from textural relationships between primary and secondary mineral is: development of nigerite-bearing quartz-andalousite-(fibrolite) marginal facies coeval with tourmalinization; greisenization then argillization.

The nigerite-bearing quartz-andalousite-(fibrolite) marginal facies is most of time limited to enrichment in andalousite, quartz and nigerite in restricted part of the recrystallized zone but is sometimes well developed with a thickness which can be up to 5 cm. In that case, biotite and ilmenite are no more observed whereas cassiterite, Fe, Sn, Ta, Nb-rich rutile and chrysoberyl become characteristic accessory minerals.

Tourmalinization is limited to a narrow aureole (10 to 20cm wide) at pegmatite-host rock contact. Tourmaline is systematically more abundant just beyond the nigerite-bearing quartz-andalousite-(fibrolite) marginal facies. The greisenization aureole (sometimes up to 1 m thick) generally extends beyond the tourmalinization aureole.

-Nigerite in the GSP facies: Nigerite is occasionally found in samples of the GSP facies which contain abundant tourmaline and andalousite and accessory sillimanite (fibrolite). An important feature is that this facies generally contain no tourmaline neither nigerite. Andalousite and sillimanite are systematically replaced by muscovite and often occur as optically continuous relics in muscovite flakes. Fe, Sn, Ta, Nb-rich rutile occurs as small scattered grains, enclosed in muscovite. Nigerite is most of time enclosed in margin of muscovite flakes replacing andalousite but can occasionally be observed enclosed in margin of primary albite and interstitial (late-magmatic) cassiterite. No corrosion or replacement of nigerite by muscovite has taken place.

IV. NIGERITE IN OUTEIRO GRANITE

The top of Outeiro granite sometimes contains strongly greisenized pelitic xenoliths which consist of quartz and muscovite replacing biotite and sillimanite that occurs as sheaf-like aggregates of fibrolite. Nigerite forms euhedral crystals always enclosed in sillimanite near muscovite or in this latter. Both Outeiro granite and its xenoliths have recorded three episodes of hydrothermal alteration: transformation of primary biotite, high in TiO_2 to secondary green biotite, low in TiO_2; greisenization and argillization. Ti liberated be recrystallization and alteration of biotite forms rutile. Primary ilmenite has reacted to form rutile.

V. NIGERITE STRUCTURAL FORMULA

Bennister and al. (1947) showed that nigerite has the approximate formula $(Zn, Mg, Fe^{2+})(Sn,Zn)_2(Al,Fe^{3+})_{12}O_{22}(OH)_2$. It may be represented as $AB_2C_{12}O_{22}(OH)_2$ structure type.

Structural formulas were calculated on the basis of 24 (O,OH). Fe is allocated to the C sites to bring the total, with Al (and accessory Si), to 12 (there is some replacement of Al by Fe^{3+}), and the remainder (Fe^{2+}) is assigned to the A site which is occupied by Fe^{2+}, Mn and Mg. Since calculated Fe^{2+} is low, structural formulas were recalculated considering that iron is essentially ferric. Ti is allocated to B site: the close similarity in ionic radius between Sn^{4+} and Ti^{4+} enables the latter to enter into stanniferous minerals. Since the sum of Fe^{2+}, Mn and Mg atoms is lower than 1 (lower than 0.35 in our nigerites), Zn is allocated to the A site (Zn_A) to bring the total, with these metal atoms, to 1, and the remainder (Zn_B) (close to 1 a./f.u. in Zn-rich nigerites of Outeiro granite) has been assigned, as advocated by Bannister and al. (1947), to complete the Sn (and Ti) positions because Zn has a near ionic radius to Sn.

The sum of metal atoms is often appreciably greater than 15. Bannister et al. (1947) indicated that this excess over the ideal repeat is possible because the structure of nigerite has ample interstitial vacancies. This excess of metal atoms is positively correlated to Zn (a./f.u.). This correlation clearly better when we consider that iron is essentially ferric. This is consistent with Al deficit in C sites and with the analysis of nigerite given by Bannister and al. (1947). In all known compounds the valency of Zn is two. We can exclude the substitution of the one Sn^{4+} by one Zn^{2+} since the number of Si atoms is to low to think that the structure can be electrostatically balanced by the complementary substitution of Al^{3+} by Si^{4+}. The slope (-0.5) of the correlation in the diagrams (Sn+Ti) versus Zn_B (Fig.1) and the value of the abscissa intercept (Zn_B=4) lead us to propose the substitution:

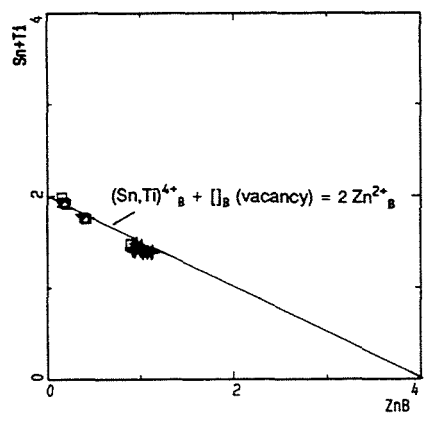

Fig.1. Chemical compositions (a./f.u.) of nigerites. Nigerite from: ✣ Outeiro granite; ▫ Seixoso pegmatites; ▼ Nigeria (Bannister and al., 1947).

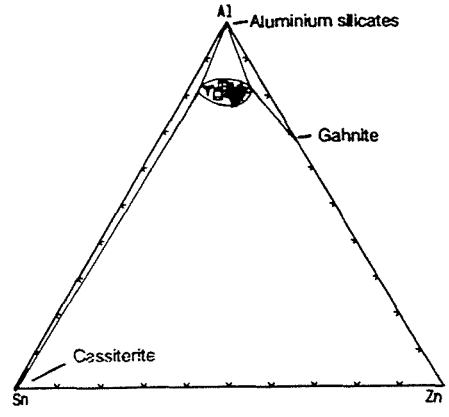

Fig.2. Chemical compositions (a./f.u.) of nigerites. Nigerite from: ✣ Outeiro granite; ▫ Seixoso pegmatites; ▼ Nigeria (Bannister and al., 1947).

$$(Sn,Ti)^{4+}_B + []_B\ (vacancy) = 2\ Zn^{2+}_B$$

We propose that four B sites are available. B sites occupancy is variable: when Sn is ideally absent, B sites are occupied by four Zn, whereas Zn_B equals zero two B sites are occupied by Sn and two others B sites are vacant.

In conclusion, nigerite must have the approximate formula:
$(Zn,Mg,Fe^{2+})\ [Zn_{4-2x},(Sn,Ti)_x,[]_x](Al,Fe^{3+})_{12}O_{22}(OH)_2$.

VI. DISCUSION AND CONCLUSIONS

Nigerite is a peraluminous mineral. In Seixoso area and in all known occurrences, nigerite is associated with aluminium silicate (sillimanite and/or andalousite) and/or muscovite, so nigerite is only stable in peraluminous environments. In Outeiro granite nigerite is found in strongly greisenized metapelitic xenoliths. Nigerite have probably been formed by reaction of sillimanite and biotite with a Sn, Zn-rich fluid also responsible for the greisenization of the top of Outeiro granite. Pegmatites and their metasedimentary country rocks are characterized by strongly peraluminous bulk compositions so it is not alumina which controls nigerite repartition in that case.

In Seixoso area, nigerite occurs in four different situations: internally (generally in stocksheider-like marginal facies) and externally along pegmatites contacts with pelitic (biotite-rich) wallrocks, in pelitic xenoliths found in top of Outeiro granite and occasionally in samples of the GSP facies. Except the latter case, nigerite is obviously a secondary mineral originate by the action of a Sn, Zn-enriched fluid since pelitic rocks are Zn and Sn poor. However, part of Zn can originally be present in primary biotite of pelitic rocks.

Nigerite found in the GSP facies is always associated with andalousite, sillimanite, tourmaline and Fe, Sn, Ta, Nb-rich rutile. This assemblage is analogous to that of the nigerite-bearing quartz-andalousite-(fibrolite) marginal facies developed on pelitic rocks suggesting that it is represents transformed xenoliths derived by stoping of pelitic wallrocks. The Seixoso pegmatites contain no tourmaline. The systematic late-stage tourmalinization of wallrocks shows that the original B content of the peraluminous pegmatite magma was probably high but tourmaline saturation was not reached on account of the low Fe and Mg content of the magma. Nigerite is a relatively iron-rich mineral. Samples of GSP where nigerite was found have a high enough Fe and Mg content to stabilize tourmaline and nigerite, on account of contamination by Fe, Mg rich pelitic wallrocks. In that case, it seems that nigerite have crystallized in late-magmatic stage: it is observed as inclusions in rim of primary albite and in interstitial Nb-rich cassiterite which crystallize just before the magmatic-hydrothermal transition (Helal, 1992).

Nigerite is the Zn-bearing phase in Seixoso pegmatites, their wallrocks and in Outeiro granite xenoliths whereas greisenized samples of Seixoso granite showing enrichment in Zn are characterized by the lack of nigerite: sphalerite is the Zn-bearing phase. It should be noted that sulphides never occur in Seixoso pegmatite and in Outeiro granite. The crystallization of nigerite is probably controlled by the activity of the S in the fluids or in the pegmatite magma (nigerite in GSP facies). In sulphide rich environment, Zn usually forms sphalerite because the large affinity of Zn for sulphur. Since pelitic rocks from Seixoso area originally contain some sulphides, the activity of S in the fluid from which pegmatites margins nigerite originate was probably controlled by the S-poor pegmatite magma. In the same way the

fluids responsible for the greisenization of Outeiro granite was S-poor.

The composition of the nigerite is related to that of the host rock: pegmatite nigerites have distinctly higher Sn/Zn ratio that Outeiro nigerites. In the case of nigerite-bearing samples of contaminated Outeiro granite, this relation is due to the fact that nigerite is the only Sn, Zn-bearing phase. In nigerite-bearing samples of GSP facies, nigerite has a high Sn/Zn ratio because it has crystallized in the presence of primary cassiterite. The similar and high Sn/Zn ratio of nigerite found in altered pelitic wallrocks (characterized by the lack of cassiterite) along pegmatites contacts shows that pegmatite cassiterite was capable of buffering Sn activity in the fluid expelled from the pegmatite.

The Sn-Al-Zn triangular diagram showing presumed mineral compatibilities in the system Sn,Al,Zn together with the observed phase assemblages in nigerite-bearing samples of contaminated Outeiro granite or Seixoso pegmatite suggest that the Sn/Zn ratio of the solution (or the magma for GSP nigerite) is a critical factor as indicated by Kloosterman (1974). In the presence of sillimanite and/or andalousite, with a progressive increase in the value of the Sn/Zn ratio of the solution (or the magma for GSP nigerite), the paragenetic succession is as follows: Gahnite, -gahnite and nigerite, nigerite alone then nigerite and cassiterite.

The nigerite-sillimanite and/or andalousite stability region is large on account of the effect of Sn substitution by two Zn in B sites: for Seixoso nigerite, the atomic Sn/Zn ratio varies from approximately 0.3 to 2 whereas for Nigeria nigerite (Bannister et al., 1947) it is about 3. It is important note that Outeiro nigerite have atomic Sn/Zn ratio lower that nigerite from the other known occurrences probably because it is not associated with cassiterite. the existence of alluvial nigerite is reported (Kloosterman, 1974): the hardness is between 8 and 9 (Bennister et al., 1947) and permit nigerite to support transport. Since nigerite is easily identifiable by its habit, its composition can be utilised as a rule for cassiterite prospection: nigerite in equilibrium with cassiterite have a high atomic Sn/Zn ratio.

Compared to nigerite from the other known occurrences, Seixoso nigerite have high content of Ti because it is always associated with rutile. It is consistent with the fact that Ti-rich nigerite described by van Tassel is associated with rutile too.

We concluded that nigerite found in the GSP facies is formed during the interaction of pegmatite magma and xenoliths derived by stoping of pelitic wallrocks. Nigerite found along pegmatites margins is formed during the interaction of a fluid expelled from the pegmatite in the late metasomatic stage of its internal evolution and pelitic wallrocks. this fluid is Sn,Zn-rich and S-poor and characterized by a high Sn/Zn ratio imposed by the pegmatite cassiterite. Outeiro nigerite is formed during the interaction of a Sn, Zn-rich and S-poor fluid responsible for the greisenization of Outeiro granite and its pelitic xenoliths.

REFERENCES:

Bennister, F.A., Hey, H.M., Standler, H.P. 1947. Nigerite a new tin mineral. *Mineral. Mag.*, 28, 129-136.

Ginzburg, A.I., Nazarova, A.S., Sukhomazova, L.L. 1961. Nigerite from pegmatites. In, New data on rare mineralogy, 42, Translation 1963, New York.

Helal, B. 1992. Granitoïdes, granites à metaux rares et hydrothermalisme associé: géologie, minéralogie et géochimie de plusieurs suites tardi-hercyniennes (Nord du Portugal). *Thèse de Doctorat Ecole des Mines de Paris*, 495 p.

Jacobson, R. Webb, J.S. 1947. The occurrence of nigerite, a new tin mineral in quartz-sillimanite rocks from Nigéria. *Mineral. Mag.*, 28, 118-128.

Kloosterman, J.B. 1974. Nigerite in the tin-tantalum pegmatites of Amapa, Brazil. *Mineral. Mag.*, 39, 837-845.

Maijer, C. 1965. Geological investigations in the Amarante region (Northern Portugal) with special reference to the mineralogy of the cassiterite-bearing albite pegmatites. *Thesis, Univ. Amsterdam, Deltro, Roterdam.* 155 p.

Pereira, E.S. 1987. Estudo geologico-estrutural da regiao de Celorico de Basto e sua interpretacao geodinâmica. Thèse doct. Univ. de Lisboa., *Serv. Geol. do Portugal.*

Van Tassel, R. 1965 Nigerite from Lixa, near Felgueiras, Douro Litoral province, Portugal. *Mineral. Mag.*, 483-486.

Current Research in Geology Applied to Ore Deposits. Fenoll Hach-Alí, Torres-Ruiz & Gervilla (eds) (1993). ISBN 84-338-1772-8

ACCESSORY MINERALS OF THE CINOVEC GRANITIC CUPOLA; BEHAVIOUR OF REE IN F- AND CO_2-RICH FLUIDS

Johan, Z. & Johan, V.
BRGM, BP 6009, 45060 Orléans, France

ABSTRACT: The following accessory minerals from a 1596 m deep borehole in the Sn-W- mineralized Cínovec (Zinnwald) granite cupola, Czech Republic, were studied: zircon, monazite, xenotime, columbite, ilmenorutile, rutile, pyrochlore, thorite, bastnaesite, synchysite. Early crystallized accessory phases (zircon, monazite, thorite, xenotime) underwent strong hydration and fluorination due to the interaction with a fluid phase. After precipitation of fluorite and bastnaesite, a late fluid phase appeared, destabilizing columbite and precipitating pyrochlore and synchysite.

1. INTRODUCTION. - In 1961-1963 the Czechoslovakian Geological Survey drilled a 1596 m deep borehole in the Sn-W mineralized Cínovec (Zinnwald) granite cupola. The hole intersected quartz veins with W-Sn mineralization and greisens in the apical part of the cupola, then traversed zinnwaldite granite (ZG) underlain by protolithionite granite (PG). The ZG extends to a depth of 730 m; its contact with PG is gradual, the transition zone (TZ) being about 10 m thick. Cores from the hole were studied in detail by Stemprok and Sulcek (1969) and Cocherie et al. (1991). However, little attention was paid to accessory minerals and several of them, essential for the understanding of fluid-rock interactions, were not found. To fill this gap, 56 core samples have been studied in polished sections and 37 were examined by SEM, the accessory minerals being analysed by electron microprobe.

2. ACCESSORY MINERALS. - Studied were: zircon, monazite, xenotime, thorite, columbite, pyrochlore, ilmenorutile, rutile, bastnaesite, synchysite.

Zircon. - Crystals are complexely zoned and strongly hydrated. The analytical totals indicate up to 18 wt% H_2O. On the H_2O-ZrO_2-SiO_2 diagram, the analyses plot beside the $ZrSiO_4$-H_2O tie-line, being displaced towards $Zr(OH)_4$. This indicates, in addition to molecular water, the presence of OH in the O structural site. The F concentration reaches 2.4 wt% in the uppermost part of the intrusion, and varies from 0.2 to 1.1 wt% in the deepest section of the PG. A strong enrichment in F persists down to a depth of 275 m.

The maximum HfO_2 concentration is 5.24 wt%. The cores of zircon crystals in ZG are enriched in Hf compared with the rims, whilst in the PG the zoning is inversed. The inversion occurs at the TZ (740 m). The UO_2 concentration varies irregularly with depth (3.36 wt% at 1107 m). ThO_2 content is less than 1 wt%. Microprobe analyses revealed up to 0.38 wt% Sc_2O_3 in zircon from the ZG and the TZ; in the deepest part of the PG, Sc_2O_3 is generally below the detection limit. Among the REE, Dy, Er and Yb contents are noticeable. Zircon from the apical part of the cupola is enriched in Y_2O_3 (3.3-4.3 wt%); extremely high Y-values were recorded at 1100 m (8.9wt%). Y_2O_3 concentration does not correlate with P_2O_5, which remains low and

nearly constant along the borehole profile.

In order to obtain the number of OH in the O site, the formulae were calculated on the basis of the A site fully occupied by M^{4+}, M^{3+} and M^{2+}, where M^{4+} = Zr,Hf,Th,U; M^{3+} = REE,Y,Sc; M^{2+} = Fe,Ca. This calculation shows vacancies in the Si site. A new model of substitution of Zr^{4+} by M^{3+} and M^{2+} in hydrated zircon is proposed, implying that the appearance of (OH,F) in the O site is related to the introduction of M^{3+} and M^{2+} into the A structural site.

Monazite. - It forms anhedral grains (about 20 μm) and aggregates (100 - 200 μm) included in protolithionite (PG) and/or in plagioclase and quartz (ZG). The average F concentration in monazite corresponds to 0.127 at. per formula unit. Two types of monazite were distinguished: (1) Th-rich monazite (up to 9.3 wt% ThO_2) characteristic of the ZG; (2) Th-poor monazite (< 2 wt% ThO_2) in the PG. The number of Th atoms per formula unit positively correlates with $[Ca+Si]_{at}$. This indicates the substitution mechanism $Ca^{2+} + Th^{4+} \Leftrightarrow 2REE^{3+}$, and miscibility with $ThSiO_4$ (huttonite). Th-rich monazite is poor in Y, whilst that from the PG contains up to 1.5 wt% Y_2O_3. $[Ce/La]_{at}$ decreases with depth. The distribution of REE is characterized by a strong negative anomaly in Eu, especially for monazite from the ZG showing Eu/Eu* = 0.009. The monazite from the PG is characterized by 0.028 < Eu/Eu* < 0.059.

Thorite. - Euhedral crystals in the TZ and PG (50-70 μm in size), are included in mica and/or plagioclase. Thorite is strongly hydrated; microprobe analyses indicate 12-14 wt% H_2O. Fluorine is systematically detected. The calculation of formulae on the basis of a fully occupied A site (see zircon), shows a deficit in the Si site and the presence of F and OH in the O site.The UO_2 is generally below the detection limit. However, uranothorite (26.31 wt% UO_2) appears at 1558 m. An extensive solid solution $ThSiO_4$ - YPO_4 was observed, reaching 56 mol% $(Y,REE)PO_4$.

Xenotime. - Rare in the PG, but absent in the upper part of the ZG, is commonly associated with zircon, in places in epitaxial overgrowth. Analyses indicate a strong hydration (8 - 9 wt% H_2O). Similar to zircon and thorite, the B site is not fully occupied. Fluorine is systematically present (< 1 wt%). ThO_2 is generally < 1 wt% ZrO_2 concentration is always below the detection limit. $[Dy/Yb]_{at}$ ratio varies from 0.59 to 1.97.

Columbite. - The main carrier of Nb and Ta in the ZG, it is absent in the upper part of the PG and appears again at a depth of 1558 m. The crystals are strongly zoned, reflecting variations in Nb/(Nb+Ta) and in W distribution. The Fe/(Fe+Mn+Ca) ratio increases with depth (0.576 to 0.906), as well as Ti, Zr and Sn concentrations. The maximum occupation of the B site by Ti and Sn is respectively 12.36 and 8.55%; the highest ZrO_2 content is 1.34 wt%. Nb/(Nb+Ta) ratio is virtually constant in the ZG. WO_3 content generally is less than 4 wt% in the apical part of the cupola, but W-rich columbite crystals (up to 32.62 wt% WO_3) were observed in the TZ. Two groups of columbite crystals can be distinguished with respect to their WO_3 concentration:

$W^{6+} < \Sigma M^{4+}$ and $W^{6+} > \Sigma M^{4+}$, where M^{4+} = Ti,Sn,Th,U,Zr. The first group shows the number of ΣM^{4+} atoms in excess to the substitution scheme $W^{6+} + M^{4+} \Leftrightarrow 2(Nb,Ta)^{5+}$. The ratio $[(\Sigma M^{4+})_{excess}/(Sc^{3+}+ Y^{3+})]_{at}$ is remarkably constant and close to 2. This implies a mode of substitution $6M^{4+} + 3M^{3+} \Leftrightarrow 4Fe^{2+} + 5(Nb,Ta)^{5+}$. The chemical formulae of columbite with $W^{6+} > \Sigma M^{4+}$, when calculated on 6 O, show an excess in the A site and a correspondig deficit on the B site. The deficit in the number of charges on the B site has to be compensated by Fe^{3+}, and the substitution scheme $2W^{6+} + Fe^{3+} \Leftrightarrow 3(Nb,Ta)^{5+}$ can be proposed. The introduction of W^{6+} into columbite is controlled by fO_2.

Ilmenorutile. - It appears in the ZG, forming strongly zoned subhedral crystals; the complex zoning is due to variations in Ti/(Nb+Ta) ratio and W content. The occupation of Ti-sites by Nb and Ta ranges from 11.2 to 16.4 %. (Fe+Mn)/(Nb+Ta) varies between 0.71 and 0.82. The plot of analytical results on the (Nb,Ta) - (Fe,Mn) - (Ti,Sn) triangle indicates the presence of Fe^{3+}; the formula of the "end-member" towards which the ilmenorutile tends is $Fe^{2+}Fe^{3+}Nb_3O_{10}$. This composition results in the simultaneous appearance of the following substitutions: $Fe^{3+} + (Nb,Ta)^{5+} \Leftrightarrow 2Ti^{4+}$; $(Fe,Mn)^{2+} + 2(Nb,Ta)^{5+} \Leftrightarrow 3Ti^{4+}$, leading respectively to the end-members $Fe^{3+}(Nb,Ta)O_4$ and $Fe^{2+}(Nb,Ta)_2O_6$.

Rutile. - Rare in the PG, and absent in the ZG, is only weakly Nb-bearing (maximum 4.06 wt% Nb_2O_5). Among the minor elements, W, Sn, Zr and Sc are systematically present.

Pyrochlore. - Irregular grains of U-rich pyrochlore are included in protolithionite. Fluorine was not detected. The high total deficit (average 85.58 wt%) indicates strong hydration. Silica is systematically present in amounts that correlate negatively with Σ(Nb,Ta,W,Ti,Sn,Zr), and its content is remarkably constant within the same grain. This is the first time that such concentrations of SiO_2 are reported for natural pyrochlore; however, the incorporation of Si into the B site of the pyrochlore lattice was shown experimentally (Subramanian et al., 1983). The calculation leads to the general formula AB_2O_6, corresponding to a defect (2+,5+)-pyrochlore $A^{2+}\square B_2^{5+}(O_6\square)$. The U concentration is much higher than that previously reported for natural pyrochlore. This implies a significant substitution in the A site by U^{4+} which permits the introduction of M^{4+} (Si^{4+}) in the B site, leading to a hypothetical end-member $U^{4+}\square B_2^{4+}(O_6\square)$. The calculation of cationic charges implies the presence of OH in the X sites. The total analytical deficit indicates the degree of hydration of about 2.2 - 3.7 molecules of H_2O.

Bastnaesite. - Anhedral to subhedral grains, generally associated with fluorite and sometimes with monazite, occur in both types of granite. Microprobe analyses show high ThO_2 concentrations correlated with CaO, and suggest the substitution $Th^{4+} + Ca^{2+} \Leftrightarrow 2REE^{3+}$. Formulae calculated on the basis of Σ(REE,Y,Th,Ca) = 1 indicate the presence of OH in the F site, the ratio $[F/(F+OH)]_{at}$ varying from 0.74 to 0.96. $[Ce/La]_{at}$ and $[Sm/Nd]_{at}$ increase with depth from 1.2 to 3.3, and from 0.17 to 0.46

respectively. The distribution of REE normalized to chondrites shows an important negative Eu anomaly.

Synchysite. - Radial aggregates of platy crystals (60-80 m) are commonly associated with fluorite, zircon and uranpyrochlore, more rarely with bastnaesite. Synchysite is absent in the apical part of the cupola and appears below 378.0 m. When calculated on the basis of Σ(Ca,REE,Y,Th) = 2, the number of F atoms is lower than 1 and the number of O atoms is higher than 6. Attributing the excess of O atoms to OH, the equilibrium of charges is satisfied, but the occupation of F site is in excess, suggesting the presence of O in this site. The substitution $Th^{4+} + Ca^{2+} \Leftrightarrow 2REE^{3+}$ plays only a minor role. The presence of O in F site allows the substitution $REE^{3+} + F^{-} \Leftrightarrow Th^{4+} + O^{2-}$. Among the REE, Ce, Nd and La are predominant, followed by Sm, Pr and Gd. $[Ce/La]_{at}$ decreases with depth from 5.2 to 3.1. Synchysite-(Y) occurring at 1558 m is considerably impoverished in LREE, shows a positive anomaly in Eu, and is the richest in OH ever observed in the Cínovec cupola.

3. DISCUSSION. - The following steps in the evolution of the Cínovec cupola can be inferred from the study of accessory minerals: (1) emplacement of granitic magma enriched in volatiles and incompatible elements; (2) transfer of volatiles into the apical part of the intrusion, lowering the liquidus temperature; (3) early crystallization of zircon, monazite, xenotime, thorite and columbite, at lower temperature in the ZG than in the PG, as inferred from zoning in zircon and columbite crystals; (4) strong variations in the fO_2 at the interface between ZG and PG; (5) interaction of early crystallized accessory phases with a F- and CO_2- rich fluid leading to their strong hydration and fluorination; (6) precipitation of CaF_2 causing an increase of fCO_2 in fluid phase; (7) crystallization of $CeCO_3F$ (bastnaesite); (8) interaction of previously crystallized minerals with a late F- , CO_2 - and Ca- bearing fluid causing instability of columbite and crystallization of pyrochlore and synchysite.

4. REFERENCES.

Cocherie, A., Johan, V., Rossi, P. & Stemprok M. 1991. Trace elements variations and lanthanide tetrad effect studied in a Variscan lithium albite granite: case of the Cínovec granite (Czechoslovakia). In: Pagel, M., Leroy, J.L. (eds) Source, Transport and Deposition of Metals. Balkema Rotterdam, pp 745-749

Stemprok, M. & Sulcek, Z. 1969. Geochemical profile through an ore-bearing lithium granite. Econ. Geol. 64:392-404

Subramanian, M.A., Aravamudan, G. & Rao G.V.S. 1983. Oxide pyrochlores - a review. Prog. Solid State Chem. 15:55-143

Current Research in Geology Applied to Ore Deposits. Fenoll Hach-Alí, Torres-Ruiz & Gervilla (eds) (1993). ISBN 84-338-1772-8

REE IN PLAGIOGRANITES OF THE KUYUL OPHIOLITE MASSIF (KORYAKYA, RUSSIA)

Luchitskaya, M.V.
Geological Inst., Russian Academy of Sciences, Pyzhevsky per. 7, Moscow 109017, Russia

Plagiogranite complex of Kuyul ophiolite massif was probably formed at the fore-arc position. It is confirmed by data on REE in plagiogranites and geological and geochemical data on basaltic rocks of sheeted dyke and pillow-lava complexes.

The Kuyul ophiolite massif is a huge serpentinite melange containing a fragments of ophiolite sequence. Within the melange Gankuvayame tectonic slice is distinguished. It is composed of a weakly tectonized full ophiolite sequence of the Late Jurassic - Early Cretaceous age. It contains upwards: 1) harzburgites (420 m); 2) apodunite serpentinites (50 m); 3) layered troctolite-wehrlite-olivine gabbro complex (430 m); 4) plagiogranites (50 m); 5) a sheeted dyke complex (400 m); 6) pillow lavas (300 m) (3).

Plagiogranites form an individual complex which occurs along the contact of gabbroides and a sheeted dyke complex. In the upper part of plagiogranite body there are many "inclusions" in forms of boudinaged layers, lenses and divergent bodies, which are composed of diorite porphyrites and have a typical dyke ophitic texture and probably are the fragments of sheeted dyke complex.

Petrographically plagiogranites are composed of euphedral plagioclase (andesine-oligoclase), quartz and hornblende. Accessory minerals are represented by apatite, zircon, sphene, ore minerals (magnetite?). From the secondary minerals albite, epidote, chlorite, minerals of phrenite-pumpellyite group and zeolites are developed. Plagiogranites are characterized by hypidiomorphic texture with widely graphic intergrowths of albite and quartz, suggesting their magmatic origin.

Petrochemical characteristics. Plagiogranites plot along the tholeitic and calc-alcaline trends on the AFM diagram. On the O'Connor diagram they plot into tonalite and trondhjemites fields. Characteristic features of Kuyul plagiogranites (KP) as well as ophiolite plagiogranites of other regions are their low contents of K_2O (0,1-0,8%) and AL_2O_3 (11-14%).

Geochemical characteristics. KP have low contents of K and Rb and are depleted in HFSE in comparison with ocean-ridge granite (ORG) by Pearce. On polycomponental diagram by Pearce the KP graphics are like that of supra-subduction zone granites (Troodos ophiolite massif) (see fig.1) and that of eusimatic island-arcs granites (Late Intrusive complex of Oman and complex Little Port, Newfoundland) (see fig.2) by Pearce. Low $^{87}Sr/^{86}Sr$=0,70369-0,70460 indicates that the parental rocks for plagiogranites have mantle origin. On the chondrite normalized graphics of REE KP are weakly enriched in LREE and have nearly horizontal part of HREE spectrum (La/Yb=0,8-1.37). KP have negative Eu-anomaly (Eu*/Eu=0,76-0,98) which indicates the intensity of plagioclase fractionation process. The KP chondrite normalized graphics are like that of Troodos granites and granites of Late Intrusive complex, Oman (see fig.3).

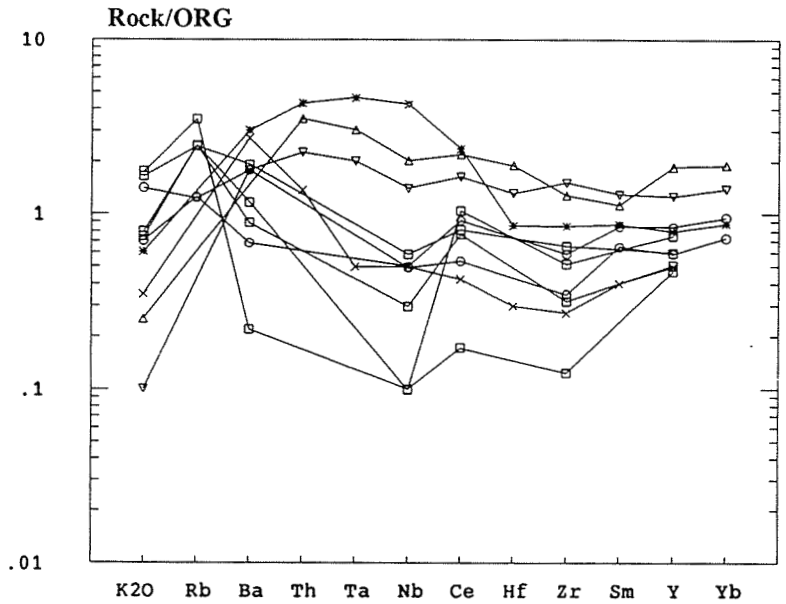

fig.1. ○ - plagiogranites, Kuyul ophiolite massif; △ - granites of Tuscany, Italy; ▽ - granites of Smartville, Sierra-Nevada; ✱ - quartz diorites, 45° n.l.MAR; × - trondhjemites, Troodos massif.

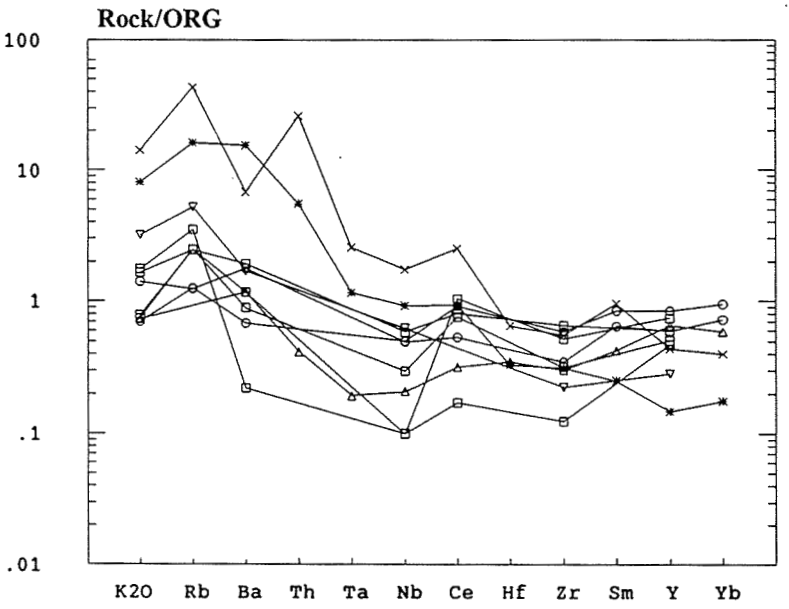

fig.2. ○ - plagiogranites, Kuyul ophiolite massif; △ - granites, Late Intrusive complex of Oman; ▽ - trondhjemites Little Port, Newfoundland; ✱ - granites, Jamaica; x - granites, Chili.

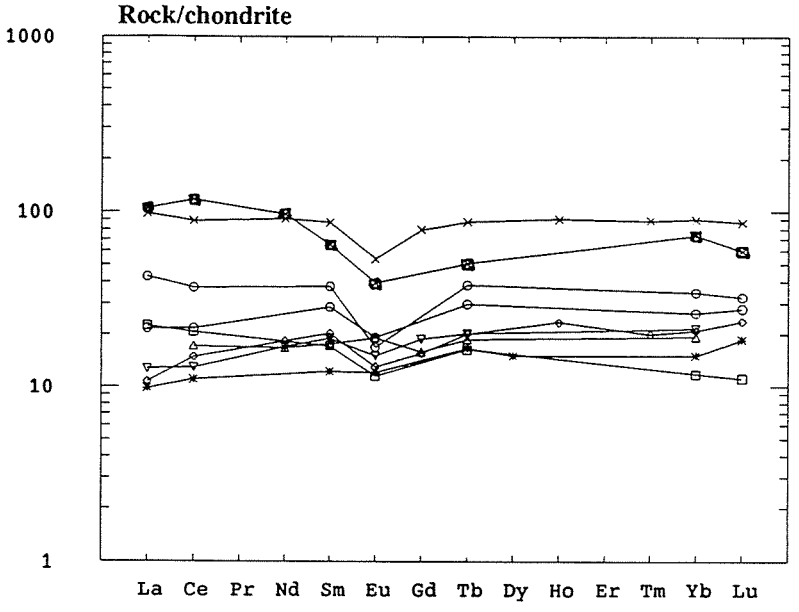

fig.3. ○ - plagiogranites, Kuyul ophiolite massif; □ - trondhjemites, Troodos massif; △ - granites, Late Intrusive complex of Oman; ✱ - trondhjemites, ophiolites Canyon Mountin, Oregon; ⊠ - granophyre, Miocene ophiolites Tihana Asir, Saudian Aravia; ✕ - Lower level plagiogranites, Nicoya complex, Costa Rica.

Similarity of KP REE graphics, intermediate-basic rocks of sheeted dike complex indicates that all rocks are cogenetic.

Small amount (5-10%) of KP with regards to mafic rocks of ophiolite sequence; inconsiderable quantity of intermediate rocks; existense of eutectic quartz-albite intergrowths in hornblende gabbro in the upper part of gabbroides; existense of common trend for plagiogranites, acid-intermediate rocks of sheeted dike complex and hornblende gabbro with quartz-plagioclase intergrowths on Harker's diagrams; similarity of REE graphics for plagiogranites, rocks of sheeted dike and pillow-lava complexes (from basic to acid) allow to suggest a model of fractional crystallization for the explanation of their origin. Qualitative comparison of experimental datd on partial melting of tholeite and olivine tholeite (2) and on liquid immiscibility (1) on Harker's diagram shows that these processes can't lead to the KP formation. Besides that acid liquids that are produced by the process of liquid immiscibility must be enriched in 4-6 times in REE in comparison with basic liquids (5), but for the rocks of Gankuvayame ophiolite slice REE contents for basic and acid rocks are not distinguished considerably. It is shown in (4), that the position of low-K and low-Ti depleted in HFSE basaltic rocks of sheeted dyke and pillow-lava complexes is fore-arc. Formation of KP may be linked with this stage of ophiolite development.

1) Dixon S., Rutherford M.J. 1979. Plagiogranites as late-stage

mmiscible liquids in ophiolite and mid-ocean ridge suites: Earth and Planetary Science Letters, 45:45-60.
2) Helz R.T. 1976. Phase relations of basalts in their melting ranges at P_{H2O}=5 kb. Part 2. Melt compositions. Journal of petrology, 17:139-193.
3) Krylov K., Grigoriev V. 1992. Kuyul ophiolite complex, Northern Kamchatka, USSR (age, composition, structure). 29th IGC, Kyoto, Japan, 24 aug-3 sept., 1 of 3:137-138.
4) Kuyul ophiolite terrane. 1990. Vladivostok, Far East Branch of USSR Academy of sciences, 108 p.
5) Watson E.B. 1976. Two-liquid partition coefficient experimental dates and implication. Contrib. Mineral. Petrology,.56:119-134.

Current Research in Geology Applied to Ore Deposits.Fenoll Hach-Alí, Torres-Ruiz & Gervilla(eds)(1993).ISBN 84-338-1772-8

SPACIO-TEMPORAL RELATIONSHIP OF MULTIPLE PHASES OF GRANITIC ROCK TO MULTIPLE PERIODS OF MINERALIZATION IN THE SHIZHUYUAN W-POLYMETALLIC DEPOSIT, SOUTH HUNAN, CHINA

Mao, J. (1); Li, H. (1); Perrin, M. (2); Raimbault, L. (2) & Guy, B. (3)
(1) Inst. of Mineral Deposits, Chinese Academy of Geological Sciences, China
(2) Centre de Geologie Generale et Miniere, Ecole des Mines de Paris, France
(3) Dept. Geologie, Ecole des Mines de Saint-Etienne, France

Abstract: Metallogenesis of the Shizhuyuan super-giant W-Polymetallic deposit can be divided into three periods, of which, the second period, being the strongest one, consists of four metallogenic stages which are responsible for the zoning of W-polymetallic mineralization. The three metallogenic periods are spacio-temporally associated with the former three phases of granitic rocks in the Qianlishan granite rock series.

Introduction

The Shizhuyuan W-polymetallic deposit in south China is well known as a "museum of nonferrous metls" all over the world. It has 800,000 tons of tungsten metal, 500,000 tons of tin, more than 200,000 tons of bismuth, about 100,000 tons of molybdenum and huge reserve of fluorine as well as beryllium, lead, zinc and silver. Wang Changlie *et al.* (1982, 1987), Yang Chaoqun (1982), Wang Shufeng *et al.* (1988) have described its geologic setting and metallogenesis. The spacio-temporally evolutional relationship of the multiple phases of granitic rock to multiple periods of mineralizations is studied in the present paper.

1. Geological setting

The Shizhuyuan W-polymetallic deposit is situated in the south Hunan depressive area of the south China Paraplatform. In the district of the Shizhuyuan deposit, the stratigraphic sequence consists of Precambrian metagraywacke, Middle Devonian sandstone of the Tiaomajian Group, dolomitic limestone of the Qiziqiao Group and Upper Devonian limestone and marls of the Shetianqiao Group, and dolomitic limestone of the Xikuangshan Group. The Devonian system, especially the Shetianqiao Group, is mainly the country rock for the mineralizations.

The Qianlishan Yanshanian biotite granite stock in the Shizhuyuan area is a composite one and its outcrop is about 10 km^2. The granitic stock is composed of, from early to late, pseudoporphyritic biotite granite (182 Ma), medium-coarse grained biotite granite (140 Ma), fine-grained muscovite granite (120 Ma), granite porphyry (80 Ma) and diabase. The three earlier phases of the granite are apparently associated with the W-polymetallic deposit.

2. Spacio-temporal distribution of rock forming and metallogenesis

2.1. The first phase of granitic rock and related mineralization

The pseudoporphyritic biotite granite, having a total 1.4 km^2 of outcrop, occurs as apohyses distributed in the marginal parts of the granite stock (Fig. 1) or as remainders scattered in the roof pendants of medium-coarse grained biotite granite. It is mainly composed of K-feldspar, albite, oligoclase, quartz and minor biotite with the phenocrystals of quartz and K-feldspar. Owing to mineralization and alteration, the phenocrystals in K-feldspar of the rock have almost disappeared. That is perhaps why the pseudoporphyritic biotite granite used to be classified into quartz porphyry and greisenized granite.

There develops garnet vesuvianite skanr around the apophyses of this phase of granite. The most of the apophyses are so extensively greisenized and mineralized that they have formed economic orebodies, which can be grouped into massive greisn type W-Sn-Mo orebodies and stringer vein-disseminated type Sn-Cu orebodies. The former develops in Dajiling area (Fig. 1), south of the Qianlishan granite stock and exists as remainders in the cupolas of the medium-coarse grained biotite granite under the Shizhuyuan major massive skarn in southeast of the stock. It dominantly contain muscovite, biotite and quartz as well as major ore minerals of wolframite, cassiterite and molybdenite. Whereas the original phenocrysts of quartz in pseudoporphyritic biotite granite are still remained in the greisen. In some localities, there develops a

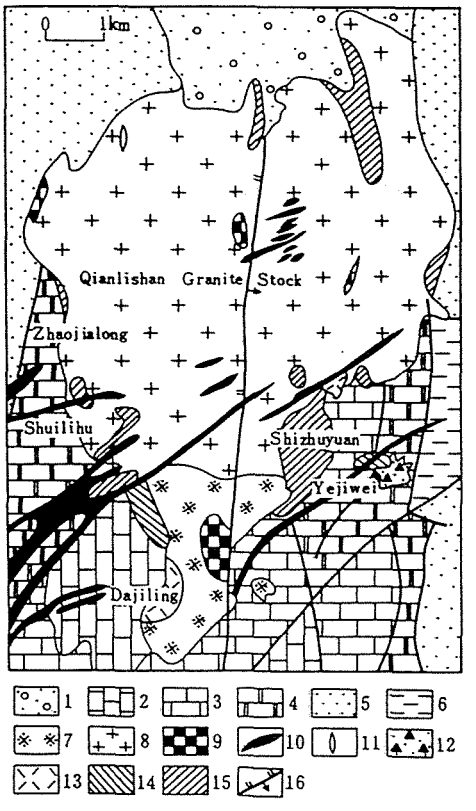

Fig. 1 Schematic map of the Qianlishan granite stock and skarn

1. Quaternary System, 2. Upper Devonian Xikuangshan Group, 3. Upper Devonian Shetianqiao Group, 4. Middle Devonian Qiziqiao Group, 5. Middle Devonian Tiaomajian Group, 6. Sinian System, 7. Pseudoporphyritic biotite granite, 8. Medium–coarse grained biotite granite, 9. Fine grained muscovite granite, 10. Granite porphyry, 11. Diabase, 12. Fine vein and disseminated Sn–Cu (W) ore body, 13. Massive W–Sn–Mo orebody, 14. Skarn, 15. Skarnizated and greisenized areas, 16. Faults

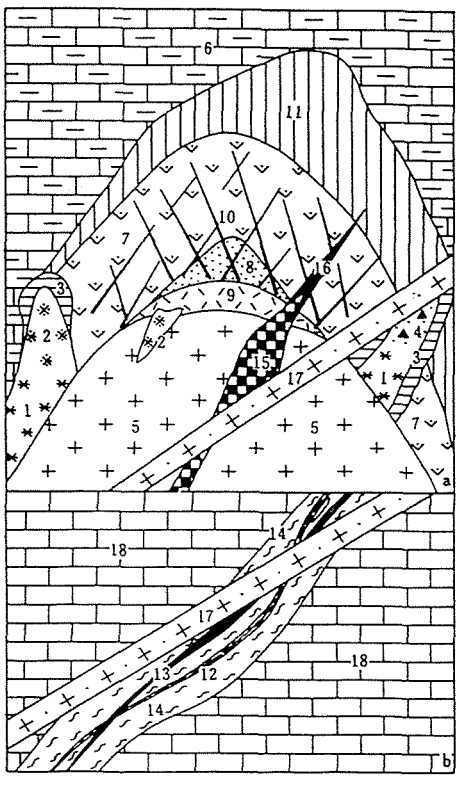

Fig. 2 Diagram showing the relationship between multiple phases of granitic rock and multiple periods of W–polymetallic mineralization

1. Pseudoporphyritic biotite granite, 2. Massive greisen W–Sn orebodies, 3. Garnet skarn, 4. Fine veins and disseminated Sn–Cu (W) orebody, 5. Medium–coarse grained biotite granite, 6. Hornfels and hornfelsic marble, 7. Massive skarn (W–Bi orebody), 8. Retrograde altered rock (W–Bi–Sn–Mo orebody), 9. Massive greisen W–Sn–Mo orebody, 10. Stockwork greisen veins of W–Sn–Mo–Bi orebody, 11. Fine stockwork greisen veins of Sn–Be (Cu) orebody, 12. Distal greisen veins of W–Be–Sn mineralization, 13. Pb–Zn lodes, 14. Altered rock, 15. Fine grained muscovite granite, 16. Garnet vesuvianite W–Mo ore vein, 17. Granite porphyry, 18. Carbonate

laminated greisen which is made up of dark laminations of dominant biotite alternated with white laminations of dominant quartz. The latter only occurs in Yejiwei apophysis (Fig. 1) and contains major ore minerals of cassiterite, chalcopyrite, scheelite, pyrrhotite, pyrite and gangue mineals of fluorite, muscovite, chlorite, quartz and margarite.

2.2 The second phase of granitic rock and related mineralization

The medium–coarse grained biotite granite has an outcrop of 8.4 km^2, being predominant part of the

Qianlishan granite stock. It mainly consists of K-feldspar, albite, quartz and biotite. During the empalcement of this phase of granite, a strong skarnization develops between it and Devonian carbonates, which is frequently superimposed on hornfels or hornfelsic marble. The hornfelses, being composed of wollastonite, vesuvianite (MgO/FeO = 0.50–0.78), grossular (And 0–10), diopside (Hed 0–10) and locally minor andalusite and scapolite, were formed from lars or the argillaceous stripes of limestone by thermal metamorphism. Almost all of the skarn in the Shizhuyuan deposit is exoskarn. Its major mineals are garnet (And 20–80), vesuvianite (MgO/FeO = 0.2–0.3), wollastonite and pyroxene (Hed 50–80) and it was apparently formed by infiltration metasomatism. The skarn is about 200–500 meters of thickness in the Shizhuyuan mine, but there is not clear zoning. In general, it seems that there is a zoning of garnet zone, garnet pyroxene zone, garnet vesuvianite zone and vesuvianite wollastonite zone from the contact outwards. After the skarnization, retrograde alteration of the skarn strongly develops nearby the contact, especially along fractures. During the retrograde alteration, the minerals, such as garnet and pyroxene of the skarn are first altered into the mineral assemblage of fine grained salite and magnetite. The salite is characterized by fresh green in color, anhedral and/or subhedral form and colorful interference color. Then the salite is altered into the assemblage of pargasite, fluorite, chlorite, biotite, quartz, magnetite, etc. It should be emphasized that the skarnization and the retograde alteration are respectively accompanied by W-polymetallic mineralizations. The primary skarn partly contains scheelite, bismuthinite, minor molybdenite, pyrite, pyrrhotite, magnetite and chalcopyrite. The retrograde altered rock is frequently enriched in magnetite, cassiterite, scheelite and molybdenite. After the retrograde alteration of the skarn, greisen type W-polymetallic mineralization extensively and broadly develops. The greisenization apparently exhibits a zoning in space. From the cupolas of medium-coarse grained biotite granite outwards or upwards, the zoning of greisenization is massive greisen type W-Sn-Mo-Bi ore zone in the roof pendants of the granite, stockwork greisen vein type W-Sn-Mo-Bi ore zone superimposed on the skarn, fine stockwork greisen vein type Sn-Be-Cu ore zone superimposed on marble and weak greisen vein type W-Sn-Be mineralized zone in distal contact along the SW-striking fractures. The massive greisen in this phase is different in enrichment of components of muscovite and protolithonite from the former one. Owing to the control of fracture system in the upper of the granitic stock, the width of stockwork veins of greisen type W-Sn-Mo-Bi mineralization gradually changes from several decades of centimeters to millimeters upward. In this zone, the greisen can be recognized to be four types of normal greisen (muscovite and quartz), protolithonite grisen, feldspar greisen and topaz greisen. The fine stockwork veins of greisen type Sn-Be-Cu mineralization generally exhibit width ranging from 0.1 to several millimeters. Within this zone, there are many minerals mainly including fluorite, muscovite, chlorite, margarite, corundum, cassiterite, scheelite and ten pieces of berium-bearing mineral. The three zones above are ditributed in the range of six hundred meters from the contact of the granitic stock. Along the SW-striking fractures, the greisenization reaches about several kilometers in space. Although containing scheelite, cassiterite, helvite, phenacite, etc., the distal greisen does not form an economic orebody. It is herein necessary to mention that the greisen in this period is generally acompanied by a suite of minerals of manganoan skarn (Mao Jingwen *et al.*, 1993) including spessartinic-almandinic garnet, spessartine, Mn-bearing salite, Mn-rich hedenbergite, helvite, rhodonite, Mn-rich phlogopite and Mn-rich grossular. The minerals of manganoan skarn usually occur beside the greisen veins or rare superimposed on them. And they also serve as gangue minerals in the fine greisen veins. After the greisenization Pb-Zn (Ag) veins develop within or beyond the greisenization area. The base metal ore mainly contains sphalerite, galena, pyrrhotite, pyrite, arsenopyrite, fluorite, calcite, tourmaline and muscovite. The Pb-Zn lodes tend to be accompanied by manganoan skarn including rhodonite, spessartine, helvite, tephroite, tephroitic-faylitic olivine, johannsenite, rhodochroist and alabandite.

2.3 The third phase of granitic rock and related mineralization

The third period of mineralization is spacio-temporally associated with the fine grained muscovite granite, which occur as apophyses and dikes superimposed on the earlier phases of granite (Fig. 1). The component of fine grained muscovite granite is similar to that of medium-coarse grained biotite granite except for mica. It can be found that the apophyses of fine grained granite gradually change into skarn veins enriched in scheelite, molybdenite and minor cassiterite by emplacement. This kind of skarn veins, 10–50 centimeters in width, consists of coarse grained garnet (And 40–60 mole %), vesuvianite and fluorite. In some localities, the

minerals in the skarn veins show a clear zoning, i.e. dominant garnets in the center and predominant vesuvianite in the margins. Fluorite and ore minerals are interstial among the skarn minerals. The mineralization of this period is relatively weak and is limited near the contct. But its tungsten grade is generally higher than 0.5%, even locally reaches 6%.

Furthermore, there are granite porphyry and diabase dikes which are supposed to be magmatic activities of postmineralizations in the Shizhuyuan mine. Wang Changlie *et al.* (1987) considered the granite porphyry is responsible for the Pb–Zn (Ag) mineralization, but it is almost always found that the granite porphyry without any mineralizations cut through the Pb–Zn lodes anyway.

The spacio–temporal relationship of the emplcements of the biotite granites to the W–polymetallic mineralizations is modeled as Fig. 2.

3. Conclusions

The south Hunan province situated in the middle part of the Nanling nonferrous metal metallogenic belt is enriched in W–polymetallic deposits. Almost all of the Yanshanian granite intrusions in the region are accompanied by W–polymetallic mineralizations. The outcrop of the Qianlishan granitic stock is just about 10 km^2 in the Shizhuyuan area, but geophysical data (Xu Youzhi *et al.*, 1989) show that it gradually enlarged at depth.

Except for the dikes of granite porphyry and diabase, other three phases of granite in the Qianlishan composite granitic stock show that they have experienced strong differentiations characterized by more than 88 of differentiation index and enrichments in K, Na, Si, Li, Rb, Ga, Be, W, Sn, Mo, Bi, F, HREE components. And the three former phases of granite emplacement are respectively responsible for one period of W–polymetallic mineralization. Of them, the second period of mineralization is strongest and can be divided into several stages which exhibit a clear spacio–temporal distribution.

In general, the granitoids, associated with tungsten and/or tin deposits, are frequently emplaced as granitic rock series. The W–Sn mineralization is usually related to the latest phase of granitic series (Groves, 1978; Mao Jingwen, 1989 and Lehmnann, 1990). Whereas apparently multiple phases of granitic rock and relative multiple period of W–Polymetallic mineralization, develop in the Shizhuyuan area. That is perhaps one of the major reasons why the super–giant W–polymetallic deposit occurs there.

References

Groves, D.I. and Mccarthys, S. (1978). Fractional crystallization and the origin of tin deposits in granitoids. Mineral. Deposit., vol. 13, 11–26.

Lehmann, B. (1990). Metallogeny of tin. Springer–Verlag, 211 p.

Mao Jingwen (1989). The igneous rock series and tin polymetallic mineraogenetic series in the Tengchong area, Yunnan. Acta Geologica Sinica, vol. 2, 175–187.

Mao Jingwen, Guy, B., Perrin, M., Raimbault, L. (1993). Manganoan skarn in the Shizhuyuan W–polymetallic deposit, south Hunan, China. Mining Geology (in press).

Wang Changlie, Xu Youzhi, Xie Ciguo and Xu Wenguang (1982). The geological characteristics of Shizhuyuan W–Sn–Mo–Bi deposit. Tungsten Geology Symposium, Jiangxi, China, 413–425.

Wang Changlie, Luyo Shihui, Xu Youzhi, Sun Yihong, Xie Ciguo, Zhang Zhongming, Xu Wenguang and Ren Xiangmei (1987). Geology of the Shizhuyuan tungsten–polymetallic deposit. Geological Publishing House, 173 p (in Chinese with English abstract).

Wang Shufeng and Zhang Qiling (198). Introduction of Geology of the Shizhuyuan tungsten tin–bismuth–molybdenum ore deposit. Beijing Publishing House of Sciences and Technology, 134 pp.

Xu Youzhi (1989). Prospecting for blind Sn–Pb–Zn deposits in the Dongpo ore district and its vicinity. Xiangnan Geological Team of Hunan Bureau of Geology, 144–158.

Yang Chaoqun (1982). Mineralization of the composite–greisen stockwork skarn type W (scheelite and wolframite) Bi–Mo deposit of Shizhuyuan, Dongpo, Southern Hunan, China. Tungsten Geology Symposium, Jiangxi, China, 503–520.

Current Research in Geology Applied to Ore Deposits.Fenoll Hach-Alí, Torres-Ruiz & Gervilla(eds)(1993).ISBN 84-338-1772-8

GENETIC MODEL FOR THE FIRST OCCURRENCE IN SPAIN OF BERYLLIUM GEMSTONES (ALEXANDRITE-EMERALD-PHENAKITE): METASOMATIC REACTIONS BETWEEN PEGMATITIC AND DUNITIC ROCKS.

Martín-Izard, A.; Moreiras, D.; Acevedo, R.; Paniagua, A. & Marcos-Pascual, C.
Dept. de Geología, Universidad de Oviedo, 33005, Oviedo, Spain

ABSTRACT: Exometasomatic interaction of Be-rich pegmatitic bodies with dunitic wall-rocks leads to the development of gemstone deposit, several meters thick, formed essentially of emerald, phenakite and chrysoberyl (alexandrite) in phlogopite gangue. From fluid inclusion studies, clearly no great differences exist among the fluid inclusion populations of emerald and phenakite, and two discontinuous hydrothermal stages can be distinguished. Structural similarities between forsterite and chrysoberyl could favour the epitaxial growth of alexandrite on olivine relicts.

REGIONAL GEOLOGY

The studied mineralization is located in the Galicia-Tras Os Montes area (Matte, 1968) which is made up of the Schist and the granitic domains. The former is composed of metamorphic rocks and the Lalín-Forcarey Unit -the southern end of the Ordenes large complex (Barrera et al, 1989; Monterrubio, 1991)-. In accordance with Barrera et al, (1989), rocks forming the schist domain, were deformed by the different phases of the Hercynian Orogeny, three of which are the most important. The second phase generates sub-horizontal axial-plane overthrust faults and recumbent folds. During this phase are emplaced the Cabo Ortegal and Ordenes Complexes (in Galicia), and Bragança and Morais Complexes (in Portugal). The studied area is located between the Portuguese complexes and the Ordenes complex (Fig. 1). These Complexes are made up of rocks ophiolitic in nature and belong to oceanic crust fragments overthrust during the Hercynian Orogeny (Barrera et al, 1989) and including, among other lithologies, dunitic type rocks.

The hercynian granites make up the greatest percentage of rocks in the region. Three types of granites have been singled out (Barrera et al, 1989). Into them, the peraluminous inhomogeneous two mica granitoids are syncinematic in nature and also being the ones associated with the studied pegmatites. In the work area they outcrops like small points related to the massif of La Cañiza (Fig. 1). It is characteristic of these granites the abundant remains of materials from the schist domain, either as xenoliths or at the top of the intrusions.

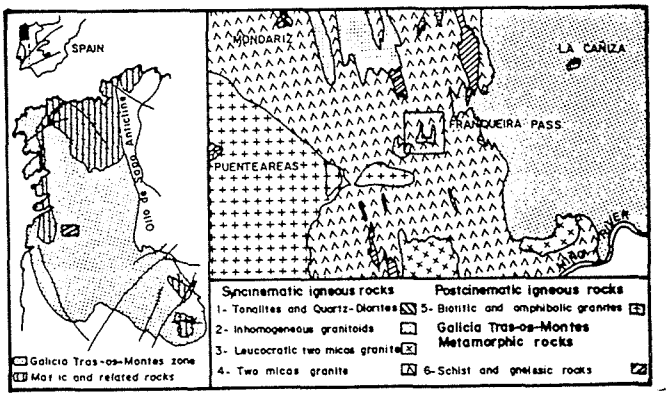

Fig. 1 Situation and generalized geologic map of the Franqueira ore.

THE PEGMATITES. LOCAL GEOLOGY.

The studied pegmatite here outcrops in the area on the top of La Franqueira pass (Fig. 1), constituting a network of small subvertical pegmatitic dikes of an anastomosate lenticular geometry, running from E to W direction, about 15-20 meters in length and up to 40 cm thick. These pegmatitic bodies fit into the materials of the schist domain of Galicia-Tras Os Montes. Each of these bodies has a simple interior zonation, showing an edge of an aplitic character, made up of quartz, albite, muscovite and scarce potassic feldspar, with garnets, tourmaline, apatite and zircon as accessory minerals. The pegmatite main zone is composed by coarsed grains than in the border. Within the pegmatitic bodies of greater thickness, a banding can be observed in which a coarse grained rock alternates with another of saccharoidal appearance. The plagioclases are partially sericitized.

HOST ROCKS

PHLOGOPITITES (phlogopite hornfels). The host rocks have a clear contact with the pegmatites and are of a micaceous nature. The mica is phlogopite (table 1), being the most abundant mineral in this facies. The rock has a markedly lepidoblastic texture, sometimes banded and occasionally crenulated. The accessory minerals are chrysoberyl (alexandrite), phenakite, beryl (emerald), tourmaline, garnet (almandine), apatite (fluorapatite), and zircons. Chrysoberyl appears as subhedral porphyroblasts isolated in the phlogopite or as skeletal intergrown within emerald, phenakite and apatite. The twinned porphyroblasts, up to 1 in size cm, shows the pronounced pleochroism and the color change phenomenon of the alexandrite variety. Its average chrome content is 0.3wt%. Phenakite appears as subhedrals and colorless prismatic crystals, up to 3 cm in size. Phenakite has associated frequently apatite crystals. Beryl appears as euhedral prismatic crystals sometimes larger than 10 cm, very intense green color and Cr content (up to 0.2wt%) gives it its emeraldlike character. This phlogopitic facies grades to an amphibolic facies where amphibolite pockets within the phlogopitites are found.

AMPHIBOLITES (tremolite hornfels). It is an amphibolic rock with nematoblastic texture and chiefly made up by tremolite, always with some phlogopite and locally, along with a dunitic rock, anthophyllite (Table 1), accompanied by sphene, as an abundant accessory. The amphibole is subhedral and does not show a defined orientation, as it is partially altered to phlogopite and zoisite. As accessory minerals zircon, apatite and ilmenite are observed. Gradually, though quickly, it passes, through an orthoamphibolic facies with anthophyllite, on to a dunitic type rock.

DUNITE. This rock is composed chiefly by olivine (Mg 87) which forms a hypidiomorphic, partially serpentinized aggregate. Some grains are partially replaced by titanoclinohumite. Chromite is found as an accessory mineral, usually disseminated, although occasionally it forms small aggregates. Also sulphides are found, generally filling cavities. This paragenesis, of a clearly accessory character, is made up of nickeline, maucherite and pyrrhotite with small quantities of pentlandite, westerveldite, millerite and chalcopyrite. The concentrations of Cr and Ni in the rock are very similar, reaching 0.125wt% of each one.

OTHER MELANOCRATIC ROCKS. Locally, and without showing any clear spatial relation with the others rocks, an amphibolic gabbro is observed. It is constituted by an assemblage of calcic amphibols (Mg-hornblende), plus plagioclase (An 92) and some ferrohyperstene

and quartz. As accessory minerals ilmenite, rutile and circon are found. This rock is cross-cutted by the pegmatite, giving rise on the primary gabbro assemblage to a secondary mineral association made up by hornblende, with almandine, zoisite, sphene and albite.

Mineral Rock(N)	Olivine (8)	Chromite (20)	Phlogopite Dunite (10)	Phlogopite Amph. (8)	Phlogopite Phlog. (10)	Tremolite Dunite (10)	Tremolite Phlog. (8)	Amphibol Gabb. (11)	Tourmal. (9)	Hipers. (4)	Anorth. (4)	Garnet (16)	Hematite (22)	Antoph. (1)
SiO_2	40.80	0.01	41.60	42.50	41.10	56.40	54.40	40.60	37.40	51.70	44.10	36.70	36.40	63.90
TiO_2	0.10	0.81	0.44	0.40	0.67	0.15	0.06	0.65	0.31	0.21	0.02	0.03	3.32	0.01
Al_2O_3	0.00	7.73	12.40	12.70	14.10	2.00	2.85	11.60	30.60	0.80	34.60	20.10	0.00	0.03
Cr_2O_3	0.00	55.5	0.70	0.71	0.13	0.43	0.15	0.02	0.18	0.04	0.00	0.02	0.05	0.00
Fe_2O_3	0.00	4.52	0.00	0.00	0.00	2.17	4.52	5.61	0.00	0.00	0.00	2.27	0.00	0.00
FeO	13.10	29.7	3.60	4.43	8.33	0.54	3.86	22.90	4.15	28.70	0.40	25.80	12.00	1.48
MnO	0.15	0.45	0.03	0.04	0.11	0.07	0.55	0.20	0.06	0.84	0.00	1.45	0.19	0.02
NiO	0.08	0.03	0.00	0.00	0.00	0.00	0.00	0.00	0.06	0.04	0.00	0.00	0.07	0.11
MgO	47.30	2.81	26.20	24.20	20.70	22.90	19.20	2.90	9.95	13.80	0.02	0.34	46.2	30.50
CaO	0.02	0.01	0.04	0.05	0.03	13.40	12.70	11.60	1.60	1.01	19.20	13.10	0.01	0.05
Na_2O	0.01	0.00	0.06	0.13	0.26	0.36	0.45	0.66	1.89	0.02	0.77	0.00	0.01	0.09
K_2O	0.00	0.00	9.16	9.30	9.04	0.06	0.15	0.70	0.02	0.00	0.01	0.00	0.01	0.00
H_2O	0.00	0.00	4.28	4.28	4.21	2.20	2.16	1.91	13.80	0.00	0.00	0.00	0.00	0.00
Total	101.5	101.6	98.43	98.79	98.64	100.60	100.90	99.32	100.00	97.21	99.14	99.81	98.28	96.17

Table 1. Selected microprobe analyses on samples of the Franqueira deposit. N=number of points analysed. $H_2O+Fe_2O_3$ calculated by stoichiometry.

FLUID INCLUSION STUDIES

To define the hydrothermal evolution of the fluids trapped in the metasomatic minerals, fluid inclusion studies in samples of emerald and phenakite were made up. From the microthermometrical data clearly no great differences exist among the fluid inclusion populations of emerald and phenakite, and two discontinuous hydrothermal stages can be distinguished. The first hydrothermal stage was characterized by the circulation and trapping of aqueous fluid with some volatiles of the type 1 and 2 inclusions (complex CH_4 and CO_2 aqueous inclusions), with densities between 0.005 and 0.034 gr/cc for type 1 and 0.07 to 0.14 for type 2. Salinities are below 10 wt% eq. NaCl (Potter et al, 1978). Homogenization temperatures range between 318 and 381ºC and the lithostatic or hydrostatic pressure was high enough to prevent boiling. These inclusions could be contemporaneous and this fact suggest some stage of heterogeneous entrapment (immiscibility) in the H_2O-NaCl-CH_4-CO_2-other volatiles system. The characteristics of type 3 inclusions suggests an independent episode of fluid circulation. Densities range from 0.9 to 1.15 gr/cc (Bodnar, 1983), and salinity lies below 24.7 wt% eq. NaCl, at minimum trapping temperatures ranging between 160 and 265ºC. The results are summarized in the following Table:

samples	type	Nº	$TmCO_2$	TmICE	TmHyd	$ThCO_2$	$ThCH_4$	Th
Emerald	1	39	-----	-3/-5.2	11.5/19	----	-82/-90 L -83/-106 G	318/369 L 354 G
Emerald	2	31	-60.8/-62.1	-3/-7	11.9/22	-11.2/10G	----	320/378 L 381 G 381 C
Emerald	3	7	-----	-1.3/-23	----	-----	----	160/245 L
Phenakite	1	40	-----	-3.5/-5.2	14.8/18.3	-----	-88.6/-109 L -86/-106 G -86.7/-89 C	322/350 L 363/373 G
Phenakite	3	8	-----	-2.1/-11	----	-----	----	193/265 L

Table 2. Microthermometric results.

GENETIC MODEL AND DISCUSSION

As for the ultramaphic rock, the presence in NW of Iberian Peninsula of the Ordenes, Braganza and Morais, all of which are overthrust complexes of an ophiolitic nature (IGME, 1990), and to

which, among other rocks, abundant dunitic rocks are associated, leads to the belief that the dunite and hornblende gabbro considered here may belong to a remnant of peridotitic and gabbroic rocks from the overthrust complexes. The compositional characteristics of the spinels and olivines (Fig. 7) are agree closely with those analyzed by Monterrubio (1991) in the Ordenes and the Herberia complexes and the olivines from peridotites alpines (Jan, Q.M. & Windley, B.F.,1990). Later, during the intrusion of the hercynian granites, the considered maphic rocks could have remained at the top of the intrusions of the non-homogeneous two micas granite bodies.

Formation of Be-rich pegmatites, which cut the dunitic rocks of Franqueira, is related to the above mentioned granites. These pegmatites, rich in fluids and volatile elements (Be, B,P, H_2O), yield a metasomatic phenomenon in contact with the dunite. In the zones closest to the pegmatite, the dunitic rock would transform entirely (chiefly due to the water, Si, Al and K from the pegmatite) into a rock mainly constituted of phlogopite, the Mg of which is provided by the dunite. In the zones farthest from the pegmatite, its influence would be less. Therefore, the dunite is transformed into an amphibolitic (tremolite) rock, in which the Mg is provided by the dunite itself. In zones which are close to the dunite (and therefore magnesium-rich) orthoamphibol (anthophyllite) is formed.

These rocks are also characterized by their high content of chromium, which comes from the dunitic rock. The phlogopite present in the dunitic (table 1) rocks is the richest in MgO (26.2wt%) and Cr_2O_3 (0.7wt%); those related to tremolite are somewhat poorer in MgO (24.2wt%), with practically the same content in Cr_2O_3. Phlogopite located near of the pegmatites has lesser content in MgO (20.7wt%) and Cr_2O_3 (0.13wt%). Beryl, chrysoberyl and phenakite appear in the last facies above mentioned.

As for the volatile elements B, P and Be, the first two forms mineralogical phases in the metasomatic facies with phlogopite, giving rise to the crystallization of tourmalines and abundant apatites. Beryllium spreads out in the system favouring the development of beryl porphyroblasts among the phlogopites. The fact that emerald is the variety of beryl present is due to the chromium content of these minerals. Chromiun comes from the dunite. The reason that chrysoberyl (alexandrite variety) is formed is probably due to the fact that this mineral and the olivine are isostructural. Therefore, the growth of the chrysoberyl could be favoured by a decrease in the energy threshold necessary for its nucleation in epitaxy on olivine relicts.

BIBLIOGRAPHICAL REFERENCES

Bodnar R.J.(1983). A metod to calculated fluid-inclusion volumes based on vapor bubble diameters and P-V-T-X properties of F.I. Econ. Geol. 78: 535-542

Barrera, J; Farias, P; Gonzalez Lodeiro, F; Marquinez, J; Martin-Parra, L. Martinez Catalan, J; Olmo, A del; Pablo, J.G de (1989) Mem. Mapa Geol España E 1:200.000 Ourense. I.T.G.E. Madrid, 284p.

Jan, Q.M. & Windley, B.F. (1990). Chromian spinel-silicate chemistry in ultramaphic rocks of the Jijal complex, Pakistan. Jour Petro 31:667-715.

Matte, PH (1968). La estructure de la virgation hercynienne de Galicia (Spain). Trav. Lab. Geol. Fac. Sci. Grenoble. Rev Geol Alp, 44:1-128.

Monterrubio, S (1991): Mineralizaciones asociadas a rocas ultrabásicas en el hercínico español. Tes.Doc.U.C.M.:337p.

Potter, R.W.; Clytnne, M.; Brown, D.L. (1978). Freezing point depression of aqueous sodium chloride solutions. Econ Geol. 73:284-285.

This paper has been financed by the CICYT GEO 91/1077 and Oviedo University proyect f91/21527.

Current Research in Geology Applied to Ore Deposits.Fenoll Hach-Alí, Torres-Ruiz & Gervilla(eds)(1993).ISBN 84-338-1772-8

POLYTYPISM AND RHENIUM-CONTENTS OF MOLYBDENITES FROM TWO Mo-DEPOSITS IN NORTHERN GREECE.

Michailidis, K.; Filippidis, A. & Kassoli-Fournaraki, A.
Aristotle University of Thessaloniki, Thessaloniki, GR-540 06 Greece

ABSTRACT: The nature of molybdenite polytypes in relation to the Re-contents is studied, by means of XRD and electron microprobe analyses, on samples from two Mo-deposits associated with magmatic rocks in Northern Greece. Molybdenite in both deposits forms disseminations, veinlet-fillings and open space botryoidal encrustations within the host rocks. The granite-hosted molybdenite consists solely of the $2H_1$ modification and has very low Re-contents (0.00-0.10 wt%). A mixture of the $2H_1$+3R polytypes of molybdenite is found within a granitic-porphyry. The higher Re-contents (0.94-1.27 wt%) of the latter molybdenite are correlated with the presence of the 3R-polytype.

INTRODUCTION

Molybdenite is known naturally occurring in either of two structures, the common hexagonal ($2H_1$) and the rare rhombohedral (3R) polytype. The presence of only one polytype or the coexistence of both in varying proportions, has been confirmed at several localities in the world (e.g., Clark 1970, Watanabe and Soeda 1981).

Molybdenite serves, to date, as the most important mineral host of the rare element rhenium. A general trend found in the literature is that high Re-contents can be correlated with high 3R-polytype contents (e.g., Ayres 1974, Newberry 1979b). So, the additional finds of 3R-molybdenite will lead to new sources of the rare element rhenium.

Previous works in Greece have dealed mainly with the presence of Mo-mineralization (e.g., Walenta and Pantzartzis 1969, Arikas 1979, 1981) and some of them on the relation between polytypism and Re-content of molybdenite (Filippidis et al. 1986, Melfos et al. 1991). The purporse of this work is to study the polytypism and the Re-contents of molybdenites from the Mo-deposits associated with the Axiopolis granite and the Melitena granitic-porphyry in Northern Greece (Fig. 1).

OCCURRENCE AND GEOLOGICAL SETTING

The Axiopolis Mo-deposit has been mined during the years 1940-44 by underground excavations. The area (Fig. 1) lies ≈90Km NW of Thessaloniki in Macedonia county, and belongs to the Peonia geotectonic zone. The Mo-deposit is related to the Jurassic leucocratic biotite-granite of Fanos which is distinguished into three rock-types, namely aplitic granite, granite and microgranite (Christofides et al., 1990). Molybdenite is found mainly within aplitic-pegmatitic veins crosscutting the altered marginal zones of the Fanos granite. It occurs as disseminations of single laths or flaky aggregates, filling veinlets and small nests. Botryoidal massive encrustations on the wall of fissures or cavities are also observed. Associated minerals are pyrite, galena, quartz, sericite, chlorite, epidote, fluorite and partly kaolinized feldspars.

The Melitena area is situated ≈22Km NW of Komotini in Thrace county of Northern Greece, and belongs geotectonically to the Rhodope massif. A Mo-deposit has been recently discovered (Filippidis et al., 1986) within the upper parts of a Tertiary subvolcanic intrusion of trachyandesitic composition being converted into a granitic-porphyry as a result of an intense silicification. Molybdenite forms disseminations, fissure-fillings and encrustations, as in the Axiopolis area. Associated minerals are pyrite replacing initial pyrrhotite, quartz, sericitized feldspars, micas and epidote.

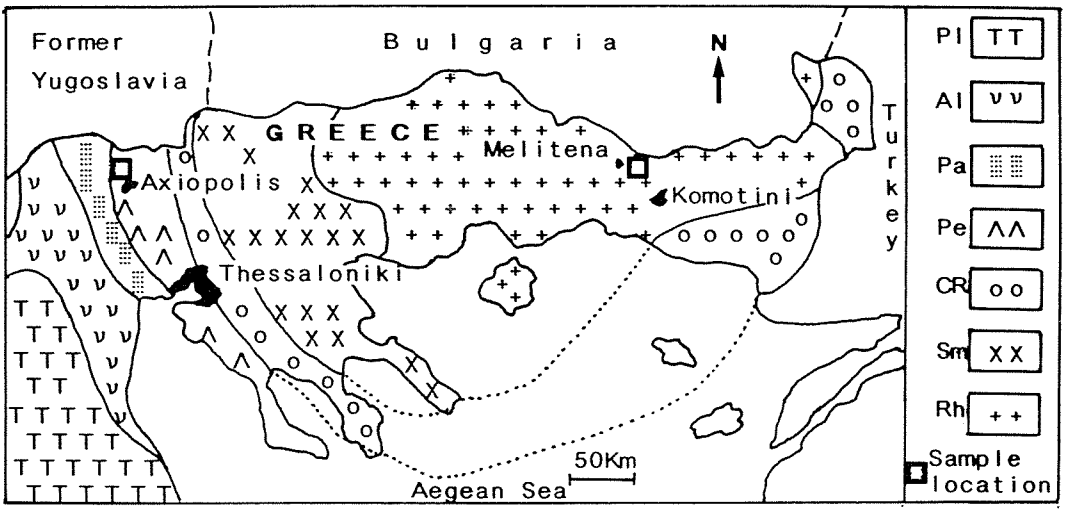

Fig. 1. Geotectonic sketch-map of a part of Northern Greece showing the sampling locations. Pl:Pelagonian zone, Al:Almopia zone, Pa:Paikon zone, Pe:Peonia zone, CR:Circum-Rhodope belt, Sm:Serbomacedonian massif, Rh:Rhodope massif.

Table 1. Electron microprobe analyses, structural formulae and cell parameters of the studied molybdenites.

Location	Axiopolis		Melitena			
Polytype	$2H_1$		$2H_1$		3R	
	Range	Average*	Range	Average*	Range	Average*
Mo	59.61-61.01	60.47	58.99-60.02	59.67	58.77-59.55	59.20
Re	0.00- 0.10	0.04	0.12- 0.25	0.18	0.94- 1.27	1.18
Zn	0.00- 0.08	0.03	0.02- 0.06	0.04	0.00- 0.05	0.03
Cu	0.00- 0.15	0.04	0.00- 0.06	0.04	0.00- 0.05	0.03
Fe	0.01- 0.21	0.14	0.05- 0.11	0.09	0.00- 0.02	0.01
W	0.00	0.00	0.00- 0.06	0.03	0.00	0.00
S	38.72-40.69	39.93	39.56-40.11	39.78	39.90-40.39	40.17
Total		100.65		99.83		100.62
			Calculation on 2(S)			
Mo		1.01		1.00		0.99
Re		-		-		0.01
S		2.00		2.00		2.00
Σ		3.01		3.00		3.00
			Cell parameters			
a(A)		3.160(1)**		3.163(1)		3.166(1)
c(A)		12.290(3)		12.297(2)		18.421(5)
V(A^3)		106.30(5)		106.56(4)		159.92(5)

*) Average of 10 analyses. **) Estimated standard deviation in parentheses; thus, 3.160(1) indicates estimated standard deviation of 0.001.

EXPERIMENTAL WORK

Powder X-ray diffraction studies on purified molybdenite concentrates were done using a Philips diffractometer (Ni-filtered CuKα radiation, scanning over the interval of 13 to 70° 2θ, scanning speed 1°and 1/4° per minute, silicon as external standard).

Polytypes of molybdenites and their contents were determined following the calculated patterns of Wickman and Smith (1970), the XRD patterns for naturally occurring molybdenites by Frondel and Wickman (1970) and the indexing in ASTM cards. Cell parameter refinements (Table 1) of molybdenites were performed using the 12 strongest and well defined reflections and the computer program of Appleman and Evans (1973).

Electron microprobe analyses (Table 1) of molybdenites were carried out in a C.A.M.E.C.A. CAMEBAX probe (Dept. of Geology, University of Manchester, U.K.) equipped with two wavelength dispersive spectrometers (W.D.S.).

RESULTS AND DISCUSSION

XRD studies revealed that the $2H_1$ polytype was alone present in the Axiopolis granite-hosted molybdenite mineralization. This supports previous suggestions (e.g., Clark 1970, Frondel and Wickman 1970) that the majority of the $2H_1$ molybdenites comes from pegmatites or quartz veins associated with granites. A mixture of both types $2H_1$+3R, in nearly equal proportions, was found in the Melitena porphyry-hosted molybdenite mineralization. Molybdenites with 3R-polytype dominant, or present in a significant amount, were found in a variety of geological environments in the world. However, Clark (1970) considered that 3R-molybdenites, actually are most likely to be accountered in quartz-feldspar porphyries, as happens in the studied Melitena area.

Many arguments have so far been made on the possible factors controlling the molybdenite polytype formation, like: differences in composition, trace element admixtures, pressure and temperature, cooling rate during formation, sulfidation state, growth processes e.t.c. (e.g., Clark 1970, Frondel and Wickman 1970, Newberry 1979a,b, Watanabe and Soeda 1981). Among these factors, the presence of Re in the molybdenite structure has been generally considered as one of the most important and its concentration was positively correlated with the 3R-polytype formation.

Electron microprobe analyses of the studied molybdenites are given in Table 1. Rhenium is considered as the major admixture in the molybdenite structure. The Re-content of the Axiopolis granite-hosted molybdenite is very low varying within the range 0.00-0.10 wt%. The analyzed Melitena molybdenites show two chemically different groups, one Re-poor (0.12-0.15 wt% Re) and another Re-rich (0.94-1.27 wt% Re), which were respectively combined with the $2H_1$ and the 3R polytypes determined by the XRD studies. Thus, the higher Re-content of the Melitena molybdenite is attributed to the participation of the 3R modification.

The presence of the 3R modification with high Re-content in the Melitena subvolcanic intrusion, confirms Ishihara's (1988) statement that the Re-contents of molybdenites increase as the depth of mineral formation decreases. Besides, these results confirm the view of Todorov and Staikov (1985) that the Re concentration increases in time from older to younger Mo-mineralizations.

The coexistence of the two polytypes of molybdenite has been confirmed at several localities. Clark (1970) considered that the occurrence in ores of the two modifications may be an indication of initial crystallization below, very approximately, 500°C. Evidence for the conversion of one polytype to the other, either during the hypogene development of an ore, or during supergene alteration has also been presented (e.g., Clark 1970, Newberry 1979b).

The textural features of the Melitena molybdenite are not diagnostic of any replacement of one polytype by the other. However, the replacement of the initial pyrrhotite by pyrite during the ore-mineralization process, may indicate a conversion of rhombohedral molybdenite to the hexagonal form, as stated by Clark

(1970).

In summary, the results of XRD and electron microprobe analyses of the studied molybdenites indicate that molybdenite associated with the older Axiopolis plutonite is represented by the Re-poor $2H_1$ modification, while that from the younger Melitena subvolcanic intrusion consists of Re-poor $2H_1$ and Re-rich 3R modifications. Thus, the Re-content seems to play a determinant role in molybdenite-polytype formation in the studied Mo-deposits of Northern Greece.

REFERENCES

Appleman, D.E. & Evans Jr., H.T. 1973. Job 9214: Indexing and least-squares refinement of powder diffraction data. U.S. Geol. Surv., Computer contribution 20, U.S. Nat. Techn. Infor. Serv. Doc., PB2-16188.

Arikas, A. 1979. An occurrence of porhyry copper and molybdenum ores near Kirki (Thracia, Northern Greece). N. Jb. Miner. Abh. 137(1):74-82.

Arikas, A. 1981. Subvolcanic hydrothermal Mo-Cu-Zn-Pb-mineralization, South-Eastern Rhodope Mts., Northern Greece: Petrography and geochemistry. Tschermaks Min. Petr. Mitt. 28:189-205.

Ayres, D. 1974. Distribution and occurrence of some naturally occurring polytypes of molybdenite in Austalia and Papua New Guinea. J. Geol. Soc. Australia. 21:273-278.

Christofides, G., Soldatos, T. & Koroneos, A. 1990. Geochemistry and evolution of the Fanos granite, N. Greece. Mineral. Petrol. 43:49-63.

Clark, A.H. 1970. Compositional differences between hexagonal and rhombohedral molybdenite. N. Jb. Miner. Mh. 33-38.

Filippidis, A., Vavelidis, M., Michailidis, K. & Evagelou, E. 1986. Re-rich and Re-poor molybdenite in the Melitena porphyritic intrusion, Rhodope massif (Greece). Fortschr. Miner. 64(1):47.

Frondel, J.W. & Wickman, F.E. 1970. Molybdenite polytypes in theory and occurrence. II. Some naturally occurring polytypes of molybdenite. Amer. Miner. 55:1857-1875.

Ishihara, S. 1988. Rhenium contents of molybdenites in granitoid-series rocks in Japan. Econ. Geol. 83:1047-1051.

Melfos, V., Vavelidis, M., Filippidis, A., Christofides, G. & Evagelou, E. 1991. Re-rich and Re-poor molybdenite in the Maronia rhyolitic intrusion, North-eastern Greece. In: Pagel, M. & Leroy, J.L. (eds). Source Transport and Deposition of Metals. Balkema, Rotterdam, pp 775-777.

Newberry, R.J.J. 1979a. Polytypism in molybdenite (I): a non-equilibrium impurity-induced phenomenon. Amer. Miner. 64:758-767.

Newberry, R.J.J. 1979b. Polytypism in molybdenite (II): relatioships between polytypism, ore deposition/alteration stages and rhenium contents. Amer. Miner. 64:768-775.

Todorov, T. & Staikov, M. 1985. Rhenium content in molybdenite ore mineralizations in Bulgaria. Geol. Balcanica 15(6):45-58.

Walenta, K. & Pantzartzis, P. 1969. Die molibdanglanz-lagerstatte von Kimeria bei Xanthi in Nordgriechenland. Erzmetall 22(6):272-278.

Watanabe, M. & Soeda, A. 1981. Distribution of polytype contents of molybdenites from Japan and possible controlling factor in polytypism. N. Jb. Miner. Abh. 141(3):258-279.

Wickman, F.E. & Smith, D.K. 1970. Molybdenite polytypes in theory and occurrence. I. Theoretical considerations of polytypism in molybdenite. Amer. Miner. 55:1843-1856.

Current Research in Geology Applied to Ore Deposits. Fenoll Hach-Alí, Torres-Ruiz & Gervilla (eds) (1993). ISBN 84-338-1772-8

GRANITE PEGMATITES IN SARDINIA - PRELIMINARY REPORT

Pani, E. & Valera, R.G.
Inst. di Giacimenti Minerari, Piazza D'Armi, 09123 Cagliari, Italy

ABSTRACT: Three groups of granite pegmatites, differentiated according to their composition, belong to the magmatic sequence of the Hercynian Sardinia-Corsica batholith. The characteristics and the distribution of the studied pegmatites suggest the existence of an increasing northward fractionation trend parallel to the gradient of the Hercynian regional metamorphism.

INTRODUCTION

According to the most recent views (Carmignani et al.,1992, with bibliography) the Sardinian crystalline basement is interpreted as a segment of the South-European Hercynian chain, brought about by a continent-continent collision, oceanic crust subduction, nappe accumulation, metamorphism, and magmatism. The Sardinia-Corsica batholith is formed by a heterogeneous plutonic complex emplaced at the end of the Hercynian tectonometamorphic events, according to a magmatic sequence spaced during syn-, late- and post-tectonic activity.
Pegmatites are very common in the Paleozoic crystalline basement of the island. They are genetically associated with all the granitoids and reveal a variable composition, also showing a broad evolutionary trend which controls their distribution. According to the results of the studies carried out on a wide sample of Sardinian granite pegmatites, we will describe their mode of occurrence and propose a first approach to their classification.

GEOLOGICAL OUTLINE

Paleozoic metasedimentary and metavolcanic sequences were intruded by the stocks and plutons of variable composition of the Sardinia-Corsica batholith, generally emplaced at high crustal levels. The magmatic products extensively crop out all over the island covering an area of about 6,000 sq. km.
The structural fabric of the crystalline basement is characterized by three parallel belts, respectively called (from south to north) "External Zone", "Nappe Zone", and "Axial Zone". The three belts have a NW-SE trend and show a tectonometamorphic zoning developed from a low-grade greenschist facies (SW Sardinia) to an intermediate pressure amphibolite facies, with migmatites (NE Sardinia).
The External Zone is confined to SW Sardinia. Cambrian to Lower Carboniferous formations in low-grade greenschist facies prevail, overlying micaschists and orthogneisses of supposed Precambrian age, visible in few outcrops near the southern coast. Hercynian magmatism products are also present, with the large plutons of the Sulcis and Arburese districts. The simplest pegmatites observed in the island belong to the External Zone.
The Nappe Zone makes up the central belt, according to the general NW-SE trend. Its structures are characterized by an "accumulation zone" of allochthonous units overthrusting from NE to SW. Volcano-sedimentary sequences of Cambrian to Lower Carboniferous age bear the imprint of a regional metamorphism in greenschist facies, Chlorite zone (biotite appears in the deepest tectonic units). The Hercynian batholith is widely represented by the large plutons of central and SE Sardinia. The pegmatites of the Nappe Zone are frequently hosted in the metamorphic cover, sometimes in the parent granitoid,

always close to the contacts. The crystalline basement of northern Sardinia belongs to the Axial Zone of the Hercynian chain. It is essentially formed by the late magmatic Hercynian products, intruding the highest grade metamorphic sequence. Metamorphism increases from the Chlorite zone in the SW part of the belt to the Sillimanite + K -feldspar zone, associated with migmatites, in the NE (Franceschelli et al., 1982). The boundaries between low-/medium- and high-grade metamorphic complexes are marked by a regional shear-zone, the "Posada-Asinara Line", recently interpreted as a segment of the "South -European Hercynian Suture". Some of the higly fractionated pegmatites occur in the Axial Zone.

One of the most important features of the Sardinian crystalline basement is given by the Hercynian batholith. It is described as a calc-alkaline suite of metaluminous intrusives with some peraluminous representatives (Di Vincenzo & Ghezzo, 1992).

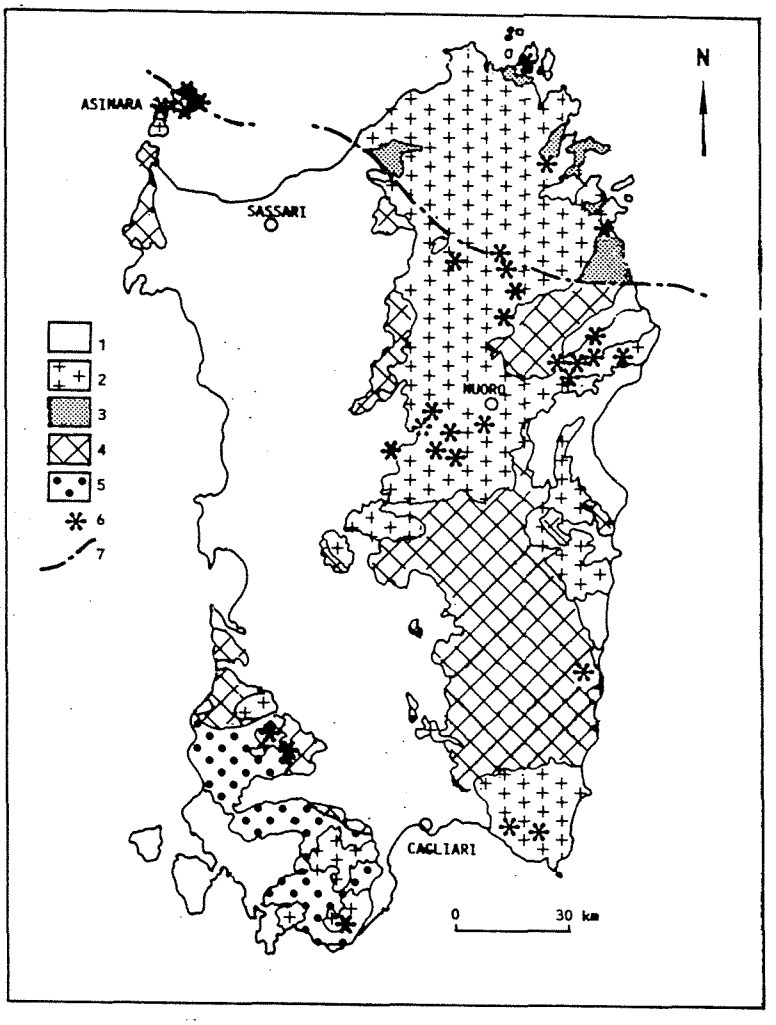

Fig. 1. Distribution of the studied pegmatites in Sardinia. 1: Post-Hercynian sedimentary and volcanic complexes. 2: Hercynian batholith. 3: Axial Zone. 4: Nappe Zone. 5: External Zone. 6: Pegmatites. 7: Asinara-Posada Line.

Different phases are recognized in the evolution of this activity, starting from early syn- to late- and post-tectonic intrusions. The genetic dependence of the Sardinian pegmatites on the Hercynian magmatic activity is clear.

The syn-tectonic magmatic activity produced some small intrusions and dikes of granodiorites, monzogranites and rare tonalites. They settled during the last phase of the most intense orogenic movements and mainly occur in the Axial Zone as generally semiconformable bodies within migmatites and high-grade metamorphites. The synkinematic origin is witnessed by the strongly foliated structures, which also affect the associated pegmatites. The composition of the pegmatites bound to the syn-tectonic intrusions is rather simple, with quartz, K-feldspar and muscovite.

The late-tectonic magmatic activity accounts for the largest proportion of the batholith-forming stocks and plutons. The position in the orogenic sequence is indicated by structures and attitude suggesting an emplacement still controlled (at least partially) by compressive conditions. The composition changes along with the age, ranging from tonalites and tonalitic granodiorites of the oldest phases, with flow structures and foliated fabric, to discordant monzogranitic granodiorites and leucocratic monzogranites of the younger intrusions. The oldest plutons of the late-tectonic suite particularly occur as small intrusions within the low-grade metamorphites (Chlorite- and Biotite-zone) of the Nappe Zone. The youngest plutons contribute to the largest frame of the batholith both in the Nappe Zone and in the Axial Zone. However, some of them also appear in the low-grade metamorphic areas of the External Zone. Most of the Sardinian pegmatites are associated with late-tectonic granitoids.
The post-tectonic magmatic activity produced perfectly discordant, biotite-bearing leucogranites, scattered in each belt and intruded in all the other plutons and in the metamorphic complexes. They are frequently altered by albitization, sericitization, and muscovitization due to late hydrothermal processes, which also produced mineralization (molybdenite, wolframite, fluorite). The associated pegmatites normally appear as small lenses, pockets, and stockworks close to the contacts with the metamorphic cover.

THE PEGMATITES. DISTRIBUTION

The occurrence of pegmatites is strictly bound to the close proximity of the parent granitoids, which normally are also the host rocks. Under such a constraint they practically crop out all over the island, although they show some changes in frequency and characteristics from south to north. Actually they are rather rare in the southern areas, and appear with very simple composition in peripheral and marginal position within the plutons, essentially leucogranites. The pegmatites are more frequent in the central part of the island, showing increased size and variety of composition. In this region they are mainly bound to monzogranites and granodiorites, but association with leucogranites is also recorded. More to the north they maintain the same characteristics of composition variety but start decreasing in number of occurrences, being associated with different types of parent granitoids (monzogranites, granodiorites, and leucogranites).

THE PEGMATITES. DESCRIPTION

The Sardinian pegmatites belong to a sequence marked by a northward increasing fractionation, which corresponds to a northward deepening of the intrusive levels, consequently followed by the emplacement of the crystallization products in periplutonic environment, the farther from the marginal facies of the parent melts.
The mineral association characterizes the different pegmatite types. Quartz + K-feldspar are the common denominator, and can be accompanied by other minerals according to the fractionation level and to their position in the metamorphic belts. It is possible to distinguish three pegmatite groups according to the mineral assemblage, i.e. according to the fractionation level.
The first group is typical of South Sardinia. Simple pegmatite bodies are essentially composed of quartz + K-feldspar, with some albite and minor muscovite. Their size is generally very small.
The pegmatites of the second group crop out in Central and Northern Sardinia. In addition to quartz and K-feldspar, they contain abundant muscovite booklets, garnet (either andradite or almandine), and minor biotite. The size of the pegmatite bodies increases and some zoned and layered structures start to appear.
The third group is characterized by the highest differentiation level. A fairly

rich mineral assemblage can be observed in a single pegmatite body, even if small in size: quartz, K-feldspar, albite-cleavelandite, muscovite, Li-mica, tourmaline var.schorl, almandine, Mn-tantalite, microlite and phosphates of the alluaudite series. This group is well developed in Central-Northern Sardinia, however the complete mineral assemblage to date is only recognized in few bodies near Nuoro. The most common association is given by quartz, K-feldspar, albite, muscovite, tourmaline, garnet and is particularly typical of many pegmatites cropping out in the Asinara island.
Referring to Cerny's pegmatite classification (1991) we preliminarly propose to assign Group 1 and 2 to the Muscovite class, and Group 3 to the Rare-element class, LCT type.

AKNOWLEDGEMENTS
This research has been carried out with grants from the Italian National Council of Researches, throught the Centro Studi Geominerari e Mineralurgici, Università di Cagliari.

REFERENCES

Carmignani, L., Barca, S., Carosi, R., Di Pisa, A., Gattiglio, M., Musumeci, G., Oggiano, G. & Pertusati, P.C. 1992. Schema dell'evoluzione del basamento sardo. In: Geologia della Catena Ercinica in Sardegna, Guida all'Escursione sul Basamento Paleozoico della Sardegna. Gruppo Informale Geologia Strutturale, maggio 1992, pp. 11-38

Černý, P. 1991. Rare Element Granitic Pegmatites.Part I: Anatomy and Internal Evolution of Pegmatite Deposits. Geoscience Canada, 18, 2:49-67

Di Vincenzo, G. & Ghezzo, C. 1992. Peraluminous Hercynian granitoids in Sardinia, Corsica and Provence: a preliminary note. Contr. to the Geol. of Italy with special regards to Paleozoic basements. A volume dedicated to Tommaso Cocozza. L. Carmignani & F.P. Sassi Eds., I.G.C.P. n° 276, NEWSLETTER vol. 5, Siena, pp. 469-472

Franceschelli, M., Memmi, I. & Ricci C.A. 1982. Zoneografia metamorfica della Sardegna Settentrionale. In: Guida alla Geologia del Paleozoico Sardo; Guide Geologiche Regionali. Soc. Geol. It., pp. 137-149

Current Research in Geology Applied to Ore Deposits.Fenoll Hach-Alí, Torres-Ruiz & Gervilla(eds)(1993).ISBN 84-338-1772-8

ON THE EMPLACEMENT OF GRANITE AND A METALLOGENETIC MODEL OF THE DAJISHAN TUNGSTEN DEPOSITS, JIANGXI PROVINCE, CHINA

Pei, R. & Wu, L.
Inst. of Mineral Deposits, Chinese Academy of Geological Sciences, 26 Baiwanzhuang Road, Beijing 100037, P.R. China

Abstract: The emplacement of granite and metallogenetic model of Dajishan tungsten deposits can be recognized as a pulse emplacement of comagmatic complementary differentiation in multi-stage and the metallogenetic model as the mineralization association with different type in two stage during the pulse emplacement of granite in same period.

Introduction

China is one of the largest tungsten produces in the world and has a great variety of different types of tungsten deposits. The major production of tungsten comes from quartz-vein and skarn deposits which are distributed among five provinces in southern China. The largest tungsten resources are found in the southern Jiangxi province where the Dajishan deposits is situated (Fig. 1).

1. Tectonic location

The tectonic location of Dajishan deposit is assigned to the post-caledonian uplift domain of south China paraplatform and belongs since Mesozoic to a mobile belt along the continental margin of West Pacific plate. Such geotectonic position has brought that the developing block faulting, during this period divided the uplift domain into several parallel NE-NNE trending upwarped and downwarped zones. The Dajishan granite and related tungsten deposits occur in one of these upwarped zones (Fig. 1).

2. Emplacement of granite

2.1. Characteristics of granite

The Dajishan granite is a Yanshanian composite intrusion which composed of biotite granite, two-mica granite and muscovite granite. The intrusion was controlled by the NE and NNE trending structures of the upwarp and emplaced into Cambrian meta-sandstones. Among them, the biotite granite, Wuliting granite is exposed over a great area. The two-mica and muscovite granite are not exposed at the surface. They are occurred as a hidden cupola on the rise of the Wuliting granite, the muscovite granite accompanying Nb, Ta, W, Be mineralization, as a small laccolith occur in the roof of the cupola.

The Rb-Sr isochron ages of these three granite are 167±1, 161±3, and 159±5 Ma, respectively, and the have initial $^{87}Sr/^{86}Sr$ ratios of 0.7189, 0.7128 and 0.7143. K-Ar dating of the mineralized vein system gives around 142 Ma. The biotite granite is comparable with the Ca-rich granite, two mica granite with the Ca-low granite and the muscovite granite has a low content of Ca, Ti, Fe and Mg and is enriched in Na and Mn. The normalized values show an increase in Rb, Cs, Be, Nb and Ta and a decrease in Sr and Ba when plotted in the succession biotite granite-two mica granite-muscovite granite.

The biotite granite has the highest total REE content, averaging 274 ppm. It is relatively enriched in LREE (LREE/HREE = 15.4). The chondrite normalized pattern for the biotite granite reveals a small negative Eu anomaly ($Eu/Eu^* = 0.62$). In contrast, the muscovite granite has a much lower total content of REE and is depleted in HREE (LREE / HREE = 3.5). The chondrite normalized pattern shows an extremely negative Eu anomaly ($Eu / Eu^* = 0.03$). Both the total REE content (av. 70 ppm) and the chondrite normalized pattern ($Eu / Eu^* = 0.22$) of the two-mica granite are transitional to the other granite.

The $\delta^{18}O$ values for the biotite granite, the two-mica granite and the muscovite granite fall in the range from +10.3 to +10.9‰ , +9.5 to +10.4 ‰ and +10.1 to +11.4 ‰ , respectively. The δD values range from -60.7‰ in the biotite granite to -75.1‰ in the muscovite granite. Stable isotope data as well as initial $^{87}Sr/^{86}Sr$ ratios are in accordance with a crustal source for the granitoid magma. The chondrite-normalized REE pattern of the biotite granite is very similar to that of the Cambrian meta-sandstone.

2.2. Feature of emplacement

Based on the tectonic sittings, mode of occurrence, and geochemistry, the emplaced feature of Dajishan granite can be recognized as that there is a deep genetic relation between this three granite and they are all the products of comagmatic complementary differentiation in polystage. The comagmatic sources probably originated by anatexis of sialic sedimentary rocks which may include the Cambrian meta-sandstone and parts of the underlying Precambrian rocks. As a result of the comagmatic complementary differentiation in poly-stage, the pulse emplacement of Dajishan granite was formed in the upwarping tectonic setting of this area. This pulse emplaced granite is very favourable for poly-phase mineralization.

3. Model of metallogeny

3.1. Characteristics of deposits

The muscovite granite, No. 69 body, is an ore-bearing granite body with Nb-Ta-Be showing uniform mineralization an ascending order, the mineralization becomes better. The essential ore minerals are microlite and Fe-niobiotantalite. It is suggested that the ore-forming process is closely related to albitization, greisenization and alkali-metasomatism.

Tungsten occurs both as dissemination in the No. 69 body together with Nb-Ta-Be and as quartz-wolframite veins in overlying Cambrian meat-sandstone. The occurrence of the quartz-wolframite veins generally show a swarm with NNW-trending, which can be divided into nort, central and south group and downward transect

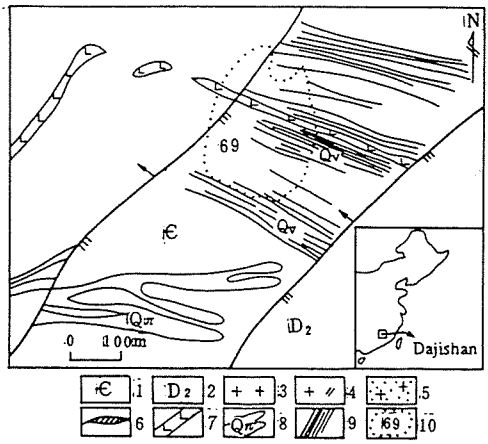

Fig.1 Sketch geological map of Dajishan deposits (revised from Dajishan mine 1977).

1. Cambrian metasandstone; 2. Devonian sandstone; 3. biotite granite; 4. two-mica granite; 5. muscovite granite; 6. pegmatite; 7. gabbro-diabase; 8. quartz-porphyry(Qπ); 9. quartz-wolframite vein(Qv); 10. horizontal projection of the mineralized muscovite granite;

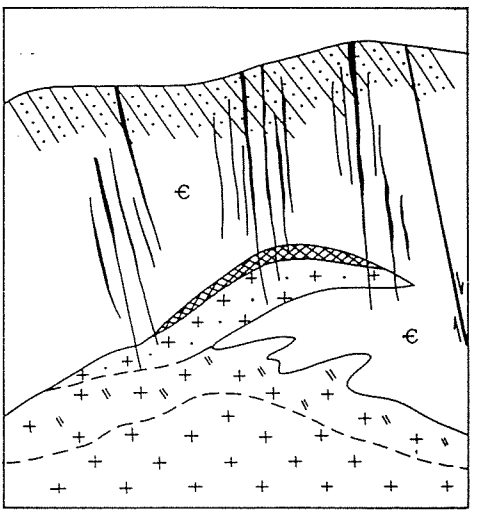

Fig.2 Schematic map of metallogenific model of Dajishan tungsten deposits

Legend same Fig.1.

the No. 69 body and two-mica granite (Fig. 2). It is believed that the quartz-wolframite veins are controlled by the tension fractures transection wall-rocks and granite. Based on our studies of paragenesis and texture of ores as will as stable isotope and fluid inclusion, the wolframite divided into two stages. The early stage is low-grade dissemination wolframite together with Nb, Ta and Be minerals which were precipitated towards the end of the crystallization of the granite. The late stage comprises a period of hydrothermal activity with precipitation of quartz and wolframite both in the muscovite granite and in the wall-rocks. Dajishan tungsten deposits is a composite type.

3.2. Metallogenetic model

The metallogenetic model of Dajishan tungsten deposits can be concluded that the deposits occurs associated with a composite granite intrusion which is composed of biotite granite, two-mica granite and muscovite granite. The granitic magma was formed by partial melting of the continental crust and was emplaced into the Cambrian meta-sandstones during the Yanshanian period. Progressive differentiation of the magma gave as an end product the muscovite granite which mainly hosts Nb, Ta, Be and W. The Cambrian meta-sandstone overlying the Dajishan granite contains an abundant swarms of quartz-wolframite veins which locally at depth transect the muscovite granite and some of which transect the two-mica granite (Fig. 2). The mineralization of tungsten is a composite type including dissemination and ore vein. The former is a low grade and was formed during an early stage when crystallization of the muscovite granite was nearly ended, i.e. late-magmatic. The latter is a high grade and mainly are abundant quartz-wolframite veins in the meta-sandstone which were formed by hydrothermal solution of deep-seat origin permeated the granite, i.e. post-magmatic. Accordingly, it is believed that the abundant quartz-wolframite veins with muscovite and two-mica granite probably are fraternal in relationship.

4. Conclusions

Finally, it can be suggested that the petro-minerogenetic model of Dajishan Nb-Ta-Be-W deposits belongs to the emplacement of granite in multistage (three stage granite) and the mineralization associated with different type (disseminate and vein) in two stage (late-magmatic and post-magmatic) during the comagmatism in same period (Yanshanian) (Pei Rongfu, 1989).

References

Pei Rongfu and Mao Jingwen (1989). On Petro-Mineragenetic models of Tin-Tungsten Granite in South China. *28th IGC Abstracts*, vol. 2 of 3.

Chen Yuchuan, Pei Rongfu *et al.* (1989). The Geology of Non-ferrous and Rare Metal Deposits related to Mesozoic granitoids in Nanling region. *Geological Publishing House, Beijing*.

Pei Rongfu and Wu Liangshi (1989). Regional metallogenetic environments and basic features of ore-forming. Progress in Geosciences of China (1985-1988). *Papers to 28th IGC, vol. III. Geological Publishing House, Beijing.*

Current Research in Geology Applied to Ore Deposits. Fenoll Hach-Alí, Torres-Ruiz & Gervilla (eds) (1993). ISBN 84-338-1772-8

MICA AND K-FELDSPAR AS INDICATORS OF PEGMATITE EVOLUTION IN THE FREGENEDA AREA (SALAMANCA, SPAIN)

Roda, E.; Pesquera, A. & Velasco, F.
Dept. de Mineralogía y Petrología, Universidad del País Vasco/EHU, Bilbao, Spain

ABSTRACT: Micas and blocky K-feldspars, selected from the different groups of pegmatites in the Fregeneda area, were studied to determine wether the pegmatites can be related by a common fractionation path, and how different pegmatite types are related to the spatially associated Lumbrales granite. Compositional variations in the micas and K-feldspars depend on the pegmatite type. Cs, Li, and Rb increase with distance from the Lumbrales granite, whereas K/Rb decreases. According to this, the exterior Li-bearing pegmatites are the most evolved, whereas the simple comformable pegmatites seem to be the less evolved.

Introduction

The element distribution in K-feldspar and white mica is a good indicator of pegmatite fractionation, and it has often been used as geochemical recorders of pegmatite petrogenesis (Trueman and Cerny, 1982; Shearer et al, 1992; Cerny, 1992). So, in this study, representative micas and blocky K-feldspars, selected from the different groups of pegmatites, were studied to determine wether the pegmatites can be related by a common fractionation path, and how different pegmatite types are related to the spatially associated Lumbrales granite.

Pegmatites of the Fregeneda area lie in the western part of a narrow metamorphic band, bordered by the Lumbrales granite to the south, and by the Saucelle granite to the NE (Fig. 1), in north-western Salamanca (Spain). Both units are two-mica, peraluminous granites, and belong to a group of syntectonic massifs, which have been deformed during the third phase of Hercynian deformation (López Plaza & Carnicero, 1988).

The studied pegmatites intrude into metamorphic rocks of the Schist-Metagraywacke Complex (Fig. 1). In this area, this Complex consists of an alternation of quartzites, graywackes, micaschists and pelites, with abundant thin calcsilicate layers. These materials have undergone several phases of Hercynian deformation and metamorphism (Martínez, 1974). The earliest phase of the regional metamorphism localy reaches the sillimanite zone, whereas the biotite zone is the most extensive.

Geology of pegmatites

Several groups of pegmatites have been distinguished, according to their mineralogy, morphology, internal relationships, etc. With increasing distance from the Lumbrales granite the groups are (Roda et al. 1991), (Fig. 1):

(1) Intragranitic pegmatites consisting of quartz, K-feldspar, muscovite, albite and schorl, that are relatively abundant in the border zones of the granite.

(2) Dykes composed mainly of quartz, andalusite and minor muscovite, schorl and K-feldspar. They are conform to the host-rock, showing a relevant deformation with boudinage structures. These bodies appear close to the Lumbrales granite, in the andalusite-cordierite zone.

(3) Dykes and apophyses showing aplitic and pegmatitic facies, consisting of quartz, K-feldspar, muscovite and minor albite, schorl and biotite. Their forms are greatly variable. These bodies are located S-E of the studied area, near the Lumbrales granite, associated with the sillimanite, andalusite and even biotite zones.

(4) Conformable pegmatites of narrow width, sometimes showing internal zoning. They are mainly composed of quartz, muscovite, K-

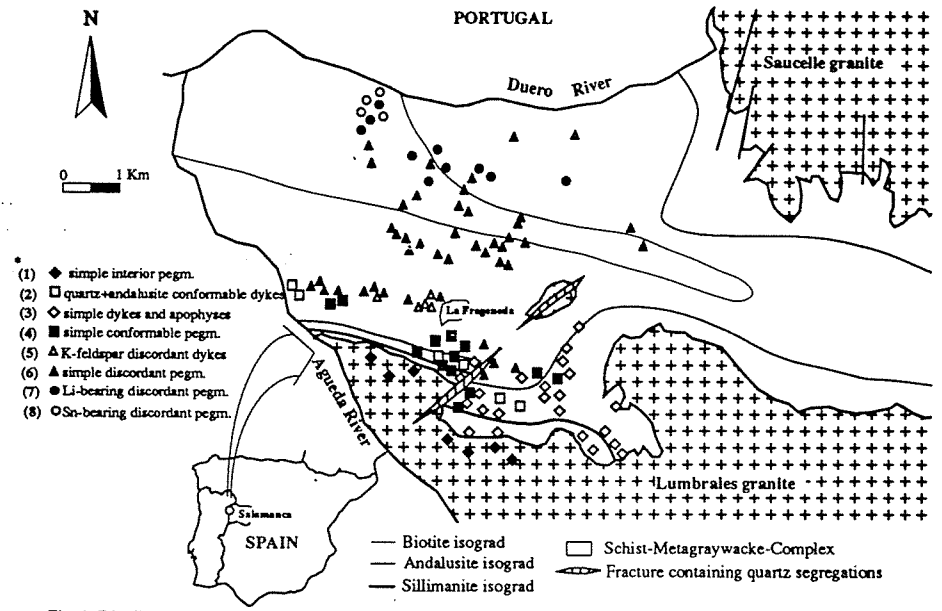

Fig. 1: Distribution of the pegmatite groups differentiated in the Fregeneda area. (*numbers as in "Geology of pegmatites").

feldspar, schorl, albite and minor andalusite, chlorite, garnet and biotite. These pegmatites are located close to the Lumbrales granite, in the andalusite zone, and to a lesser extent in the sillimanite zone.

(5) Pegmatites mainly composed of pink K-feldspar. Other phases that can be present are quartz, muscovite and pyrite. They are discordant to the host-rock, and very scarce, appearing near the contact with the Lumbrales granite, associated to the biotite zone.

(6) Discordant pegmatites that in some cases show a layered internal structure. They consist of quartz, K-feldspar, muscovite and albite. In the pegmatites furthest from the Lumbrales granite, amblygonite may appear. Situated in an area between 1 and 4 km to the north of the Lumbrales granite, this group is the most abundant. Their host rock exhibits a low grade regional metamorphism (biotite and chlorite zones).

(7) Discordant Li-mica-bearing pegmatites. These bodies usually display a zoned internal structure. They are composed of quartz, Li-mica, albite, K-feldspar, muscovite and minor amblygonite, spodumene, cassiterite, apatite, etc. These dykes outcrop along a narrow band, 4-6 Km north from the Lumbrales granite. Similar to the previous category, these pegmatites are associated with the biotite and chlorite zones.

(8) Pegmatites consisting of quartz and minor fine-grained muscovite, albite, microcline and cassiterite. These dykes sometimes show internal zonation, being folded with an important reduction in the vertical length. They appear in the north zone of the studied area, associated with the chlorite zone.

Analytical procedures and results

Micas were analysed for F by X-ray fluorescence (XRF); for Li by inductively coupled plasma (ICP) and atomic absorption (AA); for Rb and Cs by instrumental neutron activation (INAA) and XRF; and for Ba, Sr, Sn and Zn by ICP and XRF. Blocky K-feldspar was analysed for Li, Be, Zn, Sr, Zr, Sn, Ba, Pb, and Bi by inductively coupled plasma (ICP); for Rb and Cs by instrumental neutron activation (INAA); and finally, K was analysed by X-ray fluorescence (XRF).

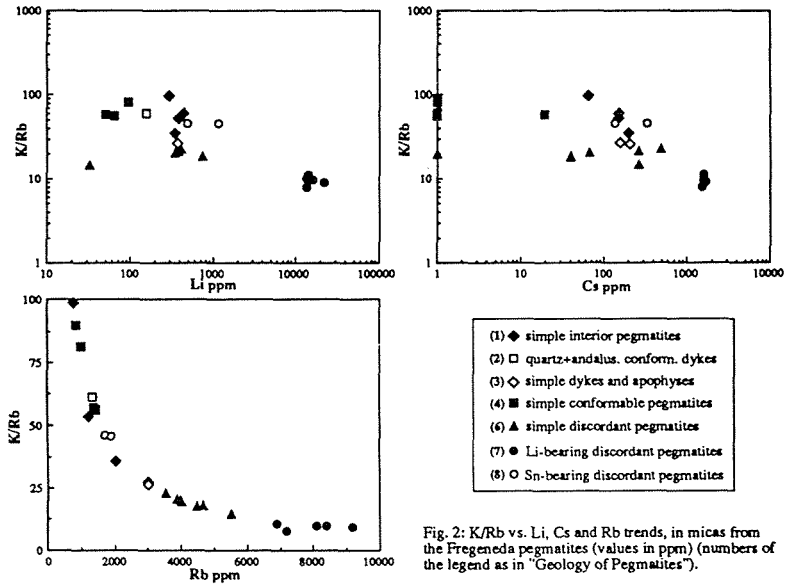

Fig. 2: K/Rb vs. Li, Cs and Rb trends, in micas from the Fregeneda pegmatites (values in ppm) (numbers of the legend as in "Geology of Pegmatites").

In Fig. 2 and 3 compositional variations in micas and K-feldspars, depending on the pegmatite type are illustrated.

The content in trace elements of micas shows differences among the different pegmatite types (Fig. 2). Muscovites from simple conformable pegmatites (4 type) are the poorest in Cs, Zn and F, the richest in Ba, and they show high values in the K/Rb ratio, whereas Li-micas from the Li-bearing pegmaties (7 type) are the richest in Cs, F, Rb and Ni, and they show the lowest values in the K/Rb ratio. Muscovites of the simple discordant pegmatites (6 type) show the highest Zn contents, and are the richest muscovites in Rb and Ni. With regard to the Sn-bearing pegmatites, their K/Rb ratio shows intermediate values, whereas the contents in Ba and Sr are high in comparison with the rest of the types.

On the other hand, trace elements contents in K-feldspars are illustrated in (Fig. 3). According to these graphs, simple comformable pegmatites (4 type) are the poorest in Cs, Li, Rb and Zn, whereas they show the highest K/Rb ratios. On the contrary, K-feldspars from the Li-bearing pegmatites (7 type) are the richest in Li, Cs and Rb, and the poorest in Ba. They also show the lowest K/Rb ratios. It is also notable that the K-feldspars from the simple discordant pegmatites (6 type) are the richest in Zn, and that they show low values in the K/Rb ratio. With regard to the Sn-bearing pegmatites (8 type), their K/Rb ratio shows intermediate values, whereas their contents in Ba and Sr are the highest.

General discussion

Alkali fractionation in K-feldspar and micas shows apparent congruent trends. The degree of alkali fractionation in pegmatite minerals as shown in Figs. 2 and 3, enables a first distinction between barren and highly fractionated pegmatites, with intermediate levels of fractionation. So, the less evolved ones are the simple conform pegmatites (type 4) and the quartz-andalusite dykes (type 2). Next, an intermediate fractionation zone, where simple interior pegmatites (type 1), simple dykes and apophyses (type 3), and K-feldspar discordant dykes (type 5) overlape, is observed. This intermediate zone is followed by other of higher level of fractionation, corresponding to the simple discordant pegmatites

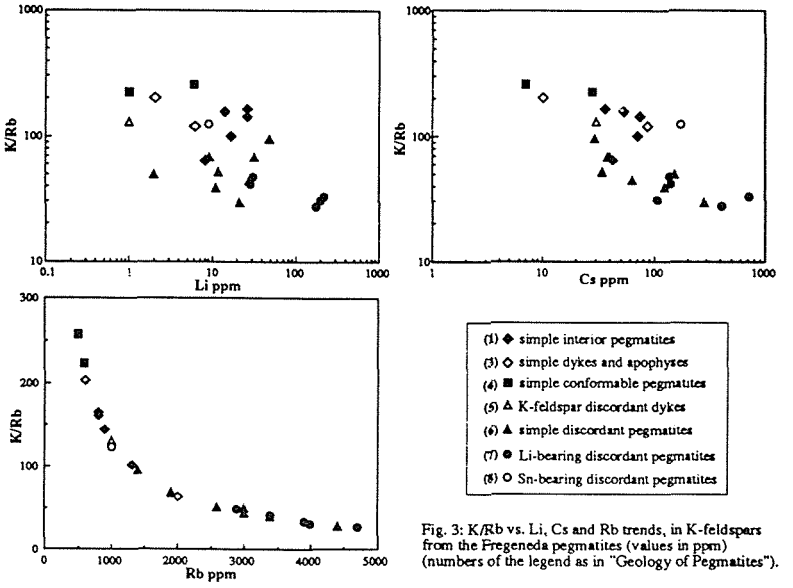

Fig. 3: K/Rb vs. Li, Cs and Rb trends, in K-feldspars from the Fregeneda pegmatites (values in ppm) (numbers of the legend as in "Geology of Pegmatites").

(type 6). Finally, the most evolved pegmatites are the Li-bearing discordant ones (type 7).

Sn-bearing pegmatites (type 8) plot in the intermediate fractionation zone, although their mineral assemblage is characteristic of the most diferentiated terms in a given pegmatitic sequence. This suggests that this group of pegmatites is not related by simple fractional crystallization to the other types. In contrast, the congruent trends showed for the rest of the pegmatites (Figs 2 and 3) suggest that they, to a first aproximation, are genetically, as well as spatially related to each other.

According to the trends showed in Figs. 2 and 3, a continous crystallization model could explain the different pegmatite compositions and mineral assemblages in the Fregeneda area, except for the Sn-bearing pegmatites. In this way, we have to bear in mind that there are individual pegmatite fields formed under different conditions and belong to different classes (Cerny, 1991).

References

Cerny, P. 1991. Rare-element granitic pegmatites, Part II. Anatomy and internal evolution of pegmatite deposits. Geoscience Canada, 18: 46-67

-1992. Geochemical and petrogenetic features of mineralization in rare-element granitic pegmatites in the light of current research. Applied Geoch. 7:393-416

López Plaza, M.; Carnicero, M. A. 1988. El plutonismo Hercínico de la penillanura salmantino-zamorana (centro-oeste de España): Visión de conjunto en el contexto geológico regional. In Geología de los granitoides y rocas asociadas del macizo Hespérico: 53-68. Rueda, Madrid

Martinez Fernandez, F. J. 1974. Estudio del área metamórfica y granítica de los Arribes del Duero (Prov. de Salamanca y Zamora). Ph. D Thesis. Salamanca Univ.

Roda, E.; Pesquera, A.; Velasco, F. 1991. The pegmatites of the Fregeneda area, Salamanca, Spain. in Source, transport and deposition of metals, Pagel & Leroy (eds) Balkema, Rotterdam, pp 801-806.

Shearer, C. K.; Papike, J. J.; Jolliff, B. L. 1992. Petrogenetic links among granites and pegmatites in the Harney peak rare-element granite-pegmatite system, Black Hills, South Dakota. Can. Miner. 30:785-809

Trueman, D. L. & Cerny, P. 1982. Exploration for rare-element granitic pegmatites. In MAC Short Course Handbook, Vol. 8: 463-493.

Current Research in Geology Applied to Ore Deposits.Fenoll Hach-Alí, Torres-Ruiz & Gervilla(eds)(1993).ISBN 84-338-1772-8

POTENTIAL OF COLUMBITE U-Pb DATING IN RECONNAISSANCE EXPLORATION FOR Nb-Ta-MINERAL OCCURRENCES

Romer, R.L.
Dept. Appl. Geol., Luleå University, S-951 87 Luleå, Sweden.

Abstract Columbite occurs in most kinds of Nb-Ta mineralizations and it yields very precise U-Pb ages. Yet, U-Pb dating of columbite involves a leaching procedure, which may cause laboratory induced U-Pb fractionation. Therefore, a single columbite fraction is insufficient to yield the age of the mineral. Instead, the age must be assessed by showing its reproducibility or by demonstrating the constancy of the $^{207}Pb^*/^{206}Pb^*$ from several fractions that were leached at a different extent. Properly performed U-Pb dating on detrital columbite gives in regional reconnaissance exploration surveys clear indications on which age group of parent rocks to concentrate exploration efforts.

Among economically significant Nb-Ta minerals, columbite-tantalite $(Fe,Mn)(Nb,Ta)_2O_6$ is the most widespread type and it occurs in most kinds of Nb-Ta deposits (Cerny & Ercit 1989). Other economically important Nb-Ta minerals are pyrochlore, microlite, wodgingite, and strüverite. Ta occurs, furthermore, in cassiterite (Roethe 1989). Common to Nb-Ta minerals is their genetic association with (1) alkaline anorogenic complexes (carbonatites, alkaline granites and their associated pegmatites), (2) late- to post-tectonic calcalkaline to peraluminous granites from orogenic settings, and (3) rare-element granitic pegmatites from orogenic settings (cf. Cerny & Ercit 1989).

The density of columbite-tantalite grains varies from 5.2 g/cm^3 to 7.9 g/cm^3 dependent on $MnFe_{-1}$ and $NbTa_{-1}$ substitutions. Columbite-tantalites are complex solid solutions into which W, Ti, Sn, and U can substitute to highly variable extent. Some of these substitutes exsolve subsequently and form tiny inclusions of, e.g., rutile, wolframite, cassiterite, and uraninite (e.g., Ramdohr, 1975). The common metamictization of columbite suggests that not all U is exsolved into uraninite, and U may remain to some extent in the crystal lattice. Columbite is generally U-rich (several 100 to several 1000 ppm) and it has very low Pb contents (often less than 1 ppm). Therefore, it is potentially suited as a U-Pb geochronometer.

Columbite is mechanically and chemically very resistant and, therefore, it can be concentrated in heavy mineral sands and placers. Detrital columbite is only economically significant in residual soil deposits in tropic areas (e.g., Nigeria; Matheis & Küster 1989). However, subordinately it can occur in placer deposits and black sands with ilmenite, rutile, cassiterite, monazite, zircon, and magnetite. Detrital columbite indicates that columbite-bearing rocks occur in the source area of the investigated drainage system. In drainage areas that cover several potential parent lithologies of contrasting age, exploration efforts could be optimized if the age of the potential mineralization is known. U-Pb dating of detrital columbite gives the age of the columbite-bearing rock as well as the one of the associated magmatic parent rocks. As the ore mineral itself is dated, the U-Pb age of detrital columbites gives a direct indication on which group of potential parent rocks to concentrate.

Columbite U-Pb dating involves a leaching procedure, which could result in laboratory induced U-Pb fractionation and erroneous ages. Therefore, this paper (1) describes the dating procedure and its inherit problems and uncertainties, (2) presents methods to test the validity of columbite U-Pb ages, and (3) suggests the use of U-Pb dating of detrital columbite in regional reconnaissance exploration.

U-Pb dating of columbites

With respect to U-Pb dating, columbite is a two-component system. One U-Pb system is represented by the uraninite inclusions, the other by the unexsolved U in the columbite crystal lattice. These two systems behave differently: The U-Pb system of uraninite is enclosed in columbite, which prevents U and Pb from interacting with the surrounding. This system may yield concordant ages. In contrast, because of the metamictization of the crystal lattice of columbite, the lattice-bound U-Pb system may interact with the surrounding and behave as an open system (see Romer & Wright 1992). Early dating yielded, because of the multi-system nature of columbite, highly discordant data (Aldrich

et al. 1956; Welin & Blomqvist 1964). With the development of zircon for U-Pb dating and the adaptation of this method for micro-samples (see Faure 1986), the dating of U-rich phases (such as columbite, euxenite, samarskite), which generally yield strongly discordant age data, became increasingly less common.

To obtain closely constrained, reliable U-Pb columbite ages, the uraninite inclusions have to be separated from columbite and only the potentially closed U-Pb system of the inclusions should be used for dating. In U-Pb dating of, e.g., zircon, baddeleyite, and rutile, increased concordance is generally obtained by abrasion (Krogh 1982). My abrasion experiments on columbites did, so far, not yield increased concordance of the age data. Romer & Wright (1992) used a leaching procedure to improve the concordance of columbite age data and to increase the precision of the upper intercept age of the discordia line. They used variably diluted HF to dissolve partially the columbites. The undissolved residue was used for U-Pb dating. Romer & Wright (1992) showed that leaching increased the measured $^{206}Pb/^{204}Pb$, i.e., preferentially removed common lead, and that stronger leached fractions were more concordant. Their upper intercept ages coincide with the ages obtained by other methods.

Analytical problems associated with columbite U-Pb dating

Romer & Wright (1992) leached columbite fractions to obtain more concordant data and to closer constrain upper intercept ages. During the acid attack, (1) metamict parts of the columbite should dissolve more readily than the non-metamict ones and (2) uraninite inclusions in contact to fractures of crystal surfaces should dissolve. The undissolved parts used for the U-Pb dating are (1) little or non-metamict columbite and (2) uraninite inclusions without surface contact. Although the leaching procedure is highly successful to increase the concordance of the data and to yield a well-defined discordia with a closely constrained upper intercept age, there are several inherit problems associated with leaching (e.g., Todt & Büsch 1981, Claesson 1987). Most important, leaching may result in an artificial fractionation of U and Pb. For grains with a single stage history and no surface Pb-loss, this laboratory-induced U-Pb fractionation does not affect the upper intercept age. Laboratory induced U-Pb fractionation will move the data points along trajectories through the origin of the concordia diagram (Fig. 1, double-ended arrows). Previously concordant points would fall on an artificial discordia that, nonetheless, yields the correct age. However, if columbites had previously suffered from Pb-loss during metamorphism, i.e., the data fall on a discordia between the formation age and the disturbance age (Fig. 1, line B-C), laboratory induced U-Pb fractionation would result in increased scatter about the discordia. Laboratory induced U-Pb fractionation would move each point to an arbitrary extent along trajectories through the origin of the diagram. In this case, leaching could result in erroneous upper intercept ages.

Assessment of correctness of U-Pb ages

In absence of precise and reliable age data from other geochronometers, the validity of U-Pb columbite ages can be evaluated along two lines of evidence. First, the $^{207}Pb^*/^{206}Pb^*$ ratio for various fractions should be independent on the extent of leaching. Second, the upper intercept age should be reproducible.

In a closed system, the $^{207}Pb^*/^{206}Pb^*$ is only dependent on the age of the specimen. For columbites with a single-stage history this ratio is independent on the extent of leaching and remains constant. Constant $^{207}Pb^*/^{206}Pb^*$ could also be obtained from homogeneous, yet discordant U-Pb systems. This possibility, however, is in contrast with the heterogeneous nature of columbite as demonstrated by mineralogical studies (e.g., Ramdohr 1975, Cerny & Ercit 1989). Therefore, a $^{207}Pb^*/^{206}Pb^*$ that is independent on the extent of leaching is sufficient to demonstrate that the upper intercept age is correct. Columbites with a two-stage or poly-stage history, during which the $^{238}U/^{204}Pb$ of the mineral changed or radiogenic lead was lost, show a contrasting behavior. Their $^{207}Pb^*/^{206}Pb^*$ depends on the formation and disturbance ages and the proportion of lead that was acquired before and after the disturbance. During the leaching procedure, various parts of the mineral will be dissolved to a different extent. It is unlikely that the two U-Pb lead systems are affected to the same extent, and therefore the $^{207}Pb^*/^{206}Pb^*$ will not remain constant for different extents of leaching.

In this case, the age of the columbite should be assessed by demonstrating reproducibility of the upper intercept age.

The reproducibility of the age implies that the sample had a single-stage history or that there occurred no U-Pb fractionation in the laboratory. For samples with a single-stage history, this information is redundant as it already is contained in the constant $^{207}Pb^*/^{206}Pb^*$. However for samples with a multi-stage history, the argument of reproducibility of the intercept ages is very essential: Dating several primary columbites from the same rock must yield the same upper **and** lower intercept age within analytical uncertainties. Reproducible intercept ages of poly-stage grains demonstrate that there was no fractionation of U and Pb during the leaching procedure in the laboratory.

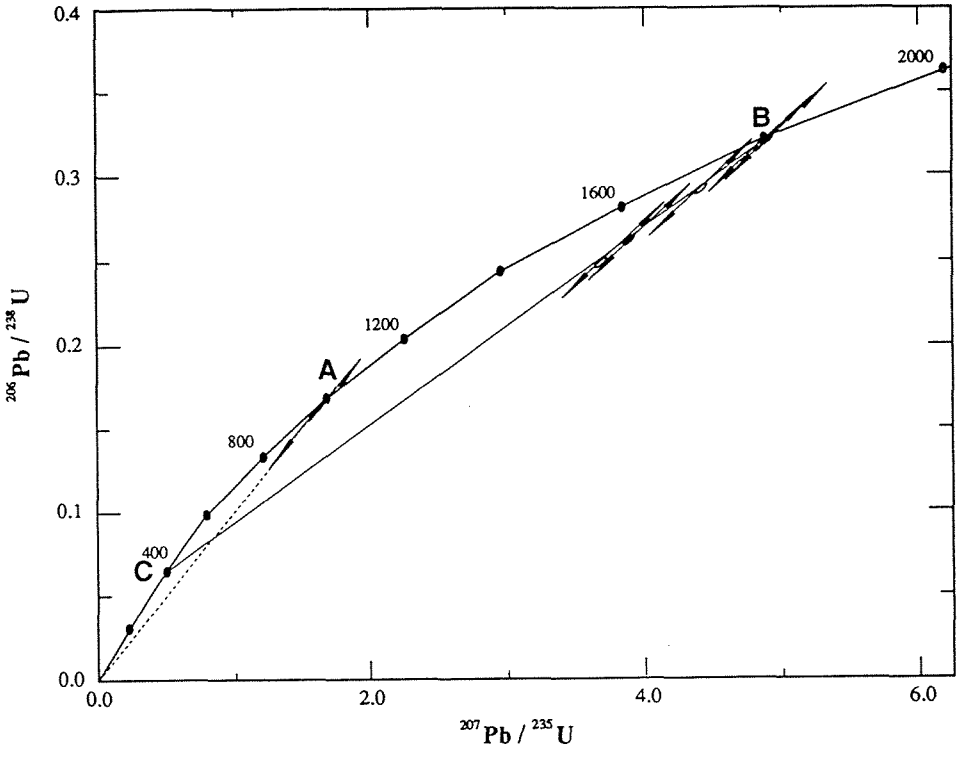

Fig. 1: Concordia diagram illustrating the effect of laboratory induced U-Pb fractionation on the upper intercept age. A = concordant sample, B, C = upper, lower intercept of a sample with two-stage evolution. Laboratory induced U-Pb fractionation would move each data along trajectories (arrows) through the origin of the diagram. For discussion see text.

Potential use in reconnaissance exploration investigations for Ta and Nb

Detrital columbite illustrates that there is a potential for Nb-Ta mineralizations in the drainage area from which the sediments are derived. If only one group of potential parent rocks for Nb-Ta-mineralizations occurs in that area, there is no need to know the age of the detrital columbites, as exploration anyhow directly will focus on the only suitable lithologic unit. However, if several different potential parent rocks with contrasting age occur within the drainage area, the age of detrital columbites will clearly outline on which age group of potential parent rocks (and their surrounding) to focus exploration efforts.

Gulson & Jones (1992) suggest a similar use of cassiterite dating in reconnaissance exploration. As columbite and cassiterite often occurs in the same kind of deposit, they may yield similar information. Cassiterite generally does not dissolve completely (Gulson & Jones 1992) and

suffers, therefore, from the same analytical problems as columbite, i.e., the possibility of laboratory induced U-Pb fractionation. The large impetus of U-Pb dating of columbite (and cassiterite) is that the ore mineral itself is dated. In the study of the genesis of Ta-Nb (and Sn) deposits, this allows to determine the time of columbite (and cassiterite) mineralization as well as later mobilizations. In the context of exploration for Ta-Nb (and Sn) mineralizations, dating of detrital ore minerals, despite analytical problems, is a powerful tool to select among exploration targets.

References

Aldrich, L.T., Davis, G.L., Tilton, G.R. & Wetherill, G.W. 1956. Radioactive ages of minerals from the Brown Derby Mine and the Quartz Creek Granite near Gunnison, Colorado. J. Geophys. Res. 61: 215-232

Cerny, P. 1989. Exploration strategy and methods for pegmatite deposits. In: Möller, P., Cerny, P., Saupé, F. (eds.) Lanthanides, Tantalum and Niobium. Springer Berlin, pp 274-302

Cerny, P. & Ercit, S.T. 1989. Mineralogy of niobium and tantalum: crystal chemical relationships, paragenetic aspects and their economic implications. In: Möller, P., Cerny, P., Saupé, F. (eds.) Lanthanides, Tantalum and Niobium. Springer Berlin, pp 27-79

Claesson, S. 1987. Isotopic evidence for the Precambrian provenance and Caledonian metamorphism of high-grade paragneisses from the Seve Nappes, Scandinavian Caledonides. Contrib. Mineral. Petrol. 97: 196-204

Faure, G. 1986. Principles of isotope geology (2nd ed.). Wiley & Sons, New York, 589 pp

Gulson, B.L. & Jones, M.T. 1992. Cassiterite: Potential for direct dating of mineral deposits and a precise age for the Bushveld Complex granites. Geology 20: 355-358

Krogh, T.E. 1982. Improved accuracy of U-Pb zircon ages by the creation of more concordant systems using an air abrasion technique. Geochim. Cosmochim. Acta 46: 637-649

Matheis, G. & Küster, D. 1989. Geochemical exploration guide for rare-metal pegmatites – Examples from Nigeria and Sudan. In: Möller, P., Cerny, P., Saupé, F. (eds.) Lanthanides, Tantalum and Niobium. Springer Berlin, pp 321-328

Ramdohr, P. 1975. Die Erzmineralien und ihre Verwachsungen. Akademie-Verlag, Berlin.

Roethe, G. 1989. Processing of tantalum and niobium ores. In: Möller, P., Cerny, P., Saupé, F. (eds.) Lanthanides, Tantalum and Niobium. Springer Berlin, pp 27-79

Romer, R.L. & Wright, J.E. 1992. U-Pb dating of columbites: A geochronologic tool to date magmatism and ore deposits. Geochim. Cosmochim. Acta 56: 2137-2142

Todt, W.A. & Büsch, W. 1981. U-Pb investigations of zircons from pre-Variscan gneisses - I. A study from the Schwarzwald, West Germany. Geochim. Cosmochim. Acta 45: 1789-1810

Welin, E. & Blomqvist, G. 1964. Age measurements on radioactive minerals from Sweden. Geol. Fören. Stockholm Förh. 86: 33-50

Current Research in Geology Applied to Ore Deposits. Fenoll Hach-Alí, Torres-Ruiz & Gervilla (eds) (1993). ISBN 84-338-1772-8

ZIRCONOSILICATE PHASE RELATIONS IN THE STRANGE LAKE PLUTON, QUEBEC-LABRADOR, CANADA

Salvi, S. & Williams-Jones, A.E.
Earth & Planet. Sci. McGill University, 3450 University St., Montreal, QC, Canada H3A 2A7

ABSTRACT: Petrographic observations at Strange Lake indicate that the sodium zirconosilicate elpidite crystallized under magmatic conditions, but that the calcium zirconosilicates armstrongite (minor) and gittinsite are secondary. Both minerals show textural evidence of having replaced elpidite, and in the case of gittinsite, with major volume loss. A model is proposed in which external Ca-rich, quartz-undersaturated fluids dissolved elpidite, replacing it primarily with gittinsite (and locally with armstrongite, or armstrongite + gittinsite). This created extensive pore space which, higher in the pluton, was subsequently filled when the fluids become saturated with quartz as a result of increased $a_{H_4SiO_4^0}$ and decreased pressure and temperature.

Introduction

Zirconium is present as a trace constituent in most igneous rocks, where it typically displays incompatible geochemical behaviour and is accommodated as the accessory phase zircon. In peralkaline rocks, however, zirconium can reach concentrations of several percent in various exotic alkali and alkaline-earth minerals that in some cases are sufficiently abundant to be potentially economic (e.g., Ilímaussaq, Karup-Møller, 1978; Lovozero, Kogarko, 1990; in Canada at Strange Lake, Birkett et al., 1992, and Thor Lake, Trueman et al., 1988). Information on the paragenesis of these minerals is important in understanding the petrogenesis of peralkaline rocks, and is essential if we are to establish the factors that could lead to economic concentrations of zirconium.

In the more evolved units of the Strange Lake complex, zirconium is contained mainly in the minerals gittinsite ($CaZrSi_2O_7$), elpidite ($Na_2ZrSi_6O_{15}\cdot 3H_2O$) and armstrongite ($CaZrSi_6O_{15}\cdot 3H_2O$). These minerals vary greatly in their relative proportions; locally, any one of them may be the principal or sole Zr mineral. Significantly, the highest concentrations of Zr are found in rocks containing only gittinsite. This paper provides preliminary data on, and an explanation for, the distribution of gittinsite, elpidite and armstrongite, in core from a diamond drill hole located near the main exploration trench in the centre of the complex.

Geological Setting

The peralkaline Strange Lake pluton was emplaced in Aphebian gneisses and Elsonian rocks of the eastern Rae province of the Canadian Shield (Bélanger, 1984), and is believed to represent the western extension of the Gardar anorogenic igneous event (Currie, 1985; Pillet *et al.*, 1989). Rocks to the north of the pluton consist of metadiorites, calc-silicate gneisses, meta-amphibolites, quartzofeldspathic and graphitic paragneisses (Bélanger, 1984). To the south, the pluton intrudes a large body of quartz monzonite.

The pluton has been subdivided into hypersolvus granite and more evolved, volatile-saturated, subsolvus granite (Nassif & Martin, 1991). The complex also contains numerous pegmatites mainly associated with subsolvus granite. The hypersolvus granite consists mostly of perthite, interstitial quartz and late arfvedsonite, whereas the subsolvus granite is characterized by idiomorphic quartz, arfvedsonite and late alkali feldspars. Rare-metal-bearing minerals comprise between 5 and 30% of the rock, with the highest concentrations occurring in the subsolvus granite and pegmatites. A potential ore zone has been delineated containing approximately 30 million tonnes grading 3.25% ZrO_2, 1.3% REE oxides, 0.66% Y_2O_3, 0.56% Nb_2O_5 and 0.12% BeO.

Geology of DDH SL-182

Hole SL-182 (87.02 m deep) was drilled by the Iron Ore Company of Canada in 1982, in the subsolvus granite, very near the potential ore zone. All the lithologies intersected contain quartz phenocrysts, arfvedsonite, fine-grained alkali feldspars, zirconosilicate minerals and medium- to coarse-grained idiomorphic pseudomorphs of titanite + quartz ± fluorite after narsarsukite ($Na_2[Ti,Fe^{3+}]Si_4\ [O,F]_{11}$). Most samples contain rare perthite phenocrysts (replaced almost entirely by microcline and rimmed by albite), at least two generations of fluorite in varied proportions, and small idiomorphic crystals of pyrochlore. Hematite, zircon, thorite, allanite, bastnæsite, kainosite, yttrian milarite, and several unidentified minerals occur locally.

The granitic host rocks are invariably altered, as indicated by the replacement of arfvedsonite by aegirine, replacement textures involving the zirconosilicates (see below), hematitic alteration, cloudiness and red Fe^{3+}-activated cathodoluminescence of feldspars, and the development of extensive secondary porosity.

The top half and final 10 m of the hole are composed of medium-grained granite that is distinguished by a bimodal distribution of arfvedsonite crystal size and the presence of inclusions of melanocratic granite. In the central portion of the hole, the granite is equigranular, fine- to medium-grained and inclusion-free. Several metre-wide pegmatites also are present in this part of the hole.

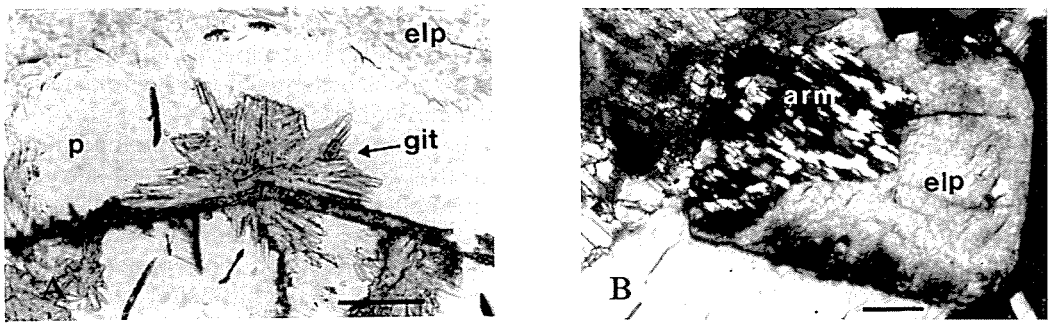

Fig. 1. A) Radiating gittinsite crystals attached to a string of zircon spherules, and growing in pore space (p) adjacent to elpidite. B) Partial replacement of elpidite by armstrongite. Scale bars 0.1 mm.

Zirconosilicate Minerals

Elpidite, gittinsite and armstrongite have distinctly different distributions and modes of occurrence. In the first 10 m of drill core, gittinsite occurs to the exclusion of elpidite and armstrongite. It forms radiating feathery crystals up to ≈0.25 mm in length and, together with interstitial anhedral quartz, forms coherent aggregates in the groundmass. Although lacking regular shapes, these aggregates have sharp boundaries, suggesting that they are restricted to interstitial volumes formerly occupied by crystals of a precursor phase. In this zone, the granite lacks porosity and displays a patchy red coloration due to the presence of abundant fine-grained hematite in the gittinsite-quartz aggregates. Similar rocks from the exploration trench contain pseudomorphs of gittinsite + quartz after euhedral crystals with an elpidite-like morphology (cf. Salvi & Williams-Jones, 1990).

Further down hole (10-40 m depth), elpidite is the dominant zirconosilicate; it forms interstitial pockets of tiny interlocking crystals in the groundmass, with a habit very similar to the shapes of the gittinsite-quartz aggregates higher in the hole. Commonly, radiating sprays of gittinsite partly replace elpidite. The porosity in this interval is high, due to the

dissolution of elpidite. Gittinsite rosettes occur in the cavities left by elpidite dissolution, and grow preferentially on secondary zircon and titanite (Fig. 1A). Quartz does not accompany the gittinsite, and hematite is rare. Minor armstrongite occurs locally as small overgrowths on, or replacements of elpidite.

In the equigranular granite, elpidite occurs as euhedral crystals of up to 2 mm long and comprises 10% to 30% of the rock by volume. It displays varying degrees of rim and core replacement by armstrongite (Fig. 1B), gittinsite or, most commonly, a mixture of armstrongite and gittinsite. In some cases, the elpidite has been completely destroyed. Where the replacement involved armstrongite alone, volume was conserved, i.e., there is no added porosity. Crystals replaced by gittinsite, or armstrongite + gittinsite, all contain pore space. Interestingly, although armstrongite can be found in contact with both elpidite and gittinsite, the latter minerals rarely occur in contact with each other.

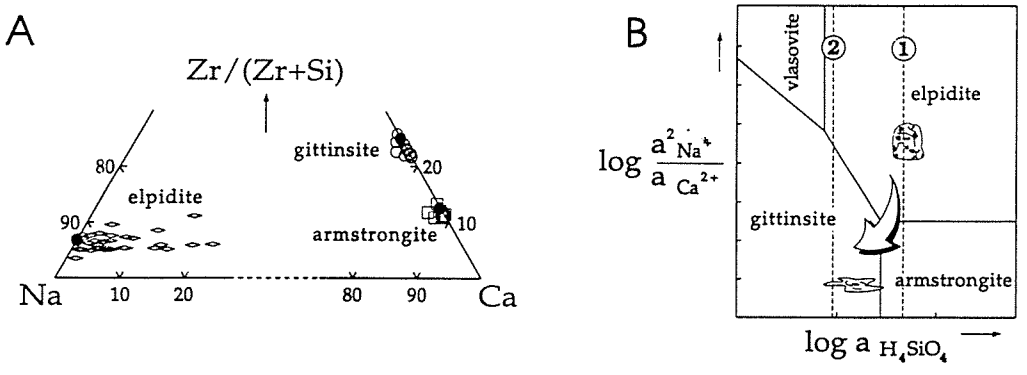

Fig. 2. A) A plot of the cation proportions in the Strange Lake zirconosilicate minerals calculated on the basis of 7 and 15 atoms of oxygen for anhydrous and hydrous species, respectively. Filled circles indicate end-member compositions. B) A schematic log $a^2_{Na^+}/a_{Ca^{2+}}$ vs. log $a_{H_4SiO_4^0}$ diagram showing zirconosilicate stability fields, and hypothetical compositions of unaltered elpidite-bearing granite and hydrothermal fluid. Lines 1 & 2 represent respective quartz saturation at deep and shallow levels in the drill hole.

Below the equigranular granite, elpidite again occurs as interstitial aggregates of small grains. Armstrongite is absent, and gittinsite is rare The rock has a fresher appearance, and porosity is minor.

Discussion

The euhedral habit of elpidite in the equigranular granite suggests that this mineral crystallized relatively early, whereas its occurrence as interstitial anhedra in the porphyritic granite indicates relatively late-stage crystallization. In both rock types, however, elpidite is clearly a magmatic mineral and was the first zirconosilicate to form. In contrast, both armstrongite and gittinsite occur only as secondary subsolidus minerals, largely as a replacement of elpidite. The formation of armstrongite is readily explained by the reaction

$$Na_2ZrSi_6O_{15}\cdot 3H_2O + Ca^{2+} \rightleftharpoons CaZrSi_6O_{15}\cdot 3H_2O + 2Na^+ \qquad (1)$$

which has very small negative ΔV (-11.01 ml; 4.8% volume reduction) thereby permitting the essentially constant volume pseudomorphism of elpidite euhedra by armstrongite (Fig. 1B). The replacement of elpidite by gittinsite can be explained either by the reaction

$$Na_2ZrSi_6O_{15}\cdot 3H_2O + Ca^{2+} \rightleftharpoons CaZrSi_2O_7 + 2Na^+ + 4SiO_2 + 3H_2O \quad (2)$$

or

$$Na_2ZrSi_6O_{15}\cdot 3H_2O + Ca^{2+} + 5H_2O \rightleftharpoons CaZrSi_2O_7 + 2Na^+ + 4H_4SiO_4^0. \quad (3)$$

Both these reactions are associated with large negative values of ΔV (reaction 2, -58.42ml or 25% volume reduction; reaction 3, -149.1 ml or 65% volume reduction), and thus explain the considerable porosity associated with the replacement of elpidite by gittinsite in the central part of the hole. The absence of accompanying quartz suggests that replacement proceeded via reaction 3 not 2, i.e., that the altering fluid was undersaturated with respect to quartz. In the top 10 m of the hole, gittinsite is accompanied by quartz, and there is no evidence of porosity. This requires that replacement of the precursor zirconosilicate, whether by reaction 2 or 3 or analogous reactions involving armstrongite, was accompanied or followed by precipitation of additional quartz. The preservation of delicate rosettes of gittinsite suggests that replacement occurred prior to the precipitation of quartz precipitation, i.e., by reaction 3.

In a previous study, Salvi & Williams-Jones (1990) reported the presence of primary fluid inclusions in gittinsite-quartz pseudomorphs from trench samples. On the basis of data collected from these inclusions, we proposed that the pseudomorphism was effected by Ca-rich brines at temperatures of $\approx$200°C. It seems probable that the textures observed in core from DDH SL-182, involving the replacement of magmatic elpidite by gittinsite or armstrongite or both, were caused by a similar fluid (such low-temperature formation of gittinsite and armstrongite is consistent with the near-end-member compositions of these minerals, and contrasts with the extensive solid-solution displayed by elpidite, Fig. 2A).

We propose that groundwaters heated by the pluton equilibrated with adjacent calc-silicate gneisses and gabbros, thereby producing Ca-rich quartz-undersaturated fluids (Fig. 2B, undersaturated with respect to line 1) which subsequently entered the granite (quartz saturated, Fig. 2B). These fluids dissolved elpidite, replacing it primarily with gittinsite, but locally with gittinsite + armstrongite, or armstrongite alone where $a_{H_4SiO_4^0}$ was greater. Higher in the pluton, cavities left by the replacement of elpidite with gittinsite were later filled by quartz due to decreased silica solubility at lower temperatures and pressures, and evolution of the fluid to higher $a_{H_4SiO_4^0}$.

References

Bélanger, M. 1984. Région du lac Brisson: Ministère Énergie Ressour. Qué., DP 84-20 (carte annotée)

Birkett, T.C., Miller, R.R., Roberts, A.C. & Mariano, A.N. 1992. Zirconium-bearing minerals of the Strange Lake intrusive complex, Quebec-Labrador. Can. Mineral. 30:191-205

Currie, K.L. 1985. An unusual peralkaline granite near Lac Brisson, Quebec-Labrador. Geol. Sur. Can. Rpt. 85-1A:73-90

Karup-Møller, S. 1978. The ore minerals in the Ilímaussaq intrusion: their mode of occurrence and their conditions of formation. Bull. Grønl. Geol. Unders. 127:1-51

Kogarko, L.N. 1990. Ore-forming potential of alkaline magmas. Lithos 26:167-175

Pillet, D., Bonhomme, M., Duthou, J.L. & Shenevoy, M. 1989. Chronologie Rb/Sr et K/Ar du granite peralkalin du lac Brisson, Labrador central, Nouveau-Québec Can. J. Earth Sci. 26:328-332

Salvi, S. & Williams-Jones, A.E. 1990. The role of hydrothermal processes in the granite-hosted Zr, Y, REE deposit at Strange Lake, Quebec/Labrador: Evidence from fluid inclusions. Geochim. Cosmochim. Acta 54:2403-2418

Trueman, D.L., Pedersen, J.C., de St. Jorre, L. & Smith, D.G.W. 1985. The Thor Lake, N.W.T. rare-metal deposits. In: Taylor, R.P. & Strong, D.F. (eds.) Granite-related mineral deposits: Geology, petrogenesis and tectonic setting. CIM Spec. Vol. 39. pp 279-284

Current Research in Geology Applied to Ore Deposits.Fenoll Hach-Alí, Torres-Ruiz & Gervilla(eds)(1993).ISBN 84-338-1772-8

CONDITIONS OF THE SEPARATION ORE FORMING FLUIDS CONNECTED WITH RARE METALS GRANITES

Sobolev, R.N.
Geological Faculty, Moscow State University, 119899 Moscow, Russia

ABSTRACT. On the basis of glass inclusions investigations and experimental data is established that separetion of the ore forming fluids connected with rare metal granites occurs by high temperature (higher than 1100 C). This process is result of immisibility: starting silicate melt disintegrats into silicate melt and saline melt (brine) with very high concentration of ore elements. This saline melt is a sort of "saline ore magma", which forms ore deposits.The hydrothermal solutions (fluids) separated from silicate melt by rather low temperature don't form industrial ore deposits.

For investigators who study problem of magma(rock) - ore concen tration relations is clear that the nature of these concentrations is not sporadic but regular for hydrothermal types of rare metal ore deposits (W, Sn etc.). The basis for this is that: 1. ore deposits of this type, as a rule, are situated in the apical parts of granitic bodies; 2. the ore and granitic veins very often alternate with each other in time; 3. common isotopic composition of elements. All this shows that there are space and genetical con nections between granites and hydrothermal proceses,- the latters usually consider as derivatives of crystallizing granitic magma. Nevertheless there are some questions: fluid's source in magma and how occurs it separation from melt. As a possible sources of fluids in magma usually admit: 1. mantle and 2. rocks of the earth crust (mostly for phanerozoic granites). Exists also poin of view that fluids, from which have formed hydrothermal ore deposits, have no relations with magma, but represent solutions which existed in wall rocks before magma intrusion. Under influence of magma's heat they attain capacity to take ore elements from wall rocks and granite itself and transporte these elements to place of deposit. Many scientists believe that fluids have mixed origine. Possibly that this idea is the most correct (Sobolev, 1992a).

Problem of relation between granite (granitic melt) and ore concentrations becomes yet more complicated because granites itself

have different genesis and tectonic setting. Usually, according to these criterions, granites divide into 4 types: M,I,S,A(Sobolev, 1992b). Rare metal ore deposits are connected with all 4 types but they form different types of deposits. It is possible to consider this question on the W, as example. Average concentration of W in granitoids varies from 1.5 to 2 g/t. The highest concentration are in muscovite (rock forming mineral) - 45 and rutil (accessory mineral) - 600 g/t. Principal minerals of tungsten are wolframite and scheelite which forme on magmatic, late magmatic and post magmatic stages. Average concentration both minerals in granitoids is less than 3 g/t; usually in granites is wolframit but in granodiorites - scheelite.

Concentrations of W formed on the magmatic stage are very rare - these are plots in granites there W associate with Sn (Russia, USA, S. Africa etc.); these concentrations have not industrial significance. Late magmatic stage of W concentrations (pegmatites) are tin-tungsten (usually) and rare metal - molibden - tin (exeptional) formations. Scarns, greizens and quartz veins are the most frequent types of W ore deposits. They generate onthe post magmatic stage. Ore deposits of scarn type are related with granodiorite and quartz diorite (I- and M-types) - these are scheelite ore deposits. Greizens type of ore deposits arerelated mostly with leucocratic granites (S-type) - these are wolframite ore deposites. Ore deposits of hydrothermal types are very diverse: quartz-tin-wolframite type is connected with leucocratic granites /S-type), quartz-wolframite - with leucocratic andbiotite granites (S- and, rarely, I-type), quartz-wolframite-molibdenite - with biotite granites and granodiorites (I-type).

In the process of the crystallizing differentiation W concentrates increase in 1.5-2 times - the evident of this is it's concentration in mineral-phenocrysts and in the same minerals of the ground mass. In some succession's phases of injections in the same granitic body concentration of W in the last injection is about 6 times higher than in the first. Many scientists suppose what then the temperature decrease and redox potential increase the W4+ transfer to W6+ , which has lithophyle properties. Accocding to this it has close relation with silicium, that is why it concentrates in acide differenciates of granitic magma, greizens and quartz veins (Sobolev, 1992c).

The result of studing glass inclusions (in quartz) from granites

and experimental investigations gave the matirial for new ideas. It is very important that in the rare metal ore forming granites in glass inclusions are two unmixed (but in equilibrium) melts: silicate and saline (brine); in non-ore forming granites there is only silicate melt. Saline melts of the ore forming (rare metal) granites are very rich in chlorides, fluorides and borides (especially chlorides). In these saline melts there are also very soluble tungsten's salts. Concentration of salts in saline melt-brine is very high - till 70-90 mas.%. That is very important what when the temperature decrease on 15 - 20^0 below the temperature of immisibility, the composition of the salt melt (which is in equilibrium with silicate melt) principally chang: salt's concentration is only 20-30 mas % and high concentration's melt-brine changes into undersaturated solution. There are also experiments which demonstrate disintegration (immisibility) of the silicate melt into two phases: high concentrated melt-brine and silicate melt (Marakushev et all, 1991).

It is established (on the basis of glass' inclusions studing) what in the rare metal ore bearing granites desintegration of the starting silicate melt occurs in the interval 1235 (united starting melt) - 1130^0C (silicate melt and melt-brine). Water's concentration in the rare metal ore bearing granitic magma is 3.3 - 6.6 whereas in non-ore bearing granites only about 2.4 mas. %. In melt's inclusions of ore bearing granites we have almost constantly muscovite as a solid phase. Homogenisation's yemperature of glass inclusions in quartz in non-ore bearing granites is about 1000^0C. So, rare metal ore bearing granites in comparison with non-ore bearing granites, have: 1) higher temperature of crystallisation, 2) disintegration of the starting melt (when the temperature decrease) into two: silicate and saline melts, 3) higher water's concentration in saline melt than in silicate melt, 4) high concentration of halogenides (especially chlorides) and borides in saline melt, 5) high W's concentration in saline melt, as well as, others rare metals in the form of the easy soluble salts, 6) in inclusions are constantly quartz and muscovite.

It is possible to say now what it is established what saline melts have capacity to extract W and other rare metals from silicate melt by very nigh temperature - when temperature decrease this capasity decrease also. Saline melt is a type of a special "ore saline magma" which transport ore elements. In this "magma" tungsten is in the form W6+. When this "ore saline magma" migrates it can be dilute by water (mostly) and in this case we have normal hydrothermal solution.

From the above mentioned we can conclud what extraction of W (and others rare metal elements) from the granitic melts occur in two ways: 1) During the

desintegration of the starting silicate melt on silicate and saline melts most part of W is extracted from the starting silicate melt to the saline melt-brine. Then this high temperature phase migrates indipendently , can be dilutes by underground waters and becomes hydrothermal solution with high (or low) concentration of W - from such solution forms W ore deposites. 2) Granitic melt evolutions (without disintegration) and on the final stage from it separates fluids (solutions) with relatively low concentration of W. Such fluids migrate through granite as a rock (not as a melt) and extract from it W and others ore elements and precipitate its or as a non-indastrial concentrations or as dispersed ore minerals in rock - in this way don't form ore deposits.

So the most important condition for formation rare metal ore deposits, related with granites is melt's separetion (by the high temperature conditions) into two parts: silicate melt and brine. If this mechanism does not work, there are no prerequistes for formation idustrial ore concentrations.

References

Marakushev, A.A. & Schapovalov,J.B. 1991.Acid-alkali differentiation granitic salt-melts. Reports of Russian Academy of Sciences. 321,3: 574-579

Sobolev,R.N. 1992. Granites' genesis. Moscow University Geology Bulletin (Vestnik Moskovskogo Universiteta. Geologiya).1:3-23 / a /

Sobolev,R.N. 1992. Reasons for hydrothermal ore deposits relation's with the granites of the definite's phazies of depth. Proceedings of USSR Academy of Sciences. Geology. 2:62-70 / b /

Sobolev,R.N. 1992. Tungsten bearing granites.Moscow Society of Nature Investigators Bulletin. Geology. 67,5:109-119. / c/

5 Industrial mineral deposits

Current Research in Geology Applied to Ore Gervilla.Fenoll Hach-Alí, Torres-Ruiz & Gervilla(eds)(1993).ISBN 84-338-1772-8

APPLIED CLAY MINERALOGY OF THE DOLERITE-CONTACT SEDIMENTS OF THE PONT DE SUERT FM. (CATALONIAN PYRENEES, SPAIN)

Bastida, J. (1); Berastegui, X. (2); Lago, M. (3); Serrano, J. (1); Signes, M. (4) & Tritlla, J. (5)
(1) Dept. de Geología, Universidad de Valencia, Burjasot, Valencia, Spain
(2) Servei Geologic de Catalunya, Barcelona, Spain
(3) Dept. de Ciencias de la Tierra, Universidad de Zaragoza, Zaragoza, Spain
(4) AIMPLAS. Parque Tecnológico, Paterna, Valencia, Spain
(5) Dept. de Cristal.lografia, Mineralogia i Diposits Minerals, Universitat de Barcelona, Barcelona, Spain

Abstract. The materials of the Keuper marls in the Pyrenees belongs to the Pont de Suert Fm. which includes sedimentary rocks as well as volcanoclastic deposits and igneous bodies of dolerites. Lutites and marls as well as argillized igneos rocks of this formation have been mineralogically and technologically characterized . The recognized mineralogical assemblage is ±quartz ±calcite ± dolomite ±feldspars ±gypsum ±talc ± chlorite ±illite ±vermiculite ±smectite ± kaolinite ±mixed layers chlorite-smectite ± mixed layers illite- smectite (± pyroxenes, ± amphiboles, in argillized igenous rocks). Ceramic applications are not recomended; good characteristics can eventually be achieved for fillers or for absorvents (technological data are provided for selected representative materials).

The Pont de Suert Fm. was defined by MEY et al (1968) in the Southern Pyrenees, between the Esera and Llobregat rivers , grouping the materials of the Middle and Upper Triassic, and sandwiched between the Bunter Fm., in the base, and the Bonansa Fm. at the top.This formation includes a great number of dolerite bodies (the nature of the corresponding magmatism was studied in AZAMBRE et al 1987) , and the aim of this work is to characterize , from the mineralogical, and technological point of view, the materials of contact with these dolerite bodies.

The Figure 1 show the distributions of outcrops of Bunter Fm. and Pont de Suert Fm. in the Southern Pyrenees, according to LOSANTOS et al (1989); the outcrops at the north of the line Berga- Campo belong to the Lower Thrust Sheets (or Nogueres Zone) and those situated at the south of that line, belong to the Upper Sheets of MUÑOZ et al. (1986).

The Figure 2 show the main evaporitic triassic basins at the East Spain (based in ORTI,1982). The Figure 3 is a correlation sketch between the different formations recognized in the Keuper .succesion: in the based in Nogueras Zone of MUÑOZ et al(1983), in the Sierras Exteriores of MUÑOZ et al (1983) and in the Catalonian Ranges, and in the Valencia basin , according to data of SALVANY (1986, 1989) and ORTI (1974), in SALVANY (1990) Concerning the nature of materials not affected by the emplacement of dolerites, the observed variety of lithologies to which lutites are vasociated does not allow to establish a general model of clay minerals origin in the sedimentary environment (BERASTEGUI et al.,1991).

AMIGO et al (1986) found the mineralogical assemblage talc± smectite ± chlorite ± calcite, in chilled margins of dolerites and its contact sediments in the Pont de Suert Fm. in the Estopiñán area (W of Figure 1B). In the present worck , the sampling (106 samples , corresponding to 30 localities) has beeen limited to distances above 0.25 m from the wall of the dolerite rocks, but extended to lutites and marls of different formations as well as argilllized dolerite rockcs and volcanoclastic deposits , in the area between the Esera and Segre rivers.

The observed mineralogical assemblages are : a) ±quartz ± calcite ±dolomite ± feldspars ± gypsum ± talc ± smectite ± vermiculite ± illite ± ± kaolinite ± mixed layers chlorite - smectite ± mixed layers illite- smectite b) The same ± pyroxenes ± amphiboles. These assemblages can be recognized in contact sediments, external boundaries of chilled margins of dolerites andin more or less argillized materials belonging to alterated dolerites as well as to cataclasites and/or breccias and /or volcanoclastic deposits of contact zones .

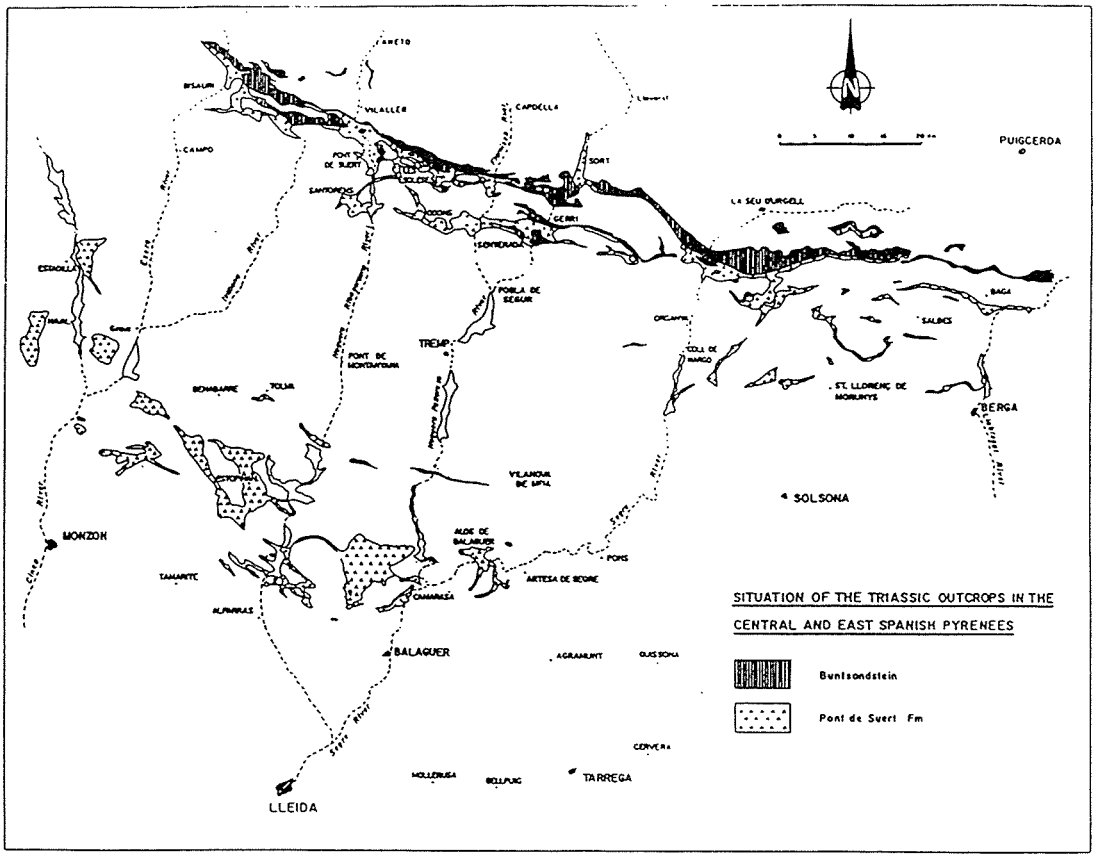

Figure 1. Situation of the triassic outcrops in the Catalonian Pyrinees. The situated northward of the line Berga-Campo belong to the Upper thrust sheets of the MUÑOZ *et al.* (1986), those situated at the south, correspond to Lower thrust sheet.

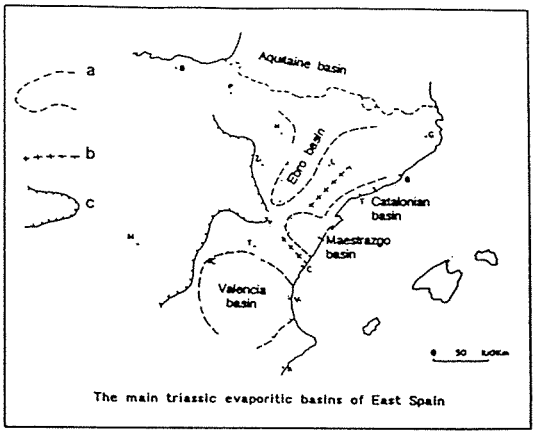

Figure 2. Sketch of the main triassic evaporitic basins of East Spain (based on ORTI, 1982). a. Subsident evaporitic triassic and liassic basins; b. Paleogeographic positive threshold; c. W edge of triassic-liassic evaporites.

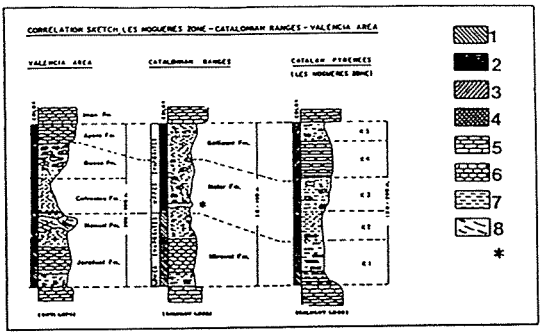

Figure 3. Correlation sketch of the Keuper units (based on SALVANY, 1991). 1. Grey; 2. Red; 3. Grey-green; 4. Versicolor; 5. Lime and dolostones; 6. Gypsum; 7. Lutites; 8. Sandstones; *. Volcanoclastic deposits.

Table 1 shows some mineralogical, petrographical, and technological properties of selected representative samples.

TABLA 1..

Ref.	Sh/L	%C*	%Q*	%T*	%f	%S	%NS	PS	OA	L%
GC-18	327 / A00	34.3	0.4	1.0	25.4	5.3	20.1	24.0	43.0	74.3
GC-38	328 / AR2	2.4	1.5	3.9	89.7	85.6	4.1	30.0	37.0	80.3
GC-46	252 / BT3	11.7	5.6	1.0	57.8	58.8	0.0		38.4	83.2
GC-65	327 / A05	50.3	1.4	0.5	10.8	0.5	10.3	15.4	26.5	78.3
GC-82	253 / LB1	46.8	0.6	3.0	41.7	41.7	0.0	19.8	44.4	78.7
GC-93	253 / GA4	56.9	0.3	15.6	22.1	0.0	22.1	10.1	23.6	-
GC-102A	214 / PM2	8.0	10.0	1.8	91.6	90.7	0.9	42.9	33.3	73.0
GC-V1	327 / A20	11.1	0.3	23.1	98.8	30.5	58.3	8.5	32.5	88.7
GC-T1	327 / A11	4.1	0.3	8.4	97.0	11.9	87.9	9.6	44.4	92.3
GC-A2	327 / A08	2.7	9.6	11.0	88.7	26.5	51.2	10.1	34.0	83.1

Ref = Refrence sample; Sh= Nr. of sheet of the Nat. map. scaled 1/50.000; L= locality.
C= calcite; Q = quartz; T= talc; *, refers to quantiative x - ray diffration analysi s (method of CHUNG, 1974)
f= sheet silicates; S= swelling sheet silicates; NS= not swelling sheet silicates (semiquantiative x-ray diffraction procedures, BARAHONA, 1980).
PS = Particle size average (laser diffraction, Culter LS 100).
OA= Oill absortion (ASTM D281-31,1980)
L=Huntterlab lightness (from hundred to zero)(in a Minolta CR-200, spectrocolorimeter UV-V).

Table 2 shows the corresponding chemical analysis.These materials ranges from lutites to marls, so high values of ignition loss (IL) and CO_2 can be found. The analized materials have low S content, because materials related with sulphate bearing rocks were avoided in the sampling Cu, Zn, Ni, Pb, Co, As and Mo no were found in greater than trace quantities.

TABLE 2.

REF.	Na_2O %	MgO %	Al_2O_3 %	SiO_2 %	K_2O %	CaO %	TiO_2 %	Cr ppm	MnO %	Fe_2O_3 %
GC18	.05	9.34	9.06	22.1	.51	23.9	.44	14	.13	7.66
GC38	.28	22.6	11.0	40.0	.62	3.14	.540	65	.09	4.27
GC46	.15	12.0	14.4	42.2	6.17	8.50	.678	34	.03	2.83
GC65	.08	2.64	3.04	8.36	.74	46.1	.114	<10	.03	.64
GC82	.02	13.4	3.33	19.8	.02	29.6	.208	<10	.06	4.05
GC93	.04	9.50	2.67	12.9	.05	39.6	.122	<10	.05	1.33
GC102A	.21	17.7	12.3	41.4	1.36	5.31	.613	75	.04	5.60
GCV1	.23	19.0	12.2	37.1	.66	8.82	.549	62	.03	1.27
GCT1	.44	23.5	13.1	40.5	.52	3.14	.584	90	.07	.75
GCA2	.89	10.9	14.8	52.7	2.67	2.88	.836	80	.04	2.81

REF.	CO_2 %	P_2O_3 %	S %	Cl ppm	Ba ppm	IL %
GC18	18.7	.13	.04	856	<10	27.0
GC38	.99	.06	<.01	1460	36	17.7
GC46	6.26	.11	.02	1190	14	13.0
GC65	36.8	.07	.02	133	<10	38.3
GC82	23.1	.08	.03	726	<10	29.8
GC93	31.4	.19	<.01	<50	<10	34.0
GC102A	2.83	.15	<.01	<50	160	15.7
GC-V1	5.91	.09	.02	1640	415	20.3
GC-T1	1.85	.10	<.01	556	86	17.8
GC-A2	1.34	.18	<.01	585	746	11.3

Analysis by X-RAL (SGS Group) Major elements : reference method WR; detection limit, 0.01; CO2: ref. method WR; detection limit,0.01; S: ref. method LECO; detection limit,0.01; Minors: ref. method WR; detection limit, 10 ppm.; Cl: ref. method XRF; detection limit, 50 ppm

Sulphates and halides were no detected by x- ray diffraction, but the observed Cl contents can affect the dispersing processes of these materials.

According to their chemical compositions (BERTON & LE BERRE,1983), these materials are no suitables for fine ceramics and neither for heavy ceramics formulations if the content of swelling sheet silicates is greater than 10% (mainly, in order to avoid drying problems).

The quartz contents are variable (Table 1) but usually, low. The values of bright can be high, in the range of natural ground calcium carbonates and of air - classified kaolins. (Mc VEY & HARBEN,1989). The values of oil absortion are in the range of those of natural ground calcium carbonates , talcs , slates and kaolins.(HARBEN,1992). So applications as fillersand extenders can be expected, and as absorvents if the swelling sheet silicates content is high.

REFERENCES

AMIGO,J.M; et al.(1986).**Cuad. Geol.. Ibérica,**87,.11, 83-96.

AZAMBRE,Bet al. (1987) **Bull. Minéralogie** , 110, 4, pp.83-96.

BARAHONA,J (1980) Arcillas de ladrillería de la provincia de Granada..Tesis Doct. Univ.de Granada, n° 49.

BASTIDA,J; et al.(1989) **Acta Geol. Hispánica,** 24, pp.115-130.

BERASTEGUI, X;et al. (1991).**Terra Abstracts,** 3, 1, pp. 106.

BERTON, Y et LE BERRE, P (1983). Guide de prospectio des matériaux de carrière. BRGM, Orléans.

CHUNG, F.M (1974) **Journ. App. Cryst.**, 7, 519-525.

HARBEN, P.W (1992) The Industrial Minerals HandyBook. Metal Bulletin PLC, London.

LOSANTOS, M; et al.(1989). Mapa Geológic de Catalunya 1/250.000. Servei Geologic de Catalunya.

Mc VEY H. & HARBEN P. (1989). Industrial minerals in paper. **Industrial Minerals**, dec. pp.41-49.

MEY, P.H.W; et al.(1969).**Leid. Geol. Med.,**V..41, pp.221-228.

MUÑOZ,J.A; et al. (1986).**Journ. Struct. Geol.**, 8, 399-405.

ORTI,F (1982). **Sciences de la Terre,** 25, 2, 179-199.

SALVANY, J.M (1990) Introducción a las evaporitas triásicas de las cadenas periféricas de la Cuenca del Ebro. In ORTI, F. y SALVANY, J.M , Edits. (1990) "Formaciones evaporíticas de la Cuenca del Ebro y cadenas periféricas y de la zona de Levante". Enresa- GPPG. Barcelona, 1990.

WARSHAW, C. AND ROY, R. (1961) **Geol.Soc. Amer. Bull.** 72, 1455-1492.

Current Research in Geology Applied to Ore Gervilla.Fenoll Hach-Alí, Torres-Ruiz & Gervilla(eds)(1993).ISBN 84-338-1772-8

ISOTOPIC STUDY OF THE DIAGENETIC AND HYDROTHERMAL ORIGINS OF THE BENTONITE DEPOSITS AT LOS ESCULLOS (ALMERIA, SPAIN)

Delgado, A. & Reyes, E.
Estación Experimental del Zaidín, C.S.I.C., Granada, Spain.

ABSTRACT: The isotopic study of carbonates and clays from the Los Escullos zone (Almería, Spain) reveals the meteoric origin of the carbonates distributed between the bentonite and the filling of the fissures (-3.7‰>δ^{18}O>-6.4‰; -8.3‰>δ^{13}C>-13.1‰). The marine carbonates must have been deposited in water up to 60°C. (δ^{13}C ≈ 0‰; -2.3‰>δ^{18}O>-8.7‰). Bentonitization would have occurred at temperatures between 70 and 90°C (+10‰<δ^{13}C<+19‰). δ^{2}H values show that postdepositional isotopic exchange took place between the hydrogen of the $(OH)^-$ in the clays and meteoric water.

INTRODUCTION

The aim of this paper is to determine the type of water and temperatures involved in the bentonitization of the pyroclastic materials at Los Escullos (Almería, Spain). We therefore studied the isotopic composition of the mineral phases created throughout the diagenetic and/or hydrothermal history of the area. The original tuff with abundant pumice fragments and marine carbonate intercalations had a high diagenetic potential due to the high porosity and high glass content in the tuff, and because the carbonate intercalations are bioclastic calcarenites mainly consisting of aragonite and Mg-rich calcite. Alteration must therefore have begun in a marine environment with high geothermal gradients, typical of an active volcanic zone in which dome intrusion had been frequent. After emersion, the zone would have been affected by meteoric water and alteration processes would have continued, causing new mineral phases in equilibrium with the new conditions.

An interesting aspect of the geochemical evolution of these materials, and the subject of debate, is the susceptibility of the clay minerals to isotopic exchanges of hydrogen, occurring in different temperature conditions and water of different isotopic composition to those present during genesis (Lawrence & Taylor, 1972; Wilson et al, 1987; Longstaffe & Ayalón, 1990, etc.). In the case studied here, the porosity and high specific surfaces of the smectites may have encouraged isotopic exchanges of the hydrogen with the meteoric water affecting these materials over the past 2-3 Ma.

GEOLOGICAL BACKGROUND

The materials are located in the volcanic region of Cabo de Gata (Almería, SE Spain). This is a calc-alkaline volcanism aging from 15 to 7.5 Ma (Bellón et al., 1983; Di Battistini et al., 1987). The predominant type of structure is dome fields of andesite-dacite composition, that form clearly distinguishable volcano-stratigraphic units. Pyroclastic episodes composed of rhyolite and dacite are abundant (Fernández Soler, 1992).

A pyroclastic unit outcrops in the vicinity of Los Escullos, which is several km^2 in size and varies in depth up to over 70 m. These materials, which are mainly made up of pumice fragments, occasionally present marine carbonate intercalations several metres thick. The pyroclastic materials are of hydromagmatic origin with facies characteristic of base surge and co-surge falls (Fernández Soler, 1992). A dacite dome intrudes these materials and at present outcrops as a small hill 181 m high, known as the Morrón de Mateo. Abundant bentonitised zones are found around the dome, which was dated by Di Battistini et al. (1987) as 10,8 Ma. Quartz and/or cristobalite fillings in fissures are frequently found, whose isotopic composition clearly indicates a hydrothermal origin (Delgado et al., 1992).

One of the most highly bentonitised zones in the Los Escullos area is located beside the Morrón de Mateo and is at present commercially exploited. The bentonite

has smectite contents of normally over 70%, and variable quantities of plagioclase, K-feldspar, quartz and amphiboles. Zeolites, cristobalite and tridymite are also present as secondary minerals (Caballero, 1985; Linares et al., 1993). The smectites are mainly dioctahedral with an average structural formula: $[Si_{7.61}Al_{0.39}][Al_{2.57}Fe_{0.51}Mg_{1.10}]X_{0.91}O_{20}(OH)_4$ that locates them in the field of montmorillonites (Linares et al., 1993).

ANALYTICAL METHODS

The isotopic determinations were carried out in the Geochemical Isotopic Laboratory in the Estación Experimental del Zaidín (C.S.I.C., Granada). Oxygen was extracted from the clay minerals by leaching with ClF_3, following a method similar to that described by Borthwick & Harmon (1982). Hydrogen was extracted by heating 15 g of sample (previously desiccated at 200°C) at 1000°C in a quartz tube. The water extracted was used to determine the δ^2H following the method of Coleman et al., (1982). The McCrea (1950) method was used for analysis of the carbonate samples. The isotopic ratios were determined using a Finnigan Mat 251 mass spectrometer. Experimental error for $\delta^{13}C$ and $\delta^{18}O$ was lower than 0.05‰ in carbonates and lower than 0.2‰ in silicates. The experimental error for δ^2H was lower than 4‰.

RESULTS

56 carbonate samples were analysed, 24 of which belong to the Tortonian calcarenites intercalated in the pyroclastic materials at Los Escullos. The others were calcites located in fissures or disseminated through the bentonite. The marine carbonates showed higher dispersion in $\delta^{18}O$ values (-2.68‰ to -8.69‰) than in $\delta^{13}C$ values (around 0‰ with a maximum +1.01‰ and a minimum -1.56‰). The disseminated carbonates together with those filling the fissures showed more negative $\delta^{13}C$ values, varying from -13.07‰ to -8.26‰, and, unlike the marine carbonates, showed closer grouping of $\delta^{18}O$ values (-3.65‰ to -6.37‰). The isotopic data are represented graphically in Fig. 1.

The < 2 μm fractions of Morrón de Mateo bentonites were also analysed. 49 samples presenting over 95% smectite were chosen for isotopic analysis. The isotopic ratios of H were also analysed in eight sample from the same site. The $\delta^{18}O$ values are shown as frequency histograms in Fig. 1 B, where it can be seen that over 30 samples are located in the +16‰ - +18‰ interval. The δ^2H values of the samples analysed are between -90‰ and -70‰.

DISCUSSION

The isotopic data ($\delta^{13}C$, $\delta^{18}O$) of the marine carbonates indicate that isotopic changes occurred in oxygen in comparison to typical seawater values. This shift to more negative values may have been due to both processes of meteoric diagenesis and the action of seawater at higher than environmental temperatures, possibly up to 60°C (Fig. 1A). The action of light meteoric water can be discounted, since the carbon isotope values of around 0‰ are typical of marine environments and are very dissimilar to those of the carbonates precipitated in meteoric environments, with values around -12‰ (Cerling, 1984). On the other hand, the carbonates disseminated in the bentonitised materials show both carbon and oxygen values typical of meteoric carbonates. The carbon values (-8‰ to -13‰) indicate an important pedogenic component, with clear influence of carbon from the decomposition of C_3 plants. The $\delta^{18}O$ values are grouped round the meteoric calcite line (MCL) of the region (calcite precipitated at 20°C in equilibrium with water whose $\delta^{18}O_{(SMOW)}$ = -4‰).

The smectites present values that clearly indicate a low temperature (<100°C) hydrothermal origin. Even considering the action of meteoric water, the lowest acceptable temperature would be 35°C (Fig. 1C). However, the presence of later marine materials, deposited on the tops of the volcanic structures 200 m above the materials examined, together with the evidence of processes of diagenesis and/or hydrothermalism with the seawater mentioned above, seems to indicate that alteration began with this water and temperatures between 70 and 90°C. These values

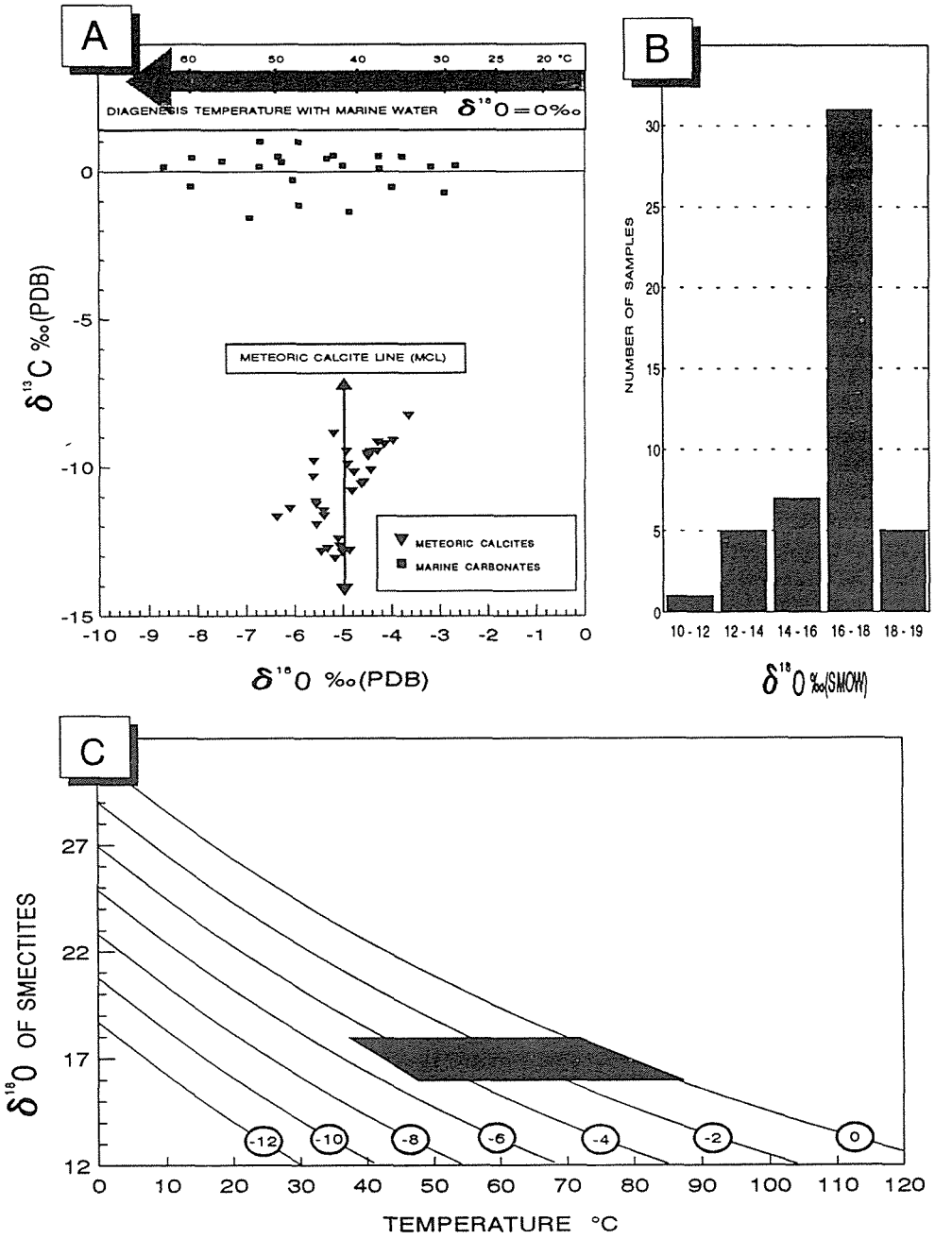

Fig. 1. A: Isotopic composition of marine and meteoric carbonates. Temperatures were calculated using the Anderson & Arthur (1983) equation. B: Histogram of the frequency distribution of the isotopic composition of oxygen in the smectites studied. C: The curves represent the theoretical isotopic composition of smectites in equilibrium with water whose $\delta^{18}O_{(SMOW)}$ is indicated in the corresponding circles. The Savin & Lee (1988) equation was used for calculation. The shaded area represents the most common smectite compositions.

are relatively coincident with the temperatures affecting the diagenesis of the calcarenites intercalated between the pyroclastic materials in the zone (Fig. 1A,C). Therefore, the low, disperse δ^2H values may be due to isotopic exchange of hydrogen with meteoric water at environmental temperature occurring simultaneously with deposition of the meteoric calcites filling the fissures or disseminated throughout the bentonite (Fig. 1A). This agrees with the theoretical calculations of Kyser & Kerrich (1992), which indicate that the <2μm fraction of clayey materials can exchange hydrogen isotopes at 25°C in under 2 Ma. If this hypothesis were confirmed, the case studied here would provide one of the best natural examples of hydrogen isotope exchange in relatively short periods.

ACKNOWLEDGMENTS

The authors wish to thank Minas de Gádor for their help in sampling the sites.

REFERENCES

Anderson, T.F. & Arthur, M.A. 1983. Stable isotopes of oxygen and carbon and their application to sedimentologic and palaeoenviromental problems. In Stable Isotopes in Sedimentary Geology (eds M.A. Arthur et al.). I:1-151. Society of Economic Palaeontologists and Mineralogists Short Course nº 10.

Bellon, H., Bordet, P. & Montenat, C. 1983. Choronlogie du magmatisme néogene des Cordillères Bétiques (espane meridionale). Bull.Soc.Geol. France. 25:205-217.

Borthwick, J. & Harmon, R.S. 1982. A note regarding ClF_3 as an alternative to BrF_5 for oxygen isotope analysis. Geoquim. Cosmochim. Acta. 27:43-52.

Caballero, E. (1985). Quimismo del proceso de bentonitización en la región volcánica de Cabo de Gata (Almeria). Ph.D. diss. Univ. Granada. pp. 328.

Cerling, T.E. 1984. The stable isotopic composition of modern soil carbonate and its relationship to clime. Earth Pla. Sci. Letters. 71:229-240.

Coleman, M.L., Shepherd, T,J., Durham, J.J., Rouse, J.E. & Moore, G.R. 1982. Reduction of water with zinc for hydrogen isotope determination. Anal. Chem. 54:993-995.

Delgado, A., Nuñez, R. & Reyes, E. 1992. Composición isotópica de polimorfos de sílice hidrotermal en la región volcánica de Cabo de Gata (Almeria). Bol. Soc. Esp. Min. 15-1:161-165.

Di Battistini, G., Toscani, L., Iacarino, S. & Villa, I.M. 1987. K/Ar ages and the geological setting of cal-alcaline volcanic rocks from Sierra de Gata, SE Spain. N. Jb. Miner. Mh. H8:337-383.

Fernandez Soler, J.M. 1987. Análisis e interpretación de los materiales volcánicos del Cerro de Los Frailes (Cabo de Gata, Almería). Estud. Geol. 43:359-366.

Fernandez Soler, J.M. 1992. El volcanismo calco-alcalino de Cabo de Gata (Almeria). Ph.D. dissertation, Universidad de Granada. pp. 243.

Kyser, T.K. & Kerrich, R. 1991. Retrograde exchange of hydrogen isotopes between hydrous minerals and water at low temperatures. In: Stable Isotope Geochemistry: A Tribute to Samuel Esptein. The Geochemical Society, Special Publication. 3:409-422.

Lawrence, J.R. & Taylor, H.P., Jr. 1972. Hydrogen and oxygen isotope systematics in weathering profiles. Geoquim. Cosmochim. Acta. 35:1377-1393.

Linares,J., Huertas,F., Reyes,E., Caballero,E., Barahona,E., Guardiola,J.L., Yañez,J., Romero,E. & Delgado,A. (1993) Investigaciones de bentonitas como material de sellado para almacenamiento de residuos radiactivos de alta actividad. Edit. ENRESA. pp. 324.

Longstaffe, F.J. & Ayalon, A. 1990. Hydrogen-isotope geochemistry of diagenetic clay minerals from Cretaceuos sandstones, Alberta, Canada: evidence for exchange. 1990. Applied Geochemistry. 5:657-668.

McCrea, J.M. (1950) On the isotopic chemistry of carbonates and a paleotemperature scale. J. Chem. Phys. 18:849-857.

Savin, S.M. & Lee, M. 1988. Isotopic Studies of phyllosilicates. In "Hydrous phyllosilicates (exclusive of micas)". (Bailey, S.W. Ed.). Rev. in Min. of Min. Soc. Amer. 19:189-223.

Wilson M.R., Kyser, T.K., Mehnert, H.H. & Hoeve, J. 1987. Changes in the H-O-Ar isotope composition of clays during retrograde alteration. Geoquim. Cosmochim. Acta. 51:869-878.

Current Research in Geology Applied to Ore Gervilla.Fenoll Hach-Alí, Torres-Ruiz & Gervilla(eds)(1993).ISBN 84-338-1772-8

GENETIC LINKS BETWEEN ALBITE AND CHLORITE-TALC MINERALIZATIONS IN CENTRAL SARDINIA, ITALY

Garbarino, C. (1); Fiori, M. (2); Grillo, S.M. (1); Marcello, A. (1); Marini, C. (3); Pretti, S. (1)
(1) Ist. Giacimenti Minerali, Cagliari, Italy
(2) Centro Studi Geominerari e Mineralurgici del CNR, Cagliari, Italy
(3) Dip.to Scienze della Terra, Universita' di Cagliari, Italy

Abstract
The discovery of economically important albitite deposits near the already known talc-chlorite deposits in Central Sardinia (Italy) reopened the debate about the genesis of these deposits.The Na-metasomatism and the Mg-metasomatism which originated the two deposit types appear spatially related,with a W-E flow direction of the fluids.It is likely that the Na-replacement in Mg-bearing rocks generated the Mg front responsible for the chlorite-talc formation.

Foreword
In the region of Barbagia (Central Sardinia,Italy) talc and chlorite occurrences are long known and exploited. More recently, important albitite deposits of ceramic grade have been discovered and are now actively exploited. This last discovery reopened the debate about the genesis of the deposits (Massoli Novelli,1971; Uras,1973). The genetic problem is not merely speculative, since it has important implications for industrial research.

Geological setting
The main rocks of Central Sardinia are the Hercynian granites, locally covered by pre-Carboniferous Palaeozoic roof-pendants.
In the examined area these roof-pendants extend for some 25 km by 12 km, the main axis being directed NE-SW, parallel to an important regional structure, active during the Hercynian orogeny and reactivated during the Alpine cycle (Fig.1). The granitoid rocks are mostly granodiorites, monzogranites and tonalites. The metamorphic rocks include mainly terms of terrigenous origin, with locally interbedded carbonatic lenses. The metamorphic facies derive from an overlapping of contact and regional metamorphism.

The ore bodies
They may occur both in intergranitic position and at the granitoids-metamorphics contact.
In the first position only albitite bodies occur, predominantly along NE-SW structures. Albitites are also present along the contacts, associated with the chlorite-talc bodies, which only occur in this position. Also in the latter, the ore bodies are mostly elongated NE-SW.
The size of the bodies of economic interest ranges from a few tens of metres in length by a few metres in width for the talc-chlorite bodies to about ten times more for many albitite bodies.

The mineralizations
The albitite mineralization derives from Na-metasomatism of both granitoid and metamorphic rocks. Albitization typically gives a rock composed of albite (up to 11% Na2O) and quartz. Locally, minerals such as chlorite and epidote also occur. Relics of the protolith are sometimes represented by plagioclases (granitoids) and muscovite (metamorphics). Immobile element minerals, such as zircon and rutile, are also commonly present. All the degrees of metasomatic transformation are often visible (Fig. 2). Also the texture of the original rock is often well recognizable. Microscopically, the metasomatic albite may display ches-

sboard twinning, plagioclase relics in the newly formed individuals and phantoms of the polysynthetic twinning. Besides the original untouched individuals, the quartz may form epigenetic veinlets.

The chlorite-talc mineralization clearly follows the albitization. The Mg-metasomatism affects all the pre-existing lithologies, i.e. granitoids, albitites and metamorphics.

The species by far most abundant are the Mg-chlorites (clinochlore) followed by talc and Ca-Mg silicates such as diopside, tremolite, epidote, vesuvianite and garnets.

Another mineral very abundant in the massive chloritic bodies is quartz, which commonly occurs as lenses and thick veins of big, milky crystals. Microscopically, the metasomatism appears massive, with total destruction of the pre-existing minerals. Only Ti minerals, such as rutile and titanite, survive. At the electron microprobe the transformation biotite-chlorite-talc has been cleary observed (Fig.3).

Discussion

On observing the location of the known occurrences in Fig.1, the following characteristics are evident. The bodies in which only albitite is present (with local, very slight chloritization) also occur west of the map.

The occurrences inside the dotted line are characterized by important occurrences of both Na- and Mg-metasomatism, while outside that line the Mg-minerals predominate.

Thus it appears that, in addition to the already mentioned temporal sequence (Na-metasomatism earlier than Mg-metasomatism), a spatial array also exists, with the Mg-minerals increasing from W to E, apparently in relation with the main NE-SW regional structures.

This seems to indicate that the flow of the metasomatizing fluids had a horizontal component directed W-E,i.e.from the granitic core to the metamorphic cover.

These fluids were initially charged with Na and the physico-chemical conditions were favourable to albitization (Bornioli et al., in preparation).

This phenomenon achieved huge proportions, as is evident from the number and size of the albitite bodies, from the granitic core to the metamorphics, with several millions of tons of already measured ore grade reserves.

The albitization displaced several metals, in particular K, Ca and Mg. While the first metal did not apparently reprecipitate, at least in significant quantities, the other two, particularly Mg, gradually reached sufficient activity to metasomatize both the already formed albitites and the metamorphics. In fact, no other source of Mg is available for the formation of Mg-silicates, since the absence of mafic rocks is total and the mean Mg content of the carbonatic metasediments low, quite similar to that of the terrigenous metasediments (an estimate on a group of samples of metamorphic rocks gave a mean content of about 1,5% MgO).

It is not impossible that small lenses of silica- and magnesium-rich carbonatic rock occurred, since the bodies of Ca-Mg-silicates (inosilicates and epidotes) are likely to derive from such rocks, but the largest carbonatic bodies suffered normal skarn transformation (with predominantly Ca-garnets and vesuvianite). In turn the Ca-Mg-silicate bodies sometimes suffered a further transformation in talc and calcite. Another possibility of talc formation is given by the reaction of Mg-rich fluids with the excess of silica in the chlorite bodies, deriving both from the original quartz present in the albitites and micaschists and from the silica released by the chlorite formation (Moine et al.,1982).

The envisaged hypothesis on the origin of the Mg is quite acceptable. In fact, if a figure of about 6 million tons of total Mg-silicates (deriving from the production data of the talc and chlorite mines) is fixed, since the mean MgO content in talc and chlorites is about 30%, the albitization of some 120 million tons of preexisting rocks would supply the necessary Mg,if it werecompletely utilized in the metasomatic reactions. Obviously, since the "efficiency" of the real phenomenon is not 100%, an additive quantity of albitizing,Mg-

releasing rocks is necessary. The abundance of albitites, both the numerous large bodies of economic interest and the innumerable low-grade and minor bodies, can easily satisfy the required tonnage.

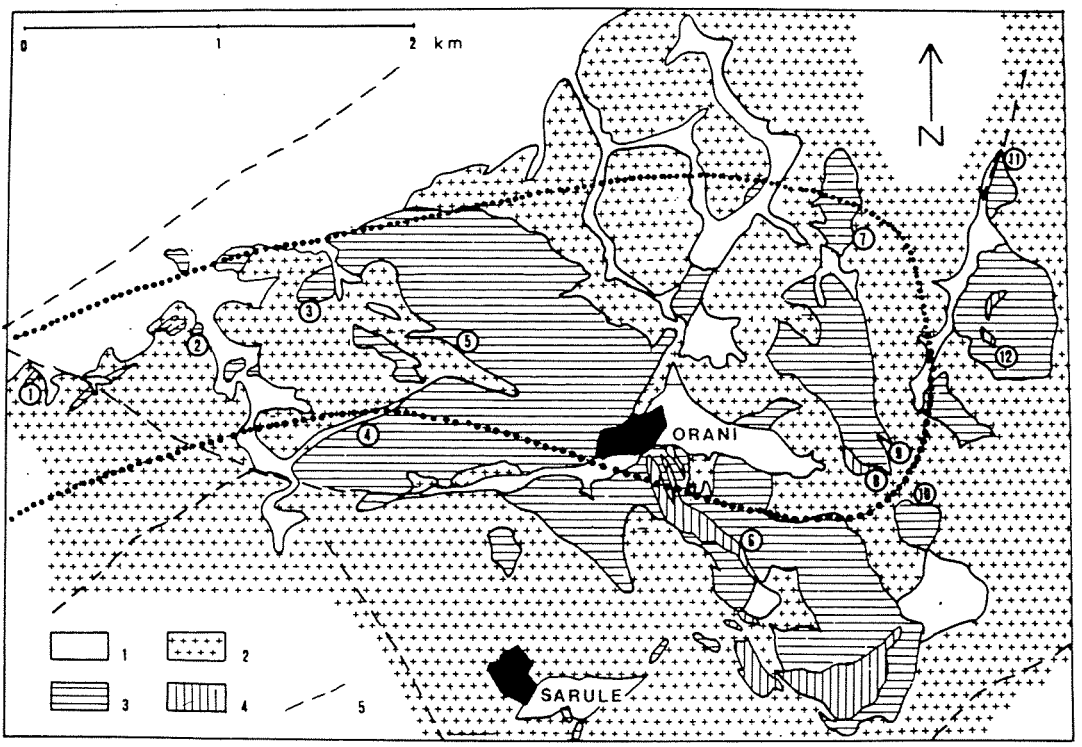

Fig.1 Geological sketch map,with the main indications and mining sites. The only albitite (Ab) domain lies just left (W) of the represented area.The dotted line separates the domain of contemporaneous Na- and Mg-silicate occurrences (inside) from that of predominantly chlorite-talc (Chl,Ta) occurrences outside.
Geology: 1-Tertiary volcanics and sediments, Quaternary covers; 2-Carboniferous granitoids; 3-Pregranitic metamorphics, mostly of terrigenous origin; 4-Mappable metalimestone lenses; 5-Main faults.
Sites: 1-Istiarvu (Ab, Chl, Ta); 2-Monte Nule (Ab,Chl); 3-Ispaduleddas (Ab, Chl); 4-Sa Matta (Chl,Ta); 5-Predas Biancas (Ab,Chl,Ta); 6-San Francesco (Chl,Ta,Ab); 7-Lasasai-Bonucoro (Ab,Chl); 8-Istellaeddu (Ab,Chl); 9-Istellai (Ab,Chl); 10-Monte Berchialo' (Chl,Ab);11-Spirito Santo (Chl);12-San Sebastiano (Chl).

Fig.2 Monte Nule: Albitization front on micaschist. Relics (darker grey around the hammer) and textural phantoms of the protolith are well recognizable in the albitite (various shades of grey). The white veins are of pure (hydrothermal) albite.

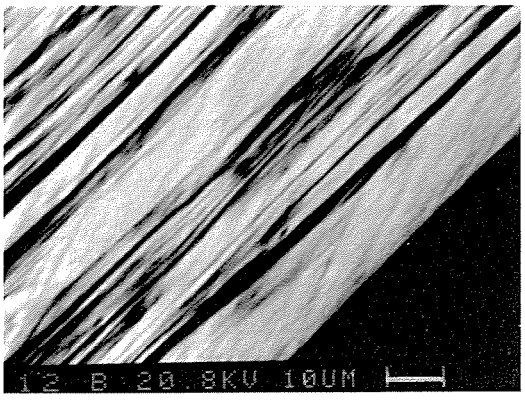

Fig. 3. BSE image of chlorite lamellae (light grey) with talc forming along cleavage planes (dark grey).

Acknowledgments
Study supported by the contribution of "Centro Studi Geominerari e Mineralurgici del CNR", Piazza D'Armi, Cagliari, Italy

References

Bornioli R., Fadda S., Fiori M., Grillo S.M., Marini C. 1993. Genetic aspects of albitite deposits from Central Sardinia:mineralogical and geochemical evidences.(in preparat).

Massoli Novelli R. 1971. Contributo allo studio genetico del talco di Orani (Nuoro). A.M.S.2,9-39.

Moine B., Gavoille B. & Thiebaut J. 1982.Geochimie des transformations metasomatiques a l'origine du gisement de talc et chlorite de Trimouns (Luzenac, Ari?ge, France). I - Mobilite des elements et zonalites. Bull. Mineral., 105, 62-75.

Uras I. 1973. Guida per l'escursione ai giacimenti di talco di Orani. In E.M.Sa. ed. "Itinerari geologici, mineralogici e giacimentologici in Sardegna". 63-72.

Current Research in Geology Applied to Ore Gervilla.Fenoll Hach-Alí, Torres-Ruiz & Gervilla(eds)(1993).ISBN 84-338-1772-8

GEOCHEMISTRY AND MINERALOGENESIS OF THE BARITE DEPOSITS IN SOUTHWESTERN SPAIN

Hernández, M.J. & Miras, A.
Dept. de Cristalografía, Mineralogía y Química Agrícola. Universidad de Sevilla. Sevilla, Spain

ABSTRACT: Mineralogical and chemical characterization of barite deposits at the SW of Spain has been carried out. Four different mineralization types have been determined by field and geological criteria. $^{87}Sr/^{86}Sr$ and geochemical data suggest different origins and sources of Ba for each barite deposits.

Introduction

The Ossa Morena Zone, at the South of the Iberian Massif, abounds with barite occurrences and deposits which have been given little attention in terms of geochemical and minerallogenetic research and traditionally were considered vein. However, besides the barite veins associated with the occurrence of igneous rocks, field observation reveals numerous stratiform outcrops together with recrystallizations and other epigenetic features hosted within Precambrian to Upper Carboniferous materials.

This set of barite mineralizations offers an economical potential of great importance, since it contains the largest amounts of barite in the Iberian Peninsula, its estimated reserves being over 700,000 ton.

Geological Setting

The Ossa Morena Zone, the most complex segment of the Iberian Massif, constitutes the general setting where the mineralizations occur; due to its complexity, it has been divided in different tecto-sedimentary «domains». The barites studied occur mainly in the Zafra-Alanís-Córdoba domain and within the Villaviciosa de Córdoba-La Coronada magmatic belt (fig. 1).

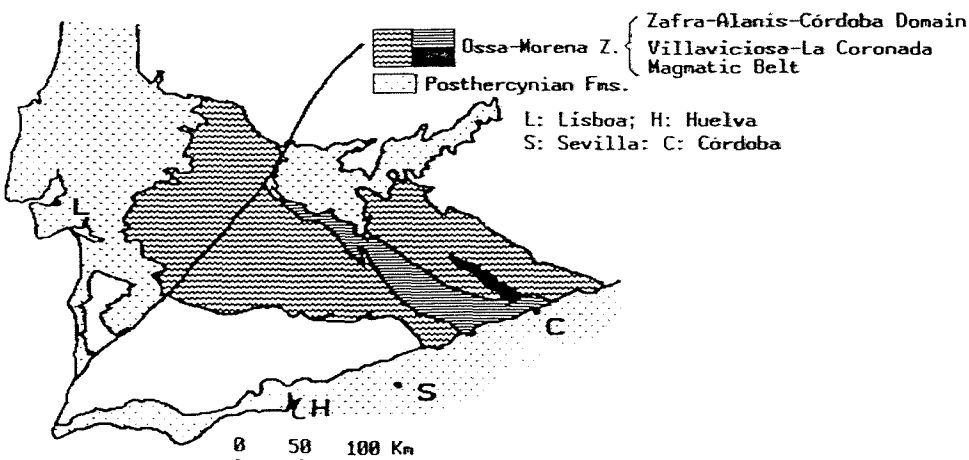

Fig. 1.- General geologic outline of the SW of the Iberian Massif.

This domain shows at its base a thick upper Proterozoic vulcano-sedimentary set, which supports unconformable detrital, carbonate, and vulcano-sedimentary Lower and Middle Cambrian materials.

The Villaviciosa de Córdoba-La Coronada magmatic belt (Middle Tournaisien to Upper Westfalian) consists of volcanic and plutonic rocks of a varied nature, the most abundant being diverse granites generally shallow seated and showing alcaline tendency, granofidic texture with scarce mafics and Fl and Ba mineralizations.

Features of the mineralizations

The following types have been observed:

a) Stratiform mineralizations, composed by massive and laminar barite, their most significant impurities being quartz and phyllosilicates (illite). They are associated to vulcanosedimentary Upper Proterozoic materials and to Lower Cambrian shale-carbonate formations. These have the highest economical potential, since some layers reach over 10 km and are up to 3 m thick.

b) Karstic mineralizations; these are barites within ferruginous mud filling karstic cavities in Cambrian limestones, associated to Fe- oxy·hydroxids, quartz, phyllosilicates (illite) and carbonates (siderite, calcite and ankerite); short amounts of Fe and Cu sulphurs are also present.

c) Vein mineralizations associated to Upper Carboniferous igneous rocks; they are formed by many subvertical veins of a diverse entity, related to the fracturing systems developed along the late period of the Hercynian evolution (N70°-80°E & N45°-55°E). In spite of the different host-rocks, these veins are always associated to granitic rocks of an alkaline tendency. Quartz and fluorite, often below 10 %, are the most frequent impurities, plus a low content of Fe and Cu oxydes and sulphurs, and carbonates.

d) Vein barite deposits related to Posthercynian fractures (N170°-190°E & N120°-130°E). Undeformed barite is associated to quartz and less to Fe, Cu and Pb sulphurs and carbonates.

Geochemistry of barites and associated rocks

161 barite and 77 host rock samples were analyzed, from the most representative types and deposits in each of the areas studied.

Mineralizations are rather pure in general, especially the vein barite occurrences associated to igneous rocks, where SO_4 (Ba,Sr) rates up to 97-98 % are found.

Silica is the most abundant impurity for the whole area ($\bar{x}$=6%), linked to the intense silicification affecting all the deposits studied. Ca may be found in a significant proportion, but only in the case of some stratiform barites associated to carbonate rocks, or due to the fluorite present in some veins. In any case, the low rate of impurities make these barites highly interesting from an industrial point of view.

The average SrO contents are close to 1%, but a general tendency is observed towards lower contents of strontium in vein than in stratiform barites, and in the latter than in karstic barites, which indicates low temperatures in the formation of vein mineralizations.

Among the other elements analyzed, a low presence of metals must be pointed out.

A principal-component factor analysis showed the geochemical relationships among the different elements (fig. 2). The first component shows an inverse relationship between sulphate and silica, and a positive correlation between silica and Al, Fe and Cr contents.

The second component shows two different populations. One with a larger Sr content associated with the pair Pb-Cu, corresponding to stratiform and karstic deposits, versus one richer in Ca and Cl related to the vein barites associated to igneous rocks. The inverse relationship between Sr and Cl shows that the highest amount of Sr included in barite occurs with a decrease of salt content in the solutions.

About the host rocks, a large content of Ba is seen in almost all rocks from that area, which may indicate a general positive anomaly for this element (Fisher & Puchet, 1972). It is remarkable that in general there is no increase of Ba near the mineralizations. This fact, plus the presence of primary barite in some igneous rocks in the Villaviciosa-La Coronada magmatic belt, are criteria to be considered when establishing a genetic hypothesis.

The Sr content stays within the regular limits for igneous rocks, but its proportion increases largely in carbonate rocks; this fact, together with the presence of barite in a scattered phase, shows that these rocks carry mineralizing elements.

Fig. 3 shows the isotopic ratios $^{87}Sr/^{86}Sr$ versus 1/Sr of 42 significant samples from the different barite deposits studied. First of all, the heterogeneous set of values obtained (0.70873-0.71394) must be pointed out, which shows that this Sr, and consequently the Ba, may not come from the same source, but rather various mineralizing fluids with different isotopic ratios may be involved.

The homogeneous isotopic ratio of vein Posthercynian barites is significant (0.7104), opposed to the other mineralizations.

Most of the results obtained stay within the established limits for the values of continental and sea barite (Goldberg et al., 1969) which supports the idea of diverse origins.

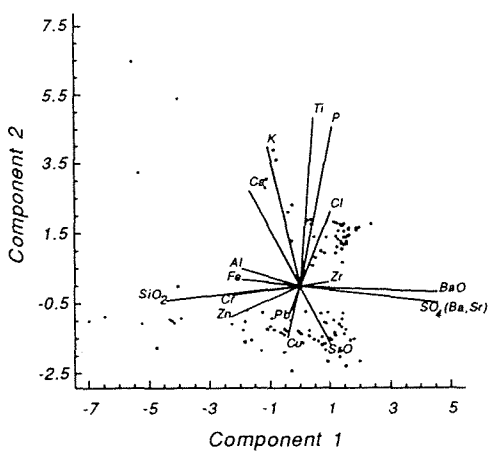

Fig. 2.- Plot of principal component of barite composition in the SW of the Iberian Massif.

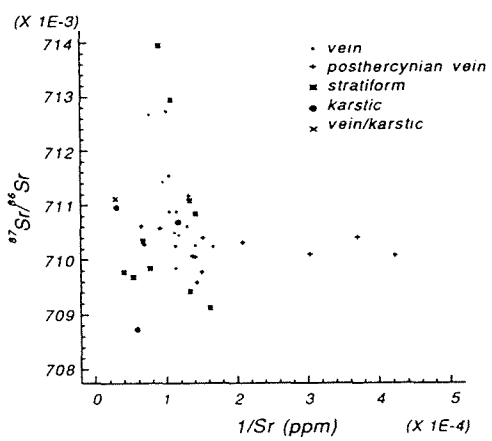

Fig. 3.- $^{87}Sr/^{86}Sr$ vs. 1/Sr plot, also showing the various types of barite.

Conclusions

Firstly, the barium content in the central part of the Ossa-Morena Zone is anomalously high from a geochemical point of view, as found in a number of barite mineralizations and deposits of various types.

On the other hand, field relationships and geochemical and isotopic data reveal various origins and different sources for the Ba, depending on the types of the deposits studied.

The barite veins associated to igneous rocks can be considered low temperature veins to which Ba and Sr are provided by the granitoids where mineralizations are hosted, forming the lithologic *"mineralotecte"* that controls their presence.

A primary vulcanosedimentary and/or diagenetic origin can be established for the stratiform mineralizations, as shown by textural relationships and the Sr isotopic content.

As for the other cases, they may have been formed by recrystallization from previous mineralizations and from the leaching out of host rocks.

Bibliography

Fischer, K. & Puchelt, H. 1972. Barium. In: K.H. Wedepohl (ed). Handbook of Geochemistry, 56, Springer Verlag., Heidelberg, 100 pp.

Goldberg, E.D.; Somayajulu, B.L.K.; Galloway, J.; Kaplan, I.R. & Faure, G. 1969. Differences between barites of marine and continental origins. Geochimica et Cosmochimica Acta, 33:287-289.

Current Research in Geology Applied to Ore Gervilla.Fenoll Hach-Alí, Torres-Ruiz & Gervilla(eds)(1993).ISBN 84-338-1772-8

LITHMOLOGY IS A NEW TREND IN GEOLOGY

Karogodin, Yu.
Inst. of Geology, Geophysics and Mineralogy, University pr.3 630090 Novosibirsk-90 Russia

Abstract. Lithmology is a new integrating science of geology, which continues the hierarchical sequence: mineralogy-lithology-lithmology.The object and subject of this trend are the rocky associations, integral in time and their structure, substance,process and genesis, respectively.

The author formulated principles and rules to distinguish bodies - structures on the super-rocky level of their organization and has developed their classification and hierarchical model of lithmosphere. This new trend permits to improve regional, basin stratigraphic schemes, providing more accurate determination of structural sequences and different reconstructions (paleotectonic, paleogeodynamic,lithologo-paleogeographic,paleogeomorphologic, etc).In its turn, these sequences permit to reveal regular placements and the formation conditions of a great variety of deposits and pools, different ores,gold,bauxites,oil,gas,building materials, etc. It is just the well-grounded way for the fossil prediction and the optimization of the prospecting works.

Lithmology is a new integrating science of geology. The final aim of this new science is to develop and formulate the laws of organization and origin of layer associations.

The formulation of the evolution laws of objects of any nature (living or not living) needs the investigation of the integrating objects - systems.Thus, the system approach is the methodological basis of lithmology. Layer associations are first considered as the integrating systems. Their integrating property (system-forming) is involved in the connection (sequence) of its elements (layers) through the time. In contrast to other types of layer associations,which connection is not considered as the most important phenomenon, the above mentioned layer associations were called cyclites, parachronolites. Thus, cyclites are the layer bodies - systems, integrating in time and space and testifying the resulting substance of sedimentary cyclites.

Such principle to set off the rocky bodies - systems can be extended to sedimentary - effusive, effusive - metamorphic thickness. They can be called endocyclites, while the trend - endolithmology.

Lithmology didn't appear on the blank space. Its close parents were sedimentary cyclicity ("mother") and the formation analysis ("father"), according to N.S. Shatsky, N.P. Charaskov, B.E.Chain A.L. Yanshin et al.,; its precusors were the lithology (the first half of XX century), sedimentology (the second half of XIX century) and stratigraphy (XYII century of its origin). The origin and the development of geological sciences exhibit quite obvious regularities: from the investigation and the development of sciences on the most obvious objects (crystals,minerals) towards the most scaled, large bodies on rocky and super-rocky levels. Thus, this hierarchical sequence: mineralogy - lithology - lithmology is quite logical and regular. Principles of subordination (and coordination) are the most important in such system approach.

Different approaches and principles can be used to set off cyclites as layer systems, integral in time in the outcrops' sections, mines, wells and quarries. The author has used the structure - substance approach and the following four rules:the direc - tionality and permanency of the change of the main property from the element (layer) to the element (layer), the body structure between elements and the binary structure of the body (system). The last property is characteristic of all integrating systems and is recognizable on any signs.

Basing on these formal rules, elementary layer systems - cyclites can be distinguished within any layer section.

Layers and cyclites are not spatially divided within the section, thus, the problem of their borders extisted and still existed.To solve this problem one should reveal the connection intensity between the elements, which will be more intensive within the system, than on the systems' border. The mentioned four rules and some additional approaches serve to reveal the connection intensity between elements (layers) of the system. This connection can be expressed as quantitatively so qualitatively.

There is an infinitive number of lithologic combinations of the rocky layers in nature. Thus, their classification is very im - portant. To classify these combinations it was used the sign of the directionality of change of the main structure - substance

property of the layer system. According to such directionality all cyclites can be comprized into two groups: A - single-directed and B - differently-directed changes of the main property from layer to layer towards the top of the section. Each group comprises two types of cyclites: one type with the direct "progressive" orientation and the other one - with the reverse "regressive" orientation. Cyclites are called progressive and regressive, respectively. The second group also involves two types of the cyclite structure : the first one with the progressive-regressive and the second - with regressive-progressive orientation of the change of the main property. They are called progressive-regressive and regressive-progressive types of cyclites, respectively. This classification permits not only the information to be expressed compactly, but to decipher the hierarchical organization of the layer associations.

Using some approaches and coefficients, developed on the given classification it was revealed quite valid hierarchical organization of Vend-Phanerozoic part of the sedimentary cover of the Earth: elementary cyclites (two and more layers) zonal (and subzonal) regional (8 - 10 million yrs $\pm$ 2) nexocyclites (contain not less than 9 regocyclites) galcyclites (two nexocyclites) trigalcyclite (three galcyclites).

This approach and the given model of the hierarchical sequence of organization of the sedimentary cover of the Earth (lithmos - phere) provide new development of regional, basin stratigraphic and planetary schemes. The system-lithmologic approach provides different degree of the detailed revealing and correlation of sedimentary thickness of different genesis and age, including the ancient thicknessess, lacking faunas, continental ones, ashes, etc.

The stratigraphy, based on the given scheme provides more accurate determination of geological body structure and permits to realize different reconstructions (paleotectonic, lithologo -paleogeographic, paleogeomorphologic, etc). It is the direct way to decipher regular placements and the formation coefficient of different fossils (iron ore, gold, bauxites, phosphorites, oil, gas, salts, building materials, etc).

New trends, such as an engineering lithmology (Ya.E. Shaevitch

and others), coal lithmology (T.A. Yakubjanu and others), seismo-lithmology, lithmostratigraphy and many others have been recently developed.

Lithmology is a new trend in geology, it is deeply rooted in the past and opens new horizonts in the cognition of the Earth evolution. It provides more complete understanding of regular placements and of the formation conditions of a great variety of fossils. In its turn, it is the direct way for the optimization of the prospecting works.

Current Research in Geology Applied to Ore Gervilla.Fenoll Hach-Alí, Torres-Ruiz & Gervilla(eds)(1993).ISBN 84-338-1772-8

THE GEOLOGY AND ORE DEPOSITS OF SOUTHERN ISPARTA (TURKEY)

Kumral, M. & Gedikoğlu
Süleyman Demirel Üniversitesi, Jeoloji Müh. Böl. Isparta, Turkey

ABSTRACT : In this study it is investigated the geology of Shouthern Isparta (Turkey) and the economic potantial of the region. As a result of the studies it was determined the geological and ore deposits properties of the mentioned area. The lowest the geological sequence was consist of Triassic radiolarite-chert complex. At the top of this serie Plio-Quaternary volcanics were determined. It was estimated that Toros Mauntains has covered richest economic potantial in the studied area.

This investigation aims at a reconstraction of the geology of Isparta (Türkiye) and to estimate its economic potantial. Investigatin area cover a approximately 200 km^2 area between Isparta and Ağlaşan administrative districts. In this area geological units are divided in to two groups, namely allocthonous and autochthonous. The autochthonous units we as follows in order. At the bottom, the Ispartaçay formation of Triassic age prevents. The formatio presention a highly folded structure may be divided in to three major litologies. These are layers limestone, radiolarite-cherts and massive limestones.

Over the Ispartaçay Formation lies the Cretaceous aged Davras limestones. These are locally moved massive limestone and affected by the tectonic forces in the region. Over the Davras Formation, Savköy Formation of Upper Paleocene-Lower Eocene age lies. The Formation consist of sandstone, marl and limestone layers. It was been affected by the tectonism that took place often Miocene. Over the Savköy Formation Lower Miocene İmrezi limestone. The formation was formed in a shallow marine environment subject to a transgression.

Burdugalien age Ağlaşan Formation which is above İmresi limestone Formation exhibits tin-middle of layer sandstone-marl and it has determined most extensively in investigation area. Middle-Upper Miocene Gavurdüzü Formation is the top. This formation laying comformably with Ağlaşan Formation consist of conglomeras of unconsolidated cements and polioecenic shallow marina debris.

Gölcük volcanices which appear in investigation area exist of this units cut-down and consist of mainly tufa-tuffite type of volcanic ash, Andesite-trachi-andesite and hand tufa units. Being the product of deep Volcanism, been focus of our these volcanic rocs has the study.

Hand tufa which shows ignimbrite character setting paleogeographic, actual alluvion and drift of side exist above this units.

Allocthonous units in investigation area Isparta ophiolite complex is under and Akdağ limestones is above. The Isparta ophiolite complex, consist of serpantinized peridotites which had settled in the region after the Eocene and later deposited over the Burdugalien by a new tectonism after Miocene.

The Akdağ limestones which settle down Isparta ophiolite complex studied area is in age Jurassic-Cretaceous. These suppose the area with came tectonic of compression which finally Miocene proved to be true. Ruins of Sagalassus exist above limestones which show the feature of recristaline units explained from economic point of view in investigation area and ordered that shape units which will carred economic value.

The single economics material in the area is the trass which have been used for years in Göltaş cement plant in Isparta as a raw material. The chemical properties of the trass as follows.

The contents of $SiO_2+Al_2O_3+Fe_2O_3$ is 74-84 %, of MgO 0.27-0.76 % and of SO_3 0.00-0.30 %.

These properties are very suitable for industrial marketing and as a result of geological, geochemical and other properties it has been conceded that the material can be used productivelly for cement industry as raw material.
Except these, other economical units in the area andesite and limestones. The andesites are used in the quarries as bulding-ballast materials. They are investigated in being and having marble features. However, it can be seen that they are not suitable for large block cuttings. After laboratuary studies, the andesites are found as soft rock group.
The limestones have the widest outcroups in the area. The Akdağ Limestones has suitable marble features due to their cyristalization.That is why, they were used as the building material in the ancient period. These limestones can also be used in mosaics after breaking them in the quarries.

REFERENCES

KARAMAN, M.E., 1990, The Geology of the Southern Isparta (Turkey), Bulletin of TJK, Ankara.

KUMRAL, M., 1992, The Geology and Ore Deposits Investigation of the Southern Isparta (Turkey), Isparta.

YALÇINKAYA, S., 1986, The Geology of Isparta-Burdur (Turkey) University of Ankara Ph.D.

Current Research in Geology Applied to Ore Gervilla.Fenoll Hach-Alí, Torres-Ruiz & Gervilla(eds)(1993).ISBN 84-338-1772-8

CHARACTERIZATION OF SEPIOLITE FROM THE CERRO CANTUEÑA DEPOSIT (PARLA, MADRID): MICROSTRUCTURE AND RHEOLOGICAL PROPERTIES

Medina, J.A.(1); Santarén, J.(2); Martín Rubí, J.A.(3); Casas, J.(2); Cuevas, J.(1); Alvarez, A.(2) & Leguey, S.(1)

(1) Dept. Química Agrícola, Geología y Geoquímica, Facultad de Ciencias, Universidad Autónoma, Madrid, Spain

(2) Tolsa, S.A., Madrid, Spain

(3) ITGE, Rios Rosas 23, 28003 Madrid, Spain

Abstract: Sepiolitic materials from a sedimentary sequence have been studied in order to relate the variable proportions in detrital minerals and the different textural arrangments with some technological and rheological properties.

The study of mineral fabric by means of optical microscopy and SEM has been shown a zonal distribution of textures across the characterized levels: Coatings and Plasmic Textures, Massive Textures and Nodular textures.

The following characteristics with technological interest have been studied: disintegration ability, rheological properties, liquid absorption capacity and surface area.

Some sepiolitic materials interbedded between arkosic lutites and micaceous sands from the miocene Madrid Basin have been studied. Three levels can be observed in a vertical sequence: A greenish lower level (1 m of thickness, 50% Sepiolite), an intermediate white level (1.7 m) and an upper brown level (0.5 m, both levels with more than 90% of sepiolite).

Quartz and feldspars (10-30%) , hydrous mica (5 %) and smectites (5-10%) are present in the lower level. These minerals and calcite are the main accessory minerals in the upper levels. Chemical analysis of major and some trace elements has been performed. Si, Al, Ti, K, Ba, Y and Pb are strongly correlated with the presence of detrital minerals while F and Mg are associated to sepiolite . Cr and Fe contents exhibit dependence on stratigraphic position, both elements growing upwards, indicating , possibly, a selective dissolution and mobilization process.

The study of mineral fabric by means of optical microscopy and SEM has been shown a zonal distribution of textures across the characterized levels from the bottom to the top:

1.- Coatings and Plasmic Textures

In the lower levels dissolution aureoles of detrital minerals are the main features observed. Silica glomerular coatings and sepiolite have been observed to develop on quartz surfaces (Figure 1), while fibrous illite develops on feldspars as substitution of crystals or as birefringent cement coatings. The cements show sepiolitic composition but with significant contents of Al, Fe, K and Ti.

2.- Massive Textures

In the intermediate level, sepiolite quasi-monomineral materials are conformed by imbricated arrays of plain-parallel fiber aggregates (10-15μm size) (Figure 2). These units show a very uniform texture and occasionally corroded quartz grains can be observed.

3.- Nodular textures

These textures are developed in association with a fissural pattern in which sepiolite overgrowths fill the internodular spaces (Figure 3). The nodulization is more advanced to the top levels where internodular voids are occupied in some cases with sparitic calcite. Nodules have a massive nuclei being more birefringent and compact towards the border where the sepiolite aggregates are parallel to the surface. The ratio SiO2%/MgO% and the Fe content increase from the nuclei to the edges of the aggregates while Al decreases.

The structural formulae of sepiolites fitted to an ideal unit cell (Bailey, 1980) ($Si_{12-x}Al_x$ Mg_{8-y-z} R^{3+}_y $\blacksquare_z$ O_{30} $(OH)_4$ $(OH_2)_4$) were performed in samples composed

virtually only by sepiolite. Chemical analyses were corrected for K_2O, Fe_2O_3, and Al_2O_3 by means of subtracting the appropriate proportions of a celadonitic analysis taking into account previous EDX analyses of micaceous fibers from SEM observations (Table 1). All of the sepiolites show no tetrahedral substitutions. Massive texture sepiolite (as CC5 in Table 1) has no octahedral vacancies while in those with nodular textures a 0.2 to 0.3 unit cell octahedral vacancies were calculated. Octahedral aluminium remains fairly constant in the sepiolites analyzed.

Table 1:

Structural Formulae of Sepiolite							
	Si^{IV}	Al^{IV}		Al^{VI}	Fe^{VI}	Mg^{VI}	Sum
CC5	12.00	-		0.177	0.016	7.816	8.009
CC2S	12.00	-		0.202	0.112	7.481	7.795
CC3S	12.00	-		0.174	0.026	7.595	7.795
CC6I	12.00	-		0.135	0.009	7.568	7.712

Anionic Base : $O_{30}(OH,F)_4\ (OH_2)_4$

Some environmental factors related to weathering processes as the composition of parent materials, the chemical evolution of phreatic waters and the level oscillations of the water table, among others, can be taken into account for explaining textural and chemical differences in the sepiolites under characterization. the dissolution-precipitation processes and the development of cementing phases occurs mainly in transitional vadose-phreatic zones where rich magnesium-alkaline waters interacting with lutitic sediments yields the formation of magnesium phylosilicates. Ba and Li are commonly associated with magnesium trioctahedral smectites formed in those environments.

The textural and mineralogical homogeneity observed in massive sepiolite implies an active process of dissolution-precipitation. Such process develops in high permeability phreatic environments where low concentration trace elements as F (with a regional level of 2 ppm, Santaren et al., 1990) experiment a significant enrichment up to 7000-9000 ppm related to sepiolite lattice. These materials react with bicarbonated superficial waters, being responsible of the fissural "karstification" of massive materials, yielding nodular textures and Fe mobilization into the voids.

Technological properties of a mineral are mostly determined by the mineralogical composition and texture of a mineral. These properties are of paramount importance regarding the potential industrial uses of the mineral, and therefore their economical value. Thus, the following characteristics with technological interest have been studied: disintegration ability, rheological properties, liquid absorption capacity and surface area.

The rheological properties of the materials depend, among other factors, on the mineralogical composition, basically on sepiolite content, and on the particle size distribution of the final product. In the tested conditions, particle size distribution is a function not only of the elemental particle size but also of the disintegration ability, and therefore of the aggregation state.

Sepiolites with nodular texture, that show a lesser degree of aggregation and consequently can be disintegrated more easily, are the materials which give products with higher viscosity values, higher than 40,000 cP.

Massive sepiolites, more crystalline and more difficult to disintegrate due to the interlocking of the microfibrous individual particles, have lower viscosity values, in the range of 20.000 to 30,000 cP.

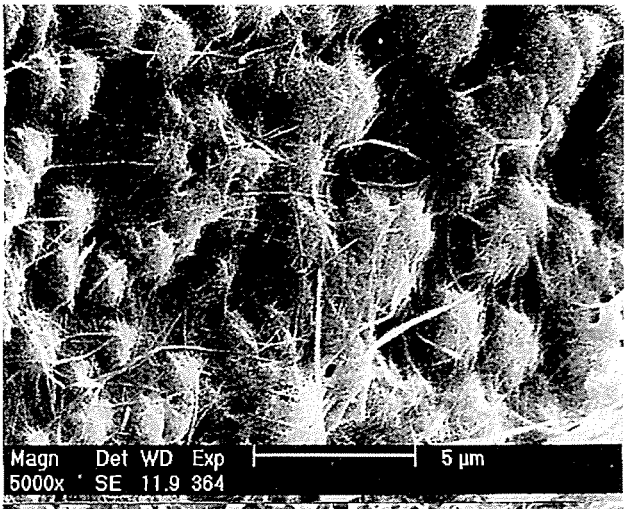

Figure 1

Growth of sepiolite fibers coating globular forms of silica

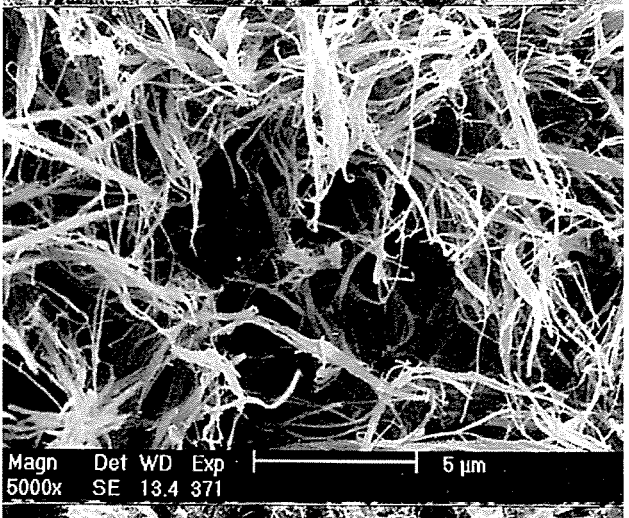

Figure 2

Sepiolite fibers in the massive textures

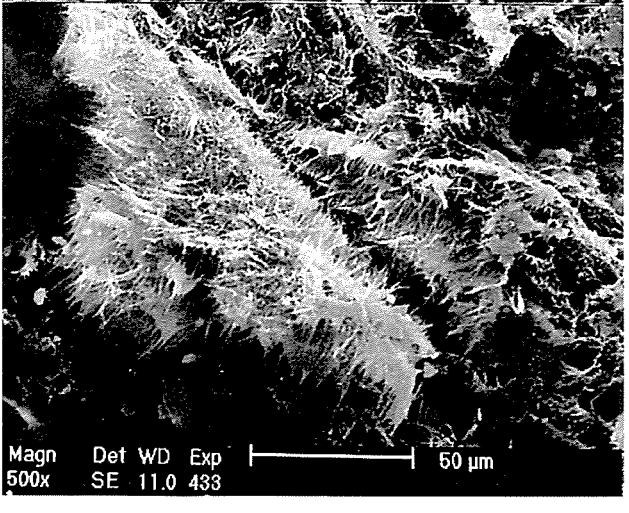

Figure 3

View of a fissure with overgrowths of sepiolite.

Sepiolite content in the material is also an important factor that determines the rheological properties. Thus, the presence of detritic materials significantly reduces the viscosity. The materials mostly composed by non-sepiolitic clays (lutites) give very low viscosity values, ranging from 50 to 1,200 cP.

Another important characteristic concerning the industrial application of the materials is the liquid absorption capacity. This characteristic is directly related to the surface area and porosity of the mineral that also depends of the mineralogical composition and texture of the material. In general, non-sepiolitic materials show a low absorption capacity meanwhile sepiolite with nodular texture have the highest absorption. Massive sepiolites, due to their texture, show an absorption capacity somewhat lower than nodular sepiolites. Liquid absorption capacity also decreases as the detritic minerals content increases.

References:

Bailey, S.W., (1980). Structures of Layer Silicates. In G.W. Brindley and G. Brown (Editors): "Crystal Structures of Clay Minerals and their X-Ray Identification". Mineralogical Society Monograph, 5. 1-125.

Santaren, J., Sanz, J. and Ruiz-Hitzky, E. (1990). Structural Fluorine in Sepiolite. Clays and Clay Minerals., 38, 1, 63-68.

Current Research in Geology Applied to Ore Gervilla.Fenoll Hach-Ali, Torres-Ruiz & Gervilla(eds)(1993).ISBN 84-338-1772-8

TALC DEPOSITS IN THE ITALIAN WESTERN ALPS

Sandrone, R.
Dip.to di Georisorse e Territorio, Politecnico di Torino, Torino, Italy

ABSTRACT: Talc deposits in the Western Alps primarily occur in the serpentinites of the Piedmontese Zone and the micaschists of the Dora-Maira Massif. The former were probably formed during a late-Alpine hydrothermal-metasomatic event at about 300 °C and 1.5-2 kbar, the second from pre-Alpine and/or Alpine metamorphic evolution of an original Mg-rich pelitic sediment reshaped by the Alpine tectonics.

INTRODUCTION

Talc deposits in the Western Alps belong to two structural contexts. A first group (devoid of any economic significance) is associated with the Piedmontese Zone, and is mainly hosted in serpentinites (Sandrone & Zucchetti, 1991), or subordinately in dolomitic facies within the metasedimentary sequence (Mastrangelo et al., 1983). A second group occurs as a discontinuous horizon within the Dora-Maira crystalline massif (Sandrone et al., 1990; 1992), and is the source of Italy's well-known high-quality talc.

THE DEPOSITS ASSOCIATED WITH SERPENTINITES

The geological setting of these deposits is composed of portions of an oceanic lithosphere with minor remnants of a sedimentary cover of Ligurian affinity. The lithologies of these portions bear witness to a complex metamorphic history comprising an early-Alpine event under eclogitic conditions, followed by multistage decompression in blueschist, barroisite and greenschist conditions. The mineralisations present as "dykes" that are sharply unconformable with respect to the regional foliation and develop along shear zones. They always consist of only a few phases (talc, chlorite or carbonates ± sphene ± opaque ores), often organised in single-mineral domains. The stable associations are talc + carbonates and/or talc + chlorite, though small sphene blasts, too, seem to be in equilibrium with the talc in some cases. This geological and sedimentological picture points to very close analogies with the much more important deposits in Val Malenco (Central Alps), where talc formation appears to be due to a hydrothermal-metasomatic event during the retrograde phases of the meso-Alpine metamorphism at about 2 kbar and 350-530 °C. The metasomatic fluids were rich in SiO_2, CO_2 and CaO, and may have been of metamorphic origin or the outcome of remobilisation resulting from intrusion of the Bregaglia pluton into the serpentinites (Beaulieu, 1983; 1985).

In the Western Alps, too, the field evidence shows that the mineralisations are younger than the Alpine tectonic and metamorphic events. The origin of the fluids, however, must be metamorphic. Furthermore, if it is assumed that talc and sphene coexist in equilibrium, the calculation programs of Perkins et al. (1986) give a temperature of no more than 350 °C for this paragenesis. Identical or slightly lower maxima have been proposed for chrysotile (Zucchetti et al., 1988, with references) and sepiolite (Belluso & Sandrone, 1989) mineralisations developing in late faults or fractures produced by a post-collisional extension tectonics (Borghi & Sandrone, 1990). The pressure values at which the talc mineralisations were formed cannot be determined as yet. The only evidence available consists of preliminary data regarding fluid inclusions. These suggest pressures of the order of 1.5-2 kbar. Lastly, there is the question of the composition of the fluids that produced the metasomatosis. In addition to what has been said above with respect to the Val Malenco deposits, some conclusions can be drawn from the composition and distribution of the opaque ores in the

mineralised horizons. The host ultramafics display magnetite, Fe-Ni alloy, pentlandite, and pyrrhotite ± heazlewoodite associations indicative of distinctly reducing environment (Rossetti & Zucchetti, 1988), whereas the transition to the talc vein is nearly always emphasised by abundant pyrite and sometimes by magnetite ± haematite ± pyrite. This points to a strong fO_2 (and fS_2) gradient between the host rock and the veins, referable to remobilisation and/or transformation of mineral associations typical of the former's reducing environment on the part of relatively oxidising fluids during the hydrothermal event.

THE DEPOSITS IN THE DORA-MAIRA MASSIF

Italian high-quality cosmetic talc is produced at the Fontane mine near Pinerolo (Province of Torino, Piedmont). This mine is the only active survivor of a series of workings along a mineralized horizon forming part of the polymetamorphic terrains of the Dora-Maira Massif.

This Massif is a Pennidic unit of continental crust, formed of an upper element consisting of pre-Carboniferous metapelites, marbles and metabasites, and a lower one consisting of metasediments of probably (Permo)-Carboniferous age; both elements contain metagranitoids with granite to diorite chemistry. All these lithologies have clearly undergone metamorphic re-equilibration into greenschist facies of meso-Alpine age, although early-Alpine high-pressure parageneses and occasional relics of a pre-Alpine metamorphic event are preserved locally.

The talc occurs in the pre-Carboniferous terrains near the contact with the overthrusted Piedmontese Zone as a conformable, sheetlike body.

The Fontane lithological series consists (from bottom to top) of marbles (interbedded on the regional scale in the basement micaschists), followed by micaschists, augengneisses and more micaschists enclosing the mineralized body.

On an average, this body trends N25°W and dips WSW at an angle of 30°. Its workable thickness is usually 1-3 m, but is sometimes more than 10 m.

Structural analysis of the Fontane area has enabled a distinction to be drawn between three superposed folding phases. The first of these (F1) is marked by the presence of uprooted millimetric to centimetric isoclinal folds displaying thickened bends and thin, parallel flanks. The b1 axes are usually no more than slightly inclined and directed more or less constantly E-W. F1 is also associated with a well-developed axial plane foliation dipping a few degrees to the West. Its distribution is confined to the lower structural levels, whereas in the higher levels it is completely obliterated by the following phase.

The second folding phase (F2) is characterised by crenulated folds that become increasingly serrated at the higher structural levels, where they take on the typical geometries of transpositive isoclinal folds. Its intensity of expression increases as it approaches the tectonic contact with the Piedmontese Zone. The b2 axes, too, are subhorizontal and their orientation (N-S) is roughly at right angles to that of the b1 axes and prevalently dipped to the South. F2 has been responsible for the transpositive folding of the previous planar anisotropy (S1) and the development of a new tectonic foliation (S2) that is also characterised by a weak Westward dip. F1 and F2 thus display a large orientation angle between their axes and a marked coplanarity of their axial surfaces.

In the Fontane area, F2 displays a constant Z-type asymmetry direction on looking towards the North. This can be seen at all scales of expression and is regarded as responsible for the hectometric structure of a thick layer of marbles that outcrops on the left-hand side of the Germanasca stream below the village of Fontane. The worked horizon lies in the long flank of this structure.

The third folding phase (F3) displays a rather spaced out crenulation cleavage that deforms the earlier foliation and gives rise to millimetric-hectometric folds. The subhorizontal b3 axes are oriented roughly NE-SW and the axial surfaces dip about 60° to the North-West. The distribution of F3 is poorly pervasive, but ubiquitous, and involves both the Dora-Maira Massif and the Piedmontese Zone lithologies.

The geometry and thickness of the body appear to be mainly governed by F2 and F3. The second deformation phase is of major importance with respect to the attitude of the deposit, because the talc is located on the long side of a hectometric F2 fold, and its development in area is probably controlled by the

fold itself. By contrast, its anomalous variations in thickness and local attitude seem to be substantially controlled by the last deformation phase.

The talc is usually found in the form of finely felty-scaly, white to milk-white aggregates. Two other types are variously distributed: a snow-white type composed of large, lamellar crystalline individuals with a distinctly schistous texture and a bright, pearly luster; the other greenish-white or ivory-white, with a microgranular structure and isotropic texture, a massive appearance, and a strikingly greasy feel.

The talc includes several accessory minerals. These are sometimes visible to the naked eye, though they are usually first observed under the microscope. Chlorite, carbonates (mostly magnesite and dolomite), zoisite, clinozoisite/epidote, rutile, sphene, tremolitic amphibole, quartz, and pyrite are fairly frequent. Albite, apatite, tourmaline, graphite, pyrrhotite, calchopyrite, and ilmenite are uncommon or subordinate.

Variously sized inclusions also occur in the mineralized body. These are generally ellipsoid or lenticular (known as "rognoni" = "kidneys"), or in bands that sometimes alternate with the talc. Leaving aside those composed of rocks hosting the mineralization, their chemical composition is mostly carbonatic (magnesite and/or dolomite + talc + chlorite + tremolite + quartz), or siliceous (quartz + talc + dolomite + tremolite + chlorite).

Even in the absence of a comprehensive geochemical picture, on the basis of the data set out above Sandrone et al. (1987) and Sandrone & Zucchetti (1988) proposed that the genesis of the Fontane talc be sought in the regional metamorphism of a protolith with an appropriate chemical composition, e.g. an Mg-rich clay such as sepiolite.

A more recent isotopic study of the pyrite associated with the talc (Ferrini et al., 1991) has not produced any evidence against this hypothesis.

As far as the age of the deposit is concerned, if one extrapolates for the Hercynian metamorphism of the Dora-Maira Massif the medium-high grade conditions recognised in other sectors of the Pennidic Domain, one must admit that the talc was formed during this event. The Alpine metamorphic evolution (Sandrone & Borghi, 1992) would thus have been solely responsible for its recrystallizations and the re-equilibrations of the parageneses within which it occurs.

REFERENCES

Beaulieu, P. 1983. Contribution à l'étude géologique des gisements de talc du Val Malenco (Alpes Italiennes).Thèse, Univ. Franche-Comté, Besançon

Beaulieu, P. 1985. Les gisements de talc du Val Malenco (Italie du Nord). Chron. rech. min. 478:5-20

Belluso, E. & Sandrone, R. 1989. Occurrence of sepiolite in the marbles of Dora--Maira Massif (Italian Western Alps). Miner. Petrogr. Acta 32:67-74

Borghi, A. & Sandrone, R. 1990. Structural and metamorphic constraints to the pre-collisional evolution of a NW sector of Dora-Maira Massif (Western Alps). Mem. Soc. Geol. It. 45:in press

Ferrini, V., Masi, U. & Monticelli, F. 1991. Geochemistry of pyrite from the talc deposit of Val Germanasca (Western Alps, Italy) and genetic implications. Miner. Petrogr. Acta 34:153-158

Mastrangelo, F., Natale, P. & Zucchetti, S. 1983. Quadro giacimentologico e metallogenico delle Alpi occidentali italiane. Boll. Ass. Min. Subalpina 20:203-248

Perkins, E.H., Brown, T.H. & Berman, R.G. 1986. PTX-SYSTEM: Three programs for calculation of pressure-temperature-composition phase diagrams. Computers & Geosciences 12:749-755

Rossetti, P. & Zucchetti, S. 1988. Occurrence of native iron, Fe-Co and Ni-Fe alloys in the serpentinite from Balangero asbestos mine (Western Italian Alps). Ofioliti 13:43-56

Sandrone, R. & Borghi, A. 1992. Zoned garnets in the northern Dora-Maira Massif and their contribution to a reconstruction of the regional metamorphic evolution. Eur. J. Mineral. 4:465-474

Sandrone, R. & Zucchetti, S. 1988. Geology of the Italian high-quality cosmetic talc from the Pinerolo district (Western Alps). Zuffar'days Symposium, Cagliari, October 10-15 1988, 105-113

Sandrone, R. & Zucchetti, S. 1991. Osservazioni su alcune mineralizzazioni a

talco associate alle ultramafiti della Zona Piemontese (Alpi Occidentali). Boll. Ass. Mineraria Subalpina 28:487-491

Sandrone, R., Trogolo Got, D., Respino, D. & Zucchetti, S. 1987. Osservazioni geo-giacimentologiche sulla miniera di talco di Fontane (Val Germanasca, Alpi Cozie). Mem. Sci. Geol. Padova 39:175-186

Sandrone, R., Borghi, A., Carosso, G., Morsetti, C., Tagliano, C. & Zucchetti S. 1990. Geometry of the Fontane talc deposit, and structural evolution of the area (Dora-Maira Massif, Western Alps). Boll. Ass. Mineraria Subalpina 27:45-62

Sandrone, R., Cadoppi, P., Sacchi, R. & Vialon, P. 1992. The Dora-Maira Massif. In: von Raumer, J.F. & Neubauer, F. (Eds.) The pre-Mesozoic geology in the Alps. Springer, Berlin, *in press*

Zucchetti, S., Mastrangelo, F., Rossetti, P. & Sandrone, R. 1988. Serpentinization and metamorphism: their relationships with metallogeny in some ophiolitic ultramafics from the Alps. Zuffar'days Symposium, Cagliari, October 10-15 1988, 137-159.

Current Research in Geology Applied to Ore Gervilla.Fenoll Hach-Alí, Torres-Ruiz & Gervilla(eds)(1993).ISBN 84-338-1772-8

APPLIED MINERALOGY OF THE STEPHANIAN-AUTUNIAN KAOLINITE BEARING ROCKS OF THE ATECA MASSIF (EASTERN IBERIAN RANGE, SPAIN)

Serrano, J. (1); Sanz, A. (1); Plana, F. (2); Lago, M. (3) & Bastida, J. (1)
(1) Dept. de Geología. Universidad de Valencia. Burjasot, Valencia, Spain
(2) Inst. Jaume Almera (CSIC), Barcelona, Spain
(3) Dept. de Ciencias de la Tierra, Facultad de Ciencias, Universidad de Zaragoza, Zaragoza, Spain

ABSTRACT. Kaolinitic materials derived from stephanian - autunian acid volcanic and hypabisal rocks of the East Iberian Range (Ateca Massif, W Zaragoza, Spain) had been analysed and compa, red to other well known kaolins derived from paleozoic rocks of other areas of the same range at NW Spain.The recognized mineralogical assemblage is + quartz +feldspars + kaolinite ± metahalloysite ± llite ± hematites /goethite + alunite . Some mineralogical, chemical and technological data are provided.Concentration and washing of these materials is needed in order to obtain marketable material.

Three groups of kaolins (A. Sedimentary B. Hydrothermal C. Weathering) are recognized in the typology of Galán & Espinosa (1974) for the spanish kaolins.These different groups includekaolins of several paleozoic formations.;the group A includes, for example , the type II, subtype Sierra del Pedroso, constituted by ordovician flintclays of the Barrios Fm. (García Ramos, et el.,1984, Sanz et al. 1987), as well as other kaolins belonging to different ordovician, silurian and devonian formations enriched in kaolinite by processes B. or C.

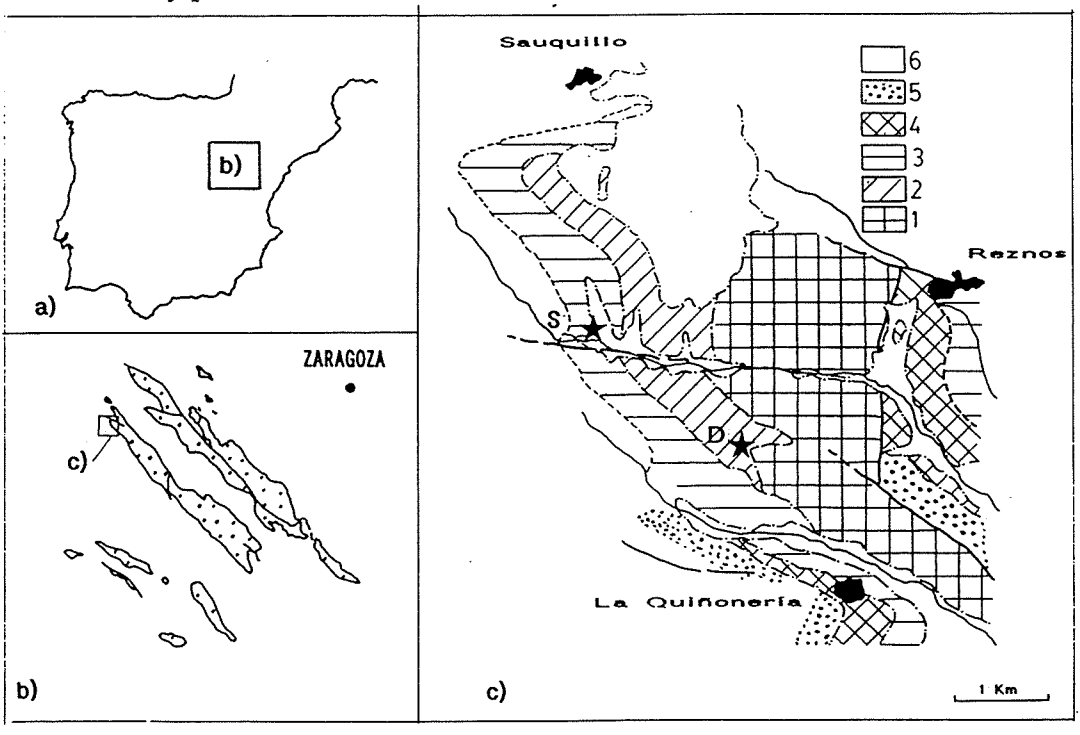

FIG.1. Geographical and geological situation. b) Iberian Chain hercynian outcrops at W Zaragoza, Spain. c) 6= Covered. 5= Cretaceous 4= Muschelkalk 3= Buntsandstein 2= Stephanian- Permian. 1= Paleozoic.

The gropup C includes the type VI (Burela) formed from acid volcanic rocks, the more representative locality of wich is the mining district Regovello, of ECESA (Caolines de Burela), in Burela (Lugo). The outcrop show a succesion of quarzitic schists, and grey, white and brown clays with an interbedded kaolinized felsite, belonging to the Capas de Tránsito Unit , downward the Begadeo Fm. (IGME,1984), in the Cambrian of the Mondoñedo Domain (Perez Estaún, 1978) of the Astur-Occidental - Leonesa Zone of the Iberian Range Julivert at al, 1972). This is the more important mine in a deposit in a deposit of volcanic origin in Spain.The main components of the kaolin are : metahalloysite, kaolinite and quartz., and the genetic processes involved include an alteration syngenetic to the setting or the deposit of the volcanic material previouly to the recent "in situ" weathering.The little knowledge of other similar deposits in Spain justifies the developping of the present work., cocerning kaolinized igneous bodies of the Stephanian - Autunian of the same zone of the Iberian Range, but in the East area, in the Ateca Massif, near Sauquillo (Zaragoza).

The presence of permian pyroclastic deposits (cinerites, lutites and pyroclastic sandstones more or less transformated., with diagenetic neoformation of hematite, albite, quartz, illite and dolomite, an kaolinite and illite, in lutites, as a result of lateritic alteration of volcanic rocks was recognized by Marfil & Peña (1973) and Peña et Marfil (1975).

The Figure 1 is a geological sketch of the studied area A volcanosedimentary succesion with an isolated rhyolitic body and a basaltic andesite are recognized on surface; paleoflora found at the top of the succesion as well as radiometric data (Rb-Sr, Nd-Sa) allows to date this magmatic activity as Stephanian - Autunian.(Lago et al. in ITGE,1991). The cal-alkaline nature of these manifestations has been stablished in the context of calc-alkaline rocks associations with high K enrichment in an intraplate domain characteristic of the East Iberian Range (Lago et al., 1988;ITGE,1991)

The aim of the work is the previous applied caracterization (mineralogical and technological) of materials provided by two points of sampling (S, surface and D, drill, in the area of Figure 1). The field and petroghraphical descriptions of the materials can be found in ITGE (1991) Lago et al. (1991).

The Table 1 shows the identification (procedure of Warshaw and Roy, 1964) semiquantitative mineralogical analysis of the samples, obtained trough X - ray diffraction analysis of unoriented powder of the bulk rock and of oriented aggregates , according the procedures of Barahona(1980).The same table show the data of (2ω), used as crystallinity index for the 001 reflections of illite and kaolinite.The Table 2 show the corresponding chemical analysis The first five samples of these tables correspond to autunian surface samples (Point S, Fig.1); the other correspond to different samples of rhyolitic tuffs samples from drill (point D, Fig.1), samples 29 and 40 (related to thin coal beds) can correspond to evolutions of the rhyolitic tuffs to underclays, so a depletion in some major elements (mainly Fe) can be observed (table 2) and an enrichment in sheet silicates.

The mineralogical assemblages recognized are + quartz +feldspars ± kaolinite ± metahalloysite ± llite ± hematites /goethite + alunite ,for the studied autunian materials and quartz + feldspars + kaolinite ± illite ± siderite ± pyrite ± hematites /goethite+ alunite , for the stephanian Hematite/goethite are quite unfrequent, and the opposite is true for siderite and pyrite, so the Fe_2O_3 contents are quite high, mainly for the autunian surface samples

Some materials (for example, selected samples 1,5, 14, 23, 28 of the tables1 and 2) show a clay fraction made of only kaolinite minerals (including kaolinite,

Mineralogical analysis

Table 1

Sample	f	Q	FK	I	K	Pi	Si	HG	(2w)10	(2w)7
42	31	46	15	13	11	6	*		,37	,32
45	21	53	22	7	15	3	*		,32	,31
43	25	75	23	6	19		*			,32
11	46	50	3	11	35		*		,33	,38
33	,41	22	56	21	17	5			,44	,31
19	18	36	45	7,80	10,20				,31	,37
27	31	54	14	14	17	*			,47	,33
04	24	64	12	7	17	*			,30	,36
02	23	65	11	7	16				,27	,30
29	69	23	80	19	50			*		,32
49	16	73	7	2	14	*				,29
10	10	81	8	1,50	8,50					,36
13	27	69	3	4	23				,43	,31
17	24	73	11	4	20	*	*		,29	,34
09	24	70	5	4	20		*		,30	,31
36	16	58	6	14	6		19		,30	,34
40	69	25	5	4	65				,27	,30
20	22	55	22	6	16				,30	,36
35	36	57	6	27	9				,41	,32
25	16	60	24	7	8				,34	,30
1	24	61	14	0	24					,30
5	7	72	20	0	7					,28
14	19	72	8	0	19	*				,29
23	20	72	8	0	20			*		,27
28	16	68	15	0	16	*	*			,32

Chemical analysis

Table 2

Sample	SiO2	Al2O3	Fe2O3	MnO	MgO	CaO	Na2O	K2O	TiO2	LOI
42	52,12	13,21	12,96	,24	1,96	,64	,13	9,11	,49	9,14
45	59,43	15,23	5,24	,12	1,76	2,40	,13	8,65	,29	6,75
43	61,64	13,97	4,06	,10	1,40	2,03	,13	9,95	,32	6,40
11	65,80	15,91	4,71	,03	1,35	,33	,28	5,73	,45	5,41
33	63,52	15,93	2,64	,08	,93	1,13	,10	12,04	,42	3,21
19	73,44	12,75	2,03	,01	,38	,14	,25	7,85	,14	3,01
27	71,14	12,90	2,65	,05	,50	,09	,23	6,33	,09	6,02
04	75,19	13,13	1,72	,01	,36	,08	,23	5,94	,08	3,26
02	72,28	15,55	1,57	,02	,37	,81	,27	5,20	,09	3,84
29	76,36	13,65	,77	,01	,19	,06	,19	4,35	,07	4,35
49	74,48	13,43	,43	,00	,10	,65	,27	6,48	,08	4,08
10	75,29	13,29	1,84	,05	,36	,08	,17	4,22	,11	4,59
13	73,50	9,28	6,20	,18	1,10	,18	,16	2,79	,10	6,51
17	75,53	12,39	,90	,02	,24	,14	,12	3,55	,14	6,97
09	74,28	15,55	1,18	,02	,30	,08	,14	4,31	,16	3,98
36	79,25	13,64	,34	,03	,13	,06	,21	3,01	,12	3,21
40	76,21	13,59	,62	,01	,19	,17	,15	3,81	,12	5,13
20	68,83	12,72	5,34	,16	1,07	,07	,10	4,68	,07	6,96
35	69,30	14,85	1,13	,03	,45	,68	,11	6,93	,08	6,44
25	63,43	18,69	3,14	,01	1,28	,23	,20	7,80	,51	4,71
1	73,68	13,60	,50	,03	,37	,67	,17	7,15	,17	3,66
5	70,42	13,18	1,68	,03	,50	,90	,16	8,24	,14	4,75
14	74,17	12,51	1,36	,01	,28	,26	,18	8,08	,11	3,04
23	75,83	12,25	1,45	,02	,20	,07	,11	4,17	,07	5,83
28	71,24	16,01	1,82	,07	,62	,16	,14	7,12	,11	2,71

metahalloysite and nacrite); the kaolinite content is high enough in order to consider the materials as kaolins (Berton and Leberre, 1983); they show high quartz contents , and the quality is lowered by the presence of allunite, so a concentration and washing is required in order to recover marketable kaolin; if particle size was a problem for that (usual in solfatara related kaolins), the applications would be limited to the manufacture of white cement (Bristow,1989).

In the natural state these materials show low brightness;. the table 3 show brightness data according to the Hunter system. (for relations to CIE sytem, see Khan et al 1982).

Table 3.

SAMPLE	L	a	b	SAMPLE	L	a	b
1	77.12	4.58	14.38				
5	83.84	4.99	15.44	40	83.14	1.84	9.0
14	70.56	4.38	7.02	29	82,67	0.43	5.27
23	71.41	5.93	8.83	10	77.42	0.96	8.68
28	76.24	6.53	18.96				

Lightness measurements (Equipment Color Quest 45/0; software Specware 1.01). Parameters Huntterlab; L=lightness (from hundred to zero), a (+= redness, 0= grey, -+greennes), b (+= yellowness, 0= grey, -= blueness)

References

Amigó et al. (1987) 6 th. Meeting European Clays Groups. p.74.
Barahona,E (1980) Arcillas de ladrillería de la prov. de Granada. Tesis Doct. Univ. Granada,N°49.
Bertton, Y and Le Berre, P (1983) Guide de prospection des matériaux de carrière. BRGM, 160 pp.
Bristow, C.M (1989) World kaolins: Genesis, exploitation and application. Industrial Clays. A special review. pp. 8-19. Metal Bulletin PLC.
Galán, E and Espinosa, J (1974) El caolín en España, ICV (C.S.I.C).230 pp.
García Ramos J.C et al. (1984) Trab. Geol. 14. 27-33.
IGME(1984). Mapa Geológico de España, Esc. 1/200.000. Hoja N°1(2-1).
ITGE (1991) Mapa Geológico de España, Serie 2. Hoja, N°380 (Borobia). Madrid, 82 pp.
Julivert, M et al. (19720 Mapa tectónico de la península Ibérica y Baleares. Memoria anexa, 212 pp. IGME, Madrid.
Khan,M et al. (1982). Interceram, 1, 17-20.
Lago M et al., (1991)b, EUG VI Meeting. OS. XI/41. Terra Abstracts, 3, 429.
Lago, M et al., (1988) II Cong. Geol. de España, Vol.2, pp.35-39
Lago, M et al., (1991).IV Congreso de Geoquímica de España, t.1, pp.35-46.
Marfil, R y Peña, J.A De la (1973) Est. Geol. XXIX, 83-98.
Peña, J.A De la y Marfil, R (1975) Est. Geol. XXXI, 513-530.
Perez Estaún, A (1978) Mem. Inst. Geol. y Min. de España, N°92, 1-151.
Pocovi, A et al. (1991)EUG VI Meeting. OS. XI/40. Terra Abstracts, 3, 428.
Rey, D y Ramos, A (1991) Rev. Soc. Geol. de España, 4, (1-2), 104-125.
Sanz, A et al. (1987).6 th. Meeting European Clays Groups. pp.490-491.
Warhaw C & Roy,R (1961). Geol. Soc. of America Bull.72, 1455-1492.

Current Research in Geology Applied to Ore Gervilla.Fenoll Hach-Alí, Torres-Ruiz & Gervilla(eds)(1993).ISBN 84-338-1772-8

GEOCHEMISTRY OF SPANISH, TERTIARY, FIBROUS CLAY DEPOSITS

Torres-Ruiz, J. (1); López-Galindo, A. (1); Gónzalez, M. (2) & Delgado, A. (3)
(1) Dept. de Mineralogía y Petrología & IAGM, Universidad de Granada-CSIC, Granada, Spain
(2) Dept. de Ciencias de la Tierra, Universidad de Zaragoza, Spain.
(3) Estación Experimental del Zaidin, CSIC, Granada, Spain

ABSTRACT

The mineralised intervals of fibrous clay deposits are made up of neoformed phyllosilicates (sepiolite, palygorskite, stevensite), detrital silicates (quartz, feldspars, illite, interstratified smectite-illite, Al-smectite, kaolinite) and carbonates (calcite, dolomite). Opal-A, gypsum and halite also appear sporadically. REE, transition trace elements, F and Li contents can be used to distinguised between phyllosilicates formed by chemical precipitation, detrital phyllosilicates, and those formed by transformation of the latter during early diagenesis. The contents in these elements and the isotope data indicate the formation of sepiolite and stevensite as chemical precipitates whereas palygorskite would derive from diagenetic transformation of other inhereted clay minerals.

INTRODUCTION

Spain has abundant, large sedimentary deposits of sepiolite and/or palygorskite (cf. Galán & Castillo, 1984, and references). This paper aims to present a geochemical characterisation of this type of mineral deposits (including data on Rare Earth elements and isotopes of C and O). Eighty eigtht samples form the Vicálvaro, Cerro Batallones, Parla, Pareja, Maderuelo, Almazán, Calatayud and El Cuervo deposits (numbers 1 to 8 in figure 1), belonging to Tajo, Duero, Calatayud-Teruel and Guadalquivir basins, have been studied. These samples represent the principal, most characteristic mineral facies present in mineralised intervals of these deposits. All the deposits studied are Neogene and were formed in restricted continental or perimarine lacustrine basins. The sedimentological characteristics of these deposits, and in particular the associations of the neoformed clay minerals, indicate that they were formed in alkaline continental lacustrine environments during periods of tectonic calm, in a warm climate with semiarid or seasonal arid conditions (Galán & Castillo, 1984).

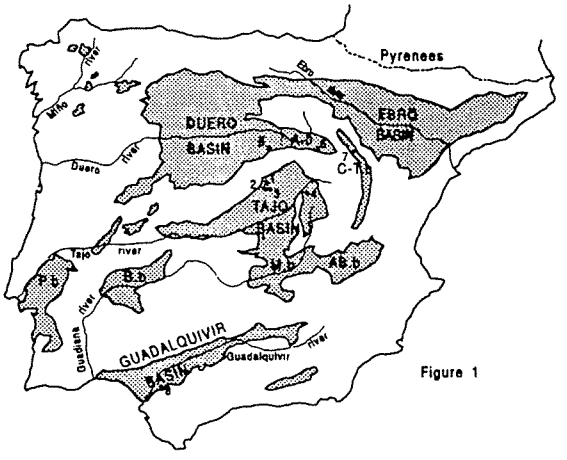

Figure 1

METHODOLOGY

Mineralogical characterisation.- Determination of mineral phases was carried out by X-ray diffraction, using a Philips PW1710, CuKα radiation and automatic slit, and by the powder method and oriented aggregates treated with ethylene-glycol, dimethyl-sulphoxide and heating to 350°C. The quantitative mineralogical analysis was carried out using information from chemical analyses and from X-ray diffraction (area measurement of peaks and reflective power, e.g. Schultz, 1964; Biscaye, 1965), according to the mineralogical pecularities of each sample.

Chemical analyses.- All the chemical elements except Si, F, Cl and REE were analysed by ICP Thermo Jarrel Ash-Plasma 300 equipment. Silicon was determined by atomic absorption using IL-257 equipment. F and Cl were analysed using selective electrodes. The analyses were carried out in the TOLSA, S.A. laboratories (Madrid). REE analyses were carried out at the X-Ray Assay Laboratories (Ontario, Canada) using the ICP-

MS technique. Isotope analyses were carried out at the Stable Isotope Laboratorie of the Estación experimental del Zaidín (CSIC, Granada, Spain). Isotopic ratios were measured in a FINNIGAN MAT 251 mass spectrometer.

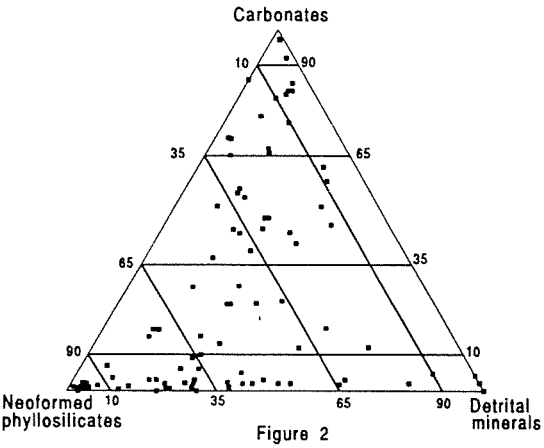

Figure 2

RESULTS

A) Mineralogy

The main mineral components of the samples from all deposits belong to three groups: detrital silicates (quartz, feldspars, illite, interstratified smectite-illite, dioctahedral smectite and kaolinite); neoformed phyllosilicates (sepiolite, palygorskite and Mg-smectite) and carbonates (calcite and dolomite). Opal-A, gypsum and/or halite also appear sporadically. In some layers, the neoformed phyllosilicates are the major components of the samples, reaching percentages of up to 97% (sepiolite), 94% (trioctahedral smectite) and 71% (palygorskite). On the whole, either only one of these neoformed phyllosilicates is present, or the sepiolite-trioctahedral smectite or sepiolite-palygorskite associations are found. Palygorskite and trioctahedral smectite do not coexist in any of the samples. The trioctahedral smectite corresponds to the stevensite end-member.

B) Chemistry

B.1. Major and trace elements

The major and trace elements make up three clearly differentiated group accorging to their source. High positive correlations are obtained among Al, Fe, Mn, K, Ti, REE and trace elements of the first transition series (V, Cr, Co, Ni, Cu and Zn) which are mainly found as part of the detrital fraction of the samples (figure 3). On the other hand, Mg, Ca, Cl, F and Li are basically found in the neoformed minerals (neoformed phyllosilicates, carbonates, gypsum and halite) and correspond to elements in solution in the depositional basins. F show a high positive linear correlation coefficient for the Mg and neoformed phyllosilicates as a whole (figure 3). However, sepiolite and stevensite contain more F than palygorskite. Li is preferentially concentrated in tne stevensite. This selective concentration of Li is a well documented fact (Tardy et al., 1972). As these authors point out, for similar Mg contents in the neoformed phyllosilicates, Li is retained more readily in laminar than in fibrous minerals.The third group consists of Si, Na, Sr and Ba which are found in both the detrital fraction and the neoformed minerals. At the level of individual deposits, Sr and Ba are positively correlated. Neither element shows highly sifnificant correlations as regard the rest of the chemical components and/or the different mineral phases. However, on considering the deposits at a whole, correlation between both elements is not significant. On the other hand, it can be observed that Sr correlates positively with the Cl content, with the highest concentrations of Sr and Cl in the El Cuervo deposit, where halite is a neoformed phase that is frequently present.

In all the deposits REE/Chondrite patterns show a negative trend with a negative anomaly in Eu, similar to those of the NASC. However, REE contents range from 1 to 0.05 times the NASC values, according to the mineralogy of the samples. Furthermore, in comparison with the NASC pattern, most of the clayey samples show a noticeable progressive depletion in HREE. The REE are mainly supplied by detrital minerals. REE contents of the main minerals are ordered as follows: illite > interstratified smectite-illite > palygorskite > stevensite ≈ sepiolite ≈ carbonates.

REE, transition trace elements (TRTE) and F contents of the diferents neoformed phyllosilicates, detrital Al-silicates and carbonates are shown in figure 4. The values were calculated on the basis of the chemical and mineralogical analyses of samples very rich in each of these minerals. It can be seen that palygorskite presents higher ΣREE and ΣTRTE and minor F values than stevensite and sepiolite.

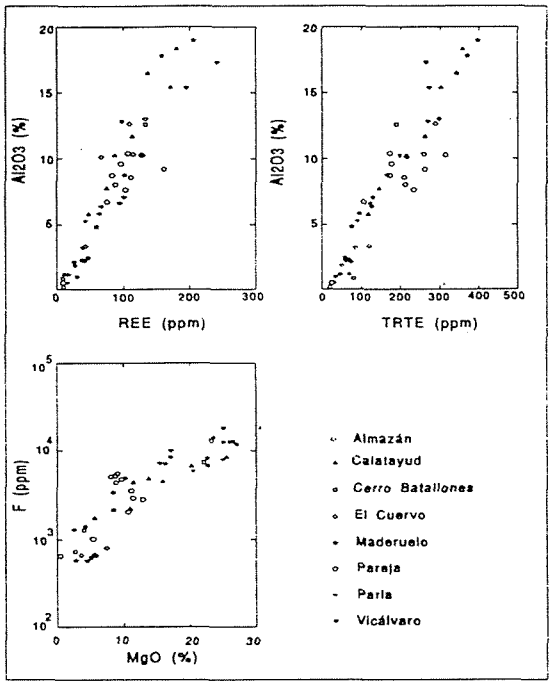

Figure 3

B.2. Isotope data

B.2.1.Carbon

The $\delta^{13}C$ values have a wide range (-4.28 to -11.15‰ PDB) and are typical od carbonates originating in continental environments and strongly affected by supplies of highly negative carbon (-10 to -25‰), which must have originated in the decomposition of the plant cover and in the breathing of plant roots, under the majority presence of *C3 plants* (Salomons et al., 1978; Deines, 1980).

B.2.2. Oxygen

$\delta^{18}O$ values for neoformed minerals are: calcite (-1.06 to -6.54‰ PDB), dolomite (1.07 to -2.38‰ PDB), silica (23.6 to 30.4‰ V-SMOW), sepiolite (18.0 to 18.8‰ V-SMOW), stevensite (16.0 to 17.0‰ V-SMOW), palygorskite (21.0 to 22.0 ‰ V-SMOW). The analysis of isotope data from the equations of fractionation of the diferents mineral-water systems indicate that silica, stevensites and sepiolites were formed in equilibrium with the same type of solutions which would correspond to meteoric waters. Such solutions are differents of those in equilibrium with palygorskites and carbonates which have heavier values related to more evaporated solutions.

GENETIC CONSIDERATIONS AND CONCLUSIONS

The conditions of formation of magnesian clay minerals in sedimentary environments continues to be the subject of considerable debate. The main question is to determinate whether these minerals formed by direct precipitation, from the solutions in the depositional basins or from diagenetic solutions, or whether they are the result of diagenetic reactions between solutions and solids and, therefore, products of the transformation of preexisting material (see Velde, 1985 and Jones, 1986). In most cases, the evidence on which workers base their attempts to discover the origin of magnesian minerals in the sediments of continental or marine basins derives from experimental work and electronic microscope observation of certain mineral transformations. In this work we propose to use the amounts of certain trace elements (F, Li, REE and transition elements) as discriminating parameters. Clay minerals produced by weathering and/or transformation, tend to inherit and level out the distributions of residual trace elements (REE and transition elements) of their source rocks or minerals. On the other hand, directly precipitated clay minerals show very low REE content and distributions coherent with those of the solutions in the depositional basins, where the amount in true solution is very small in comparison to that transported by particles. Furthermore, in contrast to detrital minerals, neoformed clay minerals in evaporitic basins could retain higher quantities of migratory elements (such as F and Li) during continental weathering.

REE and trace elements of the first transition series (TRTE) on the one hand, and F and Li contents on the other can be used to distinguish between inherited phyllosilicates and phyllosilicates formed by chemical

precipitation in the depositional basins. The former present high ΣREE and ΣTRTE values and very low values of F and Li, whereas the latter have low ΣREE and ΣTRTE values and high F values. The latter also have high Li content in laminar minerals, as is the case of stevensite, which distinguishes it clearly from inhereted dioctahedral smectites. The contents of these elements in sepiolite and stevensite are consistent with an origin by chemical precipitation. Moreover, the contents of these elements in palygorskite are intermediate between those of sepiolite and stevensite and those of detrital Al-silicates. This fact suggests a genesis of palygorskite other than by direct precipitation from the solutions in the depositional basins. Actually, the REE, TRTE and F contents, together with the high Al content of palygorskite, rather suggest a genesis of this mineral by transformation from detrital phyllosilicates. These genetic considerations are supported by the results of the analyses of isotopic fractionation. The data obtained indicate that sepiolite, stevensite and silica were formed in equilibrium with waters of similar isotopic composition and that these waters are different to those with which palygorskite and carbonates were formed in equilibrium.

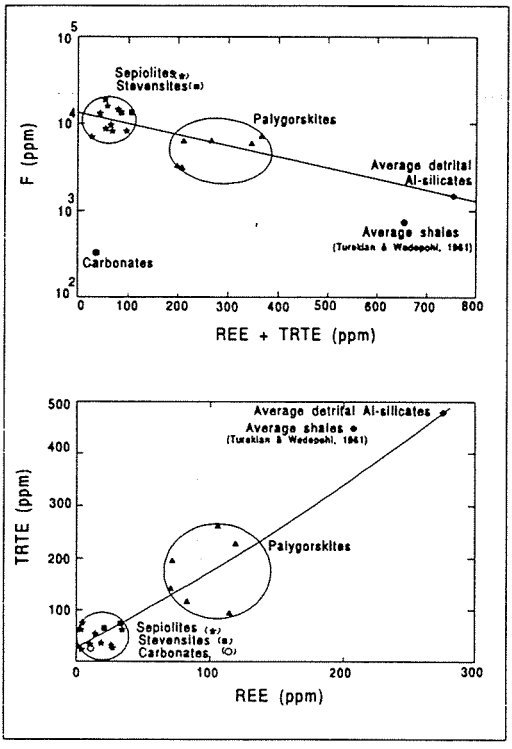

Figure 4

The isotopic data also indicate that the main source of C in the carbonates was edafic, mainly provided by decomposition of C3 plants. The values calculated for the fractionation factors of the sepiolite-water and palygorskite-water systems at 20°C are:

α (sepiolite-water) = 1.030

α (palygorskite-water) = 1.027

ACKNOWLEDGEMENTS

We thank A. Alvarez and J. casas (TOLSA, S.A., Madrid) for their collaboration in the field work and Dr. E. Reyes (Estación Experimental del Zaidín, CSIC, Granada) for his help in the results and discussion of isotope data. We also thank TOLSA, S.A for the analytical data of major and trace elements. This research has been partially financed by groups 4065 and 4028 of the Autonomous Goverment of Andalucía.

REFERENCES

Deines P (1980). The isotopic composition of reduced organic carbon. In: "Handbook of Environmental Geochemistry" (Fritz P & Fontes J Ch, Eds.), 1, Elsevier, Amsterdam. 329-406.

Galán E & Castillo A (1984). Sepiolite-palygorskite in Spanish Tertiary basins: genetical patterns in continental environments. In: "Palygorskite-Sepiolite: Occurrences, Genesis and Uses" (Singer A & Galán E, Eds). Dev. in Sedim., 37. Elsevier, Amsterdam. 87-124.

Jones B F (1986). Clay mineral diagenesis in lacustrine sediments. U.S. Geol. Surv. Bull., 1578, 291-300.

Salomons W, Goudie A & Mook W G (1978). Isotopic composition of calcrete deposits from Europe, Africa and India. Earth Surf. Proc., 3, 43-57.

Tardy Y, Krempp G & Trauth N (1972). Le lithium dans les minéraux argileux des sédiments et des sols. Geochim. Cosmochim. Acta, 36, 397-412.

Velde B (1985). Clay minerals. A physico-chemical explanation of their occurrence. Dev. in Sedim., 40. Elsevier, New York. 427 pp.

6 Open session

Current Research in Geology Applied to Ore Deposits.Fenoll Hach-Alí, Torres-Ruiz & Gervilla(eds)(1993).ISBN 84-338-1772-8

THE TIN BEARING ENDOSKARN VEINS OF MATA AZUL (GOIAS, BRAZIL)

Bilal, E. (1); Moutte, J. (1); Botelho, N. (2) & Andrade, G. de (2)
(1) Ecole des Mines de Saint Etienne, France
(2) Universidade de Brasilia, Brazil

ABSTRACT

In Mata Azul, economic tin concentrations are found in biotitic- and pyroxenitic veins. These were formerly considered as trondhjemitic or granulitic enclaves in the granitic massif of Serra Dourada, but the chemical data suggest that they actually result from metasomatic transformations of granitic rocks, and that the original materials were acidic differentiates of the enclosing granitic suite. The mineralogical zonation of the veins is similar to the structure of endoskarns; it reflects as important change of oxygen fugacity, which can be responsible for the precipitation of large amounts of tin as cassiterite in the outer zone and in the silicates in the inner zone. The same kind of transformations may be also observed in several parts of the Serra Dourada massif, in the NW part of the Serra da Mesa massif, and in granite prophyry dykes intruded in the Serra d'Encosto. It is thus suggested that the tin mineralizations are closely related to the anorogenic magmatism of the Goias district.

I. INTRODUCTION

The Serra Dourada granite massif contains two types of vein: cassiterite-bearing biotite veins, and pyroxenitic veins. Because of their lenticular shape, these veins have been formerly interpreted as enclaves, the biotitic veins as restitic material (Macambira, 1983), and the pyroxenitic as trondhjemitic (Macambira, 1983) or granulitic (Pierantoni Campos & Marmos, 1986) enclaves. However, the shapes can be explained by the pervasive deformation also found in the host granites. Moreover, the pyroxenitic veins contain tin, both as cassiterite in outer biotitic rims and in the silicates (sphene and garnet) in the inner part, and the biotitic veins may be thus considered as equivalent to the outer zones of the pyroxenitic veins. In this paper, we will describe the mineralogical and chemical features of the veins, and we will interpret them as representing tin-bearing vein endoskarns. Such a skarnization process is not restricted to the Serra Dourada: similar features are also found in granite prophyries that crosscut the Serra d'Encosto, in the NW part of Serra da Mesa, and in carbonate-bearing horizons of the host series (Bilal, 1991).

II. GEOLOGICAL OUTLINE

The Serra Dourada massif, located 500 km North of Brasilia, is emplaced in metasediments derived from greywackes and pelites, and its Rb-Sr age is 1.68 Ga (Macambira, 1983). It is composed mainly of biotite-granite; amphibole-biotite granite is found at the periphery, garnet-bearing granite forms small stocks within the biotite-granite mass, which is also intruded by dykes of granite-porphyry. All the granites suffered deformations of Uruaçuano age (1.3-1.1 Ga, Hasui *et al.*, 1980). The major and trace element compositions, e.g. the Fe/Mg, Mg/Ti, Ga/Al ratios, of all these rocks are comparable to those of A-type granites (Bilal, 1991).

Tin mineralizations are located in a strongly fractured zone (the subvertical fractures are oriented N-S and N-160). The ore consist of N-S oriented veins, 1 to 2 m thick (sometimes up to 8 m), 10 to 20 m long, which can be followed for 350 m along strike; the minerals (biotite, amphibole, sphene) are oriented parallel to the foliation of the host biotite granite.

III. THE PROTOLITHS OF THE VEINS

The pyroxenitic veins show a mineralogical zoning; from shell to core, three zones can be distinguished: biotite zone, amphibole zone, pyroxene zone.

As the biotite is associated with sphene, the very low Ti content of the biotite (0.45 to 1.12 wt. %

TiO_2) is considered as a clue for rather low equilibration temperatures (Robert & Maury, 1980), especially when compared with biotites from granulites (2.6 to 6 % TiO_2, cf. Leelanandam, 1970). The garnets contain no pyrope, they have almandine–grossular compositions similar to garnets from tin or tungsten skarn deposits (Einaudi & Burt, 1982). The pyroxenes are hedenbergites, with no Ti, low Al content, and high Ca contents, which are also typical features of clinopyroxenes from skarns (e.g. Deer *et al.*, 1978; Burton *et al.*, 1982). The pyroxenitic this cannot be considered as granulitic enclaves. On the contrary, the mineral chemistry, the textural features, and the presence of tin as cassiterite (biotite zone) and in the silicates favour the hypothesis that the veins are the result of by metasomatic processes.

In order to identify the protoliths these rocks are derived from, we have to find immobile components. Considering the presence of zircon and sphene all over the zonation, we suppose that Zr and Ti stayed immobile during the transformations. In a Zr–TiO_2–Th diagram, the mineralised rocks plot on the same domain as unaltered granites of Serra Dourada; this suggests that the veins are derived from granitic rocks, and that these 3 elements were inert. Moreover, on the TiO_2–Th diagram, the compositions of the different zones of a pyroxenitic vein plot on the same straight line as the granite porphyry samples.

We conclude here that the pyroxenitic and biotitic rocks are metasomatic rocks (endoskarns) developed on granitic rocks of the Serra Dourada massif. They cannot be considered as granulitic or trondhjemitic enclaves.

The vein endoskarns:

Only the pyroxene veins are described here: the biotitic veins are considered as the lateral equivalent of the biotite zone of the former, the contain the same mineral associations and have the same mineral chemistry. The pyroxene veins are 1 to 2 m thick, they are foliated like the host granite. The following zonation is observed from the rim to the core of the zone.

Biotite zone: This outer zone, 30 cm thick, consists of biotite (= 90 vol. %), quartz, some plagioclase (An_{20-16}), and disseminated pyrrhotite. At the contact with the biotite granite, the potash feldspar is altered to green biotite. The brown biotite also gradually disappears, and its replacement by green biotite accompanied by the accumulation of sphene. Biotite and sphene are oriented parallel to the foliation of the granite. Compared to the green biotites, the few brown biotites remaining in the veins have relatively low contents of Fe, Al, Mn, and high contents of Ti, Mg. compared to the biotites of the host granites, the green biotites are low in Ti and high in Fe. Remnants of ilmenite from the granite are observed as relicts in the sphene grains. The garnet is of almandine composition (Alm_{76} $Spess_{11}$ $Gross_{12}$ $And_{0.93}$ $Pyr_{0.07}$). The plagioclase has the same composition (An_{19-16}) as in the observed in the granite, is found in this zone as inclusions in the green biotite or associated with sphene. Hypidiomorphic cassiterite (5–8 mm) forms chapelets.

Granite	**Bio zone**	**Amph zone**	**Prx zone**
Plg (An_{20-16})	Plg (An_{19-16})	Plg (An_{27-23})	
KF			
Bio	Bio		
3% TiO_2	1% TiO_2		
			Hedenber
Ilmenite			
Sphene	Sphene	Sphene	Shpene
	0.8% SnO_2	1.9% SnO_2	3% SnO_2
Quartz	Quartz	Quartz	Quartz
	Garnet	Garnet	Garnet
	76% alm	60% alm	45% alm
	12% gros	30% gros	45% gros
	11% spess	7% spess	7% spess
	0.93% and	0.78% and	2.33% and
	0.07% pyr	2.22% pyr	0.48% pyr
Monazite			
Zircon	Zircon	Zircon	Zircon
	Allanite	Allanite	Allanite
	Pyrrhotite	Pyrrhotite	Pyrrhotite

Amphibole zone: This zone is 30 cm thick. The amphibole (ferropargasite) first appears as small crystals (0.14 mm) and then develops against the green biotite, which finally completely disappears. Compared with the ferropargasites of the granites, those from the veins are characterised by relatively high F content (not found in the granite, lower Cl, Mg, Ti contents, and higher Al and Fe contents.

Garnet (Alm_{60} $Spess_{07}$ $Gross_{30}$ $And_{0.78}$ $Pyr_{2.22}$) replaces plagioclase (An_{27-24}). The high content of sphene is explained by the destabilisation of the biotite. It is associated with allanite, which is also found as inclusions in the amphiboles. No cassiterite is found in this zone, but tin is present in the silicates (SnO_2 amounts 0.6 % in garnet, 1.9 % in sphene).

Pyroxene zone: This zone, 23 cm thick, is limited by a sharp front where amphibole is replaced by clinopyroxene (Di_{11} Hd_{86} Jo_{03}) with Ti not detected and Al very low). Garnet megacrysts (1–2 cm), together with clinopyroxene, replaces plagioclase An_{27}. Its composition (Alm_{45} $Spess_{07}$ $Gross_{45}$ $And_{2.33}$ $Pyr_{0.48}$) is characterised by higher andradite and grossular contents than in the amphibole zone. They contain some fluorine, not detected in the other zones. Spessartite content is somewhat lower than in the biotite zone. The pyrrhotite is here also the only sulphide present. To the pyroxenes are often associated sphenes, and allanite inclusions. The sphenes contain up to 7 % malayite, they are thus characterised by high contents in Sn (3.3 % SnO_2, compared to 1.9 % in the amphibole zone and 0.02 % in the biotite zone), in Al, Fe, F, and by low Ti contents.

IV. THE CHEMICAL EVOLUTION OF THE VEINS

Ti, Th, Zr, and, with some limitations, P may be considered as inert. Zr and Th contents are similar in the granite and in the biotite zone, they are 15 % higher in the amphibole and in the pyroxene zones: these variations can be explained by the mobility of other elements. Ca, Mn, Sr increase from the biotite zone inward; Fe and Mg increase from the granite to the biotite amphibole zones and them decrease in the pyroxene zone; Si, Al, Na, and K decrease from the biotite zone to the pyroxene zone; Si, Al, Na, and K decrease from the biotite zone to the pyroxene zone. The mineralogical zoning of the vein system is illustrated chemically in the Ca–Fe–Al diagram (in atom numbers): from rim to core, Ca increases whereas Fe and Al decrease. Li, Zn, Ga, Nb, Sn, and Pb contents increase from the biotite granite to the biotite zone, and them decrease in the other two zones. Th, Rb and Ba contents are lower in the vein than in the granite; they decrease from the biotite zone inward to the pyroxene zone. Yttrium and the REE show the following behaviour: the biotite and amphibole zones have chondrite–normalised REE contents of about 700 for the LREE and 50 to 60 for the HREE. $(La/Yb)_N$ changes from 12 in the biotite zone to 16 in the amphibole zone to 6.5 in the pyroxene zone. This ratio is inversely correlated with the amount of garnet. As the high REE contents cannot be explained by mass variation alone, we may infer that the REE's have been transported by the fluids. The fluorine content is higher in the veins (0.33, 0.22 0.19 wt. % in the biotite, amphibole, and pyroxene zones respectively) then in the granites (0.17 wt. %). Tin is strongly concentrated in the biotite zone (8600 ppm) as cassiterite; it is present also as silicates (garnet and sphene) in the amphibole and pyroxene zones (resp. 630 and 860 ppm Sn). The high F and low Cl contents in the vein–forming silicates (sphenes, biotite, amphibole) reflect the strong fluorine activity and low salinity of the ore–forming fluids. It is thus inferred that tin has precipitated from fluorine–rich fluids.

V. DISCUSSION AND CONCLUSIONS

According to several studies (Einaudi & Burt, 1982; Van Marcke & Verkaeren, 1987), the biotite–ferropargasite–hedenbergite zonation reflects conditions of low fO2. The Fe /(Fe+Mg) ratio of the mafic minerals stays around 0.92 (atomic) across the different zones of the veins. This implies that the mineralogical zonation of the vein has to be explained mainly by the variation of the activity of CaO. As ferropargasite is stable only at low fO2 (Gilbert, 1966; Thomas 1982), we infer that higher fO2 would promote direct replacement of biotite by hedenbergite, and there would be no amphibole zone in–between (Van Marke & Verkaeren, 1987). This type of skarn has been described at El Hammam, Morocco (Sonnet, 1980), and at Flamanville, France (Chang, 1979). The formation of purely biotitic veins may also be explained by a very high fO2 preventing even hedenbergite formation.

We conclude that the skarnification observed al Mata Azul has been produced by F^- and Ca–rich fluids, under low fO2 and fS2. The elements brought in are Ca, Sr, F, Sn, Nb, REE, and Y; those brought out

are Si, Al, Ga, Mg, Mn, Ba, and the alkalis; those inter are Ti, Zr, Th, P. This vein system developed on a granitic protolith may be called endoskarn.

REFERENCES

Bilal, E. (1991): Etude de deux massifs de la province granitique stannifère de l'état de Goias (Brésil) et des formations métasometiques associées aux minéralisations en Sn et Be. Thèse de Doctorat Ecole des Mines de Paris, 480 pp.

Burton, J.C.; Taylor, L.A. & Chou, I. (1982): The fO2–T and fS2–T stability relations of hedenbergite and of hedenbergite–johannsenite solid solution. Econ. Geol., 77: 764–783.

Chang Ho Wan (1979): Pétrologie et métallogénie des formations de l'auréole métamorphique du granite de Flamanville dans la région de Diélette (Cotentin, France). Thèse U.C.L. Belgique.

Deer, W.A.; Howie, R. A. & Zussman, J. (1962): Rock–forming minerals, 1: 270 pp.

Einaudi, M.T. & Burt, D.M. (1982): A special issue devoted to skarn deposits: introduction–terminology, classification and composition of skarn deposits. Econ. Geol., 77–4: 745–754.

Gilbert, C.M. (1966): Synthesis and stability relations of the hornblende ferropargasite. Am. J. Sci., 264: 698–742.

Hasui, Y. & Alii (1990): Dataçoes Rb–Sr e K–Ar do centro–norte do Bresil e seu significado geologico–tectonico. Congresso Barsileiro de geologia. Anais SBG, 5: 2659–2678.

Leelanandam, C. (1970): Chemical mineralogy of hornblendes and biotites from the charnockitic rocks of Kondapalli, India. Journal of petrology, 11–3: 475–505.

Macambira, M.J.B. (1983): Ambiente geologico e mineralizaçoes associadas ao granito Serra Dourada (extremidade meridional) –Goias. Tese de Mestrado, universidade Fedérale de Para, 132 pp.

Pierantoni Campos, G.E. & Marmos, D.L. (1986): Geologia revisada do deposito estanifero de Mata Azul. Anais do XXXIV Congresso Brasileiro de Geologia, Goias, 5: 2367–2382.

Robert, J.L. & Maury, R.C. (1980): Natural occurence of (Fe, Mn, Mg) tetrasilicic potassium mica. Contrib. Mineral. Petrol., 68: 117–123.

Sonnet, Ph. (1981): Les skarns à tungstène, étain et bore de la région d'El Hamman Maroc central. Thèse à U.C.L. Belgium, 347 pp.

Thomas, W.M. (1982): Stability relations of the amphibole hastingsite. Am. J. Sci. 282, 136–164.

Van Marcke de Lummen, G. & Verkaeren, J. (1987): Ca–K matasomatism in the system $CaO–K_2O–MgO–Al_2O_3–SiO_2–H_2O$ and skarn formation in pelitic rocks. In Hegelson H.C. (ed.), Chemical transport in metasomatic processes, 669–679.

Current Research in Geology Applied to Ore Deposits. Fenoll Hach-Alí, Torres-Ruiz & Gervilla (eds) (1993). ISBN 84-338-1772-8

THE PHOSPHATE MINERALIZATIONS FROM GAVA, CATALONIA, SPAIN

Costa, F.; Camprubi, A.; Salvany, M.C.; Saez, G.; Arcas, A. & Melgarejo, J.C.
Dept. Cristal.lografia, Mineralogia i Diposits Minerals, Universitat de Barcelona, Barcelona, Spain

ABSTRACT: Lower Silurian series of Gavà area contain exhalative stratiform levels of variscite and apatite, which are associated to shales that contain disseminations of Ti, Cu, Ba, V and REE-bearing minerals. Phosphate remobilization by hydrothermal fluids occurred during the late Hercynian, producing veins with variscite, turquoise and jarosite, as well as limestone replacements by Fe-rich phosphates.

INTRODUCTION: Many deposits and showings containing Al-Fe phosphates (mostly variscite) are known in the Iberian Peninsula (Moro et al., 1992), and many of them are stratiform. Although some of these mineralizations occur into Carboniferous series (Melgarejo, 1992), the more significant examples are Silurian.

In the Catalonian Coastal Ranges Al-Fe-Cu phosphate mineralizations have also been described into Carboniferous series (Melgarejo, 1992), but the more interesting deposits occur into Silurian materials (Mata et al., 1983, Fernández Turiel et al., 1990, Melgarejo, 1992). Two mines exist on the most significative deposits in Silurian materials: the so-called Can Tintorer mine and the Rocabruna mine.

The Can Tintorer deposit was mined during the Neolithic (3500 b. C.) with the aim to obtain variscite for ornamentation. A complex system of underground mining, the oldest of this type discovered to the present in Europe (Villalba et al., 1990), is in process of archaeological excavation. The Rocabruna deposits have been mined for Fe since the middle age up to early in this century. In both deposits the phosphates occur in several types of morphologies.

The aim of this paper is to stablish the different types of phosphate mineralization and their paragenetic sequence.

GEOLOGICAL SETTING: The Paleozoic basement of the Gavà area comprises Silurian, Devonian and Carboniferous series (Fernández Martos, 1980) but all the phosphate mineralizations are located in the Silurian materials. These are made of 20-25 m of quartzites and shales (Lower LLandoverian?), 20 m of black and gray shales, chert, and tuffs which are thinly interbedded with phospahate levels (Lower LLandoverian), and 20-40 m of black shales (that can be locally enriched in pyrite disseminations or nodules) that correspond to Ludlowian-Wenlockian age. The Upper Silurian and Lower Devonian are made of 40 m of massive, nodulose limestones (Julivert & Martínez, 1983). The upper part of the Devonian series (50 m thick) is made of argillaceous limestones, that in their upper part change to marls with calcareous nodules and finally to green shales with some thin limestone beds (Emsian-Eifelian).

The base of the Silurian series in neighbouring areas contains, in addition, basaltic alkali rocks, with thickness comprised between

several meters to a few decameters. According to their geochemistry, Ibarguchi et al. (1990) suggest a distensive/anorogenic geodynamic environment active during the Lower Silurian.

The Carboniferous series unconformably cover the older materials, and they are constituted by interbedded shales and sandstones (Culm facies).

The Hercynian regional metamorphism is a very low-grade one in this sector of the Catalan Coastal Ranges, and the greenschist facies was achieved only locally. Three main phases of Hercynian deformation have been distinguished (Fernández Martos, 1980): phase 1 generated folds with axial plane cleavage dipping towards the North, and thrusts; phase 2 generated mainly tight folds with axial planes dipping towards the North; and phase 3 originated crenulations, kink bands and slack folds. Finally, a late Hercynian episode of fracturing must be distinguished.

Triasic materials (red beds in Buntsandstein facies and limestones in Muschelkalk facies) unconformably cover all the elder materials.

TYPES OF PHOSPHATE MINERALIZATION: Three main types of phosphate mineralization can be stablished: stratiform, veins and limestone replacements.

Stratiform mineralization: Such a mineralization occurs into the gray Silurian shales in Can Tintorer mine. The mineralogy of these shales consists mainly of V-enriched sericite and quartz. Rutile and ilmenite crystals are very abundant in them, and other accessory minerals relatively common are pyrite, chalcopyrite, barite and REE-bearing phosphates (xenotime and monazite).

Apatite forms in centimetric nodules into the shales, or occurs in mm-thick levels interbedded with shales and cherts.

Monomineralic variscite beds with thickness ranging between less than 1 mm and 2-3 cm are interbedded with centimetric-thick gray shales. The total thickness of this ensemble can achieve 2 m. The variscite levels have been deformed by all phases of deformation, and many of the original textures have been oblitered by cleavage and late replacements by red strengite. Variscite nodules, up to 2 cm thick, flattened by Hercynian deformation, also occur into the lower part of the Silurian black shales (Rocabruna mine).

Vein mineralization: A rich phosphatic assemblage is placed in irregular veinlets with sharp contacts that crosscut all the Hercynian cleavages. Despite these veins are placed into the Paleozoic materials (and specially close to the stratiform phosphatic mineralization), these veins do not occur into fractures across the triasic materials. This fact suggests a late-Hercynian emplacement, after folding and before the pretriasic unconformity.

The vein thickness ranges from few millimeters up to 2 cm. Variscite and ferrovariscite are the most common phosphates in these veins, and they occur as radial-shaped groups. They have been sometimes partially replaced by strengite. Turquoise also occurs alternatively to variscite as primary mineral in some discrete veins. Jarosite, alone or forming intergrowths with variscite, is the other significant primary mineral in these veins.

A late phosphate association comprises montgomeryite, strengite, crandallite, beraunite, phosphosiderite, kingsmountite

and, finally, radial groups of apatite and goethite. These phosphates are filling porosity or replacing the above mineral associations.

Limestone replacements: This mineralization type occurs mainly at the Rocabruna mine. The phosphates, associated to Fe oxides and sulphates, are replacing the Upper Silurian-Lower Devonian limestones. The replacements are associated to strong dolomitization and ankeritization of these limestones. The ore bodies shape is very irregular, and they are developed closely to the Hercynian thrusts. Furthermore, some of their primary minerals display evidences of deformation, so that the mineralization would be formed by hydrothermal fluids related to the thrusts.

The primary mineral assemblage has been very disturbed by late alterations, but is formed by earthy tinticite nodules embedded into goethite and jarosite. In addition, montgomeryite occurs as crosscutting late veinlets or replacing the outermore part of the tinticite nodules (Melgarejo et al., 1988). Dufrenite and apatite radial groups also occur as late filling of these veinlets.

CONCLUDING REMARKS: Variscite beds and disseminations occur laterally to Cu-Pb-Zn-Ag sedimentary-exhalative deposits in the Carboniferous series from the Southern part of the Catalan Coastal Ranges (Melgarejo, 1992), where basic alkali vulcanism also occurs. In spite of the fact that in Gavà area volcanic rocks or massive sulfide deposits directly associated to the phosphate levels can not be found, alkali basic volcanism is present in neighbouring areas. Furthermore, exhalative-sedimentary Cu-deposits are common through the Silurian series from the Catalan Coastal Ranges (Ayora et al., 1990), and they are rich in Ti, V, Cr, REE and PGE minerals and apatite levels (Melgarejo, 1992). So, in absence of favorable conditions for biogenic-sedimentary phosphate accumulations, and according to the geochemical anomaly in Ti-V-Ba-REE, precipitation from exhalative hydrothermal solutions related to the volcanism must be taken in consideration for its origin.

These preconcentrations were remobilized by late Hercynian hydrothermal solutions. These solutions were strongly oxidizing and acidic, leaching Al and P from the sediments, and probably Fe and Cu from the disseminated sulfides. Jarosite, variscite or turquoise formed into veins; Fe-rich phosphates as late vein fillings or replacing limestones were the mineral phases able to precipitate in more oxidizing conditions, according to the criteria of Warry and Kramer (1976).

The Silurian phosphate levels occur interbedded into sediments with disseminations of minerals with Ti, Ba, V, Cu and REE. Similar enrichments also occur in equivalent series in the Southern part of Catalan Coastal Ranges (Melgarejo, 1992). This apparently close association open suggestive possibilities for REE exploration in equivalent Silurian series in the Iberian Peninsula when stratiform variscite mineralization is also present.

AKNOWLEDGEMENTS: This research has been financed by a "Jóvenes Investigadores" grant from the Spanish Instituto de la Juventud-CICYT.

REFERENCES:

Ayora, C., Soler, A., Melgarejo, J.C. 1990. The Hercynian ore deposits from the Catalonian Coastal Ranges. Acta Geol. Hisp. 25, 1-2:5-74.

Fernández Martos, J.G. 1980. Estudio del Paleozoico al oeste del rio LLobregat entre Gava y Palleja. Unpub. Bach. thesis, Univ. Autònoma de Barcelona, 85 p.

Fernández Turiel, J.L., Gimeno, D., Plana, F., Blasco, A., Edo, M., Villalba Gordo, J. 1990. Estudio de las mineralizaciones fosfáticas del complejo minero de Can Tintorer (Gavà, Barcelona) y comparación con las cuentas procedentes de ajuares arqueológicos. Bol. Soc. Esp. Min. 13-1: 86-87.

Julivert, M., Martínez, F. J. 1983. El Paleozoico de las Cordilleras Costeras Catalanas. In: J.A. Comba (ed.): Geología de España. I.T.G.E. Vol I pp 529-535.

Mata, J.M., Plana, F., Traveria, A. 1983. Estudio mineralógico del yacimiento de fosfatos de Gavà. Bol. Soc. Esp. Min. 6, pp 257-258.

Melgarejo, J.C. 1992. Estudio geológico y metalogenético del Paleozoico del Sur de las Cordilleras Costeras Catalanas. Col. Memorias ITGE, 103. 605 p.

Melgarejo, J.C., Galí, S., Ayora, A. 1988. Tinticite: new chemical and structural data. N. Jb. Miner. Mh. 10: 446-453.

Moro, M.C., Gil Agero, M., Cembranos, M. L., Pérez del Villar Guillén, L., Montero, J.M., Fernández, A., Hernández, E. 1992. Aluminofosfatitas silúricas de la Península Ibérica: síntesis preliminar. Bol. Soc. Esp. Min. 15-1: 227-232.

Villalba, M.J., Bañolas, L., Arenas, J. 1990. Can Tintorer, Gavà (Catalunya). Une exploitation néolithique de phosphates et silicates. In: Séronie-Vivien, M.R. & Lenoir, M. (eds.): Le silex: de sa genèse à l'outil. Cahiers du Quaternaire nº 17. Actes V Colloque International sur le silex. C.N.R.S., Bordeaux: pp 275-285.

Warry, N.D., Kramer, J.R. 1976. Some factors affecting the synthesis of cryptocrystalline strengite from an amorphous phosphate complex. Canad. Mineral. 14: 40-46.

Current Research in Geology Applied to Ore Deposits.Fenoll Hach-Ali, Torres-Ruiz & Gervilla(eds)(1993).ISBN 84-338-1772-8

FORMATION OF HYDROTHERMAL FLUORITE VEIN DEPOSITS IN THE SOUTHERN BLACK FOREST/GERMANY. PART 1: STRUCTURAL CONTROL

Franzke, H.J. (1) & Lüders, V. (2)
(1) Inst. f. Geologie und Paläontologie, TU Clausthal, Leibnizstr. 10, 3392 Clausthal-Zellerfeld, Germany
(2) Geoforschungszentrum Potsdam, Telegrafenberg A50 1561 Potsdam, Germany

Abstract: The numerous fluorite/barite vein structures of the Black Forest were formed under an extensional stress-regime in relation to the updoming of the Rhenish shield during the Mesozoic. Most of the vein structures follow older shear zones of Variscan age.

Geological setting and older mineralisations

In the area of the Black Forest numerous SSW-NNE and E-W trending shear zones of Variscan origin are widespread phenomena. Of fundamental importance is the WSW-ENE striking NW verging crustal deep shear zone of Lalaye-Lubine-Baden-Baden in the northern Black Forest (Fig. 1), which seperates the Moldanubian zone of the Central Gneiss Complex (CGC) from the Saxothuringian zone of the Variscides (EISBACHER et al., 1989). In the southern Black Forest the SSE verging Todtnau fault (Badenweiler-Lenzkirch Zone) forms the boundary between the CGC and the Southern Gneiss Complex (CGC).
The polyphase Variscan tectono-metamorphic evolution in the central and southern Black Forest is distinguished by a sharp change in the tectonical regime from collisional shortening and crustal stacking to crustal extension and thinning since the earliest Upper Carboniferous (KROHE & EISBACHER, 1988, ECHTLER & CHAUVET, 1992). Former oblique convergent ductile shear zones were inverted to ductile-kataclastic high-angle normal faults, which bordered subsided and uplifted block units. This change in the tectonic regime coincided with the widespread intrusion of syn- and postkinematic Variscan granites and porphyric extrusions.
The timing of the extension tectonics is well controlled by the age of the deformed Albtal granite (Rb/Sr, 326 ± 2 Ma, SCHULER & STEIGER, 1978) and the Malsburg granite (U/Pb, 328 ± 6 Ma, TODT, 1976).
The oldest fault controlled mineralisations are scheelite (WERNER et al., 1990) and fine-dispersed sulphides in cherts, which mineralised ductile-cataclastic shear zones of probably Variscan origin. Radiometric dating of WENDT et al. (1979) and HOFMANN et al. (1991) from the Krunkelbach vein-type uranium deposit (occurrence 10 in Fig. 1) hint for hydrothermal circulations of Upper Carboniferous generated by the Variscan thermal field and an extensional regime of faulting.
We concentrated our investigations on the structural control, fault kinematics and geochemical aspects (LÜDERS & FRANZKE, this vol.) of the widespread fluorite-barite vein structures in the Black Forest, mainly in its southern part.

Structural control

In the sketch map (Fig. 1) 12 in detail investigated fluorite/barite bearing vein structures are shown. In Fig. 2 (occurrence No 5 in Fig. 1) the precursor of the SSW-NNE trending "Caroline" vein structure is mapped as an sinistral transpressional ductile shear zone with a 10-20 m wide anticlockwise rotation zone of the gneiss foliation. This shear zone was reactivated as highly altered kataclastic normal fault zone and mineralised by a sequence of sulphidic ores and barite. This shear zone is positioned in the eastern shoulder of the later opened (Eocene) Rhein Graben and geometry and the kinematics of reactivation is coinciding with the rift tectonics of the Rhein Graben. But the lack of radiometric data hinders the solution of this problem.

Remarkable are the very low up to missing fault throws during the fluorite/barite mineralisations which are presented in an example from the same vein structure (Fig. 3). This hints for dominating extensional stresses and very low shear stresses during the opening of the vein structures.
In contrast to the more complex figured and poly-phase activated vein structures in basement rocks the mineral veins in the cover rocks of Triassic are simple constructed. They follow one of the joint groups in the cover rocks, which was predestinated to be opened under the applied stress-field (Fig. 4, occurrence 2 in Fig. 1). The joints were integrated to large fracture planes through destruction of bridges between neighbouring joints. Breccia-textures (hydro-fracturing) indicate high

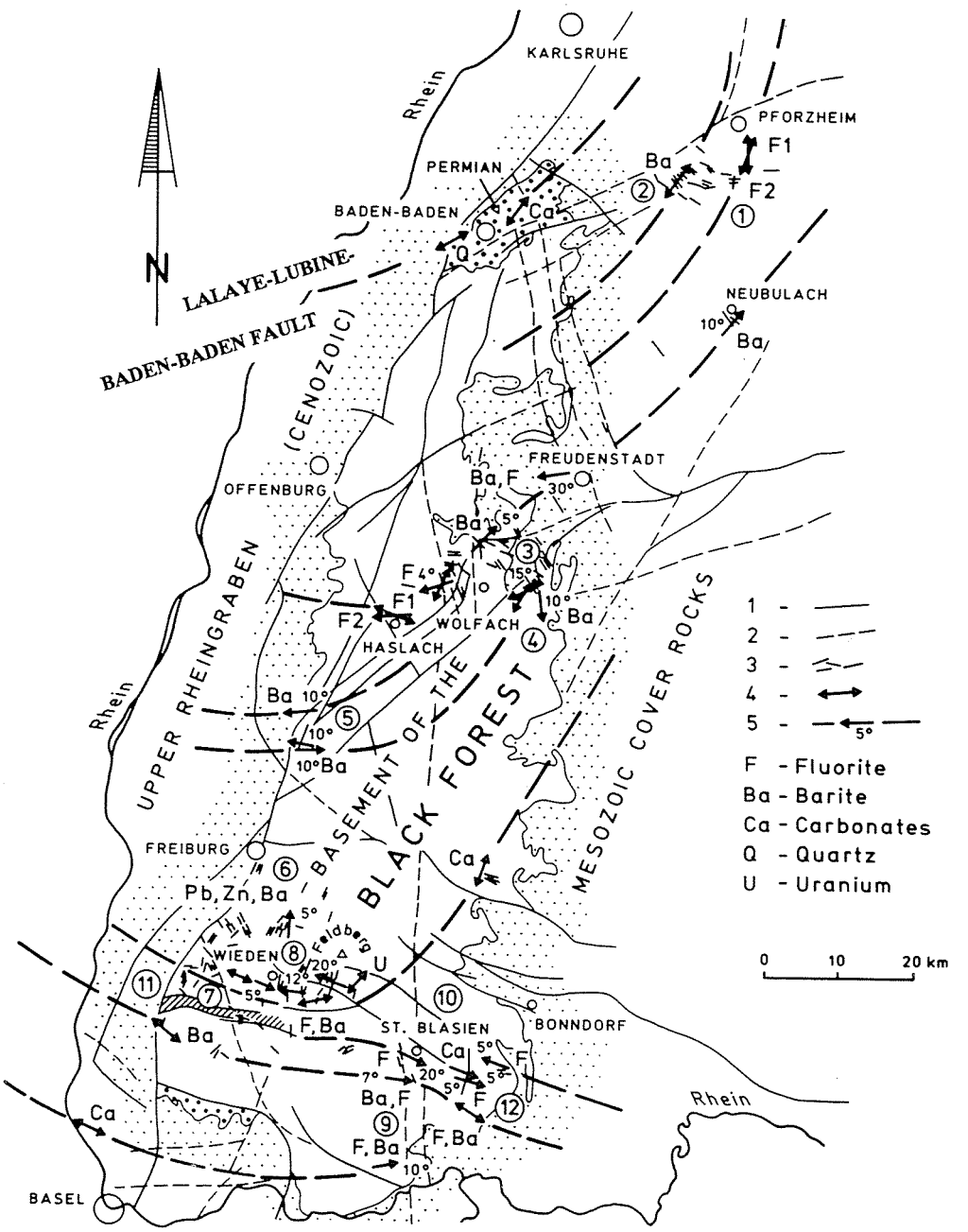

Fig.1. Stress-field of the fluorite-barite mineralisation in the Black Forest/Germany. 1 - principal fault zones, 2 - fault zones after remote sensing informations, 3 - mineral veins, 4 - minimal principal stress-axes in horizontal position, 5 - inclined stress-axes and trajectories. Numbers in circles: 1 - "Käfersteige" mine, 2 - Neuenbürg vein district, 3 - "Clara"mine, 4 - Wittichen vein district., 5 - "Caroline"mine, 6 - "Schauinsland" vein field, 7 - "Teufelsgrund"mine, 8 - Wieden vein district, 9 - "Gottesehre"mine, 10 - "Krunkelbach"mine, 11 - Badenweiler Lenzkirch Zone, 12 - Brenden vein district

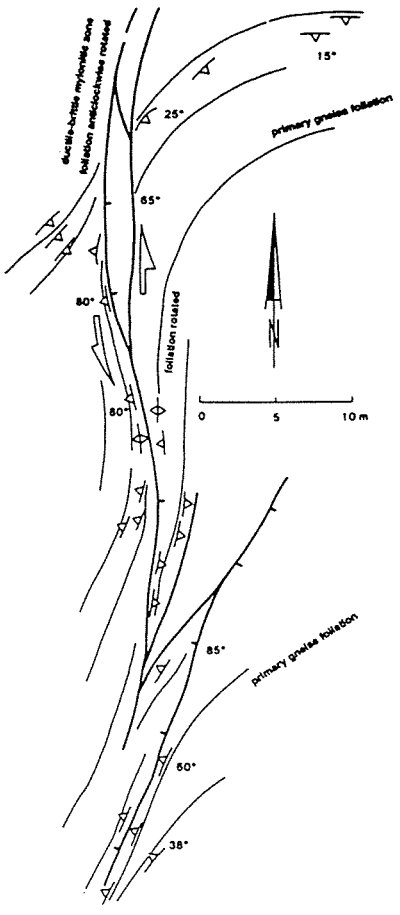

Fig. 2: Variscan structural pattern of the upper level of the "Caroline" mine NNE of Freiburg/Br.
Sinistral transpressional shear zone.

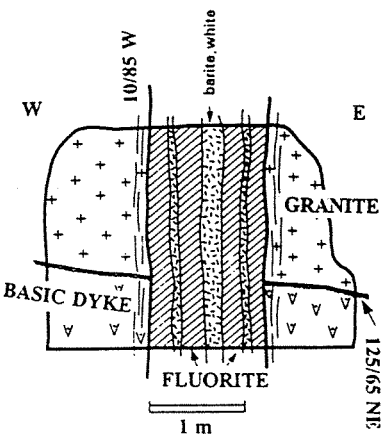

Fig. 3: Cross section through the mine "Brenden", Southern Black Forest. Basic dyke as control for fault kinematics.

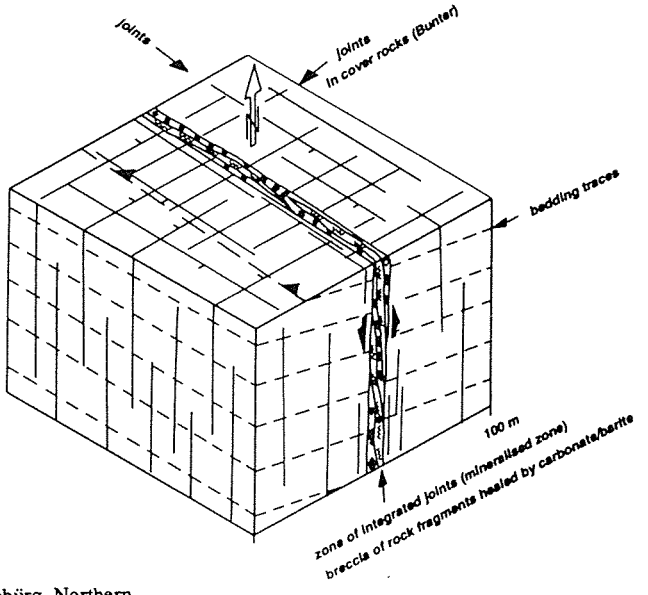

Fig. 4: "Frisch Glück" mine near Neuenbürg, Northern Black Forest. Block diagramm shows two joints set in Triassic sandstone and the vein structure (carbonate, barite).

Discussion

Exceptionally the reactivation of the Krunkelbach-uranium deposit at Lower Tertiary (WENDT et al, 1979, HOFMANN et al, 1991) the published radiometric data of the mineralisations range between 250 and 100 Ma (LIPPOLT, 1984). That means, that the fluorite/barite-vein mineralisation in the basement and Triassic cover rocks of the Black forest was formed under an increasing layer of cover rocks up to 0.8-1.0 km up to Lower Jurassic. HUCK (in MERTZ et al, 1986) found out, that the older fluorite in the "Clara" mine (occurrence 3 in Fig. 1) penetrated unconsolidated sands of the lowermost Triassic as a clear indication for synchronous sedimentation/mineralisation during the Lower Triassic.
In Fig. 1 are drawn the minimal principal stress axes from 35 vein structures compiled from the position of barite/fluorite tensional fractures, mineral fibre growth-directions, slickenside-striae and other kinematic indications. The interpolated stress-trajectories show evidences to a regional updoming of the Rhenish shield (CLOOS, 1939). Remarkable is the fact, that the orientation of the minimal principal stresses are approximately perpendicular orientated to the trace of the Upper Rhein Graben. We conclude from these observations, that a connection between the updoming of the Rhenish shield and the repeated generation of hydrothermal circulation cells took place in the time-span between Zechstein/Lower Triassic (250 Ma) and Cenomanian (100 Ma) and to the later following breaking-down of the Rhein Graben under the described stress situation since the Upper Eocene.

References

CLOOS, H. (1939): Hebung, Spaltung, Vulkanismus. Elemente einer geometrischen Analyse irdischer Großformen. - Geol. Rdsch., 30:401-527.

ECHTLER, H.P. & CHAUVET, A. (1992): Carboniferous convergence and subsequent crustal extension in the southern Schwarzwald (SW Germany). - Geodinamica Acta (Paris) 1991-1992, 5, 1-2: 37-49.

EISBACHER, G.H., LÜSCHEN, E. & WICKERT, F. (1989): Crustal-scale thrusting and extension in the Hercynian Schwarzwald and Vosges, Cental Europe. - Tectonics, 8, No 1: 1-21.

HOFMANN, B. & EIKENBERG, J. (1991): The Krunkelbach Uranium Deposit, Schwarzwald, Germany. - Econ. Geol., 86: 1031-1049.

KROHE, A. & EISBACHER, G.H. (1988): Oblique crustal detachment in the Variscan Schwarzwald, southwestern Germany. - Geol. Rdsch., 77, 1: 25-43.

LIPPOLT, H. (1984): Experimentelle Datierungen von postvaristischen Mineralisationen, Möglichkeiten und Grenzen. - In: "Postvaristische Gangmineralisationen in Mitteleuropa", ed. by the Gesellschaft Deutscher Metallhütten- und Bergleute: 305-360.

MERTZ, D.F., LIPPOLT, H.J. & HUCK, K.-H. (1986): K-Ar, Ar/Ar and Rb-Sr investigations on the genesis of the Clara vein deposit/central Schwarzwald. - Abstr. DGG/ILP meeting Karlsruhe: p. 235.

SCHULER, C. & STEIGER, R.H. (1978): On the genesis of feldspar megcrysts in granites: an Rb-Sr isotopic study. - 4th Conf. Geochron. Isotope Geology, Ed. R.E. ZARTMANN: 386-387.

TODT, W. (1976): Zirkon-U/Pb-Alter des Malsburger Granits vom Süd-Schwarzwald. - N. Jb. Miner., Mh., H. 12: 532-544.

WENDT, I., LENZ, H., HÖHNDORF, A., BÜLTEMANN, H. & BÜLTEMANN, W.-D. (1979): Das Alter der Pechblende der Lagerstätte Menzenschwand, Schwarzwald. - Z. dt. Geol. Ges., 130: 619-626.

WERNER, W., SCHLAEGEL-BLAUT, P. & RIEKEN, R. (1990): Verbreitung und Ausbildung von Wolframmineralisationen im Kristallin des Schwarzwaldes. - Jh. geol. L.-Amt Baden-Württemberg, 32: 17-61.

Current Research in Geology Applied to Ore Deposits. Fenoll Hach-Alí, Torres-Ruiz & Gervilla (eds) (1993). ISBN 84-338-1772-8

A MINERALIZED KARSTIC ANATOMY: THE MOUTHOUMET BARITIC ORES (AUDE-FRANCE)

Giannoni-Pasco, A.
Lab. de Geologie Appliquée. Universite de Paris VI, Tour 26, 4 Place Jussicu, 75 252 Paris, France

ABSTRACT : The paleozoic dolomites of the Mouthoumet massif (Aude, France) hosted baritic and Cu sulfosalts ores. Karstic evolution can be proposed : (i) ante-triassic peneplanation, dolomization and dissolution of paleozoïc fractured limestones ; (ii) the triassic transgression invades depressed zones, filling small tectonics basins with clastic deposits. Internal deposits show silicified polygenic sandstones. (iii) Anisian : the sedimentation becomes more lacustrine, with evaporitic events. The karstic fillings show authigenic and banded barite ; (iv) Ladinian : basin sediments become marine. The phreatic level is high and the karstic evolutions stops. Later, diagenetic basinal brines migrates and invades the unconformity surface : an epigenetic mineralisation affects most of the top of the palezoic hoests, the karstic network and the first triassic layers . The epigenetic baritic event occurred between lower Hettangian (the last mineralized layer) and Albo-aptian stage. Comparison between karstic paleo-phenomenons and mineralizing circulations with current karstic events shows that polystaged evolutions in the Mouthoumet are roughly similar to contemporaneous and pene-contemporaneous phenomenons in binary karsts.

INTRODUCTION

The baritic (Cu, Pb, Zn) karstic ores have been largely described in numerous deposits linked with unconformity surfaces (Ferrand & Thibieroz, 1978, Mansouri, 1980, Marini, 1986, Soler y Ayora, 1985, etc...). As they include large metal tonnage, these type of deposits have been the center of a numerous discussions dealing with the origins of fluids which leads to dissolution phenomenons, or with the mineralisation processes and their origins (Lagny & Rouvier, 1976). The Mouthoumet's karstic orebodies, object of this study provides an excellent case for a detailed analysis of the metallogenical processes which lead to the formation of these concentrations.
The paleozoic Mouthoumet massif is a North Pyrenean massif, composed by volcano-sedimentary tangential units. A long emersion phase succeeded the hercynian paroxysm. Mesozoïc transgression invaded the southern part of the massif, with red continental deposits, overlied by Anisian sebkha facies. Ladinian layers show marine dolomitic limestones. Triassic deposits occurred in small sized basins generated along synsedimentary faults inherited from the hercynian phases and reactivated in an extension context. Uppermost deposits consists in a well developped Keuper, overlied by thick marine deposits until Albo-aptian emersion.
Orebodies outcrop as subvertical lenticular lodes, with moderated vertical extension, or as stratiform bodies, linked with silicified crusts. The paragenesis is quite simple : barite, quartz, Cu, Pb sulfosallts and accesory sphalerite and galena. The ore is strictly hosted within paleozoïc dolomites and first transgressive triassic deposits. The latest mineralized stages are lower hettangian breccias.

II - A KARSTIC BARITIC ORE : THE AURIAC MINE

In the massif, the Auriac mine (100 000 t) is certainly the most illustrative of karstic dissolution phenomenons : baritic mineralisations are hosted by brecciated visean dolomites limited by two N-S auxiliary faults, satellites of a major N20 trend. Trace elements analysis (Sr, Cu, Zn, Pb) shows an impoverishment of visean dolomites close to the ore. In parallel, the hostrock becomes sandy and crumbly, spotted with manganese oxides (giraffe like) while its content in Fe_2O_3 increases. We can identify three generations of barite among which the two first generations (authigenic and banded barite) represent only a small part of the mineral weight.
The Auriac karstic body exhibits : (i) an apical zone underlying paleo-surface, poorly mineralized, rubefied and silicified with lack of karstic fillings; (ii) mineralized zone, with collapse breccias vertical dissolution features, breack-down sediments and exogenous deposits, and last (iii) the saturation zone, with horizontal dissolution zones filled by vadose sediments, dolomitic muds, and chemical fillings.The basis of this zone is also the wall of mineralisation, aproximatively at 50 meters under the surface.

- **Ba I** : rosettes and authigenic limpid barite needles growing in altered dolomite, dolarenite fillings and pelites.
- **Ba II** : banded barite with sulfosalts, baritic concretions on collapse breccia and dolomite fillings elements. Petrographic analysis shows bacterial relics, algal velums, etc... (Giannoni, 1990).
- **Ba III** : Main baritic epigenetic event, affecting the paleozoïc hostrock beyond karstic cavities, and invading locally triassic stratas. This event is **post-hettangian** and **ante-cenomanian**
- **Ba IV**, the last barite generation is composed by geodic cask-like cristals, associated with a post-tectonic spathic calcite, post-tectonic, associated with a post-tectonic spathic calcite, and linked with basin sediments diagenesis.

Erosion resumptions, sedimentation cycles and sediments destabilisation shows that the saturation zone level fluctuated during the karst's evolution. Detailed analysis of fillings shows synsedimentary episodes such as breakdown sediments, sediments and mineralisation early rework, slumpings and synsedimentary brecciation of already hardened sediments. All this phenomenons can be related to tectonic pulses recorded also in triassic basin fillings. The different kinds of sediments and the attached chronological sequence are synthetised in Fig. 1. Spherical baritic and sulphide concretions (**Ba II**) can be considered as chemical sediments : microscopical studies allowed J.P. Adolphe (Dept. de Géomicrobiologie appliquée, Laboratoire de Géodynamique des Milieux continentaux), and the author (Giannoni, 1990) to identify, extract and cultivate mineralized bacterial relics and velums. Only exogenous detritical sediments (polygenic conglomerates and sandstones) can be correlated with basin sedimentary deposits. The other types of internal sediments, such as dolomitic sandstones result from in situ dissolution of host-rock, and are **heterochronous**.

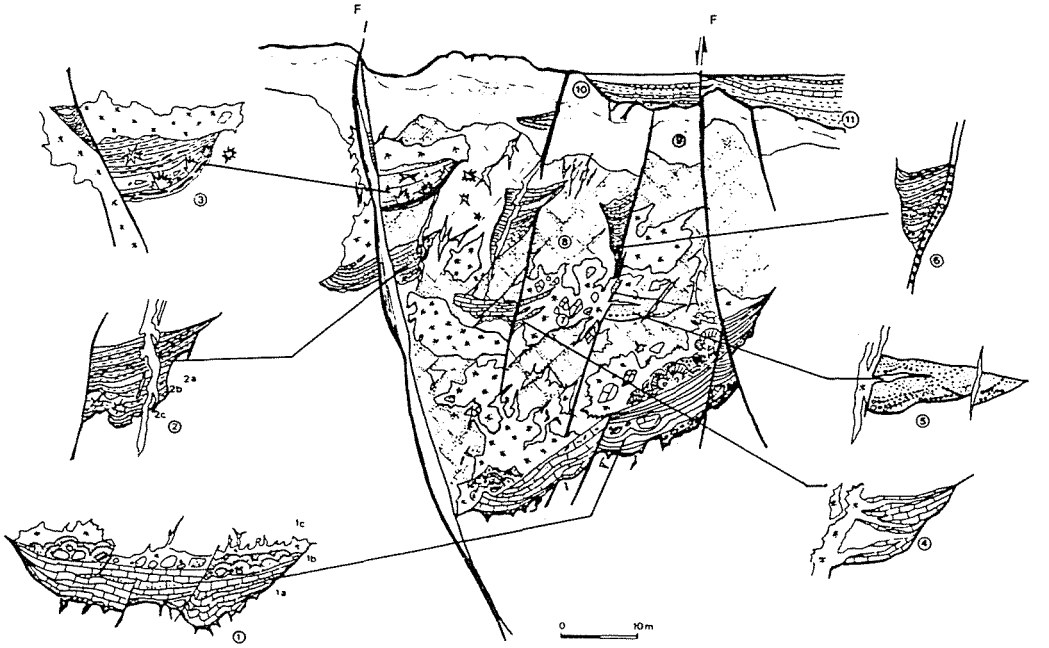

1 - Basal dolomitic filling
  1 a Layered dolomitic sandstone and authigenic baritic needles (Ba I)
  1 b Banded barite (Ba II)
  1 c Massive barite (Ba III)
2 - Pelitic filling
  2 a Arenaceous and pelitic sediment
  2 b Authigenic barite (Ba I)
  2 c Ba III cross-cutting vein
3 - Arenaceous silicified pelites, with synsedimentary barite (Ba I),sphalerite and galena.
4 - Fine varved dolomitic mud epigeneised by massive barite (Ba III)
5 - Silicified polygenic microconglomerates (Grès d'Auriac) cut by a baritic vein (Ba III)
6 - Post-tectonic argillaceous sediment with baritic clasts.
7 - Collapse breccia with Ba III cement
8 - Altered bedrock, brecciated visean dolomite
9 - Silicified crust underlying unconformity.
10 - Paleo-surface, lapiaz
11 - Transgressive upper triassic sediments (Keuper).

Fig. 1 . Karstic fillings spatial organisation in a baritic ore-body from the Mouthoumet Massif. (Giannoni, 1990, modified).

III- MORPHOGENETICAL INTERPRETATION

The Mouthoumet's mineralized karsts are located in a very strictly defined paleogeographical context, at the top of triassic paleohorsts, along extension faults. Polystaged tectonic activities on the fault network determined both basin deposits and paleozoic horsts uplift, drainage circulations and phreatic levels during Trias.
As a matter of fact, the very high position of the karst excludes any kind of connexion with the triassic cover : as a result, polygenic sandstones and conglomerates (grès d'Auriac) are not clastic sediments infiltrated from a sedimentary cover but represent a sedimentary clastic drift in the karstic caves, equivalent of basin triassic conglomerates. Recurrents floods overflowed the basin margins, invading the dissolution channels in visean dolomites, eroding the open pits and filling karstic caves. Between two flooding phases, decantation processes, confinement and sursaturation of internal brines lead to pelitic, argillaceous, then chemical deposits leading to evaporitic authigenesis. Only a small part of dolomitic sands and dolomites are linked with triassic deposits : chemical analysis shows that the result from *in situ* desagregation of visean dolomites, and the settling of such sediments are heterochronous. Most internal sediments and ores are intersected by blue pelites and chocolate clays sediments : they are connected with surface and results from withdrawal of material coming from the upper levels. All this sediments, ante, syn and post-baritic ore are affected by a fracturation phase, associated with a progressive uplift of the massif, and an intense erosion, at the Albo-aptian stage. This erosion affects the sedimentary cover, stripping the basement off, and reactivating the triassic karstic network. The fillings linked with this phase contain triassic bipyramidal quartz cristals and rubefacted mylonitic barite elements.

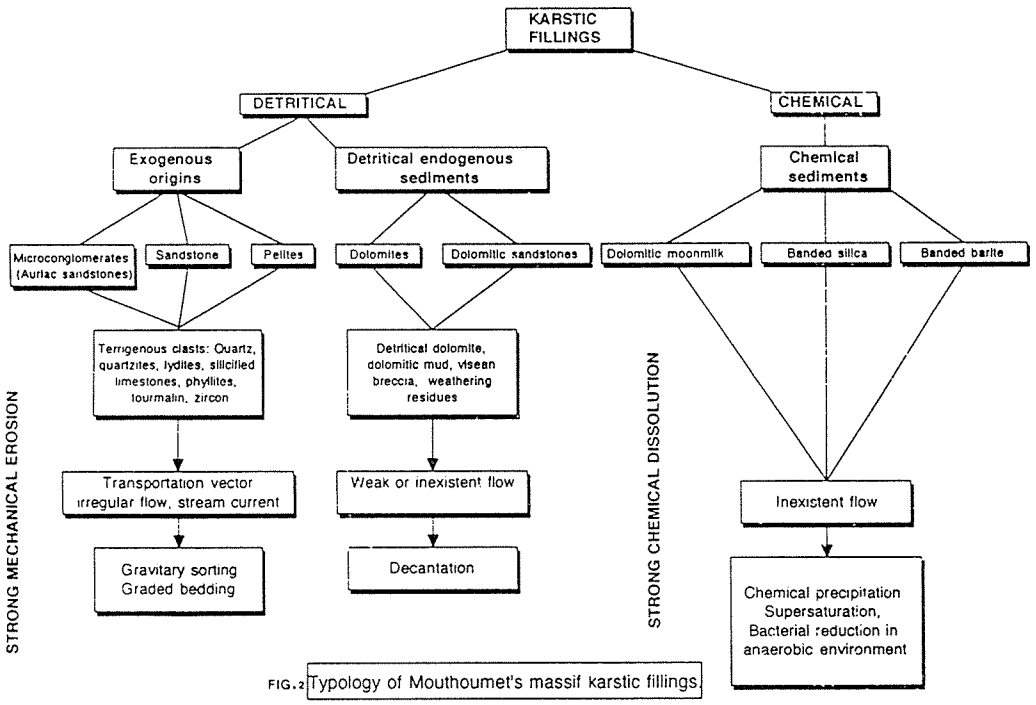

FIG.2 Typology of Mouthoumet's massif karstic fillings.

IV - CONCLUSION : KARSTIC ANATOMY, CONTEMPORANEOUS AND PENE-CONTEMPORANEOUS MODELS COMPARISONS

The reasoning applied to current karstic phenomenons either in this geographical area (Sorriaux, 1982), or more largely in Europe, North America or China (White, 1988) can be transposed to the morphological evolution and filling of mineralized karsts of Mouthoumet, provided that the last glaciation stages (and the eustatic variations) are taken into account. Thus, a karst formation history can be traced : dissolution and digging along joints and hercynian inherited fracturation network by

meteoritic paleocirculations. Ante-triassic paleosurface was subject to silicification and rubefaction phenomenons. The triassic transgression invades the depressed areas, reaching sporadically the karstified paleo-horsts. Tectonic pulses reactivate internal dissolution. Between two sedimentary and tectonic events, vadose sedimentation, confinement and chemical processes lead to early mineralized features (**Ba I, II**). This karstic evolution can be assimilated to a binary karst in extension context.

Very often, mineralized karsts are related to hydrothermal circulations, and present rounded shapes, linked with carbonate dissolution by hot and aggressive solutions. This is not the case in the Mouthoumet massif at all. Most of the other karstic orebodies contain internal sediments (i.e; Marini, 1986 ; Smati, 1987, Macquar & *al*, 1990) but exogenous sediments are extremely rare (described in the Asturrias , Ferrand & Thibieroz, 1978, at the Pourtalet fluorite mine, Martin, 1979). The most complete sedimentary sequences are found in the Mouthoumet massif, with evident relations between triassic basin transgressive sediments and syngenetic mineralisations.

It is often alleged that ore bearing solutions bring about both the mineralisation and the karstic dissolution of the host-rock. This hypothesis must be balanced in the case of the Mouthoumet mineralized karsts. The dissolution and karstic sediments filling stage, syn-triassic, are clearly anterior to the main epigenetic mineralisation, post-hettangian and due to diagenetic basinal brines migration along basement-cover unconformity.

However, evidence of early mineralized occurrences can be found that are linked with intrakarstic confinement of trapped solutions in the saturation level of the karst.

BIBLIOGRAPHIC REFERENCES

FERRAND A., THIBIEROZ J. 1978. Les gîtes de fluorine de l'Ouest de la province Asturrienne (Arlòs, La Moscona, Casa del Cura, Villabona, Cucona, Ural) résultent d'une même succession de circulations paleohydrologiques au sein d'un horizon calcaire triasique. *Bull. B.R.G.M.*, IIème série, Section II, n°4, pp. 335-355.

GIANNONI A. 1990. Les gîtes à barytine et sulfosels associés des Corbières (Aude). Un exemple de concentrations épigénétiques à l'interface socle/couverture. Thèse Université de Paris VI, 2 vol., cartes h.t.

1992. Minéralisations polyphasées à barytine et sulfosels de Cu et Pb du Sud de la France, Corbières (Aude) : Incidences métallogéniques et implications géodynamiques. In Source, Transport and Déposition of Metals, Proceedings of the 25 Years SGA anniversary Meeting, Nancy, 30 August - 3 September 1991, M. Pagel & J.L. Leroy eds, A.A. Balkema, Rotterdam, pp. 177-180

LAGNY Ph. & ROUVIER H. 1976. Les gisements Pb-Zn en roches carbonatées sous inconformité : gisements paleokarstiques ou gisements dans les paléokarsts ? *Mém. h. Sér. Soc. géol. France*, n° 7, pp. 57-69.

MACQUAR J.C., ROUVIER H., THIBIEROZ J. 1990, Les minéralisations Zn, Pb, Fe, Ba, F, péri-cevenoles : cadre structuro-sédimentaire et distribution spatio-temporelle, in "Mobility and Concentration of base metals in sedimentary cover rocks. Manifestations, Mechanisms, Prospection." Document du BRGM n° 183, 442 p.

MARINI D. 1986. Etude des minéralisations Zn, Pb, Ba des conglomérats triasiques de la bordure du gisement des Malines (Gard-France). Comparaison sédimentologique, minéralogique et géochimique des séries sulfatées et de leurs équivalents latéraux à l'aplomb des gîtes minéralisés. Thèse Université de Paris VI, 448 p.

MARTIN F. 1979. Les gisements de fluorine post-hercyniens (karstiques et filoniens) dans le Paléozoïque de la région du Pourtalet (Pyrénées Orientales, province de Huesca). Thèse IIIème cycle, Paris VI, Géol App., 190 p.

SOLER A.,& AYORA C. 1985. La mineralitzaciò kàrstica (Ba, Cu, Pb, Zn, Sb) de Rocabruna i de can Pubill, Pirineu Oriental : geologia, morfologia i gènesi. *Acta Geologica Hispanica*, v. 20, n° 2, pàgs. 107-122.

SORRIAUX P. 1982. Contribution à l'étude de la sédimentation en milieu karstique. Le système de Niaux-Lombrives-Sabart (Pyrénées Ariégeoises). Thèse IIIème cycle, Toulouse, 255 p.

WHITE W.B. 1988. Geomorphology and Hydrology of Karst Terrains. Oxford University Press. New York, Oxford, 464 p.

Current Research in Geology Applied to Ore Deposits. Fenoll Hach-Ali, Torres-Ruiz & Gervilla (eds) (1993). ISBN 84-338-1772-8

MORPHOLOGY, MINERALOGY AND CHEMISTRY OF THE RESPIRABLE-SIZE (<5μm), FLY-ASH FRACTION FROM THE MAIN AND NORTHERN LIGNITE FIELDS IN PTOLEMAIS, MACEDONIA, GREECE.

Kassoli-Fournaraki, A.; Georgakopoulos, A.; Michailidis, K. & Filippidis, A.
Aristotle University of Thessaloniki, Thessaloniki, GR-540 06 Greece

ABSTRACT: The respirable-size (<5μm) fly ash fraction from the Main and Northern lignite fields of Ptolemais, is investigated for its morphological, mineralogical and chemical features. This fraction represents the 8% of the bulk fly ash and consists mainly of calcite and gypsum. Chemically, CaO and SO_3 account for >60wt% in the respirable fly ash, while the most abundant trace elements are Sr, Ba and Cr. Compared to the bulk fly ash, the respirable-size fraction is enriched in gypsum (sponge-like), its Sr-content remains approximately in the same levels, while the rest analyzed trace elements are depleted.

INTRODUCTION

A considerable number of studies has been carried out recently, concerning the morphology, mineralogy and chemistry of the fly ash derived from the coal combustion (e.g. Coles et al. 1979, Gay and von Rosenstiel 1982, Gay et al. 1984, Gay and Davis 1987). The interest of the researchers concentrates mainly on the biological effects of fly ash emission, in the general framework of environmental pollution. The state of trace elements in the respirable-size fraction of fly ash is of important concern, since a considerable number of them is potentially toxic with undesirable effects on human health.

Nowadays, some fourteen steam generated electric power stations are working in the Ptolemais basin, Northern Greece, and the environmental impact is considerably high due to the continuous fly ash emission. In order to reduce environmental hazards in this area, it is necessary to have a detailed and integrated knowledge of the burnt lignite and its fly ash composition.

Previous works have dealed with the investigation of the morphology, mineralogy and chemistry of the fly ash derived from the lignite combustion in the Ptolemais power plants (Filippidis and Georgakopoulos 1992, Georgakopoulos et al. 1992). The present study concerns the morphology, mineralogy and chemistry of the <5μm fly ash fraction from the Main and Northern lignite fields of Ptolemais. This size fraction, behaving in the atmosphere like gas, is considered as respirable (Gay and Davis 1987) and is of high biological importance.

GEOLOGICAL SETTING

The Ptolemais basin is situated 160 Km west of Thessaloniki, in Macedonia county of Northern Greece. The Neogene-Quaternary sediments of the Ptolemais basin are divided into three lithostratigraphic formations: the lowest (Upper Miocene to Lower Pliocene), the middle (Pliocene) and the upper (Quaternary) formations. The middle formation contains the exploited lignite beds, alternating with clays, marls and sands. The deposition of the lignite beds took place in four stages, each representing a separate combination of sedimentation, neotectonics and paleogeographic features.

MATERIALS AND METHODS

Samples of the Ptolemais lignite fly ash derived from the Main and Northern lignite fields, were studied in terms of their morphological, mineralogical and chemical features. Five fractions (<63, 63-125, 125-250, 250-500 and >500μm) were obtained by dry sieving. The respirable-size fraction (<5μm) was separated from the bulk fly ash by the following treatment: equal quantities of each sample were disaggregated in distilled water by means of ultrasonic techniques and then centrifugated four times at 500 RPM for 80 sec. The obtained <5μm fraction was left to dry at room temperature.

XRD studies of all fractions were done using a Philips diffractometer (Ni-filtered CuKα radiation, scanning over the interval of 3° to 63° 2θ, scanning speed 1° and 1/4° per minute, silicon as external standard). Mineral abundances in the fractions are given in Table 1. Because of the unsignificant compositional variation, the mean mineralogical composition between Main and Northern fields is given. The discrimination in major, intermediate and minor/trace phases, was made taking into account individual XRD reflections, the density and mass absorption coefficient of each mineral as well as the chemistry of the samples.

The morphology of the fly ash particles, as well as their mineralogy were studied by a JEOL JSM-840 scanning electron microscope equipped with a LINK AN 10000 EDS microanalyzer, using carbon coated samples.

Chemical analyses of the bulk fly ash and its <5μm fraction were carried out in the Analytical Lab of the Swedish Geological Co., Lulea, Sweden. The analytical methods used were Plasma emission- and Plasma mass- spectrometry. Table 2 lists the average geochemical compositions (major and trace elements) of the examined samples.

RESULTS AND DISCUSSION

The weight percentages of each size fraction are given in Table 1. The 63-125μm size is the most abundant. The respirable-size fraction represents the 8% of the bulk fly ash and was found to contain traces of unburnt lignite particles.

XRD analyses showed that calcite and anhydrite are major phases in all fractions between 5 and >500μm (Table 1). Quartz, melilites and portlandite decrease, while lime increases towards the smaller fraction of the above range. Feldspars, total clays, hatrurite, ettringite, gypsum and brownmillerite appear in minor/trace amounts in nearly all the above fractions, while bassanite and tobermorite are minor/trace detectable only in the coarser fractions.

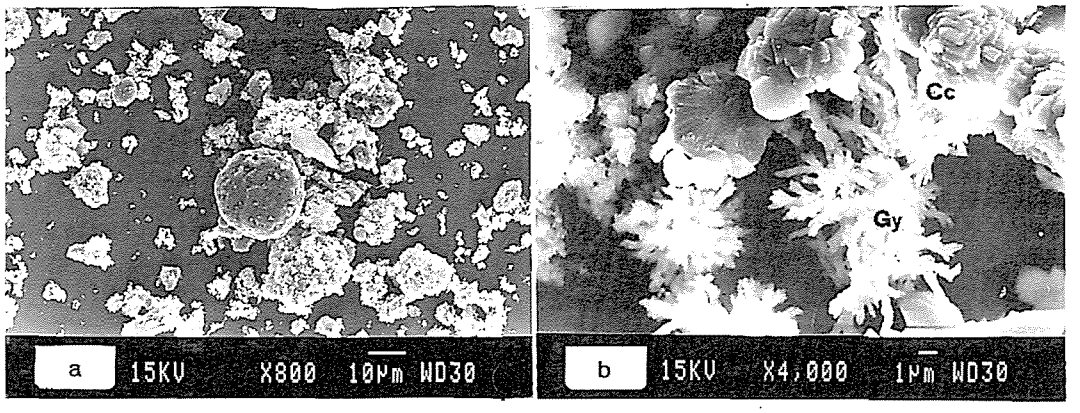

Fig. 1. SEM micrograph of the bulk fly ash (a) and its respirable-size fraction (b). Cc=calcite, Gy=gypsum.

Considerable mineralogical differences are observed in the respirable-size fly ash fraction, compared to the rest of the fly ash (Table 1): Anhydrite, lime, feldspars, hatrurite, portlandite, ettringite, bassanite, tobermorite and brownmillerite are no longer detectable, while calcite remains as a major phase and gypsum appears significantly enriched constituting also a major phase. Quartz and melilites are only minor/trace detected, while total clays remain as minor/trace phases.

Table 1. The mineralogy of the respirable- and not respirable-size fly ash fractions.

Fraction (μm)	<5	5-63	63-125	125-250	250-500	>500
wt%	8	29	44	15	3	1
Calcite	+M	+M	+M	+M	+M	+M
Quartz	+tr	+I	+I	+M	+M	+M
Feldspars	-	+tr	+tr	+tr	+I	+tr
Total clays	+tr	+tr	+tr	+tr	+tr	+tr
Anhydrite	-	+M	+M	+M	+M	+M
Lime	-	+M	+M	+M	+I	-
Melilites	+tr	+I	+M	+M	+M	+M
Hatrurite	-	+tr	+tr	+tr	+tr	+tr
Portlandite	-	+tr	+tr	+I	+I	+M
Ettringite	-	+tr	+tr	+tr	+tr	+tr
Gypsum	+M	+tr	+tr	+tr	+tr	+tr
Bassanite	-	-	-	+tr	-	+tr
Tobermorite	-	-	-	-	-	+tr
Brownmillerite	-	+tr	+tr	-	+tr	+tr

+M=present as major phase, +I=present as intermediate phase, +tr=present as minor/trace phase, -=not detected.

Table 2. The chemistry of the respirable- and not respirable-size fly ash fractions.

	fraction <5μm (wt%)	bulk fly ash (wt%)		fraction <5μm (ppm)	bulk fly ash (ppm)	det. limit (ppm)
SiO_2	2.30	29.90	Ba	138	354	2
TiO_2	0.03	0.71	Co	1.1	15	0.04
Al_2O_3	0.96	13.50	Cr	57	198	10
Fe_2O_3	0.28	5.47	Cu	3.5	56	0.04
MnO	0.00	0.05	La	<10	26	10
MgO	0.23	2.62	Nb	<5	14	5
CaO	55.91	32.40	Ni	7.4	140	0.4
K_2O	0.08	1.10	Sc	<2	11	2
Na_2O	0.08	0.54	Sr	360	325	1
P_2O_5	0.02	0.25	V	17	151	5
SO_3	12.25	7.87	Y	<2	28	2
LOI	26.96	4.73	Zn	21	74	1
Total	99.10	99.14	Zr	27	130	5

Scanning electron microscopy revealed that the samples of the bulk fly ash consist of irregularly shaped, oval and spherical particles of a varying size (Fig. 1a). The participation of spherical particles in the respirable-size fraction diminishes considerably. Calcite , with nearly isometrical grains and sponge-like gypsum crystals (Fig. 1b), are the dominant minerals in the respirable-size fraction.

Calcite being a constituent of the mined lignite, can be also recomposed by lime-CO_2 reaction and thus, is a major phase in all fractions. Gypsum was formed during soaking of the fly ash, at temperatures within the range of 42-200° C. Since soaking is a very quick process, gypsum grains are very small in size en-

riching thus the respirable-size fraction.

From Table 2 results that CaO and SO_3 are significantly increased in the respirable-size fraction, compared to the bulk fly ash, accounting for >60% of the major element oxide content, while SiO_2 considerably decreases. A more or less decrease is also observed for the other oxides. The chemical composition both of the bulk fly ash and its respirable-size fraction, is in good agreement with the corresponding mineralogical composition.

Concerning the trace elements, we could say that although some of them in the bulk fly ash composition exceed relatively the clark's of the earth (Fairbridge, 1972), e.g. Cr and Ni, the overall geochemical signatures of the Ptolemais lignite fly ash represent rather low levels of trace elements.

It is well known that high concentrations of some trace elements, e.g. Cr, Ni, Co and Ba are considered of high health risk. In this study, Ba, Co, Cr, Cu, La, Nb, Ni, Sc, V, Y, Zn and Zr are depleted in the respirable-size fraction compared to the bulk fly ash (as depleted elements we consider those whose ratios to the bulk fly ash concentrations are <0.5). Only Sr remains approximately in the same levels. The amount of Sr seems to be balanced by the constant presence of calcite in all fractions, compared to the other calcium-bearing phases.

Furthermore, we must not forget the potential health effects of inhaled minerals which may be responsible for a series of biological activities mainly due to their morphology and chemistry (Guthrie, 1992). Exposure to mineral dust for long periods may result in considerable lung diseases (e.g. pneumoconiosis, fibrosis and lung cancer). Of course human response relates to a number of factors (e.g. mineral species, exposure time, physical condition of the person).

From this study results that the morphology of the respirable-size fly ash (sponge-like particles of gypsum) might play a significant role on probable damage of the lung system. The trace elements concentrations, though ranging in low levels, might be of human health risk in cases of long exposure periods.

REFERENCES

Coles, D.G., Ragaini, R.C., Ondov, J.M., Fisher, G.L., Silberman, D. & Prentice, B.A. 1979. Chemical studies of stack fly ash from a coal-fired power plant. Environ. Sci. Technol. 13(4):455-459.

Fairbridge, R.W. 1972. The Encyclopedia of Geochemistry of Environmental Sciences, Encyclopedia of Earth Sciences Series, Van Nostrand Reinhold Co., New York.

Filippidis, A. & Georgakopoulos, A. 1992. Mineralogical and chemical investigation of fly ash from the Main and Northern lignite fields in Ptolemais, Greece. Fuel, 71:373-376.

Gay, A.J. & Davis, P.B. 1987. Some environmental aspects of coal fly ash. In: Volborth, A.(ed.) Coal science and chemistry. Elsevier, Amsterdam, pp221-243.

Gay, A.J. & von Rosenstiel, A.P. 1982. A study of the composition and morphology of fly ash from coal-burning installations. TNO Report CL 82/55.

Gay, A.J., Van Duin, P.J. & van den Burgh, N. 1984. A convenient method combining the morphological and chemical analysis of coal fly ash with particle size determination. Proc. 2nd Int. Ash. Tech. 84:9-12.

Georgakopoulos, A., Kassoli-Fournaraki, A. & Filippidis, A. 1992. Morphology, mineralogy and chemistry of fly ash from the Ptolemais lignite basin (Greece) in relation to some problems in human health. Trends in Mineralogy, 4p (in press).

Guthrie, G. 1992. Biological effects of inhaled minerals. Amer.Miner. 77:225-243.

Current Research in Geology Applied to Ore Deposits.Fenoll Hach-Alí, Torres-Ruiz & Gervilla(eds)(1993).ISBN 84-338-1772-8

THE Sb-Pb "SAN JOSE" MINE AT LANZUELA (TERUEL, SPAIN): AN EXAMPLE OF Pb-METASOMATISM

López-Ciriano, A.; Subías, I. & Fernández-Nieto, C.
Dept. de Cristalografía y Mineralogía, Universidad de Zaragoza, Zaragoza, Spain

ABSTRACT: The Sb-Pb mineralization at Lanzuela was formed by two main ore-forming phases and a final remobilization. During the phase 1, Sb-(As-Fe), stibnite was deposited; this phase was probably late Hercynian. The phase 2 (Pb-Zn-Ba) forming fluid dissolved and replaced the stibnite crystals and formed zinkenite; this process probably took place in Mesozoic times. The final remobilization caused the precipitation of semseyite. Therefore, the Sb-Pb "San José" deposit is probably a "metallogenetic superimposition" example.

INTRODUCTION

In the Iberian Mountain Range, the base metals (Pb, Zn, Cu) vein deposits are the most important ones. They are frequently associated with barite which is often benefited. These mineralizations are hosted by rocks whose ages range from the Cambrian to the Lower Cretaceous. The scarce antimony ore deposits in the Iberian Mountain Range are always located next to large deep-seated NW-SE basement fractures, formed or reactivated in late Hercynian times. These antimony ores are hosted by Cambrian to Westphalian sedimentary rocks.

GEOGRAPHICAL AND GEOLOGICAL SETTING

The "San José" abandoned mine is located 2,5 km eastward from Lanzuela (Teruel province, northeastern Spain). It is situated in the Iberian Mountain Range.

From a geological point of view, the "San José" mine is located in the northeastern paleozoic branch of the Iberian Chains, at about 100 m northward from the Datos fault, a large NW-SE fracture which is the southern boundary of the Cantabrian Zone belonging to the Iberian Massif in the Iberian Chains (Gozalo & Liñán, 1988). These major fracture was reactivated as a dextral wrench fault in late Hercynian times (related to calc-alkaline magmatism), as a normal fault during the Mesozoic and as a thrust during the Oligocene. The ore deposit is located in the periclinal end of a Hercynian NNW-SSE anticline which is overthrusted by the Cambrian along the Datos fault.

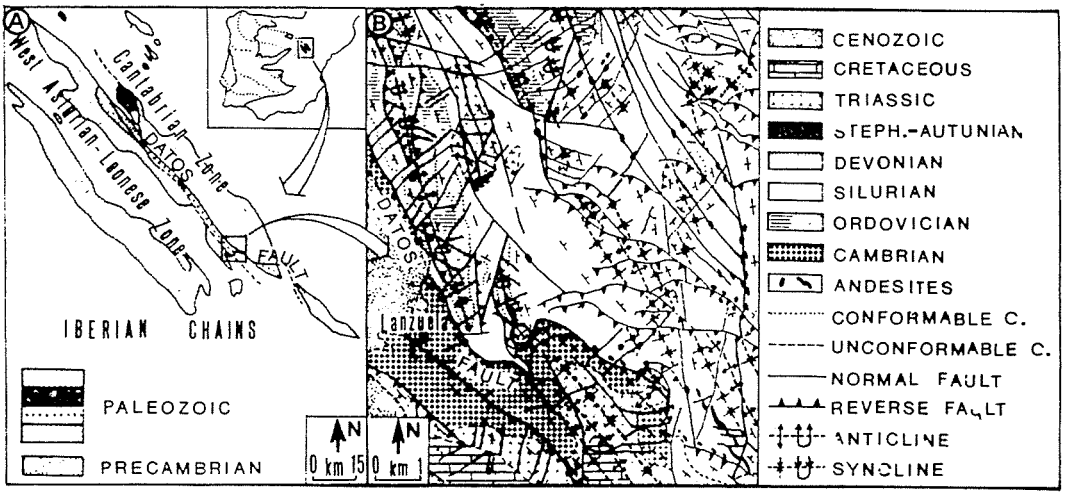

In the surroundings of the mine Lower Paleozoic materials, predominantly detritic, crop out and, resting unconformably on them, Stephanian-Autunian volcanoclastic deposits, Triassic rocks (in germanic facies) and Cretaceous ones appear. Southward to the Datos fault Cambrian occurs as an isoclinal sequence with southwestly dip. To the N of the quoted fault Ordovician, Silurian and Devonian rocks are strongly folded (Hercynian N-S to NNW-SSE axis and Alpine WNW-ESE to NW-SE ones) and fractured (NNW-SSE and NE-SW late Hercynian conjugated strike-slip faults, WNW-ESE to E-W and NNE-SSW to N-S post-Muschelkalk normal ones, and Alpine inverse faults and overthrusts, which are compatible with a NE-SW to NNE-SSW compression).

MORPHOLOGY

The mineralization is hosted by the Cystoid Limestone Formation, Ashgillian in age. At large-scale, its morphology may be considered as a discontinuous vein; nevertheless, it can be observed different ore ocurrences as described below. In the lower zone of the mine, the Sb-ores occur as disseminated stibnite related to a 5 m width sinistral 030,70E shear zone whose R (Riedel) fractures are filled by white spathic dolomite. This structure is cut by two narrow subvertical N-S fractures filled by Zn, Fe and Pb sulphides.

In the upper zone of the deposit, the mineralization occurs either as lenticular bodies making up by sulphosalts and sulphides or as millimetric to centimetric quartz (containing Pb, Zn, Cu sulphides) and barite veins. Both quartz and barite veins are hosted by a thick cataclastic dolomitic bed which is located at the top of Cystoid Limestones Formation. Moreover, the ore also appears as disseminated sulphosalts enclosed by cataclastic carbonatic fragments related to an inverse fault.

MINERALOGY

The determination of the mineralogy and paragenesis of the deposit has been carried out by means of X-ray Diffractrometry, Transmitted and Reflected light Microscopy and Electron Microprobe.

The host rock, Cystoid Limestone Fm., is mainly made up by dolomite; calcite and detritic minerals (quartz and muscovite) occur as minor constituents. The wall rock is highly recrystallized and is affected by the following hydrothermal alterations: silicification, pyritization, chloritization and argillitization.

The most important ore-minerals are zinkenite, semseyite, sphalerite and pyrite with minor stibnite, arsenopyrite, marcasite, chalcopyrite, galena, fülöppite, miargyrite and bournonite. Dolomite, quartz and minor barite are the gangue minerals. On the other hand, bindheimite, cerussite, goethite and malachite are the main minerals formed by meteoric alteration.

PARAGENESIS AND GENETIC DISCUSSION

The deposit sequence has been split into two principal ore-forming phases and a final remobilization:

At the beginning of the phase 1 minor amounts of arsenopyrite and pyrite crystallized before the deposition of the stibnite, which is the main ore of this stage. The ore-forming fluid caused a intensive host rock dissolution. At the end, the dissolved carbonate precipitated as big dolomite crystals, filling the shear zone Riedel extension joints quoted in the morphological description. This remobilization process has been confirmed by the host rock and dolomite REE patterns. The studied dolomite two-phase fluid inclusions yield Th from 55 to 85°C (mode 75°C). Eutectic temperatures below -21°C point out to the existence of several salts in solution. Total salinities of 5.5 % wt eq NaCl is deduced from last ice melting temperatures.

During the phase 2, quartz, pyrite, sphalerite and chalcopyrite was firstly deposited. The ore-forming fluid caused a partial pseudomorfic replacement of stibinite by high Sb/Pb ratio sulfosalts: zinkenite and fülöppite, and by miargyrite. It can be supposed that there was no external Sb batches since the

volume of the so formed sulphosalts do not surpass the volume of the replaced stibinite. Galena deposition took probably place when there has no Sb left in the ore-forming fluid. Barite is the latest formed mineral of this association. The quartz fluid inclusions are two-phase as those in dolomite. They have similar salinities (6.0 % wt eq NaCl) but clearly higher Th which range from 155 to 205°C (mode 185°).

Finally, a dissolution of the previous minerals took place due to an intensive fracturation episode; as a result of this process dolomite, sphalerite, low Sb/Pb ratio sulfosalts (bournonite and semseyite) and barite precipitated. A marcasitization of the pyrite occured, mainly in the upper zone of the mine. According to Moëlo (1982) the precipitation of semseyite and not of boulangerite suggests relatively low temperatures and it is characteristic of an epithermal process. This last stage has been considered as a remobilization process since a new chemical element supply does not seem necessary for the formation of the quoted minerals.

METALLOGENETIC CONSIDERATIONS

Both the phase 1, Sb-(As,Fe), mineralogical association and the physico-chemical characteristics of the ore-forming fluids for Lanzuela mine are similar to those which appear in other Sb deposits from Western Europe and Morocco (Munoz et al. 1992; Jaillard, 1980). On the other hand, the geological setting of studied deposit is also similar to many of the refered Sb-ores, especially to those from the Armorican Massif (Fouquet, 1980), i.e., it also occurs in a secondary fault close to a large deep-seated basement fracture that moved as dextral wrench fault in late Hercynian times. The striking and sense of movement of the phase 1 shear zone demand a NNW-SSE subhorizontal compression, that coincides with the late Hercynian strike-slip stage compression direction in the European Hercynian Belt (Arthaud & Matte, 1975). These all common features suggest that the phase 1 of the "San José" mine could belong to the "First ore-forming Cycle", as defined by Perichaud (1980). The Stephanian-Autunian calc-alkaline magmatism, mainly developed through large NNW-SSE and NE-SW fractures in the area, could favour the phase 1 formation.

If the deposit conditions had been favorable and the phase 2 ore-forming fluid had not found the phase 1 mineralization, it would probably have produced a classical base metal hydrothermal ore, with barite at the top, similar to those which occur in the Iberian Mountain Range, specially in the studied area. Some of the latter deposits are filling late Hercynian striking faults, but most of them are filling either N-S to NNE-SSW or E-W to WNW-ESE subvertical normal faults. The strikes of the latter faults are in agreement with the post-Muschelkalk faulting trend. Both the perpendicularity of these two fault systems and their big dip suggest a distensive regime. Capote (1983) points out that during the Mesozoic the Iberian Range domain evolved as an aulacogene whose rifting stage was controlled by the large late Hercynian faults striking. At the end of the Triassic times the more intensive thermal subsidence and the intrusion of alkaline magmas (ophites) took place (flexure stage).

On the other hand, the Triassic and Jurasic times are a very important metallogenetic period for the emplacement of Pb-Zn-Ba-F ores (p-pol association of Bernard, 1980) in the European Variscan Megazone. According to this author, in the Iberian Massif the p-pol association (220-190 m.y.) is represented by BGPC-ore type. Cardellach et al. (1990) point out a triassic age to the barite veins at the Catalonian Coastal Ranges. All these considerations suggest that the phase 2 fluid could be one of these BGPC type ore-forming solution, and therefore it probably belongs to the "Second ore-forming Cycle" (Perichaud, 1980).

If the proposed emplacement ages for both phases was confirmed, the Sb-Pb ore at Lanzuela would be thus a "metallogenetic superposition" Spanish example similar to the existing ones in France (Perichaud, 1980) and Central Morocco (Kosakevitch & Moëlo, 1978).

REFERENCES

Arthaud, F. & Matte, P. 1975. Les décrochements tardiherciniens du Sud-Ouest de l'Europe. Géométrie et essai de reconstitution des conditions de la déformation. Tectonophysics 25:139-171.

Bernard, J.H. 1980. Paragenetic units of the Variscan megazone. Freib. Forsch.H.-C Leipzig 352:55-117.

Capote, R. 1983. La tectónica de la Cordillera Ibérica. In: Comba, J.A. (ed.) Libro Jubilar J.M. Rios. Geología de España I, pp 513-529.

Cardellach, E.; Canals, A.; Tritlla, J. 1990. Late and post-Hercynian low temperature veins in the Catalonian Coastal Ranges. Acta Geol. Hispanica 25:75- 81.

Fouquet, Y. 1980. Les districts antimonifères de Quimper et du Cap Sizun (Finistère). Leur place dans la mètallogénie de l'antimoine dans le Massif Armoricain (France). Th. Doct. 3ème Cycle. Univ. Clermont-Ferrand, 227 pp.

Gozalo, R. & Liñán, E. 1988. Los materiales hercínicos de la Cordillera Ibérica en el contexto del Macizo Ibérico. Estudios Geol. 44:399-404.

Jaillard, L. (1980). Les gisements d'antimoine du champ minier de Kef-N'Sour (Maroc central). Chron. Rech. Min. 456:65-81.

Kosakevitch, A. & Moëlo, Y. 1978. Les mineralisations á antimoine du Massif hercynien de Maroc central: leurs paragenèses et leur place dans le cadre métallogénique régional. In: B.R.G.M. (ed.) Résume des principaux résultats scientifiques et techniques du Service Géologique National pour 1978. Orléans, pp 92-93.

Moëlo, Y. 1982. Contribution á l'étude des conditions naturelles de formation des sulfures complexes d'antimoine et plomb (sulfosels de Pb/Sb). Signification métallogénique. Th. Doct. D'Etat Sci. Nat. Univ. Paris VI, 624 pp.

Munoz, M.; Courjault-Rade, P.; Tollon, F. 1992. Physico-chemical and geodynamic constraints on genesis of masve stibnite veins in the southwestern european variscan belt. Act. III Cong. Geol. España 3:224-227.

Perichaud, J.J. 1980. L'antimoine, ses minerais et ses gisements. Synthèse gitologique sur les gisements du Massif central français. Chr. Rech. Min. 456:5-64.

Current Research in Geology Applied to Ore Deposits. Fenoll Hach-Alí, Torres-Ruiz & Gervilla (eds) (1993). ISBN 84-338-1772-8

RELATIONSHIPS BETWEEN TECTONICS AND BASE- AND PRECIOUS-METAL MINERALIZATION IN THE VERA-GARRUCHA AREA (S.E. SPAIN)

López-Gutierrez, J. (1); Martinez-Frías, J (2) & Lunar, R. (3)
(1) ITGE, Madrid, Spain
(2) IAGM, CSIC-Universidad de Granada, Granada, Spain
(3) Dept. de Cristalografía y Mineralogía, Universidad Complutense, Madrid, Spain

ABSTRACT: The comparison between the geo-structural organization and the metallogenetic characteristics of the base- and precious metal-deposits of the Vera-Garrucha area (SE Spain) suggests that they are forming part of a Basin and Range-type Province. In addition, it is proposed that the tectonic and mineralizing processes developed in this area could be extrapolated to other similar deposits which are also present in the South-Iberian Mediterranean border.

INTRODUCTION

The structural arrangement of some areas in the eastern Betic Cordillera (SE Spain) can be described as a simple series of Sierras and Basins trending ENE-WSW (e.g. the Vera-Garrucha area) (Fig.1). These areas are characterized by the interference of various tectonic episodes as well as by the presence of base- and precious-metal mineralization associated with volcanics, which were emplaced in various hydrothermal stages during the Neogene-Quaternary. This recent volcanic activity is especially important inside the basin zones (e.g. Vera-Garrucha basin, and Cabo de Gata area), probably as a consequence of their greater crustal thinness. In fact, these two areas are the main places where volcanics crop out.

METALLOGENY IN THE VERA-GARRUCHA BASIN

The Vera-Garrucha basin is bounded to the NW. by Sierra de Almagro, to the W. by Sierra de Bedar, to the S. by Sierra Cabrera and to the E by Sierra Almagrera (Fig.1). Volcanism bearing base- and precious-metal mineralization in the Vera-Garrucha Basin can be grouped as: 1) deep-sea hydrothermal deposits rich in Fe, Mn, Ag and base metal sulphides ("black smoker-type") (Herrerías area) which are associated with Upper Miocene marine sediments (Martínez Frías et al, 1992), and 2) Pb-Zn-Cu-Fe-Sb-(±Ag) hydrothermal veins rich in base metal sulphides and silver sulphosalts, which cut Permian-Triassic phyllites and schists (metamorphic basement, Sierra areas) (Martínez Frías et al, 1989, Martínez Frías, 1991). Mineralization in these areas possesses very similar characteristics (tectonic control, mineralogy, paragenetic sequences, hydrothermal alterations, temperatures etc) in spite of that the morphology of the deposits is different (dissemination and stratabound ores in the basin, and of vein-type in the surrounding Sierras).

From a regional tectonic point of view, Doblas & Oyarzun (1989) suggest the existence of an extension period, of Upper Miocene age, for the Neogene Alpine Almería region of southeastern Spain, that they explain as a consequence of the gravitational collapse of the Betic Orogen toward SSE. Later on, the Pliocene compressive events (Sanz de Galdeano, 1990) transformed the whole set due to the first movements of the great strike - slip faults of the Eastern Betics (e.g. Lorca Fault, Palomares Fault, Cádiz-Alicante Fault). This last

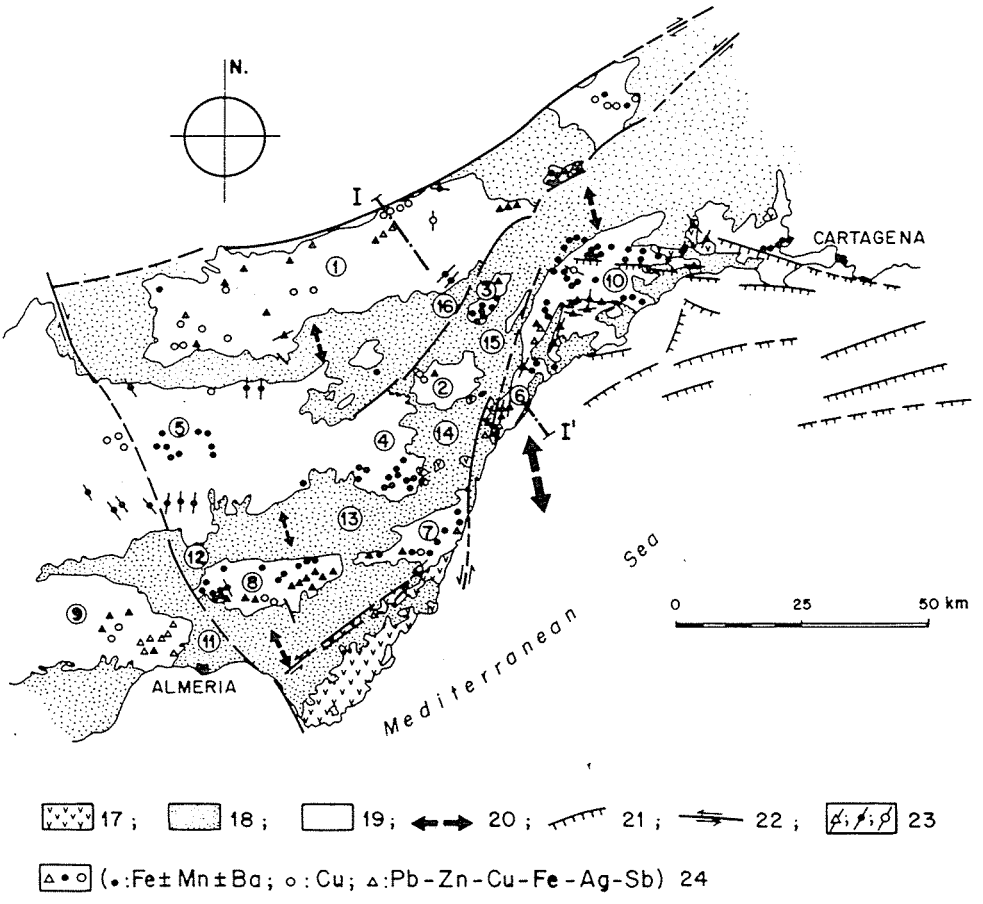

Fig.1.- Geo-structural organization of "Basin and Range-type" in the Eastern Betic Cordillera.

1: Sierra de las Estancias, 2: Sierra de Almagro, 3: Sierra de Enmedio, 4: Sierra de Bédar, 5: Sierra de Filabres, 6: Sierra Almagrera, 7: Sierra Cabrera, 8: Sierra Alhamilla, 9: Sierra de Gador, 10: Sierra Almenara, 11: Almería Basin, 12: Tabernas Basin, 13: Sorbas Basin, 14: **Vera-Garrucha Basin**, 15: Pulpi Basin, 16: Huercal Overa Basin, 17: Neogene volcanism, 18:Neogene Basins, 19: Sierras ("Nevado-Filábride" and/or "Alpujárride" materials), 20: Neogene extension, 21: Neogene normal faults, 22: Pliocene-Pleistocene strike-slip faults, 23: vein-type mineralization, 24: Other mineral deposits (indeterminate morphology). I-I': interpretative cross section (see figure 2).

event is specially important in two concrete areas (basins of Vera-Garrucha and Pulpi) (Fig.2), as they were clearly affected by the Lorca and Palomares wrench faults. These two faults lengthened the basins to NNE, and generated a shear zone between them. The stress régime (transpression-transtension) inside this shear zone (López Gutiérrez et al, 1992) conditioned that small pieces of basin get separated as fault controlled-troughs.

We interpret that a "Basin and Range-type" model can be proposed in the Vera-Garrucha area to explain both the morphology of high zones (Sierras) and depressed zones (basins) and the structural relationships between the volcanic and mineralizing processes. For instance, Las Herrerías trough inside the Vera-Garrucha Basin, is controlled by both NNE-SSW and N150E normal faults and WNW-ESE wrench reverse faults (Fig.2). Likewise, the model of fluid circulation proposed by Martínez Frías et al, (1993, *this SGA Meeting*) for the convective hydrothermal system "Las Herrerías-Sierra Almagrera-Sierra Almenara" fits well this structural scheme of Basin and Range Province. According to this model, the Sierras act as recharge zones for meteoric waters while the discharge takes place in the basin zones, where a mixture of meteoric, marine and magmatic waters occurs. The convective movements of the mineralizing fluids (Fig.2) would be conducted by the Upper Miocene magmatic source of shoshonitic character (López Ruiz & Rodríguez Badiola, 1980) which, as previously defined, is spatially and temporally associated with the base- and precious-metal deposits.

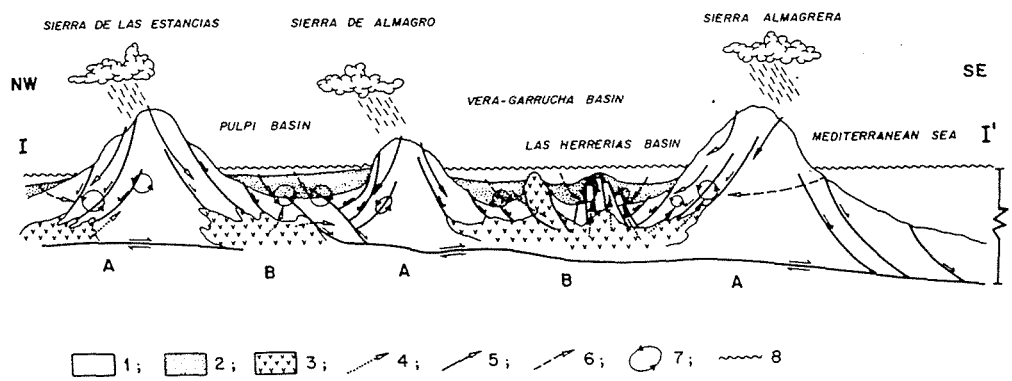

Fig.2.- Interpretative cross section (I-I') (see figure 1), which represents the geo-structural disposition during the Upper Tortonian - Messinian (vertical scale is overstated).

1: "Nevado-Filábride" and/or "Alpujárride" basement
2: Neogene sediments
3: Volcanics
4: Magmatic waters
5: Meteoric waters
6: Marine waters
7: Groundwater convective cells
8: Sea level

Finally, it is important to take into account that Oyarzun et al (1992) also suggest this type of tectonic model to describe the structural evolution of the nearby mineralized district of Rodalquilar (Cabo de Gata area).

So, considering the data described above, our hypothesis is the following: The relationships between mineralizing hydrothermal processes, volcanism and tectonics, which have been well described in the Vera-Garrucha area, could have a more regional character. Thus, the model of Basin and Range-type Province could be also used, at least in part, to explain both the structural organization and the relationships between the other similar deposits which occur in SE Spain.

ACKNOWLEDGEMENTS

This work forms part of the research project AMB92-0408 and it was completed in cooperation with IGCP Project 318 (IUGS/UNESCO) and with the Spanish Working Group on Geology and Metallogeny of Hydrothermal Seafloor Deposits.

REFERENCES

Doblas, M. and Oyarzun, R. 1989. Neogene extensional collapse in the western Mediterranean (Betic-Rif Alpine orogenetic belt): Implications for the genesis of the Gibraltar Arc and magmatic activity. Geology, 17: 430-433.

López Gutiérrez, J., Martínez Frías, J., Lunar, R. and López García, J. 1992. Geología y control tectónico de la mineralización hidrotermal submarina de Herrerías (Cordilleras Béticas). Com. III Cong. Geol. Esp. and VIII Cong. Lat. Geol. T.3: 181-186.

López Ruiz, J. & Rodríguez Badiola, E. 1980. La región volcánica neógena del sureste de España. Estudios Geológicos, V.36: 1-63.

Martínez Frías, J., García Guinea, J., López Ruiz, J., López García, J.A. and Benito, R. 1989. Los yacimientos epitermales de Sierra Almagrera y de la cuenca sedimentaria de Herrerías (Cordilleras Béticas). Rev. Soc. Esp. Min. V.12: 261-271.

Martínez Frías, J. 1991. Sulphide and sulphosalt mineralogy and paragenesis from the Sierra Almagrera veins, Betic Cordillera. Estudios Geol., 47 (5-6): 271-279.

Martínez Frías, J.; García Guinea, J.; López Ruiz, J. y Reynolds, G.A. 1992. "Discovery of fossil fumaroles in Spain". Economic Geology, 87: 444-446.

Oyarzun, R., Doblas, M. and Lunar, R. 1992. "Unconventional regional targets" for the exploration of precious epithermal deposits: An extensional tectonic model. (Abstract). 29th International Geological Congress. Kyoto, Japan. V.3: 771.

Sanz de galdeano, C. 1990. Geologic evolution of the Betic Cordilleras in the western Mediterranean, Miocene to the present. Tectonophysics, 172:107-119.

Current Research in Geology Applied to Ore Deposits.Fenoll Hach-Alí, Torres-Ruiz & Gervilla(eds)(1993).ISBN 84-338-1772-8

FORMATION OF HYDROTHERMAL FLUORITE DEPOSITS IN THE SOUTHERN BLACK FOREST (S.W. GERMANY). PART II: GEOCHEMICAL FEATURES

Lüders, V. (1) & Franzke, H.J. (2)
(1) GeoForschungZentrum Potsdam, Telegrafenberg A50, 1561 Potsdam, Germany
(2) Geological Inst. TU Clausthal, Leibnizstr. 10, 3392 Clausthal-Zellerfeld, Germany

ABSTRACT: The development of vein systems in the southern Black Forest can by traced back to Hercynian times. During the Mesozoic, extensional tectonics caused first opening of the veins and penetration of NaCl brines from Triassic evaporites into deeper crustal levels where they equilibrated with crystalline rocks of the basement. Due to the late Mesozoic uplift of the basement the structures extended and high-temperature high-salinity F-Ba-bearing brines ascended and deposited fluorite at higher vein levels along with cooling. Decreasing temperature during fluid migration caused oxydation of Eu^{2+} in the parental fluid and coprecipitation with fluorite, thus leading to positive Eu anomalies in most of the REE patterns. Subsequently, barite was deposited by mixing of the ascending brine with SO_4^{2-}-rich solutions from the residual evaporite of the Mesozoic cover.

1. INTRODUCTION

In the last 40 years, geochemical investigations of ore and gangue minerals have revealed that the genesis of the hydrothermal vein deposits of the Black Forest cannot be uniquely related to a single mineralizing event. The evolution of fluid regimes and the deposition of differently composed mineralizations within the Black Forest are strongly related to the development and activation of the vein systems of the area (Franzke & Lüders, ibid.). Variscan mineralizations in the southern Black Forest such as quartz-scheelite within the Badenweiler-Lenzkirch zone (#11 in Fig.1, Franzke & Lüders, ibid.) or uranium (Krunkelbach deposit #10 in Fig.1 Franzke & Lüders, ibid.) precipitated from low-salinity fluids and are related to late Variscan shear zone tectonics (Werner et al., 1990) or regional fluid circulation caused by a regional high heat flow, respectively (Hofmann & Eikenberg, 1991).
The majority of the mineral deposits in the southern Black Forest (e.g. #6, #7, #8, #9, #12 in Fig.1 Franzke & Lüders, this issue) is of post-Variscan age as shown by numerous radiometric datings of different minerals. A compilation of radiometric datings is given by v. Gehlen (1987). The fluid systems from which post-Variscan mineralizations of central Europe precipitated can also be clearly distinguished from those which deposited the Variscan mineralizations. Numerous investigations of fluid inclusions have shown that the majority of post-Variscan mineralizations were deposited by highly-saline brines (Behr et al., 1987). Detailed geochemical investigations focusing on the Mesozoic fluorite-(barite) mineralization of the southern Black Forest have been performed in order to develop a minerogenetic model in accordance with the regional tectonic evolution.

2. RESULTS

2.1. REE distribution patterns of fluorites

Several profiles across fluorite veins have been sampled, and analysed by ICP-MS. The European Shale-normalized REE distribution patterns of fluorite from different occurrences in the southern Black Forest are very similar (Fig.1). Small variations can only be observed for the LREE and Eu. Fluorites which precipitated first, show more or less flat patterns without significant Eu anomalies

similar to those of locally preceding calcite mineralization (Fig. 1a). Fluorites from the more central parts of the veins show HREE values similar to the older fluorites but decreasing LREE values and positive Eu anomalies (Fig. 1b).
REE distribution patterns of fluorites from veins which are hosted by gneisses (such as # 7-9 in Fig. 1 (Franzke & Lüders, this issue)) do not differ significantly from those of fluorite veins hosted by less fractionated granites (#12 in Fig. 1 Franzke & Lüders, this issue).

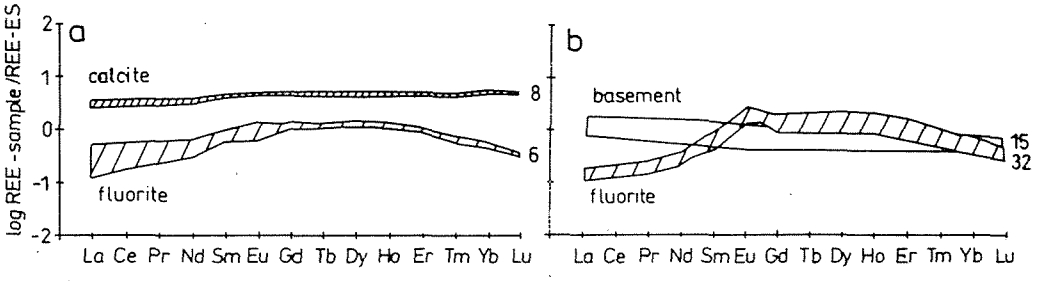

Fig. 1: REE distribution patterns of calcites and early fluorite (a) Gottesehre (# 9 in Fig. 1) and fluorites of the main fluorite stage (b) Wieden district (# 8 in Fig. 1). The light hatched band in Fig. 1b represents REE distribution patterns of gneisses and less-fractionated granites of the southern Black Forest. (Localities refer to Fig. 1 Franzke & Lüders, this issue).

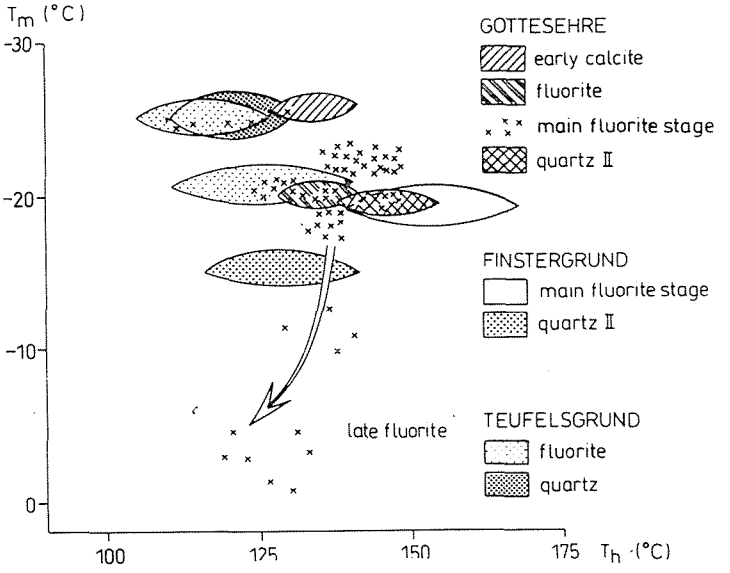

Fig. 2: Ice melting (T_m) vs. homogenization temperatures (T_h) of fluid inclusions in fluorites and other gangue minerals from Mesozoic fluorite veins from the southern Black Forest. Key to localities: Teufelsgrund (# 7), Finstergrund (Wieden district # 8), Gottesehre (# 9). Locality numbers refer to Fig. 1 (Franzke & Lüders, this issue).

2.2. Fluid inclusion studies

Excluding barite, minerals of the Mesozoic mineralization of the southern Black Forest always contain 2-phase fluid inclusions (FI) with an aqueous solution and a vapour bubble at room temperature. The liquid/vapour ratios of these FI is very consistent (about 95:5). Barite only contains liquid inclusions.
FIs in fluorite are different in shape and size. Primary FI occur in growth zones and are about 30 up to 120 µm in size, with either irregular or negative crystal shape. In contrast, secondary FI in fluorite are smaller (5 to 35 µm) and have rounded to elongated forms.
Fluorite as well as other Mesozoic mineralizations (e.g., Pb-Zn-Ba veins, Behr et al., 1987) of the area precipitated from highly-saline brines at temperatures below 200°C (Fig.2). Traces of gas such as CO_2, CH_4, H_2S etc. were not detected microthermometrically in FI contained in the investigated samples of calcite, fluorite and quartz. It is conspicuous that towards the end of the fluorite stage the salinity of the FI decreases (Fig.2). Liquid inclusions contained in the subsequent barite mineralization point to salinities between 5 and 15 wt.% NaCl equivalent.

3. DISCUSSION

The ES-normalized REE distribution patterns of fluorites (and calcites) indicate a deep homogeneous crustal source of the mineral-forming fluids. Calcite and early fluorite show patterns which are very similar in their trend compared with those of gneisses and authochtonous granites of the basement (Fig.1b). The observed positive Eu anomalies in the patterns of fluorites from the main stage indicate that Eu was in the trivalent stage during fluorite precipitation because Eu^{2+} is more likely to follow large ions such as Sr^{2+} during fluorite crystallization, consequently resulting in negative Eu anomalies. The positive Eu anomalies are best explained by changes of the P-T-X conditions in the fluids at higher vein levels. In high-temperature fluids, even at fO_2 close to the hematite-magnetite buffer, Eu^{2+} dominates over Eu $^{3+}$ (Bau, 1991). Since remobilizations at high temperatures always cause partial thermochemical Eu reduction, Eu^{2+} becomes enriched in the ascending fluids due to the fact that Eu^{2+} is less sorbed than Eu^{3+}. Consequently, fluorite (and other Ca-minerals) derived from fluids that mobilized REE at elevated temperatures (> 250°C) show REE patterns with either a positive Eu anomaly provided that Eu^{2+} was re-oxydized with decreasing temperature prior to fluorite precipitation or a negative anomaly if crystallization occurred at high temperatures (Bau & Möller, 1992). The widely distributed patterns with a positive Eu anomaly of fluorites from the southern Black Forest indicate that re-oxydation of Eu^{2+} must have occurred during fluid migration from the source of the parental fluids into higher vein levels, most probably induced by decreasing temperature.
The extreme salinity of fluid inclusions in fluorite indicates chlorinities of about 120 to 160 g Cl^-/l (Lüders & Möller, 1992) of the parental fluids. Such chlorinities cannot be explained by chloritization of biotite even at low water-rock ratios and long-term equilibration (max. 100 g Cl^-/l). Therefore, it is more plausible that Cl^- was derived from evaporites. Since the middle Triassic (Muschelkalk) the Black Forest was covered by an evaporitic sequence. Extensional tectonics caused opening of the vein systems and allowed NaCl-rich brines from the Mesozoic cover to penetrate into deep crustal levels where they equilibrated with rocks of the crystalline basement. Intensive water-rock interactions caused chloritization of biotites and albitization of plagioclase and the release of Ca^{2+}, Ba $^{2+}$, F^-, REE and other metal ions (Fig.3a).
The uplift of the basement in late Mesozoic times caused the opening of the vein structures, re-ascending of the brines into higher vein levels, and precipitation of fluorite by cooling of the fluids. Towards the end of the fluorite stage SO_4^{2-}-rich fluids originating from residual Triassic evaporites

mixed with the ascending brines, and barite precipitated (Fig.3b). Decreasing salinity of fluid inclusions in barite and $\delta^{34}S$ values in the range of 8.3 to 16.8 $^{o}/_{oo}$ (von Gehlen, 1987) are in good agreement with the assumption of a near-surface sulfate source.

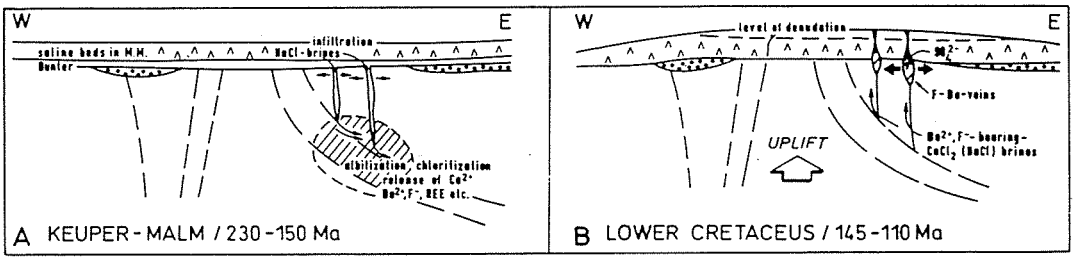

Fig. 3: Geotectonic-minerogenetic model of the southern Black Forest indicating the origin of the mineral-forming fluids.-A) Infiltration of NaCl-rich fluids during the late Triassic to late Jurassic. -B) Uplift and formation of hydrothermal fluorite deposits in the Lower Cretaceous (for details see text).

REFERENCES

Bau, M. 1991. Rare-earth element mobility during hydrothermal and metamorphic fluid-rock interaction and the significance of the oxidation state of europium. Chem. Geol. 93:219-230

Bau, M. & Möller, P. 1992. Rare earth element fractionation in metamorphogenic hydrothermal calcite, magnesite and siderite. Mineralogy and Petrology. 45:231-246

Behr, H.-J., Horn, E.E., Frentzel-Beyme, K. & Reutel, C. 1987. Fluid inclusion characteristics of the Variscan and post-Variscan mineralizing fluids in the Federal Republic of Germany. Chem. Geol. 61:273-285

Franzke, H.J. & Lüders, V. ibid.. Formation of hydrothermal fluorite deposits in the southern Black Forest (SW Germany): Part I - Structural control

Gehlen, K. v. 1987. Formation of Pb-Zn-F-Ba mineralizations in SW Germany a status report. Fortschr. Min. 65:87-113

Hofmann, B & Eikenberg, J. 1991. The Krunkelbach uranium deposit, Schwarzwald, Germany: correlation of radiometric ages U-Pb, U-Xe-Kr, K-Ar, ^{230}Th-^{234}U) with mineralogical stages and fluid inclusions. Economic Geology. 86:1031-1049

Lüders, V. & Möller, P. 1992. Fluid evolution and ore deposition in the Harz Mountains (Germany). Eur. J. Mineral. 4:1053-1068

Schürenberg, H. 1957. Die Blei-Zinkergänge des Südschwarzwaldes. In: Metz, R., Richter, M. & Schürenberg, H.: Die Blei-Zinkerzgänge des Südschwarzwaldes. Geol. Jb. 29:33-188

Werner, W., Schlaegel-Blaut, P. & Riecken, R. 1990. Verbreitung und Ausbildung von Wolfram-Mineralisationen im Kristallin des Schwarzwaldes. Jh. geol. Landesamt Baden-Würtemberg, 32:17-61

Current Research in Geology Applied to Ore Deposits.Fenoll Hach-Alí, Torres-Ruiz & Gervilla(eds)(1993).ISBN 84-338-1772-8

NEW DATA ON THE MIOCENE, FUMAROLIC HOT-SPRING SYSTEM OF HERRERIAS (BETIC CORDILLERA, S.E. SPAIN)

Martínez-Frías, J.
Instituto Andaluz de Geología Mediterránea (CSIC-Universidad de Granada), 18002 Granada, Spain

ABSTRACT: The Miocene, fumarolic hot-spring system of Herrerías is an interesting example of seafloor hydrothermal chimneys, and it constitutes a perfect natural laboratory to study the relationships between tectonics, mineralizing processes and volcanism. Mineralogy and geochemical distribution patterns in the fumarolic vents have been defined, and data obtained point out to its probable genetic association with the underlying Fe-Mn-Ag deposit of Herrerías.

INTRODUCTION

Much has been written on ancient and active hydrothermal systems at different seafloor environments over the past ten years. The present contribution offers new data on the fossil fumarolic, hot-spring field recently discovered in Spain, at the Fe-Mn-Ag seafloor hydrothermal deposit of Herrerías (Betic Cordillera) (SE Spain) (Martínez Frías et al, 1992). The fumaroles, which are similar to the black smoker-type structures from the East Pacific Rise, 21°N provide direct evidence of recently active geothermal processes (Upper Miocene), which presumably led to the formation of the Herrerías deposit and appear to be related in space and time to the Neogene volcanism in this area. Moreover, to our knowledge, these fossil fumaroles are the best examples in Europe of this type of structures.

GEOTECTONIC SETTING, AND CHARACTERISTICS OF THE FUMAROLE STRUCTURES

According to Martínez Frías et al (1992), the fumarole field is located between two faults, which bound the Herrerías trough, within the Neogene Vera basin (Almería, southeast Spain), and it extends, on the surface, over an area of approximately 130 m north-south by 10 m east-west. The sedimentary sequence of the Herrerías trough (sandstones, limestones, exhalites, sandy marls, and conglomerates) has been well described by Alvado (1986), although light modifications were added by Martínez Frías et al (1989), relative to the incidence of the hydrothermal process on these sediments. The Tortonian marine sediments are the host rocks of the Herrerías mineralization and the Messinian sandy marls constitute the substrate in which the fumarole chimneys occur. Laterally, these sandy marls pass to be alteration zones rich in quartz and alunite. Small conduits of millimetric size have been also detected in the Tortonian exhalites, which resemble the pyrite chimneys described by Boyce et al (1983) from the Silvermines deposit (Ireland). In relation with the local tectonics, the position of the fumarole field corresponds, exactly, to narrow zones of scape of fluids which are located along extensional faults with strikes N-S and N150°E (López Gutiérrez et al, 1992).

Mineralogy of the fumarole structures is represented by the occurrence of primary calcite and quartz (as main mineral phases

which constitute the composition of the sandy marls), as well as by other new minerals generated, probably, under the influence of the hydrothermal process: idiomorphous crystals of quartz, amorphous silica, Fe oxides and hydroxides, sulphates, carbonates, micas, native silver, and gold and silver sulphides and sulphosalts. Some of these minerals can be considered as the result of the simple alteration of the marls taking into account the addition of new chemical elements from the hydrothermal solution (e.g. sericite, cerusite, anglesite), while the remaining ones would represent new mineral phases (e.g. native silver, goethite, calaverite, pyrargyrite). Calcite and quartz were found in all the samples studied as major minerals. Minor and trace minerals (moscovite, goethite, spangolite, cerussite, dyscrasite, hetaerolite, anglesite, hausmannite, cobaltoan pickeringite, pyrargyrite and calaverite) only were detected along the cross sections of these fumarole structures (from the center orifice to the outer ring). However, in vertical section, their composition only consist of calcite and quartz.

Geochemical features of the fumaroles do not differ from those of the sandy marls substrate. Nevertheless, chemical distribution patterns reflect certain significative tendencies: 1) *from the central orifice to the outer ring*: Fe against As presents a contrary distribution trend, ranging from 0.88 to 10.76% and from 3 to 27 ppm, respectively; a similar case can be described for Cd against Ag (Cd:0.3-2.6 ppm and Ag:0.2-0.9 ppm), 2) *from top to bottom*: the chemical distribution patterns of these fumarolic chimneys are very homogeneous. Only Na presents a light variation from 0.05 to 0.46 ppm.

HYDROTHERMAL PROCESS AND MINERALIZATION

Volcanics: In Herrerías, volcanism appears to be as responsible, at least in part, for the hydrothermal fluids. The volcanic formation consists of domes and lavas of shoshonitic nature which outcrop westernwards from the Herrerías mine. According to López Ruiz and Rodríguez Badiola (1980) these rocks present high contents of K_2O, TiO_2, P_2O_5, uncompatible trace elements, and Sc, V, Cr, Co and Ni. Their isotopic ratio $^{87}Sr/^{86}Sr$, and their $\delta^{18}O$ values are also high (0.709 and from +13.88 to +15.1, respectively) (Hertogen et al, 1985; López Ruiz & Wasserman, 1991). Moreover, Alvado (1986) describes zones in these same volcanic rocks with a whitish colour and a powdery texture, which he ascribes to fumarolic alteration.

Time: The maximum duration of the mineralizing hydrothermal process is limited, in the Herrerías area, to between the Upper Tortonian and the Upper Messinian (the shoshonitic and ultrapotassic volcanism of the Vera district occurred between 7.6 and 8.6 m.y.b.p. (Nobel et al. 1981)). This lifetime can be considered as normal (Criss, 1991), because data on fossil hydrothermal systems demonstrate their great variance in size and longevity

Size and Location: Black smoker mineralization is commonly spatially restricted to a relatively small area, centered around the discharge site which is often located at intersections of fracture zones. These dimensions coincide with the size of both the deposit and the

fumarole field (at the surface, the area of the fumarole field is ≈ 1300 m^2 and the area corresponding to the Herrerías deposit is ≈ 1.5 km^2). In addition, as previously defined, its location corresponds exactly to intersection of faults with strikes N-S and N150°E (López Gutiérrez et al, 1992).

Temperature: Analyses of fluid inclusions in late barite which cuts the top mineralized layers of the Herrerías deposit, just under the fumaroles, indicate temperatures between 230-250°C (Martínez Frías et al, 1989). New data (in preparation at present moment) indicate, however, that, in a first stage, the temperature of the fluids was higher than 300°C.

Hydrothermal system and mineralization: Taking into account the morphology and the geotectonic setting of the fumarole field, as well as the shape of the vent structures, the hydrothermal system developed in this area appears to fit the model of "convection through crack zones" (Strens & Cann, 1982). In the case of Herrerías, at the period of time in which the hydrothermal process took place (Upper Tortonian-Upper Messinian), the depositional environment was marine with a depth of aprox. 200 m. Within this physical setting of the hydrothermal process, and in accordance with the paragenesis of the Herrerías deposit, the rapid decrease of temperature and the pH change, which are bound to occur at discharge, would propably tend to favor rapid sulphide precipitation (sphalerite, galena and pyrite) from solutions which were already supersaturated by adiabatic expansion during ascent. Oxidation during discharge of a fraction of the Fe and Mn dissolved in the hydrothermal fluids would cause deposition of oxide-hydroxides in the vicinity of the vents, giving rise to the ferromanganese crusts and pipes, which are located just under the fumaroles. Finally, clogging tends to self-seal leakage from the crack zone directly under the vents.

So, in accordance with this depositional system, and attending to the Bonatti (1983) classification, both the geothermal field and the Herrerías deposit appear to have formed in undersea environment, in accordance with a syn-discharge hydrothermal system. Ba, Fe, Mn, Ag and minor base metal sulphides would form part of very concentrated solutions, by which mineral deposition took place close to the hydrothermal vents probably under a relatively short residence time in sea water of these elements. The hydrothermal process continued until after the deposition of the Messinian sandy marls, although with very much reduced mineralizing capacity.

ACKNOWLEDGEMENTS

This work forms part of the research project AMB92-0408 and it was completed in cooperation with IGCP Project 318 (IUGS/UNESCO) and with the Spanish Working Group on Geology and Metallogeny of Hydrothermal Seafloor Deposits. The author thanks to Prof. Steven E. Kesler his help and suggestions about the fumaroles. Thanks also to Profs. James R. Hein, Barrie Bolton and Steven D. Scott for sending me very interesting references about this type of hydrothermal processes.

REFERENCES

Alvado, J.C. 1986. Sédimentation et manifestations magmatiques néogénes associés au coloir de décrochement de Palomares: Bassin de Vera (Sud-Est de l'Espagne). Unpub. Sc. thesis, Mem. Sc. Terre, Paris, Univ. Pierre and Maria Curie, 232 p.

Bonatti, E. 1983. Hydrothermal Metal Deposits from the oceanic rifts: A classification". In: Rona, P.A., Boström, K., Lambier, L., and Smith, K.L. eds. 1983: Hydrothermal processes at seafloor spreading centers. Plenum Press, 796 p.

Boyce, A.J., Coleman, M.L. and Russell, M.J. 1983. Formation of fossil hydrothermal chimneys and mounds from Silvermines, Ireland. Nature, V.306: 545-550.

Criss, R.E. 1991. Association of ore deposition with oxygen isotope anomalies in the Earth's crust, with particular reference to zones of high ^{18}O gradients. In: GSA 1991 Annual Meeting, San Diego (Abstract), p.A30.

Hertogen, J., López Ruiz, J., Rodríguez Badiola, E., Demaiffe, D. and Weiss, D. 1985. Petrogenesis of ultrapotassic volcanic rocks from SE Spain: Trace elements and Sr-Pb isotopes. Terra Cognita, 5: 215-216.

López Gutiérrez, J., Martínez Frías, J., Lunar, R. and López García, J. 1992. Geología y control tectónico de la mineralización hidrotermal submarina de Herrerías (Cordilleras Béticas). Com. III Cong. Geol. Esp. and VIII Cong. Lat. Geol. T.3: 181-186.

López Ruiz, J. & Rodríguez Badiola, E. 1980. La región volcánica neógena del sureste de España. Estudios Geológicos, V.36: 1-63.

López Ruiz, J. and Wasserman, M.D. 1991. Relaciones entre la hidratación/desvitrificación y el ^{18}O en las rocas volcánicas neógenas del SE de España. Estudios Geológicos, 47: 3-11.

Martínez Frías, J., García Guinea, J., López Ruiz, J., López García, J.A. and Benito, R. 1989. Los yacimientos epitermales de Sierra Almagrera y de la cuenca sedimentaria de Herrerías (Cordilleras Béticas). Rev. Soc. Esp. Min. V.12: 261-271.

Martínez Frías, J., García Guinea, J., López Ruiz, J. and Reynolds, G.A. 1992. Discovery of fossil fumaroles in Spain. Scientific Communications. Economic Geology, Vol.87: 444-446.

Nobel, F.A., Andriessen, P.A.M., Hebeda, E.H., Priem, H.N.A. and Rondell, H.E. 1981. Isotopic dating of the post-alpine Neogene volcanism in the Betic Cordillera, southern Spain. Geol. Mijnbouw. V.60: 209-214.

Strens, M.R. & Cann, J.R. 1982. A model of hydrothermal circulation in fault zones at mid-ocean ridge crests. Geophys. J.R. Astron. Soc., 71: 225-240.

Current Research in Geology Applied to Ore Deposits. Fenoll Hach-Alí, Torres-Ruiz & Gervilla (eds) (1993). ISBN 84-338-1772-8

PRELIMINARY MODELLING OF THE "HERRERIAS-ALMAGRERA-ALMENARA" CONVECTIVE HYDROTHERMAL SYSTEM (BETIC CORDILLERA, SPAIN)

Martínez-Frías J. (1); Navarro A. (2); Font X.(3) & Viladevall M. (3)
(1) IAGM (CSIC-Universidad de Granada) Granada, Spain
(2) ETSEIT (UPC), Tarrasa, Spain
(3) Dept. Geoquímica, Petrología y Prospección Geológica, Universidad de Barcelona, Spain

ABSTRACT: The epithermal mineralizations of Herrerías-Almagrera-Almenara are genetically related to the Miocene volcanism. These deposits form part of a hot spring-type, hydrothermal system, whose convective cells are fed by meteoric or magmatic waters (depending on the their geotectonic situation). The hydrodynamic model is based on: 1) the numerical simulation of regional groundwater flow, and 2) the theoretical estimation of the hydrothermal process.

INTRODUCTION

The Herrerías-Almagrera-Almenara (HAA) deposits are located in the eastern border of the Betic Cordillera, just in the central part of a wide volcano-tectonic and metallogenetic belt, which extends from Cabo de Gata to Sierra de Cartagena. The host rocks in Herrerías are marine sediments, of Upper Miocene age, while the Almagrera and Almenara mineralizations are placed in the metamorphic basement. In broad terms, their parageneses consist of Fe-Mn oxides and hydroxides, Ba and Fe sulphates, quartz, native gold and silver, base metal sulphides and silver sulphosalts, and the ore mineral deposition occurred in, at least, three paragenetic stages (Martínez Frías, 1991). The HAA deposits are genetically associated to the regional, Neogene volcanism, of shoshonitic character (Martínez Frías et al, 1989, Navarro et al, 1992, Martínez Frías et al, 1992).

The epithermal ore deposits of "hot spring" type are generally related to convective hydrothermal systems. In our case, a theoretical modelling of regional groundwater flow was made - in accordance with the characteristics of the epithermal model (Buchanan, 1981, Berger and Eimon, 1982) -, taking into account that these convective systems produce the solute accumulation in the discharge zone (Herrerías) of the geothermal area, and the solute dispersion in the lateral flow areas (Almagrera and Almenara).

REGIONAL GROUNDWATER FLOW: THEORETICAL MODELLING

Regional groundwater features as well as topographic and hydraulic conductivity influence, in a hypothetical, groundwater flow system (recharge and discharge areas), were determined by using a numerical model. We simulated groundwater flow and solute transport, by means of a stationary model, in finite differences with two-dimensional flow, that utilizes: a) an iterative, implicit method (ADI) to resolve the flow equation, and b) the classical method to resolve the advection-dispersion equation. The numerical simulation of regional groundwater flow had a qualitative character, without temperature coupled phenomenon analysis. The results suggest the existence of 1) topographically elevated areas, which coincide with groundwater recharge zones, and 2) depression areas in relation with groundwater discharge zones. In our case, these depression areas correspond to the the Herrerías and Valle del Azogue

mineralized zones (HAA hydrothermal system). This numerical model executes a mass balance, and computes the evolution of chloride concentration in the hydrothermal system, in a two-dimensional grid.

We consider that it represents an ideal hydrogeologic regional profile. This analysis displays a significative mass transport in the discharge areas near a magmatic source, whereas the solute accumulation is very low in the recharge and lateral flow areas in spite of the presence of the magmatic source.

THE HERRERIAS DEPOSIT: DISCHARGE AREA

Martínez Frías (1993, *this SGA Meeting*) proposes that the discharge system developed in the Herrerías area appears to fit the model of "convection through crack zones" (Strens & Cann, 1982). According to this model, the pressures associated with the flow of fluids through fractures do not modify greatly their form. Likewise, the critical flow rate necessary for hot fluid to vent can be obtained from a dimensional aproximation comparing the conductive heat loss from the upwelling fluid to the total amount of heat carried by the fluid following Sleep & Wolery (1978). The vents are fed by a narrow tubular crack zone. Hot water already present in cracks is tapped by the vents. Throug going recharge occurs on planar crack zones at the ridge axis. In the case of Herrerías - at the period of time in which the hydrothermal process took place (Upper Tortonian-Upper Messinian) -, the depositional environment was marine with a depth of aprox. 200 m (Montenat & Seilacher, 1978). The planar crack zones would correspond to the two faults which constitute the eastern and western boundaries of the Herrerías trough (Martínez Frías et al, 1992). Following this argument, Sleep (1983) proposes that if the size of the crack zone is comparable to the size of the heated region then the distance of heating away from the crack zone is proportional to $((kt)^{1/2}$, k = thermal diffusivity and t = time). The heated area is thus Area = πkt (eq.1), and the heat loss is $Q = \pi KTht$ (eq.2), where T is temperature in the upwelling water, K is the thermal conductivity, and h is the vertical extent of the crack zone (h ≈ 1 km).

Thus, an aproximation of the thermal diffusivity (k) can be made, both for the Herrerías fumarole field (Martínez Frías et al, 1992), and the adjacent deposit (*see Appendix*). These aproximations must be taken as theoretical in relation to the dimensions and to the other characteristics of the hydrothermally affected zone, given that geothermal and seismic activity is known to occur in the general area (Vera basin). For this reason, it is difficult to ascertain if the thermal source exhibits values of increasing or decreasing magnitude. In addition, values of K (thermal conductivity) and W (critical flow rate) obtained by applying of the model of "convection through crack zones" (*see calculations in Appendix*), can be considered similar to those of other geothermal zones although higher than those defined by Sleep (1983) at these crack zones (K = 0.006 cal/cm sec °C and W = 0.6 l/sec).

ACKNOWLEDGEMENTS

This work forms part of the research project AMB92-0408 and it was completed in cooperation with IGCP Project 318 (IUGS/UNESCO) and

with the Spanish Working Group on Geology and Metallogeny of Hydrothermal Seafloor Deposits.

APPENDIX (Herrerías area)

k = thermal diffusivity,
A = area (in this case, area visible which is affected by the hydrothermal process):
A1(fumarole field) = *1300 m²*
A2(mineralized area of Herrerías) = *1,5 km²*,
h = vertical extent of the crack zone (= *1 km*) (from Sleep, 1983)
K = thermal conductivity,
t = time (*Upper Tortonian-Upper Messinian*),
T = temperature (°C) (*230-250°C*),
Q = heat loss,
W = critical flow rate.

Attending to the Strens and Cann (1982) model, the following theoretical estimation of the hydrothermal process can be made:

Using eqn (1) (see text)

$k_{(fumarole\ field)} = 4.4 \times 10^{-8}$ cm²/sec

$k_{(mineralized\ area\ of\ Herrerías)} = 5 \times 10^{-5}$ cm²/sec

Similarly, following the model of "convection through crack zones" the thermal conductivity (K) and the heat loss (Q) can be calculated in accordance with the temperature range determined from the fluid inclusion studies. Hence, from eqn (2) (see text)

K = 0.019 cal/cm sec °C

Therefore, Q varies between 4.1×10^{19} and 4.5×10^{19} in Herrerías. In addition, the heat loss per unit time is defined as $F \equiv Q/t = KTh$ (cal/sec)

which, for this area, gives results of 4.3×10^{5} to 4.7×10^{5}.

Finally, the critical flow rate (W) for venting water is the flux (F) divided by the amount of heat per volume of water (≈ 1 cal/cm³ °C), which for this zone is

W = 1.9 cm³/sec

REFERENCES

Berger, B. & Eimon, P. 1982. Comparative models of epithermal silver-gold deposits. Society of Mining Engineers-AIME preprint no 82-13, 25 p.

Buchanan, L. 1981. Precious metal deposits associated with volcanic environments in the southwest. In: Dickinson, W.R., Payne, W.D. (eds.). Relations of tectonics to ore deposits in the Southern Cordillera. Arizona Geological Society, 237-262.

Martínez Frías, J., García Guinea, J., López Ruiz, J., López García, J.A. and Benito, R. 1989. Las mineralizaciones epitermales de Sierra Almagrera y de la cuenca de Herrerías. Rev. SEM, 12:261-271.

Martínez Frías, J. 1991. Sulphide and sulphosalt mineralogy and paragenesis from the Sierra Almagrera veins, Betic Cordillera. Estudios Geol., 47 (5-6): 271-279.

Martínez Frías, J., García Guinea, J., López Ruiz, J. and Reynolds, G.A. 1992. Discovery of fossil fumaroles in Spain. Scientific Communications. Economic Geology, Vol.87: 444-446.

Montenat, C. & Seilacher, A. 1978. Les turbidites messinienses à Helminthoides et Paleodictyon du bassin de Vera (Cordillère bétiques orientales). Indications Paléobathymetriques. Bull. Soc. Géol. Fr., 7, T.XX, No.3: 319-322.

Navarro, A., Font, X, Viladevall, M. and Rodríguez, P. 1993. Las mineralizaciones auríferas de S^{a} Almagrera. Estudio geoquímico y modelos de yacimientos. Bol. ITGE (in press).

Sleep, N.H. & Wollery, T.J. 1978. Thermal and chemical constraints on venting of hydrothermal fluids at mid-ocean ridges. J. Geophys. Res., 83: 5913-5922.

Sleep, N.H. 1983. Hydrothermal Convection at Ridge Axes. In: Rona, P.A., Bostrôm, K., Laubier, L., and Smith, K.L. Jr. (eds) (1983): Hydrothermal processes at seafloor spreading centers. Plenum Press, 796p.

Strens, M.R. & Cann, J.R. 1982. A model of hydrothermal circulation in fault zones at mid-ocean ridge crests. Geophys. J.R. Astron. Soc., 71: 225-240.

Current Research in Geology Applied to Ore Deposits.Fenoll Hach-Alí, Torres-Ruiz & Gervilla(eds)(1993).ISBN 84-338-1772-8

GOLD PLACERS OF THE LONQUINAY MINING DISTRICT, IX REGION, CHILE

Peebles, F.
Dept. de Geología, Universidad de Chile, Castilla 13518, Correo 21, Santiago, Chile

ABSTRACT At the Eastern Subandean Region (Lonquimay Range) between the parallels 37º to 38º south latitude, outcrop an intrusive body named Lonquimay Batholit of Terciary age, intruding marine jurasic sedimentary rocks. In the region beside these rocks, also outcrop, sedimentaries secuences of lake origen, fluvial, fluvial-glacials and moraines deposits. Also can be observed volcanics rocks or andesitic-basaltic composition, corresponding to Terciary and Quaternary volcanism.

In the present Bio Bio river bed, in fluvial and fluvial-glaciar terraces, related with its hidrographic system and in remnants of moraines deposits, numerous glacer gold deposits are distributed. These deposits probable were originated by the erosion of hydrothermal veins located in altered hydrothermal halos, formed in the contact zone between jurasic marine rocks and intrusive rocks of Lonquimay Batholit.

INTRODUCTION On the upper watercourse of the Bio-Bio river, and in an extension of 30 kilometers in North-South direction, numerous gols bearing placers are located, distributed a) in the current river-bed b) in three levels of terraces adjoining the river and in the remnants of some moraines that rise 300 meters above the Bio-Bio river.

The Lonquimay mining district has an average elevation of 800 meters above sea level. The most important town is located northe of the area and its center has the following geographical coordinates: 38020' latitude South and 71015' longitude West (Figure 1). This town is located 130 kilometers west of the city of Victoria in the Pan-American Highway to the South, and is connected to that city by means of a road that is 60% paved. All the area where the gold mills are located is linked by a gravel road that heads in a North-South direction, and connects with the Argentine through the Pino Hachado pass (Figure 1).

The relief on the West side is abrupt with altitudes of over 2.800 meters above sea level. In the center area the landscape is characterized by a mature landscape with rolling hills and river terraces, towards the east is a large basaltic plateau, with an average altitude of 1.200 meters above sea level.

The area where the gold mills are located is drained by the Bio-Bio river hydrographical system. Said river starts in lake Galletué, in the Lonquimay mountain range (Figure 2) and follows a general course in a South-North direction. Throughout is course, the Bio-Bio receives water from its tributary rivers Huallepulli, Pedregoso, Quilén, Lolén and Lonquimay on its west side and from the rivers Tue-Tue, Trolhue, Pehuenco, Pichipehuenco, Mitraquén and Rehue on the east side (Figure 2).

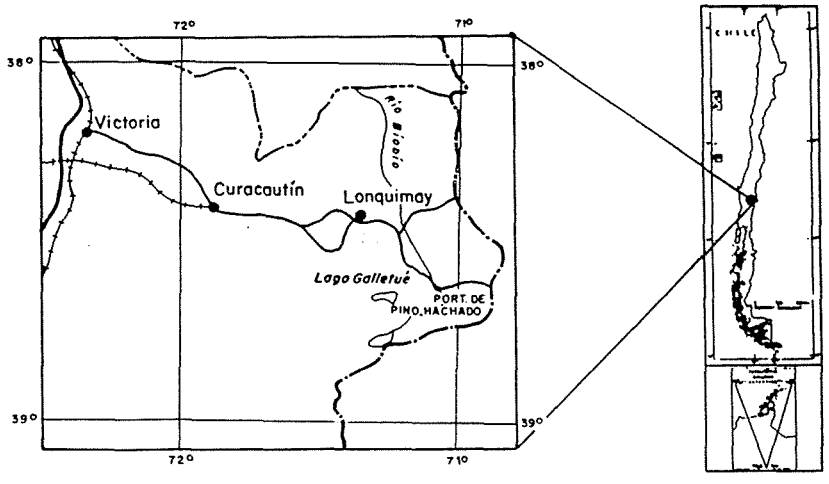

Fig. 1

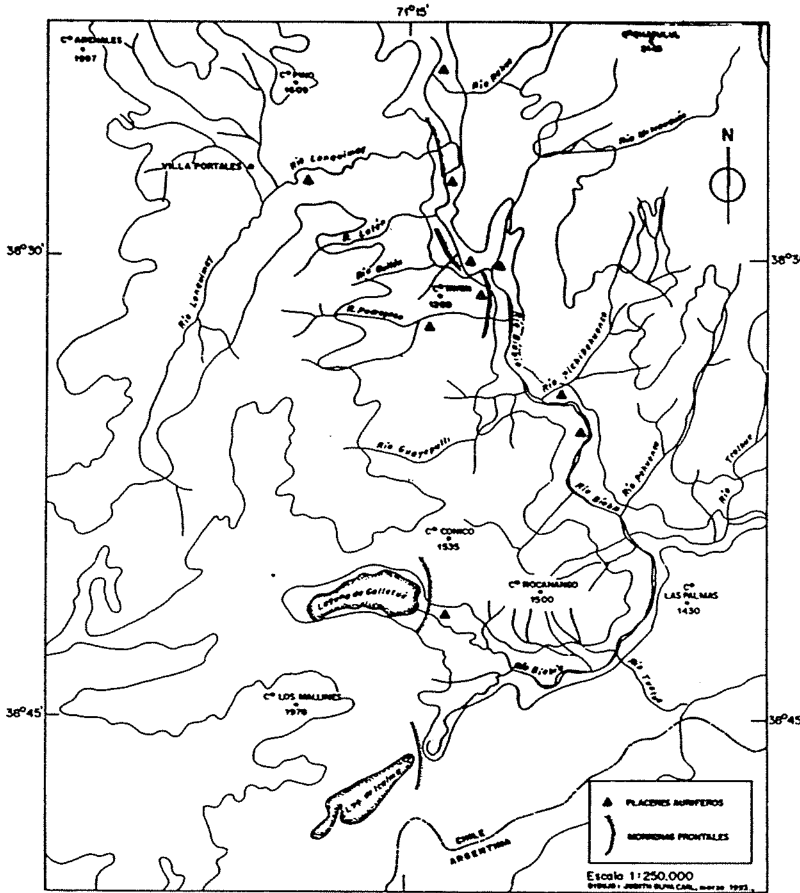

Fig. 2

On the western sector of the area, outcrop (Sandoval, 1977) a lower-tertiary age pluton know as the Lonquimay Batholith, consisting mainly of granodiorite and smaller proportions of granite and tonalite Said pluton is distributed in a strip in a north-south direction, and intrudes in its north-central area marine sedimentary rock of the jurassic period, known as Lolén-Pancunto bed. Consequence of this pluton, those sedimentary rocks have been altered by hydrometasomatism, and a large area of contact metamorphism with the presence of hematite, epidote, iron oxides, and some pyrite. In the sediment from the rivers that drain the area there are also small veins of quartz and pyrite.

On the Lonquimay Batholith and the Lolén-Pancunto bed the so-called Rio Pedregoso Formation was deposited, which is of the lower and middle miocene periods, and are lake sediments, bituminous rocks and coal, clastic and calcareous rock. Said sequence is the basis or circa of the Lonquimay gold-bearing placers (Rodríguez y Muñoz Cristi 1931).

Ice has played an important role in the distribution of gold in Lonquimay, as ice has been the physical agent that has carried large amounts of gold-bearing material from the Lonquimay mountain range. From the mountain ranges glaciers came down following the course of what are today the Pedregoso, Guelén and Lonquimay rivers. One can see today the remnants of end moraines at the point where these rivers flow into the Bio-Bio river (Portigliati, Emparan, Vogel 1988).

GOLD BEARING PLACERS

General Aspects The watershed of the upper course of the Bio-Bio river together with the Rio del Oro in the XII Region and the Madre de Dios river in the X Region is one of the areas in Chile with one of the largest volumes of gold-bearing alluvial material (Ruiz y Peebles 1988).

Almost without exception, evidence of alluvial gold can be found in all Bio-Bio sediments and in its adjoining terraces, from its origin in the Galletué lake up to the south of the Rahue river (40 kilometers to the North). Alluvial gold is found all the way to Santa Barbara, beyond the Lonquimay mountain range. In this sector, the valley becomes narrower and gold-bearing mineralization is limited to the Bio-Bio river bed. Gold here is very fine and alluvial (Peebles y Salinas 1973) (Alfaro 1974).

Throughout the upper course of the Bio-Bio there are several mills, most are abandoned. The most important, listed from North to South are: Tucapel bridge, Pichipehuenco river, Pedregoso river, Cerro Tallón, Quillén river, La Gloria, Mitrauquén river, Lolén, Las Juntas and Rahue river (Figure 2). Aside from these, in the mid-course of the Pedregoso and Lonquimay rivers, tributaries of the Bio-Bio, there are ancient gold exploitation facilities.

All placers are distributed into threee levels of terraces:

T-1 Current level of the Bio-Bio flood plain

T-2 Located 10 to 25 meters above the current water course of the Bio-Bio river. This terrace has most of the mining works.

T-3 Higher Terrace, 50 meters above the current level of the Bio-Bio river bed. The exploitation of the Cerro Tallón mil concentrated on this terrace.

Aside from the gold disseminated in the terraces indicated above, alluvial gold has been exploited in the top section of the Cerro Tallón moraine, approximately 300 meters above the level of the Bio-Bio river.

PHYSICAL CHARACTERISTICS OF THE LONQUIMAY GOLD

The following physical characteristics of the gold nuggets collected from the various different mills will be studied to determine the distance travelled by the gold particles from their point of origin:

a. Size of the nuggets
Based on the theory that the size of the nuggets is directly related to the distance from the point of origin.

b. Nugget morphology
The longer the distance travelled by the nuggets, their roundness will increase. In places close to their point of origin, nuggets have angular and pointed shapes.

c. Textural characteristics
Nuggets that are deposited close to their point of origin will have a rough surface, whereas those that have moved for a long time will have smooth surfaces and frequently will have grooves caused by friction against rocks of other particles of with the river bed or the river bank.

d. The Corey Shape factor (C.S.F.) used to define particle flatness
This measures the gold's lamination making a relating the fragment's surface to its thickness. A fragment with low flatness is thicker, which implies a shortes distance travelled and a closer proximity to the primary source, and a highly flattened particle is not very thick, which indicates a greater distance from the point of origin and therefore a longer distance travelled.

The study of all these physical characteristics may give an aproximate idea of the primary source from which the gold comes.

The following table summarizes the physical characteristics of the various different gold-bearing placers studied in the upper Bio-Bio area.

The following can be concluded from the survey in Table 1:

TABLE I	GALLETUE	PICHIPEHUENCO	PEDREGOSO	CO TALLON	LAS JUNTAS
Size of the nuggets	1,5 - 2 mm	1,0 mm	1,5 - 2 mm	1,5 - 2 mm	< 1 mm
Textural characteristics	Rough	Rough	Rough	Rough	Smooth and grooved
The Corey Shape Factor (C.S.F.)	Very Low Flatness	Low flatness	Very low flatness	Very low Flatness	Very high flatness

1. The gold particles collected in the Galletué area and the upper watercourse of the Pedregoso river were deposited very close to their point of origin. Evidence of this are the size of the particles - between 1.5 - 2 mm, their rough texture and very low flatnee factor.
2. Samples from Cerro Tallón moraine indicate a slightly longer distance travelled, with a higher flatness factor.
3. Gold particles from the Pichipehuenco area are of a smaller size- around 1 mm - than those from the Galletué area. This is an indication of a longer distance travelled than the Galletué deposits.
4. Gold particles collected at the Las Juntas mills are less than 1 mm in size, with smooth, grooved textures and a very high flatness factor. All this is evidence that the gold in these mills was deposited at a great distance from their point of origin.

General Conclusions

This survey permits to make the following general conclusions about the origin of the Lonquimay gold:

1. The gold comes from the erosion of gold, bismuth and pyrite-bearing quartz veins located in the contact metamorphosing zone between jurassic marine and granitoid rocks of the lower tertiary period (Lonquimay Batholith).
2. Another source is the Galletué granite where small gold bearing veins can be noticed.
3. The gold was carried by glaciers that eroded the hydrometasomatism zone and deposited the gold ore in the end moraines at lake Galletué, Cerro Tallón and the mouth of Lonquimay river where it joins the Bio-Bio.
4. The glaciers moved from the west to the East, following the ancient waterways of the Bio-Bio at its origin, Pedregoso, Quilen and Lonquimay.
5. End moraines were subsequently eroded by river water and deposited their gold content once again, this time in the present-day terraces of the Lonquimay river, and therefore there are mixed deposits, mainly at the Las Juntas mills where, at the top of the terrace, fluvial characteristics are predominant, and in the lower section, where moraine characteristics are found.

REFERENCES

ALFARO, G., 1974. Exploración de las pertenencias auríferas "Diego" 1-200 de Lonquimay, Instituto de Investigaciones Geológicas, Inédito.

PEEBLES, F. y SALINAS, M., 1973. Prospección de lavaderos auríferos, sector Bio Bio-Pichipehuenco, Lonquimay, Instituto de Investigaciones Geológicas, Inédito.

PORTIGLIATI, C., EMPARAN, C. y VOGEL, S., 1988. Las agentes geológicos en la formación de placeres auríferos en el sur de Chile. V Congreso Geológico Chileno. Actas Tomo I, B393-B418. Santiago.

RODRIGUEZ, M. y MUÑOS CRISTI, J., 1931. Estudio geológico y económico de los esquistos bituminosos de Lonquimay. Boletín del Departamento de Minas y Petróleo, pag. 78-79.

RUIZ, C. y PEEBLES, F., 1988. En Geología, Distribución y Génesis de los yacimientos metalíferos chilenos. Yacimientos auríferos secundarios, pp. 231-234. Editorial Universitaria. Santiago de Chile.

SANDOVAL, R., 1977. Estudio geológico de la región del Alto Bio Bio, Comuna de Lonquimay, Departamento de Curacautín, IX Región, Chile. Memoria de Geólogo, Universidad de Chile.

Current Research in Geology Applied to Ore Deposits.Fenoll Hach-Alí, Torres-Ruiz & Gervilla(eds)(1993).ISBN 84-338-1772-8

CHEMICAL EVOLUTION OF TRIOCTAHEDRAL MICAS FROM THE SALSIGNE MINE, FRANCE: SULPHIDE-BIOTITE EQUILIBRIA

Piantone, P. (1); Moine, B. (2) & Ohnenstetter, D. (1)

(1) GDR/CNRS/BRGM/1A, Rue de la Férollerie, 45071 Orleans Cedex 2, France

(2) Lab. de Minéralogie, Université Paul Sabatier, Toulouse III, 39 Allées J. Guesde, 31400 Toulouse, France

ABSTRACT: The X_{Fe} and X_F chemical variations of the biotites and mineral associations determined from the "traditional mine" of Salsigne (Aude, France) show that the high-temperature hydrothermal parageneses are dependant on a process of sulphuration related to the sulphur-arsenic phase I. This process involves progressive enrichment of the black micas in Mg which occurs according to two substitutions :
(i) $\square + {}^{[6]}Al + {}^{[4]}Al + 2Fe^{2+} + Ti^{4+} <----> {}^{[4]}Si + 5Mg^{2+}$ for biotites *s.l.* and (ii) ${}^{[4]}Si + Fe^{2+} <----> {}^{[6]}Al + {}^{[4]}Al$ for phlogopites. The physicochemical conditions assessed from the biotite sulphuration model (for 450°C and 4 kb) indicates very reducing conditions for deposition from the fluids (fO_2 between the Py-Po-Mag triple point and the FMQ buffer), for an H_2S(aq) concentration of between 0.01 and 0.50 moles.

INTRODUCTION

Unlike sulphides (pyrite-pyrrhotite), which can go undergo late-stage re-equilibrium in response to maximum P and T, the ferromagnesian silicate phases are reliable equilibrium markers for interactions between a sulphur-bearing fluid and the transformed rock. The typical scheme invoked for these sulphuration processes is a systematic decrease in the Fe/Fe+Mg ratio with the increasing fS_2 in the vicinity of ore mineralization. This phenomenon is well documented for phyllosilicates; it has been invoked for sulphur-rich metamorphic rocks in the vicinity of metamorphosed sulphide deposits and has been described from synthetic hydrothermal experiments from which it was modelled (Tso et al., 1979; Bryndizia and Scott, 1987). Application of such a scheme can be easily envisaged for the biotites of the "traditional mine" at Salsigne (Aude, France).

GEOLOGICAL SETTING

The Salsigne sulpho-arseniferous gold mine lies on the southern slope of the Montagne Noire, at the southern end of the French Massif Central (Fig. A). It contains the "traditional mine" hosted by the Cambrian-Ordovician North Minervois unit and the "2x" deposit hosted by the underlying X schist. Numerous studies of the structures and textures, as well as of the mineralogy and isotopes (Le Guen et al., 1992), favour a common Late Hercynian synkinematic hydrothermal origin for both deposits, with two very contrasted phases of mineralization: (i) a first phase (phase I) of medium- to high-pressure (4-6 kb), medium-temperature (400-500°C) sulphur-arsenic mineralization with pyrrhotite-pyrite-arsenopyrite+löllingite, and (ii) a second phase (phase II) of low-pressure (a few hundred bars), low-temperature (about 250°C) gold mineralization with bismuth-bismuthinite-Au. The hydrothermal silicate parageneses vary according to the chemical characteristics of the host rock - (i) potassic, ferriferous and magnesian for the "traditional mine" and (ii) aluminous for the X schist. Thus the "traditional mine" shows a phase I paragenesis of phengite-biotite-Kfeldspar (calcite-ankerite) that is limited strictly to the formations of the North Minervois unit (Demange et al., 1991), whereas the phase I paragenesis in the vicinity of the "2x" ore is represented only by a dominant chlorite+phengite (calcite-ankerite+chloritoid?) alteration. Phase II is only well marked at the expense of the biotite that it alters into patches of chlorite closely linked with gold and bismuth.

MINERAL HABITS AND ASSOCIATIONS

Three main types of biotite are recognised on the basis of habit and ore deposit: (i) intergranular biotites in siltite, (ii) biotite clusters in hydrothermal fissures and (iii) metasomatic biotites

accompanying the submassive pyrrhotite and pyrite mineralization.
The intergranular biotites in siltite form patches or bundles aligned along the [001] plane and, in places, outline a crude schistosity. They form halos around hydrothermal fissures and 'puffs' in the rock mass where, in places, they are associated with arsenopyrite and disseminated iron sulphides (pyrrhotite and/or pyrite).
The hydrothermal-fissure biotites show a cluster- or fan-shape habit, and are associated with quartz, allanite, ankerite or calcite, and more rarely with arsenopyrite and iron sulphides. They form dark monomineral zones around the massive sulphide bodies; these zones blend with the sulphides since they were stretched by the shear deformation that affected the sulphide bands.
The hydrothermal potassium feldspar ($Ort._{97.4\text{-}74.08}Ab._{1.57\text{-}18}Cel._{0\text{-}7.92}$) is well developed in the country rock of the "traditional mine". It is generally anhedral and associated to various degrees with the biotite neogenesis, although in places in the veins it is euhedral. The type of oxides depends on the intensity of the potassic alteration and associated sulphuration that accompanied the replacement of ilmenite by rutile or leucoxene.

CHEMICAL FEATURES

Two groups of biotite have been determined from their crystallochemical features. The first group incorporates the intergranular and the hydrothermal-fissure biotites whose Fe/Fe+Mg (X_{Fe}) ratios of >0.33 (Fig. B) place them in the biotite field. The second group is richer in Mg and corresponds to the metasomatic phlogopites. Variation in the X_{Mg}/X_{Fe} and X_F/X_{OH} ratios (respectively 0.06 to 0.28, and 0.83 to 3.31),due to the concomitant entry of fluor and magnesium into the biotite lattice, spreads the second group between the greenschist metamorphic biotite field and the hydrothermal biotite field (Ague and Brimhall, 1988) in which the Salsigne metasomatic biotites plot.

SUBSTITUTION SCHEME

In addition to being distinguished by their X_{Fe} ratio variations, the biotites show two radically different substitution patterns. The substitutions, which start from an aluminium-free end member in the octahedral position $K_2(Fe_{1.8}Mg_{4.2})(Si_6Al_2)O_{20}(OH)_4$ (Fig. B, Mg-Fe side of the triangle), veer respectively towards a Ti-siderophyllite or an aluminous eastonite end member according to the following equations:

(i) $\square + {}^{[6]}Al + {}^{[4]}Al + 2Fe^{2+} + Ti^{4+} <\text{-----}> {}^{[4]}Si + 5Mg^{2+}$ for the biotites *s.l.*, and

(ii) ${}^{[4]}Si + Fe^{2+} <\text{-----}> {}^{[6]}Al + {}^{[4]}Al$ (Tschermak substitution) for the phlogopites *s.l.*

The first scheme (i) agrees with the experimental results of Robert (1976) and the data of numerous other authors who note an increase in Ti solubility in the phlogopites with increasing Fe content. The second scheme (ii) shows that the phlogopite *s.s.* end member, $K_2(Si_6Al_2)(Mg_6)O_{20}(OH)_4$, is nowhere reached at Salsigne: a Tschermak substitution enabling the entry of Al into the octahedral position is seen after 4.20 atoms of Mg.

EQUILIBRIUM MODEL

The strong X_{Fe} variations in the biotites, related to the transformation of ilmenite to rutile indicate a biotite-sulphide-oxide equilibrium. Calculations of ilmenite/sulphides+rutile and sulphides-K-feldspar-biotite equilibria (Fig. C), using pressure-temperature conditions of 450°C and 4 kb in agreement with the data obtained on the pyrrhotite-arsenopyrite pair and with the minimum pressure-temperature measurements for trapping fluid inclusions of the phase I quartz, show that the fluids giving rise to the phase I deposition were very reducing (fO_2 between the Py-

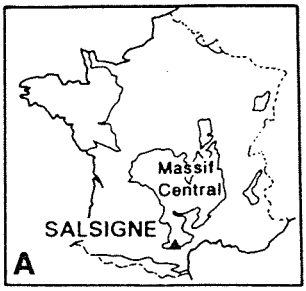

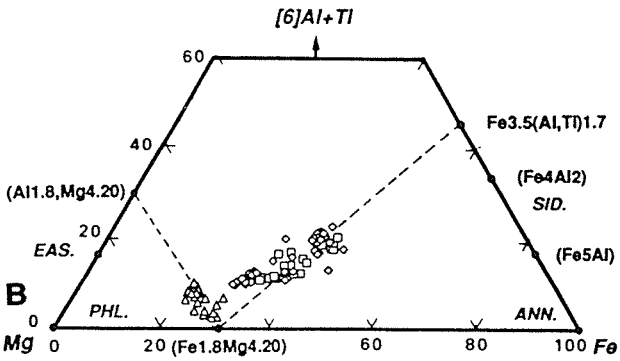

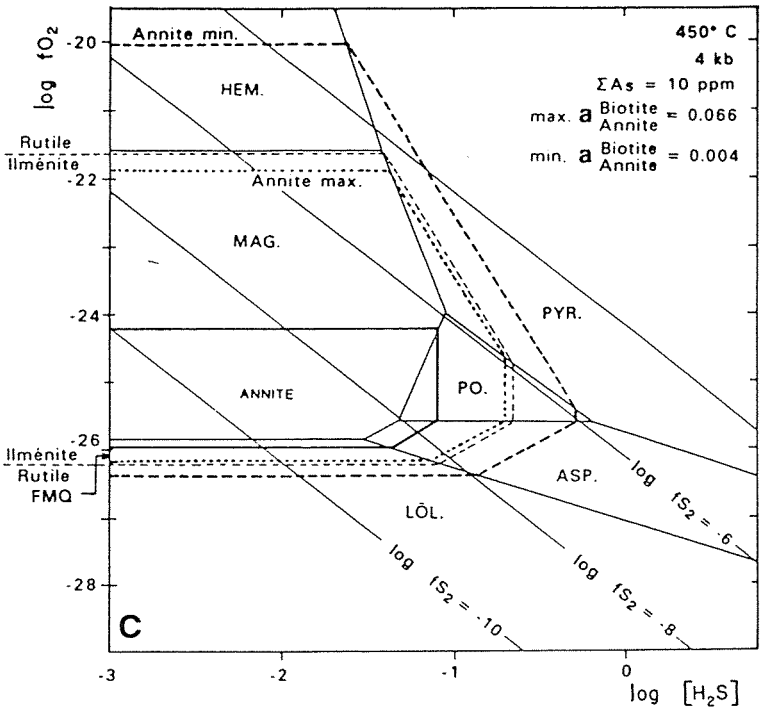

A- Map outlining the Massif Central with the location of the Salsigne mine.

B- Black micas of the "traditional mine"; main substitutions (projection on the $^{[6]}Al+Ti$-Fe-Mg plane). Major end members: PHL., phlogopite; ANN., annite; EAS., eastonite. Symbols: squares, hydrothermal fissure biotites; diamonds, phengite replacement biotites whether or not associated with sulphide mineralization; triangles, metasomatic biotites associated with the submassive sulphide mineralization.

C- Biotite stability in the Fe-Ti-O-S-H-K system at 450°C and 4 kb; log[H_2S] versus logfO_2 diagram. HEM, hematite; MAG., magnetite; LÖL., löllingite; ASP. arsenopyrite; PO., pyrrhotite; PYR., pyrite; FMQ., $FeSiO_4$-Fe_3O_4-SiO_2 buffer. Data for the sulphide species, the annite, H_2O and the potassic feldspar from SUPCRT92 (Johnson et al., 1991); data for the rutile-ilmenite equilibria from Robie et al, (1978); data concerning $H_3AsO_3°$ were estimated from the data of Helgeson (1969) and from the density model proposed by Anderson et al. (1991).

Po-Mag triple point and the FMQ buffer) with a $H_2S(aq)$ molality estimated between 10^{-1} and $10^{-0.3}$.

CONCLUSIONS

Evolution in the chemical composition (X_{Fe}, X_F) of all the biotites of the Salsigne mine was controlled by a process of sulphuration. The extent of the biotitic metasomatism that accompanied the deposition of the massive sulphide orebodies shows beyond doubt that all the biotites were contemporaneous with the potassic hydrothermalism brought about by the deposition of the type I mineralization. Two substitution schemes have been established :

(i) $\square + {}^{[6]}Al + {}^{[4]}Al + 2Fe^{2+} + Ti^{4+} <--> {}^{[4]}Si + 5Mg^{2+}$ for the biotites *s.l.*,

(ii) ${}^{[4]}Si + Fe^{2+} <--> {}^{[6]}Al + {}^{[4]}Al$ (Tschermak substitution) for the phlogopites *s.l.*.

The sulphuration model established for a temperature of 450°C and a pressure of 4 kb shows that the fluids were reducing (fO_2 between the Py-Po-Mag triple point and the FMQ buffer) for an $H_2S(aq)$ molality estimated at between 10^{-1} and $10^{-0.3}$ moles.

REFERENCES

Ague, J.J and Brimhall, H. 1988. Regional variations in bulk chemistry, mineralogy, and the composition of mafic accessory minerals in the batholiths of California. Geol. Soc. of Americ. Bull., 100, p.891-911.

Bryndzia T.L and Scott S. T. 1987. The composition of chlorite as a function of sulfur and oxygen fugacity: an experimental study. Am. Jour. of Science, 287, p. 50-76.

Demange, M., Serment, R and Touil. A. 1991, Caractérisation des fluides minéralisateurs aurfères par les altérations hydrothermales de l'encaissant: L'exemple des minéralisations de type grès riches de Salsigne (Aude, France): in Source Transport and Deposition of Metals, M., Pagel, and J.L., Leroy, (eds), Balkema, Rotterdam, p. 21-24..

Le Guen, M., Lescuyer, J.L and Marcoux, E. 1992. Lead-isotope evidence for a Hercynian origin of the Salsigne gold deposit (southern Massif central, France). Mineral. Deposita.

Anderson, G.M., Castet, S., Schott, J. and Mesmer, R.E. 1991. The density model for estimation of thermodynamic parameters of reactions at high temperatures and pressures. Geoch. et Cosmoch. Acta, 55, p.1769-1779.

Johnson, J.W., Oelkers, E.H. and Helgeson H.C., 1991. SUPCRT92: a sofware package for calculating the standard molal thermodynamic properties of minerals, gases, aqueous species, and reaction from 1 to 5000 bars and 0° to 100°C. Earth Sciences Department, L-219, Lawrence Livermore National Laboratory, CA 94550

Powell, R. and Evans, J. 1983. A new geobarometer for the assemblage biotite-muscovite-chlorite-quartz. J. Metamorphic Geol., 1, p. 331-336.

Robert, J.L. 1976. Titanium solubility in synthetic phlogopite solid solution: Chem. Geol., 17, p. 213-227.

Robie, R.A., Hemingway, B.S. and Fisher, J.R., 1978. Thermodynamic properties of minerals and related substances at 298.15 K and 1 bar (105 Pascals) pressure and at higer temperatures . U. S. Geol. Survey Bull., 1452, 456 p.

Shock E.L and Helgeson H.C., 1988. Calculation of the thermodynamic and transport properties of aqueous species at high pressures and temperatures : correlation algorithms for ionic species and équation state prediction to 5 kb and 1000°C. Geoch. et Cosmoch. Acta, 52, p.2009-2036.

Tso, J. L., Gilbert, M.C. et Craig J., 1979. Sulfidation of synthetic biotites. Am. Mineral., 64, p. 304-316.

Current Research in Geology Applied to Ore Deposits.Fenoll Hach-Alí, Torres-Ruiz & Gervilla(eds)(1993).ISBN 84-338-1772-8

IMAGE TRANSFORMATIONS OF LANDSAT TM AND ILLUMINATION CORRECTION IN THE OJEN ULTRAMAFIC MASSIF (S.W. SPAIN)

Polvorinos del Rio, A.J.; Cabrera, J. & Almarza, J.
Dept. de Cristallografía, Mineralogía y Química Agrícola, Universidad de Sevilla, Sevilla, Spain

ABSTRACT: Delineation of litology associated with ultramafic rocks in the Ojen intrusion (Betic Massif, SW of Spain) by remotely sensed Landsat TM is obscured by illumination variability produced by relief shadow casting. Principal component filtering, and hyperspherical cosine transformation have been applied to isolate the spectral content of the scene and evercome the negative topographic effects. Mapping of spectrally contrasted rocks, and alteration spots on the transformed bands can be carried out by conventional image procedures such as RGB, IHS composites, index ratios or classification.

INTRODUCTION

Rock discrimination by remotely sensed imagery relies on the knowledge of relationships between reflectance properties of the sensed materials and their mineralogical composition.

Several intrinsic factors to the area sensed, such as topography and vegetation cover, joined to other aspects dependent on the sensing conditions, frequently confuses and renders the interpretation of geological prospects difficult (Siegel and Goetz,1977; Fraser and Green, 1987). Particularly important is the high illumination variability observed in the sensed images of rugged terrains.

Different empirical methods to model such effects include the use of DEM to correct the images according to a Lambertian behaviour of the reflectance surface (Civco, 1989), or non-Lambertian (Colby, 1991); other proposed methods to avoid topography effects such as ratio calculation are confusing in their interpretation.

In this application we focused on two procedures that without a DEM extracts the topographic effects from the spectral response. The objective of hyperspherical directional cosine transformation (Pouch and Compagna,1990) and the PC inversion filter is to enhance the spatial continuity of features, preserving their radiometric characteristics independently of the illumination conditions. The enhanced results of other image processing techniques to display or classification on the filtered spectral bands is the final purpose of the methodology.

With the aim of an integrated study of the ultramafic formations in the SW of Spain, Ojen Massif has been chosen as a test area to develop a systematic of image analysis for a zone influenced by high variability in topography and vegetation cover.

GEOLOGICAL SETTING

A series of ultramafic rock exposures is spread along 60 Km of the Serrania de Ronda (Malaga, Spain). Synthesis of the regional geology made by Navarro Vila and Tubia (1983) indicates that the lithologic column has in the top a monotone sequence of micaceous schistes underlaid by gneises and migmatitic rocks with folded structures.Diabase dikes of variable size up to a metre can be found in these two upper sequences, with extensively distributed granitoide and silimanite gneises. At the bottom of the column are ultramafic

rocks, which in the Ojen massif are mainly lherzolites in their upper part.

According to Gervilla (1990), of the two subfacies of lherzolite with spinel named Seiland and Ariegite, only the former is abundant and surrounds the northern and southern parts of the pluton, the most abundant facies of lherzolite with plagioclase.

The exixtence of these rocks with variable dark to dark-green tones are due to mineralogical composition and their degre of alteration. Rhytmic layering can be observed to a centrimetric scale of alternates, and variable supergenic alteration shows preferential transformation of olivine. The surface of the rocks may apperar with variable red-dark colours covering the original aspect of fresh peridotites.

Local formations of serpentine and crisotile can be found distributed in small scale fractures and closely packed diaclase;such serpentinization is found to be abundant due to the high tectonic deformation; asociated with fractures N70E the hydrothermal alteration of peridotites can be found asbest and talc deposits.

Other alterations knowns as "listwaenites" can be found in the southern contact of the intrusion, characterized by the interaction of several processes of silicification and carbonatization of serpentines, apparently associated with an important concentration of Au (Buisson and Leblanc, 1985). Abundant mineralization of Cr, Ni, Cu and Fe can be found and several quarries of industrial materials such as talc are being mined.

IMAGE ANALYSIS

The scene studied was sensed by Landsat TM on August 29 1989 with respective elevation and azimutal angles to the Sun of 52.5° and 129.6°.

Initial estimation of atmospheric scattering of radiation in the six reflective bands shows that a model of clear atmosphere (Chavez, 1988) is adequate to the reality in the moment of sensing. As a consequence the corrections in the DN of each band are found to be very close to simple substraction of the smallest digital number.

Geometric correction of the scene has been carried out with enough ground control points to provide a correct fitting to the 1:50000 geological map of the studied area. Digital terrain model (Fig.1.d) was obtained by appropiate interpolation of digitised contour lines.

Delineation of different petrological units in the scene has been carried out by several types of image processing for the six reflectance bands of the Landsat TM images. Gneises and marbles surrounding the ultramafic intrusion have in general good spectral response contrast for their discrimination and the band combinations TM7-4-1 and TM5-4-2 show the highest contrast between peridotites and the rest of the geological materials of the area; the shadowing of extensive areas (mainly over the ultramafic rocks) is the more pronounced negative effect found, as can be seen in the NIR TM4 band (Fig.1.a).

Principal component filtering is a scene dependent topographic correction procedure; so it can be applied with different results to previously masked zones of the whole studied area. The method recover the spectral variables after fixing the principal components of high illumination variability; basically the linear combination of selected principal components with the transpose of the loading matrix obtained by PCA. Applied to the whole scene, and after inspection of the component images, the first (or brightness), third,

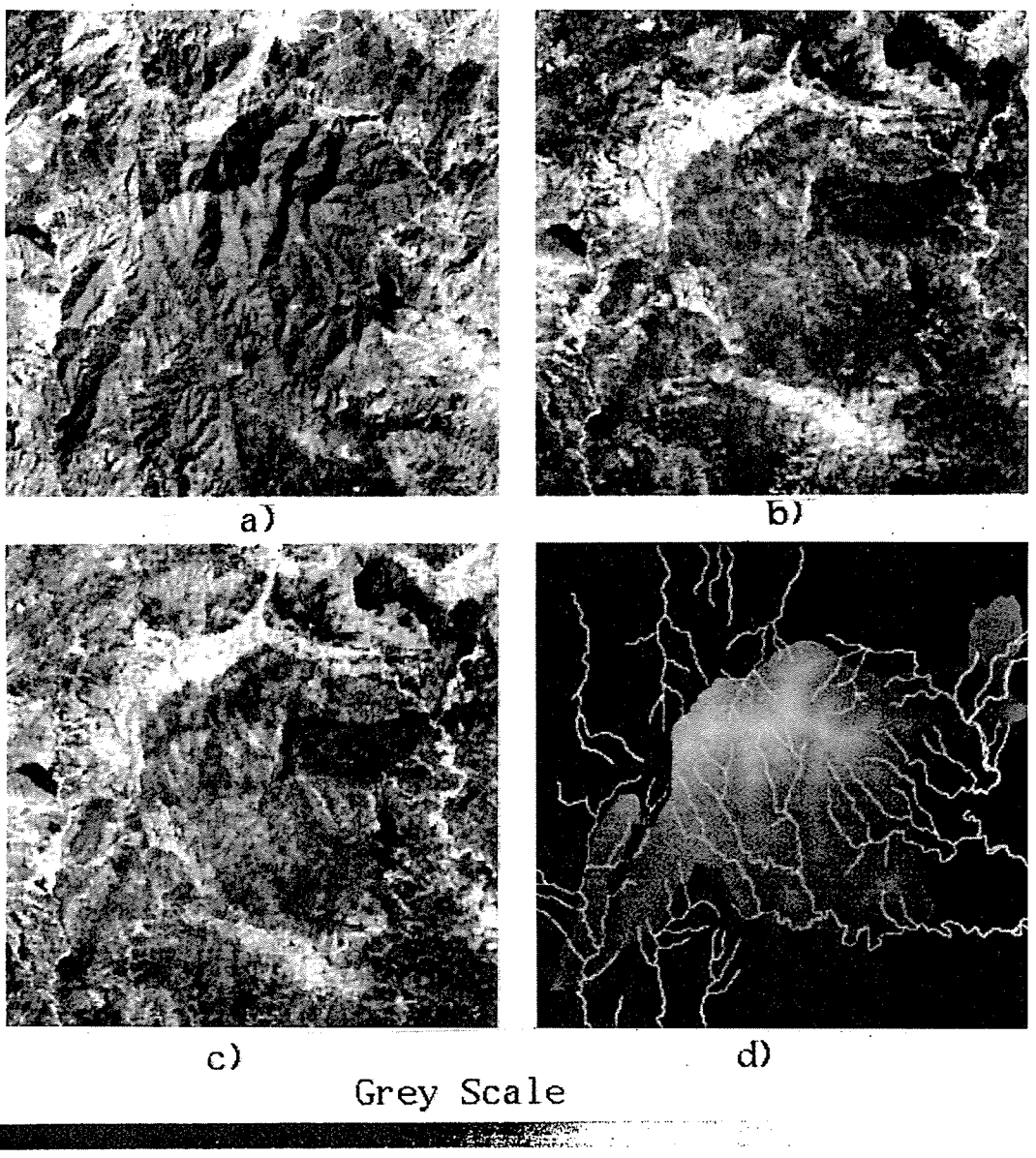

Fig.1.- a) Original georeferenced NIR band (0.76-0.90μm) TM4, with intense shadowing in the center of the image. b) Hiperspherical transformed TM4, with the topographic effect filtered, and enhancement of distinctive features in the eastern bord of the peridotitic rocks. c) The same band as in cases a) and b), without ilumination effects recovered after removing PC1-PC3 and PC6. d) Masked DEM of the peridotitic rocks superimposed to the stream network of the area.

and sixth component (mainly noise) can be removed prior to the inverse transformation. In Fig.1.c the filtered TM4 and the disappearance of shadows and enhancement of spectral contrast not seen in the original band (Fig.1.a) are shown.

Application of the procedure to the peridotitic rocks using their PCA and to other masked zones in the studied area has been tested with different contrast enhancement.

Hipercosine transformation (Pouch and Compagna,1990) isolates topographic effects by a normalization $[dn_j]=\frac{255}{R}[DN_j]$; $R=\left[\sum_{i}^{n} DN_i^2\right]^{1/2}$ applied to each pixel in the image, and in consequence is a scene independent transformation.

Applied to the studied area the visible and near infrared (NIR) (Fig1.b) bands are very efficiently filtered, although a worst case result is obtained for the TM5 and TM7 bands. Normalization by $R=\left[\sum_{i=1}^{4} DN_i^2\right]^{1/2}$ or $[dn_j]=\frac{255}{R_j}[DN_j]$; $R_j=\left[\sum_{i\neq j}^{n} DN_i^2\right]^{1/2}$ leads to improved results.

CONCLUSIONS

The proposed methods filter illumination effects in remotely sensed images and enhance the spatial continuity and contrast of patterns and features of interest for their identification. Methods that integrate the two procedures described can be easily implemented and improve the obtained results.

BIBLIOGRAPHY

Buisson,G. and Leblanc,M. (1985) Gold in carbonatized ultramafic rocks from the ophiolite complexes. Econ. Geology v. 80, p. 2028-2029.

Civco, D. (1989) Topographic normalization of Landsat Thematic Mapper digital imagery. Photogrammetric Engineering and Remote Sensing, v. 55, no. 9, p. 1303-1309.

Colby, J.D. (1991) Topographic normalization in rugged terrain. Photogrammetric Engineering and Remote Sensing, v. 57, no. 5, p. 531-537.

Fraser,S.J. and Green, A.A. (1987) A software defoliant for geological analysis of band ratios. Internationla Journal of Remote Sensing, v.8, p. 525-532.

Gervilla Linares,F.(1990) Mineralizaciones magmáticas ligadas a la evolución de las rocas ultramáficas de la Serrania de Ronda (Malaga-España). PhD Thesis. University of Granade. Spain.

Navarro-Vila,F. and Tubia,J.M. (1983) Essai d'une nouvelle differentiation des Nappes Alpujarrides dans le secteur occidental des Cordillères Betiques (Andalousie, Espagne). C.R. Acad. Sc.Paris, v. 296(II), p. 111-114.

Pouch,G. and Compagna,D. (1990) Hiperspherical directional cosines for separation of spectral and illumination information in digital scanner data. Photogrammetric Engineering and Remote Sensing, v. 56, no. 4, p. 475-479.

Siegal,B.S. and Goetz,A.F.H. (1977) The effects of vegetation on rock and soil type discriminations. Photogrammetric Engineering and Remote Sensing, v.43, p. 191-196.

Current Research in Geology Applied to Ore Deposits.Fenoll Hach-Alí, Torres-Ruiz & Gervilla(eds)(1993).ISBN 84-338-1772-8

EFFECTS OF MOBILISATION AND METAMORPHISM ON THE SCHEELITE-MAGNESITE DEPOSIT TUX, EASTERN ALPS, AUSTRIA

Raith, J.G. (1); Grum, W. (2) & Prochaska, W. (1)
(1) Inst. für Geowissenchaften, Montanuniversität, Leoben, Austria
(2) Lab. für Geochronologie, BVFA-Arsenal, Wien, Austria

ABSTRACT

The sediment-hosted stratabound scheelite magnesite deposit of Tux occurs in low-grade polymetamorphic and polyphase deformed Paleozoic sequences of the Lower Austroalpine tectonic units (Innsbrucker Quartzphyllite Zone) of the Eastern Alps. Integration of the structural geology with fluid inclusion studies and Sr, C, O, H isotope data documents a complex mobilisation history for this deposit during the metamorphic evolution of this terrain.

INTRODUCTION

Several scheelite deposits (Tux, Klamm Alm, Mühlbach/ Neukirchen) are known from the Lower Austroalpine tectonic unit in the Eastern Alps, the largest being the scheelite-magnesite deposit at Tux/Lanersbach, Northern Tyrol. These deposits occur in metaclastic-metacarbonate rocks of the Lower Austroalpine Innsbrucker Quartzphyllite Zone (IQZ) in its stratigraphically youngest sequences (Black Schist-Carbonate Series) of Upper Silurian/Lower Devonian age (Höll&Maucher, 1967; Raith, 1991). Metacarbonate rocks (Fe-dolomite, magnesite), and ±carbon-bearing metapelitic/ metapsammopelitic (black schists, chlorite±sericite phyllites) rocks representing a special facies within the IQZ are the immediate host rocks of mineralisation.
These deposits have been classified as stratabound and genetic concepts have been favoured which related tungsten (pre)concentration to sedimentary-exhalative hydrothermal processes. The close genetic relationship between mobilisation of tungsten and the metamorphic and deformational evolution will be demonstrated in this paper.

MINERALISATION RELATED TO METAMORPHISM AND DEFORMATION

The Tux deposit represents a polyphase deformed and low-grade polymetamorphic (Variscan?, Alpine) ore deposit. Three scheelite generations can be distinguished (Wenger, 1964). Scheelite I (grey) is associated with tungstenite, pyrite etc. and crystallised prior to magnesite. Scheelite II (brown) occurs together with quartz, dolomite, apatite and minor sulfides and scheelite III only forms small rims around older scheelite grains.
These generations can be related to the deformational events as follows (Fig. 2): A first scheelite generation already crystallized pre-D2. In metapelites this pre-D2 metamorphic event is indicated by rutile ("sagenite") exsolution produced after breakdown of biotite.

The main deformational event (D2) developed a penetrative crenulation cleavage (S2) under greenschist facies conditions. During this deformation isoclinal scheelite I folds were produced. Subsequent D3 deformation resulted in a tight folding (B3) and a weak S3 crenulation cleavage. Scheelite II-quartz mobilisates postdate D2 and were weakly deformed during D3. Late open folds were produced during D4 as well as crosscutting quartz carbonate veins.

FLUID INCLUSION STUDIES

Two main types of fluid inclusions (Type 1, a and b and Type 2) were distinguished:
Type 1a: These are aqueous, undersaturated but relatively saline two-phase (L+V) inclusions of the H_2O-NaCl-$CaCl_2$ system with a large variation in T_h (160-240 °C) and salinity (13-22 wt.% NaCl equiv.); this variation is explained with mixing of two aqueous fluids of different temperature and salinity. The inclusions occur as <5-25 µm large secondary and pseudosecondary inclusions in scheelite I.
Type 1b: These are aqueous, undersaturated moderately saline two-phase (L+V) inclusions of the H_2O-NaCl-$CaCl_2$-($MgCl_2$) system occurring as secondary/pseudosecondary inclusions in scheelite and quartz. They are defined as the lower saline (8-12 wt.% NaCl equiv.) and lower temperature (T_h 150-170 °C) mixing fluid of type 1 fluids.
Type 2: These are aqueous, undersaturated low saline two-phase (L+V) inclusions of the H_2O-NaCl-(KCl) system, their average size ranging from 10-25 µm. They occur as primary and secondary inclusions in vein quartz and dolomite and in scheelite; primary inclusions were found in clear scheelite III rims. Type 2 fluids are characterised by low salinities (1-7, average 3.5 wt.% NaCl equiv.) and T_h in the range of 92-176 °C (average 156±16).

ISOTOPE STUDIES

Sr isotopes. 39 analysed samples cluster into two $^{87}Sr/^{86}Sr$ groups: (a) 0.728-0.735: scheelite II in quartz ± carbonate mobilisates, discordant vein carbonate (b) 0.715-0.728: intensely deformed scheelite I, fine-grained ferroan dolomite and magnesite. All samples reveal a metamorphic isotope signature; late Paleozoic seawater isotope ratios ($^{87}Sr/^{86}Sr$ < ca. 0.709) were not detected. The variation in $^{87}Sr/^{86}Sr$ accords to the inhomogeneous isotopic exchange during D2 to D3 and to increasing $^{87}Sr/^{86}Sr$ of the mobilizing fluids respectively. Surrounding quartzphyllites are the most likely source for radiogenic Sr.

C-O isotopes were mainly analysed from scheelite-free and scheelite-bearing Fe-dolomites and sparry magnesite; a few analyses were performed on (±quartz-bearing) vein type carbonates and carbonate mobilisates. Combined ^{13}C-^{18}O data allow distinction of three major groups. (a) Unmineralised, scheelite-free ferroan dolomites are marked by only slightly negative and restricted ^{13}C values (-0.76 to -1.23‰ PDB) and variable ^{18}O values (13.2 to 16.5‰ SMOW). (b) Fine-

grained scheelite-bearing dolomites vary in their ^{13}C from -3.1 to -8.27‰ and in their ^{18}O values between 12.9 and 17.1‰. (c) Magnesites exhibit a smaller ^{13}C range (-4.5 to -2.53‰; average -3.34±0.62‰) and generally lighter ^{18}O (range: 11.65-16.47‰; average 13.23±1.55‰).

O-H isotopes of quartz-scheelite mobilisates. $\partial^{18}O$ values of quartz cluster between 16.3 and 18‰; the scheelite values vary within a range of 5.41 to 7.98‰. Oxygen isotopes analysed from coexisting quartz and scheelite II yielded formation temperatures of ca. 280 °C. Fluid compositions calculated on the basis of these temperatures are shown in Fig. 1. It is noteworthy, that fluids of carbonate-hosted mineralisation were significantly heavier (approx. 1.3‰, Fig.1) compared to those hosted by metapelites; this indicates isotopic exchange between the mobilizing fluids and the corresponding hostrock on a relatively small scale and low fluid/rock ratios. ∂D investigations from the youngest discordant quartz veins yielded light ∂D values between -80‰ and -90‰ indicating the influence of meteoric water. In contrast, the ∂D signature of the quartz-scheelite (II) veins (-45‰) is consistent with a metamorphic origin of these fluids.

Post-D3: discordant quartz-carbonate veins
$^{87}Sr/^{86}Sr$: up to 0.735
$\delta^{18}O_{Fl}$: ~ -2‰. δD_{Fl}: -85‰.
FI: type 2, ~ 3.5 wt.% $NaCl_{equiv}$, T_h 100-170°C
"meteoric" fluid signature

Pre-D3: folded Scheelite II-quartz mobilisates concordant s2
$^{87}Sr/^{86}Sr$: 0.729-0.733
$\delta^{18}O_{Fl}$: -8.5‰. δD_{Fl}: -45‰. 270-290°C (quartz-scheelite pairs)
FI: type 2, 1-7wt.% $NaCl_{equiv}$, T_h 100-170°C
"metamorphic" fluid signature

Syn-D2: isoclinally folded lenses of scheelite I
$^{87}Sr/^{86}Sr$: <0.728
FI: type 1a, 8-12 wt.% $NaCl_{equiv}$, T_h 150-170°C:
type 1b, 13-22 wt.% $NaCl_{equiv}$, T_h 160-240°C, fluid mixing

Pre-D2: crystallisation of scheelite I
$^{87}Sr/^{86}Sr$: ≤0.719

scheelite I
scheelite II
quartz-carbonate vein

Fig. 1. Fluid characteristics of the different stages of scheelite mineralization in relation to the deformational events.

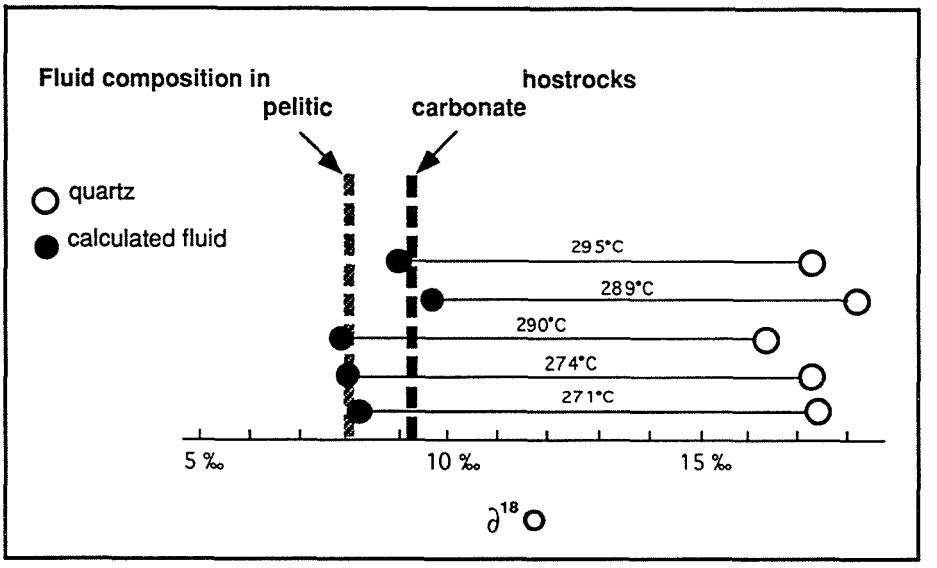

Fig.2.Isotope equlibrium temperatures of coexisting scheelite and quartz and calculated $\partial^{18}O$ fluid composition in different host rock lithologies.

REFERENCES

Höll, R.& Maucher, A. 1967. Genese und Alter der Scheelit-Magnesit-Lagerstätte Tux. Sitz. ber. Bayr. Akad. Wiss. math.-naturwiss. Kl, 1967: 1-11

Raith, J.G. 1991. Strata-bound scheelite in metacarbonate rocks - example from Lower Austroalpine Klamm Alm mineralization, Navis, Tyrol, Austria. Transactions Instn. Mining Metall., Sect. B., 99: B81-B90

Wenger H. (1964): Die Scheelitlagerstätte Tux. Radex Rundschau, 1964, 109-132

Current Research in Geology Applied to Ore Deposits. Fenoll Hach-Alí, Torres-Ruiz & Gervilla (eds) (1993). ISBN 84-338-1772-8

GEOLOGY AND GEOCHEMISTRY OF THE RIVIERA PORPHYRY-SKARN W-Mo-(Cu) DEPOSIT, SOUTH AFRICA

Scheepers, R.; Rozendaal, A. & Hallbauer, D.K.
Dept. of Geology. University of Stellenbosch. Stellenbosch 7600, South Africa

ABSTRACT: W-Mo(Cu) mineralization of the Riviera deposit is spatially and genetically related to late Precambrian granites of the Cape granite suite (500 to 630Ma). The deposit is classified as a porphyry-skarn deposit. Ore elements were transported along a repeatedly reactivated veining system in the higher part of the pluton. The hostrock is a late tectonic high K calc alkaline granite, with geochemical characteristics of both I- and A-type granites, intrusive into calcareous metasediments.

Introduction

The Riviera deposit is the only base metal occurrence of significant tenor and grade in the western and southwestern Cape Province of South Africa and is clearly of strategic importance. The deposit was discovered in 1975 by reconnaissance stream sediment sampling for tungsten by the Union Carbide Exploration Corporation. A joint venture agreement was concluded with the Anglo American Corporation during 1983. An extensive drilling program followed which outlined the ore zone and allowed feasibility studies to be conducted.

Setting

Economic minerals are mainly hosted by a late tectonic granite related to the Cape Granite Suite (518-632 Ma), a suite of rocks intrusive into the late Proterozoic Malmesbury Group metasediments. After a period of planation the sediments of the Paleozoic Cape Supergroup were deposited unconformably on these metamorphites and granites. Following the tectonostratigraphic classification of the Malmesbury Group by Hartnady et al. (1974) and Theron (1990), the deposit is located within the fault bounded Boland Terrane underlain by the Piketberg Formation (Fig. 1).

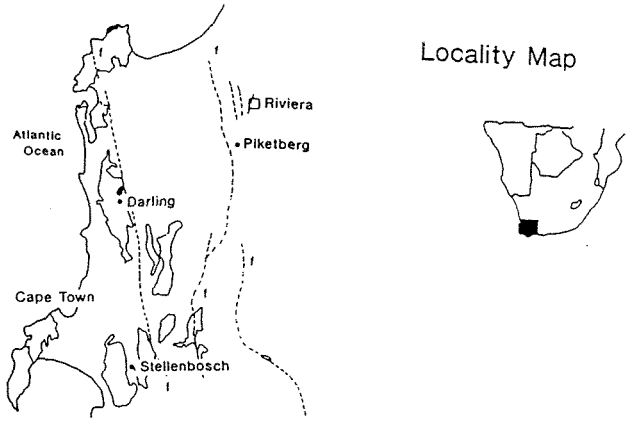

High K-calcalkaline granites plot predominantly in the fields of quartz monzonite, granodiorite and granite on the Streckeisen diagram. They have biotite hornblende as the predominant ferromagnesian minerals and typically vary from metaluminous to slightly peraluminous. The Riviera granitoids conform to these characterstics, the least altered samples classify as granodiorites to adamellites and the altered samples as quartz monzonites (loss of Si), granites (gain in K) and quartz syenites (loss of Si and gain in K). Major and trace element compositions of the Riviera granites are not corresponding to those of typical I- and S-type granites on discrimination diagrams according to Eby (1992) (Fig. 2). The stable element geochemistry of the Riviera granitoids are typical of either highly fractionated I-type granites or a mixture between typical I- and A-type granites.

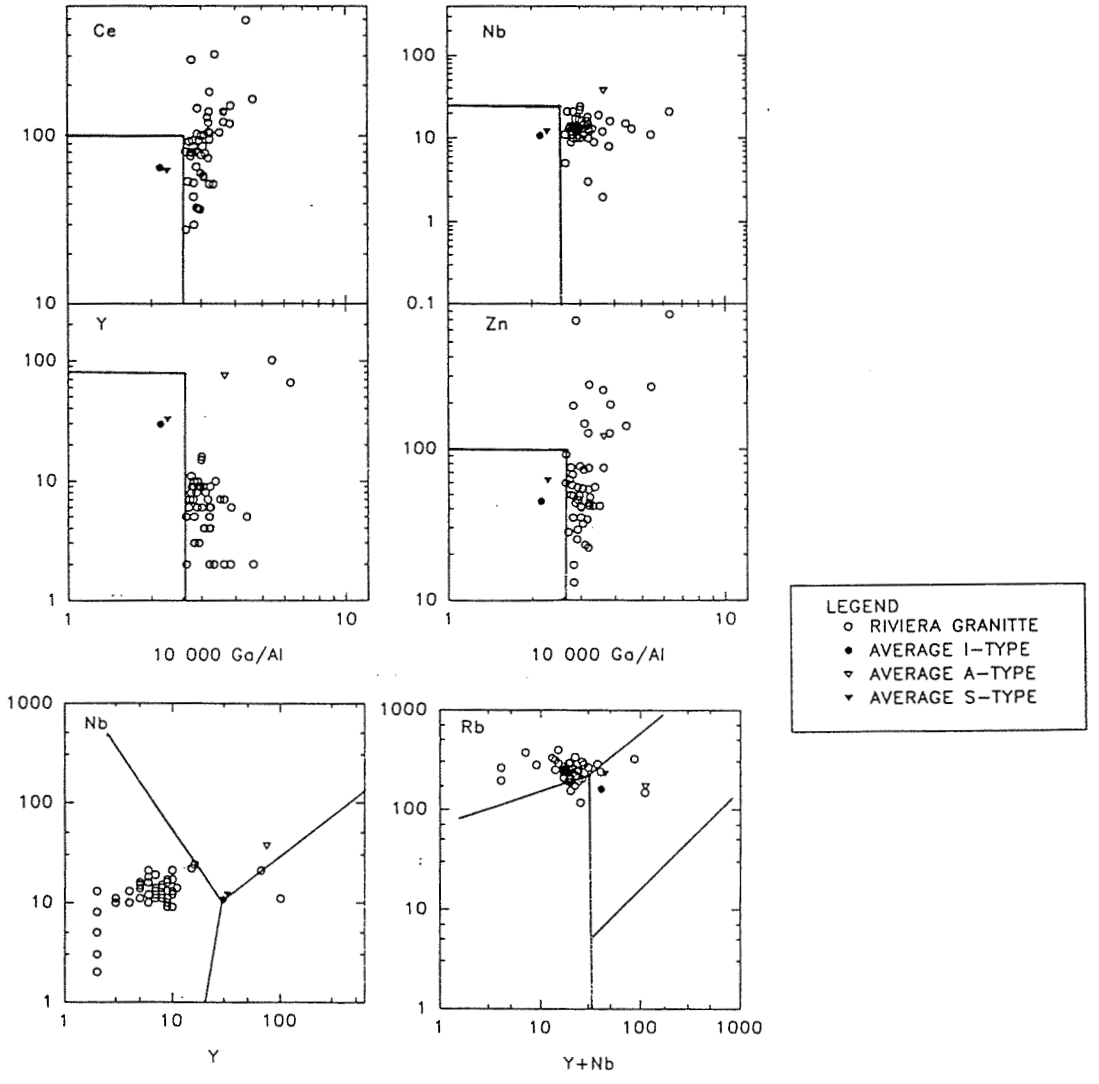

Tectonically the rocks of the Malmesbury Group lie within the Pan-African Saldania belt (Gresse, 1991) and have been subjected to polyphase deformation. Regional metamorphism which ranges from low to medium grade, is related to the Saldanian orogeny and predates the intrusion of the granites, including the Riviera granite. Two deformational episodes controlled the intrusion of granites, namely, an early F1 event (intrusion of peraluminous calkalkaline S-type granites at 620 to 630 Ma) and a later F2 event (intrusion of peraluminous to metaluminous granites with a predominantly I - type character at 540 - 580 Ma). Later granites exploited either the anticlinal structures resulting from the two deformational episodes (including the Riviera granite), or are associated with tension along well developed left lateral fault zones (Robertson and Klipberg plutons). The present spatial position of the Riviera granite, the only known granite in the Boland tectonic terrane, is considered the result of Mesozoic high angle normal faulting with an upthrow to the east.

Mineralization

Scheelite and molybdenite, the only economically significant ore minerals, are mainly associated with the roof zone (cupola) of the Riviera granite pluton and immediate contact with the Malmesbury Group wallrocks. Associated sulphides include pyrrhotite, pyrite, chalcopyrite and sphalerite.

Molybdenite occur either as fine disseminations or within quartz and calcite veinlets in the granite. These veinlets often extend into the wallrocks. Skarn-type mineral assemblages have been found either as xenoliths (endoskarns) in the granite or as metasomatized calcareous metasediments in contact with the granite. Although the latter may locally exhibit significant scheelite mineralization the ore zone is essentially confined to the granite. The highest scheelite concentrations are spatially related to dark patches in the granite containing pyroxene (diopside), garnet (andradite with a grossular component in places), calcite, epidote, scapolite, sphene and chlorite. Pervasive hydrothermal alteration is typical of the granite and zones of sericitisation, argillisation and silicification have been identified. Sphalerite pods are closely related to calcite and sericite zones in the granite.

Hostrock petrochemistry and mineralogy

The Riviera granitoids are related to the SALKL (monzonitic or high K calc alkaline) association of Debon and Le Fort (1988) and they typically classify as K-series rocks according to Wilson (1989). The subalkaline trend is defined by rocks changing in composition from gabbro to monzogabbro and monzodiorites, eventually reaching adamellitic and granitic composition in the most felsic members. The calc alkaline as opposed to tholeiitic affinity of these rocks is evident on an AFM-diagram (Wilson 1989), they are separated from normal calc-alkaline associations using the QBF-triangle of Debon and Le Fort (1988).

The low Y/Nb ratios (<1) are typical of granites with a large mantle component (Taylor and Mclennan 1985). Application of the Nb vs. Y tectonic discrimination diagram of Pearce et al. (1984) indicated a syn-collision or volcanic arc environment for the Riviera granitoids (Fig. 2). Potassic alteration increased Rb values significantly, resulting in the shifting of data points into the syn-collision field on the Y+Nb vs Rb diagram (Fig.2).

Alteration assemblages are spatially closely related to a system of quartz-calcite veins. Enrichment of the granite in ore elements (especially Mo and Cu) as well as supposedly stable elements including the rare earths took place along these veins.

References.

Debon F. and Le Fort P. (1988). A cationic classification of common plutonic rocks and their magmatic association: principles, methods, applications. Bull. Mineral. 111, p. 493-510.
Eby G.N. (1992). Chemical subdivision of the A-type granitoids: Petrogenetic and tectonic implications. Geology, 20, p. 641-644.
Gresse P.G. (1991). The Pan-African Saldania Belt in Southern Africa. Abstract. Gondwana 8 Symposium; Tasmania.
Hartnady C.J., Newton A.R. and Theron J.N. (1974). Stratigraphy and structure of the Malmesbury Group in the southwestern Cape. In Contr. to the Precambrian geology of southern Africa. Ed. Kröner A., Bull. of the P.R.U. Univ. Cape Town.
Pearce J.A., Harris N.B.W. and Trindle A.G. (1984). Trace element discrimination diagrams for the tectonic interpretation of granitic rocks. Jnl. Petrol., 25, p. 956-983.
Taylor S.R. and Mclennan S.M. (1985). The continental crust: Its composition and evolution: Oxford, England, Blackwell, 312 p.
Theron J.N. (1990). Geology of sheet 3318 Cape Town. Geological Survey, South Africa.

Current Research in Geology Applied to Ore Deposits.Fenoll Hach-Alí, Torres-Ruiz & Gervilla(eds)(1993).ISBN 84-338-1772-8

THE ANDEAN MINERALIZATIONS REVISITED: OROGENESIS, SUBDUCTION -RELATED CALC-ALKALINE MAGMATISM, AND METALLOGENESIS IN THE CENTRAL PERUVIAN ANDES

Soler, P.
ORSTOM (URIH-TOA), 213 rue Lafayette, 75010 Paris, France and Mission ORSTOM, Casilla 9214, La Paz, Bolivia

ABSTRACT: The study of the evolution of the geochemical and isotopic features of the Cretaceous to Neogene granitoids along a traverse of the central Peruvian Andes and of the metallogenetic zonation in the same segment of the Andes suggests that the evolution of the metallogenesis in the central Andes corresponds to a progressive distillation of the continental crust associated with the development of the orogenesis and with the progressive increase of the crustal component in the arc magmas. The lateral (along-strike) extensions of the different metallogenetic provinces would be controlled by the heterogeneities of the lower and middle crust.

The Andean metallogenesis is considered as the archetype of metallogenesis at ocean-continent convergent margins (e.g. Sillitoe, 1976; Mitchell and Garson, 1981; Sawkins, 1984). In the central Andes a close relationship appears both at regional and local scale between most of the Mesozoic and Cenozoic ore deposits and the subduction process, via the subduction-related calc-alkaline magmatism generating the Fe, Cu, and polymetallic ores, but the distribution of the metallogenetic provinces in space and time shows that such relations are not simple. The complete "classical" transversal zonation (from the coast towards the Brazilian shield: Fe province, Cu province, polymetallic province, tin province - Sillitoe, 1976, Clark et al., 1990) is observed only within one segment of the Andean range (southern Peru, Bolivia, northern Chile). In the other parts of the central Andes either a similar but uncomplete zonation (e.g. central Peru) or a quite different zonation (e.g. central Chile) are observed. The lateral (along-strike) limits are roughly the same for a set of parallel metallogenetic provinces, which permits to define a succession of segments along the Andean range. Each province is associated with a portion of a magmatic arc of a given age but this arc is not necessarily (economically) mineralized in the adjacent segments.

The observed metallogenetic zonation is diachronous: in central Peru (e.g. Soler et al., 1986; Vidal, 1987) the coastal Cu-province is associated with the Albian Casma volcanism and to the late Cretaceous Coastal Batholith while the eastern polymetallic province is associated with Oligo-Miocene volcanics and intrusive stocks. In southern Peru (e.g. Soler et al., 1986; Clark et al., 1990) the Fe-province is linked to Jurassic and lower Cretaceous plutons, the Cu-province (mainly porphyry-type deposits) is associated with the Paleocene part of the Coastal Batholith, the polymetallic province is linked to Miocene volcanics and intrusive stocks, and the Sn-(W)-base metals-Ag province of the Eastern Cordillera is associated with Oligo-Miocene peraluminous felsic intrusions.

The close spatial and genetical relationship between the calc-alkaline magmas and most of the Mesozoic and Cenozoic (Fe), Cu, and polymetallic ore deposits is demonstated by the metallogenetic types of deposits (porphyry deposits, contact metasomatic deposits,

intra-plutonic hydrothermal veins, ...) and by geochemical data. As an example, lead isotopic data for the Cenozoic intrusive stocks (barren and mineralized) and the galena from the associated ores (Tilton et al., 1981; Soler and Rotach-Toulhoat, 1988 and unpub. data; Gunnesch et al., 1990; Macfarlane and Petersen, 1990; Macfarlane et al., 1990; Mukasa et al., 1990; Soler, 1991) show that the lead (and by extension the other base metals and silver) of the ores proceeds from two sources: 1) mainly from the intrusive stocks themselves; and 2) secondarily from the early Paleozoic sedimentary rocks. These data show that the pre-existing Mesozoic stratabound Pb-Zn deposits are not a significant source for the lead of the Cenozoic polymetallic ore deposits.

Various models have been proposed to explain the observed metallogenetic zonation across the Andes. The diachronous pattern of this zonation and many geochemical considerations permit to disregard the ultra-simplistic model initially proposed by Sillitoe (1976) of a progressive down-dip distillation of the subducted slab as the motor of such a zonation. Differences in the level of erosion or in the level of emplacement of the arc magmas do not seem neither to be good explicative candidates. The close relationship between the arc magmas and the Andean ore deposits induces to look for possible changes in the geochemical features of the arc magmas with time (and space) that would correlate with the metallogenetic evolution: systematic differences in the degrees of differentiation with time are not observed, but changes in the chemistry of the arc magmas at a given stage of differentiation with time are evidenced and appear to be the best candidates to explain the observed metallogenetic zonation, as shown by our study of the geochemistry of the Cretaceous to Neogene magmatism of central Peru (Soler, 1991).

During the Andean orogeny (Albian to Present) the space and time distribution of the calc-alkaline magmatic rocks in this segment of the Andes have been tightly controlled by the features of the subduction of the Nazca (previously Farallon) plate under the South American continent (Soler and Bonhomme, 1990; Sébrier and Soler, 1991; Soler, 1991). Over this time span, the geochemical and isotopic features of the calc-alkaline volcanic rocks and the I-type granitoids display complex variations. For a given period of time, overall similarities in their space distribution and compositions imply that both the volcanic and plutonic arc suites were derived from the same source, an enriched mantle modified by fluids (or melts?) extracted from the subducted slab. The variations in their compositions in time correspond mostly to MASH-like (Hildreth and Moorbath, 1988) lower crustal processes in deep magma chambers which include (Soler, 1991): (1) selective diffusive exchanges between the mafic magmas and their crustal country rocks; a general increase of the K content with time (at a same stage of differentiation) is not observed however. The calc-alkaline suites jump in the medium to high-K fields as soon as the crustal contamination is significant so that the K-content evolves quickly (at a same stage of differentiation) only during the first stage of the orogenic maturation of the arc (transition from the Casma volcanism to the Coastal Batholith). This is considered as a consequence of the self-limiting nature of the diffusive exchanges; (2) assimilation of the country rock at an early stage of differentiation of the magmas; (3) modification of the mineralogy of the crystallizing phases, with the appearance of garnet at the liquidus and a later

crystallisation of plagioclase which lead in particular to lower HREE, Sc, Mn, and higher Sr and LREE in the intermediate and felsic rocks. The observed evolution corresponds to a succession of compositionnal jumps (for a given stage of differentiation) which are contemporaneous with the main tectonic events (e.g. Mégard, 1987; Sébrier and Soler, 1991) and the associated crustal thickening, and are interpreted as the result of an increasing degree of crustal assimilation (which is particularly well illustrated by the evolution of the Sr-, Nd-, and Pb-isotopic compositions of the granitoids - Mukasa, 1986; Soler and Rotach-Toulhoat, 1990ab; Soler, 1991) and of an evolution under higher pressure at an early stage of differentiation (appearance of garnet at the liquidus) (Soler, 1991). The most conspicuous of these compositionnal jumps took place at nearly 100 Ma (early Mochica tectonic event - change from the Casma volcanism to the Coastal Batholith granitoids), 50-40 Ma (Inca tectonic events - transition from the Coastal Batholith to the post batholith magmatism), 30-20 Ma (Aymara and early Quechua tectonics), and 10-6 Ma (late Quechua tectonic events) (Soler, 1991). Thus, the evolution of the chemical and isotopic features of the calc-alkaline magmatic rocks of central Peru may be regarded as the geochemical fingerprint of the orogenic processes upon mantle-derived magmas the primary compositions of which do not appear to have changed significantly with time.

It is tempting to draw a parallel between this evolution of the calc-alkaline magmas and the time (and space) distribution of the (Fe), Cu, and polymetallic provinces of central and southern Peru: the evolution Fe --> Cu --> polymetallic ores would correspond to a progressive distillation of the continental crust associated with the development of the orogenesis and the progressive increase of the crustal component in the arc magmas. This explanation is not sufficient however, because it does not account for the lateral (along-strike) extensions of the different metallogenetic provinces. The heterogeneities of the lower and middle crust must be taken into account. For example, the Oligo-Miocene polymetallic ore deposits of central Peru have developped at the space-time conjonction of highly crust-contaminated calc-alkaline arc magmas and the early Paleozoic basin; in the same way, the southern Peruvian Paleocene porphyry copper deposits would have formed at the conjonction of slightly contaminated arc magmas (Lebel et al., 1985) and an abnormal MORB-like underplated material (the "Mollendo Ridge" of Soler et al., 1989). Finally, the central Andean eastern tin belt would not be directly linked to the subduction process. Tin deposits, which are restricted to the area where the A-type subduction of the Brazilian shield under the Andean range is observed, are genetically associated with Oligo-Miocene peraluminous granitoids and sub-volcanic stocks, the mixed mantellic-crustal origin of which (Carlier et al., 1992; Soler et al., 1992) is probably associated with this peculiar geodynamic setting wich corresponds to the latest stage of the orogenic evolution.

REFERENCES:

Carlier, G. et al. 1992. Orígen y significado tectónico del volcanismo shoshonítico neógeno a cuaternario en los Andes. Bol. Soc. Geol. Boliviana 27: 173-175

Clark, A.H. et al. 1990. Geologic and geochronologic constraints on the metallogenic evolution of the Andes of Southeastern Peru. Econ. Geol. 85:1520-1583

Gunnesch, K.A. et al. 1990. Lead isotope variations across the Central Peruvian Andes. Econ. Geol. 85:1384-1401
Hildreth, W. & Moorbath, S. 1988. Crustal contributions to arc magmatism in the Andes of Central Chile. Contrib. Mineral. Petrol. 98:455-489
Lebel, L. et al. 1985. A high-K, mantle-derived, plutonic suite from Linga, near Arequipa, Peru. J. Petrology 26:124-148.
Macfarlane, A.W. & Petersen, U. 1990. Pb isotopes of the Hualgayoc area, Northern Peru: Implications for metal provenance and genesis of a Cordilleran polymetallic mining district. Econ. Geol. 85:1303-1327
Macfarlane, A.W. et al. 1990. Lead isotope provinces of the central Andes inferred from ores and crustal rocks. Econ. Geol. 85:1857-1880
Mégard, F. 1987. Structure and evolution of the Peruvian Andes. In: Schaer, J.P. et Rodgers J. (eds.) The anatomy of mountain ranges. Princeton Univ. Press, Princeton, pp179-210
Mitchell, A.H.G. & Garson, M.S. 1981. Mineral deposits and global tectonic setting. Academic Press, London
Mukasa, S.B. 1986. Common Pb isotopic compositions of the Lima, Arequipa and Toquepala segments in the Coastal Batholith, Peru: implications for magmagenesis. Geochim. Cosmochim. Acta 50:771-782.
Mukasa, S.B. et al. 1990. Pb isotope bearing on the metallogenesis of sulfide ore deposits in Central and Southern Peru. Econ. Geol. 85:1438-1446.
Sawkins, F.J. 1984. Metal deposits in relation to plate tectonics. Springer-Verlag, Berlin Heidelberg New York
Sébrier, M. & Soler, P. 1991. Tectonics and magmatism in the Peruvian Andes from late Oligocene to Present. G.S.A. Spec. Paper 265:259-278
Sillitoe, R.H. 1976. Andean mineralization: a model for the metallogeny of convergent plata margins. Geol. Assoc. Canada Spec. Paper 14:59-100
Soler, P. 1991. Contribution à l'étude du magmatisme associé aux marges actives. Pétrographie, géochimie et géochimie isotopique du magmatisme crétacé à pliocène le long d'une transversale des Andes du Pérou central. Implications géodynamiques et métallogéniques. Unpub. Doctorat d'Etat thesis, Univ. Paris 6, Paris, 857 p.
Soler, P. & Bonhomme, M. G. 1990. Relation of magmatic activity to plate dynamics in central Peru from late Cretaceous to recent. G.S.A. Special Paper 241:173-192.
Soler, P. & Rotach-Toulhoat, N. 1988. Pb-isotopic compositions of intrusive stocks and associated ore minerals from the Oligo-Miocene polymetallic belt of central Peru. Chemical Geology 70:137.
Soler, P. & Rotach-Toulhoat, N. 1990a. Implications of the time dependent evolution of Pb- and Sr-isotopic compositions of Cretaceous and Cenozoic granitoids from the coastal region and the lower Pacific slope of the Andes of Central Peru. G.S.A. Special Paper 241:161-172.
Soler, P. & Rotach-Toulhoat, N. 1990b. Sr-Nd isotope compositions of Cenozoic granitoids along a traverse of the Central Peruvian Andes. Geological Journal (Liverpool) 25:351-358
Soler, P. et al. 1986. Essai de synthèse sur la métallogénie du Pérou. Géodynamique 1:33-68.
Soler, P. et al. 1989. Evidences for the subduction and underplating of an oceanic plateau beneath the South Peruvian Andes during the late Cretaceous-Structural implications. Tectonophysics 163:13-24
Soler, P. et al. 1992. An alternative model for the origin and the tectonic significance of the Neogene and Quaternary shoshonitic volcanism of the Andes. EOS Trans. AGU, Spring Meeting Suppl. 73(14):341.
Vidal, C. E. 1987. Kuroko-type deposits in the middle Crataceous marginal basin of central Peru. Econ. Geol. 82:1409-1430
Tilton, G.R. et al. 1981. Isotopic composition of Pb in central Andean ore deposits. Geol. Soc. Amer. Memoir 154:791-816

Current Research in Geology Applied to Ore Deposits. Fenoll Hach-Alí, Torres-Ruiz & Gervilla (eds) (1993). ISBN 84-338-1772-8

CHANGES IN TEMPERATURE AND SALINITY IN A ZONE OF LATERAL FLOW IN THE ALUTO-LANGANO GEOTHERMAL FIELD, ETHIOPIA: EVIDENCE FROM CLAY MINERALS AND FLUID INCLUSIONS

Teklemariam, M. (1); Battaglia, S. (2); Gianelli, G. (2) & Ruggieri, G. (2)
(1) Dipto. di Scienze della Terra, Pisa, Italy
(2) International Institute for Geothermal Research, Pisa, Italy

ABSTRACT: The zones of lateral flow in the Aluto-Langano geothermal field are characterized by temperature inversions, mixing between geothermal and cold waters, persistence of high-temperature alteration minerals, secondary fluid inclusions with high homogenization temperatures and occurrence of low temperature chlorite-smectite mixed layers. The upflow zone is characterized by waters with up to 14 ppb of Au and up to 3.4 ppb of Ag. These metals can be deposited in the zones of lateral flow.

INTRODUCTION

Aluto-Langano is a high-temperature (350°C) water-dominated geothermal system hosted in alkaline basalt to rhyolite lavas and pyroclastics within the Main Ethiopian Rift (Fig. 1). Exploratory and production wells identified an upflow zone (wells LA-6 and LA-3) with temperatures of 300-350°C and partial pressures of CO_2 of the order of 1.3 MPa. The zone of lateral outflow is characterized by more diluted waters with temperatures in the range of 150-270°C, local temperature inversions at the margin of the field and very high pCO_2 (3-5 MPa). Previous works (Valori et al., 1992; Gianelli & Teklemariam, 1993) hypothesize a rise in temperature in the discharge zone (as indicated by fluid inclusion data), and a general stabilization of the mineral assemblage at temperatures comparable to the present in-hole values, but at lower pCO_2 values. Important changes in the hydrothermal regime in the outflow zones are indicated by the presence of relict high-temperature mineral assemblages at temperatures as low as 170°C. Fluid inclusions and clay minerals from wells LA-7 and LA-4, drilled in the outflow zone, were studied for evidence of major changes in the hydrothermal regime. A preliminary hypothesis is also proposed for the transport and deposition of gold and silver in the Aluto-Langano geothermal system, based on fluid chemical data (wells LA-3, LA-6, LA-8).

ROCK ALTERATION

The alteration mineral assemblages are characterized by the presence of calcite and quartz associated with calc-alumina silicates, such as frequent epidote and minor prehnite, garnet and amphibole. Biotite and clay minerals are also present. In the hottest part of the wells the clay minerals are distributed in four zones (Teklemariam, 1986): 1) illite smectite mixed-layers ($T < 150°C$); 2) illite + chlorite ($170<T<210°C$); 3) illite ($300<T<320°C$) and chlorite ($T > 320°C$). However, in the wells drilled outside the upflow zone (LA-4 and LA-7) the sequence of the clay mineral assemblages in order of increasing depth is characterized by illite-smectite mixed layers ($T<150°C$), illite + chlorite ($150<T<200°C$) and chlorite-smectite mixed layers, vermiculite, chloritic-intergrades and kaolinite at a temperature less than 200°C and in the zones of temperature inversion (Fig. 2).

Table 1) gives the X-ray diffraction data for basal reflection d(001)A for the chlorite-smectite mixed-layers and chloritic intergrades. The latter minerals show reduced expandibility and resistance to collapse upon heating or K-saturation. Thermal treatment at 550°C leaves a broad basal peak (001) at 12.7 A and no collapse at 10 A. Collapse to approx. 17 A, after Mg-saturation and ethylene glycol solvation, is inhibited, as shown by the (001) peak value of 15.7 A. The chlorite-smectite mixed layers are identified on the basis of peak positions (14.6, 7.20 and 3.54) as interstratified trioctahedral chlorite-smectite (saponite), with a chlorite percentage of about 85-90% (Reynolds, 1980). Application of the chlorite geothermometer of Cathelineau (1988) indicates a computed temperature of 200-240°C in well LA-7 at a depth of 798 m, in agreement with in-hole data.

Table 1.- Basal spacings (A) for clay minerals: CHLI=chloritic intergrade; CHL/SM=chlorite-smectite mixed layer.

Mineral	Well/depth (m)	T°C	Treatment			
			Air-dried	Mg-E.G.	K-300°	K-550°
CHLI	LA-7/1791	150	14.2	15.7	13.9	12.7
CHL/SM	LA-4/ 759	220	14.7	15.3	14.2	14.2

FLUID INCLUSIONS

Secondary fluid inclusions in magmatic quartz from core samples of well LA-7 (798 and 2040 m depth) were studied. Most of the inclusions are aqueous two-phase (L+V) or polyphase (L+V+S) liquid-rich. The polyphase inclusions contain one or more solids, which are interpreted as accidentally trapped minerals. Secondary two-phase (L+V) vapour-rich and one-phase vapor inclusions, sometimes coexisting with the liquid-rich inclusions, also occur, indicating that the hot fluids were boiling a some time in the system. The vapour-rich inclusions were not suitable for microthermometric determination. Preliminary microthermometric measurements on the liquid-rich inclusions show a first ice melting temperature in the range of -22.5 to -20.0°C, suggesting the presence of Na^+, Cl^- and possibly K^+ in the inclusion fluids. Final ice melting temperatures (Tm) are in the range of -1.3 to -2.0°C for the sample at 798 m and -1.3 to -1.7 for the sample at 2040 m, corresponding to apparent salinities of 2.2 - 3.4 wt% NaCl eq. and 2.2 - 2.9 wt% NaCl eq., respectively. These salinities are substantially similar to those reported by Valori et al. (1992) for inclusions in core samples from wells LA-3 and LA-6, and higher than the present salinity of 0.3-0.4 wt%. Clathrate was not observed in the studied inclusions. Homogenization temperatures (Th) are between 215 and 256°C for the sample at 798 m and between 248 and 297°C for the sample at 2040 m. Assuming that all inclusions have trapped fluids close to boiling conditions, the Th values may be considered as representative of the true trapping temperature.

Au AND Ag CONTENT IN GEOTHERMAL FLUIDS

The geothermal fluids from wells LA-3, LA-6 and LA-8 contain <10, 14, <10 ppb of Au and <0.5, <0.5, 3.4 ppb of Ag, respectively. Using thermodynamic data for gold aqueous species (Hayashi & Ohmoto, 1991), our calculations indicate that the LA-6 fluid is

near saturation in gold, assuming the $HAu(HS)^{\circ}_2$ and $AuHS^{-}$ complexes as dominant aqueous phases for gold. Theoretical calculations indicate that the LA-8 fluid cannot carry this amount of gold to reach saturation. The preliminary conclusion could therefore be that the upflow zone of the field is a zone in which gold can be transported in solution whereas the more diluted and relatively cold water of LA-8 can deposit this metal. Significant amount of Ag has been found in the LA-8 water and the computed values of the saturation indexes for silver and argentite are 4.1 and 8.1 respectively. These minerals are undersaturated in wells LA-3 and LA-6. Silver in well LA-8 is transported as chloride complexes, according to the results of a computed species distribution.

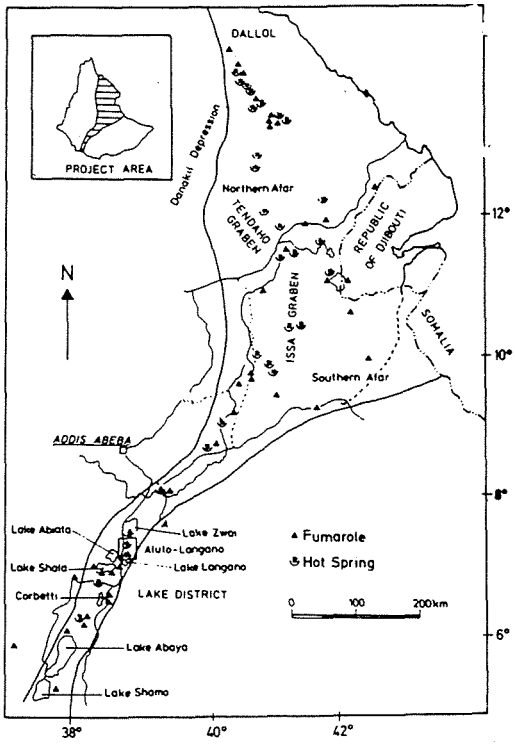

Fig. 1 - Location map of the Aluto-Langano geothermal field.

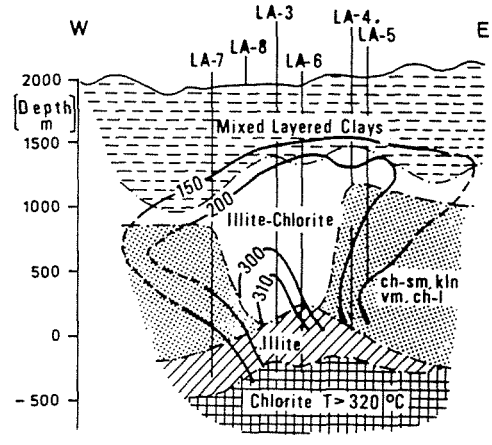

Fig. 2 - Clay minerals and temperature distribution in the Aluto-Langano geothermal field. Ch-sm=chlorite-smectite mixed layers; kln=kaolinite; ch-I= chloritic intergrades; vm=vermiculite; LA = geothermal well.

CONCLUSIONS

The only petrographic evidence of a lateral flow of cold water into the reservoir is the existence of chlorite-smectite mixed layers and chlorite intergrades. The occurrence of these clay minerals in zones with cooling conditions has also been reported in other geothermal fields (Tomasson & Kristmannsdottir, 1972; Harvey & Browne, 1991; Gianelli et al., 1992); the temperatures there are very close to those measured in well LA-7 in the zone of temperature inversion. The temperature recorded by fluid inclusions in this zone is about 120°C higher than the in-hole temperature, indicating a significant cooling process after fluid inclusion formation. The presence of epidote, garnet and biotite in association with these low-temperature clay minerals represents the relict phases of a previous high temperature stage of the hydrothermal system. Preliminary data on the Ag and Au contents in the Aluto-Langano geothermal waters indicate that the water of well LA-6 could transport Au but not Ag, whereas Au could deposit in the zones of lateral outflow.

REFERENCES

Cathelineau, M. 1988. Cation site occupancy in chlorites and illites as a function of temperature. Clay Min. 23:471-485

Hayashi, K. & Ohmoto, H. 1991. Solubility of gold in NaCl- and H_2S-bearing aqueous solutions at 250-350°C. Geochimica Cosmochim. Acta. 55:2111-2126

Gianelli, G. & Teklemariam, M. 1993. Water - rock interaction processes in Aluto-Langano geothermal field, Ethiopia. J. Volc. Geotherm. Res. in press

Gianelli, G., Yusa, Y., Battaglia, S. & Takemura, K. 1992. Water-rock interaction in a zone of lateral flow: a natural example from the active geothermal field and gold-mineralized zone of Beppu (Kyushu Island, Japan). Mineralogy and Petrology.45:247-259

Harvey, C. & Browne, P. 1991. Mixed layer clay geothermometry in the Wairakei geothermal field, New Zealand. Clays and Clay Minerals. 39:614-621

Reynolds, R. 1980. Interstratified clay mineral. In: Brindley, G.W.& Brown, G.(eds) Crystal structures of clay minerals and their identification, pp 249-303

Teklemariam, M. 1986. Hydrothermal alteration in wells LA-3, LA-4 and LA-6, Aluto-Langano geothermal field, Ethiopia. Ext. Abst. Fifth Int. Symp. on Water - rock interaction, Reykjavik, Iceland, pp 565-566

Tomasson, J. & Kristmannsdottir, H. 1972. High temperature hydrothermal minerals and thermal brines, Reykjanes, Iceland. Contr. Mineral. Petrol. 36:123-134

Valori, A., Teklemariam, M. & Gianelli, G. 1992. Evidence of temperature increase of CO2-bearing fluids from Aluto-Langano geothermal field (Ethiopia): a fluid inclusion study of deep wells LA-3 and LA-6. Eur. J. Mineral. 4:907-919

Current Research in Geology Applied to Ore Deposits.Fenoll Hach-Ali, Torres-Ruiz & Gervilla(eds)(1993).ISBN 84-338-1772-8

PETROLOGICAL CHARACTERISTICS OF THE PTOLEMAIS LIGNITE, GREECE. A PRELIMINARY STUDY.

Valceva, S. (1) & Georgakopoulos, A. (2)
(1) University of Sofia, Bulgaria
(2) University of Thessaloniki, Greece

ABSTRACT: Lignite samples from the Southern field of Ptolemais basin in Northern Greece are investigated for their petrological characteristics. The lignites are characterized by a complex petrographic composition and consist of nearly all macerals of the three maceral groups: huminite (86-90%), inertinite (5-8%) and liptinite (1-2%). The mineral matter (4-5%) consists of framboidal pyrite and clay minerals. The reflectance of the individual macerals and maceral groups is variable (0,07-1,01%) and is predetermined by the type of the original flora and the degree of its decomposition and gelification.

INTRODUCTION AND GEOLOGICAL SETTING

Lignite occurs in more than sixty basins in Greece, four of them, including Ptolemais basin, being under intensive exploitation and the exploited lignite is used mainly for electric power generation. The Neogene-Quaternary sediments of the Ptolemais basin (Fig.1) are divided into three lithostratigraphic formations: the lowest (Upper Miocene to Lower Pliocene), the middle (Pliocene) and the Upper (Quaternary) formations (Koufos & Pavlides 1988). The middle formation contains the exploited lignite beds alternating with clays, marls and sands. The lignite beds are divided into the upper lignite seam, with an average thickness of 25 m and the lower lignite seam, with an average thickness of 40 m. The intermediate sterile band has an average thickness of 12 m.

Few papers have so far been devoted to the study on petrology of Greek coals. Attention has been essentially focused on the presence of uranium in some lignites from coal fields in Northern Greece (Taupitz 1984, Psilovikos and Karistineos 1986). Cameron et al. (1984) reported the complex petrological characteristics of Greek coals from different basins. The present work aims to investigate, for the first time, the petrological characteristics of selected lignite samples through a borehole from the Southern lignite field in Ptolemais basin.

MATERIALS AND METHODS

The investigations were carried out with three samples from the borehole KNP-20 from the Southern lignite field of Ptolemais basin. Sample 1 (69 m depth) and sample 2 (74 m depth) belong to the upper lignite seam, while sample 3 (113 m depth) belongs to the lower one.

The coals were characterized using the following petrographic analyses: lithotype determination, maceral analysis and reflectance measurements. Polished sections of the samples were prepared for microscopic examination. The blocks were prepared according to the standard method, following the procedure outlined in the Stach's Textbook (Stach et al., 1975).

The microscopic measurements and the lithotype analysis were carried out according to the Bulgarian standard lithotype classification for lignites and brown coals (Siskov & Valceva 1983). In accordance with it, the lithotypes that are visually recognizable in the low coalified coals, are divided into homogeneous and heterogeneous. The latter include humoclarain, humodurain and liptain and the former xylain, humovitrain, semifusain and fusain.

The quantitative maceral analysis was carried out under reflected light and oil immersion, using a microscope equipped with point automatic integrator. The maceral classification and terminology adopted in the Stach's Textbook, was followed. The reflectance was determined using a Standard Universal MPM "Opton" microscope-photometer with Antiflex Epi $40/0.65_{oel}$ objective, in immersional

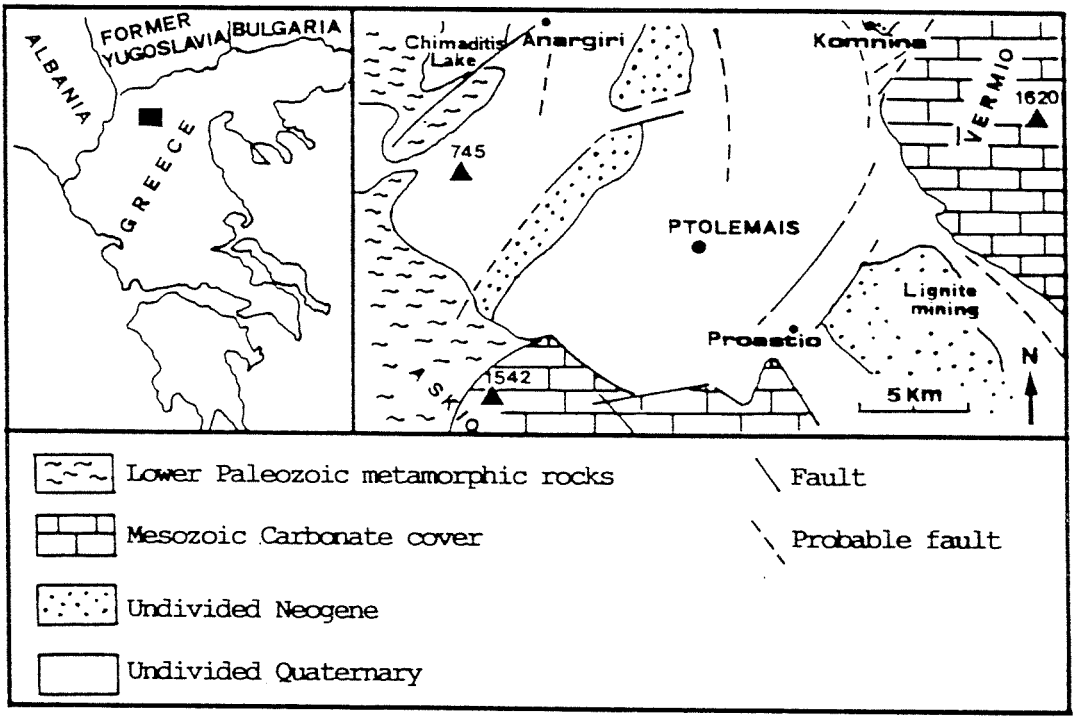

Fig. 1. Geological map of the Ptolemais area (after Pavlides & Mountrakis 1987).

cedar oil medium with reflectivity N=1.515 at a monochromatic light (λ=546 nm). A reference with reflectance capacity of 0.299% (R_o) was used for huminite and liptinite group macerals, while for those of the inertinite group, a reference with R_o=0.94% was applied.

RESULTS AND DISCUSSION

Lithotype composition: The coals studied, represent dark-brown semi-bright lignites, consisting mainly of the coal lithotype humoclarain. The latter contains fragments of xylain, humovitrain or humodurain bands of various size. The separate samples have their own specific lithotype characteristics. Thus, sample 1 comprises greyish brown lignites with associated sections of cinnamon-brown xylain with distinct cell structure. Xylain occurs not only as fragments but also in the form of bands and strias with thickness up to 1-2 mm, rarely to 1cm. Humovitrain represents a black, bright material with mussel texture. Fusain and semifusain exist as small inclusions that dirty the hands and have a sooty and silky appearance. The basic humoclarain mass is dark brown, with compact or striated texture in humovitrain. In humoclarain, inclusions of 2-5 mm as spots of lake chalk, are identified. The latter is a white pink dusty material that dirties the hands and is probably formed by the shell decay.

Sample 2 appears as black, compact, striated coal with mussel texture, which is characteristic for the geleous humoclarain. Rare striations and bands of bright humovitrain and darker humodurain have been identified. Sample 3 consists of black semibright humoclarain coal with humovitrain bands.

Maceral composition: The petrographic composition of the lignites under

study was determined by quantitative maceral analysis. The representatives of the three maceral groups and mineral matter have been identified. The maceral differentiation is based on colour, reflectance, morphological and other properties. Table 1 reveals the great variation in the quantitative presence of maceral groups-huminite (86-90%), liptinite (1-2%), inertinite (5-8%) and mineral matter (4-5%).

Table 1. Petrographic composition (%) of Ptolemais lignites, from borehole KNP-20, of Southern field.

Sample No	Huminite Group								
	Textinite		Texto-ulminite		Ulminite		Attrinite	Corpo-huminite/ phlobaphinite	Total
	A	B	A	B	A	B			
1	10	1	1	28	2	2	42	1	87
2	tr	1	3	7	6	7	61	1	86
3	tr	1	13	7	8	10	50	1	90

Sample No	Liptinite Group	Inertinite Group				Mineral matter		
	Resinite-Sporinite	Semi-fusinite	Inerto-detrinite	Sclero-tinite	Total	Pyrite	Clay minerals	Total
1	2	1	4	1	6	3	2	5
2	1	2	6	-	8	3	2	5
3	1	1	4	tr	5	tr	4	4

Two varieties (A and B), of textinite, ulminite and texto-ulminite macerals have been distinguished in the huminite group. The other huminite macerals identified in this study are attrinite (in some places changing to densinite), phlobaphinite and corpohuminite. Textinite represents remnants of well preserved, ungelified woody and grass tissues and is characterized by clearly defined cell structure and open cell lumina that are partially filled by resinite or phlobaphinite. Texto-ulminite is a partially gelified plant tissue, and some of the cell lumina are closed and filled by humic substance or resinite and corpohuminite.

The gelified macerals are more rarely identified and ulminite A varies from 2% in sample 1 to 8% in sample 3, while for the light ulminite B the content ranges from 2 to 10% for the same samples. Attrinite is the most abundant maceral of the huminite group in all samples studied. It represents a mixture of fine to small comminuted humic particles and often plays the role of a basic mass.

Corpohuminite is identified as rounded, oval or oblong bodies with reflectance equal to/or higher than that of the surrounding huminite. The bodies included in the cell lumina of the plant tissue are indicated as phlobaphinite and can be clearly seen both in the dark (A) and in the light (B) varieties of textinite and texto-ulminite.

The liptinite group includes the coalified debris of the durable parts of the plant tissue with characteristic morphological properties. Resinite is the most abundant maceral from the liptinite group. Sporinite is found in minor

amounts in nearly all samples. The inertinite group macerals are found in minor amounts (5-8%). The following macerals have been identified: semifusinite/ fusinite (1-2%), inertodetrinite (4-6%) and sclerotinite (up to 1%). Fusinite and semifusinite are characterized by separate small fragments with clearly defined cell structure, at some places with ring-like appearance. Pyrite, in framboidal form, is found in minor amounts (up to 3%).

Maceral reflectance: The macerals of the liptinite group show the lowest mean reflectance R_o=0.07-0.13% and those of the huminite group ranges from 0.10 to 0.41% depending on the degree of gelification of the lignin-cellulose tissues. In accordance to the degree of oxidation of the original wood, the inertinite group macerals have the highest reflectance, R_o=0.44 to 1.01%.

The results obtained in the study of the reflectance measurements unambiguously confirm the general concept (e.g., Valceva 1979), that the reflectance variations of the individual macerals and maceral groups depend essentially on the type of the original flora and the degree of its decomposition and gelification.

CONCLUSIONS

The lignites from the Ptolemais basin are characterized by a complex petrographic composition and consist of nearly all macerals of the three maceral groups: huminite, liptinite and inertinite. The macerals of the huminite group (86-90%), especially attrinite as basic constituent followed by the A (dark) and B (light) varieties of textinite, texto-ulminite and ulminite are among the most abundant compositional entities identified in the samples studied. The investigated samples are characterized by minor amounts of macerals of the inertinite group (5-8%) and low amounts of macerals of the liptinite group (1-2%).

The reflectance of the individual macerals and maceral groups is variable and is predetermined both by the botanical nature of the original plant material and by the degree of gelification and fusination of the lignin-cellulose tissue during the peatification.

REFERENCES

Cameron, A.R., Kalkreuth, W.D. & Koukouzas, C. 1984. The petrology of Greek brown coals. Int. J. Coal Geology 4:173-207.

Koufos, G.D. & Pavlides, S.B. 1988. Correlation between the continental deposits of the lower Axios valley and Ptolemais basin. Bull. Geol. Soc. Greece XX/2:9-19.

Pavlides, S.B. & Mountrakis, D.M. 1987. Extensional tectonics of northwestern Macedonia, Greece, since the late Miocene. J. Struct. Geology 9(4):385-392.

Psilovikos, A. & Karistineos, N. 1986. A depositional sedimentary model for the Neogene uraniferous lignites of the Serres graben, Greece. Paleogeography, Paleoclimatology, Palaeoecology 56:1-16.

Siskov, G.D. & Valceva, S.P. 1983. Petrological nomenclature of lignites and brown coals. Comptes rendus de l' Acad. bulg. des Sciences 36(6):799-801.

Stach, E., Mackowsky, M-Th., Teichmuller, M., Taylor, G.H., Chandra, D. & Teichmuller, R. 1975. Stach's Textbook of Coal Petrology. Gebruder Borntraeger, Berlin, Stuttgart.

Taupitz, K. Ch. 1984. Uraniferous coals in the Neogene of NE-Macedonia (Greece). Erzmetall 37(2):57-65.

Valceva, S.P. 1979. Reflectance of macerals from bright brown coal, Pernik basin. Fuel 58(1):55-57.

Current Research in Geology Applied to Ore Deposits.Fenoll Hach-Alí, Torres-Ruiz & Gervilla(eds)(1993).ISBN 84-338-1772-8

Author index